Proceedings

17th Applied Stochastic Models and Data Analysis International Conference with Demographics Workshop

ASMDA2017

Editor

Christos H Skiadas

6 - 9 June 2017

De Morgan House, London, UK

Imprint
Proceedings of the 17th Applied Stochastic Models and Data Analysis International Conference with the 6th Demographics Workshop
London, UK: 6-9 June, 2017
Published by: ISAST: International Society for the Advancement of Science and Technology.
Editor: Christos H Skiadas

ISBN (e-book) 978-618-5180-23-2

Preface

It is our pleasure to welcome the guests, participants and contributors to the International Conference (ASMDA 2017) on Applied Stochastic Models and Data Analysis and (DEMOGRAPHICS2017) Demographic Analysis and Research Workshop.

The main goal of the conference is to promote new methods and techniques for analyzing data, in fields like stochastic modeling, optimization techniques, statistical methods and inference, data mining and knowledge systems, computing-aided decision supports, neural networks, chaotic data analysis, demography and life table data analysis.

ASMDA Conference and DEMOGRAPHICS Workshop aim at bringing together people from both stochastic, data analysis and demography areas. Special attention is given to applications or to new theoretical results having potential of solving real life problems.

ASMDA 2017 and DEMOGRAPHICS 2017 focus in expanding the development of the theories, the methods and the empirical data and computer techniques, and the best theoretical achievements of the Applied Stochastic Models and Data Analysis field, bringing together various working groups for exchanging views and reporting research findings.

We thank all the contributors to the success of these events and especially the authors of this Proceedings Book. Many thanks to the honorary guest Gilbert Saporta and the Colleagues contributed in his special session on data analysis. Special thanks to the Plenary, Keynote and Invited Speakers, the Session Organisers, the Scientific Committee, the ISAST Committee, Yiannis Dimotikalis, Aristeidis Meletiou, the Conference Secretary Mary Karadima, and all the members of the Secretariat.

November 2017

Christos H. Skiadas
Conference Chair

ASMDA Conferences and Organizers

1st ASMDA 1981 Brussels, Belgium. Jacques Janssen

2nd ASMDA 1983 Brussels, Belgium. Jacques Janssen

3rd ASMDA 1985 Brussels, Belgium. Jacques Janssen

4th ASMDA 1988 Nancy, France. J. Janssen and Jean-Marie Proth

5th ASMDA 1991 Granada, Spain. Mariano J. Valderrama

6th ASMDA 1993 Chania, Crete, Greece. Christos H Skiadas

7th ASMDA 1995 Dublin, Ireland. Sally McClean

8th ASMDA 1997 Anacapry, Italy. Carlo Lauro

9th ASMDA 1999 Lisbon, Portugal. Helena Bacelar-Nicolau

10th ASMDA 2001 Compiègne, France. Nikolaos Limnios

11th ASMDA 2005 Brest, France. Philippe Lenca

12th ASMDA 2007 Chania, Crete, Greece. Christos H Skiadas

13th ASMDA 2009 Vilnious,Lithouania. Leonidas Sakalauskas

14th ASMDA 2011 Rome, Italy. Raimondo Manca

15th ASMDA 2013 Mataró (Barcelona), Spain. Vladimir Zaiats

16th ASMDA 2015 Piraeus, Greece. Sotiris Bersimis

17th ASMDA 2017 London, UK. Christos H Skiadas

SCIENTIFIC COMMITTEE

Plenary/Keynote Talks For ASMDA Conference

In celebration of Gilbert Saporta's 70th birthday and in honour of his contributions to Applied Statistics and Data Analysis and his support to ASMDA activities

Gilbert Saporta
Emeritus Professor of Applied Statistics
Conservatoire National des Arts et Métiers (CNAM)
Paris, France

N. Balakrishnan
Department of Mathematics and Statistics
McMaster University
Hamilton, Ontario, Canada

Robert J. Elliott
Haskayne School of Business,
University of Calgary, Canada and
Centre for Applied Financial Studies,
University of South Australia,
Adelaide, Australia

Sally McClean
School of Computing and Information Engineering
Ulster University
Coleraine
Northern Ireland

Fabrizio Ruggeri
CNR IMATI
Via Bassini 15
Milano, Italy

Anatoliy Swishchuk
Department of Mathematics and Statistics
University of Calgary, Canada

P.-C.G. VASSILIOU
Department of Statistical Sciences,
University College London, UK

For Demographics Workshop

Jean-Marie Robine
Université Montpellier 2, Place Eugène Bataillon
Montpellier, France

Rebecca Kippen
Rural Health,
Monash University
Victoria, Australia

Contents **Page**

Saporta at Seventy

Pieter M. Kroonenberg,

Emeritus Professor at the Department of Education and Child Studies, Leiden University and The Three-Mode Company, Leiden

Abstract. This paper is an introduction to the Keynote lecture by Prof. Gilbert Saporta at the occasion of his seventieth birthday. An overview of this major publications, his citation record, his academic non-statistical interests is presented as well as a pictorial overview.

1. Introduction

The *Applied Stochastic Models and Data Analysis International Society* (ASMDA) decided to pay a special tribute to Prof. Gilbert Saporta of the *Centre National des Arts et Métiers*, Paris at the occasion of his 70th birthday. Clearly such a tribute is not bestowed upon just any septuagenarian. If his contributions to applied statistics and data analysis and his support to ASMDA activities themselves were not already enough for such a tribute, his nomination as Président d'Honneur de la Société Française de Statistique, made just before the conference, is additional proof that Prof. Saporta is not an average man.

.

In his keynote lecture entitled "50 Years of data analysis: from EDA to predictive modelling and machine learning" Prof Saporta sketches what has taken place in data analysis during his academic career, but this introduction will concentrate on some of the highlights of his publishing career, looking at his key publications, his citation record and his presence at various statistical gremia. A full curriculum vitae of Prof. Saporta can be found at the CNAM site: *http://cedric.cnam.fr/~saporta/CVSaporta_english_April2017.pdf*.

2. Publication records and their citations

There are at present several organisations, publishers and individuals who provide citation records of individual academics and academic groups. Two of the older ones are the ISI *Web of Science* and *Google Scholar*. Given that the latter includes books and more publications in languages other than English, I have taken Google Scholar as the basis for the information presented in this article -- although its use is not without difficulty. Anne-Wil Harzing has created a program *Publish or Perish*, which uses Google Scholar as its data base. In this program she calculates various statistics about publications, satisfying specific search terms (authors, subjects, research groups, etc.). One unfortunate circumstance is that academics are human, too, and not uncommonly references to their colleagues' work are not completely accurate. Given the automated character of data gathering by Google Scholar, such inaccuracies are generally not detected, so that multiple variants of the same publications can be found in the data base, and hence also in that of Harzing's *Publish or Perish* database. Therefore, this article contains such inaccuracies as well, but they would be too time-consuming and too difficult to rectify. I have tried to eliminate some of the more glaring ones, but more will have remained.

ResearchGate indicates that Prof. Saporta obtains a (albeit somewhat ResearchGate-specific) score which exceeds the scores of 70% of other researchers on its site. I would imagine that if all his publications were uploaded on this site he would easily score in the 90s.

Incidentally, it turns out that references to Prof. Saporta's work also appear under "S. Gilbert" (see Table 1). The probable reason is that algorithms gathering information on a person need to allocate publications of "G. Saporta", "Gilbert Saporta", "Saporta, Gilbert", "Saporta, G" to the same person, but "Saporta Gilbert" (without

the ",") also occurs. How is the algorithm to know what which is the first name and which is the family name? Note that on the same line Jean-Marie Bourouche has been reduced to a mere Mr. B.

Table 1. Citations to publications by S. Gilbert (Source: *Publish or Perish*, 18/6/2017)

Cites	Per year	Rank	Authors	Title	Year	Publication	Publisher
h 19	0.70	2	S Gilbert	Probabilités, analyse des données et statistique	1990	Paris, Éditions Technip	
h 8	1.00	1	H Wang, M Ye, S Gilbert	Classification for Multiple Linear Regression Methods [J]	2009	Journal of System Simulation	en.cnki.com.cn
h 7	0.30	4	B Jean-Marie, S Gilbert	L'analyse des données	1994	Que Saisje	
2	0.06	3	S Gilbert	Multidimensional data analysis for categorical variables	1985		Matrtinus Nujholf Publishe
2	1.00	7	D Jean-Jacques, S Gilbert, TA Christine	Méthodes robustes en statistique	2015		books.google.com

An additional aspect is that Prof. Saporta has published in both French and English and that for the casual investigator such as me it is unclear whether some English publications are straightforward translations of the French ones or vice versa. Finally, do we count various editions of the same book as different publications, or as the same publication? I have merged the results of the citation analysis so that in these cases all references were to the same publication. This leads to higher citation counts for those books, but I think this is only proper.

3. Saporta's productivity

Let us first look at Prof. Saporta's productivity as found in *Publish or Perish* (Fig. 1), but only counting those publications which have been cited at least once.

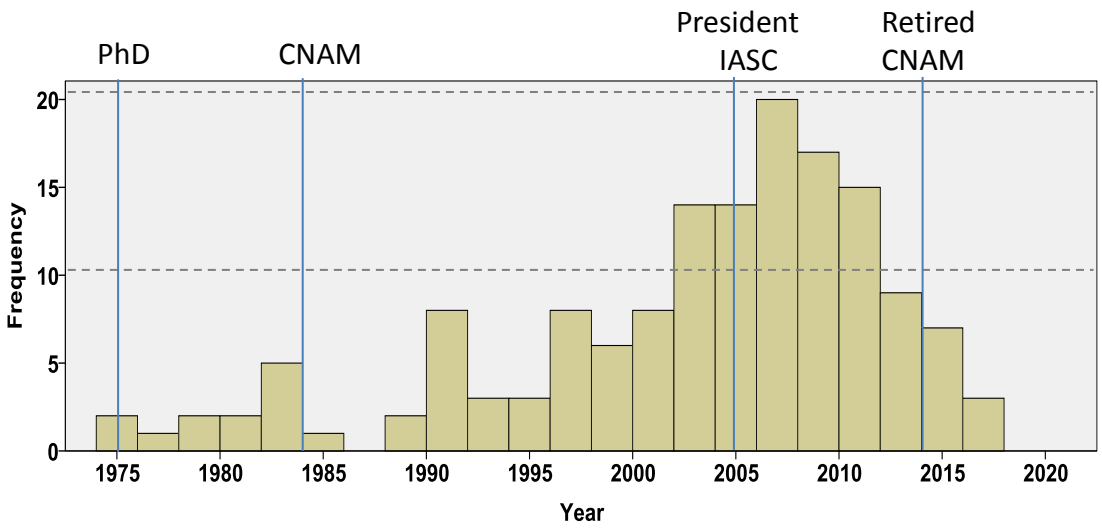

Figure 1. Number of publications cited at least once, arranged per year.

Figure 1 clearly shows that Prof. Saporta's peak productivity was in his sixties. His publications included not only cited journal papers but also several books, including textbooks from which many generations of French students were taught (and hopefully learned) statistics; in particular *Probabilités, analyse des données et statistique*, which so far has known three editions (2006, 1991, 2011).

As a slightly frivolous exercise I asked Google to produce images of the covers of his books, which resulted in Figure 2. I have not edited the results, so there are some rogue and fantasy 'covers' included here as well. The one I loved best was the second from the right on the top row. It reads "*L'Analyse des données* (French Edition)". Why 'French Edition'? Who would have been surprised that this book was not written in English? The solution to this riddle is that it is actually not a real cover (as stated almost illegibly in this figure), but a place holder for the real one, as is the first one of the same row. The actual covers of the two books from the *Que sais-je* series are given in Figure 3.

Figure 2. Covers of books (co)authored and/or (co)edited by Gilbert Saporta.

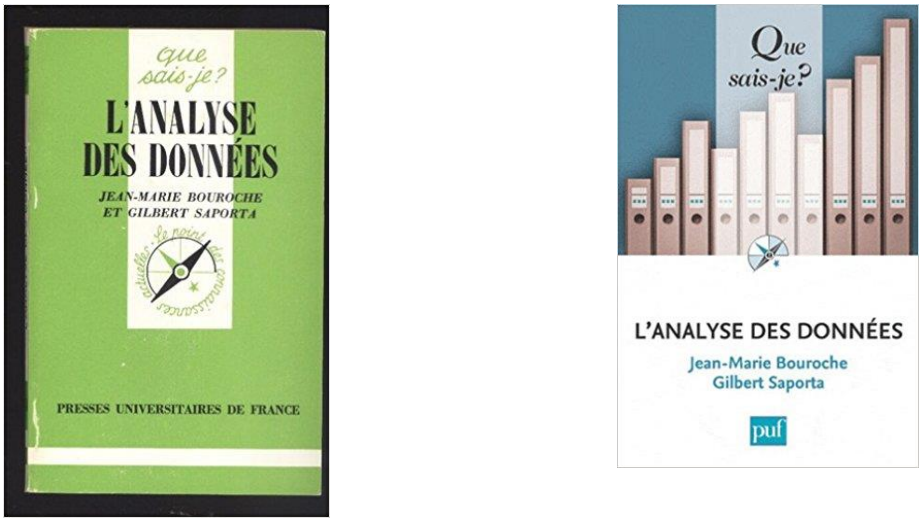

Figure 3. The real covers of the first and last editions of *L'Analyse des Données* from the *Que sais-je* series.

4. Saporta's prominent publications

In Table 2 below I present the results of a search for "Gilbert Saporta" in *Publish or Perish*. The outcomes are ranked according to frequency of citation. Prof. Saporta has an *h* index of 24, which means that on 17 June 2017, 24 of his publications had 24 citations or more, and it is those publications which are included in the list. The number of citations is a lower bound, because incorrect referencing has created new entries in the database. However, these citations should be part of the record of the correctly referenced publications.

The results in Table 2 make very clear that Prof. Saporta's books have been widely used, and one could even wonder what their citation count would have been had they also been available in English, the *lingua franca* of the scientific world. Finally, it is interesting to note how widely read and cited his two academic *thèses* have been. Not many scholars have that honour; of course it may be that this more usual in France than in the English-speaking world, but this does not diminish the acknowledged importance of these theses.

Table 2. Number of citations to publications (co)authored by Prof. Saporta (17/6/2017). Books are in **bold**

Nr.	**Cites**	**Cites/Year**	**Authors**	**Title**
1	**2101**	191.3	G Saporta (1990, 2006, 2011)	**Probabilités, analyse des données et statistique.** Paris : Editions Technip (3 editions).
2	**140**	11.7	C Preda, G Saporta (2005)	Clusterwise PLS regression on a stochastic process. *Computational Statistics & Data Analysis*, *49*, 99-108.
3	**123**	3.2	G Saporta (1978)	**Théories et méthodes de la statistique.** Paris : Editions Technip.
4	**121**	3.5	JM Bouroche, G Saporta, (2006)	**L'analyse des données (Que sais-je ?)** (9 editions).Presses Universitaires de France. (translated in Arabic, Italian and Portuguese).
5	**110**	5.5	JJ Droesbeke, J Fine, G Saporta (Eds.) (1997)	**Plans d'expériences: Applications à l'entreprise.** Paris : Editions Technip.
6	**99**	2.4	G Saporta (1975)	*Liaisons entre plusieurs ensembles de variables et codage de données qualitatives*. Thèse de 3^{e} Cycle Université Pierre et Marie Curie - Paris VI.
7	**90**	9.0	C Preda, G Saporta, C Lévéder (2007)	PLS classification of functional data. *Computational Statistics*, *22*, 223–235.
8	**77**	2.1	G Saporta (1981)	*Méthodes exploratoires d'analyse de données temporelles*. Thèse de doctorat d'état Université Pierre et Marie Curie - Paris VI.
10	**72**	3.4	F Dazy, JF Le Barzic, G Saporta, F. Lavallard (Eds.). (1996).	**L'analyse des données évolutives-Méthodes et applications.** Paris : Editions Technip.
11	**68**	6.8	M Plasse, N Niang, G Saporta, A Villeminot, L Leblond (2007)	Combined use of association rules mining and clustering methods to find relevant links between binary rare attributes in a large data set. *Computational Statistics & Data Analysis*, *52*, 596-613.
12	**60**	4.0	G Saporta (2002)	Data fusion and data grafting. *Computational Statistics & Data Analysis*, *38*, 465-473.
13	**54**	6.0	S Zaugg, G Saporta, E. van Loon, H. Schmaljohann, F. Liechti (2008)	Automatic identification of bird targets with radar via patterns produced by wing flapping. *Journal of the Royal Society Interface, 5*, 1041-1053.
14	**48**	6.0	M Vichi, G Saporta (2009)	Clustering and disjoint principal component analysis. *Computational Statistics & Data Analysis*, *53*, 3194-3208.
15	**48**	3.4	D Karlis, G Saporta, A Spinakis (2003)	A simple rule for the selection of principal components. *Communications in Statistics - Theory and Methods*, *32*, 643-666.

16	**42**	2.8	G Saporta, G Youness (2002)	Comparing two partitions: Some proposals and experiments (pp. 243-248). In W. Härdle, B. Rönz (Eds), *Compstat 2002*. Heidelberg: Physica, Verlag.
17	**40**	3.1	G Youness, G Saporta (2004)	Une méthodologie pour la comparaison de partitions. *Revue de Statistique Appliquée, 52*, 97-120.
18	**29**	2.4	JJ Droesbeke, M Lejeune, G Saporta (2005)	**Modèles statistiques pour données qualitatives.** Paris : Editions Technip.
19	**27**	2.7	A Tenenhaus,, A Giron, E viennet, M Bera, G Saporta, & B Fertil (2007)	Kernel logistic PLS: A tool for supervised nonlinear dimensionality reduction and binary classification. *Computational Statistics & Data Analysis, 51*, 4083-4100.
20	**29**	4.1	AM Aguilera, M Escabias, C Preda, G. Saporta (2010)	Using basis expansions for estimating functional PLS regression: Applications with chemometric data. *Chemometrics and Intelligent Laboratory Systems,104*, 289-305
21	**28**	2.3	V Stan, G Saporta (2005)	Customer satisfaction and PLS structural equation modeling. An application to automobile market . Presented at the Applied Stochastic Models and Data Analysis. Conference (ASMDA 2005).
22	**26**	1.1	L Jaupi, G Saporta (1993)	Using the influence function in robust principal components analysis.. S. Morgenthaler, E. Ronchetti (Eds.), *New directions in statistical data analysis and robustness*. Basel: Birkhäuser.
23	**25**	1.7	C Preda, G Saporta (2002)	Régression PLS sur un processus stochastique. *Revue de Statistique Appliquée, 50,*. 27-45.
24	**24**	3.0	G. Saporta, N Niang(2010)	Principal component analysis: Application to statistical process control. In G. Govaert (Ed.), *Data analysis*. Wiley Online Library.

5. Gilbert Saporta: A man for all disciplines.

"The best thing about being a statistician is that you get to play in everyone's backyard." (J. W. Tukey). Clearly Prof. Saporta likes to play in other people's backyards, but more to the point, he likes to play with the owners of the yards as well. This is evident from his co-authorship in backyard papers such as:

- applications à l'entreprise [business applications]
- bird targets with radar via patterns produced by wing flapping
- chemometric data
- automobile market
- radioactive waste produced at hadron accelerators
- psychosocial factors impacting stress level
- radiological characterization of historical waste
- vascular surgery
- vieillissement cutané chez femmes caucasiennes adultes [skin aging by adult Caucasian women]

6. Gilbert Saporta in the picture

Jan de Leeuw, Gilbert Saporta and Yutaka Tanaka
Calcutta, December 1985, International Conference on Advances in Multivariate Statistical Analysis (from JSS 2016 Festschrift De Leeuw)

Groningen, European Meeting Psychometric Society 1980
(with, amongst others, Gerhard Fischer, Herman Wold, Jan-Berndt Lohmöller)

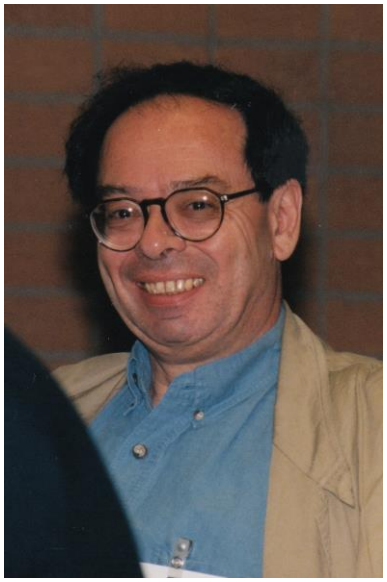

Leiden, European Meeting Psychometric Society 1995

Rennes: Carme 2011

Rennes: Carme 2011

Napoli: Carme 2015

Napoli: Carme 2015

Photos by Pieter M. Kroonenberg, except Groningen – photographer unknown

Gilbert Saporta at Pieter Kroonenberg's Farewell Symposium: 14-11-14

Photos by Jan Piet Hartman (https://www.4fotos.eu/)


At the ASMDA 2017 conference: Saporta and Skiadas, Organiser. Last-minute adjustments before his keynote lecture. Photos: Pieter M. Kroonenberg

Evaluation of Stopping Criteria for Ranks in Solving Linear Systems

Benard Abola[1], Pitos Biganda[1,2], Christopher Engström[1], and Sergei Silvestrov[1]

[1] Division of Applied Mathematics, The School of Education, Culture and Communication (UKK), Mälardalen University, Box 883, 721 23, Vsterås, Sweden (E-mails: benard.abola@mdh.se, christopher.engstrom@mdh.se, sergei.silvestrov@mdh.se)

[2] Department of Mathematics, College of Natural and Applied Sciences, University of Dar es Salaam, Box 35062, Dar es Salaam, Tanzania (E-mail: pitos.biganda@mdh.se)

Abstract. Linear systems of algebraic equations arising from mathematical formulation of natural phenomena or technological processes are common. Many of these systems of equations are large, the matrices derived are mainly sparse and need to be solved iteratively. Moreover, interpretation is crucial in making decision. Bioinformatics, internet search engines (web pages) and social networks are some of the examples with large and high sparsity matrices. For some of these systems only the actual ranks of the solution vector is interesting rather than the vector itself. In this case, it is desirable that the stopping criterion reflects the error in ranks rather than the residual vector which might have a lower convergence. In this paper, we evaluated stopping criteria on Jacobi, successive over relaxation and power series iterative schemes. Numerical experiments was performed and results show that Kendall's correlation coefficient, τ gives good stopping criterion of ranks for linear system of equations. Numerical experiments have been performed and results presented.
Keywords: stopping criteria, networks, rank.

1 Introduction

Sparse and large linear systems of equations are common in many physical applications. In particular, internet search engines is one of the area where such systems are encountered and have been studied intensively. The concepts have been deployed in areas such as social networks, bioinformatics and infectious disease management (Wills *et al.*[23]). With growing technology, the size of data from these fields are reaching billions and numerical computations are becoming more demanding (Boldi *et al.*[7]). Moreover, for the case of search engines, only a few relevant pages for query are provided, which is literally termed as ranking of web pages as explained by Kohlschületter *et al.*[3]. Indeed, ranking requires efficient algorithms, understanding parameter influence on convergence and stability or error tolerance as suggested by Engström and

17^{th} *ASMDA Conference Proceedings, 6 – 9 June 2017, London, UK*

Silvestrov [24]. Recently, PageRank, connecting a Line of nodes with a complete graph was studied and explicit formula to determine of ranks were proposed, which was mainly aimed at minimizing errors in estimating ranks as pointed out in Engström and Silvestrov [25]. Much as these attempt have been made to improve ranking processes by increasing convergence rate and formulating formulas, the issue on the quality of ranks obtained still remain unresolved. As a matter of fact, paying much attention to the accurate solutions of linear system of equations underscore the practical significance for ranking in areas where they are applied.

In this paper, we focus on the termination criterion as means of obtaining good ranks. We first outline some studies made on stopping criteria in solving linear system.

Bennani and Braconnier[4] studied convergence detection of iterative solvers. They pointed out that such criterion may allow excessive number of iterations to be performed. Geometric distance such as absolute error and normalized residual for linear systems have been preferred as terminating criteria when using Jacobi iterative schemes (Gleich *et al.*[6]). Another study was done by Qiu and Cho [19] who applied ranking distance as termination criterion to approximate PageRank vector. They noted that there are instance in which the relative error may be large but the ranks are pretty good.

Essential goal in PageRank computing is to rank webpages (Gong *et al.*[18]), while accuracy of the PageRank vectors is secondary. In the view of Haveliwala [21], if Pagerank vector is to be used for establishing the importance of pages the convergence should be measured based on how the ordering changes as the number of iterations increases. Berklin [22] questioned the sense to iterate beyond the accuracy that establishes the order of the pages in search engines analysis. Boldi *et al.*[7] said 'it is the relative order of pages with respect to PageRank that is actually interesting for search engines'. Rank ordering as an algorithm provides few number of iterations sufficient for the purpose of identifying important webpages and moreover, time complexity of algorithm can be drastically reduced (Bidoki *et al.*[13]). In fact with the advancement in technology and adaptation of PageRank algorithm in areas like object tracking or target filtering, the importance of stopping criterion for ranks should not be underscored. This motivates the need to evaluate stopping criteria in relation to ranks. This paper aims to answer the following questions:- 1) Which stopping criterion out performs the others? 2) Which criteria are similar? and 3) Is there any link between the stopping criterion and the iterative methods in ranking problems?

2 Methods

This section describes some notions used in the methods to an easy understanding. Preliminaries of concepts such as key definitions and theorems are outlined. Also, iterative methods and stopping criteria are briefly described.

2.1 Preliminaries

Consider a large sparse system of equation

$$A\mathbf{x} = \mathbf{b}, \tag{1}$$

where $A \in \mathbb{R}^{n\times n}$ is a nonsingular matrix and $\mathbf{x}$, $\mathbf{b} \in \mathbb{R}^n$ are vectors. To avoid confusion all the matrices and vectors are real numbers unless otherwise stated.

Definition 1. (Hadjidimos [16]) If a matrix A satisfies $A \geq 0$, then it is said to be non-negative. The matrix A is said to be an L-matrix if and only if $a_{i,i} > 0$, $i = 1, \cdots, n$ and $a_{i,j} \leq 0$, $i \neq j$. A matrix, A is said to be a M-matrix if it is both an L-matrix and invertible.

Theorem 1. *(Perron-Frobenius Theorem [27]) Let A be an $n \times n$ positive matrix with spectral radius ρ. Then the following statements holds:*

1. *There is a positive real eigenvalue $\lambda_1 = \rho = \max\{|\lambda| : \lambda \in \mathbb{C}\}$*
2. *There is an eigenvector $\boldsymbol{\varsigma} > 0$ such that $A\boldsymbol{\varsigma} = \lambda_1\boldsymbol{\varsigma}$.*
3. *The eigenvalue λ_1 has multiplicity 1.*
4. *Apart from $\boldsymbol{\varsigma}$ there are no positive eigenvector of A other than positive scalar multiples of $\boldsymbol{\varsigma}$.*

Having stated some essential definitions and a theorem that will be referred to in this work, we next present the formulation of two iterative schemes, that is the Jacobi and Successive overrelaxation methods. Solving Equation (1) iteratively involves splitting matrix A as

$$A = M - N, \tag{2}$$

where M is nonsingular. It is also a convergent splitting of A if the spectral radius of iterative matrix, $M^{-1}N$, is less than 1 (Li and Wu [8]). Following representation (2), the iterative solution of Equation (1) becomes

$$\begin{aligned} \mathbf{x}^{(m+1)} &= M^{-1}N\mathbf{x}^{(m)} + M^{-1}\mathbf{b}, \\ &= T\mathbf{x}^{(m)} + \mathbf{g}, \end{aligned} \tag{3}$$

where $T = M^{-1}N$ is called iterative matrix and $\mathbf{g} = M^{-1}\mathbf{b}$ is a vector.

2.2 Iterative methods

This subsection presents iterative techniques applied in solving large sparse linear systems, namely Jacobi method, Successive Overrelaxation method and Power series method. Note that the performance of iterative solver(s) depends mostly on the structure of iterative matrix which we have taken into account without much details described in this paper, see Young [9].

Jacobi Iterative method: To derive the Jacobi iterative formula, the matrix A is split as $A = D - (L + U)$. Using representation (2), $M = D$, where $D = \text{diag}(A)$, and $N = L + U$, where L and U are respectively strictly lower and upper triangular $n \times n$ matrices, whose entries are the negatives of the entries of A respectively below and above the leading diagonal of A. It follows from Equation (3) that

$$\mathbf{x}^{(m+1)} = D^{-1}(L + U)\mathbf{x}^{(m)} + D^{-1}\mathbf{b}, \quad m \geq 0, \tag{4}$$

where $\mathbf{x}^{(0)}$ is the initial estimate of the unique solution $\mathbf{x}$ of (1). Equation (4) is called the point Jacobi iterative method (Varga[15]) and the matrix

$$J = D^{-1}(L + U) \tag{5}$$

is called the point Jacobi iterative matrix associated with the matrix A. The method requires a simultaneous storage of all the components of the vector $\mathbf{x}^{(m)}$ while computing the components of the vector $\mathbf{x}^{(m+1)}$.

Successive Overrelaxation (SOR) Iterative method: In a similar way as the Jacobi method, we split matrix A as $A = M - N$, but $M - N \equiv D - L - U = (\frac{D}{\omega} - L) - ((\frac{1}{\omega} - 1)D + U)$, where the quantity ω is called the relaxation factor (Young [9]). From (3), we have

$$(D - \omega L)\mathbf{x}^{m+1} = [(1 - \omega)D + \omega U]\,\mathbf{x}^{m} + \omega\mathbf{b}. \tag{6}$$

Since $D - \omega L$ is a nonsingular, (6) is equivalent to

$$\mathbf{x}^{(m+1)} = (D - \omega L)^{-1}\,[(1 - \omega)D + \omega U]\,\mathbf{x}^{(m)} + \omega(D - \omega L)^{-1}\mathbf{b}, \tag{7}$$

which is called the point SOR iterative method. The matrix J_{SOR} is given by

$$J_{SOR} = (D - \omega L)^{-1}\,[(1 - \omega)D + \omega U]\,,$$

is called the point SOR matrix. To find an optimal value of ω, it is assumed that the decomposed matrix has Property 'A' (Hadjidimos [16]), and the optimal choice of the parameter can be obtained from the theorem below.

Theorem 2. *(Optimal Successive Overrelaxation parameter (Young[9]) Let J and J_{SOR} be Jacobi and SOR iterative matrices respectively and derived from a matrix A. If $\mu(J)$ is the eigenvalues of J and the spectral radius, $\rho(J) < 1$, then the optimal SOR parameter, $\omega_o = \frac{2}{1+\sqrt{1-\rho^2(J)}}$.*

Before, we have a look at how to approximate ω_o, it is important to note that explicit formula that compute the optimal parameter for SOR method in general does not exist. There are some special form of matrices such as tri-diagonal, property A and weakly-cyclic their relaxation parameters can be derived precisely. This implies that determining $\rho(J)$ is practically challenging so one need to approximate ω_o which was the case in this problem. Now, by Equation 5 and Equation 13, the matrix, $J = L + U = cP$, taking 1-norm of J,

we have $\rho(J) \leq c$, and using this bound, one gets an estimate of the parameter as $\omega_o = \frac{2}{1+\sqrt{1-c^2}}$. Since the damping factor $c = 0.85$, an approximate value of $\omega_o = 1.3099$. This value works only if the matrix has property 'A'.

Alternatively, if J is weakly-cyclic then for each eigenvalue of J, $\mu(J)$ with $\frac{1}{2} < \mu(J) < 1$, set $\omega_o = \frac{2}{1+\sqrt{2c-1}}$, where $c = \mu(J)$ as earlier mentioned. Hence, a better choice of ω_o is 1.0889. Exploring connectivity of the graph that generated a iterative matrix J is important to avoid extreme initial guest of ω_o.

Power Series method: The formulation of Power series iterative method arise from Equation (12), that is multiplying both sides by $(I - cP)^{-1}$, we obtain

$$\boldsymbol{\pi} = (1 - c)(I - cP)^{-1}\mathbf{v}. \tag{8}$$

Expressing the term $(I - cP)^{-1}$ as geometric series yields

$$(I - cP)^{-1} = I + cP + c^2P^2 + \cdots = \sum_{j=0}^{\infty}(cP)^j.$$

Substituting in Equation (8) gives

$$\boldsymbol{\pi} = (1 - c)[\sum_{j=0}^{\infty}(cP)^j]\mathbf{v}. \tag{9}$$

3 Formulation of linear system

Linear systems of equations that is considered in this paper are those arising from PageRank problems (Langville and Meyer[10]). We briefly describe how one can formulate the system from a web link graph $\mathcal{G}$ with n vertices. That is we let P be weighted adjacency (stochastic) $n \times n$ matrix derived from outgoing vertices of the graph. If $\mathcal{G}$ has no outgoing links in some vertices, then P is a sub-stochastic matrix. We remedy this by adding to P rows corresponding to dangling vertices (vertices without outgoing links) a positive probability distribution $\mathbf{v}$ over all vertices. A stochastic matrix $\mathcal{P}$, obtained after adjustment for dangling vertices is defined as

$$\mathcal{P} = P + \mathbf{d}\mathbf{v}^T,$$

where $\mathbf{d}$ is a column vector such that

$$d_i = \begin{cases} 1, & \text{if vertex } i \text{ is dangling,} \\ 0, & \text{otherwise,} \end{cases} \tag{10}$$

and $\mathbf{v} = \frac{\mathbf{e}}{n}$, n is the dimension of $\mathcal{P}$ and $\mathbf{e} = (1, 1, \cdots, 1)$.

Suppose $c \in (0, 1)$ is the probability that a web surfer follows the link as described by $\mathcal{P}$ and jump to any vertex in the graph according to $\mathbf{e}\mathbf{v}^T$ with probability $(1 - c)$, then the matrix defined in PageRank problem becomes

$$\mathcal{T} = c(P + \mathbf{d}\mathbf{v}^T) + (1 - c)\mathbf{e}\mathbf{v}^T. \tag{11}$$

By Theorem 1 we can formulate the problem to determining a stationary distribution of the web link graph by multiplying (11) by an eigenvector $\boldsymbol{\pi}$ corresponding to eigenvalue 1. Rearranging, we get

$$(I - cP)\boldsymbol{\pi} = (1 - c)\mathbf{v}, \tag{12}$$

where c is damping factor, P is a stochastic matrix and $(I - cP)$ is M-matrix. This is the version of linear system defined in Engström and Silvestrov [24] as the eigenvalue problem. However, the version of the system considered is the one in which $\|\boldsymbol{\pi}\|_1 \neq 1$ and is given as

$$(I - cP)\boldsymbol{\pi} = n_g\mathbf{v}, \tag{13}$$

where n_g is the size of the one vector $\mathbf{e}$ in case $\mathbf{v}$ is uniform.

Remark 1. From Equation (13), and comparing it with Equation (1), then $A \equiv (I - cP)$, $\mathbf{x} = \boldsymbol{\pi}$ and $\mathbf{b} = n_g\mathbf{v}$.

4 Stopping Criteria

Whenever one attempt to solve large linear system of equations, the solution is always approximated because of round off errors. Therefore, some degree of accuracy need to be adopted which will depend on stopping criteria among others. This section briefly outlines five stopping criteria used in large linear system solvers. We intend to use them based on their popularity in PageRank problem which is a sister problem to linear system of equations (12).

(I) Assume that the residual vector at the $(m+1)^{th}$ iteration is $r^{(m)}$, then the norm of the residual is

$$\|\mathbf{r}^{(m)}\|_1 = max_i|\mathbf{x}^{(m)} - A\mathbf{x}^{(m-1)}|, \tag{14}$$

where $\mathbf{x}^{(m)}$ is the approximate solution vector at m^{th} iteration.

(II) Componentwise backward error: The criterion allowed for determination of finite bound when the matrix A is sparsed Arioli *et al.*[1] is

$$max_i \frac{|\mathbf{r}^m|_i}{(|A|.|\mathbf{x}^m| + |\mathbf{b}|)_i}. \tag{15}$$

At this point, the use of 1-norm appears in many literature but infinity norm and 2-norm may also work. However, one must be conscious on technical reasons to use a norm or combination of norms. We highlight this in the next criterion.

(III) Normwise backward stopping criterion: the ideal to include this bound stem from the fact that in most iterative methods their convergence solely depends on eigensystem of iteration matrix where the backward error is also unknown. Moreover such iteration involves successive computation matrix-vector; this result to dense matrix. Hence, a solution obtained may be quite near machine precision, which in turn result to stoping iteration

to early. To remedy this one would need to choose some larger threshold to determine termination, i.e.

$$\frac{\|\mathbf{r}^m\|_\infty}{\|A\|_\infty.\|\mathbf{x}^m\|_1 + \|\mathbf{b}\|_\infty}. \tag{16}$$

(IV) The ratio of residual to infinity norm of vector $\mathbf{b}$ neglecting the effect of matrix A:

$$\frac{\|\mathbf{r}^m\|_\infty}{\|\mathbf{b}\|_\infty}. \tag{17}$$

This criterion has been discussed in Arioli *et al.*[1] in detail.

(V) Before defining the criterion, let us consider the following lemma:

Lemma 1. *If $J \in \mathbb{R}^{n\times n}$ and $\|J\| < 1$, then $I - J$ is nonsingular and $(I-J)^{-1} = \sum_{k=0}^{\infty} J^k$ with $\|(I-J)^{-1}\| \leq \frac{1}{1-\|J\|}$.*

Proof. To proof nonsingularity, we use proof by contradiction. Let $I-J$ be singular, then for some vector $\mathbf{x} \in \mathbb{R}^n$ we have $(I-J)\mathbf{x} = 0$ but $\|\mathbf{x}\| = \|J\mathbf{x}\|$, hence $\|J\| \geq 1$. Thus $I - J$ is nonsingular.
To prove the second part of the lemma, consider the identity $\sum_{k=0}^{N} J^k(I - J) = I - J^{N+1}$, since $\|J\| < 1$, it follows that $J^k \to 0$ as $k \to \infty$ because $\|J^k\| \leq \|J\|^k$ for some k. Therefore $\lim_{N\to\infty} \sum_{k=0}^{N} J^k(I-J) = I$. This is equivalent to $(I-J)^{-1} = \lim_{N\to\infty} \sum_{k=0}^{N} J^k$.
Taking matrix norm on both sides, we get $\|(I-J)^{-1}\| \leq \frac{1}{1-\|J\|}$.

In the second lemma, we derived the bound of successive residual which will turn out to be stopping criterion.

Lemma 2. *Suppose a stationary iterative scheme is defined as $\mathbf{x}^{(m+1)} = J\mathbf{x}^{(m)} + \mathbf{d}$, where $\|J\| < 1$, $\mathbf{d}$ is a constant and $m = 1, 2, \cdots,$. Then the estimate $\frac{\|J\|}{1-\|J\|}\|\mathbf{x}^{(m)} - \mathbf{x}^{(m-1)}\| < \epsilon$.*

Proof. Let $\mathbf{x}$ be the exact solution obtained when using the iterative scheme, then at the m-th iteration, we can write the residual as

$$\begin{aligned}\mathbf{x} - \mathbf{x}^{(m)} &= J\mathbf{x} - J\mathbf{x}^{(m-1)} \\ &= J\mathbf{x} - J\mathbf{x}^{(m)} + J\mathbf{x}^{(m)} - J\mathbf{x}^{(m-1)}.\end{aligned}$$

Collecting similar terms and taking vector norm on both sides yields

$$\begin{aligned}\|(\mathbf{x} - \mathbf{x}^m) - J(\mathbf{x} - \mathbf{x}^m)\| &= \|J(\mathbf{x}^m - \mathbf{x}^{(m-1)})\| \\ \|(\mathbf{x} - \mathbf{x}^m)(I - J)\| &\leq \|J\|\|(\mathbf{x}^m - \mathbf{x}^{(m-1)})\|, \\ \|(\mathbf{x} - \mathbf{x}^m)\| &\leq \|J\|\|(I-J)^{-1}\|\|(\mathbf{x}^m - \mathbf{x}^{(m-1)})\|,\end{aligned}$$

using lemma 1, we get $\frac{\|J\|}{1-\|J\|}\|\mathbf{x}^{(m)} - \mathbf{x}^{(m-1)}\|$ which is less or equal to some tolerance, ϵ. Now, we write criterion V as $\frac{c}{1-c}\|\mathbf{x}^{(m)} - \mathbf{x}^{(m-1)}\|$, where c (damping factor) is approximated by $\|J\|$.

(VI) Kendall's τ rank correlation: This is one of the many correlation indices for comparing orders. It is a non parametric correlation index and widely used for ranking aggregation in the web community (Dwork *et al.*[14]). It also helps to determine how fast the computation of PageRanks converges (Kamvar *et al.*[17]). Kendall's τ is defined as follows:

Definition 2. Let $\mathbf{x} \in \mathbb{R}^n$ and $\mathbf{y} \in \mathbb{R}^n$ be two vectors of rank values. Given a pair (x_i, y_i) and (x_j, y_j), $1 \leq i, j \leq n$, then the pair is said to be
- concordant iff $x_i > x_j$ and $y_i > y_j$ or $x_i < x_j$ and $y_i < y_j$;
- discordant iff $x_i > x_j$ and $y_i < y_j$ or $x_i < x_j$ and $y_i > y_j$;
- neither concordant nor discordant iff $x_i = x_j$ (x- tie) or $y_i = y_j$ (y- tie) or $x_i = x_j = y_i = y_j$ (joint tie).

Let n_c and n_d be the number of concordant pairs and discordant pairs, respectively. Kendall's τ is calculated as

$$\tau = \begin{cases} \frac{n_c - n_d}{n(n-1)/2}, & \text{if no tie} \\ \frac{n_c - n_d}{\sqrt{(n_0 - n_1)(n_0 - n_2)}}, & \text{otherwise,} \end{cases} \tag{18}$$

where $n_0 = n(n-1)/2$, $n_1 = \sum_i t_i(t_i - 1)/2$, $n_1 = \sum_j u_j(u_j - 1)/2$, t_i is the number of ties in the i^{th} group of ties for $\mathbf{x}$ and u_j is the number of ties in the j^{th} group of ties for $\mathbf{y}$.

Kendall's correlation range between 1 and -1. If $\tau = 1$, there are no non-joint ties and the two total orders induced by the vectors are the same. The converse is true for $\tau = -1$, i.e., no non-joint ties and the two total orders are of opposite signs. When $\tau = 0$, the pairs are not correlated.
Top k lists: This technique was introduced by Fagin *et al.*[12]. It is understood as a ranking metric in which the first k elements are considered in the list of n, where $k \leq n$. The top k lists can be ranked in many ways [12]. However, due to its simplicity, Kendall's metric is mostly used.
Let $N = \{1, \ldots, n\}$ be a set of size n. Suppose that r_1 and r_2 are two top k rankings on N. According to Rolland[11] and Fagin *et al.*[12], Kendall's distance metric is defined as $d_K(r_1, r_2) = \sum_{\{i,j\} \in N} K_{i,j}(r_1, r_2)$,
where

$$K_{i,j}(r_1, r_2) = \begin{cases} 0, & \text{if } i \text{ and } j \text{ appear in the same order in } r_1 \text{ and } r_2, \\ 1, & \text{if } i \text{ and } j \text{ appear in the opposite order,} \\ 0, & \text{if } i \text{ is ahead of } j \text{ in } r_1 \ . \end{cases} \tag{19}$$

Alternatively, $d_K(r_1, r_2)$ is the total sum of pairwise discordances between two k lists.
To determine the stoping criterion of the iterative methods, one assumes that $r_1^{(m)}$ and $r_2^{(m+1)}$ are the ranks at m^{th} and $(m+1)^{th}$ iterations, respectively. Then, the Kendall's distance for top k lists is expressed as

$$d_K\left(r_1^{(m)}, r_2^{(m)}\right) = \sum_{\{i,j\} \in N} K_{i,j}\left(r_1^{(m)}, r_2^{(m+1)}\right).$$

We normalized d_K, hence we obtain Kendall's τ correlation.

5 Numerical experimentation of stopping criteria

In this section, we evaluate the stopping criteria for ranks of linear system of equations. We feel that it is essential to base the stopping criteria on intended purpose, that is induced ranks rather than solution of the equation. To that effect, good evaluation framework should be carried out to ensure sound stopping criteria for ranks. We set up the evaluations as follows:-

- Convergence of five stopping criteria.
- Quantize and ranks at different iterations.
- Kendall's coefficient τ against number of iterations for different stopping criteria by iterative method.
- Top-k list (100 and 300) against number of iterations by iterative method.

5.1 Convergence of stopping criterion

In this section, we present evaluation of five criteria mostly used in iterative schemes. We performed 20-100 iterations and results presented in Table 1, and Figure 1. The findings revealed that criterion I (1-norm of residual $\|\mathbf{x}^{(m)} - A\mathbf{x}^{(m-1)}\|$) and criterion IV ($\frac{\|\mathbf{x}^m - A\mathbf{x}^{m+1}\|_\infty}{\|\mathbf{b}\|_\infty}$) seem to suit convergence of ranks of linear system, since their error tolerance were within the range as suggested in Engström and Silvestrov [24] and Steward [26]. Also, criteria V ($\frac{c}{1-c\|}\|\mathbf{x}^{(m)} - \mathbf{x}^{(m-1)}\|$) is good alternative if one wishes choose any other, more specifically for slow convergence scheme. While criterion II and III performed badly because they rather have faster convergence than expected.

Method	Error by criterion	No. of Iteration			
		20 ($\times 10^{-3}$)	40 ($\times 10^{-4}$)	60 ($\times 10^{-6}$)	100 ($\times 10^{-9}$)
Power series and Jacobi	I	38.8	15.0	58.0	86.8
	II	6.0	2.25	8.70	1.30
	III	15.6	3.26	7.75	5.51
	IV	38.8	15.0	58.0	86.8
	V	219.6	85	328.0	492.0
SOR	I	37.1	14.0	48.9	64.68
	II	5.7	2.07	7.34	9.68
	III	14.7	2.87	6.36	3.96
	IV	37.1	14.0	48.9	64.68
	V	210.5	77.0	277.6	366.0

Table 1. Error tolerance and stopping criteria by iterative methods.

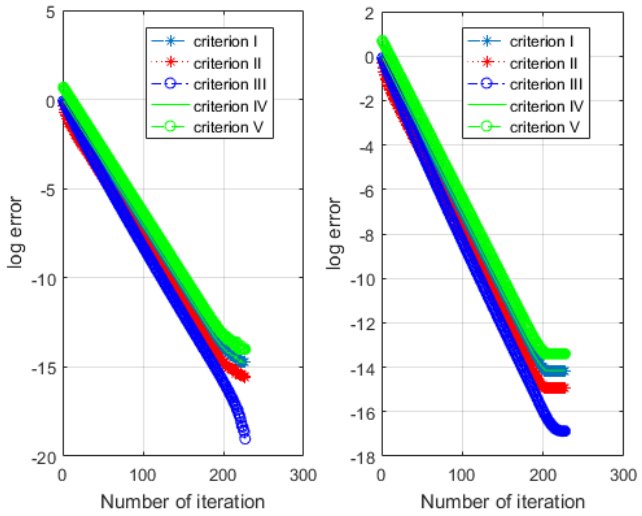

Fig. 1. Convergence of the 5 criteria using Power Series /Jacobi iterative method (left) and SOR (right)

The behavior of error around 10^{-15} could probably be due to machine precision being similar. In Matlab software, double precision in IEEE format can store up to 16 digits only.

5.2 Quantiles

The quantiles (10%, 25%, 50%, 75% and 90%) of solutions for the iterative methods on four sets of iteration were performed and results presented in Table 2. Criterion I was used a stopping requirement because it is simple and found to be better as noted earlier. We found that no significant difference in solutions at different quantiles points. Further, lower ranks seem to converge much faster than higher ranks, see Table 2.

When the numbers of iteration was increased to 60, we noted that ranks seem to have stabilized. To get a better picture, we gave a plot in Figure 1. It can be clearly seen that in the early states of iterations ranks were unstable; however after at least 50 iterations most ranks achieved their limiting values. Moreover, the iterative scheme had converge already in at most 30 iterations. Hence, the scheme had converged before the ranks.

5.3 Kendall correlation coefficient as stopping criterion

Further, we explored the use of Kendall correlation coefficient, τ as a stopping criterion. We first assumed that the exact solution vector is known, then we determined its correlation at different iteration points. To avoid heavy computation, the top 100 and 300 list were considered for analysis of correlation. Taking an interval of 10 and considering the 10th iterations as the starting

		No. of Iteration	
Method	Quartiles	40	60
		solution	solution
Power series and Jacobi	10%	3.5630	3.5637
	25%	4.6043	4.6051
	50%	5.4261	5.4273
	75%	5.9494	5.9515
	90%	6.2534	6.2565
SOR	10%	3.5630	3.5637
	25%	4.6045	4.6051
	50%	5.4263	5.4273
	75%	5.9497	5.9516
	90%	6.2539	6.2565

Table 2. Quartiles, number of iterations and solutions using stopping criterion I & II

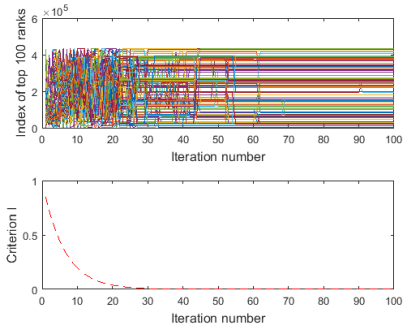

Fig. 2. Index of first 100 top ranks and error (criterion I) against iteration number using power series method

point and ending at 220th iterations. The followings were observed:- the first time convergence of rank was at about 60th iterations shown in Figure 3. This has been revealed by both iterative methods and this could be the stopping point which match with the finding using criterion I and II.

Secondly, we observed that a proper rank can be achieved at a particular iteration and lost as iteration progresses. This seem to be pronounced in SOR as compared to Jacobi or power series methods, particularly with Top-100 ranks. However, for Top-300 ranks it seems to achieve their convergence once and this can be seen in Figure 3. Based on this results, determining convergence rate of ranks using Kendall, τ coefficient seem to be an effective technique as compared the others, in particular, when two Top-k lists are compared and where they

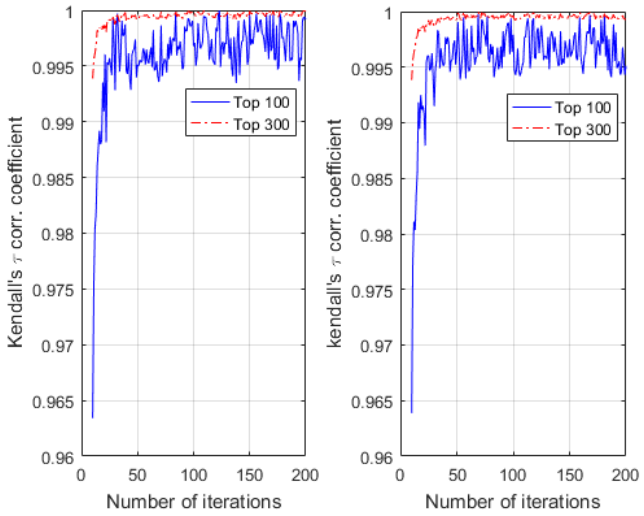

Fig. 3. Convergence of Top-100 and Top-300 ranks using Kendall's τ correlation coefficient with Jacobi (left) and SOR (right) iterative schemes

coupled is the best stopping point. We evaluated this argument using Top-100 and Top-300, in all cases the results were promising. The number of iterations required were 85 and 69 for Jacobi and SOR methods respectively as presented in Figure 3.

6 Conclusions

Stopping criterion of ranks for linear system of equations is of practical significance, particularly if ranking is to be meaningful and applicable in areas like search engine, financial networks, bioinformatics and many others. In this paper, we evaluated several criteria and the findings revealed that Kendall's τ method seem to be an effective stopping criterion for ranks of linear system of equations as compared to the others. It was found that this technique which is based on correlation coefficient between successive iterates of solution vectors together with two Top-k lists (for example, Top-100 & 300) has good convergence, we named it Kendall's τ 2 Top-k list method. Comparing the method with other stopping criteria, it was observed that stopping point can easily be identified as shown in Figure 3.

Further, criterion I and IV were found to competitor with Kendall's τ 2 Top-k list method while criterion V seem to be relevant for slow convergence linear system problem. We think that the contribution of this paper should play a complementary role when the purpose is to determine ranks in linear system of equations.

Acknowledgements This research was supported by the Swedish International Development Cooperation Agency (Sida), International Science Programme (ISP) in

Mathematical Sciences (IPMS), Sida Bilateral Research Program (Makerere University and University of Dar-es-Salaam). We are also grateful to the research environment Mathematics and Applied Mathematics (MAM), Division of Applied Mathematics, Mälardålen University for providing an excellent and inspiring environment for research education and research.

References

1. M. Arioli.,I. Duff and D. Ruiz. Stopping criteria for iterative solvers. *Journal SIAM Journal on Matrix Analysis and Applications*, 13, 1, 138–144, 1992.
2. P. Berkhin. A survey on pagerank computing, *Internet Mathematics*, 2, 73–129, 2005.
3. C. Kohlscütter., P. Chirita and W. Nejdl. Efficient Parallel Computation of PageRank
4. M. Bennani and T. Braconnier. Stopping criteria for eigensolver, *Submitteto IMA Num. Annal*, 1993
5. J.C. Mielou, P. Spiteri and D. El Baz. A new stopping criterion for linear pertubed asyncronous iterations, *Journal of Computational and Applied mathematics*, 219, 471–483, 2008.
6. D. Gliech, L. Zhukov and P. Berhim. Fast Parallel PageRank: A Linear System Approach, *WWW2005,* Chiba and Japan, 2005
7. P. Boldi., M. Santini, and S. Vigna: Paradoxical Effects in PageRank Incremental Computations, *Internet mathematics*, 2, **3**, 387–404, 2005.
8. C. Li and S. Wu. Some New Comparison Theorems for Double Splitting of matrices, *Applied mathematics and Information Sciences*, 8, **5**, 2523–2526, 2014.
9. D.M. Young. Iterative solutions for Linear Systems, Academic Press, New York, 1971.
10. A.N. Langville and C.D. Meyer. A Reoredering for PageRank problem,SIAM J. Sci. Comput, 6, **27**, 2112–2120, 2006.
11. A. Rolland. A Note on Top-K Lists: Aveage Distance between Two Top-K Lists,
12. R. Fagin, R. Kumar and D. Sivakumar. Comparing top lists, *J. Discrete mathematics*, 18, **1**, 134–160, 2003.
13. Z. Bidoki, A. Mohammand and N. Yazdani. DistanceRank: An intelligent ranking algorithm for web pages, *Information Processing and management*, 18, **1**, 134–160, 2007.
14. C. Dwork, R. Kumar, M. Naor and D. Sivakamar. Rank Aggregation Methods for the Web, *World Wide Web,* 10, 613-622, 2001.
15. R.S. Varga. *Matrix iterative Analysis,* Prentice-Hall, Englewood Cliffs, NJ, 1962.
16. A. Hadjidimos. Successive overrelaxation (SOR) and related methods, *Journal of Computational and Applied Mathematics*, 123, 177-199, 2000.
17. S.D. Kamvar, T.H. Haveliwala, C.D. Manning and G.H. Golub. Extrapolation methods for accelarating PageRank computations, *World Wide Web,* 12, 261-270, 2003
18. C. Gong, K. Fu, A. Loza, Q. Wu, J. Liu, and J. Yang. PageRank tracker: From Ranking to Tracking, *IEEE TRANSACTIONS ON CYBERNETICS,* 44, **6**, 882-893, 2014
19. F. Qiu abd J. Cho. Automatic identification of user interest for personalised search, *in WWW '06: PROC.15th International Conference on World Wide Web, ACM Press,* New York 727-736, 2006.
20. R.S. Wills. When ranks trumps precion: Using the power method to compute Google's Pagerank, *http : //www.lib.ncsu.edu/theses/available/etd − 061220007 − 173712/*, 2007.

21. T.H. Haveliwala. Efficient computation pf Pagerank, *Tech. Rep, 31,* Stanford University, 1999.
22. P. Berkhin. A survey on pagerank computing, *Internet Mathematics*, 2, 73-120, 2005.
23. R.S. Wills and I.C.F. Ipsen. Ordinal Ranking for Google PageRank. *SIAM J. MATRIX ANAL. APPL.*, 30, **4**, 1677-1696, 2009.
24. C. Engström and S. Silvestrov. A Componentwise PageRank agorithm. *16 th ASMDA Conference Preceedings, 30 June - 4 th July 2015*,ISAST.
25. C. Engström and S. Silvestrov. PageRank, Connecting a Line of Nodes with a Complete Graph. *Engineering Mathematics II. Springer Proceedings in Mathematics & Statistics, vol 179. Springer*,Cham, 2016
26. W.J. Stewart. Introduction to the Numerical Solution of Markov Chains. Princeton University Press, 1994.
27. C.D. Meyer. *Matrix Analysis and Applied Linear Algebra*, Society for Industrial and Applied Mathematics, Philadelphia, PA, USA, 2000.

Asymptotic Analysis of Queueing Models based on Synchronization Method

Afanasyeva L.G.[1]

Department of Probability Theory, Lomonosov Moscow State University, GSP-1, 1 Leninskiye Gory, Main Building, 119991; (E-mail: l.g.afanaseva@yandex.ru)

Abstract. This paper is focused on the stability conditions of the multiserver queueing system with heterogeneous servers and a regenerative input flow $X(t)$. The main idea is constructing an auxiliary service process $Y(t)$ which is also a regenerative flow and defining the common points of regeneration for the both processes $X(t)$ and $Y(t)$. Then the traffic rate of the system is defined in terms of the mean of the increments of these processes on the common regeneration period. It allows to use well-known results from the renewal theory to find the instability and stability conditions. The possibilities of the proposed approach are demonstrated by examples.
Keywords: regenerative flow, synchronization, stability condition, service discipline.

1 Introduction

Studying of queueing models is an appealing part of applied mathematics because queues are familiar and intuitively clear and they can be need to model many real systems. This paper deals with the study of stability conditions for a heterogeneous multiserver queueing system with a regenerative input flow.

We consider queueing systes with regenerative input flow for three reasons. Firstly, a process describing the system under some natural conditions turns out to be a classical regenerative process [see Asmussen [4], Thorisson [28]] and the renewal theory gives very effective tools for asymptotic analysis of the system. Secondly, the class of regenerative flows is rather wide and includes fundamental flows from queueing theory. Finally, a regenerative flow has some useful properties that allow us to investigate various applied models.

The main objective of our study is to determine conditions under which the process describing the performance of the system is a stochastically bounded one and therefore under some additional assumptions a stable process.

Let us note that stability results for the classical homogeneous multiserver queue are very well known. We refer to the works of Kiefer and Wolfowitz [18] for the $GI|GI|m$ system and the general ergodicity results of Loynes [19]. As it was shown in Sadowsky [24] the proposed approach could not be applied for heterogeneous systems. Instead, in the work of Sadowski [24] the stability is examined from the point of view of Harris recurrent Markov chain theory. Basing on the works of Malyshev [20], Meyn and Tweedy [21], Georgiadis and

17^{th} *ASMDA Conference Proceedings, 6 – 9 June 2017, London, UK*

Szpankowski [15], Szapankowski [26] the author obtained two results concerning the irreducibility and positive Harris recurrence of the corresponding process.

The heterogeneous multiserver queueing system with a regenerative flow was investigated in the paper of Afanasyeva and Tkachenko [3]. Under some assumptions necessary and sufficient stability condition was obtained there. Here we study more general model with a regenerative input flow $X(t)$ and an auxiliary service process $Y(t)$ that is the number of customers which can be served during the interval $[0, t)$ under the assumption that there are always customers for service. We consider the discrete-time as well as continuous-time models assuming that $Y(t)$ is a regenerative flow not depending on the input flow $X(t)$.

The basic idea is constructing the common points of regeneration for the both processes $X(t)$ and $Y(t)$. Then we define the traffic rate of the system in terms of the first moments of increments of these processes on the common regeneration period. Under some conditions we estimate the increments of the real service process $\tilde{Y}(t)$ (that is the number of customers really served at the system up to time t) with the help of increments of an auxiliary process $Y(t)$. It allows us to prove instability results and to find conditions of stochastic boundedness of the number of customers $Q(t)$ at the system at time t as $t \to \infty$. One may think that our conditions are too restrictive to be useful in applications therfore we consider three models with service interruptions as examples. In particular, in Section 6 a discrete-time heterogeneous multiserver queueing system with a regenerative input flow and interruptions of the service which are described by independent renewal processes for various servers, is discussed. It is shown that the traffic rate ρ is not expressed in terms of the first moments of the random variables defining the model for the preemptive repeat service discipline (see Gaver [14]). We also prove that $Q(t) \to \infty$ as $t \to \infty$ when $\rho \geq 1$ and $Q(t)$ is a stochastically bounded process when $\rho < 1$.

Let us note that the model with service interruptions occurs in numerous applications including manufactoring process, multi-processor computer networks, telecommunicating networks and various types of service counters. Service interruptions occur from resource sharing or service breakdowns, priority assignment, some external events and others. Queueing models with service interruptions have been investigated by many authors, in continuous as well as in discrete-time.

White anf Christie [29] were the first to study queueing systems with interruptions. Those authors investigated the $M|M|1$ model with preemptive resume priority discipline. Their results were later extended by Avi-Itzhak and Naor [5] and Thiruvengadam [27] who study queues with general service times. Gaver [14] studied single-server queues with batch Poisson arrivals and generally distributed service times. Assuming that a breakage of the server may appear only when it is busy by service this author introduced a notion "completion time" which turns out to be very efficient since it allows to reduce the analysis of the system with interruptions to a classiscal model $M|G|1$. So far there is extensive literuture concerning queueing systems with interruptions. There are some review papers that cover most of the literature in this sphere.

Some of important papers on the single-server case are presented in the work of Fiems and Bruneel [12].

The most extensive literature survey on systems with interruptions both for single-server and multiserver cases is given by Krishnamoorthy *et al* [17]. This paper also covers some non-Markovian multichannel systems with homogeneous servers. There are some other articles with extensive literature survey as well, see e.g. Pechinkin *et al* [23], Morozov *et al* [22]. To the best of our knowledge, there are no papers that study stability problem for multichannel queueing systems with heterogeneous servers in non-Markovian case with general input flow and service times. Synchronization method combined with the regenerative theory is one of the powerful approaches to obtain stability conditions for such systems. Basing on this method Morozov *et al* [22] considered the multichannel queueing system with identically distributed service times by different servers, renewal input flow, alternating renewal-type servers' interruptions in the discrete-time case. Authors established some sufficient conditions of stability for preemeptive repeat different and preemptive resume service disciplines but for preemptive resume service discipline the obtained condition is not necessary.

Let us also mention the fluid approximation approach as an alternative to the synchronization approach followed here. Such an approach has lent to significant progress in stability analysis of multiclass queueing networks (see Dai [10], Chen [8], Chen and Yao [9]). See also Foss and Konstantopoulos [13] for a survey of various approaches to stability of queueing systems with a focus on the fluid approach. Nevertheless, this paper does not rely on a fluid approach since to the best of our opinion, the synchronization method with regard to regenerative structure of the processes turns out to be suitable to obtain complete ana transporent proofs as well as natural stability conditions for the model at hand.

The paper is organized as follows. In the next section the queueing system under consideration is described in detail and basic notions are given. In Scetion 3 instability results are obtained. Section 4 is devoted to the conditions of the stochastic boundedness. In the rest sections we give examples of systems with service interruotions and use obtained results to asymptotical analysis of these systems.

2 Model description

We consider a queueing system with n servers and a regenerative input flow $X(t)$ (see Afanasyeva and Bashtova [1], Thorisson [28]). Suppose an integer-valued stochastic process $\{X(t), t \geq 0\}$ be defined on the probability space $(\Omega, \mathscr{F}, P)$. Assume that $X(t)$ has non-decreasing right-continuous sample paths and $X(0) = 0$. There exists filtrarion $\{\mathscr{F}^X_{\leq t}\}_{t\geq 0}$, $(\mathscr{F}^X_{\leq t} \in \mathscr{F}$ for all $t \geq 0)$ such that $X(t)$ is measurable with respect to $\{\mathscr{F}^X_{\leq t}\}_{t\geq 0}$.

Definition 1. The stochastic flow $X(t)$ is called regenerative one if there is an increasing sequence of Markov moments $\{\theta^{(1)}_j, j \geq 0\}(\theta^{(1)}_0 = 0)$ with respect to

$\{\mathscr{F}^X_{\leq t}, t \geq 0\}$ such that the sequence

$$\{\varkappa_j\}_{j=1}^{\infty} = \{X(\theta_{j-1}^{(1)} + t) - X(\theta_{j-1}^{(1)}), \theta_j^{(1)} - \theta_{j-1}^{(1)}, t \in (0, \theta_j^{(1)} - \theta_{j-1}^{(1)}]\}_{j=1}^{\infty}$$

consists of independent identically distributed (iid) random elements on $(\Omega, \mathscr{F}, P)$.

The random variable $\theta_i^{(1)}$ is said to be the ith regeneration point of $X(t)$ and $\tau_i = \theta_i^{(1)} - \theta_{i-1}^{(1)}$ is the ith regeneration period ($i = 1, 2, \ldots$). Let $\xi_j^{(1)} = X(\theta_j^{(1)}) - X(\theta_{j-1}^{(1)})$ be the number of customers arrived during the ith regeneration period. Assume that $\mathbf{E}\tau_1^{(1)} < \infty, \mathbf{E}\xi_1^{(1)} < \infty$. The limit $\lambda_X = \lim\limits_{t\to\infty} \frac{X(t)}{t}$ with probability 1 (w.p.1) is called the rate of $X(t)$. It is easy to prove that $\lambda_X = \frac{\mathbf{E}\xi_1}{\mathbf{E}\tau_1^{(1)}}$ (see Smith [25], Thorisson [28]). The class of regenerative flows contains most of fundamental flows that are exploited in the queueing theory. First of all, the doubly stochastic Poisson process(see Grandell [16]) with stochastic regenerative intensity is a regenerative flow. There are many other examples of the regenerative flows, for instance, semi-Markovian, Markov-arrival, Markov-modulated and other processes, (see Afanasyeva *et al* [2]). Define an auxiliary process $Y(t)$ as the number of customers that can be served during the interval $[0, t)$ under assumption that there are always customers for service during this interval.

We consider the discrete-time queueing systems as well as continuous-time(see Avi-Itzhak and Naor [5]). In the first case time divided into fixed length intervals or slots and all arrivals and departures are synchronized with respect to slot boundaries. Moreover, in the case of some events synchronization at one slot these events are ordered as follows: arrival and departure. System is observed at the end of a slot. For the discrete and continuous-time cases we assume that an auxiliary process $Y(t)$ is a regenerative flow with regeneration points $\{\theta_n^{(2)}\}_{n=1}^{\infty}$ ($\theta_0^{(2)} = 0$). We also need additional assumptions.

Condition 1 *For the continuous-time case $Y(t)$ is the strongly regenerative flow not depending on $X(t)$ with the sequence $\{\theta_n^{(2)}\}_{n=1}^{\infty}(\theta_0^{(2)} = 0)$ as points of regeneration.*

We call the regenerative flow $Y(t)$ strongly regenerative if the regeneration period $\tau_n^{(2)} = \theta_n^{(2)} - \theta_{n-1}^{(2)}$ has a form

$$\tau_n^{(2)} = v_n^{(1)} + v_n^{(2)} \tag{1}$$

where $P(v_n^{(1)} > x) = e^{-\delta x}(\delta \in (0, \infty))$, $v_n^{(1)}$ and $v_n^{(2)}$ are independent random variables and $Y(\theta_{n-1}^{(2)} + v_n^{(1)}) = Y(\theta_{n-1}^{(2)})$.

Condition 2 *for the discrete-time case processes $X(t)$ and $Y(t)$ are independent regenerative aperiodic flows. As usually, aperiodicity means that the greatest common divisor(GCD)*

$$GCD\{k : P(\theta_1^{(i)} = k) > 0\} = 1, \quad i = 1, 2.$$

Then we may determine common points of regeneration $\{T_n\}_{n=1}^{\infty}$ for the both processes $X(t)$ and $Y(t)$ putting in the discrete-time case

$$T_n = \min\left\{\theta_j^{(1)} > T_{n-1} : \bigcup_{l=1}^{\infty}\{\theta_j^{(1)} = \theta_l^{(2)}\}\right\}, T_0 = 0 \tag{2}$$

and in the continuous-time case

$$T_n = \min\{\theta_j^{(1)} > T_{n-1} : \bigcup_{l=1}^{\infty}\theta_{l-1}^{(2)} < \theta_j^{(1)} \le \theta_{l-1}^{(2)} + \nu_l^{(1)}\}, T_0 = 0. \tag{3}$$

Lemma 1. *Let for the continuous-time (discrete-time) Condition 1 (Condition 2) be fulfilled. Then the sequence $\{T_n\}_{n=1}^{\infty}$ consists of common regeneration points for $X(t)$ and $Y(t)$ and*

$$\boldsymbol{E}(T_n - T_{n-1}) = \boldsymbol{E}T_1 = \delta\,\boldsymbol{E}\tau_n^{(1)}\boldsymbol{E}\tau_n^{(2)} < \infty \tag{4}$$

for the continuous-time case,

$$\boldsymbol{E}T_1 = \boldsymbol{E}\theta_1^{(1)}\boldsymbol{E}\theta_1^{(2)} < \infty \tag{5}$$

for the discrete-time case.

Proof. Since the proof (4) is similar for the proof (5) we consider the discrete-time case only. Let

$$\nu_k = \min\left\{j > \nu_{k-1} : \bigcup_{l=1}^{\infty}\{\theta_j^{(1)} = \theta_l^{(2)}\}\right\}, \nu_0 = 0,$$

so that $T_k = \theta_{\nu_k}^{(1)}$. Then $\{\nu_k - \nu_{k-1}\}_{k=1}^{\infty}$ is a sequence of iid random variables and in accordance with Wald's identity $\mathbf{E}T_1 = \mathbf{E}\theta_1^{(1)}\mathbf{E}\nu_1$(see Feller [11]). Therefore, we need to prove the finiteness of $\mathbf{E}\nu_1$. Denote by $h_2(t)(h(t))$ the mean number of renewals up to time t for the renewal process $\{\theta_n^{(2)}\}_{n=0}^{\infty}$ ($\{\nu_k\}_{k=0}^{\infty}$) so that

$$h_2(t) = \sum_{l=0}^{\infty} P(\theta_l^{(2)} = t)$$

and

$$h(t) = \sum_{k=0}^{\infty} P(\nu_k = t).$$

Taking into account Condition 2 we derive from Blackwell's theorem (see Thorisson [28])

$$h_2(t) \xrightarrow[t\to\infty]{} \frac{1}{\mathbf{E}\theta_1^{(2)}}, \quad h(t) \xrightarrow[t\to\infty]{} \frac{1}{\mathbf{E}\nu_1}$$

if $\mathbf{E}\nu_1 < \infty$ and $h(j) \to 0$ as $j \to \infty$ if $\mathbf{E}\nu_1 = \infty$.

In view of $X(t)$ and $Y(t)$ independence

$$h(j) = P(\bigcup_{l=0}^{\infty}\{\theta_j^{(1)} = \theta_l^{(2)}\}) = \mathbf{E}\left(\sum_{l=0}^{\infty} P(\theta_j^{(1)} = \theta_l^{(2)}|\theta_j^{(1)})\right) = \mathbf{E}h_2(\theta_j^{(1)}).$$

Since $\theta_j^{(1)} \xrightarrow[j\to\infty]{} \infty$ w.p.1, then $h_2(\theta_j^{(1)}) \xrightarrow[j\to\infty]{} \frac{1}{\mathbf{E}\theta_1^{(2)}}$ w.p.1. Therefore, from Lebesgue;s dominated convergence theorem we obtain $\mathbf{E}\nu_1 = \mathbf{E}\theta_1^{(2)} < \infty$.

Later we consider the both cases (discrete-time and continuous-time) together. One only has to take Condition 2 instead of Condition 1.

Let

$$\Delta_Y(n) = Y(T_n) - Y(T_{n-1}),$$
$$\Delta_X(n) = X(T_n) - X(T_{n-1}).$$

Then

$$\lambda_X = \frac{E\Delta_X(n)}{E(T_n - T_{n-1})}, \lambda_Y = \frac{E\Delta_Y(n)}{E(T_n - T_{n-1})}.$$

We define the traffic rate as follows.

$$\rho = \frac{\lambda_X}{\lambda_Y} = \frac{E\Delta_X(n)}{E\Delta_Y(n)}. \tag{6}$$

We think of λ_X and λ_Y as the arrival and service rate respectively. Intuitively, it is clear that the traffic rate of the system is given by (6). The main stability result of the paper consists of the formal proof of this fact.

We define the stochastic flow $\tilde{Y}(t)$ as the number of customers really served at the system during time interval $[0, t)$.

Condition 3 *The following stochastic inequalities take place*

$$\tilde{\Delta}_Y(n) = \tilde{Y}(T_n) - \tilde{Y}(T_{n-1}) \le \Delta_Y(n), \ (n = 1, 2, ...).$$

Let $Q(t)$ be the number of customers at the system including the customers on the srvers at time t so that

$$Q(t) = Q(0) + X(t) - \tilde{Y}(t).$$

Condition 4 *There are two possible cases:*

(i) $Q(t)$ *is a stochastically bounded process, i.e.*

$$\lim_{x\to\infty} \liminf_{t\to\infty} P(Q(t) \le x) = 1;$$

(ii) $Q(t) \xrightarrow[t\to\infty]{P} \infty$.

Let us define the event

$$A_n = \{Q(t) \ge m \text{ for all } t \in [T_n, T_{n+1}]\}.$$

Condition 5 *If Condition 4(ii) takes place then for any* $\epsilon > 0$ *there is* n_ϵ *such for* $n > n_\epsilon$

$$E\tilde{\Delta}_Y(n)\mathbb{I}(A_n) \ge E\Delta_Y(n) - \epsilon. \tag{7}$$

Here $\mathbb{I}(A_n)$ *is an indicator function of the event* A_n.

3 Instability results for the case $\rho \geq 1$

Theorem 1. *Let Condition 3 and Condition 1(2) for the continuous-time (for the discrete-time) case be fulfilled. If $\rho \geq 1$ then*

$$Q(t) \xrightarrow[t\to\infty]{P} \infty. \tag{8}$$

Proof. The statement of the Theorem is almost evident for the case $\rho > 1$. Consistent with Condition 3 we have the stochastic inequality

$$Q(T_n) \geq X(T_n) - Y(T_n) + Q(0). \tag{9}$$

Since w.p.1

$$\lim_{n\to\infty} T_n^{-1}(X(T_n) - Y(T_n)) = \lambda_X - \lambda_Y > 0$$

then $Q(T_n) \xrightarrow[n\to\infty]{P} 0$ and therefore (8) holds. For the case $\rho = 1$ consider the embedded process $Q_n = Q(T_n)$ and denote by $Z_k = \sum_{j=1}^{k}(\Delta_X(j) - \Delta_Y(j))$ ($Z_0 = 0$). Define the auxiliary sequence $\{\hat{Q}_k\}_{k=0}^{\infty}$ by the recursion

$$\hat{Q}_k = \max[0, \hat{Q}_{k-1} + \Delta_X(k) - \Delta_Y(k)],\ \hat{Q}_0 = 0.$$

Because of the equality $Q_k = Q_{k-1} + \Delta_X(k) - \tilde{\Delta}_Y(k)$ and Condition 3 we get the stochastic inequality $Q_k \geq \hat{Q}_k$. It is well-known(see Feller [11]) that in distribution

$$\hat{Q}_k = \max_{0\leq j\leq k} Z_j.$$

For $\rho = 1$ the sequence $\{Z_j\}_{j\geq 0}$ is a random walk with zero drift. Hence, except when $\Delta_X(1) = \Delta_Y(1) = c$ (c is a constant), $\max_{0\leq j\leq k} Z_j \xrightarrow[k\to\infty]{} \infty$ (w.p.1) (see Feller [11]) that completes the proof.

4 Stochastic boundedness for the case $\rho < 1$

Our objective here is to establish stochastic boundedness of the process $Q(t)$ when the traffic rate $\rho < 1$. Under some additinal assumptions providing the regenerative structure of the process $Q(t)$ this property has a consequence its stability.

Theorem 2. *Let Conditions 4 and 5 and Condition 1(2) for the continuous-time (for the discrete-time) case be fulfilled. If $\rho < 1$ then $Q(t)$ is a stochastically bounded process.*

Proof. Because of Condition 4 there are two possible cases: Q_n is either stochastically bounded or $Q_n \xrightarrow[n\to\infty]{P} \infty$. Assume that the second case takes place and $\rho < 1$. For $0 < \epsilon < E\frac{\Delta_Y(1)-\Delta_X(1)}{2}$ we take n_ϵ such that for $n > n_\epsilon$

$$E\Delta_Y(n)\mathbb{I}(\overline{A}_n) < \epsilon.$$

Because of Condition 5 there is $\tilde{n}_\epsilon$ such that for $n > \max(\tilde{n}_\epsilon, n_\epsilon)$

$$EQ_{n+1} = EQ_n + E\Delta_X(1) - E\tilde{\Delta}_Y(n) \leq$$
$$\leq EQ_n + E\Delta_X(1) - E\Delta_Y(n)\mathbb{I}(A_n) + \epsilon \leq$$
$$\leq EQ_n + E\Delta_X(1) - E\Delta_Y(1) + 2\epsilon \leq EQ_n$$

that contradicts our assumption that $Q_n \xrightarrow[n\to\infty]{P} \infty$.

In the next sections we discuss some examples to verify our results and to compare them with previous works.

5 Queueing system with unreliable servers

We consider a continuous-time queueing system with a regenerative input flow $X(t)$ and m heterogeneous servers which may be not available for operation from time to time. We also propose that the velocity of the service may be dependent on the state of the server. Assume that for the ith server a stochastic process $n_i(t)$ with state space $(0; r_1^{(i)}; \ldots; r_{k_i}^{(i)})$, $r_j^{(i)} > 0$, $j = \overline{1, k_i}$ is defined. If $n_i(t) = 0$ then the ith server is in unavailable state, for instance it is broken, if $n_i(t) = r_j^{(i)}$ then the ith server is working with the velocity $r_j^{(i)}$ ($j = \overline{1, k_i}$, $i = \overline{1, m}$). Service times of customers by the ith server in the case when the velocity of the service is equal to one constitute a sequence $\{\eta_{in}\}_{n=1}^{\infty}$ of iid random variables that does not depend on the input flow and service times by other servers, $b_i = E\eta_{in} < \infty$, $B_i(x) = P(\eta_{in} \leq x)$, $i = \overline{1, m}$.

It is possible that an unavailable period starts while a customer is receiving service. Then service of the customer is immediately interrupted. There are various disciplines for continuation of the service after restotation (see Gaver [14]). Here we consider the preemptive resume service discipline assuming that interrupted service continues when the server returns from a blocked period and the service velocity is the next state of the process $n_i(t)$.

Condition 6 *The stochastic process $\overrightarrow{n}(t) = (n_1(t), \ldots, n_m(t))$ is a strongly regenerative one with regeneration points $\{\theta_n^{(2)}\}_{n=1}^{\infty}$ ($\theta_0^{(2)} = 0$), $\tau_n^{(2)} = \theta_n^{(2)} - \theta_{n-1}^{(2)}$, $E\tau_n^{(2)} < \infty$ with an exponential phase $v_n^{(1)}$ so that $\tau_n^{(2)} = v_n^{(1)} + v_n^{(2)}$. We also assume that $n_i(\theta_{n-1}^{(2)} + t) = 0$ for $t \in [0, v_n^{(1)}]$, $i = \overline{1, m}$.*

It follows from the Condition 6 and Smith Theorem [25] that there exist the limits

$$\lim_{t\to\infty} P(\overrightarrow{n}(t) = (j_1, \ldots, j_m)) = \pi_{j_1,\ldots,j_m} > 0$$

and

$$\lim_{t\to\infty} P(n_i(t) = j) = \pi_j^{(i)},$$

where j_i takes values $0, r_1^{(i)}, \ldots, r_{k_i}^{(i)}$, $i = \overline{1, m}$.

To define an auxiliary process $Y_i(t)$ for the ith server we introduce a counting process

$$K_i(t) = \max\{j : \sum_{l=1}^{\infty} \eta_{il} \le t\}.$$

Then

$$Y_i(t) = K_i(\int_0^t n_i(y)dy) \tag{10}$$

and

$$Y(t) = \sum_{i=1}^{m} Y_i(t).$$

Condition 7 *Service times have the first exponential phase, i.e.*

$$\eta_{in} = \eta_{in}^{(1)} + \eta_{in}^{(2)}$$

where $\eta_{in}^{(1)}$ *and* $\eta_{in}^{(2)}$ *are independent random variables and* $P(\eta_{in}^{(1)} \le x) = e^{-\alpha_i x}$ $(\alpha_i \in (0, \infty))$.

As regeneration points for $Y(t)$ we take subsequence $\{\theta_{n_k}^{(2)}\}_{k=1}^{\infty}$ of the sequence $\{\theta_n^{(2)}\}_{n=1}^{\infty}$ such that at time $\theta_{n_k}^{(2)}$ interrupted services for processes $Y_i(t)$ $(i = \overline{1,m})$ were in the exponential phase. Because of the Conditions 6 and 7 $Y(t)$ is a strongly regenerative flow and we may define the common sequence $\{T_n\}_{n=1}^{\infty}$ of regeneration points for the both processes $X(t)$ and $Y(t)$ with the help of formula (3). We need only to take $\{\theta_{n_k}^{(2)}\}_{k=1}^{\infty}$ instead of $\{\theta_n^{(2)}\}_{n=1}^{\infty}$.

Because of (10) we can easily obtain from the renewal theory the formula for the rate of the auxiliary process

$$\lambda_Y = \sum_{i=1}^{m} b_i^{-1} \sum_{j=1}^{k_i} r_j^{(i)} \pi_j^{(i)}. \tag{11}$$

Now we may calculate the traffic rate ρ and under some assumptions we get the necessary and sufficient stability condition for the system , basing on Theorems 1 and 2. As an example, we consider the famous case (see Morozov *et al* [22]) when $r_i^{(j)} = 1$, $j = \overline{1,k_i}$, $i = \overline{1,m}$, i.e. a server may be in an available or unavailable state. Let $\{s_{i,n}^{(2)}\}_{n=1}^{\infty}$ be moments of break-downs and $\{s_{i,n}^{(1)}\}_{n=1}^{\infty}$ be moments of restorations for the ith server. Here

$$0 = s_{i,0}^{(2)} < s_{i,1}^{(1)} < s_{i,1}^{(2)} < \dots. \tag{12}$$

Then $u_{i,n}^{(1)} = s_{i,n}^{(1)} - s_{i,n-1}^{(2)}$ and $u_{i,n}^{(2)} = s_{i,n}^{(2)} - s_{i,n}^{(1)}$ denote the length of the nth blocked and the nth available period of the ith server respectively $(i = \overline{1,m})$. The sequence $\{u_{i,n}^{(1)}, u_{i,n}^{(2)}\}_{n=1}^{\infty}$ consists of iid random vectors (for all $(i = \overline{1,m})$) that do not depend on the input flow $X(t)$ and service times. Let $u_{i,n} = u_{i,n}^{(1)} + u_{i,n}^{(2)}$ be the length of the nth cycle for the server i. A cycle consists of a blocked period followed by an available period. We assume that $Eu_{i,n}^{(1)} = a_i^{(1)} <$

∞, $Eu_{i,n}^{(2)} = a_i^{(2)} < \infty$, $a_i = a_i^{(1)} + a_i^{(2)}$ $(i = \overline{1,m})$. We put $n_i(t) = 0$ if the ith server is in an unavailable state at time t and $n_i(t) = 1$ otherwise $(i = \overline{1,m})$. If a blocked period $u_{i,n}^{(1)}$ has an exponential phase i.e. $u_{i,n}^{(1)} = v_{i,n}^{(1)} + v_{i,n}^{(2)}$ where $v_{i,n}^{(1)}$ and $v_{i,n}^{(2)}$ are independent random variables and $v_{i,n}^{(1)}$ has an exponential distribution with a parameter α_i then we may define the sequence $\{\theta_n^{(2)}\}_{n=1}^{\infty}$ of regeneration points for the regenerative process $\overrightarrow{n}(t) = (n_1(t), \ldots, n_m(t))$ as above. Therefore, Condition 6 holds. Under Condition 7 the auxiliary process $Y(t)$ is also regenerative one and we can construct the common points of regeneration $\{T_n\}_{n=1}^{\infty}$ for $X(t)$ and $Y(t)$ and apply Theorems 1 and 2 for this model. Since

$$\pi_i = \lim_{t\to\infty} P(n_i(t) = 1) = \frac{a_i^{(2)}}{a_i}$$

we have from (11)

$$\rho = \frac{\lambda_X}{\sum\limits_{i=1}^{\infty} b_i^{-1} \frac{a_i^{(2)}}{a_i}}.$$

If $b_i = b$ then we get the same stability condition as obtained in Morozov *et al* [22] for a queueing system $GI|G|m$ with a common distribution function of service times for all servers.

Corollary 1. *For a queueing system with* $r_j^{(i)} = 1$, $j = \overline{1,k_i}$, $i = \overline{1,m}$

$$Q(t) \xrightarrow[t\to\infty]{P} \infty$$

if $\rho > 1$.

Under Condition 4 the process is stochastically bounded if $\rho < 1$.

Proof. Let, as before, $\tilde{Y}_i(t)$ be the number of customers really served on the ith server up to time t. It is evident that stochasic inequality

$$Y_i(t) \geq \tilde{Y}_i(t),\ i = \overline{1,m}$$

for $t \geq 0$ takes place and hence

$$Q(t) = Q(0) + X(t) - \tilde{Y}(t) \geq Q(0) + X(t) - Y(t).$$

Since $\rho > 1$, then $Q(t) \xrightarrow[t\to\infty]{P} \infty$.

To prove the second statement we firstly assume that Conditions 6 and 7 hold. Then Condition 1 for the process $Y(t)$ takes place. We also may organize the performance of the system in such a way that inequaity (7) is realized when $Q(t) \xrightarrow[t\to\infty]{P} \infty$. Thus, Conditions 1, 4 and 5 are satisfied and because of Theorem 2 the process Q(t) is stochastically bounded.

If Conditions 6 and 7 (or one of them) do not hold, we construct a system S_δ satisfying Conditions 6 and 7 and majorising our system S, so that in distribution

$$Q(t) \leq Q_\delta(t) + m. \tag{13}$$

Here $Q_\delta(t)$ is the number of customers in the system S_δ at instant t. Let us introduce independent sequences $\{\{\nu_{i,n}\}_{n\geq 1}, \{\gamma_{i,n}\}_{n\geq 1}\}_{i=1}^m$ of iid random variables with exponential distribution with a rate δ. Assume that repair time $\tilde{u}_{i,n}^{(1)}$ in the system S_δ has a form $\tilde{u}_{i,n}^{(1)} = \nu_{i,n}^{(1)} + u_{i,n}^{(1)}$ and service time $\tilde{\eta}_{i,n}$ by the ith server has a form $\tilde{\eta}_{i,n} = \eta_{i,n} + \gamma_{i,n}$.

Then S_δ satisfies Conditions 6 and 7. Since $\rho_\delta = \lambda_X (\sum\limits_{i=1}^{m} \frac{\delta}{1+\delta b_i} \frac{a_i^{(2)}\delta}{1+\delta a_i})^{-1}$ and $\rho = \rho_\delta < 1$ we may choose δ so that $\rho_\delta < 1$.

The proof (13) is based on so-called one probability space method (see Belorusov [6]).

Let us note that Condition 4 may be provided in various ways. For instance, assume that blocked (or available) period has an exponential phase and

$$B_1(x) > 0 \text{ for all } x > 0. \tag{14}$$

Then $Q(t)$ is a regenerative process with points of regeneration $\{\theta_{n_k}^{(1)}\}_{k=1}^\infty$ that is a subsequence of the sequence $\{\theta_n^{(1)}\}_{n=1}^\infty$ such that $Q(\theta_{n_k}^{(1)}-) = 0$ and all servers are in the exponential phase of their blocked (or available) periods. Now Condition 4 follows directly from Theorem 1 in Afanasyeva and Tkachenko [3]. We also note that in this case $Q(t)$ is a stable process if $\rho < 1$. If only assumption (14) takes place by defining the majorising system S_δ we obtain the stochastic boundedness $Q(t)$ when $\rho < 1$.

6 Discrete-time queueing system with interruptions and preemptive repeat different service discipline

Here we consider the system with interruptions described in the end of the previous section for the discrete-time case. The moments of breakdowns $\{s_{i,n}^{(2)}\}_{n=1}^\infty$ and moments of restorations $\{s_{i,n}^{(1)}\}_{n=1}^\infty$ for the ith server satisfy (12). The input flow $X(t)$ is an aperiodic discrete-time regenerative flow with rate λ_X.

We consider the preemptive repeat different service discipline that means that the service is repeated from the start after restoration of the server and the new service time is independent of the original service time (see Gaver [14]).

To define the auxiliary processes $Y_i(t)$ for the ith server we introduce the collection $\left\{\{\eta_{i,n}^{(j)}\}_{n=1}^\infty\right\}_{j=1}^\infty$ of independent sequences $\{\eta_{i,n}^{(j)}\}_{n=1}^\infty$ consisting of iid random variables with distribution function $B_i(x)$. Let $\mathscr{K}_{i,j}(t)$ be the counting process associated with the sequence $\{\eta_{i,n}^{(j)}\}_{n=1}^\infty$ i.e. $\mathscr{K}_{i,j}(t) = \max\{k : \sum\limits_{n=1}^{k} \eta_{i,n}^{(j)} \leq t\}$, $(\mathscr{K}_{i,j}(0) = 0)$ and $\mu_i(t)$ be the number of cycles for the ith server during $[0,t]$, i.e. $\mu_i(t) = \max\{j : \sum\limits_{n=1}^{j} \eta_{i,n} \leq t\}$, $(\mu_i(0) = 0)$. Then the process $Y_i(t)$ is defined be the relation

$$Y_i(t) = \sum_{j=1}^{\mu_i(t)} \mathscr{K}_{i,j}(u_{i,j}^{(2)}) + \mathscr{K}_{i,\mu_i(t)+1}(\max[0, t - s_{i,\mu_i(t)+1}^{(1)}]) \tag{15}$$

and $Y(t) = \sum\limits_{i=1}^{m} Y_i(t)$. By $H_i(t)$ we denote the renewal function for $\mathscr{K}_{i,j}$, i.e. $H_i(t) = \mathbf{E}\mathscr{K}_{i,j}(t)$.

Lemma 2. *There exists the limit*

$$\lambda_{Y_i} = \lim_{t\to\infty} \frac{Y_i(t)}{t} = \frac{\boldsymbol{E}H_i(u_{i,n}^{(2)})}{a_i} \quad w.p.1.$$

The proof easily follows from the evident inequalities

$$g_i(\mu_i(t)) \le Y_i(t) \le g_i(\mu_i(t)+1)$$

where $g_i(n) = \sum\limits_{j=1}^{n} \mathscr{K}_{i,j}(u_{i,j}^{(2)})$, the strong law of large numbers and convergence $t^{-1}\mu_i(t) \xrightarrow[t\to\infty]{} a_i^{-1}$ w.p.1.

From Lemma 2 we have

$$\lambda_Y = \lim_{t\to\infty} \frac{Y(t)}{t} = \sum_{i=1}^{m} \frac{\mathbf{E}H_i(u_{i,1}^{(2)})}{a_i}.$$

We introduce the counting processes

$$N_0(t) = \max\{k : \theta_k^{(1)} \le t\},$$

$$N_i(t) = \max\{k : s_{i,k}^{(2)} \le t\}, i = \overline{1,m}$$

Condition 8 *The counting processes $N_0(t)$ and $N_i(t)$ ($i = \overline{1,m}$) are aperiodic.*

Then $Y(t)$ is a regenerative aperiodic flow with points of regeneration

$$\theta_j^{(2)} = \min\{t > \theta_{j-1}^{(2)} : \bigcap_{i=1}^{m} [N_i(t) - N_i(t-1) > 0]\}, \theta_0^{(2)} = 0.$$

In other words, $\theta_j^{(2)}$ is a point of regeneration of $Y(t)$ if all the servers get out of the order simultaneously at this moment. Taking into account Condition 8 we conclude from Lemma 1 that $\mathbf{E}(\theta_j^{(2)} - \theta_{j-1}^{(2)}) < \infty$. Now we construct the sequence $\{T_n\}_{n=1}^{\infty}$ of common points of regeneration for processes $X(t)$ and $Y(t)$ with the hepl of (1). In view of Lemma 1 $\mathbf{E}(T_n - T_{n-1}) < \infty$ and the traffic rate ρ of the system is defined by (4). It is also evident that Conditions 3 and 5 are realized.

Corollary 2. *Let Condition 8 be fulfilled. Then*

(i) $Q(t) \xrightarrow[t\to\infty]{P} \infty$ *if* $\rho \ge 1$;
(ii) $Q(t)$ *is a stochastically bounded process if* $\rho < 1$.

Proof. The first statement follows from Theorem 1 since Conditions 2 and 3 are realized.

Let $\rho < 1$. We introduce the embedded process $x_n = (Q_n, \zeta_1(n), \ldots, \zeta_m(n))$, $n \geq 0$, where Q_n is the number of customers at the system on time T_n and $\zeta_i(n) = 1$ if there is a customer on the ith server and $\zeta_i(n) = 0$ otherwise. In view of the service discipline after service restoration and properties of the synchronization epochs $\{T_n\}_{n\geq 0}$ the process $\{x_n\}_{n\geq 1}$ is a Markov chain with countable set of states $\mathscr{R} = \big\{\{0\}, (j, e_1, \ldots, e_m), j = \overline{1, m-1}; \{j\}, j \geq m\big\}$. Let R_0 be the set of unessential states and R_j $(j = \overline{1, r})$ irreducible classes of communicating states. It follows from the condition $\rho < 1$ that the number of classes $r < \infty$.

For any aperiodic class $\mathscr{K}_l$ of states basing on Foster's criterion (see Meyn And Tweedie [21]) and Condition 5 one may easily prove that this class is ergodic. Therefore, the process Q_n is stochastically bounded if $Q_0 \in \mathscr{K}_l$. It is also true if $\mathscr{K}_l$ is a periodic class. Since the number of classes $r < \infty$ we obtain the stochastic boundedness of the process Q_n and therefore $Q(t)$.

We may obtain the upper bound of the traffic rate ρ providing the stochastic boundedness of the process $Q(t)$. It is known from Borovkov [7] that

$$H_i(t) \geq \frac{t}{b_i} - 1.$$

Therefore

$$\sum_{i=1}^{m} H_i(u_{i,n}^{(2)}) \geq \sum_{i=1}^{m} \frac{a_i^{(2)}}{b_i a_i} - \sum_{i=1}^{m} \frac{1}{a_i}$$

and suddicient condition of the stochastic boundedness of $Q(t)$ has the following form

$$\lambda_k + \sum_{i=1}^{m} a_i^{-1} \leq \sum_{i=1}^{m} \frac{a_i^{(2)}}{b_i a_i}.$$

If $b_i = b$ then we have the same condition as obtained in Morozov *et al* [22]

7 Queueing system with a preemptive priority discipline

Here we study a continuous-time queueing system with two independent regenerative input flows $X_1(t)$ and $X_2(t)$ with intensities λ_1 and λ_2 and m servers. The customers of the second type (which belong to $X_2(t)$) have an absolute priority with respect to customers of the first type. Service interruption for the low priority customer occurs when a high priority customer arrives during a low priority customer's service time. If at an arrival time of the second type customer there are m_1 free servers, m_2 servers occupied by customers of the first type and $m - m_1 - m_2$ servers occupied by customers of the second type, then an arriving customer randomly chooses any server from $m_1 + m_2$ servers which are not busy by customers of the second type. Service times by the ith server for high(low) priority customers have distribution function $B_0(x)$ ($B_i(x)$, $i = \overline{1, m}$) with mean b_0 (b_i, $i = \overline{1, m}$). Therefore for high priority customers we have a system $Reg|G|m$ with homogeneous servers and for low priority customers a system with interruptions considered in Section 5..

Denote by $Q_i(t)$ the number of customers of the ith type at the system including the customers on the servers at time t ($i = 1, 2$). Let $\{\theta_j^{(1)}\}_{j=1}^{\infty}$ ($\theta_0^{(1)} = 0$) and $\{\theta_j^{(2)}\}_{j=1}^{\infty}$ ($\theta_0^{(2)} = 0$) be the sequences of regeneration points for $X_1(t)$ and $X_2(t)$ respectively. Under some additional conditions, for example, when the inequality (14) is valid for the function $B_0(x)$ (other sufficient assumptions are given in Afanasyeva and Tkachenko [3]. the process $Q_2(t)$ is a regenerative one with points of regeneration

$$S_n^{(2)} = \min\{\theta_j^{(2)} > S_{n-1}^{(2)} : Q_2(\theta_j^{(2)}) = 0\},\ n > 0;$$

$$S_0^{(2)} = 0.$$

At first we also assume that Condition 7 holds for service time distribution $B_i(x)$, $i = \overline{1, m}$, i.e. service times have an exponential phase.

Stability condition for the process $Q_2(t)$ has a form [11]

$$\rho_2 = \frac{\lambda_2 b_0}{m} < 1 \tag{16}$$

that is supposed to be fulfilled. We now want to get stability condition for the process $Q_1(t)$.

We start with the definition of the process of interruptions. Let $n_i(t) = 0$ if at instant t the ith server is occupied by a high priority customer and $n_i(t) = 1$ otherwise, $i = \overline{1, m}$. As regeneration points for $\overrightarrow{n}(t) = (n_1(t), \ldots, n_m(t))$ we take subsequence $\{\theta_{k_j}^{(2)}\}_{j=1}^{\infty}$ of the regeneration points sequence $\{\theta_j^{(2)}\}_{j=1}^{\infty}$ for the input flow $X_2(t)$ such that $Q_2(\theta_{k_j}^{(2)} + 0) = m$ and all service times are in the exponential phase. For simplicity we suppose that $X_2(t)$ is a strongly regenerative flow. Then an auxiliary process $Y(t)$ for low priority customers defined by (10) is strongly regenerative with regeneration points $\{\theta_{\tilde{k}_j}^{(2)}\}_{j=1}^{\infty}$ that is a subsequence of the sequence $\{\theta_{k_j}^{(2)}\}_{j=1}^{\infty}$ such that at time $\theta_{\tilde{k}_j}^{(2)}$ all interrupted services of low priority customers are in the exponential phase.

To obtain the traffic rate for low priority customers we need to find $\pi_i = \lim\limits_{t\to\infty} P(n_i(t) = 1)$. Because of the rule of the server choose by an arriving high priority customer we have $\pi_i = \pi_1 = \pi$ for all $i = \overline{1, m}$. To calculate π we define for high priority customers the following processes. Let $w_i(t)$ be the residual service time (virtual waiting time) on the ith server at instant t and $Z_i(t)$ the total service time of customers which arrived up to time t and have to be served on the ith server. Thus

$$\sum_{i=1}^{m} Z_i(t) = \sum_{j=1}^{X_2(t)} \eta_j$$

where η_j is the service time of the jth arrived customer. Since w.p.1

$$\lim_{t\to\infty} \frac{Z_i(t)}{t} = \frac{1}{m} \lim_{t\to\infty} \sum_{j=1}^{X_2(t)} \eta_j = \frac{\lambda_2 b_0}{m}$$

and

$$\frac{w_i(t)}{t} \xrightarrow[t\to\infty]{} 0$$

because of the stability Condition (16).

We note that

$$w_i(t) = Z_i(t) - \int_0^t (1 - n_i(y))dy$$

and

$$\lim_{t\to\infty} t^{-1} \int_0^t (1 - n_i(y))dy = 1 - \pi.$$

Therefore $\pi = 1 - \frac{\lambda_2 b_0}{m}$ and traffic rate for low priority customers has a form

$$\rho_1 = \lambda_1((1 - \frac{\lambda_2 b_0}{m}) \sum_{i=1}^{m} b_i^{-1})^{-1}.$$

We get from Corollory 1

Corollary 3. *Assume that $X_2(t)$ is a strongly regenerative flow, $B_0(x)$ satisfies the inequality (14) and $\rho_2 = \frac{\lambda_2 b_0}{m} < 1$. Then $Q_1(t) \xrightarrow[t\to\infty]{P} \infty$ if $\rho_1 > 1$. If additionally $B_i(x)$ satisfies (14) and $\rho_1 < 1$ then $Q_1(t)$ is a stochastically bounded process.*

Basing on results from Section 4 one may obtain sufficient conditions providing stability of the process $Q_1(t)$.

8 Conclusion

In this paper we considered stability problem for multiserver queues with a regenerative input flow. Let us note that stability analysis is an essential and challenging stage of the investigation of stochastic models. However stability conditions may be of independent interest. In particular, the stability criterion of the multi-server model can be used for the capacity planning of a model and estimation of the upper bound of potential energy saving. The main contribution of this paper is an extension of the stability criterion to the model with a regenerative input flow. The method we use has the following steps. Firstly, we define an auxiliary process $Y(t)$ that is the number of customers which are served at the system if always there are customers for service. Secondly, assuming that this process is a regenerative flow not depending on the input flow $X(t)$ under some additional conditions we construct the common points of regeneration of $Y(t)$ and $X(t)$. This step we call synchronization of the processes. This approach allows us to use results from the renewal theory for the stability analysis of the systems satisfying additional conditions. One may think that these conditions are too restrictive to be useful for the analysis of the real models. Therefore we apply our approach to stability analysis of three classical systems with interruptions of the service. It follows from our results that the structure of the input flow does not effect on the stability condition.

One has to know only the intensity of this flow to estimate the traffic rate. But for the preemptive repeat different service discipline the distribution of the service time plays an essential role, since the traffic rate is expressed with the help of the renewal function corresponding to this distribution. We obtain the upper bound for traffic rate providing the sufficient stability condition. Note, that this condition is the same as obtained in Morozov *et al* [22] for the more simple model.

Acknowledgement. The research was partially supported by RFBR grant 17-01-00468.

References

1. L.G.Afanasyeva, E.E. Bashtova. Coupling method for asymptotic analysis of queues with regenerative input and unreliable server. *Queueing Systems*, 76, 2, 125–147, 2014.
2. L. Afanasyeva, E. Bashtova and E. Bulinskaya. Limit Theorems for Semi-Markov Queues and Their Applications. *Communications in Statistics Part B: Simulation and Computation*, 41 **6**, 688–709, 2012.
3. L.Afanasyeva, A.Tkachenko. Multichannel queueing systems with regenerative input flow. *Theory of Probability and Its Applications*, 58 **2**, 174–192, 2014.
4. S.Asmussen *Applied Probability and Queues*, **51**, Springer-Verlag, 2003.
5. B.Avi-Itzhak and P.Naor. Some queueing problems with the service station subject to breakdown. *Operations Research*, 11 **3**, 303–320, 1963.
6. T.Belorusov. Ergodicity of a multichannel queueing system with balking. *Theory of Probability and Its Applications*, 56 **1**, 120–126, 2012.
7. A.A.Borovkov. *Stochastic Processes in Queueing Theory*, **4**, Springer-Verlag. 1976.
8. H.Chen. Fluid approximation and stability of multiclass queueing networks: work-conserving disciplines. *Annals of Applied Probability*, 5, 637–665, 1995.
9. H.Chen, D.Yao. *Fundamentals of queueing networks*, Springer, 2001.
10. J.Dai. On positive Harris recurrence of multiclass queueing networks: a unified approach via fluid limit models. *Annals of Applied Probability*, 5, 49–77, 1995.
11. W.Feller. *An introduction to probability theory and its applications*, 2nd Edition, Wiley, New York, NY, USA, 1957.
12. D.Fiems, H.Bruneel. Discrete-time queueing systems with Markovian preemptive vacations. Mathematical and computer modeling, 57 **3-4**, 782792, 2013. doi: 10.1016/j.mcm.2012.09.003.
13. S.Foss, T.Konstantopoulos. An overview on some stochastic stability methods. *Journal of the Operations Research Society of Japan*, 47 **4**, 275–303, 2004.
14. D.Gaver Jr. A waiting line with interrupted service, including priorities. *Journal of the Royal Statistical Society. Series B (Methodological)*, 24, 7390, 1962.
15. L.Georgiadis, W.Szpankowski. Stability of token passing rings. *Queueing systems*, 11, 7–33, 1992.
16. J.Grandell *Double Stochastic Poisson Process*, Lect.Notes.Math., **529**, Springer, Berlin 1976.
17. A.Krishnamoorthy, P.Pramod, S. Chakravarthy. Queues with interruptions: a survey, TOP 1-31doi:10.1007/s11750-012-0256-6, 2012.
18. J.Kiefer and J.Wolfowitz. On the theory of queues with many servers. *Trans. Amer. Math. Soc.*, 78, 1–18, 1955.
19. R.M.Loynes. The stability of a queue with non-independent inter-arrival and service times. *Proc. Cambr. Phil. Soc.*, 58 **3**, 497–520, 1962.

20. V.A.Malyshev, M.V.Menshikov. Ergodicity continuity and analyticity of countable Markov chains. *Trans Moscow Math*, 1, 1–48, 1982.
21. S.P.Meyn and R.L.Tweedie. Markov chains and stochastic stability. *Cambridge University Press.*, 2009.
22. E.Morozov, D.Fiems, H.Bruneel. Stability analysis of multiserver discrete-time queueing systems with renewal-type server interruptions. *Performance Evaluation*, 68 **12**, 1261–1275, 2011. doi:10.2016/j.peva.2011.07.002.
23. A.Pechinkin, I.Socolov, V.Chaplygin. Multichannel queueing system with refusals of servers groups. *Informatics and its Applications*, 3 **3**, 4–15, 2009.
24. J.S.Sadowsky. The probability of large queue lengths and waiting times in a heterogeneous multiserver queue: positive recurrence and logarithmic limits. *Adv. Appl. Prob.*, 27, 567–583.
25. W.Smith. Regenerative stochastic processes. *Proceedings of the Royal Society of London. Series A. Mathematical and Physical Scinces*, 232 **1188**, 6–31, 1955.
26. W.Szpankowski. Stability conditions for some distributed systems. Buffered random access systems. *Adv. Appl. Prob.*, 26, 498–515, 1994.
27. K.Thiruvengadam. Queueing with breakdowns. *Operations Research*, 11 **1**, 62–71, 1963.
28. H.Thorisson *Coupling, Stationary and Regeneration*, Springer, New York. 2000.
29. H.White. Lee S. Christie, Queueing with preemptive prioriries or with breakdown. *Operations Research*, 6 **1**, 79–95 1958.

Stability Analysis of a Multiserver model with Simultaneous Service and a Regenerative Input Flow

Larisa Afanaseva[1], Elena Bashtova[2], and Svetlana Grishunina[3]

[1] Department of Probability, Faculty of Mathematics and Mechanics, Lomonosov Moscow State University, Moscow, Russia
(E-mail: lafanaseva@yandex.ru)
[2] Department of Probability, Faculty of Mathematics and Mechanics, Lomonosov Moscow State University, Moscow, Russia
(E-mail: bashtovaelena@rambler.ru)
[3] Department of Probability, Faculty of Mathematics and Mechanics, Lomonosov Moscow State University, Moscow, Russia; Moscow Institute of Electronics and Mathematics, National Research University Higher School of Economics, Moscow, Russia
(E-mail: svetagri@live.ru)

Abstract. We study the stability conditions of the multiserver system in which each customer requires a random number of servers simultaneously. The input flow is supposed to be a regenerative one and a random service time is identical at all occupied servers. The service time has an exponential or a phase-type distribution. We define an auxiliary service process that is the number of served customers under assumption that always there are customers at the system. Then we construct the sequence of common regeneration points for the regenerative input flow and the auxiliary service process. Basing on relation between the real and auxiliary service processes we obtain the upper and lower estimates for the mean of the really served customers during the common regeneration period. It allows us to deduce the stability criterion of the model under consideration. It turns out that the stability condition does not depend on the structure of the input flow, only the rate of this process plays a role. Nevertheless the distribution of the service time is a very important factor. We give an example which shows that the stability condition can not be expressed in terms of the mean of the service time.
Keywords: Stability criterion, Cluster systems, Regeneration, Queueing systems.

1 Introduction

This paper is devoted to the stability analysis of a multiserver queueing system in which each new customer requires a random number of servers simultaneously and a random service time identical at all occupied servers. For this model with a regenerative input flow we deduce stability criterion using synchronization method. The most crucial attribute of the systems which provide

17^{th} *ASMDA Conference Proceedings, 6 – 9 June 2017, London, UK*

a random number of servers per customer is that a customer cannot begin service until all required servers are available. Therefore servers may be idle even when there are customers waiting to enter service. Queueing systems belonging to this class are found in a variety of contexts. In computer systems, buffers and other temporary storage devices are used for programs and date of varying dimensions. The increasing interest to multiserver systems with simultaneous service is motivated by the modeling of high performance clusters (HPC) and cloud/distributed computing containing a huge number of servers working in parallel.

The class of systems with simultaneous service can be divided into two subclasses. The first one is class of systems with independent service (service times of a given customer on occupied servers are independent) and the second subclass contains systems with concurrent service (service times of a customer on occupied servers are identical) (see Van Dyk[23]). For the former subclass, the stablity condition as well as some performance measures, have been obtained in a number of papers, see Green[9], Seila[21], Federgruen and Green[11], Ittimakin and Kao[13], Schaack and Larson[20]), Gillent and Latonche[7].

Queueing systems with concurrent service have been also considered in a number of works. Here we refer to pioneering papers Brill and Green[6], Whitt[24] and more late works, Rumyantsev and Morozov[19], Morozov and Rumyantsev[15]. Detail analysis of available results in this domain of the queueing theory and extensive list of references are given in the paper Rumyantsev and Morozov[19].

Let us note that the mentioned papers (except Morozov and Rumyantsev[15] where $MAP|M|s$ cluster model is considered) deal with exponential distributions of inter-arrival and service times and authors use the matrix analysis of the system.

The main contribution of the represented paper is an extension of the stability criterion to the cluster model with a regenerative input flow. The class of these flows is very broad and includes MMP, MAP, DSPP with intensity that is a regenerative process. The detail description of the regenerative flows and processes one may find in Thorisson[22] and Afanaseva and Bashtova [1].

We consider two models. In the first one the service time has an exponential distribution (system S_1), in the second the service time is a summ of r independent exponentially distributed random variables (system S_2). We define an auxiliary service process $Y(t)$ that is the number of served customers under the assumption that always there are customers in the system. We construct the sequence of common regeneration points for the input flow $X(t)$ and an auxiliary process $Y(t)$. Then basing on relation between the real service process $\widetilde{Y}(t)$ and $Y(t)$ we obtain the upper and lower estimates for the mean of the served customers during the constructed regeneration period. It allows us to deduce the stability criterion.

Let us note that the stability condition does not depend on the structure of the regenerative input but only its intensity plays a role. Also our stability condition for the system S_1(exponentially distributed service time) is the same as obtained by Rumyantsev and Morozov[19]. Nevertheless, as it is shown by

pur example the distribution of the service time plays the important role in the stability condition.

The rest of the paper is organized as follows. We describe the model in Section 2 and define an auxiliary process $Y(t)$ in Section 3. We also find the rate of this process in this section. Section 4 is devoted to synchronization of the input flow and an auxiliary service process. Basing on the relation between the real and auxiliary service processes we proof the stability criterion in Section 5. Next, in section 6 we give an example(the system $Reg|PH|2$) and show that the stability condition depends on the service time distribution. Some concluding comments are given in Section 7.

2 Description of the model

We consider an $m-$server queueing system with a regenerative input flow $X(t)$ with the rate λ and FCFS service discipline.

Let $\{\theta_j\}_{j=1}^{\infty}$ be a sequence of regeneration points of the input flow $\tau_j = \theta_j - \theta_{j-1}$, $(\theta_0 = 0)$ regeneration periods and $\xi_j = X(\theta_j) - X(\theta_{j-1})$ the number of arrived customers on the jth regeneration period, so that $\lambda = \frac{\mathsf{E}\xi}{\mathsf{E}\tau}$. For more details on these types of flows see, for instance, Afanaseva and Bashtova[1] and Thorisson[22].

We consider two models: S_1 and S_2. Customer i occupies ζ_i servers simultaneously for an exponentially distributed service time η_i with rate μ, $(i \geq 1)$ for the model S_1 and for the model S_2

$$\eta_i = \eta_i^{(1)} + \ldots + \eta_i^{(r)} (r > 1),$$

where $\{\eta_i^{(n)}\}_{n=1}^{r}$ are independent identically distributed(iid) random variables with rate μ_k for $\eta_i^{(k)} (k = \overline{1,r})$. We call $\eta_i^{(l)}$ the lth phase of the service time. All ζ_i servers occupied by customer i are simultaneously released upon completion of their service. The sequence $\{\zeta_i\}_{i=1}^{\infty}$ consists of iid random variables with given distribution

$$p_j = \mathsf{P}(\zeta = j), \quad j = 1, \ldots m, \quad \sum_{j=1}^{m} p_j = 1.$$

(We omit the serial index to denote a generic element of an iid sequence.) Let us note that for the model S_2 the service time distribution has a phase type. The probability distributions of this type (PH) have been introduced by Neuts [16–18].

Let $Q(t)$ be the number of customers in the system at instant t, $t \geq 0$. Our goal is the extension of the stability criterion for this process to the cluster model with a regenerative input flow.

3 Auxiliary process and related results

In this section we define an auxiliary process $Y(t)$ that will be used in our analysis. We think $Y(t)$ as the number of customers that can be served in the

system if there are always customers for service. It means that $Y(t)$ is defined by sequences $\{\eta_n\}_{n=1}^{\infty}$ and $\{\zeta_n\}_{n=1}^{\infty}$ and does not depend on the input flow $X(t)$.

Customer n occupies ζ_n servers simultaneously. We call customer n class-i one if $\zeta_n = i$. For the model S_1 we introduce the stochastic process $U_1(t)$ with state space

$$\mathcal{K}_1 = \{\overrightarrow{k} = (k_1, \ldots, k_j, k_{j+1}); \quad \sum_{i=1}^{j} k_i \le m, \quad \sum_{i=1}^{j+1} k_i > m\}$$

and for the model S_2 the stochastic process $U_2(t)$ with state space

$$\mathcal{K}_2 = \{\overrightarrow{k} = (k_1, e_1, \ldots, k_j, e_j, k_{j+1}); \quad \sum_{i=1}^{j} k_i \le m, \quad \sum_{i=1}^{j+1} k_i > m, e_i = \overline{1,r}\}$$

Under condition that there are always customers for service we put $U_1(t) = \overrightarrow{k} = (k_1, \ldots, k_j, k_{j+1})$ if there are j customers on the servers at instant t, the ith serving customer has a class $k_i (i = \overline{1,j})$ and the first customer in the queue has a class k_{j+1}. For the process $U_2(t)$ coordinates $k_i (i = \overline{1,j+1})$ have the same meaning and e_i is the number of the phase of the service time for the ith customer at instant t. We note that $U_i(t)(i = 1, 2)$ is a Markov chain with a finite set of states and there are limits

$$\lim_{t\to\infty} \mathsf{P}(U_i(t) = \overrightarrow{k}) = \mathsf{P}_i(\overrightarrow{k}), \quad (i = 1, 2).$$

The auxiliary process $Y_i(t)(i = 1, 2)$ is a regenerative flow(see, e.g. Afanaseva and Bashtova [1]) and there exists the rate

$$\lambda_{Y_i} = \lim_{t\to\infty} \frac{Y_i(t)}{t} \quad w.p.1.$$

For the state $\overrightarrow{k} = (k_1, \ldots, k_j, k_{j+1})$ of the Markov chain $U_1(t)$ define $j(\overrightarrow{k}) = j$ as the number of customers on the servers and for $U_2(t)$ define $g(\overrightarrow{k})(\overrightarrow{k} \in \mathcal{K}_2)$ as the number of customers on the servers which are in the last (the rth) phase of the service time, i.e.

$$g(\overrightarrow{k}) = g(k_1, e_1, \ldots, k_j, e_j, k_{j+1}) = \sum_{i=1}^{j} \mathbb{I}(e_i = r).$$

Here $\mathbb{I}(A)$ is an indicator function of the event A. Then the rates of the auxiliary processes $Y_1(t)$ and $Y_2(t)$ are given by the formulas

$$\lambda_{Y_1} = \mu \sum_{\overrightarrow{k}\in\mathcal{K}_1} j(\overrightarrow{k})\mathsf{P}_1(\overrightarrow{k}), \lambda_{Y_2} = \mu_r \sum_{\overrightarrow{k}\in\mathcal{K}_2} g(\overrightarrow{k})\mathsf{P}_2(\overrightarrow{k}). \tag{1}$$

Now we define the traffic rate for the system S_i as follows

$$\rho_i = \frac{\lambda_X}{\lambda_{Y_i}}, \quad (i = 1, 2). \tag{2}$$

Intuitively, it is clear that the system is stable when $\rho_i < 1$ and it is unstable otherwise. The main stability result of the paper consists of the formal proof of this fact. The key element of our proof is the procedure which we call the synchronization of the processes $X(t)$ and $Y_i(t)(i = 1, 2)$.

In order to calculate the traffic rates we need to find the limit distributions of the control processes $U_i(t)(i = 1, 2)$. Unfortunately, for $U_2(t)$ we could not do it up to now but late we give an example demonstrating how it can be done.

Now consider the process $U_1(t)$. In the rest of this section we consider only the system S_1 therefore index 1 will be omitted.

Let t_n be the moment of departure of the nth customer. Consider the embedded Markov chain $U_n = U(t_n + 0)$ with state space $\mathcal{K}_1$.

Lemma 1. *There are limits*

$$\lim_{n\to\infty} \mathsf{P}(U_n = \overrightarrow{k}) = \pi_{\overrightarrow{k}} = p_{k_1} \cdot \cdots \cdot p_{k_{j+1}}. \tag{3}$$

Proof. Consider another Markov chain $\widetilde{U}_n$ with the state space

$$\mathcal{K} = \{\widetilde{k} = (k_1, \ldots, k_m), k_i = 1, 2, \ldots, m\}$$

and put

$$j(\overrightarrow{k}) = \max\{i : k_1 + \cdots + k_i \le m\}.$$

Transition probabilities are given by the formula

$$\mathsf{P}(\widetilde{U}_{n+1} = (k_1, \ldots, k_{i-1}, k_{i+1}, \ldots, k_m, s) | \widetilde{U}_n = (k_1, \ldots, k_m)) = \frac{p_s}{j(\overrightarrow{k})}.$$

Limit distribution

$$\widetilde{\pi}_{\overrightarrow{k}} = \lim_{n\to\infty} \mathsf{P}(\widetilde{U}_n = \overrightarrow{k})$$

satisfies the system of the equations

$$\widetilde{\pi}_{\overrightarrow{k}} = \sum_{s=1}^{m} \sum_{j=1}^{j(\overrightarrow{k},s)} p_{k_m} \frac{1}{j(\overrightarrow{k}, s)} \widetilde{\pi}_{k_1,\ldots,k_{i-1},s,k_i,\ldots,k_{m-1}}.$$

Here

$$j(\overrightarrow{k}, s) = \max\{i : s + k_1 + \cdots + k_i \le m\}.$$

One may easily verify that

$$\widetilde{\pi}_{\overrightarrow{k}} = \prod_{j=1}^{m} p_{k_j}.$$

Since for $j < m$

$$\pi_{(k_1,\ldots,k_j,k_{j+1})} = \sum_{k_{j+1},\ldots,k_m} \widetilde{\pi}_{(k_1,\ldots,k_j,k_{j+1},\ldots k_m)} = \prod_{i=1}^{j+1} p_{k_i}$$

and $\pi_{(1,\ldots,1)} = \widetilde{\pi}_{(1,\ldots,1)}$. the Lemma is proved.

Let

$$\tilde{\mathcal{K}}_i = \{\overrightarrow{k} : j(\overrightarrow{k}) = i\}, \quad \text{so that} \quad \mathcal{K}_1 = \bigcup_{i=1}^{m} \tilde{\mathcal{K}}_i.$$

Then we have from (1)

$$\lambda_y = \lim_{t\to\infty} \frac{Y(t)}{t} = \mu \sum_{j=1}^{m} j \sum_{\overrightarrow{k}\in\tilde{\mathcal{K}}_j} \mathsf{P}(\overrightarrow{k}). \tag{4}$$

Now we find $\mathsf{P}(\overrightarrow{k})$ with the help of $\pi_{\overrightarrow{k}}$ obtained in Lemma 1.

Markov chain $U(t)$ is situated in the state $\overrightarrow{k}$ the exponentially distributed time $\tau^{(U)}_{\overrightarrow{k}}$ with mean

$$\mathsf{E}\tau^{(U)}_{\overrightarrow{k}} = \frac{1}{j(\overrightarrow{k})\mu}.$$

Also the response time $\tau^{(U)}$ in a state for the stationary process $U(t)$ has the mean

$$\mathsf{E}\tau^{(U)} = \frac{1}{\mu} \sum_{\overrightarrow{k}\in\mathcal{K}_1} \frac{1}{j(\overrightarrow{k})} \pi_{\overrightarrow{k}}.$$

It is well known (see, e.g. Borovkov[4]) that for any $\overrightarrow{k}_0 \in \mathcal{K}_1$

$$\lim_{t\to\infty} \mathsf{P}(U(t) = \overrightarrow{k}_0) = \mathsf{P}(\overrightarrow{k}_0) = \frac{\pi_{\overrightarrow{k}_0} \mathsf{E}\tau^{(U)}_{\overrightarrow{k}_0}}{\mathsf{E}\tau^{(U)}} =$$

$$= \pi_{\overrightarrow{k}_0} \frac{1}{j(\overrightarrow{k}_0)} \left(\sum_{\overrightarrow{k}\in\mathcal{K}_1} \frac{1}{j(\overrightarrow{k})} \pi_{\overrightarrow{k}} \right)^{-1}.$$

Therefore we get from (4)

$$\lambda_Y = \mu \left(\sum_{\overrightarrow{k}\in\mathcal{K}_1} \frac{1}{j(\overrightarrow{k})} \pi_{\overrightarrow{k}} \right)^{-1}.$$

Consider a renewal process $\{\zeta_j\}_{j=1}^{\infty}$ and a counting process

$$N(n) = \max\{j : Z_j \le n\}, \quad \text{where} \quad Z_j = \zeta_1 + \cdots + \zeta_j, \quad Z_0 = 0.$$

Taking into account (3) we have

$$\lambda_Y = \mu \left(\sum_{j=1}^{m} \frac{1}{j} \sum_{\overrightarrow{k}\in\mathcal{K}_|} \prod_{i=1}^{j+1} p_{k_i} \right)^{-1} = \mu \left(\sum_{j=1}^{m} \frac{1}{j} \mathsf{P}(Z_j \le m, Z_{j+1} > m) \right)^{-1} =$$

$$= \mu \left(\sum_{j=1}^{m} \frac{1}{j} \mathsf{P}(N(m) = j) \right)^{-1} = \mu \left(\mathsf{E} \frac{1}{N(m)} \right)^{-1}.$$

Now we define the traffic rate for the system S_1 as follows

$$\rho_1 = \frac{\lambda_X}{\lambda_Y} = \frac{\lambda_X}{\mu}\mathsf{E}\frac{1}{N(m)}. \tag{5}$$

4 Synchronization of the input flow and auxiliary service processes

First we construct the common regeneration points for the input flow $X(t)$ and auxiliary process $Y_i(t)$. We fix an arbitrary state $\overrightarrow{k}$ of the Markov chain $U_i(t)$ assuming that $\mathsf{P}_i(\overrightarrow{k}) > 0$. Let $\{t_n^{(\overrightarrow{k})}\}_{n=1}^{\infty}$ be the moments of hits $U_i(t)$ into the state $\overrightarrow{k}$ so that

$$t_n^{(\overrightarrow{k})} = \min\{t_j > t_{n-1}^{(\overrightarrow{k})} : U_i(t_j + 0) = \overrightarrow{k}\}, \quad (t_0^{(\overrightarrow{k})} = 0), \quad n = 1, 2, \ldots$$

Here $\{t_j\}_{j=1}^{\infty}$ is the sequence of the timing of each jump $U_i(t)$. Then $\{t_{n+1}^{(\overrightarrow{k})} - t_n^{(\overrightarrow{k})}\}_{n=1}^{\infty}$ is a sequence of iid random variables and $t_n^{(\overrightarrow{k})}$ is the nth regeneration point of $Y_i(t)$. Moreover $\mathsf{E}(t_{n+1}^{(\overrightarrow{k})} - t_n^{(\overrightarrow{k})}) < \infty$ and $Y_i(t)$ is the strongly regenerative flow. It means that its regeneration period is of the form

$$t_{n+1}^{(\overrightarrow{k})} - t_n^{(\overrightarrow{k})} = \eta_n^{(\overrightarrow{k})} + v_n^{(\overrightarrow{k})}.$$

Here $\eta_n^{(\overrightarrow{k})}$ and $v_n^{(\overrightarrow{k})}$ are independent random variables and $\eta_n^{(\overrightarrow{k})}$ is the time which $U_i(t)$ is in the state $\overrightarrow{k}$. Since $U_i(t)$ is a Markov chain, $\eta_n^{(\overrightarrow{k})}$ has an exponential distribution with rate $j(\overrightarrow{k})\mu$ for $U_1(t)$ and $\sum\limits_{i=1}^{j}\mu_{e_i}$ for $U_2(t)$. We note that any time within the interval $[t_n^{(\overrightarrow{k})}, t_n^{(\overrightarrow{k})} + \eta_n^{(\overrightarrow{k})})$ can be considered as a point of regeneration for $Y_i(t)$. Later the interval $[t_n^{(\overrightarrow{k})}, t_n^{(\overrightarrow{k})} + \eta_n^{(\overrightarrow{k})})$ we call the first phase of the regeneration period of $Y_i(t)$. Let us define the common regeneration points $\{T_n^{(\overrightarrow{k})}\}_{n=1}^{\infty}$ for $Y_i(t)$ and $X(t)$ with regeneration points $\{\theta_n\}_{n=1}^{\infty}$ as

$$T_n^{(\overrightarrow{k})} = \min\{\theta_l > T_{n-1}^{(\overrightarrow{k})} : \bigcup_{i=1}^{\infty}(t_j^{(\overrightarrow{k})} \le \theta_l < t_j^{(\overrightarrow{k})} + \eta_j^{(\overrightarrow{k})})\}, n = 1, 2, \ldots, \tag{6}$$

$$T_0^{(\overrightarrow{k})} = 0.$$

Lemma 2. *For any state $\overrightarrow{k}$ such that $\mathsf{P}_i(\overrightarrow{k}) > 0$ the sequence $\{T_n^{(\overrightarrow{k})}\}_{n=1}^{\infty}$ consists of regeneration points for the both flows $X(t)$ and $Y_i(t)$ $(i = 1, 2)$ and*

$$\mathsf{E}(T_{n+1}^{(\overrightarrow{k})} - T_n^{(\overrightarrow{k})}) = \alpha(\overrightarrow{k})\delta_{\overrightarrow{k}}\mathsf{E}\tau_1 < \infty, \tag{7}$$

where

$$\delta_{\overrightarrow{k}} = \mathsf{E}(t_{n+1}^{(\overrightarrow{k})} - t_n^{(\overrightarrow{k})}), \quad \mathsf{E}\tau_1 = \mathsf{E}(\theta_{j+1} - \theta_j)$$

and

$$\alpha(\overrightarrow{k}) = \begin{cases} j(\overrightarrow{k})\mu \text{ for } U_1(t) \\ \sum\limits_{i=1}^{j} \mu_{e_i} \text{ for } U_2(t) \end{cases} .$$

Remind that $\overrightarrow{k} = (k_1, \dots, k_j, k_{j+1}) \in \mathcal{K}_1$ for $U_1(t)$ and $\overrightarrow{k} = (k_1, e_1, \dots, k_j, e_j, k_{j+1}) \in \mathcal{K}_2$ for $U_2(t)$.

Proof. The first statement of the Lemma follows from the definition (6) of $T_n^{(\overrightarrow{k})}$. To prove the second statement we note that $\delta_{\overrightarrow{k}} < \infty$ since $\mathsf{P}_i(\overrightarrow{k}) > 0$ and introduce the function

$$h_{\overrightarrow{k}}(t) = \mathsf{P}\left(\bigcup_{l=0}^{\infty}(t \in [t_l^{(\overrightarrow{k})}, t_l^{(\overrightarrow{k})} + \eta_l^{(\overrightarrow{k})}))\right).$$

Let $\beta_{\overrightarrow{k}}(t) = \min(i : t_i^{(\overrightarrow{k})} > t)$ and $H_{\overrightarrow{k}}(t) = \mathsf{E}\beta_{\overrightarrow{k}}(t)$. Then we have

$$h_{\overrightarrow{k}}(t) = \sum_{i=0}^{\infty} \mathsf{P}\left(t - \eta_i^{(\overrightarrow{k})} < t_i^{(\overrightarrow{k})} \le t\right) = \int_0^t e^{-\alpha(\overrightarrow{k})(t-y)} dH_{\overrightarrow{k}}(y). \qquad (8)$$

It follows from the key renewal theorem (see e.g. Thorisson[22]) that there exists

$$\lim_{t\to\infty} h_{\overrightarrow{k}}(t) = \frac{1}{\delta_{\overrightarrow{k}}} \int_0^{\infty} e^{-\alpha(\overrightarrow{k})y} dy = \left(\alpha(\overrightarrow{k})\delta_{\overrightarrow{k}}\right)^{-1}. \qquad (9)$$

Denote

$$\nu_n = \min(i > \nu_{n-1} : \bigcup_{l=1}^{\infty}(\theta_i \in [t_l^{(\overrightarrow{k})}, t_l^{(\overrightarrow{k})} + \eta_l^{(\overrightarrow{k})}))), \quad \nu_0 = 0.$$

Then $\{\nu_{n+1} - \nu_n\}_{n=1}^{\infty}$ is a sequence of iid random variables and $T_n^{(\overrightarrow{k})} = \theta_{\nu_n}$. In accordance with Wald's identity we get

$$\mathsf{E}(T_{n+1}^{(\overrightarrow{k})} - T_n^{(\overrightarrow{k})}) = \mathsf{E}\tau_1 \mathsf{E}(\nu_2 - \nu_1).$$

Therefore we need to prove the finiteness of $\mathsf{E}(\nu_2 - \nu_1)$. Let

$$h(n) = \sum_{l=0}^{\infty} \mathsf{P}(\nu_l = n)$$

so that $h(j)$ is a probability that θ_j is in the first phase of the regeneration period of $Y_i(t)$. From Blackwell's Theorem (see e.g. Thorisson[22]) we have

$$\lim_{n\to\infty} h(n) = \frac{1}{\mathsf{E}(\nu_2 - \nu_1)}$$

if $\mathsf{E}(\nu_2 - \nu_1) < \infty$ and $h(n) \to 0$ otherwise.

On the other hand in accordance with (8)

$$h(n) = \mathsf{P}\left(\bigcup_{l=0}^{\infty}(\theta_n \in [t_l^{(\overrightarrow{k})}, t_l^{(\overrightarrow{k})} + \eta_l^{(\overrightarrow{k})}))\right) =$$

$$= \mathsf{E}h_{\overrightarrow{k}}(\theta_n) = \mathsf{E}\int_0^{\theta_n} e^{-\alpha(\overrightarrow{k})(\theta_n - y)} dH_{\overrightarrow{k}}(y).$$

From (9) and Lebesgue's dominated convergence theorem we obtain

$$\mathsf{E}(\nu_2 - \nu_1) = \alpha(\overrightarrow{k})\delta_{\overrightarrow{k}} < \infty.$$

These concludes the proof of Lemma 2.

For fix $\overrightarrow{k} \in \mathcal{K}_i$ with $P_i(\overrightarrow{k}) > 0 (i = 1, 2)$ we define

$$\Delta_X^{(\overrightarrow{k})}(n) = X(T_{n+1}^{(\overrightarrow{k})}) - X(T_n^{(\overrightarrow{k})}),$$

and

$$\Delta_{Y_i}^{(\overrightarrow{k})}(n) = Y_i(T_{n+1}^{(\overrightarrow{k})}) - Y_i(T_n^{(\overrightarrow{k})})$$

$n = 1, 2, \ldots$. Then $\{\Delta_X^{(\overrightarrow{k})}(n)\}_{n=1}^{\infty}$ and $\{\Delta_{Y_i}^{(\overrightarrow{k})}(n)\}_{n=1}^{\infty}$ are sequences of iid random variables and w.p.1

$$\lambda_X = \lim_{t\to\infty}\frac{X(t)}{t} = \frac{\mathsf{E}\Delta_X^{(\overrightarrow{k})}(1)}{\mathsf{E}(T_2^{(\overrightarrow{k})} - T_1^{(\overrightarrow{k})})},$$

$$\lambda_{Y_i} = \lim_{t\to\infty}\frac{Y_i(t)}{t} = \frac{\mathsf{E}\Delta_{Y_i}^{(\overrightarrow{k})}(1)}{\mathsf{E}(T_2^{(\overrightarrow{k})} - T_1^{(\overrightarrow{k})})}.$$

Therefore the traffic rate defined by (2) can be rewritten as follows

$$\rho_i = \frac{\mathsf{E}\Delta_X^{(\overrightarrow{k})}(1)}{\mathsf{E}\Delta_{Y_i}^{(\overrightarrow{k})}(1)}. \tag{10}$$

Note that it is true for any state $\overrightarrow{k} \in \mathcal{K}_i$ such that $\mathsf{P}_i(\overrightarrow{k}) = \lim_{t\to\infty}\mathsf{P}(U_i(t) = \overrightarrow{k}) > 0 (i = 1, 2)$.

5 Stability criterion

Theorem 1. *Let $Q(t)$ be the number of customers at the system $S_i (i = 1, 2)$ at instant t. Then $Q(t)$ is a stable process if and only if*

$$\rho_i < 1.$$

Remark 1. We call $Q(t)$ a stable process if there is

$$\lim_{t\to\infty} \mathsf{P}(Q(t) \le x) = F(x)$$

and $F(x)$ is a distribution function which does not depend on the initial state of the system.

Proof. Let $\widetilde{Y}_i(t)$ be the number of customers really served in the system during time interval $[0,t)$. Note that any server may be empty time to time and therefore $\widetilde{Y}_i(t)$ is not the same as $Y_i(t)$. Denote $Y_i^{(\overrightarrow{k})}(t)$ the process $Y_i(t)$ under the condition that $U_i(0) = \overrightarrow{k}$, $(\overrightarrow{k} \in \mathcal{K}_i)$. Let $\overrightarrow{k_0}$ be the state of $U_1(t)$ such that $P_1(\overrightarrow{k_0}) > 0$ and $j(\overrightarrow{k_0}) \ge j(\overrightarrow{k})$ for any $\overrightarrow{k} \in \mathcal{K}_1$ with $P_1(\overrightarrow{k}) > 0$. For the process $Y_2^{(\overleftrightarrow{k_0})}(t)$ we additionally assume that $e_i = r$ for all $i = \overline{1, j(\overrightarrow{k_0})}$. It is evident that $\overrightarrow{k_0}$ is an $m+1$ dimensional vector $(1,\dots,1)$ if $p_1 > 0$ for $Y_1^{(\overleftrightarrow{k_0})}(t)$ and $\overrightarrow{k_0} = (1, r, \dots, 1, r, 1)$ for $Y_2^{(\overleftrightarrow{k_0})}(t)$. Then the following stochastic inequality takes place

$$\widetilde{Y}_i(t) \le Y_i^{(\overrightarrow{k_0})}(t) \quad (t \ge 0). \tag{11}$$

Let $\rho_i > 1$. Without loss of generality assume that $Q(0) = 0$. Because of (11) we have

$$\frac{Q(t)}{t} = \frac{X(t)}{t} - \frac{\widetilde{Y}_i(t)}{t} \ge \frac{X(t)}{t} - \frac{Y_i^{(\overrightarrow{k_0})}(t)}{t}.$$

Since $\lambda_X > \lambda_{Y_i}$ this inequality means that $Q(t) \xrightarrow[t\to\infty]{} \infty$ w.p.1. For the case $\rho_i = 1$ note that the stochastic inequality

$$\widetilde{\Delta}_{Y_i}^{(\overrightarrow{k_0})}(n) \le \Delta_{Y_i}^{(\overrightarrow{k_0})}(n) \tag{12}$$

is fulfilled. Here

$$\widetilde{\Delta}_{Y_i}^{(\overrightarrow{k_0})}(n) = \widetilde{Y}_i(T_{n+1}^{(\overrightarrow{k_0})}) - \widetilde{Y}_i(T_n^{(\overrightarrow{k_0})}).$$

For the sake of brevity assume that $T_0^{\overrightarrow{k_0}} = 0$, $\widetilde{Y}_i(0) = 0$. Consider the embedded process

$$Q_n = Q(T_{n+1}^{(\overrightarrow{k_0})}) = \sum_{j=1}^{n} \left(\Delta_X^{(\overrightarrow{k_0})}(j) - \widetilde{\Delta}_{Y_i}^{(\overrightarrow{k_0})}(j) \right).$$

Thus

$$Q_n = Q_{n-1} + \Delta_X^{(\overrightarrow{k_0})}(n) - \widetilde{\Delta}_{Y_i}^{(\overrightarrow{k_0})}(n).$$

We define the auxiliary sequence $\{\widehat{Q}_n\}_{n=1}^{\infty}$ by the recursion

$$\widehat{Q}_n = \widehat{Q}_{n-1} + \Delta_X^{(\overrightarrow{k_0})}(n) - \Delta_{Y_i}^{(\overrightarrow{k_0})}(n)$$

In view of (12) we have the stochastic inequality $\widehat{Q}_n \le Q_n$. Since $\{\widehat{Q}_n\}_{n=1}^{\infty}$ is a random walk with zero drift then w.p.1

$$\sup_{n\ge 0} \widehat{Q}_n \underset{n\to\infty}{\to} \infty. \tag{13}$$

We also note that $Q(t)$ is a regenerative process with the sequence of regeneration points $\{\theta_{n_s}\}_{s=1}^{\infty}$ that is a subsequence of the sequence $\{\theta_n\}_{n=1}^{\infty}$ such that

$$Q(\theta_{n_s} - 0) = 0.$$

It follows from Theorem 1 in Afanaseva, Tkachenko[2] that there are two possible cases: $Q(t)$ is a stable process or $Q(t) \underset{t\to\infty}{\overset{\mathsf{P}}{\to}} \infty$. Because of (13) the second case takes place when $\rho_i = 1$.

Consider the case $\rho_i < 1$. Let $\overrightarrow{k_1}$ be the state $U_1(t)$ such that

$$j(\overrightarrow{k_1}) \le j(\overrightarrow{k})$$

for any $\overrightarrow{k} \in \mathcal{K}_1$ with $\mathsf{P}_1(\overrightarrow{k}) > 0$. For $Y_2^{(\overrightarrow{k_1})}(t)$ we additionally assume that $e_l = 1$ for all $l = \overline{1, j(\overrightarrow{k_1})}$. It is clear that $\overrightarrow{k_1} = (m, m)$ when $p_m > 0$ for $U_1(t)$ and $\overrightarrow{k_1} = (m, 1, m)$ for $U_2(t)$.

Assume that $Q(t)$ is an unstable process. Then in the case under consideration

$$Q(t) \underset{t\to\infty}{\overset{\mathsf{P}}{\to}} \infty. \tag{14}$$

We define the event

$$A_n = \{Q(t) > m \,\text{for any}\, t \in [T_n^{(\overrightarrow{k_1})}; T_n^{(\overrightarrow{k_1})})\}.$$

In view of (14) and finiteness of $\mathsf{E}\Delta_{Y_i}^{(\overrightarrow{k_1})}(n)$ there exists n_δ such that for $n > n_\delta$

$$\mathsf{E}\Delta_{Y_i}^{(\overrightarrow{k_1})}(n)\mathbb{I}(\overline{A_n}) < \delta = \frac{1-\rho}{2\rho}\mathsf{E}\Delta_X^{(\overrightarrow{k_1})}(n). \tag{15}$$

Taking into account the choice $\overrightarrow{k_1}$ and distribution of the service time we have the stochastic inequality

$$\Delta_{Y_i}^{(\overrightarrow{k_1})}(n)\mathbb{I}(A_n) \le \widetilde{\Delta}_{Y_i}^{(\overrightarrow{k_1})}(n)\mathbb{I}(A_n). \tag{16}$$

Now estimate

$$\begin{aligned} Q_{n+1}^{(\overrightarrow{k_1})} = Q(T_n^{(\overrightarrow{k_1})}) = Q_n^{(\overrightarrow{k_1})} + \Delta_X^{(\overrightarrow{k_1})}(n) - \widetilde{\Delta}_{Y_i}^{(\overrightarrow{k_1})}(n) \le \\ \le Q_n^{(\overrightarrow{k_1})} + \Delta_X^{(\overrightarrow{k_1})}(n) - \widetilde{\Delta}_{Y_i}^{(\overrightarrow{k_1})}(n)\mathbb{I}(A_n) \le \\ \le Q_n^{(\overrightarrow{k_1})} + \Delta_X^{(\overrightarrow{k_1})}(n) - \Delta_{Y_i}^{(\overrightarrow{k_1})}(n)\mathbb{I}(A_n) - \Delta_{Y_i}^{(\overrightarrow{k_1})}(n)\mathbb{I}(\overline{A_n}) + \Delta_{Y_i}^{(\overrightarrow{k_1})}(n)\mathbb{I}(\overline{A_n}). \end{aligned}$$

In view of (14) we have for $n > n_\delta$

$$\begin{aligned} \mathsf{E}Q_{n+1}^{(\overrightarrow{k_1})} \le \mathsf{E}Q_n^{(\overrightarrow{k_1})} + \mathsf{E}\Delta_X^{(\overrightarrow{k_1})}(n) - \mathsf{E}\Delta_{Y_i}^{(\overrightarrow{k_1})}(n) + \delta = \\ = \mathsf{E}Q_n^{(\overrightarrow{k_1})} - \frac{1-\rho_i}{\rho_i}\mathsf{E}\Delta_X^{(\overrightarrow{k_1})}(n) + \delta < \mathsf{E}Q_n^{(\overrightarrow{k_1})} \end{aligned}$$

that contradicts (13).

6 Example. Queueing systems with two servers

Here we consider the systems S_1 and S_2 with two servers and two-phase distribution of the service time in S_2. Thus, the service time η in S_2 has a form $\eta = \eta^{(1)} + \eta^{(2)}$ where $\eta^{(1)}$ and $\eta^{(1)}$ are independent exponentially distributed random variables with rates μ_1 and μ_2 respectively. The service time in S_1 has an exponential distribution with the same mean $\mu^{-1} = \frac{1}{\mu_1} + \frac{1}{\mu_2} = \frac{1+\delta}{\mu_2}$ where $\delta = \frac{\mu_2}{\mu_1}$. We shall compare traffic rates for these systems and show that $\rho_2 > \rho_1$ if $0 < \delta < \infty$. For S_1 we get from (5)

$$\rho_1 = \lambda_X \frac{(1+\delta)(2-p_1^2)}{2\mu_2} \tag{17}$$

where $p_1 = \mathsf{P}(\zeta = 1)$.

To obtain ρ_2 we have to calculate the limit distribution $\mathsf{P}_2(\overrightarrow{k}) = \lim\limits_{t\to\infty} \mathsf{P}(U_2(t) = \overrightarrow{k})$. As the state space for $U_2(t)$ we take the set $\mathcal{K}_2 = \{(2, e_1), (1, e_1, 1, e_2), (1, e_1), e_i = 1, 2\}$. The state $(2, e_1)$ means that there is one serving customer which occupies two servers and e_i is the phase of the service time. The interpretation of the residual states is evident. Let us enumerate the states by such a way

$$\{1\} = (2,1); \quad \{2\} = (2,2); \quad \{3\} = (1,1,1,1); \quad \{4\} = (1,2,1,2);$$

$$\{5\} = (1,2,1,1); \quad \{6\} = (1,1); \quad \{7\} = (1,2).$$

Then infinitesimal generator R has a form

$$R = \begin{pmatrix} -\mu_1 & \mu_1 & 0 & 0 & 0 & 0 & 0 \\ (1-p_1)\mu_2 & -\mu_2 & p_1^2\mu_2 & 0 & 0 & p_1(1-p_1)\mu_2 & 0 \\ 0 & 0 & -2\mu_1 & 0 & 2\mu_1 & 0 & 0 \\ 0 & 0 & 0 & -2\mu_2 & 2\mu_2 p_1 & 0 & 2\mu_2(1-p_1) \\ 0 & 0 & \mu_2 p_1 & \mu_1 & -(\mu_1+\mu_2) & (1-p_1)\mu_2 & 0 \\ 0 & 0 & 0 & 0 & 0 & -\mu_1 & \mu_1 \\ (1-p_1)\mu_2 & 0 & p_1^2\mu_2 & 0 & 0 & p_1(1-p_1)\mu_2 & -\mu_2 \end{pmatrix}.$$

Let $x_i = \lim\limits_{t\to\infty} \mathsf{P}(U_2(t) = i)(i = \overline{1,7})$ and $\overrightarrow{x} = (x_1, \ldots, x_7)$. Then we have the system of equations

$$\overrightarrow{x} R = 0, \quad \sum_{i=1}^{7} x_i = 1.$$

One may easy verify that

$$x_1 = \frac{2\delta(1+\delta)(1-p_1)}{(2-p_1^2)(1+2\delta)+2\delta^2}, \quad x_2 = \frac{x_1}{\delta}, \quad x_3 = \frac{(1+\delta-p_1)p_1^2}{2(1+\delta)(1-p_1)}x_1,$$

$$x_4 = \frac{p_1^2}{(1+\delta)(1-p_1)}x_1, \quad x_5 = \frac{p_1^2}{2\delta(1+\delta)(1-p_1)}x_1,$$

$$x_6 = \frac{p_1(1+\delta-p_1)}{1+\delta}x_1, \quad x_7 = \frac{p_1}{\delta}x_1$$

and

$$\lambda_{Y_2} = \mu_2(x_2 + 2x_4 + x_5 + x_7) = 2\mu_2 \frac{1+\delta}{(2-p_1^2)(1+\delta)^2 - p_1^2\delta(1-p_1)}.$$

Therefore, the traffic rate

$$\rho_2 = \rho_1 \left(1 - \frac{\delta p_1^2(1-p_1)}{(2-p_1^2)(1+\delta)^2}\right).$$

We see that ρ_2=ρ_1 in the four cases: 1) $p_1 = 0$; 2) $p_1 = 1$; 3) $\delta = 0$; 4) $\delta = \infty$.

In the first case we have a classical model $Reg|G|2$, in the second case the system $Reg|G|1$ and in the rest cases service time in the system S_2 has an exponential distribution. In the rest cases the traffic rate ρ_2 is less then ρ_1. We also note that $\rho_2(\delta)$ takes the maximum value when $\delta = 1$, that is $\mu_2 = \mu_1$.

7 Concluding comments

In this paper, a multiserver queueing system in which each customer requires a random number of servers simultaneously and a random but identical service time at all occupied servers is considered. The input flow is assumed to be regenerative one and service time has an exponential or a phase-type distribution. By means of the synchronization method we establish stability criterion of such systems. The main contribution of this paper is an extension of the stability criterion to the model with a regenerative input flow. Note that the class of regenerative flows is broad and includes MAP, doubly stochastic Poisson process with a regenerative process as intensity, MMP, and others. It turns out that the stability condition depends only on the intensity of the input flow and the structure of this flow does not play any role. The flow has to be regenerative with finite means of the regeneration period and the number of customers arrived during this period.

But the distribution of the service time plays the important role in stability condition. We give an example which shows that stability condition can not be expresses in terms of the mean of the service time.

Aknowlegement. Work is partially supported by RFBR grant 17-01-00468.

References

1. L.G.Afanasyeva, E.E. Bashtova Coupling method for asymptotic analysis of queues with regenerative input and unreliable server. *Queueing Systems*, 76, 2, 125–147, 2014.
2. L.Afanasyeva, A.Tkachenko Multichannel queueing systems with regenerative input flow *Theory of Probability and Its Applications*, 58, 2, 174–192, 2014.
3. S.Asmussen *Applied Probability and Queues*, **51**, Springer-Verlag. 2003.
4. A.A.Borovkov *Stochastic Processes in Queueing Theory*, **4**, Springer-Verlag. 1976.
5. P.Brill, L.Green. Queues in which customers receive simultaneous service from a random number of servers: A system point approach. *Management Science*, 30, 1, 51–68, 1984.

6. P.Brill and L.Green. Queues in which customers receive simultaneous service from a random number of servers: a system point approach. *Management Science*, 30,1,51–58,1984.
7. L.Gillent, G.Latouche. Semi-explicit solutions for $M|PH|1$-like queueing systems. *European Journal of Operations Research*, 13, 2, 151–160, 1983.
8. J.Grandell *Double Stochastic Poisson Process*,Lect.Notes.Math., **529**, Springer, Berlin 1976.
9. L.Green. Comparing operating characteristics of queues in which customers require a random number of servers. *Management Science*, 27, 1, 65–74, 1980.
10. L.Green. Comparing operating characteristics of queues in which customers require a random number of servers. *Operations Research*, 28, 6, 1335–1346, 1980.
11. A.Federgruen, L.Green. An $M|G|c$ queue in which the number of servers required is random. *Journal of Applied Probability*, 21, 3, 583, 1984.
12. G.Y.Fletcher, H.Perros, D.Stewart A queueing system where customers require a random number of servers simultaneously. *European Journal of Operations Research*, 23, 331–342, 1986.
13. P.Ittimakin, E.P.C.Kao. Stationary waiting time distribution of a queue in which customers require a random number of servers. *Operations Research*, 39, 4, 633–638, 1991.
14. S.Kim *$M|M|s$ queueing system where customers demand multiple server use.*, Ph.D.Thesis, Southern Methodist University. 1979.
15. E.Morozov, A.Rumyantsev. Stability Analysis of a $MAP|M|s$ Cluster model by Matrix-Analytic Method. *European Workshop on Performance Engineering*, 63-76, 2016.
16. M.F.Neuts. Probability distributions of phase-type. *Liber Amicorum Prof. Emeritus H. Florin (Universite de Louvain, Belgium)*, 173–206, 1975.
17. M.F.Neuts. Renewal processes of phase-type. *Naval Res. Logist. Quart.*, 25, 445–454, 1978.
18. M.F.Neuts. Matrix-geometric solution in Stochastic Models. An Algoritmic Approach. *The Johns Hopkins University Press. Baltimore*, 1981.
19. A.Rumyantsev, E.Morozov. Stability criterion of a multi-server model with simultaneous service. *Annals of Operations Research*, 1-11, 2015.
20. G.Schaack, R.C.Larson. An N server cutoff priority queue where arriving customers request a random number of servers. *Management Science*, 35, 5, 614–634, 1989.
21. A.F.Seila. On waiting times for a queue in which customers require simultaneous service from a random number of servers. *Operations Research*, 32, 5, 614–639, 1984.
22. H.Thorisson *Coupling, Stationary and Regeneration*, Springer, New York. 2000.
23. N.M. Van Dyk. Blocking of finite inputs which require simultaneous servers with general think and holding times *Operation Research Letters*, 8, 1, 45–52, 1989.
24. W.Whitt. Blocking when service is required from several facilities simultaneously. *AT and T Technical Journal*, 64,8, 1807-1856 1985.

The Problem of the SARIMA Model Selection for the Forecasting Purpose

Josef Arlt, Peter Trcka, and Markéta Arltová

Department of Statistics and Probability, Faculty Informatics and Statistics, University of Economics, Prague, nám. W. Churchilla 4, 130 67 Prague 3, Czech Republic
(E-mail: arlt@vse.cz, trcp00@vse.cz, arltova@vse.cz)

Abstract: The goal of the work is the study of the ability to choose the proper models for the time series generated by SARIMA processes with different parameter values and to analyze the accuracy of the forecasts based on the selected models. The work is based on the simulation study. For this purpose a new automatic SARIMA modelling method is proposed and used. Also the other competing automatic SARIMA modelling procedures are applied and the results are compared. The important question to which the reference should be made is the relation of the magnitude of the SARIMA process parameters i. e. the size of the systematic part of the process and the ability to select a proper model. Another addressed problem is the relationship between the quality of the selected model and the accuracy of forecasts achieved by its application. The simulation study leads to the results that can be generalized to most empirical analyses in various research areas.
Keyword: SARIMA, forecast, simulation, automatic identification

1 Introduction

The principle of the SARIMA time series modeling has been well known for many years. Its practical applications can be found in many areas where empirical analyses are needed and it has become the basis for modern econometric analysis of time series. The crucial phase of the practical application of the Box-Jenkins methodology is the identification and the verification of the suitable model. There are two approaches to the process of finding a suitable SARIMA model. The first, classical "manual" approach is difficult and subjective, and it depends on the person who has built the model. Important is the knowledge of the method, as well as training in empirical statistical analysis and good knowledge of the field of application in addition to experience of using specialized statistical or econometric software. The development of the computer technology and software, these are the main

17th *ASMDA Conference Proceedings, 6 - 9 June 2017, London, UK*

reasons which justified the attempts to develop the second, automatic SARIMA modelling and forecasting approach.

The goal of this article is to identify the time series for which it is relatively easy to find the proper model and the time series for which it is difficult, regardless of which approach, manual or automatic, is chosen. Another goal is to analyze the forecasting abilities of the SARIMA models for different kinds of time series. A convenient way to verify the aforementioned is the simulation study with the application of the automatic SARIMA modelling approach.

The article is divided into four sections (excluding the Introduction). In the first section the SARIMA models are briefly described. In the second section, the simulation study as well as the Auto.SARIMA and Auto.AIC procedures for the automatic model selection are explained. The results of the simulation study are the subject of the third section. The fourth section contains the conclusion, along with the summary of the work.

2 SARIMA Modeling and Forecasting

The ARMA(p, q) proces (Auto-Regressive-Moving-Average proces of orderes p, q) is defined as $\phi(B)y_t = c + \theta(B)a_t$, where B ($B^{\,j}y_t = y_{t-j}$) is the backshift operator and $\phi(B)$ and $\theta(B)$ are the polynomials of the order p and q respectively. It is stationary, if the roots of the autoregressive polynomial $\phi(B)$ lie outside of the unit circle and it is invertible if the roots of the moving average polynomial $\theta(B)$ lie outside of the unit circle.

The SARMA(p, q)(P, Q) proces (Seasonal ARMA process of orders p, q, P, Q) can be written in the form $\phi(B)\Phi(B^s)y_t = c + \theta(B)\Theta(B^s)a_t$, where s is the number of seasons (usually 4 or 12) and $\Phi(B^s)$ and $\Theta(B^s)$ are seasonal polynomials of the order P and Q respectively. It is denoted as SARMA(p,q)(P,Q). If the roots of all polynomials lie outside of the unit circle, the proces is stationary and invertible.

The special form of the nonstationary proces is the so called integrated process („I“ in acronym). Such a proces is stationary after some degree of differencing. The SARIMA(p,d,q)(P,D,Q) proces is the general form of the integrated proces and can be written as $\phi(B)\Phi(B^s)\Delta^d\Delta_s^{\,D}y_t = c + \theta(B)\Theta(B^s)a_t$, where $\Delta^d = (1 - B)^d$ is the nonseasonal difference of the order d and $\Delta_s^{\,D} = (1 - B^s)^D$ is the seasonal difference of the order D.

The forecasting of the future values of the time series is an important role of the SARIMA modelling. The optimal forecast, i. e., the forecast with the minimum mean square error, is the conditional mean of the future random variable, which is conditioned on the historical information available in the observed values of the applied time series. The computing of the SARIMA forecasts is based on the recursive principle. If the model with the estimated parameters is used, the recursion leads to the point, and to the interval forecasts

(the point and the interval estimates of the conditional means of the future random variables).

The SARIMA time series modelling methodology has been well known for many years and there exists a vast amount literature devoted to this topic, *inter alia*, Box, Jenkins, Reinsel and Ljung [2], Brockwell and Davis [3], Wei [16], Hamilton [8], Enders [6], Pesaran [14].

Simulation study

The goal of the simulation study is to analyze the relationship of the magnitude of the SARIMA process parameters; i. e., the size of the systematic part of the process, which is used for time series generation and the ability to select the proper model for the generated time series. This question is general in scope, and the qualified and substantiated answers can be important for the empirical analyses in the different fields of the research. Another goal is to analyze the quality of the forecasts for the time series generated by the processes with different systematic parts. Important is also the analysis of the ability to select suitable model and reach the relatively accurate forecasts for the time series generated by the near nonstationary and the nonstationary processes.

In the simulation study the results of the two automatic procedures for SARIMA model selection and forecasting are compared. The first one is based on the classic model selection process, i.e. the model identification, the parameters estimation, the diagnostic controll. The second one is based on the minimazitation of the AIC criterion (Akaike [1]). Both procedures were created in the R software.

3.1 Procedure Auto.SARIMA

The Auto.SARIMA is fully automated procedure, whose goal is to find the best model with respect to predefined parameters for the analyzed time series. In the first stage, the order of the nonseasonal and the seasonal differencing i. e. the numbers d and D, after which the analyzed time series is stationary, has been found. For the nonseasonal unit root testing, the ADF (Dickey and Fuller [5]), the PP (Phillips and Perron [15]) and the KPSS (Kwiatovski, Phillips, Schmidt and Shin [11]) tests are used. The seasonal unit root is tested by the CH (Canova and Hansen [4]) test.

The procedure will analyze the quality of the SARIMA(p,d,q)(P,D,Q) models for the given order of the nonseasonal differencing d, as well as the seasonal differencing D, and for all possible combinations of values p, q, P, Q. It is therefore possible to skip the identification stage and to estimate the parameters for all the possible model forms. After the parameters estimation, the procedure continues with the diagnostic checking, which is mainly based on residual analysis. The statistical significance of the parameter estimates is verified by the standard t-tests. The autocorrelation is assessed by the residual

autocorrelation function, and the Ljung-Box test (Ljung and Box [12]). In order to test the seasonal autocorrelation, the heuristic function called the Big_ACF was designed, which is in the fact the modification of the statistical tolerance limits. The conditional heteroscedasticity is tested by the ARCH test (Engle [7]). The normality is tested by the Jarque-Bera test (Jarque and Bera [10]).

If the parameter estimates are statistically significant and the hypotheses of no autocorrelation, no conditional heteroscedasticity and normality are accepted, than the value 1 is assigned to the particular property (autocorrelation, heteroscedasticity, normality, parameter significance). Otherwise, the value 0 is assigned. The suitability criterion of the model is computed as the weighted average of the results of the individual tests. The weighting system is set so that the two models with the different test results have to have different values of suitability criterion. The final value of each model is computed as a function of the value of the model suitability criterion and the value of the AIC criterion.

3.2 Procedure Auto.AIC

The model selection on the basis of the AIC criterion is the content of the Auto.AIC procedure. The course of the procedure can be divided into four steps. In the first step, the stationarity of the time series is analyzed. The order of differencing is determined by the same methods as in the Auto.SARIMA procedure (see part 3.1). After the determination of the order of differencing and on the basis of the SARIMA model maximal orders, the set of the possible models is generated. Furthermore, the optimization criterion is set to such value which the AIC criterion cannot reach. In the third step, adjustments are made so that all the models lead to the same number of residuals. On the basis of the adjusted time series, the model parameters are estimated, and the value of the AIC criterion is computed. In the following step, the actual value of the AIC criterion is compared with the value of the optimalization criterion. If the model is better that the last one, i. e. if its value of the AIC criterion is smaller than the value of the optimalization criterion, than it is denoted as the optimal and the value of the optimization criterion is updated. Thus, there are checked the whole set of possible models.

3.3 Data generation

In the simulation study, the time series generated by the SARIMA proces of the first order are analyzed. This process has the following form

$$(1 - \phi_1 B)(1 - \Phi_1 B^{12}) y_t = (1 - \theta_1 B)(1 - \Theta_1 B^{12}) a_t.$$

The basic elements for the simulations are the time series generated by the normal white noise process with the variance $\sigma_a^2 = 1$. The parameters ϕ_1, θ_1, Φ_1, Θ_1 take the all possible combinations of the following values: 0.0, 0.1, 0.2, 0.3, 0.4, 0.5, 0.6, 0.7, 0.8, 0.9, 1.0. When $\phi_1 = 1$, the process is nonseasonally nonstationary, when $\Phi_1 = 1$, the process is seasonally nonstationary, when $\phi_1 = 1$ and $\Phi_1 = 1$, the process is both non-seasonally and seasonally

nonstationary. When $\theta_1 = 1$, the process is seasonally noninvertible, when $\Theta_1 = 1$, it is seasonally noninvertible or both, when $\theta_1 = 1$ and $\Theta_1 = 1$. Overall, the time series from 14 641 different generating processes are analyzed. Each process generates 100 time series with a length of 150 values. The time series generator was created in the R software.

4 Results

The results of the simulation study are presented in a two-dimensional spece, whose structure is shown in Table 1. The rows of table represent an ordered combination of values of the seasonal parameters Φ_1 and Θ_1 and the columns of table represent an ordered combination of values of the nonseasonal parameters ϕ_1 and θ_1. In this way the whole set of the all possible generating processes is arranged.

The table is conditionally formatted to be able to visually evaluate the results and the success of the individual automatic procedures when comparing their ability to find a suitable model. This feature is referred to as the quality criterion. The quality criterion can take the values in the interval from 0 to 100 and it represents the percentage success rate of the selection of the correct model by the given procedure.

The forecasts are computed as the point estimates of the conditional expectations of the future random variables. The analyzed time series with a length of 150 values, which is about 24 observations longer than the series used for model selection, is the input of this function. In the first step, the forecasts with the horizon $h = 24$ values are computed on the basis of the model estimated from the first 126 values. In the second step, the RMSE criterion is computed. The resulting RMSE value is computed as the average from the all partial RMSE values of 100 time series forecasts with a horizon of 24 values. This criterion is presented in the same way as the quality criterion.

Tab. 1. The Detail of Arrangement of Values in Table

	A	B	C	D	E	F	G
1							
2		XX	AR	0	0	0	0
3		SAR	SMA/MA	0	0.1	0.2	0.3
4		0	0	0.937542	0.93019	0.919874	0.919377
5		0	0.1	0.904717	0.767206	0.898254	0.902059
6		0	0.2	0.877652	0.861469	0.859324	0.863639
7		0	0.3	0.81858	0.823727	0.831057	0.808163
8		0	0.4	0.776119	0.783348	0.778838	0.760929
9		0	0.5	0.723514	0.730076	0.741064	0.748346
10		0	0.6	0.691472	0.708557	0.692079	0.684466
11		0	0.7	0.672497	0.6694	0.661066	0.685954
12		0	0.8	0.648874	0.659905	0.667023	0.652519
13		0	0.9	0.644479	0.62838	0.648453	0.642565
14		0	1	0.629243	0.639511	0.637589	0.627531
15		0.1	0	0.914029	0.897469	0.898585	0.898266
16		0.1	0.1	0.868774	0.861418	0.872823	0.861606

Source: own calculations

4.1 Quality of the selected model

First, in the simulation study, the Auto.SARIMA and the Auto.AIC procedures were compared from the point of view of the quality criterion. The results with the percentage quantifications are shown in Figure 1.

It is seen that the Auto.AIC is better than the Auto.SARIMA in 75.38% of cases. The Auto.SARIMA achieves better results in 23.03% of cases. Identical results are found in 1.58% of cases. But it is clear that there is a general group of the generating processes for which the Auto.SARIMA is better than the Auto.AIC. They are mainly the seasonal and the non-seasonal non-stationary (integrated) processes, and those processes that do not contain the non-seasonal and the seasonal autoregressive parts (AR respectively SAR). Furthermore, this procedure is superior to the processes that partly do not contain the nonseasonal and the seasonal moving average parts (MA, SMA). All these processes can be denoted as marginal. The results show that, mainly there, the "classical" model identification analysis represented by the Auto.SARIMA procedure (unit root testing, residual autocorrelation testing, normality and conditional heteroscedasticity testing and parameters estimate testing) has considerable importance.

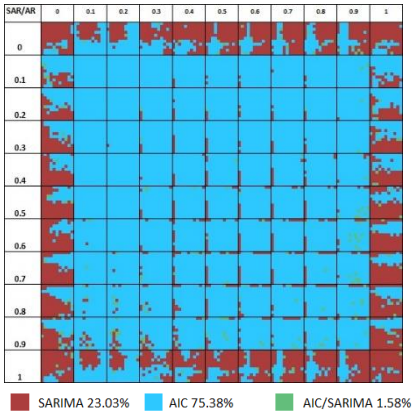

Fig. 1. Quality Comparison of AIC, SARIMA

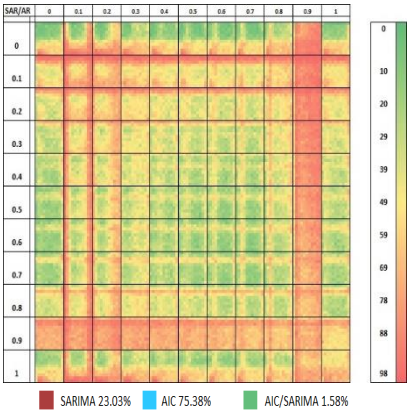

Fig. 2: The Quality – Auto.SARIMA

Source: own calculations

The Figure 2 shows the quality criterion (the percentage of the correct model selections) for the Auto.SARIMA procedure. It can be seen that this procedure has problems with the near nonseasonal and the near seasonal nonstationary processes; i. e., for the processes with the parameters $\phi_1 = 0.9$ and $\Phi_1 = 0.9$. In the first case, the success rate is 29.05%, and in the second it is 22.49%. The processes with the low values of the parameters; i. e., when the parameters ϕ_1 and Φ_1 lie between 0.1 and 0.2 together with the parameters θ_1, and Θ_1 between 0 and 0.2, while on the contrary, the seasonally nonstationary processes, when $\Phi_1 = 1$, create more problem areas. For the proceses with parameters ϕ_1 and Φ_1 between 0.3 and 0.7, the Auto.SARIMA gives good results regardless of the

values of θ_1 and Θ_1. The success rate in this area is 66.14%. The average overall success rate of this procedure is 50.64%.

Figure 3 shows the quality criterion for the Auto.AIC procedure. Also, this procedure has problems with the near nonseasonal and the near seasonal nonstationary processes. In the case of $\phi_1 = 0.9$, the success rate is 37.76%, and when $\Phi_1 = 0.9$, the rate is 34.03%. The problematic areas are also for $\phi_1 = 0$ and $\phi_1 = 1$, and $\Phi_1 = 0$ and $\Phi_1 = 1$, together with practically any values of parameters θ_1 and Θ_1. For the processes with parameters ϕ_1 and Φ_1 between 0.1 and 0.8, the Auto.AIC gives good results regardless of the values of θ_1 and Θ_1. The success rate in this area is 82.75%. The average overall success rate of this procedure is 66.68%. In comparison with the Auto.SARIMA, the Auto.AIC procedure is better.

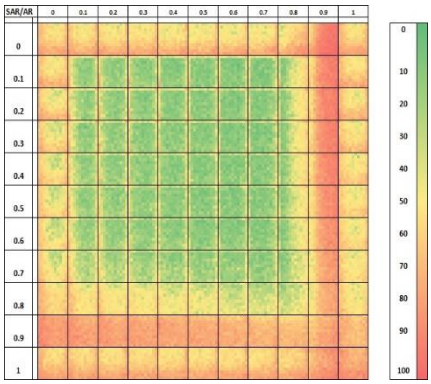

Fig. 3. The Quality – Auto.AIC

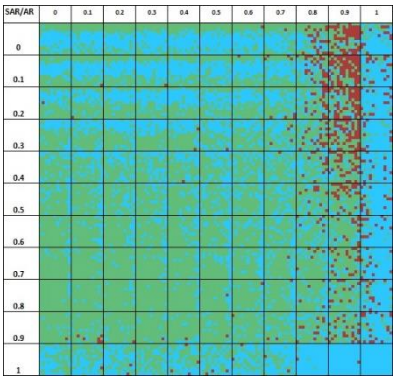

Fig. 4. RMSE – 1% tolerance

Source: own calculations

4.2 Forecasts

The forecasts RMSE criterion is presented in the same way as the quality criterion. For each generating process, the procedure, which gives the the minimal value of the forecast RMSE, has been selected.

As the differences in the RMSE for the Auto.AIC and the Auto.SARIMA procedures are often very small, and the forecasts are very similar, it is suitable to compare them based on the tolerance limit of 1.0%. It means that the forecasts which are different in the RMSE up to 1.0% will be considered to be the same. Figure 4 ilustrates the results according which that the Auto.SARIMA procedure gives the best forecasts in 5.02% of cases; the Auto.AIC in 36.66% cases. There are similar forecasts by both procedures in 58.32% cases. The Auto.AIC is better mainly for the nonseasonally nonstationary processes and the Auto.SARIMA for the near nonseasonally nonstationary processes.

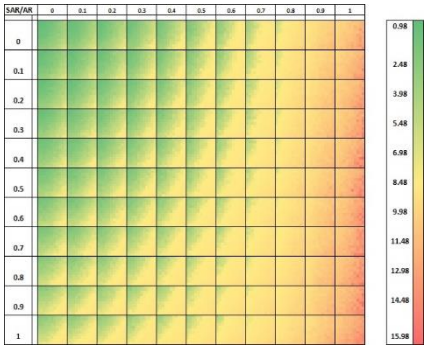

Fig. 5: RMSE - Auto.AIC

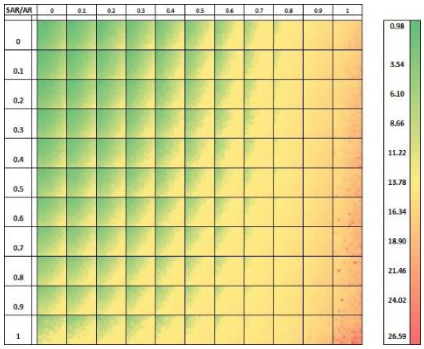

Fig 6: RMSE – Auto.SARIMA

Source: own calculations

Figure 5 shows the RMSE of the forecasts computed by the Auto.AIC procedure for the individual processes. It can be seen that along with the growing parameter values, the RMSE grows also. The best results are either for the processes with zero, or small, values of the parameters. The worst results are for the nonseasonal nonstationary processes. It is interesting that the seasonal nonstationarity does not have such a strong influence on the forecasts from the RMSE like the nonseasonal nonstationarity. Figure 6 contains the RMSE of the forecasts computed by the Auto.SARIMA. The pattern is similar to that in Fig. 5.

4.3 Forecasting of the nearly integrated time series

Figure 7 depicts the forecasting success of the nonseasonal integrated model of the SARIMA(0,1,1)(1,0,1) type for the integrated and nearly integrated, but still stationary, processes, irrespective of the forecasting procedure. It can be seen that even for the non-seasonally stationary processes with ϕ_1 from 0.90 to 0.95, the integrated model is more suitable for forecasting than the correct stationary model. This result is consistent with the result for the example of Medel and Pincheira [13]. The possible explanation is that the estimates of the parameters of the correct models for the time series generated by the nearly nonstationary processes have greater variability and are thus less accurate.

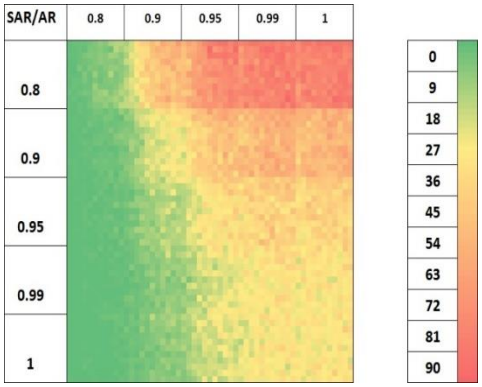

Fig. 7: The Forecasting Success of SARIMA(0,1,1)(1,0,1)
Source: own calculations

5 Conclusion

The goal of the simulation study was to analyze the relationship of the size of the systematic part of the process, which is used for time series generation and the ability to select the proper model for the generated time series. The second goal was to analyze the quality of the forecasts for the time series generated by the processes with different systematic parts. In this connection it was important also the analysis of the ability to select suitable model and reach the relatively accurate forecasts for the time series generated by the near nonstationary and the nonstationary processes.

As a results of the simulation study, these interesting facts have been found:

1. The Auto.AIC procedure is better for the selection of models for the time series generated by the stationary and invertibe processes. The Auto.SARIMA procedure is better for the modelling the time series from so called marginal processes; i. e., mainly from the nonstationary processes and the processes that do not contain the non-seasonal and the seasonal autoregressive parts.
2. For both procedures it is difficult to find the correct model for the time series generated by processes with low values of the autoregressive parameters, and by the near nonstationary processes. In the first case, the systematic part in the data is very weak and the property which we are looking for does not show sufficient transparency, so it is possible to overlook it. In the second case, the two different and incompatible situations have the same, or very similar phenomanal effects, so it is difficult to distinguish between them.
3. The Auto.AIC procedure leads to the better forecasts, but for near to nonstationary processes the Auto.SARIMA procedure is more suitable. The differences in accuracy between the Auto.SARIMA and Auto.AIC procedures are relatively small. With the growing magnitude of parameters, the accuracy of forecasts decreases in both procedures.

4. For the forecasting of the time series generated by the nonseasonally nearly integrated processes, the nonseasonally integrated models are more suitable than the correct stationary ones.

Acknowledgement

This paper was written with the support of the Czech Science Foundation project No. P402/12/G097 *DYME - Dynamic Models in Economics*.

References

1. H. Akaike. A new look at the statistical model identification", IEEE Transactions on Automatic Control, 19 (6): 716–723, 1974.
2. G. E. P. Box, G. M. Jenkins, G. C. Reinsel, and.G. M. Ljung. Time Series Analysis: Forecasting and Control, Wiley 2015.
3. P. J. Brockwell, and R. A. Davis. Introduction to Time Series and Forecasting, Springer, 2010.
4. F. Canova, and B. E. Hansen. Are Seasonal Patterns Constant Over Time? A Test for Seasonal Stability, Journal of Business and Economic Statistics, 13, 237-252, 1995.
5. D. A. Dickey, and W. A. Fuller. Distribution of the Estimators for Autoregressive Time Series with a Unit Root, Journal of the American Stat. Association 74, 427-431, 1979.
6. W. Enders. Applied Econometric Time Series, Wiley 2014.
7. R. Engle. Autoregressive conditional heteroscedasticity with estimates of the variance of UK inflation, Econometrica, 50, 987–1008, 1982.
8. J. D. Hamilton. Time Series Analysis, Princeton University Press, (1994).
9. E. J. Hannan, and B. G. Quinn. The Determination of the Order of an Autoregression, Journal of Royal Statistical Society, 41, 190 – 195, 1978.
10. C. Jarque, and A. Bera.: Efficient Tests for Normality, Heteroscedasticity, and Serial Independence of Regression Residuals, Economics Letters 6, 255-259, 1980.
11. D. Kwiatovski, P. C. B. Phillips, P. Schmidt, and Y. Shin. Testing the Null Hypothesis of Stationarity Against the Alternative of a Unit Root, Journal of Econometrics, 54, 159-178, 1992.
12. G. M. Ljung, and G. E. P. Box. On a Measure of Lack of Fit in Time Series Models, Biometrika 65, 297-303, 1978.
13. M. H. Pesaran.: Time Series and Panel Data Econometrics, Oxford University Press, 2015.

14. P. C. B. Phillips, and P. Perron. Testing for a Unit Root in Time Series Regression, Biometrika 75, 335-346, 1988.
15. C. A. Medel and P. M. Pincheira. The out-of-sample performance of an exact median-unbiased estimator for the near-unity AR(1) model," Applied Economics Letters, vol. 23(2), pages 126-131, 2016.
16. W. W. S. Wei. Time Series Analysis : Univariate and Multivariate Methods (2nd Edition), 2005.

The Extended Flexible Dirichlet model: a simulation study

Roberto Ascari[1], Sonia Migliorati[2], and Andrea Ongaro[2]

[1] Department of Statistics and Quantitative Methods (DISMEQ) Via Bicocca degli Arcimboldi, 8, Università di Milano-Bicocca, Milano, Italy
(E-mail: r.ascari@campus.unimib.it)
[2] Department of Economics, Management and Statistics (DEMS) P.zza dell'Ateneo Nuovo, 1, Università di Milano-Bicocca, Milano, Italy
(E-mail: sonia.migliorati@unimib.it; andrea.ongaro@unimib.it)

Abstract. Compositional data are prevalent in many fields (e.g. environmetrics, economics, biology, etc.). They are composed by positive vectors subject to a unit-sum constraint (i.e. they are defined on the *simplex*), proportions being an example of this kind of data. A very common distribution on the simplex is the Dirichlet, but its poor parametrization and its inability to model many dependence concepts make it unsatisfactory for modeling compositional data. A feasible alternative to the Dirichlet distribution is the Flexible Dirichlet (FD), introduced by Ongaro and Migliorati [14]. The FD is a generalization of the Dirichlet that enables considerable flexibility in modeling dependence as well as various independence concepts, though retaining many good mathematical properties of the Dirichlet. More recently, the Extended Flexible Dirichlet (EFD, [15]) distribution has been proposed in order to generalize the FD. The EFD preserves a finite mixture structure as the FD, but it exhibits some relevant advantages over the FD, such as a more flexible cluster structure and a (even strong) positive dependence for some pairs of variables. The aim of this contribution is twofold. First we propose and investigate sophisticated EM algorithms for parameters estimation, with particular emphasis on the initialization problem, which is a crucial issue. Furthermore, we devise a simulation study to evaluate the performances of the MLE of the parameters as well as of a procedure proposed to compute their standard errors.
Keywords: Compositional Data, Dirichlet Mixture, EM algorithm.

1 Introduction

In many fields (e.g. environmetrics, economics, biology, etc.) data consist of vector of proportions and thus are constrained to unit-sum and non-negative constraints. Their support is the simplex, defined as:

$$\mathcal{S}^D = \left\{ \mathbf{x} \in \mathbb{R}^D : x_i > 0, \;\; i = 1, \ldots, D, \;\; \sum_{i=1}^{D} x_i = 1 \right\}.$$

In order to model these "compositional data", an appropriate distribution built on this particular subset of $\mathbb{R}^D$ is required. The Dirichlet is the most known simplex distribution: it has several mathematical properties and it is characterized by an intuitive interpretation of parameters, but it is often unsatisfactory

in fitting real compositional data due to its poor parametrization and its implied strict forms of independence.

In the literature there are different proposals for managing such type of data [1,2,7,10,11,16]. Recently Ongaro and Migliorati [14] proposed a new probabilistic model, called Flexible Dirichlet (FD). This model not only preserves the properties of the Dirichlet distribution, but it also enables considerable flexibility in modeling covariance among components of the composition. A useful particularity of the FD is that it can be represented as a finite mixture of specific Dirichlet distributions; it follows that this new model allows for multimodality. A generalization of the FD was introduced recently, namely the Extended Flexible Dirichlet (EFD) [15]. This new simplex distribution allows for positive dependence among components of the composition and it removes the symmetry constraints on the cluster means displayed by the FD.

Some inferential issues in the EFD model have already been tackled in [12], where a standard EM estimation procedure has been adopted. In the current paper, we propose new ad hoc initialization strategies for the EM algorithm and we introduce a stochastic version of the EM procedure aimed at weakening the dependence of the maxima on the starting points. The performances of these estimation procedures are evaluated via simulation. Furthermore, we provide an efficient procedure to derive MLE standard errors. A further simulation study has been implemented in order to assess the behavior of MLE and of the proposed standard errors under different settings of parameters and different configurations of clusters.

2 The Flexible Dirichlet Distribution

The Flexible Dirichlet distribution derives from the normalization of a particular basis $\mathbf{Y} = (Y_1, \ldots, Y_D)$. Each element of this vector is obtained as:

$$Y_i = W_i + Z_i U \qquad\qquad i = 1, \ldots, D,$$

where $W_i \sim \text{Gamma}(\alpha_i, \beta)$ are independent r.v., $U \sim \text{Gamma}(\tau, \beta)$ is an additional independent r.v. and $\mathbf{Z} = (Z_1, \ldots, Z_D) \sim \text{Multinomial}(1, \mathbf{p})$ is independent of W_i's and U. A realization of $\mathbf{Z}$ is the vector $\mathbf{e}_i$ with probability p_i, where $\mathbf{e}_i$ is the vector whose elements are equal to 0 except for the i^{th} element which is equal to 1. Then, the normalized vector $\mathbf{X} = \mathbf{Y}/Y^+$ is FD distributed and its density function is:

$$f_{FD}(\mathbf{x}; \boldsymbol{\alpha}, \tau, \mathbf{p}) = \frac{\Gamma(\alpha^+ + \tau)}{\prod_{r=1}^{D} \Gamma(\alpha_r)} \left(\prod_{r=1}^{D} x_r^{\alpha_r - 1} \right) \sum_{i=1}^{D} p_i \frac{\Gamma(\alpha_i)}{\Gamma(\alpha_i + \tau)} x_i^{\tau},$$

where $\mathbf{x} \in \mathcal{S}^D = \left\{ \mathbf{x} : x_i > 0, i = 1, \ldots, D, \sum_{i=1}^{D} x_i = 1 \right\}$, $\alpha^+ = \sum_{i=1}^{D} \alpha_i$, $\boldsymbol{\alpha} = (\alpha_1, \ldots, \alpha_D)$, $\alpha_i > 0$, $\tau > 0$, $0 \leq p_i < 1$ and $\sum_{i=1}^{D} p_i = 1$. An attractive aspect of the FD is that its distribution function can be written as a finite mixture, where each cluster is characterized by a particular Dirichlet component:

$$FD(\mathbf{x}; \boldsymbol{\alpha}, \tau, \mathbf{p}) = \sum_{i=1}^{D} p_i \mathcal{D}(\mathbf{x}; \boldsymbol{\alpha}_i),$$

where $\mathcal{D}(\mathbf{x};\boldsymbol{\alpha})$ is the distribution function of a D-dimensional Dirichlet with parameter $\boldsymbol{\alpha}$ and $\boldsymbol{\alpha}_i = \boldsymbol{\alpha}+\tau\mathbf{e}_i$. It follows that the density of the FD can assume various shapes, including a number $k \leq D$ of different modes. The parameter τ regulates the distance of each cluster mean from the common barycenter $\boldsymbol{\alpha}/\alpha^+$. Since all the cluster means have the same distance from the barycenter, the density function of the FD shows a sort of symmetry. It can be proved that the FD coincides with a Dirichlet distribution if $\tau = 1$ and $p_i = \alpha_i/\alpha^+$, $\forall i = 1,\ldots,D$.

Finally, the additional parameters introduced in this model (i.e. the weights $\mathbf{p}$ and τ) allow for a more flexible modeling of the covariance matrix. In particular, unlike the Dirichlet, it allows to have components with equal means but different variances. Moreover, covariances may not be proportional to the product of the means. However, all the covariances are negative: this is partly due to the unit-sum constraint but it may be a limitation in real data problems where positive correlation between some of the components occurs.

3 The Extended Flexible Dirichlet Distribution

A further generalization of the FD has been introduced in order to relax the independence/dependence assumptions induced by the Dirichlet model: the Extended Flexible Dirichlet (EFD). This new model is generated by the normalization of a basis that is similar to the FD's one:

$$Y_i = W_i + Z_i\, U_i,$$

where $U_i \sim \text{Gamma}(\tau_i, \beta)$ are independent random variables and independent of $\mathbf{W} = (W_1,\ldots,W_D)$ and $\mathbf{Z} = (Z_1,\ldots,Z_D)$, which are defined as in the FD. The new vector $\boldsymbol{\tau} = (\tau_1,\ldots,\tau_D)$ is composed by positive elements. It is immediately observable that when $\tau_1 = \tau_2 = \cdots = \tau_D = \tau$, the EFD coincides with the FD. Once again, the distribution function of this random vector can be written as mixture of Dirichlet components:

$$EFD(\mathbf{x};\boldsymbol{\alpha},\boldsymbol{\tau},\mathbf{p}) = \sum_{i=1}^{D} p_i \mathcal{D}(\mathbf{x};\boldsymbol{\alpha}_i),$$

where $\boldsymbol{\alpha}_i = \boldsymbol{\alpha} + \tau_i\mathbf{e}_i$. This finite mixture structure leads to the following mixture density function:

$$f_{EFD}(\mathbf{x};\boldsymbol{\alpha},\boldsymbol{\tau},\mathbf{p}) = \frac{1}{\prod_{r=1}^{D}\Gamma(\alpha_r)}\left(\prod_{r=1}^{D} x_r^{\alpha_r-1}\right)\sum_{i=1}^{D}\frac{\Gamma(\alpha_i)\Gamma(\alpha^+ + \tau_i)}{\Gamma(\alpha_i+\tau_i)}x_i^{\tau_i}p_i.$$

Thanks to the mixture representation, it is straightforward to compute joint moments of the EFD:

$$\mathbb{E}\left[\prod_{i=1}^{D} X_i^{n_i}\right] = \prod_{i=1}^{D}\alpha_i^{[n_i]}\sum_{i=1}^{D}\frac{(\alpha_r+\tau_r)^{[n_r]}}{\alpha_r^{[n_r]}(\alpha^+ + \tau_r)^{[n^+]}},$$

where n_i are arbitrary nonnegative integers, $n^+ = \sum_{i=1}^{D} n_i$, $x^{[n]} = x(x+1)\dots(x+n-1)$ and $x^{[0]} = 1$. The richer parametrization of the EFD compared to the FD has two important consequences. The first one is an even larger flexibility in modeling the implied cluster structure: with different τ_i's, this model allows to have clusters with different distances from the common barycenter. In particular, each τ_i has an effect only on $\boldsymbol{\mu}_i$, the mean vector of the generic i^{th} cluster:

$$\boldsymbol{\mu}_i = \frac{\boldsymbol{\alpha} + \tau_i \mathbf{e}_i}{\alpha^+ + \tau_i} = \left(\frac{\alpha^+}{\alpha^+ + \tau_i}\right)\frac{\boldsymbol{\alpha}}{\alpha^+} + \left(\frac{\tau_i}{\alpha^+ + \tau_i}\right)\mathbf{e}_i.$$

The cluster mean is a weighted average of the common barycenter $\boldsymbol{\alpha}/\alpha^+$ and $\mathbf{e}_i$: the higher τ_i is, the closer the i^{th} cluster is to the i^{th} vertex of the simplex. In order to understand the effect of the τ_i's, we graphically compare two EFD models with equal $\boldsymbol{\alpha}$ and $\mathbf{p}$ but with different $\boldsymbol{\tau}$ (Fig. 1 and Fig. 2): the first model has $\boldsymbol{\tau} = (20, 20, 20)$ (i.e. it coincides with a FD model with parameter $\tau = 20$) and the second one has $\boldsymbol{\tau} = (10, 30, 100)$. It is easy to see that in the first scenario there is a common distance between each cluster mean and the common barycenter $\boldsymbol{\alpha}/\alpha^+$, whereas in the second case these distances are different.

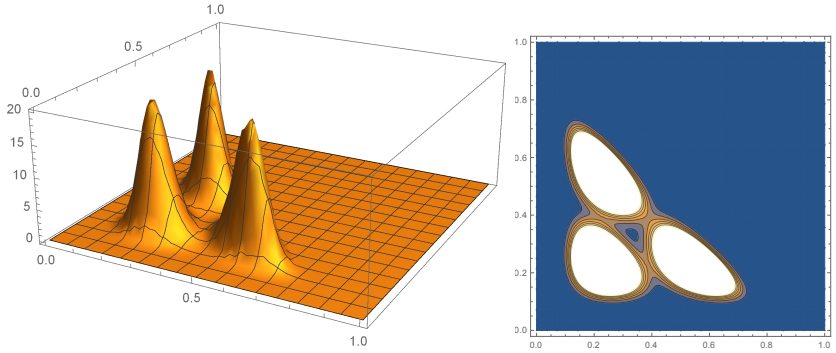

Fig. 1. EFD density (left) and contour plots (right) with $\boldsymbol{\alpha} = (15, 15, 15)$, $\mathbf{p} = (1/3, 1/3, 1/3)$ and $\boldsymbol{\tau} = (20, 20, 20)$

The second consequence of the richer parametrization of the EFD is that it allows for a more flexible modeling of the covariance matrix; in particular it allows to have a positive correlation among components of the composition [12].

4 Maximum Likelihood Estimation via the EM algorithm

4.1 EM Type Algorithm

Given the mixture structure of the EFD model, Migliorati and Ongaro [12] proposed an EM algorithm for maximizing the likelihood function [8]. Suppose

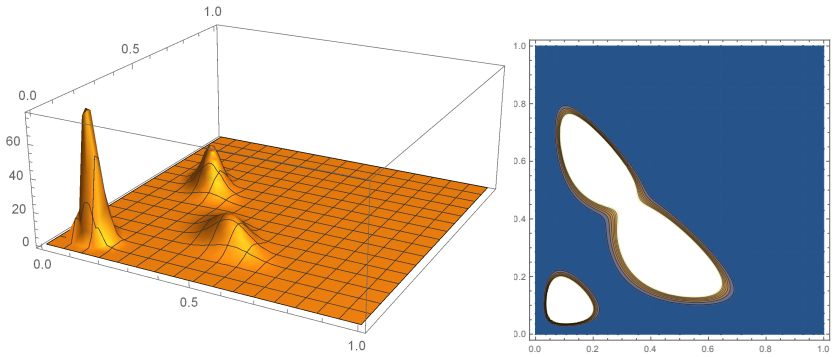

Fig. 2. EFD density (left) and contour plots (right) with $\boldsymbol{\alpha} = (15, 15, 15)$, $\mathbf{p} = (1/3, 1/3, 1/3)$ and $\boldsymbol{\tau} = (10, 30, 100)$

to have a sample of n independent observations $\mathbf{x} = (\mathbf{x}_1, \ldots, \mathbf{x}_n)$ from an EFD distribution; the true log-likelihood can be thought as originated from the following complete-data log-likelihood [12]:

$$\log L_C(\boldsymbol{\alpha}, \boldsymbol{\tau}, \mathbf{p}) = \sum_{j=1}^{n} \sum_{i=1}^{D} z_{ji} \left\{ \log p_i + \log f_{\mathcal{D}}(\mathbf{x}_j; \boldsymbol{\alpha}_i) \right\}, \tag{1}$$

where z_{ji} is equal to 1 if the j^{th} observation has arisen from the i^{th} cluster of the mixture and 0 otherwise; $f_{\mathcal{D}}(\mathbf{x}_j; \boldsymbol{\alpha}_i)$ is the density function of a Dirichlet with parameter $\boldsymbol{\alpha}_i = \boldsymbol{\alpha} + \tau_i \mathbf{e}_i$ evaluated in the data point $\mathbf{x}_j$. We can apply the EM algorithm if we think of the vector $\mathbf{z}_j = (z_{j1}, \ldots, z_{jn})$, $j = 1, \ldots, n$, as the missing component-labels.

The generic $(k+1)^{th}$ step of this iterative method is composed as follows:

- **E-step**: Given $(\boldsymbol{\alpha}^{(k)}, \boldsymbol{\tau}^{(k)}, \mathbf{p}^{(k)})$ (the parameter estimates obtained at step k), compute the conditional expectation of the complete-data log-likelihood given $\mathbf{x}$ as:

  $$\sum_{i=1}^{D} \sum_{j=1}^{n} w_i \left(\mathbf{x}_j; \boldsymbol{\alpha}^{(k)}, \boldsymbol{\tau}^{(k)}, \mathbf{p}^{(k)} \right) \left\{ \log p_i^{(k)} + \log f_{\mathcal{D}} \left(\mathbf{x}_j; \boldsymbol{\alpha}^{(k)} + \tau_i^{(k)} \mathbf{e}_i \right) \right\},$$

  where:

  $$w_i \left(\mathbf{x}_j; \boldsymbol{\alpha}^{(k)}, \boldsymbol{\tau}^{(k)}, \mathbf{p}^{(k)} \right) = \frac{p_i^{(k)} f_{\mathcal{D}}(\mathbf{x}_j; \alpha_i^{(k)})}{\sum_{h=1}^{D} p_h^{(k)} f_{\mathcal{D}}(\mathbf{x}_j; \boldsymbol{\alpha}_h^{(k)})}, \quad i = 1, \ldots, D \tag{2}$$

  is the "posterior" probability that $\mathbf{x}_j$ belongs to the i^{th} cluster of the mixture given $(\boldsymbol{\alpha}^{(k)}, \boldsymbol{\tau}^{(k)}, \mathbf{p}^{(k)})$.

- **M-step**: Maximize the above conditional expectation to update the maximum likelihood estimates of the parameters. In order to obtain new values of $\hat{\boldsymbol{\alpha}}^{(k+1)}$ and $\hat{\boldsymbol{\tau}}^{(k+1)}$ we require a numeric maximization method (e.g. Newton-Raphson), whereas a closed-form expression of $\hat{p_i}^{(k+1)}$ exists: $\hat{p_i}^{(k+1)} = \frac{1}{n} \sum_{j=1}^{n} w_i \left(\mathbf{x}_j; \boldsymbol{\alpha}^{(k)}, \boldsymbol{\tau}^{(k)}, \mathbf{p}^{(k)} \right), \qquad i = 1, \ldots, D-1.$

The E-step and the M-step alternate each other until a convergence criterion is reached (e.g. the algorithm can be stopped when there is a small difference between the log-likelihood of two consecutive steps or d is lower than a threshold, where $d = \left|\boldsymbol{\alpha}^{(k+1)} - \boldsymbol{\alpha}^{(k)}\right| + \left|\boldsymbol{\tau}^{(k+1)} - \boldsymbol{\tau}^{(k)}\right| + \left|\mathbf{p}^{(k+1)} - \mathbf{p}^{(k)}\right|$).

Unfortunately, the EM algorithm typically leads to solutions highly dependent on the starting point; this means that the algorithm often gets trapped in a local maximum close to the starting point. In order to weaken this dependence, we introduce a Stochastic EM (SEM) algorithm [3,5,6]. This is a modified version of the classic EM which is likely to explore a large region of the parameter space. We therefore implement a SEM algorithm followed by an EM one: the results of SEM are used as starting points of a proper EM algorithm, which is very precise in finding maxima close to initial values.

In SEM, after the E step, a new partition of data into D groups $\{\mathcal{G}_1, \ldots, \mathcal{G}_D\}$ is generated, with a draw from the current conditional distribution of $\mathbf{z}_j$ ($j = 1, \ldots, n$) given the observed data (it coincides with a draw from a multinomial distribution with parameters equal to the current estimates of the conditional probabilities $w_i(\cdot)$ given by (2), $i = 1, \ldots, D$). In this way, we give the algorithm a chance to escape from a path of convergence to a local maximizer. Finally, the M step of the SEM consists in updating the weights $\mathbf{p}$ as the relative number of observations in each cluster. Updatings of $\boldsymbol{\alpha}$ and $\boldsymbol{\tau}$ are obtained maximizing the classified likelihood (i.e. the likelihood computed by assuming knowledge of which mixture component each observation comes from):

$$\prod_{i=1}^{D} \prod_{j \in A_i} f_{\mathcal{D}}(\mathbf{x}_j; \alpha_i),$$

where $A_i = \{j : \mathbf{x}_j \in \mathcal{G}_i\}$. This maximization problem can be approached numerically (i.e. with Quasi-Newton optimization algorithms [4]).

4.2 Initialization Issues

The speed of convergence of the EM algorithm can be influenced by the initial values required for the first steps of the algorithm. In general this choice can even influence the ability to locate the global maximum of the log-likelihood function. To address these critical issues, we develop suitable ad hoc initialization strategies.

Usually, the first step of the initialization is to obtain a partition of the n observations into D clusters by means of a clustering method (e.g. the k-means algorithm). Here, following results presented in [13], we shall adopt two different type of clustering. The first one, called barycenter method, is based on the peculiar cluster structure of the EFD: observation $\mathbf{x}_j$ is assigned to group i if $x_{ji}/x_{jh} > B_i/B_j$, $\forall h = 1, \ldots, D, h \neq i$, where $\mathbf{B} = (B_1, \ldots, B_D)$ is a data barycenter (e.g. mean or median). The second method applies a k-means algorithm to a regular simplicial transformation of data. The latter is a linear transformation which is particularly suitable for compositional data (see [13] for more details). Since the k-means algorithm assigns the group labels randomly, we relabel the groups on the basis of the structure imposed by the EFD model:

group i will show the largest mean of component i. In case a single group shows two or more components with maximum sample means, we consider permutations of labels compatible with the largest sample mean positions and choose the one that maximizes the corresponding likelihood. Then, given this partition, a possible value for p_i is the proportion of observations that are assigned to cluster i.

An open problem regards the initialization of $\boldsymbol{\alpha}$ and $\boldsymbol{\tau}$. For this problem, we consider the initialization method used for the FD model and two new ad hoc strategies. We thus compare the performances of the following three methods:

1) The procedure used for the FD in [13], where initialization values for $\boldsymbol{\alpha}$ and τ were obtained using the method of moments: in the EFD context we thus initialize $\boldsymbol{\tau} = (\tau, \tau, \ldots, \tau)$. This method imposes the cluster means' symmetry and therefore can be expected to produce inaccurate results if data do not show this symmetry.
2) Given a partition, we can compute the sample mean of each cluster: $\bar{\mathbf{x}}_h = (\bar{x}_{h1}, \ldots, \bar{x}_{hD})$, $h = 1, \ldots, D$, where $\bar{x}_{hi} = \sum_{j=1}^{n} z_{hj} x_{ji}$. We can obtain values of $\boldsymbol{\alpha}$ and $\boldsymbol{\tau}$ minimizing the distance between $\bar{\mathbf{x}}_h$ and $\boldsymbol{\mu}_h$:

$$\arg\min_{\boldsymbol{\alpha},\boldsymbol{\tau}} \sum_{h=1}^{D} \delta_h (\boldsymbol{\mu}_h - \bar{\mathbf{x}}_h)'(\boldsymbol{\mu}_h - \bar{\mathbf{x}}_h),$$

where δ_h are suitable weights (e.g. the size of each group). Let $\tilde{\boldsymbol{\alpha}} = \boldsymbol{\alpha}/\alpha^+$ and $\tilde{\boldsymbol{\tau}} = \boldsymbol{\tau}/\alpha^+$ be the "relative" counterparts of $\boldsymbol{\alpha}$ and $\boldsymbol{\tau}$, then:

$$\boldsymbol{\mu}_h = \frac{\tilde{\boldsymbol{\alpha}}}{1 + \tilde{\tau}_h} + \frac{\tilde{\tau}_h}{1 + \tilde{\tau}_h} \mathbf{e}_h.$$

Since the constraints $\sum_{h=1}^{D} \tilde{\alpha}_h = 1$, $\tilde{\alpha}_h > 0$, $\tilde{\tau}_h > 0$. $h = 1 \ldots, D$ should hold, this is a constrained minimization problem and could be fulfilled numerically with a Quasi-Newton algorithm [4].
3) The above constrained minimization can be approached analytically. Setting the partial derivatives of the target function (with respect to $\tilde{\alpha}_h$ and $\tilde{\tau}_h$) equal to zero one obtains:

$$\tilde{\alpha}_h \left[\sum_{l=1}^{D} \frac{\delta_l}{(1 + \tilde{\tau}_l)^2} \right] = \sum_{l=1}^{D} \bar{x}_{lh} \frac{\delta_l}{(1 + \tilde{\tau}_l)} - \frac{\tilde{\tau}_h \delta_h}{(1 + \tilde{\tau}_l)^2} \tag{3}$$

and

$$\tilde{\tau}_h = \begin{cases} \dfrac{b_h}{c_h} & \text{if } b_h > 0 \\ 0 & \text{otherwise} \end{cases} \tag{4}$$

where $b_h = (\bar{\mathbf{x}}_h - \tilde{\boldsymbol{\alpha}})'(\mathbf{e}_h - \tilde{\boldsymbol{\alpha}})$ and $c_h = \sum_{r=1}^{D} \tilde{\alpha}_r \bar{x}_{hr} + 1 - \tilde{\alpha}_h - \bar{x}_{hh}$ (c_h is always positive). It can be immediatly observed that the solutions for the $\tilde{\alpha}_h$'s depend on the $\tilde{\tau}_h$'s and viceversa. The final algorithm is:

- initialize the $\tilde{\alpha}_h$'s (i.e. initializing $\boldsymbol{\alpha}^*$ with the FD method and computing $\tilde{\boldsymbol{\alpha}}^* = \boldsymbol{\alpha}^* / \sum_{k=1}^{D} \alpha_k^*$)
- calculate the $\tilde{\tau}_h$'s on the basis of (4)
- calculate the $\tilde{\alpha}_h$'s on the basis of (3)
- repeat until a convergence criterion is satisfied

Methods 2 and 3 have some technical issues: whereas the constraint $\sum_{h=1}^{D} \tilde{\alpha}_h = 1$ is automatically satisfied, other constraints could be violated:

- $\tilde{\tau}_h$ could be equal to 0. In this case we set $\tilde{\tau}_h$ equal to a very small positive quantity (e.g. 0.00001).
- $\tilde{\alpha}_h$ could be negative: if this happens, we set $\tilde{\alpha}_h$ equal to a very small positive quantity and re-normalize the remaining $\tilde{\alpha}_h$'s.

Note that methods 2 and 3 only allow for initialization of the relative quantities $\tilde{\boldsymbol{\alpha}}$ and $\tilde{\boldsymbol{\tau}}$: in order to initialize α^+ one can resort to the variances:

$$\mathbf{Var}(X_k|\mathcal{G}_h) = \sigma_{hk}^2 = \frac{\mu_{hk}(1-\mu_{hk})}{\alpha^+ + \tau_h + 1}$$

where $\mathcal{G}_h$ indicates group h ($h = 1, \ldots, D$). We can estimate each σ_{hk}^2 with s_{hk}^2, the sample variance of component k among group h. With some algebra, we can obtain:

$$\widehat{\alpha^+ + \tau_h} = \frac{1 - \sum_{k=1}^{D} \bar{x}_{hk}^2}{\sum_{k=1}^{D} s_{hk}^2} - 1, \qquad h = 1, \ldots, D.$$

The sum of variances in the denominator permits to have stable estimates whenever some s_{hk}^2 is close to zero. We can use these estimates to obtain several estimates of α^+:

$$\widehat{\alpha^+}_{(h)} = \frac{\widehat{\alpha^+ + \tau_h}}{1 + \tilde{\tau}_h}, \qquad h = 1, \ldots, D$$

where $\tilde{\tau}_h$ was obtained with one of the above methods. Finally, we can aggregate the $\widehat{\alpha^+}_{(h)}$'s using a weighted mean.

4.3 MLE Covariance Matrix

A well known result from statistical theory is that the asymptotic covariance matrix of the ML Estimator $\hat{\boldsymbol{\theta}}$ of $\boldsymbol{\theta} = (\boldsymbol{\alpha}, \boldsymbol{\tau}, \mathbf{p})$ can be approximated, under regularity conditions, by the inverse of the observed information matrix $\mathbf{I}(\hat{\boldsymbol{\theta}}; \mathbf{x})$. In order to compute this matrix, the second-order derivatives of the incomplete log-likelihood are required; unfortunately, their evaluation is quite complicated. We then generalize the method adopted by Migliorati, Ongaro and Monti [13] to the EFD: an evaluation of $\mathbf{I}(\hat{\boldsymbol{\theta}}; \mathbf{x})$ can be obtained via decomposition of complete-data into observed and missing ones, so that we can write:

$$\mathbf{I}(\hat{\boldsymbol{\theta}}; \mathbf{x}) = \left\{ \mathbb{E}_{\boldsymbol{\theta}} \left[\mathbf{I}_c(\boldsymbol{\theta}; \mathbf{X}_c) | \mathbf{x} \right] \right\}_{\boldsymbol{\theta}=\hat{\boldsymbol{\theta}}} - \left\{ \mathbb{E}_{\boldsymbol{\theta}} \left[\mathbf{S}_c(\boldsymbol{\theta}; \mathbf{X}_c) \mathbf{S}_c^T(\boldsymbol{\theta}; \mathbf{X}_c) | \mathbf{x} \right] \right\}_{\boldsymbol{\theta}=\hat{\boldsymbol{\theta}}} \qquad (5)$$

where $\mathbf{S}_c(\boldsymbol{\theta}; \mathbf{X}_c)$ is the complete-data score statistics and $\mathbf{I}_c(\boldsymbol{\theta}; \mathbf{X}_c)$ is the negative of the Hessian matrix of the complete-data log-likelihood (1). Evaluation of the conditional expected value in (5) can be based on conditional bootstrap [9], noting that, conditionally on $\mathbf{x}$, the random vectors $\mathbf{Z}_j$, $j = 1, \ldots, n$ are distributed as independent multinomials with parameters $(p^*_{j1}, \ldots, p^*_{jD})$, where $p^*_{ji} = w_i(\mathbf{x}_j; \hat{\boldsymbol{\theta}})$ is given by (2). Consequently we can approximate the conditional expectations by averaging over B independent bootstrap samples $\mathbf{z}_{jb}$ from $\mathbf{Z}_j$ $(j = 1, \ldots, n; b = 1, \ldots, B)$ for a sufficiently high value of B.

5 The Simulation Study

Two simulation studies have been set up. The first one is aimed at investigating the behavior of the initialization procedures proposed in sections 4.1 and 4.2, whereas the second one is aimed at evaluating the performance of the Maximum Likelihood Estimator and its variance estimate.

In order to implement these studies, 21 parameter configurations were investigated. More precisely, the following values were chosen: for the α_i's and τ_i's $5, 10, 15, 20, 25, 30, 40, 45, 50, 70, 80, 100$ and for the p_i's 0.05, 0.1, 0.15, 0.2, 1/3, 0.35, 0.6, 0.65, 0.75. The chosen parameter configurations allow to cover a great variety of cases, including well-separated as well as overlapped clusters, according to the Symmetrized Kullback-Leibler divergence. This metric is of the form:

$$d_{SKL}(f_1, f_2) = d_{KL}(f_1, f_2) + d_{KL}(f_2, f_1),$$

where:

$$d_{KL}(f_1, f_2) = \int f_1(\mathbf{x}) \ln \frac{f_1(\mathbf{x})}{f_2(\mathbf{x})} d\mathbf{x},$$

with f_1 and f_2 two arbitrary density functions. In our case, f_1 and f_2 are the densities of the Dirichlet components and:

$$\ln \frac{f_{\mathcal{D}}(\mathbf{x}; \boldsymbol{\alpha}_i)}{f_{\mathcal{D}}(\mathbf{x}; \boldsymbol{\alpha}_h)} = \ln C_{i,h} + \tau_i \ln x_i - \tau_h \ln x_h,$$

where $C_{i,h} = \frac{\Gamma(\alpha^+ + \tau_i)}{\Gamma(\alpha^+ + \tau_h)} \frac{\Gamma(\alpha_i)}{\Gamma(\alpha_h)} \frac{\Gamma(\alpha_h + \tau_h)}{\Gamma(\alpha_i + \tau_i)}$ and $\boldsymbol{\alpha}_i = \boldsymbol{\alpha} + \tau_i \mathbf{e}_i$. Remember that if $\mathbf{X} \sim \mathrm{Dir}(\alpha_1, \ldots, \alpha_D)$, then $\mathbb{E}[\ln X_i] = \psi(\alpha_i) - \psi(\sum_k \alpha_k)$, where $\psi(\cdot)$ denotes the digamma function. With some algebra one can then show that:

$$\begin{aligned} d_{KL}(f_{\mathcal{D}}(\mathbf{x}; \boldsymbol{\alpha}_i), f_{\mathcal{D}}(\mathbf{x}; \boldsymbol{\alpha}_h)) = \tau_i \left[\psi(\alpha_i + \tau_i) - \psi(\alpha^+ + \tau_i)\right] + \\ - \tau_h \left[\psi(\alpha_h) - \psi(\alpha^+ + \tau_i)\right] + \ln C_{i,h}. \end{aligned}$$

Then:

$$\begin{aligned} d_{SKL}(f_{\mathcal{D}}(\mathbf{x}; \boldsymbol{\alpha}_i), f_{\mathcal{D}}(\mathbf{x}; \boldsymbol{\alpha}_h)) = \tau_i \left[\psi(\alpha_i + \tau_i) - \psi(\alpha_i)\right] + \tau_h \left[\psi(\alpha_h + \tau_h) - \psi(\alpha_h)\right] + \\ + (\tau_i - \tau_h) \left[\psi(\alpha^+ + \tau_h) - \psi(\alpha^+ + \tau_i)\right]. \end{aligned}$$

Graphical investigation shows that values of d_{SKL} larger than 15 entail well-separated clusters. For space constraints, we report only the results of five representative configurations, shown in Table 1.

ID	α_1	α_2	α_3	τ_1	τ_2	τ_3	p_1	p_2	p_3	$d_{SKL}(1,2)$	$d_{SKL}(1,3)$	$d_{SKL}(2,3)$
1	15	15	15	20	20	20	1/3	1/3	1/3	34.666	34.666	34.666
2	10	40	80	5	30	25	1/3	1/3	1/3	14.801	6.176	23.627
3	50	50	50	5	30	25	0.2	0.6	0.2	10.945	8.267	24.292
4	15	15	15	10	20	15	1/3	1/3	1/3	20.892	15.456	27.581
5	5	30	70	10	25	15	0.1	0.75	0.15	25.180	14.400	17.472

Table 1. Configurations of parameters

5.1 Initialization Method Simulation

In order to evaluate which of the three methods described in subsection 4.2 provides the best initialization, we simulated $K = 100$ datasets for each parameter configuration and applied to them both the clustering methods described in subection 4.2, selecting each time the one which is performing better. Given the resulting data partition, an initial estimate for $\mathbf{p}$ is obtained (subsection 4.2). Then we applied to each dataset the three methods devised for initializing $\boldsymbol{\alpha}$ and $\boldsymbol{\tau}$. With these initializations, we started a SEM+EM procedure obtaining the final estimates for $\boldsymbol{\alpha}$ and $\boldsymbol{\tau}$. Table 2 shows the results of these simulations for each initialization method (rows):

- the first column "Perc." reports the percentage of times that the EFD likelihood evaluated at the initial values is the highest one; the second column "Perc" reports the percentage of times that the final estimates maximize the likelihood function
- columns "Lik. mean" represent the mean of the likelihoods evaluated at the initial values and at the final estimates
- columns "d_2 mean" represent the mean of the euclidean distances between the initial values (or the final estimates) and the true parameter values.

Method 3 generally provides the best starting points, with method 2 displaying only slightly worse performances. On the contrary, method 1 behaves rather poorly compared to the other two, except in the symmetric case 1, as expected. Remarkably, after the SEM+EM step the differences between the three methods are not significant. This evidentiates a strong robustness of the SEM phase with respect to the choice of the initial value. In the following, we shall employ method 3, which is also the one converging faster.

5.2 MLE and Standard Error Simulation

In this section we show the results of a simulation study whose purpose is the evaluation of the performance of the MLE and its estimated variance. For each of the 21 parameter configurations used in subsection 5.1 we simulated $K = 1000$ samples of size $n = 100$. After every estimation procedure, a bootstrap algorithm has been launched (with $B = 3000$ bootstrap samples), in order to have an estimate of the standard errors that can be used to compute confidence intervals as well (based on the asymptotic normal distribution of the ML estimator). In Table 3 we can see the results of the simulations. Rows

Case 1: $\boldsymbol{\alpha} = (15, 15, 15)$, $\boldsymbol{\tau} = (20, 20, 20)$, $\mathbf{p} = (1/3, 1/3, 1/3)$

	Initial Values			Final Estimates		
Meth.	Perc.	Lik. mean	d_2 mean	Perc.	Lik. mean	d_2 mean
1	0.02	209.76901	5.14892	0.32	211.06737	5.61060
2	0.38	210.86665	6.10219	0.35	211.06731	5.61591
3	0.60	210.90500	5.51940	0.33	211.06734	5.61096

Case 2: $\boldsymbol{\alpha} = (10, 40, 80)$, $\boldsymbol{\tau} = (5, 30, 25)$, $\mathbf{p} = (1/3, 1/3, 1/3)$

	Initial Values			Final Estimates		
Meth.	Perc.	Lik. mean	d_2 mean	Perc.	Lik. mean	d_2 mean
1	0.00	285.82046	23.34352	0.38	349.49176	13.41457
2	0.61	347.33590	12.47437	0.33	349.49008	13.19208
3	0.39	347.26455	11.93005	0.29	349.49127	13.08968

Case 3: $\boldsymbol{\alpha} = (50, 50, 50)$, $\boldsymbol{\tau} = (5, 30, 25)$, $\mathbf{p} = (0.2, 0.6, 0.2)$

	Initial Values			Final Estimates		
Meth.	Perc.	Lik. mean	d_2 mean	Perc.	Lik. mean	d_2 mean
1	0.00	300.47035	27.26236	0.34	325.76015	11.90573
2	0.00	316.19300	19.01524	0.38	325.76017	11.92682
3	1.00	316.81200	15.52419	0.28	325.76004	11.76126

Case 4: $\boldsymbol{\alpha} = (15, 15, 15)$, $\boldsymbol{\tau} = (10, 20, 15)$, $\mathbf{p} = (1/3, 1/3, 1/3)$

	Initial Values			Final Estimates		
Meth.	Perc.	Lik. mean	d_2 mean	Perc.	Lik. mean	d_2 mean
1	0.00	194.93455	9.05571	0.34	204.83934	5.15334
2	0.11	204.18551	5.88219	0.35	204.83930	5.14925
3	0.89	204.29076	5.30722	0.31	204.83936	5.11252

Case 5: $\boldsymbol{\alpha} = (5, 30, 70)$, $\boldsymbol{\tau} = (10, 25, 15)$, $\mathbf{p} = (0.1, 0.75, 0.15)$

	Initial Values			Final Estimates		
Meth.	Perc.	Lik. mean	d_2 mean	Perc.	Lik. mean	d_2 mean
1	0	323.9595	23.94387	0.25	376.7433	11.61793
2	0.05	337.6969	23.48097	0.37	376.7447	11.42953
3	0.95	339.0964	21.73839	0.38	376.7442	11.51620

Table 2. Simulation results: initialization

"MLE mean" and "MLE sd" represent the simulated mean and standard deviation of the ML estimator (namely, the Monte Carlo approximation of its expected value and standard error). The quantity "se mean" shows the mean of the bootstrap based simulated standard errors and the row "arb" represents its absolute relative bias (i.e. the mean of the absolute deviations between such standard errors' estimates and the simulated standard deviation - row "MLE sd" - divided by this last quantity). Lastly, "coverage" reports the simulated coverage levels of confidence intervals against a 95% nominal one.

Despite the mixture nature of the EFD model and the relatively small sample size, the performance of the MLE appears rather satisfactory: in most scenarios we considered, small bias and standard deviation are obtained. Furthermore, the bootstrap estimates of the standard errors are remarkably close

Case 1	p_1	p_2	α_1	α_2	α_3	τ_1	τ_2	τ_3
True	1/3	1/3	15	15	15	20	20	20
MLE Mean	0.333	0.332	15.561	15.549	15.6	20.757	20.841	20.828
MLE sd	0.047	0.047	1.655	1.674	1.673	2.793	2.784	2.798
se mean	0.047	0.047	1.618	1.617	1.623	2.744	2.753	2.749
arb	0.028	0.029	0.080	0.083	0.083	0.080	0.079	0.080
coverage	0.951	0.952	0.946	0.943	0.942	0.944	0.947	0.951

Case 2	p_1	p_2	α_1	α_2	α_3	τ_1	τ_2	τ_3
True	1/3	1/3	10	40	80	5	30	25
MLE Mean	0.336	0.331	10.491	41.982	83.890	5.388	31.506	26.901
MLE sd	0.073	0.051	1.259	5.166	10.007	1.461	4.545	6.742
se mean	0.07	0.05	1.228	5.006	9.834	1.376	4.500	6.491
arb	0.168	0.048	0.083	0.080	0.078	0.135	0.075	0.105
coverage	0.919	0.936	0.939	0.942	0.950	0.935	0.947	0.931

Case 3	p_1	p_2	α_1	α_2	α_3	τ_1	τ_2	τ_3
True	0.2	0.6	50	50	50	5	30	25
MLE Mean	0.201	0.595	52.496	52.643	52.555	5.808	31.499	26.607
MLE sd	0.058	0.057	6.091	6.458	6.211	3.814	4.539	5.080
se mean	0.056	0.054	5.900	6.155	5.907	3.750	4.437	4.966
arb	0.166	0.076	0.085	0.088	0.088	0.198	0.087	0.112
coverage	0.922	0.933	0.946	0.943	0.937	0.962	0.941	0.930

Case 4	p_1	p_2	α_1	α_2	α_3	τ_1	τ_2	τ_3
True	1/3	1/3	15	15	15	10	20	15
MLE Mean	0.333	0.333	15.626	15.624	15.626	10.408	20.935	15.700
MLE sd	0.050	0.047	1.702	1.695	1.718	1.991	2.914	2.454
se mean	0.050	0.048	1.691	1.700	1.694	1.941	2.876	2.411
arb	0.044	0.038	0.078	0.075	0.079	0.078	0.077	0.076
coverage	0.950	0.944	0.958	0.949	0.943	0.952	0.950	0.95

Case 5	p_1	p_2	α_1	α_2	α_3	τ_1	τ_2	τ_3
True	0.1	0.75	5	30	70	10	25	15
MLE Mean	0.100	0.750	5.212	31.598	73.177	10.531	25.942	16.764
MLE sd	0.031	0.045	0.582	4.021	8.177	2.193	3.820	8.670
se mean	0.032	0.045	0.555	3.827	7.878	2.048	3.761	8.232
arb	0.132	0.059	0.090	0.098	0.086	0.164	0.086	0.147
coverage	0.936	0.936	0.943	0.940	0.945	0.928	0.957	0.941

Table 3. Simulation results: MLE

to the Monte Carlo approximations and the coverage levels of the confidence intervals are fairly precise. It is also worth noting that the results relative to the other parameter configurations not included in the paper are similar to the reported ones. As a consequence, we can conclude that the proposed estimation procedure appears to be both accurate and reliable.

References

1. J. Aitchison. The Statistical Analysis of Compositional Data. *The Blackburn Press, London*. 2003.
2. O.E. Barndorff-Nielsen, B. Jorgensen. Some parametric models on the simplex. *J. Multivariate Anal.*, 39, 106-116, 1991.
3. C. Bieracki, G. Celeux, G. Govaert. Choosing starting values for the EM algorithm for getting the highest likelihood in multivariate Gaussian mixture models. *Comput. Stat. Data Anal.*, 41, 561-575, 2003.
4. R. H. Byrd, P. Lu, J. Nocedal. A Limited Memory Algorithm for Bound Constrained Optimization. *SIAM Journal on Scientific and Statistical Computing*, 16, 5, 1190-1208, 1995.
5. G. Celeux, G. Govaert. A classification EM algorithm for clustering and two stochastic versions. *Comput. Stat. Data Anal.*, 4, 315-332, 1992.
6. G. Celeux, D. Chauvean, J. Diebolt. Stochastic versions of the EM algorithm: an experimental study in the mixture case. *J. Stat. Comput. Simul.*, 55, 287314, 1996.
7. J.R. Connor, J.E. Mosimann. Concepts of independnece for proportions with a generalization of the Dirichlet distribution. *J. Am. Stat. Assoc.*, 64, 194-206, 1969.
8. A. P. Dempster, N. M. Laird, D. B. Rubin. Maximum Likelihood from Incomplete Data via the EM Algorithm. *Journal of the royal Statistical Society. Series B (Methodological)*, 39, 1, 1-38, 1997.
9. J. Diebolt, E. Ip. Stochastic EM: method and application. *WR Gilks, S.R. Spiegelhalter, D. (eds) Markow Chain Monte Carlo in Practice, Chapman & Hall, London*, pp. 259-273, 1996.
10. S. Favaro, G. Hadjicharalambous, I. Prunster. On a class of distributions on the simplex. *J. Stat. Plan. Infer.*, 141, 2987-3004, 2011.
11. R.D. Gupta, D.St.P. Richards. Multivariate Liouville distributions. *J. Multivariate Anal.*, 23. 233-256, 1987.
12. S. Migliorati, A. Ongaro. Inferential issues in the Extended Flexible Dirichlet model. *16th ASMDA Conference Proceedings*, Greece, 2015.
13. S. Migliorati, A. Ongaro, G. S. Monti. A structured Dirichlet mixture model for compositional data: inferential and applicative issues. *Stat Comput*, 2016.
14. A. Ongaro, S. Migliorati. A generalization of the Dirichlet distribution. *Journal of Multivariate Analysis*, 114, 412–426, 2013.
15. A. Ongaro, S. Migliorati. A Dirichlet mixture model for compositions allowing for dependence on the size. In M. Carpita, E. Brentari and E.M. Qannari (Eds), *Advances in Latent Variables Methods, Models and Applications*, Springer, 2014.
16. W.S. Rayens, C. Srinivasan. Dependence properties of generalized Liouville distributions on the simplex. *J. Am. Stat. Assoc.*, 89, 1465-1470, 1994.

Numerical Stability of the Escalator Boxcar Train under reducing System of Ordinary Differential Equations

Tin Nwe Aye[1] and Linus Carlsson[2]

[1] Division of Applied Mathematics, Mälardalen University, Box 883, 721 23, Västerås, Sweden and University of Mandalay, Myanmar
(E-mail: tinnweaye211@gmail.com)
[2] Division of Applied Mathematics, Mälardalen University, Box 883, 721 23, Västerås, Sweden
(E-mail: linus.carlsson@mdh.se)

Abstract. The Escalator Boxcar Train (EBT) is one of the most popular numerical methods used to study the dynamics of physiologically structured population models. The original EBT-model accumulates an increasing system of ODEs to solve for each time step. In this project, we propose a merging procedure to overcome computational disadvantageous of the EBT method, the merging is done as an automatic feature. In particular we apply the model including merging to a colony of Daphnia Pulex.
Keywords: Escalator Boxcar Train, physiologically structured population models, Daphnia, merging.

1 Introduction

Physiologically structured population models (PSPMs) describe the dynamics of an arbitrary number of biological populations. The basic idea of the EBT-technique is to group individuals of similar state into cohorts, in which the dynamics is prescribed by ODEs which are tracked throughout their entire life history. The individual population dynamics in physiologically structured population models are given by birth rates, death rates, and growth rates, which are dependent of the environment and their physiological state. These states can describe any data of individual physiology, for example; length, size, age, height or weight (Metz and Diekmann[8]).
In this paper, we will for convenience work with a one-dimensional state space describing an individual's length. In the PSPMs, the death rate, the growth rate and the birth rate of the individuals are assumed to have the form $\mu(x, E_t)$, $g(x, E_t)$ and $b(x, E_t)$ respectively, where x is the length of the individual at time t and E_t is the environment. Furthermore, offspring are assumed to have the same birth size x_b. With these assumptions, one can show (see, e.g., de Roos[2]) that the density $u(x, t)$ of individuals of state x at time t satisfies the first order, nonlinear, nonlocal hyperbolic partial differential equation with

nonlocal boundary condition

$$\frac{\partial}{\partial t}u(x,t) + \frac{\partial}{\partial x}\big(g(x,E_t)u(x,t)\big) = -\mu(x,E_t)u(x,t), \tag{1a}$$

$$g(x_b,E_t)u(x_b,t) = \int_{x_b}^{\infty} b(\xi,E_t)u(\xi,t)d\xi, \tag{1b}$$

$$u(x,0) = u_0(x), \tag{1c}$$

where $x_b \leq x < \infty$ and $t \geq 0$.
The EBT method, developed by de Roos[3], solves these kind of partial differential equations, using an increasing system of ODEs. In this article, we propose a procedure of merging internal cohorts in order to reduce the system of ordinary differential equations. We show that this merging procedure does not affect the properties of the solution and in addition, the computation time decreases from polynomial to linear time when the EBT of Daphnia is simulated.
The convergence of the Escalator Boxcar Train has been established in a series of papers, see for example; de Roos and Mets[4], Brännström *et al.*[1], and Carrillo *et al.*[7]. This report consists of four parts. The first part consists of concept, definitions and formulations of the EBT model in Section 2. In the second part, Section 3, Daphnia's model specifications is described. The third part, Section 4, presents a mathematical proof of convergence. And, in the last part, Section 5, we present results from simulations of the Daphnia model, with and without merging.

2 The Escalator Boxcar Train

The Escalator Boxcar Train is a numerical method for solving physiologically structured population models (PSPMs). This method is widely used in theoretical biology since the components of the numerical scheme can be given a biological interpretation. To study the dynamics of a PSPMs numerically, the structured population is subdivided into distinct groups of individuals that are similar, these groups are called cohorts.
The cohorts are separated into internal cohorts and a boundary cohort, where the latter has the unique property that the numbers of individuals may be growing because of newborn individuals. The newly born individuals are assumed to have the same physiological properties and are accumulated in the boundary cohort. The remaining cohorts are called internal cohorts. We set the index of the boundary cohort to be zero and the internal cohorts are indexed by $i = 1, 2, \ldots, N$.
The number of individuals in the i^{th} cohort is denoted by $N_i(t)$. As the sizes of the individuals in each cohort are similar, the mean individual state will be used and is denoted by $X_i(t)$.
We consider the numerical solution of the one-dimensional PSPM with a single birth state x_b defined by Equation (1). The EBT method approximates the measure induced by the solution rather than approximating the solution

directly. The approximation is given by linear combination of Dirac measures, and the approximated measured-value solution ζ_t^N to the PSPMs is

$$\zeta_t^N = \sum_{i=0}^{N} N_i(t)\delta_{X_i(t)}. \tag{2}$$

We biologically interpret each of the terms in the approximation as a cohort composed of N_i individuals with average individual state X_i at time t (see for example Brännström et al[1]). The environment E_t is often directly or in-directly dependent of the solution ζ_t^N.

2.1 The dynamics of internal cohorts

The internal cohorts can be characterized by the number of individuals and by a representative size for these individuals. We will adopt the mean length as the characteristic measure of body size, since even within a cohort the individuals are not completely identical. The dynamics of the size in the internal cohorts follows the differential equation

$$\frac{dX_i}{dt} = g(N_i, E_t), \tag{3}$$

which is simply the growth equation for an individual.
The dynamics of the number (density) of individuals in the internal cohort is defined by:

$$\frac{dN_i}{dt} = -\mu(X_i, E_t)N_i. \tag{4}$$

2.2 The dynamics of the boundary cohort

The boundary cohort is characterized by the number of individuals it contains and by a representative size measure. The number of individuals and length of individuals in the boundary cohort are denoted by $N_0(t)$ and $X_0(t)$, respectively. If there is no reproduction at all, the boundary cohort could be identical to all other cohorts as the dynamics $N_0(t)$ and $X_0(t)$ is described by

$$\frac{dN_0}{dt} = -\mu(X_0, E_t)N_0,$$
$$\frac{dX_0}{dt} = g(X_0, E_t).$$

If reproduction does occur, the contribution is summed for the offspring in all cohorts, where the offspring, produced in cohort i, equals $b(X_i, E_t)N_i$. Thus the total population fecundity will be $\sum_{i=0}^{N} b(X_i^t, E_t)N_i^t$.
This total population birth rate is represented by the newborn individuals which are all accumulated into the current boundary cohort. Hence the dynamics of the number of individuals in the boundary cohort become:

$$\frac{dN_0}{dt} = -\mu(X_0, E_t)N_0 + \sum_{i=0}^{N} b(X_i, E_t)N_i,$$

which depends upon the one hand for the mortality process of the individuals that have recently been born and on the other hand for the addition of offspring.
The dynamics of the size $X_0(t)$ in the boundary cohort, follow the same equation as the dynamics of the size in the internal cohort, i.e.,

$$\frac{dX_0}{dt} = g(X_0, E_t).$$

This dynamics was introduced in [1], and have been shown to have the same convergence rate as the original dynamics in [3], see [12].

2.3 Process of internalizing the boundary cohort

In the course of time, both the number and size of individuals in the boundary cohort change according to the reproduction of individuals and the environment. If the size of the boundary cohort grows to large, it will produce an inapplicable large approximation error. Therefore, the boundary cohort must be internalized sufficiently often.
At each time step, we check if the current boundary cohort's density is zero (no reproduction has occurred), in this case we reset the size of individuals in the boundary cohort to x_b, otherwise, we will introduce a new boundary cohort. Whenever a new boundary cohort is introduced, the old boundary cohort is transformed into an internal cohort. For this reason, the number of internal cohorts will be increased due to internalization. This will be inconvenient for computational purposes, (see Table 5.1). To overcome the growing number of internal cohorts, we apply a merging procedure for internal cohorts containing a small number of individuals.

2.4 Process of merging internal cohorts

If the number of individuals in an internal cohort falls below a certain threshold, and that the size of the internal cohort closest to this one, is close enough, then we merge the two cohorts together. We do this in such a way that the expected number of offspring stays the same, compared to if we had not merged the cohorts. The reason why the two merging cohorts must have similar size is explained in the proof of convergence given in Section 4.

3 The Daphnia's model specifications

To illustrate that the solution when merging cohorts converges, we will exemplify this with an EBT-model applied to the water flea, Daphnia pulex, which is the structured population in the model. The Daphnia pulex feeds on the algae Chlamydomonas reinhardtii, which specify the amount of food, the environment in the model. Biologists have been studying the behaviour of Daphina extensively (see for example Hebert[13], Ebert[6]), and hence, the biological information is vast, we will therefore introduce a simple size-structured model for

Symbol	Value	Unit	Interpretation
ν	0.007	mgC/mm^2	maximum ingestion rate per surface area
f_h	0.164	mgC/L	half saturation food density
x_b	0.6	mm	length at birth
x_j	1.4	mm	length at maturity
l_{max}	3.5	mm	maximum length
r_g	0.11	d^{-1}	growth rate
r_{max}	1.0	mm^2	maximum reproduction rate
μ	0.05	d^{-1}	mortality rate
ρ	0.5	d^{-1}	resource regrowth rate
k	0.25	mgC/L	maximum resource density

Table 3.1. Interpretation of constants used for the Daphnia's life history model was presented by De Roos in (de Roos and Persson *et al.*[5]). The values are developed from practical experiments. Milligram of carbon (mgC), millimeter (mm), liter(L), and day (d) are used in units.

the life history of individual Daphnia. We will use the EBT-model, with the constants in the simulation, as given in Table 3.1. The length of the Daphnia depends on the environment, i.e., the amount of food available. More specifically, larger individuals have higher food consumption, basal metabolism and reproduction rate (Diekmann *et al.*[10]). If they can't get enough food, their growth rate will decelerate and they may even decrease in size. In particular, this implies that the mature Daphnia individuals can shrink under particular conditions (de Roos and Persson[5]) to a juvenile state, in which they do not produce any offspring.
We denote the length of an individual Daphnia by X. The reproduction of adult Daphnia is directly proportional to food ingestion. The reproduction is described by the function

$$b(X,F) = \begin{cases} r_{max} X^2 \frac{F}{f_h+F} & \text{if } X > x_j \ , \\ 0 & \text{if } X \leqslant x_j, \end{cases} \tag{5}$$

where $b(X,F)$ denotes the birth rate of adult Daphnia per unit of time, f_h is the half-saturation food density F (the environment) and r_{max} is the maximum reproduction rate per unit of surface area.
For the growth rate of Daphnia, the von Bertalanffy growth equation (see von Bertalanffy[9]) will be applied. This growth rate is represented by:

$$\frac{dX}{dt} = r_g(l_{max}\frac{F}{f_h+F} - X), \tag{6}$$

where r_g is growth rate constant and l_{max} can be interpreted as the maximum length of Daphnia reaches under actual food condition. Note that the value of the growth rate can be negative when the value of F is small. This reflects that individuals can shrink under low food apply, as mentioned above.
We assume that all Daphnia individuals have the same risk for mortality rate, $\mu(X,F)$, that will be defined by a constant.

$$\mu(X,F) = \mu. \tag{7}$$

4 Error bounds when merging two cohorts

In this section, we present a proof of convergence to the general solution when merging two cohorts, sufficiently close together, i.e., we prove that the reduced system of ODEs will not give rise to large changes in the general solution.
We consider two cohorts (X_a, N_a) and (X_b, N_b), where N denotes the number of individuals in a cohort and X the mean size.
In a small time step, Δt, the food available in the system is assumed to be constant, which implies that the growth rate and fecundity rate are both constant in the time interval $0 \leq t \leq \Delta t$. In this model, the death rate, μ is constant, see Equation (7).
For notational purpose, we assume that $X_b \geq X_a$ at time $t = 0$. At the start of the time step, we denote the initial data with a sub-index zero, e.g., $X_{a_0} = X_a(0)$, $N_{a_0} = N_a(0)$ and so on. The difference, $\Delta x_0 = X_{b_0} - X_{a_0}$, between the sizes of these cohorts is assumed to be sufficiently small.
With the above assumptions, the dynamics of the internal cohorts become simplified. From Equation (4) we get

$$N'(t) = -\mu N(t), \tag{8}$$

and from Equation (6) we get

$$X'(t) = c_1 \left(1 - \frac{X(t)}{K}\right), \tag{9}$$

with parameters $K = l_{max} \frac{F}{f_h + F}$ and $c_1 = r\,K$.
When we consider the reproduction from the two cohorts, without merging, we get from Equation (5) the contribution to the boundary cohort as

$$b_w(t) = c_2 N_a(t) X_a^2(t) + c_2 N_b(t) X_b^2(t), \tag{10}$$

where $c_2 = r_{max} \frac{F}{f_h + F}$.
When merging the two cohorts (X_a, N_a) and (X_b, N_b) into one merged cohort (X_m, N_m), we naturally add the number of individuals in both cohorts, i.e.,

$$N_{m_0} = (N_{a_0} + N_{b_0}) \tag{11}$$

and, in view of Equation (10), we initialize the merged cohort size to

$$X_{m_0} = \sqrt{\frac{N_{a_0} {X_{a_0}}^2 + N_{b_0} {X_{b_0}}^2}{N_{a_0} + N_{b_0}}}, \tag{12}$$

since this formula best preserves the expected number of offspring. In the case when we merge the two cohorts, we get the dynamics of the fecundity, Equation (5), as

$$b_m(t) = c_2 N_m(t) X_m^2(t). \tag{13}$$

We will now show that the general solution of the merged cohort converges to the general solution without any merging, this is the main result of the paper.

Theorem 1. *Under the above assumptions we get*

$$b_m(\Delta t) = b_w(\Delta t) + \ O(\Delta x_0 \cdot \Delta t)$$

Proof. For non-merging cohort, we get an expression for the newborn individuals, b_w, by using Maclaurin expansion in Δt

$$\begin{aligned} b_w(\Delta t) &= b_{w_0} + b'_{w_0}\Delta t + O(\Delta t^2) \\ &= c_2(N_{a_0}X_{a_0}^2 + N_{b_0}X_{b_0}^2) \\ &\quad + c_2(N'_{a_0}X_{a_0}^2 + 2N_{a_0}X_{a_0}X'_{a_0} + N'_{b_0}X_{b_0}^2 + 2N_{b_0}X_{b_0}X'_{b_0})\Delta t \\ &\quad + O(\Delta t^2) \end{aligned}$$

Where we used Equation (10) and its derivative in the last equality. To proceed, we substitute Equation (8) and Equation (9) in the above equation. Thus

$$\begin{aligned} b_w(\Delta t) &= c_2(N_{a_0}X_{a_0}^2 + N_{b_0}X_{b_0}^2) \\ &\quad + c_2\left(-\mu N_{a_0}X_{a_0}^2 + 2N_{a_0}X_{a_0}c_1\left(1 - \frac{X_{a_0}}{K}\right) - \mu N_{b_0}X_{b_0}^2 + 2N_{b_0}X_{b_0}c_1\left(1 - \frac{X_{b_0}}{K}\right)\right)\Delta t \\ &\quad + O(\Delta t^2) \\ &= c_2\left(N_{a_0}X_{a_0}^2 + N_{b_0}X_{b_0}^2\right) - \mu c_2\left(N_{a_0}X_{a_0}^2 + N_{b_0}X_{b_0}^2\right)\Delta t \\ &\quad + 2c_1c_2\left(N_{a_0}X_{a_0} + N_{b_0}X_{b_0}\right)\Delta t - \frac{2c_1c_2}{K}\left(N_{a_0}X_{a_0}^2 + N_{b_0}X_{b_0}^2\right)\Delta t \\ &\quad + O(\Delta t^2) \end{aligned}$$

In the case when we merge cohorts, we get an expression for the newborn individuals, using similar calculations as above

$$\begin{aligned} b_m(\Delta t) &= b_{m_0} + b'_{m_0}\Delta t + O(\Delta t^2) \\ &= c_2N_{m_0}X_{m_0}^2 + c_2(N'_{m_0}X_{m_0}^2 + 2N_{m_0}X_{m_0}X'_{m_0})\Delta t \\ &\quad + O(\Delta t^2) \end{aligned}$$

We substitute equations (8), (9), (11), and (13) in the above equation.

$$\begin{aligned} b_m(\Delta t) &= c_2(N_{a_0} + N_{b_0})\frac{N_{a_0}X_{a_0}^2 + N_{b_0}X_{b_0}^2}{N_{a_0} + N_{b_0}} \\ &\quad + c_2\left(-\mu N_{m_0}\frac{N_{a_0}X_{a_0}^2 + N_{b_0}X_{b_0}^2}{N_{a_0} + N_{b_0}} + 2(N_{a_0} + N_{b_0})X_{m_0}c_1\left(1 - \frac{X_{m_0}}{K}\right)\right)\Delta t \\ &\quad + O(\Delta t^2) \\ &\quad = c_2\left(N_{a_0}X_{a_0}^2 + N_{b_0}X_{b_0}^2\right) \\ &\quad + c_2\left(-\mu\left(N_{a_0}X_{a_0}^2 + N_{b_0}X_{b_0}^2\right) + 2c_1(N_{a_0} + N_{b_0})X_{m_0} - 2c_1(N_{a_0} + N_{b_0})\frac{X_{m_0}^2}{K}\right)\Delta t \\ &\quad + O(\Delta t^2) \end{aligned}$$

$$
\begin{aligned}
b_m(\Delta t) &= c_2\left(N_{a_0}X_{a_0}^2 + N_{b_0}X_{b_0}^2\right) - \mu c_2\left(N_{a_0}X_{a_0}^2 + N_{b_0}X_{b_0}^2\right)\Delta t \\
&\quad + 2c_1c_2(N_{a_0}+N_{b_0})\sqrt{\frac{N_{a_0}X_{a_0}^2 + N_{b_0}X_{b_0}^2}{N_{a_0}+N_{b_0}}}\Delta t \\
&\quad - \frac{2c_1c_2}{K}(N_{a_0}+N_{b_0})\frac{N_{a_0}X_{a_0}^2 + N_{b_0}X_{b_0}^2}{N_{a_0}+N_{b_0}}\Delta t + O(\Delta t^2) \\
&= c_2\left(N_{a_0}X_{a_0}^2 + N_{b_0}X_{b_0}^2\right) - \mu c_2\left(N_{a_0}X_{a_0}^2 + N_{b_0}X_{b_0}^2\right)\Delta t \\
&+2c_1c_2N_{a_0}\sqrt{\frac{N_{a_0}X_{a_0}^2 + N_{b_0}X_{b_0}^2}{N_{a_0}+N_{b_0}}}\Delta t + 2c_1c_2N_{b_0}\sqrt{\frac{N_{a_0}X_{a_0}^2 + N_{b_0}X_{b_0}^2}{N_{a_0}+N_{b_0}}}\Delta t \\
&\quad - \frac{2c_1c_2}{K}\left(N_{a_0}X_{a_0}^2 + N_{b_0}X_{b_0}^2\right)\Delta t + O(\Delta t^2).
\end{aligned}
$$

Subtracting the equation for b_m from the equation for b_w gives

$$
\begin{aligned}
b_w - b_m &= 2c_1c_2\left(N_{a_0}X_{a_0} + N_{b_0}X_{b_0}\right)\Delta t \\
&-2c_1c_2N_{a_0}\sqrt{\frac{N_{a_0}X_{a_0}^2 + N_{b_0}X_{b_0}^2}{N_{a_0}+N_{b_0}}}\Delta t - 2c_1c_2N_{b_0}\sqrt{\frac{N_{a_0}X_{a_0}^2 + N_{b_0}X_{b_0}^2}{N_{a_0}+N_{b_0}}}\Delta t \\
&\quad + O(\Delta t^2).
\end{aligned}
$$

Finally, using the continuity of the square root function, we get that both

$$
X_{a_0} = \sqrt{\frac{N_{a_0}X_{a_0}^2 + N_{b_0}X_{b_0}^2}{N_{a_0}+N_{b_0}}} + O(\Delta x_0)
$$

and

$$
X_{b_0} = \sqrt{\frac{N_{a_0}X_{a_0}^2 + N_{b_0}X_{b_0}^2}{N_{a_0}+N_{b_0}}} + O(\Delta x_0)
$$

Thus, the number of newborn individuals for merging cohorts converges to the number of newborn individuals for non-merging cohort when the difference between the size of individuals for these two cohorts and that the time step goes to zero. Which completes the proof.

5 Simulation of the EBT and Daphnia model

The EBT of the Daphnia's life model was simulated using MATLAB. To solve the system of ODEs in each time step, we use the function ode45 because of its accuracy and speed.
In this section, we present the behavior of a solution to the model with merging in Fig.5.1. In Table 5.1 we present simulation times, both for merging respectively non-merging of cohorts. In the simulation, at the beginning of each time step, we introduce a new boundary cohort, and internalize the old boundary

cohort. We used a least square method to fit the best monomial for the simulation time depending on the number of time steps. We found that when we simulated without merging, the power was close to 1.7, whereas, when the simulations was done with merging of cohorts, the power was close to one, i.e., the relationship between the simulation time and the number of time steps was linear.
In addition, as a consequence of Theorem 1, we see that the biomass of juveniles and adults for merging cohorts converges to the corresponding values for the non-merging simulations as Δt approaches to zero.

Time Span(days)	Merging	Elapsed Time(seconds)	Internal Cohorts	$j(mgC/L)$	$m(mgC/L)$	$v(mgC/L)$
2	Yes	14	45	0.3088	0.0330	0.3418
1	Yes	26	57	0.3072	0.0326	0.3398
1/2	Yes	47	72	0.3137	0.0382	0.3518
1/4	Yes	95	120	0.3132	0.0391	0.3523
2	No	21	749	0.3088	0.0330	0.3418
1	No	53	1367	0.3062	0.0335	0.3398
1/2	No	128	1681	0.3137	0.0382	0.3519
1/4	No	467	3165	0.3132	0.0392	0.3523

Table 5.1. Data for merging and non-merging of cohorts. The column, Elapsed Time, shows the running time for simulations, and the column, Internal Cohorts, the total number of internal cohorts for merging respectively non-merging cohorts. We also represent the value of the biomass of juvenile, j , mature, m, and the value of the total biomass of juvenile and mature, v.

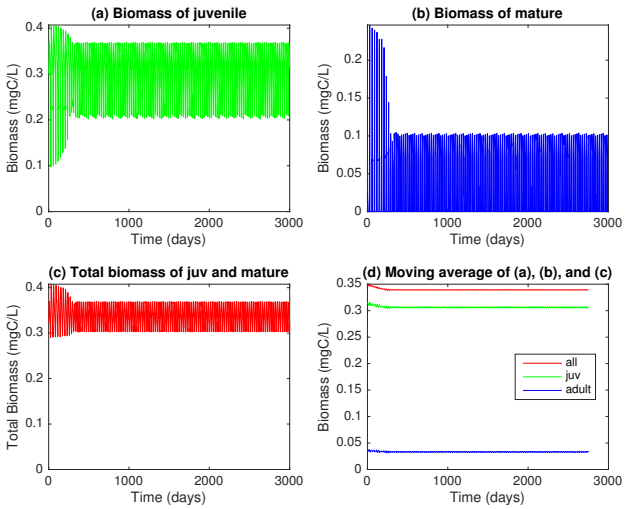

Fig. 5.1. A graphical representation of a simulation with merging of cohorts. While (a) and (b) show juvenile and mature biomass, (c) represents total biomass of juvenile and adult. In addition, the moving average of figures (a), (b), and (c) is presented in (d) to compare for all these biomass, the moving average was taken over 250 days

Conclusion and Future work

Physiologically structured population models are used to study biological systems. The Escalator Boxcar Train method is one of the commonly used numerical methods to find solutions to PSPMs but there are computational disadvantageous of the EBT method. In this project, we have shown how to overcome the problem of the increment of ODEs over time. The main objective for this project is to present a way of how to merge cohorts in order to stabilize the number of ODEs to solve in each time step. We also constructed an EBT-solver that reduces the number of ODEs by an automatic feature of merging cohorts, in which we showed that we get a linear relationship between the number of time steps and the execution time.
The Escalator Boxcar Train method was first published in 1988 by A. de Roos[3], and a first proof of convergence appeared in 2013 by Å. Brännström, L. Carlsson, and D. Simpson[1]. The important reason for merging cohorts is that the maximum number of cohorts can be held under a certain level to make the simulation run faster. In this project, we compare the number of newborn individuals between merging and non-merging of cohorts, where we also prove that the number of newborn individuals for merging cohorts converges to the number of newborn individuals for non-merging cohorts.
Furthermore, this project uses MATLAB to simulate the Daphnia model and present graphs for the biomass of mature and juvenile.
In the future work, we want to establish EBT-solver which includes the automatic feature of merging and splitting cohorts, not only for the Daphnia model,

but for more general models as well, where we also aim to prove convergence for the merging and splitting of cohorts.

Acknowledgements

This research was supported by International Science Programme (ISP) in collaboration with South-East Asia Mathematical Network (SEAMaN). We would like to convey thanks to Professor Sergei Silvestrov. Tin Nwe Aye is also grateful to the research environment Mathematics and Applied Mathematics (MAM), Division of Applied Mathematics, Mälardalen University for providing an excellent and inspiring environment for research education and research.

References

1. Å. Brännström, L. Carlsson, and D. Simpson. On the convergence of the Escalator Boxcar Train. *SIAM Journal on Numerical Analysis,*, 51(6):3213-3231, 2013.
2. A. M. de Roos, *A gentle introduction to models of physiologically structured populations*, in Structured-Population Models in Marine, Terrestrial, and Freshwater Systems, S .Tuljapurkar and H.Caswell, eds., Chapman & Hall, NewYork, 1997, pp. 119-204.
3. A. M. de Roos. Numerical methods for structured population models: the Escalator Boxcar Train. *Numerical methods for partial differential equations*, 4(3), 173-195, 1988.
4. A. M. de Roos and J.A.J. Metz. Towards a numerical analysis of the Escalator Boxcar Train. *Differential Equations with Applications in Biology, Physics, and Engineering*, 133, 1991, pp 91-113
5. A. M. de Roos and L. Persson. From individual life history to population dynamics using physiologically structured models. https:// staff fnwi.uva.nl/a.m. deroos/downloads/EBT/EBT syllabus pdf, 2004, Accessed:2014-19-09.
6. D. Ebert. Ecology, epidemiology and evolution of parasitism in daphnia [internet]. page http:// www.ncbi. nim.nih.gov/books/NBK 2036/, 2005. Accessed:2014-09-19.
7. J. A. Carrillo, P. Gwiazda, K. Kropiclnicka, and A. Marciniak-Czochra. The escalator Boxcar Train method for a system of aged-structured equations in the space of measures: The convergence, 2017.
8. J. A. J. Metz and O. Diekmann. The dynamics of physiologically structured populations, volume 68 of Lecture Notes in Biomathematics. Springer-Verlag Berlin Heidelberg, 1986.
9. L. von Bertalanffy. Quantitative laws in metabolism and growth. *Quarterly Review of Biology*, pages 217-231, 1957.
10. O. Diekmann, M. Gyllenberg, J. A. J. Metz, and A. M. de Roos. The dynamics of physiologically structured populations: A mathematical framework and modelling explorations. 2012.
11. O. Diekmann, J. A. J. Metz, and A. M. de Roos. Studying the dynamics of structured population models: a versatile technique and its application to daphnia. *American Naturalist* , pages 123-147, 1992.
12. P. Gwiazda, K. Kropielnicka, and A. Marciniak-Czochra. The Escalator Boxcar Train method for a system of agestructured equations. Netw. Heterog. Media, 11(1), 2016.

13. P. D. Hebert. The population biology of Daphnia(crustacea, daphnidae), pages 387-426, 1977.

Semiparametric consistent estimators for recurrent event times models based on parametric virtual age functions

Eric Beutner[1], Laurent Bordes[2], and Laurent Doyen[3]

[1] Department of Quantitative Economics, Maastricht University, P.O. Box 616, NL-6200 MD Maastricht, The Netherlands
(E-mail: e.beutner@maastrichtuniversity.nl)
[2] Univ. Pau & Pays Adour, Laboratoire de Mathématiques et de leurs Applications, UMR 5142, IPRA, 64000 Pau, France
(E-mail: laurent.bordes@univ-pau.fr)
[3] Univ. Grenoble Alpes, CNRS, LJK, F-38000 Grenoble, France
(E-mail: laurent.doyen@imag.fr)

Abstract. We consider a large class of semiparametric models for recurrent events based on virtual ages. Modeling recurrent events lifetime data using virtual age models has a long history, this rich class of model contains standard model families as non homogeneous Poisson processes and renewal processes and may include covariates or random effects (see for instance Peña (2006) for a large overview on these models). In many non- or semi-parametric works the virtual age function is supposed to be known, this weakness can be overcome by parametrizing the virtual age function (see for instance Doyen and Gaudoin, 2004). Then the model consists of an unknown hazard rate function, the infinite-dimensional parameter of the model, and a parametrically specified virtual age (or effective) function. Recently Beutner *et al.* (2016) derived conditions on the family of effective age functions under which the profile likelihood inference method for the finite-dimensional parameter of the model leads to inconsistent estimates. Here we show how to overcome the failure of the profile likelihood method by smoothing the pseudo-estimator of the infinite-dimensional parameter of the model, by adapting a method proposed by Zeng and Lin (2007) for the accelerated failure time model.
Keywords: Recurrent events, Virtual age, Semiparametric, Consistency.

1 Introduction

Virtual age models are useful to understand the dynamic of recurrent events in reliability (for instance). The strength of theses models is their ability to account both dependency between inter-arrival times of successive events as well as the evolution of the inter-arrival times distributions with easy interpretation. Virtual age models have been introduced by Kijima et al. (1988), Kijima (1989) and basically they assume that the intensity at time t of a counting process $N(t) = \sum_{j\geq 1} \mathbb{1}_{\{X_j \leq t\}}$, where $X_0 = 0 < X_1 < X_2 < \cdots$ are the event times, can be written $(\lambda \circ \varepsilon)(t)$ where λ is a deterministic function and ε is a random function depending (at least) on the history of the process. When $\varepsilon(t) \equiv t$, the process N is a non homogeneous Poisson process with intensity λ, while if $\varepsilon(t) = t - X_{N(t^-)}$, the process N is a renewal process. As a consequence

we see that the function ε specifies a virtual age just after an event which has to reflect the efficiency of maintenance action in industry. However, genrally this effect is unknown, and even we may want to measure it. To succeed in it Doyen and Gaudoin (2004) introduced some parametrized versions ε^{θ} of the effective age function ε where the Euclidean parameter θ measure the efficiency of a an industrial maintenance policy.

In the semiparametric or nonparametric setting all the existing results assume that the virtual age function is known. For instance Dorado et al. (1997) proposed an estimator of Λ for general (but known) effective age function and studied its asymptotic properties. During the last two decades this class of virtual age models has been enriched by adding covariates effects and frailties. One of the most complex version of these models has been proposed by Peña (2006) and recent semiparametric estimation and asymptotic results based on the profiled likelihood estimation method have been obtained by Adekpedjou and Stocker (2015) and Peña (2016). However, as we mentioned previously, considering that the effective age function is known impedes a large application of these models. One way to overcome this difficulty is therefore to either consider virtual age models for which both the virtual age function and λ are parametric and then applying the usual maximum likelihood approach, or consider parametric virtual age functions with nonparametric assumption on λ. Unfortunately it is especially difficult to fit the later class of models. Indeed, Beutner et al. (2016) recently shown that the usual profile likelihood method fails to lead to consistent estimators. This phenomena has even been observed for the semiparametric accelerated failure time model where the profile likelihood function does not depend on the unknown Euclidean parameter. To overcome this difficulty, Zeng and Lin (2007) shown that profiling out with a smoothed version of the pseudo-estimator of the unknown baseline hazard rate function is enough to restore the consistency and efficiency of the profile likelihood estimator at the price of adding a new parameter required to define the level of regularization. These authors generalized their approach to the case of recurrent events in Zeng and Lin (2010).

In this paper we show that the expected consistency property is recovered by smoothing the profiled log-likelihood function. These results are obtained for a large class of models including most of the relevant virtual age models of the literature like for instance the Doyen and Gaudoin (2004) Arithmetic Reduction of Age (ARA) models that include Kijima (1989) Type–I and Type–II models. Up to our knowledge all the asymptotic results obtained for these models are based on adaptation of martingale methods. This adaptation is due to the necessity of switching from the calendar time scale to the effective age scale following an idea introduced by Selke and Siegmund (1983) and where the martingale properties are no longer true (see e.g. Peña et al. 2001). In addition to overcome the limitation of known effective age functions our approach also show that empirical processes tools may be an efficient alternative to martingale methods to study the asymptotic properties of these inference methods. Basically our empirical processes are based on independent and identically copies of $\boldsymbol{Z} = (\mathcal{T}, \boldsymbol{X})$ with probability distribution P where $\mathcal{T}$ is a right censoring time and $\boldsymbol{X} = (X_1, X_2, \dots)$ is the non decreasing sequence of event times. The

right censored counting process N is defined by $N(t) = \sum_{j\geq 1} \mathbb{1}_{\{X_j \leq t\wedge\mathcal{T}\}}$ for $t \in [0, s]$ where $[0, s]$ is the period of study. Then defining the class of functions $\mathcal{H}_s = \{\boldsymbol{z} = (\tau, x_1, x_2, \dots) \mapsto h_t(\boldsymbol{z}) = \sum_{j\geq 1} \mathbb{1}_{\{x_j \leq t\wedge\tau\}}; t \in [0, s]\}$ and using the usual empirical processes notations (see van der Vaart and Wellner 1996, or van der Vaart 1998) we can identify $(N(t))_{t\in[0,s]}$ and $(\delta_{\boldsymbol{Z}} h)_{h\in\mathcal{H}_s}$ where $\delta_{\boldsymbol{Z}}$ is the Dirac measure at the random (infinite dimentional) point $\boldsymbol{Z}$.

2 Model and estimators

Let $\mathcal{X}$ be the set of non decreasing sequences of non negative real numbers without accumulation point, thus $\boldsymbol{x}$ in $\mathcal{X}$ is defined by $\boldsymbol{x} = (x_n)_{n\in\mathbb{N}}$ with $x_n \in [0, +\infty)$ for all $n \in \mathbb{N} = \{1, 2, \dots\}$ and $0 \leq x_1 < x_2 < \cdots$. In addition we set $x_0 = 0$. Let $\mathcal{Z} = \mathbb{R}^+ \times \mathcal{X}$, then $\boldsymbol{z} \in \mathcal{Z}$ means $\boldsymbol{z} = (\tau, \boldsymbol{x})$ with $\tau \in \mathbb{R}^+$ and $\boldsymbol{x} \in \mathcal{X}$.

Let $\boldsymbol{X} = (X_1, X_2, \dots)$ be a sequence of non decreasing event times and $\mathcal{T}$ is a censoring time. Thus $\boldsymbol{Z} = (\mathcal{T}, \boldsymbol{X})$ is a random element on $\mathcal{Z}$ such that $\boldsymbol{Z} \sim P$ where P is a probability measure on a probability space $(\Omega, \mathcal{F})$. Here we consider recurrent event time models for which the counting process N, defined by $N(t) = \sum_{j\geq 1} \mathbb{1}_{\{X_j \leq t\wedge\mathcal{T}\}}$ for $t \geq 0$ has compensator $A(t) = \int_0^t Y(u)\lambda(\varepsilon^\theta(u))du$ with respect to the natural flitration, where $Y(u) = \mathbb{1}_{\{\mathcal{T}\geq u\}}$ is predictable, where the virtual age function $u \mapsto \varepsilon^\theta(u)$ is predictable and defined up to an unknown Euclidean $\theta \in \Theta$ and where $\lambda \in \Gamma$ the set of hazard rate functions on $\mathbb{R}^+$. The restriction of ε^θ to $(X_{j-1}, X_j]$ is denoted by ε^θ_{j-1} for $j \geq 2$ and ε^θ_0 is defined on $[0, X_1]$ (we note $X_0 = 0$). Note that $\varepsilon^\theta_{j-1}(t)$ may depend on $X_1, \dots, X_{j-1}$.

We assume that ε^θ_0 is the identity function and that P–almost surely $t \mapsto \varepsilon^\theta_{j-1}(t, \omega)$ is continuous on $(X_{j-1}(\omega), X_j(\omega)]$, differentiable on $(X_{j-1}(\omega), X_j(\omega))$ with derivative equal to 1 for all $j \geq 2$.

Let us fix the period of study to $[0, s]$. We know that $M(t) = N(t) - \int_0^t Y(u)\lambda(\varepsilon^\theta(u))du$ is a square integrable martingale with respect to the natural filtration. Under the previous assumptions, by a change in variables (see for instance Peña (2006)) the above martingale process M can be transformed into the following doubly indexed process

$$M^\theta(s, t) = N^\theta(s, t) - \int_0^t Y^\theta(s, u)\lambda(u)du$$

where $N^\theta(s, t) = f_{\theta,t}(\boldsymbol{Z})$ and $Y^\theta(s, t) = g_{\theta,t}(\boldsymbol{Z})$ are defined by

$$f_{\theta,t}(\boldsymbol{z}) = \sum_{j\geq 1} \mathbb{1}_{\{\varepsilon^\theta_{j-1}(x_j)\leq t; x_j \leq s\wedge\tau\}}$$

and

$$g_{\theta,t}(\boldsymbol{z}) = \mathbb{1}_{\{t\leq x_1\wedge s\wedge\tau\}} + \sum_{j\geq 2} \mathbb{1}_{\{\varepsilon^\theta_{j-1}(x_{j-1}+)<t\leq\varepsilon^\theta_{j-1}(x_j\wedge s\wedge\tau); x_{j-1}<s\wedge\tau\}}.$$

Although it has moment properties comparable to those of martingales (in particular $PM^\theta(s,t) = 0$ if $\theta = \theta_0$), the process $t \mapsto M^\theta(s,t)$ is no longer a martingale, making the study of estimators based on $t \mapsto M^\theta(s,t)$ rather complicated (see e.g. Dorado *et al.* (1997) or Peña (2014)).

Now we consider $\mathbb{Z}_n = \{\boldsymbol{Z}_1, \ldots, \boldsymbol{Z}_n\}$ where the $\boldsymbol{Z}_i = (\mathcal{T}_i, \boldsymbol{X}_i)$ are $n > 1$ independent and identically distributed copies of $\boldsymbol{Z} = (\mathcal{T}, \boldsymbol{X})$. We write $\boldsymbol{X}_i = (X_{i,j})_{j\geq 1}$ and $X_{i,0} = 0$.

Because s is a constant we omit to indicate that both f and g depend on s. Let $\mathbb{P}_n = \frac{1}{n}\sum_{i=1}^n \delta_{\boldsymbol{Z}_i}$ we write

$$\bar{N}_n^\theta(s,t) = \mathbb{P}_n f_{\theta,t} = \frac{1}{n}\sum_{i=1}^n N_i^\theta(s,t) \quad \text{and} \quad \bar{Y}_n^\theta(s,t) = \mathbb{P}_n g_{\theta,t} = \frac{1}{n}\sum_{i=1}^n Y_i^\theta(s,t),$$

where $N_i^\theta(s,t) = f_{\theta,t}(\boldsymbol{Z}_i)$ and $Y_i^\theta(s,t) = g_{\theta,t}(\boldsymbol{Z}_i)$.

Since the process

$$t \mapsto \bar{N}_n^\theta(s,t) - \int_0^t \bar{Y}_n^\theta(s,u)\lambda(u)du$$

is centered, a "method-of-moment" type estimator for $\Lambda(t) = \int_0^t \lambda(u)du$ is defined by

$$\Lambda_n^\theta(s,t) = \int_0^t \frac{\bar{N}_n^\theta(s,du)}{\bar{Y}_n^\theta(s,u)}.$$

Here we call $\Lambda_n^\theta(s,t)$ a pseudo–NPMLE of Λ since for θ known it is a NPMLE of Λ as proved in Beutner *et al.* (2016).

Let us define for $t \in [0,s]$

$$\lambda_n^\theta(s,t) = \frac{1}{b_n}\int_{\mathbb{R}} \kappa\left(\frac{t-u}{b_n}\right)\Lambda_n^\theta(s,du),$$

where $\Lambda_n^\theta(s,du) \equiv 0$ on (s,∞), κ is a kernel function (here a probability density function) and b_n is a bandwidth such that $b_n \to 0$ and $nb_n \to \infty$. Then introducing

$$\ell_{n,s}(\theta) = \int_0^M \log(\lambda_n^\theta(s,t))\bar{N}_n^\theta(s,dt),$$

we estimate θ and $\Lambda(t)$ by $\theta_n = \arg\max_{\theta\in\Theta}\ell_{n,s}(\theta)$ and $\Lambda_n(s,t) = \Lambda_n^{\theta_n}(s,t)$ respectively. We show that the resulting estimators are asymptotically consistent and their behavior for finite sample size is illustrated by a simulation study.

3 Arithmetic Reduction of Age models

Arithmetic Reduction of Age (ARA) models has been introduced by Doyen and Gaudoin (2004). These models simply assume that an event effect adds a certain quantity to the virtual age, also called effective age. For ARA models ε_0^θ is the identity function on $[x_0, x_1]$ (where $x_0 = 0$, thus $\varepsilon_0^\theta(x_0+) = 0$) and for $j \in \mathbb{N}$ and $t \in (x_j, x_{j+1}]$, $\varepsilon_j^\theta(t) = t - x_j + \varepsilon_j^\theta(x_j+)$. A specific ARA

model is thus characterized by the j–th event effect, that is by the rejuvenation $\varepsilon_{j-1}^{\theta}(x_j) - \varepsilon_j^{\theta}(x_j+)$ just after time x_j. As we said in the introduction ARA models propose several parametrization with $\theta \in [0,1]$ of Kijima [7] effective age functions. For instance a Kijima Type–I effect at the j–th event corresponds to a reduction proportional to the supplement of age accumulated since the last event: $\varepsilon_{j-1}^{\theta}(x_j) - \varepsilon_j^{\theta}(x_j+) = \theta(\varepsilon_{j-1}^{\theta}(x_j) - \varepsilon_{j-1}^{\theta}(x_{j-1}+))$. That amounts to an ARA_1 model verifying $\varepsilon_j^{\theta}(t) = t - \theta x_j$. A Kijima Type–II effect corresponds to a reduction proportional to the value of the effective age at the last event time: $\varepsilon_{j-1}^{\theta}(x_j) - \varepsilon_j^{\theta}(x_j+) = \theta\varepsilon_{j-1}^{\theta}(x_j)$. That amounts to an ARA_∞ model verifying $\varepsilon_j^{\theta}(t) = t - \theta\sum_{i=0}^{j-1}(1-\theta)^i x_{j-i}$. More generally ARA_m models, for $m \in \overline{\mathbb{N}} \equiv \mathbb{N} \cup \{+\infty\}$, integrate both previous models by assuming that the effective age functions verifies

$$\varepsilon_j^{\theta}(t) = t - \theta \sum_{i=0}^{(j-1)\wedge(m-1)} (1-\theta)^i x_{j-i},$$

with the convention that $\sum_{i=a}^{b} \cdot = 0$ for $a > b$. Thus, for any $j \geq 1$ and $t \in (x_j, x_{j+1}]$, the function $\theta \mapsto \varepsilon_j^{\theta}(t)$ is non increasing, it means that the greater θ is, the less aged the system is. As a consequence the parameter $\theta \in [0,1]$ represents the efficiency of events effects. Indeed notice that $\theta = 0$ corresponds to the well known "as bad as old" situation in reliability applications, for which events have no effects on the effective age since $\varepsilon_j^0(x_j+) = x_j$, while $\theta = 1$ corresponds to the "as good as new" situation, for which each event renews the system since the effective age verifies $\varepsilon_j^1(x_j+) = 0$. The corresponding random processes are respectively a non homogeneous Poisson process and a renewal process.

Let us now index the true model parameters by 0 (the true values of the unknown parameters θ, Λ, etc. are thus noted θ_0, Λ_0, etc.) and introduce the assumptions under which our main result is obtained.

A. Assumptions on the functional parameter
The baseline hazard rate λ_0 is non constant, upper and lower bounded with non null lower bounds on $[0, M]$ for some constant $M > 0$ (defined in Assumption C below). In addition, the corresponding probability density function f_0 is continuous and bounded on $\mathbb{R}^+$ and $\mathrm{BV}_{[0,s]}(f_0) < \infty$ and the associated survival function S_0 verifies $S_0(s) > 0$.

B. Technical assumptions on the kernel and the bandwidth
- (i) The bandwidth $(b_n)_{n\in\mathbb{N}}$ verifies $b_n = cn^{-d}$ for $d \in (0, 1/2)$ and a fixed real number $c > 0$.
- (ii) The kernel function κ is a pdf with support in $[-1, 1]$ and $\mathrm{BV}_{[-1,1]}(\kappa)$ is finite.

Theorem 1. *Suppose that Assumptions* **A** *and* **B** *are satisfied, that the effective age function satisfies an ARA_m models for one $m \in \overline{\mathbb{N}}$, and that $\mathcal{T}$ is a positive random variable, independent of $\boldsymbol{X}$, with pdf $f_{\mathcal{T}}$ bounded on $[0, s]$, survival function $S_{\mathcal{T}}$ such that $S_{\mathcal{T}}(s) > 0$, and for all $c \in [0, s]$ and $\epsilon > 0$,*

$P(\mathcal{T} \in [c-\epsilon, c+\epsilon] \cap [0,s]) > 0$. *Then with probability one*

$$\theta_n \to \theta_0 \quad \textit{and} \quad \sup_{t\in[0,s]} |\Lambda_n(t) - \Lambda_0(t)| \to 0.$$

4 Numerical illustration

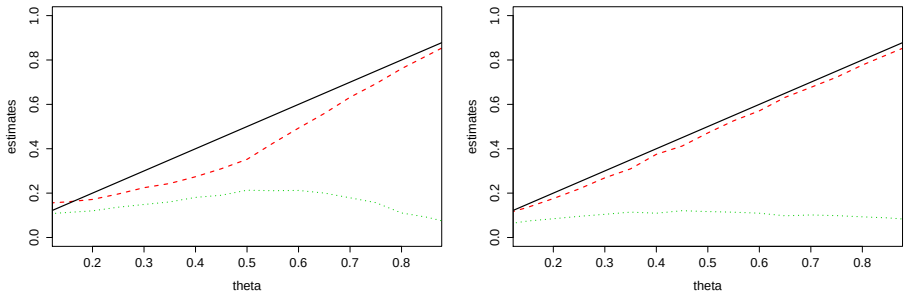

Fig. 1. Empirical mean (red dashed line) and standard deviation (green dotted line) of $N = 1000$ estimates of θ_0 varying in $[0.1, 0.9]$ (black solid line) for an ARA_1 model (left) and an ARA_∞ model (right) with sample size $n = 100$, Type–I censoring with $\tau = s = 7$ and bandwidth $b = 0.5$.

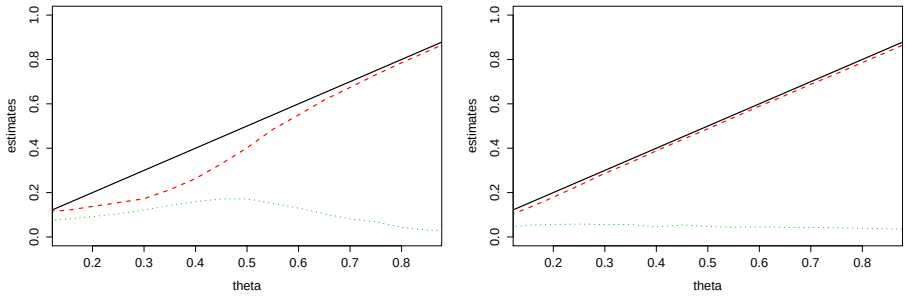

Fig. 2. Empirical mean (red dashed line) and standard deviation (green dotted line) of $N = 1000$ estimates of θ_0 varying in $[0.1, 0.9]$ (black solid line) for an ARA_1 model (left) and an ARA_∞ model (right) with sample size $n = 400$, Type–I censoring with $\tau = s = 7$ and bandwidth $b = 0.5$.

The first objective of this section is to give a numerical illustration of our consistency results for ARA_m models focalizing on the estimation of θ_0. Indeed due to a wide range of situations to illustrate (e.g. sample size effect, censoring effect, bandwidth effect, s effect, m and θ effects for ARA_m models) we focus on the estimation of parametric effective age functions which is the main innovation of the paper. In our simulations the baseline hazard rate function λ_0 is Weibull and defined by $\lambda_0(t) = 0.1 \times t^2$ which does not verify the assumption

$\inf_{[0,s]} \lambda_0 > 0$ required in Theorem 1. All the simulation results are based on $N = 1000$ simulated samples. We consider two types of censoring schemes: Type-I censoring for which $\mathcal{T}_i = \tau$ for all $1 \leq i \leq n$ where τ is a constant, and Type-II censoring for which $\mathcal{T}_i = X_{i,k}$ for all $1 \leq i \leq n$ where k is a constant integer. Indeed we can show that Theorem 1 still holds for these types of censoring schemes.

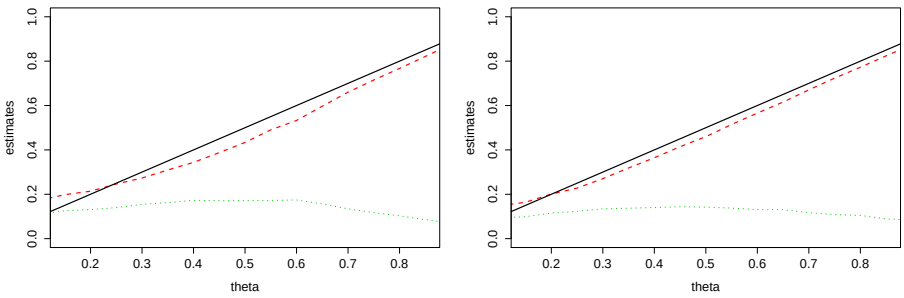

Fig. 3. Empirical mean (red dashed line) and standard deviation (green dotted line) of $N = 1000$ estimates of θ_0 varying in $[0.1, 0.9]$ (black solid line) for an ARA_1 model (left) and an ARA_∞ model (right) with sample size $n = 100$, Type–II censoring with $k = 3$ and bandwidth $b = 0.5$.

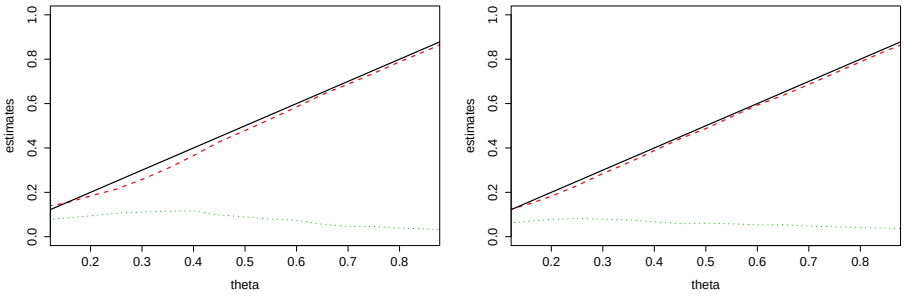

Fig. 4. Empirical mean (red dashed line) and standard deviation (green dotted line) of $N = 1000$ estimates of θ_0 varying in $[0.1, 0.9]$ (black solid line) for an ARA_1 model (left) and an ARA_∞ model (right) with sample size $n = 400$, Type–II censoring with $k = 3$ and bandwidth $b = 0.5$.

Consistency results are illustrated for both ARA_1 and ARA_∞ models, for two sample sizes $n \in \{100, 400\}$ and two censoring schemes i.e. Type–I censoring with $s = \tau = 7$ and Type–II censoring with $k = 3$. The combination of 2 models $\times$ 2 sample sizes $\times$ 2 censoring schemes leads to the 8 graphs given in Figures 1–4.

5 Concluding remarks

There are many perspectives to this work. The first one is theoretical, it concerns the study of the central limit behavior of estimators and the way to derive confidence intervals and bands for the unknown parameters of the model. The second one is both computational and theoretical since the simulation study has shown that even if the consistency can be illustrated numerically, the finite sample behavior of the estimators depends on several tuning parameters (especially s and the bandwidth b), for which a data-driven selection criterium should be provided. An additional perspective we want to mention is the possibility to extend the model by adding covariates at several places in the model.

References

1. Adekpedjou, A. and Stocker, R. (2015). A general class of semiparametric models for recurrent event data. *Journal of Statistical Planning and Inference*, 156, 48–63.
2. Dorado, C., Hollander, M. and Sethuramam, J. (1997). Nonparametric estimation for a general repair model. *Annals of Statistics*, 25, 1140–1160.
3. Beutner, E., Bordes, L. and Doyen, L. (2016). The failure of the profile likelihood method for a large class of semi-parametric models. *Bernoulli*, to appear.
4. Dorado, C., Hollander, M. and Sethuramam, J. (1997). Nonparametric estimation for a general repair model. *Annals of Statistics*, 25, 1140–1160.
5. Doyen, L. and Gaudoin, O. (2004). Classes of imperfect repair models based on reduction of failure intensity or virtual age. *Reliability Engineering and System Safety*, 84, 45–56.
6. Kijima, M., Morimura, H. and Suzuki, Y. (1988). Periodical replacement problem without assuming minimal repair. *European Journal of Operational Research*, 37, 194–203.
7. Kijima, M. (1989). Some results for repairable systems with general repair. *Journal of Applied Probability*, 26, 89–102.
8. Peña, E. (2006). Dynamic modeling and statistical analysis of event times. *Statistical Science*, 21, 487–500.
9. Peña, E.A., Strawderman, R.L. and Hollander, M. (2001). Nonparametric estimation with recurrent event data. *Journal of the American Statistical Association*, 96, 1299–1315.
10. Peña, E.A. (2016). Asymptotics for a class of dynamic recurrent event models. *Journal of Nonparametric Statistics*, 28, 716–735.
11. Selke, T. and Siegmund, D. (1983). Sequential Analysis of the Proportional Hazards Model. *Biometrika*, 70, 315–326.
12. van der Vaart, A. W. (1998). *Asymptotic Statistics*. Cambridge University Press, Cambridge.
13. van der Vaart, A. W. and Wellner, J. A. (1996). *Weak Convergence and Empirical Processes*. Springer, New York.
14. Zeng, D. and Lin, D.Y. (2007). Efficient estimation for the accelerated failure time model. *Journal of the American Statistical Association*, 102, 1387–1396.
15. Zeng, D. and Lin, D.Y. (2010). A general asymptotic theory for maximum likelihood estimation in semiparametric regression models with censored data. *Statistica Sinica*, 20, 871–910.

Measuring Latent Variables is space and/or time: A Gender Statistics exercise

Gaia Bertarelli[1], Franca Crippa[2], and Fulvia Mecatti[3]

[1] University of Perugia, Perugia, Italy
(E-mail: gaia.bertarelli@unipg.it)
[2] University of Milano-Bicocca, piazza dell'Ateneo Nuovo 1, 20126, Milano, Italy
(E-mail: franca.crippa@unimib.it)
[3] University of Milano-Bicocca, via Bicocca degli Arcimboldi 8, 20126, Milano, Italy
(E-mail: fulvia.mecatti@unimib.it)

Abstract. This paper concerns a Multivariate Latent Markov Model recently introduced in the literature for estimating latent traits in social sciences. Based on its ability of simultaneously dealing with longitudinal and spacial data, the model is proposed when the latent response variable is expected to have a time and space dynamic of its own, as an innovative alternative to popular methodologies such as the construction of composite indicators and structural equation modeling. The potentials of the proposed model and the added value with respect to the traditional weighted composition methodology, are illustrated via an empirical Gender Statistics exercise, focused on gender gap as the latent status to be measured and based on supranational official statistics for 30 European countries in the period 2010-2015.

Keywords: Latent clustering, Longitudinal data, Spatial ordering, Gender Gap.

1 Introduction

Composite indicators have the advantage of synthesizing a latent, multidimensional construct in a single number, usually included in the interval (0; 1). They can be derived as a weighted sum of simple indexes, as it is often the case in social statistics, specially when the set of indexes needs to stay unchanged in several geographic areas and/or time periods. In complex settings, the synthetic indicator is conceivable as a latent variable, typically estimated applying Structural Equation Models (SEM) in order to obtain a single measure.
When the latent variable is thought to have a time and-or space dynamic of its own, Multivariate Latent Markov Models (LMMs) may represent a valuable innovation to the construction of composite indicators. LMMs are a particular class of statistical models for the analysis of longitudinal data which assume the existence of a latent process affecting the distribution of the response variables [2] for a review). The rationale of this methodology considers the latent process as fully explained by the observable behaviour of some items, together with available covariates. The main assumption is conditional independence of the response variables given the latent process, which follow a first order discrete Markov chain with a finite number of states. The model is composed of two parts, analogously to SEM: the *measurement model*, concerning the conditional distribution of the response variables given the latent process, and the *latent*

model, pertaining the distribution of the latent process. LMMs can account for measurement errors or unobserved heterogeneity between areas in the analysis. LMMs main advantage is that the unobservable variable is allowed to have its own dynamics and it is not constrained to be time constant. In addition, when the latent states are identified as different subpopulations, LMMs can identify a latent clustering of the population of interest, with areas in the same subpopulation having a common distribution for the response variables. Under this respect, a LMM may be seen as an extension of the latent class (LC) model, in which areas are allowed to move between the latent classes during the observational period. Available covariates can be included in the latent model and then they may affect the initial and transition probabilities of the Markov chain. When covariates are included in the measurement model, the latent variables are used to account for the unobserved heterogeneity and the main interest is on a latent variable which is measured through the observable response variables (e.g., health status or gender inequalities) and on the evaluation of this latent variable depending on covariates. We focus on an extended model of the second type, as we are interested in ordinal latent states.
Very recently, Markov models for latent variables have contributed to in-depth investigations in highly specific and therefore narrow topics [**?**]. Extensive analyses of LMMs, both methodological and applicative, have been performed in the case of small area estimation, taking also into account several points in time [**?**]. Our viewpoint aims to adjust the LMMs approach to a wider area of synthetic social indicators in different geographical areas and in time, namely for national gender gap between countries. Gender statistics are defined as statistics that adequately reflect differences and inequalities in the situation of women and men in all areas of life [8]. Composite gender indicators are usually computed as weighted sum of simple indexes reflecting the multidimensionality of the phenomena and they are periodically released by supranational agencies (see for instance [6] for a comparative review.
We focus on gender gap as the latent status, since this construct is actually a latent trait, measurable only indirectly through a collection of observable variables and indicators purposively selected as micro-aspects that contribute to the latent macrodimension, aiming to add sensitiveness and discrimination power with respect to current indicators.

2 The proposed model

In this paper we use an extension of LMM proposed by Bertarelli [**?**]. The existence of two process is assumed: an observed process ca be expressed as:

$$Y_{jit}, \quad j = 1, \ldots, J, \quad i = 1, \ldots, n \text{ and } t = 1, \ldots, T \tag{1}$$

where Y_{itj} denote the response variable j for unit i at time t, and an unobservable finite-state first-order Markov Chain

$$U_{it}, \quad i = 1, \ldots, n \text{ and } t = 1, \ldots, T \text{ with state space } \{1, \ldots, m\}. \tag{2}$$

We assume that the distribution of Y_{jit} depends only on U_{it}; specifically the Y_{jit} are conditionally independent given U_{it}.

We also denote by $\tilde{\boldsymbol{U}}_{it} = \{U_{jt}, j \in \mathcal{G}_\rangle\}$, where $\mathcal{G}_i$ is the set of the neighbours, the latent states realisations in the neighborhood units.

In the *measurement model* we consider two Gaussian state-dependent distributions:

$$\begin{aligned} Y_{1it}|U_{it} &\sim N(\mu_1, \nu_1), \\ Y_{2it}|U_{it} &\sim N(\mu_2, \nu_2). \end{aligned} \tag{3}$$

The set of parameters of the *structural model*, corresponding to the latent Markov chain, includes the vector of initial probabilities

$$\boldsymbol{\pi} = (\pi_1, \ldots, \pi_u, \ldots, \pi_m)', \tag{4}$$

where

$$\pi_u = P(U_{i1} = u)$$

is the probability of being in state u at the initial time for $u = 1, \ldots, m$ and the elements of the transition probability matrix

$$\boldsymbol{\Pi} = \{\pi_{u|\bar{u}},\ \bar{u}, u = 1, \ldots, m\}, \tag{5}$$

where

$$\pi_{u|\bar{u}} = P(U_{it} = u|U_{i,t-1} = \bar{u})$$

is the probability that unit i visits state u at time t given that at time $t-1$ it was in state $\bar{u}$.

Considering spatial dependence is a crucial point in our field of application [**?**]. As in [**?**], we propose to handle spatial dependence introducing a covariate in the structural model based on the information from a neighboring matrix and depending on the latent structure itself. In this way, the influence of spatial structure depends on the latent process, therefore it is not fixed during the observation period.

For each unit i we know the number of neighbouring units, g_i and their corresponding labels which are collected in the sets G_i. Let $\tilde{\boldsymbol{U}}_{it}$ be the vector of latent states at occasion t for the neighbours of unit i. We suppose to handle ordinal latent states in order to model the severity of the gender gap. Let us consider a function $\boldsymbol{\eta}(\cdot)$ that maps the g_i-dimensional vector $\tilde{\boldsymbol{U}}_{it}$ onto a $d-$dimensional covariate, the choice of $\boldsymbol{\eta}$ depending on the nature of latent states (ordinal or not). Due to our application context, we decide to work with the mean of neighbourhood latent states. Then, this time-varying covariate affects the initial and transition probabilities through the following multinomial logit parametrization:

$$\log \frac{p(U_{i1} = u|\tilde{\boldsymbol{U}}_{i1} = \tilde{\boldsymbol{u}}_{i1})}{p(U_{i1} = 1|\tilde{\boldsymbol{U}}_{i1} = \tilde{\boldsymbol{u}}_{i1})} = \beta_{0u} + \boldsymbol{\eta}(\tilde{\boldsymbol{u}}_{i1})'\boldsymbol{\beta}_{1u} \quad \text{for } u \geq 2, \tag{6}$$

$$\log \frac{p(U_{it} = u|U_{i,t-1} = \bar{u}, \tilde{\boldsymbol{U}}_{it} = \tilde{\boldsymbol{u}}_{it})}{p(U_{it} = \bar{u}|U_{i,t-1} = \bar{u}, \tilde{\boldsymbol{U}}_{it} = \tilde{\boldsymbol{u}}_{it})} = \gamma_{0u\bar{u}} + \boldsymbol{\eta}(\tilde{\boldsymbol{u}}_{it})'\boldsymbol{\gamma}_{1u\bar{u}}, \quad \text{for } t \geq 2 \text{ and } u \neq \bar{u}, \tag{7}$$

where $\boldsymbol{\beta_u} = (\beta_{0u}, \boldsymbol{\beta}'_{1u})'$ and $\boldsymbol{\gamma}_{u\bar{u}} = (\gamma_{0u\bar{u}}, \boldsymbol{\gamma}'_{1u\bar{u}})'$ are vectors of parameters to be estimated. An individual covariate has been introduced, accordingly both the assumptions of local independence and of a first order latent process still hold.

3 Estimation and Inference

To estimate the proposed model. we adopt the principle of data augmentation (Tanner et al, 1987) in which the latent states are introduced as missing data and augmented to the state of the sampler [**?**]. In this way we can simplify the process of sampling from the posterior distribution: we can use a Gibbs sampler for the parameters of the measurement model and we can estimate the initial and the transition probabilities by means of a Random Walk Metropolis-Hastings step. We then need to introduce a system of priors for the unknown model parameters. In particular, a system of Dirichlet priors is set on the initial and on the transition probabilities, while for the vectors $\boldsymbol{\beta_u}$ and $\boldsymbol{\gamma}_{u\bar{u}}$ we assume that they are a priori independent with distribution $N(0, \sigma^2_\beta \boldsymbol{I})$ and $N(0, \sigma^2_\gamma \boldsymbol{I})$, respectively. The choice for σ^2_β and σ^2_γ depends on the context of the application, typically $5 \leq \sigma^2_\beta = \sigma^2_\gamma \leq 10$. The prior distribution for the parameters of the measurement model depends on the distribution assumed for the state-dependent distribution. We choose a Gaussian distribution for the priors of μ_1 and μ_2 and inverse gamma distributions for the variances ν_1 and ν_2.

The choice of the number of latent states of the unobserved Markov chain, underlying the observed data, is part of the model selection procedure and is a very important step of the estimation process. We adopt the Bayesian information criterion (BIC) [**?**] among a restricted set of models ($m = 3, 4, 5$).

4 LMMs Composite Indicators. A Gender Statistics exercise

Gender inequality - both in space and time - is indirectly measurable through a collection of observable variables. Gender composite indicators are commonly constructed as statistics indicators, i.e. linear combinations of a collection of simple indexes, such as means and proportions, which represent observable items, aggregated by means of a weighing system. The choice of both indexes and weight introduce a certain level of arbitrariness. Their case-specific technical limitations [12],[6] often lead to internal inconsistency since the ranking of a single country can vary in relation to the indicator considered. Moreover, few simple indexes, as well as the weighing system, can outweigh the overall results..

LMMs is liable to offer a sound methodology for estimating the latent trait, i.e. the gender gap, in time and in space, resulting in a synthetic indicator. We move from existing source, namely from supranational official statistics, providing different indicators for all nations worldwide. In particular, we take into account the Gender Inequality Index (GII)[9] and the Global Gender Gap Index

(GGGI)[10]. The GII was introduced by UNDP in 2010 and it measures gender inequalities in three aspects of human development: reproductive health, empowerment and economic status. It focus on inequality, therefore a balanced women/man situation is represented by a zero value. The Global Gender Gap Index (GGGI)was introduced by the World Economic Forum in 2006 with the aim of capturing the magnitude of gender-based disparities. It comprises four dimensions: economic participation and opportunity, educational attainment, health and survival, political empowerment. Perfect parity leads to the value 1. Our applicative viewpoint intends to adapt the LMM approach to Gender synthetic index. Gender Inequality Index (GII) and Global Gender Gap Index (GGGI) are composite indicators which aim to capture differences between man and woman in several areas of life. In our case, we focus on gender gap as the latent status, both in space and time. The gap is in fact a latent trait, namely only indirectly measurable through a collection of observable variables and indicators purposively selected as micro-aspects contributing to the latent macro-dimension. To make the interpretation of results easier and more accessible to non-statisticians, we transformed the value of $\boldsymbol{\beta_u} = (\beta_{0u}, \boldsymbol{\beta}'_{1u})'$ and $\boldsymbol{\gamma}_{u\bar{u}} = (\gamma_{0u\bar{u}}, \boldsymbol{\gamma}'_{1u\bar{u}})'$ in order to obtain an unique set of initial and transition probabilities for all the countries and time occasion. That is, our values represent a cross-national, inter-temporal synthesis.

Applying LMMs to $n = 30$ European countries, with respect to $T = 6$ time points (from 2010 to 2015), we investigate the unobservable latent gender gap summarizing the GGGI and GII information in a single value and rearranging two distinct and rather different ranking into a single one, as the multivariate latent Markov model identifies latent statuses of countries. The model selects $k = 4$ latent states, allowing us to organize countries in 4 ordinal latent statuses through the proposed multivariate spatial Latent Markov model with multinomial logit parametrization, where 1 reflects a situation relatively closest to equality and 4 denotes the highest level of Gender Gap severity. The vector of estimated initial probabilities of latent states at the first measurement occasion is

$$\boldsymbol{\pi} = (0.212, 0.483, 0.139, 0.167).$$

These values can be interpreted as sort of relative frequency [1] in the first year of observation. On the whole, European countries under consideration are more likely to be in latent status 1 and 2, with a relatively low gender gap, with initial probability status of 0.212 and 0.483 respectively. The higher imparity condition, present in status 3 and 4 is less common, accounting for slightly more then 20%, i.e. 0.139 and 0.167 jointly considered.

The Transition Probabilities matrix Π for geographical areas is the following, where the identified latent status are denoted $S1 \cdots S4$

$$\begin{array}{lcccc} & \text{to S1} & \text{to S2} & \text{to S3} & \text{to S4} \\ \text{from S1} & 0.98 & 0.02 & 0 & 0 \\ \text{from S2} & 0.1 & 0.9 & 0 & 0 \\ \text{from S3} & 0 & 0.14 & 0.85 & 0.01 \\ \text{from S4} & 0 & 0.3 & 0.2 & 0.4 \end{array} \tag{8}$$

It is noticeable that we obtained a matrix close to diagonality, with more sub-diagonal elements than over-diagonal. Such a matrix implies that on the whole countries did not undergo relevant changes in the ten-year observational periods. Probabilities of improving or worsening with respect to the gender gap are low, except for latent status 4, whose diagonal value is equal to 0.4, meaning that 60% or countries improved their gender gap since 2010. When moving, it is often to a better condition, the probability of joining a worse latent status being limited to the shift from latent status 1 to 2, with probability 0.02, and from latent status 2 to 3, with probability 0.02. This reflects, on the one side, a relatively high starting point in gender equality, under the constitutional rights perspective and under aspects such as educational opportunities. On the other side, in so called developed countries, gender disparities tend to stay, when not to worsen, even in the most advanced countries. To this respect, some remarks can be posed on the basis of spacial results.

Figure 1 shows the geography of latent gap in Europe in 2010 and 2015 (at the beginning and at the end of the observational time period we considered for our exercise). The 4 latent statuses identified by our models are represented in darkening shades of gray from status $S1$ to $S4$, meaning a worsened gender gap situation.

In 2010 we obtain the following distribution: (i) Latent status 4: Bulgaria, Greece, Hungary, Italy, Malta, Turkey; (ii) Latent status 3: Ireland, Romania, Spain; (iii) Latent status 2: Austria, Cyprus, Croatia, Czech Republic, Germany, Estonia, France, Latvia, Lithuania, Luxembourg, Poland, Portugal, Slovenia; (iv) Latent status 1: Belgium, Finland, Island, Netherlands, Norway, Sweden, Switzerland, United Kingdom.
Despite the almost diagonal transition matrix, some changes in latent status structure are highlighted in 2015: (i) Latent status 4: Bulgaria, Hungary, Malta; (ii) Latent status 3: Romania, Turkey; (iii) Latent status 2: Austria, Cyprus, Croatia, Czech Republic, Estonia, France, Greece, Ireland, Italy, Latvia, Lithuania, Luxembourg, Poland, Portugal, Spain, United Kingdom; (iv) Latent status 1: Belgium, Finland, Germany, Island, Netherlands, Norway, Slovenia, Sweden, Swiss.
Latent status 2 becomes the most crowded. The ten-year span appears to have allowed some countries, like Italy, Greece, Spain, to narrow the gap especially in the educational and, to a lesser extent, in political representation. In the case of Slovenia, the upward shift was impressive. The downward shift experimented by the United Kingdom seems to reflect a general trend in economic conditions that cuts across all European countries, even the ones that are regarded as the most socially fair, like Norway, for instance. The overall change in time signals this aspect in a more concise and sharp form by the transition matrix in time, as discussed below.
Under a spacial point of view, then, a first relevant LMMs contribution can be identified in the synthetic single ranking from the information in two different preexisting ones, GGGI and GII respectively. The LMMs ranking establishes relations of equivalence and order that make a complex situation more accessible and readable to the public. For instance, with reference to 2015, the first latent status establishes that the relative best situation in terms of gender par-

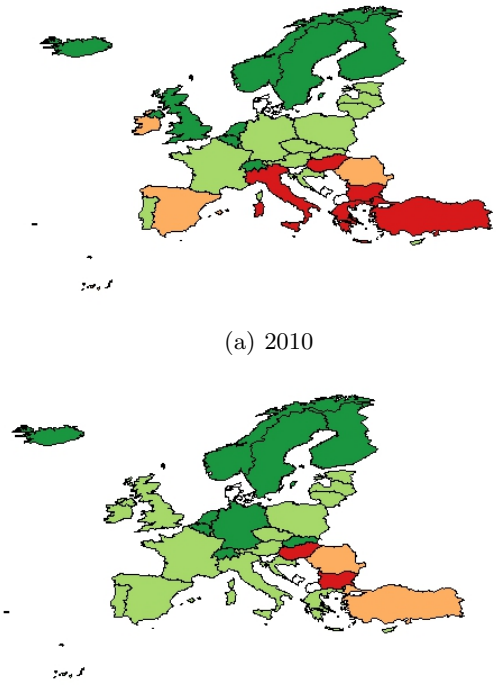

(a) 2010

(b) 2015

Fig. 1. Latent Gender Gap Classification in 2010 and 2015

ity is reached with GGGI values in the interval [0.861; 0.947] and GII values in [0.044; 0.076]. Within this general framework, we gain a better understanding of individual countries changes or stability. As aforementioned, Slovenia upward shift from latent status 2 in 2010 to latent status 1 in 2015 relates to a remarkable increase in GGGI, from .698 to .874, as well as in GI, from .139 to .057. Table 1 shows values for countries that changed their ordinal clustering ranking in the five-year period.

Official statistics provide the two measure annually. With reference to time latent states, LMMs estimation showed an overall stability of the gender gap in the observational time, since the indicators transitional matrix (8) is almost diagonal. On the first hand, the widespread, general access to education and health has been experimented with different times and speed. Therefore, at the initial time point of our investigation (2010) some countries see slower, if not almost nonexistent, progress rates after 2010. On the other hand, GII has being decreasing far more slowly since 2010 not only in countries with a longer record of low GII values, like Switzerland, but also for countries that reached these goals more recently, like Greece. Furthermore, GGGI trend is generally very modest (fig.2) and it has often come to a halt after 2008 in

Country	2010 GGGI	2010 GII	2015 GGGI	2015 GII	2010 status	2015 status
Germany	0,7449	0,117	0,7790	0,073	2	1
Greece	0,6662	0,179	0,6850	0,121	4	2
Ireland	0,7597	0,192	0,8070	0,135	3	2
Italy	0,6798	0,175	0,7260	0,085	4	2
Slovenia	0,6982	0,139	0,7840	0,057	x	1
Spain	0,7345	0,118	0,7420	0,087	3	2
Turkey	0,5828	0,564	0,6240	0,340	4	3
United Kingdom	0,7402	0,206	0,7580	0,149	1	2

Table 1. GGGI, GII and latent status for countries with an upward shift in ordinal clustering

a specific dimension, Economic Opportunity and Political Empowerment, as signalled by the World Economic Forum's Global Gender Gap Report 2016, that states that the gap in the economic pillar is currently larger since 2008 [11]. Besides the disparities in opportunities and salary, a major critical issue is posed by the perspective need for women to acquire Stem (Science, Technology, Engineering and Mathematics) skills, with several implications for everyday social and personal lives.

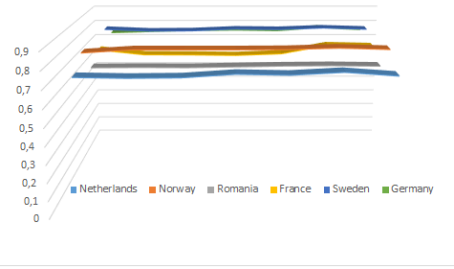

Fig. 2. GGGI trend from 2010 to 2016 in some European countries

5 Conclusion

LMMS have been recently applied to estimate latent traits in time and/or space in social sciences, mainly to highly specific research areas that did not respond adequately to other techniques. Adapting the model in [**?**] to a wider context of social sciences, our proposal consist in the application of LMMS to a more extensive and explored field, Gender Statistics. By means of an empirical exercise, we showed how these models can provide a relevant contribution, since they produced a latent ordinal classification of gender gap between 30 European countries from 2010 to 2015 using two different social composite indicators. They allowed us to obtain synthetic information from the transition matrix that, when diagonal, expresses absence of change. In our exercise, the matrix was nearly diagonal, with reduced margins of improvement for several

countries and in time, especially in the economic sector.
Given the complexity and the multidimensionality of social phenomena, LMMs can contribute highly to a unitarian view. Their latent approach, both in space and in time, can summarise information from different sources. As a matter of fact, both space and time components proved valuable in our application. As far as the former component is concerned, LMMs allowed to identify at a glance areas that are homogeneous or different with respect to gender equality and, in case of differences, permitted to set and order of such a divergence. With respect to the time component, LMMS returned a valuable, concise measure the trend to stagnation that gender parity is experimenting in western countries, due to the rigidness of the economic sector, in particular of the labour market. These models provided also information of national changes in time, i.e. if, how fast and how well some countries were able to set women and men more equal.
Further developments can focus on covariates, especially when expressing opportunities in everyday routines. The persistence of disparities in economic treatment, in fact, can rarely be attributed to explicit law discriminations in western countries, but they can be more often retrieved in availability and in simplification of services to the person and to parenthood, as well as in customs and in mental habits.

References

1. D.J. Bartholomew. *Stochastic Models for Social Processes* 2nd Edition, Wiley, New York, 1973.
2. F. Bartolucci, F. Pennoni and B. Francis. A latent Markov model for detecting patterns of criminal activity. *Journal of the Royal Statistical Society, Series A*, 170, 151-132, 2007
3. G. Bertarelli. Latent Markov models for aggregate data: application to disease mapping and small area estimation. *Ph.D Thesis* `https://boa.unimib.it/handle/10281/96252`, 2015.
4. H. Crane. A hidden Markov model for latent temporal clustering with application to ideological alignment in the US Supreme Court. *Computational Statistics Data Analysis*, 110, 19-36, 2017.
5. B. Fisher and R. Naidoo. The Geography of Gender Inequality, *PlosOne*, 11(3), 0145778, 2016.
6. S.H. Germain. Bayesian spatio-temporal modelling of rainfall through non-homogenous hidden Markov models, *PhD thesis*, University of Newcastle Upon Tyne, 2010.
7. P.F. Lazarsfeld and N.W. Henry. *Latent Structure Analysis*, Houghton Mifflin, Boston, 1968.
8. F. Mecatti, F.Crippa and P. Farina. A special gen(d)re of statistics: roots, development and methodological prospects of gender statistics. *International Statistical Review*, 80(3), 452–467, 2012.
9. M.A. Tanner and W.H. Wong. The calculation of posterior distributions by data augmentation, *Journal of the American statistical Association*, 82, 528–540, 1987.
10. I. ˜Permanyer. The measurement of multidimensional gender inequality: continuing the debate. *Social Indicators Research*, 95(2):181–198, 2010.

11. G.E. Schwarz. Estimating the dimension of a Model, *Annals of Statistics*, 6(2), 461-464, 1978.
12. United Nation. *What are Gender Statistics?*, http://unstats.un.org/unsd/genderstatmanual/What-are-gender-stats.ashx.
13. United Nations Development Programme. *Human Development Reports*, http://hdr.undp.org/en/content/gender-inequality-index-gii/, 2016.
14. World Economic Forum. *The Global Gender Index*, https://www.weforum.org, 2015.
15. World Economic Forum. *The Global Gender Gap Report 2016* http://reports.weforum.org/global-gender-gap-report-2016/, 2016.
16. W. Zucchini and I. MacDonald. *Hidden Markov models for time series*, Springer-Verlag, New York, 2009

PageRank, connecting a line of nodes with multiple complete graphs

Pitos Seleka Biganda[1,2], Benard Abola[2], Christopher Engström[2], and Sergei Silvestrov[2]

[1] Department of Mathematics, College of Natural and Applied Sciences, University of Dar es Salaam, Box 35062 Dar es Salaam, Tanzania
(E-mail: pitos.biganda@mdh.se)

[2] Division of Applied Mathematics, The School of Education, Culture and Communication (UKK), Mälardalen University, Box 883, 721 23, Västerås, Sweden
(E-mails: benard.abola@mdh.se, christopher.engstrom@mdh.se, sergei.silvestrov@mdh.se)

Abstract. PageRank was initially defined by S. Brin and L. Page for the purpose of ranking homepages (nodes) based on the structure of links between these pages. Studies has shown that PageRank of a graph changes with changes in the structure of the graph. In this article we examine how the PageRank changes when two or more outside nodes are connected to a line directed graph. We also look at the PageRank of a graph resulting from connecting a line graph to two complete graphs. In this paper we demonstrate that both the probability (or random walk on a graph) and blockwise matrix inversion approaches can be used to determine explicit formulas for the PageRanks of simple networks.
Keywords: Graph, PageRank, Random walk.

1 Introduction

PageRank was first introduced by Brin and Page [1] to rank homepages (nodes) on the Internet, based on the structure of links between these pages. When a person is interested in getting a certain information from the internet, he is most likely going to use a search engine (eg. Google search engine) to look for such information. Moreover, he will be interested in getting the most relevant ones. What PageRank aims to do, is to sort out and place the most relevant pages first in the list of all information displayed after the search.

It is known that the number of pages on the internet is very large and keeps on increasing over time. For this reason, the PageRank algorithm need to be very fast to accommodate the increasing number of pages and at the same time retaining the requirement for quality of the ranking results as one carries out an internet search [1].

Algorithms similar to PageRank are available, for instance, EigenTrust algorithm, by Kamvar *et al.*[2], applied to reputation management in peer-to-peer networks, and DeptRank algorithm, which is used to evaluate risk in financial networks (Battiston *et al.*[10]). These imply that PageRank concept can be adopted to various networks problem.

Usually PageRank is calculated using power method. The method has been found to be efficient for both small and large systems. The convergence speed

of the method on a webpage structure depends on the parameter c, where c is a real number such that $0 \leq c \leq 1$ (Haveliwala and Kamvar[12]), and the problem is well conditioned unless c is very close to 1 (Kamvar and Haveliwala[4]). However, many methods have been developed for speeding up the calculations of PageRank in order to meet the increasing number of pages on the internet. Some of these methods include aggregating webpages that are close and are expected to have similar PageRank (Ishii *et al.*[7]), partitioning the graph into components as in (Engström and Silvestrov[14]), removing the dangling nodes before computing PageRank and then calculate their ranks at the end or use a power series formulation of PageRank (Anderson and Silvestrov[8]), and not computing the PageRank of pages that have already converged in every iteration as suggested by Sepander *et al.*[13].

There are also studies on a large scale using PageRank and other measure in order to learn more about the Web. One of them is looking at the theoretical and experimental perspective of the distribution of PageRank as by Dyani *et al.*[11].

The theory behind PageRank is built from Perron-Frobenius theory (Berman and Plemmons[9]) and the study of Markov chains (Norris [3]). But how PageRank changes with changes in the system or parameters is not well known. Engström and Silvestrov[5,6] investigated the changes of PageRank of the nodes in the system consisting of a line of nodes and an outside node and/or a complete graph connected to the line of nodes in different ways. In this article, we will extend their work by looking at a line graph connected to multiple outsides nodes, and a line graph connected to two complete graphs. For instance, we will consider what happens when two or more nodes are linked to a line graph. Like in (Engström and Silvestrov[5]), we will consider PageRank as the solution to a linear system of equations as well as probabilities of a random walk through the graph. In the similar way, non-normalized PageRank will be considered.

2 Preliminaries

This section describes important notations and definitions. We start by giving some notations and thereafter essential definitions that are used throughout the article.

- S_G: The system of nodes and links for which we want to calculate PageRank. It contains both the system matrix A_G and a weight vector $\boldsymbol{v}_G$. A subindex G can be either a capital letter or a number in the case of multiple systems.
- n_G: The number of nodes in system S_G.
- A_G: A system matrix of size $n_G \times n_G$ where an element $a_{ij} = 0$ means there is no link from node i to node j. Non-zero elements are equal to $1/r_i$ where r_i is the number of links from node i.
- $\boldsymbol{u}_G$: Non-negative weight vector, not necessary with sum one. Its size is $n_G \times 1$.
- c: A parameter $0 < c < 1$ for calculating PageRank, usually $c = 0.85$.

- $\boldsymbol{g}_G$: A vector with elements equal to one for dangling nodes and zero otherwise in S_G. Its size is $n_G \times 1$.
- M_G: Modified system matrix, $\mathrm{M}_G = c(\mathrm{A}_G + \boldsymbol{g}_G \boldsymbol{u}_G^\top)^\top + (1-c)\boldsymbol{u}_G \boldsymbol{e}^\top$ used to calculate PageRank, where $\boldsymbol{e}$ is the unit vector. Size $n_G \times n_G$.
- S: Global system made up of multiple disjoint subsystems $S = S_1 \cup S_2 \ldots \cup S_N$, where N is the number of subsystems.

In the cases where there is only one possible system the subindex G is omitted. For the systems making up S we define disjoint systems in the following way.

Definition 1. Two systems S_1, S_2 are disjoint if there are no paths from any nodes in S_1 to S_2 or from any nodes in S_2 to S_1.

PageRank can be defined in various versions, for instance in [5] where two versions were presented. However, in this paper we will use the non-normalized PageRank, denoted as $\boldsymbol{R}_j$ for node j, and it is defined as

Definition 2. $\boldsymbol{R}_G$ for system S_G is defined as $\boldsymbol{R}_G = (\mathrm{I} - c\mathrm{A}_G^\top)^{-1} n_G \boldsymbol{u}_G$, where I is an identity matrix of same size as A_G.

Definition 3. Consider a random walk on a graph described by A_G, which is the adjacency matrix weighted such that the sum over every non-zero row is equal to one. In each step with probability $c \in (0,1)$, move to a new vertex from the current vertex by traversing a random outgoing edge from the current vertex with probability equal to the weight on the corresponding edge weight. With probability $1-c$ or if the current vertex have no outgoing edges, we stop the random walk. The PageRank $\boldsymbol{R}$ for a single vertex v_j can be written as

$$\boldsymbol{R}_j = \left(\sum_{v_i \in V, v_i \neq v_j} w_i P_{ij} + w_j \right) \left(\sum_{k=0}^{\infty} (P_{jj})^k \right), \tag{1}$$

where P_{ij} is the probability to hit node v_j in a random walk starting in node v_i described as above. This can be seen as the expected number of visits to v_j if we do multiple random walks, starting in every node once and weighting each of these random walks by $\boldsymbol{w}$ [5].

Next, let us define graph-structures we will encounter in the section that follows.

Definition 4. A simple line is a graph with n_L nodes where node n_L links to node n_{L-1} which in turn links to node n_{L-2} all the way until node n_2 link to node n_1.

Definition 5. A complete graph is a group of nodes in which all nodes in the group links to all other nodes in the group.

The following well known lemma for blockwise inversion will be used in this article. A proof can be found, for example in Bernstein [15].

Lemma 1.

$$\begin{bmatrix} \mathrm{B} & \mathrm{C} \\ \mathrm{D} & \mathrm{E} \end{bmatrix}^{-1} = \begin{bmatrix} (\mathrm{B} - \mathrm{C}\mathrm{E}^{-1}\mathrm{D})^{-1} & -(\mathrm{B} - \mathrm{C}\mathrm{E}^{-1}\mathrm{D})^{-1}\mathrm{C}\mathrm{E}^{-1} \\ -\mathrm{E}^{-1}\mathrm{D}(\mathrm{B} - \mathrm{C}\mathrm{E}^{-1}\mathrm{D})^{-1} & \mathrm{E}^{-1} + \mathrm{E}^{-1}\mathrm{D}(\mathrm{B} - \mathrm{C}\mathrm{E}^{-1}\mathrm{D})^{-1}\mathrm{C}\mathrm{E}^{-1} \end{bmatrix} \tag{2}$$

where B, E *is square and* $\mathrm{E}, (\mathrm{B} - \mathrm{C}\mathrm{E}^{-1}\mathrm{D})$ *are nonsingular.*

3 Changes in PageRank when connecting the simple line graph with multiple outside nodes

In this section, we presents four graphs and associated PageRanks lemma and theorem. We will start with a lemma from where explicit PageRank for each vertex of the graph considered can be determined.

3.1 Connecting the simple line with multiple links from m outside nodes to one node in the line

Consider a simple line graph that has L vertices. Suppose vertex $n_j, j \in [1, L]$ is linked to m outside vertices as shown in Figure 1. It can be seen that if $j = 1$, then the node is said to be an authority node.

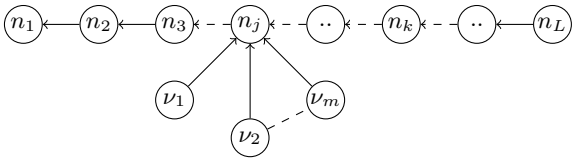

Fig. 1. A simple line directed graph with m outside vertices

Lemma 2. *The PageRank of a node e_i belonging to the line in a system containing a simple line with m outside nodes linking to one node j in the line when using uniform weight vector $\boldsymbol{u}$ can be expressed as*

$$\begin{aligned} \boldsymbol{R}_i &= \sum_{k=0}^{n_L - i} c^k + b_{ij} = \frac{1 - c^{n_L - i + 1}}{1 - c} + b_{ij} \\ b_{ij} &= \begin{cases} mc^{j-i+1}, & \text{if } i \leq j \\ 0, & \text{if } i > j \end{cases} \end{aligned} \tag{3}$$

where $m \geq 1$ and n_L is the number of nodes in the line. The new nodes each have rank 1.

Proof. Applying the notion of probability, the PageRank for a node when a uniform $\boldsymbol{u}$ is used can be written in the form Equation (1). Let e_i and e_j be the nodes on the line. Suppose that P_{ji} is the probability of hitting node e_i starting at node e_j. Considering a random walk on a graph described by $c\mathrm{A}_G$, i.e. we walk to the new node with probability c and stop with probability $1-c$, therefore P_{ji} becomes

$$P_{ji} = c^{j-i}, \quad j > i$$

and zero, otherwise. It follows that the expected numbers of visits to e_i if multiple random walks is performed starting at any node e_j, for $j > i$ is

expressed as

$$\sum_{\text{all}j:e_j \neq e_i} P_{ji} + 1 = \sum_{j=i+1}^{n_L} c^{j-i} + 1 = \frac{1 - c^{n_L - i + 1}}{1 - c},$$

where n_L is the number of nodes in the line. Next we show that the m outside nodes linking to node e_j on the line adds $b_{ij} = mc^{j-i+1}$ for $j \geq i$. The proof of this part is similar to Theorem 2 in [14], only that we need to show that it is generally true for m nodes. By induction; for $m = 1$, it is exactly the same as in [14]. Next, assume that it is true for $m = k$, then

$$b_{ij}(k) = \underbrace{c^{j-i+1} + c^{j-i+1} + \cdots + c^{j-i+1}}_{k \text{ times}} = kc^{j-i+1}.$$

It follows that for $m = k + 1$,

$$b_{ij}(k+1) = b_{ij}(k) + c^{j-i+1} = (k+1)c^{j-i+1}.$$

Finally, it is obvious that the PageRank of the m nodes is 1 each since no node links to each of the nodes.

Remark It is essential to note that we are dealing with simple line graph as given in Definition 4 thus it is not possible to hit node i from the left, that is., $i - 1$ if one takes a random walk from any node j such that $j < i$ as shown in Figure 1.

3.2 Connecting a simple line with multiple links from multiple outside nodes to the line

Assume that the nodes $n_1, n_2, \cdots, n_5$ on the line are linked to outside nodes $m_1, m_2, \cdots, m_5$ respectively, where $m_j \geq 0$ (the number of outside nodes linked to node j on the line graph). Suppose $m_j = 1$ for all $j \in \{1, 2, \cdots, 5\}$ as shown in the Figure 2. To gain a better understanding of how to obtain the

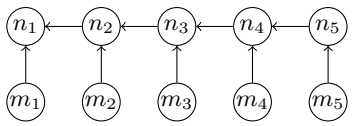

Fig. 2. A simple line graph with one outside vertex linked to one vertex on the line

PageRanks of Figure 2, let us have a look at $\boldsymbol{R}_4$ and $\boldsymbol{R}_5$ on the line graph which correspond to nodes n_4 and n_5 respectively. Using Definition 2, the Pagerank $\boldsymbol{R}_5 = 1 + m_5 c$. Similarly, we get $\boldsymbol{R}_4 = 1 + m_4 c + c\boldsymbol{R}_5$ and substituting for $\boldsymbol{R}_5$ yields $\boldsymbol{R}_4 = \frac{1-c^2}{1-c} + m_4 c + m_5 c^2 = \frac{1-c^2}{1-c} + \sum_{j=4}^{5} m_j c^{j-3}$. In overall PageRank

$\boldsymbol{R}_{S_L}$ on the line graph before substituting for m_j is

$$\begin{pmatrix} \boldsymbol{R}_1 \\ \boldsymbol{R}_2 \\ \boldsymbol{R}_3 \\ \boldsymbol{R}_4 \\ \boldsymbol{R}_5 \end{pmatrix} = \begin{pmatrix} 1+c+c^2+c^3+c^4+m_1c+m_2c^2+m_3c^3+m_4c^4+m_5c^5 \\ 1+c+c^2+c^3+m_2c+m_3c^2+m_4c^3+m_5c^4 \\ 1+c+c^2+m_3c+m_4c^2+m_5c^3 \\ 1+c+m_4c+m_5c^2 \\ 1+m_5c \end{pmatrix} \tag{4}$$

and the PageRank of each of the outside node is equal to 1.
It can be seen that a better approach to find the PageRank would be to start with $\boldsymbol{R}_5$, $\boldsymbol{R}_4$ and so on, that is, recursively then generalization can easily be made. In the theorem that follows, the PageRanks for such general network is proposed for $m_j \geq 0$.

Theorem 1. *The PageRank of a node e_i belonging to the line in a system containing a simple line with multiple outside nodes, $m_1, m_2, \cdots, m_i, \cdots, m_L$ linking to every nodes $n_1, n_2, \cdots, n_i, \cdots, n_L$ in that order respectively in the line when using uniform weight vector $\boldsymbol{u}$ can be written as*

$$\begin{aligned} \boldsymbol{R}_i &= \frac{1-c^{n_L-i+1}}{1-c} + b_i, \quad \textit{where} \\ b_i &= \begin{cases} \sum_{j=i}^{n_L} m_j c^{j-i+1}, & \textit{if } j \geq i \\ 0 & \textit{if } i < j. \end{cases}, \end{aligned} \tag{5}$$

The outside nodes each have rank 1.

Proof. We start by calculating the PageRank of the nodes i on the directed line graph, we have partially shown how to achieve this in Lemma 2. However, the Pagerank $\boldsymbol{R}_i$ on the line graph is obtained by dividing the overall nodes of the graph into two: along the line and outside. Then writing the PageRank using Definition 3 while taking into account the weight $w_i = 1$. Hence, $\dfrac{1-c^{n_L-i+1}}{1-c}$ is the expected number of visit to node i when arbitrary random walks are performed starting from any node j. The term b_i is the expected number of visits to node i starting from each outside nodes e_j, for $j \geq i$. Recall that if you are along the line, you can hit node $L-1$ while starting from node L but not the vice verse. Now, without loss of generality, take the node L on the line, then

$$\begin{aligned} R_L = 1 + m_L c &= \frac{1-c}{1-c} + m_L c = \frac{1-c^{L-L+1}}{1-c} + m_L c^{L-L+1}, \\ &= \frac{1-c^{L-L+1}}{1-c} + \sum_{j=L}^{L} m_j c^{j-L+1}. \end{aligned} \tag{6}$$

This proves that the formula is correct for the last node L in the line.

Next we prove that if the formula is correct for R_k then it is correct for R_{k-1} as well, which by induction proves that it is correct for all vertices in the line.

Now, assume that its true for k node on the line whose rank is $\boldsymbol{R}_k$, then

$$\boldsymbol{R}_k = \frac{1 - c^{n_L - k + 1}}{1 - c} + \sum_{j=k}^{n_L} m_j c^{j-k+1}.$$

Thus to find $\boldsymbol{R}_{k-1}$, we add the weight $w_{k-1} = 1$, the influence of PageRank $\boldsymbol{R}_k$ due to one-step probability, $c\boldsymbol{R}_k$ and the expected number of visits to node $k-1$ starting from each outside nodes e_{L-1}, $m_{k-1}c$. Therefore $\boldsymbol{R}_{k-1}$ becomes

$$\begin{aligned} \boldsymbol{R}_{k-1} &= 1 + c\boldsymbol{R}_k + m_{k-1}c, \\ &= 1 + c\left(\frac{1 - c^{n_L - k + 1}}{1 - c}\right) + c\sum_{j=k}^{n_L} m_j c^{j-k+1} + m_{k-1}c. \end{aligned} \tag{7}$$

Combining the first two terms and rewriting the last two gives

$$\boldsymbol{R}_{k-1} = \frac{1 - c + c - c^{n_L - k + 2}}{1 - c} + \sum_{j=k}^{n_L} m_j c^{j-(k-1)+1} + m_{k-1}c^{k-1-(k-1)+1}.$$

Finally moving the last term into the sum and simplifying, we get

$$\boldsymbol{R}_{k-1} = \frac{1 - c^{n_L - (k-1) + 1}}{1 - c} + \sum_{j=k-1}^{n_L} m_j c^{j-(k-1)+1}.$$

For the outside nodes, each has PageRank equal to 1.

3.3 Connecting the simple line with two links from two outside nodes to the line.

In this graph we let two vertices n_j and n_k for $k > j$, be linked to two outsides vertices as shown in Figure 3. It worth mentioning that this graph is one of the types presented in the previous subsection where two of the outside nodes are non-zero and the rest are zeros. Hence, it can be proved using Theorem 1. But to avoid repetition, we show that the PageRanks of such graph can be obtained using matrix approach in Lemma 1.

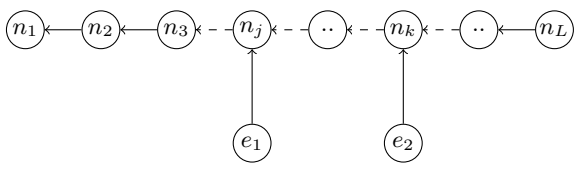

Fig. 3. A simple line directed graph with two outside vertices linked to the line

Proposition 1. *The PageRank of a node e_i belonging to the line in a system containing a simple line with two outside nodes linking to two arbitrary nodes, j and k with $j < k$, respectively in the line when using uniform weight vector $\boldsymbol{u}$ can be written as*

$$\begin{aligned} \boldsymbol{R}_i &= \frac{1 - c^{n_L - i + 1}}{1 - c} + b_{ik} \quad \textit{for} \quad i \geq k \\ b_{ik} &= \begin{cases} c, & \textit{if } i = k \\ 0, & \textit{if } i > k \end{cases}, \end{aligned} \tag{8}$$

$$\begin{aligned} \boldsymbol{R}_i &= \frac{1 - c^{n_L - i + 1}}{1 - c} + c^{k - i + 1} + b_{ij} \quad \textit{for} \quad j \leq i < k \\ b_{ij} &= \begin{cases} c, & \textit{if } i = j \\ 0, & \textit{if } i > j \end{cases} \end{aligned} \tag{9}$$

$$\boldsymbol{R}_i = \frac{1 - c^{n_L - i + 1}}{1 - c} + c^{1 - i} \left(c^j + c^k \right), \quad \textit{for} \quad i < j, \tag{10}$$

where n_L is the number of nodes in the line. The new nodes each have rank 1.

Proof. Let B be part of the matrix $(I - cA_G^{\mathrm{T}})$ corresponding to the nodes in the line such that

$$(I - cA_G^{\mathrm{T}}) = \begin{bmatrix} B & C \\ D & E \end{bmatrix}. \tag{11}$$

It follows that, B is an $n_L \times n_L$ matrix of the form

$$B = \begin{bmatrix} 1 & -c & 0 & \cdots & 0 \\ 0 & 1 & -c & & \vdots \\ \vdots & & \ddots & \ddots & -c \\ 0 & \cdots & \cdots & \cdots & 1 \end{bmatrix}$$

and C is an $n_L \times 2$ matrix of the form

$$C = \begin{bmatrix} 0 & 0 \\ \vdots & -c \\ -c & 0 \\ 0 & \vdots \\ 0 & 0 \end{bmatrix}.$$

The non-zero entries of C correspond to the positions j and k in the line at which the two outsides nodes link to. The matrix D is a $2 \times n_L$ zero matrix, and E is an identity matrix of order 2. From (11), we write

$$(I - cA_G^{\mathrm{T}})^{-1} = \begin{bmatrix} B^{\mathrm{inv}} & C^{\mathrm{inv}} \\ D^{\mathrm{inv}} & E^{\mathrm{inv}} \end{bmatrix}$$

and using Lemma 1 for blockwise inversion, we have

$$B^{\text{inv}} = (B - CE^{-1}D)^{-1} = B^{-1}.$$

Since B is the matrix for the simple line, we get

$$B^{\text{inv}} = \begin{bmatrix} 1 & c & c^2 & \cdots & c^{n_L-1} \\ 0 & 1 & c & \cdots & c^{n_L-2} \\ 0 & 0 & 1 & \cdots & c^{n_L-3} \\ \vdots & \vdots & \ddots & \ddots & \vdots \\ 0 & 0 & \cdots & 0 & 1 \end{bmatrix}. \tag{12}$$

Also, using Lemma 1,

$$C^{\text{inv}} = -B^{\text{inv}}CE^{-1} = -B^{\text{inv}}C = \begin{bmatrix} c^k & c^j \\ c^{k-1} & c^{j-1} \\ c^{k-2} & \vdots \\ \vdots & c \\ c & 0 \\ 0 & 0 \\ \vdots & \vdots \\ 0 & 0 \end{bmatrix}$$

since $E^{-1} = I$. Note also that $D^{\text{inv}} = O$. Since the weight vector $\boldsymbol{u}$ is uniform we get the PageRank of a node as the sum of corresponding row in $(I - cA_G^{\text{T}})^{-1}$ as given by (8), (9) and (10).

3.4 Connecting the simple line with two links from the line to two outside nodes

Suppose we consider a graph where two nodes in the line link to two outside nodes as in Figure 4. We formulate the following to obtain the pageRank

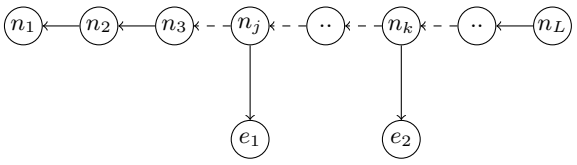

Fig. 4. A simple line with two links from the line to two outside nodes

Theorem 2. *The PageRank $\boldsymbol{R}_i$ of a node e_i belonging to the line in a system containing a simple line with two outside nodes, e_1 and e_2, whose links are*

from node j and k, $j < k$, respectively in the line when using uniform weight vector $\boldsymbol{u}$ can be expressed as

$$\boldsymbol{R}_i = \sum_{m=i}^{n_L} c^{m-i} = \frac{1 - c^{n_L - i + 1}}{1 - c}, \quad for \quad i \geq k, \tag{13}$$

$$\begin{aligned} \boldsymbol{R}_i &= \sum_{m=i+1}^{k} c^{m-i-1} + \frac{1}{2} \sum_{m=k}^{n_L} c^{m-i} \\ &= \frac{2 - c^{k-i} \left(1 + c^{n_L - k + 1}\right)}{2(1-c)}, \quad for \quad j \leq i < k, \end{aligned} \tag{14}$$

$$\begin{aligned} \boldsymbol{R}_i &= \sum_{m=i+1}^{j} c^{m-i-1} + \frac{1}{2} \sum_{m=j}^{k-1} c^{m-i} + \frac{1}{4} \sum_{m=k}^{n_L} c^{m-i}, \quad for \quad i < j \\ &= \frac{4 - c^{k-i} - c^{j-i} \left(2 + c^{n_L - j + 1}\right)}{4(1-c)}, \end{aligned} \tag{15}$$

where n_L is the number of nodes in the line. The PageRank of the new nodes e_1 and e_2 are respectively,

$$\boldsymbol{R}_{e_1} = 1 + \frac{1}{2} c \left(\frac{1 - c^{k-j}}{1 - c} \right) + \frac{1}{4} c^{k-j+1} \left(\frac{1 - c^{n_L - k + 1}}{1 - c} \right) \tag{16}$$

and

$$\boldsymbol{R}_{e_2} = 1 + \frac{1}{2} c \left(\frac{1 - c^{n_L - k + 1}}{1 - c} \right). \tag{17}$$

Proof. Consider nodes v_j and $v_k, k > j$ on the line graph G_L. The PageRank, for the node $i \geq k$ can be found in the same way as the PageRank on directed line graph. By Theorem 1 and using the fact that $\mathbf{u}$ is the uniform vector. The probability of hitting node e_i starting at node e_j in the line is

$$P_{ji}, j > i$$

Then, the overall PageRank, $\boldsymbol{R}_i$ if $i \geq k$ is determined by summing over all nodes for which $i \geq k$ is true.

$$\begin{aligned} \boldsymbol{R}_i &= \sum_{e_m \in S, e_m \neq e_i} P_{mi} + 1, \\ &= \sum_{m=i+1}^{n_L} c^{m-i} + 1 = \frac{1 - c^{n_L - i + 1}}{1 - c}. \end{aligned}$$

This ends the proof of the first part (Equation (13)).

To find the PageRank in the line graph for which $j \leq i < k$. We observe that

$$P_{kk-1} = \frac{1}{2} c \boldsymbol{R}_k,$$

where $\boldsymbol{R}_k$ is the PageRank at the node labeled k. Using this argument, the overall PageRank for $j \leq i < k$ is $\frac{1}{2}c^{k-i}\boldsymbol{R}_k$ plus the PageRank of a directed line graph between j and k, i.e.

$$\frac{1-c^{k-i}}{1-c}.$$

Adding and simplifying the two terms

$$\begin{aligned}\boldsymbol{R}_i &= \frac{1-c^{k-i}}{1-c} + \frac{1}{2}c^{k-i}\boldsymbol{R}_k, \\ &= \frac{2-c^{k-i}\left(1+c^{n_L-k+1}\right)}{2(1-c)}, \quad \text{for} \quad j \leq i < k.\end{aligned}$$

Further, to obtain the PageRank for $i < j$, we first look at the probability of the nodes labeled j and k hitting its neighboring nodes on the line, say e_i. These can be presented as

$$P_{ki} = \frac{1}{4}c^{k-i} \quad \text{and} \quad P_{ji} = \frac{1}{2}c^{j-i},$$

respectively. Also, we need to consider the PageRank on the nodes n_1 to n_{j-1} for the portion of directed line graph. This is essentially equal to

$$\sum_{m=i+1}^{j} c^{m-i-1} + 1 = \frac{1-c^{j-i}}{1-c}.$$

The overall $\boldsymbol{R}_i$ for $i < j$, is

$$\boldsymbol{R}_i = \sum_{m=i+1}^{j} c^{m-i-1} + \sum_{m=j}^{k-1} P_{mi} + \sum_{l=k}^{n_L} P_{li},$$

where

$$P_{mi} = \frac{1}{2}c^{m-i} \quad \text{and} \quad P_{li} = \frac{1}{4}c^{l-i}.$$

Substitute and simplify to obtain

$$\begin{aligned}\boldsymbol{R}_i &= \sum_{m=i+1}^{j} c^{m-i-1} + \frac{1}{2}\sum_{m=j}^{k-1} c^{m-i} + \frac{1}{4}\sum_{l=k}^{n_L} c^{l-i}, \\ &= \frac{4-c^{k-i}-c^{j-i}\left(2+c^{n_L-j+1}\right)}{4(1-c)}.\end{aligned}$$

Finally, the PageRank of $\boldsymbol{R}_{e_2}$ is equal to

$$P_{k1} + 1 = 1 + \frac{1}{2}c\boldsymbol{R}_k, \quad \text{therefore} \quad \boldsymbol{R}_k = \frac{1-c^{n_L-k+1}}{1-c}.$$

Similarly,

$$\begin{aligned}\boldsymbol{R}_{e_1} &= P_{j1} + 1,\\ &= \frac{1}{2}c\boldsymbol{R}_j + 1,\\ &= 1 + \frac{1}{2}c\left(\frac{1-c^{k-j}}{1-c}\right) + \frac{1}{4}c^{k-j+1}\left(\frac{1-c^{n_L-k+1}}{1-c}\right)\end{aligned}$$

and this completes the proof.

4 Connecting the simple line with two links from the line to two complete graphs

Consider a network S in which a directed line graph G_L is connected to two complete graphs S_{G_1} and S_{G_2} such that $S = S_L \cup S_{G_1} \cup S_{G_2}$. Assume that subgraph S_{G_1} and $S_{G_2}$is linked to nodes j and k respectively as shown in Figure 5.

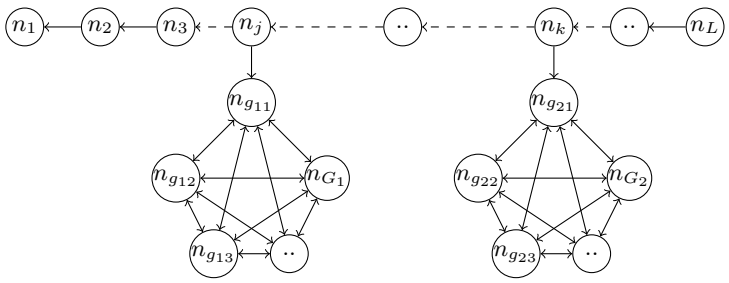

Fig. 5. A simple line with two links from the line to two complete graphs

Theorem 3. *Let S be a system made up of three systems: a simple line S_L with n_L nodes, two complete graphs, S_{G_1} and S_{G_2}, with n_{G_1} and n_{G_2} nodes, respectively. We add two links from nodes j and k, $j < k$ in the line to nodes g_j and g_k in the first and second complete graph, respectively. Assuming uniform weight vector $\boldsymbol{u}$, we get the PageRank $\boldsymbol{R}_{L,i}$, where $S_G = S_{G_1} \cup S_{G_2}$, for the nodes in the line after the new links, $\boldsymbol{R}_{G_1,i}$ for the nodes in the first complete graph S_{G_1} and $\boldsymbol{R}_{G_2,i}$ for the nodes in the second complete graph S_{G_2} as:*

$$\boldsymbol{R}_{L,i} = \sum_{m=i}^{n_L} c^{m-i} = \frac{1-c^{n_L-i+1}}{1-c}, \quad \textit{for} \quad i \geq k, \tag{18}$$

$$\begin{aligned}\boldsymbol{R}_{L,i} &= \sum_{m=i+1}^{k} c^{m-i-1} + \frac{1}{2}\sum_{m=k}^{n_L} c^{m-i}, \quad \textit{for} \quad j \leq i < k\\ &= \frac{2 - c^{k-i}\left(1 + c^{n_L-k+1}\right)}{2(1-c)}, \quad \textit{for} \quad j \leq i < k,\end{aligned} \tag{19}$$

$$\boldsymbol{R}_{L,i} = \sum_{m=i+1}^{j} c^{m-i-1} + \frac{1}{2}\sum_{m=j}^{k-1} c^{m-i} + \frac{1}{4}\sum_{m=k}^{n_L} c^{m-i}, \quad for \quad i<j$$
$$= \frac{4 - c^{k-i} - c^{j-i}\left(2 + c^{n_L-j+1}\right)}{4(1-c)}, \tag{20}$$

where n_L is the number of nodes in the line. The PageRank of the nodes in the complete graphs are given by

$$\boldsymbol{R}_{G_2,g_k} = \frac{c}{2}\left(\frac{1-c^{n_L-k+1}}{1-c}\right)\left(\frac{(n_{G_2}-1)-c(n_{G_2}-2)}{(n_{G_2}-1)-c(n_{G_2}-2)-c^2}\right) + \frac{1}{1-c} \tag{21}$$

$$\boldsymbol{R}_{G_2,i} = \left(\frac{c^2(1-c^{n_L-k+1})}{2(1-c)}\right)\left(\frac{1}{(n_{G_2}-1)-c(n_{G_2}-2)-c^2}\right) + \frac{1}{1-c} \tag{22}$$

$$\boldsymbol{R}_{G_1,g_j} = \left[\frac{2c - c^{k-j+1} - c^{n_L-j+2}}{4(1-c)}\right]\left[\frac{(n_{G_1}-1)-c(n_{G_1}-2)}{(n_{G_1}-1)-c(n_{G_1}-2)-c^2}\right] + \frac{1}{1-c} \tag{23}$$

$$\boldsymbol{R}_{G_1,i} = \left[\frac{2c^2 - c^{k-j+2} - c^{n_L-j+3}}{4(1-c)}\right]\left[\frac{1}{(n_{G_1}-1)-c(n_{G_1}-2)-c^2}\right] + \frac{1}{1-c} \tag{24}$$

where $\boldsymbol{R}_{G_1,g_j}$ is the PageRank for the node in the complete graph S_{G_1} linked by the line and $\boldsymbol{R}_{G_1,i}$ is the PageRank of the other nodes in S_{G_1}. Similarly, $\boldsymbol{R}_{G_2,g_k}$ is the PageRank for the node in the complete graph S_{G_2} linked by the line and $\boldsymbol{R}_{G_2,i}$ is the PageRank of the other nodes in S_{G_2}.

Proof. The prove of Equations (18), (19) and (20) can be done in the similar way as in Theorem 2 parts (13) and (14).

In addition, the proofs of Equations (21), (22), (23) and (24) are similarly done using Theorem 2 and blockwise inversion of line and complete graphs as in Engström and Silvestrov[5].

5 Conclusions

We have observed that these simple construction of networks can be used to understand common graph such as star, complete graph and many others. Their PageRanks are determined with minimum numerical consideration and this is advantageous for visual identification of important nodes in a simple directed networks. We have noted that probability approach to determine the PageRank of simple graphs seem to be straight forward compared to blockwise matrix inversion approach, particularly to line directed graphs with multiple outside nodes and complete graphs.

Acknowledgements This research was supported by the Swedish International Development Cooperation Agency (Sida), International Science Programme (ISP) in Mathematical Sciences (IPMS), Sida Bilateral Research Program (Makerere University and University of Dar es Salaam). We are also grateful to the research environment Mathematics and Applied Mathematics (MAM), Division of Applied Mathematics, Mälardålen University for providing an excellent and inspiring environment for research education and research.

References

1. S. Brin and L. Page. The anatomy of a large-scale hypertextual Web search engine. *Computer Networks and ISDN Systems* **30**(1-7), 107-117 (1998). Proceedings of the Seventh International World Wide Web Conference.
2. S.D. Kamvar, M.T. Schlosser and H. Garcia-Molina. The eigentrust algorithm for reputation management in p2p networks. In: Proceedings of the 12th international conference on World Wide Web, WWW '03, pp. 640-651, 2003
3. J.R. Norris. *Markov chains*. Cambridge University Press, New York, 2009.
4. S.D. Kamvar and T. Haveliwala. The Condition Number of the PageRank Problem. *Technical Report*, Stanford InfoLab, 2003.
5. C. Engström and S. Silvestrov. PageRank, a look at small changes in a line of nodes and the complete graph. In: Silvestrov S., Rančić M. (eds) Engineering Mathematics II. *Springer Proceedings in Mathematics & Statistics*, vol 179. Springer, Cham,2016.
6. C. Engström and S. Silvestrov. PageRank, connecting a line of nodes with a complete graph. In: Silvestrov S., Rančić M. (eds) Engineering Mathematics II. *Springer Proceedings in Mathematics & Statistics*, vol 179. Springer, Cham, 2016.
7. H. Ishii, R. Tempo, E.W. Bai and F. Dabbene. Distributed randomized pagerank computation based on web aggregation. In: Decision and Control, 2009 held jointly with the 2009 28th Chinese Control Conference. CDC/CCC 2009. *Proceedings of the 48th IEEE Conference* on, pp. 3026-3031, 2009.
8. F. Anderson and S. Silvestrov. The mathematics of Internet search engines. *Acta Appl. Math.* **104**, 211-242, 2008.
9. A. Berman and R.J. Plemmons. *Nonnegative Matrices in the Mathematical Sciences*. Society for Industrial and Applied Mathematics, 1994.
10. S. Battiston, M. Puliga, R. Kaushik, P. Tasca and G. Calderelli. DeptRank: Too central to fail? Financial networks, the fed and systemic risk. *Tech. rep.*, 2012.
11. D. Dhyani, S.S. Bhowmick and WK. Ng. Deriving and Verifying Statistical Distribution of a Hyperlink-Based Web Page Quality Metric. *Data Knowl. Eng.* **46**(3), 291-315, 2003.
12. T. Haveliwala and S. Kamvar. The second eigenvalue of the google matrix. *Technical Report* 2003-20, Stanford InfoLab, 2003.
13. S. Kamvar, T. Haveliwala and G. Golub. Adaptive methods for the computation of pagerank. *Linear Algebra and its Applications* **386**(0), 51-65, 2004.
14. C. Engström and S. Silvestrov. A componentwise pagerank algorithm. In: Applied Stochastic Models and Data Analysis (ASMDA 2015). The 16th Conference of the ASMDA International Society, p. (in press) (2015).
15. D. Bernstein. Matrix Mathematics. Princeton Unversity Press, (2005).

Designing critical infrastructure network with cascading for predefined safety level

Agnieszka Blokus-Roszkowska[1] and Krzysztof Kołowrocki[2]

[1] Gdynia Maritime University, Gdynia, Poland
(E-mail: a.blokus-roszkowska @wn.am.gdynia.pl)
[2] Gdynia Maritime University, Gdynia, Poland
(E-mail: k.kolowrocki@wn.am.gdynia.pl)

Abstract. The multistate approach to cascading effect modeling in critical infrastructure (CI) networks is proposed. Describing cascading effects in CI networks both the dependencies between subnetworks of this network and between their assets are considered. Proposed theoretical models are applied to the safety analysis of the exemplary network of transmission lines regarding dependencies of its lines and subnetworks. For presented exemplary network, the intensities of departure from the safety state subsets of transmission lines are estimated for arbitrarily assumed values of the network mean lifetimes.
Keywords: multistate approach, ageing network, cascading effects, dependency model.

1 Introduction

In the paper we describe and analyse local load sharing (LLS) model of dependency for a series network, equal load sharing (ELS) model of dependency for a parallel network and mixed load sharing (MLS) rule for a parallel-series network. In such networks, taking into account dependencies between assets and subnetworks, after changing the safety state subset by some of assets or subnetworks to the worse safety state subset, the lifetimes of remaining assets, respectively subnetworks, in the safety state subsets decrease. Models of dependency and behavior of components can differ depending on the structural and material properties of the network, operational conditions and many other factors, as for example natural hazards. According to the equal load sharing rule [15], [16], after changing the safety state subset by some of assets to the worse safety state subset, the lifetimes of remaining assets in the safety state subsets decrease equally depending, inter alia, on the number of these assets that have left the safety state subset [3], [4], [6]. In the local load sharing model of dependency [8], [9], after departure from the safety state subset by one

of assets the safety parameters of remaining assets are changing dependently of the coefficients of the network load growth [1], [5], [6]. These coefficients are concerned with the distance from the asset that has got out of the safety state subset and can be interpreted in the metric sense as well as in the sense of relationships in the functioning of the network. Apart from the dependency of assets' departures from the safety states subsets, the dependencies between subnetworks are also taken into account in this paper [5]-[7].

2 Multistate series CI network with dependent assets

Describing cascading effects in a series network we can consider a network composed of n ageing assets denoted by E_i, $i = 1,\ldots,n$. We assume all assets and a CI network have the safety state set $\{0,1,...,z\}$, $z \geq 1$, where the safety state 0 is the worst and the safety state z is the best [11], [12]. Further, we assume that after changing the safety state subset by one of assets in a network to the worse safety state subset, the lifetimes of remaining assets in the safety state subsets decrease dependently of the distance from the asset that has left the safety state subset. More exactly, we assume that these lifetimes decrease mostly for neighbour components in first line, then less for neighbour components in second line and so on and we call this rule of components dependency a local load sharing (LLS) rule. The local load sharing rule for a multistate series network is described in [5], [7].

We denote by $E[T_i(u)]$ and $E[T_{i/j}(u)]$, $i = 1,2,...,n$, $j = 1,2,...,n$, $u = 1,2,\ldots,z$, the mean values of components' lifetimes $T_i(u)$ and $T_{i/j}(u)$, respectively, before and after departure of one fixed component E_j, $j = 1,\ldots,n$, from the safety state subset $\{u,u+1,\ldots,z\}$, $u = 1,2,\ldots,z$. With this notation, in considered LLS rule, the mean values of components lifetimes in the safety state subset $\{\upsilon,\upsilon+1,\ldots,z\}$, $\upsilon = u,u-1,\ldots,1$, $u = 1,2,\ldots,z$, are decreasing according to the following formula:

$$T_{i/j}(\upsilon) = q(\upsilon, d_{ij}) \cdot T_i(\upsilon), \quad E[T_{i/j}(\upsilon)] = q(\upsilon, d_{ij}) \cdot E[T_i(\upsilon)],$$
$$i = 1,\ldots,n, j = 1,\ldots,n, \ \upsilon = u, u-1,\ldots,1, \tag{1}$$

where the coefficients of the network load growth $q(\upsilon, d_{ij})$, $0 < q(\upsilon, d_{ij}) \leq 1$, $i = 1,\ldots,n$, $j = 1,\ldots,n$, and $q(\upsilon,0) = 1$ for $\upsilon = u,u-1,\ldots,1$, $u = 1,2,\ldots,z-1$, are functions of components' distance $d_{ij} = |i-j|$ from the component that has got out of the safety state subset $\{u,u+1,\ldots,z\}$, $u = 1,2,\ldots,z$. The distance between network assets can be interpreted in the metric sense as well as in the sense of relationships in the functioning of the network components.

The safety function of a multistate series network with assets dependent according to LLS rule is given in [7] and in case of assets with exponential safety functions the results can be found in [5]. In [5] the safety analysis of a multistate series network with dependent subnetworks and of a multistate series network with dependent assets of its subnetworks is also presented.

We consider a multistate series network composed of assets having identical

exponential safety functions

$$S(t,\cdot) = [1, S(t,1), \ldots, S(t,z)],\ t \geq 0, \tag{2}$$

with the coordinates

$$S(t,u) = \exp[-\lambda(u)t], t \geq 0, \lambda(u) \geq 0,\ u = 1,2,\ldots,z, \tag{3}$$

where $\lambda(u)$, $u = 1,2,\ldots,z$, are components' intensities of departure from the safety state subset $\{u,u+1,\ldots,z\}$, $u = 1,2,\ldots,z$. Then, the intensities $\lambda_{i/j}(\upsilon)$, $i = 1,\ldots,n$, $j = 1,\ldots,n$, $\upsilon = u,u-1,\ldots,1$, of components' departure from this safety state subset after the departure of the jth component E_j, $j = 1,\ldots,n$, from (1), are given by

$$\lambda_{i/j}(\upsilon) = \frac{\lambda(\upsilon)}{q(\upsilon, d_{ij})},\ \upsilon = u, u-1,\ldots,1. \tag{4}$$

In this case from results presented in [7] we can obtain the following proposition.

Proposition 1. If in a multistate series network assets are dependent according to the local load sharing rule and have identical exponential safety functions (2)-(3), then its safety function is given by the vector

$$\boldsymbol{S}_{LLS}(t,\cdot) = [1, \boldsymbol{S}_{LLS}(t,1), \ldots, \boldsymbol{S}_{LLS}(t,z)],\ t \geq 0, \tag{5}$$

with the coordinates

$$\boldsymbol{S}_{LLS}(t,u) = \exp[-n\lambda(u+1)t]$$

$$+\frac{1}{n}\sum_{j=1}^{n}[\exp[-\lambda(u)\sum_{i=1}^{n}\frac{1}{q(u,d_{ij})}t] - \exp[-(n\lambda(u+1) - n\lambda(u) + \lambda(u)\sum_{i=1}^{n}\frac{1}{q(u,d_{ij})})t]],$$

$$u = 1,2,\ldots,z-1, \tag{6}$$

$$\boldsymbol{S}_{LLS}(t,z) = \exp[-n\lambda(z)t]. \tag{7}$$

From *Proposition 1*, we immediately obtain a corollary concerned with the mean values and standard deviations of the lifetimes in the safety state subsets of a multistate series network.

Corollary 1. If in a multistate series network components are dependent according to the local load sharing rule and have identical exponential safety functions (2)-(3), then its mean lifetime in the safety state subset $\{u,u+1,\ldots,z\}$, $u = 1,2,\ldots,z$, is given by

$$\mu_{LLS}(u) = \frac{1}{n\lambda(u+1)} + \sum_{j=1}^{n}\frac{1}{n}$$

$$\cdot[\frac{1}{\lambda(u)\sum_{i=1}^{n}\frac{1}{q(u,d_{ij})}} - \frac{1}{n\lambda(u+1) - n\lambda(u) + \lambda(u)\sum_{i=1}^{n}\frac{1}{q(u,d_{ij})}}], \; u = 1,2,\ldots,z-1, \tag{8}$$

$$\mu_{LLS}(z) = \frac{1}{n\lambda(z)}, \tag{9}$$

and the standard deviation of the network sojourn time in the safety state subset $\{u,u+1,\ldots,z\}$, $u = 1,2,\ldots,z$, is given by

$$\sigma_{LLS}(u) = \sqrt{n_{LLS}(u) - [\mu_{LLS}(u)]^2}, \; u = 1,2,\ldots,z-1, \tag{10}$$

where

$$n_{LLS}(u) = \frac{2}{[n\lambda(u+1)]^2}$$

$$+ 2\sum_{j=1}^{n}\frac{1}{n} \cdot[\frac{1}{[\lambda(u)\sum_{i=1}^{n}\frac{1}{q(u,d_{ij})}]^2} - \frac{1}{[n\lambda(u+1) - n\lambda(u) + \lambda(u)\sum_{i=1}^{n}\frac{1}{q(u,d_{ij})}]^2}], \tag{11}$$

and

$$\sigma_{LLS}(z) = \frac{1}{n\lambda(z)}. \tag{12}$$

Further, knowing the mean lifetimes $\mu_{LLS}(u)$ in the safety state subsets $\{u,u+1,\ldots,z\}$, $u = 1,2,\ldots,z$, of a multistate series network, using formulae (8)-(9), we can determine the intensities $\lambda(u)$, $u = 1,2,\ldots,z$, of assets' departure from the safety state subset $\{u,u+1,\ldots,z\}$. Namely, from (9) we can estimate the intensity $\lambda(z)$

$$\lambda(z) = \frac{1}{n\mu_{LLS}(z)}, \tag{13}$$

and substituting it into formula (8) for $u = z-1$ we get

$$n\mu_{LLS}(z-1)-n\mu_{LLS}(z)$$

$$=\sum_{j=1}^{n}\left[\frac{1}{\lambda(z-1)\sum_{i=1}^{n}\frac{1}{q(z-1,d_{ij})}}-\frac{1}{\frac{1}{\mu_{LLS}(z)}-n\lambda(z-1)+\lambda(z-1)\sum_{i=1}^{n}\frac{1}{q(z-1,d_{ij})}}\right]. \quad (14)$$

Next, from formula (14), for assumed values of the coefficients of the network load growth $q(z-1,d_{ij})$, we can estimate the intensity $\lambda(z-1)$. Similarly, using (8) for $u = z$-2,…,1, we can estimate the intensities $\lambda(z-2),\ldots,\lambda(1)$.

Then, according to the well known relationship between the lifetime mean value in this safety state subset and the intensity of departure from this safety state subset we can determine the mean values of assets' lifetimes in the safety state subsets $\{u,u+1,\ldots,z\}$, $u = 1,2,\ldots,z$.

3 Multistate parallel CI network with dependent assets

For a parallel network composed of n assets we assume that after decreasing the safety state by one of the assets the increased load can be shared equally among the remaining assets. More generally, we assume that after leaving the safety state subset by some of assets, the lifetimes of remaining assets decrease equally depending on the number of these assets that have left the safety state subset. Additionally these changes are influenced by the component stress proportionality correction coefficient, concerned with features of particular network and its assets. More exactly, if $\omega, \omega = 0,1,2,\ldots,n-1,$ assets are out of the safety state subset $\{u,u+1,...,z\}$, the mean values of the lifetimes $T_i'(u)$ in the safety state subset $\{u,u+1,...,z\}$ of the remaining assets become less according to the formula

$$E[T_i'(u)] = c(u)\frac{n-\omega}{n}E[T_i(u)],\ i=1,2,\ldots,n,\ u=1,2,\ldots,z, \quad (15)$$

where $c(u)$ is the component stress proportionality correction coefficient for each u, $u=1,2,\ldots,z$, [4], [6].

Hence, for case of network with dependent assets having identical exponential safety functions (2)-(3), we get following formula for intensities of departure from the safety state subset $\{u,u+1,...,z\}$, of remaining assets

$$\lambda^{(\omega)}(u) = \frac{n}{n-\omega}\frac{\lambda(u)}{c(u)},\ \omega=0,1,\ldots,n-1,\ u=1,2,\ldots,z. \quad (16)$$

Proposition 2. If in a multistate parallel network assets are dependent according to the equal load sharing rule and have identical exponential safety functions

(2)-(3), then its safety function is given by the vector

$$\boldsymbol{S}_{ELS}(t,\cdot) = [1, \boldsymbol{S}_{ELS}(t,1), \ldots, \boldsymbol{S}_{ELS}(t,z)],\ t \geq 0, \tag{17}$$

with the coordinates

$$\boldsymbol{S}_{ELS}(t,u) = \sum_{\omega=0}^{n-1} \frac{\left[\frac{n\lambda(u)}{c(u)}t\right]^{\omega}}{\omega!} \exp[-\frac{n\lambda(u)}{c(u)}t],\ u = 1,2,\ldots,z. \tag{18}$$

Corollary 2. If in a multistate parallel network assets are dependent according to the equal load sharing rule and have identical exponential safety function given by (2)-(3), then the system lifetime in the safety state subset $\{u,u+1,\ldots,z\}$, $u = 1,2,\ldots,z$, has Erlang distribution with the shape parameter n and the scale parameter $n\lambda(u)/c(u)$, $u = 1,2,\ldots,z$.

Corollary 3. If in a homogeneous multistate parallel system components are dependent according to the equal load sharing rule and have identical exponential safety functions (2)-(3), then its mean lifetime in the safety state subset $\{u,u+1,\ldots,z\}$ is given by

$$\mu_{ELS}(u) = \frac{c(u)}{\lambda(u)},\ u = 1,2,\ldots,z, \tag{19}$$

and the standard deviation of the networks sojourn time in the safety state subset $\{u,u+1,\ldots,z\}$ is given by

$$\sigma_{ELS}(u) = \frac{c(u)}{\sqrt{n}\cdot\lambda(u)},\ u = 1,2,\ldots,z. \tag{20}$$

4 Multistate parallel-series network with dependent subnetworks and dependent assets of these subnetworks

Considering cascading effects in networks with more complex structures we can link the results of safety analysis for previously described dependency models. Then, apart from the dependency of subnetworks' departures from the safety states subsets we can take into account the dependencies between assets in subnetworks. This way we can proceed with parallel-series network assuming the dependence between its parallel subnetworks according to the local load sharing rule and the dependence between their assets in subnetworks according to the equal load sharing rule. Further, such model of dependency we will call a mixed load sharing (MLS) model [6], [7].

In this section, we propose MLS model of dependency between subnetworks and between assets in these subnetworks. We consider a multistate parallel-series network composed of k parallel subnetworks N_i, $i = 1,2,\ldots,k$, connected in series, illustrated in Figure 1. Further, by E_{ij}, $i = 1,2,\ldots,k$, $j = 1,2,\ldots,l$, we denote the jth asset being in the ith subnetwork N_i, and we assume that all assets have identical exponential safety functions, given by (2)-(3).

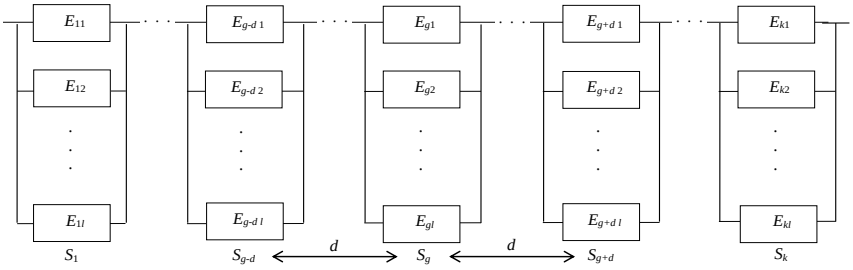

Figure 1. The scheme of a regular parallel-series system.

In each parallel subnetwork we consider dependency of its l assets according to ELS model, presented in Section 3. Then, after departure from the safety state subset $\{u,u+1,\ldots,z\}$, $u = 1,2,\ldots,z$, by $\omega, \omega = 0,1,2,\ldots,l-1$, assets of the subnetwork, the intensities of departure from this safety state subset of the remaining assets in the subnetwork from (16) are given by

$$\lambda^{(\omega)}(u) = \frac{l}{l-\omega}\frac{\lambda(u)}{c(u)},\ \omega = 0,1,\ldots,l-1,\ u = 1,2,\ldots,z. \tag{21}$$

Further, between these subnetworks, linked in series, we assume LLS model of dependency, presented in Section 2. Then, we assume that after departure from the safety state subset $\{u,u+1,\ldots,z\}$, $u = 1,2,\ldots,z$, by the subnetwork N_g, $g = 1,2,\ldots,k$, the safety parameters of assets of remaining subnetworks are changing dependently of the distance from the subnetwork that has got out of the safety state subset $\{u,u+1,\ldots,z\}$, $u = 1,2,\ldots,z$, expressed by index d. However, within a single subnetwork the changes of the safety parameters for all of its assets are on the same level according to the equal load sharing rule. The meaning of the distance d in MLS model is illustrated in Figure 1.

We denote by $E[T_{i,j}(u)]$ and $E[T_{i/g,j}(u)]$, $i = 1,2,...,k$, $g = 1,2,...,k$, $j = 1,2,...,l$, $u = 1,2,\ldots,z$, the mean values of the lifetimes of ith subnetwork assets $T_{i,j}(u)$ and $T_{i/g,j}(u)$, respectively, before and after departure of one fixed subnetwork N_g, $g = 1,\ldots,k$, from the safety state subset $\{u,u+1,\ldots,z\}$, $u = 1,2,\ldots,z$. With this notation, in LLS model used between subnetworks, the mean values of their components lifetimes in the safety state subset $\{\upsilon,\upsilon+1,\ldots,z\}$, $\upsilon = u,u-1,\ldots,1$, $u = 1,2,\ldots,z$, are decreasing, using (1), according to the following formula

$$E[T_{i/g,j}(\upsilon)] = q(\upsilon, d_{ig}) \cdot E[T_{i,j}(\upsilon)],\ i = 1,2,...,k,\ g = 1,2,...,k,\ j = 1,2,...,l, \tag{22}$$

where the coefficients of the network load growth $q(\upsilon,d_{ig})$ for $\upsilon = u,u\text{-}1,\ldots,1$, $u = 1,2,\ldots,z\text{-}1$, are functions of subnetworks' distance $d_{ig} = |i - g|$ from the subnetwork N_g that has got out of the safety state subset $\{u,u+1,\ldots,z\}$, $u = 1,2,\ldots,z$.

Considering Corollary 2 and results given in [6], concerned with Erlang distribution of network lifetime in the safety state subset $\{u,u+1,\ldots,z\}$, $u = 1,2,\ldots,z$, in case assets of parallel network are dependent according to ELS rule, and linking this result with the safety function of a series network with assets dependent according to LLS rule and having Erlang safety functions, presented in [6], we can obtain the safety function of a multistate parallel-series network with mixed model of dependency.

Proposition 3. If in a multistate parallel-series netowork, there are k parallel subnetworks dependent according to the local load sharing rule and assets of these parallel subnetworks are dependent according to the equal load sharing rule and have exponential safety functions (2)-(3), then its safety function is given by the vector

$$\boldsymbol{S}_{MLS}(t,\cdot) = [1, \boldsymbol{S}_{MLS}(t,1), \ldots, \boldsymbol{S}_{MLS}(t,z)],\ t \geq 0, \tag{23}$$

with the coordinates

$$\boldsymbol{S}_{MLS}(t,u) = \prod_{i=1}^{k}[\sum_{\omega=0}^{l_i-1}\frac{[\frac{l_i\lambda_i(u+1)}{c_i(u+1)}t]^{\omega}}{\omega!}]\cdot\exp[-\frac{l_i\lambda_i(u+1)}{c_i(u+1)}t]$$

$$+\sum_{g=1}^{k}\int_0^t \tilde{f}_g(a,u+1)\cdot\prod_{\substack{i=1\\i\neq g}}^{k}[\sum_{\omega=0}^{l_i-1}\frac{[\frac{l_i\lambda_i(u+1)}{c_i(u+1)}a]^{\omega}}{\omega!}]\cdot\sum_{\omega=0}^{l_g-1}\frac{[\frac{l_g\lambda_g(u)}{c_g(u)}a]^{\omega}}{\omega!}$$

$$\cdot\exp[-(\sum_{\substack{i=1\\i\neq g}}^{k}\frac{l_i\lambda_i(u+1)}{c_i(u+1)}+\frac{l_g\lambda_g(u)}{c_g(u)})a]$$

$$\cdot[\prod_{i=1}^{k}\frac{\sum_{\omega=0}^{l_i-1}\frac{[\frac{l_i\lambda_i(u)}{c_i(u)q(u,d_{ig})}t]^{\omega}}{\omega!}}{\sum_{\omega=0}^{l_i-1}\frac{[\frac{l_i\lambda_i(u)}{c_i(u)}a]^{\omega}}{\omega!}}\cdot\exp[-\frac{l_i\lambda_i(u)}{c_i(u)q(u,d_{ig})}t+\frac{l_i\lambda_i(u)}{c_i(u)}a]]da,$$

$$u = 1,2,\ldots,z-1, \tag{24}$$

where $\tilde{f}_g(a,u+1)$ is given by

$$\tilde{f}_g(a,u+1) = [[\sum_{\omega=0}^{l_g-1} \frac{[\frac{l_g\lambda_g(u+1)}{c_g(u+1)}a]^\omega}{\omega!} \cdot \sum_{\omega=0}^{l_g-2} \frac{[\frac{l_g\lambda_g(u)}{c_g(u)}]^{\omega+1}a^\omega}{\omega!}$$

$$- \sum_{\omega=0}^{l_g-2} \frac{[\frac{l_g\lambda_g(u+1)}{c_g(u+1)}]^{\omega+1}a^\omega}{\omega!} \cdot \sum_{\omega=0}^{l_g-1} \frac{[\frac{l_g\lambda_g(u)}{c_g(u)}a]^\omega}{\omega!}] \,/\, [\sum_{\omega=0}^{l_g-1} \frac{[\frac{l_g\lambda_g(u)}{c_g(u)}a]^\omega}{\omega!}]^2$$

$$+ \sum_{\omega=0}^{l_g-1} \frac{[\frac{l_g\lambda_g(u+1)}{c_g(u+1)}a]^\omega}{\omega!} (\frac{l_g\lambda_g(u+1)}{c_g(u+1)} - \frac{l_g\lambda_g(u)}{c_g(u)}) / \sum_{\omega=0}^{l_g-1} \frac{[\frac{l_g\lambda_g(u)}{c_g(u)}a]^\omega}{\omega!}]$$

$$\cdot \exp[-(\frac{l_g\lambda_g(u+1)}{c_g(u+1)} - \frac{l_g\lambda_g(u)}{c_g(u)})a],\ u = 1,2,\ldots,z-1, \tag{25}$$

and

$$\boldsymbol{S}_{MLS}(t,z) = \prod_{i=1}^{k} [\sum_{\omega=0}^{l_i-1} \frac{[\frac{l_i\lambda_i(z)}{c_i(z)}t]^\omega}{\omega!}]^k \cdot \exp[-\sum_{i=1}^{k} \frac{l_i\lambda_i(z)}{c_i(z)}t]. \tag{26}$$

Further, knowing the mean lifetimes $\mu_{MLS}(u)$ in the safety state subsets $\{u,u+1,\ldots,z\}$, u = 1,2,…,z, of a multistate parallel-series network, from (13)-(14), we can estimate the intensities $\lambda_{N_i}(u)$, u = 1,2,…,z, of departure from the safety state subset $\{u,u+1,\ldots,z\}$ of subnetworks N_i, i = 1,2,…,k.

Namely, from (13) we get $\lambda_{N_i}(z)$ given by

$$\lambda_{N_i}(z) = \frac{1}{k \cdot \mu_{MLS}(z)} \tag{27}$$

and $\lambda_{N_i}(u)$, u = z-1, z-2,…,1, can be estimated from

$$k \cdot \mu_{MLS}(u) - \frac{1}{k \cdot \lambda_{N_i}(u+1)} =$$

$$\sum_{g=1}^{k}\left[\frac{1}{\lambda_{N_i}(u)\sum_{i=1}^{k}\frac{1}{q(u,d_{ig})}}-\frac{1}{k\cdot\lambda_{N_i}(u+1)-k\cdot\lambda_{N_i}(u)+\lambda_{N_i}(u)\sum_{i=1}^{k}\frac{1}{q(u,d_{ig})}}\right]. \quad (28)$$

Then, for each parallel subnetwork with assets dependent according to ELS rule, from Corollary 2 about Erlang distribution of the subnetwork lifetime, we can obtain the intensities $\lambda(u)$, $u = 1,2,\ldots,z$, of this subnetwork assets' departures. The intensity of departure from the state z, using (27), is

$$\lambda(z)=\frac{c(z)}{kl\cdot\mu_{MLS}(z)} \quad (29)$$

and the intensities of departure from the state subsets $\{u,u+1,\ldots,z\}$, $u = z-1, z-2, \ldots,1$, are given by

$$\lambda(u)=\frac{c(u)\cdot\lambda_{N_i}(u)}{l}, \quad (30)$$

where $\lambda_{N_i}(u)$ can be estimated from (28).

4 Application – Exemplary CI Network

As an example of a critical infrastructure network [2] we consider a network of transmission lines between distribution substations. Authors in [10] present reliability and risk analysis of power systems including cascading interruptions. Here, we analyze safety of a network N of transmission lines between eight substations ($k = 8$). We assume that subsystems N_i, $i = 1,2,\ldots,8$, of lines between substations form a series safety structure and are dependent according to LLS rule. Each to substations are connected by two or three transmission lines in parallel safety structure and we assume ELS model of dependency between them. In first case we assume that there are two lines in operation between each two substations i.e. $l = 2$. Thus, we can conclude that an exemplary CI network can be analyzed as a parallel-series network under MLS model of dependency, described in Section 3.

We assume that the network N is a 5-state system ($z = 4$) and we arbitrarily distinguish the following four safety states of the network and its assets:

- a safety state 4 – the transmission line is new and fully effective, the network operation is fully effective,
- a safety state 3 – the transmission line is not new but fully effective and the network operation is fully effective,
- a safety state 2 – the transmission line is in operation, but it is suitable for further use, the network operation is less effective because of ageing,

- a safety state 1 – advanced ageing processes in the transmission lines and there is a high risk of failure, the network operation is less effective and does not provide sufficient transmission capacity,
- a safety state 0 – the network or transmission line is destroyed.

Further, knowing the mean lifetimes $\mu_{MLS}(1)$, $\mu_{MLS}(2)$, $\mu_{MLS}(3)$, $\mu_{MLS}(4)$, of a network N, respectively in the safety state subsets {1,2,3,4}, {2,3,4}, {3,4}, {4}, from (27)-(28), we can estimate the intensities $\lambda_{N_i}(1)$, $\lambda_{N_i}(2)$, $\lambda_{N_i}(3)$, $\lambda_{N_i}(4)$, of departure from these subsets of subnetworks N_i, i = 1,2,…,8. We arbitrarily assume that

$$\mu_{MLS}(1)=5,\ \mu_{MLS}(2)=4,\ \mu_{MLS}(3)=3,\ \mu_{MLS}(4)=1 \text{ years.} \tag{31}$$

Namely, from (27) the intensity $\lambda_{N_i}(4)$ takes value

$$\lambda_{N_i}(4)=\frac{1}{8\cdot\mu_{MLS}(4)}=0.1250. \tag{32}$$

And substituting (31) and (32) into (28), we get

$$23=\sum_{g=1}^{8}\left[\frac{1}{\lambda_{N_i}(3)\sum_{i=1}^{8}\frac{1}{q(3,d_{ig})}}-\frac{1}{1-8\lambda_{N_i}(3)+\lambda_{N_i}(3)\sum_{i=1}^{8}\frac{1}{q(3,d_{ig})}}\right]. \tag{33}$$

We assume LLS model of dependency between subnetworks N_i, i = 1,2,…,8, with following coefficients of load growth

$$q(\upsilon,d_{ig})=1-\frac{1}{d_{ig}+1},\ i,g=1,2,\ldots,8,\ i\neq g,\ q(\upsilon,0)=1, \tag{34}$$

where d_{ig} denotes the distance between subnetwork N_i, i = 1,2,…,8, and the subnetwork N_g, g = 1,2,…,8, that has got out of the safety state subset.
From (33) and using (34) we can estimate the intensity $\lambda_{N_i}(3)$ of subnetworks' departure from the subset {3,4}

$$\lambda_{N_i}(3)\cong 0.0230. \tag{35}$$

Similarly, applying (28) and substituting (31), (32), (34), (35), the intensities of subnetworks' departure from the subset {2,3,4} and {1,2,3,4}, respectively account

$$\lambda_{N_i}(2) = 0.0112,\ \lambda_{N_i}(1) = 0.0071. \tag{36}$$

Next, using (31) and the results (32), (35), (36), for assumed ELS model of dependency between transmission lines in subnetworks we can estimate the intensities of departure from the safety state subsets of transmission lines. Namely, from (29), the intensity of departure from the state 4 is

$$\lambda(4) = \frac{c(4)}{16\mu_{MLS}(4)}. \tag{37}$$

For the component stress proportionality correction coefficient $c(u) = 1$, $u = 1, 2,3,4$, it takes value

$$\lambda(4) \cong 0.0625, \tag{38}$$

and the intensities of departure from the subsets {3,4}, {2,3,4} and {1,2,3,4}, from (30), are given by

$$\lambda(3) \cong 0.0115,\ \lambda(2) \cong 0.0056,\ \lambda(1) \cong 0.00355. \tag{39}$$

In second case, considering also transmission lines under construction, we assume that there are three lines between each two substations i.e. $l = 3$. Then, the intensities of departure from the safety state subsets of transmission lines are

$$\lambda(4) \cong 0.04167,\ \lambda(3) \cong 0.00767,\ \lambda(2) \cong 0.00373,\ \lambda(1) \cong 0.00237. \tag{40}$$

The failure coefficients of AC power lines by type of structure can be found, for example, in [14].

Conclusions

In this paper a multistate approach [11], [12], [17], [18] to safety analysis of series, parallel and parallel-series ageing networks with different models of dependency is presented. Estimation of intensities of assets' departures from the safety state subsets for predefined safety level can be helpful in designing of CI networks. As an application a network of transmission lines is considered assuming dependencies between its subnetworks and between lines in these subnetworks. Components of transmission and distribution networks require constant maintenance and their insulation properties degrade over time. Thus, multistate approach to the safety analysis of such a network seems to be reasonable. Further, such approach can help to capture the critical points and critical operations that can cause voltage collapse of the whole network.

Acknowledgements

The paper presents the results developed in the scope of the EU-CIRCLE project titled "A pan – European framework for strengthening Critical Infrastructure resilience to climate change" that has received funding from the European Union's Horizon 2020 research and innovation programme under grant agreement No 653824.
http://www.eu-circle.eu/

References

1. A. Blokus-Roszkowska. Reliability analysis of the bulk cargo loading system including dependent components. In Simos T, Tsitouras Ch (eds), *Proceedings of the International Conference of Numerical Analysis and Applied Mathematics 2015 (ICNAAM 2015)*: 440002-1−440002-4. AIP Publishing, AIP Conf. Proc. 1738, 2016.
2. A. Blokus-Roszkowska and P. Dziula. An approach to identification of critical infrastructure systems. In Simos T, Tsitouras Ch (eds), *Proceedings of the International Conference of Numerical Analysis and Applied Mathematics 2015 (ICNAAM 2015)*: 440006-10−440006-13. AIP Publishing, AIP Conf. Proc. 1738, 2016.
3. A. Blokus-Roszkowska and K. Kołowrocki. Reliability analysis of complex shipyard transportation system with dependent components. *Journal of Polish Safety and Reliability Association, Summer Safety and Reliability Seminars* 5(1): 21-31, 2014.
4. A. Blokus-Roszkowska and K. Kołowrocki. Reliability analysis of ship-rope transporter with dependent components. In Nowakowski et al. (eds), *Safety and Reliability: Methodology and Applications – Proceedings of the European Safety and Reliability Conference, ESREL 2014*: 255-263. London: Taylor & Francis Group, 2015.
5. A. Blokus-Roszkowska and K. Kołowrocki. Modelling dependencies in critical infrastructure networks. In *Safety and Reliability – Theory and Application: ESREL 2017*, Taylor and Francs, CRC Press (to appear).
6. EU-CIRCLE Report D3.3-GMU1, *Modelling inside dependences influence on safety of multistate ageing systems - Modelling safety of multistate ageing systems*, 2016.
7. EU-CIRCLE Report D3.3-GMU6, *Interconnected critical infrastructures cascading safety model*, 2016.
8. D.G. Harlow and S.L. Phoenix. The chain-of-bundles probability model for the strength of fibrous materials. *Journal of Composite Materials* 12: 195-214, 1978.
9. D.G. Harlow and S.L. Phoenix. Probability distribution for the strength of fibrous materials under local load sharing. *Adv. Appl. Prob.* 14: 68-94, 1982.
10. G.H. Kjølle, I.B. Utne and O. Gjerde. Risk analysis of critical infrastructures emphasizing electricity supply and interdependencies. *Reliability Engineering and System Safety* 105: 80-89, 2012.
11. K. Kołowrocki. Reliability of Large and Complex Systems. Elsevier, 2014.
12. K. Kołowrocki and J. Soszyńska-Budny. Reliability and Safety of Complex Technical Systems and Processes: Modeling – Identification – Prediction – Optimization. Springer, 2011.

13. S.L. Phoenix and R.L. Smith. A comparison of probabilistic techniques for the strength of fibrous materials under local load sharing among fibres. *Int. J. Solids Struct.* 19(6): 479-496, 1983.
14. A. Rakowska. The necessity of dynamic development of the cable network – technical and social conditions. *XX Konferencja Szkoleniowo-Techniczna KABEL, 12-15 March 2013* (*in Polish*), 2013.
15. R.L. Smith. The asymptotic distribution of the strength of a series-parallel system with equal load sharing. *Ann. of Prob.* 10: 137-171, 1982.
16. R.L. Smith. Limit theorems and approximations for the reliability of load sharing systems. *Adv. Appl. Prob.* 15: 304-330, 1983.
17. J. Xue. On multi-state system analysis. *IEEE Trans on Reliab.* 34: 329-337, 1985.
18. J. Xue and K. Yang. Dynamic reliability analysis of coherent multi-state systems. *IEEE Trans on Reliab.* 4(44): 683-688, 1995.

Analysis of the crude oil transfer process and its safety

Agnieszka Blokus-Roszkowska[1], Bożena Kwiatuszewska-Sarnecka[2], and Paweł Wolny[3]

[1] Gdynia Maritime University, Gdynia, Poland
(E-mail: a.blokus-roszkowska @wn.am.gdynia.pl)
[2] Gdynia Maritime University, Gdynia, Poland
(E-mail: b.sarnecka@wn.am.gdynia.pl)
[3] Naftoport Ltd, Poinca 1, 80-561 Gdańsk, Poland
(E-mail: Pawel.Wolny@naftoport.pl)

Abstract. Considering the operation process of oil port terminal the paper focuses on processes related to the cargo movement inside the pipeline system. Technical parameters during all stages of crude oil transfer process are described. Processes of crude oil loading, discharging and internal recirculation are described. Analyzing the crude oil transfer process and its influence on the oil port terminal and operating environment safety, potential threats of oil spill during oil transfer are identified. The accidental events that can cause oil spill in the terminal are in the paper classified with distinction of internal and external as well as root and contributing causes. Finally, the discussion on protection of marine facilities against hydraulic transient pressure surges that can occur during crude transfer is performed. Some recommendations, including safety culture recommendation, are given.
Keywords: oil port terminal, oil transfer, operation process, oil spill, pressure upsurge.

1 Introduction

In the Baltic Sea region, there are many oil terminals, which perform transshipment of crude oil and refined petroleum products. Oil terminals are a key element of the petroleum supply logistics of crude oil to refineries and oil transit. The accident in the oil terminal during unloading/loading of tankers may have a long or short-term consequences for the work of the terminal, that may be associated with the socioeconomic losses and environmental costs consequences.
One of important causes of oil spill, is pressure upsurge inside the pipelines as a hydraulic hammer's consequence. These pressure surges can be generated by anything that causes the liquid velocity in a line to change quickly e.g., valve

17*th* *ASMDA Conference Proceedings, 6 - 9 June 2017, London, UK*

closure, pump trip, Emergency Shut Down (ESD) closure occurs and subsequently packing pressure. In the paper the particular attention is paid to the pressure upsurge inside the pipelines caused by sudden valve closure on the oil reloading installation in port terminal.

2 Processes related to the crude oil transfer inside the pipeline system

The operation process of the crude oil transfer has an influence on oil terminal safety and environment safety. Considering system composed of a single pipeline we can distinguish following operational states during its operation process:
z_1 − loading cargo with initially slow rate,
z_2 − laboratory tests of exported crude oil,
z_3 − loading cargo with full rate,
z_4 − loading cargo with reduced rate,
z_5 − unloading cargo with initially slow rate,
z_6 − unloading cargo with full rate,
z_7 − unloading cargo with reduced rate,
z_8 − terminal idle mode, there is no transfer of cargo,
z_9 − internal recirculation process.
We describe below all listed operational states of crude oil transfer process specifying technical parameters.
First, a tanker vessel arriving at oil terminal have to be properly moored for cargo handling process and its position has to be continuously controlled during the unloading/loading time. Moreover the ship's and the terminal's representatives have to discuss all technical issues and procedures before the transhipment process may begin.

Fig. 1. Loading arms for loading/unloading tankers in the oil terminal [6]

To start the crude oil loading process a piping system line up agreement between tank farm and terminal and between vessel and terminal have to be set. Before tanker loading cargo from the oil terminal, the vessel marine loading arms are connected, for crude oil usually 3 or 4 arms are connected (Fig. 1). Next the line is set by choosing dedicated tanks and pumps ashore and by opening or closing relevant line's valves. Marine terminal leaves per one valve closed on each loading arm. After receiving readiness confirmation for starting loading process from the vessel, the last valves on marine loading arms are opened and the process of crude oil loading with initially slow rate begin (state z_1). Cargo starts to flow due to gravity, if needed the pumps start to obtain agreed initial rate.

Technical parameters (pinpoint loading parameters) during initial state of crude oil loading include inter alia:

- initial rate (usually abt. 1000 cbm/h),
- pressure 0,1 – 0,5 Mpa,
- temperature max 35°C.

After some laboratory tests of exported crude oil (state z_2) and relevant checks on cargo tanks and lines against leakages and aberrations, the terminal receive agreement from the vessel to increase loading rate to agreed maximum rate and the process of loading crude oil with full rate start (state z_3). During loading the parameters and infrastructure integrity have to be inspected on a regular basis and tanker receives cargo from the terminal in accordance with agreed parameters (pressure, temperature, rate).

Below there are given technical parameters of crude oil loading process during state z_3:

- maximum loading rate (usually approx. 10000 cbm/h),
- pressure 0,3 – 0,4 Mpa,
- temperature max 35°C.

Tanker's tanks are loaded usually to their 95-98% capacities. Final stage of each tank's filling is named "topping". On this stage, for oil spill avoidance reasons, loading rate is decreased to approx. 1000 cbm/h (state z_4). When one tank is already full other tank goes to open position to let the cargo pass inside, then the full tank is closed. When the last cargo tank is topped up, tanker asks terminal for pump stoppage and valve closure. When this happens, terminal gives confirmation regarding stoppage and the ships manifold valves are closed. When tankers and terminal's valves on loading lines are closed, the terminal goes into idle mode (state z_8).

Technical parameters in the final stage of crude oil loading process are:

- topping rate (usually 1000 cbm/h),
- pressure 0,1 – 0,2 Mpa,
- temperature max 35°C.

Parameters of planned cargo operations stoppages (ex. Line Displacement; One Foot Sample) are:

- maximum pressure limits 1 Mpa,
- cargo temperature limits 1 – 35°C.

The process of crude oil discharging is similar. Before staring the unloading process, a piping system line up agreement between tank farm and terminal and an agreement between vessel and terminal have to be set. Then, the vessel marine loading arms are connected; during unloading process for crude oil usually 3 loading arms are connected. The line has to be set by choosing dedicated tanks and pumps on vessel and by opening or closing relevant line's valves. After fixing the readiness notice between vessel, marine terminal and tank farm, the loading process from the tank farm starts. The last valves on marine loading arms are opened and the pumps on vessel start with initial rate (state z_5). If there are no aberrations, after obtained from the vessel agreement to increase discharging rate to agreed maximum rate, the unloading cargo starts with full rate (state z_6). During discharging the parameters and infrastructure integrity have to be inspected on a regular basis. In a simplistic way, in the final stage the unloading cargo with reduced rate takes place and tanker finishes discharging cargo, by stripping all cargo tanks (state z_7). At the end of the transshipment we are dealing with the process of washing tankers from the sediment COW (Crude Oil Washing). Then the pumps stop, relevant valves are closed and the loading arms are disconnected.
Below there are given technical parameters of crude oil discharging process.
During the state z_5:
- initial rate (usually 1000 cbm/h),
- pressure 0,1 – 0,5 Mpa,
- temperature max 35°C,

during the state z_6:
- maximum discharging rate (usually approx. 10000 cbm/h),
- pressure 0,3 – 0,5 Mpa,
- temperature max 35°C,

planned cargo operations stoppages (ex. Line Displacement) in the state z_7:
- maximum pressure limits 1 Mpa,
- cargo temperature limits 1 – 35°C.

To start the internal recirculation process (state z_9) a piping system line up agreement between tank farm and terminal has to be set. Relevant valves are opened or closed; one valve on each tank has to be still closed. After confirming readiness of both sides, i.e. terminal and tank farm, the valves on dedicated tanks are opened and the recirculation by gravity commences. Next, relevant checks against line integrity and aberrations are made and cargo pumps start. During recirculation the parameters and infrastructure integrity have to be also inspected on a regular basis. When the process of recirculation is finished the pumps stop and the line valves are closed.
Technical parameters of internal recirculation of crude oil are:
- recirculation rate 5000 cbm/h,
- maximum pressure limits 1 Mpa,
- cargo temperature limits 1 – 35°C.

In terminal idle mode, there is no transfer of cargo, however cargo is still inside shore pipelines.

3 Scenarios and classification of accidents during crude oil transfer process

For this article needs, we divided oil related incidents into three types. These are oil leakage, overflow and most dangerous oil spill. Types of accidents are concerned with the volume of oil spilled and are strictly related to the states of the operational process (Fig. 2):

- oil leakage – minor incident, that may occur during the state z_1, z_2, z_5, z_8 and z_9,
- oil overflow – medium incident something between leakage and spill, that may occur during the state z_4 and z_7,
- oil spill – major incident, that may occur during the state z_3 and z_6.

Most of oil related incidents are not very serious and they are connected to leakages group, however serious accidents also occur.

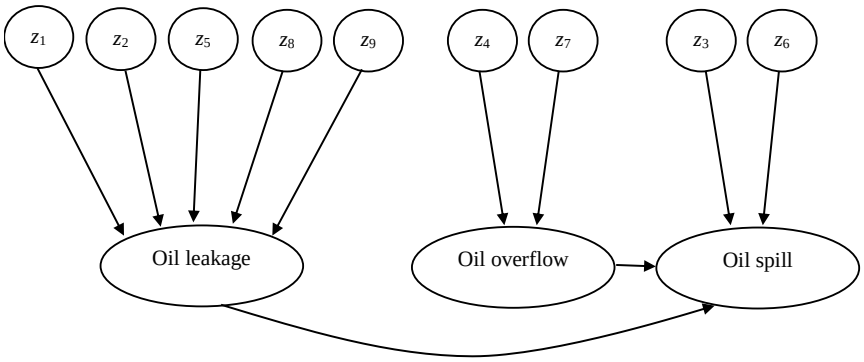

Fig. 2. Spill incidences in terms of oil transfer operational states.

The main causes of oil leakage include:

- Disconnecting the ship's manifold from the loading arm during the transshipment due to technical drawbacks or human error (defect) in connecting the arm to the manifold;
- Hydraulic impact due to a sudden valve closure on the ship in case of loading, or a valve closure at the terminal in case of unloading from the ship.

For example, PDVSA, oil company in Venezuela, confirmed that a crude spill occurred from a pipeline, on March 28th, 2017. The crude oil leak was a result of a break in the line running from a crude terminal to a single buoy mooring, but it did not affect terminal operations though [9].

Oil overflow may be the result of no stopping loading onto the ship at the right time. Then, the overflowing of tanks and oil spills with P/V valves or mastraiser may occur. As a consequence of inadequate level monitoring the gasoline tank was overfilled in Buncefield, UK, in 2005. The overflow occurred due to the defect of the system that should detect a high level and shut-off the inflow. During that incident more than 250,000 l of gasoline was spilled from an

atmospheric pressure storage tank [4]. Oil overflow on shore storage tank can happen also during ship discharging.
Oil spill on board of the ship or on terminal pipeline infrastructure may occur during transfer cargo with full rate, but uncontrolled oil leakage can also result in oil spill and pollution of marine ecosystems. For example, the bunker tanker spilled about 70 tons of fuel at the ATB Vitol oil terminal in Malaysia on August 24, 2016. The spill occurred as the result of a leaking hose during bunkering of the vessel [5].
According to "Oil Tanker Spill Statistics 2016", oil spills during loading and discharging account for 40% of all small sized spills (below 7 tonnes), classified by operation at time of incident, in 1974-2016. In medium sized spills (7-700 tonnes), 29% occurred during loading and discharging operations. Large spills during oil transfer operations are less frequent and account for 9% of all incident recorded in 1970-2016. Considering these large spills in terms of cause, it can be noticed that 31% are caused by fire or explosion, 26% by equipment failure and 19% by other causes that include heavy weather damage and human error [3].

5 Oil spill threats related to crude oil transfer in the terminal

Considering the causes and circumstances of oil spills during oil transfer operations we propose in this paper classification for internal and external reasons.
Internal causes may include:
- technical conditions of oil terminal's infrastructure,
- technical conditions of equipment on tanker vessels,
- human error made by vessel or terminal workers involved in the transshipment process.

Causes associated with technical conditions of oil terminal's infrastructure may include failure of different systems: main oil line, flow line, arms, hoses, hose joints, flange joints, block valves. They can depend on various factors, such as, insufficient maintenance level of pipes, devices, technological appliances and sensors, carried out hot works in sensitive areas. Among human errors we can mention errors made during technological process, maintenance and other activities, abstractedness or measurement errors, errors in setting valves or errors related to insufficient technological knowledge.
Sometimes oil spills during the crude oil transfer can be caused by both human error and mechanical damage. Pressure upsurge inside the pipelines as a hydraulic hammer's consequence can be caused by:
Pump startup – a starting pump can generate high pressures;
Pump power failure – it can cause a pressure upsurge on the suction side and a pressure down-surge on the discharge side;
Valve opening and closing – sudden valve closure changes the velocity quickly and results in a pressure surge. The pressure surge resulting from a sudden valve opening is usually not as excessive. Closing a valve at the downstream end of a

pipeline creates a pressure wave that the moves back toward the reservoir; improper operation or incorrect design of surge protection devices [2].
Accidents may also occur during the crude oil transfer process due to following external causes:

- technical conditions of oil terminal's infrastructure, associated with abrupt temperature changeover within arrangement: pipeline-liquid-ambient, damage caused by other objects operating in the vicinity of pipelines (ashore/sea), damage to installation and technological appliances due to external forces,
- human factor including terrorism,
- weather condition such as thunderstorm, winds, icing, very high or low temperatures.

Causes of oil spills can be also divided into two other categories. These are generic failures associated with mechanical component of the facility or terminal and specific operating failures prime cause of which is human error. Specific operating failures can include also accidents.
Causes of oil spills in investigation reports are often classified as root causes and contributing causes or factors. Contributing factors can be associated with environment, equipment, safety policy and management, work practice, supervision, training. Contributing factors can be also classified as behavioral, medical, task errors and other. Root causes can be also grouped to immediate causes (unsafe acts, unsafe conditions and miscellaneous causes) and contributing caused (safety management performance, mental and physical condition of worker) [7]. Scheme of different classifications of oil spill causes is presented in Figure 3.
The effects of accidents, which occur at time of oil transfer, can be divided in following categories:

- damage to oil terminal’s infrastructure and/or ship,
- short or long term breaks in the functioning of the oil terminal,
- endanger to human health and life,
- environmental pollution that is the most important and financially significant for the polluter.

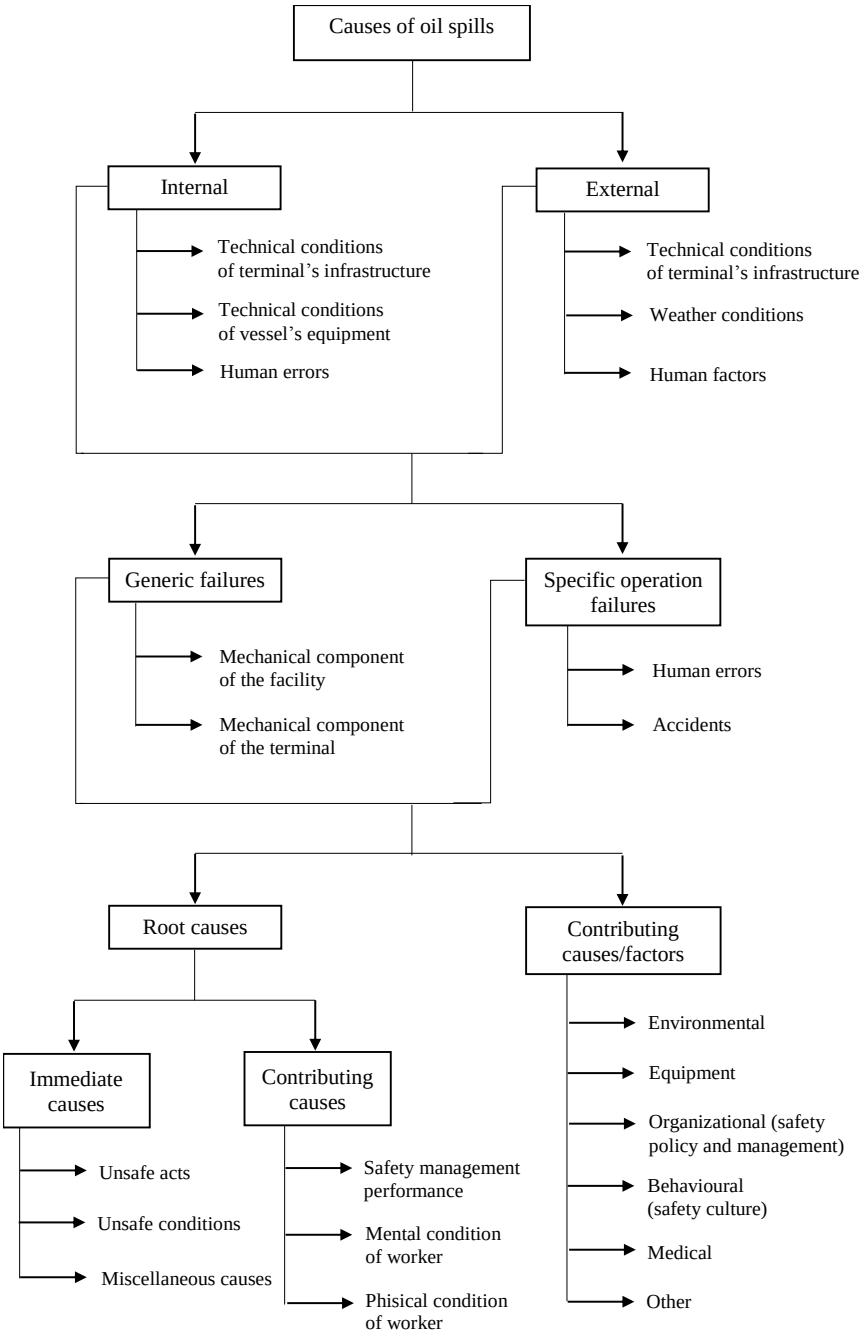

Fig. 3. Types of oil spill causes.

6 Prevention of pressure upsurge inside the pipelines

One of important causes of oil spill, mentioned before, is pressure upsurge inside a pipeline generated by an abrupt change in the rate of flow of liquid in the line i.e. as a hydraulic hammer's consequence. A hydraulic hammer can be caused by the ship's breakaway couplings when the ship disconnects or from an Emergency Shut Down (ESD) valve closure. Both can cause damage to loading hoses or arms, loading buoys, and feed pipework. Sudden valve closure on the reloading installation may occur e.g. on a ship that has all the cargo tanks full. Such situation may take place when there is no space to accept additional volumes of crude oil and there is not able to pass the terminal to stop the transshipment for example by communication errors. In this case, if there is an emergency system to stop handling, not to cause overflow tanks and bottling, the ship decides to close the valve connecting it to the mainland, resulting in the so-called "hammering" resulting in discontinuity of installation and spill [2].
The pressure surge in the pipeline may result in pressure stresses or displacement stresses, and as a consequence it may cause a rupture leading to an extensive oil spill. According to [10], a pressure surge during tanker loading can occur as a result of:

- closure of an automatic shut down valve,
- slamming shut of a shore non-return valve,
- slamming shut of a butterfly type valve,
- rapid closure of a power operated valve.

To protect terminal from the potential damage that can be caused by pressure surges, some pressure relief systems are often used. Excessive surge pressures result from a sudden change in fluid velocity and, without surge relief, they can damage pipes, other piping components, equipment and personnel. These pressure surges can be generated by anything that causes the liquid velocity in a line to change quickly (e.g., valve closure, pump trip, ESD closure occurs) and subsequently packing pressure. The task of crude oil surge-relief system is to protect marine facilities against hydraulic transient pressure surges that can occur during loading and unloading of crude oil to and from vessels. Such system should be able to open very quickly high capacity valves to remove surge pressures from the line and then return to the normal state. Typical tank and pressure vessel systems are required to release pressure without passing large volumes of liquid. These valves are often fully open to allow the entire stream flowing. Closing of these valves should also be done quickly but without causing additional pressure surge. To prevent hydraulic shock and secondary surge during a valve closing, some surge relief systems include damping or slowing systems on valve closing [1].
Investigation reports after oil spills in ports or terminals indicate also a problem of organizational and safety culture. We also analyzed the investigation report on a refinery explosion caused by a raffinate splitter tower overflow.
In order to prevent oil spills accidents following recommendations can be given:

- adequately addressed controlling major hazard risk,
- creating an effective reporting and learning culture after oil spill incidents,

- incorporating human factor considerations in its training, staffing, and work schedule for operations personnel,
- training courses including abnormal and emergency situations and procedures of reaction in such situations,
- proper communication (eliminating problems associated with communication) between operators from the vessel and terminal responsible for oil transfer,
- providing effective safety culture leadership and oversight,
- providing adequate resources to prevent major accidents,
- avoiding excessive cost-cutting.

Conclusions

The paper describes operations during oil transfer process in a terminal and associated with them threats and potential oil spill accidents. Various classifications of causes of oil spill accidents have been proposed in the paper, which may help to identify oil spill threats. Determining the causes of oil spill accidents and identification of potential spill sources can help to avoid or mitigate the effects of potential spills during oil transfer in a terminal in the future. As a continuation of the outlined problem, recommendations and procedures to prevent oil spill accidents will be given. In this scope, training on recognizing and handling abnormal situations during oil transfer will be proposed.

Acknowledgements

The paper presents the results developed in the scope of the HAZARD project titled “Mitigating the Effects of Emergencies in Baltic Sea Region Ports” that has received funding from the Interreg Baltic Sea Region Programme 2014-2020 under grant agreement No #R023. https://blogit.utu.fi/hazard/

References

1. Emerson Process Management. An Introduction to Liquid Pipeline Surge Relief, Technical Guide, 2015.
2. T. Gupta. Specifying surge relief valves in liquid pipelines, Emerson Process Management, 2012.
3. International Chamber of Shipping, Oil Companies International Marine Forum, International Association of Ports and Harbors. International Safety Guide for Oil Tankers & Terminals (ISGOTT), 2006.
4. International Labour Office. Encyclopaedia of Occupational Health and Safety 4th Edition, Part VIII - Accidents and Safety Management, http://www.ilocis.org/en/default.html, last accessed 22.03.2017.
5. The International Tanker Owners Pollution Federation Limited. Oil Tanker Spill Statistics 2016, http://www.itopf.com/fileadmin/data/Photos/Publications/Oil_Spill_Stats_2016_low.pdf, last accessed 22.03.2017.

6. Sakhalin Energy. Summary of Oil Spills Prevention and Response Plan for Prigorodnoye Asset Onshore Operations, 2011, http://www.sakhalinenergy.ru/media/1dbd9f2d-e253-4d71-ad43-b20f6d152158.pdf, last accessed 22.03.2017.
7. http://shipandbunker.com/news/apac/538654-70-tonne-bunker-spill-from-tanker-responsible-for-vtti-terminal-closure-reports, last accessed 22.03.2017.
8. http://www.green4sea.com/crude-oil-leak-at-venezuela-port/, last accessed 30.03.2017.
9. http://www.macgregor.com/en-global/macgregor/products/Woodfield%20Loading%20Arms/Pages/Ambient%20marine%20loading%20arms.aspx, last accessed 22.03.2017.
10. http://www.thechemicalengineer.com/~/media/Documents/TCE/lessons-learned-pdfs/861lessonslearned.pdf, last accessed 22.03.2017.

Statistical identification of critical infrastructure accident consequences process
Part 1
Process of initiating events

Magda Bogalecka[1], and Krzysztof Kołowrocki[2]

[1] Department of Industrial Commodity Science and Chemistry, Gdynia Maritime University, 81-87 Morska Str., 81-225 Gdynia, Poland
(E-mail: m.bogalecka@wpit.am.gdynia.pl)
[2] Department of Mathematics, Gdynia Maritime University, 81-87 Morska Str., 81-225 Gdynia, Poland
(E-mail: k.kolowrocki@wn.am.gdynia.pl)

Abstract. The statistical methods such as the method of moments, the maximum likelihood method and the chi-square goodness-of-fit test are applied to the identification of the process of initiating events generated either by the critical infrastructure accident or by its loss of required safety critical level. The unknown parameters of this process are evaluated on the basis of statistical data coming from its realizations.
Keywords: critical infrastructure, sea accident, potential consequences, initiating events.

1 Introduction

Some kinds of critical infrastructure accidents concerned with its safety level decrease may occur during its operation Kołowrocki[5], Kołowrocki and Soszyńska-Budny[6]. Those accidents may bring various dangerous consequences for the environment and have disastrous influence on the human health and activity. Each critical infrastructure accident can generate the initiating event causing dangerous situations in the critical infrastructure operating surroundings. The process of those initiating events can result in this environment threats and lead to the environment dangerous degradations (Fig. 1).

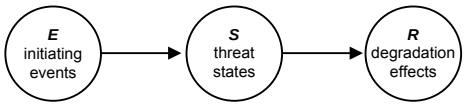

Fig. 1. Interrelations of the critical infrastructure accident consequences general model

To involve the interactions between the initiating events, the environment threats and environment degradation effects, semi-Markov general model of a critical infrastructure accident consequences was built by Bogalecka and Kołowrocki[1].
This paper is concerned with the identification of the first one of those three processes.The process of initiating events and its states are defined. The unknown parameters of semi-Markov model of the process of initiating events are estimated. Next, based on the statistical data of ship accidents at world seas 11-years-observation, the vectors of initial probabilities of the process of initiating events staying at its particular states, the matrix of probabilities of this process transitions between its particular states are estimated. Next, the parameters of the process of initiating events conditional sojourn times at particular states were evaluating and forms of their distributions fixed. Finally, the mean values of the process conditional sojourn times at its particular states are estimated.

2 Process of initiating events modelling

We assume, that the process of initiating events is taking ω, $\omega \in N$, different initiating events states $e^1,e^2,\ldots,e^{\omega}$. Next, we mark by $E(t)$, $t \in <0,\infty)$, the process of initiating events, that is a function of a continuous variable t, taking discrete values in the set $\{e^1,e^2,\ldots,e^{\omega}\}$ of the initiating events states. We assume a semi-Markov model Grabski[2], Kołowrocki[3-4], Kołowrocki and Soszyńska[7], Limnios and Oprisan[8], Macci[9], Mercier[10] of the process of initiating events $E(t)$, and we mark by θ^{lj} its random conditional sojourn times at the initiating events states e^l, when its next state is e^j, $l, j = 1,2,\ldots,\omega$, $l \neq j$.
Under these assumption, the unknown parameters of the process of initiating events semi-Markov model are:
– the vector $[p^l(0)]_{1x\omega}$ of probabilities of the process of initiating events staying at the particular initiating events states at the initial moment $t = 0$,
– the matrix $[p^{lj}(t)]_{\omega x\omega}$ of probabilities of transitions between the initiating events states
– the matrix $[H^{lj}(t)]_{\omega x\omega}$ of the distribution functions of the conditional sojourn times θ^{lj} of the process $E(t)$ at the initiating events states or equivalently by the matrix $[h^{lj}(t)]_{\omega x\omega}$ of the density functions of the conditional sojourn times θ^{lj}, $l, j = 1,2,\ldots,\omega$, $l \neq j$, of the process of initiating events at the initiating events states,
– the mean values M^{lj}, of the conditional sojourn times θ^{lj}, $l, j = 1,2,\ldots,16$, $l \neq j$.
The marine traffic across the world and the ship accidents were observed and analysed. Based on that analysis and the maritime authorities classification of the initial events caused by sea accidents, seven initiating events that generate dangerous situations for the sea environment were distinguished. These initial events are marked by E_i, $i = 1,2,\ldots,7$, and defined as follows: E_1 – collision (a ship striking another ship), E_2 – grounding (a ship striking the sea bottom, shore

or underwater wreck), E_3 – contact (a ship striking an external object *e.g.* pier or floating object), E_4 – fire or explosion on board, E_5 – shipping without control (drifting of ship) or missing of ship, E_6 – capsizing or listing of ship, E_7 – movement of cargo in the ship.
Further, we introduce the set of vectors

$$E = \{e: \quad e = [e_1, e_2, ..., e_7],\ e_i \in \{0,1\}\},$$

where

$$e_i = \begin{cases} 1, \text{ if the initiating event } E_i \text{ occurs,} \\ 0, \text{ if the initiating event } E_i \text{ does not occur,} \end{cases}$$

for $i = 1,2,\ldots,7$.
Next, we distinguish $\omega = 16$ following states of the process of initiating events $E(t)$:

$e^1 = [0,0,0,0,0,0,0]$, $e^2 = [1,0,0,0,0,0,0]$, $e^3 = [0,1,0,0,0,0,0]$, $e^4 = [0,0,1,0,0,0,0]$,
$e^5 = [0,0,0,1,0,0,0]$, $e^6 = [0,0,0,0,1,0,0]$, $e^7 = [0,0,0,0,0,1,0]$, $e^8 = [0,0,0,0,0,0,1]$,
$e^9 = [0,1,0,1,0,0,0]$, $e^{10} = [0,0,0,1,1,0,0]$, $e^{11} = [0,0,0,0,1,1,0]$,
$e^{12} = [0,0,0,1,0,0,1]$, $e^{13} = [0,0,0,0,0,1,1]$, $e^{14} = [0,0,0,1,1,1,0]$,
$e^{15} = [0,0,0,0,1,1,1]$, $e^{16} = [0,0,0,1,0,1,0]$.

Moreover, it is assumed that there are possible the transitions between all states of the process of initiating events.

3 Statistical identification of the process of initiating event

The experiment was performed across the world seas and oceans in the years 2004-2014. The number of the observed ship accidents that generated the distinguished states of the process of initiating events was $n(0) = 1630$. The initial moment $t = 0$ of the process of initiating event for each ship was fixed at the moment when the ship after an accident generated one of the distinguished states.

3.1 Data collection for estimating unknown parameters of the process of initiating events

To identify unknown parameters of the process of initiating events, described in Section 2, the statistical data coming from the process $E(t)$ realization are used:

– the process of initiating observation/experiment time $\Theta = 11$ years (2004-2014);
– the vector of realizations $n^l(0)$, $l = 1,2,\ldots,16$, of the numbers of the process $E(t)$ of initiating events staying at the particular states e^l at the initial moment $t = 0$

$[n^l(0)]_{1x16} = [1630, 0, 0, 0, 0, 0, 0, 0, 0, 0, 0, 0, 0, 0, 0, 0]$;

– the number of the process of initiating events realizations at the moment $t = 0$

$$n(0) = \sum_{l=1}^{16} n^l(0) = 1630 + 0 + \ldots + 0 + 0 = 1630.$$

The collected statistical data necessary for evaluating the probabilities of transitions between initiating events states are:

– the matrix of realizations n^{lj}, $l, j = 1,2,\ldots,16$, of the numbers of the process $E(t)$ transitions from the state e^l into the state e^j during the experimental time (the numbers of transitions that are not equal to 0 are presented only):

$n^{1\,2} = 401$, $n^{1\,3} = 369$, $n^{1\,4} = 123$, $n^{1\,5} = 268$, $n^{1\,6} = 234$, $n^{1\,7} = 205$, $n^{1\,8} = 30$;

$n^{2\,1} = 237$, $n^{2\,3} = 125$, $n^{2\,4} = 3$, $n^{2\,5} = 4$, $n^{2\,6} = 22$, $n^{2\,7} = 40$, $n^{2\,10} = 2$, $n^{2\,11} = 1$;

$n^{3\,1} = 753$, $n^{3\,2} = 2$, $n^{3\,6} = 4$, $n^{3\,9} = 1$;

$n^{4\,1} = 111$, $n^{4\,2} = 3$, $n^{4\,3} = 13$, $n^{4\,6} = 9$, $n^{4\,7} = 13$;

$n^{5\,1} = 210$, $n^{5\,9} = 18$, $n^{5\,10} = 39$, $n^{5\,12} = 1$, $n^{5\,16} = 5$;

$n^{6\,1} = 127$, $n^{6\,2} = 28$, $n^{6\,3} = 88$, $n^{6\,4} = 22$, $n^{6\,10} = 4$, $n^{6\,11} = 14$;

$n^{7\,1} = 107$, $n^{7\,3} = 141$, $n^{7\,4} = 1$, $n^{7\,8} = 3$, $n^{7\,11} = 3$, $n^{7\,13} = 5$;

$n^{8\,1} = 28$, $n^{8\,13} = 4$;

$n^{9\,1} = 19$;

$n^{10\,1} = 22$, $n^{10\,6} = 15$, $n^{10\,14} = 1$;

$n^{11\,1} = 8$, $n^{11\,3} = 10$;

$n^{12\,1} = 1$;

$n^{13\,1} = 4$, $n^{13\,3} = 3$, $n^{13\,15} = 2$;

$n^{14\,1} = 1$;

$n^{15\,3} = 2$;

$n^{16\,1} = 2$, $n^{16\,3} = 2$, $n^{16\,7} = 1$;

– the vector of realisations of total numbers of the process $E(t)$ departures from the state e^l, $l = 1,2,\ldots,16$, during the experimental time

$[n^l] = [1630, 434, 760, 149, 273, 283, 260, 32, 19, 38, 18, 1, 9, 1, 2, 5]$.

The collected statistical data necessary to evaluate the unknown parameters of the distributions of the conditional sojourn times θ^{lj} at the states of the processes of initiating events are as follows:

– the numbers n^{lj}, $l, j = 1,2,\ldots,16$, $l \neq j$, of the realizations θ_γ^{lj}, $\gamma = 1,2,\ldots, n^{lj}$ of the conditional sojourn times θ^{lj} of the process of initiating events state e^l when the next transition is to the initial events process state e^j during the experimental time;

– the realizations θ_γ^{lj}, $\gamma = 1,2,\ldots,n^{lj}$ of the conditional sojourn times θ^{lj} of the process of initiating events state e^l when the next transition is to the initial events process state e^j during the experimental time.

For instance, the collected statistical data for the sojourn time θ^{27} are as follows:

– the number of realizations $n^{27} = 40$;

– the realizations θ_γ^{27}, $\gamma = 1,2,\ldots,40$: 1, 10, 30, 60, 10, 1, 10, 10, 10, 15, 1, 1, 10, 1, 1, 1, 5, 1, 1, 1, 10, 1, 5, 10, 1, 1, 1, 1, 1, 1, 1, 60, 1, 1, 1, 1, 1, 10, 1, 1.

3.2 Estimating parameters of the process of initiating events

On the basis of the statistical data from Section 3.1, using the formulae given in Section 4.2.3 in Kołowrocki and Soszyńska-Budny[7], it is possible to evaluate the following unknown basic parameters of the process of initiating events:

– the vector

$[p(0)]_{1x16} = [1, 0, 0, 0, 0, 0, 0, 0, 0, 0, 0, 0, 0, 0, 0, 0]$,

of the initial probabilities $p^l(0)$, $l = 1,2,\ldots,16$ of the process of initiating events at the particular states e^l at the moment $t = 0$;

– the matrix $[p^{lj}]$, $l, j = 1,2,\ldots,16$, of the probabilities of transitions of the process $E(t)$ from the state e^l into the state e^j during the experimental time (the probabilities of transitions that are not equal to 0 are presented only):

$p^{1\,2} = 0.2460$, $p^{1\,3} = 0.2264$, $p^{1\,4} = 0.0754$, $p^{1\,5} = 0.1644$, $p^{1\,6} = 0.1436$,
$p^{1\,7} = 0.1258$, $p^{1\,8} = 0.0184$;

$p^{2\,1} = 0.5461$, $p^{2\,3} = 0.2880$, $p^{2\,4} = 0.0069$, $p^{2\,5} = 0.0092$, $p^{2\,6} = 0.0507$,
$p^{2\,7} = 0.0922$, $p^{2\,10} = 0.0046$, $p^{2\,11} = 0.0023$;

$p^{3\,1} = 0.9908$, $p^{3\,2} = 0.0026$, $p^{3\,6} = 0.0053$, $p^{3\,9} = 0.0013$;

$p^{4\,1} = 0.7450$, $p^{4\,2} = 0.0201$, $p^{4\,3} = 0.0872$, $p^{4\,6} = 0.0604$, $p^{4\,7} = 0.0873$;

$p^{5\,1} = 0.7692$, $p^{5\,9} = 0.0659$, $p^{5\,10} = 0.1429$, $p^{5\,12} = 0.0037$, $p^{5\,16} = 0.0183$;

$p^{6\,1} = 0.4488$, $p^{6\,2} = 0.0989$, $p^{6\,3} = 0.3110$, $p^{6\,4} = 0.0777$, $p^{6\,10} = 0.0141$,
$p^{6\,11} = 0.0495$;

$p^{7\,1} = 0.4115$, $p^{7\,3} = 0.5423$, $p^{7\,4} = 0.0038$, $p^{7\,8} = 0.0116$, $p^{7\,11} = 0.0116$,
$p^{7\,13} = 0.0192$;

$p^{8\,1} = 0.8750$, $p^{8\,13} = 0.1250$;

$p^{9\,1} = 1$;

$p^{10\,1} = 0.5790$, $p^{10\,6} = 0.3947$, $p^{10\,14} = 0.0263$;

$p^{11\,1} = 0.4444$, $p^{11\,3} = 0.5556$;

$p^{12\,1} = 1$;

$p^{13\,1} = 0.4445$, $p^{13\,3} = 0.3333$, $p^{13\,15} = 0.2222$;

$p^{14\,1} = 1$;

$p^{15\,3} = 1$;

$p^{16\,1} = 0.4000$, $p^{16\,3} = 0.4000$, $p^{16\,7} = 0.2000$.

The values of some probabilities existing in the vectors $[p(0)]$ and in the matrix $[p^{lj}]$, besides of those standing on the main diagonal, equal to zero do not mean that the events they are concerned with, cannot appear. They are evaluated on

the basis of real statistical data and their values may change and become more precise if the duration of the experiment is longer.

3.3 Estimating parameters of distributions of the process of initiating events

On the basis of the statistical data presented in Section 3.1, using the procedure and the formulae given in Chapter 4.2.3 from Kołowrocki and Soszyńska-Budny[7], it is possible to determine the empirical parameters of the conditional sojourn times θ^{ij} of the initiating events process at the particular initiating events states. To illustrate the application of this procedure and these formulae, we perform it for the conditional sojourn time θ^{27}, using their realizations presented in Section 3.1 are as follows.

The realization θ^{27} of mean value of the conditional sojourn time θ^{27} of the initial events process state e^2 when the next transition is to the initial events process state e^7 is

$$\bar{\theta}^{27} = \frac{1}{40}\sum_{\gamma=1}^{40}\theta_{\gamma}^{27} = 7.25.$$

The number $\bar{r}^{27}$ of the disjoint intervals $I_z =< a_z^{27}, b_z^{27})$, $z = 1,2,\ldots,\bar{r}^{27}$, that include the realizations θ_{γ}^{27}, $\gamma = 1,2,\ldots,40$ of the conditional sojourn time θ^{27} of the initial events process state e^2 when the next transition is to the initial events process state e^7

$$\bar{r}^{27} \cong \sqrt{40} \cong 6.$$

The length d^{27} of the intervals $I_z =< a_z^{27}, b_z^{27})$, $z = 1,2,\ldots,6$, that after considering

$$\bar{R}^{27} = \max_{1\le\gamma\le 40}\theta_{\gamma}^{27} - \min_{1\le\gamma\le 40}\theta_{\gamma}^{27} = 60 - 1 = 59,$$

is

$$d^{27} = \frac{\bar{R}^{27}}{\bar{r}^{27} - 1} = \frac{59}{5} = 11.8.$$

The ends a_z^{27}, b_z^{27}, of the intervals $I_z =< a_z^{27}, b_z^{27})$, $z = 1,2,\ldots,6$, that after considering

$$\min_{1\le\gamma\le 40}\theta_{\gamma}^{27} - \frac{d^{27}}{2} = 1 - \frac{11.8}{2} = -5.9,$$

are

$$a_1^{27} = \max\{-5.9, 0\} = 0 \qquad b_1^{27} = a_1^{27} + 11.8 = 0 + 11.8 = 11.8,$$

$$a_2^{27} = b_1^{27} = 11.8, \qquad b_2^{27} = a_1^{27} + 2\cdot 11.8 = 0 + 23.6 = 23.6,$$

$a_3^{27} = b_2^{27} = 23.6,$ $b_3^{27} = a_1^{27} + 3 \cdot 11.8 = 0 + 35.4 = 35.4,$

$a_4^{27} = b_3^{27} = 35.4,$ $b_4^{27} = a_1^{27} + 4 \cdot 11.8 = 0 + 47.2 = 47.2,$

$a_5^{27} = b_4^{27} = 47.2,$ $b_5^{27} = a_1^{27} + 5 \cdot 11.8 = 0 + 59 = 59,$

$a_6^{27} = b_5^{27} = 59,$ $b_6^{27} = a_1^{27} + 6 \cdot 11.8 = 0 + 70.8 = 70.8.$

The numbers n_z^{27} of the realizations θ_γ^{27} in particular intervals $I_z =< a_z^{27}, b_z^{27})$, $z = 1,2,\ldots,6,$

$n_1^{27} = 36,\ n_2^{27} = 1,\ n_3^{27} = 1,\ n_4^{27} = 0,\ n_5^{27} = 0,\ n_6^{27} = 2.$

3.4 Identifying distribution functions of initiating events conditional sojourn times at states

Using the procedure given in Section 4.2.4 in Kołowrocki and Soszyńska-Budny[7] and the results partly presented in Section 3.3, we verify the hypotheses on the distributions of the process of initiating events conditional sojourn times θ^{lj}, $l, j = 1,2,\ldots,16$, $l \neq j$, at particular states. To make the procedure familiar to the reader, we perform it for the conditional sojourn time for θ^{27} preliminary analyzed in Section 3.3.

The realization $h^{27}(t)$ of the histogram of the process of initiating events conditional sojourn time θ^{27} defined by

$$\overline{h}^{n^{lj}}(t) = \frac{n_z^{lj}}{n^{lj}} \text{ for } t \in I_z,$$

is presented in Table 1 and illustrated in Figure 2.

Table 1. The realization of the histogram of the process initiating events conditional sojourn time θ^{27}.

Histogram of the conditional sojourn time θ^{27}						
$I_z =< a_z^{27}, b_z^{27})$	0-11.8	11.8-23.6	23.6-35.4	35.4-47.2	47.2-59	59-70.8
n_z^{27}	36	1	1	0	0	2
$\overline{h}^{27}(t) = n_z^{27} / n^{27}$	36/40	1/40	1/40	0/40	0/40	2/40

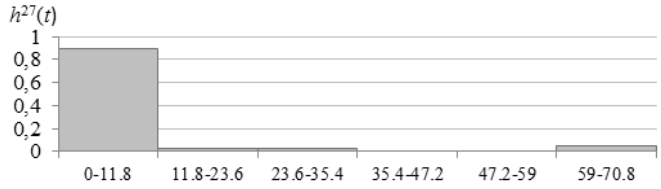

Fig. 2. The graph of the histogram of the process of initiating events conditional sojourn time θ^{27}

After analyzing and comparing the realization $h^{27}(t)$ of the histogram with the graphs of the density functions $h^{27}(t)$ of the previously distinguished in Chapter 2 from Kołowrocki and Soszyńska-Budny[7] distributions, we formulate the null hypothesis H_0 in the following form.

H_0: the process of initiating events conditional sojourn time θ^{27} at the state e^2 when the next transition is to the operation state e^7, has the chimney distribution with the density function of the form

$$h^{27}(t) = \begin{cases} 0, & t < x^{27} \\ \dfrac{A^{27}}{z_1^{27} - x^{27}}, & x^{27} \le t < z_1^{27} \\ \dfrac{C^{27}}{z_2^{27} - z_1^{27}}, & z_1^{27} \le t < z_2^{27} \\ \dfrac{D^{27}}{y^{27} - z_2^{27}}, & z_2^{27} \le t < y^{27} \\ 0, & t \ge y^{27}. \end{cases} \tag{1}$$

Since, according to (4.16)-(4.17) from Kołowrocki and Soszyńska-Budny[7] we have

$$\hat{n}^{27} = \max_{1 \le z \le 11} \{n_z^{27}\} = 36 \text{ and } n_1^{27} = \hat{n}^{27} = 36,$$

then $i = 1$ is the number of interval including the largest number of realizations. Moreover, by (4.19) in Kołowrocki and Soszyńska-Budny[7] we get

$$n_2^{27} = 1, \text{ and } \frac{n_1^{27}}{n_2^{27}} = \frac{36}{1} > 3.$$

Therefore, we estimate the unknown parameters of the density function of the hypothetical chimney distribution using the formulae (4.15) and (4.18) from Kołowrocki and Soszyńska-Budny[7] and we obtain the following results

$$x^{27} = a_1^{27} = 0,$$

$$y^{27} = x^{27} + \bar{r}^{27} d^{27} = 0 + 6 \cdot 11.8 = 70.8,$$

$$z_1^{27} = x^{27} + (i-1) d^{27} = 0 + (1-1) \cdot 11.8 = 0,$$

$$z_2^{27} = x^{27} + i d^{27} = 0 + 1 \cdot 11.8 = 11.8,$$

$$A^{27} = 0, \quad C^{27} = \frac{n_1^{27}}{n^{27}} = \frac{36}{40},$$

$$D^{27} = \frac{n_2^{27} + n_3^{27} + \ldots + n_6^{27}}{n^{27}} = \frac{1+1+0+0+2}{40} = \frac{4}{40}.$$

Substituting the above results into (1), we get completely defined the hypothetical density function in the form

$$h^{27}(t)=\begin{cases}0, & t<0\\ \dfrac{36/40}{11.8-0}, & 0\le t<11.8\\ \dfrac{4/40}{70.8-11.8}, & 11.8\le t<70.8\\ 0, & t\ge 70.8\end{cases}=\begin{cases}0, & t<0\\ 0.076271186, & 0\le t<11.8\\ 0.001694915, & 11.8\le t<70.8\\ 0, & t\ge 70.8\end{cases} \quad (2)$$

Hence the hypothetical distribution function $H^{27}(t)$ of the conditional sojourn time θ^{27}, after taking the integral of the hypothetical density function $h^{27}(t)$ given by (2), takes the following form

$$H^{27}(t)=\int_0^t h^{27}(t)dt=\begin{cases}0, & t<0\\ 0.076271186\,t, & 0\le t<11.8\\ 0.001694915\,t+0.879999995, & 11.8\le t<70.8\\ 1, & t\ge 70.8\end{cases}$$

Next, we join the intervals defined in the realization of the histogram $h^{27}(t)$ that have the numbers n_z^{27}, of realizations less than 4 into new intervals and we perform the following steps:

– we fix the new number of intervals

$$\bar{\bar{r}}^{27}=2;$$

– we determine the new intervals

$$\bar{I}_1=<0,11.8),\quad \bar{I}_2=<11.8,70.8);$$

– we fix the numbers of realizations in the new intervals

$$\bar{n}_1^{27}=36,\quad \bar{n}_2^{27}=4;$$

– we calculate, using (4.46) from Kołowrocki and Soszyńska-Budny[7], the hypothetical probabilities that the variable θ^{27} takes values from the new intervals

$$p_1=P(\theta^{27}\in\bar{I}_1)=P(0\le\theta^{27}<11.8)=H^{27}(11.8)-H^{27}(0)\cong 0.9-0=0.9,$$

$$p_2=P(\theta^{27}\in\bar{I}_2)=P(11.8\le\theta^{27}<70.8)=H^{27}(70.8)-H^{27}(11.8)$$

$$\cong 1-0.9=0.1;$$

– we calculate, using (4.47) from Kołowrocki and Soszyńska-Budny[7], the realization of the χ^2 (chi-square)-Pearson's statistics

$$u_{27}=\sum_{z=1}^{2}\frac{(\bar{n}_z^{27}-n^{27}p_z)^2}{n^{27}p_z}=\frac{(36-40\cdot 0.900)^2}{40\cdot 0.900}+\frac{(4-40\cdot 0.100)^2}{40\cdot 0.100}=0+0=0;$$

– we assume the significance level $\alpha=0.05$;

– we fix the number of degrees of freedom

$$\bar{\bar{r}}^{27}-j-1=2-0-1=1;$$

– we read from the Tables of the χ^2 – Pearson's distribution the value u_α for the fixed values of the significance level $\alpha = 0.05$ and the number of degrees of freedom

$$\bar{\bar{r}}^{27} - j - 1 = 1,$$

such that, according to (4.48) from Kołowrocki and Soszyńska-Budny[7], the following equality holds

$$P(U_{27} > u_\alpha) = \alpha = 0.05$$

that amounts to $u_\alpha = 3.84$ and we determine the critical domain in the form of the interval $(3.84,+\infty)$ and the acceptance domain in the form of the interval $<3.84,+\infty)$ (Fig. 3);

– we compare the obtained value $u_{27} = 0$ of the realization of the statistics U_{27} with the read from the Tables critical value $u_\alpha = 3.84$ of the chi-square random variable and since the value $u_{27} = 0$ does not belong to the critical domain, i.e.

$$u_{27} = 0 \le u_\alpha = 3.84,$$

then we do not reject the hypothesis H_0 that the sojourn time θ^{27} has the chimney distribution with the density function given by (2).

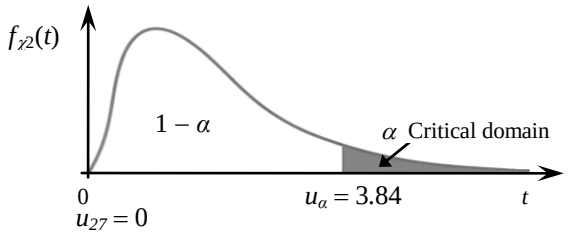

Fig. 3. The graphical interpretation of the critical interval and the acceptance interval for the chi-square goodness-of-fit test

Thus, after applying the formula (2.19) in Kołowrocki and Soszyńska-Budny[7] it is possible to find the mean value:

$$M_{27} = E[\theta^{27}] = \frac{1}{2}[A^{27}(x^{27} + z_1^{27}) + C^{27}(z_1^{27} + z_2^{27}) + D^{27}(z_2^{27} + y^{27})]$$

$$= \frac{1}{2}[0(0+0) + 0.9(0+11.8) + 0.1(11.8+70.8)] \cong 9.44.$$

For the remaining cases, when the realizations of conditional sojourn times θ^{j} are more than 28, proceedings afterwards in analogous way as in the case of the conditional sojourn time θ^{27}, we can get the following results:

– the conditional sojourn time θ^{18} has the exponential distribution with density function

$$h^{18}(t)=\begin{cases}0, & t<0\\ 0.0000000151\exp[-0.0000000151t], & t\geq 0\end{cases}$$

– the conditional sojourn time θ^{23} has the chimney distribution with density function

$$h^{23}(t)=\begin{cases}0, & t<0\\ 0.011264916, & 0\leq t<83.8\\ 0.000066826, & 83.8\leq t<921.8\\ 0, & t\geq 921.8\end{cases}$$

– the conditional sojourn time θ^{51} has the chimney distribution with density function

$$h^{51}(t)=\begin{cases}0, & t<0\\ 0.000482693, & 0\leq t<2024.625\\ 0.000001403, & 2024.625\leq t<18221.625\\ 0, & t\geq 18221.625\end{cases}$$

– the conditional sojourn time θ^{510} has the chimney distribution with density function

$$h^{510}(t)=\begin{cases}0, & t<0\\ 0.038784745, & 0\leq t<23.8\\ 0.000646412, & 23.8\leq t<142.8\\ 0, & t\geq 142.8\end{cases}$$

– the conditional sojourn time θ^{62} has the chimney distribution with density function

$$h^{62}(t)=\begin{cases}0, & t<0\\ 0.013724267, & 0\leq t<57.25\\ 0.000935745, & 57.25\leq t<286.25\\ 0, & t\geq 286.25\end{cases}$$

– the conditional sojourn time θ^{63} has the chimney distribution with density function

$$h^{63}(t)=\begin{cases}0, & t<0\\ 0.000193913, & 0\leq t<5039.75\\ 0.0000005637, & 5039.75\leq t<45357.75\\ 0, & t\geq 45357.75\end{cases}$$

– the conditional sojourn time θ^{73} has the chimney distribution with density function

$$h^{73}(t)=\begin{cases}0, & t<0\\ 0.002366234, & 0\leq t<392.64\\ 0.000016421, & 392.64\leq t<4711.68\\ 0, & t\geq 4711.68\end{cases}$$

In the case when as a result of the experiment, limited data coming from experts, we only have the number of realizations of the process of initiating events lifetimes in the states and its all realizations are equal to an approximate

value, we assume that this conditional sojourn times have the uniform distribution in the interval from this value minus its half to this value plus its half. For instance, the process initiating events the conditional sojourn time θ^{21} assumed $n^{21} = 237$ values equal to 1, we assume that it has the density function given by

$$h^{21}(t) = \begin{cases} 0, & t < 0.5 \\ 1, & 0.5 \le t < 1.5 \\ 0, & t \ge 1.5, \end{cases}$$

and the distribution function given by

$$H^{21}(t) = \begin{cases} 0, & t < 0.5 \\ t, & 0.5 \le t < 1.5 \\ 1, & t \ge 1.5. \end{cases}$$

In the case when as a result of the experiment, coming from experts, there are not any suitable distribution presented in Chapter 2 from Kołowrocki and Soszyńska-Budny[7] to describe the process of initiating events or we have less than 28 realizations of the process of initiating events, we assume that this time has the empirical distribution. For instance, the process initiating events conditional time θ^{47} assumed $n^{47} = 13$ values. The order sample realizations θ^{47} is: 1, 1, 1, 1, 1, 1, 1, 5, 5, 10, 10, 10, 15. Thus, we assume that conditional sojourn time θ^{47} has the density function given by

$$h^{47}(t) = \begin{cases} 0, & t \le 1, \\ 7/13, & 1 < t \le 5, \\ 9/13, & 5 < t \le 10, \\ 12/13, & 10 < t \le 15, \\ 0, & t > 15. \end{cases}$$

and the distribution function given by

$$H^{47}(t) = \begin{cases} 0, & t \le 1, \\ 7/13, & 1 < t \le 5, \\ 9/13, & 5 < t \le 10, \\ 12/13, & 10 < t \le 15, \\ 1, & t > 15. \end{cases}$$

We can proceeding with the remaining conditional times in the states of the process of initiating events in the same way and approximately fix they distribution.

For the distributions identified in this section, by application either the general formulae for the mean value or particular formulae given respectively by (2.12) and (2.13-2.19) in Kołowrocki and Soszyńska-Budny[7], the mean values $M^{lj} = E[\theta^{lj}]$, $l, j = 1,2,\ldots,16$, $l \ne j$, of the process of initiating events conditional sojourn times at particular states can be determined and they amount to:

$M^{18} \cong 6622516.56$, $M^{23} \cong 69.55$, $M^{27} \cong 9.44$, $M^{2\,11} = 1.00$, $M^{39} = 45.00$,

$M^{51} \cong 1073.05$, $M^{510} \cong 17.61$, $M^{5\,12} = 15.00$, $M^{61} \cong 804.66$, $M^{62} \cong 58.68$,
$M^{63} \cong 2973.45$, $M^{71} \cong 1808.15$, $M^{73} \cong 361.23$, $M^{74} = 5.00$, $M^{81} \cong 365.00$,
$M^{10\,14} = 60.00$, $M^{12\,1} = 30.00$, $M^{14\,1} \cong 120.00$, $M^{16\,7} = 60.00$.

In the remaining cases, when the distributions cannot be identified, it is possible to find the approximate empirical values of the mean values $M^{lj} = E[\theta^{lj}]$ of the conditional sojourn times at particular states that are as follows:

$M^{12} \cong 8745800.5$, $M^{13} \cong 11095287.8$, $M^{14} \cong 9005707.32$, $M^{15} \cong 11267059.7$,
$M^{16} \cong 10655753.85$, $M^{17} \cong 12392622.44$, $M^{21} \cong 1.00$, $M^{24} \cong 15.33$, $M^{25} = 5.25$,
$M^{26} \cong 1.86$, $M^{2\,10} = 3.00$, $M^{31} \cong 4500.64$, $M^{32} = 65.00$, $M^{36} = 6.50$, $M^{41} \cong 1.00$,
$M^{42} \cong 13.33$, $M^{43} \cong 79.31$, $M^{46} \cong 28.56$, $M^{47} \cong 4.77$, $M^{59} \cong 1071.67$,
$M^{5\,16} = 33.00$, $M^{64} \cong 25.91$, $M^{6\,10} = 41.25$, $M^{6\,11} \cong 53.36$, $M^{78} = 12.00$,
$M^{7\,11} = 4.00$, $M^{7\,13} = 7.40$, $M^{8\,13} = 4.25$, $M^{91} = 162.63$, $M^{10\,1} \cong 1254.77$,
$M^{10\,6} \cong 143.67$, $M^{11\,1} = 502.5$, $M^{11\,3} = 54.00$, $M^{13\,1} \cong 85.00$, $M^{13\,3} \cong 103.33$,
$M^{13\,15} = 15.00$, $M^{15\,3} = 140.00$, $M^{16\,1} = 75.00$, $M^{16\,3} = 90.00$.

Conclusions

The results presented in the paper will be used in the prediction of the considered process of initiating events generated by a ship operating at the sea waters as well as in the prediction of the entire process of the critical infrastructure accident consequences including the process of initiating events, the proces of environment threats and the process of environment degradation.

Acknowledgments

The paper presents the results developed in the scope of the EU-CIRCLE project titled “A pan – European framework for strengthening Critical Infrastructure resilience to climate change” that has received funding from the European Union’s Horizon 2020 research and innovation programme under grant agreement No 653824. http://www.eu-circle.eu/.

References

1. M. Bogalecka and K. Kołowrocki. Modelling critical infrastructure accident consequences – an overall approach, Journal of Polish Safety and Reliability Association, Summer Safety and Reliability Seminars, 7, 3, 1{13, 2016.
2. F. Grabski. Semi-Markov processes: applications in system reliability and maintenance, Elsevier, 2015.

3. K. Kołowrocki. Reliability of large systems, Elsevier, Amsterdam, Boston, Heidelberd, London, New York, Oxford, Paris, San Diego, San Francisco, Singapore, Sidney, Tokyo, 2004.
4. K. Kołowrocki. Reliability of large and complex systems, Elsevier, 2014.
5. K. Kołowrocki. Safety of critical infrastructures, Journal of Polish Safety and Reliability Association, Summer Safety and Reliability Seminars, 4, 1, 51{72, 2013.
6. K. Kołowrocki and J. Soszyńska-Budny. A general model of industrial systems operation processes related to their environment and infrastructure, Summer Safety and Reliability Seminars, Journal of Polish Safety and Reliability Association, 2, 2, 223{226, 2008.
7. K. Kołowrocki and J. Soszyńska-Budny. Reliability and safety of complex technical systems and processes: modeling – identification – prediction – optimization, Springer, London, Dordrecht, Heildeberg, New York, 2011.
8. N. Limnios and G. Oprisan. Semi-Markov processes and reliability, Birkhauser, Boston, 2005.
9. C. Macci. Large deviations for empirical estimators of the stationary distribution of a semi-Markov process with finite state space, Communications in Statistics-Theory and Methods, 37, 9, 3077{3089, 2008.
10. S. Mercier. Numerical bounds for semi-Markovian quantities and application to reliability, Methodology and Computing in Applied Probability, 10, 2, 179{198, 2008.

Statistical identification of critical infrastructure accident consequences process Part 2 Process of environment threats

Magda Bogalecka[1], and Krzysztof Kołowrocki[2]

[1] Department of Industrial Commodity Science and Chemistry, Gdynia Maritime University, 81-87 Morska Str., 81-225 Gdynia, Poland
(E-mail: m.bogalecka@wpit.am.gdynia.pl)
[2] Department of Mathematics, Gdynia Maritime University, 81-87 Morska Str., 81-225 Gdynia, Poland
(E-mail: k.kolowrocki@wn.am.gdynia.pl)

Abstract. The probabilistic general model of critical infrastructure accident consequences includes the process of initiating events, the process of environment threats and the process of environment degradation models. The statistical identification of the unknown parameters of the process of environment threats, i.e. estimating the probabilities of this process of staying at the states at the initial moment, the probabilities of this process transitions between its states and the distributions of this process conditional sojourn times at the particular states is performed.
Keywords: critical infrastructure, sea accident, potential consequences, environment threats.

1 Introduction

The risk analysis of chemical spills at sea and their consequences is proposed to be based on the general model of mutual interactions between three processes: the process of the sea accident initiating events, the process of the sea environment threats and the process of the sea environment degradation, Bogalecka and Kołowrocki [1]. This paper is concerned with the identification of the second one of these three processes.
To construct the general model of the environment threats caused by the process of the initiating events generated by critical infrastructure loss of required safety critical level, we distinguish the set of n_2, $n_2 \in N$, kinds of threats as the consequences of initiating events that may cause the sea environment degradation and denote them by

$H_1, H_2, ..., H_{n_2}$.

17th *ASMDA Conference Proceedings, 6 - 9 June 2017, London, UK*

We also distinguish n_3, $n_3 \in N$, environment sub-regions

$$D_1, D_2, \ldots, D_{n_3},$$

of the considered critical infrastructure operating environment region

$$D = D_1 \cup D_2 \cup \ldots \cup D_{n_3},$$

that may be degraded by the environment threats H_i, $i = 1,2,\ldots,n_2$. Moreover, we assume that the scale of the threat H_i, $i = 1,2,\ldots,n_2$, influence on region D depends on the range of its parameter value and for particular parameter f^i, $i = 1,2,\ldots,n_2$, we distinguish l_i ranges $f^{i1}, f^{i2}, \ldots, f^{il_i}$ of its values.

After that, we introduce the set of vectors

$$S = \{s : s = [f^1, f^2, \ldots, f^{n_2}]\}, \tag{1}$$

where

$$f^i = \begin{cases} 0, & \text{if a threat } H_i \text{ does not appear at the region } D, \\ f^{ij}, & \text{if a threat } H_i \text{ appears at the region } D \\ & \text{and its parameter is at the range } f^{ij},\ j = 1,2,\ldots,l^i, \end{cases}$$

for $i = 1,2,\ldots,n_2$.

We call vectors (1) the environment threat state of the region D.

Simultaneously, we proceed for the particular sub-regions D_k, $k = 1,2,\ldots,n_3$.

The vector

$$s_{(k)} = [f^1_{(k)}, f^1_{(k)}, \ldots, f^{n_2}_{(k)}],\ k = 1,2,\ldots,n_3, \tag{2}$$

where

$$f^i_{(k)} = \begin{cases} 0, & \text{if a threat } H_i \text{ does not appear at the sub-region } D_k, \\ f^{ij}_{(k)}, & \text{if a threat } H_i \text{ appears at the sub-region } D_k \text{ and} \\ & \text{its parameter is in the range } f^{ij}_{(k)},\ j = 1,2,\ldots,l_i, \end{cases} \tag{3}$$

for $i = 1,2,\ldots,n_2$, $k = 1,2,\ldots,n_3$,

is called the environment threat state of the sub-region D_k.

From the above definition, the maximum number of the environment threat states for the sub-region D_k, $k = 1,2,\ldots,n_3$, is equalled to

$$\upsilon_k = (l^1_{(k)} + 1), (l^2_{(k)} + 1), \ldots, (l^{n_2}_{(k)} + 1),\ k = 1,2,\ldots,n_3.$$

Further, we number the sub-region environment threat states defined by (2) and (3) and mark them by

$$s^{\upsilon}_{(k)} \text{ for } \upsilon = 1,2,\ldots,\upsilon_k,\ k = 1,2,\ldots,n_3,$$

and form the set

$$S_{(k)} = \{s^{\upsilon}_{(k)},\ \upsilon = 1,2,\ldots,\upsilon_k\},\ k = 1,2,\ldots,n_3,$$

where

$s^i_{(k)} \neq s^j_{(k)}$ for $i \neq j,\ i, j \in \{1,2,\ldots,\upsilon_k\}$.

The set $S_{(k)}$, $k = 1,2,\ldots,n_3$, is called the set of the environment threat states of the sub-region D_k, $k = 1,2,\ldots,n_3$, while a number υ_k is called the number of the environment threat states of this sub-region.
A function

$S_{(k)}(t)$, $k = 1,2,\ldots,n_3$,

defined on the time interval $t \in <0,\infty)$, and having values in the environment threat states set

$S_{(k)}$, $k = 1,2,\ldots,n_3$,

is called the sub-process of the environment threats of the sub-region D_k, $k = 1,2,\ldots,n_3$.
Next, to involve the sub-process of environment threats of the sub-region with the process of initiating events, we introduced the function

$S_{(k/l)}(t)$, $k = 1,2,\ldots,n_3$, $l = 1,2,\ldots,\omega$,

defined on the time interval $t \in <0,\infty)$, depending on the states e^l, $l = 1,2,\ldots,\omega$, of the process of initiating events $E(t)$ and taking its values in the set of the environment threat states set $S_{(k)}$, $k = 1,2,\ldots,n_3$. This function is called the conditional sub-process of the environment threats in the sub-region D_k, $k = 1,2,\ldots,n_3$, while the process of initiating events $E(t)$ is at the state e^l, $l = 1,2,\ldots,\omega$.

2 Process of environment threats modelling

We assume a semi-Markov model Grabski[3], Kołowrocki[4-5], Kołowrocki and Soszyńska[6], Limnios and Oprisan[7], Macci[8], Mercier[9] of the sub-process of environment threats $S_{(k/l)}(t)$, $k = 1,2,\ldots,n_3$, $l = 1,2,\ldots,\omega$, and denote by

$\eta^{ij}_{(k/l)}$, $i, j = 1,2,\ldots,\upsilon_k$, $i \neq j$, $k = 1,2,\ldots,n_3$, $l = 1,2,\ldots,\omega$,

its random conditional sojourn times at the state $s^i_{(k)}$ while its next transition will be done to the state $s^j_{(k)}$. This sub-process is defined by:
– the vector of probabilities of its initial states at the moment $t = 0$

$[p^i_{(k/l)}(0)]_{1x\upsilon_k}$,

– the matrix of probabilities of transitions between the states

$[p^{ij}_{(k/l)}]_{\upsilon_k x \upsilon_k}$,

– the matrix of the distribution functions of the conditional sojourn times

$[H^{ij}_{(k/l)}(t)]_{\upsilon_k x \upsilon_k}$,

or equivalently by the matrix of the density functions of the conditional sojourn times

$[h^{ij}_{(k/l)}(t)]_{\upsilon_k x \upsilon_k}$,

– the mean values of the conditional sojourn times

$M^{ij}_{(k/l)}$.

We divided the maritime environment into $k = 5$ sub-regions D_k, and defined as follows: D_1 – air, D_2 – water surface, D_3 – water column, D_4 – sea floor, D_5 – coast (shoreline). Next, we distinguished $n_2 = 6$ possible environment threats that may cause degradation in the neighbourhood region of the ship accident area as follows: H_1 – explosion of the chemical substance in the accident area, H_2 – fire of the chemical substance in the accident area, H_3 – toxic chemical substance presence in the accident area, H_4 – corrosive chemical substance presence in the accident area, H_5 – bioaccumulative substance presence in the accident area, H_6 – other dangerous chemical substances presence in the accident area. The procedure of defining states of the sea environment threats process generated by hazardous chemicals is presented in Bogalecka and Kołowrocki[2]. The number of this process states for each sub-region $\upsilon_1 = 35$, $\upsilon_2 = 33$, $\upsilon_3 = 29$, $\upsilon_4 = 29$, $\upsilon_5 = 29$ are fixed and the environment threats states $s^i_{(k)}$, $i = 1,2,\ldots,\upsilon_k$, are defined in Bogalecka and Kołowrocki[1]. Additionally, we involve the process of initiating events $E(t)$ with each sub-process of environment threats. Thus, we fix environment threats states $s^i_{(k/l)}$, $i = 1,2,\ldots,\upsilon_k$, $k = 1,2,\ldots,n_3$, $l = 1,2,\ldots,\omega$, for a particular sub-region according to the initiating event e^l, $l = 1,2,\ldots,\omega$, that causes the environment threats state. Moreover, it is assumed that there are possible transitions between all states of the sub-process of environment threats.

3 Statistical identification of the process of environment threats

The experiment was performed across the world seas and oceans in the years 2004-2014. The initial moment $t = 0$ of the process of environment threat was fixed at the moment when the initiating event causing ship accident generated one of the distinguished environment threat states.

3.1 Data collection for estimating unknown parameters of the process of environment threats

To identify unknown parameters of the sub-process of environment threats, described in Section 2, the statistical data coming from the sub-process of environment threats $S_{(k/l)}(t)$, $k = 1,2,...,n_3$, $l = 1,2,...,\omega$, realization are used:

– the process of environment threats observation/experiment time $\Theta = 11$ years (2004-2014);
– the vectors of realizations $[n^i_{(k/l)}(0)]_{1x\upsilon k}$, $k = 1,2,...,5$, $l = 1,2,...,16$, $\upsilon_1 = 35$, $\upsilon_2 = 33$, $\upsilon_3 = 29$, $\upsilon_4 = 29$, $\upsilon_5 = 29$, of the environment threats sub-processes staying at the particular states $s^i_{(k/l)}$ at the initial moment $t = 0$. For instance, the vectors of realizations for the sub-region D_1 are as follows:

$[n^i_{(1/1)}(0)]_{1x35} = [1630, 0,..., 0]$, $[n^i_{(1/2)}(0)]_{1x35} = [434, 0,..., 0]$,

$[n^i_{(1/3)}(0)]_{1x35} = [760, 0,..., 0]$, $[n^i_{(1/4)}(0)]_{1x35} = [149, 0,..., 0]$,

$[n^i_{(1/5)}(0)]_{1x35} = [273, 0,...,0]$, $[n^i_{(1/6)}(0)]_{1x35} = [284, 0,..., 0]$,

$[n^i_{(1/7)}(0)]_{1x35} = [260, 0,..., 0]$, $[n^i_{(1/8)}(0)]_{1x35} = [38, 0,..., 0]$,

$[n^i_{(1/9)}(0)]_{1x35} = [19, 0,..., 0]$, $[n^i_{(1/10)}(0)]_{1x35} = [45, 0,..., 0]$,

$[n^i_{(1/11)}(0)]_{1x35} = [18, 0,..., 0]$, $[n^i_{(1/12)}(0)]_{1x35} = [1, 0,..., 0]$,

$[n^i_{(1/13)}(0)]_{1x35} = [9, 0,..., 0]$, $[n^i_{(1/14)}(0)]_{1x35} = [1, 0,..., 0]$,

$[n^i_{(1/15)}(0)]_{1x35} = [2, 0,..., 0]$, $[n^i_{(1/16)}(0)]_{1x35} = [5, 0,..., 0]$;

– the number of the environment threats sub-process realizations at the moment $t = 0$

$n_{(k/1)}(0) = 1630$, $n_{(k/2)}(0) = 434$, $n_{(k/3)}(0) = 760$, $n_{(k/4)}(0) = 149$, $n_{(k/5)}(0) = 273$,
$n_{(k/6)}(0) = 284$, $n_{(k/7)}(0) = 260$, $n_{(k/8)}(0) = 38$, $n_{(k/9)}(0) = 19$, $n_{(k/10)}(0) = 45$,
$n_{(k/11)}(0) = 18$, $n_{(k/12)}(0) = 1$, $n_{(k/13)}(0) = 9$, $n_{(k/14)}(0) = 1$, $n_{(k/15)}(0) = 2$,
$n_{(k/16)}(0) = 5$, $k = 1,2\ldots,5$.

The collected statistical data necessary for evaluating the probabilities of transitions between environment threats states are:
– the matrices of realizations $n^{ij}_{(k/l)}$, $i, j = 1,2,\ldots,\upsilon_k$, $k = 1,2,...,5$, $l = 1,2,...,16$, $\upsilon_1 = 35$, $\upsilon_2 = 33$, $\upsilon_3 = 29$, $\upsilon_4 = 29$, $\upsilon_5 = 29$, of the numbers of the process $S_{(k/l)}(t)$ transitions from the state $s^i_{(k/l)}$ into the state $s^j_{(k/l)}$ during the experimental time. For instance, the matrices of realizations for the sub-region D_1 are as follows (the numbers of transitions that are not equal to 0 are presented only):

$n^{1\ 27}_{(1/2)} = 43$, $n^{7\ 1}_{(1/2)} = 1$, $n^{27\ 1}_{(1/2)} = 42$, $n^{27\ 7}_{(1/2)} = 1$;

$n^{1\ 23}_{(1/3)} = 1$, $n^{1\ 27}_{(1/3)} = 40$, $n^{1\ 30}_{(1/3)} = 2$, $n^{23\ 1}_{(1/3)} = 1$, $n^{27\ 1}_{(1/3)} = 40$, $n^{30\ 1}_{(1/3)} = 2$;

$n^{1\ 13}_{(1/4)} = 1$, $n^{1\ 27}_{(1/4)} = 16$, $n^{1\ 35}_{(1/4)} = 1$, $n^{5\ 1}_{(1/4)} = 1$, $n^{13\ 1}_{(1/4)} = 1$, $n^{27\ 1}_{(1/4)} = 16$,

$n^{35\ 5}_{(1/4)} = 1$;

$n^{1\ 3}_{(1/5)} = 1$, $n^{1\ 4}_{(1/5)} = 3$, $n^{1\ 27}_{(1/5)} = 5$, $n^{1\ 34}_{(1/5)} = 1$, $n^{3\ 17}_{(1/5)} = 1$, $n^{4\ 1}_{(1/5)} = 4$,

$n^{7\ 1}_{(1/5)} = 1$, $n^{17\ 7}_{(1/5)} = 1$, $n^{27\ 1}_{(1/5)} = 5$, $n^{34\ 4}_{(1/5)} = 1$;

$n^{1\,27}_{(1/6)} = 2,\ n^{27\,1}_{(1/6)} = 2;$

$n^{1\,27}_{(1/7)} = 7,\ n^{1\,30}_{(1/7)} = 1,\ n^{27\,1}_{(1/7)} = 7,\ n^{30\,1}_{(1/7)} = 1;$

$n^{1\,3}_{(1/8)} = 1,\ n^{1\,6}_{(1/8)} = 3,\ n^{1\,7}_{(1/8)} = 1,\ n^{1\,8}_{(1/8)} = 1,\ n^{1\,27}_{(1/8)} = 11,\ n^{3\,1}_{(1/8)} = 1,\ n^{6\,1}_{(1/8)} = 3,$

$n^{7\,21}_{(1/8)} = 1,\ n^{8\,1}_{(1/8)} = 1,\ n^{21\,1}_{(1/8)} = 1,\ n^{27\,1}_{(1/8)} = 11;$

– the vectors of realisation of the total numbers of the sub-process $S_{(k/l)}(t)$ transitions from the state $s^i_{(k/l)}$, $i = 1,2,...,\upsilon_k$, $k = 1,2,...,5$, $l = 1,2,...,16$, $\upsilon_1 = 35$, $\upsilon_2 = 33$, $\upsilon_3 = 29$, $\upsilon_4 = 29$, $\upsilon_5 = 29$, during the experimental time. For instance, the vectors of realizations for the sub-region D_1 are as follows:

$[n^i_{(1/2)}]_{1x35} = [43, 0, 0, 0, 0, 0, 1, 0, 0, 0, 0, 0, 0, 0, 0, 0, 0, 0, 0, 0, 0, 0, 0, 0, 0,$
$0, 43, 0, 0, 0, 0, 0, 0, 0, 0],$

$[n^i_{(1/3)}]_{1x35} = [43, 0, 0, 0, 0, 0, 0, 0, 0, 0, 0, 0, 0, 0, 0, 0, 0, 0, 0, 0, 0, 0, 1, 0, 0,$
$0, 40, 0, 0, 2, 0, 0, 0, 0, 0],$

$[n^i_{(1/4)}]_{1x35} = [18, 0, 0, 0, 1, 0, 0, 0, 0, 0, 0, 0, 1, 0, 0, 0, 0, 0, 0, 0, 0, 0, 0, 0, 0,$
$0, 16, 0, 0, 0, 0, 0, 0, 0, 1],$

$[n^i_{(1/5)}]_{1x35} = [10, 0, 1, 4, 0, 0, 1, 0, 0, 0, 0, 0, 0, 0, 0, 0, 1, 0, 0, 0, 0, 0, 0, 0, 0,$
$0, 5, 0, 0, 0, 0, 0, 0, 1, 0],$

$[n^i_{(1/6)}]_{1x35} = [2, 0, 0, 0, 0, 0, 0, 0, 0, 0, 0, 0, 0, 0, 0, 0, 0, 0, 0, 0, 0, 0, 0, 0, 0, 0,$
$2, 0, 0, 0, 0, 0, 0, 0, 0],$

$[n^i_{(1/7)}]_{1x35} = [8, 0, 0, 0, 0, 0, 0, 0, 0, 0, 0, 0, 0, 0, 0, 0, 0, 0, 0, 0, 0, 0, 0, 0, 0, 0,$
$7, 0, 0, 1, 0, 0, 0, 0, 0],$

$[n^i_{(1/8)}]_{1x35} = [17, 0, 1, 0, 0, 3, 1, 1, 0, 0, 0, 0, 0, 0, 0, 0, 0, 0, 0, 0, 1, 0, 0, 0, 0,$
$0, 11, 0, 0, 0, 0, 0, 0, 0, 0],$

$[n^i_{(1/1)}]_{1x35} = [n^i_{(1/9)}]_{1x35} = [n^i_{(1/10)}]_{1x35} = [n^i_{(1/11)}]_{1x35} = [n^i_{(1/12)}]_{1x35} = [n^i_{(1/13)}]_{1x35}$
$= [n^i_{(1/14)}]_{1x35} = n^i_{(1/15)}]_{1x35} = [n^i_{(1/16)}]_{1x35} = [0, 0,\ldots, 0].$

The collected statistical data necessary to evaluate the unknown parameters of the distributions of the conditional sojourn times $\eta^{ij}_{(k/l)}$ at the states of the sub-process of environment threats are as follows:

– the numbers $n^{ij}_{(k/l)}$, $i, j = 1,2,...,\upsilon_k$, $i \neq j$, $k = 1,2,...,5$, $l = 1,2,...,16$, $\upsilon_1 = 35$, $\upsilon_2 = 33$, $\upsilon_3 = 29$, $\upsilon_4 = 29$, $\upsilon_5 = 29$, of the realizations $\eta^{ij}_{(k/l)\gamma}$, $\gamma = 1,2,...,n^{ij}_{(k/l)}$ of the conditional sojourn times $\eta^{ij}_{(k/l)}$ of the sub-process of environment threats state $s^i_{(k/l)}$, when the next transition is to the state $s^j_{(k/l)}$ during the experimental time;

– the realizations $\eta^{ij}_{(k/l)\gamma}$, $\gamma = 1,2,...,n^{ij}_{(k/l)}$ $i, j = 1,2,...,\upsilon_k$, $i \neq j$, $k = 1,2,...,5$, $l = 1,2,...,16$, $\upsilon_1 = 35$, $\upsilon_2 = 33$, $\upsilon_3 = 29$, $\upsilon_4 = 29$, $\upsilon_5 = 29$, of the conditional sojourn times $\eta^{ij}_{(k/l)}$ of the sub-process of environment threats state $s^i_{(k/l)}$, when the next transition is to the state $s^j_{(k/l)}$ during the experimental time.

3.2 Estimating parameters of the process of environment threats

On the basis of the statistical data from Section 3.1, using the formulae given in Section 4.2.3 in Kołowrocki and Soszyńska-Budny[6], it is possible to evaluate the following unknown basic parameters of the process of environment threats:

– the vectors of the initial probabilities $p^i_{(k/l)}(0)$, $i = 1,2,...,\upsilon_k$, $k = 1,2,...,5$, $l = 1,2,...,16$, $\upsilon_1 = 35$, $\upsilon_2 = 33$, $\upsilon_3 = 29$, $\upsilon_4 = 29$, $\upsilon_5 = 29$, of the environment threats sub-process at the particular states at the moment $t = 0$. For instance, the vectors of initial probabilities for the sub-region D_1 are as follows:

$[p_{(1/l)}(0)]_{1x35} = [1,0,\ldots,0]$, $l = 1,2,...,16$;

– the matrices $[p^{ij}_{(k/l)}]$, $i, j = 1,2,...,\upsilon_k$, $k = 1,2,...,5$, $l = 1,2,...,16$, $\upsilon_1 = 35$, $\upsilon_2 = 33$, $\upsilon_3 = 29$, $\upsilon_4 = 29$, $\upsilon_5 = 29$, of probabilities of transitions of the sub-process $S_{(k/l)}(t)$ from the state $s^i_{(k/l)}$ into the state $s^j_{(k/l)}$ during the experimental time. For instance, the matrices of probabilities of transitions for the sub-region D_1 are as follows (the probabilities of transitions that are not equal to 0 are presented only):

$p^{1\ 27}_{(1/2)} = 1,\ p^{7\ 1}_{(1/2)} = 1,\ p^{27\ 1}_{(1/2)} = 0.977,\ p^{27\ 7}_{(1/2)} = 0.023;$

$p^{1\ 23}_{(1/3)} = 0.023,\ p^{1\ 27}_{(1/3)} = 0.931,\ p^{1\ 30}_{(1/3)} = 0.046,\ p^{23\ 1}_{(1/3)} = 1,\ p^{27\ 1}_{(1/3)} = 1,$

$p^{30\ 1}_{(1/3)} = 1;$

$p^{1\ 13}_{(1/4)} = 0.055,\ p^{1\ 27}_{(1/4)} = 0.890,\ p^{1\ 35}_{(1/4)} = 0.055,\ p^{5\ 1}_{(1/4)} = 1,\ p^{13\ 1}_{(1/4)} = 1,$

$p^{27\ 1}_{(1/4)} = 1,\ p^{35\ 5}_{(1/4)} = 1;$

$p^{1\ 3}_{(1/5)} = 0.1,\ p^{1\ 4}_{(1/5)} = 0.3,\ p^{1\ 27}_{(1/5)} = 0.5,\ p^{1\ 34}_{(1/5)} = 0.1,\ p^{3\ 17}_{(1/5)} = 1,\ p^{4\ 1}_{(1/5)} = 1,$

$p^{7\ 1}_{(1/5)} = 1,\ p^{17\ 7}_{(1/5)} = 1,\ p^{27\ 1}_{(1/5)} = 1,\ p^{34\ 4}_{(1/5)} = 1;$

$p^{1\ 27}_{(1/6)} = 1,\ p^{27\ 1}_{(1/6)} = 1;$

$p^{1\ 27}_{(1/7)} = 0.875,\ p^{1\ 30}_{(1/7)} = 0.125,\ p^{27\ 1}_{(1/7)} = 1,\ p^{30\ 1}_{(1/7)} = 1;$

$p^{1\ 3}_{(1/8)} = 0.059,\ p^{1\ 6}_{(1/8)} = 0.176,\ p^{1\ 7}_{(1/8)} = 0.059,\ p^{1\ 8}_{(1/8)} = 0.059,\ p^{1\ 27}_{(1/8)} = 0.647,$

$p^{3\ 1}_{(1/8)} = 1,\ p^{6\ 1}_{(1/8)} = 1,\ p^{7\ 21}_{(1/8)} = 1,\ p^{8\ 1}_{(1/8)} = 1,\ p^{21\ 1}_{(1/8)} = 1,\ p^{27\ 1}_{(1/8)} = 1.$

The values of some probabilities existing in the vectors $[p_{(k/l)}(0)]$ and in the matrix $[p^{ij}_{(k/l)}]$, besides of those standing on the main diagonal, equal to zero do

not mean that the events they are concerned with, cannot appear. They are evaluated on the basis of real statistical data and their values may change and become more precise if the duration of the experiment is longer.

3.3 Estimating parameters of distributions of the process of environment threats

On the basis of the statistical data presented in Section 3.1, using the procedure and the formulae given in Kołowrocki and Soszyńska-Budny[6], it is possible to determine the empirical parameters of the conditional sojourn times $\eta^{ij}_{(k/l)}$ of the sub-process of environment threats at the particular environment threats states. The application of this procedure and these formulae is similar to the one presented in Part 1 of the paper, than we omit it.

3.4 Identifying distribution functions of environment threats conditional sojourn times at states

Using the procedure given in Section 4.2.4 in Kołowrocki and Soszyńska-Budny[6] and proceedings in analogous way as in Section 3.4 of Part 1 of the paper, we identified the forms of the particular density function $h^{ij}_{(k/l)}(t)$ and distribution functions $H^{ij}_{(k/l)}(t)$ of the sub-process of environment threats conditional sojourn times $\eta^{ij}_{(k/l)}$, $i, j = 1,2,...,\upsilon_k$, $i \neq j$, $k = 1,2,...,5$, $l = 1,2,...,16$, $\upsilon_1 = 35$, $\upsilon_2 = 33$, $\upsilon_3 = 29$, $\upsilon_4 = 29$, $\upsilon_5 = 29$, having sufficiently numerous set of their realizations at particular states. We have got the following results:

– the quasi-trapezium distribution function for the conditional sojourn time $\eta^{27\,1}_{(1/2)}$

$$H^{27\,1}_{(1/2)}(t) = \begin{cases} 0 & t < 0 \\ -0.000000054796\,t^2 + 0.000250627\,t, & 0 \le t < 1320 \\ 0.000105985\,t + 0.0954528, & 1320 \le t < 5760 \\ 0.000000153988\,t - 0.00166796\,t + 5.204416, & 5760 \le t < 6840 \\ 0, & t \ge 6840, \end{cases}$$

– the chimney distribution function for the conditional sojourn time $\eta^{127}_{(1/3)}$

$$H^{1\,27}_{(1/3)}(t) = \begin{cases} 0, & t < 0 \\ 0.003387769\,t, & 0 \le t < 287.8 \\ 0.000017373\,t + 0.969999969, & 287.8 \le t < 1726.8 \\ 1, & t \ge 1726.8, \end{cases}$$

– the double trapezium distribution function for the conditional sojourn time $\eta^{271}_{(1/3)}$

$$H^{27\,1}_{(1/3)}(t)=\begin{cases}0, & t<0\\ -0.0000000735\,t^2+0.00035461\,t, & 0\le t<2718\\ 0.0000000467\,t^2-0.000299711\,t+0.890464, & 2718\le t<6768\\ 1, & t\ge 6768,\end{cases}$$

– the chimney distribution function for the conditional sojourn time $\eta^{331}_{(2/2)}$

$$H^{33\,1}_{(2/2)}(t)=\begin{cases}0, & t<0\\ 0.000022616\,t, & 0\le t<43164\\ 0.00000011\,t+0.971448984, & 43164\le t<258984\\ 1, & t\ge 258984,\end{cases}$$

– the chimney distribution function for the conditional sojourn time $\eta^{133}_{(2/3)}$

$$H^{1\,33}_{(2/3)}(t)=\begin{cases}0, & t<0\\ 0.003389888\,t, & 0\le t<287.8\\ 0.000016949\,t+0.970731844, & 287.8\le t<1726.8\\ 1, & t\ge 1726.8,\end{cases}$$

– the exponential distribution function for the conditional sojourn time $\eta^{331}_{(2/3)}$

$$H^{33\,1}_{(2/3)}(t)=\begin{cases}0, & t<0\\ 1-\exp(-0.0000898\,t), & t\ge 0,\end{cases}$$

– the chimney distribution function for the conditional sojourn time $\eta^{241}_{(3/2)}$

$$H^{24\,1}_{(3/2)}(t)=\begin{cases}0, & t<0\\ 0.000022616\,t, & 0\le t<43164\\ 0.00000011\,t+0.971448984, & 43164\le t<258984\\ 1, & t\ge 258984,\end{cases}$$

– the chimney distribution function for the conditional sojourn time $\eta^{124}_{(3/3)}$

$$H^{1\,24}_{(3/3)}(t)=\begin{cases}0, & t<0\\ 0.003389888\,t, & 0\le t<287.8\\ 0.000016949\,t+0.970731844, & 287.8\le t<1726.8\\ 1, & t\ge 1726.8,\end{cases}$$

– the exponential distribution function for the conditional sojourn time $\eta^{241}_{(3/3)}$

$$H^{24\,1}_{(3/3)}(t)=\begin{cases}0, & t<0\\ 1-\exp(-0.00008066\,t), & t\ge 0.\end{cases}$$

In the case when as a result of the experiment, limited data coming from experts, we only have the number of realizations of the process of environment threats lifetimes in the states and its all realizations are equal to an approximate value, we assume that this conditional sojourn times have the uniform distribution in the interval from this value minus its half to this value plus its half. On the other hand, in the case when as a result of the experiment, coming from experts, we have less than 28 realizations of the sub-process of environment threats, we assume that this time has the empirical distribution function. Then we proceeds in analogous way as in Section 3.4 of Part 1 of the paper.

For the distributions identified in this section, by application either the general formulae for the mean value or particular formulae given respectively by (2.12) and (2.13-2.19) in Kołowrocki and Soszyńska-Budny[6], the mean values $M^{ij}_{(k/l)} = E[\eta^{ij}_{(k/l)}]$, $i, j = 1,2,...,\upsilon_k$, $i \neq j$, $k = 1,2,...,5$, $l = 1,2,...,16$, $\upsilon_1 = 35$, $\upsilon_2 = 33$, $\upsilon_3 = 29$, $\upsilon_4 = 29$, $\upsilon_5 = 29$, of the sub-process of environment threats conditional sojourn times at particular states can be determined and they amount to:

$$M^{1\,27}_{(1/2)} = 1,\ M^{7\,1}_{(1/2)} = 240,\ M^{27\,1}_{(1/2)} \cong 3685.1,\ M^{1\,23}_{(1/3)} = 1,\ M^{1\,27}_{(1/3)} \cong 165.485,$$

$$M^{1\,30}_{(1/3)} = 1,\ M^{23\,1}_{(1/3)} = 240,\ M^{27\,1}_{(1/3)} \cong 3596.51,\ M^{30\,1}_{(1/3)} = 240,\ M^{1\,13}_{(1/4)} = 1,$$

$$M^{1\,27}_{(1/4)} = 1,\ M^{1\,35}_{(1/4)} = 1,\ M^{5\,1}_{(1/4)} = 300,\ M^{13\,1}_{(1/4)} = 120,\ M^{35\,5}_{(1/4)} = 120,\ M^{1\,3}_{(1/5)} = 1,$$

$$M^{1\,4}_{(1/5)} = 1,\ M^{1\,27}_{(1/5)} = 1,\ M^{1\,34}_{(1/5)} = 1,\ M^{3\,17}_{(1/5)} = 1,\ M^{7\,1}_{(1/5)} = 5,\ M^{17\,7}_{(1/5)} = 300,$$

$$M^{34\,4}_{(1/5)} = 15,\ M^{1\,27}_{(1/6)} = 1,\ M^{27\,1}_{(1/6)} = 5760,\ M^{1\,27}_{(1/7)} = 1,\ M^{1\,30}_{(1/7)} = 1,\ M^{30\,1}_{(1/7)} = 240,$$

$$M^{1\,3}_{(1/8)} = 1,\ M^{1\,6}_{(1/8)} = 1,\ M^{1\,7}_{(1/8)} = 1,\ M^{1\,8}_{(1/8)} = 1,\ M^{1\,27}_{(1/8)} = 1,\ M^{3\,1}_{(1/8)} = 40,$$

$$M^{7\,21}_{(1/8)} = 15,\ M^{8\,1}_{(1/8)} = 240,\ M^{21\,1}_{(1/8)} = 5,\ M^{1\,33}_{(2/2)} = 1,\ M^{2\,1}_{(2/2)} = 280800,$$

$$M^{33\,1}_{(2/2)} \cong 24171.84,\ M^{33\,2}_{(2/2)} = 2880,\ M^{1\,17}_{(2/3)} = 1,\ M^{1\,18}_{(2/3)} = 1,\ M^{1\,33}_{(2/3)} \cong 161.17,$$

$$M^{18\,1}_{(2/3)} = 43200,\ M^{33\,1}_{(2/3)} \cong 11135.86,\ M^{1\,33}_{(2/4)} = 1,\ M^{1\,33}_{(2/5)} = 1,\ M^{1\,33}_{(2/6)} = 1,$$

$$M^{1\,17}_{(2/7)} = 1,\ M^{1\,33}_{(2/7)} = 1,\ M^{17\,1}_{(2/7)} = 1440,\ M^{1\,2}_{(2/8)} = 1,\ M^{1\,4}_{(2/8)} = 1,\ M^{1\,5}_{(2/8)} = 1,$$

$$M^{1\,33}_{(2/8)} = 1,\ M^{2\,1}_{(2/8)} = 7200,\ M^{4\,1}_{(2/8)} = 1440,\ M^{5\,1}_{(2/8)} = 1440,\ M^{1\,24}_{(3/2)} = 1,$$

$$M^{2\,1}_{(3/2)} = 280800,\ M^{24\,1}_{(3/2)} \cong 24171.84,\ M^{24\,2}_{(3/2)} = 2880,\ M^{1\,14}_{(3/3)} = 1,\ M^{1\,15}_{(3/3)} = 1,$$

$$M^{1\,24}_{(3/3)} \cong 161.17,\ M^{15\,1}_{(3/3)} = 43200,\ M^{24\,1}_{(3/3)} \cong 12398.05,\ M^{1\,24}_{(3/4)} = 1,\ M^{1\,24}_{(3/5)} = 1,$$

$$M^{1\,24}_{(3/6)} = 1,\ M^{1\,14}_{(3/7)} = 1,\ M^{1\,24}_{(3/7)} = 1,\ M^{14\,1}_{(3/7)} = 1440,\ M^{1\,2}_{(3/8)} = 1,\ M^{1\,3}_{(3/8)} = 1,$$

$$M^{1\,4}_{(3/8)} = 1,\ M^{1\,24}_{(3/8)} = 1,\ M^{2\,1}_{(3/8)} = 7200,\ M^{3\,1}_{(3/8)} = 1440,\ M^{4\,1}_{(3/8)} = 1440,$$

$$M^{1\,2}_{(4/2)} = 1,\ M^{2\,1}_{(4/2)} = 280800,\ M^{1\,14}_{(4/3)} = 1,\ M^{1\,15}_{(4/3)} = 1,\ M^{15\,1}_{(4/3)} = 43200,$$

$$M^{1\,24}_{(4/4)} = 1,\ M^{1\,24}_{(4/5)} = 1,\ M^{1\,14}_{(4/7)} = 1,\ M^{14\,1}_{(4/7)} = 1440,\ M^{1\,2}_{(4/8)} = 1,\ M^{1\,4}_{(4/8)} = 1,$$

$$M^{1\,24}_{(4/8)} = 1,\ M^{2\,1}_{(4/8)} = 7200,\ M^{4\,1}_{(4/8)} = 1440,\ M^{1\,15}_{(5/3)} = 1,\ M^{15\,1}_{(5/3)} = 43200,$$

$$M^{1\,24}_{(5/4)} = 1,\ M^{1\,24}_{(5/5)} = 1,\ M^{24\,1}_{(5/5)} = 172800,\ M^{1\,24}_{(5/6)} = 1440,\ M^{24\,1}_{(5/6)} = 17280,$$

$$M^{1\,24}_{(5/7)} = 1,\ M^{1\,24}_{(5/8)} = 1.$$

In the remaining cases, when the distributions cannot be identified, it is possible to find the approximate empirical values of the mean values $M^{ij}_{(k/l)} = E[\eta^{ij}_{(k/l)}]$, $i, j = 1,2,\ldots,\upsilon_k$, $i \neq j$, $k = 1,2,\ldots,5$, $l = 1,2,\ldots,16$, $\upsilon_1 = 35$, $\upsilon_2 = 33$, $\upsilon_3 = 29$, $\upsilon_4 = 29$, $\upsilon_5 = 29$, of the conditional sojourn times at particular states that are as follows:

$$M^{27\,7}_{(1/2)} = 240,\ M^{27\,1}_{(1/4)} = 2546.25,\ M^{4\,1}_{(1/5)} = 1147.50,\ M^{27\,1}_{(1/5)} = 1488,$$

$$M^{27\,1}_{(1/7)} = 2185.8,\ M^{6\,1}_{(1/8)} = 1100,\ M^{27\,1}_{(1/8)} = 2648.4,\ M^{17\,1}_{(2/3)} = 24480,$$

$$M^{33\,1}_{(2/4)} = 31050,\ M^{33\,1}_{(2/5)} = 38016,\ M^{33\,1}_{(2/6)} = 12240,\ M^{33\,1}_{(2/7)} = 8640,$$

$$M^{33\,1}_{(2/8)} = 12133.63,\ M^{14\,1}_{(3/3)} = 24480,\ M^{24\,1}_{(3/4)} = 31050,\ M^{24\,1}_{(3/5)} = 38016,$$

$$M^{24\,1}_{(3/6)} = 12240,\ M^{24\,1}_{(3/7)} = 8640,\ M^{24\,1}_{(3/8)} = 10497.27,\ M^{1\,24}_{(4/2)} = 549.33,$$

$$M^{24\,1}_{(4/2)} = 35382.86,\ M^{1\,24}_{(4/3)} = 440.78,\ M^{14\,1}_{(4/3)} = 24480,\ M^{24\,1}_{(4/3)} = 32230.59,$$

$$M^{24\,1}_{(4/4)} = 70765.71,\ M^{24\,1}_{(4/5)} = 91440,\ M^{1\,24}_{(4/6)} = 720.5,\ M^{24\,1}_{(4/6)} = 20880,$$

$$M^{1\,24}_{(4/7)} = 90.75,\ M^{24\,1}_{(4/7)} = 18630,\ M^{24\,1}_{(4/8)} = 34560,\ M^{1\,24}_{(5/2)} = 351.32,$$

$$M^{24\,1}_{(5/2)} = 26441.05,\ M^{1\,24}_{(5/3)} = 288.87,\ M^{24\,1}_{(5/3)} = 22368,\ M^{24\,1}_{(5/4)} = 64260,$$

$$M^{24\,1}_{(5/7)} = 11520,\ M^{24\,1}_{(5/8)} = 87480.$$

Conclusions

The results presented in the paper will be used in the prediction of the considered process of environment threats generated by the sea accident initiating events as well as in the prediction of the entire process of the critical infrastructure accident consequences including the process of initiating events, the proces of environment threats and the process of environment degradation.

Acknowledgments

The paper presents the results developed in the scope of the EU-CIRCLE project titled “A pan – European framework for strengthening Critical Infrastructure resilience to climate change” that has received funding from the European Union’s Horizon 2020 research and innovation programme under grant agreement No 653824. http://www.eu-circle.eu/.

References

1. M. Bogalecka and K. Kołowrocki. Modelling critical infrastructure accident consequences – an overall approach, Journal of Polish Safety and Reliability Association, Summer Safety and Reliability Seminars, 7, 3, 1{13, 2016.
2. M. Bogalecka and K. Kołowrocki. The process of sea environment threats generated by hazardous chemicals release, Journal of Polish Safety and Reliability Association, Summer Safety and Reliability Seminars, 6, 1, 67{74, 2015.
3. F. Grabski. Semi-Markov processes: applications in system reliability and maintenance, Elsevier, 2015.
4. K. Kołowrocki. Reliability of large systems, Elsevier, Amsterdam, Boston, Heidelberd, London, New York, Oxford, Paris, San Diego, San Francisco, Singapore, Sidney, Tokyo, 2004.
5. K. Kołowrocki. Reliability of large and complex systems, Elsevier, 2014.
6. K. Kołowrocki and J. Soszyńska-Budny. Reliability and safety of complex technical systems and processes: modeling – identification – prediction – optimization, Springer, London, Dordrecht, Heildeberg, New York, 2011.
7. N. Limnios and G. Oprisan. Semi-Markov processes and reliability, Birkhauser, Boston, 2005.
8. C. Macci. Large deviations for empirical estimators of the stationary distribution of a semi-Markov process with finite state space, Communications in Statistics-Theory and Methods, 37, 9, 3077{3089, 2008.
9. S. Mercier. Numerical bounds for semi-Markovian quantities and application to reliability, Methodology and Computing in Applied Probability, 10, 2, 179{198, 2008.

Statistical identification of critical infrastructure accident consequences process Part 3 Process of environment degradation

Magda Bogalecka[1], and Krzysztof Kołowrocki[2]

[1] Department of Industrial Commodity Science and Chemistry, Gdynia Maritime University, 81-87 Morska Str., 81-225 Gdynia, Poland
(E-mail: m.bogalecka@wpit.am.gdynia.pl)
[2] Department of Mathematics, Gdynia Maritime University, 81-87 Morska Str., 81-225 Gdynia, Poland
(E-mail: k.kolowrocki@wn.am.gdynia.pl)

Abstract. The risk analysis of chemical spills at sea and their consequences is proposed to be based on the general model of mutual interactions between three processes: the process of the sea accident initiating events, the process of the sea environment threats and the process of the sea environment degradation. The statistical identification of the unknown parameters of the process of environment degradation, i.e. estimating the probabilities of this process of staying at the states at the initial moment, the probabilities of this process transitions between its states and the distributions of this process conditional sojourn times at the particular states is performed.
Keywords: critical infrastructure, sea accident, potential consequences, environment degradation.

1 Introduction

The probabilistic general model of critical infrastructure accident consequences includes the process of initiating events, the process of environment threats and the process of environment degradation models, Bogalecka and Kołowrocki[1]. This paper is concerned with the identification of the third one of these three processes.

The particular states of the process of the environment threats $S_{(k)}(t)$ of the sub-region D_k, $k = 1,2,\ldots,n_3$, described in Part 2 of the paper, may lead to dangerous effects degrading the environment at this sub-region. Thus, we assume that there are m_k different dangerous degradation effects for the environment sub-region D_k, $k = 1,2,\ldots,n_3$, and we mark them by

$$R_{(k)}^1, R_{(k)}^2, \ldots, R_{(k)}^{m_k}.$$

17th *ASMDA Conference Proceedings, 6 - 9 June 2017, London, UK*

This way the set

$$R_{(k)} = \{R_{(k)}^1, R_{(k)}^2, \ldots, R_{(k)}^{m_k}\}, \ k = 1,2,\ldots,n_3,$$

is the set of degradation effects for the environment of the sub-region D_k.
These degradation effects may attain different levels. Namely, the degradation effect

$$R_{(k)}^m, \quad m = 1,2,\ldots,m_k,$$

may reach $\nu_{(k)}^m$ levels

$$R_{(k)}^{m1}, R_{(k)}^{m2}, \ldots, R_{(k)}^{m\nu_{(k)}^m}, \ m = 1,2,\ldots,m_k,$$

that are called the states of this degradation effect.
The set

$$R_{(k)}^m = \{R_{(k)}^{m1}, R_{(k)}^{m2}, \ldots, R_{(k)}^{m\nu_{(k)}^m}\}, \ m = 1,2,\ldots,m_k,$$

is called the set of states of the degradation effect $R_{(k)}^m$, $m = 1,2,\ldots,m_k$, $k = 1,2,\ldots,n_3$ for the environment of the sub-region D_k, $k = 1,2,\ldots,n_3$.
Under the above assumptions, we can introduce the environment sub-region degradation process as a vector

$$R_{(k)}(t) = [R_{(k)}^1(t), R_{(k)}^2(t), \ldots, R_{(k)}^{m_k}(t)], \quad t \in <0,+\infty),$$

where

$$R_{(k)}^m(t), \quad t \in <0,+\infty), \ m = 1,2,\ldots,m_k, \ k = 1,2,\ldots,n_3,$$

are the processes of degradation effects for the environment of the sub-region D_k, defined on the time interval $t \in <0,+\infty)$, and having their values in the degradation effect state sets

$$R_{(k)}^m, \ m = 1,2,\ldots,m_k, \ k = 1,2,\ldots,n_3,$$

is called the degradation process of the environment of the sub-region D_k.
The vector

$$r_{(k)}^m = [d_{(k)}^1, d_{(k)}^2, \ldots, d_{(k)}^{m_k}], \ k = 1,2,\ldots,n_3, \tag{1}$$

where

$$d_{(k)}^m = \begin{cases} 0, & \text{if a degradation effect } R_{(k)}^m \text{ does not appear} \\ & \text{at the sub-region } D_k, \\ R_{(k)}^{mj}, & \text{if a degradation effect } R_{(k)}^m \text{ appears} \\ & \text{at the sub-region } D_k \text{ and} \\ & \text{its level is equel to } R_{(k)}^{mj}, \ j = 1,2,\ldots,\nu_{(k)}^m, \end{cases} \tag{2}$$

for $m = 1,2,\ldots,m_k$, $k = 1,2,\ldots,n_3$,

is called the degradation state of the sub-region D_k.
From the above definition, the maximum number of the environment degradation states for the sub-region D_k, $k = 1,2,\ldots,n_3$, is equalled to

$$\ell_k = (v_{(k)}^1 + 1), (v_{(k)}^2 + 1), \ldots, (v_{(k)}^{m_k} + 1), \quad k = 1,2,\ldots,n_3.$$

Further, we number the sub-region D_k, $k = 1,2,\ldots,n_3$, degradation states defined by (1) and (2) and mark them by

$$r_{(k)}^{\ell} \text{ for } \ell = 1,2,\ldots,\ell_k, \quad k = 1,2,\ldots,n_3,$$

and form the set of degradation states

$$R_{(k)} = \{r_{(k)}^{\ell}, \quad \ell = 1,2,\ldots,\ell_k\}, \quad k = 1,2,\ldots,n_3,$$

where

$$r_{(k)}^{i} \neq r_{(k)}^{j} \text{ for } i \neq j, \quad i, j \in \{1,2,\ldots,\ell_k\}.$$

The set $R_{(k)}$, $k = 1,2,\ldots,n_3$, is called the set of the environment degradation states of the sub-region D_k, $k = 1,2,\ldots,n_3$, while a number ℓ_k is called the number of the environment degradation states of this sub-region.
A function

$$R_{(k)}(t), \quad k = 1,2,\ldots,n_3,$$

defined on the time interval $t \in <0,\infty)$, and having values in the environment degradation states set

$$R_{(k)}, \quad k = 1,2,\ldots,n_3,$$

is called the sub-process of the environment degradation of the sub-region D_k, $k = 1,2,\ldots,n_3$.
Next, to involve the environment sub-region D_k, $k = 1,2,\ldots,n_3$, degradation process with the process of the environment threats, we define the conditional environment sub-region degradation process while the process of the environment threats $S_{(k)}(t)$ of the sub-region D_k, is in the state $s_{(k)}^{\upsilon}$ $\upsilon = 1,2,\ldots,\upsilon_k$, as a vector

$$R_{(k/\upsilon)}(t) = [R_{(k/\upsilon)}^1(t), R_{(k/\upsilon)}^2(t), \ldots, R_{(k/\upsilon)}^{m_k}(t)], \quad t \in <0,+\infty), \tag{3}$$

where

$$R_{(k/\upsilon)}^m(t), \quad t \in <0,+\infty), \quad m = 1,2,\ldots,m_k, \; k = 1,2,\ldots,n_3, \; \upsilon = 1,2,\ldots,\upsilon_k,$$

defined on the time interval $t \in <0,+\infty)$, and having values in the degradation effect states set $R_{(k)}^m$, $m = 1,2,\ldots,m_k$, $k = 1,2,\ldots,n_3$.
The above definition means that the conditional environment sub-region degradation process $R_{(k/\upsilon)}(t)$, $t \in <0,+\infty)$, also takes the degradation states from

the set $R_{(k)}$ of the unconditional sub-region degradation process $R_{(k)}(t)$, $t \in <0,+\infty)$, defined by (3).

2 Process of environment degradation modelling

We assume a semi-Markov model Grabski[2], Kołowrocki[3-4], Kołowrocki and Soszyńska[5], Limnios and Oprisan[6], Macci[7], Mercier[8] of the sub-process of environment degradation $R_{(k/\upsilon)}(t)$, $k = 1,2,\ldots,n_3$, $\upsilon = 1,2,\ldots,\upsilon_k$, and denote by

$\zeta^{ij}_{(k/\upsilon)}$, $i, j = 1,2,\ldots,\ell_k$, $i \neq j$, $k = 1,2,\ldots,n_3$, $\upsilon = 1,2,\ldots,\upsilon_k$

its random conditional sojourn times in the state $r^i_{(k)}$ while its next transition will be done to the state $r^j_{(k)}$. This sub-process is defined by:

– the vector of probabilities of its initial states at the moment $t = 0$

$[q^i_{(k/\upsilon)}(0)]_{1x\ell_k}$,

– the matrix of probabilities of transitions between the states

$[q^{ij}_{(k/\upsilon)}]_{\ell_k x \ell_k}$,

– the matrix of the distribution functions of the conditional sojourn times

$[G^{ij}_{(k/\upsilon)}(t)]_{\ell_k x \ell_k}$,

or equivalently by the matrix of the density functions of the conditional sojourn times

$[g^{ij}_{(k/\upsilon)}(t)]_{\ell_k x \ell_k}$,

– the mean values of the conditional sojourn times

$M^{ij}_{(k/\upsilon)}$.

We distinguished $m = 5$ possible environment degradations in the neighbourhood sub-regions D_k, $k = 5$, of a critical infrastructure (a ship) accident area that may be caused by threats coming from chemical substance released into the marine environment as a result of a sea accident as follows: R^1 – the increase of the air and water temperature in the accident area, R^2 – the decrease of oxygen concentration of the air and water of the accident area, R^3 – the disturbance of air and water pH regime in the accident area, R^4 – the aesthetic nuisance (caused by smells, litter, discoloration etc.) in the accident area, R^5 – the pollution of air and water in the accident area. Each of the environment degradation effect may attain different levels. Next, we distinguished states of the environment degradation process for particular sub-regions. The number of this process states for each sub-region $\ell_1 = 30$, $\ell_2 = 28$, $\ell_3 = 28$, $\ell_4 = 31$, $\ell_5 = 23$, are fixed and the environment degradation states $r^i_{(k)}$, $i = 1,2,\ldots,\ell_k$,

$k = 1,2,\ldots,n_3$, are defined in Bogalecka and Kołowrocki[1]. Additionally, we involve the process of environment threats $S_{(k/l)}(t)$, with each sub-process of environment degradation. Thus, we fix environment degradation states $r^{i}_{(k/\upsilon)}$, $i = 1,2,\ldots,\ell_k$, $k = 1,2,\ldots,n_3$, $\upsilon = 1,2,\ldots,\upsilon_k$, for a particular sub-region according to the environment threat that cause the environment degradation effects state. Moreover, it is assumed that there are possible the transitions between all states of the sub-process of environment degradation.

3 Identification of the process of environment degradation

The experiment was performed across the world seas and oceans in the years 2004-2014. The initial moment $t = 0$ of the process of environment degradation was fixed at the moment when the threat caused by ship accident generated one of the distinguished degradation effects states.

3.1 Parameters of the process of environment degradation

On the basis of the statistical data coming from experiment, it is possible to evaluate the following unknown basic parameters of the process of environment degradation:

– the vectors of the initial probabilities $q^{i}_{(k/\upsilon)}(0)$, $i = 1,2,\ldots,\ell_k$, $k = 1,2,...,5$, $\upsilon = 1,2,\ldots,\upsilon_k$, $\upsilon_1 = 35$, $\upsilon_2 = 33$, $\upsilon_3 = 29$, $\upsilon_4 = 29$, $\upsilon_5 = 29$, $\ell_1 = 30$, $\ell_2 = 28$, $\ell_3 = 28$, $\ell_4 = 31$, $\ell_5 = 23$, of the environment degradation sub-process at the particular states at the moment $t = 0$. For instance, the vectors of initial probabilities for the sub-region D_1 are as follows:

$[q_{(1/1)}(0)]_{1x30} = [1,0,\ldots,0]$, $[q_{(1/2)}(0)]_{1x30} = [0,0,\ldots,0]$,
$[q_{(1/3)}(0)]_{1x30} = [1,0,\ldots,0]$, $[q_{(1/4)}(0)]_{1x30} = [1,0,\ldots,0]$,
$[q_{(1/5)}(0)]_{1x30} = [1,0,\ldots,0]$, $[q_{(1/6)}(0)]_{1x30} = [1,0,\ldots,0]$,
$[q_{(1/7)}(0)]_{1x30} = [1,0,\ldots,0]$, $[q_{(1/8)}(0)]_{1x30} = [1,0,\ldots,0]$,
$[q_{(1/9)}(0)]_{1x30} = [0,0,\ldots,0]$, $[q_{(1/10)}(0)]_{1x30} = [0,0,\ldots,0]$,
$[q_{(1/11)}(0)]_{1x30} = [0,0,\ldots,0]$, $[q_{(1/12)}(0)]_{1x30} = [0,0,\ldots,0]$,
$[q_{(1/13)}(0)]_{1x30} = [1,0,\ldots,0]$, $[q_{(1/14)}(0)]_{1x30} = [0,0,\ldots,0]$,
$[q_{(1/15)}(0)]_{1x30} = [0,0,\ldots,0]$, $[q_{(1/16)}(0)]_{1x30} = [0,0,\ldots,0]$,
$[q_{(1/17)}(0)]_{1x30} = [1,0,\ldots,0]$, $[q_{(1/18)}(0)]_{1x30} = [0,0,\ldots,0]$,
$[q_{(1/19)}(0)]_{1x30} = [0,0,\ldots,0]$, $[q_{(1/20)}(0)]_{1x30} = [0,0,\ldots,0]$,
$[q_{(1/21)}(0)]_{1x30} = [1,0,\ldots,0]$, $[q_{(1/22)}(0)]_{1x30} = [0,0,\ldots,0]$,
$[q_{(1/23)}(0)]_{1x30} = [1,0,\ldots,0]$, $[q_{(1/24)}(0)]_{1x30} = [0,0,\ldots,0]$,
$[q_{(1/25)}(0)]_{1x30} = [0,0,\ldots,0]$, $[q_{(1/26)}(0)]_{1x30} = [0,0,\ldots,0]$,
$[q_{(1/27)}(0)]_{1x30} = [1,0,\ldots,0]$, $[q_{(1/28)}(0)]_{1x30} = [0,0,\ldots,0]$,

$[q_{(1/29)}(0)]_{1x30} = [0,0,\ldots,0]$, $[q_{(1/30)}(0)]_{1x30} = [1,0,\ldots,0]$,
$[q_{(1/31)}(0)]_{1x30} = [0,0,\ldots,0]$, $[q_{(1/32)}(0)]_{1x30} = [0,0,\ldots,0]$,
$[q_{(1/33)}(0)]_{1x30} = [0,0,\ldots,0]$, $[q_{(1/34)}(0)]_{1x30} = [1,0,\ldots,0]$,
$[q_{(1/35)}(0)]_{1x30} = [1,0,\ldots,0]$;

– the matrices $[q^{ij}_{(k/\upsilon)}]$, $i, j = 1,2,\ldots,\ell_k$, $k = 1,2,...,5$, $\upsilon = 1,2,\ldots,\upsilon_k$, $\upsilon_1 = 35$, $\upsilon_2 = 33$, $\upsilon_3 = 29$, $\upsilon_4 = 29$, $\upsilon_5 = 29$, $\ell_1 = 30$, $\ell_2 = 28$, $\ell_3 = 28$, $\ell_4 = 31$, $\ell_5 = 23$, of probabilities of transitions of the sub-process $R_{(k/\upsilon)}(t)$ from the state $r^i_{(k/\upsilon)}$ into the state $r^j_{(k/\upsilon)}$ during the experimental time. For instance, the matrices of probabilities of transitions for the sub-region D_1 are as follows (the probabilities of transitions that are not equal to 0 are presented only):

$q^{1\,28}_{(1/3)} = 1,\ q^{6\,1}_{(1/3)} = 1,\ q^{22\,6}_{(1/3)} = 1,\ q^{25\,22}_{(1/3)} = 1,\ q^{28\,25}_{(1/3)} = 1;$

$q^{1\,27}_{(1/4)} = 0.75,\ q^{1\,30}_{(1/4)} = 0.25,\ q^{20\,1}_{(1/4)} = 1,\ q^{21\,1}_{(1/4)} = 1,\ q^{24\,21}_{(1/4)} = 1,\ q^{27\,24}_{(1/4)} = 1,$

$q^{29\,20}_{(1/4)} = 1,\ q^{30\,29}_{(1/4)} = 1;$

$q^{1\,26}_{(1/5)} = 1,\ q^{20\,1}_{(1/5)} = 1,\ q^{23\,20}_{(1/5)} = 1,\ q^{26\,23}_{(1/5)} = 1;$

$q^{1\,2}_{(1/6)} = 0.667,\ q^{1\,19}_{(1/6)} = 0.333,\ q^{2\,1}_{(1/6)} = 1,\ q^{17\,1}_{(1/6)} = 1,\ q^{18\,17}_{(1/6)} = 1,\ q^{19\,18}_{(1/6)} = 1;$

$q^{1\,2}_{(1/7)} = 0.5,\ q^{1\,10}_{(1/7)} = 0.5,\ q^{2\,1}_{(1/7)} = 1,\ q^{6\,1}_{(1/7)} = 1,\ q^{8\,6}_{(1/7)} = 1,\ q^{10\,8}_{(1/7)} = 1;$

$q^{1\,15}_{(1/8)} = 1,\ q^{13\,1}_{(1/8)} = 1,\ q^{14\,13}_{(1/8)} = 1,\ q^{15\,14}_{(1/8)} = 1;$

$q^{1\,6}_{(1/13)} = 1,\ q^{6\,1}_{(1/13)} = 1;$

$q^{1\,28}_{(1/17)} = 1,\ q^{6\,1}_{(1/17)} = 1,\ q^{22\,6}_{(1/17)} = 1,\ q^{25\,22}_{(1/17)} = 1,\ q^{28\,25}_{(1/17)} = 1;$

$q^{1\,20}_{(1/21)} = 1,\ q^{20\,1}_{(1/21)} = 1;$

$q^{1\,2}_{(1/23)} = 1,\ q^{2\,1}_{(1/23)} = 1;$

$q^{1\,6}_{(1/27)} = 1,\ q^{6\,1}_{(1/27)} = 1;$

$q^{1\,11}_{(1/30)} = 1,\ q^{11\,1}_{(1/30)} = 1;$

$q^{1\,26}_{(1/35)} = 1,\ q^{20\,1}_{(1/35)} = 1,\ q^{23\,20}_{(1/35)} = 1,\ q^{26\,23}_{(1/35)} = 1.$

The values of some probabilities existing in the vectors $[q_{(k/\upsilon)}(0)]$ and in the matrix $[q^{ij}_{(k/\upsilon)}]$, besides of those standing on the main diagonal, equal to zero do not mean that the events they are concerned with, cannot appear. They are evaluated on the basis of real statistical data and their values may change and become more precise if the duration of the experiment is longer.

3.2 Distribution functions of environment degradation conditional sojourn times at states

Using the procedure given in Section 4.2.4 in Kołowrocki and Soszyńska-Budny[5] and proceedings in analogous way as in Section 3.4 of Part 1 of the paper, we identified the forms of the particular density function $g^{ij}_{(k/\upsilon)}(t)$ and distribution functions $G^{ij}_{(k/\upsilon)}(t)$ of the sub-process of environment degradation conditional sojourn times $\zeta^{ij}_{(k/\upsilon)}$, $i, j = 1,2,...,\ell_k$, $i \neq j$, $k = 1,2,...,5$, $\upsilon = 1,2,\ldots,\upsilon_k$, $\upsilon_1 = 35$, $\upsilon_2 = 33$, $\upsilon_3 = 29$, $\upsilon_4 = 29$, $\upsilon_5 = 29$, $\ell_1 = 30$, $\ell_2 = 28$, $\ell_3 = 28$, $\ell_4 = 31$, $\ell_5 = 23$, having sufficiently numerous set of their realizations at particular states. We have got the following results:

– the chimney distribution function for the conditional sojourn time $\zeta^{6\,1}_{(2/33)}$

$$G^{6\,1}_{(2/33)}(t) = \begin{cases} 0, & t < 0 \\ 0.0000162911\,t, & 0 \le t < 59898 \\ 0.00000008976\,t + 0.97036156, & 59898 \le t < 329439 \\ 1, & t \ge 329439, \end{cases}$$

– the exponential distribution function for the conditional sojourn time $\zeta^{9\,6}_{(2/33)}$

$$G^{9\,6}_{(2/33)}(t) = \begin{cases} 0, & t < 0 \\ 1 - \exp(-0.000175142\,t), & t \ge 0, \end{cases}$$

– the exponential distribution function for the conditional sojourn time $\zeta^{11\,9}_{(2/33)}$

$$G^{11\,9}_{(2/33)}(t) = \begin{cases} 0, & t < 0 \\ 1 - \exp(-0.000197971\,t), & t \ge 0, \end{cases}$$

– the chimney distribution function for the conditional sojourn time $\zeta^{6\,1}_{(3/24)}$

$$G^{6\,1}_{(3/24)}(t) = \begin{cases} 0, & t < 0 \\ 0.00003003\,t, & 0 \le t < 31957 \\ 0.000000126\,t + 0.95564242, & 31957 \le t < 351527 \\ 1, & t \ge 351527, \end{cases}$$

– the chimney distribution function for the conditional sojourn time $\zeta^{9\,6}_{(3/24)}$

$$G^{9\,6}_{(3/24)}(t) = \begin{cases} 0, & t < 0 \\ 0.000059866\,t, & 0 \le t < 13920 \\ 0.000004789\,t + 0.7666721, & 13920 \le t < 48720 \\ 1, & t \ge 48720, \end{cases}$$

– the chimney distribution function for the conditional sojourn time $\zeta^{1\,6}_{(4/24)}$

$$G_{(4/24)}^{1\,6}(t) = \begin{cases} 0, & t < 0 \\ 0.000984632\,t, & 0 \le t < 839.83 \\ 0.000034348\,t + 0.798077012, & 839.83 \le t < 5878.81 \\ 1, & t \ge 5878.81, \end{cases}$$

– the chimney distribution function for the conditional sojourn time $\zeta_{(4/24)}^{6\,1}$

$$G_{(4/24)}^{6\,1}(t) = \begin{cases} 0, & t < 0 \\ 0.0000242253\,t, & 0 \le t < 35485.7 \\ 0.00000056502\,t + 0.839602, & 35485.7 \le t < 283885.6 \\ 1, & t \ge 283885.6, \end{cases}$$

– the exponential distribution function for the conditional sojourn time $\zeta_{(4/24)}^{6\,9}$

$$G_{(4/24)}^{6\,9}(t) = \begin{cases} 0, & t < 0 \\ 1 - \exp(-0.000571517\,t), & t \ge 0, \end{cases}$$

– the exponential distribution function for the conditional sojourn time $\zeta_{(4/24)}^{9\,6}$

$$G_{(4/24)}^{9\,6}(t) = \begin{cases} 0, & t < 0 \\ 1 - \exp(-0.000094208\,t), & t \ge 0, \end{cases}$$

– the chimney distribution function for the conditional sojourn time $\zeta_{(5/24)}^{1\,6}$

$$G_{(5/24)}^{1\,6}(t) = \begin{cases} 0, & t < 0 \\ 0.001462496\,t, & 0 \le t < 575.8 \\ 0.000054844\,t + 0.810526022, & 575.8 \le t < 3454.8 \\ 1, & t \ge 3454.8, \end{cases}$$

– the chimney distribution function for the conditional sojourn time $\zeta_{(5/24)}^{6\,1}$

$$G_{(5/24)}^{6\,1}(t) = \begin{cases} 0, & t < 0 \\ 0.000023999\,t, & 0 \le t < 38400 \\ 0.0000003404\,t + 0.9084976, & 38400 \le t < 268800 \\ 1, & t \ge 268800, \end{cases}$$

– the exponential distribution function for the conditional sojourn time $\zeta_{(5/24)}^{9\,6}$

$$G_{(5/24)}^{9\,6}(t) = \begin{cases} 0, & t < 0 \\ 1 - \exp(-0.000073209\,t), & t \ge 0. \end{cases}$$

In the case when as a result of the experiment, limited data coming from experts, we only have the number of realizations of the process of environment degradation lifetimes in the states and its all realizations are equal to an approximate value, we assume that this conditional sojourn times have the uniform distribution in the interval from this value minus its half to this value plus its half. On the other hand, in the case when as a result of the experiment, coming from experts, there are not any suitable distribution presented in Chapter 2 in Kołowrocki and Soszyńska-Budny[5], to describe the process environment degradation or we have less than 28 realizations of the sub-process of

environment degradation, we assume that this time has the empirical distribution function. Then we proceeds in analogous way as in Section 3.4 of Part 1 of the paper.

For the distributions identified in this section, by application either the general formulae for the mean value or particular formulae given respectively by (2.12) and (2.13-2.19) in Kołowrocki and Soszyńska-Budny[5], the mean values $M^{ij}_{(k/\upsilon)} = E[\zeta^{ij}_{(k/\upsilon)}]$, $i, j = 1,2,...,\ell_k$, $i \neq j$, $k = 1,2,...,5$, $\upsilon = 1,2,\ldots,\upsilon_k$, $\upsilon_1 = 35$, $\upsilon_2 = 33$, $\upsilon_3 = 29$, $\upsilon_4 = 29$, $\upsilon_5 = 29$, $\ell_1 = 30$, $\ell_2 = 28$, $\ell_3 = 28$, $\ell_4 = 31$, $\ell_5 = 23$, of the sub-process of environment degradation conditional sojourn times at particular states can be determined and they amount to:

$$M^{1\,28}_{(1/3)} = 1,\ M^{6\,1}_{(1/3)} = 180,\ M^{22\,6}_{(1/3)} = 120,\ M^{25\,22}_{(1/3)} = 120,\ M^{28\,25}_{(1/3)} = 300,$$

$$M^{1\,27}_{(1/4)} = 1,\ M^{1\,30}_{(1/4)} = 1,\ M^{20\,1}_{(1/4)} = 20,\ M^{29\,20}_{(1/4)} = 20,\ M^{30\,29}_{(1/4)} = 40,\ M^{1\,26}_{(1/5)} = 1,$$

$$M^{20\,1}_{(1/5)} = 30,\ M^{23\,20}_{(1/5)} = 60,\ M^{26\,23}_{(1/5)} = 360,\ M^{1\,2}_{(1/6)} = 1,\ M^{1\,19}_{(1/6)} = 1,\ M^{17\,1}_{(1/6)} = 30,$$

$$M^{18\,17}_{(1/6)} = 30,\ M^{19\,18}_{(1/6)} = 180,\ M^{1\,2}_{(1/7)} = 1,\ M^{1\,10}_{(1/7)} = 1,\ M^{2\,1}_{(1/7)} = 15,\ M^{6\,1}_{(1/7)} = 180,$$

$$M^{8\,6}_{(1/7)} = 120,\ M^{10\,8}_{(1/7)} = 420,\ M^{1\,15}_{(1/8)} = 1,\ M^{13\,1}_{(1/8)} = 60,\ M^{14\,13}_{(1/8)} = 60,$$

$$M^{15\,14}_{(1/8)} = 120,\ M^{1\,6}_{(1/13)} = 1,\ M^{6\,1}_{(1/13)} = 120,\ M^{1\,28}_{(1/17)} = 1,\ M^{6\,1}_{(1/17)} = 180,$$

$$M^{22\,6}_{(1/17)} = 120,\ M^{25\,22}_{(1/17)} = 120,\ M^{28\,25}_{(1/17)} = 300,\ M^{1\,20}_{(1/21)} = 1,\ M^{20\,1}_{(1/21)} = 10,$$

$$M^{1\,2}_{(1/23)} = 1,\ M^{2\,1}_{(1/23)} = 240,\ M^{1\,6}_{(1/27)} = 1,\ M^{6\,1}_{(1/27)} = 1,\ M^{1\,11}_{(1/30)} = 1,\ M^{1\,26}_{(1/35)} = 1,$$

$$M^{20\,1}_{(1/35)} = 30,\ M^{23\,20}_{(1/35)} = 60,\ M^{26\,23}_{(1/35)} = 360,\ M^{1\,5}_{(2/1)} = 1,\ M^{5\,1}_{(2/1)} = 600,$$

$$M^{1\,2}_{(2/2)} = 1,\ M^{2\,1}_{(2/2)} = 2880,\ M^{1\,2}_{(2/4)} = 1,\ M^{2\,1}_{(2/4)} = 1440,\ M^{1\,18}_{(2/5)} = 1,$$

$$M^{13\,1}_{(2/5)} = 780,\ M^{14\,13}_{(2/5)} = 360,\ M^{18\,14}_{(2/5)} = 300,\ M^{1\,25}_{(2/17)} = 1,\ M^{1\,27}_{(2/17)} = 1,$$

$$M^{1\,11}_{(2/18)} = 1,\ M^{6\,1}_{(2/18)} = 10080,\ M^{9\,6}_{(2/18)} = 11520,\ M^{11\,9}_{(2/18)} = 21600,\ M^{1\,6}_{(2/33)} = 1,$$

$$M^{1\,9}_{(2/33)} = 1,\ M^{1\,11}_{(2/33)} = 1,\ M^{1\,23}_{(2/33)} = 1,\ M^{2\,1}_{(2/33)} = 246240,\ M^{6\,1}_{(2/33)} \cong 33935.21,$$

$$M^{9\,6}_{(2/33)} \cong 5709.65,\ M^{11\,9}_{(2/33)} \cong 5051.25,\ M^{12\,2}_{(2/33)} = 14400,\ M^{15\,12}_{(2/33)} = 7200,$$

$$M^{20\,15}_{(2/33)} = 10080,\ M^{22\,20}_{(2/33)} = 1440,\ M^{23\,22}_{(2/33)} = 1440,\ M^{1\,2}_{(3/2)} = 1,\ M^{2\,1}_{(3/2)} = 2880,$$

$$M^{1\,2}_{(3/3)} = 1,\ M^{2\,1}_{(3/3)} = 1440,\ M^{1\,18}_{(3/4)} = 1,\ M^{13\,1}_{(3/4)} = 780,\ M^{14\,13}_{(3/4)} = 360,$$

$$M^{18\,14}_{(3/4)} = 300,\ M^{1\,25}_{(3/14)} = 1,\ M^{1\,27}_{(3/14)} = 1,\ M^{1\,11}_{(3/15)} = 1,\ M^{6\,1}_{(3/15)} = 10080,$$

$$M^{9\,6}_{(3/15)} = 11520,\ M^{11\,9}_{(3/15)} = 21600,\ M^{1\,6}_{(3/24)} = 1,\ M^{1\,9}_{(3/24)} = 1,\ M^{1\,11}_{(3/24)} = 1,$$

$M^{1\,23}_{(3/24)}=1,\ M^{2\,1}_{(3/24)}=246240,\ M^{6\,1}_{(3/24)}\cong 16687.31,\ M^{9\,6}_{(3/24)}\cong 11018.72,$

$M^{12\,2}_{(3/24)}=14400,\ M^{15\,12}_{(3/24)}=7200,\ M^{20\,15}_{(3/24)}=10080,\ M^{22\,20}_{(3/24)}=1440,$

$M^{23\,22}_{(3/24)}=1440,\ M^{1\,2}_{(4/2)}=1,\ M^{2\,1}_{(4/2)}=2880,\ M^{1\,18}_{(4/4)}=1,\ M^{13\,1}_{(4/4)}=780,$

$M^{14\,13}_{(4/4)}=360,\ M^{18\,14}_{(4/4)}=300,\ M^{1\,28}_{(4/14)}=1,\ M^{1\,30}_{(4/14)}=1,\ M^{1\,11}_{(4/15)}=1,$

$M^{6\,1}_{(4/15)}=10080,\ M^{9\,6}_{(4/15)}=11520,\ M^{11\,9}_{(4/15)}=21600,\ M^{1\,6}_{(4/24)}\cong 928.66,$

$M^{1\,9}_{(4/24)}=1,\ M^{1\,11}_{(4/24)}=1,\ M^{6\,1}_{(4/24)}\cong 37664.56,\ M^{6\,9}_{(4/24)}\cong 1749.73,$

$M^{6\,24}_{(4/24)}=4320,\ M^{9\,6}_{(4/24)}\cong 10614.81,\ M^{25\,24}_{(4/24)}=30240,\ M^{26\,25}_{(4/24)}=10080,$

$M^{1\,5}_{(5/1)}=1,\ M^{5\,1}_{(5/1)}=600,\ M^{1\,11}_{(5/15)}=1,\ M^{6\,1}_{(5/15)}=10080,\ M^{9\,6}_{(5/15)}=11520,$

$M^{11\,9}_{(5/15)}=21600,\ M^{1\,6}_{(5/24)}\cong 564.28,\ M^{1\,9}_{(5/24)}=1,\ M^{1\,11}_{(5/24)}=1,$

$M^{6\,1}_{(5/24)}\cong 29741.18,\ M^{9\,6}_{(5/24)}\cong 13659.52.$

In the remaining cases, when the distributions cannot be identified, it is possible to find the approximate empirical values of the mean values $M^{ij}_{(k/\upsilon)}=E[\zeta^{ij}_{(k/\upsilon)}]$, $i,j=1,2,\ldots,\ell_k$, $i\neq j$, $k=1,2,\ldots,5$, $\upsilon=1,2,\ldots,\upsilon_k$, $\upsilon_1=35$, $\upsilon_2=33$, $\upsilon_3=29$, $\upsilon_4=29$, $\upsilon_5=29$, $\ell_1=30$, $\ell_2=28$, $\ell_3=28$, $\ell_4=31$, $\ell_5=23$, of the conditional sojourn times at particular states that are as follows:

$M^{21\,1}_{(1/4)}=680,\ M^{24\,21}_{(1/4)}=920,\ M^{27\,24}_{(1/4)}=2020,\ M^{2\,1}_{(1/6)}=1560,\ M^{11\,1}_{(1/30)}=260,$

$M^{12\,1}_{(2/17)}=2640,\ M^{16\,12}_{(2/17)}=2145,\ M^{21\,16}_{(2/17)}=1530,\ M^{25\,21}_{(2/17)}=255,\ M^{27\,25}_{(2/17)}=270,$

$M^{12\,1}_{(3/14)}=2640,\ M^{16\,12}_{(3/14)}=2145,\ M^{21\,16}_{(3/14)}=1530,\ M^{25\,21}_{(3/14)}=255,\ M^{27\,25}_{(3/14)}=270,$

$M^{6\,9}_{(3/24)}=2448,\ M^{9\,11}_{(3/24)}=3780,\ M^{11\,9}_{(3/24)}=8177.14,\ M^{12\,1}_{(4/14)}=2640,$

$M^{16\,12}_{(4/14)}=2145,\ M^{21\,16}_{(4/14)}=1530,\ M^{28\,21}_{(4/14)}=300,\ M^{30\,28}_{(4/14)}=270,\ M^{9\,11}_{(4/24)}=2010,$

$M^{9\,25}_{(4/24)}=7080,\ M^{11\,9}_{(4/24)}=6189.6,\ M^{11\,26}_{(4/24)}=5160,\ M^{24\,6}_{(4/24)}=5760,$

$M^{25\,6}_{(4/24)}=15120,\ M^{26\,9}_{(4/24)}=30763.64,\ M^{6\,9}_{(5/24)}=1418.18,\ M^{9\,11}_{(5/24)}=1483.64,$

$M^{11\,9}_{(5/24)}=27552.$

Conclusions

The results presented in the paper will be used in the prediction of the considered process of environment degradation generated by the threat caused

by ship accident as well as in the prediction of the entire process of the critical infrastructure accident consequences including the process of initiating events, the proces of environment threats and the process of environment degradation.

Acknowledgments

The paper presents the results developed in the scope of the EU-CIRCLE project titled “A pan – European framework for strengthening Critical Infrastructure resilience to climate change” that has received funding from the European Union’s Horizon 2020 research and innovation programme under grant agreement No 653824. http://www.eu-circle.eu/.

References

1. M. Bogalecka and K. Kołowrocki. Modelling critical infrastructure accident consequences – an overall approach, Journal of Polish Safety and Reliability Association, Summer Safety and Reliability Seminars, 7, 3, 1{13, 2016.
2. F. Grabski. Semi-Markov processes: applications in system reliability and maintenance, Elsevier, 2015.
3. K. Kołowrocki. Reliability of large systems, Elsevier, Amsterdam, Boston, Heidelberd, London, New York, Oxford, Paris, San Diego, San Francisco, Singapore, Sidney, Tokyo, 2004.
4. K. Kołowrocki. Reliability of large and complex systems, Elsevier, 2014.
5. K. Kołowrocki and J. Soszyńska-Budny. Reliability and safety of complex technical systems and processes: modeling – identification – prediction – optimization, Springer, London, Dordrecht, Heildeberg, New York, 2011.
6. N. Limnios and G. Oprisan. Semi-Markov processes and reliability, Birkhauser, Boston, 2005.
7. C. Macci. Large deviations for empirical estimators of the stationary distribution of a semi-Markov process with finite state space, Communications in Statistics-Theory and Methods, 37, 9, 3077{3089, 2008.
8. S. Mercier. Numerical bounds for semi-Markovian quantities and application to reliability, Methodology and Computing in Applied Probability, 10, 2, 179{198, 2008.

Asymptotic Analysis and Optimization of Some Insurance Models

Ekaterina Bulinskaya

Faculty of Mechanics and Mathematics, Department of Probability Theory,
Lomonosov Moscow State University, Leninskie gory 1, 119234 Moscow, Russia
(E-mail: ebulinsk@yandex.ru)

Abstract. The aim of the paper is to discuss some problems arising in insurance, finance and other applications of probability theory. To this end we consider two insurance models (one continuous-time and one discrete-time). The first one is a dual insurance model with dividends. The main attention is paid to investigation of a new strategy of dividends payment. The second model deals with short-term credit policy in discrete-time case. We focus here on system optimization in the framework of cost approach.
Keywords: Insurance models, Cost approach, Dividends.

1 Introduction

It is well known to all researchers dealing with applications that it is desirable to construct the mathematical model of a real-life process (or system) for its investigation. There can exist a lot of models describing the system with different degrees of accuracy. Moreover, the same model can arise in various research fields. Thus, methods applied in one domain can be useful in others.

The models considered in such applications of probability theory as insurance, finance, queueing, reliability, inventory, dams, transport networks, population dynamics and many others are of input-output type. In order to describe these models, see, e.g., Bulinskaya[9], one has to ascertain input and output processes (or flows) and time horizon. To evaluate the system performance one needs an objective function (target, valuation criterium, risk measure). It is also necessary to introduce a set of feasible controls and carry out the optimization.

The most widely used approaches are reliability and cost ones, see, e.g., Bulinskaya[6], Afanasyeva and Bulinskaya[1]. Thus, objective functions considered by researchers are either survival probability of the system under consideration and its life-time until failure or costs (losses and profits) associated with the system functioning, see, e.g., Bulinskaya[7].

The paper is organized as follows. In Section 2 we consider a discrete-time model with short-term credit. On the contrary, the model treated in Section 3 is a continuous-time dual model with dividends. The Section 4 contains conclusions and further research directions.

17^{th} *ASMDA Conference Proceedings, 6 - 9 June 2017, London, UK*

2 Short-term credits

We consider a discrete-time insurance system (or other organization) which is interested in short-term credits (or bank loans). It is supposed that at the beginning of each period (year, month or week) it is possible to apply to a bank in order to obtain a credit card valid for a fixed number of periods. The card is provided immediately. The upper limit z of the credit is chosen by the applicant who pays bank at once the amount cz where c is the interest rate. The aim of loan is to satisfy the claims flow described by a sequence of nonnegative i.i.d. random variables $\{\xi_n\}_{n\geq 1}$. We assume that each claim ξ has a known distribution function $F(t)$ possessing a density $\varphi(t) > 0$ for $t > 0$ and a finite expectation. If a claim amount ξ is larger than the cash amount u available for payment then another loan is obtained at the interest rate p, $p > c$, its size is $\xi - u$. The amount $u - \xi$, not used for payment before the card expiration term, is lost. Moreover, in this case the financial loss of applicant is equal to $k(u - \xi)$. Let x be the initial cash amount of applicant. Our aim is to determine the optimal n-period strategy of applicant. Optimality means the minimization of expected discounted costs entailed by the n-step credit strategy.

2.1 One-period credit

Assume, at first, that the credit is valid for one period only. That means, the money not used for payment during the period cannot be used later. Denote by $f_n(x)$ the minimal expected discounted costs incurred by the implementation of n-period credit strategy. Here x is the cash amount available initially for claims payment if $x > 0$ and $|x|$ is the debt amount if $x < 0$. Put $H_1(y) = cy + L(y)$ with $L(y) = p\int_y^\infty (s - y)\varphi(s)\,ds + k\int_0^y (y - s)\varphi(s)\,ds$ and $y = x + z$ where z is the credit limit. Then the following statements are valid.

Lemma 1.

$$f_1(x) = -cx + \min_{y\geq x} H_1(y). \tag{1}$$

If $p > c$ then, for any x, there exists the critical level $\bar{x}_1$ defined by the relation

$$F(\bar{x}_1) = (p - c)(p + k)^{-1} \tag{2}$$

such that optimal credit limit is given by $z_1(x) = \max(0, \bar{x}_1 - x)$. The function $f_1(x)$ is twice differentiable and convex, whereas

$$f_1'(x) = \begin{cases} -c, & x \leq \bar{x}_1, \\ L'(x), & x \geq \bar{x}_1. \end{cases} \tag{3}$$

Proof. Obviously, $cz = c(y - x)$ is the interest which is paid for obtaining the credit. Moreover, $L(y)$ is the expected cost amount incurred by insufficiency or superfluity of one-period credit. Therefore relation (1) holds. It easily follows from the expression of $L(y)$ that $L'(y) = -p + (p + k)F(y)$ and $H_1'(y) = c - p + (p + k)F(y)$. Thus, $H_1''(y) = (p + k)\varphi(y) \geq 0$ for any y and $H_1'(\bar{x}_1) = 0$

for $\bar{x}_1$ defined by (2). That means, the function $H_1(y)$ is convex and attains the minimum at the point $\bar{x}_1$. Hence, $f_1(x) = H_1(y_1(x))$ for $y_1(x) = \max(x, \bar{x}_1)$ and $z_1(x) = y_1(x) - x$ has the desired form, whereas $f_1'(x)$ is defined by (3). Thus, $f_1''(x) = 0$ for $x < \bar{x}_1$ and $f_1''(x) = L''(x) > 0$ for $x > \bar{x}_1$. So, the function $f_1(x)$ is convex and the proof is completed. □

Turning to multi-period case we introduce a discount factor $\alpha \in (0, 1)$ and establish the following results.

Theorem 1. *The function $f_n(x)$ specified by*

$$f_n(x) = -cx + \min_{y \geq x} H_n(y), \tag{4}$$

where $H_n(y)$ has the form

$$H_n(y) = H_1(y) + \alpha f_{n-1}(0)F(y) + \alpha \int_y^\infty f_{n-1}(y - s)\varphi(s)\, ds, \tag{5}$$

is twice differentiable and convex for all $n > 1$. There exists $\bar{x} > \bar{x}_1$ such that the optimal credit limit $z_n(x) = \max(0, \bar{x} - x)$ for any x and $n > 1$. The critical level $\bar{x}$ is defined by the relation $F(\bar{x}) = (p - c(1 - \alpha))(p + k + \alpha c)^{-1}$.

Proof. Clearly, the n-period costs entailed by bank loans consist of the first period costs and costs arising during the following $n - 1$ periods. Since a first loan can be used during the first period only, at the beginning of the second period the insurance company either will have no cash available for future payments (that corresponds to the case $\xi_1 < y$) or its debt will be equal to $\xi_1 - y$ (that corresponds to the case $\xi_1 > y$). According to Bellman optimality principle (see, e.g., Bellman[4]) it is possible to conclude that equations (4) and (5) are valid.

Further proof is carried out by induction. Consider at first $n = 2$ and use the fact that $f_1'(x) = -c$ for $x \leq 0$. Then,

$$H_2'(y) = H_1'(y) + \alpha \int_y^\infty f_1'(y - s)\varphi(s)\, ds = c + L'(y) - \alpha c \int_y^\infty \varphi(s)\, ds.$$

Now it is obvious that the right-hand side of the last equality is $c(1 - \alpha) - p + (p + k + \alpha c)F(y)$, hence, $H_2'(\bar{x}) = 0$. So, for $n = 2$ the credit limit $z_2(x)$ has the form mentioned in the theorem statement. In other words,

$$f_2(x) = -cx + \begin{cases} H_2(\bar{x}), & x \leq \bar{x}, \\ H_2(x), & x \geq \bar{x} \end{cases}$$

and

$$f_2'(x) = -c + \begin{cases} 0, & x \leq \bar{x}, \\ H_2'(x), & x \geq \bar{x}. \end{cases}$$

Since $H_2''(y) = (p + k + \alpha c)\varphi(y) \geq 0$ for $y > \bar{x}$ and equals zero otherwise, it follows immediately that $f_2''(x) \geq 0$. Thus, the theorem statement is valid for $n = 2$. Assuming that it is true as well for $n - 1$ we easily get $H_n'(y) = H_1'(y) - \alpha c \int_y^\infty \varphi(s)\, ds = H_2'(y)$. That means, the critical number for all $n > 1$ is equal to $\bar{x}$.

Obviously $\bar{x} > \bar{x}_1$, since

$$\frac{p - c(1-\alpha)}{p+k+\alpha c} > \frac{p-c}{p+k}. \square$$

Thus, we have established that for any $n > 1$ the optimal credit strategy is determined by a single critical number $\bar{x}$ whereas for $n = 1$ one has to use $\bar{x}_1$ instead of $\bar{x}$. It is not difficult to prove the following results clarifying the dependence of critical levels on the cost parameters.

Corollary 1. *Critical level $\bar{x}_1$ is increasing function of p and decreasing function of c and k, whereas $\bar{x}$ increases in p and α and decreases in c and k.*

Proof is based on explicit form of partial derivatives of critical levels with respect to parameters. Thus,

$$\frac{\partial \bar{x}_1}{\partial p} = \frac{k+c}{\varphi(\bar{x}_1)(p+k)^2}, \quad \frac{\partial \bar{x}_1}{\partial c} = -\frac{1}{\varphi(\bar{x}_1)(p+k)}, \quad \frac{\partial \bar{x}_1}{\partial k} = -\frac{p-c}{\varphi(\bar{x}_1)(p+k)^2}.$$

On the other hand,

$$\frac{\partial \bar{x}}{\partial p} = \frac{k+c}{\varphi(\bar{x})(p+k+\alpha c)^2}, \qquad \frac{\partial \bar{x}}{\partial \alpha} = \frac{c(k+c)}{\varphi(\bar{x})(p+k+\alpha c)^2},$$

$$\frac{\partial \bar{x}}{\partial c} = -\frac{k(1-\alpha)+p}{\varphi(\bar{x})(p+k+\alpha c)^2}, \qquad \frac{\partial \bar{x}}{\partial k} = -\frac{p-c(1-\alpha)}{\varphi(\bar{x})(p+k+\alpha c)^2}.$$

Since all the cost parameters are positive, as well as density $\varphi(x)$ for $x > 0$, and $\alpha < 1$, $p > c$, the desired results are obvious. $\square$

2.2 Two-period credit

Now, let the credit be available for two periods. We begin by writing the one-step objective function

$$G_1(z,x) = cz + p\int_{x+z}^{\infty}(s-x-z)\varphi(s)\,ds + k\int_0^x (x-s)\varphi(s)\,ds. \tag{6}$$

If, as previously, we denote by $f_1(x)$ the minimal one-period additional expected costs entailed be the credit then

$$f_1(x) = \min_{z\geq 0} G_1(z,x).$$

It is possible to prove the following results.

Lemma 2. *The optimal one-step limit of credit $z_1(x)$ has the following form*

$$z_1(x) = \begin{cases} x_1 - x, & x \leq x_1, \\ 0, & x \geq x_1. \end{cases} \tag{7}$$

Here $F(x_1) = p^{-1}(p-c)$. The function $f_1(x)$ is convex twice-differentiable and

$$f_1'(x) = \begin{cases} -c + kF(x), & x \leq x_1, \\ -p + (p+k)F(x), & x \geq x_1. \end{cases} \tag{8}$$

Proof. It is clear that, for a fixed x, minimum of $G_1(z,x)$ in z is attained either on the boundary $z=0$ or at the point $z_1(x)$ being the root of the equation

$$\frac{\partial G_1}{\partial z}(z,x)=0. \tag{9}$$

Due to (6), one immediately gets $F(x+z_1(x))=p^{-1}(p-c)$ from (9). Since $p>c$, there exists such x_1 that the form (7) of $z_1(x)$ is true.

Obviously, $f_1(x)=G_1(z_1(x),x)$, therefore

$$f_1(x)=\begin{cases} c(x_1-x)+k\int_0^x(x-s)\varphi(s)\,ds+p\int_{x_1}^\infty(s-x_1)\varphi(s)\,ds, & x\le x_1,\\ k\int_0^x(x-s)\varphi(s)\,ds+p\int_x^\infty(s-x)\varphi(s)\,ds, & x\ge x_1,\end{cases}$$

whence (8) follows immediately. It is clear that $f_1'(x)$ is continuous, moreover,

$$f_1''(x)=\begin{cases} k\varphi(x), & x<x_1,\\ (k+p)\varphi(x), & x>x_1.\end{cases}$$

In view of $f_1''(x)\ge 0$, function $f_1(x)$ is convex. □

Turning to n-step case one can write, for $n>1$, using the Bellman optimality principle, see, e.g., Bellman[4],

$$f_n(x)=\min_{z\ge 0}G_n(z,x)$$

where

$$G_n(z,x)=G_1(z,x)+\alpha f_{n-1}(z)F(x)+\alpha\int_x^\infty f_{n-1}(x+z-s)\varphi(s)\,ds \tag{10}$$

and $\alpha\in(0,1)$ is a discount factor as in previous subsection.

Theorem 2. *For any $n>1$, the function $f_n(x)$ is convex and twice differentiable. Moreover, there exists the optimal credit level $z_n(x)\ge 0$ possessing the following properties*

$$-1\le z_n'(x)\le 0,\quad z_n'(x)=-1\quad \textit{for } x\le 0,\quad \textit{and } z_n(x)=0\quad \textit{for } x\ge x_0, \tag{11}$$

where $F(x_0)=p^{-1}(p-c(1-\alpha))$ and $f_n(x)=G_n(z_n(x),x)$.

Proof is based on Lemma 2 and carried out by induction. Assume that all the statements are proved for the number of steps up to $n-1$. Using (10) we obtain

$$\frac{\partial G_n}{\partial z}(z,x)=c-p\int_{x+z}^\infty\varphi(s)\,ds+\alpha f_{n-1}'(z)F(x)+\alpha\int_x^\infty f_{n-1}'(x+z-s)\varphi(s)\,ds.$$

The solution of the equation $\partial G_n(z_n(x),x)/\partial z=0$ is a differentiable implicit function $z_n(x)$ and

$$z_n'(x)=-\frac{p\varphi(x+z_n(x))+\alpha\int_x^\infty f_{n-1}''(x+z_n(x)-s)\varphi(s)\,ds}{p\varphi(x+z_n(x))+\alpha\int_x^\infty f_{n-1}''(x+z_n(x)-s)\varphi(s)\,ds+\alpha f_{n-1}''(z_n(x))F(x)}. \tag{12}$$

It is clear from (12) that properties (11) are true. Since $z_n(x)$ is decreasing, we can find such x_n that $z_n(x_n) = 0$. It has to satisfy the following relation

$$0 = \frac{\partial G_n}{\partial z}(0, x_n) = c - p + (p + \alpha f'_{n-1}(0))F(x_n) + \alpha \int_{x_n}^{\infty} f'_{n-1}(x_n - s)\varphi(s)\, ds.$$

Due to the form of $f'_{n-1}(x) = -p + pF(x + z_{n-1}(x)) + kF(x) + \alpha \int_x^{\infty} f'_{n-2}(x + z_{n-1}(x) - s)\varphi(s)\, ds$, for $x \le x_{n-1}$ (valid for $n > 2$) it is not difficult to check that $f'_{n-1}(x) = -c$ for $x \le 0$ and $pF(x_n) = p - c(1 - \alpha)$. Hence it follows immediately that $x_n = x_0$. For $n = 2$ the same reasoning can be carried out, because we need only convexity of $f_{n-1}(x)$ and equality $f'_{n-1}(x) = -c$ for $x \le 0$ which is true for $f_1(x)$. Thus, the base of induction is valid along with its steps. □

Remark. If we suppose additionally that $k \le c$ then it is possible to establish that $z_2(x) \ge z_1(x)$ for all x.

3 Dual insurance model

To emphasize the fruitfulness of cost approach, below we investigate the model with dividend payments, dual to the classical Sparre Andersen insurance model. That means, the company surplus (or capital) $X(t)$ at time t, without dividends, is described by the following relation

$$X(t) = x - ct + S(t).$$

Here x is the initial surplus, c is the expenses rate and the last term $S(t) = \sum_{n=1}^{N(t)} Y_n$ represents the company profit. It is supposed that $N(t)$ is a renewal process generated by a sequence of independent identically distributed nonnegative random variables $\{T_n\}_{n\ge1}$. The sequence $\{Y_n\}_{n\ge1}$ does not depend on $N(t)$ and also consists of nonnegative i.i.d. r.v.'s. A particular case of this model corresponding to assumption that $N(t)$ is a Poisson process, that is, interarrival times T_n, $n \ge 1$, are exponentially distributed, is called a dual Cramér-Lundberg model. There exist many possible interpretations for this model. For example, one can treat the surplus as amount of the capital of a business engaged in research and development, see, e.g. Avanzi *et al.*[3]. The company pays continuously expenses for research, and occasional profit of random amounts (such as the award of a patent or a sudden increase in sales) arises according to a Poisson process. A similar model was used in Bayraktar and Egami[5] to model the functioning of a venture capital investment company.

It was already mentioned that the object of investigation is a dual Sparre Andersen model with dividends. So, it is necessary to introduce the strategy of dividends payment. If the dividend strategy with a constant barrier level $b > 0$ is applied, the surplus and aggregate dividends have the form depicted by Figure 1. In other words, whenever the surplus exceeds the barrier the excess is paid out immediately as a dividend.

Expected discounted dividends paid until ruin time T (the first time when surplus becomes negative) are given by $V(x; b) = E(\int_0^T e^{-\delta t} dD(t))$. Here $D(t)$

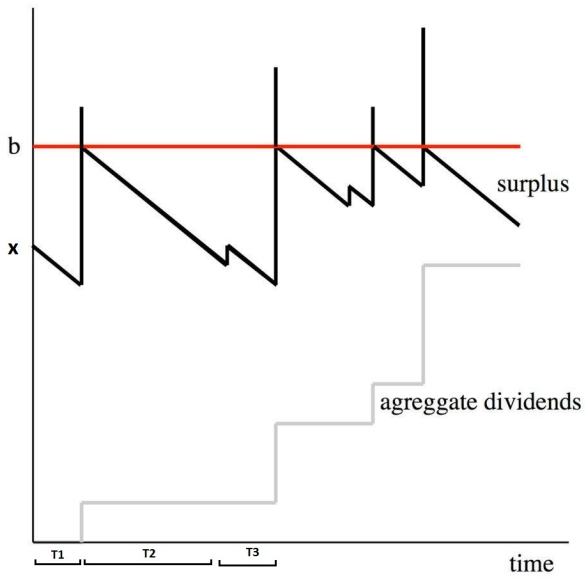

Fig. 1. Surplus and dividends under barrier strategy

is the aggregate dividends paid up to time t and $\delta > 0$ is a constant discount rate.

It was established in Avanzi *et al.*[3] that a simple barrier strategy is optimal for the model under consideration and it is possible to calculate the optimal barrier for some particular cases. However such a strategy leads almost surely to ruin, moreover, sometimes the company shareholders would like to get dividends as soon as possible setting a barrier lower than optimal. So, we are going to prove that in this case a step-function barrier introduced in Muromskaya[15] for insurance models of Cramér-Lundberg type is more advantageous.

At first, turn to the case of two barriers $b_2 \geq b_1$ and denote by $V(x; b_1, b_2)$ the expected discounted dividends until the ruin. It is supposed that barrier level b_1 is used only up to time T_1 whereas b_2 is set afterwards, see Figure 2.

Theorem 3. *For the case of one change of barrier level the relation*

$$V(x; b_1, b_2) \geq V(x; b_1)$$

is valid if $V(x; b_1) \leq V(x; b_2)$ *for any* $x \leq b_1 \leq b_2$.

Proof. If the initial state $x > b_1$ then $V(x; b_1, b_2) = x - b_1 + V(b_1; b_1, b_2)$. So further on suppose that $x \leq b_1$. Hence, it is possible to write $V(x; b_1, b_2)$ as a sum of expected dividends $V_{[0,T_1]}(x, b_1)$ obtained as a result of the first gain at time T_1 and the results of further gains for which one applies the new barrier level b_2. It is necessary to emphasize that for $T_1 > (x/c)$ the company does not obtain any dividends being ruined earlier. Thus, using the total expectation

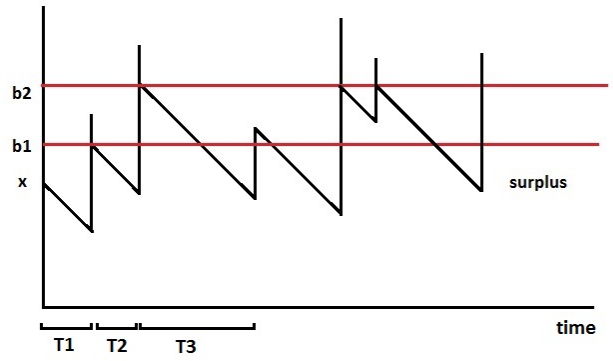

Fig. 2. Surplus under two-level barrier strategy

formula one gets

$$V(x;b_1,b_2)=\int\limits_0^{x/c} e^{-\delta t}f(t)\Bigg[\int\limits_0^{b_1-(x-ct)} V(x-ct+y;b_2)p(y)dy$$

$$+\int\limits_{b_1-(x-ct)}^{\infty} V(b_1;b_2)p(y)dy\Bigg]dt+V_{[0,T_1]}(x,b_1).$$

Here $f(t)$ is the density of the first gain arrival time T_1 and $p(y)$ is the density of the gain amount, whereas

$$V_{[0,T_1]}(x,b_1)=\int\limits_0^{x/c} e^{-\delta t}f(t)\int\limits_{b_1-(x-ct)}^{\infty}(x-ct+y-b_1)p(y)dy\,dt$$

is the expected discounted dividends paid on interval $[0,T_1]$. In fact, there are two different situations after the first profit. Either its amount is such that the surplus does not reach the dividends barrier b_1 or after the dividends payment the company starts from the level b_1. Moreover, since $V(x;b_1)=V(x;b_1,b_1)$, under the theorem assumption it is obvious that $V(x;b_1,b_2)\geq V(x;b_1)$. □

Now denote by $V(x;b_1,\ldots,b_n)$ the expected discounted dividends for the payment strategy using barrier level b_i on interval $(\sum_{k=1}^{i-1}T_k,\sum_{k=1}^{i}T_k]$, $i>1$, and b_1 is dividend barrier for $[0,T_1]$. The condition $0<b_1\leq b_2\leq\ldots\leq b_n$ defines the strategy with growing barrier level, see Figure 3.

Theorem 4. *Under assumption of Theorem 3 the strategy with growing barrier level provides the higher expected discounted dividends until ruin than the strategy with a constant barrier, that is* $V(x;b_1,\ldots,b_k)\geq V(x;b_1)$ *for any* $x\leq b_1$ *and* $n\geq k>1$.

Proof is carried out by induction. The base of induction is established by Theorem 3. Next, let relation $V(x; b_1, \ldots, b_m) \geq V(x; b_1, \ldots, b_{m-1})$ be fulfilled for any $0 < b_1 \leq b_2 \leq \ldots \leq b_m$. Using the formula of total expectation one can write by averaging on T_1 and Y_1 the following relation

$$V(x; b_1, \ldots, b_{m+1}) = \int_0^{x/c} e^{-\delta t} \Bigg[\int_0^{b_1-(x-ct)} V(x - ct + y; b_2, \ldots, b_{m+1}) p(y) dy$$

$$+ \int_{b_1-(x-ct)}^{\infty} V(b_1; b_2, \ldots, b_{m+1}) p(y) dy \Bigg] f(t)\, dt + V_{[0,T_1]}(x, b_1).$$

In view of induction assumption we obtain the desired statement of the theorem. □

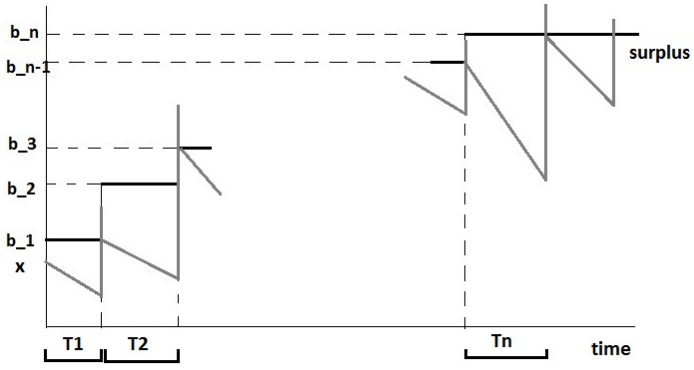

Fig. 3. Surplus under n-level barrier strategy

Integrating by parts it is easy to obtain for any $a > 0$

$$\int_a^{\infty} (y - a) dF(y) = \int_a^{\infty} \overline{F}(y)\, dy$$

where $\overline{F}(y) = 1 - F(y)$ and F is a distribution function. Thus, we get the following

Corollary 2. *The expected discounted dividends with a step-function barrier strategy can be written in the form*

$$V(x; b_1, \ldots, b_n) = \int_0^{x/c} e^{-\delta t} f(t) \left[\int_0^{b_1-x+ct} V(x - ct + y; b_2, \ldots, b_n)\, dF(y) \right.$$

$$+V(b_1;b_2,\ldots,b_n)\overline{F}(b_1-x+ct)+\int\limits_{b_1-x+ct}^{\infty}\overline{F}(y)\,dy\Bigg]\,dt$$

where $F(y)=P(Y_n\le y)$, $n\ge 1$, is the distribution function of profit amounts.

Further refinement of the obtained results is possible for the case of dual Cramér-Lundberg model. Hence, let $f(t)=\lambda e^{-\lambda t}$ for $t\ge 0$. According to Avanzi *et al.*[3] the function $V(x;b)$ satisfies the following integro-differential equation

$$cV'(x;b)+(\lambda+\delta)V(x;b)-\lambda\int\limits_0^{b-x}V(x+y;b)\,dF(y)$$

$$-\lambda\int\limits_{b-x}^{\infty}(x-b+y)\,dF(y)-\lambda V(b,b)\overline{F(b-x)}=0,\quad 0<x<b.$$

It is supposed further on that the condition of the positive surplus profit per unit time is satisfied, namely, $ES(1)-c>0$. Under additional assumption that surplus jumps have also exponential distribution $p(y)=\beta e^{-\beta y}$, $y\ge 0$, this integro-differential equation can be transformed into the second order differential equation

$$cV''(x;b)+(\lambda+\delta-\beta c)V'(x;b)-\beta\delta V(x;b)=0 \tag{13}$$

with initial condition $V(0;b)=0$. It easily follows that one can obtain the solution in explicit form

$$V(x;b)=\frac{\lambda}{\beta}\cdot\frac{e^{rx}-e^{sx}}{(cr+\delta)e^{rb}-(cs+\delta)e^{sb}}. \tag{14}$$

Here r and s are solutions of the characteristic equation corresponding to (13). Due to (14) there exists the optimal barrier

$$b^*=\frac{1}{r-s}\cdot\ln\frac{s(cs+\delta)}{r(cr+\delta)}. \tag{15}$$

Hence, assumption of Theorems 3 and 4 is valid and choosing $b_1\le b_2\le\ldots\le b_n\le b^*$ we can state that $V(x;b_1)\le V(x;b_1,\ldots,b_n)$ for all $x\le b_1$.

Moreover, since the jumps distribution is exponential one easily gets

Corollary 3. *The following relation is true*

$$V(x;b_1,b_2)=\frac{\lambda e^{-\beta(b_1-x)}}{\lambda+\delta+\beta c}\left(1-e^{-(\lambda+\delta+\beta c)(x/c)}\right)[\beta^{-1}+V(b_1;b_2)]$$

$$+\lambda\beta\int\limits_0^{x/c}e^{-(\lambda+\delta)t}\int\limits_0^{b_1-x+ct}V(x-ct+y;b_2)e^{-\beta y}\,dydt.$$

Thus, it is possible to calculate recursively $V(x; b_1, b_2, \ldots, b_n)$ using Corollaries 2 and 3 and explicit form (14) of $V(x; b)$.

Next step of investigation is to employ the recently introduced new notions such as absolute and Parisian ruin or Omega model describing the company bankruptcy. The simplest case of Parisian ruin with a fixed implementation delay means that the company surplus cannot stay negative longer than a given time d, see, e.g., Czarna and Palmowski[11], Loeffen *et al.*[14]. In relation to our model this signifies that the company stops the functioning if its surplus reaches the level $-cd$. Denote by $\tilde{V}(x; b)$ expected discounted dividends paid by the company with initial surplus x and dividend barrier b until the bankruptcy. Hence, it is not difficult to prove the following

Proposition 1. $\tilde{V}(x; b) = V(x + cd; b + cd)$ *for* $-cd \leq x \leq b$.

So, one can establish the analogues of Theorems 3 and 4, as well as Corollaries 2 and 3. Furthermore, if the gain amounts have exponential distribution the optimal dividends barrier for the new model $\tilde{b}^*$ is equal to $b^* - cd$ where b^* is given by (15).

4 Conclusion

For the credit model we have considered the short-term case (one or two periods). Further research includes treatment of longer terms models and their stability.

Summing up the investigation of the dual model we underline that under some additional assumptions a step-function barrier strategy with growing steps gives the higher expected discounted dividends than a simple barrier strategy. Moreover, if the dividends expression is known for a constant barrier it is possible to obtain the expected dividends amount for the case of step-function with any fixed number of steps. Furthermore, proceeding as in Avanzi *et al.*[3], one can get the explicit expressions for the processes with jumps having not only exponential distribution but their mixtures as well.

It was also shown how to extend these results to the models with delay of bankruptcy, that is, generalize the notion of ruin. In particular, using the Parisian ruin with a deterministic delay meaning that company becomes bankrupt only if it surplus stays negative longer than a fixed time d it is easy to obtain the results similar to the case of usual ruin.

The other case of Parisian ruin with a stochastic implementation delay (considered, e.g., in Landriault *et al.*[13] for insurance risk models) is not so obvious for the dual model and needs a special treatment.

The same is true for Omega models with a specified intensity of default depending on company surplus. Definition of Omega models one can find, e.g., in Albrecher *et al.*[2], Gerber *et al.*[12].

Thus, we have demonstrated unification of reliability and cost approaches, since the employed objective functions include the company gains as well as its ruin or bankruptcy times.

In order to complete the research it is necessary to carry out the sensitivity analysis with respect to small parameters fluctuations and underlying processes

perturbations (see, e.g., Bulinskaya[8], Bulinskaya and Gusak[10], Saltelli *et al.*[16]), in other words, to establish the models stability.

Acknowledgement. The research was partially supported by RFBR grant 17-01-00468.

References

1. L. Afanasyeva, E. Bulinskaya. Stochastic Models of Transport Flows. *Communications in Statistics: Theory and Methods*, 40, 16, 2830–2846, 2011.
2. H. Albrecher, H.U. Gerber, E.S.W. Shiu. The optimal dividend barrier in the Gamma-Omega model. *European Actuarial Journal*, 1, 43–55, 2011.
3. B. Avanzi, H.U. Gerber and E.S.W. Shiu. Optimal Dividends in the Dual Model. *Insurance: Mathematics and Economics*,41, 1, 111–123, 2007.
4. R. Bellman. *Dynamic Programming*, Princeton University Press, 1957.
5. E. Bayraktar and M. Egami. Optimizing venture capital investment in a jump diffusion model. *Mathematical Methods of Operations Research*, 67, 1, 21–42, 2008.
6. E.V. Bulinskaya. On a cost approach in insurance. *Review of Applied and Industrial Mathematics*, 10, 2, 376–386, 2003.
7. E.V. Bulinskaya. Cost and reliability approaches in inventory theory. *Cybernetics and Systems Analysis*, 41, 1, 56–66, 2005.
8. E. Bulinskaya. Stochastic Insurance Models: Their Optimality and Stability. *Advances in Data Analysis, ed. Ch.H. Skiadas*, Birkhäuser, Boston, Basel, Berlin, 129–140, 2010.
9. E. Bulinskaya. New research directions in modern actuarial sciences. *Modern problems of stochastic analysis and statistics – selected contributions in honor of Valentin Konakov, ed. V.Panov*, Springer, 2017, In press.
10. E. Bulinskaya and J. Gusak. Optimal Control and Sensitivity Analysis for Two Risk Models. *Communications in Statistics – Simulation and Computation*, 45, 5, 1451–1466, 2016.
11. I. Czarna and Z. Palmowski. Ruin probability with Parisian delay for a spectrally negative Lévy risk process. *Journal of Applied Probability*, 48, 984–1002, 2011.
12. H.U. Gerber, E.S.W. Shiu and H. Yang. The Omega model: from bankruptcy to occupation times in the red. *European Actuarial Journal*, 2, 259–272, 2012.
13. D. Landriault, J.-F. Renaud and X. Zhou. Insurance risk models with Parisian implementation delays. *Methodology and Computing in Applied Probability*, 16, 3, 583–607, 2014.
14. R. Loeffen, I. Czarna, Z. Palmowski. Parisian ruin probability for spectrally negative Lévy processes. *Bernoulli*, 19, 2, 599–609, 2013.
15. A. Muromskaya. Discounted dividends in a strategy with a step barrier function. *Moscow University Mathematics Bulletin*, 71, 5, 200–203, 2016.
16. A. Saltelli, M. Ratto, T. Campolongo, J. Cariboni, D. Gatelli, M. Saisana and S. Tarantola. *Global Sensitivity Analysis. The Primer*, Wiley, 2008.

Empirical Power Study of the Jackson Exponentiality Test

Frederico Caeiro[1] and Ayana Mateus[2]

[1] Faculdade de Ciências e Tecnologia & Centro de Matemática e Aplicações (CMA), Universidade Nova de Lisboa, Portugal
(E-mail: fac@fct.unl.pt)
[2] Faculdade de Ciências e Tecnologia & Centro de Matemática e Aplicações (CMA), Universidade Nova de Lisboa, Portugal
(E-mail: amf@fct.unl.pt)

Abstract. The exponential model is a frequently used distribution in areas such as queueing theory, reliability and survival analysis. Therefore, testing exponentiality is an important problem in Statistics. Many tests have been proposed in the literature and in this paper we revisit the exact and asymptotic properties of the Jackson exponentiality test. Using Monte Carlo computations we study and compare the Empirical Power of the Jackson test.
Keywords: Exponential distribution; exponentiality test; monte carlo simulation; power of a statistical test;.

1 Introduction

Let X be a continuous random variable with distribution function (df)

$$F(x) = P(X \leq x) = 1 - \exp(-\lambda x), \quad x > 0. \tag{1}$$

Then X has exponential distribution with parameter $\lambda > 0$ and we will use the notation $\text{Exp}(\lambda)$ to refer to this distribution. Note that if $X \sim \text{Exp}(\lambda)$, then $\lambda X \sim \text{Exp}(1)$. The exponential distribution is the adequate model for the time between two consecutive events in a Poisson process with intensity λ. This distribution has several useful statistical properties, summarized in Ahsanullah and Hamedani[2], Balakrishnan[4], Johnson *et al.*[10], among others.

The problem of testing exponentiality against other alternatives has received in the last decades a lot of attention from different researchers (see Alizadeh Noughabi and Arghami[3], Brilhante[5], Doksum[7], Henze and Meintanis[8], Kozubowski *et al.*[11], Stephens[13] and references therein). Possible alternative models, which extend the exponential distribution, are the gamma distribution, the Weibull distribution, the generalized Pareto distribution and the q-exponential distribution.

In this paper we revisit the Jackson statistic used to test exponentiality against a general alternative. In section 2 we present the Jackson statistic test and we review several exact and asymptotic properties. Section 3 is dedicated to a monte carlo simulation study to compute the power of the Jackson test. Those values are then compared to the power of the Lilliefors exponentiality test.

2 Jackson Exponentiality Test

Suppose X_1, X_2,..., X_n are independent and identically distributed random variables with common unknown continuous distribution. We wish to test the null hypothesis

$$H_0 : X \sim \text{Exp}(\lambda)$$

for some unspecified parameter $\lambda > 0$, against H_1: the distribution of X is not exponential.

The Jackson test was introduced in Jackson [9] and discussed in Caeiro *et al.*[6]. The test statistic is given by

$$J_n = \frac{\sum_{i=1}^{n} m_i X_{(i)}}{\sum_{i=1}^{n} X_i}, \tag{2}$$

with $X_{(i)}$ the i-th ascending order statistic and $m_i = \lambda E(X_{(i)}) = \sum_{j=1}^{i}(n-j+1)^{-1}$, $i = 1, \ldots, n$. Since this statistic test can be expressed as a function of the scaled random variables λX_i, the null distribution of J_n does not depend on the value of the parameter λ. With some algebra, eq. (2) could be expressed in terms of the standardized spacings $S_i = (n-i+1)(X_{(i)} - X_{(i-1)})$, $i = 1, \ldots, n$ with $X_0 \equiv 0$ (Jackson[9]), that is,

$$J_n = \frac{\sum_{i=1}^{n} c_i S_i}{\sum_{i=1}^{n} S_i},$$

with $c_i = 1 + m_{i-1}$, $i = 1, \ldots, n$ ($m_0 \equiv 0$). The exact null df was presented in [9] and is given by

$$P(J_n \leq x) = \frac{\sum_{k=1}^{n}(x - c_k)^n I_{(0,\infty[}(x - c_k)}{\prod_{j=1,\, j\neq k}^{n}(c_j - c_k)}, \quad 1 < x < c_n, \tag{3}$$

where I_A denotes the indicator function on the set A ($I_A(x) = 1$ if $x \in A$ and $I_A(x) = 0$ otherwise). This df was implemented in R programming language [14] and the computer code is available in Caeiro *et al.*[6]. Unless we use a arbitrary precision package to compute the df in eq. (3), we can obtain inaccurate values for $n > 100$, due to floating-point errors in R. In Table 1 we provide several quantiles of probability p from the df in (3). This table extends Table 1 in Caeiro *et al.*[6].

The limit distribution of $\sqrt{n}(J_n - 2)$ is the standard normal distribution (Jackson[9]). Since the rate of converge of $\sqrt{n}(J_n - 2)$ to the limit distribution is slow, Caeiro *et al.*[6] studied a more a accurate approximation for the df, for finite sample sizes. The approximation, based on Edgeworth expansion (Abramowitz and Stegun[1]), is

$$P(J_n \leq x) \approx \Phi(z) - \phi(z)\left\{\gamma_1 \frac{z^2-1}{6} + (\gamma_2 - 3)\frac{z^3 - 3z}{24} + \gamma_1^2 \frac{z^5 - 10z^3 + 15z}{72}\right\}$$

where $z = (x-\mu)/\sigma$, ϕ and Φ are the density function and the df of the standard normal distribution and $\sigma^2 = \mu_2 = \mu_2' - \mu^2$, $\gamma_1 = \mu_3/\sigma^3$ and $\gamma_2 = \mu_4/\sigma^4$ with

Table 1. Exact quantiles from the null distribution of the Jackson statistic.

	p												
n	0.005	0.01	0.025	0.05	0.1	0.25	0.5	0.75	0.9	0.95	0.975	0.99	0.995
3	1.037	1.053	1.083	1.118	1.167	1.264	1.377	1.511	1.629	1.689	1.731	1.769	1.788
4	1.092	1.116	1.158	1.199	1.251	1.346	1.468	1.600	1.727	1.801	1.859	1.918	1.952
5	1.146	1.173	1.218	1.260	1.312	1.410	1.531	1.665	1.793	1.871	1.936	2.007	2.051
6	1.192	1.220	1.266	1.308	1.361	1.458	1.579	1.712	1.840	1.920	1.988	2.066	2.115
7	1.231	1.260	1.306	1.349	1.401	1.497	1.617	1.748	1.876	1.956	2.025	2.106	2.159
8	1.264	1.294	1.340	1.382	1.435	1.530	1.647	1.777	1.904	1.983	2.053	2.135	2.190
9	1.294	1.323	1.369	1.411	1.463	1.557	1.673	1.801	1.926	2.004	2.074	2.156	2.212
10	1.320	1.349	1.395	1.437	1.488	1.581	1.694	1.820	1.943	2.021	2.090	2.172	2.229
11	1.343	1.372	1.417	1.459	1.509	1.601	1.713	1.837	1.958	2.035	2.103	2.185	2.241
12	1.364	1.393	1.438	1.479	1.529	1.619	1.729	1.851	1.970	2.046	2.114	2.195	2.251
13	1.382	1.411	1.456	1.497	1.546	1.635	1.743	1.863	1.981	2.055	2.122	2.202	2.258
14	1.400	1.428	1.473	1.513	1.561	1.649	1.756	1.874	1.989	2.063	2.129	2.208	2.263
15	1.415	1.444	1.488	1.527	1.575	1.662	1.767	1.883	1.997	2.069	2.135	2.213	2.268
16	1.430	1.458	1.501	1.541	1.588	1.674	1.778	1.892	2.004	2.075	2.139	2.217	2.271
17	1.443	1.471	1.514	1.553	1.600	1.684	1.787	1.899	2.010	2.080	2.143	2.219	2.273
18	1.456	1.484	1.526	1.564	1.611	1.694	1.795	1.906	2.015	2.084	2.146	2.222	2.274
19	1.468	1.495	1.537	1.575	1.621	1.703	1.803	1.912	2.019	2.087	2.149	2.223	2.276
20	1.478	1.506	1.547	1.585	1.630	1.711	1.810	1.918	2.023	2.090	2.151	2.225	2.276
21	1.489	1.516	1.557	1.594	1.639	1.719	1.816	1.923	2.027	2.093	2.153	2.225	2.276
22	1.498	1.525	1.566	1.603	1.647	1.726	1.822	1.927	2.030	2.095	2.155	2.226	2.276
23	1.507	1.534	1.574	1.611	1.655	1.733	1.828	1.932	2.033	2.097	2.156	2.226	2.276
24	1.516	1.542	1.582	1.619	1.662	1.740	1.833	1.935	2.035	2.099	2.157	2.226	2.276
25	1.524	1.550	1.590	1.626	1.669	1.746	1.838	1.939	2.038	2.101	2.158	2.226	2.275
30	1.559	1.584	1.622	1.657	1.698	1.771	1.858	1.954	2.047	2.106	2.160	2.224	2.270
35	1.587	1.612	1.648	1.681	1.721	1.790	1.874	1.964	2.053	2.109	2.159	2.221	2.264
40	1.611	1.634	1.669	1.701	1.739	1.806	1.886	1.972	2.056	2.110	2.158	2.216	2.258
45	1.630	1.653	1.687	1.718	1.754	1.819	1.896	1.979	2.059	2.110	2.156	2.212	2.251
50	1.647	1.669	1.702	1.732	1.767	1.830	1.904	1.983	2.061	2.110	2.154	2.207	2.245
55	1.662	1.683	1.716	1.744	1.779	1.839	1.911	1.987	2.062	2.109	2.151	2.203	2.239
60	1.675	1.696	1.727	1.755	1.789	1.847	1.916	1.991	2.063	2.108	2.149	2.198	2.233
65	1.687	1.707	1.738	1.765	1.797	1.854	1.921	1.994	2.063	2.107	2.147	2.194	2.228
70	1.697	1.717	1.747	1.773	1.805	1.860	1.926	1.996	2.063	2.106	2.144	2.190	2.223
75	1.706	1.726	1.755	1.781	1.812	1.866	1.930	1.998	2.064	2.105	2.142	2.187	2.218
80	1.715	1.734	1.763	1.788	1.818	1.871	1.933	2.000	2.064	2.104	2.140	2.183	2.214
85	1.723	1.741	1.770	1.794	1.824	1.876	1.936	2.001	2.063	2.102	2.138	2.180	2.210
90	1.730	1.748	1.776	1.800	1.829	1.880	1.939	2.003	2.063	2.101	2.136	2.177	2.206
95	1.737	1.755	1.782	1.806	1.834	1.884	1.942	2.004	2.063	2.100	2.134	2.174	2.202
100	1.743	1.761	1.787	1.811	1.839	1.887	1.944	2.005	2.063	2.099	2.132	2.171	2.198

$\mu_3 = \mu'_3 - 3\mu\mu'_2 + 2\mu^2$ and $\mu_4 = \mu'_4 - 4\mu\mu'_3 + 2\mu^2$ and

$$\mu = \mu'_1 = \frac{\sum_{i=1}^n c_i}{n}, \quad \mu'_2 = \frac{\sum_{i=1}^n c_i^2 + (\sum_{i=1}^n c_i)^2}{n(n+1)},$$

$$\mu'_3 = \frac{2\sum_{i=1}^n c_i^3 + 3(\sum_{i=1}^n c_i)\sum_{i=1}^n c_i^2 + (\sum_{i=1}^n c_i)^3}{n(n+1)(n+2)},$$

$$\mu'_4 = \frac{6\sum_{i=1}^n c_i^4 + 8(\sum_{i=1}^n c_i)\sum_{i=1}^n c_i^3 + 3(\sum_{i=1}^n c_i^2)^2 + 6(\sum_{i=1}^n c_i)^2\sum_{i=1}^n c_i^2 + (\sum_{i=1}^n c_i)^4}{n(n+1)(n+2)(n+3)}.$$

3 Power comparison and conclusions

3.1 Other test Statistic

To be able to compare the power of the Jackson exponentiality test, we also considered the Lilliefors test, which is a Kolmogorov-Smirnov type test. The test statistic is

$$D_n = \sup_x |F_n(x) - F_0(x)|, \tag{4}$$

with $F_0(x) = 1 - \exp(-x/\bar{x}),\ x > 0$ the exponential df in (1) with λ estimated by $1/\bar{x}$, where $\bar{x}$ is the sample mean and $F_n(x)$ is the empirical distribution function. The test statistic in (4) is equivalent to

$$D_n = \max\left\{D_n^+, D_n^-\right\},$$

with $D_n^+ = \max_{1\le j\le n}[i/n - Y_i]$, $\quad D_n^- = \max_{1\le j\le n}[Y_i - (i-1)/n]$ and $Y_i = 1 - \exp(-X_{(i)}/\bar{X})$. Since the parameter λ of the exponential distribution is estimated from the sample, the critical values for the Kolmogorov-Smirnov test are no longer valid. Lilliefors[12] made a Monte Carlo simulation study, based on 5000 runs, and computed critical values for the test statistic D_n in (4). Since those critical values were computed from a small number of runs and values for even sample sizes were interpolated, we also conducted a monte carlo simulation study, based on 100000 runs, to compute critical values for the statistic D_n in (4). In Table 2 we present the simulated critical values for D_n for $n = 3(1)20$, and $n = 25(5)$ at the significance level $\alpha = 0.20,\ 0.10,\ 0.05,\ 0.025,\ 0.02,\ 0.01,\ 0.005$. The values in Table 2 were computed in R language using the computer code:

```
# Function to compute critical values for Lilliefors Exponentiality test
ksexp.crit <- function(n, runs=10^5, alpha=0.05){
  set.seed(1)
  lambda <- 1
  sim.ks <- replicate(runs, {x <- rexp(1000, rate=lambda)[1:n];
                        ks.test(x,"pexp",rate=1/mean(x))$statistic} )
  return(quantile(sim.ks,  probs=1-alpha))
}
```

3.2 Possible alternatives to Exponentiality

We shall consider two alternatives to the exponential distribution: the gamma and Weibull distributions with density function given respectively by,

$$f(x) = \frac{\lambda^\theta\, x^{\theta-1}}{\Gamma(\theta)} \exp(-\lambda x), \quad x > 0 \quad (\theta > 0,\, \lambda > 0) \tag{5}$$

and

$$f(x) = \lambda\theta(\lambda x)^{\theta-1} \exp\{-(\lambda x)^\theta\}, \quad x > 0 \quad (\theta > 0, \lambda > 0). \tag{6}$$

When $\theta = 1$ those models reduce to the exponential distribution. Thus testing the exponential hypothesis is equivalent to test the null hypothesis $H_0 : \theta = 1$. For the power study, we considered $\lambda = 1$ and $\theta = 0.1(0.1)2$.

Table 2. Critical values for D_n at the significance level α and sample size n.

α	0.20	0.10	0.05	0.025	0.02	0.01	0.005
3	0.451	0.511	0.551	0.578	0.585	0.601	0.612
4	0.401	0.445	0.485	0.522	0.532	0.559	0.582
5	0.361	0.405	0.442	0.474	0.484	0.512	0.537
6	0.332	0.373	0.408	0.440	0.449	0.475	0.500
7	0.310	0.348	0.381	0.412	0.421	0.447	0.470
8	0.292	0.327	0.359	0.387	0.396	0.421	0.444
9	0.276	0.311	0.341	0.367	0.376	0.401	0.423
10	0.263	0.296	0.324	0.350	0.358	0.381	0.403
11	0.251	0.283	0.311	0.336	0.343	0.365	0.386
12	0.242	0.272	0.299	0.323	0.330	0.351	0.371
13	0.233	0.262	0.288	0.311	0.318	0.339	0.359
14	0.224	0.253	0.278	0.301	0.308	0.328	0.347
15	0.217	0.245	0.270	0.292	0.298	0.317	0.337
16	0.211	0.237	0.261	0.283	0.289	0.310	0.329
17	0.205	0.230	0.254	0.274	0.280	0.300	0.319
18	0.199	0.224	0.247	0.267	0.273	0.292	0.309
19	0.194	0.219	0.240	0.261	0.267	0.285	0.302
20	0.189	0.213	0.234	0.254	0.260	0.277	0.295
25	0.170	0.192	0.211	0.228	0.233	0.249	0.263
30	0.156	0.175	0.193	0.209	0.214	0.228	0.243
35	0.145	0.163	0.179	0.195	0.199	0.213	0.225
40	0.136	0.153	0.169	0.182	0.187	0.199	0.212
45	0.128	0.145	0.159	0.172	0.176	0.188	0.200
50	0.122	0.137	0.151	0.164	0.168	0.179	0.190
60	0.111	0.126	0.139	0.150	0.154	0.164	0.174
70	0.103	0.116	0.128	0.139	0.143	0.153	0.162
80	0.097	0.109	0.120	0.130	0.133	0.142	0.151
90	0.091	0.103	0.113	0.123	0.126	0.134	0.142
100	0.087	0.098	0.108	0.117	0.120	0.127	0.135

3.3 Results and power comparison

We present in this section the simulated Power values of the Jackson and Lilliefors tests. Results are based on a Monte Carlo simulation study with 100000 samples of size $n = 5$, 10, 20, 50 and 100 at a significance level $\alpha = 0.05$. The critical values used in the simulation study are the ones available in Tables 1 and 2. Although we considered the models in (5) and (6) we assume to have no knowledge of the alternative distribution. Therefor the critical region for Jackson test is two-tailed and for Lilliefors test is one-tailed.

In Figures 1 and 2 and in Tables 3 and 4 we present the simulated power values at a significance level $\alpha = 0.05$. Results for $n = 5$ are only available in the tables. Both tests exhibit a similar statistical power, almost identical when the alternative hypothesis was nearly exponential (θ close to 1). The studied tests have a reasonable power, for sample sizes $n \geq 50$. Lilliefors test is more powerful for the gamma alternative and θ not close to 1. For the Weibull alternative and $\theta > 1$, Jackson test is more powerful.

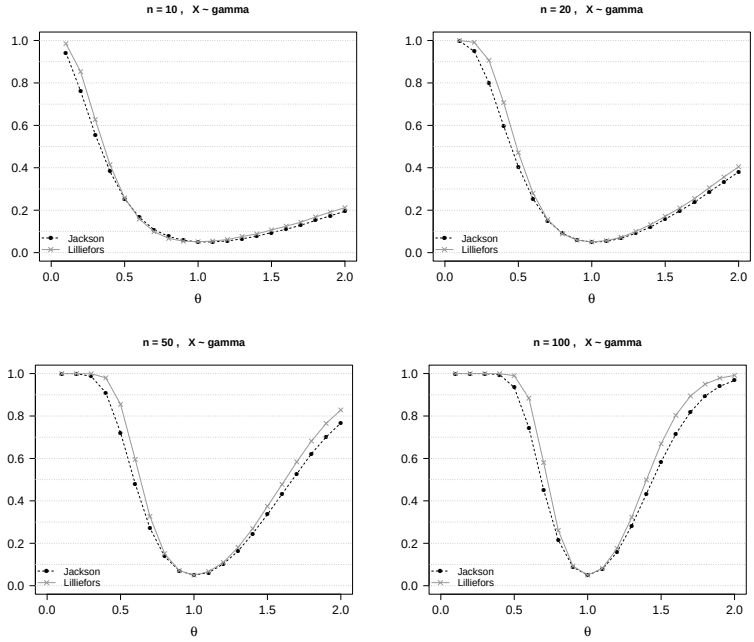

Fig. 1. Simulated Power curve for the statistic tests J_n and D_n and $\alpha = 0.05$, for the gamma model.

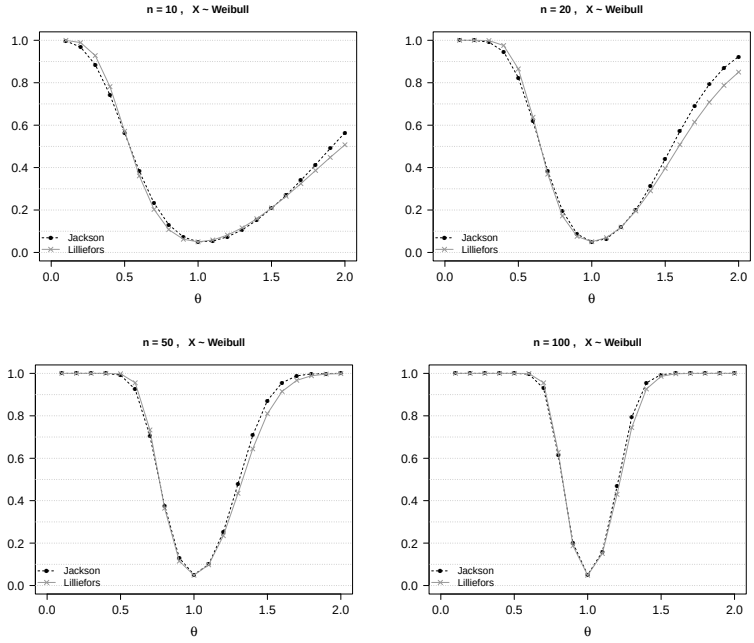

Fig. 2. Simulated Power curve for the statistic tests J_n and D_n and $\alpha = 0.05$, for the Weibull model.

Table 3. Simulated power of the tests for the gamma alternative.

	$n=5$		$n=10$		$n=20$		$n=50$		$n=100$	
θ	J_n	D_n	J_n	D_n	J_n	D_n	J_n	D_n	J_n	D_n
0.1	0.736	0.770	0.943	0.985	0.998	1.000	1.000	1.000	1.000	1.000
0.2	0.518	0.499	0.762	0.853	0.949	0.991	1.000	1.000	1.000	1.000
0.3	0.357	0.316	0.556	0.627	0.800	0.906	0.987	0.999	1.000	1.000
0.4	0.247	0.202	0.383	0.414	0.597	0.707	0.909	0.980	0.995	1.000
0.5	0.173	0.134	0.254	0.257	0.405	0.471	0.722	0.855	0.935	0.990
0.6	0.122	0.093	0.166	0.159	0.254	0.280	0.480	0.595	0.744	0.883
0.7	0.090	0.068	0.108	0.098	0.151	0.155	0.272	0.327	0.453	0.581
0.8	0.067	0.055	0.076	0.067	0.091	0.088	0.138	0.151	0.214	0.260
0.9	0.058	0.052	0.058	0.054	0.061	0.058	0.071	0.071	0.088	0.093
1.0	0.049	0.050	0.051	0.052	0.049	0.051	0.050	0.050	0.050	0.050
1.1	0.047	0.051	0.051	0.054	0.053	0.056	0.062	0.067	0.078	0.082
1.2	0.049	0.057	0.055	0.061	0.068	0.072	0.102	0.110	0.158	0.176
1.3	0.050	0.062	0.065	0.076	0.091	0.100	0.163	0.181	0.283	0.322
1.4	0.055	0.069	0.077	0.088	0.121	0.132	0.245	0.269	0.433	0.499
1.5	0.062	0.078	0.095	0.107	0.158	0.171	0.336	0.374	0.584	0.670
1.6	0.066	0.084	0.110	0.125	0.197	0.211	0.433	0.478	0.715	0.804
1.7	0.075	0.095	0.129	0.144	0.238	0.255	0.527	0.584	0.819	0.895
1.8	0.080	0.102	0.152	0.168	0.286	0.306	0.622	0.682	0.894	0.950
1.9	0.090	0.113	0.174	0.191	0.333	0.357	0.701	0.765	0.940	0.979
2	0.097	0.121	0.194	0.212	0.381	0.405	0.767	0.828	0.968	0.992

Table 4. Simulated power of the tests for the Weibull alternative.

	$n=5$		$n=10$		$n=20$		$n=50$		$n=100$	
θ	J_n	D_n	J_n	D_n	J_n	D_n	J_n	D_n	J_n	D_n
0.1	0.899	0.938	0.997	1.000	1.000	1.000	1.000	1.000	1.000	1.000
0.2	0.768	0.785	0.968	0.989	0.999	1.000	1.000	1.000	1.000	1.000
0.3	0.618	0.600	0.885	0.928	0.992	0.999	1.000	1.000	1.000	1.000
0.4	0.470	0.423	0.743	0.782	0.946	0.976	1.000	1.000	1.000	1.000
0.5	0.336	0.279	0.563	0.571	0.824	0.865	0.992	0.998	1.000	1.000
0.6	0.227	0.176	0.382	0.361	0.618	0.637	0.924	0.956	0.997	0.999
0.7	0.148	0.108	0.233	0.203	0.385	0.369	0.706	0.733	0.929	0.956
0.8	0.094	0.070	0.131	0.108	0.197	0.172	0.377	0.365	0.613	0.628
0.9	0.063	0.054	0.073	0.062	0.087	0.075	0.130	0.115	0.200	0.187
1.0	0.049	0.050	0.050	0.050	0.050	0.051	0.051	0.049	0.050	0.048
1.1	0.047	0.054	0.053	0.059	0.065	0.070	0.099	0.098	0.159	0.151
1.2	0.053	0.065	0.074	0.082	0.118	0.119	0.253	0.235	0.467	0.430
1.3	0.064	0.080	0.107	0.116	0.201	0.196	0.480	0.435	0.794	0.744
1.4	0.081	0.098	0.152	0.159	0.313	0.290	0.708	0.644	0.955	0.927
1.5	0.099	0.119	0.208	0.210	0.440	0.397	0.872	0.810	0.995	0.986
1.6	0.119	0.141	0.270	0.265	0.571	0.508	0.956	0.915	1.000	0.998
1.7	0.143	0.167	0.339	0.324	0.691	0.614	0.989	0.967	1.000	1.000
1.8	0.169	0.195	0.414	0.386	0.792	0.708	0.998	0.989	1.000	1.000
1.9	0.197	0.223	0.490	0.448	0.870	0.788	1.000	0.997	1.000	1.000
2.0	0.226	0.251	0.565	0.507	0.923	0.850	1.000	0.999	1.000	1.000

Acknowledgements. This research was partially supported by National Funds through **FCT** – Fundação para a Ciência e a Tecnologia, through the project UID/MAT/00297/2013 (Centro de Matemática e Aplicações).

References

1. M. Abramowitz and I. A. Stegun, *Handbook of Mathematical Functions*, Vol. 55 of Appl. Math. Ser., 10th edition, National Bureau of Standards, US Governement Printing Office, Washington, DC, 1972.
2. M. Ahsanullah and G.G. Hamedani. *Exponential distribution*. Nova Science Publ., 2010.
3. H. Alizadeh Noughabi and N.R. Arghami. Testing exponentiality based on characterizations of the exponential distribution, *Journal of Statistical Computation and Simulation*, **81**:11, 1641–1651, 2011. DOI: 10.1080/00949655.2010.498373
4. Balakrishnan, K. Exponential distribution: theory, methods and applications. CRC press, 1996.
5. M. F. Brilhante, Exponentiality versus generalized Pareto - a resistant and robust test, *REVSTAT - Statistical Journal* **2**(1), 2–13 2004.
6. F. Caeiro, F.J. Marques, A. Mateus, and S. Atal. A note on the Jackson exponentiality test, *AIP Conference Proceedings* **1790**, 080005, 2016. doi: 10.1063/1.4968686
7. K. A. Doksum and B. S. Yandell, Tests for exponentiality. In P.R. Krishnaiah and P. K. Sen (eds.), *Handbook of Statistics 4: Nonparametric Methods*, Vol. **4**, North-Holland, Amsterdam, 579–611, 1984.
8. N. Henze and S.G. Meintanis, Recent and classical tests for exponentiality: a partial review with comparisons *Metrica*, **61**, 29–45, 2005.
9. O. A. Y. Jackson. An analysis of departures from the exponential distribution, *J. Roy. Statist. Soc.* B, **29**, 540–549, 1967.
10. N.L. Johnson, S. Kotz and N. Balakrishnan. Continuous Univariate Distributions, Volume 1, 2nd Edition. Wiley, 1994.
11. T.J. Kozubowski, A. K. Panorska, F. Qeadan, A. Gershunov and D. Rominger, Testing Exponentiality Versus Pareto Distribution via Likelihood Ratio. *Comm. Statist. - Simulation Comput.* **38**(1), 118–139, 2009.
12. H. W. Lilliefors, On the Kolmogorov-Smirnov test for the exponential distribution with mean unknown. Journal of the American Statistical Association, **64**(325), 387–389, 1969.
13. M. A. Stephens, Tests for the exponential distribution, in: R.B. D'Agostino, M.A. Stephens (eds.), *Goodness-of-Fit Techniques*, Marcel Dekker Inc., New York, 421–459, 1986.
14. R Core Team, R: A language and environment for statistical computing. R Foundation for Statistical Computing, Vienna, Austria, 2015. URL http://www.R-project.org/.

Log Probability Weighted Moments Method for Pareto distribution

Frederico Caeiro[1] and Ayana Mateus[2]

[1] Faculdade de Ciências e Tecnologia, Universidade Nova de Lisboa, Portugal and Centro de Matemática e Aplicações (CMA)
(E-mail: fac@fct.unl.pt)[1]
[2] Faculdade de Ciências e Tecnologia, Universidade Nova de Lisboa, Portugal and Centro de Matemática e Aplicações (CMA)
(E-mail: amf@fct.unl.pt)[1]

Abstract. In this work, we introduce new estimators for the parameters of the Pareto type I distribution. These new estimators are obtained through a modification of the probability weighted moments method, in order to make the new estimators consistent for any value of the shape parameter. We also compare the finite sample behaviour of the new estimators with the most common used estimators (the moment, the maximum likelihood and the probability weighted moments estimators) with a Monte Carlo simulation study. Some asymptotic properties for the new estimators introduced in this work are also shown.
Keywords: Pareto distribution, Monte Carlo method, Maximum likelihood estimator, Moment estimator, Probability weighted moments estimators, Log probability weighted moments estimators.

1 Introduction

The Pareto [12] distribution was first introduced as a model for large incomes and nowadays has been extensively used for modelling events in fields such as bibliometrics, demography, insurance, or finance, among others. Although there are several variants of this distribution, in this work we shall consider the classic Pareto distribution also known as Pareto type I distribution. A random variable X has a Pareto type I distribution if its distribution function (d.f.) is

$$F_X(x) = P(X \leq x) = 1 - \left(\frac{c}{x}\right)^a, \quad x > c, \quad c > 0, \quad a > 0,$$

where c and a are scale and shape parameters, respectively (Arnold [1], Johnson *et al.*[10]). In this work we shall consider both parameters unknown. The parameter a measures the heaviness of the right tail and is also known as the tail index. The associated quantile function of X is obtained by inverting the d.f. and is given by

$$Q_X(p) = F_X^{\leftarrow}(p) = c(1-p)^{-1/a}, \quad 0 < p < 1, \quad c > 0, \quad a > 0,$$

where p denotes the lower tail probability. Estimation of the parameters a and c has already been extensively addressed in the literature (see Caeiro *et al.*[3] Lu and Tao[11], Quandt[13], Rytgaard [15], Singh and Guo[16] and references

therein). Under a semiparametric framework, this Pareto type I distribution is often used as an upper tail model. Under such framework, we often work with the parameter $\xi = 1/a$, usually called the Extreme Value Index. Details on the estimation of ξ for models with a Pareto upper tail can be found in (Arnold [1], Beirlant *et al.*[7] and Gomes and Guillou [9]).

In section 2 of this work, we introduce new estimators for the parameters of the Pareto distribution. These new estimators are obtained through a modification of the probability weighted moments method, in order to make the new estimators consistent for any value of the shape parameter a. In section 3 we compare the finite sample behaviour of new estimators with the most common used estimators (the moment, the maximum likelihood and the probability weighted moments estimators) with a Monte Carlo simulation study. In section 4 we present some asymptotic properties for the new estimators introduced in this work.

2 Estimation of the Pareto Distribution

Here we introduce the estimators for the parameters a and c, considered in this work.

2.1 A Brief Review of Several Popular Estimators

Let $X_1, X_2, \ldots, X_n$ be a sample of size n taken from a Pareto type I population. Here we will denote the corresponding order statistics by $X_{1:n} \leq X_{2:n} \leq \ldots \leq X_{n:n}$. The most popular moment (M) estimators are the ones proposed by Quandt[13] and given by

$$\hat{a}^M = \frac{n\overline{X} - X_{1:n}}{n(\overline{X} - X_{1:n})}, \quad \hat{c}^M = \left(1 - \frac{1}{n\hat{a}^M}\right) X_{1:n}, \quad \text{with} \quad \overline{X} = \frac{\sum_{i=1}^n X_i}{n},$$

which are consistent for $a > 1$. To avoid the restriction $a > 1$ of the previous estimators, we can use the maximum likelihood (ML) estimators

$$\hat{a}^{ML} = \left(\frac{1}{n}\sum_{i=1}^{n} \ln \frac{X_i}{X_{1:n}}\right)^{-1}, \qquad \hat{c}^{ML} = X_{1:n},$$

The probability weighted moments method (PWM), introduced in Greenwood *et al.*[5] is a generalization of the classic method of moments. In this method we work with the theoretical moments $M_{p,r,s} = E(X^p(F(X))^r(1 - F(X))^s)$ with p, r and s any real numbers, and with their corresponding sample moments. The PWM estimators are obtained by equating $M_{p,r,s}$ with their corresponding sample moments, and then solving those equations in order of the parameters. When $r = s = 0$, $M_{p,0,0}$ are the usual noncentral moments of order p. Hosking *et al.* [8] advise the use of $M_{1,r,s}$, because the relations between parameters and moments have usually a much simpler form. Also, when r and s are integers $F(X)^r(1 - F(X))^s$ can be written as a linear combination of powers of $F(X)$

or $1-F(X)$. Taken in account this considerations it is usual to work with one of the two special cases:

$$w_r = M_{1,0,r} = E(X(1-F(X))^r) \quad \text{or} \quad k_r = M_{1,r,0} = E(X(F(X))^r). \quad (1)$$

For nonnegative integer r the unbiased estimators of w_r and b_r in (1) are respectively,

$$\hat{w}_r = \frac{1}{n}\sum_{i=1}^{n-r} \frac{\binom{n-i}{r}}{\binom{n-1}{r}} X_{i:n}, \quad \text{and} \quad \hat{k}_r = \frac{1}{n}\sum_{i=r+1}^{n} \frac{\binom{i-1}{r}}{\binom{n-1}{r}} X_{i:n}. \quad (2)$$

For Pareto type I distribution, we have $M_{p,r,s}{=}c^p\mathcal{B}(s+1-p/a, r+1)$, with $s-p/a>-1$, $r>-1$, where $\mathcal{B}$ represents the complete beta function (Caeiro and Gomes[2]).
In particular, $w_r = M_{1,0,r} = c/(r+1-1/a), \quad a>1/(r+1)$. Consequently, if we consider the theoretical moments $w_0 = c/(1-1/a)$ and $w_1 = c/(2-1/a)$, with $a>1$ the PWM estimators are, respectively,

$$\hat{a}^{PWM} = \frac{1}{1-\left(\frac{\hat{w}_1}{\hat{w}_0-\hat{w}_1}\right)} \quad \text{and} \quad \hat{c}^{PWM} = \hat{w}_0\left(\frac{\hat{w}_1}{\hat{w}_0-\hat{w}_1}\right), \quad a>1, \quad (3)$$

where $\hat{w}_0$ and $\hat{w}_1$ are given in (2).

2.2 New Estimators

Since the PWM estimators in (3) use the sample mean, they are only consistent if $a>1$. In order to have consistent estimators for $a>0$, we consider another method, related to the PWM method. Let

$$l_r = E((\ln X)(1-F(X))^r)$$

be the log probability weighted moments (LPWM) of X. For nonnegative integer r, the unbiased estimator of l_r is given by

$$\hat{l}_r = \frac{1}{n}\sum_{i=1}^{n-r} \frac{\binom{n-i}{r}}{\binom{n-1}{r}} \ln X_{i:n}. \quad (4)$$

For the Pareto distribution we have

$$l_r = \frac{\ln(c)}{(1+r)} + \frac{1}{a(1+r)^2}.$$

Hence if we consider the moments $l_0 = \ln c + 1/a$ and $l_1 = \ln c/2 + 1/4a$ the LPWM estimators are respectively,

$$\hat{a}^{LPWM} = \frac{1}{2\hat{l_0} - 4\hat{l_1}} \quad \text{and} \quad \hat{c}^{LPWM} = \exp(4\hat{l_1} - \hat{l_0}) \quad (5)$$

where $\hat{l}_0$ and $\hat{l}_1$ are given in (4).

3 Finite sample behaviour of the estimators

In this section we are going to evaluate the performance of the shape and scale Pareto estimators here presented. We have implemented a Monte-Carlo simulation experiment in `R` software environment [14], to obtain the distributional behaviour of the estimators under study. The study is made with 20,000 samples of sizes $n = 10$, 15, 20, 30, 40, 50, 75, 100, 150, 200, 300 and 500 from the Pareto distribution with parameters $(a, c) = (0.5, 1)$ and $(a, c) = (2, 2)$. In Table 1 and 2 we present the simulated mean values and the root mean squared error (RMSE), to four decimal places, of the estimators under study. In both tables the "best" mean value and RMSE, for each sample size, are underlined.

n	PWM	LPWM	M	ML
		$\hat{a}$		
10	1.1605 / 0.6889	0.5765 / 0.2547	1.0771 / 0.5897	0.6233 / 0.2659
15	1.1114 / 0.6248	0.5476 / 0.1830	1.0473 / 0.5520	0.5759 / 0.1825
20	1.0885 / 0.5971	0.5354 / 0.1513	1.0346 / 0.5370	0.5549 / 0.1446
30	1.0629 / 0.5672	0.5229 / 0.1166	1.0222 / 0.5231	0.5355 / 0.1088
40	1.0502 / 0.5530	0.5166 / 0.0983	1.0165 / 0.5171	0.5258 / 0.0900
50	1.0415 / 0.5434	0.5130 / 0.0864	1.0130 / 0.5133	0.5203 / 0.0784
75	1.0300 / 0.5310	0.5082 / 0.0690	1.0085 / 0.5086	0.5132 / 0.0618
100	1.0239 / 0.5246	0.5059 / 0.0592	1.0063 / 0.5064	0.5095 / 0.0525
150	1.0174 / 0.5177	0.5040 / 0.0478	1.0042 / 0.5043	0.5065 / 0.0421
200	1.0137 / 0.5140	0.5028 / 0.0413	1.0032 / 0.5032	0.5048 / 0.0363
300	1.0098 / 0.5100	0.5018 / 0.0332	1.0021 / 0.5021	0.5031 / 0.0291
500	1.0065 / 0.5066	0.5013 / 0.0259	1.0013 / 0.5013	0.5020 / 0.0225
		$\hat{c}$		
10	9.40 / 190.63	1.0835 / 0.4953	1.1307 / 0.3150	1.2477 / 0.4016
15	10.20 / 326.36	1.0513 / 0.3533	1.0797 / 0.1858	1.1534 / 0.2359
20	8.44 / 68.85	1.0372 / 0.2955	1.0568 / 0.1311	1.1106 / 0.1662
30	8.70 / 98.38	1.0239 / 0.2302	1.0363 / 0.0826	1.0713 / 0.1047
40	8.90 / 120.33	1.0172 / 0.1934	1.0271 / 0.0611	1.0530 / 0.0772
50	8.77 / 84.19	1.0137 / 0.1719	1.0212 / 0.0474	1.0418 / 0.0601
75	8.45 / 53.30	1.0084 / 0.1384	1.0140 / 0.0314	1.0276 / 0.0396
100	11.58 / 341.40	1.0064 / 0.1193	1.0103 / 0.0229	1.0204 / 0.0291
150	11.11 / 254.57	1.0039 / 0.0964	1.0068 / 0.0152	1.0135 / 0.0192
200	63.44 / 7198.00	1.0022 / 0.0824	1.0051 / 0.0115	1.0102 / 0.0145
300	34.37 / 3195.22	1.0014 / 0.0669	1.0033 / 0.0075	1.0067 / 0.0095
500	19.13 / 1149.99	1.0010 / 0.0518	1.0020 / 0.0045	1.0040 / 0.0057

Table 1. Simulated mean value / RMSE of the shape and scale estimators, for the Pareto model with $(a, c) = (0.5, 1)$.

n	PWM	LPWM	M	ML
		$\hat{a}$		
10	2.6095 / 1.1745	2.3062 / 1.0187	2.4325 / 0.9402	2.4933 / 1.0635
15	2.4344 / 0.8627	2.1905 / 0.7321	2.2970 / 0.6833	2.3037 / 0.7299
20	2.3511 / 0.7238	2.1414 / 0.6054	2.2327 / 0.5636	2.2196 / 0.5784
30	2.2580 / 0.5672	2.0918 / 0.4665	2.1671 / 0.4430	2.1421 / 0.4354
40	2.2073 / 0.4878	2.0662 / 0.3932	2.1312 / 0.3789	2.1034 / 0.3598
50	2.1745 / 0.4327	2.0520 / 0.3455	2.1092 / 0.3366	2.0813 / 0.3136
75	2.1285 / 0.3550	2.0328 / 0.2759	2.0785 / 0.2757	2.0527 / 0.2474
100	2.1039 / 0.3116	2.0237 / 0.2369	2.0620 / 0.2411	2.0382 / 0.2098
150	2.0776 / 0.2620	2.0160 / 0.1913	2.0458 / 0.2023	2.0259 / 0.1682
200	2.0612 / 0.2321	2.0110 / 0.1651	2.0356 / 0.1795	2.0191 / 0.1451
300	2.0451 / 0.1954	2.0071 / 0.1330	2.0258 / 0.1502	2.0125 / 0.1163
500	2.0317 / 0.1603	2.0050 / 0.1037	2.0180 / 0.1227	2.0080 / 0.0899
		$\hat{c}$		
10	2.0821 / 0.2573	2.0089 / 0.2040	2.0093 / 0.1085	2.1045 / 0.1515
15	2.0651 / 0.2112	2.0060 / 0.1599	2.0048 / 0.0710	2.0688 / 0.0991
20	2.0550 / 0.1875	2.0042 / 0.1370	2.0028 / 0.0522	2.0510 / 0.0731
30	2.0429 / 0.1582	2.0028 / 0.1099	2.0014 / 0.0344	2.0338 / 0.0483
40	2.0357 / 0.1413	2.0019 / 0.0938	2.0011 / 0.0259	2.0255 / 0.0363
50	2.0309 / 0.1293	2.0016 / 0.0839	2.0007 / 0.0204	2.0203 / 0.0287
75	2.0235 / 0.1114	2.0007 / 0.0681	2.0004 / 0.0137	2.0135 / 0.0192
100	2.0195 / 0.1007	2.0006 / 0.0590	2.0002 / 0.0101	2.0101 / 0.0142
150	2.0144 / 0.0868	2.0002 / 0.0479	2.0001 / 0.0067	2.0067 / 0.0095
200	2.0112 / 0.0784	1.9998 / 0.0411	2.0001 / 0.0051	2.0050 / 0.0072
300	2.0084 / 0.0672	1.9999 / 0.0334	2.0000 / 0.0033	2.0033 / 0.0047
500	2.0058 / 0.0559	2.0000 / 0.0259	2.0000 / 0.0020	2.0020 / 0.0028

Table 2. Simulated mean value / RMSE of the shape and scale estimators, for the Pareto model with $(a, c) = (2, 2)$.

- According to the theory the PWM and M estimators are not consistent for $a \leq 1$ and the simulated mean values and the root mean squared error presented in Table 1 for these estimators confirms it.
- Regarding minimum absolute bias for both Pareto models here used, the LPWM shape estimator was always the best estimator.
- Regarding RMSE, the ML shape estimator provides the minimum value. This can be partially explained by the optimal properties of the regular maximum likelihood estimators;
- The M scale estimator was always the best estimator regarding minimum RMSE for the estimation of c.

4 Asymptotic results for the LPWM estimators

In this section, we study the asymptotic behavior of the LPWM estimators introduced in (5) for a Pareto type I distribution. We can write those estimators

using linear functions of order statistics. Indeed, we have

$$\hat{a}^{LPWM} = \frac{1}{2\hat{l_0} - 4\hat{l_1}} = \frac{1}{\frac{1}{n}\sum_{i=1}^{n}\left(4\frac{i-1}{n-1} - 2\right)\ln X_{i:n}} \tag{6}$$

and

$$\hat{c}^{LPWM} = \exp\left\{4\hat{l_1} - \hat{l_0}\right\} = \exp\left\{\frac{1}{n}\sum_{i=1}^{n}\left(3 - 4\frac{i-1}{n-1}\right)\ln X_{i:n}\right\} \tag{7}$$

Proposition 1. *Let $X_{1:n} \leq X_{2:n} \leq \ldots \leq X_{n:n}$ be the corresponding ordinal statistics of a random sample of size n taken from a Pareto type I population. Then,*

$$\ln X_{i:n} \stackrel{d}{=} \ln c + \frac{1}{a}E_{i:n}$$

where a and c are respectively the shape and scale parameter of a Pareto type I distribution and $E_{i:n}$, $(1 \leq i \leq n)$ denotes the i-th ascending order statistic of a sample of size n taken from a standard exponential population.

Proof. Let Y be a standard Pareto random variable with d.f. $F_Y(y) = 1 - 1/y$, $y > 1$. The probability integral transformation $F_Y(Y)$ produces a standard uniform distribution (Arnold *et al.*[4]). Thus, if $U_{i:n}$ $(1 \leq i \leq n)$ represents the ordinal statistic of a sample of a standard uniform population, we have,

$$F_Y(Y_{i:n}) \stackrel{d}{=} U_{i:n} \Leftrightarrow 1 - \frac{1}{Y_{i:n}} \stackrel{d}{=} U_{i:n}.$$

and,

$$X_{i:n} \stackrel{d}{=} F_X^{\leftarrow}(U_{i:n}) \stackrel{d}{=} F_X^{\leftarrow}(1 - \frac{1}{Y_{i:n}}) = cY_{i:n}^{1/a}$$

Since $\ln Y$ has a standard exponential distribution,

$$\ln X_{i:n} \stackrel{d}{=} \ln(cY_{i:n}^{1/a}) = \ln c + \frac{1}{a}\ln(Y_{i:n}) \stackrel{d}{=} \ln c + \frac{1}{a}E_{i:n}.$$

Proposition 2. *For a sample of size n, from a Pareto type I population and for $\hat{a}_{LPWM}$ and $\hat{c}_{LPWM}$ introduced in (5), we have,*

$$\sqrt{n}\left(\hat{a}^{LPWM} - a\right) \xrightarrow[n\to\infty]{d} N\left(0, \frac{4a^2}{3}\right)$$

and

$$\sqrt{n}(\hat{c}^{LPWM} - c) \xrightarrow[n\to\infty]{d} N\left(0, \frac{c^2}{3a^2}\right).$$

Proof. From Proposition 1 and since$\sum_{i=1}^{n}\left(4\frac{i-1}{n-1} - 2\right) = 0$, the denominator of

$$\hat{a}^{LPWM} = \frac{1}{\frac{1}{n}\sum_{i=1}^{n}\left(4\frac{i-1}{n-1} - 2\right)\ln X_{i:n}}$$

has the same distribution of

$$T_n = \frac{1}{n}\sum_{i=1}^{n}\frac{1}{a}\left(4\frac{i-1}{n-1}-2\right)E_{i:n}.$$

Using the asymptotic results for linear function of order statistics (Arnold *et al.* [4], p.229), we know that,

$$\sqrt{n}\,(T_n-\mu_{T_n}) \xrightarrow[n\to\infty]{d} N\left(0,\sigma^2_{T_n}\right), \tag{8}$$

where

$$\mu_{T_n} = \int_0^\infty x\frac{1}{a}(4(1-e^{-x})-2)e^{-x}dx = \frac{1}{a}$$

and

$$\sigma^2_{T_n} = \frac{2}{a^2}\int_0^\infty dx\int_x^\infty (4(1-e^{-x})-2)(4(1-e^{-y})-2)(1-e^{-x})e^{-y}dy = \frac{4}{3a^2}$$

Applying the delta method to (8), we have

$$\sqrt{n}\left(\frac{1}{T_n}-a\right) \xrightarrow[n\to\infty]{d} N\left(0,\frac{4a^2}{3}\right). \tag{9}$$

Asymptotic results for the estimator of the scale parameter

$$\hat{c}^{LPWM} = \exp\left\{\frac{1}{n}\sum_{i=1}^{n}\left(3-4\frac{i-1}{n-1}\right)\ln X_{i:n}\right\}$$

can be obtained with an analogous proof. Using the results from Proposition 1 and since, $\frac{1}{n}\sum_{i=1}^{n}\left(3-4\frac{i-1}{n-1}\right)=1$,

$$\frac{1}{n}\sum_{i=1}^{n}\left(3-4\frac{i-1}{n-1}\right)\ln X_{i:n} \overset{d}{=} \ln c + \frac{1}{n}\sum_{i=1}^{n}\frac{1}{a}\left(3-4\frac{i-1}{n-1}\right)E_{i:n}$$

Using again the asymptotic results in (Arnold *et al.* [4], p.229) with the notation $C_n = \frac{1}{n}\sum_{i=1}^{n}\frac{1}{a}\left(3-4\frac{i-1}{n-1}\right)E_{i:n}$

$$\sqrt{n}(C_n-\mu_{C_n}) \xrightarrow[n\to\infty]{d} N\left(0,\sigma^2_{C_n}\right). \tag{10}$$

where

$$\mu_{C_n} = \int_0^\infty -\frac{1}{a}xe^{-x}+4xe^{-2x}dx = 0$$

and

$$\sigma^2_{C_n} = \frac{2}{a^2}\int_0^\infty dx\int_x^\infty (3-4(1-e^{-x}))(3-4(1-e^{-y}))(1-e^{-x})e^{-y}dy = \frac{1}{3a^2}$$

Applying the delta method to (10) it follows that,

$$\sqrt{n}(c\exp C_n - c) \xrightarrow[n\to\infty]{d} N\left(0,\frac{c^2}{3a^2}\right). \tag{11}$$

References

1. B.C. Arnold. Pareto and Generalized Pareto Distributions. *In D. Chotikapanich (ed.) Modeling Income Distributions and Lorenz Curves*, Springer, New York, 119–145, 2008.
2. F. Caeiro and M. I. Gomes. Semi-parametric tail inference through probability-weighted moments.*Journal of Statistical Planning and Inference*, 141, 937–950, 2011.
3. F. Caeiro, A.P. Martins and I.j. Sequeira. Finite sample behaviour of Classical and Quantile Regression Estimators for the Pareto distribution. In T.E. Simos and C. Tsitouras (eds.), AIP Conf. Proc. 1648, 540007, 2015.
4. B. C. Arnold, N. Balakrishnan and H. N. Nagaraja. *A first course in order statistics*, New York, Wiley, 1992.
5. J.A. Greenwood, J.M. Landwehr, N.C. Matalas and J.R. Wallis. Probability Weighted Moments: definition and relation to parameters of several distributions expressable in inverse form. *Water Resources Research*, 15, 1049–1054, 1979.
6. J. Beirlant, F. Caeiro and M.I. Gomes, An overview and open research topics in statistics of univariate extremes, *Revstat* **10**:1, 1–31 2012.
7. J. Beirlant, J. Teugels and P. Vynckier, *Practical analysis of extreme values*, Leuven University Press 1996.
8. J. Hosking, J. Wallis and E. Wood. Estimation of the generalized extreme value distribution by the method of probability-weighted moments. *Technometrics*, 27(3),251–261, 1985.
9. M.I. Gomes and A. Guillou, Extreme Value Theory and Statistics of Univariate Extremes: A Review. *International Statistical Review*, 83, 2, 263–292, 2015.
10. N.L. Johnson, S. Kotz and N. Balakrishnan. *Continuous Univariate Distributions*, Wiley, New York, Vol.1, 2nd Ed., 1994.
11. H.-L. Lu and S.-H. Tao. The Estimation of Pareto Distribution by a Weighted Least Square Method, *Quality & Quantity* **41**:6, 913–926, 2007.
12. V. Pareto. Cours d'Economie Politique, Vol. 2, Lausanne, 1897.
13. R. E. Quandt. Old and new Methods of Estimation and the Pareto Distribution. *Metrika*, 10, 55–82, 1966.
14. R Development Core Team, R: A language and environment for statistical computing. R Foundation for Statistical Computing, Vienna, Austria (2014). URL: `http://www.R-project.org/`
15. M. Rytgaard. Estimation in the Pareto distribution. *Astin Bulletin*, 20, 2, 1990.
16. V. R Singh and H. Guo. Parameter Estimations for 2-Parameter Pareto Distribution by Pome. Water Resources Management 9, 81–93, 1995.

Option pricing under multiscale stochastic volatility and stochastic interest rate — an asymptotic expansion approach

Betuel Canhanga* Anatoliy Malyarenko† Ying Ni‡

Milica Rančić § Sergei Silvestrov¶

26th October 2017

Abstract Among other limitations, the celebrated Black-Scholes option pricing model assumes constant volatility and constant interest rates, which is not supported by empirical studies on for example implied volatility surfaces. Studies by many researchers such as Heston in 1993, Christoffersen in 2009, Fouque in 2012, Chiarella-Ziveyi in 2013, and the authors' previous work removed the constant volatility assumption from the Black-Scholes model by introducing one or two stochastic volatility factors with constant interest rate. In the present paper we follow this line but generalize the model by considering also stochastic interest rate. More specifically, the underlying asset process is governed by a mean-reverting interest rate process in addition to two mean-reverting stochastic volatility processes of fast and slow mean-reverting rates respectively. The focus is to derive an approximating formula for pricing the European option using a double asymptotic expansion method.

*Faculty of Sciences, Department of Mathematics and Computer Sciences, Eduardo Mondlane University, Box 257, Maputo, Mozambique, e-mail: canhanga@uem.mz

†Division of Applied Mathematics, School of Education, Culture and Communication, Mälardalen University, Box 883, SE-721 23 Västerås, Sweden, e-mail: anatoliy.malyarenko@mdh.se

‡Division of Applied Mathematics, School of Education, Culture and Communication, Mälardalen University, Box 883, SE-721 23 Västerås, Sweden, e-mail: ying.ni@mdh.se

§Division of Applied Mathematics, School of Education, Culture and Communication, Mälardalen University, Box 883, SE-721 23 Västerås, Sweden, e-mail: milica.rancic@mdh.se

¶Division of Applied Mathematics, School of Education, Culture and Communication, Mälardalen University, Box 883, SE-721 23 Västerås, Sweden, e-mail: sergei.silvestrov@mdh.se

17th *ASMDA Conference Proceedings, 6 - 9 June 2017, London, UK*

Keywords: stochastic volatility, asymptotic expansion, stochastic interest rate, European options.

1 Introduction

We consider the following risk-neutral dynamics for the underlying asset price S:

$$\begin{aligned}
\mathrm{d}S &= rS\,\mathrm{d}t + \sqrt{V_1}S\,\mathrm{d}W_1 + \sqrt{V_2}S\,\mathrm{d}W_2,\\
\mathrm{d}V_1 &= \left[\frac{1}{\varepsilon}(\theta_1 - V_1) - \lambda_1 V_1\right]\mathrm{d}t + \frac{\xi_1}{\sqrt{\varepsilon}}\sqrt{V_1}\rho_{13}\,\mathrm{d}W_1 + \frac{\xi_1}{\sqrt{\varepsilon}}\sqrt{V_1(1-\rho_{13}^2)}\,\mathrm{d}W_3,\\
\mathrm{d}V_2 &= [\delta(\theta_2 - V_2) - \lambda_2 V_2]\,\mathrm{d}t + \sqrt{\delta}\xi_2\sqrt{V_2}\rho_{24}\,\mathrm{d}W_2 + \sqrt{\delta}\xi_2\sqrt{V_2(1-\rho_{24}^2)}\,\mathrm{d}W_4,\\
\mathrm{d}r &= a(m-r)dt + \sigma_{(r)}\,\mathrm{d}W_5.
\end{aligned} \tag{1}$$

We assume that the stochastic risk free interest rate r is of Vasicek type. The long run mean is denoted by m, the speed of reversion to the long run mean is a and $\sigma_{(r)}$ is a volatility of the interest rate. V_1 and V_2 are the variance processes of Heston [11] type, $\frac{1}{\varepsilon}$, and δ are the speed of reversion for variances V_1 and V_2, respectively. The long run mean for the two variances are given by θ_1, and θ_2, while $\frac{1}{\sqrt{\varepsilon}}\xi_1$ and $\sqrt{\delta}\xi_2$ represent the instantaneous volatilities. λ_1 and λ_2 are constants that determine the market price of volatility risk and are defined more detailed in Canhanga et al. [3], Canhanga et al. [4] and Chiarella and Ziveyi [6]. $W_i,\ i = 1,2,3,4,5$ are independent Wiener processes. The variance processes are independent one from another and the correlation between the asset price and the variance $V_1(V_2)$ is given by $\rho_{13}(\rho_{24})$. ξ_1 and ξ_2 are constants.

In order to guarantee positive solutions for the second and the third equations of (1), we assume that the following Feller condition (Feller [8]) hold

$$2\theta_1 \geq \xi_1^2 \quad \text{and} \quad 2\theta_2 \geq \xi_2^2.$$

We also impose the conditions presented by Cheang et al. [5] in order to guarantee that the variances processes will be finite, therefore

$$-1 < \rho_{13} < \min\left(1, \frac{1}{\xi_1\sqrt{\varepsilon}}\right) \quad \text{and} \quad -1 < \rho_{24} < \min\left(1, \frac{\sqrt{\delta}}{\xi_2}\right).$$

We consider an *European option* with maturity T, strike price of K. The payoff function is given by $h(S_T) = \max(S_T - K, 0)$. The task is to price the European option using a double asymptotic expansion approach.

2 Pricing formula for European option

It was proved by Andersen and Piterbarg [1] and Kac [13] that, given a function $U^{\varepsilon;\delta}$ with continuous first order derivatives with respect to variable t and continuous second order derivative with respect to variables $s,\ v_1,\ v_2, r$ the option price can be given by the unique solution of a boundary value problem (BVP) which is constructed from the system (1). To obtain the BVP we need to construct the correlation matrix and perform some calculations.

$$\Sigma = \begin{pmatrix} S\sqrt{V_1} & S\sqrt{V_2} & 0 & 0 & 0 \\ \frac{\xi_1\sqrt{V_1}\rho_{13}}{\sqrt{\varepsilon}} & 0 & \frac{\xi_1\sqrt{V_1(1-\rho_{13}^2)}}{\varepsilon} & 0 & 0 \\ 0 & \rho_{24}\xi_2\sqrt{\delta V_2} & 0 & \xi_2\sqrt{\delta(1-\rho_{24}^2)V_2} & 0 \\ 0 & 0 & 0 & 0 & \sigma_{(r)} \end{pmatrix},$$

and the product of Σ and $\Sigma^\top$ (the transpose of Σ) is given by

$$\Sigma\Sigma^\top = \begin{pmatrix} S^2(V_1+V_2) & \frac{\xi_1\rho_{13}SV_1}{\sqrt{\varepsilon}} & \rho_{24}\xi_2 SV_2\sqrt{\delta} & 0 \\ \frac{\rho_{13}\xi_1 SV_1}{\sqrt{\varepsilon}} & \frac{V_1\xi_1^2}{\varepsilon} & 0 & 0 \\ \rho_{24}\xi_2 SV_2\sqrt{\delta} & 0 & \delta\xi_2^2 V_2 & 0 \\ 0 & 0 & 0 & (\sigma_{(r)})^2 \end{pmatrix}.$$

Let s, v_1, v_2, r be the values of $S(t), V_1(t), V_2(t), r(t)$ at time t. With the above matrix, let us now consider $U = U(t, s, v_1, v_2, r)$ as a function that has continuous second derivatives with respect to variables s, v_1, v_2 and r. As indicated above, the European option price on the asset (1) will be given by the following BVP

$$\left(\frac{1}{\varepsilon}\mathscr{L}_0 + \frac{1}{\sqrt{\varepsilon}}\mathscr{L}_1 + \mathscr{L}_2 + \sqrt{\delta}\mathscr{M}_1 + \delta\mathscr{M}_2\right)U^{\varepsilon,\delta} = 0, \tag{2}$$

$$U^{\varepsilon,\delta}(T, s, v_1, v_2) = h(S_T).$$

where

$$
\begin{aligned}
\mathscr{L}_0 &= (\theta_1 - v_1)\frac{\partial}{\partial v_1} + \frac{\xi_1^2 v_1}{2}\frac{\partial^2}{\partial v_1^2}, \qquad \mathscr{L}_1 = \rho_{15} s v_1 \xi_1 \frac{\partial^2}{\partial s \partial v_1}, \\
\mathscr{L}_2 &= \frac{\partial}{\partial t} + (r-q)s\frac{\partial}{\partial s} + \frac{1}{2}(v_1+v_2)s^2\frac{\partial^2}{\partial s^2} - r - \lambda_1 v_1 \frac{\partial}{\partial v_1} - \lambda_2 v_2 \frac{\partial}{\partial v_2} \\
&\quad + a(m-r)\frac{\partial}{\partial r} + \frac{(\sigma_{(r)})^2}{2}\frac{\partial^2}{\partial r^2}, \\
\mathscr{M}_1 &= \rho_{24} s v_2 \frac{\partial^2}{\partial s \partial v_2}, \qquad \mathscr{M}_2 = (\theta_2 - v_2)\frac{\partial}{\partial v_2} + \frac{1}{2}\xi_2^2 v_2 \frac{\partial^2}{\partial v_2^2}.
\end{aligned} \tag{3}
$$

The coefficients of first order derivatives are coefficients of the dt terms in the stochastic differential equations (1) and the coefficients of second order derivatives come from $\Sigma\Sigma^\top$.

3 Regular and singular perturbation

In order to find the option price *(the solution for (2))*, we introduce perturbation in the solution following the procedure presented by Fouque et al. [9] and Fouque et al. [10]. We start by performing a regular perturbation with respect to δ, followed by a singular perturbation with respect to ε.

We assume that the solution for (2) can be expressed in the following form

$$
U^{\varepsilon,\delta} = U_0^\varepsilon + \sqrt{\delta} U_1^\varepsilon + \delta U_2^\varepsilon + \cdots \tag{4}
$$

and using this expansion in (2) we will have

$$
\left(\frac{1}{\varepsilon}\mathscr{L}_0 + \frac{1}{\sqrt{\varepsilon}}\mathscr{L}_1 + \mathscr{L}_2 + \sqrt{\delta}\mathscr{M}_1 + \delta\mathscr{M}_2\right)(U_0^\varepsilon + \sqrt{\delta}U_1^\varepsilon + \delta U_2^\varepsilon + \cdots) = 0.
$$

Collecting terms with the same power of $\sqrt{\delta}$, the above equation can be rearranged into

$$
\begin{aligned}
&\left(\frac{1}{\varepsilon}\mathscr{L}_0 + \frac{1}{\sqrt{\varepsilon}}\mathscr{L}_1 + \mathscr{L}_2\right)U_0^\varepsilon \\
&\quad + \sqrt{\delta}\left[\left(\frac{1}{\varepsilon}\mathscr{L}_0 + \frac{1}{\sqrt{\varepsilon}}\mathscr{L}_1 + \mathscr{L}_2\right)U_1^\varepsilon + \mathscr{M}_1 U_0^\varepsilon\right] \\
&\quad + \delta\left[\left(\frac{1}{\varepsilon}\mathscr{L}_0 + \frac{1}{\sqrt{\varepsilon}}\mathscr{L}_1 + \mathscr{L}_2\right)U_2^\varepsilon + \mathscr{M}_1 U_1^\varepsilon + \mathscr{M}_2 U_0^\varepsilon\right] + \cdots = 0
\end{aligned} \tag{5}
$$

which is true only if all coefficients of δ are equal to zero and if we consider appropriate final conditions, i.e.

$$\begin{aligned}
&\left(\frac{1}{\varepsilon}\mathscr{L}_0+\frac{1}{\sqrt{\varepsilon}}\mathscr{L}_1+\mathscr{L}_2\right)U_0^\varepsilon=0, \qquad U_0^\varepsilon(T,s,v_1,v_2,r)=h(S_T);\\
&\left(\frac{1}{\varepsilon}\mathscr{L}_0+\frac{1}{\sqrt{\varepsilon}}\mathscr{L}_1+\mathscr{L}_2\right)U_1^\varepsilon+\mathscr{M}_1U_0^\varepsilon=0, \qquad U_1^\varepsilon(T,s,v_1,v_2,r)=0;\\
&\left(\frac{1}{\varepsilon}\mathscr{L}_0+\frac{1}{\sqrt{\varepsilon}}\mathscr{L}_1+\mathscr{L}_2\right)U_2^\varepsilon+\mathscr{M}_1U_1^\varepsilon+\mathscr{M}_2 \quad U_0^\varepsilon U_1^\varepsilon(T,s,v_1,v_2,r)=0
\end{aligned} \tag{6}$$

4 Leading term of the approximation

After the regular perturbation, we introduce a singular perturbation for each term in (4), i.e.

$$\begin{aligned}
U_0^\varepsilon &= U_{0,0}+\sqrt{\varepsilon}U_{1,0}+\sqrt{\varepsilon}U_{2,0}+\cdots\\
U_1^\varepsilon &= U_{0,1}+\sqrt{\varepsilon}U_{1,1}+\sqrt{\varepsilon}U_{2,1}+\cdots\\
U_2^\varepsilon &= U_{0,2}+\sqrt{\varepsilon}U_{1,2}+\sqrt{\varepsilon}U_{2,2}+\cdots
\end{aligned} \tag{7}$$

Therefore the first order approximation is given by

$$U^{\varepsilon,\delta}\approx U_{0,0}+U_{1,0}^\varepsilon+U_{0,1}^\delta \tag{8}$$

where $U_{1,0}^\varepsilon=\sqrt{\varepsilon}U_{1,0}$ and $U_{0,1}^\delta=\sqrt{\delta}U_{0,1}$.

We start by computing $U_{0,0}$. Equation (6) and (7) implies that

$$\begin{aligned}
&\frac{1}{\varepsilon}\mathscr{L}_0U_{0,0}+\frac{1}{\sqrt{\varepsilon}}\left(\mathscr{L}_0U_{1,0}+\mathscr{L}_1U_{0,0}\right)+\left(\mathscr{L}_0U_{2,0}+\mathscr{L}_1U_{1,0}+\mathscr{L}_2U_{0,0}\right)\\
&\quad+\sqrt{\varepsilon}\left(\mathscr{L}_0U_{3,0}+\mathscr{L}_1U_{2,0}+\mathscr{L}_2U_{1,0}\right)+\cdots=0.
\end{aligned}$$

which is true only if all coefficients of ε in the above equation are equal to zero, and we consider proper boundary conditions, i.e.

$$\begin{aligned}
\mathscr{L}_0U_{0,0}&=0 \qquad & U_{0,0}(T,s,v_1,v_2,r)&=h(S_T)\\
\mathscr{L}_0U_{1,0}+\mathscr{L}_1U_{0,0}&=0 \qquad & U_{1,0}(T,s,v_1,v_2,r)&=0\\
\mathscr{L}_0U_{2,0}+\mathscr{L}_1U_{1,0}+\mathscr{L}_2U_{0,0}&=0 \qquad & U_{2,0}(T,s,v_1,v_2,r)&=0\\
\mathscr{L}_0U_{3,0}+\mathscr{L}_1U_{2,0}+\mathscr{L}_2U_{1,0}&=0 \qquad & U_{3,0}(T,s,v_1,v_2,r)&=0.
\end{aligned} \tag{9}$$

The operator $\mathscr{L}_0$ is a Poisson partial differential operator, therefore, the first equation in (9) is a homogeneous Poisson equation which has constant solutions or exponential form solutions. In order to avoid exponential growth of the option price components, we impose that $U_{0,0}$ is constant with respect to v_1, which suggests that we can write $U_{0,0}$ as $U_{0,0}(t,\ s,\ v_2, r)$. Another motivation of this choice is given in [9] by the fact that we want to have the leading-order price independent of the current value of the fast factor.

Since $U_{0,0}$ does not depend on v_1 and the operator $\mathscr{L}_1$ contains only the mixed partial derivative with respect to the cross term of s and v_1 then, $\mathscr{L}_1 U_{0,0} = 0$ and the second equation in (9) will be

$$\mathscr{L}_0 U_{1,0} = 0$$

which implies that

$$U_{1,0} = U_{1,0}(t,\ s,\ v_2, r)$$

for the same reasons as we explained for $U_{0,0}$.

Again, the fact that $\mathscr{L}_1 U_{1,0} = 0$ implies that the third equation in (9) is transformed to

$$\mathscr{L}_0 U_{2,0} + \mathscr{L}_2 U_{0,0} = 0, \tag{10}$$

which is a Poisson equation for $U_{2,0}$ with $\mathscr{L}_2 U_{0,0}$ as a source. Denote Γ as the invariant distribution of the process V_1. The solvability condition of Poisson equation (Fouque et al. [10]) implies that

$$\langle \mathscr{L}_2 U_{0,0} \rangle = 0, \tag{11}$$

where

$$\langle \cdot \rangle = \int \cdot \Gamma(dv_1)$$

denotes averaging over the invariant distribution Γ.

Since $U_{0,0}$ does not depend on v_1 it follows that

$$\begin{aligned} &\frac{\partial U_{0,0}}{\partial t} + rs\frac{\partial U_{0,0}}{\partial s} - \lambda_2 v_2 \frac{\partial U_{0,0}}{\partial v_2} + \frac{1}{2}\bar{\sigma}^2(v_2)s^2\frac{\partial^2 U_{0,0}}{\partial s^2} \\ &a(m-r)\frac{\partial U_{0,0}}{\partial r} + \frac{(\sigma_{(r)})^2}{2}\frac{\partial^2 U_{0,0}}{\partial r^2} - rU_{0,0} = 0 \end{aligned} \tag{12}$$

$$U_{0,0}(T, s, v_2, r) = h(S_T)$$

where $\bar{\sigma}^2(v_2) = \int (v_1 + v_2)\Gamma(dv_1)$.

By Feynman-Kac theorem we recognize the BVP (12) as the European option pricing problem under the following risk-neutral model

$$\begin{aligned} dS &= rSdt + \bar{\sigma}(V_2)dW_2 \\ dV_2 &= -\lambda_2 V_2 dt \\ dr &= a(m-r)dt + \sigma_{(r)}dW_5. \end{aligned} \tag{13}$$

This is Black-Scholes model with local volatility (time-dependent deterministic volatility) under stochastic interest rate.

It is known that the zero coupon bond price $P(r,t,T)$ under the above Vasicek short rate dynamics takes the form (Vasicek [16])

$$P(r,t,T) = A(t,T)e^{-rB(t,T)} \tag{14}$$

where

$$\begin{aligned} B(t,T) &= \frac{1-e^{-a(T-t)}}{a} \\ A(t,T) &= \exp\left[\frac{(B(t,T)-T+t)(a^2m-\sigma_{(r)}^2/2)}{a^2} - \frac{\sigma_{(r)}^2 B(t,T)^2}{4a}\right]. \end{aligned}$$

For simplicity we write $B = B(t,T), P = P(r,t,T)$, applying Itô lemma we obtain the risk-neutral bond price dynamics

$$\frac{dP}{P} = rdt + \sigma_{(r)}BdW_5.$$

Denote $\mathbb{Q}$ as the traditional risk-neutral measure, $\mathbb{Q}^{\mathbb{T}}$ as the *forward risk-neutral measure* induced by numeraire $P(r,t,T)$. We shall also use notations $\widehat{W}_2$,$\widehat{W}_5$ for Wiener processes under the $\mathbb{Q}^{\mathbb{T}}$-measure. Denote the denominated asset price by $\widehat{S}(t) := S(t)/P(r,t,T)$. Using the equivalent martingale theory, the denominated option price is given by

$$\widehat{U}_{0,0} := \frac{U_{0,0}(t,s,v_2,r)}{P(r,t,T)} = E^{\mathbb{Q}^{\mathbb{T}}}\left[h\left(\widehat{S}_T\right)|\mathscr{F}_t\right] \tag{15}$$

Using Girsanov theorem we can derive the $\mathbb{Q}^{\mathbb{T}}$-dynamics for $S(t)$ and $P(r,t,T)$ then using Itô quotient rule we find $\mathbb{Q}^{\mathbb{T}}$-dynamics for the denominated asset price

$$\frac{d\widehat{S}}{\widehat{S}} = \bar{\sigma}(V_2)d\widehat{W}_2 + \sigma_{(r)}Bd\widehat{W}_5 \tag{16}$$

By (15) and (16) we see that $\widehat{U}_{0,0} = \widehat{U}_{0,0}(t,\hat{s},v_2)$. This motivates the following change of variables from $(S,U_{0,0})$ to $(\widehat{S},\widehat{U}_{0,0})$, i.e. in the BVP (12) we make the change

$$s = \hat{s}P(r,t,T), \quad U_{0,0}(t,s,v_2,r) = \widehat{U}_{0,0}(t,\hat{s},v_2)P(r,t,T),$$

and using the following relationships:

$$\begin{aligned}
&\frac{\partial U_{0,0}}{\partial t} = \widehat{U}_{0,0}\frac{\partial P}{\partial t} + P\frac{\partial \widehat{U}_{0,0}}{\partial t} - \hat{s}\frac{\partial \widehat{U}_{0,0}}{\partial \hat{s}}\frac{\partial P}{\partial t}\\
&\frac{\partial U_{0,0}}{\partial s} = \frac{\partial \widehat{U}_{0,0}}{\partial \hat{s}}\\
&\frac{\partial U_{0,0}}{\partial v_2} = P\frac{\partial \widehat{U}_{0,0}}{\partial v_2}\\
&\frac{\partial U_{0,0}}{\partial r} = \widehat{U}_{0,0}\frac{\partial P}{\partial r} - \hat{s}\frac{\partial \widehat{U}_{0,0}}{\partial \hat{s}}\frac{\partial P}{\partial r}\\
&\frac{\partial^2 U_{0,0}}{\partial s^2} = \frac{1}{P}\frac{\partial \widehat{U}_{0,0}}{\partial \hat{s}}\\
&\frac{\partial^2 U_{0,0}}{\partial r^2} = \widehat{U}_{0,0}\frac{\partial^2 P}{\partial r^2} - \hat{s}\frac{\partial \widehat{U}_{0,0}}{\partial \hat{s}}\frac{\partial^2 P}{\partial r^2} + \frac{\hat{s}^2}{P}\frac{\partial^2 \widehat{U}_{0,0}}{\partial \hat{s}^2}\left(\frac{\partial P}{\partial r}\right)^2.
\end{aligned} \tag{17}$$

This allows us to transform (12) into

$$\begin{aligned}
&\frac{\partial \widehat{U}_{0,0}}{\partial t} + \frac{1}{2}\left[\bar{\sigma}^2\frac{S^2}{P^2} + (\sigma_{(r)})^2\hat{s}^2\frac{1}{P^2}\left(\frac{\partial P}{\partial r}\right)^2\right]\frac{\partial^2 \widehat{U}_{0,0}}{\partial \hat{s}^2}\\
&+ \frac{1}{P}\left[\frac{\partial P}{\partial t} + a(m-r)\frac{\partial P}{\partial r} + \frac{(\sigma_{(r)})^2}{2}\frac{\partial^2 P}{\partial r^2} - rP\right]\hat{s}\frac{\partial \widehat{U}_{0,0}}{\partial \hat{s}}\\
&+ \frac{1}{P}\left[\frac{\partial P}{\partial t} + a(m-r)\frac{\partial P}{\partial r} + \frac{(\sigma_{(r)})^2}{2}\frac{\partial^2 P}{\partial r^2} - rP\right]\widehat{U}_{0,0}\\
&- \lambda_2 v_2 P\frac{\partial \widehat{U}_{0,0}}{\partial v_2} = 0.
\end{aligned} \tag{18}$$

According to Vasicek [16] the bond price P satisfies the following PDE

$$\begin{aligned}
&\frac{\partial P}{\partial t} + a(m-r)\frac{\partial P}{\partial r} + \frac{(\sigma_{(r)})^2}{2}\frac{\partial^2 P}{\partial r^2} - rP = 0,\\
&P(r,T,T) = 1.
\end{aligned} \tag{19}$$

Using (19) into (18) we obtain

$$\frac{\partial \widehat{U}_{0,0}}{\partial t}+\frac{1}{2}\left[\bar{\sigma}^2(v_2)\frac{S^2}{P^2}+(\sigma_{(r)})^2\hat{s}^2\frac{1}{P^2}\left(\frac{\partial P}{\partial r}\right)^2\right]\frac{\partial^2\widehat{U}_{0,0}}{\partial \hat{s}^2} \quad -\lambda_2 v_2 P\frac{\partial \widehat{U}_{0,0}}{\partial v_2}=0. \tag{20}$$

As explained in the authors previous work (Ni et al. [15]), we can replace the average effective volatility $\bar{\sigma}(v_2)$ by a *corrected effective average volatility* $\bar{\sigma}^*$ given by

$$(\bar{\sigma}^*)^2=\frac{1}{\tau}\int_t^T \theta_1+v_2e^{-\lambda_2 s}ds=\theta_1+\frac{v_2}{\tau}\int_t^T e^{-\lambda_2 s}ds, \quad \tau:=T-t \tag{21}$$

to transform (20) into

$$\frac{\partial \widehat{U}_{0,0}}{\partial t}+\frac{1}{2}\left[\hat{\sigma}^2(t)\right]\frac{\partial^2\widehat{U}_{0,0}}{\partial \hat{s}^2}=0 \tag{22}$$

where

$$\hat{\sigma}(t)=\sqrt{(\bar{\sigma}^*)^2+(\sigma_{(r)})^2\left(\frac{1}{P}\frac{\partial P}{\partial r}\right)^2} \text{ and } \widehat{\mathrm{U}}_{0,0}(\mathrm{T},\hat{\mathrm{s}},\mathrm{v}_2)=\mathrm{h}(\widehat{\mathrm{S}}_{\mathrm{T}}).$$

Note that by (14), the quantity $-\frac{1}{P}\frac{\partial P}{\partial r}=B(t,T)$ does not depend on r is therefore a function of t.

The solution $\widehat{U}_{0,0}$ of (22) can be obtained by Black–Scholes formula

$$\widehat{U}_{0,0}=\hat{s}N(d_1)-KN(d_2) \tag{23}$$

where

$$d_1=\frac{\ln\frac{\hat{s}}{k}+\frac{1}{2}\int_t^T\hat{\sigma}(\tau)d\tau}{\sqrt{\int_t^T\hat{\sigma}^2(\tau)d\tau}} \qquad \text{and} \qquad \mathrm{d}_2=\mathrm{d}_1-\sqrt{\int_{\mathrm{t}}^{\mathrm{T}}\hat{\sigma}^2(\tau)\mathrm{d}\tau}$$

or

$$U_{0,0}(s,t,v_2,r)=sN(d_1^*)-KP(r,t,T)N(d_2^*) \tag{24}$$

for

$$d_1^*=\frac{\ln\frac{S}{K}-\ln P(r,t,T)+\frac{1}{2}\int_t^T\hat{\sigma}^2(\tau)d\tau}{\sqrt{\int_t^T\hat{\sigma}^2(\tau)d\tau}} \quad \text{and} \quad \mathrm{d}_2^*=\mathrm{d}_1^*-\sqrt{\int_{\mathrm{t}}^{\mathrm{T}}\hat{\sigma}^2(\tau)\mathrm{d}\tau},$$

with $P(r,t,T)$ given in (14).

Remark 1. Using the formula for bond price $P(r,t,T)$ (14), we can compute the following partial derivatives

$$\begin{aligned}
\frac{\partial P}{\partial t} &= \frac{\partial A}{\partial t}e^{-B(t,T)r} - A\frac{\partial B}{\partial t}re^{-B(t,T)r} \\
\frac{\partial P}{\partial r} &= -BAe^{-B(t,T)r)} \\
\frac{\partial^2 P}{\partial r^2} &= B^2Ae^{-B(t,T)r}.
\end{aligned}$$

Substituting the above partial derivatives into (19) we easily see that (19) is satisfied. Under the J. C. Cox and Ross [12] interest rate model, the bond price takes the same form of (14) with different $A(t,T), B(t,T)$ functions. Hence the above approach works for both the CIR model as well. If we consider CIR interest rate model instead of the Vasicek model in our system (1), the corresponding pricing problem can be solved in a almost identical way.

5 Fast and slow time scale correction

Now we need to find the other two terms of the approximation. The fast time scale correction term $U_{1,0}$ and the slow time correction term $U_{0,1}$. We use the ideas and detailed computation presented in Canhanga et al. [3], Canhanga et al. [4] and Ni et al. [15] to express the two correction terms as

$$U^{\varepsilon}_{1,0} = -(T-t)\mathscr{B}^{\varepsilon}U_{0,0} \tag{25}$$

and

$$U^{\delta}_{0,1} = (T-t)\mathscr{A}^{\delta}U_{0,0}. \tag{26}$$

Here

$$\begin{aligned}
&\mathscr{B}^{\varepsilon} = -\Upsilon^{\varepsilon}(v_2)D_1D_2, \quad \Upsilon^{\varepsilon}(v_2) = -\frac{\sqrt{\varepsilon}\rho_{13}}{2}\left\langle v_1\frac{\partial\phi(v_1,v_2)}{\partial v_1}\right\rangle; \\
&\mathscr{A}^{\delta} = \Theta^{\delta}(v_2)D_1\frac{\partial}{\partial v_2}, \quad \Theta^{\delta}(v_2) = \frac{1}{2}\rho_{24}v_2\sqrt{\delta}, \quad D_i = s^i\frac{\partial^i}{\partial s^i}; \quad \tau = T-t.
\end{aligned}$$

The function ϕ is a smooth function that solves the following equation

$$\mathscr{L}_0\phi(v_1,v_2) = v_1 - \theta_1.$$

6 Approximation formula

We now summarize the asymptotical results obtained in the previous sections into the following main theorem.

Theorem 1 *Consider an asset whose price evolves according to* (1) *where* V_1 *and* V_2 *are stochastic variance processes of mean reversion type. Consider also that the rates of reversion of the two variance processes are given by* $1/\varepsilon$ *and* δ *respectively where* $0 < \varepsilon << 1$ *and* $0 < \delta << 1$. *If* $h(S_T)$ *is the payoff of an European option on this asset with maturity time* T, *then the price of this option can be approximated by* $U^{\varepsilon,\delta}$ *given below.*

$$U^{\varepsilon,\delta} = U_{0,0} - (T-t)\left[\mathscr{B}^{\varepsilon} - \mathscr{A}^{\delta}\right] U_{0,0}.$$

for $U_{0,0}$ *defined in (24). When* $\varepsilon \to 0$ *and* $\delta \to 0$ *the approximated option price converges to the Black-Scholes option price.*

7 Conclusion and future work

Previous studies for example from Fouque et al. [9], Fouque et al. [10], Chiarella and Ziveyi [6], Canhanga et al. [3], Christoffersen et al. [7] improved Black–Scholes approach by considering two stochastic volatilities models. These models assume constant interest rate. In this paper we have presented an alternative to the previous models by introducing stochastic interest rate (Vasicek type). By using asymptotic expansion approach we have derived an approximating solution to the European option pricing problem. The ideas presented in this paper can also be applied to stochastic interest rate of CIR type. In the future we plan to make the model calibration with real market data and introduce some numerical analysis.

References

[1] L. Andersen and V. Piterbarg. *Interest rate modeling, Foundations and vanilla models*. Atlantic Financial Press, 2010.

[2] F. Black and M. Scholes. The pricing of options and corporate liabilties. *Journal of Political Economy*, 81:637–654, 1973.

[3] B. Canhanga, A. Malyarenko, Y. Ni, and S. Silvestrov. Perturbation methods for pricing european options in a model with two stochastic volatilities. In R. Manca, S. McClean, and C. Skiadas, editors, *New Trends in Stochastic Modelling and Data Analysis*, pages 199–210. ISAST, 2015.

[4] B. Canhanga, A. Malyarenko, Y. Ni, and S. Silvestrov. Second order asymptotic expansion for pricing european options in a model with two stochastic volatilities. pages 37–52, Piraeus Greece, June 2015. Applied Stochastic Models and Data Analysis International Society.

[5] G. Cheang, C. Chiarella, and A. Ziogas. *An Analysis of American Options Under Heston Stochastic Volatility and Jump-Diffusion Dynamics*. Quantitative and Finance Research Center, 2011.

[6] C. Chiarella and J. Ziveyi. American option pricing under two stochastic volatility processes. *Applied Mathematics and Computation*, 224:283–310, 2013.

[7] P. Christoffersen, S. Heston, and K. Jacobs. The shape and term structure of the index option smirk: Why multifactor stochastic volatility models work so well. *Management Science*, 55(12):1914–1932, 2009.

[8] W. Feller. Zur Theorie der stochastischen Prozesse. *Math. Ann.*, 113(1): 113–160, 1937.

[9] J.-P. Fouque, G. Papanicolaou, and K. R. Sircar. *Derivatives in financial markets with stochastic volatility*. Cambridge University Press, Cambridge, 2000.

[10] J.-P. Fouque, G. Papanicolaou, R. Sircar, and K. Sølna. *Multiscale stochastic volatility for equity, interest rate, and credit derivatives*. Cambridge University Press, Cambridge, 2011.

[11] S. L. Heston. A closed-form solution for options with stochastic volatility with applications to bond and currency options. *Rev. Financ. Stud.*, 6(2): 327–343, 1993.

[12] J. I. J. C. Cox and S. Ross. A theory of the term structure of interest rates. *Econometrica*.

[13] M. Kac. On distributions of certain Wiener functionals. *Trans. Amer. Math. Soc.*, 65:1–13, 1949.

[14] M. Kijima. *Stochastic Processes with Applications to Finance*. Capman and Hall/CRC, 2013.

[15] Y. Ni, B. Canhanga, A. Malyarenko, and S. Silvestrov. Approximation methods of european option pricing in multiscale stochastic volatility model.

[16] O. Vasicek. An equilibrium characterization of the term struture. *Journal of Financial Economics*, 5:177–188, 1977.

Flexible retirement scheme for the Italian mortality experience

Mariarosaria Coppola[1], Maria Russolillo[2], and Rosaria Simone[1]

[1] Department of Political Sciences, Via Leopoldo Rodinò, 22, 80133, Università degli Studi di Napoli Federico II, Napoli, Italy
(E-mail: m.coppola@unina.it, rosaria.simone@unina.it)
[2] Department of Economics and Statistics, University of Salerno, Fisciano, Italy
(E-mail: mrussolillo@unisa.it)

Abstract. Many countries have set up Social Security Systems which link retirement age and/or pension benefits to life expectancy, considering a mechanism for indexing the retirement age and/or pension benefits. The issue is a subject of great interest in recent literature; the debate outlines new directions in pension scheme developments and presents experiences with flexible pension schemes from various countries.
In this context, we consider an indexing mechanism based on the residual life expectancy to adjust the retirement age and keep a constant Expected Pension Period Duration (EPPD). The motivation is to focus on the recent and spread need to create flexible retirement schemes for facing global ageing and the prolonging working lives.
We implement that approach referring to the classical Lee Carter Model (no cohort effect) and Haberman and Renshaw model considering the cohort effect. We assess the impact of the two mortality models for the Italian male and female populations.
Keywords: Longevity risk, mortality projections, cohort effect.

1 Introduction

For National Social Security systems, it is of growing importance to account for longevity risk in programming retirement schemes. Specifically, as the mean life expectancy is increasing, at different rates for males and females and for different cohorts, longevity risk should be dynamically managed over time.
In this framework it is clear the necessity of reforming pension systems projected in the context of lower mortality rates and higher fertility rates. Some important considerations need to be made to achieve a proper reform of the pension system.
The dynamics of mortality for the industrialized countries over the last fifty years show: 1) an increase in life expectancy at old ages (over 65 years); 2) an increase in the mode of the age of death distribution; 3) a decrease in mortality rates at old ages. As consequence in terms of the shape of the survival function we can observe: it tends to shift towards a rectangular shape (due to the

17th *ASMDA Conference Proceedings, 6 - 9 June 2017, London, UK*

increasing concentration of deaths around the mode (at old ages) of the curve of deaths) and it expands to the right, i.e. the mode of the curve of deaths moves towards very old ages.
From a financial point of view, rectangularization and expansion have different effects. The concentration of deaths around the mode reduces the variance of the distribution and then the related risk. The expansion phenomenon, generating the risk of systematic deviations of mortality from the assumed projected behavior, together with the accelerating trend of mortality decline at old ages, increases risk for the Social Security System (Visco et al, 2006).
From these considerations emerges the need of accurate mortality projections based on stochastic analysis in order to provide reliable measures of mortality and of its uncertainty which are essential for proper pension reforms.
In this vein, we propose a flexible retirement scheme based on the indexation of the retirement age to reach a prescribed Expected Pension Period Duration (EPPD). In particular, we test that approach considering two stochastic projection mortality models: the classical Lee Carter Model (no cohort effect) and the Renshaw-Haberman model specifying the cohort effect. We refer to Italian males and females population. The aim is measuring the impact of the mortality model selection on the retirement age settings by gender. The paper is organized as follows: in Section 2 we introduce the stochastic mortality models that will be used for our analysis. Section 3 describes the Italian pension system and discusses the proposal of an indexed retirement mechanism. Section 4 is devoted to apply our proposal to the Italian mortality experience. Concluding remarks on forthcoming developments end the paper.

2 Stochastic Mortality Models

The aim of this contribution is to compare the impact that mortality projection for males and females has on a flexible retirement scheme when different stochastic mortality models are considered. In particular, we refer to the Lee-Carter model and the Renshaw-Haberman model, because the LC model has become a milestone and it is largely used in the actuarial literature, whilst the RH model allows us to take into account the cohort effect.
Consider mortality rates at time *t* for people aged *x*. For age effects α_x, period effects k_t, age-period modulating terms β_x and cohort effects γ_{t-x}, we take into account the Lee and Carter (LC) model and the Renshaw and Haberman (RH) model, which is an extension to the first one, but with an extra parameter depending on year of birth. They both are two of the selected stochastic mortality models belonging to the GAPC (Villegas et al 2016) class. The unifying design for these models prescribes a predictor $\eta_{x,t}$, which is related to mortality rates according to a log or logit link, generally. In this framework, the predictor structure proposed by Lee and Carter (1992) is given by:

$$\eta_{x,t} = \alpha_x + \beta_x k_t$$

The LC model is widely used because of its simplicity and robustness despite its inability to model specific cohort effects. In 2006, Renshaw and Haberman proposed an extended version of the LC model with an extra parameter, γ_{t-x} expressing a random cohort effect. They introduced one of the first stochastic models for population mortality with a cohort effect to obtain the predictor:

$$\eta_{x,t} = \alpha_x + \beta_x k_t + \gamma_{t-x}$$

In order to project mortality, the time index k_t and the extra parameter γ_{t-x} modelled and forecasted using ARIMA processes.

3 A Flexible retirement scheme

Societies across the world are ageing, with challenges for sustainable adequate pension systems. Governments and pension funds have largely responded by postponing pension ages and by discouraging early retirement. In many countries, for example, pension legislations has been reformed during the last decade, moving from Defined Benefits (DB) to Notional Defined Contributions (NDC) system, the last one considering particularly important the rules to take into account in the pension formulae life expectancies and their changes (Belloni, Maccheroni, 2006). The Italian pension system is composed by three pillars:1) Public, compulsory and unfunded pay-as-you-go system (PAYG); 2) The private, voluntary and collective funded system; and 3) Private, voluntary and individual savings related to social security schemes. The first pillar, the dominant one in Italy, passed through two main reforms during the nineties. The first reform, introduced by Law 335/95, determined a shift from DB to NDC scheme, in which notional accumulated contributions on individual accounts were converted into an annuity at retirement. Unlike the previous method, the latter takes into account the amount of contribution paid throughout the whole working life accumulated at the expected GDP (Gross Domestic Product) growth rate, the life expectancy of the pensioner at retirement age and the number of years that a survivor's benefit will be withdrawn by any widow or widower, according to actuarial equivalence principle. The second reform, introduced by Fornero with Law 214/2011, had two directives: the rise of the pensionable age and the calculation of the requirements for retirement on the basis of the number of years of social security contributions made and no longer on the average salary earned in the last years before retirement. In particular, among the others, the reform will see the retirement age increased to 66 for both men and women in the public and private sector by 2018; future retirement ages increasing in line with life expectancy from next year. For all workers, in accordance with Law Number 122/2010, age and service requirements will be

periodically reviewed based on the actual increases in life expectancy published by ISTAT. Moreover, pensions calculated under the NDC system will be affected by the application of periodically reviewed annuity conversion factors. In this framework, we proposed an indexing mechanism for retirement age based on the period life expectancy $e_{x_0,C}^{(M)}$ at age $x_0 = 65$, for selected cohorts and the chosen stochastic mortality models M. We consider cohorts of males/females born from 1952 to 2012, setting the cohort 1952 as benchmark. Those individuals will be aged 65 in 2017, which was the retirement age prescribed by law until the Fornero Reform.

We follow an age-period approach in the sense that life expectancy is considered as function of the age x and the calendar year t. Specifically, let us consider an individual belonging to the cohort C, aged x_0 on the first of January of year t_0, when the expected lifetime provided by a given stochastic mortality model M is equal to $e_{x_0,C}^{(M)}$. Let us suppose that the pension system we refer to foresees that x_0 is the fixed retirement age for all subsequent cohorts. The individual aged x_0 receives a constant monthly payment B as long as he/she survives. We can say that $e_{x_0,C}^{(M)}$ represents the Expected Pension Period Duration according to model M (EPPD$^{(M)}$), that is the expected number of years during which pension payments are due.

Then, for a fixed mortality model M and for each of the selected cohort C, we determine the age at which life expectancy equals the EPPD$^{(M)}$. For a fixed mortality model M and for each of the selected cohort C, we evaluate $e_{x_0*j,C}^{(M)}$ for j=1,2…., and we index the retirement age considering a shift $s_C^{(M)}$ so that:

$$s_C^{(M)} = \min_j e_{x_{0+j},C}^{(M)} \leq EPPD^{(M)} \tag{7}$$

In this way, the Social Security System will be obliged for an expected number of years that does not exceed the fixed EPPD$^{(M)}$ and will keep pension costs to budgeted level.

4 Application: Italian dataset

As aforementioned, we consider cohorts of individuals born from 1952 to 2012 for ages from 55 up to 89 years. The data are downloaded from the Human Mortality Database (Human Mortality Database 2014) by single calendar year and by single year of age. We focus on ages 55 to 89 since we are interested in mortality dynamics at old ages. The numerical application is performed considering the LC and RH mortality models according to the following steps: we fit the selected models, assess goodness of fit, forecast mortality and calculate the indexed retirement age both for males and females.

The goodness-of-fit of mortality models is typically analyzed by inspecting the residuals of the fitted model.

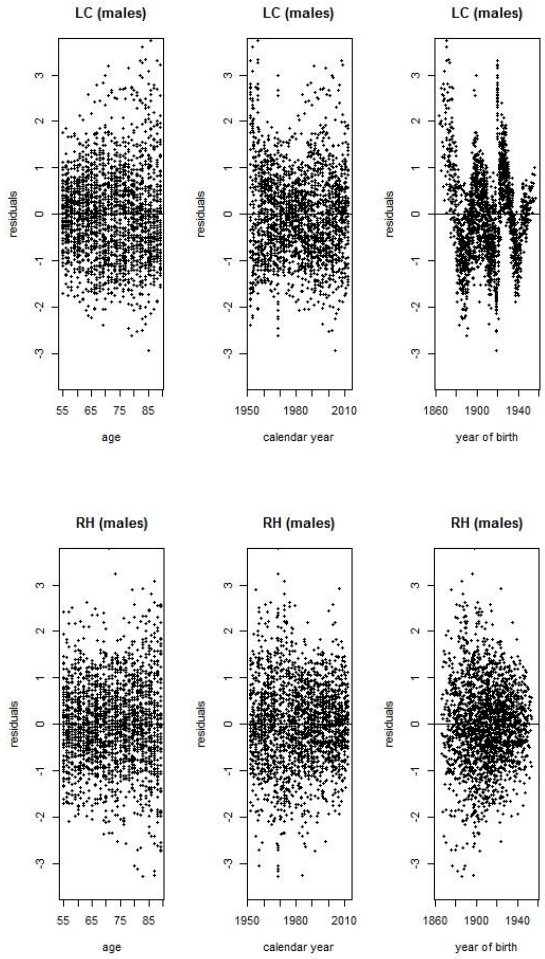

Fig.1. Scatter plots of deviance residuals for LC and RH models fitted to the Italian male population for ages 55-89 and the period 1952 to 2012.

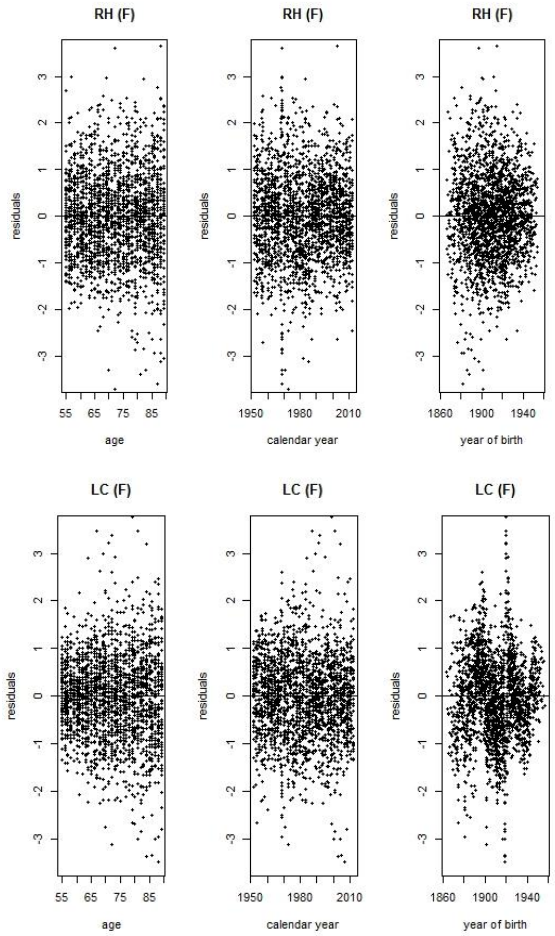

Fig. 2. Scatter plots of deviance residuals for LC and RH models fitted to the Italian female population for ages 55-89 and the period 1952 to 2012.

In fig.1 and fig. 2 scatter plots of residuals by age, period and cohort for both males and females in case of LC and RH model are reported. As well known, regular patterns in the residuals indicate the inability of the model to describe all the features of the data appropriately. In our case the scatter plots of deviance residuals show the inability of LC model to capture the well-known cohort effect. On the contrary the residuals of RH model look more reasonably random. Table 1 reports the results obtained calculating the BIC index for LC and RH models both for females and males. According to that results the RH is the best fitting one.

Table 1: BIC index for selected mortality models

	Males	Females
RH	27839.01	27584.65
LC	43772.54	29778.88

For mortality projections, we consider a forward time span of h=30 years. As customarily, we assume that the period index k_t follow a random walk with drift and the cohort index γ_{t-x} follows a univariate ARIMA process, independent of the period indexes. Then, for each mortality model, the forecasting procedure is based on the best ARIMA process fitting the observed data, as obtained from the auto.arima() function of the R Package "forecast" (Hyndman et al 2008). Table 2 reports the ARIMA(p,d,q) process that are assumed for the cohort effects both for females and males.

Table 2: Selected ARIMA process for forecasting cohort effect

Males		Females	
RH	ARIMA (1,2,2)		ARIMA(1,2,2)

According to these forecasts, the central projections of death rates and the expected residual life span at age 65 are computed for the two selected models and different genders (see Figures 3a and 3b, 4a and 4b; tables 3a and 3b).

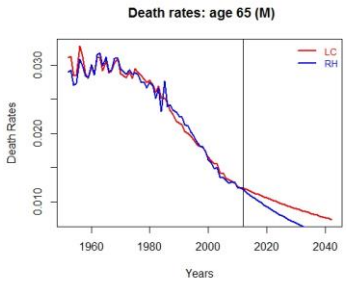

Fig. 3a. Fitted and forecasted death rates for males aged 65

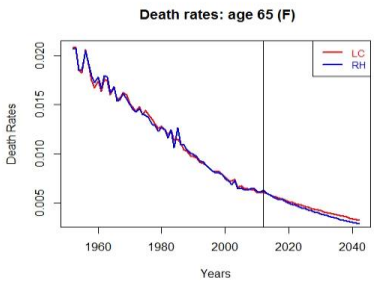

Fig. 3b. Fitted and forecasted death rates for females aged 65

Cohort	LC	RH
1952	12.97	12.80
1956	13.16	13.16
1960	13.42	13.31
1964	13.74	13.70
1968	14.22	14.37
1972	14.81	15.12
1976	15.47	15.63
1980	16.11	15.86
1984	16.73	16.61
1988	17.30	17.52
1992	17.82	18.55
1996	18.24	19.20
2000	18.59	19.89
2004	18.91	20.71
2008	19.23	21.40

Tab. 3a. Life expectancy at age 65 for male cohorts for the selected mortality models

Cohort	LC	RH
1952	15.90	15.76
1956	16.41	16.51
1960	16.97	16.98
1964	17.57	17.54
1968	18.22	18.28
1972	18.85	19.05
1976	19.47	19.56
1980	20.00	19.95
1984	20.47	20.58
1988	20.91	21.18
1992	21.32	21.88
1996	21.71	22.35
2000	22.08	22.80
2004	22.46	23.40
2008	22.84	23.86

Tab. 3b. Life expectancy at age 65 for female cohorts for the selected mortality models

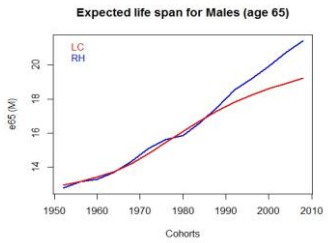

Fig. 4a. Life expectancy for males aged 65

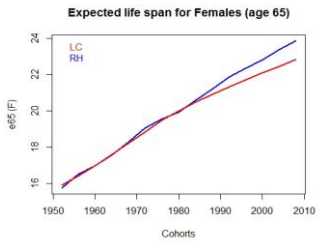

Fig. 4b. Life expectancy for females aged 65

The indexation mechanism will assume, for each mortality model M, the expected life span for cohort 1952 as $EPPD^{(M)}$. Table 4a and 4b report the computed lag as the minimum forward shift that should be applied to the retirement age (say, set at age 65), in order to reach the threshold EPPD(M). Results are represented in fig.5.a and 5.b. Different patterns are observed for different genders. Specifically, for females residual life expectancy is globally higher than for males, although the specification of the cohort effects (which is supported by the data) yields a steeper increase in expected lives for males than for females. This circumstance yields that in the case of RH model the lags requested for females are lower than for males for younger generations. Finally

we note that the cohort effect is stronger for the male population (lags are higher in case of RH model respect the LC model for males), and also the RH more sharply improves the fitting performances for males than for females.

Table 4a: Required lags by the indexation mechanism for Males

	Lag													
	1956	**1960**	**1964**	**1968**	**1972**	**1976**	**1980**	**1984**	**1988**	**1992**	**1996**	**2000**	**2004**	**2008**
LC	1	1	2	3	4	5	5	6	7	7	8	8	8	9
RH	1	1	2	3	4	5	5	6	8	9	10	10	11	12

Table 4b: Required lags by the indexation mechanism for Females

	Lag													
	1956	**1960**	**1964**	**1968**	**1972**	**1976**	**1980**	**1984**	**1988**	**1992**	**1996**	**2000**	**2004**	**2008**
LC	1	2	3	4	4	5	6	6	7	7	7	8	8	9
RH	2	2	3	4	5	5	6	7	7	8	8	9	10	10

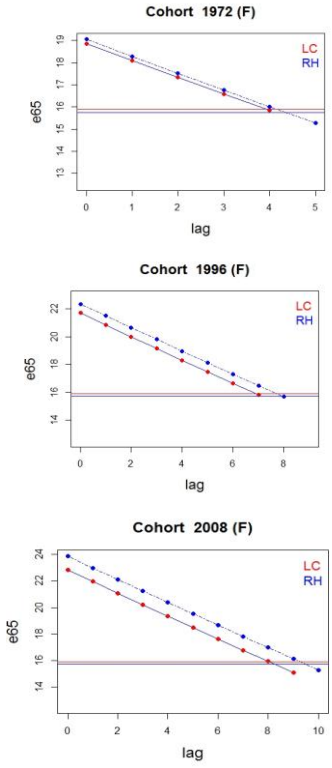

Fig. 5a. Lag to reach EPPD for LC (red) and RH (blue) females

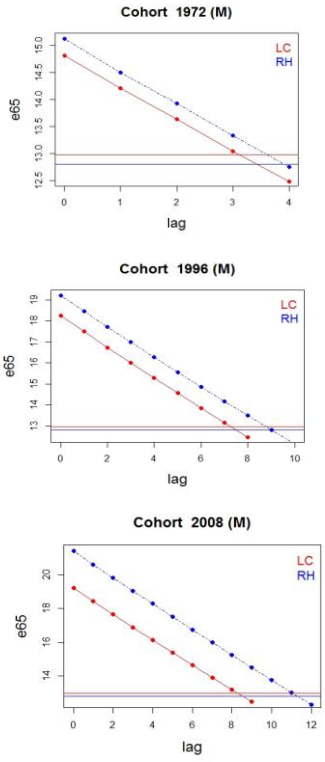

Fig. 5b. Lag to reach EPPD for LC (red) and RH (blue) males

Conclusions

The paper suggests a flexible pension scheme based on the expected residual life to adjust the retirement age for keeping a constant Expected Pension Period Duration (EPPD) and containing the pension costs to a fixed level. In this context the choice of the stochastic mortality model is crucial. So, we applied the indexing mechanism to the Italian male and female populations in case of the LC and RH models. In this way we show the impact of the selected models on the indexed retirement age when the cohort effect is considered or not. Moreover results highlight different cohort effects for males and females. The paper represents the first step of a work in progress. Future developments will extend the mortality projection topic to the choice of the best mortality model in terms of fitting and forecasts among the family of GAPC models. Finally we will measure the impact of different stochastic mortality projection models on the Social Security System costs introducing a suitable index, while accounting for uncertainty of both estimation and prediction.

References

1. Bisetti, E. and Favero, C.A.. 2014. Measuring the impact of longevity risk on pension Systems: the case of Italy. North American Actuarial Journal (18) 1.
2. Human Mortality Database, 2014. University of California, Berkeley (USA), and Max Planck Institute for Demographic Research (Germany). URL www.mortality.org
3. Lee, R. D., Carter, L. R., 1992. Modeling and forecasting U.S. mortality. Journal of the American Statistical Association 87 (419), 659-671.
4. Pitacco, E., Denuit, M., Haberman, S., Olivieri, A. 2009. Modelling Longevity Dynamics for Pensions and Annuity Business. Oxford University Press
5. Renshaw, A., Haberman, S., 2003. Lee-Carter mortality forecasting with age-specific enhancement. Insurance: Mathematics and Economics 33 (2), 255-272.
6. Villegas A.R., V. Kaishev, P. Millossovich. 2016. Under review or revision. StMoMo: An R Package for Stochastic Mortality Modelling, 38 pages.
7. Visco I., Longevity risk and financial markets, 2006. https://www.bancaditalia.it/pubblicazioni/interventi-vari/int-var-2006/visco_12_10_06.pdf

Risk factors of Severe Cognitive Impairment in the Czech Republic

Kornélia Cséfalvaiová[1] and Jitka Langhamrová[2]

[1] Department of Demography, University of Economics, Prague, Czech Republic
(E-mail: kornelia.csefalvaiova@vse.cz)
[2] Department of Demography, University of Economics, Prague, Czech Republic
(E-mail: langhamj@vse.cz)

Abstract. Expected dramatic increase in the number of people with cognitive impairment will put high demands on health and social care in the Czech Republic. Population aging and the increase of elderly persons aged 65+ evoked a need to address this issue, since age is the major risk factor for dementia and severe cognitive impairment. Conflicting conclusions of European studies confirm the difficulties of quantifying the disease. This article includes the analysis of risk factors of severe cognitive impairment, based on socio-demographic and health variables in the Czech Republic. The method of logistic regression was used for the analysis of risk factors.

Keywords: Population Ageing, Severe Cognitive Impairment, Risk Factors, Czech Republic.

1 Introduction

Due to an expected increase of demented persons, another objective of the PhD thesis is to find risk factors for the occurrence of dementia. In the event that is known as risk factors associated with dementia, and medicine can find a way to delay disease or prevented. The aim is to evaluate the applied statistics and draw conclusions regarding the demographic and medical issues associated with dementia. It is as important as the mathematical (theoretical) statistics. Application statistics troubleshooting from another department is equally important for statistics, demography and biomedicine. In the Czech Republic lacks an effective national measures in the field of dementia and mental disorders - National Action Plan for Alzheimer's disease was accepted until the beginning of 2016.

In general, particular disease, e.g., diabetes, cardiovascular disease or poor physical and mental condition, also increase the risk of occurrence. The situation is complicated by the fact that the individual may suffer at the same time at more than one simultaneously disease: diabetes, hypertension or heart disease. Equally important is appreciated that not all AIDS patients with a given

disease visit the practitioner and are introduced into the statistics. Therefore, a number of diseases which are characterized by, but not limited too course of the patient, e.g., Elevated blood pressure, it can be seen only very roughly. One approach to solving this problem is to try to model development morbidity from chronic disease on the basis of knowledge of the risk factors.
The source of data used is the SHARE database (The Survey of Health, Aging and Retirement in Europe), which by its multidisciplinary nature provides a comprehensive picture of the aging process in Europe. The results in the dissertation are of significance with respect to the issue of dementia useful material for future analysis and professionals.

2 Data – The Survey of Health, Ageing and Retirement in Europe (SHARE)

The aim of SHARE (The Survey of Health, Aging and Retirement in Europe) is creating a longitudinal data set across Europe consisting of persons older than 50 years and their families.
Among the main topics of multidisciplinary research include demography, family, education, physical and mental health, cognitive function, medical care and risks, quality of life, employment and income, housing, income and consumption of households, social support, etc. Data set SHARE provides full advice socio-demographic variables, variables relating to lifestyle and physical and mental health, which help to elucidate acting factors. The investigation so far to the 5 waves in different European countries, including CR. It was on a panel database of microdata from the area of the economic situation, health, social and family bonds. It provides real-tracking data on a sample of 123 000 individuals (more than 293 000 interviews) 27 European countries and Israel older than 50 years. Czech Republic was involved in the project in a second wave of investigations in 2006. The variables characterizing the state of physical and mental health and variables from which it was possible to calculate a variable cognitive function, found only in the second, fourth and fifth wave investigation, were therefore used in the dissertation data exclusively from these waves. One drawback SHARE investigation that do not include people in social devices. Estimates of the incidence of dementia seniorskej population differ. In institutionalized senioroch it is always higher than in senioroch living alone (Nikolai et al., 2013). As shown Jagger et al. (2000). The prevalence of dementia is significantly increased in social and health devices as in households. Since demented persons require intensive care, it is in a certain phase of the disease necessary to have these persons transferred to social facilities (Hallauer, 2002). The most frequent group of respondents were consisted of age less than 60 years (37.62%), followed by annual 60-69 (35.16%), annual 70-79 (19.23%), annual 80-89 (7.64%) and the smallest proportion represented persons older than 90 years (0.35%). The relative proportions of the age categories are shown in Figure 1.

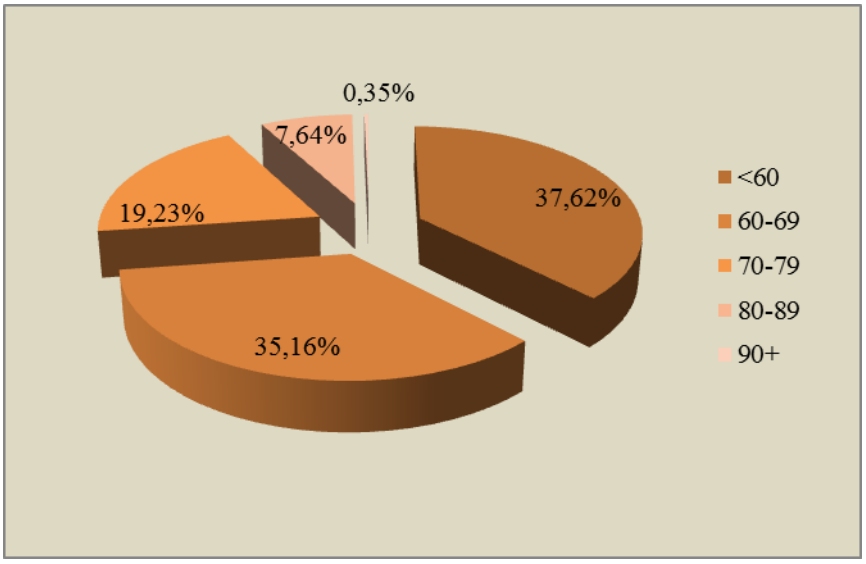

Figure 1. Age structure of the respondents
Source: data SHARE (2015), own construction

3 Determinants of occurrence of dementia

In the literature there exist several risk factors of dementia. From these results it can be assumed that higher education and active lifestyle reduce the chance of developing dementia. Furthermore, some diseases such as diabetes and cardiovascular diseases or poor physical and mental health should generally increase the chances of developing dementia. The aim of this part is the analysis and identification of factors that affect the risk of severe cognitive impairment in the Czech Republic. Researchers question is whether there are any assumptions or risk factors, which when exposed to a certain person more frequently, thereby increasing their chances of developing a cognitive disorder? Admission variables related to socio-demographic characteristics, physical and mental health and lifestyle were drawn from the SHARE, which were described in section 2.
Multi-dimensional analysis can exclude relationships that exist between the explanatory variables. To determine associations between basic demographic characteristics and other variables, and severe cognitive impairment model was constructed logistic regression. Alltogether we constructed 4 models of logistic regression.

After the analysis of risk factors for severe cognitive impairment and by looking for associations between socio-demographic variables, variables of physical and

mental health, social characteristics and development of severe cognitive impairment the fourth model was created that includes variables, which were in the previous models confirmed as significant.

In all models, it was shown that the chances of developing severe cognitive impairment increases rapidly with age. Also higher education positively affects cognition. It is important to highlight the factors which appeared in most models as significant (higher than e.g., education) and the family status (living with a partner). Starting from a model there is about 6 times higher risk of dementia for persons who live without a partner.

4 ROC curve

To illustrate the discriminating capabilities of the model we used ROC curve (Received Operation Characteristic Curve; see Figure 2). ROC curve enables the ability of the diagnostic assay depending on the sensitivity (sensitivity) and specificity (accuracy) and minimize the consequences of erroneous diagnostic decisions. In a square of a unit we receive content: diagonal (and area under the diagonal size of about 0.5), when the model has no ability to classify and units are classified into groups randomly; a curve under the diagonal (defining the area of greater than 0.5) for certain models with better or worse discrimination capability; ROC curve confluent with the left upright and the upper horizontal side of the square in a situation where model classifies perfectly and the quality is best expressed by the entire unit area of a square (Hebák et al., 2015). The closer the ROC curve in the upper left corner, the higher the overall accuracy of the test (Zweig, Campbell, 1993). In case the model no discriminatory property and units are randomly assigned to the given categories, the ROC curve has a diagonal shape (dashed line).

Value of McFadden's pseudo R-square is in this case, it was 0.41, and the value of Kendal tau is equal to 0.14. Statistics AUC value is 0.938 (see Figure 3). By these criteria, the best is the final model (see Figure 3).

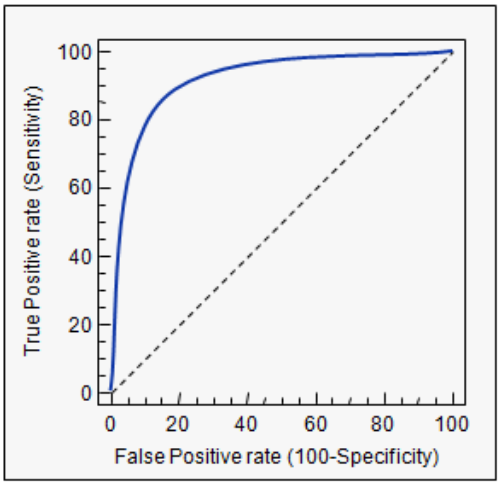

Figure 2. ROC Curve
Source: MedCalc, 2016

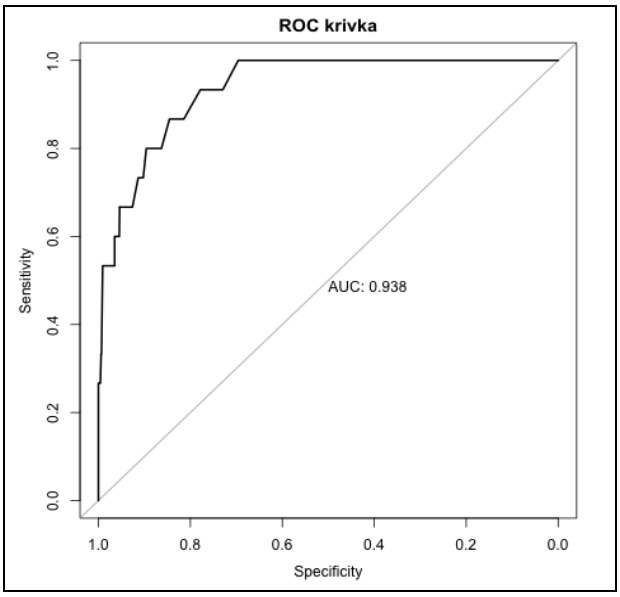

Figure 3. ROC Curve
Source: own calculation

5 Risk factors of dementia in the literature

Due to the complexity of dementia syndrome, and factors that increase the risk of disease, has heretofore been unambiguously identified relatively few risk factors. Risk factors, such as e.g., Age, family history and inheritance can not be changed, but recent investigations indicate that there are other risk factors that can be influenced. Some factors are still debatable and others have been repeatedly confirmed in the existing studies. Jorm (1994) is under research and Short form of the Informant Questionnaire on Cognitive Decline in the Elderly (IQCODE): Development and cross-validation discloses Down syndrome as a possible risk factors for Alzheimer's disease. During the 60s and 70s of the 20th century the aluminum appeared to be a possible risk factor causing Alzheimer's disease. This suspicion led to concerns about the everyday use of aluminum through Pot film beverage cans antiperspirants. Since then, studies have not confirmed the statistical significance of aluminum in the incidence of dementia and Alzheimer's disease. Attention therefore focuses scientists to other research and aluminum is now possible to exclude from the list of risk factors of dementia.
Regardless of the form of dementia, personal, economic and societal consequences of this disease can be devastating. The following portion provides a comprehensive summary of the results of international studies of the risk factors of dementia using statistical methods.

Conclusions

Age was demonstrated (in accordance with literature) as the major risk factor of severe cognitive impairment. The risk of severe cognitive impairment increases with age, some studies have suggested that the highest age groups is slower increase. Pliant factors, such as. Lifestyle, can prevent and slow down the development of cognitive disorders. Lifestyle also affected by the presence of other diseases such as hypertension, diabetes, heart attack, vascular disease of the brain which are also associated with severe cognitive impairment. It can be concluded that healthy diet reduces the risk of developing severe cognitive impairment, both directly and indirectly. There is no direct correlation between the different pathologies and pursued the development of severe cognitive impairment, but generally it can be said that a combination of factors, the monitored increases the likelihood of its development. A higher level of education and healthy lifestyle appear to be the factors which delay disease incidence in the higher age group.
People with higher education had access i greater cognitive reserve and are able to work longer and with a decrease in brain function. Interestingly finding that partner coexistence indirectly protects against the development of dementia: it is well known that persons in Partnership live longer, healthier, have more social bonds more emotional stimuli aid like. Support partnerships may thus become

one of the instruments preventing dementia (and other chronic diseases in the elderly).
Aging of the population with particular emphasis on more than two-fold increase in the number of dementing and those with severe cognitive impairment in a population must be understood as a call for the entire company and invites public and private institutions to action. In addition to the necessary medical care must be a target for aging society, increase the capacity of long-term care. The necessity of social services depending on age and level of dependency has been discussed in the first chapter of the thesis. The company must be aware of these changes that will belong not only to increase the number of demented people and increased costs associated with the care of patients and their treatments, but also the associated problems, such as the varying structure of the population and the load, which will represent for the family caregiver or pre-set institutional care.

Acknowledgments

This article was supported by the Czech Science Foundation, No. GA ČR 15-13283S under the title "Projection of the Czech Republic Population According to Educational Level and Marital Status."

References

1. HALLAUER, J. F. (2002). Epidemiologie für Deutschland mit Prognose. In J. Hallauer and A. Kurz (Eds.), Weissbuch Demenz. Versorgungssituation relevanter Demenzerkrankungen in Deutschland, Stuttgart, pp. 15-18. Georg Thieme Verlag.

2. HEBÁK, P. A kol. (2015). Statistické myšlení a nástroje analýzy dat. Informatorium: 2015. Vyd. 1. 880 s. ISBN: 978-80-7333-105-4

3. JAGGER, C., A. M. D., M. M. B. BRETELER, J. R. M. COPELAND, C. HELMER, M. BALDERESCHI, L. FRATIGLIONI, A. LOBO, H. SOININEN, A. HOFMAN, AND L. J. LAUNER (2000). Prognosis with dementia in Europe: a collaborative study of population-based cohorts. Neurology 54, 16.

4. JORM, A. F. (1994). A short form of the Informant Questionnaire on Cognitive Decline in the Elderly (IQCODE): development and cross-validation. Psychological Medicine 1994; 24 (1), s. 145−153.

5. NIKOLAI, T., VYHNÁLEK, M., ŠTĚPÁNKOVÁ, H., HORÁKOVÁ, K. (2013). Neuropsychologická diagnostika kognitivního deficitu u Alzheimerovy choroby. Praha: Psychiatrické centrum Praha 2013, 64 s. ISBN: 978-80-87142-25-7.

6. ZWEIG, M. H., CAMPBELL, G. (1993). Receiver-operating characteristic (ROC) plots: a fundamental evaluation tool in clinical medicine. Clinical Chemistry. 1993. Apr. 39 (4): 561−77.

An intervention analysis regarding the impact of the introduction of budget airline routes to Maltese tourism demographics

Maristelle Darmanin[1] and David Suda[2]

[1] National Statistics Office, Lascaris Wharf, Valletta VLT1920
(E-mail: maristelle.darmanin@gov.mt)
[2] Room 511 Mathematics and Physics Building, University of Malta, Msida MSD8020
(E-mail: david.suda@um.edu.mt)

Abstract. Intervention analysis is an important method for analysing temporary or long-lasting effects of sudden events on time series data. We use monthly data of the National Statistics Office's Tourstat survey covering the years 2003 up to 2012. This contains a number of time series regarding tourist demographics, the type of tourism, and other variables of economic relevance. We apply intervention analysis to determine the impact of the introduction of budget airline routes to Maltese tourism related time series. We consider two main interventions. The first is the introduction of Italy and UK bound routes in October 2006. The second is the introduction of a considerable number of routes in March 2010, in particular the Marseille route. In addition to the standard types of intervention introduced by Box and Tiao [1], the step and the pulse intervention, we also use a periodic pulse intervention which allows us to cater for any seasonality in the intervention effect, with the corresponding transfer function possibilities. We conclude with a critique of this method for this data.
Keywords: Time series analysis, intervention analysis, tourism.

1 Introduction

Intervention analysis looks for dynamic changes in a time series following an intervention. The seminal paper related to intervention analysis is that by Box and Tiao [1]. This intervention, in actual practice, could take the form of an event, procedure, law or policy intended to change a particular trend. Transportation and tourism time series are time series which are expected to be impacted by external events that are known to have occurred at a particular point in time. By understanding the extent of the impact of an intervention on a time series, policy makers would be able to quantify the exent of the impact and adjust policy to cater for inferred change. Intervention analysis has often been used to study the effects of policy, procedure or other events on transportation and tourism. In [6], the impact of fare and service changes on transportation in Kentucky during the period 1975-1985 is studied. In [5], the impact on passenger ridership of the opening of a new railway line in Soeul is investigated. A study from a tourism perspective is found in [4], where the impact of SARS in 2003 on Japanese tourism to Taiwan is assessed.

The relatively small size of the Maltese islands means that changes in policies and interventions may prove to have a significant effect on the economy. Tourism is an important pillar of the Maltese economy, and the impact of the introduction of low cost carriers, which have been introduced in 2006, to Maltese tourism has never before been studied. In this paper we look at how the introduction of these new routes has impacted on the volume and profile of tourists visiting Malta during the above mentioned period. The analysis is based on variables derived from the Tourstat survey [8] carried out by the National Statistics Office in Malta. This is a tourism survey carried out monthly using a two-stage sampling technique consisting of clustering and systematic sampling stages. The survey is carried out at departure terminals at randomly picked time-intervals, and tourists visiting Malta are selected systematically and interviewed as they are entering the departures lounge towards the end of their stay. The results from this survey are then projected for the whole tourist population. For the analysis, we consider the period 2003-2012 on a monthly basis. We shall be looking at two interventions - the introduction of low cost routes to Pisa and London in October 2006, and a considerable addition of new routes (namely Bologna, Marseille and other European airports in Spain, Denmark and Poland) in March 2010. Due to numerous time series datasets at our disposal, from here onwards we shall only present those series where intervention eventually proved to be significant.

When carrying out intervention analysis, some assumptions need to be taken into consideration. First of all, apart from the noise of the series, the only exogenous impact shall be presumed to be that of the event or the intervention itself. Secondly, the temporal delimitations of the intervention are presumed to be known, such as the time of onset, the durations and the time of termination of the input event. Lastly, a sufficient number of observations in the series should be available before and after the onset of the event for the researcher to separately model the pre-intervention time series and the post-intervention time series.

2 Building the intervention model

Building an intervention model typically follows these steps. A model is constructed for change, which describes what is expected to occur given knowledge of the known intervention (or interventions). Data analysis is then worked out appropriately based on that model. A pre-intervention model is first obtained, based on the data prior to the first intervention. A SARIMA (seasonal autoregressive moving average) model is typically used at this stage, but not exclusively. This is then followed by an analysis on the whole dataset including the intervention. This is usually chosen after the selected model is used to generate forecasted values for the period after the intervention, and the differences between the actual values after the interention and the forecasted values are visually analysed. The typical intervention model is given by

$$Y_t = f(\theta, \mathbf{I}, t) + N_t \tag{1}$$

where Y is the original or appropriately transformed series, f represents the dynamic model for the intervention effects and is a function of the parameter set θ, the intervention variables $\mathbf{I}$ and the time t, and N represents the underlying time series with no intervention, which may either be completely random or modeled by some time series model of endogenous variables. Diagnostic checks are then carried out on the fitted model, and if serious deficiencies are uncovered, the model needs to be modified. Typical diagnostic checking which occurs at this stage is the significance of model parameters, where one also includes post-intervention data, and analysis of residuals. In this paper we shall assume that N is modeled by SARIMA. A SARIMA $(p,d,q)\left(P,D,Q\right)_s$ with no constant term is given by the equation

$$\left(1-B\right)\left(1-B^s\right)\phi\left(B\right)\Phi\left(B^s\right)N_t=\theta\left(B\right)\Theta\left(B^s\right)Z_t \tag{2}$$

where B is the backward operator, Z is a white noise process and:

1. $\phi\left(z\right)=1-\phi_1 z-...-\phi_p z^p$
2. $\Phi\left(z\right)=1-\Phi_1 z-...-\Phi_P z^P$
3. $\theta\left(z\right)=1+\theta_1 z-...-\theta_q z^q$
4. $\Theta\left(z\right)=1+\Theta_1 z-...-\Theta_Q z^Q$

If we include the constant term, we replace N_t in (2) with $\tilde{N}_t\equiv N_t-\mu$ for non-zero constant term μ. We now look into possible ways of modelling intervention.

2.1 Dynamic Models for Intervention

A model for intervention can contain both single and multiple interventions. For a single intervention, the dynamic model in (1) is given by

$$f\left(\theta,I,t\right)=\chi_t=\frac{\omega\left(B\right)}{\delta\left(B\right)}I_t \tag{3}$$

where

1. $\omega\left(z\right)=1-\omega_1 z-...-\omega_r z^r$
2. $\delta\left(z\right)=1-\delta_1 z-...-\delta_s z^s$
3. $\omega\left(z\right)$ and $\delta\left(z\right)$ have roots outside the unit circle
4. χ_t represents the dynamic transfer from a single intervention I
5. $\theta=\left(\omega_1,...,\omega_r,\delta_1,...,\delta_s\right)$

Furthermore, we call the term $\frac{\omega(z)}{\delta(z)}$ in (3) the transfer function, as it relates the exogenous input I_t with the observed process Y at time t. The generalisation of (3) for multiple interventions is given by

$$f\left(\theta,\mathbf{I},t\right)=\sum_{j=1}^{k}\chi_{tj}=\sum_{j=1}^{k}\frac{\omega_j\left(B\right)}{\delta_j\left(B\right)}I_t^{(j)} \tag{4}$$

where

1. $\omega_j(z) = 1 - \omega_{1j}z - ... - \omega_{r_j j}z^{r_j}$
2. $\delta_j(z) = 1 - \delta_{1j}z - ... - \delta_{s_j j}z^{s_j}$
3. for all j, $\omega_j(z)$ and $\delta_j(z)$ have roots outside the unit circle
4. $\mathbf{I} = \left(I^{(1)}, ..., I^{(j)}\right)$
5. χ_{tj} represents the dynamic transfer from the j^{th} intervention $I^{(j)}$
6. $\theta = (\omega_{11}, ..., \omega_{r_k k}, \delta_{11}, ..., \delta_{s_k k})$

The two most common types of intervention variables I_t^j are the step intervention and the pulse intervention. The step intervention $S^{(T,j)}$ represents an intervention at time T that remains in effect thereafter, hence causing a permanent change in state. In this case:

$$S_t^{(T,j)} = \begin{cases} 0, t < T \\ 1, t \geq T \end{cases} \tag{5}$$

The pulse intervention $P^{(T,j)}$, on the other hand, represents an intervention at time T whose change in state is only temporary. In this case

$$P_t^{(T,j)} = \begin{cases} 0, t \neq T \\ 1, t = T \end{cases} \tag{6}$$

Sometimes, however, the intervention effect may also be seasonal. This is likely to cause model misspecification if not catered for. Specifically devised for our purpose, we shall also consider a periodic pulse intervention to model one of our time series. Denoting it by $P^{(d,t,j)}$, we define this as follows

$$P_t^{(d,T,j)} = \begin{cases} 1, t = T + j + bd \\ 0, t \neq T + j + bd \end{cases} \tag{7}$$

where $a \in \{0, 1, ..., d-1\}$ and $b \in \mathbb{Z}^+$. To cater for multiple periodic pulse intervention effects, one can consider these within the context of a multiple intervention model of the type (4).

We next discuss the polynomial terms in (3) and (4). The ω_j-polynomials are responsible for the delay in the effect of the intervention variable, while the δ_j-polynomials are responsible for the type of change in the mean after the effect of the intervention. For example, if $\omega_j(z) = \tilde{\omega}$, then the effect of the intervention of the mean is immediate, while if $\omega_j(z) = \tilde{\omega}z^k$ for $k > 0$, then the effect of the intervention is delayed by k. On the other hand, $\delta_j(z) = 1$ suggests an abrupt change in mean after the effect of the intervention, $\delta_j(z) = 1 - \tilde{\delta}z$ where $\tilde{\delta} \in (0, 1)$ suggests a gradual change in mean after the effect of the intervention, while $\delta_j(z) = 1 - z$ suggests a linear increase/decrease without bound. For illustrations of the different effects to the mean level for different combinations of ω_j-polynomials and δ_j-polynomials applied to interventions of the type (5) and (6), see [1], Section 2. For interventions of the type (7), we shall only apply $\omega_j(z) = \tilde{\omega}_j$, due to the fact that the intervention effect for a particular month will only be expected to occur in that month. On

the other hand, in the denominator, we shall assume either that $\delta_j(z) = 1$, $\delta_j(z) = 1 - \tilde{\delta}_j z^d$ or $\delta_j(z) = 1 - z^d$. In the latter, we allow for gradual change along the seasonal streaks of the intervention. The forms for $\omega_j(z)$ and $\delta_j(z)$ mentioned in this paragraph are the only ones we shall consider moving forward.

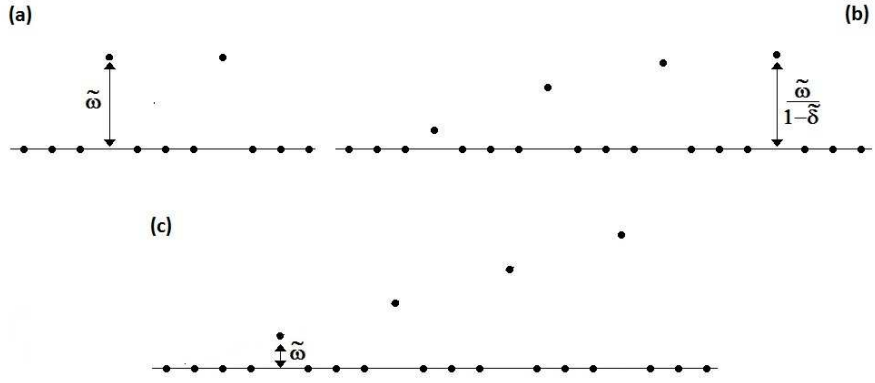

Fig. 1. The response to a periodic pulse intervention with $d = 4$ for the following transfer functions: (a) $\omega(z) = \tilde{\omega}$, $\delta(z) = 1$, (b) $\omega(z) = \tilde{\omega}$, $\delta(z) = 1 - \tilde{\delta}z^4$ and (c) $\omega(z) = \tilde{\omega}$, $\delta(z) = 1 - z^4$.

Preliminary analysis for deciding which intervention model is most appropriate is not unique. One approach for selecting an adequate intervention model is through plots of the differences between the actual values after intervention and the forecasted values. We opt to use moving average plots which have smoothed out the noise and seasonal effects, hence bringing to the fore the underlying patterns of the data. This will be elaborated on in Section 3. Ultimately, these are just graphical indications, and the resulting model may not correspond to what one expects from preliminary analysis.

2.2 Inference for the intervention model

We now discuss estimation for the intervention model in 1. Given a time series of length $N + d + sD$, the likelihood may be obtained in terms of an N-dimensional vector $\mathbf{W}$ whose t^{th} element is given by

$$W_t = (1 - B)^d (1 - B^s)^D (Y_t - f(\theta, \mathbf{I}, t))$$

where

$$W_t = \left\{ \frac{\theta(B)\Theta(B^s)}{\phi(B)\Phi(B^s)} \right\} Z_t$$

is stationary. Let β be the vector SARIMA and intervention parameters in 1. Then the likelihood function is

$$L\left(\beta, \sigma_z^2 | \mathbf{W}\right) = \left(2\pi\sigma_z^2\right)^{-\frac{N}{2}} |\mathbf{M}|^{\frac{1}{2}} \exp\left\{-\frac{S\left(\beta\right)}{2\sigma_z^2}\right\}$$

where $\sigma_z^2 \mathbf{M}^{-1}$ is the covariance matrix of $\mathbf{W}$ and

$$S\left(\beta\right) = \mathbf{W}'\mathbf{M}\mathbf{W} = \sum_{t=0}^{N} E\left[Z_t | \mathbf{W}, \beta\right]$$

Least squares estimation may be applied as a good alternative when MLE becomes infeasible to implement because of the model's strong nonlinearity. Furthermore, two alternative approaches to estimation are suggested by [1]. The first approach uses the same parameters obtained at pre-intervention stage and just estimates the intervention parameters. In this case we would be looking at a quasi-likelihood or quasi-least squares problem. This appears to be less ideal but may sometimes lead to more manageable optimisation, however this was never necessary in our case. The second approach, on the other hand, will apply maximum likelihood estimation or least squares estimation (typically non-linear least squares estimation) to the whole model. When the intervention is abrupt or gradual, i.e. $\delta\left(z\right) = 1$, $\delta\left(z\right) = 1 - \tilde{\delta}z$ or $\delta\left(z\right) = 1 - \tilde{\delta}z^d$, maximum likelihood may be used by applying a number of available software packages. When $\delta\left(z\right) = 1 - z$ or $\delta_j\left(z\right) = 1 - z^d$, estimating (1) becomes a restricted least squares problem. For the purpose of restricted least squares estimation, (1) may be rewritten as

$$\left(1 - B\right)^d \left(1 - B^s\right)^D \left\{\frac{\phi\left(B\right)\Phi\left(B^s\right)}{\theta\left(B\right)\Theta\left(B^s\right)}\right\} \left(Y_t - f\left(\theta, \mathbf{I}, t\right)\right) = Z_t \tag{8}$$

Methods for transforming (8) into regression form can be found in [2], Chapter 11, and the parameters are then estimated via the Levenberg-Marquardt algorithm or other alternatives.

2.3 Goodness of fit measures and residual diagnostics

The following goodness of fit measures are used to select the best intervention model. In the following, we denote by $\hat{Y}_t$ the one-step ahead predictor of Y_t.

1. Mean absolute error (MAE): $MAE = \frac{1}{T}\sum_{t=1}^{T}\left|Y_t - \hat{Y}_t\right|$;
2. Mean absolute percentage error ($MAPE$): $MAPE = \frac{100}{T}\sum_{t=1}^{T}\left|\frac{Y_t - \hat{Y}_t}{Y_t}\right|$;
3. Maximum absolute error ($MaxAE$): $MaxAE = \max_t\left|Y_t - \hat{Y}_t\right|$;
4. MaxAPE ($MaxAPE$): $MaxAPE = 100\max_t\left|\frac{Y_t - \hat{Y}_t}{Y_t}\right|$;

5. Normalised BIC ($NBIC$): $NBIC = p \ln T - 2 \ln L$, where L is the model likelihood and p is the number of parameters to be estimated. When the likelihood is not known, we can approximate this by $NBIC = \ln(MSE) + p \ln(T)$, where $MSE = \frac{1}{T} \sum_{t=1}^{T} \left(Y_t - \hat{Y}_t \right)^2$. For independent identically distributed normal disturbances, the two are equivalent.

Furthermore, we shall also apply the Ljung-Box test on the error terms to ensure that the white noise hypothesis is satisfied. For further details on the Ljung-Box test see [3].

3 Results

The limitation with intervention analysis is that it is based on the assumption that the model specification is correct and no other exogenous occurrences have influenced the data. Furthermore, the size of the pre-intervention and post-intervention data set may also hinder a proper specification of the model. A more detailed discussion of the limitations of intervention analysis can be found in e.g. [7]. We shall therefore perform preliminary analysis on the data to identify some characteristics of the data after the noise and seasonality have been smoothed, to avoid having gross misspecifications in the model and erroneous identification of the intervention.

3.1 Preliminary analysis using moving averages

We shall plot prior moving averages of order 12 over the French tourism series, package tourism series and Italian tourism series - three series that we have identified to be influenced by the mentioned interventions. We opt for prior moving averages rather than centred ones, as these are better for identifying the exact occurence of the intervention effect. From Fig. 2, we can see from the moving average that the French tourism model appears to show a linear and unbounded increase in tourism following the addition of new routes, including Marseille, in March 2010. The package tourism moving averages, after the March 2010 intervention, shows a gradual increase which quickly reaches a plateau. The Italian tourism model, on the other hand, also appears to show an increase which reaches a plateau after a few years.

Despite the characteristics evident in Fig. 2, the modelling aspect may lead us to different models altogether. Sometimes, what appears to be the ideal model ends up not being estimable. Furthermore, there are instances where it may be difficult to capture all features, and we may be forced to opt for some features rather than others. Nonetheless, in this paper we present intervention models where the white noise hypothesis via the Ljung-Box test is not rejected at the 0.05 level of significance and, furthermore, we shall ensure that the SARIMA part of the model is causal and invertible after first order and seasonal differencing.

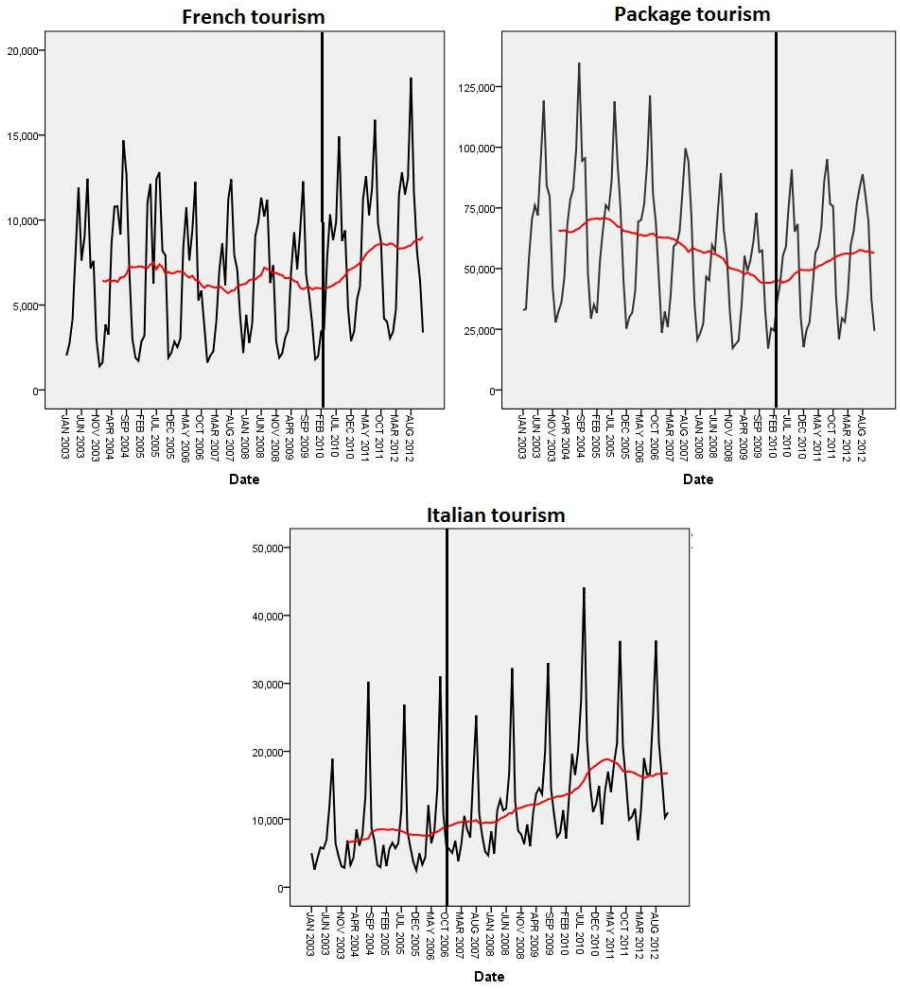

Fig. 2. Original series (black solid line) and prior moving average of order 12 (red solid line) for the following tourism series: French (top left), package (top right) and Italian (bottom). Black vertical line denotes the time of the intervention.

3.2 Model fitting and diagnostics

In this section we discuss models and their diagnostics for the aforementioned series where this was estimable. We select the model with the best goodness of fit criteria which satisfies the required model assumptions. Due to the permanent nature of our interventions, we have not considered the pulse interventions in (5), but the step interventions in (4) where appropriate. Where step interventions failed, we applied the periodic pulse interventions in (6) for each month. When implementing an intervention model of the type (4), we have attempted estimation for $\omega(z) = \tilde{\omega} z^k$ for various lags k and $\delta(z)$ for all the aforementioned forms. We take $k = 0, 1, 2, 3$ when $\delta(z) = 1$ and $k = 0, 1$ otherwise. For some cases, the parameters for the models could not be esti-

mated due to numerical instability. For an intervention model of the type (6), we have considered $\omega(z) = \tilde{\omega}$ in conjunction with $\delta(z) = 1$, $\delta(z) = 1 - \tilde{\delta} z^d$ and $\delta(z) = 1 - z^d$. We have also allowed for multiple interventions, however none of the time series considered found more than one intervention to be significant. The time series where intervention was deemed to have a significant impact were monthly French tourist numbers, monthly package tourist numbers and monthly Italian tourist numbers. For the French tourism series and package tourism series, the step intervention model was sufficient and the significant intervention was the one occurring in March 2010. This was expected for the French tourism time series, as this corresponded to the intervention where the Marseille route was introduced. On the other hand, for the Italian tourist time series, the periodic pulse intervention model was found to be more appropriate and the significant intervention was the one occurring in October 2006. This means that the introduction of the Pisa route in October 2006 left an impact on Italian tourism volumes, but the introduction of the Bologna route in March 2010 does not appear to have had a significant impact. The fitted models and the results are the following.

We first look at the step intervention model for French tourism time series. With reference to the model in (1), N is represented by a $SARIMA(0,0,0)(1,1,0)_{12}$. On the other hand, we take $\omega(z) = \omega z$ and $\delta(z) = 1 - z$. The two coefficients that need estimating, Φ and $\tilde{\omega}$, we obtained through non-linear least squares estimation after transforming (7) into regression form. The parameters, standard errors and corresponding 95% confidence intervals are found in Table 1.

Parameter	Estimate	Standard Error	95% Lower Bound	95% Upper Bound
Φ	-0.45	0.09	-0.62	-0.27
$\tilde{\omega}$	656.79	132.33	394.04	919.53

Table 1. Parameter estimates for the French tourism intervention model.

The goodness of fit statistics for this model are $MAE = 1120.74$, $MAPE = 14.9$, $MaxAE = 4903.4$, $MaxAPE = 92.92$, $NBIC = 14.46$ and $R^2 = 0.86$. The Ljung-Box statistic for the 18^{th} lag is 18.898 and the p-value is 0.4. Fitting a similar model but with $\omega(z) = \tilde{\omega}$ was unsuccessful. Models with $\omega(z) = \tilde{\omega} z^k$ for $k = 0, 1, ...3$ and $\delta(z) = 1$ were also successfully fitted, but the Ljung-Box test was rejected at 0.05 level of significance in all cases, p-values extremely close to zero.

The next series we look into is the package tourism time series, again applying the step intervention model. With reference to the model in (1), N is represented by a $SARIMA(1,0,0)(1,1,0)_{12}$. On the other hand, we take $\omega(z) = \tilde{\omega} z^k$ for $k = 0, 1, 2, 3$ and $\delta(z) = 1$. Other types of intervention models were also attempted but the model fitting was unsuccessful. There are three coefficients that needed estimating: ϕ, Φ and $\tilde{\omega}$. These are obtained via maximum likelihood estimation. To select the optimal k, we look at the goodness

of fit statistics for various $k = 0, 1, 2$ in Table 4 when maximum likelihood estimation is applied.

k	R^2	MAE	MAPE	MaxAE	MaxAPE	NBIC	Ljung-Box
0	0.93	5166.58	9.63	18642.62	**40.4**	17.81	16.44 ($p = 0.42$)
1	**0.94**	5128.23	9.53	**18462.64**	40.68	17.81	18.29 ($p = 0.31$)
2	**0.94**	**5075.65**	**9.44**	18741.43	**40.4**	**17.79**	17.31 ($p = 0.37$)
3	**0.94**	5111.37	9.51	18542.7	40.87	**17.79**	18.62 ($p = 0.29$)

Table 2. Goodness of fit tests and Ljung-Box statistic for the package tourist intervention model at $k = 0, 1, 2, 3$.

Parameter	Estimate	Standard Error	p-value
ϕ	0.57	0.08	0
Φ	-0.46	0.09	0
$\tilde{\omega}$	4686.06	2028.95	0.02

Table 3. Parameter estimates for the package tourism intervention model at $k = 2$.

In Table 2, the superior goodness-of-fit statistics are marked in bold. Since the intervention model at $k = 2$ had the best MAE and $MAPE$, and the joint best R^2, $MaxAPE$ and $NBIC$ with other models having different k, we opt for this model. The parameters, standard errors and p-values for the intervention model at $k = 2$ are found in Table 3.

We finally look at the Italian tourism time series. The first attempt was to fit intervention models with $\omega(z) = \tilde{\omega} z^k$ and all possible $\delta(z)$. While the models were estimable when $\delta(z) = 1$ and $\delta(z) = 1 - z$, these led to residuals with significant short term correlation. An analysis of raw monthly pre-intervention and post-intervention means led us to suspect that seasonality i the intervention effect was the issue. The post-intervention increase in the raw mean for the month of July was 8402.58 (the highest) in comparison to the pre-intervention raw mean, while the increase for February was 3283. We therefore implement the periodic pulse intervention model, and we shall assign a periodic pulse to each month of the year. Hence we have a model of the type (1), where the dynamic model is of the multiple type in (3). We consider combinations of the cases where $\omega_j(z) = \tilde{\omega}_j$, and $\delta_j(z)$ is either equal 1, $1 - \tilde{\delta}_j z^{12}$ or $1 - z^{12}$. Hence, we look at an intervention model of the form

$$f(\theta, \mathbf{I}, t) = \sum_{j=1}^{12} \frac{\tilde{\omega}_j}{\delta_j(z)} P_t^{(12,T,j)}$$

where T corresponds to October 2006, the 46^{th} data point. With reference to the model in 1, N is represented by a $SARIMA(1,0,0)(0,0,1)_{12}$ with constant term. On the other hand, the best model is obtained when $\omega(z) = \tilde{\omega}$

and $\delta(z) = 1$ for July and September, while $\delta(z) = 1 - \tilde{\delta} z^{12}$ for August. We use maximum likelihood estimation to estimate μ, ϕ, Θ_1, Θ_2, the $\tilde{\omega}_j$'s and $\tilde{\delta}_8$. The periodic pulse interventions for July, August and September were found to be significant. The significant parameters, standard errors, and p-values are found in Table 4.

Parameter	Estimate	Standard Error	p-value
μ	10734.55	1173.76	0
ϕ	0.52	0.09	0
Θ	-0.52	0.11	0
$\tilde{\omega}_7$	8335.69	2253.92	0
$\tilde{\omega}_8$	12271.77	3510.25	0
$\tilde{\delta}_8$	0.51	0.18	0.01
$\tilde{\omega}_9$	4743.29	2241.27	0.04

Table 4. Parameter estimates for the Italian tourism intervention model.

The goodness of fit statistics for this model are $MAE = 2572.57$, $MAPE = 29.77$, $MaxAE = 18175.44$, $MaxAPE = 165.56$, $NBIC = 16.92$ and $R^2 = 0.77$. The Ljung-Box staistic for the 18^{th} lag is 13.17 and the p-value is 0.66.

Based solely on the obtained model fits, we deduce the following. French tourism has increased linearly after removing the SARIMA dynamics of the model, at an estimated rate of 656.79 every month. The response to the intervention appears to have occurred with a delay of one month, as $k = 1$ for the dynamic model explaining intervention. On the other hand, after removal of the SARIMA dynamics, package tourism appears to have increased by an estimated 4686.06 in the post-intervention months. The response to the interventions appears to have happened with a two month lag ($k = 2$). This occurrence may appear strange, considering that low cost airline routes are not associated with package tourism, since these travel options have made self-organised travel affordable. Indeed, package tourism appeared to have been on the decline for quite a few years prior to the 2010 intervention. However, what we may be seeing here is the response of the tourism industry to the introduction of a significant number of low cost routes in March 2010, by offering more worthwhile deals to the potential Maltese tourism market. It is also likely that package deals have now been making use of these inexpensive routes to lower their prices. Finally, for the Italian tourism market, the periodic pulse intervention was found to be significant for the months of July, August, and September. We have a sudden estimated increase of 8115.29, on removal of the SARIMA effect, in the post-intervention July months. For September, the sudden estimated increase is of 4571.45. On the other hand, for August, the post-intervention effect is increasing gradually to an estimated asymptote of 25044.43. Interestingly, intervention was not found to have led to a significant increase in British tourists in 2006, or a significant increase in tourists from other EU countries in 2010, despite the addition of new routes from Spain,

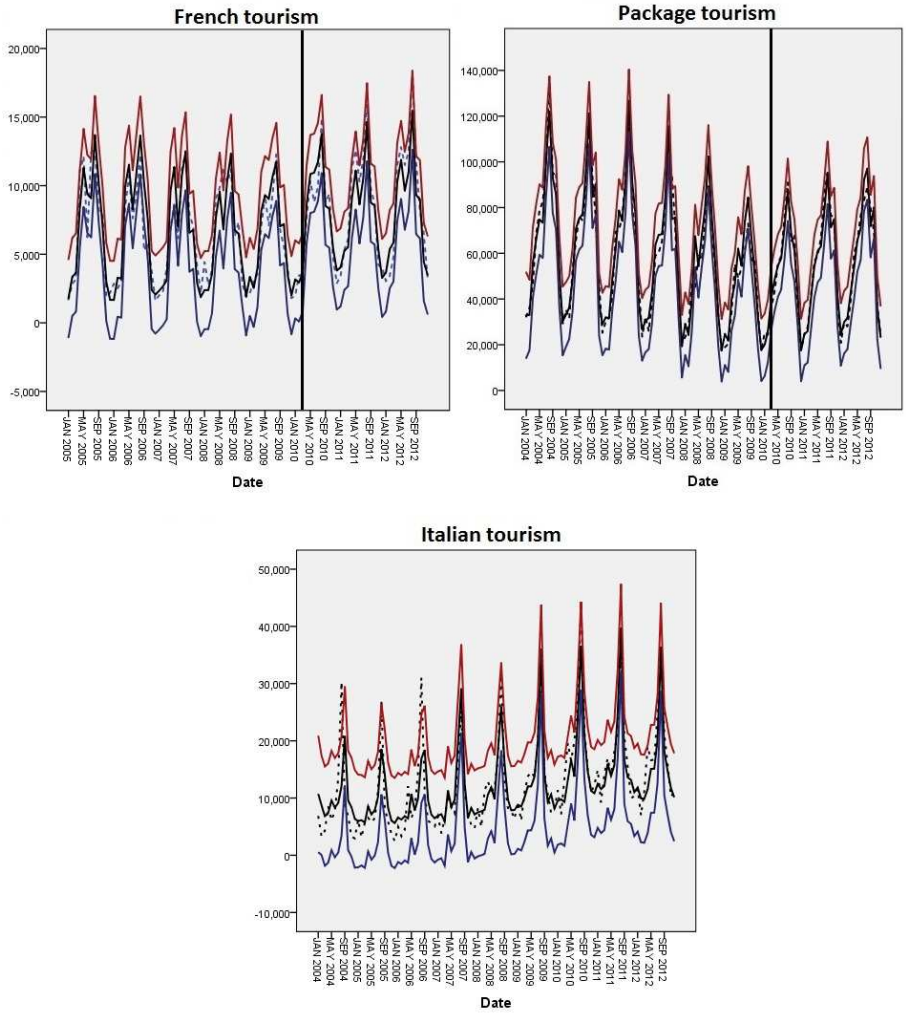

Fig. 3. Original series (black dashed line), fitted series (black solid line), lower 95% confidence levels (blue solid line) and upper 95% confidence levels (red solid line) for the following tourism series: French (top left), package (top right) and Italian (bottom). Black vertical line denotes the time of the intervention.

Denmark and Poland. A plot of the original series, fitted values of one-step predictors and lower/upper 95% confidence levels can be seen in Fig. 3.

4 Conclusion

Intervention analysis is a useful way of assessing the impact of policy on time series. In this paper, we have presented three cases where the introduction of new routes was found to have a significant impact, either on the intended

tourism market or on other areas. Intervention was found to be significant for French and Italian tourism, where an increase in tourists from this country is detected, and package tourism, where the tourism industry appears to have responded to the introduction of low cost airlines. Furthermore, we see that the intervention did not affect Italian tourism equally for all months - only the effects for the months of July, August and September were found to be significant.

Intervention analysis is not without its pitfalls. The amount of data available pre-intervention and post-intervention may affect both model selection and estimation. A complex transfer function may also complicate the estimation problem. Indeed, sometimes we may need to settle for simpler and less informative models. Furthermore, we need to be careful not to falsely attribute changes in the dynamics of a time series to intervention effects. These are all issues we have encountered when performing the analysis. A careful exploratory analysis of the data and being well informed about the context that one is dealing with may help avoid these mistakes. Nonetheless, intervention analysis is an effective and important tool for detecting effect of a sudden change, whether intended or unintended, and is also capable of influencing future policy and decision-making.

References

1. G.E.P. Box and G.C. Tiao. Intervention analysis with applications to economic and environmental problems. *Journal of the American Statistical Association*, 70, 349, 70-79, 1975.
2. J.D. Cryer and K.S. Chan. *Time series analysis: with applications in R (Second Edition).* Springer, 2010.
3. G.M. Ljung and G.E.P. Box. On a Measure of a Lack of Fit in Time Series Models. *Biometrika*, 65, 2, 297303, 1978.
4. J.C.H. Min, C. Lim and H.H. Kung. Intervention analysis of SARS on Japanese tourism demand for Taiwan. *Quality and Quantity*, 45, 1, 91-102, 2011.
5. M.S. Park, J. K. Eom, T.Y. Heo and J. Song. Intervention analysis of the impact of opening a new railway line on passenger ridership in Soeul. *KSCE Journal on Civil Engineering*, 20, 6, 2524-2534, 2016.
6. M. Vaziri, J. Hutchinson and M. Kermanshah. Short-term demand for specialized transportation. *Journal of Transportation Engineering*, 116, 1, 105-121, 1990.
7. R.A. Yaffee and M. McGee. *An Introduction to Time Series Analysis and Forecasting: With Applications of SAS and SPSS.* Academic Press, 2000.
8. https://nso.gov.mt/en/nso/Sources_and_Methods/Unit_C3/Population_and_Tourism_Statistics/Pages/Inbound-Tourism.aspx

Displaying empirical distributions of conditional quantile estimates: an application of symbolic data analysis to the cost allocation problem in agriculture

Dominique Desbois

Joint Research Unit *Economie publique*, INRA-AgroParistech, 16 rue Claude Bernard, 75732 Paris Cedex 05, France
(E-mail: desbois@agroparistech.fr, dominique.desbois@inra.fr)

Abstract: This paper uses the symbolic data analysis tools in order to display and analyze the conditional quantile estimates, with an application to the cost allocation problem in agriculture. After recalling the conceptual framework of the estimation of agricultural production costs, the first part presents the empirical data model, the quantile regression approach and the interval data techniques used as symbolic data analysis tools. The second part presents the comparative analysis of the econometric results for wheat between twelve European member states, using principal component analysis and hierarchic clustering of estimates and range of estimation intervals, discussing the relevance of the displays obtained for inter-country comparisons based on specific productivity.
Keyword: agricultural production, cost allocation, micro-economics, quantile regression, symbolic data analysis, confidence intervals

1 Conceptual framework and methodological aspects of cost allocation

Successive reforms of the Common Agricultural Policy (**CAP**), the integration of agriculture in the 28 Member States resulting from enlargement of the European Union (**EU**) have raised both in the context of competitive markets as markets subject to regulation, recurring needs for estimating costs of production of major agricultural products. The analysis of agricultural production costs, whether retrospective or prospective, is also a tool for analyzing margins for farmers. It allows to assess the price competitiveness of farmers, one of the major elements for development and sustainability of food chains in the European regions. Thus, the estimation of production costs provides partial but certainly needed lightings on the issues raised by the adaptation of European agriculture to the context of agricultural markets, whether they are national, European or international.

17th *ASMDA Conference Proceedings, 6 - 9 June 2017, London, UK*

Given these issues, in contexts of either ex ante or ex post scenarios, for evaluation of eventual options of public agricultural policy, we must be able to provide information on the entire distribution of production costs and to meet the needs of simulations and impact assessment in the various common market organizations. In this perspective, based on the observation of asymmetry and heteroskedasticity within the empirical distribution of agricultural inputs, we propose a methodology adapted to the problem of estimating the specific costs of production for the main agricultural products in a European context where agricultural holdings remain mainly oriented towards multiple productions, despite a preponderance of farms specializing in some of the more integrated agricultural production sectors.

To this end, we propose a methodology to obtain and analyze estimates of these quantile specific costs that are conditioned by the product mix of farmers. To demonstrate the relevance of this approach, we will apply this methodology to estimate the specific costs of wheat, agricultural commodity most commonly produced in the EU28, to a set of twelve European countries (**EU12**) where this production is significant in 2006.

We first present the empirical estimation of specific production cost model derived from an econometric approach to cost allocation, using a microeconomic model to build an input-output matrix (Divay and Meunier [6]). Second, we introduce the methodology for estimating conditional quantiles as proposed by Koenker and Bassett [8]. Third, we present the symbolic data analysis tools used in our procedures, mainly based on the concepts and methods described in Bock and Diday [1], using symbolic principal component and divisive clustering analyses. Fourth, the various displays provided by these symbolic tools are commented and discussed based on the conditional quantile estimates obtained for wheat production at the European level. Eventually, we conclude on the effectiveness of this approach for the wheat production with a proposal to extend it to other main agricultural products.

2 The empirical model of specific production cost estimates

In the EU-Farm Accounting Data Network (**FADN**) survey, the input recording occurs in aggregated form at the farm level and does not provide direct estimates of production costs incurred by each agricultural commodity produced. In contrast, the EU-FADN survey provides at the farm level, on one hand, the amount of gross product generated by each of the various commodities and, on the other hand, the sum of expenses for all the specific agricultural inputs recorded. So, it becomes possible to estimate, with an econometric model regressing the specific inputs on the gross products, the allocation coefficients of agricultural inputs to the main agricultural products, denoted as "specific coefficients" of production.

Following Desbois, Butaut and Surry [5], the econometric model decomposes linearly *x* the sum of specific inputs for each farm holding *i* according to the gross product *Y* of each agricultural commodity *j*, expressed by the following stochastic equation:

$$x_i = \sum_{j=1}^{P} \gamma_j Y_i^j + \varepsilon_i \; with \; \varepsilon_i \; iid \qquad (\mathbf{1}).$$

3 The conditional quantile estimation

To take into account the intrinsic heterogeneity of the distribution of the specific costs, we estimate the specific production coefficients of equation (1) accordingly with the methodology of quantile regression (Koenker and Bassett [8]), the solution being expressed in terms of conditional quantile of order *q*:

$$\hat{\mu}_q(i) = \sum_{j=1}^{P} \hat{\gamma}_j^{(q)} Y_i^j \qquad (\mathbf{2})$$

As [2], we assume that the data generator process is a linear model with multiplicative heteroscedasticity characterized in matrix form by:

$$x = Y'\beta + u \text{ with } u = Y'\alpha \times \varepsilon \quad \text{and} \quad Y'\alpha > 0 \qquad (\mathbf{3})$$

where $\varepsilon \sim iid[0, \sigma]$ is a random-vector identically and independently distributed with zero mean and constant variance σ^2. Under this assumption,

$$\mu_q(x|Y, \beta, \alpha),$$

the q^{th} conditional quantile of the production cost *x*, the production cost, conditioned by *Y* and the α and β parameters, is derived analytically as follows:

$$\mu_q(x|Y, \beta, \alpha) = Y'[\beta + \alpha \times F_e^{-1}(q)] \qquad (\mathbf{4}),$$

where F_ε is the cumulative distribution function (CDF) of the errors.

At least, two kinds of model can be distinguished:

i) $x = Y'\beta + u$ with $u = K\epsilon$, homoscedastic errors $V(\epsilon|Y) = \sigma^2$, denoted as the *location-shift* model, *i.e*. the linear model of conditional quantile with homogeneous slopes; while $Y'\alpha = K$ is constant, the conditional quantiles $\mu_q(x|Y, \beta, \alpha) = Y'\beta + KF_e^{-1}(q)$ get all the same slope, but differ only by a constant gap, growing as *q*, the quantile order, increases;

ii) $x = Y'\beta + (Y'\alpha) \times \varepsilon$ and $Y'\alpha > 0$ with heteroscedastic residuals, referred as the *location-scale shift* model, *i.e*. the linear model of heterogeneous conditional quantile slopes.

Weighted conditional quantiles were proposed as weighted L-estimates in heteroscedastic linear models (Koenker and Zhao [9]) defined by the weighting $\{\omega_i; i = 1, \cdots, n\}$. Those weights correspond to the inverse of the FADN sampling frequency in order to ensure the country representativeness of the estimates.

The observation weighting leads to a quantile regression scheme solving the minimization problem (**5**):

$$\hat{\beta}_{\omega}(q) = \underset{\beta \in R^p}{Argmin} \left\{ \sum_{i; y_i \geq x_i' \beta} [\omega_i q | y_i - x_i' \beta|] + \sum_{i; y_i < x_i' \beta} [\omega_i (1-q) | y_i - x_i' \beta|] \right\}$$

Given the FADN sample size and its non-random selection, we opt for the method of resampling based procedure based on the Markov Chain Marginal Bootstrap (**MCMB**) because no assumption on distributions of hazards is needed; this method gives robust empirical confidence intervals in a reasonable computation time (He and Hu [7]).

4 Symbolic analyses of the empirical distributions of specific costs

The symbolic data analysis tools used in this paper are mainly based on the vertices principal component analysis (**V-PCA**, Cazes *et al*. [3]) and the PCA of the range transformation of interval data (**RT-PCA**, Lauro and Palumbo [10]), with the divisive clustering method (Chavent [4]) chosen to ensure the best mathematical coherency for the display and analysis of the conditional quantile estimates.

Let us denote $\Delta = \{\partial_1, \cdots, \partial_i, \cdots \partial_n\}$, the empirical distributions of specific costs, as symbolic objects described by a set of *p* conditional quantile estimators $X = \{x_1, \ldots, x_j, \ldots, x_p\}$. for *p*=6 give the following quantile estimates $\{Q_{0,10}, Q_{0,25}, Q_{0,50}, Q_{0,75}, Q_{0,90}\}$. This feature is referred to as the quality criterion. The [*inf ; sup*] estimation intervals of MCMB conditional quantiles are denoted $\underbrace{\widetilde{x_{ij}}} = \left[\underbrace{x_{ij}}; \widetilde{x_{ij}}\right]$.

These estimation intervals can be represented by the pair $(m_{ij}; z_{ij})$ where m_{ij} is the conditional central estimate, and $\bar{z_i^j} = \widetilde{x}_{ij} - \underbrace{x_{ij}}$ is the interval range transformation.

However, because the MCMB intervals are not symmetric, we shall rather consider the hyper-volume, associated with the description of the Symbolic Objects (**SO**),

$\delta_i, 1 \leqslant i \leq N,$

computed as the Cartesian product $z_i^j \times \cdots \times z_i^j \times \cdots \times z_i^p$ of the *p* associated quantile descriptors.

The Description Potential (**DP**) measurement is defined by:

$$\pi(\omega_i) = \prod_{j=1}^{p} \mu\left(\bar{z}_i^j\right) \quad (6)$$

where is the normalized range with respect to the domain s_j. However, if the measurement of one of the descriptors tends to zero, then the DP tends to zero.

To overcome this problem, the Linear Description Potential (**LDP**), is used by De Carvalho [11] for the instance a_i of symbolic object δ_i, as:

$$(a_i) = \sum_{j=1}^{p} \mu\left(\bar{z}_i^j\right) \quad (7).$$

The Range Transformation Principal Component Analysis (RT-PCA) is defined by the factorial decomposition of the total LDP:

$$LDP_{tot} = \sum_{i=1}^{n} \sigma(a_i) \quad (8),$$

allowing a geometric representation of hyper-volumes in which the *inf* vertices are translated to the origin. With regards to the orthogonality between couples of sides of each hypercube, the search of the optimal subspace to visualize the size and the shape of each quantile distribution as a SO can be implemented by a non centered PCA with respect to the *sup* vertices. The non centered PCA performed on the matrix $\sqrt{\bar{z}_i^j}$ is decomposing the LDP_{tot} criterion.

Hence, our mixed strategy of PCA of the distribution of specific costs (**DSC-PCA**) combines the V-PCA and the RT-PCA in the three steps approach of the symbolic PCA defined by Lauro and Palumbo [10], to take into account the differences in scale and shape between empirical distributions of specific costs.

Also based on the estimation intervals of conditional quantiles, we use **DIV**[1], a divisive hierarchical clustering procedure (Chavent [4]), to obtain criteria for classifying countries according to their specific wheat costs.

The DIV evaluation criterion of the partition P_K with K clusters

$P_K = (C_1, \cdots, C_k, \cdots, C_K)$

is the sum of the homogeneity indices, such as:

$$W(P) = \sum_{C_k \in P} Q(C_k) \quad (9),$$

with the homogeneity index $Q(C_k) = \frac{1}{2n_k} \sum_{\omega_i \in C_k} \sum_{\omega_j \in C_k} d^2\left(\delta_i, \delta_j\right)$,

and the euclidean distance $d(\omega_i, \omega_k) = \left(\sum_{j=1}^{p} d_j^2 \left(\underbrace{\overbrace{x_i^j}}, \underbrace{\overbrace{x_k^j}} \right) \right)^{1/2}$.

[1] DIV is the divisive hierarchical clustering procedure of the **Sodas 2.5** software

5 The visualization and the analysis of econometric results

In 2010, according to Eurostat estimates, the EU27 accounts for 21% of world wheat production. The EU12 countries are among the largest producers in terms of amounts collected, descending countries: France (FRA, 27.9%), Germany (DEU, 17.6%), United Kingdom (UKI, 10.9%), Poland (POL, 6.9%), Italy (ITA, 5.0%), Spain (ESP, 4.3%), Denmark (DNK, 3.7%), Hungary (HUN, 2.7%), Sweden (SVE, 1.6%), Belgium (BEL, 1.4%), and (1.1%) for Austria (OST) and Netherlands (NLD), either 84.3% of the European production.

The Table 1 presents estimates of conditional quantiles (the first decile D1, the lower quartile Q1, the median Q2, the upper quartile Q3, the ninth decile D9) for wheat production costs, issued from Surry, Desbois and Butault [12]. They are issued from the quantile regression of specific agricultural production costs (the SE281 accounting aggregate in EU-FADN) based on the decomposition of the gross product among fifteen speculations, for a subset of 12 European countries (EU12) in 2006.

Tab. 1. The Specific Cost Estimates (€) for 1 000 € of Wheat Gross Product, EU12-FADN 2006.

Country	D1	Q1	Q2	Q3	D9
BEL	364	407	407	506	691
DNK	220	265	363	437	543
DEU	284	285	320	335	372
ESP	228	226	252	333	560
FRA	345	392	449	491	563
HUN	209	247	342	354	427
ITA	164	238	335	378	471
NLD	144	207	295	489	771
OST	204	239	277	250	305
POL	266	293	347	420	523
SVE	368	285	349	437	597
UKI	293	302	357	396	460

Source: FADN-based author's computations,

The visualization of the relative position of countries is provided by the first factorial plan (figure 1) from the V-PCA of point estimates, accounting for 90.7% of total inertia. Accounting for 64.4% of total inertia, the first principal component F1 is a size axis positively correlated (> 0.77) to all conditional estimators, especially to Q2 (0.89), and Q1 (0.90). The second principal component F2, accounting for 26.3% of total inertia, is positively correlated with D9 (0.81) and Q3 (0.52) and negatively D1 (-0.45) and Q1 (-0.37).

The hierarchical clustering procedure[2] gives two interesting partitions at low level of semi-partial R squared, P4 (8%) and P5 (4%), projected on first factorial plan (figure 2): {NLD} with highest D9 estimate, {BEL, FRA} with highest Q2 estimates, {OST, DEU} the lowest D9 estimates, {ESP, ITA, HUN} with Q2 lower values than {DNK, POL, SVE, UKI} characterised by more central estimates.

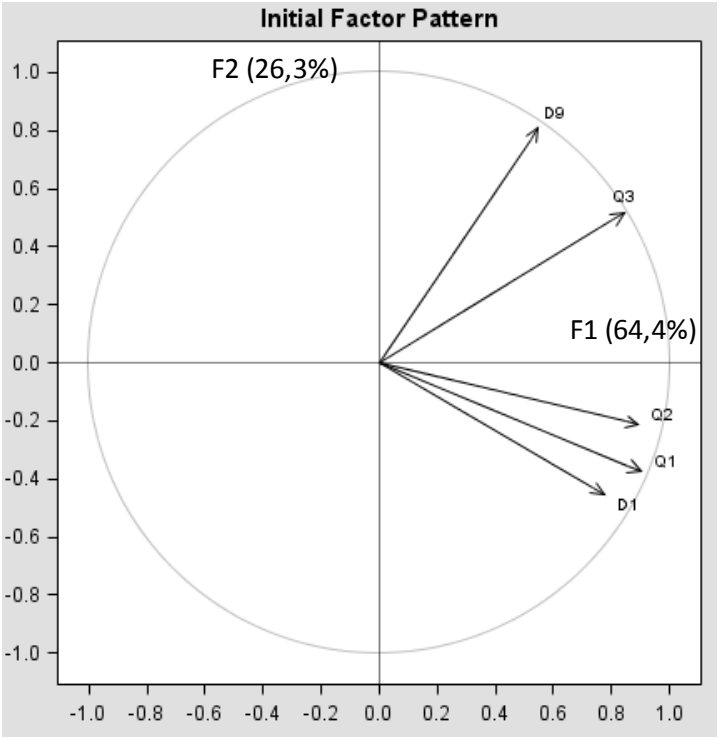

Fig. 1. The First Factorial Plan (F1xF2) of the V-PCA, with the Conditional Quantile Projections (D1, first decile; Q1, lower quartile; Q2, median; Q3, upper quartile; D9, ninth decile)
Source: FADN-based author's computations

[2] The 'proc CLUSTER' procedure of the SAS software.

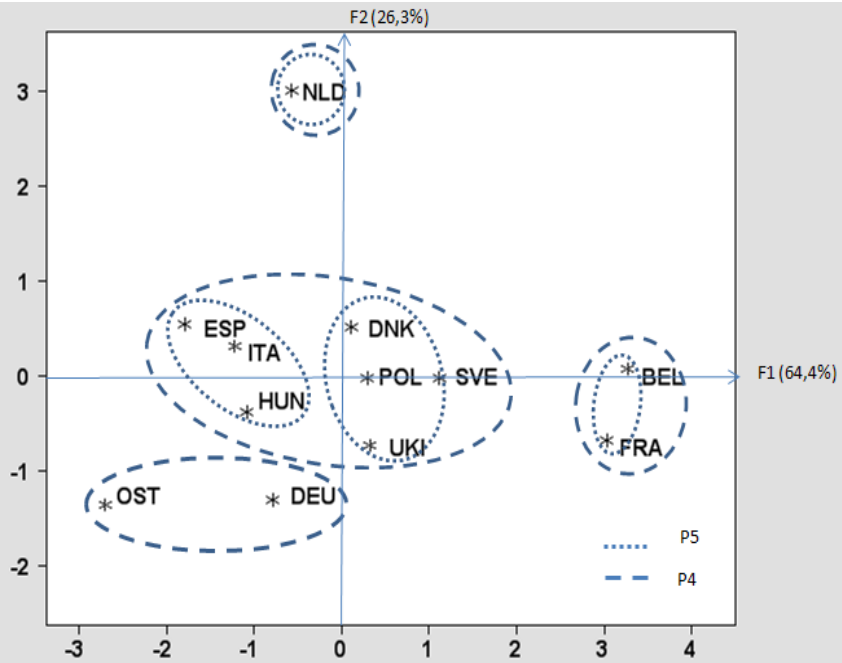

Fig. 2: The First Factorial Plan (F1xF2) of the V-PCA, with the Empirical Distributions of EU-12 Countries

Source: FADN-based author's computations

However, the RT-PCA of the interval ranges gives complementary information (figure 3).

SPCA - Variables Int Coordinates

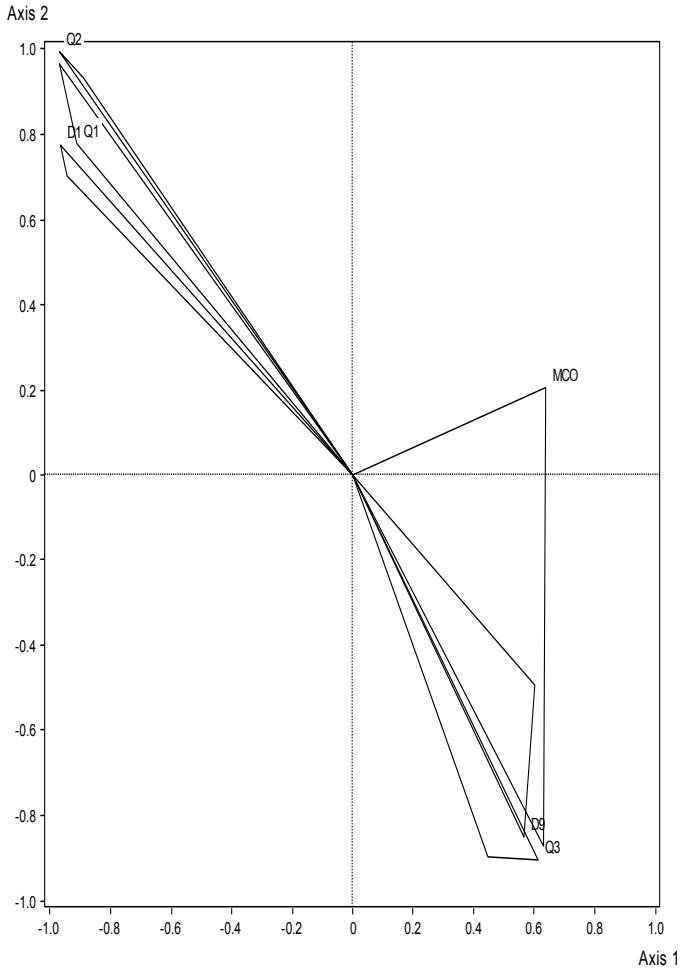

Fig. 3. The,RT-PCA of Empirical Distributions of Specific Costs, with the Projected Interval Coordinates of Quantile Estimates.
Source: FADN-based author's computations

For the F1 component, only the correlation interval of D9 is strictly positive ([0.260, 0.990]); all other correlations intervals contain origin. Meanwhile, the radii of correlation intervals of D1 and Q1 are the highest ones (0.87 and 0.88 respectively). Hence, examination of F1 correlation projections identifies D9 as an estimator indicating heteroscedasticity for conditional distributions while

appear similarities along F2, involving D1 and Q1 as indicators of skewness by lower estimates, and Q3 and D9 as indicators of skewness by higher estimates.

On the first factorial plane of symbolic objects (figure 4), rectangle of France (FRA), consisting of the projections of the edges of estimate hyper-rectangle parallel to the first two principal components, differs from that of Germany (DEU), this which means specific differences in costs both in terms of scale (along Axis1, the first principal component, whose central dispersion rather reflects the differences between median estimates) and in shape of specific costs distributions (along Axis 2, the second principal component, opposing the estimates of lower quantiles to those of the upper quantiles).

The distributional ranges may partially overlap on the lowest quantiles as indicated by the positions of the projected hyper-rectangles of Austria (OST) and France (FRA). Note also the projection of the Netherlands (NED) hyper-rectangle that includes all other projected hyper-rectangles, indicating the most heterogeneous distribution, followed in this by Sweden (SVE) and Belgium (BEL) projected rectangles whose lengths according Axis 1 are among the largest. Hence, DSC-PCA can be used as a procedure to characterize distributions of specific costs: Netherlands, Sweden and Belgium are associated to the location-scale shift model while other countries are rather belonging to the location-shift (homogeneous) model.

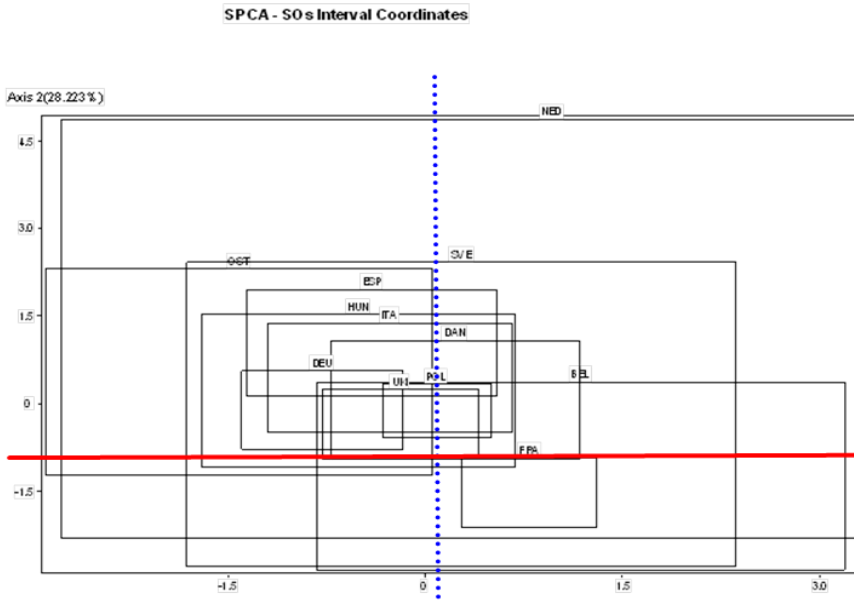

Fig. 4. The RT-PCA of Empirical Distributions of Specific Costs, with the Projected Hyper-Rectangles of EU12 Countries

Source: FADN-based author's computations

The divisive clustering procedure (Chavent [4]), applied to the confidence intervals of the quantile estimates, confirms these differences and similarities indicating the cost structure to the classes of countries (figure 5).

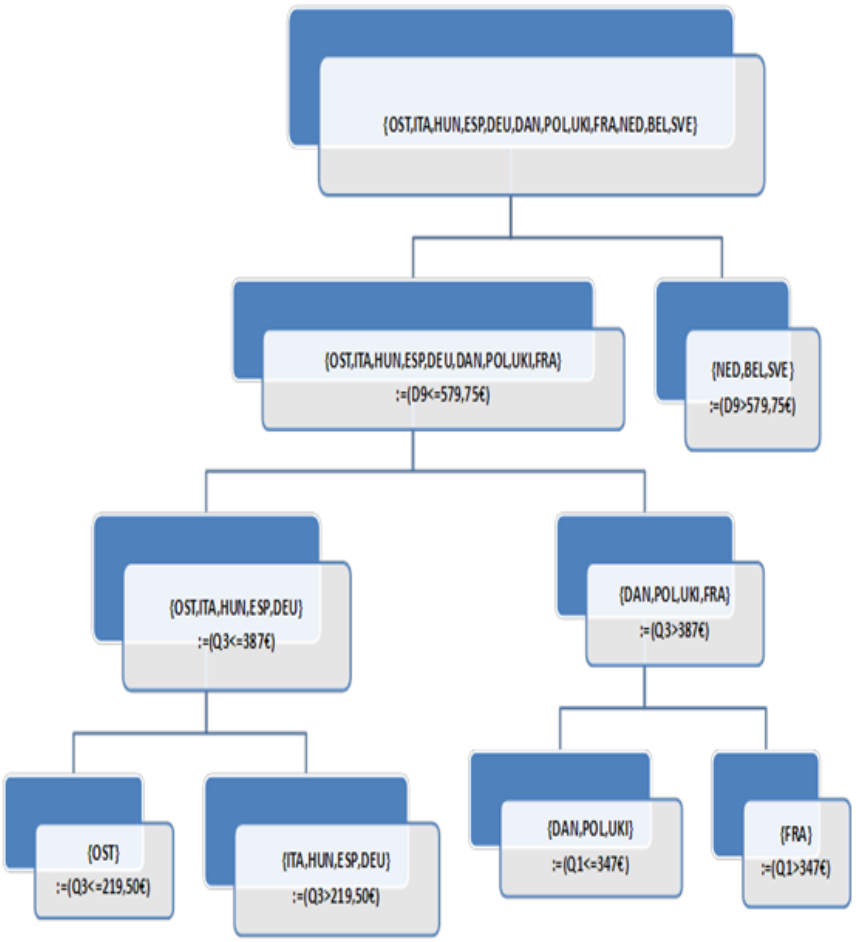

Fig. 5: The Interval Divisive Hierarchical Clustering of Empirical Distributions of Specific Cost, with the EU-12 Countries, 2006.
Source: FADN-based author's computations

First, at the first node of the divisive tree, comes a major distinction between location distributional scales: on one hand (the triplet {NED, BEL, SVE} whose D9 conditional quantiles of specific costs exceed € 579.75) and, on the other hand, other countries whose ninth decile estimates are less or equal to that value.

Second, at the bottom of the tree, the divisive clustering algorithm highlights a partial order, authorizing some local rankings based on the conditional first decile (D1): a first local ranking, between Italy, Hungary, Spain and Germany; a second one between Poland and the United Kingdom; and a third one, between the Netherlands, Belgium and Sweden.

These local rankings can be used in inter-country comparison for the purpose of specific productivity assessment, in the context of an increasingly competitive wheat market.

6 Conclusion

In this paper, we proposed a symbolic data analysis approach in order to display the distributions of quantile conditional estimates. We apply this approach to the specific costs of production for wheat in twelve European countries. This case study demonstrates the relevance of our approach in allowing the identification of significant differences particularly between France and Germany, two of the main European producers of wheat.

With regards of location and shape of the conditional quantile estimated distribution, the national differences are mainly based on the highest conditional decile and quartile, displaying the skewness by the greatest values of the empirical distribution of conditional quantile estimates.

The skewness of conditional quantile distributions for wheat production cost being inherited from the heterogeneity of conditions and techniques in agricultural production among European producers, we propose to extend our approach to other main agricultural products such as cow milk and pig.

Acknowledgement

This research has received funding from the 7th Framework Program of the European Community (FP7 / 2007-2013) under the authorization n° 212292.

References

1. H. Bock, and E. Diday. Analysis of Symbolic Data: Exploratory Methods for Extracting Statistical Information from Complex Data. Berlin, Springer-Verlag, 2000.
2. A. C. Cameron, and P. K. Trivedi. Microeconometrics. Methods and Applications. Cambridge, Cambridge University Press, 2005.
3. P. Cazes, A. Chouakria, E. Diday, and Y. Schektman. Extension de l'analyse en composantes principales à des données de type intervalle, Revue de statistique appliquée, 45(3): 5-24, 1997.
4. M. Chavent. A monothetic clustering method, Pattern Recognition Letters, 19: 989-996, 1998.
5. D. Desbois, J.-P. Butault, and Y. Surry (2015) Distribution des coûts spécifiques de production dans l'agriculture de l'Union européenne : une approche reposant sur la méthode de régression quantile, 9es Journées de Recherches en Sciences Sociales, December 10th-11th, 2015.
6. J.F. Divay, and F. Meunier: Deux méthodes de confection du tableau entrées-sorties. Annales de l'INSEE, 37:59-109, 1980.
7. X. He, and F. Hu. .Markov Chain Marginal Bootstrap, Journal of the American Statistical Association , 97:783-795, 2002.
8. R. Koenker, and G. Bassett. Regression quantiles. Econometrica, 46 : 33-50, 1978.
9. R. Koenker, and Q. Zhao. L-estimation for linear heteroscedastic models. Journal of Nonparametric Statistics, 3: 223-235, 1994.
10. C.N. Lauro, and F. Palumbo. Principal component analysis of interval data: a symbolic data analysis approach, Computational Statistics, 15(1): 73-87, 2000.
11. F. A. T. De Carvalho. Clustering of constrained symbolic objects based on dissimilarity functions, Indo–French Workshop on Symbolic Data Analysis and its Applications, University of Paris IX, 1997.
12. Y. Surry, D. Desbois, and J.-P. Butault. Quantile Estimation of Specific Costs of Production. FACEPA, D8.2, 2012.

Optimal control of a pest population through geometric catastrophes

Theodosis D. Dimitrakos[1], Epaminondas G. Kyriakidis[2]

[1] Department of Mathematics, University of the Aegean, Karlovassi 83200 Samos, Greece (E-mail: dimitheo@aegean.gr)

[2] Department of Statistics, Athens University of Economics and Business, Patission 76, 10434 Athens, Greece (E-mail: ekyriak@aueb.gr)

Abstract. We study the problem of controlling the stochastic growth of a bounded pest population by the introduction of geometric catastrophes. The damage done by the pests is represented by a cost. Another cost is also incurred when the controlling action of introducing geometric catastrophes to the population is taken. It is assumed that the catastrophe rate is constant. We aim to find a stationary policy which minimizes the long-run expected average cost per unit time. A semi-Markov decision formulation of the problem is given. It seems intuitively reasonable that the optimal policy is of control-limit type, i.e. it introduces geometric catastrophes if and only if the pest population is greater than or equal to a critical size. Although a rigorous proof of this assertion is difficult, a computational treatment of the problem is possible. Various Markov decision algorithms are implemented for the computation of the optimal policy. From a great number of numerical examples that we have tested, there is strong evidence that the optimal policy is of control-limit type.

Keywords: Pest control, Geometric catastrophes, Semi-Markov decision process, Control-limit policy, Markov decision algorithms

1 Introduction

In the last four decades, several articles have appeared dealing with population processes under the influence of catastrophes. The stochastic growth of a population has been successfully modeled by using various suitable birth/immigration/emigration-death processes. It is assumed that the catastrophe of a population may have different forms. The considered population may be controlled by some action which initiates a specific type of catastrophes.

An interesting problem that arises in biological population models controlled by catastrophes is related to the computation of a stationary policy which satisfies a predefined optimality criterion. A usual optimality criterion is the minimization of the long-run expected average cost per unit time. In some of these problems, it can be shown that the optimal stationary policy initiates the controlling action of introducing a type of catastrophe to the population if and only if the size of the biological population is greater than or equal to a critical

17th *ASMDA Conference Proceedings, 6 - 9 June 2017, London, UK*

level. Such a policy is usually called control-limit policy and the critical level is called the control-limit. The semi-Markov decision process and the Markov decision process in continuous time are appropriate mathematical models for the description of the stochastic growth of biological populations controlled by catastrophes.

The simplest form of catastrophes is the so-called total catastrophes. When such a type of catastrophes is initiated into a population then the entire population is annihilated. In the article of Kyriakidis and Abakuks [6], a simple immigration-birth process was considered to represent the stochastic growth of a pest population. It was assumed that the pest population may be controlled by an action which introduces total catastrophes. A Markov decision process in continuous time was considered and the stationary policy which minimizes the long-run expected average cost per unit time was found. It was proved that the optimal stationary policy belongs into the class of control-limit policies according to which the controlling action of introducing total catastrophes is taken if and only if the size of the pest population is greater than or equal to a critical value. In Kyriakidis [9], the problem of controlling a simple immigration-birth-death process, which represents a pest population by the introduction of total catastrophes was assumed. A suitable semi-Markov decision formulation was given which enabled the author to numerically compute the optimal policy. By applying the standard policy iteration algorithm there is strong numerical evidence that the optimal policy has a control-limit form. Economou [3] proved that the optimal policy in the problem of controlling a compound immigration process through total catastrophes is of control-limit type. In Kyriakidis and Dimitrakos [10] the same problem as in Economou's paper was studied and it was further showed that the average cost of a control-limit policy is unimodal as a function of the critical population size. This result enabled the authors to design efficient Markov decision algorithms for the numerical computation of the optimal control-limit policy.

In population processes under the influence of total catastrophes, except for the computation of the optimal policy, alternative interesting problems are also studied. Various papers deal with the computation of important descriptive measures for the population, such as its equilibrium probabilities and its extinction probability. In Kyriakidis [8], the stationary probabilities of a simple immigration-birth-death process under the influence of total catastrophes were derived using a renewal argument for the case in which the catastrophe rate is equal to one. In Swift [13], the transient probabilities for a simple immigration-birth-death process under total catastrophes were derived for the case in which the catastrophe rate is constant.

Alternative catastrophe mechanisms were introduced in the article of Brockwell *et al.* [2] in some Markov models which represent the stochastic growth of a population. In these models, it was assumed that the population size can be reduced by a random amount which was geometrically, binomially or uniformly distributed. Explicit formulas for some descriptive quantities of

interest were derived, such as the stationary distribution of the population size and the distribution of the time to population extinction. In Kyriakidis [7], an efficient special-purpose Markov decision algorithm was developed for the optimal control of the stochastic growth of a bounded pest population subjected to uniform catastrophes. There is strong numerical evidence that the designed algorithm converges to the optimal policy within the class of all stationary policies. The final policy obtained by the algorithm is of control-limit type. In Economou [4], a stochastic model was studied in which the population grows according to a compound Poisson process. Binomial catastrophes were initiated in the population. The equilibrium distribution of the process was studied and an algorithmic approach for its approximate computation was derived. In Artalejo *et al.* [1], an immigration process subjected to binomial and geometric catastrophes was studied. Explicit expressions was derived for some populations descriptors of interest such as, among others, the first population extinction time and the maximum population size reached between two consecutive extinctions. In Kapodistria *et al.* [5], a birth/immigration-death process under binomial catastrophes was studied and explicit expressions were obtained for the transient and equilibrium factorial moments which are then used to construct the transient and the equilibrium distribution of the population size.

In this article, we consider a pest population which grows stochastically according to a general birth process. The pest population is controlled by an action which introduces geometric catastrophes. Under an appropriate cost structure, a Markovian decision process is considered in which we aim to find a stationary policy which minimizes the long-run expected average cost per unit time.

The article is mainly concerned with a computational treatment of the problem and is organized as follows. In Section 2 we present the model and in Section 3 its semi-Markov decision formulation is given. In Section 4, we present two numerical examples by implementing various Markov decision algorithms such as the standard value iteration algorithm, the standard policy iteration algorithm and the modified policy iteration algorithm. From a great number of numerical examples that we have tested, there is strong evidence that the optimal stationary policy is of control-limit type.

2 The model

Consider a pest population which grows stochastically according to a general birth process in a habitat with carrying capacity N, where N is a positive integer. We assume that the birth rates $\lambda_i, 0 \le i \le N-1,$ are positive. The birth rate λ_N is necessarily equal to zero since it corresponds to the carrying capacity of the habitat. The damage done by the pests is represented by a cost $c_i \ge 0, 0 \le i \le N,$ for each unit of time during which the population size is equal

to i. It seems intuitively reasonable to assume that the sequence $\{c_i\}$ is non-decreasing and $c_0 = 0$. The pest population may be controlled by an action which introduces geometric catastrophes.

It is assumed that the rate γ of catastrophe is constant. If a catastrophe occurs, when the population size is $i, 1 \le i \le N$, the population size after the catastrophe is reduced to $j, 1 \le j \le i-1$, with probability $p(1-p)^{i-j-1}$ and is reduced to $j = 0$ with probability $(1-p)^{i-1}$, where $p \in (0,1)$.

Let the cost of taking controlling action be k per unit time where k is a positive number. Let also $f \equiv \{f_i\}, 0 \le i \le N$, denote a stationary policy under which the action f_i is taken when the process is in state i. It is assumed that $f_i = 1$ when the controlling action of introducing geometric catastrophes is being taken and $f_i = 0$ when the controlling action is not being taken. If the stationary policy $f \equiv \{f_i\}, 0 \le i \le N$, is employed, our assumptions imply that we have a continuous-time Markov chain model for the population growth of the pests with state space $S = \{0, \ldots, N\}$ and the following transition rates:

Transition	*Rate*
$i \to i+1$	$\lambda_i, 0 \le i \le N,$
$i \to j$	$\gamma p(1-p)^{i-j-1} f_i, \quad 1 \le i \le N, 1 \le j \le i-1,$
$i \to 0$	$\gamma(1-p)^{i-1} f_i, 1 \le i \le N.$

We consider a Markovian decision process in which we aim to find a stationary policy which minimizes the long-run expected average cost per unit time. An intuitively appealing class of policies is the class $\mathcal{P} \equiv \{P_x, 1 \le x \le N\}$, where P_x is the stationary policy according to which the controlling action of introducing geometric catastrophes is taken if and only if the population size is equal to or exceeds x. These policies are called control-limit policies. It seems intuitively reasonable that the optimal policy is of control-limit type. Although it seems difficult to give a rigorous proof of this assertion, a computational treatment of the problem is possible by applying various Markov decision algorithms.

3 Formulation as a semi-Markov decision model

Let $p_{ij}(a)$ be the probability that the next state of the process will be j given that the action $a \in \{0,1\}$ is taken in the present state $i, 0 \le i \le N$ and let $T(i,a)$ and $C(i,a)$ be the corresponding one-step expected transition time and cost, respectively. We assume that $a = 1$ when the controlling action which introduces geometric catastrophes is being taken and $a = 0$ when the controlling action is not being taken. These quantities are given below.

Non-zero one-step transition probabilities

$$p_{01}(0) = 1,$$

$$p_{i,i+1}(0) = 1, 1 \le i \le N-1,$$

$$p_{i,i+1}(1) = \frac{\lambda_i}{\lambda_i + \gamma}, 1 \le i \le N-1,$$

$$p_{ij}(1) = \frac{\gamma p(1-p)^{i-j-1}}{\lambda_i + \gamma}, 1 \le i \le N-1, 1 \le j \le i-1,$$

$$p_{i0}(1) = \frac{\gamma(1-p)^{i-1}}{\lambda_i + \gamma}, 1 \le i \le N-1,$$

$$p_{Nj}(1) = p(1-p)^{N-j-1}, 1 \le j \le N-1,$$

$$p_{N0}(1) = (1-p)^{N-1}.$$

One-step expected times

$$T(i,0) = \lambda_i^{-1}, 0 \le i \le N-1,$$

$$T(i,1) = (\lambda_i + \gamma)^{-1}, 1 \le i \le N-1,$$

$$T(N,1) = (\lambda_N + \gamma)^{-1} = \gamma^{-1}, \text{ since } \lambda_N = 0.$$

One-step expected costs

$$C(0,0) = 0,$$

$$C(i,0) = c_i \lambda_i^{-1}, 1 \le i \le N-1,$$

$$C(i,1) = (c_i + k)(\lambda_i + \gamma)^{-1}, 1 \le i \le N-1,$$

$$C(N,1) = (c_N + k)(\lambda_N + \gamma)^{-1} = (c_N + k)\gamma^{-1}, \text{ since } \lambda_N = 0.$$

Based on the above semi-Markov decision formulation, a direct implementation of the standard Markov decision algorithms (e.g. standard value iteration algorithm, standard policy iteration algorithm) and of the modified policy iteration algorithm is possible. For a detailed description of these algorithms we refer, for example, to the books of Puterman [12] (see Ch. 6, pp. 185-195) and Tijms [14] (see Ch. 7, pp. 284-286).

4 Numerical results

In this section, we present two numerical examples. We implemented the standard value iteration algorithm, the standard policy iteration algorithm and the modified policy iteration algorithm by running the corresponding Matlab program on a personal computer equipped with an Intel Core i5-3230M, 2.6 GHz processor and 4 GB of RAM. In all examples that we have tested, there is strong numerical evidence that the optimal stationary policy has a control-limit form.

Example 1. We assume that the pest population grows according to the Prendiville process (see e.g. Nasell (2011), Section 2.4, pp. 14-15), where the birth rates λ_i are given by $\lambda_i = v\left(1 - \frac{i}{N}\right)$, $0 \le i \le N$, where v is a positive constant. The cost rate of the damage done by the pests is assumed to be $c_i = i$. We also assume that $N = 50, v = 12, k = 15$ and $p = 0.3$. The rate of the catastrophe is assumed to be $\gamma = 5$. The control-limit policy P_N according to which the controlling action is being taken only in state N is chosen as the initial stationary policy in the initial step of the standard policy iteration algorithm. Note that if the process is never controlled the long-run average cost per unit time is equal to c_N (i.e. equal to 50 in our example), since state N is an absorbing state in this case. In Table 1, we present the successive control-limit policies P_x generated by the algorithm and their average costs. As it can be seen in the second row of Table 1 from the value of the average cost of the policy P_N which is equal to 43.5218, the policy P_N achieves a considerably

smaller average cost than the policy of never controlling. The optimal policy was obtained after 5 iterations of the algorithm.

Table 1. The successive control-limit policies P_x generated by the policy iteration algorithm

Critical value x	Average cost g_x
50	43.5218
1	18.1925
6	17.3070
3	16.8772
4	16.8314

Thus, there is strong numerical evidence that the optimal policy obtained by the algorithm is the control-limit policy P_4 according to which the controlling action of introducing geometric catastrophes is taken if and only if the population size is equal to or exceeds the critical value $x^* = 4$. The value of the minimum average cost is approximately equal to 16.8314. We also choose $\varepsilon = 10^{-3}$ as the tolerance number for the stopping criterion of the standard value iteration algorithm. The algorithm is terminated after 584 iterations. Choosing the same value of the tolerance number ε as in the standard value iteration algorithm, the modified policy iteration algorithm is stopped after only 22 iterations. This significant difference in the number of iterations between the two algorithms is consistent with the report of Puterman's [12] book in p. 193, according to which the implementation of modified policy iteration requires little additional programming effort yet attains superior convergence to value iteration algorithm.

In Table 2, for $\gamma = 10$ and for each value of p, we present the critical values x^* of the optimal control-limit policies P_{x^*} obtained by the value iteration algorithm and by the modified policy iteration algorithm, their minimum average costs g_{x^*} the required number of iterations of the value-iteration algorithm (Iterations 1) and the required number of iterations of the modified policy iteration algorithm (Iterations 2).

Table 2. The optimal control-limit policies P_{x^*} for each value of p

p	x^*	g_{x^*}	Iterations 1	Iterations 2
0.1	4	6.7464	105	10
0.2	4	7.9757	167	13
0.3	3	9.3643	234	15
0.4	3	10.8265	312	18
0.5	3	12.5068	404	20
0.6	2	14.2123	529	24
0.7	2	16.2156	679	27
0.8	1	18.5118	881	32
0.9	1	21.0820	1107	36

We observe that, as p increases, the critical number x^* that corresponds to the optimal control-limit policy P_{x^*} decreases.

In Figure 1, we present a graph that shows the variation of the minimum average cost as the probability p takes values in the set $\{0.1,\ldots,0.9\}$. We see that, as p increases, the minimum average cost increases rather linearly.

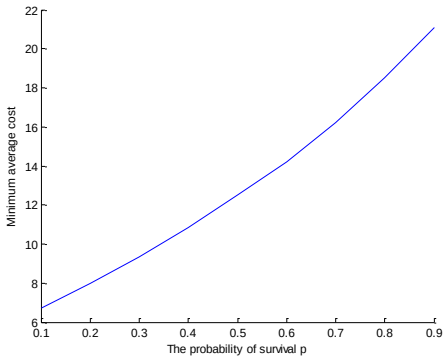

Fig. 1. The minimum average cost as parameter p varies

In Table 3, we present the optimal critical value x^* obtained by the Markov decision algorithms and the corresponding average cost g_{x^*} obtained by the policy iteration algorithm for various values of the parameters γ, v and k.

Table 3. The optimal control-limit policy P_{x^*}

A. The effect of varying γ for $p = 0.3$, $v = 12$ and $k = 15$

γ	Critical value x^*	Minimum cost g_{x^*}
0.5	50	48.7576
1	50	47.1361
5	4	16.8314
10	3	9.3598
20	3	5.4743

B. The effect of varying v for $p = 0.3$, $\gamma = 5$ and $k = 15$

v	Critical value x^*	Minimum cost g_{x^*}
1	2	2.4166
2	2	4.0931
5	3	8.0895
10	4	14.3120
20	4	27.1417

C. The effect of varying k for $p = 0.3$, $\gamma = 5$ and $v = 12$

k	Critical value x^*	Minimum cost g_{x^*}
5	2	9.3847
10	3	13.2115
15	4	16.8314
20	4	20.3035
25	5	23.6474

From Table 3, it can be seen that the optimal critical value x^* decreases as the catastrophe rate γ increases and the minimum average cost g_{x^*} decreases as γ increases. It can also be seen that the optimal critical value x^* increases as v and k increase and the minimum average cost g_{x^*} increases as v and k increase. ■

Example 2. We assume that the pest population grows according to the same Prendiville process, as in Example 1. The cost rate is now assumed to be $c_i = \sqrt{i}$. We also assume that $N = 60, v = 10, k = 16$ and $p = 0.4$. The rate of the catastrophe is assumed to be $\gamma = 15$. The control-limit policy P_1 is chosen as the initial stationary policy in the initial step of the standard policy iteration algorithm. In Table 4, we present the successive control-limit policies P_x generated by the algorithm and their average costs. The optimal policy was obtained after 7 iterations of the algorithm.

Table 4. The successive control-limit policies P_x generated by the policy iteration algorithm

Critical value x	Average cost g_x
1	8.1927
60	7.7555
2	6.6896
10	6.5482
3	6.2246
5	6.0973
4	6.0931

Thus, there is strong numerical evidence that the optimal policy obtained by the algorithm is the control-limit policy P_4 according to which the controlling action of introducing geometric catastrophes is taken if and only if the population size is equal to or exceeds the critical value $x^* = 4$. The value of the minimum average cost is approximately equal to 6.0931. We also choose $\varepsilon = 10^{-3}$ as the tolerance number for the stopping criterion of the standard value iteration algorithm. The algorithm is terminated after 278 iterations. Choosing the same value of the tolerance number ε as in the value iteration algorithm, the modified policy iteration algorithm is stopped after only 27 iterations.

In Figure 2, for $p = 0.1$, we present a graph that shows the variation of the critical number x^* that corresponds to the optimal control-limit policy P_{x^*}, as the parameter k takes values in the set $\{2, 4, \ldots, 58, 60\}$.

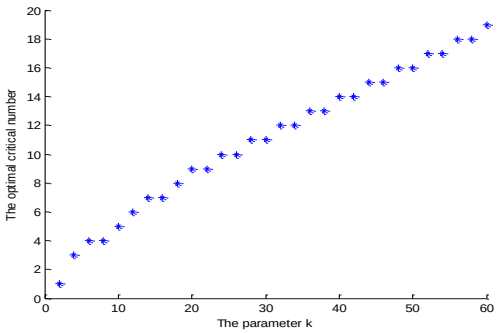

Fig. 2. The variation of the optimal critical number x^* as parameter k varies

We observe that, as k increases, the critical number x^* that corresponds to the optimal control-limit policy P_{x^*}, increases. When k takes values in the set $\{2,\ldots,10\}$, the critical number x^* increases rather rapidly while when k takes values in the set $\{12,\ldots,60\}$, the critical number x^* increases slowly.

In Figure 3, again for $p = 0.1$, we present a graph that shows the variation of the minimum average cost as the cost rate k of taking the controlling action that introduces geometric catastrophes takes values in the set $\{2,4,\ldots,58,60\}$.

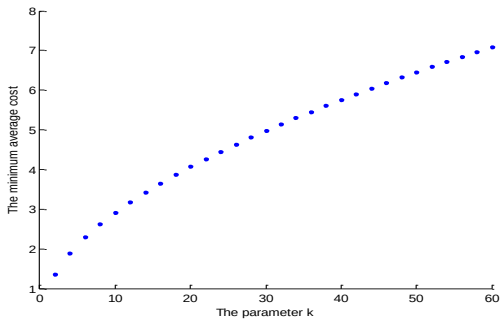

Fig. 3. The variation of the minimum average cost as parameter k varies

We observe that, as k increases, the minimum average cost increases almost linearly. The minimum average cost increase rather rapidly for $k \leq 10$, while for $k > 10$, the minimum average cost increases slowly. ■

Conclusions

In this paper we considered the problem of controlling the stochastic growth of a bounded pest population by the introduction of geometric catastrophes. It was assumed that the cost rate caused by the pests is an increasing function of their population size and that the cost rate of the controlling action which introduces geometric catastrophes is constant. We sought a stationary policy which minimizes the long-run expected average cost per unit time. It seems reasonable that the optimal policy introduces geometric catastrophes if and only if the pest population is greater than or equal to a critical level. Although a proof of this assertion seems difficult, a computational treatment of the problem is possible based on a semi-Markov decision formulation of the model. We implemented various Markov decision algorithms for the computation of the optimal policy. From a great number of numerical examples that we have tested, there is strong evidence that the optimal policy belongs to the class of control-limit policies.

References

1. J.R. Artalejo, A. Economou and M.J. Lopez-Herero. Evaluating growth measures in populations subject to binomial and geometric catastrophes. Mathematical Biosciences and Engineering, 4, 573{594, 2007.
2. P.J. Brockwell, J. Gani and S.I. Resnick. Birth, immigration and catastrophe processes, Advances in Applied Probability, 14, 709{731, 1982.
3. A. Economou. On the control of a compound immigration process through total catastrophes, European Journal of Operational Research 147, 522{529, 2003.
4. A. Economou. The compound Poisson immigration process subject to binomial catastrophes, Journal of Applied Probability, 41, 508{523, 2004.
5. S. Kapodistria, T. Phung-Duc and J. Resing. Linear birth/immigration-death process with binomial catastrophes, Probability in the Engineering and Informational Sciences 30, Issue 1, 79{111, 2016.
6. E.G. Kyriakidis and A. Abakuks. Optimal pest control through catastrophes. Journal of Applied Probability, 27, 873{879, 1989.
7. E.G. Kyriakidis. A Markov decision algorithm for optimal pest control through uniform catastrophes, European Journal of Operational Research, 64, 38{44, 1993.
8. E.G. Kyriakidis. Stationary probabilities for a simple immigration/birth-death process under the influence of total catastrophes. Statistics & Probability Letters, 20, 239{240, 1994.
9. E.G. Kyriakidis. Optimal control of a simple immigration-birth-death process through total catastrophes. European Journal of Operational Research, 81, 346{356, 1995.
10. E.G. Kyriakidis and T.D. Dimitrakos. Computation of the Optimal Policy for the Control of a Compound Immigration Process through Total Catastrophes. Methodology and Computing in Applied Probability, 7, 97{118, 2005.
11. I. Nasell. Extinction and Quasi-stationarity in the Stochastic Logistic SIS Model. Lecture Notes in Mathematics, Vol. 2022, ISBN : 978-3-642-20529-3, Springer-Verlag, Berlin, Heidelberg, 2011.

12. M.L. Puterman. Markov Decision Processes : Discrete Stochastic Dynamic Programming, John Wiley & Sons, New York, 1994.
13. R.J. Swift. Transient probabilities for a simple birth-death-immigration process under the influence of total catastrophes, International Journal of Mathematics and Mathematical Sciences, 25 (10), 689{692, 2001.
14. H.C. Tijms. A First Course in Stochastic Models, Wiley, Chichester, 2003.

Modeling of EEG Signals by Using Artificial Neural Networks with Chaotic Neurons

Dmitrieva L. A., Kuperin Yu. A., Mokin P. V.

Saint Petersburg State University, 7/9 Universitetskaya emb., St. Petersburg, 199034, Russia
(E-mail: kuperin.yury@yandex.ru)

Abstract. The aim of this paper is to use artificial neural networks in order to generate time series which reproduce the properties of the real electroencephalograms. The focus was made on manifestations of nonlinearity and deterministic chaos. The study deals with a question about the place of modeling in the study of complex systems and processes. Particular attention is paid to the definition of indicators of studied time series. The goal was to make meaningful judgments about the intrinsic properties of the generated EEG signals in comparison with the real signals. We presented and evaluated the simulation results with the help of artificial neural networks. The conclusion is that under certain conditions the neural networks with chaotic neurons may reproduce properties of real EEG signals. But at the same time the similarity between generated and real signal is not so close that there is no way to distinguish one from another by using a sufficiently informative methods including visually representing information. In other words, the concept of cybernetic black box is limited in practice by the complexity of the problem.
Keywords: artificial neural networks, models of chaotic neurons, modeling of electroencephalogram signals, deterministic chaos.

1 Introduction

It should be noted that EEG analysis methods are specific in their capabilities and purpose. There are many methods for analyzing the EEG signal: from visual expert evaluation to analysis of microstates using Markov chains (Gärtner *et al.* [4]). Moreover, nonlinear methods make it possible to obtain more accurate and nontrivial results than linear methods, in view of the nonlinearity of the EEG itself. These methods include the study of reconstructed attractor in the lag space, calculating the correlation dimension, the information entropy, the largest Lyapunov exponent, the Hurst exponent, the fractal dimensions, the recurrent diagram, and so on (see, for instance, Acharya *et al.* [1]).
It should be noted that the model can contain a stochastic component, that is, it should not be purely deterministic. This modeling can also be carried out using artificial neural networks (ANN). In this paper, we consider such ANNs, in which deterministic chaos is included a priori (Crook and Scheper [15]). Thus, the hypothesis was formulated that it is possible to construct an artificial neural network for modeling the EEG signal, in which there are layers consisting of chaotic neurons.

17th *ASMDA Conference Proceedings, 6 - 9 June 2017, London, UK*

2 General properties of electroencephalograms (EEG)

The signal consists of a set of interfering rhythms of brain activity with the addition of chaos and noise of various types. The EEG signal is nonstationary at sufficiently large time intervals (Kaplan *at al.* [2]) and nonlinear (Rombouts *at al.* [3]). This is especially noticeable in the case of external stimulation of the brain by signals from the sensory organs (Fig. 1).

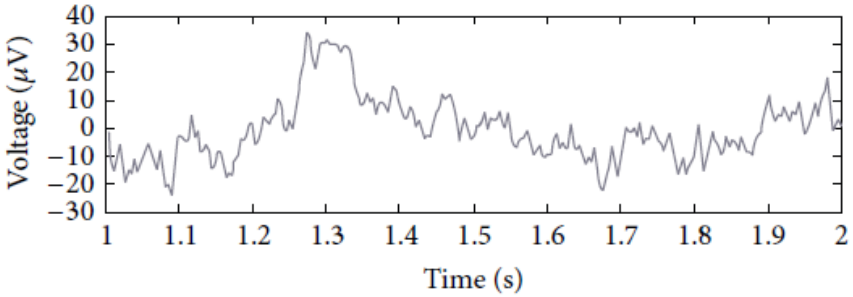

Fig. 1. EEG signal in response to a stimulus (Payal *at al.* [17])

In this figure, we can estimate what the EEG signal is. Usually it varies from -30 to 50 millivolts (μV).Changes in the EEG signal can occur in milliseconds. From a mathematical and computational point of view, the EEG is a collection of discrete time series, the number of which corresponds to the number of EEG recording channels. Each such time series can be written as follows: $X = \{x_t\}, \ t \in [1,...,N]$. Here N is the number of the EEG signal samples, t is the discrete time. The number of samples in the EEG record depends on the recording conditions. Usually the sampling frequency is 250 or 500 Hz and the recording time is 1-2 minutes.

3 Quantitative indicators of EEG analysis

Below we briefly describe some aspects of the EEG analysis and those quantitative indicators that were used in this work in assessing the quality of modeling the artificial EEG signals.

In this paper we use the fact that there are many measures, which take into account chaotic dynamics, suitable for analyzing time series in general and EEG signals, in particular. It is reasonable to use several complexity measures for EEG signals at the same time (Burns [5]). In the framework of this study, the following quantitative indicators were chosen to compare the real EEG signals with the model EEG signals:

- Hjorth Mobility;
- Hjorth complexity;
- Information entropy;

- Approximate entropy;
- Algorithmic complexity;
- Largest Lyapunov exponent;
- Hurst exponent;
- Correlation dimension.

Below we will consider in more details each of these measures.

3.1 Hjorth Parameters

These parameters were proposed specifically for EEG analysis in Hjorth [6]. For the time series $X = \{x_t\},\ t \in [1,...,N]$, they were called as Activity $HA(X)$, Mobility $HM(X)$ and Complexity $HC(X)$. The activity corresponds exactly to the sample variance of the time series, so we will not calculate it separately:

$$HA(X) = Var(X) \tag{1}$$

Mobility can be understood as the standard deviation of the signal power spectrum. That is, the standard deviation of the first time derivative of the signal, divided by the standard deviation of the signal itself:

$$HM(X) = \sqrt{\frac{Var(\frac{dX}{dt})}{Var(X)}} \tag{2}$$

Here, by the derivative, we mean its finite difference approximation, that is, the increments of the time series under study with a unit step.

The complexity is related to the change in frequency. The complexity is calculated as follows:

$$HC(X) = \frac{HM(\frac{dX}{dt})}{HM(X)} \tag{3}$$

Hjorth parameters are fairly simple and easy to calculate. They are currently used in the study of EEG signals (see, for instance, Cecchin *at al*.[7]). Therefore, we also use these measures in this paper.

3.2. Information Entropy

Calculating the information entropy (IE) of the EEG signal can be useful for quantifying the various states of the brain. It can also be regarded as a measure of the complexity of the signal in the sense of its conditional information content (Ghorbanian *at al*.[8]). Information entropy is given by the formula:

$$IE(X) = -\sum_i s_i^2 \log_2(s_i^2) \tag{4}$$

In this expressions, s_i are the coefficients of the signal X in some wavelet orthonormal basis. In this paper we also use another entropy measure. Namely, approximate entropy is used.

3.3. Approximate Entropy

This indicator determines the complexity of the signal $X = \{x_t\},\ t \in [1,...,N]$, by means of an analysis of its regularity, based on a logarithmic estimation for similarity of the compared patterns (Pincus [9]). Approximate entropy (AE) can be defined as the following difference:

$$AE(X) = \frac{1}{N-(m-1)\tau} \sum_{i=1}^{N-(m-1)\tau} \log C_i^m(r) - \frac{1}{N-m\tau} \sum_{i=1}^{N-m\tau} \log C_i^{m+1}(r) \tag{5}$$

The "correlation integral" $C_i^m(r)$ in this formula is calculated as follows:

$$C_i^m(r) = \frac{1}{N-(m-1)\tau-1} \sum_{j=1, j\neq i}^{N-(m-1)\tau} \Theta(r - |x_i - x_j|) \tag{6}$$

Here N is the number of time series samples, and $\Theta(x)$ is the Heaviside function. Accordingly, r, τ and m are parameters that can be varied during the computation process. The quantity m is called the embedding dimension of a time series in the lag space. The delay time τ determines the lag value. The methods for determining these parameters are well known and therefore are not given here The value of r is the size of the boxes of the time series reconstructed attractor covering in the lag space.

3.4. Algorithmic Complexity

Algorithmic complexity (also Kolmogorov complexity, Lempel-Ziv complexity) determines how complex a given sequence of symbols is relative to the length of the shortest computer program necessary for a complete description of this sequence of symbols. Initially, concept of Algorithmic Complexity (AC) was formulated by Kolmogorov [10].

We used the approach realized in Kugiumtzis and Tsimpiris [11]. Calculation of algorithmic complexity was performed using the MATS toolbox ("Measures of Analysis of Time Series"). This toolbox of the MatLab package was created specifically for the analysis of time series, including EEG, in Kugiumtzis and Tsimpiris [11]. It has a graphical interface, data loading capabilities and a wide range of indicators. Here we note that with the help of MATS in the present work, the Hjorth Mobility, the Hjorth Complexity, the Approximate entropy, the Hurst exponent, and the Correlation dimensions were calculated.

3.5. Largest Lyapunov Exponent

This measure is one of the key characteristics for detecting deterministic chaos in the dynamic system or time series. There is a huge literature and methods of LLE calculating. Here we do not discuss them. In general, the largest Lyapunov exponent is defined as follows:

$$\lambda = \lim_{t\to\infty} \lim_{\Delta x_0 \to 0} \frac{1}{t} \ln \frac{\left|\Delta x(x_0, t)\right|}{\Delta x_0}. \tag{7}$$

We can understand Δx_0 as the distance between two close points x_0 and $x + \Delta x$ on the attractor in the phase or lag space at the moment $t = 0$. Correspondingly, $\Delta x(x_0, t)$ is the distance between these points at the moment t. If orbits exponentially diverge with time, the LLE is positive what indicates the chaos. In the present paper the LLE of the EGG signals were calculated as in Das *at al*. [12]. To calculate the LLE of the EEG time series, we chose the embedding dimension from 5 to 20 and the time lag equal to 1.

3.6. Hurst Exponent

The Hurst exponent is a popular quantitative measure for the analysis of time series (see, for instance, Das *at al*. [12]). With its help it is possible to measure long-period memory in a time series. For the time series $X = x(t),\ t \in [0,1,...,T]$ the Hurst exponent is defined in the framework of standard R/S analysis by the formula:

$$H(X) = \frac{\log(R/S)}{\log(T)}. \tag{8}$$

R is the difference between the maximum and minimum deviation from the mean. S is the standard deviation. As a result, the ratio R/S gives the value of the normalized range. We use this indicator to compare the properties of the real EEG signal and the model EEG signals.

3.7. Correlation Dimension

In addition to the fractal dimension D_0 and the information dimension D_1, the correlation dimension D_2 has become popular as one of the fractal dimensions, applicable to a wide range of data, including EEG records (Pereda *at al*.[13]). It is given by the formula:

$$CD(X) = D_2 = \lim_{r \to 0} \frac{\log C(r)}{\log(r)}. \quad (9)$$

The value of r is the size of the boxes of the time series reconstructed attractor covering in the lag space, and $C(r)$ is the correlation integral:

$$C(r) = \frac{1}{(N-(m-1)\tau)(N-(m-1)\tau-1)} \times \\ \times \sum_{i=1}^{N-(m-1)\tau} \sum_{j=1, i \neq j}^{N-(m-1)\tau-1} \Theta(r - |x_i - x_j|) \quad (10)$$

Here, N corresponds to the number of samples in the EEG time series $X = \{x_t\}$, $t \in [1, ..., N]$, and Θ is the Heaviside step function. In fact, for carrying out such calculations, various algorithms can be used, for example, the Grassberger-Procaccia algorithm [14]. The quantity m is the embedding dimension of a time series in the lag space. The delay time τ determines the lag value.

4 Chaotic artificial neural networks

The model of the chaotic neuron and the chaotic neural network (CNN) was first proposed in 1990 by Crook and Scheper [15]. The essence of the chaotic neuron is in a special choice of its activation function. Such neurons can be added to the neural network along with other neurons, which may have other activation functions. Neurons of different types can be placed on different layers of the neural network.

In the simplest case, as an activation function f of a chaotic neuron, a chaotic logistic map can be used:

$$y(n) = f(u_n) = ru_n(1-u_n), \quad r = 4 \quad (11)$$

Here, $y(n)$ denotes the output of the neuron, and u_n is the internal state of the neuron, which is calculated as follows:

$$u_n = \sum_{j=1}^{m} w_j^n x_j^n$$

Here, w_j^n are the weights of the neuron, x_j^n is the input signal of the neuron, n is the number of the training example, and m is the number of inputs for the neuron. For such an activation function (11), the output of the chaotic neuron must be limited to a certain interval, namely the interval $0,1$ (Fig. 2).

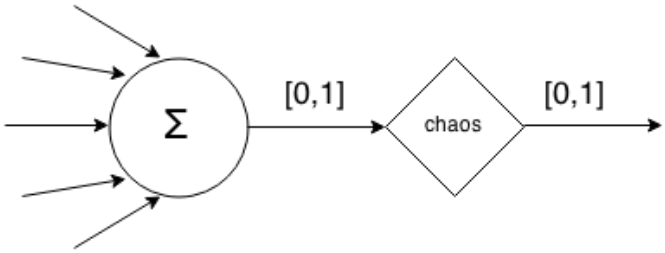

Fig. 2. Schematic representation of a chaotic neuron

Another fairly simple and effective option for choosing the activation function is a chaotic decimal mapping:

$$y(n) = f(u_n) = 10(u_n - [u_n]) \tag{12}$$

Here the function x denotes the integer part of x.

Based on what has been said above, a number of assumptions can be made about how to use CNN for the generation of an artificial EEG. The main method for generating a model EEG signal is an iterated forecast one step ahead. This means that at least one of the components of the network input vector corresponds to the output value obtained in the previous step in time:

$$x_i(t) = y(t-1) \tag{13}$$

Here, $y(t-1)$ is the output of CNN, and $x_i(t)$ are the inputs of the neural network with the iterated forecast one step in time t.

The approach in which many steps in time the output of the CNN is fed to the input can be called an iterated model, since the input can be given both an output value and an error calculated at the output. It is understood that the iterative mode of network operation will be used after the neural network training stage. A neural network trained to predict an EEG signal for one step forward can use its own calculation data to further predict the signal by one more step in time forward. When this procedure is repeated many times the network starts to generate a time series that does not depend directly on the source data, but depends on what the network has learned. It should be noted that the iterative mode is not identical with the recurrence of the neural network and can be carried out regardless of the presence or absence of recurrence in the network architecture.

5 Calculations and results

All the calculations were made in the MatLab package. For convenience and standardization of all time series of EEG, they were normalized to the interval $[0,1]$ by the formula:

$$\hat{x} = \frac{x - \min(x)}{\max(x) - \min(x)} \tag{14}$$

It is important to note that all major operations are performed on time series of 1000 samples, including network training, generation of artificial EEG and calculation of all used measures. This avoids a number of impediments that could impair the quality of the calculations. On the other hand, these are long enough time series to stably calculate all the measures. To simulate the EEG signal, a database was used with a set of EEG recordings, available for free use and described in Hoffmann *at al.*[16]. These records were provided in a pre-processed form and suitable for use in the MatLab package. The sampling frequency of each EEG record was chosen to be 128 Hz.
The next step was to choose the network training algorithm. For this study, the Bayes regularization of the error back propagation method was chosen, which minimizes the combination of quadratic errors. This regularization is based on the widely known Levenberg-Marquardt algorithm, but in some cases the chosen method exceeds Levenberg-Marquardt algorithm and gives a smaller errors (Payal *at al.*[17]).

5.1 Modeling parameters

The lag vectors composed on the basis of the EEG signal were chosen as CNN inputs. Namely, if $X = \{x_t\}, \ t \in [1,...,N]$ is the EEG time series, then the lag vector is calculated as follows:

$$L_\tau^m(t) = (x_t, x_{t-\tau}, x_{t-2\tau}, ..., x_{t-(m-1)\tau}) \tag{15}$$

Here t it is fixed in accordance with the selected time series sample, τ determines the lag value, and the embedding dimension m corresponds to the lag vector dimension, that is, the number of lag vector $L_\tau^m(t)$ components. Thus, m determines the number of CNN inputs. These two quantities τ and m must first be determined by calculating them from the original EEG time series. The procedure for calculating τ and m is well known and therefore is not described here.

5.2 Results of modeling

To standardize CNN in this series of computational experiments, a multilayer perceptron with a different number of layers was used. But in each layer the number of neurons was fixed and equal to 10. In this case, logistic and decimal

mapping can be used as an activation function in different layers, either individually or simultaneously in one neural network. In addition, as a "standard" nonchaotic activation function, a sigmoid activation function was chosen for some neurons. This activation function takes values on the interval $[0,1]$ and is defined by the formula:

$$S(x) = \frac{1}{1+e^{-x}}. \tag{16}$$

The desired dynamics of the artificial EEG was observed in the case of very good network training. The maximum achieved value of the dtermination coefficient $R^2 = 0.995$ can be considered sufficiently large to compare time series in 1000 samples. However, the comparison of the network response with the training signal is not of great importance, since the goal was to obtain time series of the artificial EEG when the network is operated independently in the iterative mode.

The most successful was a neural network with three layers and ten neurons in each layer. In this case, the first two layers as an activation function contain a decimal mapping, and the last layer contains a sigmoid activation function. As a result of computer experiments, it turned out that the number of input neurons needed to be reduced to two and use a lag equal to one. The visualization in MatLab of the used neural network is shown in Fig. 3, where F denotes a chaotic activation function.

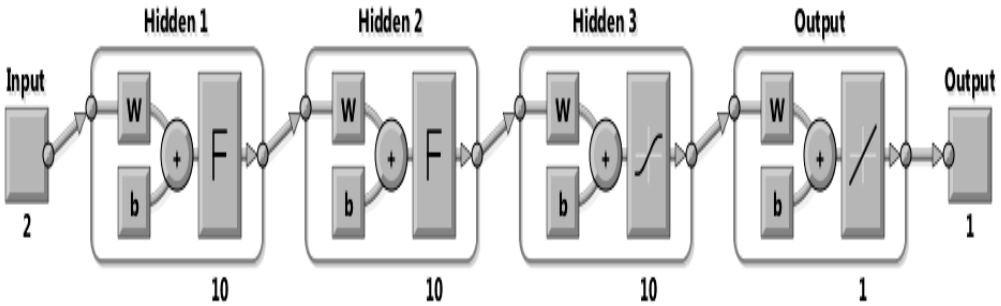

Fig. 3. Visualization of the network structure. In the third hidden layer the sigmoid activation function is selected, in the output layer the activation function is linear

To obtain the final results, three copies of such a network were created, working independently of each other. Below these chaotic neural networks are designated as CNN1, CNN2, CNN3. The results of the analysis of the time series generated by these neural networks are presented in Table 1 below. The symbol "EEG" in this table means a fragment of the real EEG, through which the neural networks were trained. For all three neural networks the parameters $m = 5$ and $\tau = 22$ were used. The results of comparison of quantitative

measures for one of the real EEG and three artificial EEG are presented in Table 1.

Symbol	Measures	EEG	CNN1	CNN2	CNN3
HM	Hjorth Mobility	0.06	0.06	0.05	0.06
HC	Hjorth complexity	0.94	0.81	0.95	0.84
IE	Information entropy	295.32	307.71	315.04	301.62
AE	Approximate entropy	0.39	0.41	0.39	0.46
AC	Algorithmic complexity	0.65	0.76	0.75	0,76
LLE	Largest Lyapunov exponent	0.59	0.27	0.20	0.61
H	Hurst exponent	0.67	0.51	0.51	0.57
CD	Correlation dimension	3.15	3.03	3.22	3.03

Table 1. Comparison of EEG modeling results

It can be seen that practically all the parameters of the simulated EEG series are very close to those of the original EEG signal. The difference in the results of three chaotic neural networks can be due to the different statistical quality of their learning. The internal variability of the real EEG can level the computational difference in quantitative indicators.

Conclusions

In this study, by means of theoretical and in computational experiments it was found that it is possible to build a model based on CNN, which would reflect some of the basic quantitative characteristics of the natural EEG signal. There are many options for constructing a model, but they are all built on the principle of an iterated forecast. To identify the most promising models, quantitative experiments are needed. In these experiments, the similarity of the model EEG signal to the natural one should be evaluated using a specially selected set of indicators.

The relevance of the development of the generator of artificial EEG is that different models and algorithms for EEG analysis can be checked on simulated time series (for example, classifiers). Classifiers can then be applied to natural EEG signals. The chaotic neural network can be reconfigured and trained on different EEG time series to obtain the desired result. Thus, the use of CNN makes it possible to simulate EEG of any type.

Refer ences

1. Acharya, R., Faust O., Kannathal N., Chua T., Laxminarayan S. Non-linear analysis of EEG signals at various sleep stages // Computer methods and programs in biomedicine. – 2005. – Vol. 80, No. 1. – P. 37–45.
2. Kaplan, A. Y., Fingelkurts A. A., Fingelkurts A. A., Borisov S. V., Darkhovsky B. S. Nonstationary nature of the brain activity as revealed by EEG/MEG: methodological, practical and conceptual challenges // Signal processing. – 2005. – Vol. 85, No. 11. – P. 2190–2212.
3. Rombouts, S. A. R. B., Keunen R. W. M., Stam C. J. Investigation of nonlinear structure in multichannel EEG // Physics Letters A. – 1995. – Vol. 202, No. 5. – P. 352–358.
4. Gärtner, M., Brodbeck V., Laufs H., Schneider G. A stochastic model for EEG microstate sequence analysis // NeuroImage. – 2015. – No. 104. – P. 199–208.
5. Burns, T. F. Combining complexity measures of EEG data: multiplying measures reveal previously hidden information // Peer J PrePrints. – 2015. – No. 3:e1369. – P. 1–8. URL: https://dx.doi.org/10.7287/peer j.preprints.1121v1.
6. Hjorth, B. EEG analysis based on time domain properties // Electroencephalography and clinical neurophysiology. – 1970. – Vol. 29, No. 3. – P. 306–310.
7. Cecchin, T., Ranta R., Koessler L., Caspary O., Vespignani H., Maillard L. Seizure lateralization in scalp EEG using Hjorth parameters // Clinical Neurophysiology. – 2010. – Vol. 121, No. 3. – P. 290–300.
8. Ghorbanian, P., Ramakrishnan S., Ashrafiuon H. Stochastic non-linear oscillator models of EEG: the Alzheimer's disease case // Frontiers in Computational Neuroscience. – 2015. – Vol. 9, No. 48. – P. 1–14.
9. Pincus, S. M. Approximate entropy as a measure of system complexity // Proceedings of the National Academy of Sciences. – 1991. – Vol. 88, No. 6. – P. 2297–2301.
10. Kolmogorov, A. N. Three approaches to the quantitative definition of information // Problems of Information Transmission. – 1965. – Vol. 1, No. 1. – P. 1–7.
11. Kugiumtzis, D., Tsimpiris A. Measures of Analysis of Time Series (MATS): A MATLAB Toolkit for Computation of Multiple Measures on Time Series Data Bases // Journal of Statistical Software. – 2010. – Vol. 33, No. i05. – P. 1–30.
12. Das, A., Das P., Roy A. B. Applicability of Lyapunov exponent in EEG data analysis // Complexity International. – 2002. – No. 9. – P. 1–8.
13. Pereda, E., Gamundi A., Rial R., González J. Non-linear behavior of human EEG: fractal exponent versus correlation dimension in awake and sleep stages // Neuroscience letters. – 1998. – Vol. 250, No. 2. – P. 91–94.
14. Grassberger, P., Procaccia I. Measuring the strangeness of strange attractors // Physica D: Nonlinear Phenomena. – 1983. – Vol. 9, No. 1. – P. 189–208.
15. Crook, N., Scheper T. O. A novel chaotic neural network architecture // Proceedings of the 9th European Symposium on Artificial Neural Networks (ESANN). – 2001. – P. 295–300.
16. Hoffmann, U., Garcia G., Vesin J. M., Diserens K., Ebrahimi T. A boosting approach to P300 detection with application to brain-computer interfaces // 2nd International IEEE EMBS Conference on Neural Engineering. Conference Proceedings. – 2005. – P. 97–100.
17. Payal, A., Rai C. S., Reddy B. V. R. Comparative analysis of Bayesian regularization and Levenberg-Marquardt training algorithm for localization in wireless sensor network // Proceedings of 15th International Conference on Advanced Communication Technology (ICACT). – 2013. – P. 191–194.

Price sensitivities for stochastic volatility models

Youssef El-Khatib[1] and Abdulnasser Hatemi-J[2]

[1] Department of Mathematical Sciences, UAE University, P.O. Box 15551, Al-Ain, United Arab Emirates
(E-mail: Youssef_Elkhatib@uaeu.ac.ae)
[2] Department of Economics and Finance, UAE University, P.O. Box 15551, Al-Ain, United Arab Emirates
(E-mail: Ahatemi@uaeu.ac.ae)

Abstract. We deal with the calculation of price sensitivities for stochastic volatility models. We consider general forms for the dynamics of the underlying asset price and its volatility. We make use of Malliavin calculus to compute the price sensitivities. Obtained results are applied to several recent stochastic volatility models as well as existing ones that are commonly used by practitioners. Each price sensitivity is a source of financial risk. The suggested formulas are expected to improve on hedging of the underlying risk.
Keywords: Asset Pricing, Malliavin Calculus, Price sensitivity, Stochastic volatility, Risk management, European options.

1 introduction

Mathematical tools are increasingly utilized by investors and financial institutions in order to neutralize or reduce the underlying financial risk. Among others, price sensitivities are commonly used in markets for financial derivatives in order to hedge against risk. This is indeed an active field of research. Recently, several papers have dealt with this important issue. It is shown in the literature that the valuation of financial derivatives is more accurate if the underlying data generating process is characterized by a stochastic volatility process. The existing literature suggests using a stochastic process for the volatility in order to determine the price of financial derivatives. The aim of this paper is to deal with the derivation of the price sensitivities. We derive price sensitivities for a general stochastic volatility model by making use of the Malliavin calculus. It should be mentioned that each financial trading position that is based on financial instruments has five price sensitivities, which are known as the Greeks in the financial literature. The precise calculation of these price sensitivities is of paramount importance for the immunization of potential financial risk of a financial trading position or a portfolio. The first price sensitivity is known as Delta, which is equal to the change of the trading position with respect to the price of the underlying asset under the

17^{th} *ASMDA Conference Proceedings, 6 – 9 June 2017, London, UK*

ceteris paribus condition. The second price sensitivity is called Gamma, which is representing the change of the Delta for a portfolio of options with respect to the price of the underlying asset. The third source of risk in this situation is known as Vega and it embodies the change of the trading position with regard to a marginal change in the volatility of the original asset. The fourth price sensitivity is called Theta, which captures the change of the value of the underlying portfolio with respect to the time factor. The last price sensitivity is commonly known as Rho in the literature and it is capturing the sensitivity of the trading position with respect to the risk free rate (i.e. the interest rate). Each of these Greek measures represent a source of risk for the portfolio and traders must calculate the pertinent Greeks for their portfolio at the end of every trading day so as to take required action if the internal risk is higher than the pre-determined levels by the underlying financial institution. The Malliaivn calculus is especially useful in this case because the price of the financial derivatives is regarded as a stochastic process that is in closed form. Consequently, dealing with the price sensitivities via this method is an appropriate approach. Through the Malliavin calculus we are able to transform the differentiation into integration and thus provide an unbiased measure of each price sensitivity. Many of the existing contributions to the price sensitivities are based on the finite difference approach, which can indeed be considered an biased methodology. Conversely, the Malliavin method is unbiased and it can also be less time-consuming in terms of convergence. The idea to make use of the Malliavin calculus for computing price sensitivities originates from [8]. This first application was within the context of a market that is characterized by information generated by the Brownian motion. Their method relies on the Malliavin derivative on the Wiener space, which contains two parts. The first part is the application of the chain rule and the second part is utilizing the fact that the derivative has an adjoint (Skorohod integral) which can be described by the Ito integral for adapted processes. Lately, this approach has been utilized by [5] for markets under stress or experiencing a financial crisis. There are also several other papers that use the Malliavin calculus for markets with jumps. For example, [7] uses the Poisson noise via the jump times. [1] takes into account both the jump timing as well as the amplitude of the underlying jumps. [3] deals with jump-diffusion models via the Malliavin calculus with regard to the Brownian motion conditional on the Poisson component. In addition, [2] permits the Poisson noise to take into account the amplitude of the jumps. However, the timing of the jumps is not taken into account. Conversely, [6] provide the price sensitivities by utilizing the Malliavin derivative on the Wiener space and the Poisson noise when the timing of the jumps is taken into account. This paper provides price sensitivities for a general stochastic volatility model that encompasses a number of well-known existing models as well as several new ones.

After this introduction the remaining part of the paper is organized as follows: Section two presents the model and an introduction to Malliavin calculus. Section three deals with deriving the price sensitivities via the Malliavin approach. A general formula is provided that encompasses different stochastic volatility

models. The formula is applied to find the price sensitivities for several new stochastic volatility models as well as for other specific stochastic volatility models that are well-known in the literature. In the last Section concluding remarks are provided.

2 Preliminaries

In this section, we describe the general stochastic volatility model and we present some tools from Malliaivin calculus needed to our study.
We consider two independent Brownian motion $(B_t)_{t\in[0,T]}$ and $(B_t^{'})_{t\in[0,T]}$ and a filtered probability space $(\Omega, \mathcal{F}, (\mathcal{F}_t)_{t\in[0,T]}, P)$, where $(\mathcal{F}_t)_{t\in[0,T]}$ is the natural filtration generated by B and $B^{'}$. Next we introduce a general framework for the stochastic volatility model.

2.1 The stochastic volatility model

We assume that the marketplace contains only two assets. The first asset is a risk free asset given by $(A_t := e^{\int_0^t r_s ds})_{t\in[0,T]}$ where r is the interest rate. The second asset is the underlying risky asset on which a European call option is built. It is assumed to have a stochastic volatility i.e the volatility is driven by a stochastic volatility model. The price of the underlying asset $(X_t)_{t\in[0,T]}$ and the volatility process are stochastic processes driven by the following stochastic differential equations

$$dX_t = \mu_t X_t dt + \sigma(Y_t) X_t dB_t, \tag{1}$$

$$dY_t = g(Y_t)dt + \beta[\rho dB_t + \sqrt{1-\rho^2} dB_t^{'}], \quad t \in [0,T], \tag{2}$$

with $X_0 = x > 0$ and $Y_0 = y \in \mathbb{R}$. μ is a deterministic function, $\beta \in \mathbb{R}$, $\rho \in [-1,1]$ and $\sigma \in \mathcal{C}^2([0,T]\times\mathbb{R})$ such that for any $t \in [0,T]$, $\sigma(.) \neq 0$. σ is the volatility of the underlying asset, β measures the volatility of the volatility and ρ represents a measure of dependency between the price of the underlying asset and its volatility. The market considered here is incomplete. There is an infinity of E.M.M -Equivalent Martingale Measure- (i.e a probability equivalent to P under which the actualized price $(X_t e^{-rt})_{t\in[0,T]}$ is a martingale). Let Q be a fixed P-E.M.M. Q is identified by its Radon-Nikodym density w.r.t P, denoted ζ_T and given by

$$\zeta_T = \exp\left(\int_0^T a_s dB_s + b_s dB_s^{'} - \frac{1}{2}\int_0^T (a_s^2 + b_s^2) ds\right),$$

where $(a_t)_{t\in[0,T]}$ and $(b_t)_{t\in[0,T]}$ are two predictable processes s.t.

$$a_t = -\frac{\mu_t - r_t}{\sigma(Y_t)}, \tag{3}$$

and b is arbitrary. Now let, for any $t \in [0,T]$, $W_t = B_t - \int_0^t a_s ds$ and $W_t^{'} = B_t^{'} - \int_0^t b_s ds$ then by the Girsanov theorem W and $W^{'}$ are two Q-Brownian

motions. In the following we work with a fixed P-E.M.M. Q and we will use $E[.]$ (instead of $E_Q[.]$) as the expectation under the probability Q. We have, under Q, for any $t \in [0,T]$

$$dX_t = r_t X_t dt + \sigma(Y_t) X_t dW_t, \tag{4}$$

$$dY_t = h(Y_t, X_t)dt + \beta[\rho dW_t + \sqrt{1-\rho^2} dW_t^{'}], \tag{5}$$

where

$$h(Y_t, X_t) := g(Y_t) + \beta\rho a_t + \beta\sqrt{1-\rho^2} b_t, \tag{6}$$

a_t is given by (3) and b_t is a predictable process, assumed depending on Y_t and X_t i.e. $b_t = b_t(Y_t, X_t)$.

2.2 Malliavin derivative

We give an introduction to Malliavin derivative in Wiener space and we list some important results . We denote by $(D_t)_{t\in[0,T]}$ the Malliavin derivative on the direction of W. We denote by $\mathbb{P}$ the set of random variables $F : \Omega \to \mathbb{R}$, such that F has the representation

$$F(\omega) = f\left(\int_0^T f_1(t)dW_t, \ldots, \int_0^T f_n(t)dW_t\right),$$

where $f(x_1, \ldots, x_n) = \sum_\alpha a_\alpha x^\alpha$ is a polynomial in n variables $x_1, \ldots, x_n$ and deterministic functions $f_i \in L^2([0,T])$. Let $\|.\|_{1,2}$ be the norm

$$\|F\|_{1,2} := \|F\|_{L^2(\Omega)} + \|D.F\|_{L^2([0,T]\times\Omega)}, \quad F \in L^2(\Omega).$$

Then Dom (D), the domain of D, is equal to $\mathbb{P}$ w.r.t the norm $\|.\|_{1,2}$. The next propositions are very useful when using the Malliavin derivative.

Proposition 1 *Given* $F = f\left(\int_0^T f_1(t)dW_t, \ldots, \int_0^T f_n(t)dW_t\right) \in \mathbb{P}$. *We have*

$$D_t^W F = \sum_{k=0}^{k=n} \frac{\partial f}{\partial x_k}\left(\int_0^T f_1(t)dW_t, \ldots, \int_0^T f_n(t)dW_t\right) f_k(t).$$

To calculate the Mallaivin derivative for Itô integral, we will use the following Proposition.

Proposition 2 *Let* $(u_t)_{t\in[0,T]}$ *be a* $\mathcal{F}_t-$*adapted process, such that* $u_t \in$ Dom (D), *we have*

$$D_t \int_0^T u_s dW_s = \int_t^T (D_t u_s) dW_s + u_t.$$

The reader can refer to [9] for more detailed description on Malliaivin calculus.

From now on, for any stochastic process u and for $F \in \text{Dom}\ (D)$ such that $u_{\cdot} D_{\cdot} F \in L^2([0,T])$ we let

$$D_u F := \langle DF, u \rangle_{L^2([0,T])} := \int_0^T u_t D_t F dt. \tag{7}$$

The next proposition presents some important results that link D and its adjoint δ, known as the Skorohod integral.

Proposition 3 *a) Let $u \in \text{Dom}\ (\delta)$ and $F \in \text{Dom}\ (D)$, we have $E[D_u F] \leq C(u)\|F\|_{1,2}$, and $E[F\delta(u)] = E[D_u F]$.*
b) Consider a $L^2(\Omega \times [0,T])$-adapted stochastic process $u = (u_t)_{t\in[0,T]}$. We have $\delta(u) = \int_0^T u_t dW_t$.
c) Let $F \in \text{Dom}\ (D)$ and $u \in \text{Dom}\ (\delta)$ such that $uF \in \text{Dom}\ (\delta)$ thus $\delta(uF) = F\delta(u) - D_u F$.

3 Price sensitivities

We consider a European option with payoff $f(X_T)$, where $(X_t)_{t\in[0,T]}$ denotes the underlying asset price given by the general stochastic volatility model (4-5). We denote by C the value of the European option. We will compute the following price sensitivities:

$$\text{Delta} = \frac{\partial C}{\partial x}, \qquad \text{Gamma} = \frac{\partial^2 C}{\partial x^2}, \qquad \text{Rho} = \frac{\partial C}{\partial r}, \qquad \text{Vega} = \frac{\partial C}{\partial \sigma},$$

The last price sensitivities Theta $= \frac{\partial V}{\partial t}$ can be obtained using the partial differential equation satisfied by C, the price of the option. In the following proposition we find the Malliaivn derivatives of X_T and Y_t w.r.t D.

Proposition 4 *For $0 \leq t \leq T$, We have*

$$D_t X_T = X_T \left(\sigma(Y_t) - \int_t^T \sigma^{'}(Y_s)\sigma(Y_s) D_t Y_s ds + \int_t^T \sigma^{'}(Y_s) D_t Y_s dW_s \right) \tag{8}$$

and

$$D_t Y_s = \beta\rho + \int_t^s D_t h(Y_\nu, X_\nu) d\nu, \tag{9}$$

where

$$D_t h(Y_\nu, X_\nu) = g^{'}(Y_\nu) D_t Y_\nu + \beta\rho(\mu_\nu - r_\nu) \frac{\sigma^{'}(Y_\nu)}{\sigma^2(Y_\nu)} D_t Y_\nu + \beta\sqrt{1-\rho^2} D_t b_\nu, \tag{10}$$

with $0 \leq t \leq \nu \leq s \leq T$.

Proof. The equality (8) can be obtained by applying the Malliavin derivative to (4). Then we use the chain rule, proposition 2, and

$$D_t \int_0^T u_s ds = \int_t^T (D_t u_s) ds, \tag{11}$$

when $(u_s)_{s\in[0,T]}$ is an adapted process.
To find D_tY_v, we have from (5), for $0 \le t \le v \le T$,

$$\begin{aligned} D_tY_v &= D_t\left(Y_0 + \int_0^v h(Y_s, X_s)ds + \beta\rho W_v + \beta\sqrt{1-\rho^2}W_v^{'}\right) \\ &= \beta\rho + \int_t^v D_t h(Y_s, X_s)ds, \end{aligned}$$

where

$$\begin{aligned} D_t h(Y_s, X_s) &= D_t(g(Y_s) + \beta\rho a_s + \beta\sqrt{1-\rho^2}b_s) \\ &= g^{'}(Y_s)D_tY_s + \beta\rho D_t\frac{r_s-\mu_s}{\sigma(Y_s)} + \beta\sqrt{1-\rho^2}D_tb_s \\ &= g^{'}(Y_s)D_tY_s + \beta\rho(\mu_s - r_s)\frac{\sigma^{'}(Y_s)}{\sigma^2(Y_s)}D_tY_s + \beta\sqrt{1-\rho^2}D_tb_s. \end{aligned}$$

□

The second and the third order derivatives of X_T w.r.t D, essential for computing the different price sensitivities are given in the following proposition.

Proposition 5 *For $0 \le t \le T$, we let $L_t^T := \sigma(Y_t) - \int_t^T \sigma^{'}(Y_\nu)\sigma(Y_\nu)D_tY_\nu d\nu + \int_t^T \sigma^{'}(Y_\nu)D_tY\nu dW_\nu$, then we have $D_tX_T = X_TL_t^T$ and*

$$D_uX_T = X_T\int_0^T u_tL_t^T dt \tag{12}$$

$$D_uD_uX_T = X_T\left(\left(\int_0^T u_tL_t^T dt\right)^2 + \int_0^T\int_s^T u_su_tD_sL_t^T dtds\right) \tag{13}$$

$$\begin{aligned} D_uD_uD_uX_T = X_T\Bigg(&\left(\int_0^T u_tL_t^T dt\right)^3 + 3\int_0^T u_tL_t^T dt\int_0^T\int_s^T u_su_tD_sL_t^T dtds \\ &+ \int_0^T\int_r^T\int_s^T u_ru_su_tD_rD_sL_t^T dtdsdr\Bigg) \end{aligned} \tag{14}$$

Proof. The equalities (12-14) are obtained using (7) and the chain rule of the Malliavin derivative. □

The derivatives $D_sL_t^T$, $D_rD_sL_t^T$, $D_sD_tY_v$ and $D_rD_sD_tY_v$ can be found using the chain rules of the Mallaivin derivative. Similar calculations can be found in [4].

3.1 First order price sensitivities: Delta, Rho, Vega

Let $C = E[f(X_T^\zeta)]$ be the price of the option, ζ can take values: the asset price x to obtain Delta, the interest rate r for Rho, and σ for Vega. We have

$$\frac{\partial}{\partial\zeta}E\left[f(X_T^\zeta)\right] = E\left[f(X_T^\zeta)\left(\frac{\partial_\zeta X_T^\zeta}{D_uX_T^\zeta}\delta(u) - D_u\left(\frac{X_T^\zeta\partial_\zeta X_T^\zeta}{D_uX_T^\zeta}\right)\right)\right].$$

Next we compute the Delta, the Rho and Vega can be computed by the same way. The Delta corresponds to $\zeta = x$, so $\partial_\zeta S_T = \partial_x S_T = \frac{1}{x} S_T$ and we have

$$\begin{aligned}
\text{Delta} &= E\left[f(X_T)\left(\frac{\partial_x X_T}{D_u X_T}\delta(u) - D_u\left(\frac{X_T \partial_x X_T}{D_u X_T}\right)\right)\right] \\
&= E\left[f(X_T)\left(\frac{X_T}{x D_u X_T}\delta(u) - D_u\left(\frac{X_T^2}{x D_u X_T}\right)\right)\right] \\
&= \frac{1}{x} E\left[f(X_T)\left(\frac{1}{\int_0^T u_t L_t^T dt}\delta(u) - 2X_T + \frac{X_T^2 D_u D_u X_T}{(D_u X_T)^2}\right)\right] \\
&= \frac{1}{x} E\left[f(X_T)\left(\frac{1}{\int_0^T u_t L_t^T dt}\delta(u) - 2X_T \right.\right. \\
&\quad \left.\left. + \frac{X_T(\int_0^T u_t L_t^T dt)^2 + X_T \int_0^T u_s D_s(\int_0^T u_t L_t^T dt) ds}{(\int_0^T u_t L_t^T dt)^2}\right)\right] \\
&= \frac{1}{x} E\left[f(X_T)\left(\frac{1}{\int_0^T u_t L_t^T dt}\delta(u) - X_T\left(1 - \frac{\int_0^T u_s(\int_s^T u_t D_s L_t^T dt) ds}{(\int_0^T u_t L_t^T dt)^2}\right)\right)\right].
\end{aligned}$$

The previous calculations can be applied to the α-hypergeometric model of [16] and most of the stochastic volatility models existing in the literature.

3.2 Gamma

The Gamma is computed using the second order derivative of $C = E[f(S_T)]$ w.r.t x given by

$$\begin{aligned}
&\frac{\partial^2}{\partial x^2} E\left[f(X_T)\right] = \frac{\partial}{\partial x}\text{Delta} = \frac{1}{x}\frac{\partial}{\partial x} E\left[f(X_T) H\right] \\
&= \frac{1}{x} E\left[f(X_T)\left(\frac{H \partial_x X_T}{D_u X_T}\delta(u) - D_u\left(\frac{H \partial_x X_T}{D_u X_T}\right) + \partial_x H\right)\right] \\
&= \frac{1}{x} E\left[f(X_T)\left(\frac{H X_T}{x D_u X_T}\delta(u) - \left(\frac{H(D_u X_T)^2 + X_T D_u X_T D_u H + H X_T D_u D_u X_T}{x(D_u X_T)^2}\right)\right.\right. \\
&\quad \left.\left. + \partial_x H)\right]\right),
\end{aligned}$$

where

$$H = \frac{1}{\int_0^T u_t L_t^T dt}\delta^W(u) - X_T\left(1 - \frac{\int_0^T u_s(\int_s^T u_t D_s L_t^T dt)ds}{(\int_0^T u_t L_t^T dt)^2}\right)$$

$$\begin{aligned} D_u H = &-\frac{\int_0^T u_s(\int_s^T u_t D_s L_t^T dt)ds}{(\int_0^T u_t L_t^T dt)^2}\delta(u) \\ &-X_T\left(\int_0^T u_t L_t^T dt - \frac{\int_0^T u_s(\int_s^T u_t D_s L_t^T dt)ds}{\int_0^T u_t L_t^T dt}\right. \\ &\left.-\frac{\int_0^T u_r \int_r^T u_s(\int_s^T u_t D_r D_s L_t^T dt)ds}{(\int_0^T u_t L_t^T dt)^2} + 2\frac{\left(\int_0^T u_s(\int_s^T u_t D_s L_t^T dt)ds\right)^2}{(\int_0^T u_t L_t^T dt)^3}\right) \end{aligned}$$

$$\partial_x H = -\frac{1}{x}X_T\left(1 - \frac{\int_0^T u_s(\int_s^T u_t D_s L_t^T dt)ds}{(\int_0^T u_t L_t^T L_t^T dt)^2}\right).$$

The above formula for Gamma is valid for most of the recent and well-know stochastic volatility models existing in the literature such as the Heston or the $\alpha-$hypergeometric volatility models.

4 Conclusions

This paper provides price sensitivities for a general stochastic volatility model that encompasses a number of recent models as well as well-known existing ones. For instance, we find the price sensitivities for recent stochastic volatility models such as the α-hypergeometric model of [16] and the linear model of [14]. In addition, we give the price sensitivities for existing models that are used regularly by practitioners such as: Hull-White [87], Stein-Stein [91] and Heston model [93]. The Malliavin calculus is used for this purpose. The advantage of this method is that it is unbiased and it requires less computational time compare to the finite difference method which is commonly used in this context.

The suggested formulas are expressed as propositions combined with pertinent proofs. Each price sensitivity is a source of financial risk that investors need to tackle. Thus suggesting alternative measures of price sensitivities is expected to improve on the management of the underlying financial risk.

References

1. V. Bally, M. Bavouzet, and M. Messaoud. Integration by parts formula for locally smooth laws and applications to sensitivity computations. *Annals of Applied probability*, 17, 1, 33-66, 2007.
2. M. Bavouzet, and M. Messaoud. Computation of Greeks using Malliavin's calculus in jump type market models. *Electronic Journal of Probability*, 11, 276-300, 2006.

3. M. Davis and M. Johansson. Malliavin Monte Carlo Greeks for jump diffusions. *Stochastic Processes and their Applications*, 116, 101-129, 2006.
4. Y. El-Khatib. Computations of Greeks in stochastic volatility models via the Malliavin calculus. *arXiv preprint arXiv:0904.3247*, 2009.
5. Y. El-Khatib, and A. Hatemi-J. Computations of Price Sensitivities after a Financial Market Crash. *IAENG International Journal of Applied Mathematics*, 41, 4, 2011.
6. Y. El-Khatib, and A. Hatemi-J. On the calculation of price sensitivities with a jump-diffusion structure. *Journal of Statistics Applications & Probability*, 1, 3, 171-182, 2012.
7. Y. El-Khatib, and N. Privault. Computations of Greeks in a market with jumps via the Malliavin calculus. *Finance and Stochastics*, 8, 2, 161-179, 2004.
8. E. Fournié, J.M. Lasry, J. Lebuchoux, P.L. Lions, and N. Touzi. Applications of Malliavin calculus to Monte Carlo methods in finance. *Finance and Stochastics*, 3, 4, 391-412, 1999.
9. B. Øksendal. *An introduction to Malliavin calculus with applications to economics*, Working paper 3, Institute of Finance and Management Science, Norwegian School of Economics and Business Administration, 1996.

Short Term Forecasting for Electricity Demand in Egypt Using Artificial Neural Networks

Mohamed A. Ismail[1], Alyaa R. Zahran[2], and Eman M. Abd El-Metaal[3]

[1] Department of Statistics, Faculty of Economics and political science, Cairo University, Giza, Egypt
(E-mail: mismail@feps.edu.eg)
[2] Department of Statistics, Faculty of Economics and political science, Cairo University, Giza, Egypt
(E-mail: azahran@feps.edu.eg)
[3] Department of Statistics, Faculty of Economics and political science, Cairo University, Giza, Egypt
(E-mail: eman_mahmoud@feps.edu.eg))

Abstract. Electricity is important for any nation. It influences not only the economy, but also the political and social aspects of a nation. Forecasting electricity demand is vital for future technical improvements. Short-term electricity demand forecasts are important for controlling of the electric power system. Recently, electricity demand series has found to contain more than one seasonal pattern. Intraday and intraweek seasonal patterns are appeared in the Egyptian electricity demand time series. This study investigates using Artificial Neural Networks in accommodating these seasonality patterns for forecasting hourly electricity demand in Egypt by using seasonal lags as inputs. Different artificial neural networks with different seasonal daily and weekly lags are used. The mean absolute percentage error is used to compare forecasting power of different artificial neural networks. Results indicate the accuracy of forecasts produced by the different artificial neural networks for different time horizons.

Keywords: Electricity demand forecasting, Mean Absolute Percentage Error, Artificial Neural Networks, Double Seasonality

1 Introduction

Electricity is one of the necessities in the ordinary life, and a major driving force for economic growth and development. The unstorable nature of electricity means that the supply of electricity must be always available to satisfy the growing demand.

In the early 2000s, Egypt has faced a major problem in its electric power sector. Egypt is in a great need of an ambitious reform program in its electric power

17th *ASMDA Conference Proceedings, 6 - 9 June 2017, London, UK*

system in order to avoid what is called "Electricity Crisis". The reason behind this problem is the rapid electricity demand growth without preplanned strategies to fulfill these needs.
Therefore, electricity utilities throughout the world have given a remarkable interest for forecasting electricity demand. Decision makers around the world widely use energy demand forecasting as one of the most important policy tools. One hour ahead forecast helps electric power utilities make correct scheduling decisions, minimize costs, maintain the balance between electricity supply and demand, and increase the reliability of electric power system (Bunn [1], Garcia and Kirschen [2]).

Artificial Neural Networks (ANNs) have been used for electricity demand forecasting. Regression approaches have criticized in that they use linear functions to forecast the load demand. However, ANN is able to perform nonlinear modeling. It does not assume any functional relationship to forecast electricity demand. In addition, the forecasts produced by ANNs are efficient and accurate (Park et al. [3]).

In 1996, ANNs was adopted to forecast electricity load for Greek Public Power Corporation (Bakirtzis et al. [4]). In (Liu et al. [5]), three short-term forecasting methods included an ANN, an autoregressive (AR) model, and fuzzy logic method were compared. They concluded that ANN and fuzzy logic outperformed AR model. In a recent study (Darbellay and Slama [6]), forecasts of short-term Czech electricity demand were obtained using ANN and autoregressive integrated moving average (ARIMA) models. The results showed the superiority of ANN.

In 2001, ANN was used to forecast electricity demand for the Republic of Ireland, while in 2009 it was used to forecast electricity load for California. ANN performed well and accurate forecasts were obtained (Ringwood et al. [7], Pindoriya et al. [8]).

Double seasonal pattern is shown in electricity demand series of many countries. A daily seasonal cycle is noticeable from the similarity of the hourly demand from one day to the other. Moreover, a weekly seasonal cycle is also found. The electricity demand of a certain day is same in different weeks. Therefore, using a forecasting method that takes into account these both seasonal patterns (daily and weekly) is vital. Double seasonal autoregressive integrated moving average (DSARIMA) model, a double seasonal Holt-Winters method and Artificial Neural Networks (ANNs) are proposed to capture the double seasonal pattern of the electricity demand series. In this paper, ANNs with different seasonal lags is investigated in accommodating these seasonal patterns and forecasting the Egyptian electricity demand series. The rest of this paper is organized as follows. Section II describes the Egyptian electricity demand series. Section III explains Artificial Neural Network (ANN). Section IV discusses the results. The conclusion closes the article.

2 Electricity demand in Egypt

A hourly data set of one year beginning from Saturday 7 January 2012 till Friday 28 December 2012 represents the Egyptian electricity demand series measured in megawatt (MW). Figure 1 shows a part of the Egyptian electricity demand series. Hour 1 till hour 24 represent the first day in this sub series that is Friday 1 June, and from hour 24 till hour 48 represents the second day and so on.

Figure 1 confirms the presence of both seasonal patterns (daily and weekly seasonal patterns). A daily seasonal cycle is apparent in this sub set. Electricity demand is similar for different days. A weekly seasonal cycle is also noticeable by comparing the electricity demand of a day in different weeks. It is observable that the weekdays have similar patterns of demand, while the weekend days that have a lower peak of demand have a different electricity demand.

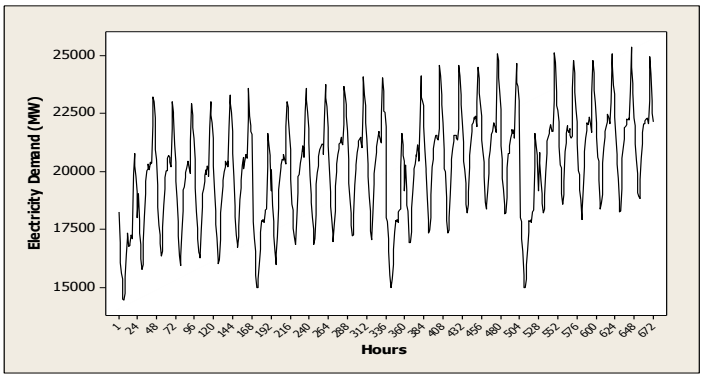

Fig. 1. Electricity demand in Egypt during the period from Friday 1 June to Thursday 28 June

3 Feed Forward Neural Network

ANNs have been developed as a mathematical model of human cognition or neural biological. ANN is based on the following assumptions:

i. Information processing occurs at elements (called neurons).
ii. Signals are passed between neurons over connection links.
iii. Each connection link has an accompanied weight.
iv. Each neuron applies an activation function to its input to determine its output signals.

Therefore, ANNs are characterized by the following components:

i. The interconnection pattern between the different layers of neurons (called its architecture)
ii. The process for setting and updating the weights of the interconnections (called its training or learning algorithm)
iii. The activation function that converts a neuron's weighted input to its output activation.

The connection patterns within and between layers is called the network architecture. An ANN has an input layer in which the activation of each neuron sends an external input signal; and an output layer that does not send an external input signals but from which the response of the net is produced. Neural networks are classified according to the number of layers into single layer networks or multilayer networks.

A single layer net has an input layer and an output layer. It has only one connection of weights. The input neurons are connected to output neurons but are not connected to other input neurons. A multilayer net contains one or more hidden layers which exist between the input layer and the output layer. Typically, there are more than one connection of weights. Multilayer nets can solve more complex problems than the single layer nets, but training algorithm may be more difficult.

A feedforward network refers to the direction of signals flow from the input units to the output units (see Figure 2). Input signals are passed through the neural network once to the output neurons. Feedforward networks with single hidden layer are the most widely used for forecasting financial and economic time series data (Kaastra and Boyd [9], Zhang et al. [10]).

Neural network behavior changes in order to adapt to the new environment. Such changes are due to changes in the weights in the network. A training algorithm is intended to model changes in the efficiency with which neurons pass information. The backpropagation algorithm is used in feedforward ANNs. The backpropagation algorithm uses supervised training, which means that we provide the algorithm with the actual values and calculate the error (difference between actual values and the forecasted values obtained by ANNs). Backpropagation algorithm aims to reduce this error, until the ANN fits the data well.

Training a feedforward network by backpropagation contains three steps: (1) the feedforward of the input training pattern, (2) the backpropagation of an error, and (3) the modification of the weigths.

The artificial neurons are arranged in layers and send their signals “forward”. The errors are calculated and then propagated backwards. The network receives inputs by neurons in the input layer, and the output of the network is given by the neurons on an output layer. The main purpose of the backpropagation

algorithm is to minimize the error. The training begins with random weights, and then modifies these weights until the error will be reduced.

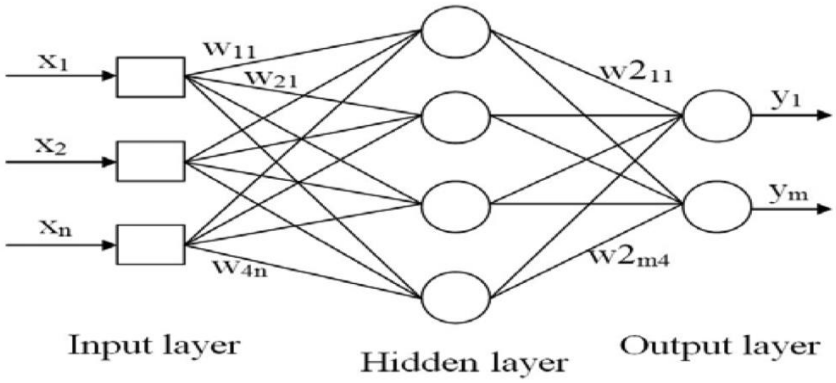

Fig. 2. Diagram of single hidden layer feed forward neural network

4 Empirical Results

In this section, we investigate the performance of ANN in forecasting the Egyptian electricity demand series taking into account different daily and weekly seasonal lags in order to accommodate the both seasonal patterns. Different number of single hidden layer feedforward ANNs were obtained using using R package version 3.1.0. Different electricity demand lagged values were used as input variables. Daily seasonal lags that are 24, 48, and 72 and weekly seasonal lags that are 168, 336, and 504 were considered. The complete Egyptian electricity demand series is used to get the ANNs except for the last 4 weeks of the series that are put aside to evaluate accuracy of post-sample forecasts.

For evaluating the forecasting accuracy of these ANNs, the mean absolute percentage error (MAPE) is calculated. The MAPE is the average of the absolute percentage prediction error (Taylor et al. [11]). Low values of this statistic are desirable. Table 1 shows different ANNs with different lags. The MAPE of the forecasts produced by these ANNs up to one week horizon, two weeks horizon, three weeks horizon and a month horizon were calculated as follows:

Table 1. The MAPE of out-sample forecasts of different ANNs

Different ANNs	MAPE (%) of the forecasts up to different time ahead			
	One week	Two weeks	Three weeks	One month
1 to 72, 168, 336, 504	3.96	3.83	3.69	4.29
1 to 72, 168, 336	3.26	3.41	4.14	4.61
1 to 72, 168	3.43	4.76	5.93	7.13
1 to 48, 168, 336, 504	3.55	3.44	3.28	3.79
1 to 48, 168, 336	3.08	3.20	3.87	4.28
1 to 48, 168	3.20	4.42	5.52	6.65
1 to 24, 168, 336, 504	2.33	2.23	2.25	2.70
1 to 24, 168, 336	2.21	2.30	2.59	2.90
1 to 24, 168	2.39	3.09	3.77	4.60

Based on the pervious results, ANNs with seasonal lags (1 to 24, 168,336, 504) and (1 to 24, 168, 336) that have the lowest MAPE for different time horizons are preferred. Figure 3 represents the forecasts produced by these two ANNs and the actual values of the Egyptian electricity demand series up to a week ahead. It is observable that the forecasts are close to the actual values. The two ANN are competitive to each other and could be considered as a good forecasting tool for the Egyptian electricity demand series.

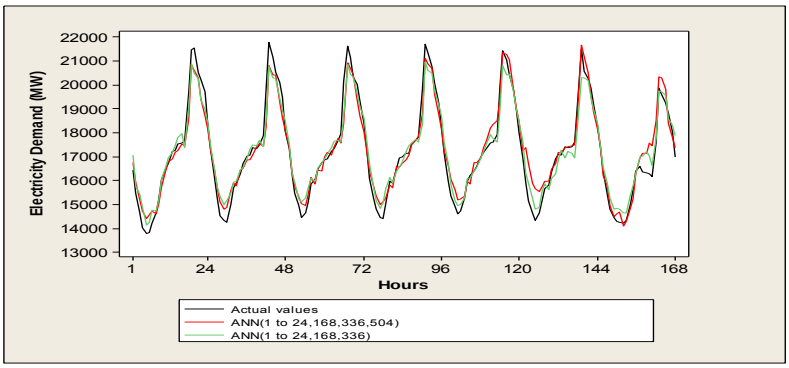

Fig. 3. Time plot of the actual values versus the forecasts produced by the selected ANN

Conclusions

Forecasting is a critical problem. The improvement of the forecasting accuracy comes from a good method that provides accurate forecasts. An observable feature of the electricity demand time series is the presence of both daily and weekly seasonal patterns. It is found that the daily electricity demand has the same pattern every day. In addition, the weekly electricity demand is not different through different weeks. Electricity demand on weekend days is observed to be similar on different weeks but different from the other days. Taking this feature into account during forecasting improves our forecasting accuracy. That is in turn will help in control and scheduling of electric sector.
In this paper, Artificial Neural Network was investigated for forecasting hourly electricity demand in Egypt taking into account different seasonal lags as inputs. Results showed that the forecasts produced by these networks were accurate for different time horizons and could be used as a recommended forecasting tool by the Egyptian electric power authority to obtain accurate forecasts for development. For future work, different other forecasting methods such as Bayesian forecasting methods could be used to analyze the Egyptian electricity demand series. In addition, controlling external effects plays an important role to improve forecasting accuracy.

References

1. D. W. Bunn. Forecasting loads and prices in competitive power markets, Proc. of the IEEE, 88, 163-169, 2000.
2. M. P. Garcia and D. S. Kirschen. Forecasting system imbalance volumes in competitive electricity markets, Power Systems, IEEE Transactions, 21, 240-248, 2006.
3. C. D. Park, A. M. El- Sharkawi, R. J. Marks, E.L. Atlas and J. M. Damborg. Electric Load Forecasting Using An Artificial Neural Network, IEEE Transadions on Power Systems, 6, 442-449, 1991.
4. A. G. Bakirtzis, V. Petrlolls, S. J. Klartzls, M. C. Alexladls and A. H. Malssls. A Neural Network Short Term Load Forecasting Model for the Greek Power System, IEEE Transactions on Power Systems, 11, 2, 858 – 863, 1996.
5. K. Liu, S. Subbarayan, R. R. Shoults, M. T. Manry, C. Kwan, F. L. Lewis and J. Naccarino. Comparison of Very Short Term Load Forecasting Techniques, IEEE Transactions on Power Systems, 11, 877– 882, 1996.
6. G. A. Darbellay and M. Slama. Forecasting the Short-term Demand for Electricity — Do Neural Networks stand A Better Chance?, International Journal of Forecasting, 16, 71– 83, 2000.
7. J. V. Ringwood, D. BocellI and F. T. Murray. Forecasting Electricity Demand on Short, Medium and Long Time Scales Using Neural Networks, Journal of Intelligent and Robotic Systems, 31, 129–147, 2001.
8. N. M. Pindoriya, S. N. Singh and S. K. Singh. One-Step-ahead Hourly Load Forecasting using Artificial Neural Network, International Conference on Power Systems (ICPS), 9, 1 – 6, 2009.

9. I. Kaastra and M. Boyd. Designing a Neural Network for Forecasting Financial and Economic Time Series, Neurocomputing, 10, 215-236, 1996.
10. G. Zhang, B. E. Patuwo and M. Y. Hu. Forecasting with Artificial Neural Networks: The state of the Art, International Journal of Forecasting, 14, 35– 62, 1998.
11. J. W. Taylor, L. M. de Menezes and P. McSharry. A Comparison of Univariate Methods for Forecasting Electricity Demand up to a day ahead , International Journal of Forecasting, 22, 1–16, 2006.

The score correlation coefficient

Z.Fabián

Institute of Computer Science, Academy of Sciences of the Czech Republic Pod vodárenskou věží 2 Prague 18200 Czech Republic
(E-mail: zdenek@cs.cas.cz)

Abstract. The t-score is a real-valued score function with a sense of likelihood score for central point of the distribution. This concept is used for definition of a distribution-dependent score correlation coefficient. Its performance is compared with some currently used correlation coefficients by means of Monte Carlo experiments.
Keywords: generalized likelihood score, t-score, heavy-tails.

1 Introduction

The usual measure of linear dependence of random variables X and Y with finite expectations EX, EY and finite variance $VarX = E(X-EX)^2$, $VarY = E(Y-EY)^2$ is their correlation coefficient

$$\rho(X,Y) = \frac{E(X-EX)(Y-EY)}{[VarXVarY]^{1/2}}. \tag{1}$$

Formula (1) can be naturally generalized for arbitrary random variables including those with heavy-tailed distributions into

$$\rho(X,Y) = \frac{E\psi_1(\tilde{X})\psi_2(\tilde{Y})}{[E\psi_1^2(\tilde{X})E\psi_2^2(\tilde{Y})]^{1/2}} \tag{2}$$

where ψ_1, ψ_2 are functions with finite first and second moments and $\tilde{X}, \tilde{Y}$ are centered versions of X and Y, respectively.

Given the observed sample $(x_1, y_1), ..., (x_n, y_n)$ of a bivariate random variable (X, Y), the finite version of (2) is

$$r(x,y) = \frac{\sum \psi_1(\tilde{x}_i)\psi_2(\tilde{y}_i)}{\left(\sum \psi_1^2(\tilde{x}_i) \sum \psi_2^2(\tilde{y}_i)\right)^{1/2}}, \tag{3}$$

where $\sum$ is either the usual sum $\sum_{i=1}^n$, which is used in this paper, or its trimmed analogue (Gnanadesikan and Kettenring, 1972).

By setting $\psi_1(z) = \psi_2(z) = z$, $\tilde{x}_i = x_i - \bar{x}, \tilde{y}_i = y_i - \bar{y}$, (3) turns into the Pearson sample correlation coefficient, r_P, say. By setting $\psi_1(z) = \psi_2(z) = \psi(z)$ where ψ is a bounded function and $\tilde{x}_i = x_i - med(x)$, $\tilde{y}_i = y_i - med(y)$, (3) turns into a robust correlation coefficient. As ψ is often taken the Huber psi-function

$$\psi(z,k) = \max[-k, \min(z,k)], \tag{4}$$

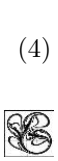

with some chosen value k. An overview of other robust variants of (2) is given i.e. by Shevlyakov and Smirnov (2011). The Spearman rank correlation coefficients is the sample correlation coefficient between the observation ranks.

All these estimates are independent of distributions of X and Y. The question is whether taking them into account could improve correlation estimates.

Example 1. Let us consider a heavy-tailed loglogistic distribution F_L with support $(0, \infty)$ and probability density

$$f_L(x;t) = \frac{1}{t}\frac{1}{(1+x/t)^2}. \tag{5}$$

Note that even the mean of F_L does not exist. The log-likelihood score for t is

$$S_L(x;t) = \frac{1}{t}\frac{x/t-1}{x/t+1}. \tag{6}$$

Clearly, $ES_L = 0$ and ES_L^2 is finite. Given an observed sample $(x_1, ..., x_n)$ from F_L, the maximum likelihood estimate $\hat{t}$ of t is the solution to the equation

$$\sum_{i=1}^{n} \frac{x_i - t}{x_i + t} = 0. \tag{7}$$

Since t can be considered in (5) as a 'central value' of F_L and the value $S_L(x_i;\hat{t})$ of the log-likelihood score actually expresses relative influence of x_i with respect to $\hat{t}$, function (6) seems to be the proper function to be used in formula (3).

As a first test of this idea we generated independent random samples of X and Z, both distributed according F_L, with $t = 1$. By setting

$$Y = \rho X + \sqrt{1-\rho^2}Z \tag{8}$$

we obtained samples (X, Y) with theoretical correlation coefficient ρ. The sample likelihood score correlation coefficient r_L was obtained by taking in (3) $\psi_1(\tilde{x}_i) = S_L(x_i;\hat{t}_1), \psi_2(\tilde{y}_i) = S_L(y_i;\hat{t}_2)$, where $\hat{t}_1$ and $\hat{t}_2$ are the corresponding solutions of (7). For each sample we computed also the Spearman rank coefficient (r_S) and the robust correlation coefficient with Huber psi-function (4) and $k = 1.75\hat{t}_j$. For illustration purposes we computed also the sample Pearson's correlation coefficient (r_P), though its use in the case of distribution (5) is not entitled.

Average values of these sample correlation coefficients after 20.000 repeated experiments are shown on Fig. 1.

Besides the expected result that Pearson r_P is of no use, we see that the likelihood r_L behaves by a similar way as Spearman and Huber estimates. Moreover, and surprisingly for the author, all the usable estimates depend on the value of ρ, overestimating it when the true correlation is low and underestimating it when the correlation is high.

Recently, Fabián (2001) introduced a scalar score function of continuous distributions with arbitrary support, taken as a likelihood (Fisher) score with respect to the 'center' of F. It makes possible to study distribution-dependent

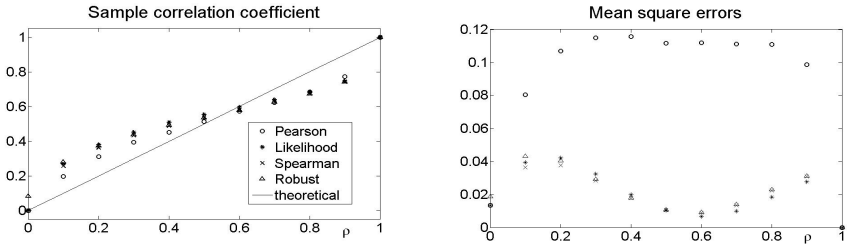

Fig. 1. Dependence of average sample correlation coefficients and mean square errors on theoretical ρ for loglogistic distribution.

score correlation coefficients (3), where psi-functions are scalar score functions of distributions.

In the paper we shortly introduce the relevant scalar scores and present a comparison of behavior of the score correlation coefficient with those mentioned above on the base of Monte Carlo experiments.

2 t-score and score correlation coefficient

The transformation-based score or shortly t-score of a (non-transformed) distribution G with support the entire real line $\mathcal{R}$ and probability density g is the usual score function $T_G(x) = -g'(y)/g(y)$. Let us state that its central point y_G^* is the mode, the solution of equation $T_G(y) = 0$. A transformed distribution $F(x) = G(\eta(x)$ with open interval support $\mathcal{X} = \varphi^{-1}(\mathcal{R})$, where $\varphi : \mathcal{X} \to \mathcal{R}$ is a smooth strictly increasing function, has t-score

$$T_F(x) = T_G(\varphi(x)) \tag{9}$$

and central point $x_F^* = \varphi^{-1}(y_G^*)$, the solution of equation $T_F(x) = 0$.

Formula (9) can be rewritten (Fabián, 2001) into aform independent on G,

$$T_F(x) = -\frac{1}{f(x)} \frac{d}{dx} \left[\frac{1}{\eta'(x)} f(x) \right]. \tag{10}$$

As the the support-dependent functions $\eta(x)$ we define mappings suggested by Johnson (1949),

$$\eta(x) = \begin{cases} \log(x-a) & \text{if } \mathcal{X} = (a, \infty) \\ \log \dfrac{(x-a)}{(b-x)} & \text{if } \mathcal{X} = (a, b). \end{cases} \tag{11}$$

The reasons for this choice and exceptions from this rule, not important for the present study, are discussed in details by Fabián (2016).

The t-scores of heavy-tailed distributions are bounded. Score moments ET_F and ET_F^2 of any distribution are finite, $ET_F = 0$. Function

$$S_F(x) = \eta'(x_F^*) T_F(x)$$

equals for a particular class of distributions with 'central' parameter, as in Example 1, the likelihood score for this parameter. ES_F^2 is thus interpreted as generalized Fisher information with respect to x_F^*. The reciprocal value

$$\omega_F^2 = \frac{1}{ES_F^2}$$

can be taken as a measure of variability of F (Fabián, 2007, 2016).

Since in (10) is differentiation with respect to the variable, all concepts concern parametric distributions as well. A parameter $\theta = (\theta_1, ..., \theta_m)$ of $F_\theta(x)$ can be estimated by means of the score moment estimating equations

$$\frac{1}{n}\sum_{i=1}^{n} T_F^k(x_i;\theta) = ET_F^k(\theta), \qquad k = 1, ..., m, \tag{12}$$

Fabián and Stehlík (2008), Fabián (2010, 2016).

Let now X, Y be random variables with (not necessarily identical) open interval supports $\mathcal{X}$ and $\mathcal{Y}$, respectively. Let F_{XY} be the joint distribution and T_X, T_Y be t-scores of marginal distributions of X and Y. The finite version of (2), the *sample score correlation coefficient*, is given by (Fabián, 2010)

$$r_F = \frac{\sum_{i=1}^{n} T_X(x_i;\hat{\theta}_X)T_Y(y_i;\hat{\theta}_Y)}{\left[\sum_{i=1}^{n} T_X^2(x_i;\hat{\theta}_X)\sum_{i=1}^{n} T_Y^2(y_i;\hat{\theta}_Y)\right]^{1/2}}, \tag{13}$$

where $\hat{\theta}_X$ and $\hat{\theta}_Y$ are estimates of corresponding vectors of parameters of marginal distributions, respectively.

For distributions with linear t-score, that is for normal, gamma and beta distributions, (13) is identical with the Pearson correlation coefficient. Properties of r_F of distributions with non-linear t-scores were studied by means of Monte Carlo experiments.

3 Results of simulation experiments

Couples (X, Y) were constructed using independent random samples of X and Z generated from one or two-parameter marginal distributions as in Example 1 with the use of (8), using routines from the MATLAB Statistics toolbox.

Rough estimates of parameters of marginal distributions were found by the solution of the corresponding equations (12). The size of samples was n=75. For $n > 25$ results practically did not depend on n.

The results are as follows.

The score correlation coefficient of distributions with support $\mathbb{R}$ and with finite interval support exhibit neither dependence on the variability of distributions nor dependence on ρ. Even in the case of a non-symmetric heavy-tailed extreme value distribution, Pearson's r_P is less biased than r_F. We conclude that for slightly skewed distributions correlation relations 'overcome' properties of distributions.

Let us present results of simulation study of distributions with support $\mathcal{X} = (0, \infty)$ with various properties of right tais: Weibull with light tail, Pareto type III ('shifted' Pareto), which is the simplest model of a heavy-tailed distribution, and Fréchet (inverse Weibull) with fat tail. The density, t-scores and score variances of these distributions are given in Table 1, Pareto III is the beta-prime distribution with $p = 1$.

F	$f(x)$	$T_F(x)$	x_F^*	ω_F^2
Weibull	$\frac{c}{x}(\frac{x}{\tau})^c e^{-(\frac{x}{\tau})^c}$	$c[(\frac{x}{\tau})^c - 1]$	τ	$\frac{\tau^2}{c^2}$
beta-prime	$\frac{1}{B(p,q)} \frac{x^{p-1}}{(x+1)^{p+q}}$	$\frac{qx-p}{x+1}$	$\frac{p}{q}$	$\frac{p(p+q+1)}{q^3}$
Fréchet	$\frac{c}{x}(\frac{x}{\tau})^{-c} e^{-(\frac{x}{\tau})^{-c}}$	$c[1 - (\frac{x}{\tau})^{-c}]$	τ	$\frac{\tau^2}{c^2}$

Table 1. Characteristics of some distributions with support $(0, \infty)$

To avoid studying of very skewed distributions generating data both either near zero or too large, we select parameters giving mild values of the score coefficient of variation, which we define by

$$scv = \frac{x_F^*}{\omega_F}.$$

It appeared that for a given *scv* results practically do not depend on x_F^*.

According to Table 1, the score coefficient of variation of Weibull and Fréchet distributions is $scv = c$ and of Pareto III is $scv = \sqrt{q/q+2}$. A decrease values of *scv* means increase of variability, generating large outliers, which are, however, in accordance with the distribution.

To estimate correlation coefficient of skewed distributions with light tail having $T_F(x) \sim x^c$ with approximately $c > 0.75$, the most suitable is the Pearson's r_P. For $c < 0.75$, the most suitable estimates affords the score correlation coefficient r_F. These results are illustrated by Fig. 2.

Fig. 3 shows the dependence of estimates of the correlation coefficient in case of the Pareto distribution. As in Example 1, the unfavorable tendency of estimates with decreasing score coefficient of variation is clearly apparent: low ρs are overestimated and high ρs are underestimated. For distributions with Pareto tails with high *scv* appears to be the best estimates the score r_F. For descending values of *cv*, that is, with increasing variability of distributions, represented by the fat-tailed Fréchet, the rank estimate r_S seems to be the best.

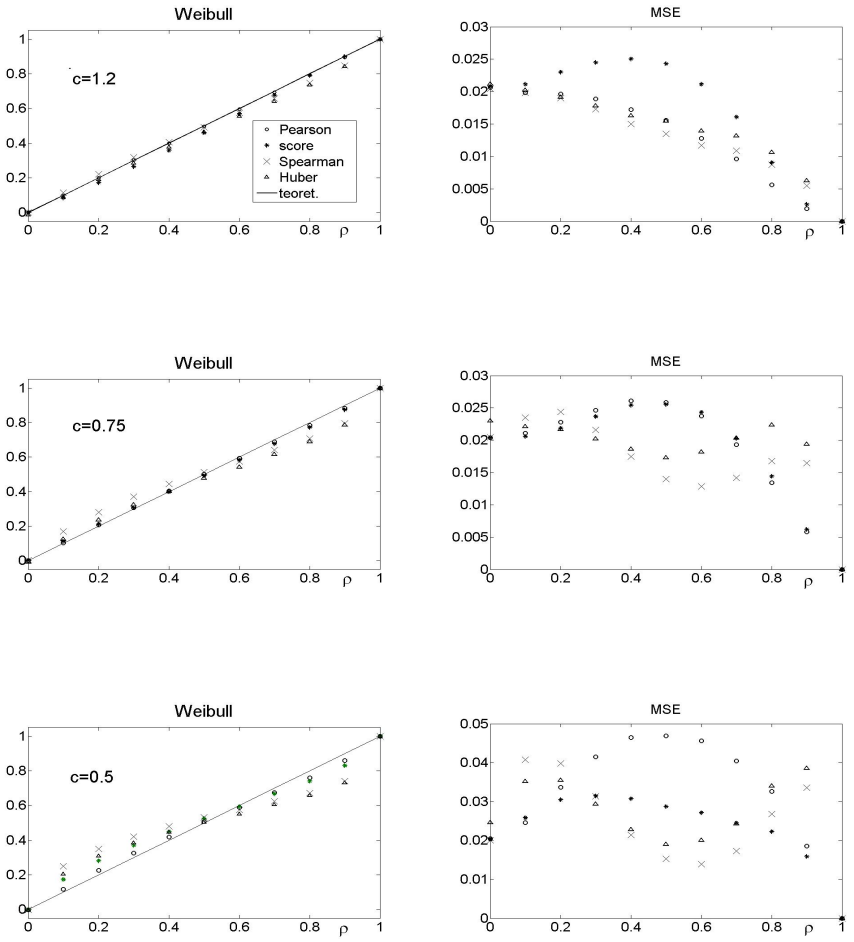

Fig. 2. Dependence of average sample correlation coefficients and mean square errors on theoretical ρ for Weibull distribution.

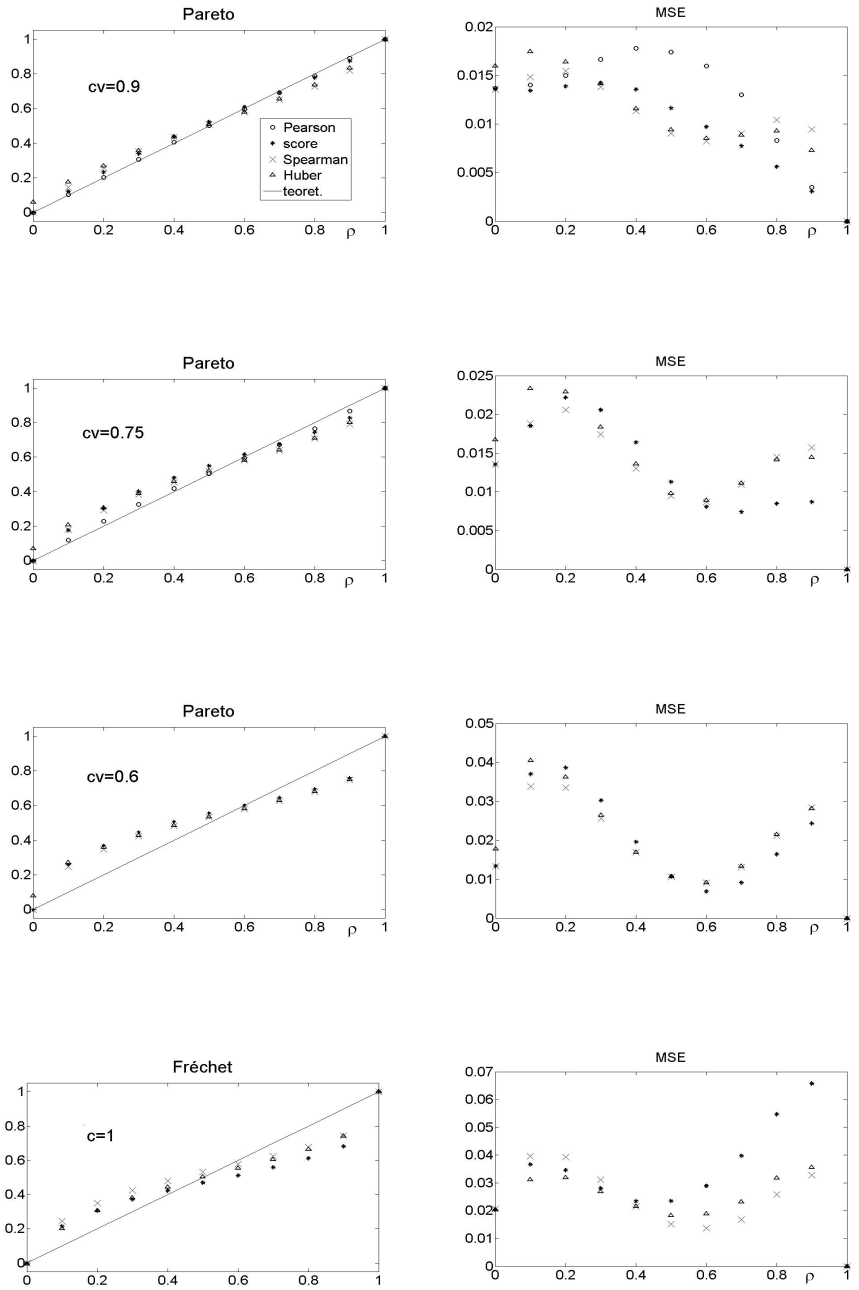

Fig. 3. Dependence of average sample correlation coefficients and mean square errors on theoretical ρ for heavy-tailed distributions.

4 Conclusions

The t-score of a continuous distribution is a function describing a relative influence of $x \in \mathcal{X}$ with respect to the central point of distribution. It makes possible to introduce a distribution-dependent correlation coefficient. This concept, perhaps theoretically interesting, seems to have a practical use only for random variables with distributions having tails of Pareto type, for which is less biased than both robust and rank correlation coefficients. On the base of our simulation experiments we conclude, that for estimation of association of data from symmetric or mildly non-symmetric distributions the best is the Pearson r_P, and for highly skewed distributions with fat tails the Spearman rank coefficient is the most robust.

Acknowledgement. The work was done by institutional support RVO:67985807.

References

1. Fabián Z. Estimation of simple characteristics of samples from skewed and heavy-tailed distributions. *Recent Advances in Stochastic Modeling and Data Analysis* Ed. C. Skiadas, Singapore: World Scientific, 43–50, 2007.
2. Fabián Z., Stehlík M. A note on favorable estimation when data is contaminated. *Comm. Depend. Quality Management*, 11, 36-43, 2008.
3. Fabián Z. Score moment estimators. *Proceedings of the conference COMPSTAT 2010*, Physica-Verlag Springer, 2010.
4. Fabián, Z. Score correlation. *Neural Network World*, 20, 793–798, 2010.
5. Fabián Z. Score function of distribution and association of random variables. *Forum Statisticum Slovakum*, 5, 10–18, 2013.
6. Fabián Z. Score function of distribution and revival of the moment method. *Comm. Statist. Theory Methods*, 45, 1118–1136,2016.
7. Gnadnadesikan R., and Kettering, J.R. Robust estimates, residuals and detection with multiresponse data. *Biometrics*, 28, 81–124, 1972.
8. Johnson, N.L. Systems of frequency curves generated by methods of translations. *Biometrika* 36, 149–176, 1949.
9. Huber P. J., Ronchetti E. M. *Robust statistics*. Hoboken: Wiley, 2009.
10. Mori, D. D., Kotz, S. *Correlation and dependence*. London: Imperial College Press, Springer, 2001.
11. Shevlyakov G., Smirnov, P. Robust estimation of the correlation coefficient: An attempt to survey. *Austrian J. of Statistic* 1, 2, 147–156, 2011.

Differences in Life Expectancy by Marital Status in the Czech Republic after 1990 and their Decomposition by Age

Tomas Fiala[1] and Jitka Langhamrova[2]

[1] Department of Demography, Faculty of Informatics and Statistics, University of Economics, Prague, nam. W. Churchilla 4, 130 67 Praha 3, Czech Republic
(E-mail: fiala@vse.cz)

[2] Department of Demography, Faculty of Informatics and Statistics, University of Economics, Prague, nam. W. Churchilla 4, 130 67 Praha 3, Czech Republic
(E-mail: langhamj@vse.cz)

Abstract. Differences in life expectancies by marital status is a well-known phenomenon. To understand better the nature of these differences it is appropriate to use the decomposition method which can detect contributions of individual age groups in adult age to the total difference.
The aim of this paper is to quantify the age-specific contributions of individual age groups to the total differences in life expectancy at births by marital status in the Czech Republic since 1990. The analysis is based on annual Czech Statistical Office data. Each five-year time period is analysed separately.
Highest contributions to the total differences in life expectancy at births were observed for males mainly in the age groups 50–59 and 60–69 years, for females usually in the age groups 60–69 and 70–79 years. In first decade studied for males under 60 single the highest contribution show single males while at higher ages divorced and widowed. In the last decade, single males have highest contribution in all age groups. For females, the development is more regular and stable. The highest contribution is observed for single females, the lowest for widowed.
Keywords: family status, life expectancy, decomposition by age, Czech Republic.

1 Introduction

Demographic studies usually analyze mortality by age and gender. However, mortality also depends on many other factors. One such factor is marital status, which is also one of the very important demographic criteria determining the demographic behavior of the population. Single people have different demographic behavior than married, divorced or widowed people. Therefore, marital status is considered an important social indicator that differentiates the population based on their link to family and marriage. Changes in marital status (marriage, divorce, widowhood) are considered very important demographic events. Marital status also provides indirect information about the lifestyle and status of an individual in society. Social status can sometimes depend on, or be

partly determined by, marital status. There is a statistical correlation between marital status and death rate.

The mortality of married people is lower than that of single, divorced or widowed people. This is what William Farr, an epidemiologist, physician and statistician of the General Register Office for England and Wales, (mostly known as the founder of medical statistics and the first classification of death causes) already claimed in the 19th century (1858). Based on the analysis of specific mortality rates by age, he showed that the mortality of single people is considerably higher than the mortality of married people of the same age and that the mortality of widowed people is even higher (Parker-Pope[4]).

The differences in mortality by marital status were confirmed by many other studies. Their explanation is based on many theories and hypotheses that can be divided into two basic groups. The first one, the so-called causality theory (protection theory), is based on the hypothesis of a "protective" effect of marriage and its positive influence on health and a longer life. On the other hand, the second theory, the so-called selection theory, is based on the hypothesis that those who get married are healthier on average, and thus their mortality is lower.

The causality theory emphasizes that marriage is an important social institution. Based on this theory, a better quality of life in wedlock stems from the fact that the spouses support each other emotionally and socially. They overcome life problems better and more easily and usually have more social contacts and thus can find necessary support or help from friends more easily in case of any problems. The causality theory also points out the fact that life in wedlock promotes a healthier lifestyle, married people have fewer bad habits, such an excessive alcohol consumption and smoking, and suffer from depression and anxiety less often. Married couples also usually keep track of each other's health condition and thus are more likely to see a physician earlier in case of any medical problem. Women in particular make sure that all family members have preventive checkups and take care of their spouse if he becomes seriously ill. Married people also have a better financial situation and usually a higher standard of living since they have joint funds and share some expenses. If one of the spouses loses work, the other spouse can financially support him or her as long as necessary. According to the causality theory, the longer a marriage lasts, the more benefits it provides. (Hamplová[2], pp. 738 -739.)

The question is whether marriage is as beneficial for men as for women, or whether marriage provides more advantages to men or women. This issue was researched by Jessie Bernardová, who concluded that marriage provided more advantages to men than to women. According to her, married women are not actually happier, but adjust their answers in different surveys to expected social norms that assume that married women are happier. (Hamplová[3], p. 133.)

An interesting question is whether marriage positively affects men about the same as women, or whether men or women benefit from marriage more. Based on some studies, marriage has a bigger impact on men because the differences in mortality between single and married men are bigger than those between single and married women. However, other studies show that women benefit

from marriage more than men, or that men and women benefit from marriage about the same but in different areas. Marriage has a positive impact on men by protecting them against depression and on women by protecting them against alcoholism. It is pointed out that men have better psychological health regardless of marital status than women. A life crisis, such as divorce or widowhood, affects men and women differently. These crises affect men much more than women.

On the other hand, the selection theory assumes that people marry or do not marry, or remain in wedlock for a shorter or longer period of time, mostly based on their personality traits. According to this theory, the mortality of married men and women is not lower because they are married. This theory stresses a favorable selective impact of marriage on mortality, e.g. people with a serious illness or a physical handicap usually do not marry, and also assumes that people with certain personality traits, e.g. temperament, optimism, etc., are better preconditioned for creating and maintaining long-term relationships, which is also positively reflected in their lower mortality. On the other hand, people suffering from depression, ill people or alcoholics, etc. (i.e. people whose mortality exceeds the average) have less chance to marry and their risk of divorce is higher.

Nevertheless, Hamplová[3], pp. 131-132, mentions three reasons why the selection theory has been called into question lately. The first reason is that the measurements of physical and psychological health either do not confirm the selectivity effect or show only a very weak selectivity effect. The second reason is that the mortality of the widowed (who were married for a rather long time) is higher than that of people who are still married, i.e. marriage decreases mortality. The third fact that calls the selection theory into question is based on the conclusions of medical research confirming that single people die more often due to their different lifestyle rather than due to their genetically conditioned illness.

The number of marriages in the Czech Republic and many European countries has currently gone down and more and more couples live together out of wedlock. This fact should also be analyzed and researched to see whether or not living out of wedlock has the same positive impact on mortality as marriage. However, the problem is that there are usually no reliable data about the number, gender and age of people living together out of wedlock and mostly that this fact is not investigated in the deceased.

2 Differences in mortality by marital status in the Czech Republic

Pechholdová and Šamanová[5] provide a very detailed analysis of the correlation between mortality and marital status in the Czech Republic for the years the population census was carried out starting in 1960. In all analyzed years, the life expectancy of married men and women aged 30 is higher than the

life expectancy of unmarried men and women, and the difference is higher in men than in women.

The trends during the socialist regime (1961–1990) and the post-socialist era were quite different. The differences in the mortality of the married and the unmarried doubled and even tripled during the 1960s, 1970s and 1980s as compared to the year 1961. During the entire analyzed time period, the mortality of single women was the highest and the mortality of widows the lowest from among unmarried women, although the mortality of divorced and widowed women gradually approximated. In the case of men, the situation was different at first. In the years 1961, 1971 and 1981, the mortality of divorced men was the highest and the mortality of single men the lowest from among unmarried men. This trend changed in 1991 where (similarly to women) the mortality of single men was the highest and the mortality of widowers the lowest (Tab. 1).

Tab. 1. Differences in life expectancy at births by marital status
Reference category: married

Year	1961	1970	1980	1991	2001	2010
Males						
Single	-3.08	-5.11	-6.59	-9.15	-8.76	-9.58
Divorced	-3.63	-5.58	-7.34	-8.24	-7.47	-7.65
Widowed	-3.54	-5.39	-7.44	-7.16	-7.24	-5.73
Females						
Single	-3.26	-4.67	-5.50	-6.65	-7.57	-7.70
Divorced	-2.46	-3.12	-3.49	-4.77	-4.67	-4.99
Widowed	-1.31	-1.64	-2.39	-3.21	-4.04	-4.69

Source: Pechholdová and Šamanová[5], Tab. 1

In her analysis of comparative indexes of mortality in individual years during 1982–1993, Rychtaříková[6] shows that the mortality of single men practically did not change, while mortality in other marital status categories decreased, in particular in married men. The mortality of women in all marital status categories decreased, but considerably less in single women.

3 Trends of life expectancy development by marital status in 1990–2014

After the year 1989, the behavior of the Czech population in terms of marriage rather considerably changed. People got married at an older age, the marriage rates dropped and the percentage of children married out of wedlock went up. For instance, while almost 79% of men and over 83% of women were married at the age of 30–39 in the year 1991, only about 50% of men and slightly over 60% of women were married at the same age in the year 2010 (Pechholdová, Šamanová[5], Tab. 2).

This chapter provides the results of the analysis of the trend in the mortality of men and women by marital status and analyzes life expectancy at birth by marital status. This life expectancy was calculated in a usual way based on complete mortality tables by marital status, using the Czech Statistical Office's data containing the number of the deceased and the number of population in the individual years of the analyzed time period classified by gender, age unit and marital status.

Specific death rates for people under the age of 16, when it is not possible to marry, were considered to be the same for all marital status categories (equal to death rates regardless of marital status). Death rates were differentiated based on marital status after the age of 16, but only if the mid-period population of the given age and marital status was higher than 100. In the case that the mid-period population of the given age and marital status was lower, the mortality of all people of the given age was used, regardless of marital status.

The life expectancy of men and women kept going up more or less linearly during the entire analyzed time period (Fig. 1). The life expectancy of all men went up (regardless of their marital status) from not quite 67.6 years to 75.7 years, i.e. by 3.9 months a year. The increase in the life expectancy of married men was slightly lower (by 3.8 months), but higher in the case of other categories of men (the average increase in the life expectancy of single men was 4.4 months a year, of divorced men 5.3 months a year and of widowers 5.7 months a year). Therefore, the differences of married and unmarried men lessened, while the differences of widowed, divorced and single men increased.

The increase in the life expectancy of women, regardless of marital status, was lower (by 3 months a year on average), from 75.5 in the year 1990 to 81.7 in the year 2014 (Fig. 2). When taking into consideration marital status, the increase was also lower in women than in men. The life expectancy of married women during the analyzed time period went up by 2.4 months a year on average, while the life expectancy of single women went up by 3.1 months a year, of divorced women by 3.3 months a year and of widows by 3.2 months a year. Similarly to men, the differences in the life expectancy of married and unmarried women lessened.

The trend in life expectancy, taking into account marital status, shows much bigger incidental deviations from the linear trend since especially the number of people of a certain marital status is very low in particular in some age groups. In order to eliminate these deviations, life expectancy for the individual five-year periods of 1990–94, 1995–99, …, 2010–14 were calculated as well. Since the goal of the trend analysis is not really the trend in life expectancy but rather the trend in life expectancy by marital status, married men and women were chosen as a reference category and the differences in life expectancy in this reference category and in the individual categories of unmarried people (i.e. single, divorced and widowed people) were analyzed.

The basic trends are the same for both men and women (Fig. 3 and 4). In all analyzed time periods, the life expectancy of single people differed from the life expectancy of married people the most, while the life expectancy of widowed

people differed the least. The difference for females was approximately 1 to 4 years less than in the relevant category of men during the same time period.

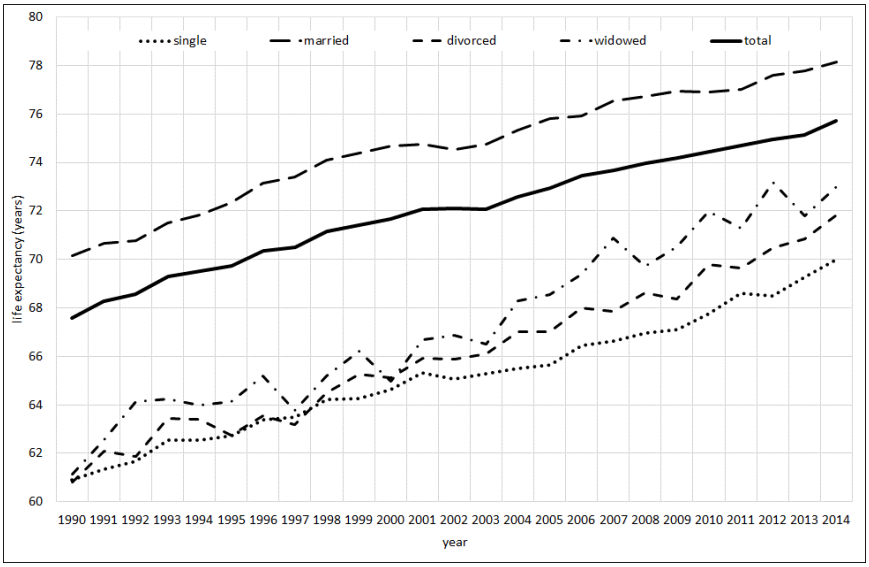

Source: data Czech Statistical Office, authors' calculation

Fig. 1. Life expectancy at births by marital status – males

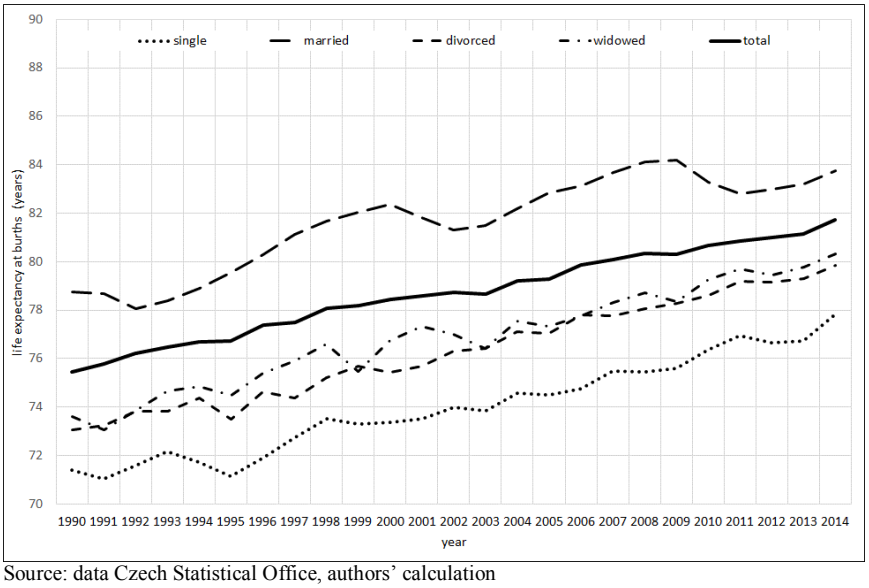

Source: data Czech Statistical Office, authors' calculation

Fig. 2. Life expectancy at births by marital status – females

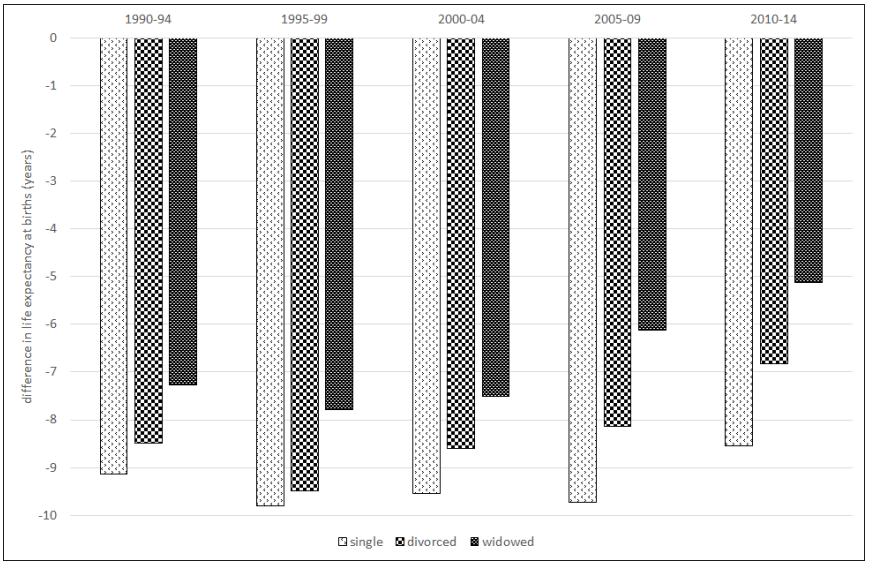

Source: data Czech Statistical Office, authors' calculation

Fig. 3. Differences in life expectancy at births by marital status – males (reference category – married)

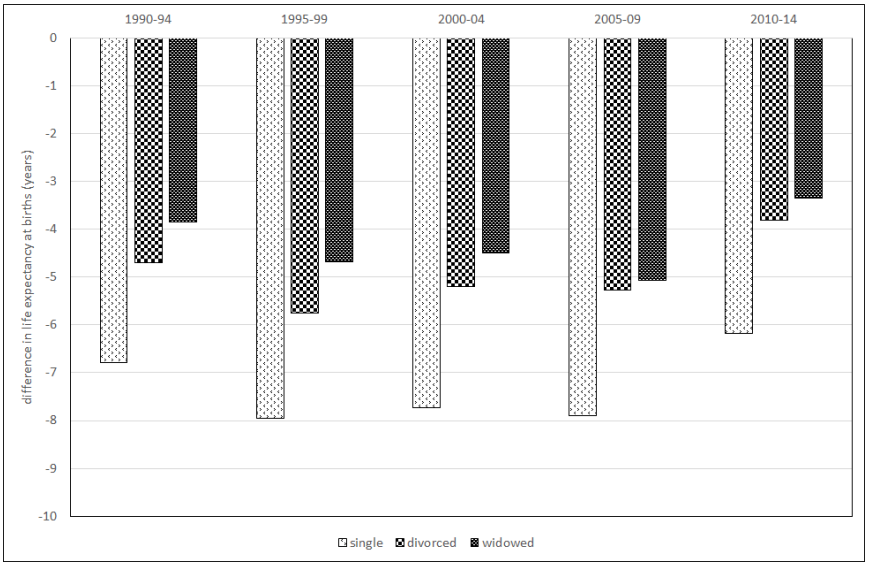

Source: data Czech Statistical Office, authors' calculation

Fig. 4. Differences in life expectancy at births by marital status – females (reference category – married)

While all differences were bigger during 1995–1999 than in the previous time period, they started lessening after 2000 and were smaller in the last analyzed time period of 2010–2014 than in the time period of 1990–1994. This may be caused by the gradual drop in the marriage rate, the higher percentage of single people in the population and thus the lower selective effect of marriage on mortality.

4 Decomposition of life expectancy differences by age

From a demographic standpoint, it is important to analyze not only the difference in overall life expectancy but also the contribution of individual age groups to this overall difference. For these purposes, the method which decomposes differences in life expectancy to the contribution of each age group is often used. This is why the decomposition of the overall difference of life expectancy by ten-year age intervals was calculated for each analyzed time period and each category of unmarried people. Of course, there cannot be any difference in the age group of 0–9, and the differences in the age group of 10–19 and 90–99 are insignificant. This is why these age groups are not shown in the following figures.

When comparing with married men and women, the biggest contributions to the difference in life expectancy at birth come mostly from men in the age groups of 50–59 and 60–69 and usually from women in the age of 60–69 and 70–79. However, the contributions differ, depending on marital status. During the first analyzed five-year time periods, the biggest contribution of men aged under 60 comes from single men, while the biggest contribution of men over 60 comes from divorced or widowed men. One of the main reasons may be the fact that young single men die more due to their irresponsibility, unhealthy lifestyle or some medical reason (which may also be why they did not get marry), while older single men are psychologically more stable than divorced or widowed men, some of whom may have a hard time dealing with the dissolution of their marriage or with the death of their long-time spouse. However, this was not the case during the past ten years, and in all age groups of men, single men contribute to the difference in life expectancy the most and widowed men the least, which corresponds to the overall difference in life expectancy at birth. The trend in women is more regular and, with some exceptions, single women always contribute the most and widows the least. See Fig. 5 – 14.

Conclusions

The life expectancy of men in the Czech Republic went up by more than 8 years and that of women by more than 6 years between 1990 and 2014. After the year 1990, the mortality of married people was lower than the mortality of single, divorced and widowed people, which corresponds to European trends.

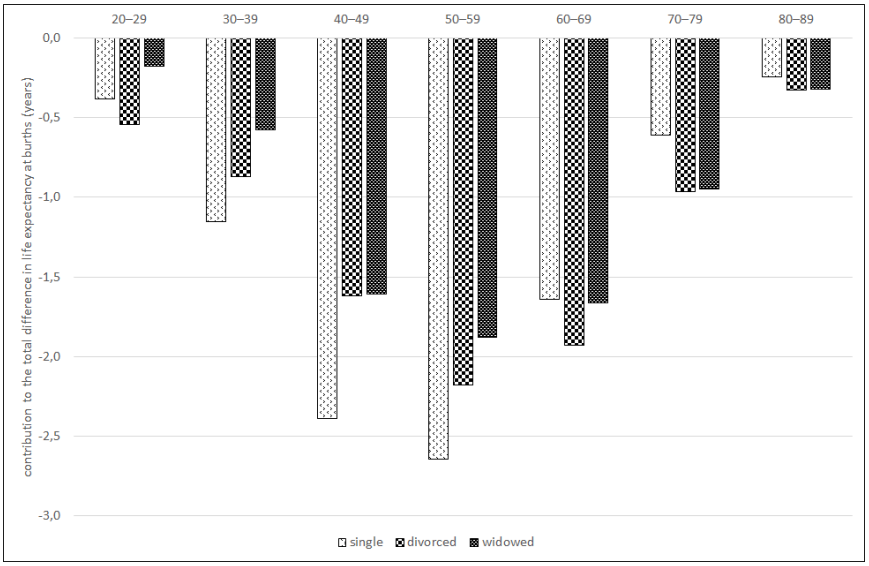

Source: data Czech Statistical Office, authors' calculation

Fig. 5. Decomposition by age in life expectancy at births by marital status – 1990–1994 males (reference category – married)

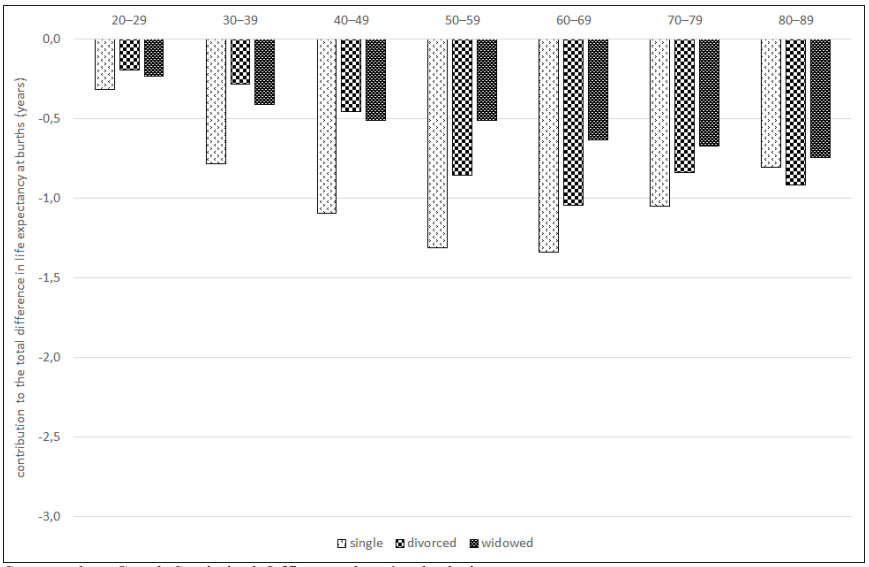

Source: data Czech Statistical Office, authors' calculation

Fig. 6. Decomposition by age in life expectancy at births by marital status – 1990–1994 females (reference category – married)

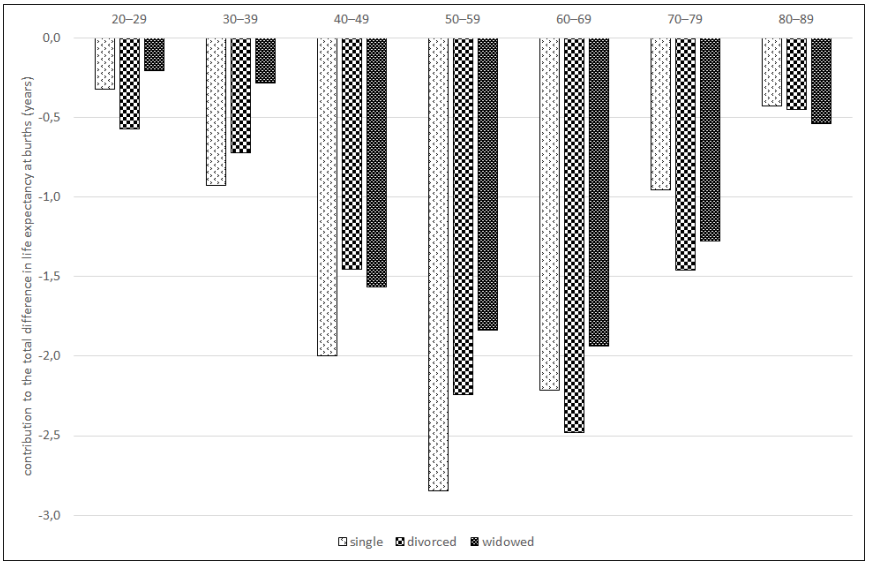

Source: data Czech Statistical Office, authors' calculation

Fig. 7. Decomposition by age in life expectancy at births by marital status – 1995–1999 males (reference category – married)

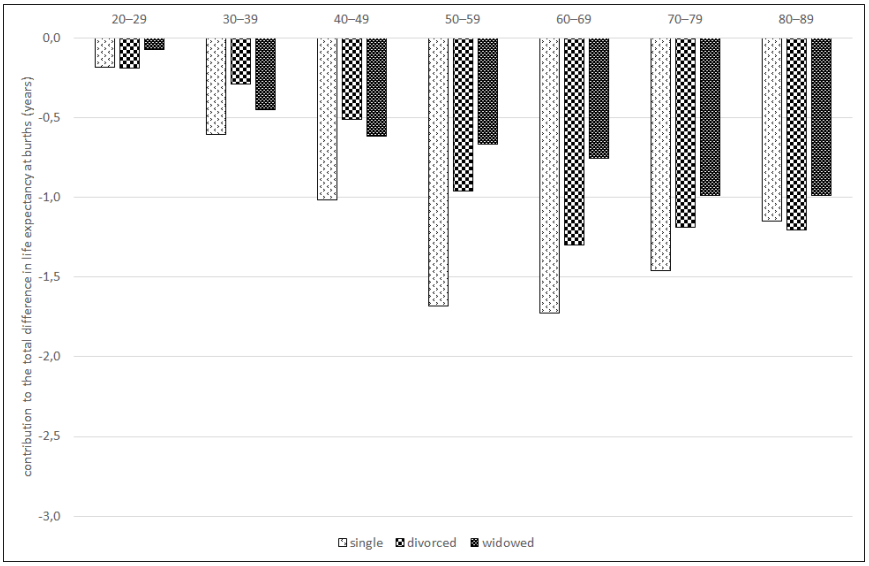

Source: data Czech Statistical Office, authors' calculation

Fig. 8. Decomposition by age in life expectancy at births by marital status – 1995–1999 females (reference category – married)

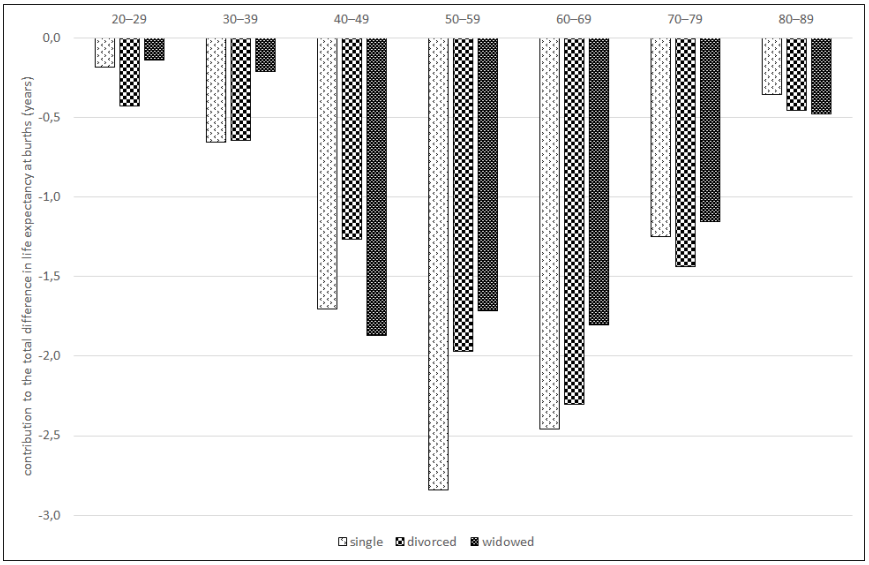

Source: data Czech Statistical Office, authors' calculation

Fig. 9. Decomposition by age in life expectancy at births by marital status – 2000–2004 males (reference category – married)

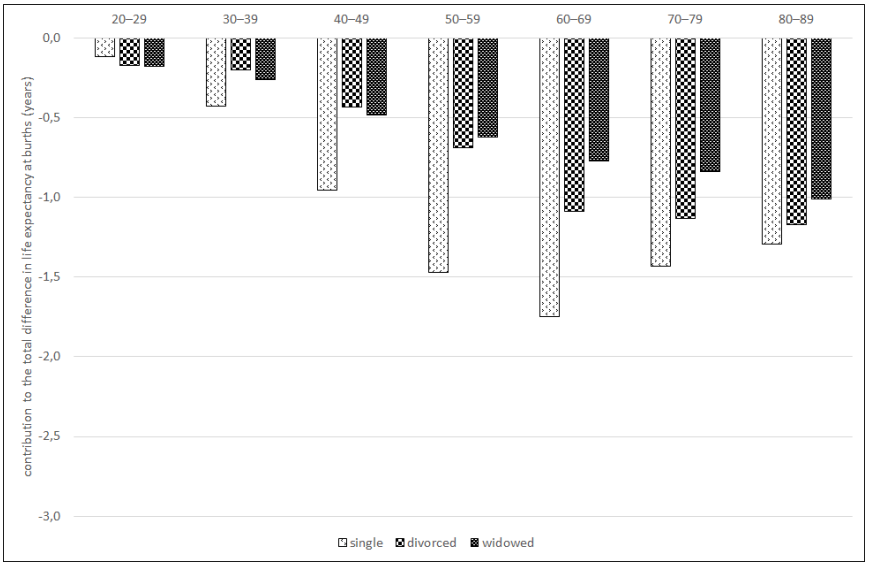

Source: data Czech Statistical Office, authors' calculation

Fig. 10. Decomposition by age in life expectancy at births by marital status – 2000–2004 females (reference category – married)

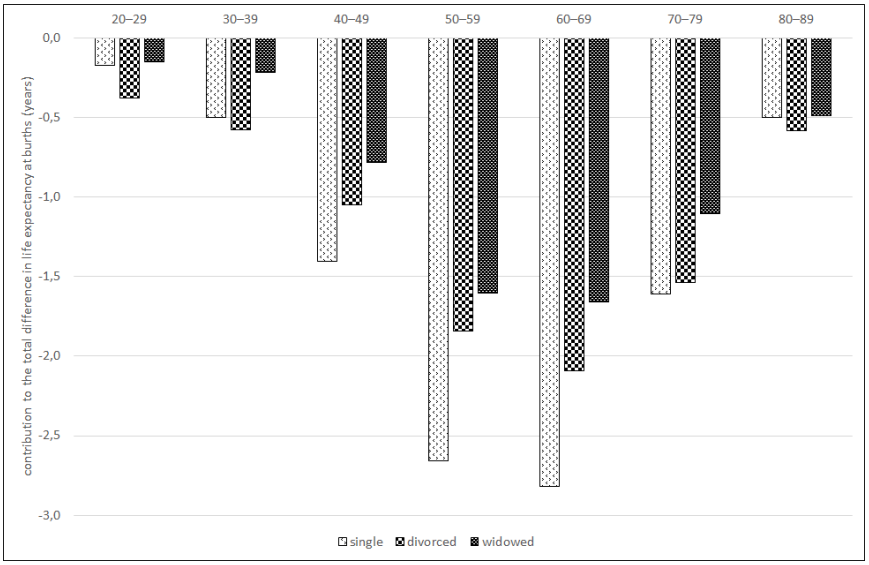

Source: data Czech Statistical Office, authors' calculation

Fig. 11. Decomposition by age in life expectancy at births by marital status – 2005–2009 males (reference category – married)

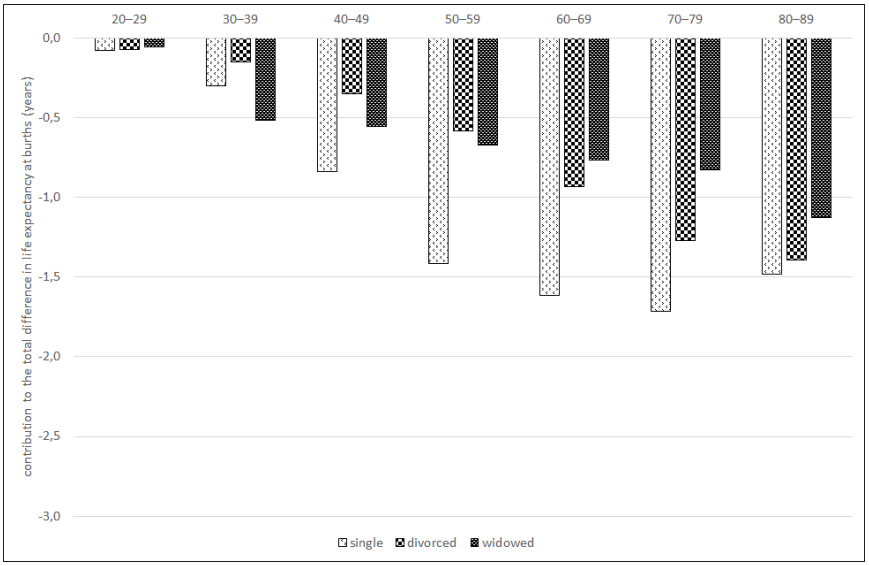

Source: data Czech Statistical Office, authors' calculation

Fig. 12. Decomposition by age in life expectancy at births by marital status – 2005–2009 females (reference category – married)

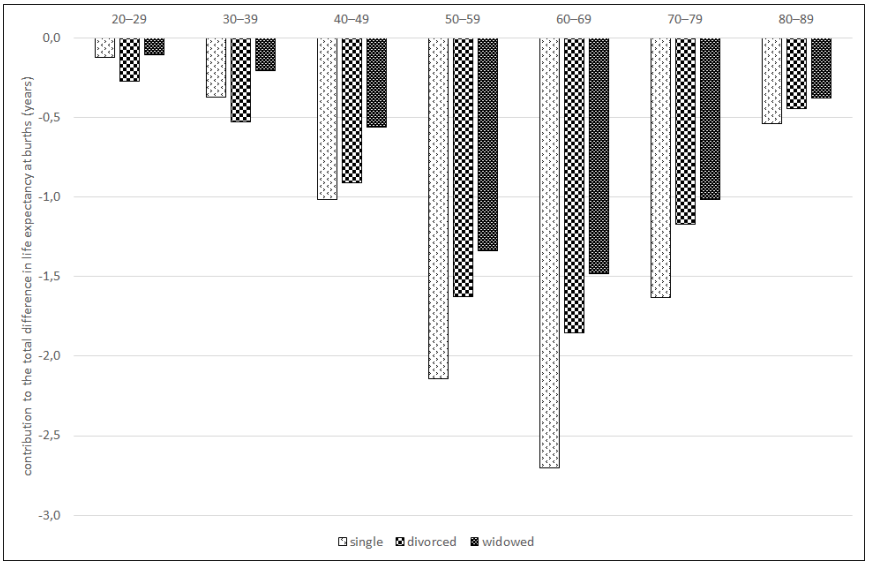

Source: data Czech Statistical Office, authors' calculation

Fig. 13. Decomposition by age in life expectancy at births by marital status – 2010–2014 males (reference category – married)

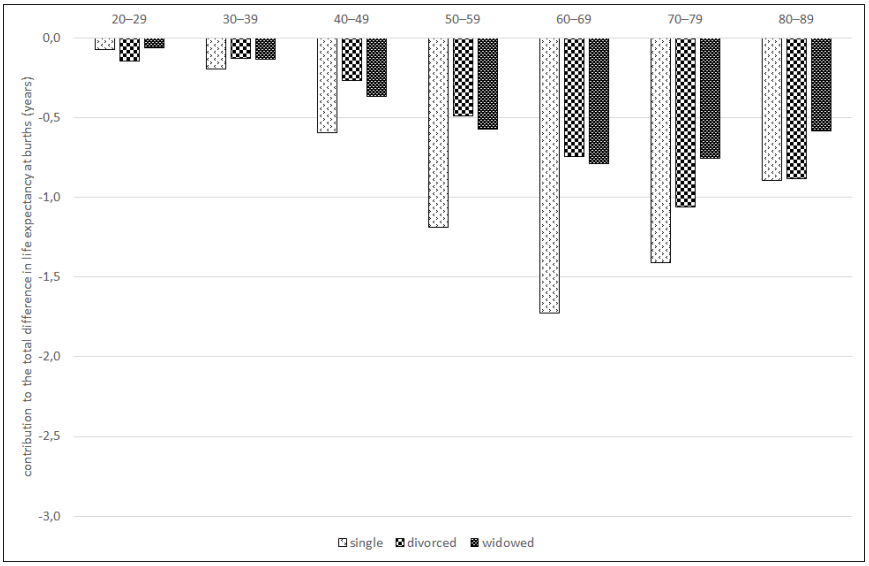

Source: data Czech Statistical Office, authors' calculation

Fig. 14. Decomposition by age in life expectancy at births by marital status – 2010–2014 females (reference category – married)

The biggest differences are between the life expectancy of married people and single people; the smallest difference is between the mortality of married people and widowed people. The difference is always bigger in men than in women. These differences were bigger in the 1990s, but this gradually changed after 2000. In 2010 –2014 in particular, the differences in life expectancy by marital status were significantly smaller than during the previous five-year time period and smaller than in 1990-94. This is also proven by the fact that the overall increase in the life expectancy of unmarried men during the analyzed period was slightly higher than that of married men and that the life expectancy of unmarried women increased more than the life expectancy of married women.
The main reason may be the lower marriage rate and thus a lower percentage of married people and a higher percentage of single people. This lessens the selective effect of marriage. While some physical or psychological handicap or an irresponsible lifestyle, which could also be the cause of the higher death rate of single people, used to often be the reason why people did not marry, nowadays there is probably a higher percentage of healthy and responsible people with an average or above-average death rate among single people.

Acknowledgment

This article was supported by the Grant Agency of the Czech Republic No. GA ČR 15-13283S under the title *Projection of the Czech Republic Population According to Educational Level and Marital Status*.

References

1. Fiala, T., Langhamrová, J. Mortality Differences by Family Status in the Czech Republic since 1993. In: *STMDA*, Valetta, Malta, 1.-4.6.2016 https://onedrive.live.com/?authkey=%21AAQ6%5FVpgAZuZB4s&cid=CB6060F40BD0FF92&id=CB6060F40BD0FF92%21348&parId=CB6060F40BD0FF92%21106&o=OneUp
2. Hamplová, D. *Zdraví a rodinný stav: dvě strany jedné mince?*. *Str. 738 -739*. 2012.
3. Hamplová, D. *Life Satisfaction, Happiness and Marital Status in Four Central European Countries. pp. 131-132.* 2009.
4. T. Parker-Pope. Is Marriage Good for Your Health? New York Times 2010-04-14. http://www.nytimes.com/2010/04/18/magazine/18marriage-t.html.
5. Pechholdová, M., Šamanová, G. Mortality by marital status in a rapidly changing society: Evidence from the Czech Republic. *Demographic research*. Vol. 29/2013, pp. 307-322. http://www.demographic-research.org/Volumes/Vol29/12/. DOI: 10.4054/DemRes.2013.29.12
6. Rychtaříková, J. Úmrtnost v České republice podle rodinného stavu. *Demografie* roč. 40, 1998, č. 2, str. 93-102.
7. Srb, V., Boris V., B. Úmrtnost obyvatelstva podle rodinného stavu 1950-1980. *Demografie*, roč. 31, 1989, č. 1, s. 37-41.

An SEM approach to modelling housing values

Jim Freeman[1] and Xin Zhao

[1] Alliance Manchester Business School, University of Manchester, Booth Street East, Manchester, UK, M15 6PB

(E-mail: jim.freeman@manchester.ac.uk)

Abstract: Though hedonic regression remains a popular technique for estimating property values, structural equation modeling (SEM) is increasingly seen as a realistic analytical alternative. The article presents an SEM analysis of a historical dataset for a large Canadian realtor. An iterative approach was adopted for the modelling. The first phase focussed on internal relationships between houses' structural characteristics and the second, on housing values and their determinants. In the final phase, advertised list prices and location details were the priority. A comprehensive evaluation of the resulting holistic model revealed a wealth of significant structural relationships - particularly between house style, structure and attributes.

Keywords: Housing Prices, Hedonic Price Theory, Structural Equation Modelling

1 Introduction

Housing is a durable, long-term asset, highly differentiated and fixed in location [1] Effective price estimation [2] is crucial to any successful property acquisition. With Hedonic Price Theory [3], a house is considered a 'basket' of attributes - $z_1, z_2, \ldots, z_n$ say – against which the house price, $P = f(z_1, z_2, \ldots, z_n)$ can be derived. Attributes here typically relate to structural, locational, neighbourhood and environmental (e.g. noise and pollution) characteristics [4]. Depending on the functional form, f adopted for computing P, various hedonic regression formulations are available for estimation purposes [5]. Some of the most common in use include the linear, semi log and log linear but a mix of these together with transformations such as the Box - Cox are becoming increasingly prevalent (see, for instance [6], [7]).

In terms of mass property appraisal modelling, the "physical – neighbourhood - location" framework has long been established. But since neighbourhood is strongly linked to location, physical (**structural**) and **locational** characteristics tend to be the focus in practice.

Structural characteristics

Structural characteristics of a house usually include the **age** of the house, the square metres of **living area**, the number, size and type of **rooms** in the house, and the attachment or lack of **garage spaces** or **chattels**. These characteristics contain both quantitative and qualitative dimensions, for example, **living area**, **lot size** and number of **rooms** are quantitative characteristics; while **chattels** can be viewed as qualitative.

Locational characteristics

Because houses are 'locationally immobile' and spatially no two properties are the same, location can have a huge impact on house values [8]. Location is often assessed in relation to accessibility – for example, proximity to a central business district (CBD; also to neighbourhood - in terms of access to educational and entertainment facilities etc [9].

Although hedonic prices models are widely employed in residential property value studies, they are frequently beset by a range of technical problems including multicollinearity, heteroscedasticity and autocorrelation [10] - all of which are actually straightforwardly handled by SEM.

This is the rationale for the modelling that follows. Using the AMOS 16 package, the SEM analysis approach is illustrated for a Canadian house sales application – details of which appear in section 2. An overview of the work is presented in Section 3 and conclusions in Section 4.

2 Data

The data was taken from Freeman and Janssen [11] and relates to houses located in ten selected neighbourhoods of Edmonton, Canada. Each home was listed and sold individually through the realtor's Multiple Listing System and relates to the eighteen month period after 1 January 1988.

Of the 240 houses that made up the sample, 90% (216) were bungalows and the remainder, two-storey homes. The mean list price for all houses was $140324.63 whilst that for bungalows was $137129.22 - compared to $169083.33 for two-story homes. Ages of houses ranged from 5 to 32 years with a mean of 22 years; correspondingly the sizes of properties ranged from 90 to 267 m^2 (the mean value was approximately 125 m^2).

Excepting list price, variables for the study were identified by house and lot attributes as follows:

Variable	*Definition*
House Attributes	
STYLE	1 if bungalow, 2 if two storey
R	Number of rooms
B	Number of bathrooms
BR	Number of bedrooms
S	Living area (square metres)
A	Age (years)
BAS	Basement (from 1 (open) to 3 (finished))
G	Number of garage spaces
ATT	Dummy variable, 1 if attached, 0 detached
F	Number of fireplaces (wood-burning)
C	Number of chattels (appliances)
Lot Attributes	
LOTS	Lot size (square metres)
CO	1 if corner lot, 0 otherwise
CUL	1 if cul-de-sac, 0 otherwise
LA	1 if lane behind, 0 otherwise
E	Exposure of yard (N, NE, E = 1, otherwise 0)
Zj	Dummy variable represents zone j (j = 0, 1, …9)
TIME	Driving time

Table 1. Definition of variables

3 Analysis

Prior to the SEM modelling, exploratory factor analysis (EFA) was conducted to help determine the underlying structure of the data and gain insight into the possible latent constructs that might exist. This provided the basis of the initial measurement model which was then tested using confirmatory factor analysis (CFA). Following on, a progression of structural relationships between latent and manifest variables were introduced and validated [12]. Three phases were involved in the SEM modelling overall.

Exploratory Factor Analysis (EFA)

Factors of interest were first identified using principal components analysis (PCA) with Varimax rotation [13].

This was then followed up with a principal axis factoring (PAF) / oblimin rotation analysis to help establish the latent structure of the model.

For the sake of practicality, it was decided not to introduce this locational variables Z0-Z9 until phase two of the modelling [14]. These were therefore omitted from the EFA which generated factors as follows:

> **Factor 1** ("House Style") linked to the STYLE (bungalow or two-storey) and ATT (attached or detached) variables
>
> **Factor 2** ("House Structure") covered the R (number of rooms), B (number of bedrooms) and BR (number of bathrooms) variables
>
> **Factor 3** ("House Attributes") represented the F (number of fireplaces), G (number of garage spaces) and C (number of chattels) variables.

Based on the latter, three research hypotheses were adopted for the study:

> H1: House style positively impacts on House structure
>
> H2: House style positively impacts on House attributes
>
> H3: House structure positively impacts on House attributes

Phase One

In the first phase of the SEM modelling, internal relationships between the structural characteristics of a house were investigated, without consideration of the value of the house – see Figure 1 which provides the formal path diagram of the theoretical (measurement) model to be evaluated.

AMOS provides a large number of standard diagnostics for assessing the effectiveness of a particular model choice. Selected values of these for model 1a) are summarised in Table 2.

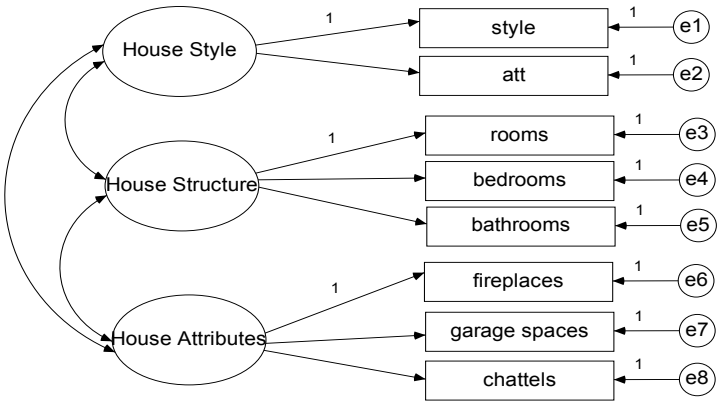

Fig 1. Measurement Model 1a)

Indices	Value	Threshold	Acceptability
χ^2	53.879 (p<.001)	Significant at 0.01 level	Unacceptable
df	17		
CMIN/DF	3.169	<2-3	Unacceptable
CFI	.911	>.9	Acceptable
GFI	.944	>.9	Acceptable
AGFI	.881	>.9	Unacceptable
RMSEA	.095	<.08	Unacceptable

Table 2. Goodness of Fit summary: Model 1a)

Though the latter model appears satisfactory according to some of the indices shown here, there is clearly room for improvement with others. As a refinement, therefore it was decided to introduce a covariance link between the error terms e2 and e4. Note that the chattels item (which turned out to have a zero regression weight) was simultaneously dropped. The resultant estimated model 1b), is shown in Figure 2 with associated diagnostics in Table 3.

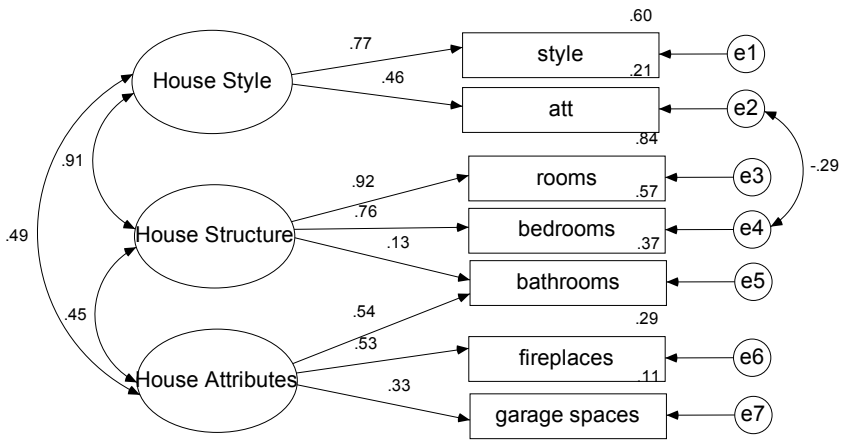

Fig 2. Estimated Model 1b)

Indices	Value	Threshold	Acceptability
χ^2	11.665 (p=.233)	Not significant	Acceptable
df	9		
CMIN/DF	1.296	<2-3	Acceptable
CFI	.994	>.9	Acceptable
GFI	.987	>.9	Acceptable
AGFI	.958	>.9	Acceptable
RMSEA	.035	<.08	Acceptable

Table 3. Goodness of Fit summary: Model 1b)

Plainly, this is a much better fit. No less importantly, all loadings here (except for bathrooms) were found to be statistically significant ($p<0.05$) and all relationships in the expected direction.

Phase 2

In the second phase, the model was modified to investigate the relationships between house values and structural and location characteristics.

A second order factor 'House Value' was therefore introduced into the model. Furthermore, the latent variable 'Location' was included as an underlying indicator of accessibility and neighbourhood. The resultant estimated model is shown in Figure 3. Unfortunately, the accompanying diagnostics in Table 4 can be seen to be far from satisfactory.

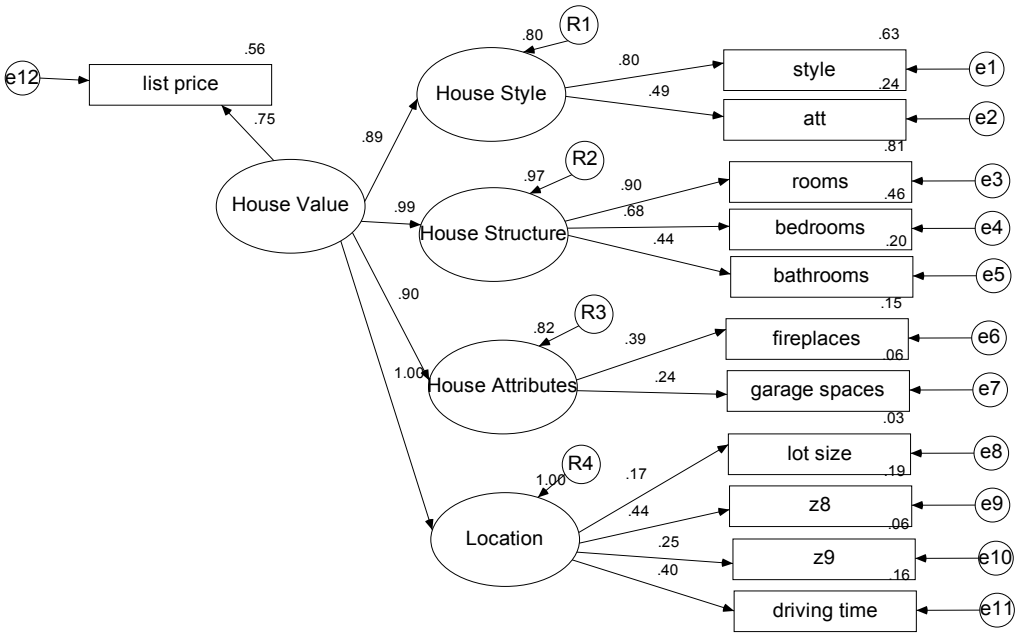

Fig 3. Estimated Model 2a)

Indices	Value	Threshold	Acceptability
χ^2	269.893 (p<.001)	Significant at 0.01 level	Unacceptable
df	53		
CMIN/DF	5.092	<2-3	Unacceptable
CFI	.737	>.9	Unacceptable
GFI	.819	>.9	Unacceptable
AGFI	.734	>.9	Unacceptable
RMSEA	.131	<.08	Unacceptable

Table 4. Goodness of Fit summary: Model 2a)

To rectify the situation, it was decided to allow for selected error terms to be correlated. This was done iteratively in line with successive AMOS modification index outputs. Details of the revised estimated model (2b) were obtained as follows:

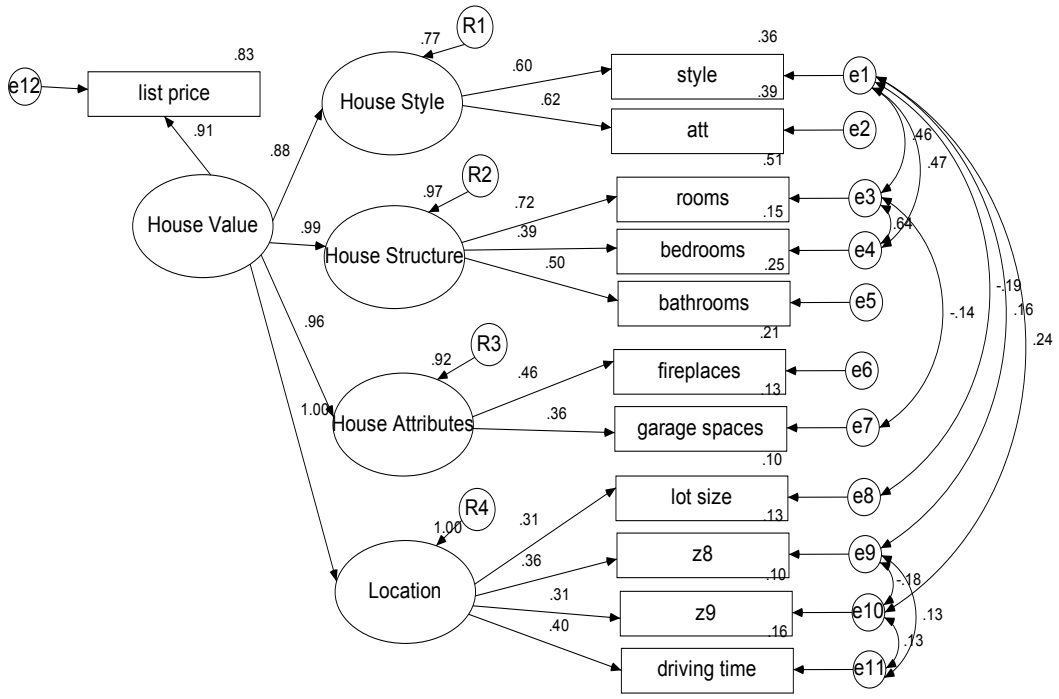

Fig 4. Estimated Model 2b)

Indices	Value	Threshold	Acceptability
χ^2	72.436 (p=.003)	Significant at 0.01 level	Unacceptable
df	43		
CMIN/DF	1.685	<2-3	Acceptable
CFI	.964	>.9	Acceptable
GFI	.955	>.9	Acceptable
AGFI	.919	>.9	Acceptable
RMSEA	.054	<.08	Acceptable

Table 5. Goodness of Fit summary: Model 2b)

Apart from the χ2 statistic, the fit results here all look satisfactory. However, because large sample sizes - as in this study - are notoriously linked to significant χ2 results, the CMIN/DF criterion (following

convention) was used as a proxy. On this basis, the model would therefore be judged to have satisfactory fit characteristics throughout. In addition, all indicator estimates are statistically significant at the 5% level with the arrow directions too in line with expectations.

Phase 3

In the third phase, the latent variable 'House Price' was introduced into the model, as estimated in Figure 5 - with corresponding diagnostics in Table 6. (The logic behind this adaptation is that list price is literally more a reflection of House Price than House Value.)

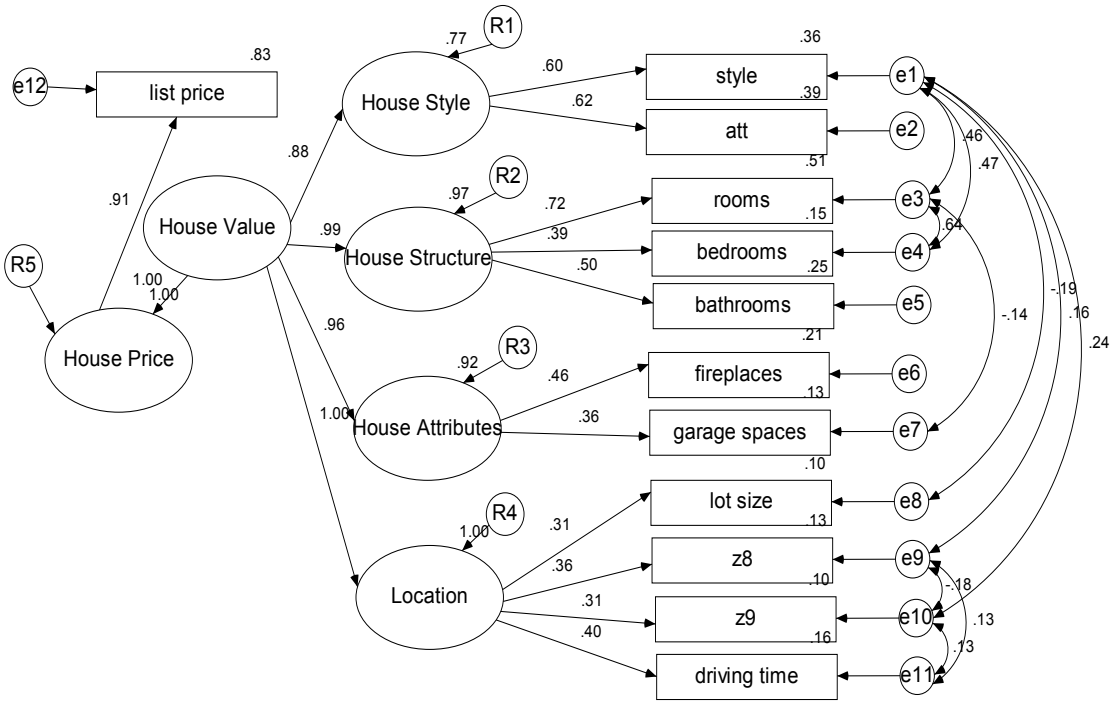

Fig 5. Estimated Model 3

Indices	Value	Threshold	Acceptability
χ^2	72.436 (p=.003)	Significant at 0.01 level	
df	43		
CMIN/DF	1.685	<2-3	Acceptable
CFI	.964	>.9	Acceptable
GFI	.955	>.9	Acceptable
AGFI	.919	>.9	Acceptable
RMSEA	.054	<.08	Acceptable

Table 6. Model 3: Goodness of Fit summary

As with Table 5, the latter diagnostics confirm that the model satisfactorily fits the data.

Similarly, the standardized estimates of all model loadings shown in Figure 5 can be shown to be highly significant (at the 0.1% level).

House Value is also found to be positively related to the four latent variables House Style, House Structure, House Attribute and Location.

In addition, supporting evidence for research hypotheses H1, H2 and H3 is provided by supplementary correlation output as follows:

	Sample Correlation	Inference
H1: House style positively impacts on House structure	0.866*	Accepted
H2: House style positively impacts on House attributes	0.432*	Accepted
H3: House structure positively impacts on House attributes	0.409*	Accepted

* $p < .05$

Finally, the squared multiple correlations in Figure 5 reveal that 77% of the variance of House Style, 97% of the variance of House Structure, 92% of the variance of House Attributes and 100% of the variance of Location are individually accounted for by House Value. Of interest the percentages here - as well as model loadings in Figure 5 are identical to those for Model 2b) (Figure 4) – suggesting that the distinction between the House Price and House Value latent constructs is probably more semantic than real.

3 Conclusions

Despite the dearth of published research on SEM modelling of house values, it is reassuring to note how strikingly in agreement the findings above are with those of Liu and Wu [15]. For their analysis of residential data from Dalian, China, two measures, house price and satisfaction degree were chosen to represent house value (not just list price as in our own case). In further contrast, a four factor (location, residential district, structure and neighbourhood environment) framework was adopted for their modelling. Notwithstanding these differences, it is salutary to find that Liu and Wu too concluded location and structure to be far and away, the most important determinants of house value.

References

1. W.N.K. Kinnard. ‘Reducing uncertainty in real estate decisions’. *The Real Estate Appraiser*, **34** 7, 10{16. 1968.
2. J. Karanka, R. O’Neill, N. Weadon, R. Sanderson and C Jenkins “Official house price statistics explained’. ONS. 2013.
3. S. Rosen. ‘Hedonic Prices and Implicit Markets: Product Differentiation in Pure Competition’. *Journal of Political Economy*, **82** 1 34{55. 1974.
4. A. Anas and S.J. Eum. Hedonic Analysis of a Housing Market in Disequilibrium. *Journal of Urban Economics*, **15** 1 87{106. 1984.
5. R.B. Palmquist. ‘Estimating the Demand for the Characteristics of Housing’. *The Review of Economics and Statistics*, **66** 3 394{404. 1984.
6. P. Linneman and R. Voith. ‘Housing Price Functions and Ownership Capitalization Rates’. *Journal of Urban Economics*, **30** 1 100{111. 1991.
7. M. Fletcher, J. Mangan and E. Raeburn. ‘Comparing hedonic models for estimating and forecasting house price’. *Property Management*, **22** 3 189{200. 2004.
8. F. Des Rosiers, M. Theriault and P. Villeneuve. ‘Sorting out access and neighbourhood factors in hedonic price modelling’. *Journal of Property Investment & Finance*, **18** 3 291{315. 2000.

9. W.J. McCluskey, W.G. Deddis, I.G. Lamont, and R.A. Borst. 'The application of surface generate interpolation models for the prediction of residential property values'. *Journal of Property Investment & Finance*, **18** 2 162{176. 2000.
10. W.M., Bowen, B.A. Mikelbank and D.M. Prestegaard. 'Theoretical and empirical considerations regarding space in hedonic house price estimation'. *Growth and Change*, **32** 4 466{490. 2001.
11. J. Freeman and C. Janssen. 'Analysis of the effect of Realtor Competition on Housing Prices'. *Research papers in Management Science. Faculty of Business University of Alberta*. 1993.
12. B.M. Byrne, 'Structural Equation Modelling with Amos: Basic concepts, applications, and programming'. (Second edn). United States of American: Routledge Academic. 2009.
13, A. Field. 'Discovering Statistics Using SPSS'. (Third edn). London: SAGE. 2009.
14. X. Zhao. 'Structural Equation Modelling Analysis of Canadian House Sales Data'. Unpublished MSc dissertation. University of Manchester. 2012.
15. Y Liu and Y.X. Wu. 'Analysis of Residential Product's Value Based on Structural Equation Model and Hedonic Price Theory'. 2009 International Conference on Management Science & Engineering (September 16th), Moscow, Russia, 1950{1956. 2009.

Stochastic Distance between Burkitt lymphoma/leukemia Strains

Jesús E. García[1], R. Gholizadeh[2], and V.A. González-López[3]

[1] Department of Statistics, University of Campinas, R. Sérgio Buarque de Holanda, 651, Campinas (CEP 13083-859), Brazil.
(E-mail: jg@ime.unicamp.br)
[2] University of Campinas, R. Sérgio Buarque de Holanda, 651, Campinas (CEP 13083-859), Brazil.
[3] Department of Statistics, University of Campinas, R. Sérgio Buarque de Holanda, 651, Campinas (CEP 13083-859), Brazil.
(E-mail: veronica@ime.unicamp.br)

Abstract. Quantifying the proximity between N-grams allows to establish criteria of comparison between them. Recently, a consistent distance d to achieve this end was proposed, see García and González-López (2017) [2]. This distance takes advantage of a model structure on Markovian processes in finite alphabets and with finite memories, called Partition Markov Models, see García and González-López (2017) [1]. In this work we explore the performance of d in a real problem, using d to establish a notion of natural proximity between DNA sequences from patients with identical diagnosis, which is: Burkitt lymphoma/leukemia. And we present a robust strategy of estimation to identify the law that governs most of the sequences considered, thus mapping out a common profile to all these patients, via their DNA sequences.
Keywords: Partition Markov Models, Bayesian Information Criterion, Robust Estimation in Stochastic Processes..

1 Introduction

The Burkitt lymphoma occurs when the chromosome 8 (locus of gene MYC) is broken, which produces a change in the cellular proliferation. The data used in this paper corresponds to the most frequent variant, produced by the translocation between chromosomes 8 and 14. It is known, so far, three variants of Burkitt lymphoma, which are (i) endemic, (ii) sporadic, (iii) produced by immunodeficiency. The first case is observed in childs in Equatorial Africa and it is associated with chronic Malaria infections. It does not exist until the moment and according to what we know, a clear notion of the profile of the Burkitt lymphoma's DNA. Considering that it is natural to expect diversity between DNA strains, we will measure the distance between 15 of them. We adopt a distance between the strains which is conditioned to each possible common string s, where s is an element of the state space. That is, suppose that $x_{1,1}^{n_1}$ and $x_{2,1}^{n_2}$ are the concatenations of elements a, c, g and t of the DNA of two patients, say 1 and 2, $d_s(1,2)$ will be the distance between the sequences in relation to s some string of interest, for instance $s = \text{aggc}$. As there are a variety of possible strings, which we should observe to measure the discrepancy between the strains, we will compute the maximum of all: $\max_s\{d_s(1,2)\}$, so

as to focus on the most extreme situation among them. This notion allows to identify which of these strings can be considered more distant of the majority, and allows us to select the strains which will be used to define the profile of the DNA. To strengthen our conclusions, we compared the model constructed with the selected strains with the model constructed using the 15 available strains. This work is organized as follows, first we introduce the notion of distance as well as the general notation. Then we will describe the strains of the 15 patients, we will inform their source. In the results we show the values calculated for the maximum distance between strains two to two. We also show the model induced by this strategy.

2 Criteria

Let (X_t) be a discrete time (order $o < \infty$) Markov chain on a finite alphabet A. Let us call $\mathcal{S} = A^o$ the state space and denote the string $a_m a_{m+1} \dots a_n$ by a_m^n, where $a_i \in A$, $m \leq i \leq n$. For each $a \in A$ and $s \in \mathcal{S}$, $P(a|s) = \text{Prob}(X_t = a | X_{t-M}^{t-1} = s)$. In a given sample x_1^n, coming from the stochastic process, the number of occurrences of s in the sample x_1^n is denoted by $N_n(s)$ and the number of occurrences of s followed by a in the sample x_1^n is denoted by $N_n(s,a)$. In this way $\frac{N_n(s,a)}{N_n(s)}$ is the estimator of $P(a|s)$. In the next paragraph, we give the notion of distance between two processes.

Definition 1. Consider two Markov chains $(X_{1,t})$ and $(X_{2,t})$, of order o, with finite alphabet A and state space $\mathcal{S} = A^o$. With sample $x_{k,1}^{n_k}$, for $k = 1, 2$ respectively; for any $s \in \mathcal{S}$,

$$d_s(1,2) = \frac{\alpha}{(|A|-1)\ln(n_1+n_2)} \sum_{a \in A} \left\{ N_{n_1}(s,a) \ln\left(\frac{N_{n_1}(s,a)}{N_{n_1}(s)}\right) + N_{n_2}(s,a) \ln\left(\frac{N_{n_2}(s,a)}{N_{n_2}(s)}\right) - N_{n_1+n_2}(s,a) \ln\left(\frac{N_{n_1+n_2}(s,a)}{N_{n_1+n_2}(s)}\right) \right\}$$

with $N_{n_1+n_2}(s,a) = N_{n_1}(s,a) + N_{n_2}(s,a)$, $N_{n_1+n_2}(s) = N_{n_1}(s) + N_{n_2}(s)$, where N_{n_1} and N_{n_2} are given as usual, computed from the samples $x_{1,1}^{n_1}$ and $x_{2,1}^{n_2}$ respectively, with α a real and positive value. In this paper we use $\alpha = \frac{1}{2}$, see García and González-López (2017) [1].

The most relevant properties of d are listed below. Both properties are consequence of results proved in García and González-López (2017) [1]:

i. *The function $d_s(1,2)$ is a distance between the Markov chains relative to the specific string $s \in \mathcal{S}$.* If $(X_{i,t}), i = 1, 2, 3$ are Markov chains under the assumptions of definition 1, with samples $x_{i,1}^{n_i}$, $i = 1, 2, 3$ respectively,

$$d_s(1,2) \geq 0 \text{ with equality } \Leftrightarrow \frac{N_{n_1}(s,a)}{N_{n_1}(s)} = \frac{N_{n_2}(s,a)}{N_{n_2}(s)} \ \forall a \in A,$$

$$d_s(1,2) = d_s(2,1),$$

$$d_s(1,2) \leq d_s(1,3) + d_s(3,2).$$

ii. *Local behavior of process Laws.* If the stochastic laws of $(X_{i,t}), i = 1, 2$ in s are the same then then $d_s(1,2) \underset{\min(n_1,n_2)\to\infty}{\longrightarrow} 0$.
Otherwise $d_s(1,2) \underset{\min(n_1,n_2)\to\infty}{\longrightarrow} \infty$.

3 DNA data

The database is composed by 15 DNA sequences, available in the repository: `https://www.ncbi.nlm.nih.gov/nuccore/`, coming from 15 patients with Burkitt lymphoma/leukemia carrying the t(8;14)(q24;q32) with IgH-MYC fusion, breakpoint in the joining region. The registers (genbank numbers) of the sequences are: AM2871z.1, where z=39, 40, 41, 46, 50, 52, 57, 58, 59, 61, 62, 65, 76, 81, 87. For each sequence, the concatenation of bases a,c,g,t observed in the code is the realization denoted by x_1^n. The size of each sequence is shown in table 1.

z	39	40	41	46	50	52	57	
n	3641	2965	4464	2731	5428	2475	3907	
z	58	59	61	62	65	76	81	87
n	3636	4291	2642	3206	2906	2635	3608	3734

Table 1. Sample sizes n of DNA sequence coming from 15 patients with Burkitt lymphoma/leukemia, AM2871z.1, where $z = 39, 40, 41, 46, 50, 52, 57, 58, 59, 61, 62, 65, 76, 81, 87$.

4 Results

In tables 2 and 3 we expose the $dmax$ values between the DNA sequences, where $dmax(i,j) = \max_{s\in\mathcal{S}}\{d_s(i,j)\}$, $i \neq j, i, j =$ AM2871z.1, with $z = 39, 40, 41, 46, 50, 52, 57, 58, 59, 61, 62, 65, 76, 81, 87$. At the end of each column we record the sum of the $dmax$, that is:

$$S(i) = \sum_j dmax(i,j), \text{ for each sequence } i = \text{AM2871}z.1,$$

where $z = 39, 40, 41, 46, 50, 52, 57, 58, 59, 61, 62, 65, 76, 81, 87$. Through d_s we have a criterion to rescue the greatest distance between two DNA sequences. From the magnitudes found, we can affirm that the processes can be considered as coming from the same stochastic law, $dmax < 1$. We also verified the above statement from the dendrograms constructed using the values recorded in tables 2 and 3, see figure 1.

$j \setminus i$	39	40	41	46	50	52	57
40	0.23625						
41	0.16160	0.25648					
46	0.22578	0.24031	0.21857				
50	0.20218	0.25847	0.17855	0.22644			
52	0.19479	0.17870	0.21143	0.16253	0.33231		
57	0.09777	0.24533	0.13885	0.22058	0.12481	0.19363	
58	0.27729	0.21783	0.30105	0.25156	0.28312	0.23041	0.25738
59	0.12485	0.32050	0.09723	0.24232	0.15545	0.21165	0.09821
61	0.20229	0.10170	0.22626	0.20598	0.30120	0.12572	0.25328
62	0.32556	0.34309	0.35858	0.26633	0.47720	0.24569	0.32362
65	0.22234	0.15183	0.26545	0.15812	0.25339	0.29264	0.27469
76	0.19421	0.24629	0.20804	0.12923	0.23960	0.12786	0.19308
81	0.16363	0.17050	0.19272	0.16614	0.22817	0.17392	0.12994
87	0.26047	0.16796	0.24704	0.25130	0.41112	0.26425	0.22481
$S(i)$	2.8890	3.13523	3.06186	2.96519	3.67203	2.94553	2.77597

Table 2. $dmax(i,j)$ values, $i \neq j, i, j =$ AM2871z.1, where $z = 39, 40, 41, 46, 50, 52, 57, 58, 59, 61, 62, 65, 76, 81, 87$.

$j \setminus i$	58	59	61	62	65	76	81	87
59	0.30177							
61	0.20284	0.32032						
62	0.27748	0.34112	0.25478					
65	0.25707	0.27412	0.21689	0.30528				
76	0.13397	0.21109	0.13318	0.27990	0.21237			
81	0.25801	0.14463	0.11904	0.23329	0.21155	0.15334		
87	0.23089	0.24762	0.20658	0.37764	0.20689	0.23144	0.19405	
$S(i)$	3.48067	3.09091	2.87007	4.40955	3.30265	2.69363	**2.53891**	3.52205

Table 3. $dmax(i,j)$ values, $i \neq j, i, j =$ AM2871z.1, where $z = 39, 40, 41, 46, 50, 52, 57, 58, 59, 61, 62, 65, 76, 81, 87$. In bold the lowest value of S, associated to the sequence with $z = 81$.

4.1 The DNA profile

The model we will apply in the data, is extensively investigated in García and González-López (2017) [1]. This is the most general model known to be used in finite order Markov chains on a finite alphabet, since this model includes fixed order Markov chains and the variable lenght Markov chains (VLMC). Essentially what this model proposes is to estimate the transition probabilities that describe the process by identifying a partition $\mathcal{L} = \{L_1, \cdots, L_{|\mathcal{L}|}\}$ in the state space $\mathcal{S}$. The state space is divided into parts $L_i, i = 1, \cdots, |\mathcal{L}|$ which constitute a partition. The strings of each part have in common the characteristic of sharing the same transition probability to any element of the alphabet. In practice, all strings included in the same part of that partition will be used for the computation of the transition probability that identifies them. The identification of such partition is done using the Bayesian Information Criterion

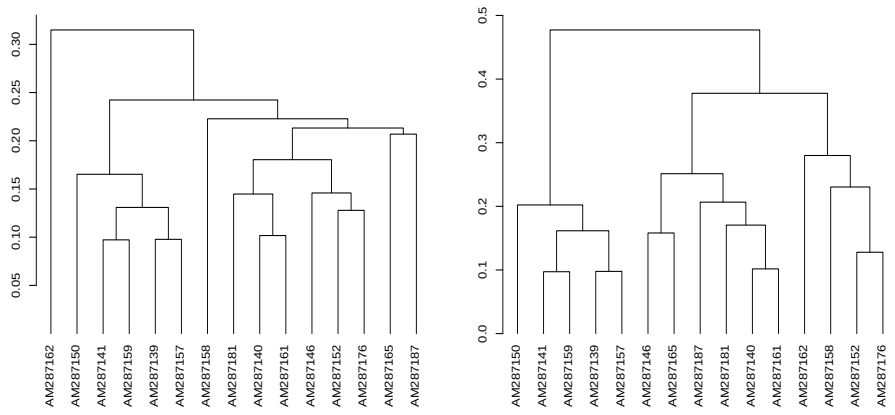

Fig. 1. Dendrograms build through the *dmax* values (tables 2-3), agglomeration method: *Average*, on the left and *Complete*, on the right.

(BIC), which also is the basis to the concept d_s, previously introduced.
Table 4 shows some general characteristics that are observed in the adjustment of the model introduced in García and González-López (2017) [1]. We include progressively (from top to bottom) the closest sequences, according to the criterion S. That is, first using the sequence 81, second, using two sequences: 81 and 61 and so on. In other words, we are increasing the sample size from one stage to the next, following as iclusion criterion the magnitude of S. We can not state unequivocally that by increasing the sample sizes we increase the parts of the estimated partition, but it seems to be a trend, as seen in the table 4. But this could also be the result of incorporating in the model gradually the more distant sequences according to criterion S.
We apply in all the adjustments the agglomerative method, whose performance is analyzed in García and González-López (2017) [1], the memory used in all the adjustments is equal to $4=\lfloor \log_{|A|}(2475) \rfloor - 1$, with alphabet $A = \{$a,c,g,t$\}$ where 2475 is the smallest sample size reported in table 1.
We describe in a comparative way the results when applying the model in: (i) the 7 closest sequences according to S, which are: AM2871z.1, where z=39, 46, 52, 57, 61, 76, 81 (see tables 5 and 6) and (ii) the 15 sequences (see tables 8 and 9). We note (see table 6) that in relation to the transition probabilities from part i to the elements of the alphabet, 3 of these parts show their highest values in the transition to a, 10 parts expose their highest values in the transition to c, 9 of those parts show their highest values in the transition to g and 5 of those parts expose their greater probabilities in the transition to t.

In table 7 we highlight the composition of the four parts 1, 16, 12 and 26 that show the highest values of transition probability for a, c, g and t respectively. We also emphasize in table 7, the part 14 that joins all those strings whose transition probability to c is zero.

z	Sample size	$\lvert\mathcal{S}\rvert$	$\lvert\mathcal{L}\rvert$
81	3604	134	6
81,76	6235	193	13
81,76,57	10138	241	18
81,76,57,61	12776	249	21
81,76,57,61,39	16413	255	27
81,76,57,61,39,52	18884	255	28
81,76,57,61,39,52,46	21611	255	27
81,76,57,61,39,52,46,41	26071	256	31
81,76,57,61,39,52,46,41,59	30358	256	33
81,76,57,61,39,52,46,41,59,40	33319	256	31
81,76,57,61,39,52,46 41,59,40,65	36221	256	34
81,76,57,61,39,52,46 41,59,40,65,58	39853	256	37
81,76,57,61,39,52,46 41,59,40,65,58,87	43583	256	39
81,76,57,61,39,52,46 41,59,40, 65,58,87,50	49007	256	40
81,76,57,61,39,52,46 41,59,40,65,58,87,50,62	52209	256	42

Table 4. Relation between the sequences used in the estimation and number of parts of the estimated partition, for AM2871z.1, where z=39, 40, 41, 46, 50, 52, 57, 58, 59, 61, 62, 65, 76, 81, 87.

We list in table 8 the elements of the partition obtained using all the strains, and then we give their transition probabilities in table 9.

According to table 9, 7 parts exhibit their highest transition probability values for the element a, 13 for the element c, 14 for the element g, and 8 for the element t. Note that the parts recorded in the selection given in table 7, where we use only 50% of the nearest strains, are combinations of those listed in table 10 with other parts, in the latter case we use all the strains. We detail the connection in the table 11. We see that the listed parts (to the left of table 11) are dispersed in several parts of the model adjusted with all the sequences. In the case of the last line, the strings listed in part 14 of table 7 occur with nonzero frequencies, when using all the sequences. This last aspect shows evidences of the natural dispersion that is imprinted to the model with only 50% of the sequences more near, when we use all the sequences.

i of part L_i	Strings
1	acgc, accg, ccag, gacg, acac, gcag, caat, atca
2	ccgc, cggt, cctc, agga, tcac, tagg, acca, gcac
3	gcgc, cgtg, ctat, tctc, cagg, cacc, taag, cgtt, ttct, cccc, ggct, gtca ctct, agac, tctt, ctta, tgcc, atgc, gttt, tatc, gctt, cttg, agct
4	tcgc, gaca, tttc, ctgc, ttgt, gata, gtta
5	aggc, aaca, agtc, agca, attc, ttcg, aagt, taca, agcg, cagc, gtcc
6	cggc, cgct, tttg, atac, gccg, caga, ttat, ctaa, tagt, ctca, gaaa
7	gggc, gtct, aatt, ttgg, cctt, ttgc, tgga, ctgt, taat, tgta, ccat tcct, ttca, ggaa, ctcg, tgtt, agaa, gtga
8	tggc, atct, gagt, gagc, aatc, tacg, ggcc, ggtt, agtg, cact, ataa
9	gtgc, gatc, catc, aaga, gctc, aaat, aata
10	actc, tgaa, acag, gtat
11	cgtc, tgtc, gtag, aggt, ttag, ttga, gtac, gcct
12	ggtc, gtaa, agtt, caaa, gttc, gaag, atag
13	cttc, taaa, ttta, catt, attt, aaag, ttaa, acat, aagc, cttt, aaac
14	caag, gcca, tgag, gcaa, aacg, acga, ccac
15	tcag, attg, agag, atcc, aact, cgat, cgta, catg, taga, tccc, ttcc, acaa
16	cgag, tccg, tcta, ggta, taac, acgg, gaga, cata
17	ggag, tgtg, tgct, tcca, tctg, tttt, ccca, ccga, ggca, gcgg, gtgg tgat, gggg
18	ctag, tcgt, ctgg, aaaa, tcgg, gtgt, gggt, tggt, gatt
19	cacg, aagg, tcaa, cgcg, actg, cgca, tgcg, tcat, ccgt
20	cccg, ctac, atcg, aggg, aatg, ggcg, cggg
21	gtcg, atta, ggat, cgaa, gagg, ggac, tact, tgca, tata, agat, acct gcga, tcga
22	ccgg, gatg, caac, cctg, atgg, tatt, tggg, tatg, accc, ggtg, cgac, atgt gcta, ggga
23	gctg, gaat, gttg, acgt, tgac, gacc
24	gcat, gact, ccta, gcgt, caca, acta, gaac, ttac
25	atat, cgga, actt, atga, ccct, cagt, aacc, ccaa, agta, ctga
26	tacc
27	gccc, cgcc, ctcc, agcc

Table 5. Parts of the partition selected through the Bayesian Information Criterion, using AM2871z.1, where z=39, 46, 52, 57, 61, 76, 81.

i of part L_i	a	c	g	t
1	**0.52430**	0.24041	0.18670	0.04859
2	0.26705	**0.53977**	0.13636	0.05682
3	**0.31714**	0.25073	0.30718	0.12495
4	0.16245	0.27557	**0.53791**	0.02407
5	**0.47689**	0.07948	0.27542	0.16821
6	0.20235	0.17204	**0.33822**	0.28739
7	0.11628	0.31924	**0.46564**	0.09884
8	0.26162	0.34661	**0.36122**	0.03054
9	0.14495	0.11376	**0.57982**	0.16147
10	0.00487	**0.42336**	0.37226	0.19951
11	0.02754	0.11864	**0.61441**	0.23941
12	0.26225	0.08357	**0.62824**	0.02594
13	0.17198	0.23406	**0.41527**	0.17869
14	0.35484	0.00000	0.18894	**0.45622**
15	0.27907	0.22161	0.12996	**0.36936**
16	0.02667	**0.72800**	0.11200	0.13333
17	0.23476	**0.35264**	0.24390	0.16870
18	0.13996	**0.43050**	0.31757	0.11197
19	0.36605	**0.38650**	0.02658	0.22086
20	0.20380	**0.51813**	0.09845	0.17962
21	0.08753	**0.43885**	0.11631	0.35731
22	0.16603	**0.35227**	0.21136	0.27034
23	0.14469	0.25736	0.23303	**0.36492**
24	0.01155	0.33949	0.22864	**0.42032**
25	0.07393	**0.47471**	0.28664	0.16472
26	0.03922	0.05882	0.03922	**0.86275**
27	0.26437	0.04310	**0.46264**	0.22989

Table 6. Transition probabilities $P(\cdot|L_i)$ with $\cdot \in$ {a,c,g,t} and $i = 1, \cdots, 27$. For each part i, listed on the left column (see table 5), we indicate in bold the highest transition probability to the elements of the alphabet.

i of part L_i	Strings	Probability
1	acgc, accg, ccag, gacg, acac, gcag, caat, atca	$P(\text{a}\|L_1)$ =0.52430
16	cgag, tccg, tcta, ggta, taac, acgg, gaga, cata	$P(\text{c}\|L_{16})$ =0.72800
12	ggtc, gtaa, agtt, caaa, gttc, gaag, atag	$P(\text{g}\|L_{12})$ =0.62824
26	tacc	$P(\text{t}\|L_{26})$ =0.86275

i of part L_i	Strings	Probability
14	caag, gcca, tgag, gcaa, aacg, acga, ccac	$P(\text{c}\|L_{14}) = 0$

Table 7. Selected parts, from table 5, which have the greater (on top)/null (on bottom) transition probabilities to each element of the alphabet {a,c,g,t}.

i of part L_i	Strings
1	acgc , accg
2	ccgc, gagt, acca, gagc, ggcg, cggt
3	gcgc, tacg, cgtg, ccca, gccg, ctat, cacc, ttat, ctaa, caga
4	tcgc, ggtt, aatc, ggcc, atca, agtg, ataa, tggc, atct
5	aggc, agtc, aaca, agca
6	cggc, cgct, tttg, atac
7	gggc, ctcg, gtct, cctt, gaca, tagc
8	atgc, gttt, cttg, tatc, ttgg, cttc, catt, taaa, gctt
9	ctgc, ctgt, gttc, tttc
10	gtgc, ggtc, gaag, atag, agtt, caaa, gtaa
11	ttgc, tgga, taat, aaac, ttca, aaag, ttaa, acat, aagc, ttta, cttt
12	catc, ctcc, gctc, aaga, gccc
13	gatc, aata, aaat, gtac, gtag, ttga, ttag, aggt
14	actc, agaa, cgga, atat, atga
15	cctc, tgcc, ggct, tcca, acac, ggag, tgat, tgtg, tgct, gcac, tctg, tttt, gtca
16	tctc, taag, cccc, cagg, ttct, ctct, tctt
17	cgtc, tgtc, gcct
18	attc, aagt, agct, taca, tagt, ctca, gaaa
19	caag, gcca, ccac
20	acag, gtat, tgaa
21	ccag, agac, agga, gcag, gacg, caat, cgtt
22	tcag, attg, aact, agag, catg, atcc, aatg, cgat, cgta
23	cgag, tccg
24	tgag, acga, gcaa, agcc, cgcc
25	ctag, ggga, accc, gctg, atgt, gaat, acgt, gttg, tgac, gacc
26	aacg, taga, acaa, tccc, ttcc
27	cacg, aagg, tcaa, cgca, actg, cgcg, tagg, tcac
28	cccg, ctac, aggg, atcg, gtcg, atta, cggg
29	agcg, cagc, gtcc, ttcg
30	tgcg, tcat, ccgt, acct
31	gagg, ggac, tgca, gcat, ttac, gact, gaac, caca, tata
32	acgg, agat
33	ccgg, gatg, tact, atgg, cctg, gcta, caac, tggg, tatg, ggtg, tatt, cgac, ggca, ccga
34	gcgg, gtgg, cact, ctta, attt, aaaa, gggg, cgaa
35	tcgg, actt, tggt, gggt, ctgg, tcgt, gatt
36	ccat, ggaa, tgta, tcct, aatt, gata, gtta, gtgt, tgtt, gtga
37	ggat, gcga, gaga, tcga
38	ccct, cagt, aacc, ccta, ccaa, agta, ctga
39	gcgt, acta
40	ttgt
41	cata, tcta, ggta, taac
42	tacc

Table 8. Parts of the partition selected through the Bayesian Information Criterion, using all the sequences AM2871z.1, where $z = 39, 40, 41, 46, 50, 52, 57, 58, 59, 61, 62, 65, 76, 81, 87$.

i of part L_i	a	c	g	t
1	**0.62162**	0.17568	0.11824	0.08446
2	0.20141	**0.52669**	0.18127	0.09063
3	**0.27795**	0.22742	0.25900	0.23563
4	0.26518	0.31020	**0.37473**	0.04989
5	**0.49296**	0.03873	0.34859	0.11972
6	0.15173	0.17569	**0.36646**	0.30612
7	0.17982	0.28801	**0.44956**	0.08260
8	0.26409	0.22741	**0.38224**	0.12625
9	0.13973	0.20960	**0.58923**	0.06145
10	0.25732	0.09728	**0.57741**	0.06799
11	0.15512	0.23870	**0.42244**	0.18373
12	0.22067	0.08288	**0.50377**	0.19268
13	0.07543	0.16140	**0.58475**	0.17843
14	0.07708	**0.49605**	0.26383	0.16304
15	0.26020	**0.34949**	0.22874	0.16156
16	**0.34054**	0.25250	0.28011	0.12685
17	0.05213	0.06398	**0.55450**	0.32938
18	0.29789	0.14042	**0.34416**	0.21753
19	0.38671	0.04532	0.09970	**0.46828**
20	0.01037	**0.41014**	0.38134	0.19816
21	**0.43774**	0.26038	0.21384	0.08805
22	0.27390	0.29363	0.11684	**0.31563**
23	0.08333	**0.82222**	0.05556	0.03889
24	0.26710	0.05375	**0.35668**	0.32248
25	0.14725	0.28990	0.24258	**0.32027**
26	0.28553	0.14211	0.18027	**0.39211**
27	**0.38189**	0.38091	0.06102	0.17618
28	0.19352	**0.51001**	0.09724	0.19924
29	**0.48899**	0.11006	0.19654	0.20440
30	0.22482	0.37230	0.02698	**0.37590**
31	0.05018	0.35636	0.17236	**0.42109**
32	0.02055	**0.66438**	0.02740	0.28767
33	0.17956	**0.35776**	0.19200	0.27069
34	0.19475	**0.34030**	0.30463	0.16031
35	0.15342	**0.42826**	0.30464	0.11369
36	0.09625	0.36320	**0.44644**	0.09401
37	0.07349	**0.48294**	0.14961	0.29396
38	0.09836	**0.36339**	0.31785	0.22040
39	0.00339	0.35254	0.28136	**0.36271**
40	0.17865	0.31828	**0.49281**	0.01027
41	0.05017	**0.63378**	0.16890	0.14716
42	0.05970	0.10448	0.12687	**0.70896**

Table 9. Transition probabilities $P(\cdot|L_i)$ with $\cdot \in \{\text{a,c,g,t}\}$ and $i = 1, \cdots, 42$. For each part i, listed on the left column (see table 8), we indicate in bold the highest transition probability to the elements of the alphabet.

i of part L_i	Strings	Probability
1	acgc, accg	$P(\mathrm{a}\|L_1)$=0.62162
23	cgag, tccg	$P(\mathrm{c}\|L_{23})$=0.82222
9	ctgc, ctgt, gttc, tttc	$P(\mathrm{g}\|L_9)$=0.58923
42	tacc	$P(\mathrm{t}\|L_{42})$=0.70896

Table 10. Selected parts, from table 8 and 9, which have the greater transition probabilities to each element of the alphabet {a,c,g,t}.

Index of part from table 7	Indices of parts - table 8
1	1,4,15,21
16	23,32,37,41
12	9,10
26	42
14	19,24,26

Table 11. Relation between the parts listed in table 7 and 10. On left we display the parts coming from the model using only 50% of the DNA sequences, on right the parts coming from the model using all the DNA strains. In the same line, on the right we list the parts in which are identified the elements into the part on the left.

5 Conclusion

In this paper we show how to use the measure d introduced in García and González-López (2017) [1] to establish a notion of proximity between strains of Burkitt lymphoma/leukemia, over the alphabet $A = \{\text{a, c, g, t}\}$, we deal with 15 strains. The state space is formed by strings that are concatenations of size 4 of elements coming from the alphabet, and the DNA sequences are identified with Markov processes of memory 4. From d it is also possible to propose a strategy of selection of strains, for the construction of a model that allows to describe the way the elements of the state space are organized. The measure d allows to select the nearest strains to build the model whose represents the majority of the strains. We estimate the transition probability of each string for any element of the alphabet A. By the conception of the model it is possible to classify the strings into 27 categories, where each category contains strings with the same transition probability to elements of the alphabet, ie within each category, the strings are stochastically equivalent. Comparing the model constructed from the closest strains to the model with all the strains, we noticed that the categories practically double. An open question is to be able to quantify with some level of significance the impact of the inclusion of each strain on the model, as the quantity S increases. An answer in that line would allow to classify the different possible models, given the 15 strains.

References

1. J.E. García and V.A. González-López. Consistent Estimation of Partition Markov Models, *Entropy* 19, **4**, 160, 2017.
2. J.E. García and V.A. González-López. *Detecting regime changes in Markov models*, New Trends in Stochastic Modeling and Data Analysis (chapter 2, page 103), 2015.

Comparison of Stochastic Processes

Jesús E. García[1], R. Gholizadeh[2], and V.A. González-López[3]

[1] Department of Statistics, University of Campinas, R. Sérgio Buarque de Holanda, 651, Campinas (CEP 13083-859), Brazil.
(E-mail: jg@ime.unicamp.br)
[2] University of Campinas, R. Sérgio Buarque de Holanda, 651, Campinas (CEP 13083-859), Brazil.
[3] Department of Statistics, University of Campinas, R. Sérgio Buarque de Holanda, 651, Campinas (CEP 13083-859), Brazil.
(E-mail: veronica@ime.unicamp.br)

Abstract. In this paper, it is explored a distance which allows to compare Markovian processes. It is shown the relationship of this distance to the divergence of Kullback Leibler and revealed its stochastic behavior in terms of the Chi-squared distribution. The distance allows to decide if there is any discrepancy between two samples of stochastic processes. When a discrepancy exist, the use of this distance allows us to find the strings where the discrepancy is manifested. We apply the distance to written texts of European Portuguese coming from two authors: Vieira-1608 and Garrett-1799. In the application the distance reveals the linguistic configurations that expose discrepancies between written texts of different genres from the same author. This type of results could characterize linguistic genres and varieties in the same language.
Keywords: Distance, Partition Markov Models, Kullback Leibler, Chi-square distribution, Computational linguistics..

1 Introduction

By comparing several processes it is possible to tackle real problems. In linguistics, for instance, different writing texts of a single language should point out identical characteristics associated with the language, common to all of them. A comparison of texts would also be useful to point out linguistic varieties existing within a language, see Galves et al. (2012) [3]. But process comparison can also be implemented to processes that operate in parallel, for example in the industrial field, often there are imposed operational constraints for processes to exhibit a similar behavior, in order to obtain a standard final material. On the other hand, the certainty that parallel processes follow the same behavior facilitates the implementation of maintenance control strategies. For this reason it is relevant to be able to measure the similarity between processes. In García and González-López (2015) [6] a criterion d is proposed to achieve this objective. d is based on the conception of Partition Markov Models formulated over discrete Markov processes with finite memory and finite alphabets, García

17^{th} *ASMDA Conference Proceedings, 6 – 9 June 2017, London, UK*

and González-López (2017) [5]. When the processes have the same law and the samples are large enough, it is possible to prove that d converges to 0 almost surely. In this work we explore other properties of this criterion, in order to construct a distance in the strict sense of the word. We show the relation that the distance d has with the divergence of Kullback Leibler and we give a notion about its behavior in terms of the Chi-square distribution. In addition, we apply this distance to a real problem.

2 Preliminaries

Let (X_t) be a discrete time (order $o < \infty$) Markov chain on a finite alphabet A. Let us call $\mathcal{S} = A^o$ the state space and denote the string $a_m a_{m+1} \dots a_n$ by a_m^n, where $a_i \in A$, $m \leq i \leq n$. For each $a \in A$ and $s \in \mathcal{S}$, $P(a|s) = \text{Prob}(X_t = a | X_{t-M}^{t-1} = s)$. In a given sample x_1^n, coming from the stochastic process, the number of occurrences of s in the sample x_1^n is denoted by $N_n(s)$ and the number of occurrences of s followed by a in the sample x_1^n is denoted by $N_n(s,a)$. In this way $\frac{N_n(s,a)}{N_n(s)}$ is the estimator of $P(a|s)$.

Definition 1. Consider two Markov chains $(X_{1,t})$ and $(X_{2,t})$, of order o, with finite alphabet A and state space $\mathcal{S} = A^o$. With sample $x_{k,1}^{n_k}$, for $k = 1, 2$ respectively. For any $s \in \mathcal{S}$,

$$d_s(x_{1,1}^{n_1}, x_{2,1}^{n_2}) = \frac{\alpha}{(|A|-1)\ln(n_1+n_2)} \sum_{a \in A} \left\{ N_{n_1}(s,a) \ln\left(\frac{N_{n_1}(s,a)}{N_{n_1}(s)}\right) + N_{n_2}(s,a) \ln\left(\frac{N_{n_2}(s,a)}{N_{n_2}(s)}\right) - N_{n_1+n_2}(s,a) \ln\left(\frac{N_{n_1+n_2}(s,a)}{N_{n_1+n_2}(s)}\right) \right\}$$

with $N_{n_1+n_2}(s,a) = N_{n_1}(s,a) + N_{n_2}(s,a)$, $N_{n_1+n_2}(s) = N_{n_1}(s) + N_{n_2}(s)$, where N_{n_1} and N_{n_2} are given as usual, computed from the samples $x_{1,1}^{n_1}$ and $x_{2,1}^{n_2}$ respectively. With α a real and positive value.

The most relevant properties of d are listed below. Both properties are consequence of results proved in García and González-López (2017) [5]:

i. *The function $d_s(x_{1,1}^{n_1}, x_{2,1}^{n_2})$ is a distance between the Markov chains relative to the specific string $s \in \mathcal{S}$.* If $(X_{i,t}), i = 1, 2, 3$ are Markov chains under the assumptions of definition 1, with samples $x_{i,1}^{n_i}$, $i = 1, 2, 3$ respectively,

$$d_s(x_{1,1}^{n_1}, x_{2,1}^{n_2}) \geq 0 \text{ with equality } \Leftrightarrow \frac{N_{n_1}(s,a)}{N_{n_1}(s)} = \frac{N_{n_2}(s,a)}{N_{n_2}(s)} \ \forall a \in A,$$

$$d_s(x_{1,1}^{n_1}, x_{2,1}^{n_2}) = d_s(x_{2,1}^{n_2}, x_{1,1}^{n_1}),$$

$$d_s(x_{1,1}^{n_1}, x_{2,1}^{n_2}) \leq d_s(x_{1,1}^{n_1}, x_{3,1}^{n_3}) + d_s(x_{3,1}^{n_3}, x_{2,1}^{n_2}).$$

ii. *Local behavior of processes laws.* If the stochastic laws of $(X_{1,t})$ and $(X_{2,t})$ are the same in s, then $d_s(x_{1,1}^{n_1}, x_{2,1}^{n_2}) \underset{\min(n_1,n_2)\to\infty}{\longrightarrow} 0$.
Otherwise, $d_s(x_{1,1}^{n_1}, x_{2,1}^{n_2}) \underset{\min(n_1,n_2)\to\infty}{\longrightarrow} \infty$.

In the following result we show the relationship between this distance and the Kullback-Leibler divergence $D(P||Q)$, a concept commonly used in the topic, but that does not constitute a distance. We also show the asymptotic behavior of the distance. We will use the following notations $D(P(\cdot)||Q(\cdot)) = \sum_{a\in A} P(a)\ln(\frac{P(a)}{Q(a)})$ and $\chi^2(P(\cdot),Q(\cdot)) = \sum_{a\in A}\frac{(P(a)-Q(a))^2}{Q(a)}$, for two distributions P and Q defined in the alphabet A, with $Q(a)\neq 0$, $a\in A$. First, we will see how the quantity $D(P(\cdot)||Q(\cdot))$ behaves under certain conditions on P and Q. Consider the function $f(x) = x\ln(x)$, near to $x=1$, by the Taylor's expansion we have $f(x) = (x-1)+\frac{(x-1)^2}{2}+\delta(x)(x-1)^2$ where $\delta(x) = -\frac{(x-1)}{6t^2}$ for some value $t\in(x,1)$ (Lagrange's form). We note that when $x\to 1, \delta(x)\to 0$. Thus, for two probability distributions P and Q in A,

$$\begin{aligned} P(a)\ln\Big(\frac{P(a)}{Q(a)}\Big) &= Q(a) f\Big(\frac{P(a)}{Q(a)}\Big) \\ &= P(a)-Q(a)+\frac{1}{2}\frac{(P(a)-Q(a))^2}{Q(a)}+\delta\Big(\frac{P(a)}{Q(a)}\Big)\frac{(P(a)-Q(a))^2}{Q(a)}, \end{aligned}$$

for $a\in A$,

$$D(P(\cdot)||Q(\cdot)) = \frac{1}{2}\chi^2(P(\cdot),Q(\cdot))+\sum_{a\in A}\delta\Big(\frac{P(a)}{Q(a)}\Big)\frac{(P(a)-Q(a))^2}{Q(a)} \tag{1}$$

and

$$\frac{D(P(\cdot)||Q(\cdot))}{\chi^2(P(\cdot),Q(\cdot))} = \frac{1}{2}+\frac{\sum_{a\in A}\delta\Big(\frac{P(a)}{Q(a)}\Big)\frac{(P(a)-Q(a))^2}{Q(a)}}{\chi^2(P(\cdot),Q(\cdot))}. \tag{2}$$

If $\frac{P(a)}{Q(a)}\to 1$, given ϵ positive and small enough, $|\delta\Big(\frac{P(a)}{Q(a)}\Big)|<\epsilon$ and
$\Big|\frac{\sum_{a\in A}\delta\Big(\frac{P(a)}{Q(a)}\Big)\frac{(P(a)-Q(a))^2}{Q(a)}}{\chi^2(P(\cdot),Q(\cdot))}\Big| < \epsilon$, so $\frac{D(P(\cdot)||Q(\cdot))}{\chi^2(P(\cdot),Q(\cdot))}\to\frac{1}{2}$.
If one of the probabilities is the empirical distribution, say $\hat{P}(a) = \frac{X(a)}{k}$, where the occurences of a in the sample of size k is denoted by $X(a)$, and the sample is generated from the law Q, $\chi^2(\hat{P}(\cdot)||Q(\cdot)) = \frac{1}{k}\sum_{a\in A}\frac{(X(a)-kQ(a))^2}{kQ(a)}$. Thus, if we introduce the quantity $\chi^{2,k}(\hat{P}(\cdot),Q(\cdot)) = \sum_{a\in A}\frac{(X(a)-kQ(a))^2}{kQ(a)}$, we can recognize the typical Chi-square statistic. From the equation (1) we obtain

$$D(\hat{P}(\cdot)||Q(\cdot)) = \frac{1}{2k}\chi^{2,k}(\hat{P}(\cdot),Q(\cdot))+\sum_{a\in A}\frac{1}{k}\delta\Big(\frac{\hat{P}(a)}{Q(a)}\Big)\frac{(X(a)-kQ(a))^2}{kQ(a)} \tag{3}$$

and when $\frac{\hat{P}(a)}{Q(a)}\to 1$,

$$\frac{D(\hat{P}(\cdot)||Q(\cdot))}{\chi^{2,k}(\hat{P}(\cdot),Q(\cdot))}\to\frac{1}{2k}.$$

If we have two samples of sizes k_1 and k_2 generated from the law W, with empririal distribution $\hat{P}(a) = \frac{X(a)}{k_1}$ and $\hat{Q}(a) = \frac{Y(a)}{k_2}$ respectively. We obtain (equation (1)),

$$D(\hat{P}(\cdot)||\hat{Q}(\cdot)) = \frac{1}{k_1}\sum_{a\in A}\Big(\frac{W(a)}{\hat{Q}(a)}\Big)\Big(\frac{1}{2}+\delta\Big(\frac{\hat{P}(a)}{\hat{Q}(a)}\Big)\Big)\frac{(X(a)-k_1W(a))^2}{k_1W(a)} + \frac{1}{k_2}\sum_{a\in A}\Big(\frac{W(a)}{\hat{Q}(a)}\Big)\Big(\frac{1}{2}+\delta\Big(\frac{\hat{P}(a)}{\hat{Q}(a)}\Big)\Big)\frac{(Y(a)-k_2W(a))^2}{k_2W(a)} + \sum_{a\in A}\Big(1+2\delta\Big(\frac{\hat{P}(a)}{\hat{Q}(a)}\Big)\Big)(\hat{P}(a)-W(a))\Big(\frac{W(a)}{\hat{Q}(a)}-1\Big). \quad (4)$$

So, when $\frac{W(a)}{\hat{Q}(a)} \to 1$ and $\frac{\hat{P}(a)}{\hat{Q}(a)} \to 1$,

$$\frac{D(\hat{P}(\cdot)||\hat{Q}(\cdot))}{\frac{1}{2k_1}\chi^{2,k_1}(\hat{P}(\cdot),W(\cdot)) + \frac{1}{2k_2}\chi^{2,k_2}(\hat{Q}(\cdot),W(\cdot))} \to 1. \quad (5)$$

These simple relationships between empirical distributions allows us to delineate the behavior of the distance d_s (definition (1)).

Theorem 1. *Let $(X_{k,t})$ be a Markov chain of order o, with finite alphabet A, state space $\mathcal{S} = A^o$ and $x_{k,1}^{n_k}$ a sample of the process for $k = 1, 2$. Consider also $s \in \mathcal{S}$. If $D\Big(\frac{N_{n_k}(s,\cdot)}{N_{n_k}(s)} \parallel \frac{N_{n_1+n_2}(s,\cdot)}{N_{n_1+n_2}(s)}\Big) < \infty$, for $k = 1, 2$, then*

$$d_s(x_{1,1}^{n_1}, x_{2,1}^{n_2}) = \frac{\alpha}{(|A|-1)\ln(n_1+n_2)}\sum_{k=1,2} N_{n_k}(s) D\Big(\frac{N_{n_k}(s,\cdot)}{N_{n_k}(s)} \parallel \frac{N_{n_1+n_2}(s,\cdot)}{N_{n_1+n_2}(s)}\Big).$$

When $\frac{N_{n_k}(s,\cdot)/N_{n_k}(s)}{W(\cdot)} \to 1$ for $k = 1, 2$,

$$2\ln(n_1+n_2)\frac{(|A|-1)}{\alpha} d_s(x_{1,1}^{n_1}, x_{2,1}^{n_2}) \sim_d$$

$$\sum_{k=1,2} \chi^{2,N_{n_k}(s)}\Big(\frac{N_{n_k}(s,\cdot)}{N_{n_k}(s)}, W(\cdot)\Big) + \chi^{2,N_{n_1+n_2}(s)}\Big(\frac{N_{n_1+n_2}(s,\cdot)}{N_{n_1+n_2}(s)}, W(\cdot)\Big),$$

where $\sim_d$ means similarity in distribution.

Proof. Note that $\ln(n_1+n_2)\frac{(|A|-1)}{\alpha}d_s(x_{1,1}^{n_1},x_{2,1}^{n_2})$ is

$$
\begin{aligned}
&= \sum_{a\in A}\Big\{N_{n_1}(s,a)\ln\left(\frac{N_{n_1}(s,a)}{N_{n_1}(s)}\right)+N_{n_2}(s,a)\ln\left(\frac{N_{n_2}(s,a)}{N_{n_2}(s)}\right)\\
&\quad -(N_{n_1}(s,a)+N_{n_2}(s,a))\ln\left(\frac{N_{n_1+n_2}(s,a)}{N_{n_1+n_2}(s)}\right)\Big\}.\\
&= \sum_{a\in A}\Big\{N_{n_1}(s,a)\Big(\ln\left(\frac{N_{n_1}(s,a)}{N_{n_1}(s)}\right)-\ln\left(\frac{N_{n_1+n_2}(s,a)}{N_{n_1+n_2}(s)}\right)\Big)\Big\}+\\
&\quad \sum_{a\in A}\Big\{N_{n_2}(s,a)\Big(\ln\left(\frac{N_{n_2}(s,a)}{N_{n_2}(s)}\right)-\ln\left(\frac{N_{n_1+n_2}(s,a)}{N_{n_1+n_2}(s)}\right)\Big)\Big\}\\
&= \sum_{k=1,2}N_{n_k}(s)\sum_{a\in A}\frac{N_{n_k}(s,a)}{N_{n_k}(s)}\ln\left(\frac{N_{n_k}(s,a)}{N_{n_k}(s)}/\frac{N_{n_1+n_2}(s,a)}{N_{n_1+n_2}(s)}\right)\\
&= \sum_{k=1,2}N_{n_k}(s)D\Big(\frac{N_{n_k}(s,\cdot)}{N_{n_k}(s)}\parallel\frac{N_{n_1+n_2}(s,\cdot)}{N_{n_1+n_2}(s)}\Big).
\end{aligned}
$$

Following the equation (5)

$$\sum_{k=1,2}N_{n_k}(s)D\Big(\frac{N_{n_k}(s,\cdot)}{N_{n_k}(s)}\parallel\frac{N_{n_1+n_2}(s,\cdot)}{N_{n_1+n_2}(s)}\Big)\sim_d$$

$$\sum_{k=1,2}\frac{N_{n_k}(s)}{2}\Big\{\frac{\chi^{2,N_{n_k}(s)}\Big(\frac{N_{n_k}(s,\cdot)}{N_{n_k}(s)},W(\cdot)\Big)}{N_{n_k}(s)}+\frac{\chi^{2,N_{n_1+n_2}(s)}\Big(\frac{N_{n_1+n_2}(s,\cdot)}{N_{n_1+n_2}(s)},W(\cdot)\Big)}{N_{n_1+n_2}(s)}\Big\}.$$

Then,

$$2\ln(n_1+n_2)\frac{(|A|-1)}{\alpha}d_s(x_{1,1}^{n_1},x_{2,1}^{n_2})\sim_d$$

$$\sum_{k=1,2}\chi^{2,N_{n_k}(s)}\Big(\frac{N_{n_k}(s,\cdot)}{N_{n_k}(s)},W(\cdot)\Big)+\chi^{2,N_{n_1+n_2}(s)}\Big(\frac{N_{n_1+n_2}(s,\cdot)}{N_{n_1+n_2}(s)},W(\cdot)\Big).$$

3 Application to Linguistic Data

Tycho Brahe corpus is an annotated historical corpus, freely accessible at Galves and Faria (2010) [2]. This corpus uses the chronological criterion of the author's birthdate to assign a time for written texts. The subset of written texts included in this study, listed in table 3 is composed by six texts from two authors. Linguistic studies show that the variability observed in different written texts of European Portuguese involves, among other aspects, changes in the proportion of occurrence of the placement of the stress in the last or in the penultimate syllable of the word and alterations in the use of monosyllables, with or without stress, see for instance Frota et al. (2012)[1]. For this reason we guide our inspection to the position in the word occupied

Author	Vieira	Vieira	Vieira
Date	1608	1608	1608
Type	dissertation	letters	sermons
Notation	1608d	1608c	1608s
Author	Garrett	Garrett	Garrett
Date	1799	1799	1799
Type	letters	narrative	theater
Notation	1799c	1799n	1799t

Table 1. The set of the Tycho Brahe corpus.

by the stress and the size of the word (number of syllables). Each written text was processed with a slightly modified version of the perl-code "silaba" by Miguel Galves, that can be freely downloaded for academic purposes at `www.ime.usp.br/~tycho/prosody/vlmc/tools/sil4.pl` . The software was used to extract two components of each orthographic word, denoted by (i, j), where i is the total number of syllables which compound the word, $i = 1, 2, ..., 8$ and j indicates the syllable (from left to right) in which is registered the stress in the word. Where, $j = 0$ means no stress in the word. The period (final of sentence) was codified as $(0, 0)$. The alphabet A used here was defined as exposed in table 3.

Orthographic word code	Element in the alphabet A	Meaning
$(0, 0)$	0	final of sentence
$(1, 1)$	1	monosyllable with stress
$(1, 0)$	2	monosyllable without stress
$(2, 2)$	3	dissyllable - stress in the last syllable
$(2, 1)$	4	dissyllable - stress in the first syllable
(i, i), $i \geq 3$	6	*oxytone* word
$(i, i-1)$, $i \geq 3$	7	*paroxytone* word
$(i, i-2)$, $i \geq 3$	8	*proparoxytone* word

Table 2. Definition of the alphabet A.

We can define

$$dmax = \max\{d_s(x_{1,1}^{n_1}, x_{2,1}^{n_2}), s \in \mathcal{S}\} \tag{6}$$

and

$$smax = \arg\max\{dmax\}. \tag{7}$$

Observe that $dmax < \epsilon$ if and only if $d_s(x_{1,1}^{n_1}, x_{2,1}^{n_2}) < \epsilon, \forall s \in \mathcal{S}$. That is, a small value of $dmax$ indicates the stochastic laws on s are similar for all $s \in \mathcal{S}$. In other words the distributions of the processes are similar.

As seen in definition 1, if the stochastic laws of $(X_{1,t})$ and $(X_{2,t})$ are the same in s, then

$$d_s(x_{1,1}^{n_1}, x_{2,1}^{n_2}) \underset{\min(n_1,n_2)\to\infty}{\longrightarrow} 0.$$

In the same way if the local laws for s are different then,

$$d_s(x_{1,1}^{n_1}, x_{2,1}^{n_2}) \underset{\min(n_1,n_2)\to\infty}{\longrightarrow} \infty.$$

We can see that if $dmax$ is large, $smax$ is exactly the string we want to recognize, as being relevant in terms of discrepancy but all the strings with a large relative value of d will reveal changes on the local laws of the processes relative to the string. In this application a value larger than 1 will be considered significant.

We note that the comparison is made between the different texts of the same author. The memory o used in this application is equal to 2.

$d_s(1608c, 1608d)$	s	$d_s(1608c, 1608s)$	s	$d_s(1608d, 1608s)$	s
1.02591	7-6	1.18101	4-7	1.07770	1-7
1.11191	1-6	1.28567	2-3	1.07883	4-4
1.13048	3-6	1.98674	2-7	1.33124	4-7
2.14046	**7-2**	**3.86756**	**2-4**	1.67395	2-4
				1.74245	**2-7**

$d_s(1799c, 1799t)$	s	$d_s(1799t, 1799n)$	s
1.13432	1-7	1.01398	1-7
1.20717	4-4	1.07517	6-2
1.29197	7-0	1.24806	1-2
2.15512	4-2	1.34589	3-2
2.35864	4-7	2.56588	2-4
2.84146	2-7	2.57690	4-7
3.40959	7-2	3.56924	4-2
3.46598	**2-4**	3.74332	2-7
		4.49460	**7-2**

Table 3. Cases with values of $d > 1$:1608c-1608d, 1608c-1608s,1608d-1608s, 1799c-1799t, 1799t-1799n. In bold the $dmax$ value (see equation (6)) and the $smax$ string (see equation (7)).

String	Meaning
2-4	a monosyllable without stress followed by a dissyllable with stress in the first syllable
2-7	a monosyllable without stress followed by a paroxytone word
7-2	a paroxytone word followed by a monosyllable without stress

Table 4. Meaning of each $smax$ detected by $dmax$.

Other studies in the area show that the strings 2-4, 7-2 and 2-7 (see tables 3, 4) are volatile configurations of the European Portuguese (from the 16th century to the 19th century) see García et al. (2017) [4]. We can see that this characteristic persists when analyzing the variability of different written texts of the same author, being that author: Vieira or Garrett.

$a \in A$	*smax*: 7-2 (2.14046)		*smax*: 2-4 (3.86756)		*smax*: 2-7 (1.74245)	
	1608c	1608d	1608c	1608s	1608d	1608s
0	0.00000	0.00000	0.02277	0.06825	0.05221	0.11444
1	0.09461	0.09927	0.06624	0.07620	0.05200	0.05488
2	0.20037	0.15025	0.31714	0.35255	0.50989	0.47124
3	0.07616	0.04350	0.04251	0.04473	0.02926	0.03284
4	0.31379	0.29417	0.20402	0.22949	0.16547	0.16809
6	0.03763	0.03986	0.02638	0.02175	0.02337	0.02203
7	0.26082	0.34266	0.31144	0.19307	0.15053	0.12464
8	0.01662	0.03028	0.00949	0.01397	0.01726	0.01183

$a \in A$	*smax*: 2-4 (3.46598)		*smax*: 7-2 (4.49460)	
	1799c	1799t	1799t	1799n
0	0.05469	0.13364	0.01100	0.00183
1	0.06448	0.10649	0.13265	0.10353
2	0.28798	0.27959	0.34777	0.15735
3	0.04389	0.04200	0.06598	0.05153
4	0.19514	0.24608	0.23505	0.29684
6	0.02971	0.01273	0.02749	0.02863
7	0.30959	0.17522	0.17113	0.32410
8	0.01452	0.00424	0.00893	0.03619

Table 5. Conditional probabilities $P(a|smax),\ \forall a \in A$ computed from each written text: 1608c, 1608d; 1608c, 1608s; 1608d, 1608s; 1799c, 1799t; 1799t, 1799n.

Table 5 shows the transition probabilities $P(a|smax)\ \forall a \in A$, for each pair of compared texts. With this information we can check the differences between the written texts in relation to the prosodic construction, for example $P(2|7-2)$ is 0.34777 in the text 1799t (theater) and it goes to 0.15735 in the written text 1799n (narrative) both texts from Garrett. Moreover, the most probable choice for the second text, since the string 7-2 has been observed is 7 ($P(7|7-2) = 0.3241$).

We can define 3 groups of strings: (i) strings that show discrepancies between Vieira's texts but not in the case of Garrett's texts, (ii) strings that show discrepancies between Garrett's texts and not in the case of Vieira's texts and strings that show discrepancies between texts for each of these authors. See the detailed description of each group in table 6.

Values of d greater than 1 have not been detected in the comparison between the texts: 1799c (letters) and 1799n (narrative). Thus, these texts can be considered as coming from the same Markovian process.

4 Conclusion

The distance proposed in this paper has a clear relation to the divergence of Kullback Leibler, we show this in theorem 1. In addition, the adequately scaled distance has its stochastic behavior described by a sum of Chi-squared dependent random variables, also seen in the theorem 1. In relation to the application, note that the distance introduced here makes it possible to decide

Author	String	Meaning
Vieira	1-6	a monosyllable with stress followed by an *oxytone* word
	2-3	a monosyllable without stress followed by a dissyllable with stress in the last syllable
	3-6	a dissyllable with stress in the last syllable followed by an *oxytone* word
	7-6	a *paroxytone* word followed by an *oxytone* word
Garrett	1-2	a monosyllable with stress followed by a monosyllable without stress
	3-2	a dissyllable with stress in the last syllable followed by a monosyllable without stress
	4-2	a dissyllable with stress in the first syllable followed by a monosyllable without stress
	6-2	an *oxytone* word followed by a monosyllable without stress
	7-0	a *paroxytone* word followed by final of sentence
Both	1-7	a monosyllable with stress followed by a *paroxytone* word
	4-4	a dissyllable with stress in the first syllable followed by a dissyllable with stress in the first syllable
	4-7	a dissyllable with stress in the first syllable followed by a *paroxytone* word

Table 6. Strings (see table 3) and meaning of the linguistic compositions that characterize the variability between the texts of the same author. We also list the strings (with $d > 1$) that are common among the authors, the constructions listed in table 4 are excluded.

whether two Markovian stochastic processes follow the same law or not. And it also allows to identify discrepancies pointing out the strings responsible for them.

References

1. S. Frota, C. Galves, M. Vigário, V.A. González-López and B. Abaurre. The phonology of rhythm from Classical to Modern Portuguese, *Journal of Historical Linguistics* (2.2) 173-207, 2012.

2. C. Galves and P. Faria. Tycho Brahe Parsed Corpus of Historical Portuguese. http://www.tycho.iel.unicamp.br/ tycho/corpus/en/index.html , 2010.
3. A. Galves, C. Galves, J.E. Garcia, N.L. Garcia and F. Leonardi, F. Context tree selection and linguistic rhythm retrieval from written texts, *The Annals of Applied Statistics* 6(1), 186-209, 2012.
4. J E. García, R. Gholizadeh and V.A. González-López. Linguistic Compositions Highly Volatile in Portuguese. *Submitted*.
5. J.E. García and V.A. González-López. Consistent Estimation of Partition Markov Models, *Entropy* 19, **4**, 160, 2017.
6. J.E. García and V.A. González-López. *Detecting regime changes in Markov models*, New Trends in Stochastic Modeling and Data Analysis (chapter 2, page 103), 2015.

Efficiency Evaluation of Multiple-Choice Questions and Exams

Evgeny Gershikov and Samuel Kosolapov

Department of Electrical and Electronic Engineering, Braude Academic College,
Carmiel, 2161002, Israel
(E-mail: eugeny11@braude.ac.il)

Abstract. Multiple-choice questions are common in Israeli institutions of higher education. They can be checked and graded automatically using artificial intelligence methods so that the answer sheets are aligned and segmented automatically into the relevant regions, and then the answers marked by the students are read. In the next step the grades can be easily calculated by comparing the marked data with the correct answers. To evaluate the efficiency of the exam in addition to the basic statistical analysis of the grades, we propose efficiency measures for each question as well as for the whole exam. These efficiency measures attempt to answer the following questions: how many of the "strong" students have answered a particular question correctly and how many of the "weak" students have failed in a particular question. A question is considered efficient if most "strong" students succeed in it while most "weak" ones fail. In a similar fashion, an exam questionnaire is considered efficient if the majority of its questions are efficient. Our measures can be used both for multiple-choice and numeric answers. We have performed the proposed statistical analysis on the grades of a number of real life examinations and our conclusion is that the proposed analysis and efficiency measures are beneficial for the purpose of estimating the quality of the exam and discovering the inefficient questions: the ones that fail to separate the "strong" and the "weak" students.
Keywords: Efficiency evaluation, Multiple-choice questions, Statistical analysis of performance, Academic exams

1 Introduction

Multiple-choice questions are a well-known method of examination often used in academic institutions of higher education (see state of the art at Wood [1]). They are easy to check and can even be graded automatically using scanners or camera-based systems that utilize image processing and computer vision techniques (Kosolapov et al. [2], Gershikov and Kosolapov [3] and [4]). Most of the automatic systems use specially tailored optical mark recognition (OMR) techniques, which are much faster and more reliable than general purpose optical character recognition (OCR) techniques (Bergeron [5]). The use of machine vision methods for applications, where visual information has to be translated to quantitative data, has accelerated in recent years due to technological advances in the areas of mobile devices and digital photography.

17th *ASMDA Conference Proceedings, 6 - 9 June 2017, London, UK*

Automatic checking of exams also has the advantage of easy statistical analysis of the students' performance in the exam at the global level as well as at the individual question level. This is because during the grading process, all the necessary data for such analysis has already been collected.

Once the grades have been derived, the grades statistics can be analyzed by a number of well-known statistical methods: classical test theory, factor analysis, cluster analysis, item response theory, and model analysis (Ding and Beichner [6]). Additionally, after the grades have been derived and analyzed, it is important to compare the performance of the group of students in this particular test or quiz to other groups of students or past examinations and determine the level of knowledge of the students versus the level of knowledge required by the exam. Clearly, a high difficulty level of the questions or a low knowledge level of the examined students may result in the same low performance in the exam. The opposite case is also true: high performance of the examinees due to an easy exam or excellent knowledge of the exam subject demonstrated by the students. To identify these cases we suggest a different kind of mathematical analysis in addition to the regular statistical analysis of the grades by calculating the average, the standard deviation, the median, the histogram of the grades, the passing/failing percent of students, and other similar values.

Our idea is to use efficiency measures for each question. One of these efficiency measures attempts to answer the following question: how many of the "strong" students answered a particular question correctly. Another measure attempts to evaluate the performance of the "weak" students: how many of them failed in a particular question. A question is considered efficient if most "strong" students succeed in it while most "weak" ones fail. In a similar fashion, an exam questionnaire is considered efficient if the majority of its questions are efficient. In the next section we present our efficiency measures. For best performance, we believe these measures have to be calculated iteratively.

2 Exam Efficiency Evaluation

2.1 Efficiency Measures and Efficiency Weighted Grades

Assume that the exams were checked and graded using the regular method of point allocation to the different questions without any other weighting. We first define $Eff33Gd_{i,0}$, the initial "good" efficiency of an exam question number i, as the ratio between the number of "strong" students that answered this question correctly N_{Gd}^{i} and the number of "strong" students in the whole exam N_{Gd}. The "strong" students are defined as those in the top 33% of the final grades. Thus

$$Eff33Gd_{i,0} = \frac{N_{Gd}^{i}}{N_{Gd}}. \qquad (1)$$

In a similar fashion, we define $Eff33Bd_{i,0}$, the initial "bad" efficiency of an exam question number i, as the ratio between the number of "weak" students that answered this question incorrectly N_{Bd}^{i} and the number of "weak" students in the whole exam N_{Bd}. The "weak" students are defined as those in the bottom 33% of the final grades. Thus

$$Eff33Bd_{i,0} = \frac{N_{Bd}^{i}}{N_{Bd}}. \qquad (2)$$

We can now define the efficiency of question i as either the minimum of the two efficiencies:

$$Eff33_{i,0} = min\left\{Eff33Gd_{i,0}, Eff33Bd_{i,0}\right\} \qquad (3)$$

or as the average of the two efficiencies:

$$Eff33_{i,0} = \frac{Eff33Gd_{i,0} + Eff33Bd_{i,0}}{2}. \qquad (4)$$

We prefer the second choice as the first option is much more demanding for a question to be considered efficient. This means that the minimum option is more suitable for readers who prefer more of a challenge.

It is reasonable to average the individual question grades by the efficiencies of Equations (3) or (4) so that an efficient question contributes more to the resulting grade than an inefficient one. We now define the efficiency weighted grade of each student as:

$$WGrades_0 = \sum_{i=1}^{N_Q} Eff33_{i,0} \cdot Grade_i. \qquad (5)$$

Here, N_Q is the number of questions in the exam and $Grade_i$ is the grade of an individual examinee of question number *i*.

2.2 Iterative Execution

To improve the performance of our efficiency measures, we suggest repeating the process described above, using the following steps in iteration k $(k = 1, 2, 3, ...)$

1. Divide the students into three classes: the "strong" students, the "weak" students, and the average ones, where the "strong" ones are the students in

the top 33% of the weighted grades $WGrades_k$ and the "weak" ones are the students in the bottom 33% of the **weighted** grades $WGrades_k$.

2. Calculate the efficiencies $Eff33Gd_{i,k}$ and $Eff33Bd_{i,k}$ for question number *i* using the classes derived in the previous stage and Equations (1) and (2). The number of students in the "strong" and "weak" classes are substituted for N_{Gd}^{i} and N_{Bd}^{i}, respectively.
3. Calculate the question efficiencies $Eff33_{i,k}$ using Equations (3) or (4).
4. Calculate the weighted grades $WGrades_k$ using Equation (5).

Repeat the process until the maximal number of iterations is reached (for example, 50) or the efficiencies converge subject to a certain stop criterion, for example,

$$\frac{1}{N_Q}\sum_{i=1}^{N_Q} | Eff33Gd_{i,k} - Eff33Gd_{i,k-1} | < TH \qquad (6)$$

and

$$\frac{1}{N_Q}\sum_{i=1}^{N_Q} | Eff33Bd_{i,k} - Eff33Bd_{i,k-1} | < TH. \qquad (7)$$

TH here is a small threshold, e. g., 0.01.
Finally, the exam efficiency score is calculated as

$$Eff33 = \frac{1}{N_Q}\sum_{i=1}^{N_Q} Eff33_{i,klast}, \qquad (8)$$

where k_{last} is the last iteration of the algorithm.

2.2 Post-Processing

The weighted grades $WGrades_{klast}$ can be adjusted to have a distribution on the same scale as the one of the non-weighted grades, given by $Grades = \sum_{i=1}^{N_Q} Grade_i$. There are several options for such an adjustment. Only one of these options should be used.

1. Adjust the weighted grades to have the desired median value $GradesMedian$, that can be chosen to be the same as for the non-weighted grades or any other value; e.g., 50 for grades on the scale of 0-100. This step is done simply by dividing $WGrades_{klast}$ by their current median, multiplying it by $GradesMedian$, and then rounding:

$$WGrades_{klast}^{new} = round\left(\frac{WGrades_{klast} \cdot GradesMedian}{median\left(WGrades_{klast}\right)}\right). \qquad (9)$$

An additional step of setting grades above the maximal possible grade (e.g., 100) to that maximal value should be added.

2. Adjust the weighted grades to have the desired maximal value $GradesMax$, which can be chosen to be the same as for non-weighted grades or another value; e.g., 100. This step is done in a similar fashion to the one above. No additional steps are required here if $GradesMax$ is chosen reasonably.
3. Adjust the weighted grades to be in the same scale as the non-weighted grades; e.g., 0-100, by scaling them using the final question efficiencies $Eff33_{i,klast}$. The maximal possible weighted grade that the student can achieve is

$$WGradesMax = \sum_{i=1}^{N_Q} Eff33_{i,klast} \cdot Points_i, \qquad (10)$$

where $Points_i$ is the number of points allocated to question number i. Thus the scaling is done simply by the following formula:

$$WGrades_{klast}^{new} = round\left(\frac{WGrades_{klast} \cdot GradesMax}{WGradesMax}\right). \qquad (11)$$

Here, $GradesMax$ is usually chosen to be the maximal value of the regular non-weighted grades; e.g., 100.

In this work we prefer the third option for post-processing the grades.

3 Real-Life Experiments and Results

We applied the algorithms described in the previous section to a number of real life examinations performed in an electrical engineering course in an academic college. The results for one of the exams are given in Fig. 1. The exam consisted of ten multiple-choice questions with five possible answers for each. We label this exam as "Exam1". When analyzing the results, the efficiencies were calculated using the average of the "good" and "bad" efficiency values, as given in Equation (4). As can be seen in Fig. 1, the efficiencies range from as low as 0.08 to as high as 0.94 before averaging, and the range is 0.5 to 0.76 after averaging. Also, there is no significant correlation between the success rate in a certain question and its efficiency score except for the radical cases of a very high success rate (close to 100%) or a very low one (close to 0%). We consider the success rate to be a poor criterion to measure efficiency since it can be the same for questions where the "strong" students succeeded and the "weak" ones failed and for questions with the opposite results.

Based on both good and bad efficiencies we can classify the questions into categories as shown in Table 1. There are 16 categories, similar to the four shown in the table. Another four categories of inefficient questions, which we find interesting, are given in Table 2 and allow the definition of very easy and very hard questions differently than just based on the success rate. The proposed efficiencies allow the comparison of two questions with exactly the same success rate, but different performance of "strong" and "weak" students.

Q1	Q2	Q3	Q4	Q5	Q6	Q7	Q8	Q9	Q10
%Success	%Success	%Success	%Success	%Success	%Success	%Success	%Success	%Success	%Success
57.97	43.48	56.52	8.70	15.94	94.20	69.57	43.48	28.99	81.16
Eff33%Gd	Eff33%Gd	Eff33%Gd	Eff33%Gd	Eff33%Gd	Eff33%Gd	Eff33%Gd	Eff33%Gd	Eff33%Gd	Eff33%Gd
0.63	0.54	0.71	0.08	0.17	1.00	0.92	0.54	0.58	0.88
Eff33%Bd	Eff33%Bd	Eff33%Bd	Eff33%Bd	Eff33%Bd	Eff33%Bd	Eff33%Bd	Eff33%Bd	Eff33%Bd	Eff33%Bd
0.76	0.53	0.53	0.94	0.82	0.24	0.59	0.71	0.82	0.41
Eff33%	Eff33%	Eff33%	Eff33%	Eff33%	Eff33%	Eff33%	Eff33%	Eff33%	Eff33%
0.70	0.54	0.62	0.51	0.50	0.62	0.76	0.63	0.70	0.65

low efficiency

high efficiency

Fig. 1. Results for Exam1: success rates and efficiencies for ten multiple-choice questions. Exam efficiency is 0.62.

Table 1. Question categories based on good and bad efficiencies.

Criterion	**"Strong" students category**	**"Weak" students category**	**Efficiency Category**
$0.25 < Eff33Gd_i < 0.5$ and $0.25 < Eff33Bd_i < 0.5$	Inefficient question	Inefficient question	Inefficient
$Eff33Gd_i < 0.25$ and $Eff33Bd_i < 0.25$	Highly inefficient question	Highly inefficient question	Highly inefficient
$0.5 < Eff33Gd_i < 0.75$ and $0.5 < Eff33Bd_i < 0.75$	Normal efficiency question	Normal efficiency question	Efficient
$0.75 < Eff33Gd_i$ and $0.75 < Eff33Bd_i$	Highly inefficient question	Highly inefficient question	Highly efficient

We can now define an efficient exam:

- The majority of questions were efficient.
- There were no questions with average efficiency below 0.5.

The results for another exam, labeled Exam2, are shown in Fig. 2. Here, the efficiencies range from 0.15 to 1 before averaging and from 0.57 to 0.87 after averaging for the 12 available multiple-choice questions. The exam scored

Table 2. Special question categories based on good and bad efficiencies.

Criterion	Category
$0.75 < Eff\,33Gd_i$ and $Eff\,33Bd_i < 0.5$	Easy question
$Eff\,33Gd_i < 0.5$ and $0.75 < Eff\,33Bd_i$	Hard question
$0.75 < Eff\,33Gd_i$ and $Eff\,33Bd_i < 0.25$	Primitive (very easy) question
$Eff\,33Gd_i < 0.25$ and $0.75 < Eff\,33Bd_i$	Challenging (very hard) question

Q1	Q2	Q3	Q4	Q5	Q6	Q7	Q8	Q9	Q10	Q11	Q12
%Success	%Success	%Success	%Success	%Success	%Success	%Success	%Success	%Success	%Success	%Success	%Success
80.49	41.46	53.66	51.22	78.05	36.59	9.76	29.27	53.66	48.78	78.05	56.1
Eff33%Gd	Eff33%Gd	Eff33%Gd	Eff33%Gd	Eff33%Gd	Eff33%Gd	Eff33%Gd	Eff33%Gd	Eff33%Gd	Eff33%Gd	Eff33%Gd	Eff33%Gd
0.92	0.85	0.69	0.38	1	0.54	0.15	0.62	0.77	0.85	0.85	0.85
Eff33%Bd	Eff33%Bd	Eff33%Bd	Eff33%Bd	Eff33%Bd	Eff33%Bd	Eff33%Bd	Eff33%Bd	Eff33%Bd	Eff33%Bd	Eff33%Bd	Eff33%Bd
0.33	0.89	0.78	0.89	0.33	0.78	1	0.89	0.78	0.78	0.33	0.67
Eff33%	Eff33%	Eff33%	Eff33%	Eff33%	Eff33%	Eff33%	Eff33%	Eff33%	Eff33%	Eff33%	Eff33%
0.625	0.87	0.735	0.635	0.665	0.66	0.575	0.755	0.775	0.815	0.59	0.76
x	v		x	x		x		v	v	x	

Fig. 2. Results for Exam2: success rates and efficiencies for ten multiple-choice questions. Exam efficiency is 0.71.

higher on the total efficiency scale, with 0.71 compared to just 0.62 for Exam1. Based on the categories in Table 1 and Table 2, we can classify questions 2, 9, and 10 as highly efficient, questions 3, 6, 8, and 12 as efficient, questions 1, 5, and 11 as easy (which is also supported by the success rate), question 4 as hard (despite the 51% success rate) and question 7 as challenging. There were no inefficient questions in Exam2, as defined in Table 1.

There were no primitive questions as well. This is supported also by the overall, relatively high, average efficiency. In Exam1, on the other hand, there was one primitive question (number 6), two challenging questions (number 4 and 5), an easy question (number 10) and one question close to being inefficient (number

2). Checking our criterion for efficiency of the whole exam, we can see that Exam2 is efficient, while Exam1 is marginally efficient.

Graphs of the non-weighted grades in ascending order and the corresponding adjusted weighted grades are shown in Fig. 3. The weighted grades were post-processed using the third method in Section 2.2. The grades change when using weighting to a small extent, but enough to see different weighted grades for students who answered the same number of questions correctly.

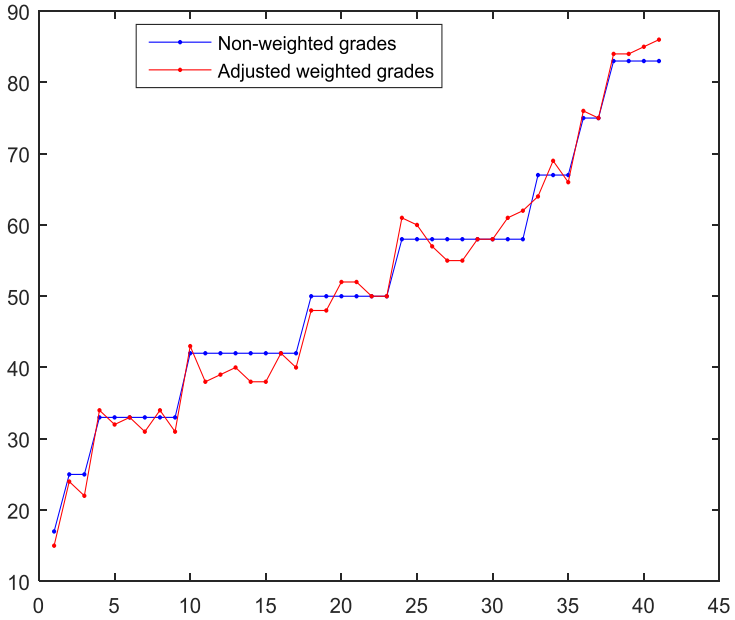

Fig. 3. Comparison of the non-weighted grades (plotted in ascending order) and the corresponding adjusted weighted grades for Exam2.

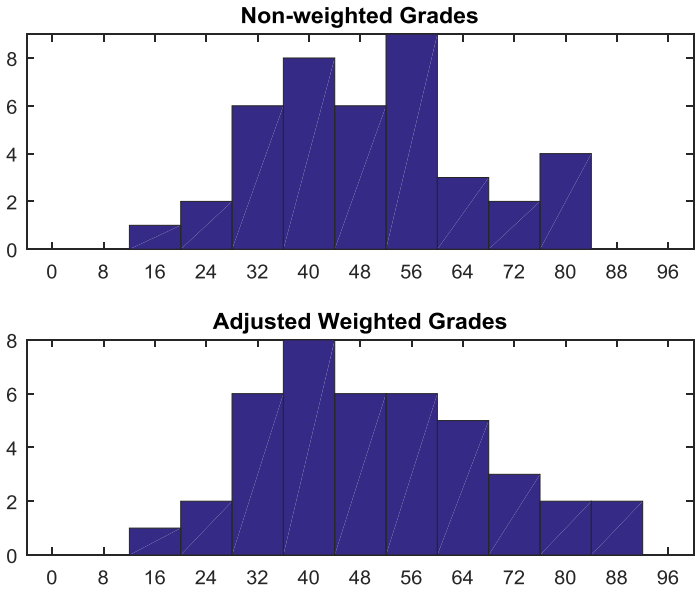

Fig. 4. Histograms of the non-weighted and adjusted weighted grades for Exam2. The average was 50.98 and the standard deviation was 18 for the weighted grades, while the average was 51.37 and the standard deviation was 17 for the non-weighted grades. The median was 50 in both cases.

A comparison of the histograms of the weighted and non-weighted grades, adjusted for efficiency, is given in Fig. 4 for Exam2. The average and median of the grades remain practically the same in both cases: with an average of around 51 and a median of 50 for grades on the scale of 0-100. The weighted grades become less discrete, meaning the differences between adjacent grades on the grade scale are smaller, allowing differentiation between two examinees that replied the same number of questions, but one of whom succeeded in questions that were more difficult for the group of examined students. This student will get a higher weighted grade than the other one by a few points, allowing the examiner to tell them apart (whether it will affect their actual final grades or not).

Conclusions

In this work we use statistical analysis of exam grades to evaluate their efficiency. The efficiency measures are proposed at both the individual question level and the exam level. One of these efficiency measures attempts to answer the following question: how many of the “strong” students have answered a particular question correctly. Another measure attempts to evaluate the

performance of the “weak” students: how many of them have failed in a particular question. A question is considered efficient if most “strong” students succeed in it while most “weak” ones fail. In a similar fashion, an exam questionnaire is considered efficient if the majority of its questions are efficient. Our measures can be used both for multiple-choice and numeric answers (where points are granted if the student writes the expected numeric value or one close to it).

We also propose a different method to grade the exams using weighted averaging using the question efficiencies as weight coefficients. This method has the benefit of differentiating between the students that successfully solve more difficult questions and those that solve the easier ones even when the non-weighted grade is the same.

We performed the proposed statistical analysis on the grades for a number of real life examinations and have presented and discussed the results. Our conclusion is that the proposed analysis and efficiency measures are beneficial for the purpose of estimating the quality of the exam and locating its weakest links: the questions that fail to differentiate between the “strong” and the “weak” students.

References

1. R. Wood, Multiple choice: A state of the art report, Evaluation in Education, International Progress, Volume 1, No. 3, pp. 191-280, 1977.
2. S. Kosolapov, N. Sabag, E. Gershikov, Evaluation of Two Camera-Based Approaches for Collecting Student Feedback", Educational Alternatives, Vol. 12, pp. 1173-1182, October 2014.
3. E. Gershikov and S. Kosolapov, On Image Based Fast Feedback Systems for Academic Evaluation, International Journal of Signal Processing Systems, Vol. 3, No. 1, pp. 19-24, June 2014.
4. E. Gershikov and S. Kosolapov, Camera-Based Instant Feedback Systems, International Journal of Advanced Computing, Vol. 47, No. 1, pp 1463-1473, June, 2014.
5. B. P. Bergeron, Optical Mark Recognition. Tallying information from filled-in “bubbles”, Postgraduate Medicine, Vol 104, No 2, pp. 23-25, August 1998.
6. L. Ding and R. Beichner, Approaches to data analysis of multiple-choice questions, Physical Review Special Topics - Physics Education Research 5, pp. 1-17, September 2009.

Topic detection using the DBSCAN-Martingale and the Time Operator

Ilias Gialampoukidis[1,2], Stefanos Vrochidis[2], Ioannis Kompatsiaris[2], and Ioannis Antoniou[1]

[1] Department of Mathematics, Aristotle University of Thessaloniki
54124 Thessaloniki, Greece
(E-mail: iliasfg@math.auth.gr; iantonio@math.auth.gr)
[2] Information Technologies Institute, Centre for Research and Technology-Hellas
6^{th} km Charilaou-Thermi road, 57001 Thessaloniki, Greece
(E-mail: heliasgj@iti.gr; stefanos@iti.gr; ikom@iti.gr)

Abstract. Topic detection is usually considered as a decision process implemented in some relevant context, for example categorization by cluster extraction. In this case, clusters correspond to topics that should be identified. Density-based clustering, for example, uses only a density level ϵ and a lower bound for the number of points in a cluster. As the density level is hard to be estimated, a stochastic process, called the DBSCAN-Martingale, is constructed for the combination of several outputs of DBSCAN for various randomly selected values of ϵ in a predefined closed interval $[0, \epsilon_{max}]$ from the uniform distribution. We have observed that most clusters are extracted in the interval $[0, \epsilon_{max}/2]$, and moreover in the interval $[\epsilon_{max}/2, \epsilon_{max}]$ the DBSCAN-Martingale stochastic process is less innovative, i.e. extracts only a few or no clusters. We found that non-symmetric skewed distributions are useful for the generation of density levels for faster cluster extraction, compared to the uniform distribution. Experiments on real datasets show that the average innovation time of the DBSCAN-Martingale stochastic process is reduced about 25% when skewed distributions are employed, so less time is needed to extract all clusters.
Keywords: DBSCAN-Martingale, Time Operator, Skewed distributions, Internal Age, Density-based Clustering, Innovation process.

1 Introduction

Journalists and media monitoring companies need to quickly detect articles relevant to a certain topic and to manage large collections of articles. Given a collection of articles the estimation of the correct number of topics is a challenging task, due to the fact that there are articles that do not belong to any of the topics. We have presented an estimation on the number of clusters (topics) using a Martingale process, namely the DBSCAN-Martingale [1]. The DBSCAN [2] algorithm is repeatedly applied using a random density parameter ϵ, while the lower bound for the number of clusters $minPts$ is kept constant. The generated stochastic process progressively estimates the number of clusters in any dataset but has been introduced in the context of text clustering to estimate the number of topics. The final number of clusters is provided by a majority vote among several realizations of the DBSCAN-Martingale process. Similarly, the DBSCAN-Martingale has also been applied in the context of image retrieval and image clustering [3] in the estimation of the number of visual

words in a set of visual descriptors, showing the wide applicability of this novel clustering approach. In all cases, the processing time is a critical aspect and needs to be minimized as much as possible.

Towards this direction, we examine whether skewed distributions are able to extract all clusters faster compared to the uniform distribution in the selection of the density level ϵ. The time needed to extract all clusters is the number of iterations, using several random choices of the density level ϵ in a pre-defined interval $[0, \epsilon_{max}]$. However, not all iterations of DBSCAN are innovative, i.e. they do not extract the same number of clusters or some iterations do not extract any clusters. The innovation probabilities at any stage of a stochastic process have been introduced in [4] and have been demonstrated in the non-stationary random walks modeling stock market prices [5] and in the fluctuations of the US economy [6], through the construction of the associated Time Operator. The Time Operator has been introduced in the context of stochastic processes [7–9], quantifying the distribution of innovations in the considered (clock) time domain. We shall examine whether the innovations of the DBSCAN-Martingale are distributed in a symmetric way or not, in order to minimize the required time stages T needed to extract all clusters (topics).

2 Density-based clustering

DBSCAN [2] provides as output a clustering vector C with values the cluster IDs $C[k]$ of each point $k = 1, 2, \ldots, n$, assigning each item k to a cluster. In case the k-th item is marked as noise, then: $C[k] = 0$. The parameters of DBSCAN are, first, a density level ϵ and, second, a lower bound for the number of clusters in a dataset $minPts$. The parameter $minPts$ is usually predefined based on the size of the expected clusters, but the density level ϵ is hard to be estimated and, if so, then the algorithm is not able to output all clusters using one unique density level, as shown, for example, in Fig. 1, where there are 10 clusters, but not of the same density level.

The OPTICS diagram [10] has been used to visualize the cluster structure, where each dent represents a cluster. Moreover, OPTICS is used to observe the density level at which the desired clusters are extracted. The OPTICS plot for the dataset of Fig. 1 is presented in Fig. 2.

The parameter $minPts$ is a pre-defined fixed value, approximately equal to 10, as initially proposed in [10]. For each density level ϵ, the output of DBSCAN is one clustering vector and is denoted by $C_{DBSCAN(\epsilon)}$. Small values of ϵ result to $C_{DBSCAN(\epsilon)} = \mathbf{0}$, where $\mathbf{0}$ is a vector of zeros, because all points are marked as noise. However, large values of ϵ, result to $C_{DBSCAN(\epsilon)} = \mathbf{1}$, where $\mathbf{1}$ is a vector of ones, since all points are reachable from any other point, hence, all points are assigned to the same cluster. A smart selection of the density level cannot ensure correct estimation in the number of clusters, with a strong impact to the performance of a news clustering approach [1], using for example Latent Dirichlet Allocation [11] to assign news articles to topics.

The estimated number of clusters in the illustrative dataset of Fig. 1 is presented in Fig. 3, where we observe that 10 clusters are correctly estimated by the majority of 1000 DBSCAN-Martingale realizations.

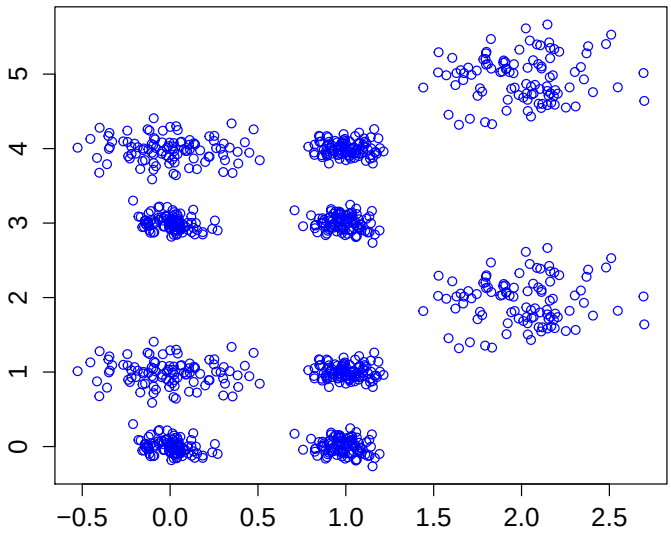

Fig. 1. A dataset with 10 clusters

3 The DBSCAN-Martingale and Time Operator

Initially, a random sample of uniformly distributed random numbers $\epsilon_t, t = 1, 2, \ldots, T$ in $[0, \epsilon_{max}]$ is generated by the DBSCAN-Martingale. The sample of $\epsilon_t, t = 1, 2, \ldots, T$ is sorted in increasing order and for each density level ϵ_t a clustering vector is provided by DBSCAN, denoted by $C_{DBSCAN(\epsilon_t)}$.

In the beginning of the DBSCAN-Martingale process, there are no clusters detected, i.e. $C^{(0)} = \mathbf{0}$. We denote by $\mathcal{F}_t$ the σ-algebra generated by $\{C_{DBSCAN(\epsilon_1)}, C_{DBSCAN(\epsilon_2)}, \ldots, C_{DBSCAN(\epsilon_t)}\}$ and let $\mathcal{F}_0$ be the trivial σ-algebra $\{\Omega, \emptyset\}$ at stage $t = 0$. At stage $t = 1$ all clusters are kept: $C^{(1)} := C_{DBSCAN(\epsilon_1)}$, extracted at lowest density level ϵ_1. At stage, $t = 2$, some of the detected clusters by $C_{DBSCAN(\epsilon_2)}$ are new and some of them have also been extracted at stage $t = 1$. DBSCAN-Martingale keeps only the newly detected clusters of the second stage, $t = 2$, by taking only groups of points of the same cluster ID with size greater than $minPts$:

$$C^{(t)}[j] := \begin{cases} 0 & \text{if point } j \text{ belongs to a previously extracted cluster} \\ C_{DBSCAN(\epsilon_t)}[j] & \text{otherwise} \end{cases} \tag{1}$$

where $C^{(1)} = C_{DBSCAN(\epsilon_1)}$. Each vector of Eq. (1) has only the newly extracted clusters and all other points are marked as noise (zero cluster ID). The cluster IDs of $C^{(t)}$ are relabeled, starting from $1 + \max_j C^{(t-1)}[j]$ to $r + \max_j C^{(t-1)}[j]$, assuming that r clusters have been extracted up to stage t.

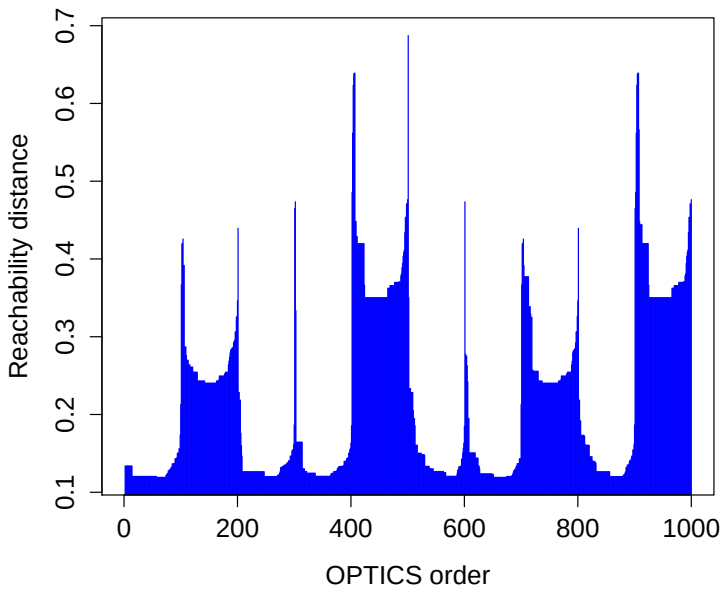

Fig. 2. OPTICS reachability distance plot for the dataset of Fig. 1

The Hilbert space $\mathcal{H}_t$ at stage t, is successively constructed by the ranges of the conditional expectations $\mathbb{E}_t = E[.|\mathcal{F}_t]$ up to stage $t, t = 1, 2, \ldots, T$, where the σ-algebras $\mathcal{F}_t, t = 1, 2, \ldots, T$ are generated by the vectors $\{C_{DBSCAN(\epsilon_1)}, C_{DBSCAN(\epsilon_2)}, \ldots, C_{DBSCAN(\epsilon_t)}\}$. Our knowledge about the final clustering vector C up to stage t is restricted to $\mathbb{E}_t C$. Moreover, the projections onto the innovation spaces $\mathcal{N}_t$ are given by:

$$\mathbb{P}_t C = E[C|\mathcal{F}_t] \ominus E[C|\mathcal{F}_{t-1}] = (\mathbb{E}_t \ominus \mathbb{E}_{t-1})C = C^{(t)} \tag{2}$$

and the final clustering vector C lives in the space of fluctuations $\mathcal{H} = \mathcal{N}_1 \oplus \mathcal{N}_2 \oplus \cdots \mathcal{N}_T$:

$$C = C^{(1)} \oplus C^{(2)} \oplus \ldots \oplus C^{(T)} \tag{3}$$

Each projection $\mathbb{E}_t C = E[C|\mathcal{F}_t], t = 1, 2, \ldots, T$ is our "best prediction" about the next $(t+1)$ outcome of the clustering vector C which needs to be determined:

$$\mathbb{E}_t C = E[C|\mathcal{F}_t] = C^{(1)} \oplus C^{(2)} \oplus \ldots \oplus C^{(t)} \tag{4}$$

Finally, at stage $t = T$, we have gained all available knowledge about the vector C, i.e. $C = E[C|C_{DBSCAN(\epsilon_1)}, C_{DBSCAN(\epsilon_2)}, \ldots, C_{DBSCAN(\epsilon_T)}]$ and all available clusters have been extracted.

The self-adjoint operator with spectral projections the conditional expectations $\mathbb{E}_t$ on the space of fluctuations $\mathcal{H}$ is the *Time Operator* of the stochastic

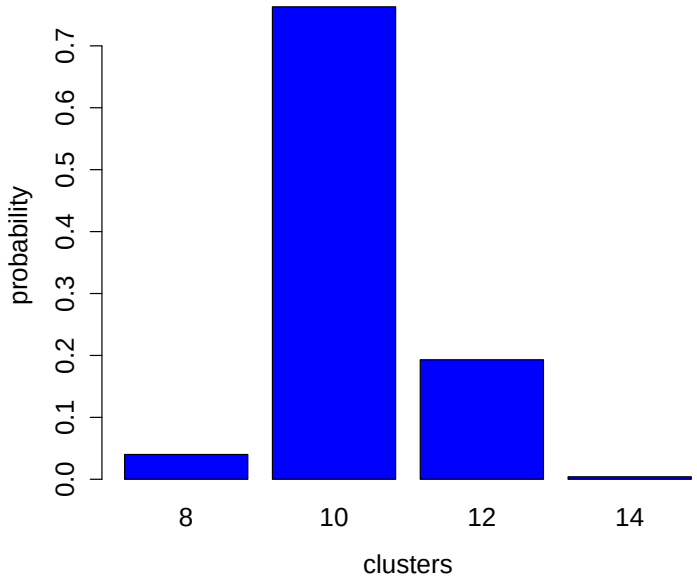

Fig. 3. 1000 realizations of the DBSCAN-Martingale in the dataset of Fig. 1

process $X_t, t = 1, 2, \ldots$:

$$\mathbb{T} = \sum_{t=1}^{\infty} t(\mathbb{E}_t \ominus \mathbb{E}_{t-1}) \tag{5}$$

The Time Operator, as defined in Eq. (5), acts on the clustering vector C in $\mathcal{H}$, defining also the distribution of innovations:

$$p_t = \text{Prob}\{C \in \mathcal{N}_t\} = \frac{\|\mathbb{P}_t C\|^2}{\|C - E[C]\|^2} = \frac{\|C^{(t)}\|^2}{\|C\|^2} \tag{6}$$

where $E[C] = 0$ because at the beginning of the process the clustering vector C is a vector of zeros and there are no expected clusters without any application of the DBSCAN algorithm.

The distribution of innovations has been assumed to be symmetric in [1], since the random sample of density levels $\epsilon_t, t = 1, 2, \ldots, T$ in $[0, \epsilon_{max}]$ has been generated from the uniform distribution. In contrast, we propose the generation of the random sample in an alternative way, having statistically significant skewness.

4 Generation of skewed samples of density levels

Motivated by the generation of random samples from the exponential distribution [12], through the transformation

$$X \leftarrow -\frac{\ln U}{\lambda}$$

where U is a random variable uniformly distributed in [0,1], we propose the following generation of a random sample of density levels as follows:

1. Generate a sample of size T from the uniform distribution in [0,1]:

$$\epsilon_1, \epsilon_2, \ldots, \epsilon_T$$

2. Transform the generated values using the natural logarithm:

$$\epsilon_t \leftarrow -\ln \epsilon_t$$

3. Normalize in [0,1]:

$$\epsilon_t \leftarrow \epsilon_t / \max_t \{\epsilon_t\}$$

4. Expand in $[0, \epsilon_{max}]$:

$$\epsilon_t \leftarrow \epsilon_t * \epsilon_{max}$$

This generation of the sample is parameter free (no rate parameter λ is required) and is in fact skewed, since it is a normalized sample of the exponential distribution, which in general has skewness equal to two. The sample skewness is usually estimated in three different ways [13], as also highlighted in the documentation of the library "e1071" of the statistical software R. We selected the typical definition used in many textbooks:

$$g_1 = \frac{m_3}{m_2^{3/2}} \tag{7}$$

where the sample moments of order r are:

$$m_r = \frac{1}{n} \sum_{i=1}^{n} (x_i - \mu)^r \tag{8}$$

and x_i are the non-missing elements of x, μ their mean value.

In the following, we shall examine whether the proposed steps 1–4 reduce the innovation time of the DBSCAN-Martingale process, by reducing the stages T needed to extract all clusters.

https://www.r-project.org/

5 Experiments

In the experiments we compare the proposed method with the result based on the uniform generation of density levels ϵ. The datasets we have used for comparison are four synthetic datasets with points in the 2-dimensional plane that contain 5,10, 15 and 20 clusters, with sizes 500, 1000, 1500 and 2000 points, respectively. We also downloaded the news articles available in the datasets WikiRef150, WikiRef186 and WikiRef220, containing, topics such as Paris attacks November 2015, Premier League, Malaysia Airlines Flight 370, Samsung Galaxy S5 and Michelle Obama (5 topics). Additional information is provided in the online dataset description. We used the online implementation of DBSCAN-Martingale.

From the text documents, numbers and punctuation are removed, as well as the English stopwords. Words are stemmed using Porter's algorithm using the R library "tm". Words are then tokenized into bi-grams as proposed in [1] and the parameter $minPts$ is set to 15 and $\epsilon_{max} = 2$. For the synthetic datasets, the parameters are set as $minPts = 55$ and $\epsilon_{max} = 0.5$. In all datasets, 1000 realizations of the DBSCAN-Martingale process were generated and skewness is averaged for the sample of generated density levels using Equation (7).

Table 1. Time needed to extract all clusters using the uniform distribution as proposed in [1] and using our proposed skewed sample. In bold we present the minimum values for the time needed to extract all clusters.

Realizations		Uniform distribution		Skewed distribution	
Dataset	Clusters	Skewness	time needed T	Skewness	time needed T
Dataset 1	5	0.02	4	1.12	**2**
Dataset 2	10	-0.01	4	0.99	**2**
Dataset 3	15	0.00	3	1.02	**2**
Dataset 4	20	-0.02	3	0.97	**2**
WikiRef150	3	0.01	**3**	0.99	**3**
WikiRef186	4	0.00	4	0.93	**3**
WikiRef220	5	0.00	4	0.96	**4**

In Table 1 we observe that the time needed to extract all clusters is remarkably (approximately 25%) reduced by our approach. This fact has a strong impact in the overall estimation of the number of clusters or topics, since the DBSCAN-Martingale process is generated several times and the final decision is taken by a majority vote scheme. Apparently, there are cases, such as the WikiRef150, where the clusters are 3 and both methods extract the clusters using the same time.

http://mklab.iti.gr/project/web-news-article-dataset
https://github.com/MKLab-ITI/topic-detection/blob/master/DBSCAN_Martingale.r

6 Concluding Remarks

We have presented a novel approach to generate the sample of density levels in the density-based clustering approach of DBSCAN-Martingale. The innovation time, as also modeled by the associated Time Operator, is reduced when skewed non-symmetric samples are employed, in all datasets examined. The proposed approach has been tested in three datasets of news articles and in four general synthetic datasets with various sizes and numbers of clusters. The skewed generation of the density levels allows to reduce the time needed to extract all clusters and therefore, provides faster estimation of the number of clusters. In the future, we shall examine whether this approach is also applicable to other clustering tasks in multimedia and social media applications.

Acknowledgements

We thank the Research Committee of the Aristotle University of Thessaloniki for awarding Dr. Gialampoukidis the "Aristeia" postdoctoral scholarship 2016. Using this scholarship we were able to compare the skewed distribution with the uniform distribution for the martingale realizations, to compute the Age and to construct the Time Operator of the DBSCAN-Martingale. The algorithm itself has been constructed in CERTH in the frame of the EC-funded project KRISTINA (H2020-645012).

References

1. Ilias Gialampoukidis, Stefanos Vrochidis, and Ioannis Kompatsiaris. A hybrid framework for news clustering based on the dbscan-martingale and lda. In *Machine Learning and Data Mining in Pattern Recognition*, pages 170–184. Springer, 2016.
2. Martin Ester, Hans-Peter Kriegel, Jörg Sander, Xiaowei Xu, et al. A density-based algorithm for discovering clusters in large spatial databases with noise. In *Kdd*, volume 96, pages 226–231, 1996.
3. Ilias Gialampoukidis, Stefanos Vrochidis, and Ioannis Kompatsiaris. Incremental estimation of visual vocabulary size for image retrieval. In *INNS Conference on Big Data*, pages 29–38. Springer, 2016.
4. Ilias Gialampoukidis, Karl Gustafson, and Ioannis Antoniou. Financial time operator for random walk markets. *Chaos, Solitons & Fractals*, 57:62–72, 2013.
5. Ilias Gialampoukidis and Ioannis Antoniou. Time operator and innovation. applications to financial data. In Lidia Filus, Teresa Oliveira, and Christos H Skiadas, editors, *Stochastic Modeling Data Analysis & Statistical Applications*, chapter 1, pages 19–31. ISAST, 2015.
6. Ilias Gialampoukidis, Karl Gustafson, and Ioannis Antoniou. Time operator of markov chains and mixing times. applications to financial data. *Physica A: Statistical Mechanics and its Applications*, 415:141–155, 2014.
7. Ioannis Antoniou and Karl Gustafson. Wavelets and stochastic processes. *Mathematics and Computers in Simulation*, 49(1):81–104, 1999.
8. Karl E Gustafson. *Lectures on computational fluid dynamics, mathematical physics, and linear algebra*. World Scientific, 1997.

9. Ioannis Antoniou and Theodoros Christidis. Bergson's time and the time operator. *Mind and Matter*, 8(2):185–202, 2010.
10. Mihael Ankerst, Markus M Breunig, Hans-Peter Kriegel, and Jörg Sander. Optics: ordering points to identify the clustering structure. In *ACM Sigmod Record*, volume 28, pages 49–60. ACM, 1999.
11. David M Blei, Andrew Y Ng, and Michael I Jordan. Latent dirichlet allocation. *Journal of machine Learning research*, 3(Jan):993–1022, 2003.
12. Luc Devroye. Sample-based non-uniform random variate generation. In *Proceedings of the 18th conference on Winter simulation*, pages 260–265. ACM, 1986.
13. DN Joanes and CA Gill. Comparing measures of sample skewness and kurtosis. *Journal of the Royal Statistical Society: Series D (The Statistician)*, 47(1):183–189, 1998.

Methodological and Operating Questions of the Three Way Lee-Carter Model

Giuseppe Giordano[1], Steven Haberman[2], Maria Russolillo[1]

[1] Department of Economics and Statistics, University of Salerno, Campus di Fisciano (Salerno), Italy (e-mail: ggiordano@unisa.it; mrussolillo@unisa.it)

[2] Faculty of Actuarial Science and Insurance, Cass Business School, City University London, United Kingdom

Abstract. The three-way model has been proposed as a development of the original Lee-Carter (LC) model when a three-mode data structure is available. The three-way LC model allows enriching the basic LC model by introducing several tools of exploratory data analysis.
Such exploratory tools allow giving a new perspective to the demographic analysis supporting the analytical results with a geometrical interpretation and a graphical representation.
From a methodological point of view, there are several issues to deal with when focusing on such kind of data. Specially, in presence of the three-way data structure, several choices on data pre-treatment could affect the whole data modelling.
The first step of a three-way mortality data investigation consists in exploring the different source of variations and highlighting the significant ones.
We will consider the three-way LC model investigated through a three-way analysis of variance with fixed effects, where each cell is given by the mortality rate in a given year of a specific age-group for a country.
Firstly, we consider the variability attached to each of the three ways main effects: age, years and countries. Then, we consider the variability induced by the interactions between each pair of the three ways. Finally, the three-way interaction could give information on which country have a specific trend (along years) in each age-group.
This kind of analysis is useful to assess the source of variation in the raw mortality data, before to extract rank-one components by the LC-model.
Keywords: Anova, Lee-Carter Model, Three-way principal component analysis, Human Mortality Database.

1 Introduction

In the last few years, the actuarial literature focused on models for detecting multiple population trends ([9], [9 b], [17], [20], etc.). In particular, an increasing interest was revealed about "connected" population dynamics categorized by similar socio-economic conditions and by geographical proximity. Investigating long-run equilibrium relationships might provide valuable information about the factors driving changes in mortality, in particular across ages and across countries. This aspect has contributed to the growth of the interest in studying cross-country longevity common trends. For this reason, we observed a development of country and age-based longevity risk models ([13], [15], [17], [20]).

In 2005, Li and Lee demonstrated the improvement of the mortality projections for individual countries by taking into account the patterns in a larger group [15]. Using the data downloaded from the Human Mortality Database, they applied the Lee-Carter model to a group of populations allowing each its own age pattern and level of mortality, but imposing shared rates of change by age. The augmented common factor LC method they derived, aimed to model and forecast mortality for a group of populations in a coherent way, taking advantage of commonalities in their historical experience and age patterns, while acknowledging their individual differences in levels, age patterns, and trends. In other words, Li and Lee proposed to model a single population in reference to another coherent population. Several other models followed the Li and Lee idea; the literature refer to these models as multi-population models or coherent mortality models. These studies suggest dependence across multiple populations and common long run relationships between countries (for instance see [13]). To handle the joint development across different populations of mortality rates [9] propose a new framework to introduce cross sectional dependence for adjacent age groups, across countries and serial/time dependence. According to [23], studying mortality experience for a group of populations with similar mortality behaviors might improve the stability of mortality modelling and allow for solving the problem of small population. Indeed some authors propose the replication of the data by mixing appropriately the mortality data from neighboring countries [18].

In this contribution, we start from the consideration that populations which are sufficiently similar to be grouped together may have experienced different mortality histories. On the basis of these findings, we believe that, in presence of disaggregated data, we may arrange a three-way data structure. Assessing the different sources of variation we may build more robust analysis also producing different sub-models for homogenous sub-populations. For instance, if we discover that mortality data can be aggregated for homogeneous countries, applying different LC-Models to any single cluster will lead more reliable result compared to the whole model with higher aggregated data.

Thus, we consider the three-way LC model [20] investigated through a three-way analysis of variance with fixed effects, where each cell is given by the mortality rate in a given year of a specific age-group for each any countries. In other words, we take into account a three-way array, given by the mortality rates for age, years and countries. In presence of these data, there are several choices on data pre-treatment that will affect the whole data modelling. Generally speaking, the advantage of introducing a third way in the analysis of a traditional years per age-class mortality data is much more clear if we can hypothesize that the decomposition along the third way brings information.

The paper is organized as follows: Section 2 illustrates the three-way LC-model. In Section 3 we present some pre-treatment steps of our strategy. In Section 4 we discuss the three-way LC model through an empirical case study.

2 The three-way LC-model

In Russolillo et.al 2011, we proposed a natural extension of the LC model to a three-way, three mode, data structure. It allows to enrich the basic LC model by introducing a third mode in the analysis. For instance, we proposed to consider the death rates aggregated for time, age-group and *Country*. Our goal is showing the capability of the 3W-LC model to deal with different sub-populations. For this reason, we specify the 3W-LC model to consider different criteria. In this way we would like to address the analyst to the proper use and the correct interpretation of the three way analysis in order to face some subjective choices implicit in the model. In this framework we have to defining an analytical framework to drive the actuary throughout the different steps of the analysis in order to providing a proper interpretation of the model components when the data structure deals with Time x Age x *Occasion*.
Let us recall the LC Model and the 3-Way LC Model. We can state both demographic models referring to the mean centred log-mortality rates:

$$\ln\left(m_{xt}\right) = \alpha_x + \beta_x \kappa_t + \varepsilon_{xt}$$

$$\ln\left(m_{xtc}\right) = \alpha_{x.c} + \beta_x \kappa_t \gamma_c + \varepsilon_{xtc}$$

where x is the generic age group, t the generic year and c is the third criterion (in our application country). As in the traditional LC model α_x is the age-specific parameter independent of time, in the 3W LC model $\alpha_{x.c}$ is the age & country death parameter independent of time. β_x and κ_t have the same interpretation as in the classical LC model, while γ_c represents the term associated to the third criterion. The final term ε_{xt} is the error term, assumed to be homoschedastic (with mean 0 and variance σ_ε^2) and reflects particular age-specific historical influences not captured by the model. Sometimes the data available can be aggregated according to a different way, for example: Countries, Ethnic groups, Causes of Death, etc
In these cases, the singular value decomposition associated to the LC model has to be reformulated to take into account the new data structure.
To solve the decomposition problem in literature are proposed several solutions which give rise to different statistical methods *(Multiple Factorial Analysis, STATIS, Generalized Canonical Analysis, PARAFAC, Tucker's Methods, etc.)*. Anyway, the natural extension of the SVD in a three way framework is the Tucker3 model *(Tucker, 1964, 1966; Kroonenberg, P.M., 1983)*, which we will take into account in our contribution.

3 Data Pre-Treatment

Our strategy involves some pre-treatment steps. With the Analysis of Variance we assess the main sources of variability considering firstly the main effects: age, year and country. Moreover, we may consider the variability induced by the paired interactions between the three ways. Lastly, the three way interaction could give information on which country has a specific trend (along years) in each age-group. This kind of analysis is recommended to assess the source of variation in the mortality data before extracting rank-one components, useful to make mortality projections. It is worthwhile to detect on which mode mortality data should be further aggregated for obtaining more homogeneous datasets. In presence of a three way data structure, pre-treatment is much more important because of several choices that will affect the whole data modelling. The advantage of introducing a third way in the analysis of a traditional year per age-group mortality data is much more clear if we can hypothesize that the decomposition along the third way brings information.
In this analysis we can distinguish three cases:

1) the third-way shows homogeneous mortality patterns
2) the third-way shows heterogeneous mortality patterns
3) Clustering effects: there are "occasions" with homogeneous trends within the same group but showing heterogeneity between two different groups

In the first case, since the mortality data are similar, it is possible to aggregate the different mortality experiences.
On the other hand, a factorial decomposition will provide a single component that will explain much of the inherent variability.
In the second case, any data aggregation is awkward and any solution could lead to unreliable results.
In this case a factorial decomposition will give a poor synthesis on the first component.
The third case is of more interest from our point of view. In this case, we may argue that a unique synthesis is not reliable, but several synthesis are possible and they can be explored. Moreover, the presence of different patterns should be indicated by a significant source of variation along the country way. Indeed, the first step of a mortality data investigation should be addressed by exploring the different sources of variation and highlighting the significant ones.

4 The Procedure at Work

We discuss the three-way LC model through an empirical case study. We make use of the mortality data downloaded from the ‘‘Human Mortality Database’’ (HMD) (www.mortality.org). The countries included are the following: *Austria*, *Sweden*, *UK*, *France*, *Belgium*, *Netherlands*, *Switzerland*, *Portugal*, *Italy*, *Norway*, *Spain*, *Finland*, *Luxembourg*, *Ireland*, *West Germany*, *East Germany*, *Czech Republic*, *Denmark*. The 18 countries have a common time range dating from 1960 to 2006; data are downloaded in age groups ranging from 0, 1-4 up to 95-99. The data array is constituted by 18 Countries x 21 Age-groups x 47 Years. As we can notice in Figures 1 and 2, each Country has its own data pattern:

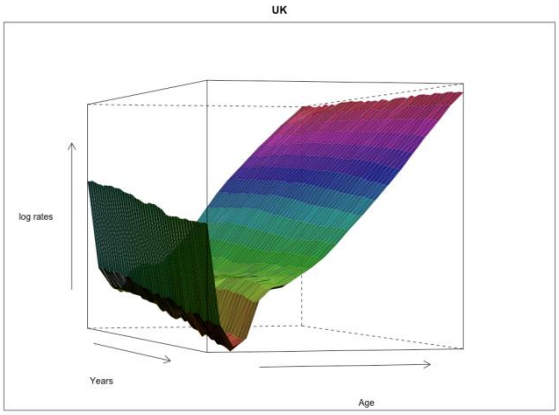

Fig. 1. Surface representation of the UK mortality data.

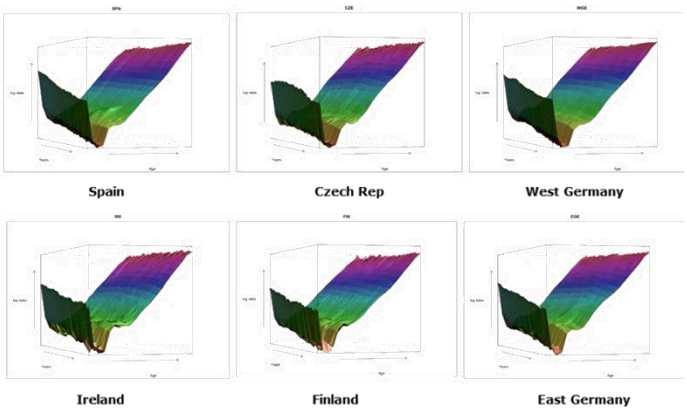

Fig. 2. Some surfaces for different Countries

In each Country, we can see how age-groups show different mortality levels: in particular, higher levels for extreme years (U-shape) can be highlighted (Fig.2). The time series seem linear decreasing along years. In order to assess the source of variability in the three modes, we perform a 3-way Analysis of Variance (ANOVA) with fixed effects. The results are shown in Table 1:

Total ssq = **91478.582**
SS_Years = 1004.892 (1.1%)
SS_Age = 89257.885 (97.57%)
SS_Country = 269.075 (0.29%)
SS_YxA = 485.150 (0.53%)
SS_YxC = 47.204 (0.05%)
SS_AxC = 219.214 (0.24%)
SS_YxAxC = 195.159 (0.21%)

Table 1. ANOVA Results

This kind of analysis allows to determine the most important sources of variability in the three-way raw data structure (i.e. the log mortality rates).
It outlines the most significant effects (it has to be specified that we are not treating with a random sample, so we do not take into account the theoretical probability distribution F, whilst we assess in a descriptive way the size of the considered statistical variables).
From this first analysis it is evident that the age-group is the one that gives raise to the most important source of variability.
Next step is a Cluster Analysis which gives useful insights on how aggregate data.

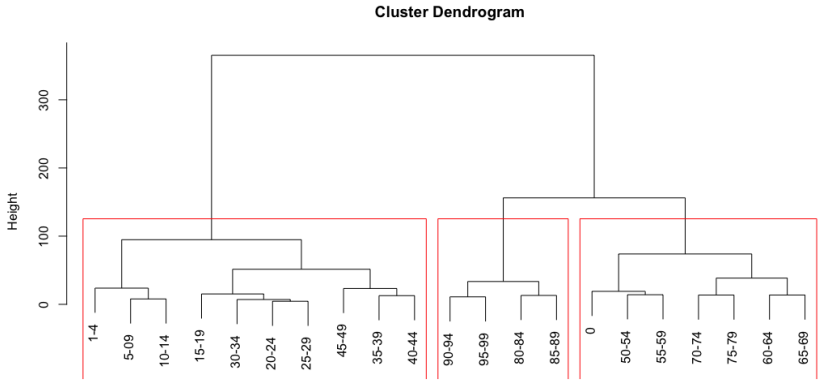

Fig. 3. Homogeneous Age-groups according to the general level of mortality across Countries

Hierarchical Cluster analysis (Ward's Method) gives useful insights on how to aggregate data. We have seen that there are different levels of age-specific mortality. In particular, we can distinguish two or three levels: Extreme young and old age-groups and adult age-groups. Looking at our data (Fig.4), we decide to remove the age-group effect considering the mean centred log-mortality rates

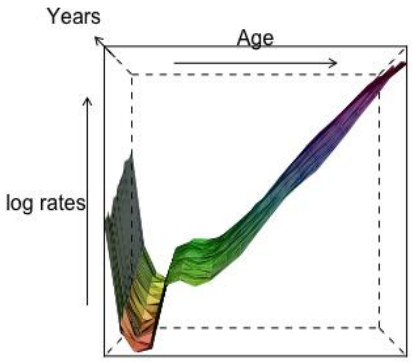

Fig. 4. Surface after removing the age-group effect

After removing the mean across age-groups, the source of variability to explore is along years, as it can be observed in Table 2.

Total ssq = 1732.40701911151
SS_a = 1004.89 (58.01 %)
SS_b = 0.00 (0 %)
SS_c = 0.00 (0 %)
SS_ab = 485.15 (28 %)
SS_ac = 47.20 (2.72 %)
SS_bc = 0.00 (0 %)
SS_abc = 195.159545 (11.27 %)

Table 2. ANOVA after Removing the Age-group Effect

We can notice that interaction now exists between years and age-groups (28%); Interaction between years and country is not evident, while it is interesting to observe the three-way interaction (11.27%). From a graphical point of view, in Fig.5 we show the cases of of UK (left) and Italy (right).

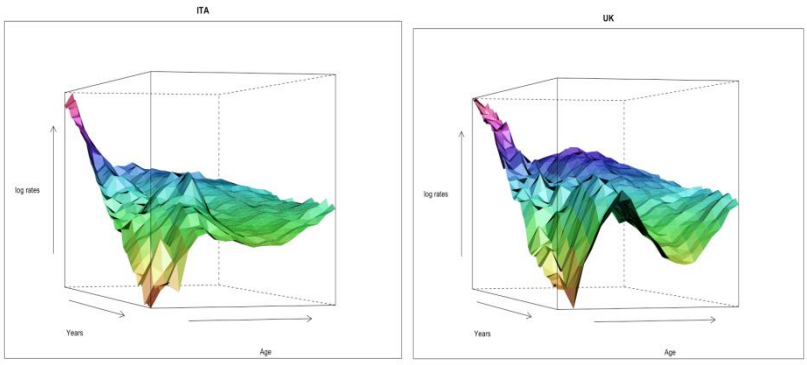

Fig. 5. Data after removing Age-group Effect

It is evident a decreasing trend along years and the interaction between years and age-groups: the slopes of the year trends vary along the age-groups. Moreover, some differences occur across countries. In Fig.6, we can notice that the age-group effect has been eliminated and the age-group are now very similar.

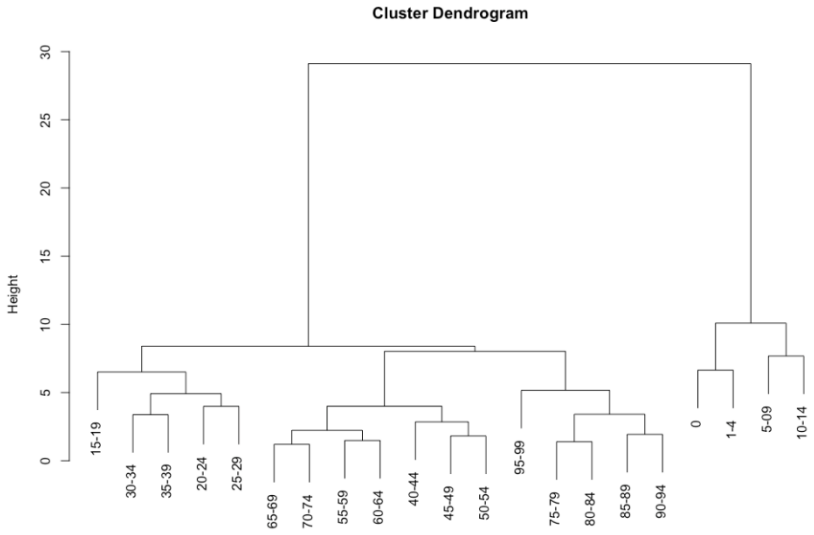

Fig. 6. Homogeneous Age-groups after removing age-group effect

Indeed, by comparing the dendrograms in Fig.6 and in Fig.3, we can see that the dissimilarity index on the vertical axis is now ten times smaller than before.

We run the Tucker3 analysis with 2x2x2 components which gives a fit of 87.5%. The results are shown in Table 3.

	Age1xCountry1	**Age2xCountry1**	**Age1xCountry2**	**Age2xCountry2**
Years1	**38.26**	0.00	0.01	-4.59
Years2	-0.01	5.45	0.99	0.65

Table 3. Tucker3 Analysis - Main Results

The Tucker3 model allows to obtain the scores related to each component for each mode. Each entry in the core matrix is used to explain the three-mode interaction measures and the percentage of explained variance. For example, 38.26 suggests that the higher variability is given by the first components. The sign specifies the type of interaction among them.
In particular, we are interested in Tucker3 Scores for Years Mode to detect the κ_{t_s}. The ones related to the first component are shown in Fig.7.

Fig. 7. Tucker3 Scores for Years Mode - first component

Fig. 7 shows a synthesis of the 18 countries from which it is possible to derive both an aggregate κ_t or a specific one.

Conclusions

In this contribution, we deal with a three-way mortality data investigation in order to explore different sources of variations and to highlight the significant ones.
The procedure allows to give a major insight into the data structure, having:
- Identified the main sources of variability
- Explored the interaction among the different modes

In further research, intermediate target will be to study how is it possible to compare mortality projections, for homogenous age-group or countries. The final aim is to build a software environment to steer the actuary in the pre-treatment choice.

References

1. Kroonenberg, P.M., (1983). Three-Mode Principal Component Analysis. DSWO Press
2. Kroonenberg, P.M., Murakami, T., Coebergh, J.W.W. 2002. Added value of the three-way methods for the analysis of mortality trends illustrated with worldwide female cancer mortality (1968-1985). Statistical Methods in Medical Research, 11: 275-292
3. Lee, R.D., Carter, L.R. (1992). Modelling and Forecasting U.S. Mortality. Journal of the American Statistical Association, 87, 659-671
4. Russolillo, M., Giordano, G., Haberman, S. (2011). Extending the Lee-Carter model: a three-way decomposition. Scandinavian Actuarial Journal, 2011: 2, 96 — 117
5. Tucker, L. R., (1964). The extension of factor analysis to three-dimensional matrices. In: Contributions to Mathematical Psychology, edited by N. Frederiksen and H. Gulliksen, New York:Holt, Rinehart & Winston, 1964, p. 110-182.
6. Tucker, L. R. (1966) Some mathematical notes on three-mode factor analysis. Psychometrika 31:279-311

Linear Approximation of Nonlinear Threshold Models

Francesco Giordano[1], Marcella Niglio[1], and Cosimo Damiano Vitale[1,2]

[1] Department of Economics and Statistics, University of Salerno, Via Giovanni Paolo II 132, 84084 Fisciano (Salerno), Italy
(E-mail: [giordano, mniglio, cvitale]@unisa.it)
[2] Universitas Mercatorum, Piazza Mattei 10, 00186 Roma, Italy

Abstract. In this paper we face the problem of the linear approximation of nonlinear time series models. After the definition of linear process, we distinguish between linear approximation and linear representation of nonlinear models, shortly giving some examples that better clarify this distinction. The attention is then given to the threshold autoregressive models whose linear approximation is discussed starting from an example (that motivate the contribution) and some theoretical issues.

Keywords: Nonlinear time series, linear approximation, threshold model.

1 Introduction

The complexity of most nonlinear models often leads to evaluate if a linear representation or a linear approximation can be admitted for this class of models. In presence of linear representation the aim can be ascribed to the need of taking advantage (under proper assumptions) of the large and strengthened literature developed in the linear domain (to cite the main references, Box and Jenkins [3], Brockwell and Davies [4]) whereas, linear approximations can be seen as a tool for model selection (or more generally to select candidate models for the data under analysis), to "filter" the dynamic relationship among variables such that the "purely" nonlinear component, obtained in output, can be properly examined.
Before to show the main advantages obtained from the linearization, it is useful to clarify when a stochastic process $\{X_t\}$, with $t \in \mathbb{Z}$, is said to be linear.
Let $\{X_t\}$ a mean zero stationary process and let $\{e_t\}$ a sequence of White Noise, with $E[e_t] = 0$ and $E[e_t^2] = \sigma^2 < \infty$. From the Wold decomposition, X_t can be expressed as:

$$X_t = \sum_{i=0}^{\infty} \psi_i e_{t-i} + D_t \tag{1}$$

with $\psi_0 = 1$, $\sum_{i=1}^{\infty} \psi_i^2 < \infty$, $E[e_t D_s] = 0$, for all $s, t \in \mathbb{Z}$, and D_t a deterministic component.
Starting from the decomposition (1), a zero mean stationary process X_t is said to be linear if it can be given as:

$$X_t = \sum_{i=0}^{\infty} \psi_i e_{t-i} \tag{2}$$

with $\{e_t\} \sim \text{IID}(0, \sigma^2)$[1].
It can be easily shown that the ARMA(p, q) model belongs to the linear class (some authors identify the linear class with ARMA models) and its widely known structure is given by:

$$X_t - \sum_{i=1}^{p} \phi_i X_{t-i} = e_t - \sum_{j=1}^{q} \theta_j e_{t-j} \tag{3}$$

where well defined assumptions are given on the parameters ϕ_i and θ_j to guarantee the stationarity and invertibility of the model (Box and Jenkins [3]).

Starting from this definition of linear process, the aim of the present paper is to show how to obtain the "best linear approximation" (in terms of $\mathbb{L}^2$ norm) of a nonlinear process. In particular in Section 2 we further clarify the difference between linear representation and linear approximation of nonlinear models and then, in Section 3 we provide new results on the linear approximation of the Threshold AutoRegressive (TAR) model (Tong [11]). Some examples with simulated data give evidence of the advantages that can be obtained from the use of the theoretical issues proposed.

2 Linear representations and linear approximations of nonlinear models

The linearization of nonlinear processes has been differently intended in the literature. Ozaki [8] proposes a local linearization of a nonlinear continuous dynamical system using (under proper requirements) a discrete time autoregressive approximation over a sufficiently small time interval Δt; Francq and Zakoïan [5] investigate on the properties of the estimators of the parameters of the so called *weak* ARMA models when some assumptions, usually given on the innovations e_t (Box and Jenkins [3]), do not hold. The estimation procedure is based on the minimization of the squared deviations about the linear conditional expectation and for this reason the estimated model is seen as weak linear representation of nonlinear models.

If we want to face organically the linearization problem of the nonlinear process Y_t, we can consider two main approaches: the first considers the *linear representation* of the nonlinear model (where the nonlinear structure is rewritten in alternative linear form, after the introduction of proper assumptions); the second approach makes a distinction between the linear (X_t) and the "purely" nonlinear (V_t) component of the process Y_t, such that it can be decomposed as:

$$Y_t = X_t + V_t. \tag{4}$$

This decomposition is usually made through linear approximations, often obtained from proper expansions of Y_t.
Examples of the first and the second approach have been differently proposed

[1]Note that is some cases $\{e_t\}$ is assumed to be a sequence of uncorrelated Gaussian random variables and so the independence is guaranteed as well.

in the literature.
Consider a GARCH(p,q) model (Bollerslev [2]) for the conditional variance of Y_t, it can be shown that this model admits a linear representation. Let $Y_t \sim$GARCH(p,q):

$$\begin{aligned} Y_t &= h_t \epsilon_t \\ h_t &= c + \sum_{i=1}^{q} \alpha_i \epsilon_{t-i}^2 + \sum_{j=1}^{p} \beta_j h_{t-j}, \end{aligned} \tag{5}$$

with ϵ_t and i.i.d. sequence with $E[\epsilon_t] = 0$ and $E[\epsilon_t^2] = 1$. If we fix $u_t = \epsilon_t^2 - h_t$, model (5) becomes:

$$\epsilon_t^2 = c + \sum_{i=1}^{\max\{p,q\}} (\alpha_i + \beta_i)\epsilon_{t-i}^2 + u_t - \sum_{j=1}^{p} \beta_j u_{t-j}$$

with $\alpha_i = 0$, for $i > q$ and $\beta_i = 0$, for $i > p$. In other words $\epsilon_t^2 \sim$ARMA$(\max\{p,q\}, p)$ model.
The distinction between the linear and the "purely" nonlinear component, introduced with the second approach, is traditionally based on the Volterra series expansion of Y_t (among the others Priestley [9], Tong [11]). In more detail, let $f(Y_t, Y_{t-1}, Y_{t-2}, \ldots) = e_t$, with $f(\cdot)$ an invertible function, then $Y_t = g(e_t, e_{t-1,\ldots})$ where $g(\cdot)$ is a well behaved nonlinear function that can be expanded, near the origin $\mathbf{0} = (0, 0, \ldots)$, in Taylor series. Under these conditions Y_t can be given as:

$$Y_t = k_0 + \sum_{i=0}^{\infty} k_i e_{t-i} + \sum_{i=0}^{\infty}\sum_{j=0}^{\infty} k_{ij} e_{t-i} e_{t-j} + \sum_{i=0}^{\infty}\sum_{j=0}^{\infty}\sum_{w=0}^{\infty} k_{ijw} e_{t-i} e_{t-j} e_{t-w} + \ldots \tag{6}$$

where $k_0 = g(\mathbf{0})$, $k_i = \frac{\partial g}{\partial e_{t-i}} \mid_{\mathbf{0}}$, $k_{ij} = \frac{\partial g}{\partial e_{t-i} \partial e_{t-j}} \mid_{\mathbf{0}}$, and so on.
It is clear that when $k_{ij} = k_{ijw} = \ldots = 0$ the linear approximation of Y_t is obtained.
An example of linear approximation of a nonlinear process can be easily shown if we consider the bilinear model (Subba Rao [10]):

$$Y_t + \sum_{j=1}^{p} a_j Y_{t-j} = \sum_{j=0}^{r} c_j \epsilon_{t-j} + \sum_{i=1}^{m}\sum_{i'=1}^{k} b_{ii'} X_{t-i} \epsilon_{t-i'} \tag{7}$$

where the "purely" nonlinear component is given by the last term on the right of equation (7). If $b_{ii'} = 0$, for $i < i'$, the "purely" nonlinear component (even called superdiagonal bilinear model) is such that its terms are (at least) uncorrelated and it makes the derivation of the linear approximation more easy. In the other cases this approximation is more difficult and for this reason has been investigated using different expansions (Guegan [7]).
The bilinear model (7) is often seen as first example of generalization of the linear ARMA model in nonlinear domain.

Another example is given by the threshold autoregressive model (Tong and Lim [12]):

$$Y_t = \sum_{j=1}^{k} \left(\phi_0^{(j)} + \sum_{i=1}^{p} \phi_i^{(j)} Y_{t-i} \right) \mathbb{I}(Y_{t-d} \in \mathcal{R}_j) + \epsilon_t \tag{8}$$

where k is the number of autoregressive regimes, p is the autoregressive order, Y_{t-d} is the threshold variable, d is the threshold delay, $\mathcal{R}_j = [r_{j-1}, r_j)$, for $j = 1, \ldots, k$, such that $\mathcal{R} = \bigcup_{j=1}^{k} \mathcal{R}_j$ and $-\infty = r_0 < r_1 < \ldots < r_{k-1} < r_k = +\infty$. When $k = 1$ the threshold model (8) degenerates to a linear autoregressive model whereas when $k > 1$ the linear approximation is not so immediate.
In the next section we present some new results of the linear approximation of model (8). It is based on the use of an alternative representation of the threshold model as discussed in the following.

3 Linear approximation of the Threshold Autoregressive model

Let Y_t be a threshold model (8) that, for easy of exposition, is assumed to have $k = 2$ regimes and null intercepts ($\phi_0^{(j)} = 0$, for $j = 1, 2, \ldots, k$):

$$Y_t = \sum_{i=1}^{p} \phi_i^{(1)} Y_{t-i} \mathbb{I}(Y_{t-d} \leq r_1) + \sum_{i=1}^{p} \phi_i^{(2)} Y_{t-i} [1 - \mathbb{I}(Y_{t-d} \leq r_1)] + \epsilon_t. \tag{9}$$

Model (9) can be alternatively written as:

$$\begin{aligned} \mathbf{Y}_t &= \boldsymbol{\Phi}_1 \mathbf{Y}_{t-1} \mathbb{I}(Y_{t-d} \leq r_1) + \boldsymbol{\Phi}_2 \mathbf{Y}_{t-1} [1 - \mathbb{I}(Y_{t-d} \leq r_1)] + \boldsymbol{\epsilon}_t, \\ &= \boldsymbol{\Phi}_2 \mathbf{Y}_{t-1} + \boldsymbol{\epsilon}_t + (\boldsymbol{\Phi}_1 - \boldsymbol{\Phi}_2) \mathbf{Y}_{t-1} \mathbb{I}(Y_{t-d} \leq r_1) \end{aligned} \tag{10}$$

where

$$\mathbf{Y}_t = \begin{bmatrix} Y_t \\ \ldots \\ Y_{t-p+1} \end{bmatrix}_{(p \times 1)}, \quad \boldsymbol{\Phi}_j = \left[\begin{array}{ccc|c} \phi_1^{(j)} & \ldots & \phi_{p-1}^{(j)} & \phi_p^{(j)} \\ \hline & \mathbf{I}_{p-1} & & \mathbf{0} \end{array} \right]_{(p \times p)}, \quad \boldsymbol{\epsilon}_t = \begin{bmatrix} \epsilon_t \\ \mathbf{0} \end{bmatrix}_{(p \times 1)}$$

for $j = 1, 2$, with $\mathbf{I}$ the identity matrix and $\mathbf{0}$ the null vector.
From equation (10) it seems easy to discriminate the linear and the nonlinear components of the threshold model: in fact if we use the same approach considered for model (7), the last term of (10) could represent the "purely" nonlinear component of the model.
Note that the bilinear and the threshold models have a not negligible difference: as remarked before, if we consider the "purely" nonlinear component of model (7) it can be shown that, under proper conditions on the values of i and i', its terms are uncorrelated (Granger and Andersen [6]) whereas similar results do not hold for the "purely" nonlinear component of the threshold model (10). It implies that the linear approximation cannot be limited to the first two terms of (10) but it needs a more detailed investigation.
In this regard consider the following example.

Example 1. Let Y_t be a threshold autoregressive model with autoregressive order $p = 2$:

$$Y_t = \begin{cases} 0.75Y_{t-1} - 0.22Y_{t-2} + \epsilon_t & Y_{t-1} \leq 0 \\ -0.10Y_{t-1} + 0.79Y_{t-2} + \epsilon_t & Y_{t-1} > 0 \end{cases} \tag{11}$$

with $\epsilon_t \sim N(0, 1)$. If we generate $T = 1000$ artificial data (with burn-in 500) from model (11), the plots of the autocorrelation function (ACF) and of the partial autocorrelation function (PACF) are given in Figure 1.

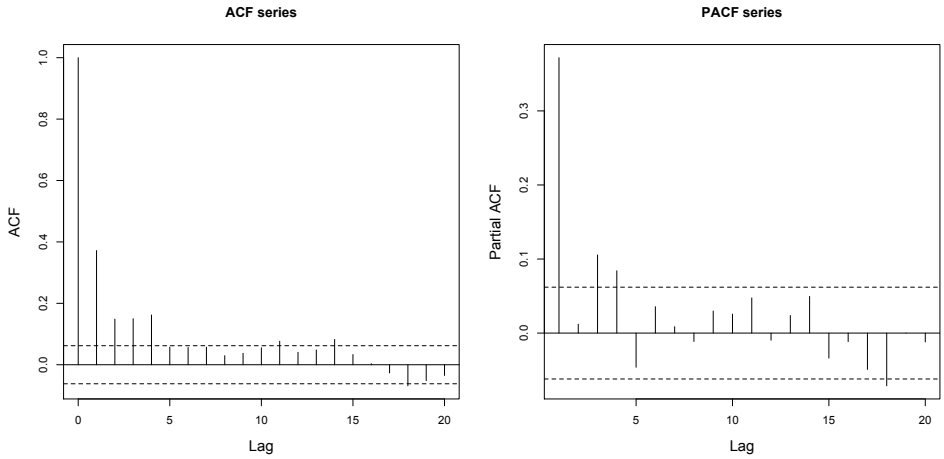

Fig. 1. ACF and PACF of the artificial data generated from model (11)

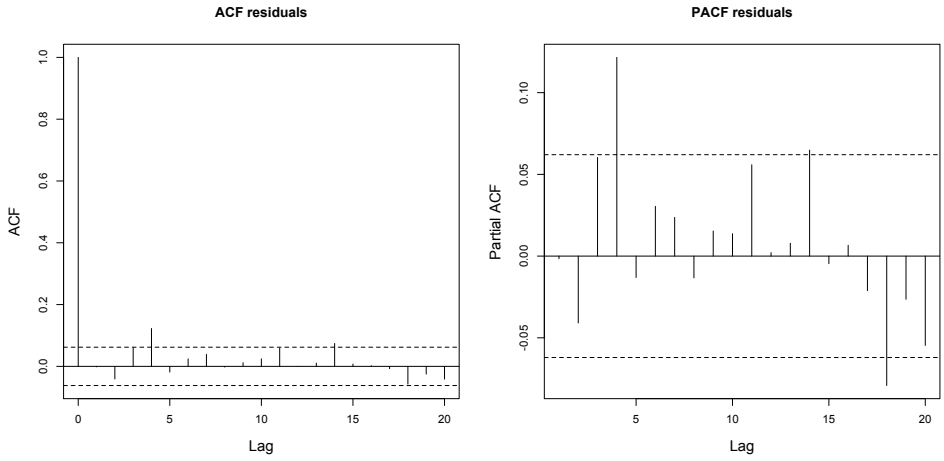

Fig. 2. ACF and PACF of the residuals obtained after fitting an AR(2) model to the artificial data generated from model (11)

Following the decomposition in equation (10), it seems that the linear component should be an AR(2) structure that, if fitted to the artificial data, does not catch all the linearity of the generating process, as can be noted if we evaluate the correlograms of the residuals in Figure 2. □

A first and naïve linear approximation of the nonlinear process Y_t, can be given defining, for the parameters of the linear model, a set of values obtained as weighted mean of the parameters of the threshold model, as illustrated in the following example.

Example 2. Let Y_t be a threshold autoregressive model:

$$Y_t = \begin{cases} 0.12Y_{t-1} + \epsilon_t & Y_{t-1} \leq 0 \\ 0.36Y_{t-1} + \epsilon_t & Y_{t-1} > 0 \end{cases} \tag{12}$$

with $\epsilon_t \sim N(0, 1)$. We generate $T = 1000$ artificial data (with burn-in 500) whose corresponding correlograms are given in Figure 3.
If we further generate $T = 1000$ artificial data from an autoregressive model $X_t = \phi X_{t-1} + \epsilon_t$ (with the same innovations of model (12)), where ϕ is a weighted mean of the parameters used in model (12), such that $\phi = 0.12 * \lambda + 0.36 * (1 - \lambda)$, with $\lambda = P[Y_{t-1} \leq 0]$, the correlograms of the simulated data are given in Figure 4.
From the comparison of Figures 3 and 4 it can be noted that the ACF and PACF of both series are similar: it gives empirical evidence of the ability of the autoregressive approximation to catch the linear component of the series Y_t such that the "purely" nonlinear component, V_t, can be properly investigated. □

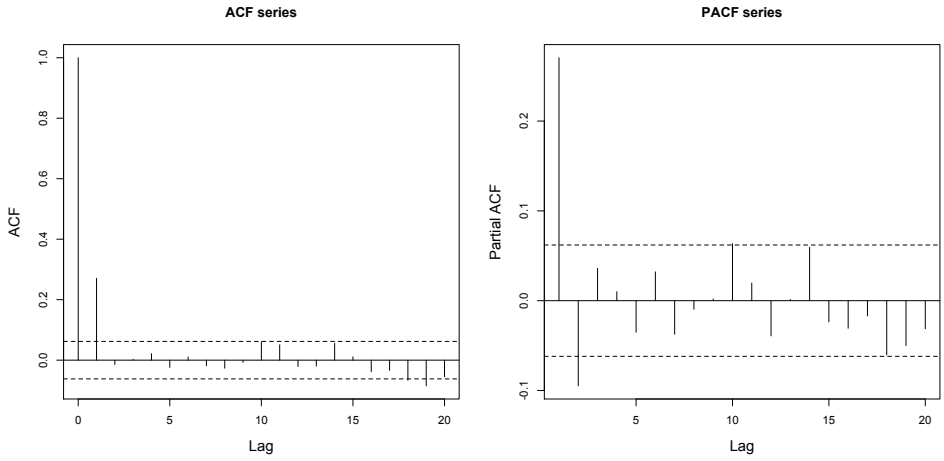

Fig. 3. ACF and PACF of the artificial data generated from model (12)

The empirical evidence of Example 1 and Example 2 introduces what we state in the following proposition (whose proof is omitted for brevity):

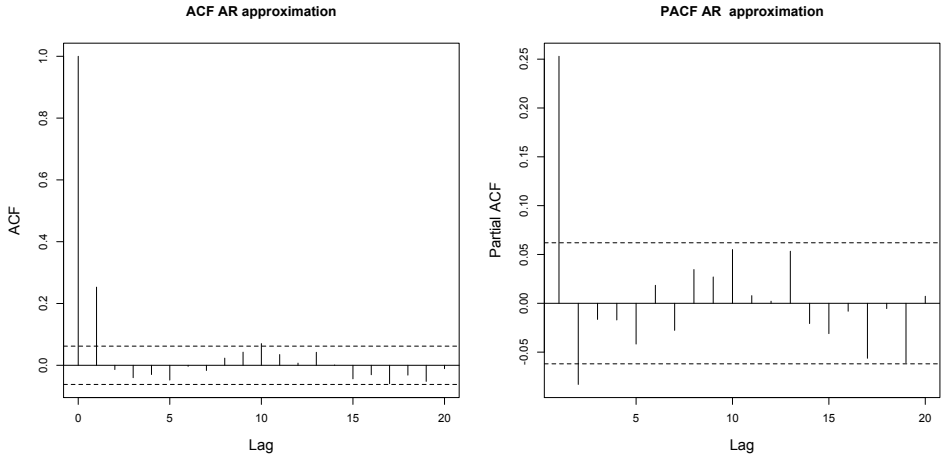

Fig. 4. ACF and PACF of the artificial data generated from the linear approximation of model (12)

Proposition 1. *Let Y_t be a stationary and ergodic threshold process (9) with $E[Y_t^2] < \infty$. The best linear approximation, in $\mathbb{L}^2$ norm, of Y_t is given by $X_t \sim ARMA(2p; 2p)$ model.*

Proposition 1 allows to further investigate and to revise the results of Example 1.

Example 1 (cont.). Given the artificial data generated in Example 1 and following the results of Proposition 1, the best linear approximation of Y_t is given by an ARMA(4,4) model whose ACF of the residuals (that represent the "purely" nonlinear component) and of the squared residuals are presented in Figure 5. It can be clearly noticed that, differently from the results in Example 1, the linear approximation completely catch the linear component, X_t, of the generating process whereas the squared residuals show the existence of a nonlinear component, V_t, that can be evaluated. □

Even the results of Example 2 can be further discussed: it can be noted that the linear AR(1) structure considered can be seen as the dominant part of the ARMA(2,2) model that, from Proposition 1, represents the best linear approximation of the generating process Y_t.

Further note that when in decomposition (4) $X_t \equiv 0$, the process Y_t becomes "purely" nonlinear and so the autocorrelations of the series cannot be significantly different from zero, as stated in the following Corollary.

Corollary 1. *Given model (9), under the assumptions of Proposition 1, there exists a threshold process where the linear component is identically null.*

It can be empirically illustrated showing that proper combinations of the parameters of the autoregressive regimes can lead to $X_t \equiv 0$ in (4).

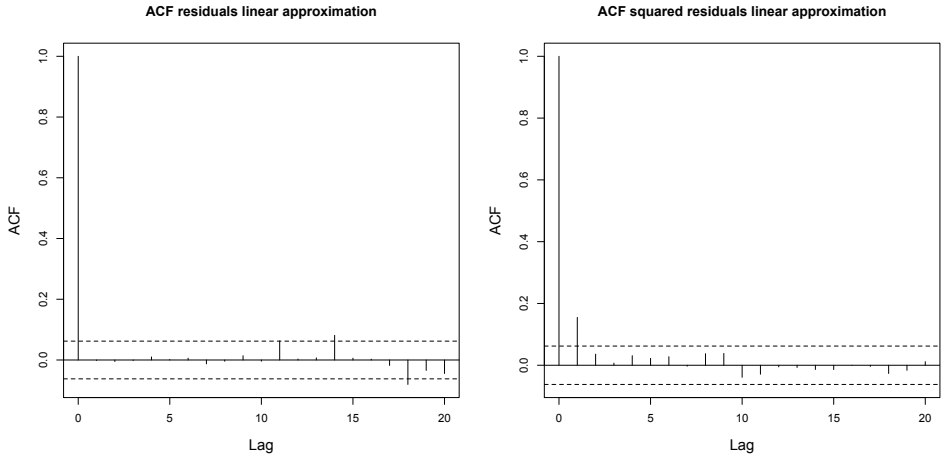

Fig. 5. On the left, ACF of the residuals of the ARMA approximation of the data generated from model (11); on the right, ACF of the squared residuals

Example 3. Let Y_t be a threshold autoregressive model:

$$Y_t = \begin{cases} 0.50Y_{t-1} + \epsilon_t & Y_{t-1} \leq 0 \\ -0.90Y_{t-1} + \epsilon_t & Y_{t-1} > 0 \end{cases} \tag{13}$$

with $\epsilon_t \sim N(0,1)$. In Figure 6, frame (a), the ACF do not show a significant linear dependence among the data that on the contrary becomes evident if we consider the ACF of Y_t^2 (frame (b)). In fact if we compute the parameter ϕ as in Example 2, its value is very near to zero and so the nonlinear structure of data prevails (it can be clearly appreciated from the correlogram of Y_t^2). □

Remark 1. What stated in Corollary 1, and empirically shown in Example 3, has a main remarkable consequence: the linear approximation of the threshold model can be seen as a proper reparametrization of the process Y_t. In fact, when the parameters of the autoregressive regimes assume well defined values of the parametric space (such that the linear component X_t becomes identically null), the process Y_t is "purely" nonlinear.

To conclude, it is interesting to note what distinguishes our results from those given in Francq and Zakoïan [5]. As said before, they consider the estimation of a linear ARMA model (3) under "weak" assumptions on the innovations e_t and their aim is to show that, under proper conditions, the strong consistency and asymptotic normality of the estimators still hold.
These results are not negligible: in fact, if applied in nonlinear domain, they allow to state that if well defined assumptions are verified on the generating process, the estimated ARMA model is a "weak" linearization of the nonlinear model. The results can be even applied to the nonlinear generating process (9) under proper assumptions related to the existence of moments and the geometric ergodicity (An and Huang [1], Theorem 3.2).

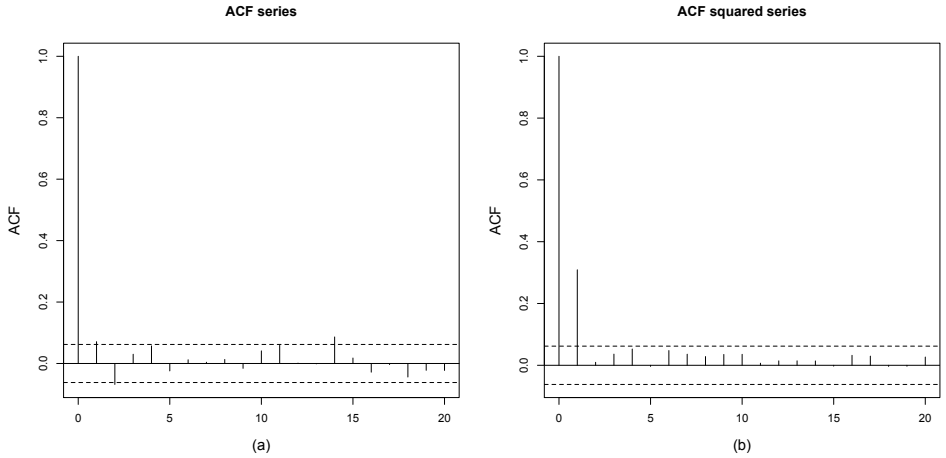

Fig. 6. Frame (a): ACF of the artificial data, Y_t, generated from model (13); Frame (b): ACF of Y_t^2

A problem that has not been faced in Francq and Zakoïan [5] is the identification of the linear approximation that on the contrary has been introduced in the present paper where, given a threshold autoregressive model, a relation between the order of the autoregressive regimes and the order of the ARMA model is stated. Further we have highlighted that the ARMA approximation is obtained, for this class of models, reparametrizing the threshold process that, under proper conditions on the values assumed by its autoregressive coefficients, becomes a "purely" nonlinear process.

References

1. H. Z. An, F. C. Huang. The geometrical ergodicity of nonlinear autoregressive models. *Statistica Sinica*, 6, 943–956, 1996.
2. T. Bollerslev. Generalized autoregressive conditional heteroskedasticity. *Journal of Econometrics*, 31, 307–327, 1986.
3. G. E. P. Box, G. M. Jenkins. *Time series analysis: forecasting and control*, Holden-Day, New York, 1976.
4. P.J. Brockwell, R.A. Davies. *Time series: theory and methods*, Springer, New York, 1991.
5. C. Francq, J.M. Zakoïan. Estimating linear representation of nonlinear processes. Journal of Statistical Planning and Inference, 68, 145–165, 1998.
6. C.W.J. Granger, A.P. Andersen. *An introduction to bilinear time series*. Vandenhoeck & Ruprecht in Göttingen, 1978.
7. D. Guegan. Different representations for bilinear models. *Journal of the Time Series Analysis*, 8, 389–408, 1987.
8. T. Ozaki. A bridge between nonlinear time series models and nonlinear stochastic dynamical systems: a local linearization approach. *Statistica Sinica*, 2, 113–135, 1992.
9. M.B. Priestley. *Non-linear non-stationary time series analysis*. Academic Press, London, 1988

10. T. Subba Rao. On the Theory of Bilinear Time Series Models. *Journal of the Royal Statistical Society (B)*,43, 244–255, 1981.
11. H. Tong. *Non-linear Time Series: A Dynamical System Approach*, Oxford University Press, New York, 1990.
12. H. Tong, K. S. Lim. Threshold Autoregression, Limit Cycles and Cyclical Data. *Journal of the Royal Statistical Society (B)*, 42, 245–292, 1980.

An Application of Data Mining Methods to the Analysis of Bank Customer Profitability and Buying Behaviour

Pedro Godinho[1], Joana Dias[2], and Pedro Torres[3]

[1] CeBER and Faculty of Economics, University of Coimbra, Av. Dias da Silva, 165, 3004-512, Coimbra, Portugal
(E-mail: pgodinho@fe.uc.pt)
[2] CeBER, INESC-Coimbra and Faculty of Economics, University of Coimbra, Av. Dias da Silva, 165, 3004-512, Coimbra, Portugal
(E-mail: joana@fe.uc.pt)
[3] CeBER and Faculty of Economics, University of Coimbra, Av. Dias da Silva, 165, 3004-512, Coimbra, Portugal
(E-mail: pedro.torres@uc.pt)

Abstract. In this paper we use a database from a Portuguese bank, with data related to the behaviour of customers, to analyse churn, profitability and next-product-to-buy. The database includes data from more than 94000 customers, and includes all transactions and balances of bank products from those customers for the year 2015. We describe the main difficulties found concerning the database, as well as the initial filtering and data processing necessary for the analysis. We discuss the definition of churn criteria and the results obtained by the application of several techniques for churn prediction and for the short-term forecast of future profitability. Finally, we present a model for predicting the next product that will be bought by a client. The models show some ability to predict churn, but the fact that the data concerns just a year clearly hampers their performance. In the case of the forecast of future profitability, the results are also hampered by the short timeframe of the data. The models for the next product to buy show a very encouraging performance, being able to achieve a good detection ability for some of the main products of the bank.
Keywords: Data Mining, Bank Marketing, Churn, Clustering, Random Forests.

1 Introduction

The huge amounts of data that banks currently possess about their customers allow them to make better decisions concerning the efforts to obtain new customers and the types of marketing campaigns they undertake. Better decisions are beneficial to the bank, since they may lead to increased profits, but they may also be beneficial to customers, who can now be targeted just by campaigns concerning products that may interest them.

One important piece of information that can sometimes be estimated from data in bank databases is the Customer Lifetime Value (CLV). CLV can be

17th *ASMDA Conference Proceedings, 6 - 9 June 2017, London, UK*

understood as the total value that a customer produces during his/her lifetime [1]. There are many models for quantifying this value (see, for instance, [2] for a review of the most prominent models). Some existing models are based on the Recency, Frequency, Monetary framework [3] and Pareto/NBD [4,5] or related models [6-7]. As pointed out by Blattberg *et al.*[8], due to the uncertainty in future customer behaviour, as well as in the behaviour of the firm's competitors and of the firm itself, CLV is indeed a random variable and methodologies should try to compute an expected CLV.

CLV prediction in the retail banking sector is especially difficult for a number of reasons, including product diversity (which can jeopardize the use of RFM based approaches [9]), the existence of both contractual and non-contractual clients (meaning that some clients are free to leave as soon as they want, while others have long-term contracts) and even the difficulty in identifying lost customers. Despite these difficulties, several authors have addressed the estimation of CLV in retail banks. Glady *et al.*[10] use a modified Pareto/NBD approach to estimate CLV in the retail banking sector. The authors show that the dependence between the number of transactions and their profitability may be used to increase the accuracy in CLV prediction. Haenlein *et al.*[11] present a model with four different groups of profitability drivers, based on a classification and regression tree. Clients are clustered into different groups, and a transition matrix is used to consider movements between clusters. A CLV model based on RFM and Markov chains is proposed in Mzoughia and Limam [12]. Calculating the churn probability for a given client or cluster of clients may support the estimation of CLV. Ali and Arıtürk[13] present a dynamic churn prediction framework that uses binary classifiers. Customer churn prediction is also tackled by He *et al.*[14], by applying support vector machines.

Another important issue in retail banking is identifying the products that a customer is most likely to be willing to purchase, in order to enhance the effectiveness of cross-selling strategies or marketing campaigns. This may be addressed by Next-Product-To-Buy (NPTB) models, which attempt to predict "which product (or products) a customer would be most likely to buy next, given what we know so far about the customer." [15]

Examples of works analysing NTBD models and cross-selling strategies in banking can be found, for example, in [15-17]. Knott *et al.*[15] compare several NTBD models in the context of a retail bank. The authors compare the use of different predictor variables, different calibration strategies and different methods, including discriminant analysis, multinomial logit, logistic regression and neural networks. The authors conclude that the use of both demographic data, information concerning the products currently owned and customer activity data increases the model accuracy, and that random sampling performs better than non-random sampling. Concerning the method, the authors do not find large differences, although neural networks seem to perform slightly better than the remaining methods, and discriminant analysis seems to perform slightly worse. Li et *al.*[16] use a structural multivariate probit model to analyse purchase patterns for bank products. Li *et al.*[17] use a

multivariate probit model and stochastic dynamic programming in order to optimize cross-selling campaigns, aiming to offer the right product to the right customer at the right time, through the right communication channel.

In this paper, we address the estimation of future profitability and churn probability as initial steps in CLV estimation, and we also aim at predicting the next product to be bought by a client. We rely both on econometric models and data mining techniques, choosing the one with the best predictive ability in the test set, that is, the one that performs better in a set that is independent from the one used to estimate the model.

The paper is organized as follows. After this introduction, we present and discuss the database in Section 2. Section 3 addresses the estimation of customer profitability, and Section 4 considers the prediction of customer churn. Section 5 focuses on next-product-to-buy models, and the conclusions and future research are discussed in Section 6.

2 Data set

The database used in this work includes data from more than 94000 customers of a Portuguese retail bank, incorporating all transactions and balances of bank products and bank-related activity of those customers in the year 2015. The database contains only anonymized data, guaranteeing the privacy of the data and preventing the identification of clients.

Socio-demographic data includes the age, the first digits of the postcode (allowing the identification of the region in which the client resides), the marital status, the job, the way the client opened the bank account (whether in a bank branch, online or in other way) and the day the client opened the account.

All bank products are associated with checking accounts, and the database also contains the transactions and balances of all products associated with the client's account, as well as the number and value of the products of each type owned by the customer. Data is aggregated at the monthly level, meaning that balances correspond to the end of the month and transactions correspond to the accumulated monthly activity. The bank products include different types of mutual funds, insurance products and credit products, as well as credit and debit cards, term deposits and stock market investments. Additionally, the number of online logins made by the customer to the bank site and the number of transactions made online are also available in the database. Other important pieces of data are the net profit the bank gained with each customer in each month, for different categories of products. The number of records concerning transactions, balances and numbers of logins is larger than 8.5 million.

The database had to be cleaned, since it contained some obviously invalid values (for example, invalid customer ages, including a few negative ages). Customers with invalid data were removed from the database.

Other pre-processing included aggregations in some categorical variables. The initial database included 486 different jobs and, using an official taxonomy of jobs for Portugal, we mapped them into a set of just 17 jobs. A similar procedure was performed for the marital status: initially, there were eleven different values for this variable (including different values for married customers, for different types of pre-marital agreements). These original values were mapped into a set of five different values.

After this initial pre-processing of the data, relations between different variables were analysed, and some expected relations were indeed found. An example is the relation between the wealth deposited in the bank and the profitability of the client for the bank. Figs. 1 and 2 show this relation, for the months of January and December, as well as a trend line. It is clear that profitability tends to increase with wealth, as was to be expected.

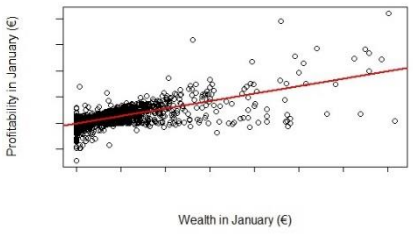

Fig. 1. Relation between customer wealth and profitability for the bank in January

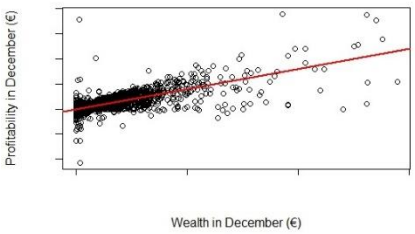

Fig. 2. Relation between customer wealth and profitability for the bank in December

Three shortcomings of the database were made evident in a preliminary analysis. The first is related to outliers in customer profitability, and it will be analysed in Section 3.

The second shortcoming is that the records that are interpreted as different customers may correspond to the same person who chose to open different accounts: for example, someone who chose to create an account for day-to-day transactions and another for retirement savings (retirement mutual funds, stock market investments and the like). Although this may create some bias, we do not expect this to happen in many cases, so the impact of such possibility will probably be limited.

Another, more serious, shortcoming is the existence of just one year of data, aggregated in monthly values. This makes it difficult to assess the medium- and long-term behaviour of the customers, for example to determine whether or not a customer is in churn. It also makes it impossible to test medium- and long-term forecasts. This shortcoming is expected to cause some problems in the estimation of customer profitability and customer churn.

In order to assess the accuracy of prediction models, data was divided into two sets. 60% of the observations were used as a training set, to estimate

the models. The other 40% of the observations constitutes a test set, used to assess the prediction accuracy in data that was not used in the estimations.

3 Short-term forecasting of customer profitability

Profitability from a client in a given month is expected to be strongly correlated with the profitability in the previous month. This is clearly shown to be the case in Fig. 3, which shows the relation between the profitability in January and February. As expected, the points in this graph are very close to the straight line $y=x$, showing that that profitability given by the client in a given month is a good forecast of the profitability given by the client in the next month. Therefore, we aimed at forecasting the changes in profitability instead of the profitability, in order to avoid getting apparently good forecasting results just because profitability shows high persistence.

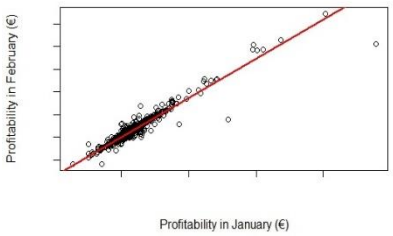

Fig. 3. Relation between the profitability of the clients in January and February

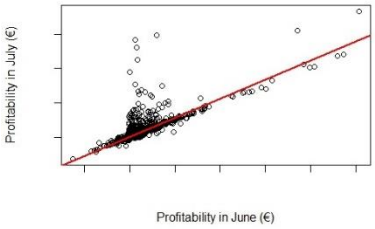

Fig. 4. Relation between the profitability of the clients in June and July

Fig. 4 shows the relation between the profitability in June and July. Once again, the relation is close to the straight line $y=x$, for the large majority of observations, but there are several important outliers, corresponding to customers whose profitability shows a visible increase. In fact, in May and July, the profitability associated with some customers has an important increase, only to show a similar decrease in the following month (June and August, respectively). This introduces outliers in the data, harming the ability to predict future profitability. According to an analysis of this situation made with bank members, this seems to be due to the way the profitability of some (very few) products is accounted. New, more realistic ways of considering the profitability of these products will be analysed with the bank but, meanwhile, we chose to use the existing values, in order to avoid the risk of introducing biases in the data.

Fig. 5 shows a histogram with the monthly values of the profitability. We can see that there is a very large number of slightly negative values of the monthly profitability.

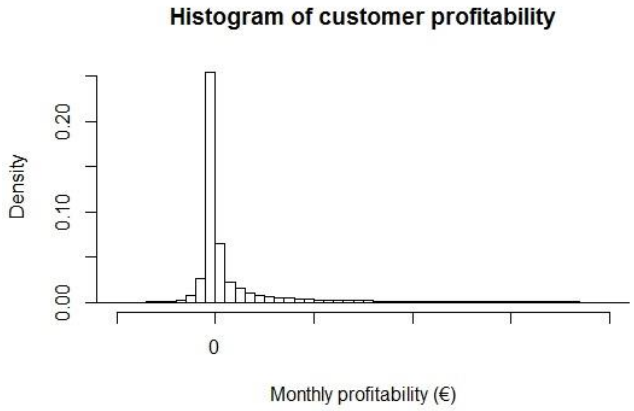

Fig. 5. Histogram with monthly values of customer profitability

We started by trying to predict the change in customer profitability one-month ahead. We used both socio-demographic data and data from the customer activity and balances in the three previous months to estimate the change in the customer profitability in the next month. For example, data concerning activity, transactions and balances from January, February and March is used to estimate the change in profitability between March and April. The goodness-of-fit measure that we chose is the Root Mean Square Error (RMSE) and we compare the obtained forecast with the naïve forecast that assumes that the change in profitability is equal to the average change in the training period (termed ModAvg).

The first types of models to be estimated were linear models. This allowed us to get a first idea of the relevance of the different variables for explaining the changes in profitability. The non-relevant variables were iteratively removed and, in the end, the model presented an adjusted R^2 of 0.4593. The performances of the model thus obtained and of the benchmark model (ModAvg), both in the training and in the test sets, are summarized in Table 1.

Table 1. Performance of the linear model and of the benchmark model

Model	RMSE in the training set	RMSE in the test set
Linear model	12.90	15.21
ModAvg	17.67	19.72

As can be seen in Table 1, the linear model is better than ModAvg, both in the training set and in the test set, and model performance deteriorates in the test set.

In order to give an idea of the impacts of the different variables, we show the sign of the coefficients and their statistical significance in Table 2, for

some of the most significant variables. Since we are considering some data from the three previous months to estimate the change in customer profitability, the coefficient signs are presented for each of these months (one, two and three months before the change in profitability we are trying to forecast).

Table 2. Sign and significance of some of the most significant variables of the linear model

	Sign and significance		
	One month before	Two months before	Three months before
Online logins	+***	+*	-
Number of online transactions	+***	-***	-***
Credit card transactions	+***	-***	+***
Number of different mutual funds in the account	+***	+	-***
Value of stock market holdings	-***	+***	+
Number of stock market transactions	-***	+**	-***
Total wealth	+***	-***	-***
Total value of loans	+***	+	-***
Value allocated to term deposits in the month	+***	+***	-
Value removed from term deposits in the month	-***	-***	-***
Amount of wages deposited in the bank	+***	-***	+**
Profitability from checking account	-***	+***	+
Profitability from term deposits	-***	+***	+
Profitability from home equity loans	-***	+***	+***
Profitability from other (non-home equity) loans	-***	+***	+***
Profitability from mutual funds	-***	+***	-***
Profitability from stock market holdings	-***	+***	+
Age	+***		

+,-: sign of the coefficient; *: Significant at the 10% level; **: Significant at the 5% level; ***: Significant at the 1% level

In some cases, the coefficient signs change from one month to the next, while remaining very significant. This is a clear indication that not only the value of the variable is relevant to forecast the change in profitability, but the

change in the value may be relevant as well. For example, wealth in the latest month has a positive sign, whereas wealth in the month before has a negative sign: this may mean that both the most recent value of the wealth and the latest change in wealth have a positive influence in the expected change in profitability.

In the cases of stock market holdings and transactions, the coefficient signs seem to be the contrary of what was expected. One possible explanation may be that customers with larger stock market holdings use the account mostly to make trades and deposit such assets (that is, as an investment account), and they do not tend to buy new products that are profitable to the bank.

Another interesting result is the negative and statistically significant sign in the last month profitability, for the different categories of products. However, this has a simple interpretation: all other things remaining constant, the larger the profitability already is, the less it is expected to increase.

Finally notice that only one socio-demographic variable is significant: age. Older clients generate more profits than younger clients. The significance of age was also found on the other models that we considered.

We also applied linear models to forecast the change of profitability at 2, 3 and 4 months horizons. The results, shown in Table 3, clearly show that the forecasting ability of the models decreases when the forecasting horizon becomes longer.

Table 3. Performance of linear models on the test set, for different forecasting horizons

Forecasting horizon	RMSE in the training set	RMSE in the test set
1 month	12.90	15.21
2 months	14.63	17.29
3 months	16.39	18.62
4 months	17.56	20.33

After this linear model, several data mining methods were applied: regression random forests, gradient boosting, naïve Bayes and linear discriminant analysis. Although these methods perform better than the linear model in the training set (sometimes very significantly), we could never improve the predictive performance in the test set, when compared with the linear model. So, there seems to be an overfitting problem with the application of these data mining techniques to predict profitability. We must, however, point out that, due to the long computation times associated with the application of these techniques, we tried a limited number of configurations for each one. In random forests, for example, it is possible that a different set of variables, or different numbers of trees or of candidates to each split, might lead to better results.

4 Churn prediction

One important initial difficulty in churn prediction was the definition of churn. The bank had no clear definition and, for this work, we chose to define churn through rules that are mostly based on common sense: there is churn if there are no relevant products and small amounts of credits and of wealth deposited in the bank. The exact rules consisted on defining that a customer was in churn if, simultaneously, he/she had no insurance contracts, no term deposits, no mutual funds and no credit or debit cards, the wealth in the bank was below 1000 € and the loans amounted to less than 100 €.

Our goal in predicting churn was mainly to predict which customers are not currently in churn but have a high probability of churning in the future. When we mention churning in the future, we are considering a reasonable amount of time; given the fact that we have data for only a year, we chose to predict churn using a 6-month horizon. In order to have enough data to try using different lags, we aimed at trying to predict which customers were not in churn in June 2015, but were in churn in December 2015. The number of customers in this situation was quite low, less than 0.7% of the customers of the database.

Churn prediction was handled as a classification problem. We used both linear models (probit and logit) and several data mining techniques (Adaboost, linear discriminant analysis, classification random forests). The best results were achieved with classification random forests, which obtained a much better performance than all the other models. We will only present the results obtained by classification random forests and logit models (the linear models with the best performance).

We started to use a large number of variables in the models, both socio-demographic and related to balances, transactions and other activity. For balances, transactions and other activity, we started by using the values from January to June 2015. We defined a variable that measures the ratio between the value of wealth in June and the average wealth in the semester, and we defined a similar variable for the amount of loans. We also defined new binary variables, for several products, to define whether or not the customer had any of that product (regardless of the amount) in each month, and also for determining whether the customer had made any online logins and transactions in each month.

Several configurations were tried (mostly in the linear models), in order to assess whether the binary variables or the initial values performed better, and then the less significant variables were iteratively removed. In the end, the number of relevant variables was much smaller than for profitability prediction. In almost all the cases, we found out that only the most recent value was relevant, the main exceptions being the two new variables that measured the relation between June values and average semester values for wealth and credits.

In general, the most relevant variables were:

- Age
- Wealth

- Ratio between the wealth in June and the average wealth on the semester
- Value of loans
- Ratio between the value of loans in June and the average value of the semester
- Profitability in the latest months
- Total balance of term deposits
- Existence of transactions and logins in the latest months

The models we used define the probability that a customer is going to churn. In order to assess the prediction ability, we calculated the average probability that the models assign to churners and to non-churners. The results are shown in Table 4, and they show that random forests assign much higher probabilities to customers that effectively end up churning, although they also assign slightly higher probabilities to non-churners.

Table 4. Performance of the best linear model (logit) and the best non-linear technique (random forests)

Model	Logit model	Random forest
Average probability assigned by the model to customers that effectively churn	3.78%	9.89%
Average probability assigned by the model to customers that end up not churning	0.66%	0.71%

We can see that random forests show some ability in differentiating future churners from non-churners. However, we must acknowledge that, due to limitations in the data that were mentioned in Section 2, we cannot be sure if the customers we are identifying as churning are, in reality, churning.

5 Next-product-to-buy

We also tried to predict, for some products, whether or not a given product from the bank will be the given customer's next buy. Since data is monthly, we are in fact identifying whether customers buy a product in the next month in which they acquire one or more products from the bank. This is also a classification problem: a product is classified as whether or not it will be bought in the month a next purchase is made. We used both linear models (probit and logit) and data mining techniques (random forests, Adaboost, linear discriminant analysis).

Three products, held by an important percentage of customers, were considered: term deposits, debit cards and credit cards. Purchase of such products was identified as an increase in the number of units of the product in the customer account. This allows us to avoid incorrectly classifying as purchases the cases in which a customer just changes a product he currently holds by another of the same kind (e.g., ending a term deposit and applying the capital in a new one).

The logic used for defining the training and test sets was somewhat different in this analysis. In the training set, the prediction was made for the next purchase in the months from May to August, using data from the previous three months (February to April). In the test set, we intended to predict the next purchase in the four-month period from September to December, using data from the previous three months (June to August). Only customers making any kind of purchase in the considered four-month period were taken into account (that is, we try to predict what is the next product to be bought, we are not making a joint prediction of the next product and of the probability of a buying occurring).

Apart from socio-demographic variables and transactions, balances and bank-related activity in the three previous months, new binary variables were added regarding the occurrence of purchases of the different types of products, for each of the three previous months.

Table 5. Performance of logit models in predicting the next product bought by a customer

Product	Percentage of customers for which the product is the next to be bought	Average probability estimated by the model, when the product is the next to be bought	Average probability estimated by the model, when the product is not the next to be bought	Percentage of customers correctly identified by the model as buying the product next	Percentage of customers, among the 5% with largest probability in the model, for which the product is the next to be bought
Term deposits	51.4%	59.7%	41.9%	71.3%	90.0%
Debit cards	11.4%	20.5%	9.7%	38.2%	60.2%
Credit cards	13.7%	19.9%	11.7%	31.6%	38.0%

The best results in the test set were obtained with logit models. In Table 5 we present the performance of these models. In order to assess the predictive ability of the models, we considered the average probability given by the model when the product is the next to be bought and when it is not, the percentage of customers correctly identified by the model as buying the product next, and also the percentage of customers, among those with the top 5% probabilities estimated by the model, who effectively buy that product next. This last measure is particularly interesting for defining targeted marketing

campaigns, since it allows the identification of the customers that will most probably buy the product. We also present the percentage of customers for which the product is the next to be bought – this is, in fact, the probability of a customer next buying that product, when you choose him/her at random.

We can see that the models perform quite well. In particular, the customers to whom the models assign higher probabilities do really have a high probability of next purchasing the product.

6. Conclusions and future research

In this paper we present the results of an analysis of churn, profitability and next-product-to-buy, obtained using a database concerning the behaviour of customers from a Portuguese bank. If it is possible to accurately predict churn probabilities and the evolution of profitability, then it is possible to estimate customer lifetime value, which is of great importance for defining marketing strategies.

As we explained, the database has some shortcomings, including not identifying the same client with different accounts, the existence of profitability outliers and the fact of there being just a year of data, aggregated in monthly values.

A linear model showed a good performance in the estimation of future short-term profitability at the 1-month horizon, but the performance of the estimated models seems to deteriorate when the prediction horizon increases, even if it is only to a few months. For churn, we had no solid reference to determine when a customer churns, so we defined a rule for identifying churning customers. A random forest seems to have an interesting ability to forecast which customers will churn in the next six months. However, given the short time period covered by the database, we cannot be completely sure that the customers identified as having churned did, indeed, churn. Therefore, given the limitations in the results concerning profitability and churn prediction, we feel that it is not yet possible to make a credible calculation of customer lifetime value. Still, the results concerning churn are interesting and may help identifying the customers whose relation with the bank is becoming very weak. The bank may thus target these customers with marketing campaigns, in order to try to avoid losing them.

The results of the models of the next-product-to-buy are very interesting, and show that a logit model has a good ability to predict the next product that a customer will buy. In particular, a large percentage of the customers to whom the model predicted the top 5% largest probabilities of purchasing each of the considered products, did indeed buy that product next. This opens the way to targeted marketing campaigns for selling the products that the customers are more likely to purchase.

At the outset, we expected data mining techniques to outperform the predictive ability of linear models. Although data mining techniques usually perform much better in the training set, only in the case of churn were they able

to beat a logit model in the test set. Possible explanations for this may be that linear models are particularly suited to this data set, that the shortcomings of the database are especially harming the performance of data mining techniques, and that different parametrizations of the techniques should be tested in order to fine-tune them to the characteristics of the data. Concerning this latter explanation, the number of tested parametrizations was indeed limited, due to very long computational running times, but we will, in the future, try new parametrizations and new approaches, in order to achieve better predictions.

As future work, we are already in contact with the bank to get a database covering a longer time period. This is expected to allow us to define a more credible identification of churning customers and better predictions of future profitability and next-product-to-buy. We will also address the estimation of customer lifetime values, both using predictions of churn probability and future profitability and also using other approaches made available by a longer database. Finally, we will try to obtain better predictions of the next-product-to-buy, and propose models for defining long-term market strategies based on these predictions.

References

[1] M. EsmaeiliGookeh and M.J. Tarokh. Customer Lifetime Value Models: A literature Survey. International Journal of Industrial Engineering, 24, 4, 317-336, 2013.

[2] S.S. Singh and D.C. Jain. Measuring Customer Lifetime Value. Review of Marketing Research (Review of Marketing Research, Volume 6) Emerald Group Publishing Limited, 6, 37-62, 2010.

[3] P.S. Fader, B.G. Hardie and K.L. Lee. RFM and CLV: Using iso-value curves for customer base analysis. Journal of Marketing Research, 42, 4, 415-430, 2005.

[4] D.C. Schmittlein, D.G. Morrison and R. Colombo. Counting Your Customers: Who-Are They and What Will They Do Next?. Management science, 33, 1, 1-24, 1987.

[5] D.C. Schmittlein and R.A. Peterson. Customer base analysis: An industrial purchase process application. Marketing Science, 13, 1, 41-67, 1994.

[6] P.S. Fader, B.G. Hardie and K.L. Lee. "Counting your customers" the easy way: An alternative to the Pareto/NBD model. Marketing science, 24, 2, 275-284, 2005.

[7] P.S. Fader, B.G. Hardie and J. Shang. Customer-base analysis in a discrete-time noncontractual setting. Marketing Science, 29, 6, 1086-1108, 2010.

[8] R.C. Blattberg, E.C. Malthouse and S.A. Neslin. Customer lifetime value: Empirical generalizations and some conceptual questions. Journal of Interactive Marketing, 23, 2, 157-168, 2009.

[9] Y. Ekinci, F. Ülengin, N. Uray and B. Ülengin. Analysis of customer lifetime value and marketing expenditure decisions through a Markovian-based model. European Journal of Operational Research, 237, 1, 278-288, 2014.

[10] N. Glady, B. Baesens and C. Croux. A modified Pareto/NBD approach for predicting customer lifetime value. Expert Systems with Applications, 36, 2, 2062-2071, 2009.

[11] M. Haenlein, A.M. Kaplan and A.J. Beeser. A model to determine customer lifetime value in a retail banking context. European Management Journal, 25, 3, 221-234, 2007

[12] M.B. Mzoughia and M. Limam. An improved customer lifetime value model based on Markov chain. Applied Stochastic Models in Business and Industry, 31, 4, 528-535, 2015.
[13] Ö.G. Ali and U. Arıtürk. Dynamic churn prediction framework with more effective use of rare event data: The case of private banking. Expert Systems with Applications, 41, 17, 7889-7903, 2014.
[14] B. He, Y. Shi, Q. Wan and X. Zhao. Prediction of customer attrition of commercial banks based on SVM model. Procedia Computer Science, 31, 423-430, 2014.
[15] A. Knott, A. Hayes and S.A. Neslin. Next-product-to-buy models for cross-selling applications. Journal of Interactive Marketing, 16, 3, 59-75, 2002
[16] S. Li, B. Sun and R.T. Wilcox. Cross-selling sequentially ordered products: An application to consumer banking services. Journal of Marketing Research, 42, 2, 233-239, 2005.
[17] S. Li, B. Sun and A.L. Montgomery. Cross-selling the right product to the right customer at the right time. Journal of Marketing Research, 48, 4, 683-700, 2011.

Penultimate Approximations in Extreme Value Theory and Reliability of Large Coherent Systems

M. Ivette Gomes[1], Paula Reis[2], Luísa Canto e Castro[3], and Sandra Dias[4]

[1] CEAUL and DEIO, Faculdade de Ciências, Universidade de Lisboa, Portugal (E-mail: ivette.gomes@fc.ul.pt)
[2] DMAT, EST-IPS, Setúbal, Portugal (E-mail: paula.reis@estsetubal.ips.pt)
[3] CEAUL, Universidade de Lisboa, Portugal (E-mail: luisa.castro@dgeec.mec.pt)
[4] Pólo CMAT-UTAD and CEMAT, Universidade de Trás-os-Montes e Alto Douro, Portugal (E-mail: sdias@utad.pt)

Abstract. The rate of convergence of linearly normalized maxima/minima to the corresponding non-degenerate extreme value (EV) limiting distribution is a relevant problem in the field of extreme value theory. Moreover, the limiting EV approximation can be asymptotically improved, through the so-called penultimate approximations, which have been theoretically studied from different perspectives. Recently, this same topic has been revisited in the field of reliability, where any coherent system can be represented as either a series-parallel or a parallel-series system, with a lifetime which can thus be written as the minimum of maxima or the maximum of minima. For large-scale coherent systems, the possible non-degenerate EV laws are eligible candidates for the finding of adequate lower and upper bounds for such system's reliability. However, since such non-degenerate limit laws are better approximated by an adequate penultimate distribution in most situations, it is sensible to assess both theoretically and through Monte-Carlo simulations the gain in accuracy when a penultimate approximation is used instead of the ultimate one.
Keywords: Extreme value theory, Monte-Carlo simulation, penultimate and ultimate approximations, system reliability.

1 Introduction and preliminaries

The main objective of this article is to put forward and discuss the existence of accurate bounds for the exact *reliability function* (RF), $R_{_T}(t) := \mathbb{P}(T > t) =: 1 - F_{_T}(t)$, of a complex system **S** with lifetime T and lifetime *cumulative distribution function* (CDF) $F_{_T}$. The derivation of the exact RF can indeed be intractable due to the large number of system's components and to the way the operating process uses such components. As examples of such structures, and among others, we mention transport networks of energy, oil, gas and water.

Any coherent system (see Barlow and Proschan[2], for details) can be represented as either a *parallel-series* (PS) system—parallel structure with components connected in series, or a *series-parallel* (SP) system—series structure with components connected in parallel. The lifetime, T, of any system **S** can thus be written as either the *maximum of minima* or the *minimum of maxima*. Just as mentioned above, let T denote now the lifetime of a coherent

structure with n components, with lifetimes $(T_1, \ldots, T_n)$. Let us denote by $(T_{1:n} \leq \cdots \leq T_{n:n})$ the sample of associated ascending *order statistics* (OSs), with $T_{1:n} = \min_{1 \leq i \leq n} T_i$, $T_{n:n} = \max_{1 \leq i \leq n} T_i$. The main importance of OSs in reliability lies on the fact that the random variable (RV) T can always be written as a function of the OSs associated with the RVs T_i, $1 \leq i \leq n$. Indeed, $T_{1:n}$ is the lifetime of a series system, the one that works if and only if (iff) all its n components work, and $T_{n:n}$ is the lifetime of a parallel system, a structure that works iff at least one of its n components work. A k-out-of-n system, i.e. the one that works iff at least k of its n components work, has a lifetime given by $T_{k:n}$, $1 \leq k \leq n$. And we always have $T = T_{I:n}$, where I is a discrete RV with support $\{1, 2, \ldots, n\}$. The vector $\underline{s} := (s_1, s_2, \ldots, s_n)$, with $s_i := \mathbb{P}(I = i)$, $1 \leq i \leq n$, is the so-called signature of the system (Samaniego[20]). To find the aforementioned representations, we need to identify the so-called *minimal paths*—paths without irrelevant components that enable the operation of the system, and the *minimal cuts*—sets of relevant components that imply the failure of the system whenever removed. Generally speaking, let $P_j, 1 \leq j \leq p = p_n$, denote the minimal paths, and C_j, $1 \leq j \leq s = s_n$, the minimal cuts. Then, and for non-necessarily *identically distributed* components,

$$\prod_{j=1}^{s} \Big(1 - \prod_{i \in C_j} F_i(t)\Big) \leq R_{\scriptscriptstyle T}(t) \leq 1 - \prod_{j=1}^{p} \Big(1 - \prod_{i \in P_j} (1 - F_i(t))\Big),$$

i.e. we can easily build lower and upper bounds for the reliability on the basis of the minimal cuts (assuming they are independent) and minimal paths (assuming they are disjoint), respectively. For sake of simplicity, we now assume that all minimal paths have the same size $l = l_n$ and that all minimal cuts have a size $r = r_n$ (the so-called *regular* system), and that $R_i(t) = R(t)$, $1 \leq i \leq n$ (the so-called *homogeneous* system). Then, with $n = r_n s_n = l_n p_n$, we get the lower/upper bounds,

$$\begin{aligned} L_{\scriptscriptstyle \rm SP} = L_{\scriptscriptstyle \rm SP}(t) = \Big(1 - (1 - R(t))^{r_n}\Big)^{s_n} &\leq R_{\scriptscriptstyle T}(t) \\ &\leq 1 - \Big(1 - R^{l_n}(t)\Big)^{p_n} = U_{\scriptscriptstyle \rm PS}(t) = U_{\scriptscriptstyle \rm PS}. \quad (1) \end{aligned}$$

In Section 2, some further details on these reliability bounds will be given, together with a simple illustration of SP and PS representations. Assuming that the number, n, of components of $\mathbf{S}$ goes to infinity, asymptotic *extreme value* (EV) ultimate or limiting models often provide a good interpretation of the RF of $\mathbf{S}$. Considering a fixed large number of components, pre-asymptotic or penultimate models can provide an improvement of the convergence rate and a better approximation to the RF of $\mathbf{S}$. In Section 3, we provide the main results in *extreme value theory* (EVT), the ones needed for the derivation of ultimate and penultimate behaviour of PS and SP systems, the topic discussed in Section 4. Following closely Reis *et al.*[19], Section 5 is devoted to providing results on a small-scale Monte-Carlo simulation and concluding remarks.

2 Some further details on reliability bounds

Apart from the reliability bounds, (L_{SP}, U_{PS}), provided in (1), we refer the most crude lower and upper bounds for the system's RF, the ones given by the RFs of the associated series and parallel systems, with all the n system's components working independently. More precisely, and with the notation used in Section 1, we get

$$L_{S} = L_{S}(t) = R^{n}(t) \leq R_{T}(t) \leq 1 - (1 - R(t))^{n} = U_{P}(t) = U_{P}. \qquad (2)$$

To see the possible accuracy of the bounds in (1), comparatively to the ones in (2), we provide the following example:

Example 1. Let us consider the simple structure in **Fig. 1**. For this struc-

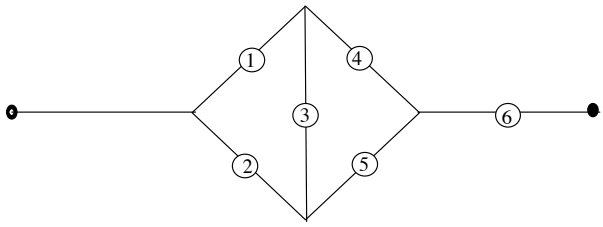

Fig. 1. A bridge-series structure

ture, we have the *minimal paths*, {1,4,6}, {2,5,6}, {1,3,5,6}, {2,3,4,6}, and the *minimal cuts*, {1,2}, {4,5}, {1,3,5}, {2,3,4}, {6}. Consequently, we have the following representations of the system under consideration:

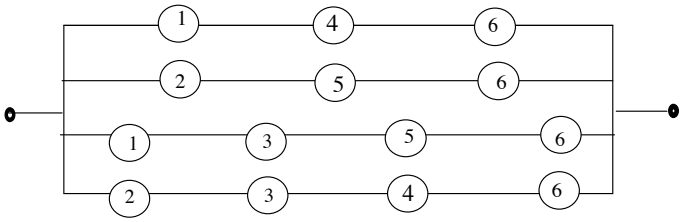

Fig. 2. PS representation of the structure in **Fig. 1**

We can thus write,

$$T = \max\Big(\min(T_1, T_4, T_6), \min(T_2, T_5, T_6), \min(T_1, T_3, T_5, T_6), \min(T_2, T_3, T_4, T_6)\Big),$$

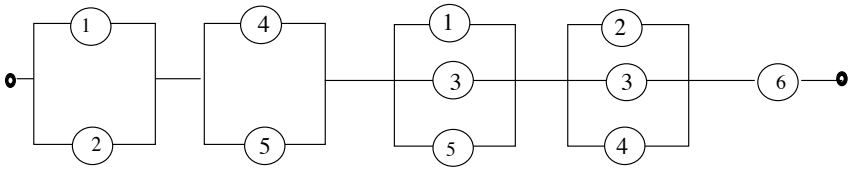

Fig. 3. SP representation of the structure in **Fig. 1**

as well as

$$T = \min\big(\max(T_1, T_2), \max(T_4, T_5), \max(T_1, T_3, T_5), \max(T_2, T_3, T_4), T_6\big).$$

We obviously need to pay attention to the strong dependence of the different RVs either in the overall max or min operators. But we can easily build reliable upper and lower bounds for the reliability, on the basis of the minimal paths (assuming they are disjoint) and the minimal cuts (assuming they are independent), respectively.

For this particular example, and considering that any of the components work independently of the others and with a probability p, we easily get the static reliability, $2p^3+2p^4-5p^5+2p^6$. And putting $R(t)=p$ in (1) and (2), we get the bounds $\mathrm{L_S} = L_{\mathrm{S}}(p) = p^6$, $\mathrm{U_P} = U_{\mathrm{P}}(p) = 1-(1-p)^6$, $\mathrm{L_{SP}} = L_{\mathrm{SP}}(p) = \big(1-(1-p)^2\big)^2\big(1-(1-p)^3\big)^2 p$, $\mathrm{U_{PS}} = U_{\mathrm{PS}}(p) = 1-(1-p^3)^2(1-p^4)^2$, all represented in **Fig. 4**.

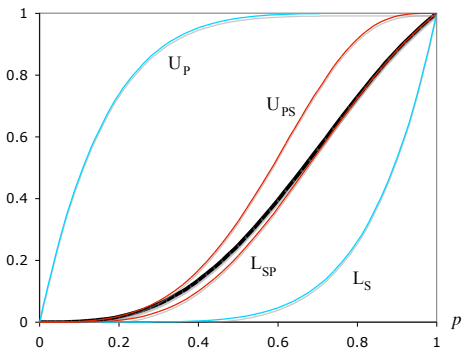

Fig. 4. Statitic reliability and lower/upper reliability bounds associated with the structure in **Fig. 1**

Just as happens in the example above, the lower and upper bounds in (1) are usually much more accurate than $L_S(t)$ and $L_P(t)$, in (2). This can also be seen in **Fig. 5**, where we consider the static counterpart of the RF, writing $p := R(t)$, representing for $l_n = r_n = 2; s_n = p_n = 10$ $(n = 20)$, $l_n = r_n = 4; s_n = p_n = 5$ $(n = 20)$ and $l_n = r_n = 4; s_n = p_n = 15$ $(n = 60)$, the

lower bounds $L_S \equiv L_S(p) = p^n$, $L_{SP} \equiv L_{SP}(p) = \left(1-(1-p)^{r_n}\right)^{s_n}$, as well as the upper bounds $U_P \equiv U_P(p) = 1-(1-p)^n$, $U_{PS} \equiv U_{PS}(p) = 1-\left(1-p^{l_n}\right)^{p_n}$, as functions of p.

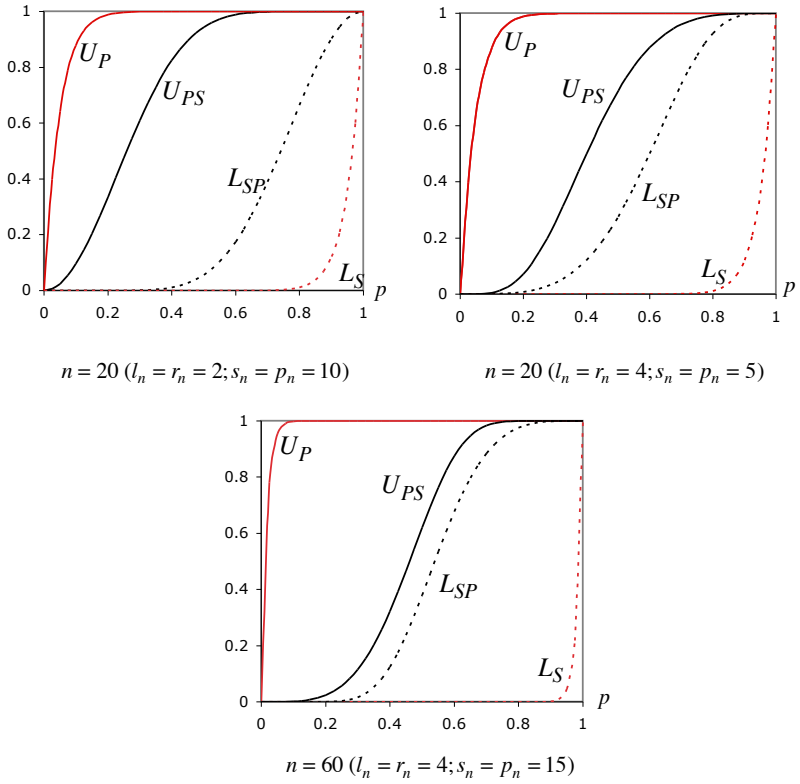

Fig. 5. Lower and upper reliability bounds associated with $l_n = r_n = 2; s_n = p_n = 10$ (*top left*), $l_n = r_n = 4; s_n = p_n = 5$ (*top right*) and $l_n = r_n = 4; s_n = p_n = 15$ (*bottom*)

Again, the SP-PS lower-upper bounds always revealed to be much more accurate than the S-P reliability bounds.

3 Limiting behavior of maxima and minima

Just as mentioned above, and whenever dealing with large-scale coherent systems, it is sensible to assume that n, the number of system components goes to infinity. Then (Gnedenko[7]), the possible non-degenerate *extreme value distributions* either for *maxima* ($\mathrm{EV_MD}$), given by

$$G(x) \equiv G_\xi(x) := \begin{cases} \mathrm{e}^{-(1+\xi x)^{-1/\xi}}, & 1+\xi x > 0, \quad \text{if} \quad \xi \neq 0, \\ \mathrm{e}^{-\mathrm{e}^{-x}}, & x \in \mathbb{R}, \quad \text{if} \quad \xi = 0, \end{cases} \tag{3}$$

or for *minima* ($\mathrm{EV_mD}$), given by

$$G^*_\theta(x) = 1 - G_\theta(-x), \quad \text{with } G_\xi(x) \text{ given in (3)}, \tag{4}$$

the symetrised version of the $EV_\mathrm{M}D$ in (3), are eligible candidates for the system reliability or at least for the finding of adequate lower and upper bounds for such a reliability on the basis of the SP and PS representations discussed in Section 1.

The shape parameter ξ, in (3), the so-called *extreme value index for maxima* ($\mathrm{EVI_M}$), measures the heaviness of the *right-tail* function (or RF), $\overline{F}(x) \equiv R(x) = 1 - F(x)$, as $x \to +\infty$, and the heavier the right-tail, the larger ξ is. The $\mathrm{EV_M}$D is sometimes separated in the three following types,

$$\begin{array}{ll} \text{Type I (Gumbel)}: & \Lambda(x) = \exp(-\exp(-x)),\ x \in \mathbb{R}, \\ \text{Type II (Fréchet)}: & \Phi_\alpha(x) = \exp(-x^{-\alpha}),\ x \geq 0, \\ \text{Type III (max-Weibull)}: & \Psi_\alpha(x) = \exp(-(-x)^{\alpha}),\ x \leq 0, \end{array}$$

$\alpha > 0$, the types considered in the aforementioned Gnedenko's paper. We have

$$\Lambda(x) = G_0(x),\ \Phi_\alpha(x) = G_{1/\alpha}(\alpha(1-x)),\ \Psi_\alpha(x) = G_{-1/\alpha}(\alpha(x+1)),$$

with G_ξ the $\mathrm{EV_M}$D, in (3).

The shape parameter θ, in (4), the so-called EVI for *minima* ($\mathrm{EVI_m}$), measures the heaviness of the *left-tail function*, $F(x)$, as $x \to -\infty$, and the heavier the left-tail, the larger θ is. Similarly to what happens in the max-scheme, the $\mathrm{EV_m}$D is sometimes separated in the three following types:

$$\begin{array}{ll} \text{Type I (min-Gumbel)}: & \Lambda^*(x) = 1 - \exp(-\exp(x)),\ x \in \mathbb{R}, \\ \text{Type II (min-Fréchet)}: & \Phi^*_\alpha(x) = 1 - \exp(-(-x)^{-\alpha}),\ x \leq 0, \\ \text{Type III (Weibull)}: & \Psi^*_\alpha(x) = 1 - \exp(-x^{\alpha}),\ x \geq 0. \end{array}$$

Remark 1. Note that the limiting result for minima, given in (4), comes from the fact that $\min_{1\leq i\leq n} X_i = -\max_{1\leq i\leq n}(-X_i)$. If the sequence $\max_{1\leq i\leq n}(-X_i)$ can be normalised, in order to admit a non degenerate limit Z, then the CDF of Z will be of the same type as G_θ, the $\mathrm{EV_M}$D, for some $\theta \in \mathbb{R}$. Hence the possible limit laws for minima, conveniently normalised, will be such that $F_{-Z}(x) = \mathbb{P}(-Z \leq x) = \mathbb{P}(Z \geq -x) = 1 - G_\theta(-x) = G^*_\theta(x)$. We then say that the CDF F, associated with the RV X, is in the min-domain of attraction of G^*_θ, using the notation $F \in \mathcal{D}_\mathrm{m}(G^*_\theta)$, and this happens if and only if the CDF of $-X$ is in the max-domain of attraction of G_θ, i.e. with the notation $H(x) = 1 - F(-x)$, $H \in \mathcal{D}_\mathrm{M}(G_\theta)$.

3.1 Rates of convergence

Thinking now on max-domains of attraction, and without loss of generality due to *Remark 1*, another relevant problem in EVT concerns the rate of convergence of $F^n(a_n x + b_n)$ to $G_\xi(x)$ or, equivalently, the finding of estimates of the difference

$$d_n(F, G_\xi, x) := F^n(a_n x + b_n) - G_\xi(x). \tag{5}$$

In EVT there exists no analogue of the Berry-Esséen theorem that, under broad conditions, gives a rate of convergence of the order of $1/\sqrt{n}$ in the central limit theorem. The rate of convergence depends strongly on the right-tail of F, on the choice of the attraction coefficients, and can be rather slow, as first detected in Fisher and Tippett[5]. A similar comment applies to the left-tail.

3.2 Penultimate approximations

To the best of our knowledge, Fisher and Tippett[5] were the first authors to provide the so-called max-Weibull penultimate approximation for $\Phi^n(x)$, with Φ the normal CDF. They observed that, despite of the fact that $\Phi \in \mathrm{D_M}(G_0)$, the convergence of $\Phi^n(a_n x + b_n)$ towards $G_0(x)$ is very slow. Through the use of skewness and kurtosis coefficients as indicators of closeness, they showed that $\Phi^n(x)$ is 'closer' to a suitable penultimate $G_{-1/\xi_n}((x-\lambda_n)/\delta_n)$, for $\xi_n > 0$, $\lambda_n \in \mathbb{R}$, $\delta_n > 0$, than to the ultimate $G_0((x-b_n)/a_n)$. Such an approximation is the so-called penultimate approximation.

The modern theory of rates of convergence in EVT began with Anderson[1], Gomes[8] and Galambos[6]. For papers on the subject prior to 1992, we refer the review in Gomes[10]. Developments have followed different directions that can be found in Beirlant*et al.*[3] and Gomes and Guillou[11]. We refer here only the study of the structure remainder $d_n(F, G_\xi, x)$, in (5), with $F \in \mathrm{D_M}(G_\xi)$, $\xi \in \mathbb{R}$, i.e. the finding of $u_n \to 0$, as $n \to \infty$, and $\varphi(x)$ such that

$$F^n(a_n x + b_n) - G_\xi(x) = u_n \varphi(x) + o(u_n).$$

We then say that the rate of convergence of $F^n(a_n x + b_n)$ towards $G_\xi(x)$ is of the order of u_n. In this same framework, the possible penultimate behaviour of $F^n(a_n x + b_n)$ has been studied, i.e. the possibility of finding $H(x) = H_n(x)$, perhaps a max-stable DF, such that

$$F^n(a_n x + b_n) - H_n(x) = O(r_n), \quad r_n = o(u_n).$$

We refer Gomes[9], Gomes and Pestana[13], and Gomes and de Haan[12], who derived, for all $\xi \in \mathbb{R}$, exact penultimate approximation rates, under the so-called von Mises-type conditions and some extra differentiability assumptions. In Kaufmann[14] a similar result was proved, but under weaker conditions. This penultimate or pre-asymptotic behaviour has further been studied by Raoult and Worms[15] and Diebolt and Guillou[4], among others.

4 Asymptotic behavior of PS and SP systems

On the basis of the main theorem in [12], and the results in [16], [17], [18] and [19], we can now state the following results, respectively given in Sections 4.1 and 4.2, and which establish the ultimate and penultimate models for a sequence of RFs of regular and homogeneous PS and SP systems.

4.1 Ultimate and penultimate models for the RF of a regular and homogeneous PS system

Let $F \in \mathrm{D_m}(G^*_\theta)$, the min-domain of attraction of G^*_θ, i.e. assume that there exist sequences $\{a_n > 0\}_{n\geq 1}$ and $\{b_n \in \mathbb{R}\}_{n\geq 1}$ such that

$$F_{1:n}(a_n x + b_n) := 1 - (1 - F(a_n x + b_n))^n \underset{n\to\infty}{\longrightarrow} G^*_\theta(x),$$

for all $x \in \mathbb{R}$ and where G^*_θ is the $\mathrm{EV_m D}$, in (4). Given an integer sequence $p_n \to \infty$, such that $p_n e_{l_n} = o(1)$, $e_n := \sup_{x\in\mathbb{R}} |F_{1:n}(a_n x + b_n) - G^*_\theta(x)|$, and $l_n \to \infty$, with $l_n p_n = n$, and as shown in Reis *et al.* [19], there exist sequences $\{\alpha_n > 0\}_{n\geq 1}$ and $\{\beta_n \in \mathbb{R}\}_{n\geq 1}$ such that

$$H_n(\alpha_n x + \beta_n) := \Big(1 - \Big(1 - F(\alpha_n x + \beta_n)\Big)^{l_n}\Big)^{p_n} \underset{n\to\infty}{\longrightarrow} \Lambda(x) \equiv G_0(x),\ \forall x \in \mathbb{R}.$$

Consequently, for a regular homogeneous PS system, composed by p_n parallel subsystems with l_n components in series, the sequence of associated RFs, suitably normalized, is such that,

$$R_n(\alpha_n x + \beta_n) := 1 - \Big(1 - \Big(1 - F(\alpha_n x + \beta_n)\Big)^{l_n}\Big)^{p_n} \underset{n\to\infty}{\longrightarrow} 1 - \Lambda(x) = 1 - G_0(x),\ \forall\, x \in \mathbb{R}.$$

If we further assume that $l_n \to \infty$ and $p_n(\ln^2 p_n)e_{l_n} = o(1)$, as $n \to \infty$, then, for all $\theta \neq -1$, there exist a sequence $\{\xi_n\}_{n\geq 1}$ such that

$$H_n(\alpha_n x + b_n) - G_{\xi_n}(x) = O(1/\ln^2 p_n),\ \forall\, x \in \mathbb{R}.$$

Moreover, we can choose $\xi_n = \xi_n(\theta) = -(\theta + 1)/\ln n$. Consequently, for a regular and homogeneous PS system, the sequence of RFs is such that

$$R_n(\alpha_n x + b_n) - (1 - G_{\xi_n}(x)) = O(1/\ln^2 p_n),\ \forall\, x \in \mathbb{R}.$$

4.2 Ultimate and penultimate models for the RF of a regular and homogeneous SP system

On the basis of a min-version of the main theorem in [12], and the results in [16] and [19], we can now state the following results:

Let $F \in \mathrm{D_M}(G_\xi)$, the max-domain of attraction of G_ξ, i.e. let us assume that there exist sequences $\{a_n > 0\}_{n\geq 1}$ and $\{b_n \in \mathbb{R}\}_{n\geq 1}$ such that

$$F_{n:n}(a_n x + b_n) := F^n(a_n x + b_n) \underset{n\to\infty}{\longrightarrow} G_\xi(x),$$

for all $x \in \mathbb{R}$ and where G_ξ is the $\mathrm{EV_M D}$, in (3). Given a sequence of integers $s_n \to \infty$, such that $s_n e_{r_n} = o(1)$, $e_n := \sup_{x\in\mathbb{R}} |F_{n:n}(a_n x + b_n) - G_\xi(x)|$ and

$r_n \to \infty$, with $r_n s_n = n$, there exist sequences $\{\alpha_n > 0\}_{n\geq 1}$ and $\{\beta_n \in \mathbb{R}\}_{n\geq 1}$ such that

$$H_n^*(\alpha_n x + \beta_n) := 1 - \left(1 - F^{r_n}(\alpha_n x + \beta_n)\right)^{s_n} \underset{n\to\infty}{\longrightarrow} \Lambda^*(x) \equiv G_0^*(x),$$

for all $x \in \mathbb{R}$. Consequently, for a regular homogeneous SP system, the sequence of associated RFs, suitably normalized, is such that,

$$R_n^*(\alpha_n x + \beta_n) := \left(1 - F^{r_n}(\alpha_n x + \beta_n)\right)^{s_n} \underset{n\to\infty}{\longrightarrow} 1 - G_0^*(x),$$

for all $x \in \mathbb{R}$. If we further assume that $r_n \to \infty$ and $s_n(\ln^2 s_n)e_{r_n} = o(1)$, as $n \to \infty$, then, for all $\xi \neq -1$, there exist a sequence $\{\theta_n\}_{n\geq 1}$ such that

$$H_n^*(\alpha_n x + b_n) - G_{\theta_n}^*(x) = O(1/\ln^2 s_n).$$

for all $x \in \mathbb{R}$. Moreover, we can choose $\theta_n = \theta_n(\xi) = -(\xi + 1)/\ln n$. Consequently, for a regular homogeneous SP system, composed by s_n series subsystems with r_n components in parallel, the sequence of RFs, $R_n(\alpha_n x + \beta_n)$, is such that, for all $x \in \mathbb{R}$,

$$R_n^*(\alpha_n x + b_n) - (1 - G_{\theta_n}^*(x)) = O(1/\ln^2 s_n).$$

5 Monte-Carlo simulation

To assess the gain in accuracy when a penultimate approximation is used instead of the ultimate one, we slightly enlarged the Monte Carlo simulations presented in [19], where several $\mathrm{PS}_{(p_n,l_n)}$ systems have been simulated, with lifetime components from different models, including the $\mathrm{EV_mD}(\theta)$, and $\mathrm{GP_mD}(\theta)$=$-\ln(1 - \mathrm{EV_mD}(\theta))$, for a few values of θ. The hypothesis $\mathcal{H}_0$: $G_n^* = 1 - (1 - F)^{l_n} \in \mathcal{D}_{\mathcal{M}}(G_\xi)$, for some $\xi \in \mathbb{R}$, was not rejected, and no typical behavior was detected on the variation of l_n, except for small values of l_n ($l_n < 20$), and lifetime parents different from the $\mathrm{EV_mD}$, as can be seen in Figure 7. The ultimate law G_0 was also tested, and the null hypothesis,

$$\mathcal{H}_0 : \; F_n(x) = \left(1 - (1 - F(x))^{l_n}\right)^{p_n} = G_0\left((x - \lambda)/\delta\right),$$

with $F_n(x)$ the CDF of the lifetime of a PS system and $(\lambda, \delta) \in \mathbb{R} \times \mathbb{R}^+$ a vector of unknown (location and scale) parameters, was rejected except for $\theta = -1$ (showing consistency between simulated and theoretical results). Estimated type I error increases as θ moves away from -1, and decreases as p_n increases.

For the simulated PS systems, a goodness of fit test for the $\mathrm{EV_MD}$ with known shape parameter and unknown location and scale parameters was applied to test the penultimate law, i.e the null hypothesis

$$H_n(x) = G_{\xi_n}\left((x - \lambda)/\delta\right), \quad \xi_n = -(\theta + 1)/\ln n,$$

with λ and δ, respectively unknown location and scale parameters. Furthermore, to see whether the estimates of ξ are closer to the penultimate parameter ξ_n rather than to the ultimate parameter zero, we have computed $\hat{\xi}$, the

maximum likelihood estimate in the GEV_ξ model, and using a Monte Carlo simulation, with $R = 1000$ runs have simulated the *root mean square error* (RMSE) and the bias (BIAS),

$$\mathrm{RMSE}_P = \sqrt{\frac{1}{R}\sum_{i=1}^{R}\left(\hat{\xi}-\xi_n\right)^2}, \quad \mathrm{RMSE}_U = \sqrt{\frac{1}{R}\sum_{i=1}^{R}\left(\hat{\xi}_i\right)^2},$$

$$\mathrm{BIAS}_P = \frac{1}{R}\sum_{i=1}^{R}\left(\hat{\xi}_i-\xi_n\right), \quad \mathrm{BIAS}_U = \frac{1}{R}\sum_{i=1}^{R}\hat{\xi}_i.$$

Figure 6 is associated with $\mathrm{EV_mD}(\theta)$ lifetime parents. The 'black' is used for BIAS_P and RMSE_P, and the 'red' is used for BIAS_U and RMSE_U. The BIAS are pictured in dashed lines.

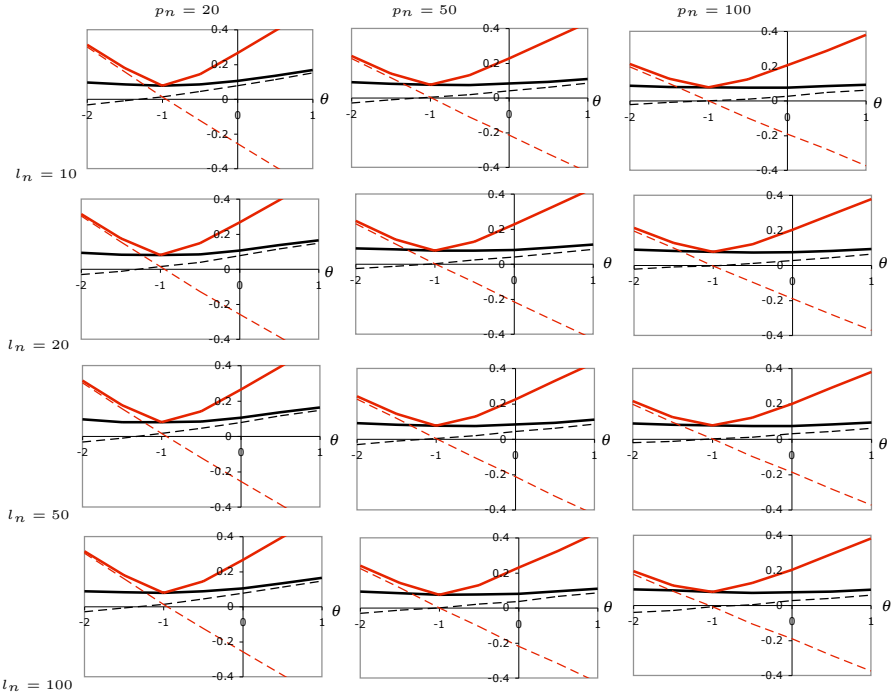

Fig. 6. $\mathrm{EV_mD}(\theta)$ lifetimes: ultimate and penultimate BIAS and RMSE

Figure 7 is similar to Figure 6, but associated with $\mathrm{GP_mD}(\theta)$ lifetime parents. For $l_n = 10$, it is here possible to note that $\mathrm{RMSE}_U < \mathrm{RMSE}_P$ for $\theta < -1$. But most of the times we indeed have $\mathrm{RMSE}_P < \mathrm{RMSE}_U$ for $\theta \neq -1$.

5.1 Concluding remarks

The gain in accuracy of a penultimate approximation comparatively to the ultimate one justifies its use in practice. We are conscious that the restriction

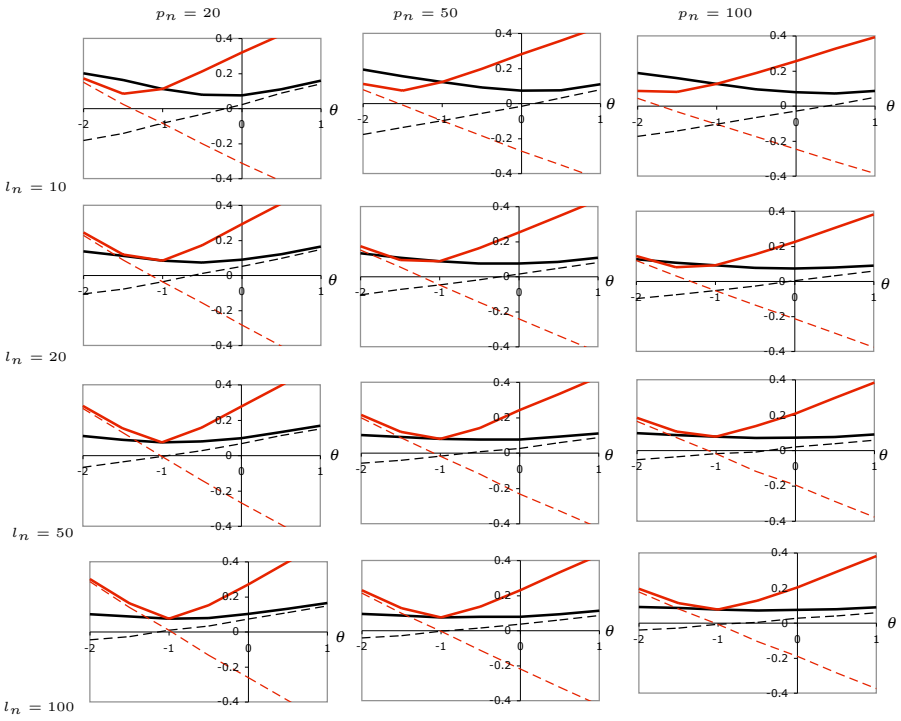

Fig. 7. $\mathrm{GP_m D}(\theta)$ lifetimes: ultimate and penultimate BIAS and RMSE

that the RF of all components of the system is the *same* is strong, but such an assumption was used *only* as a simplification. More intricate but similar work can be done for non-homogeneous systems. Applications of the developed theory are feasible, but beyond the scope of this article. Indeed, a great variety of *parametric models* can further be considered, like, for instance, the penultimate EV parametric model suggested by Smith[21],

$$\mathrm{PEV}_\xi(x;r) = \exp\left(-(1+\xi x)^{-1/\xi}\left(1+r(1+\xi x)^{-1/\xi}\right)\right),\ 1+\xi x>0$$

or the associated penultimate GP CDF,

$$\mathrm{PGP}_\xi(x;r) = 1-(1+\xi x)^{-1/\xi}\left(1+r(1+\xi x)^{-1/\xi}\right),\ 1+\xi x>0.$$

The development of inferential procedures for these models is thus welcome.

Acknowledgments

Research partially supported by National Funds through **FCT** — Fundação para a Ciência e a Tecnologia, projects UID/MAT/00006/2013 (CEA/UL), UID/MAT/00013/2013 (CMAT) and UID/Multi/04621/2013 (CEMAT).

References

1. C.W. Anderson. *Contributions to the Asymptotic Theory of Extreme Values*, Ph.D. Thesis, University of London, 1971.
2. R.E. Barlow and F. Proschan. *Statistical Theory of Reliability and Life Testing*, Holt Rinehart and Winston, Inc., New York, 1975.
3. J. Beirlant, F. Caeiro and M.I. Gomes. An overview and open research topics in the field of statistics of univariate extremes. *Revstat*, **10**,1, 1–31, 2012.
4. J. Diebolt and A. Guillou. Asymptotic behaviour of regular estimators. *Revstat*, **3**,1, 19–44, 2005.
5. R.A. Fisher and L.H.C. Tippett. Limiting forms of the frequency distributions of the largest or smallest member of a sample. *Proc. Cambr. Phil. Soc.*, **24**, 180–190, 1928.
6. J. Galambos. *The Asymptotic Theory of Extreme Order Statistics*, Wiley, New York, 1978.
7. B.V. Gnedenko. Sur la distribution limite du terme maximum d'une série aléatoire. *Ann. Math.*, **44**, 423–453, 1943.
8. M.I. Gomes. *Some Probabilistic and Statistical Problems in Extreme Value Theory*, Ph. D. Thesis, Univ. Sheffield, 1978.
9. M.I. Gomes. Penultimate limiting forms in extreme value theory. *Ann. Inst. Statist. Math.*, **36**, Part A, 71–85, 1984.
10. M.I. Gomes. Penultimate behaviour of the extremes. In J. Galambos, J. Lechner and E. Simiu (eds.), *Extreme Value Theory and Applications*, Kluwer Academic Publishers, 403–418, 1994.
11. M.I. Gomes and A. Guillou. Extreme value theory and statistics of univariate extremes: A review. *Internat. Statist. Review*, **83**,2, 263–292, 2015.
12. M.I. Gomes and L. de Haan. Approximations by extreme value distributions, *Extremes*, **2**,1, 71–85, 1999.
13. M.I. Gomes and D. Pestana. Nonstandard domains of attraction and rates of convergence. In L. Puri *et al.* (eds.), *New Perspectives in Theoretical and Applied Statistics*, Wiley, 467–477, 1987.
14. E. Kaufmann. Penultimate approximations in extreme value theory. *Extremes*, **3**,1, 39—55, 2000.
15. J.P. Raoult and R. Worms. Rate of convergence for the generalized Pareto approximation of the excesses. *Adv. Appl. Probab.*, **35**,4, 1007–1027, 2003.
16. P. Reis and L. Canto e Castro. Limit model for the reliability of a regular and homogeneous series-parallel system. *Revstat*, **7**,3, 227–243, 2009.
17. P. Reis, L. Canto e Castro, S. Dias and M.I. Gomes. A note on penultimate approximations and reliability of series-parallel structures. In K.F. Turkman *et al.* (eds.) *Symposium on Recent Advances in Extreme Value Theory: Book of Abstracts*, CEAUL editions, 99–102, 2013.
18. P. Reis, L. Canto e Castro, S. Dias and M.I. Gomes. On the penultimate approximations and reliability of parallel-series systems. In Fraga Alves, M.I. and Neves, M.M. (eds.), *Extremes in Vimeiro Today: Extended Abstracts*, CEAUL editions, 145–149, 2013.
19. P. Reis, L. Canto e Castro, S. Dias and M.I. Gomes. Penultimate approximations in statistics of extremes and reliability of large coherent systems. *Method. and Comput. in Appl. Probab.*, **17**,1, 189–206, 2015.
20. F. Samaniego. On closure of the IFR class under formation of coherent systems. *IEEE Trans. Reliab.*, **34**, 69–72, 1985.
21. R.L. Smith. *Approximations in Extreme Value Theory*, Preprint, Univ. North-Carolina, 1987.

Embedded Semi-Markov process as reliability model of two different units cold standby system

Franciszek Grabski

Department of Mathematics and Physics
Polish Naval University, Śmidowicza 69, 81 -127 Gdynia, Poland
e-mail: F.Grabski@amw.gdynia.pl

Abstract. In this paper an embedded semi-Markov stochastic process is applied in reliability problem. The problem concerns of two different cold standby system. We assume that the system consists of one operating unit *A*, the stand-by unit *B* that may have different probability distributions of the times to failure. We suppose that there is an unreliable switch in the system which is used at the moment of the working unit failure. A discrete state space and continuous time stochastic process describes work of the system in reliability aspect. To obtain the reliability characteristic and parameters of the system we construct so called an embedded semi-Markov process in this process. In our model the conditional time to failure of the system is represented by a random variable denoting the first passage time from the given state to the subset of states. To calculate the reliability function and mean time to failure of the system we apply theorems of the Semi-Markov processes theory concerning the conditional reliability functions. Often an exact reliability function of the system by using Laplace transform is difficult to calculate, frequently impossible. In those cases we apply one of theorems of Semi-Markov processes perturbation theory, to obtain an approximate reliability function of the system.

Keywords: Semi-Markov process, cold standby system, embedded stochastic process.

1 Introduction

A model presented here is an extension of the models that have been considered by Barlow and Proshan [1], Brodi and Pogosian [2], Koroluk and Turbin [7] and Grabski [4], [5]. As a model of the two different cold standby system we construct so called *embedded Semi-Markov process* by defining the renewal kernel of that one. Construction of the renewal kernel is an important first step in solving the problem. This method was presented in [2], [4], [5]. The conditional time to failure of the system is described by a random variable that means the first passage time from the given state to the subset of states. To obtain the conditional reliability functions of the system we use appropriate system of integral equations. Passing to the Laplace transforms we get system of linear equations for transforms. The solution are Laplace transforms of the conditional reliability functions of. Applying property of Laplace transform we compute the mean time to failure of the system. Very often calculating an exact reliability function of the system by using Laplace transform is a complicated matter but there is a

possibility to apply the theorem of the theory of the Semi-Markov processes perturbation [6], [7], [8], [10] to obtain an approximate reliability function of the system. We use Pavlov and Ushakov concept [9] of the perturbed SM process, which is presented in [3] by Gercbakh, for calculation approximate reliability function of the cold standby system.

2 Description and Assumptions

We assume that the system consists of one operating unit A, the stand-by unit B and a switch. We assume that a lifetime of a basic operating unit is represented by a random variable ζ_A, with distribution given by a probability density function (PDF) $f_A(x),\ x \geq 0$. When the operating unit fails, the spare B is immediately put in motion by the switch. The failed unit is renewed by a single repair facility. A renewal time of a unit A is a random variable γ_A having distribution given by a cumulative distribution function (CDF) $H_A(x) = P(\gamma_A \leq x),\ \ x \geq 0$. Lifetime of the unit B is a random variable ζ_B, with PDF $f_B(x),\ \ x \geq 0$. When unit B fails, the unit A immediately starts to work by the switch (if it is "up") and unit B is repaired. A renewal time of the unit B is a random variable γ_B having distribution given by the CDF $H_B(x) = P(\gamma_B \leq x),\ x \geq 0$.

Let U be a random variable having a binary distribution

$b(k) = P(U = k) = a^k(1-a)^{1-k},\ \ k = 0,1, \qquad 0 < a < 1,$

where $U = 0$, if a switch is failed at the moment of the operating unit failure, and $U = 1$, if the switch work at that moment.

The failure of the system takes place when the operating unit fails and the component that has failed sooner is not still ready to work or when both the operating unit and the switch have failed.

We suppose that an initial state is 5 with probability $p \geq 0$ or 6 with probability $q = 1 - p$.

We also assume that the whole system is renewable. After failure the entire system is renewed. A renewal time of whole system is random variable with distribution given by a cumulative distribution function (CDF

$H(x) = P(\gamma \leq x),\ \ x \geq 0.$

Moreover we assume that all random variables, mentioned above are mutually independent.

3 Construction of Semi-Markov reliability model

To describe the reliability process of the system, we have to define the states and the renewal kernel. We introduce the following states:

0 – failure of the whole system due to a failure of a switch;

1 – failure of the whole system due to the failure of the unit B during repair period of the unit A;

2 – failure of the whole system due to the failure of the unit A during repair period of the unit B;

3 – repair of the unit A, unit B is working;

4 – repair of the unit B, unit A is working;

5 – both unit A and unit B are "up" and unit A is working.

6 – both unit A and unit B are "up" and unit B is working.

Figure 1 shows functioning of the system. Let $0 = \tau_0^*,\ \tau_1^*, \tau_2^*, \ldots$ denote the instants of the states changes and $\{Y(t):\ t \geq 0\}$ be a random process with the state space $S = \{0, 1, 2, 3, 4, 5, 6\}$, which keeps constant values on the half-intervals $[\tau_n^*, \tau_{n+1}^*),\ n = 0,1, \ldots$ and it is right-continuous. This process is not semi-Markov, because a memory-less property is not satisfied for all instants of the state changes of it.

Operating process realization of this standby system is shown in Figure 1. We construct a new random process in a following way. Let $0 = \tau_0$ and $\tau_1, \tau_2, \ldots$ denote *instants of the unit failures or instants of the whole system failure*.

Suppose that the lines are denoted

- work of the unit A or B

- repair (renewal) of the unit A or B

- stand-by of the unit A or B

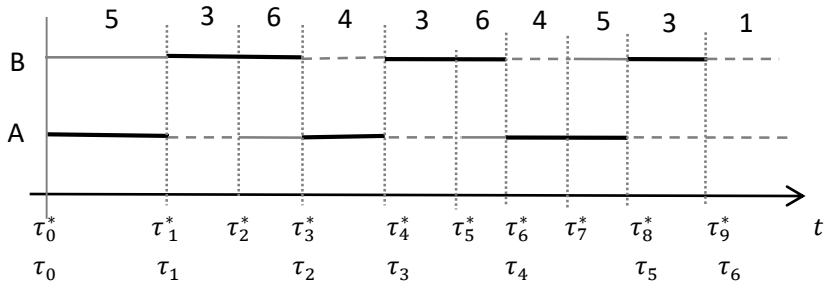

Figure 1. The cold standby system operating process evolution.

The random process $\{X(t):\ t \geq 0\}$ determining following way

$X(t) = Y(\tau_n)$ for $t \in [\tau_n, \tau_{n+1}),$ n $= 0, 1, 2, ...$

is the semi-Markov process. This process is called an *embedded semi-Markov process in the stochastic process* $\{Y(t)\colon\ t \geq 0\}$.

To determine semi-Markov process as a model we have to define its initial distribution and all elements of its kernel. Recall that the semi-Markov kernel is the matrix of transition probabilities of the Markov renewal process

$$Q(t) = [Q_{ij}(t)\colon\ i, j \in S], \tag{1}$$

where

$$Q_{ij}(t) = P(\tau_{n+1} - \tau_n \leq \mathrm{t}, X(\tau_{n+1}) = j \mid X(\tau_n) = i), \quad t \geq 0. \tag{2}$$

Let us recall that the sequence $\{X(\tau_n)\colon\ n = 0,1, ...\}$ is a homogeneous Markov chain with transition probabilities

$$p_{ij} = P(X(\tau_{n+1}) = j \mid X(\tau_n) = i) = \lim_{t\to\infty} Q_{ij}(t). \tag{3}$$

The function

$$G_i(t) = P(T_i \leq t) = P(\tau_{n+1} - \tau_n \leq t \mid X(\tau_n) = i) = \textstyle\sum_{j\in S} Q_{ij}(t) \tag{4}$$

is the CDF distribution of a waiting time T_i denoting the time spent in state i when the successor state is unknown, the function

$$F_{ij}(t) = P(\tau_{n+1} - \tau_n \leq t \mid X(\tau_n) = i, X(\tau_{n+1}) = j) = \frac{Q_{ij}(t)}{p_{ij}} \tag{5}$$

is the CDF of a random variable T_{ij} that is called a holding time of a state i, if the next state will be j. It is easy to see that

$$Q_{ij}(t) = p_{ij} F_{ij}(t). \tag{6}$$

In this case the semi-Markov kernel takes the form

$$Q(t) = \begin{bmatrix} 0 & 0 & 0 & 0 & 0 & Q_{05}(t) & Q_{06}(t) \\ 0 & 0 & 0 & 0 & 0 & Q_{15}(t) & Q_{16}(t) \\ 0 & 0 & 0 & 0 & 0 & Q_{25}(t) & Q_{26}(t) \\ Q_{30}(t) & Q_{31}(t) & 0 & 0 & Q_{34}(t) & 0 & 0 \\ Q_{40}(t) & 0 & Q_{42}(t) & Q_{43}(t) & 0 & 0 & 0 \\ Q_{50}(t) & 0 & 0 & Q_{53}(t) & 0 & 0 & 0 \\ Q_{60}(t) & 0 & 0 & 0 & Q_{64}(t) & 0 & 0 \end{bmatrix} \tag{7}$$

Construction of the semi-Markov model consists in determining of the matrix $Q(t)$ components on the basis of assumptions. We begin from determining of the transition probabilities from the "dawn" states. According to (2) and (3) we have

$$Q_{05}(t) = Q_{15}(t) = Q_{25}(t) = p\, H(t)\,, \tag{8}$$

$Q_{06}(t) = Q_{16}(t) = Q_{26}(t) = q\, H(t),$ where $p, q > 0, \quad p + q = 1;$

Transition probability from the state 3 we calculate the following way:

$$Q_{30}(t) = P(U = 0, \zeta_B t) = (1 - a) F_B(t), \tag{9}$$

$Q_{31}(t) = P(U = 1, \zeta_B \le t, \quad \gamma_A > \zeta_B) = a \iint_{C_{31}} f_B(x)dx\, dH_A(y),$ where

$C_{31} = \{(x, y):\ x \le t, y > x\}$

and finally

$$Q_{31}(t) = a \int_0^t f_B(x)[1 - H_A(x)]dx\ . \tag{10}$$

Similarly

$Q_{34}(t) = P(U = 1, \zeta_B \le t, \gamma_A < \zeta_B) = a \iint_{C_{34}} f_B(x)dx\, dH_A(y),$ where

$C_{34} = \{(x, y):\ x \le t, y < x\}.$

Hence

$$Q_{34}(t) = a \int_0^t f_B(x)\, H_A(x)dx \tag{11}$$

In a similar way we get

$$Q_{40}(t) = P(U = 0, \zeta_A \le t) = (1 - a)F_A(t), \tag{12}$$

$$Q_{42}(t) = P(U = 1, \zeta_A \le t,\ \gamma_B > \zeta_A) = a \int_0^t f_A(x)[1 - H_B(x)]dx, \tag{13}$$

$$Q_{43}(t) = P(U = 1, \zeta_A \le t, \gamma_B < \zeta_A) = a \int_0^t f_A(x)\, H_B(x)dx, \tag{14}$$

$$Q_{50}(t) = P(U = 0, \zeta_A \le t) = (1 - a)F_A(t), \tag{15}$$

$$Q_{53}(t) = P(U = 1, \zeta_A \le t) = a\, F_A(t), \tag{16}$$

$$Q_{60}(t) = P(U = 0, \zeta_B \le t) = (1 - a)F_B(t), \tag{17}$$

$$Q_{64}(t) = P(U = 1, \zeta_B \le t) = a\, F_B(t) \tag{18}$$

All elements of the kernel $Q(t)$ have been defined, hence the semi-Markov process $\{X(t):\ t \ge 0\}$ describing the reliability of the cold standby system is constructed.

For all states we need to calculate the transition probabilities of the embedded Markov chain and also distributions of the waiting and holding times. Applying (3), (7) - (18) we can determine the transition probabilities matrix of the embedded Markov chain $\{X(\tau_n):\ n = 0,1, \dots\}$

$$\boldsymbol{P} = \begin{bmatrix} 0 & 0 & 0 & 0 & 0 & p & q \\ 0 & 0 & 0 & 0 & 0 & p & q \\ 0 & 0 & 0 & 0 & 0 & p & q \\ p_{30} & p_{31} & 0 & 0 & p_{34} & 0 & 0 \\ p_{40} & 0 & p_{42} & p_{43} & 0 & 0 & 0 \\ 1 - a & 0 & 0 & a & 0 & 0 & 0 \\ 1 - a & 0 & 0 & 0 & a & 0 & 0 \end{bmatrix}, \tag{19}$$

where

$$p_{30} = 1 - \mathrm{a},\ \ p_{31} = a \int_0^\infty f_B(x)[1 - H_A(x)]dx,\ p_{34} = a \int_0^\infty f_B(x)H_A(x)\, dx,$$

$$p_{40} = 1 - \mathrm{a}\,,\ \ p_{42} = a\int_0^\infty f_A(x)[1 - H_B(x)]dx,\ \ p_{43} = a\int_0^\infty f_A(x)H_B(x)dx.$$

Using formula (4) and equalities (8)-(18)we obtain CDF's of the waiting times for the states $i \in S$.

$$G_0(t) = Q_{05}(t) + Q_{06}(t) = p\,H(t) + q\,H(t) = H(t), \tag{20}$$

$$G_1(t) = Q_{15}(t) + Q_{16}(t) = p\,H(t) + q\,H(t) = H(t), \tag{21}$$

$$G_2(t) = Q_{25}(t) + Q_{26}(t) = p\,H(t) + q\,H(t) = H(t), \tag{22}$$

$$G_3(t) = Q_{30}(t) + Q_{31}(t) + Q_{34}(\mathrm{t}) = \tag{23}$$

$$= (1-a)F_B(t) + a\int_0^t f_B(x)[1 - H_A(x)]dx + a\int_0^t f_B(x)\,H_A(x)dx = F_B(t),$$

$$G_4(t) = Q_{40}(t) + Q_{42}(t) + Q_{34}(\mathrm{t}) = \tag{24}$$

$$= (1-a)F_A(t) + a\int_0^t f_A(x)[1 - H_B(x)]dx + a\int_0^t f_A(x)\,H_B(x)dx = F_A(t),$$

$$G_5(t) = Q_{50}(t) + Q_{53}(t) = (1-a)F_A(t) + a\,F_A(t) = F_A(t)\,, \tag{25}$$

$$G_6(t) = Q_{60}(t) + Q_{64}(t) = (1-a)F_B(t) + a\,F_B(t) = F_B(t). \tag{26}$$

Applying the equality (5) and (8)-(19) we calculate CDF's of the holding times.

$$F_{05}(t) = F_{15}(t) = F_{25}(t) = F_{06}(t) = F_{16}(t) = F_{26}(t) = H(t),$$

$$F_{30}(t) = F_B(t),\quad F_{31}(t) = \frac{\int_0^t f_B(x)[1-H_A(x)]dx}{\int_0^\infty f_B(x)[1-H_A(x)]dx}\,, \tag{27}$$

$$F_{34}(t) = \frac{\int_0^t f_B(x)H_A(x)dx}{\int_0^\infty f_B(x)H_A(x)dx}$$

$$F_{40}(t) = F_A(t),\ \ F_{42}(t) = \frac{\int_0^t f_A(x)[1-H_B(x)]dx}{\int_0^\infty f_A(x)[1-H_B(x)]dx}, \tag{28}$$

$$F_{43}(t) = \frac{\int_0^t f_A(x)H_B(x)dx}{\int_0^\infty f_A(x)H_B(x)dx},$$

$$F_{50}(t) = F_{53}(t) = F_A(t),\qquad F_{60}(t) = F_{64}(t) = F_B(t). \tag{29}$$

.

4 Reliability characteristics

Assume that evolution of a system reliability is describe by a finite states pace S semi-Markov process $\{X(t)\colon t \geq 0\}$. Elements of a set S represent the reliability states of the system. Let S_+ consists of the functioning states (up states) and S_- contains all the failed states (down states). The subset S_+ and S_- form a partition of S, i.e., $S = S_+ \cup S_-$ and $S_+ \cap S_- = \emptyset$. Suppose that $i \in S_+$ is an initial state of the process. The conditional reliability function is defined by

$$R_i(t) = P(\forall u \in [0,t],\ X(u) \in S_+ | X(0) = i),\ i \in S_+. \tag{30}$$

Let $S_- = D$, and $S_+ = D'$. From (30) and the Chapman-Kolmogorov property of a two dimensional Markov chain $\{(X(\tau_n), \tau_n)\colon\ n = 0,1,2, \ldots\}$, we obtain

$$R_i(t) = 1 - G_i(t) + \sum_{j\in D'} \int_0^t R_j(t-u)dQ_{ij}(u), \quad i \in D'. \tag{31}$$

Passing to the Laplace transform we get

$$\tilde{R}_i(s) = \frac{1}{s} - \tilde{G}_i(s) + \sum_{j\in D'} \tilde{q}_{ij}(s)\tilde{R}_j(s), \quad i \in D', \tag{32}$$

where $\tilde{R}_j(s) = \int_0^\infty e^{-st}R_j(t)dt.$

The matrix form of the equation system is

$$(I - q_{D'}(s))R(s) = W_{D'}(s), \tag{33}$$

where

$$R(s) = [\tilde{R}_i(s)\colon\ i \in D']^T, \qquad W_{D'}(s) = [\frac{1}{s} - \tilde{G}_i(s)\colon\ i \in D']^T$$

are one column matrices, and

$$q_{D'}(s) = [\tilde{q}_{ij}(s)\colon\ i,j \in D', \qquad I = [\delta_{ij}\colon\ i,j \in D']$$

are square matrices. Note that

$$\tilde{G}_i(s) = \frac{1}{s}\sum_{j\in D'} \tilde{q}_{ij}(s).$$

Elements of the matrix $\widetilde{R}(s)$ are the Laplace transforms of the conditional reliability functions. We obtain the reliability functions $R_i(t),\ i \in D'$ by inverting the Laplace transforms $\tilde{R}_i(s),\ i \in D'$.

Now the equation (33) takes the form

$$\begin{bmatrix} 1 & -\tilde{q}_{34}(s) & 0 & 0 \\ -\tilde{q}_{43}(s) & 1 & 0 & 0 \\ -\tilde{q}_{53}(s) & 0 & 1 & 0 \\ 0 & -\tilde{q}_{64}(s) & 0 & 1 \end{bmatrix} \begin{bmatrix} \tilde{R}_3(s) \\ \tilde{R}_4(s) \\ \tilde{R}_5(s) \\ \tilde{R}_6(s) \end{bmatrix} = \begin{bmatrix} \frac{1}{s} - \tilde{F}_B(s) \\ \frac{1}{s} - \tilde{F}_A(s) \\ \frac{1}{s} - \tilde{F}_A(s) \\ \frac{1}{s} - \tilde{F}_B(s) \end{bmatrix} \tag{35}$$

The solution is

$$\tilde{R}_3(s) = \frac{\tilde{q}_{34}(s)\big(1-s\widetilde{F}_A(s)\big)+\big(1-s\widetilde{F}_B(s)\big)}{s(1-\tilde{q}_{34}(s)\,\tilde{q}_{43}(s))}, \tag{36}$$

$$\tilde{R}_4(s) = \frac{\tilde{q}_{43}(s)\big(1-s\tilde{F}_B(s)\big)+\big(1-s\widetilde{F}_A(s)\big)}{s(1-\tilde{q}_{34}(s)\,\tilde{q}_{43}(s))}, \tag{37}$$

$$\tilde{R}_5(s) = \frac{a\big(1-s\,\tilde{F}_B(s)\big) + a\,\tilde{q}_{34}(s)\big(1-s\,\tilde{F}_A(s)\big)+(1-s\,\tilde{F}_A(s))(1-\tilde{q}_{34}(s)\,\tilde{q}_{43}(s))}{s(1-\tilde{q}_{34}(s)\tilde{q}_{43}(s))}, \tag{38}$$

$$\tilde{R}_6(s) = \frac{a\big(1-s\,\tilde{F}_A(s)\big) + a\,\tilde{q}_{43}(s)\big(1-s\,\tilde{F}_B(s)\big)+(1-s\tilde{F}_B(s))(1-\tilde{q}_{34}(s)\,\tilde{q}_{43}(s))}{s(1-\tilde{q}_{34}(s)\,\tilde{q}_{43}(s))}. \tag{39}$$

The Laplace transform of unconditional reliability function of the system is

$$\widetilde{R}(s) = p\,\widetilde{R}_5(s) + q\tilde{R}_6(s) \tag{40}$$

A conditional means to failure of the system we can calculate using equalities

$$E(\,\Theta_i) = \lim_{s\to 0^+} \tilde{R}(s),\ \ s \in (0,\infty). \tag{41}$$

Therefore, from (38) and (39) and (40) we obtain

$$E(\Theta_5) = \frac{a\,E(T_3)+ap_{34}\,E(T_4)+E(T_5)-p_{34}p_{43}\,E(T_5)}{1-p_{34}p_{43}} = E(\zeta_A) + \frac{a\,E(\zeta_B)+ap_{34}\,E(\zeta_A)}{1-p_{34}p_{43}}, \tag{42}$$

$$E(\Theta_6) = \frac{a\,E(T_4)+ap_{43}\,E(T_3)+E(T_6)-p_{34}p_{43}\,E(T_6)}{1-p_{34}p_{43}} = E(\zeta_B) + \frac{a\,E(\zeta_A)+ap_{34}\,E(\zeta_B)}{1-p_{34}p_{43}}. \tag{43}$$

According to (40), (41) and (42) we get the mean time to failure of the system.

$$E(\,\Theta) = p\,E(\zeta_A) + q\,E(\zeta_B) + p\,a\frac{E(\zeta_B)+p_{34}\,E(\zeta_A)}{1-p_{34}p_{43}} + q\,a\frac{E(\zeta_A)+p_{34}\,E(\zeta_B)}{1-p_{34}p_{43}}, \tag{44}$$

where

$$p_{34} = a\int_0^\infty f_B(x)\,H_A(x)dx, \qquad p_{43} = a\int_0^\infty f_A(x)\,H_B(x)dx. \tag{45}$$

5 An approximate reliability function

In general case calculating an exactly reliability function of the system by means of Laplace transform is a complicated matter. Finding an approximate reliability function of that system is possible by using results from the theory of semi-Markov processes perturbations. The perturbed semi-Markov processes are defined in different ways by different authors. We introduce Pavlov and Ushakov [9] concept of the perturbed semi-Markov process presented by Gercbakh [3]

Let $D' = S - D$ be a finite subset of states and D be at least countable subset of S. Suppose $\{X(t):\ t \geq 0\}$ is SM process with the state space $S = D \cup D'$ and the kernel $\mathrm{Q}(t) = [Q_{ij}(t): i,j \in S]$, the elements of which have the form

$$Q_{ij}(t) = p_{ij}F_{ij}(t). \tag{46}$$

Assume that

$$\varepsilon_i = \sum_{j\in D} p_{ij} \ \text{ and } \ p_{ij}^0 = \frac{p_{ij}}{1-\varepsilon_i}, \quad i,j \in D'. \tag{47}$$

Let us notice that $\sum_{j\in D'} p_{ij}^0 = 1$

A semi-Markov process $\{X(t):\ t \geq 0\}$ *with the discrete state space* S *defined by the renewal kernel* $Q(t) = [\,p_{ij}F_{ij}(t): i,j \in S\,]$, *is called the perturbed process with respect to SM process* $\{X^0(t): t \geq 0\}$ *with the state space* D' *defined by the kernel*

$$Q^0(t) = [\,p_{ij}^0F_{ij}(t): i,j \in D'\,]. \tag{48}$$

We quote our version of I.V. Pavlov and I.A. Ushakov [9] theorem. The random variable $\Theta_{iD} = \inf\{t: X(t) \in D \mid X(0) = i\}$, $i \in D'$ denotes the first passage time from the state $i \in D'$ to the subset D. The function $G_i^0(t) = \sum_{j \in D}, Q_{ij}^0(t)$ denotes CDF of the waiting time in the state $i \in D'$. The number $m_i^0 = \int_0^\infty x\, dG_i^0(t)$, $i \in D'$, is the expected value of the waiting time in state i for the process $\{X^0(t): t \geq 0\}$. Denote the stationary distribution of the embedded Markov chain in SM process $\{X^0(t): t \geq 0\}$ by $\pi^0 = [\pi_i^0: i \in D']$. Let

$$\varepsilon = \sum_{i \in D}, \pi_i^0 \varepsilon_i \quad \text{and} \quad m^0 = \sum_{i \in D} \pi_i^0 m_i^0. \tag{49}$$

We are interested in the limiting distribution of the random variable $\Theta_{iD}, i \in D'$.

Theorem 1. *If the embedded Markov chain defined by the matrix of transition probabilities* $P = [\, p_{ij}: i, j \in S]$ *satisfies following conditions*

- $f_{iA} = P(\Delta_D < \infty | X(0) = i) = 1, \quad i \in D'$,
  $\Delta_D = \min\{n: X(\tau_n) \in D\}$,
- $\underset{i \in D}{\forall} \mu_{iD} = \sum_{n=1}^{\infty} n f_{iD}(n) < \infty$, and
- $\underset{c>0}{\exists} \underset{i,j \in S}{\forall} 0 < E(T_{ij}) \leq c$,

then

$$\lim_{\varepsilon \to 0} P(\varepsilon \Theta_{iD} > x) = e^{-\frac{x}{m^0}}, \tag{50}$$

where $\pi^0 = [\pi_i: i \in D']$ is the unique solution of the linear system of equations

$$\pi^0 = \pi^0 P^0, \quad \pi^0 \mathbf{1} = 1. \tag{51}$$

The considered SM process $\{X(t): t \geq 0\}$ with the state space $S = \{0,1,2,3,4,5,6\}$ we can assume to be the perturbed process with respect to the SM process $\{X^0(t): t \geq 0\}$ with the state space $D' = \{3,4,5,6\}$ and the kernel

$$Q^0(t) = \begin{bmatrix} 0 & Q_{34}^0(t) & 0 & 0 \\ Q_{43}^0(t) & 0 & 0 & 0 \\ Q_{53}^0(t) & 0 & 0 & 0 \\ 0 & Q_{64}^0(t) & 0 & 0 \end{bmatrix}, \tag{52}$$

where

$Q_{34}^0(t) = p_{34}^0 F_{34}(t)$, $Q_{43}^0(t) = p_{43}^0 F_{43}(t)$, $Q_{53}^0(t) = p_{53}^0 F_{53}(t)$,
$Q_{34}^0(t) = p_{63}^0 F_{63}(t)$.

From (4) , (7) and (52) we obtain

$$p_{34}^0 = 1, \quad p_{43}^0 = 1, \quad p_{53}^0 = 1, \quad p_{64}^0 = 1.$$

The transition matrix of the embedded Markov chain of SM process is $\{X^0(t): t \geq 0\}$ is

$$P^0 = \begin{bmatrix} 0 & 1 & 0 & 0 \\ 1 & 0 & 0 & 0 \\ 1 & 0 & 0 & 0 \\ 0 & 1 & 0 & 0 \end{bmatrix}.$$

Taking under consideration presented above the CDF's $F_{ij}(t)$, $t \geq 0$, we get

$$Q_{34}^0(t) = F_{34}(t) = \frac{\int_0^t f_B(x)\, H_A(x)\, dx}{\int_0^\infty f_B(x) H_A(x)\, dx}, \quad (53)$$

$$Q_{43}^0(t) = F_{43}(t) = \frac{\int_0^t f_A(x)\, H_B(x)\, dx}{\int_0^\infty f_A(x) H_B(x)\, dx}, \quad (54)$$

$$Q_{50}^0(t) = F_{50}(t) = F_A(t), \quad Q_{60}^0(t) = F_{60}(t) = F_B(t)$$

From (19) and (47) we have

$$\varepsilon_3 = p_{30} + p_{31} = 1 - \mathrm{a} + a\int_0^\infty f_B(x)[1 - H_A(x)]dx = 1 - a\int_0^\infty f_B(x)H_A(x)dx, \quad (55)$$

$$\varepsilon_4 = p_{40} + p_{42} = 1 - \mathrm{a} + a\int_0^\infty f_A(x)[1 - H_B(x)]dx = 1 - a\int_0^\infty f_A(x)H_B(x)dx, \quad (56)$$

$$\varepsilon_5 = p_{50} = 1 - a, \qquad \varepsilon_6 = p_{60} = 1 - a.$$

From the system of equations

$$[\pi_1^0 \quad \pi_2^0 \quad \pi_3^0 \quad \pi_4^0\,]\, P^0 = [\pi_1^0 \quad \pi_2^0 \quad \pi_3^0 \quad \pi_4^0], \quad \pi_1^0 + \pi_2^0 + \pi_3^0 + \pi_4^0 = 1$$

we get

$$\pi_3^0 = 0.5, \quad \pi_4^0 = 0.5, \quad \pi_5^0 = 0\,, \quad \pi_6^0 = 0\,.$$

From (47), (48) , (50) - (56) and from the presented above theorem it follows that for small ε

$$R(t) = P(\Theta_{iD} > t) = P(\varepsilon\Theta_{iD} > \varepsilon t) \approx \exp\left[-\frac{\varepsilon}{m^0}\, t\right], \quad t \geq 0, \quad (57)$$

where

$$\varepsilon = 0.5(\varepsilon_3 + \varepsilon_4) = 1 - 0.5\, a\left(\int_0^\infty f_B(x)H_A(x)dx + \int_0^\infty f_A(x)H_B(x)dx\right) \quad (58)$$

and

$$m^0 = 0.5(m_3^0 + m_4^0) = 0.5\frac{\int_0^\infty x f_B(x)H_A(x)dx}{\int_0^\infty f_B(x)H_A(x)dx} + 0.5\frac{\int_0^\infty x f_A(x)H_B(x)dx}{\int_0^\infty f_A(x)H_B(x)dx}. \quad (59)$$

From the shape of the parameter ε it follows that we can apply this formula only if the numbers $P(\gamma_B \geq \zeta_A)$, $P(\gamma_A \geq \zeta_B)$ denoting probabilities of the components failure during the repair periods of an earlier failed components, are small.

6 Conclusions

- The reliability model of the cold standby system consist of two different units is constructed by using the concept of the embedded semi-Markov process.
- Results of semi-Markov process theory allowed us to compute reliability characteristics of the system.
- The Laplace transform of unconditional reliability function of the system is

$$\widetilde{R}(s) = p\,\widetilde{R}_5(s) + q\tilde{R}_6(s),$$

where the Laplace transform of conditional reliability functions $\widetilde{R}_5(s)$, $\tilde{R}_6(s)$ are given by (38) and (39).

- The mean time to failure of the considered cold standby system depend on of the both components probability distribution of the lifetimes and renewal times and also on initial distribution of the process and the switch reliability

$$E(\Theta) = p\,E(\zeta_A) + q\,E(\zeta_B) + p\,a\frac{E(\zeta_B) + p_{34}\,E(\zeta_A)}{1 - p_{34}p_{43}} + q\,a\frac{E(\zeta_A) + p_{34}\,E(\zeta_B)}{1 - p_{34}p_{43}},$$

$$p_{34} = a\int_0^\infty f_B(x)H_A(x)\,dx, \quad p_{43} = a\int_0^\infty f_A(x)H_B(x)\,dx.$$

- If operating process starts from the state 5 with probability $p = 1$ then mean time to failure is

$$E(\Theta) = E(\zeta_A) + a\frac{E(\zeta_B)+p_{34}\,E(\zeta_A)}{1-p_{34}p_{43}}.$$

This results was presented in [5].

- If distributions of times to failure and renewal times of components A and B are identical: $f_A(x) = f_B(x) = f(x)$, $H_A(x) = H_B(x) = H(x)$, we obtain result shown in [4]

$$E(\Theta) = E(\zeta) + a\,\frac{E(\zeta)}{1-c} \quad \text{where} \quad c = a\int_0^\infty f(x)H(x)\,dx.$$

The cold standby causes the increase of the mean time to failure $1 + \frac{a}{1-c}$ times in this case.

- If moreover the switch is reliable ($a = 1$) we get well known result presented in [1], [2], [7].

- The approximate reliability function of the system is exponential (58)

$$R(t) \approx \exp\left[-\frac{\varepsilon}{m^0}\,t\right], \quad t \geq 0$$

where according to (58) and (59)

$$\varepsilon = 1 - 0.5\,a\left(\int_0^\infty f_B(x)H_A(x)dx + \int_0^\infty f_A(x)H_B(x)dx\right),$$

$$m^0 = 0.5\frac{\int_0^\infty xf_B(x)H_A(x)dx}{\int_0^\infty f_B(x)H_A(x)dx} + 0.5\frac{\int_0^\infty xf_A(x)H_B(x)dx}{\int_0^\infty f_A(x)H_B(x)dx}.$$

References

1. R.E. Barlow , F.Proshan , Statistical theory of reliability and life testing. Holt, Rinchart and Winston, Inc., New York 1975.
2. S.M Brodi, J.A. Pogosian, Embedded stochastic processes in theory of queue. Naukova Dumka, Kiev 1977 (in Russian).
3. B. Gertsbakh, Asymptotic methods in reliability theory: a review. *Adv. Appl. Prob.*, 16, 1984, p. 147-175.
4. F. Grabski, Semi-Markov models of reliability and operation. Warszawa 2002, IBS PAN, pp.161, (in Polish).
5. F. Grabski, *Semi-Markov Processes: Applications in Systems Reliability and Maintenance*. Elsevier; Amsterdam, Boston, Heidelberg, London, New York, Oxford, Paris, San Diego, San Francisco, Sydney, 2015.
6. Gyllenberg, D.S Silvestrov, Quasi-Stationary Phenomena in Nonlinearly Stochastic System. De Gruyter Exposition in Mathematics, 44, Walter de Gruyter, Berlin, 2008, XII , 579 pages.
7. V.S.Korolyuk, A.F. Turbin, Semi-Markov processes and their applications. Naukova Dumka,Kiev 1976, (in Russian).
8. N. Limnios G. Oprisian, Semi-Markov Processes and Reliability, Boston, Birkhauser, 2001.
9. I.V. Pavlov and I.A. Ushakov : The asymptotic distribution of the time until a semi-Markov process gets out of the kernel. Engineering Cybernetics, 1978,20 (3).
10. D.C. Silvestrov, Semi-Markov processes with a discrete state space. Sovetskoe Radio, Moskov 1980, (in Russian).

Limit theorems for queueing systems with different service disciplines

Grishunina Svetlana[1]

Department of Probability Theory, Lomonosov Moscow State University, GSP-1, 1 Leninskiye Gory, Main Building, 119991; Moscow Institute of Electronics and Mathematics, National Research University Higher School of Economics, 34 Tallinskaya Street, 123458, Moscow, Russia
(E-mail: svetagri@live.ru)

Abstract. In this paper a multi-server queueing system with regenerative input flow and independent service times with finite means is studied. We consider queueing systems with various disciplines of the service performance: systems with a common queue and systems with individual queues in front of the servers. In the second case an arrived customer chooses one of the servers in accordance to a certain rule and stays in the chosen queue up to the moment of its departure from the system. We define some classes of disciplines and analyze the asymptotical behaviour of a multi-server queueing system in a heavy-traffic situation (traffic rate $\rho \geq 1$). The main result of this work is limit theorems concerning the weak convergence of scaled processes of waiting time and queue length to the process of the Brownian motion for the case $\rho > 1$ and its absolute value for the case $\rho = 1$.
Keywords: Queueing System, Heavy-traffic, Limit Theorems, Service Disciplines.

1 Introduction

A wide class of multi-channel queueing models appears to be useful in practice. Queues are an everyday occurance: people waiting an available seller in a supermarket, uploading internet pages. Queues can be used to model many different systems in various areas of our life: computer systems, supermarkets, transport systems, finance and insurance and others. There are three basic characteristics of a queueing process: the input flow of customers, the service discipline and the service facilities. The simplest of such systems can be analysed by assuming Poisson input flow, independent identically distributed exponential service times and discipline FIFO. The more common but more complicated case is a regenerative input flow. Note that the most part of the flows under consideration in the queueing theory are regenerative. For example, Double stochastic Poisson process with a regenerative random intensity (see Grandell[9]), Markov modulated (see Asmussen[4]), semi-markov. Many others processes belong to this class. The description of such processes and their properties one may find in Afanasyeva *et al.*[3].

In this paper we analyze the asymptotical behaviour of a queueing system with a regenerative input flow and r identical parallel servers in a heavy-traffic situation (traffic rate $\rho \geq 1$). To the best of our knowledge multi-channel queueing systems in the case when the traffic rate $\rho \geq 1$ are studied since the

17^{th} *ASMDA Conference Proceedings, 6 - 9 June 2017, London, UK*

late 1970s (see Foley and McDonald[8], Eschenfeldt and Gamarnik[7], Liu *et al.*[12]).

Afanasyeva and Bashtova[2] proved the convergence of the scaled processes of the queue length and waiting time for the queueing system with a single server.

We extend this result to queueing systems with various disciplines of the service performance: systems with a single queue and systems with individual queues in front of the servers. In the second case an arriving customer chooses one of the servers according to defined rule and stays in the chosen queue up to the moment of the departure from the system. So we have r single-server queueing systems.

Although there is a huge literature on multi-channel queueing systems the asymptotical behaviour for the scaled processes of the waiting time and queue length in a heavy-taffic situation for a multi-channel queueing system with a regenerative input flow has not been considered yet. The scientific novelty of this work is that we consider quite general input flow and broad classses of disciplines.

2 Model Description

We consider a queueing system with a regenerative input flow. Assume a stochastic process $\{A(t), t \geq 0\}$, $A(0) = 0$, taking values 0,1,2,..., to be defined on a probability space (Ω, F, P). The process has non-decreasing and left-continuous sample paths.

Definition 1. The input flow $A(t)$ is regenerative if there exists an increasing sequence of random variables $\{\theta_j\}_{j=1}^{\infty}$, $\theta_0 = 0$, such that the sequence $\{\kappa_j\}_{j=1}^{\infty} = \{\theta_j - \theta_{j-1}, A(\theta_{j-1} + t) - A(\theta_{j-1}), t \in [0, \theta_j - \theta_{j-1})\}_{j=1}^{\infty}$ consists of independent identically distributed(iid) random elements.

Then θ_j is the j-th point of regeneration and $\tau_j = \theta_j - \theta_{j-1}$ is the j-th regeneration period, $\xi_j = A(\theta_j) - A(\theta_{j-1})$ and $\mu = \mathbf{E}\tau_1 < \infty,\ a = \mathbf{E}\xi_1 < \infty$.

The service times $\{\eta_j\}_{j=1}^{\infty}$ are supposed to be independent identically distributed (iid) random variables with distribution function $B(x)$ and finite mean $b = \int_0^{\infty} x dB(x)$. Furthermore, the sequence $\{\eta_j\}_{j=1}^{\infty}$ doesn't depend on $A(t)$. There are r identical servers in the system. We consider queueing systems with various rules (disciplines) of the service performance. Firstly, it is the systems with a single queue. Another case - systems with individual queues in front of the servers. An arriving customer chooses one of the servers for service according to defined rule and stays in the chosen queue up to the moment of the departure from the system. So we have r single-server queueing systems. For disciplines with interruptions of the service we assume that the service that was interrupted is continued after return the customer to a server from the point at which it was interrupted. So that all the customers are characterized by their residual service times.

The following disciplines may be considered as examples.

(i) There exists a single queue. We consider a class of so-called conservative disciplines such that the number of working servers at time t is equal to $min(r, Q(t))$, where $Q(t)$ is the total number of customers at the system at time t.
Denote D_0 discipline FIFO(first in - first out) and introduce two disciplines D_1 and D_2 with interruptions of service. For D_1 (D_2) at any time t the residual service time of the customer that is on a server is not more(less) than residual service times of the customers waiting in the single queue(if there are).

(ii) An arriving customer is served by the j-th server with probability $\frac{1}{r}$ independently of others(discipline D_3).

(iii) The n-th customer is directed for service to the j-th server if $n = rm + j$, where $m = 0, 1, 2, \ldots, j = \overline{1, r}$ (cycled discipline D_4).

(iv) A server has its own queue and an arriving customer chooses a server with minimal queue in front of it(discipline D_5). If there are several servers with minimal queues an arriving customer chooses each of them randomly with equal probabilities.

Let $q_i(t)$ be the number of customers which have to be served by the i-th server at time t in accordance with a discipline under consideration and $\eta_{ji}(t)$ be the residual service time of the j-th customer on the i-th server ($j = 1, \ldots, q_i(t), i = 1, \ldots, r$). We put $\eta_{ji}(t) = 0$ if $q_i(t) = 0$.

Denote

$$\overrightarrow{q}(t) = (q_1(t), \ldots, q_r(t)),$$
$$\overrightarrow{W}(t) = (W_1(t), \ldots, W_r(t)), \text{ where } W_i(t) = \sum_{j=1}^{q_i(t)} \eta_{ji}(t).$$

We also consider embedded processes

$$\overrightarrow{Q}_n = \overrightarrow{q}(\theta_n - 0) = (q_{n1}, \ldots, q_{nr}),$$
$$\overrightarrow{W}_n = \overrightarrow{W}(\theta_n - 0) = (W_{n1}, \ldots, W_{nr}),$$

and sums of coordinates

$$W(t) = \sum_{j=1}^{r} W_j(t), \qquad W_n = W(\theta_n - 0),$$
$$Q(t) = \sum_{j=1}^{r} q_j(t), \qquad Q_n = Q(\theta_n - 0).$$

Proposition 1. *For each server $i = \overline{1, r}$*

$$P\{\xi_1 = 0, \tau_1 > 0\} + P\{\xi_1 = 1,\ t_1 + \eta_{i1} < \tau_1\} > 0.$$

Here t_1 is the arrival time of the first customer.

To formulate our results we separate classes of disciplines.

Definition 2. Discipline D belongs to the class K_0, if the convergence $Q_n = \sum_{i=1}^{r} q_{ni} \xrightarrow{P} \infty$ as $n \to \infty$ involves the convergence $q_{ni} \xrightarrow{P} \infty$ as $n \to \infty$ for all $i = 1, \ldots, r$. (Property 1a)

Definition 3. Discipline D belongs to the class K_1, if it has property 1a and additionally the convergence $Q_n \to \infty$ (w.p.1.)(with probability 1) as $n \to \infty$ involves the convergence $q_{ni} \to \infty$ (w.p.1) as $n \to \infty$ for all $i = \overline{1,r}$ (Property 2a)

We say that a discipline has a property of symmetry if for any permutation $(i_1, \ldots, i_r)$ of numbers $(1, 2, \ldots, r)$ and $t > 0$ following equalities take place in distribution

$$(q_{i_1}(t), \ldots, q_{i_r}(t)) \stackrel{d}{=} (q_1(t), \ldots, q_r(t)),$$

$$(W_{i_1}(t), \ldots, W_{i_r}(t)) \stackrel{d}{=} (W_1(t), \ldots, W_r(t)),$$

provided that these equalities hold an initial time $t = 0$.

Definition 4. A symmetry discipline D belongs to the class K_2, if the flow $A_i(t)$ of customers that have to be served by the i-th server is a regenerative one for any $i = \overline{1,r}$. Additionally, the sequence $\{\theta_n^{(i)}\}_{n=1}^{\infty}$ of regeneration points is a subsequence $\{\theta_{n_\alpha(i)}^{(i)}\}_{\alpha=1}^{\infty}$ of the sequence of regeneration points $\{\theta_n\}_{n=1}^{\infty}$ of the input flow $A(t)$.

3 Limit theorem in the case $\rho > 1$

A regenerative flow has the following important property (see Afanasyeva and Bashtova[2]).

Property 1. There exists $\lambda = \lim\limits_{n\to\infty} \frac{A(t)}{t} = \frac{a}{\mu}$ (w.p.1) and λ is the intensity of input flow $A(t)$.

The stability condition for the processes W_n and Q_n for the disciplines from the class K_0 is $\rho = \lambda b r^{-1} < 1$ as it was shown in Grishunina[10].

Here our problem is to investigate the asymptotical behaviour of the system in a heavy-traffic situation in a case when $\rho > 1$.

Theorem 1. *Let*

$$E\tau_1^{2+\delta} < \infty, \quad E\xi_1^{2+\delta} < \infty, \quad E\eta_1^{2+\delta} < \infty \tag{1}$$

for some $\delta > 0$. If $\rho > 1$ then for any discipline from class K_1 processes

$$\tilde{W}_T(t) = \frac{W(tT) - (\lambda b - r)tT}{\sigma_W \sqrt{T}}, \quad \tilde{Q}_T(t) = \frac{Q(tT) - (\lambda - \frac{r}{b})tT}{\sigma_Q \sqrt{T}}$$

converge weakly as $T \to \infty$ to Brownion motion on any interval $[\alpha, \beta]$. Here

$$\sigma_W^2 = b^2\sigma_Q^2, \quad \sigma_Q^2 = \sigma_A^2 + r\sigma_\eta^2 b^{-3}, \quad \sigma_A^2 = \sigma_\xi^2/\mu + a^2\sigma_\tau^2/\mu^3 - 2acov(\xi,\tau)/\mu^2 \tag{2}$$

and σ_ξ^2 and σ_τ^2 - are variances of ξ and τ respectively.

Proof. It is sufficient to prove the convergence only for the process $\tilde{Q}_T(t)$ because of the results by Borovkov [6] (ch. 4 par. 25) concerning the connection between processes $W(t)$ and $Q(t)$. Our proof will be based on the result from Borovkov[5](Par. 2 Th. 1). The process $\tilde{Q}_n(t)$ converges to Brownian motion if and only if:

1. Finite-dimensional distributions of the process $\tilde{Q}_n(t)$ converge weakly to the finite-dimensional distributions of the Brownian motion;
2. For any $\epsilon > 0$

$$\lim_{\Delta \to 0} \limsup_n P(\sup_{|t_1 - t_2| < \Delta} |\tilde{Q}_T(t_1) - \tilde{Q}_T(t_2)| > \epsilon) = 0$$

Consider the workload process $\overset{\circ}{W}(t)$ for a single-server system wth input flow $A(t)$ and $B(rt)$ as a distribution function of the service time. If $W(0) = \overset{\circ}{W}(0) = 0$, then for any discipline from K_1 we have

$$W(t) \geq \overset{\circ}{W}(t),\ t \geq 0. \tag{3}$$

It was proved in Afanasyeva[1]), that $\overset{\circ}{W}(t) \to \infty$ if $t \to \infty$ and $\rho > 1$. In view of inequality (3) and definition of class K_1 we get

$$q_i(t) \xrightarrow[t \to \infty]{} \infty \text{ (w.p.1)},\ i = \overline{1, r}$$

for any rule of choice from K_1. Therefore for any ε there exists t_ε such that

$$P(A_\varepsilon) > 1 - \varepsilon$$

where the event A_ε is determined as follows

$$A_\varepsilon = \{q_i(t) > 0,\ i = \overline{1, r},\ \forall t \geq t_\varepsilon\}.$$

Let us introduce the sequence $\{Y_j^{(i)}\}_{j=1}^{\infty}$ of independent random variables. Here $Y_1^{(i)}$ is the residual service time of the customer serving by the ith server at time t_ε if $q_i(t_\varepsilon) > 0$ and 0 otherwise.

The sequence $\{Y_j^{(i)}\}_{j=2}^{\infty}$ consists of service times of customers starting their service on the ith server after t_ε. Denote

$$Y_i(t) = max\{k \geq 0 : \sum_{j=1}^{k} Y_j^{(i)} < t\},\ Y_i(0) = 0,\ i = \overline{1, r} \text{ and } Y(t) = \sum_{i=1}^{r} Y_i(t).$$

It follows from the Central Limit Theorem for renewal processes (see Borovkov[6]) that scaled process

$$\tilde{Y}_T(t) = \frac{Y_i(tT) - tTb^{-1}}{\sqrt{T\sigma_\eta^2 / b^3}}$$

converges weakly to Brownian motion as $T \to \infty$ on any finite interval $t \in [0, h]$. Here σ_η^2 is the variance of η_j. Moreover, from the properties for a regenerative input flow (see Afanasyeva and Bashtova[2]) we get that

$$\tilde{A}_T(t) = \frac{A(tT) - \lambda tT}{\sigma_A \sqrt{tT}} \tag{4}$$

converges weakly to Brownian motion. Let $Z(t) = A(t) - Y(t)$. Then the scaled process

$$\tilde{Z}(tT) = \frac{Z(tT) - (\rho - 1) r b^{-1} tT}{\sigma_Q \sqrt{T}}$$

converges weakly to Brownian motion $V(t)$ as $T \to \infty$. Here σ_Q^2 is defined by (2).

We see that the process $Z(t)$ is costructed in such a way that on the set A_ε the following inequality holds

$$Q(tT) = Q(t_\varepsilon) + Z(tT) - Z(t_\varepsilon).$$

We introduce the multi-dimensional distribution functions for $t_1 \le t_2 \le \cdots \le t_n$

$$F(\overrightarrow{t}, \overrightarrow{x}) = P(\tilde{Z}(t_1) \le x_1, \ldots, \tilde{Z}(t_n) \le x_n),$$

$$G(\overrightarrow{t}, \overrightarrow{x}) = P(\tilde{Q}(t_1) \le x_1, \ldots, \tilde{Q}(t_n) \le x_n),$$

$$\Phi(\overrightarrow{t}, \overrightarrow{x}) = P(V(t_1) \le x_1, \ldots, V(t_n) \le x_n).$$

We remind that $V(t)$ is a standard Brownian motion. Now we have

$$|G(\overrightarrow{t}T, \overrightarrow{x}) - \Phi(\overrightarrow{t}, \overrightarrow{x})| \le |G(\overrightarrow{t}T, \overrightarrow{x}) - F(\overrightarrow{t}T, \overrightarrow{x})| + |F(\overrightarrow{t}T, \overrightarrow{x}) - \Phi(\overrightarrow{t}, \overrightarrow{x})| = \\ = I_1(T) + I_2(t).$$

Here $I_2(t) \to 0$ as $T \to \infty$.

Let $t_1 T > t_\varepsilon$.

For the first term we have

$$I_1(t) = \left| P\left(\frac{Q(t_\varepsilon) - Z(t_\varepsilon)}{\sigma_Q \sqrt{T}} + \tilde{Z}(\overrightarrow{t}T) \le \overrightarrow{x};\ A_\varepsilon \right) + P(\tilde{Q}(\overrightarrow{t}T) < \overrightarrow{x};\ \overline{A}_\varepsilon) - \right.$$

$$\left. - P(\tilde{Z}(\overrightarrow{t}T) < \overrightarrow{x}) \right| \le 2P(\overline{A}_\varepsilon) + \left| P\left(\frac{Q(t_\varepsilon) - Z(t_\varepsilon)}{\sigma_Q \sqrt{T}} + \tilde{Z}(\overrightarrow{t}T) \le \overrightarrow{x} \right) - \right.$$

$$\left. - P(\tilde{Z}(\overrightarrow{t}T) < \overrightarrow{x}) \right| \to 0 \text{ as } T \to \infty$$

Therefore Condition 1 from the Theorem by Borovkov is fulfilled.

Now we prove that the second condition of the Theorem that is for any $\epsilon > 0$

$$\lim_{\Delta \to 0} \limsup_n P\Big(\sup_{|t_1 - t_2| < \Delta} |\tilde{Q}_T(t_1) - \tilde{Q}_T(t_2)| > \epsilon \Big) = 0.$$

We note that $|\tilde{Q}_T(t_1) - \tilde{Q}_T(t_2)| = |\tilde{Z}_T(t_1) - \tilde{Z}_T(t_2)|$ and since $\tilde{Z}_T(t)$ converges weakly to Brownian motion then from the mentioned Theorem by Borovkov for any $\epsilon > 0$

$$\lim_{\Delta \to 0} \limsup_n P(\sup_{|t_1 - t_2| < \Delta} |\tilde{Z}_T(t_1) - \tilde{Z}_T(t_2)| > \epsilon) = 0.$$

Therefore this statement is true for the process $\tilde{Q}_T(t)$.

The conditions of Borovkov theorem are fulfilled for the process $\tilde{Q}_T(t)$ and thus this process converges weakly to Brownian motion.

4 Corollaries

Corollary 1. *Let (1) be fulfilled and $\rho > 1$. Then for a multi-channel system with a single queue and any conservative discipline the statements of the Theorem 1 are true.*

Proof. First we note that disciplines D_1 and D_2 belong to class K_1. Therefore Theorem 1 is true for these disciplines. Let $W^D(t)$ be a process $W(t)$ for a system with a single queue and conservative discipline D. For the simplicity let the queue start out empty, i.e. $W^D(0) = 0$. Then one can easy verify that stochastic inequalities

$$W^{D_2}(t) \leq W^D(t) \leq W^{D_1}(t),\ t \geq 0 \tag{5}$$

take place for any conservative discipline. Therefore the proof is completed.

Lemma 1. *Let $\rho > 1$ and Proposition 1 be fulfilled. Then for a system with any discipline from class K_2 the convergence*

$$q_i(t) \xrightarrow[t \to \infty]{} \infty \text{ (w.p.1)},\ i = \overline{1, r} \tag{6}$$

takes place, i.e. $K_2 \in K_1$. Therefore Theorem 1 is fulfilled for disciplines from class K_2.

Proof. Since the proof is almost evident we omit it here.

Corollary 2. *Let (1) be fulfilled and $\rho > 1$. Then the statements from Theorem 1 are true for disciplines D_3, D_4, D_5.*

Proof. The result for disciplines D_3 and D_4 follows from Lemma 1. For D_5 this statement is proved by Grishunina[10].

5 Limit theorem for the case $\rho = 1$

First we consider a system with a single queue and FIFO discipline.

Theorem 2. *Let (1) be fulfilled and $\rho = 1$. Then for a system with a single queue and FIFO discipline the scaled process*

$$\hat{Q}_T(t) = \frac{Q(tT)}{\sigma_Q \sqrt{T}}$$

converges weakly as $T \to \infty$ to absolute value of the Brownian motion on any finite interval $[\alpha, \beta]$. Here σ_Q is given by (2).

Proof. In view of Property of the regenerative flow (4) one may apply the approach proposed in Iglehart and Whitt[11] for a system with a recursive flow. The modification is perfectly not significance.

For a queueing system with separate queues in front of the servers and with a discipline D from class K_2 denote $A_j^D(t)$ the input flow for the ith server. Since $A_j^D(t)$ is a regenerative flow, under (1) there exists

$$\lim_{t\to\infty} \frac{VarA_j^D(t)}{t} = \sigma^2_{A_D}$$

not depending on j for $D \in K_0$.

Corollary 3. *Let (1) be fulfilled and $\rho = 1$. Then for a system with discipline $D \in K_2$ scaled number of customers in the jth server*

$$\hat{q}^T_{j_D}(t) = \frac{q_{j_D}(tT)}{\sigma_{q_D}\sqrt{T}}$$

converges weakly as $T \to \infty$ to absolute value $v_j(t)$of the Brownian motion on any finite interval $[\alpha, \beta]$. Here

$$\sigma^2_{q_D} = \sigma^2_{A_D} + \frac{\sigma^2_\eta}{b^3}. \tag{7}$$

Proof. Since $D \in K_2$ the process $A_j^D(t)$ is a regenerative flow the statement of the Corollary follows from Theorem 2.

To employ the result we have to calculate $\sigma^2_{A_D}$. Let us give some examples.

Example 1.

Consider discipline D_3. Let $\xi_n^{(j)}$ be the number of customers arriving to the jth server during the nth regeneration period of A(t). Then we have the stochastic equality

$$\xi_n^{(j)} = \sum_{i=1}^{\xi_n} \delta_{ij}^{(n)},$$

where $\{\delta_{ij}^{(n)}\}$ is a sequance of i.i.d. random variables and $P(\delta_{ij}^{(n)} = 1) = r^{-1}$, $P(\delta_{ij}^{(n)} = 0) = 1 - r^{-1}$. One can easily get $E\xi_n^{(j)} = r^{-1}a$, $Var\xi_n^{(j)} = ar^{-1}(1 - r^{-1}) + r^{-2}\sigma^2_\xi$, $cov(\tau_n, \xi_n^{(j)}) = r^{-1}cov(\tau_n, \xi_n)$. It follows from (2).

$$\sigma^2_{A_{D_3}} = \frac{\sigma^2_\xi}{r^2\mu} + \frac{a(r-1)}{r^2\mu} + \frac{a^2\sigma^2_\tau}{r^2\mu^3} - 2\frac{cov(\tau,\xi)}{r\mu^2}. \tag{8}$$

For a renewal process $A(t)$ ($a = 1$, $cov(\tau, \xi)) = 0$, $\sigma_\xi^2 = 0$)

$$\sigma^2_{A_{D_3}} = \frac{\sigma^2_\tau}{r^2\mu^3} + \frac{r-1}{r^2\mu} \tag{9}$$

and for a Poisson flow with an intensity λ

$$\sigma^2_{A_{D_3}} = \frac{\lambda}{r}. \tag{10}$$

Corollary 4. *Let (1) be fulfilled, $\rho = 1$ and $A(t)$ be a Poisson process with an intensity λ. Then for a system with the discipline D_3 scaled number of customers in the system*

$$\hat{Q}^{D_3}_T(t) = \frac{\sum\limits_{j=1}^{r} q_{j_{D_3}(tT)}}{\sigma_{q_{D_3}}\sqrt{T}}$$

converges weakly as $T \to \infty$ to $\overline{V}_{D_3}(t) = \sum\limits_{j=1}^{r} V_j(t)$ where $V_j(t)$ ($j = \overline{1,r}$) are independent processes and each of them is the absolute value of the Brownian motion. Normalized coefficient is given by the formula

$$\sigma_{q_{D_3}} = \frac{\lambda}{r} + \frac{\sigma^2_\eta}{b^3}. \tag{11}$$

Proof. We note that input flows $A^{D_3}_j(t)$ ($j = \overline{1,r}$) are independent Poisson flows intensity λ/r. Therefore processes $\hat{q}^{(T)}_{j_{D_3}}(t)$ ($j = \overline{1,r}$) are mutially independent and the statement follows from Corollary 3.

Example 2.

Here we consider a system with the discipline D_4 and a renewal input $A(t)$. Then

$$\sigma^2_{A_{D_4}} = \frac{\sigma^2_\tau}{r^2\mu^3} \tag{12}$$

and for a Poisson process with the intensity λ

$$\sigma^2_{A_{D_4}} = \frac{\lambda}{r^2}. \tag{13}$$

Now assume that $A(t)$ is a renewal process ($a = 1$, $\sigma^2_\xi = 0$). Let us compare mathematical expectation of $\sigma_Q V(t)$ for a system with a single queue and the mean of the sum of limiting processes $\sigma_{Q_{D_4}} \sum\limits_{j=1}^{r} V_j(t)$ for disciplines D_3 and D_4. Since $EV(t) = \sqrt{\frac{2}{\pi}}t$, we get from (9), (10) and (11).

$$m_{D_0}(t) = E\sigma_Q V(t) = \sqrt{\frac{2}{\pi}}t\sqrt{\frac{\sigma^2_\tau}{\mu^3} + r\frac{\sigma^2_\eta}{b^3}};$$

$$m_{D_3}(t) = E\sigma_{q_{D_3}} \sum_{j=1}^{r} V_j(t) = \sqrt{\frac{2}{\pi}} t \sqrt{\frac{\sigma_\tau^2}{\mu^3} + \frac{r-1}{\mu} + r^2 \frac{\sigma_\eta^2}{b^3}};$$

$$m_{D_4}(t) = E\sigma_{q_{D_4}} \sum_{j=1}^{r} V_j(t) = \sqrt{\frac{2}{\pi}} t \sqrt{\frac{\sigma_\tau^2}{\mu^3} + r^2 \frac{\sigma_\eta^2}{b^3}}.$$

We see that these functions coincide when $r = 1$ but for the case $r > 1$

$$m_{D_0}(t) < m_{D_3}(t) < m_{D_4}(t).$$

Futhermore, $m_{D_0}(t) = m_{D_4}(t)$ if $\sigma_\eta^2 = 0$ We also note that all these functions for any fix t tend to infinity as $r \to \infty$ if $\sigma_\eta^2 > 0$. In point of view of this criteria disciplines D_3 and D_4 are asimptotically equivalent for large r, namely,

$$\frac{m_{D_3}(t)}{m_{D_4}(t)} \to 1 \text{ as } \tau \to \infty.$$

But discipline D_0(general queue) is essentially better since

$$\frac{m_{D_0}(t)}{m_{D_3}(t)} = O(\frac{1}{\sqrt{r}}) \to 0 \text{ as } \tau \to \infty.$$

6 Conclusion

In this paper we considered a queueing system with regenerative input flow and various service disciplines in the heavy-traffic situation($\rho \geq 1$). We proved the convergence of the scaled queue length and waiting time processes to the Brownian motion and gave some examples. There are many good directions for the future research.

Aknowlegement. Work is partially supported by RFBR grant 17-01-00468.

References

1. L. G. Afanaseva. Queueing Systems with Cyclic Control Processes. *Cybernetics and systems analysis* 41 **1**, 43–55, 2005.
2. L. G. Afanaseva and E. E. Bashtova. Coupling method for asymptotic analysis of queues with regenerative input and unreliable server, *Queueing Systems* 76 **2**, 125–147, 2014.
3. L. Afanasyeva, E. Bashtova and E. Bulinskaya. Limit Theorems for Semi-Markov Queues and Their Applications, *Communications in Statistics Part B: Simulation and Computation* 41 **6**, 688–709, 2012.
4. S. Asmussen. Ladder heights and the Markov-modulated M|G|1 queue, *Stochastic Process and its Applications* 37, 313–326, 1991.
5. A. Borovkov. *Asymptotic methods in Queueing Theory*, Chichester:Wiley, 1984.
6. A. Borovkov. *Stochastic processes in Queueing Theory*, Springer-Verlag, 1976.
7. P. Eschenfeldt and D. Gamarnik, *Join the Shortest Queue with Many Servers. The Heavy Traffic Asymptotics*, Preprint, arXiv:1502.00999.

8. R. D. Foley and D. R. McDonald, Join the Shortest Queue: Stability and Exact Asymptotics, *Ann. Appl. Probab.* 11, 569–607, 2001.
9. J.Grandell. *Double stochastic poisson processes*, Lecture Notes in Mathematics, Springer Berlin Heidelberg, New York, 1976).
10. S. A. Grishunina. *Queueing systems with different service disciplines*, International Conference "Supercomputer Simulations in Science and Engineering", Moscow, 2016.
11. D. L. Iglehart and W. Whitt. The Equivalence of Functional Central Limit Theorems for Counting Processes and Associated Partial Sums. *Ann. Math. Statist.* 42 **4**, 1372–1378, 1971.
12. Y. Liu, W. Whitt and Y. Yu. Approximations for heavily loaded $G/GI/n + GI$ Queues. *Naval Research Logistics* 63 **3**, 187–217, 2016.

Some asymptotic results for Truncated-Censored and Associated data

Zohra Guessoum[1] and Abdelkader Tatachak[2]

[1] Lab. M.S.T.D., Faculté de Mathématiques,
U.S.T.H.B., BP 32, El Alia, 16111, Algeria
(E-mail: zguessoum@usthb.dz)
[2] Lab. M.S.T.D., Faculté de Mathématiques,
U.S.T.H.B., BP 32, El Alia, 16111, Algeria
(E-mail: atatachak@usthb.dz)

Abstract. Left truncation and right censoring (LTRC) arise frequently in practice for life data. Under LTRC model, the product limit estimator (PLE) was proposed and investigated in the i.i.d. case by Tsai et al [11]. In the presence of covariates, the conditional version was studied in the α-mixing setting by Liang et al [9]. Our focus in the present paper is to assess strong uniform consistency rates for the cumulative hazard and the product limit estimates when the lifetime observations form an associated sequence. Then, as an application we derive a strong uniform consistency rate for the kernel estimator of the hazard rate function introduced and studied in the i.i.d. case by Uzuno$\bar{g}$ullari and Wang [12].
Keywords: Associated data, Left truncation, Right censoring, Strong uniform consistency rate, Truncated-censored data.

1 Introduction

Suppose that $\{Y_i;\ i = 1, \ldots, N\}$ forms a strictly stationary associated sequence. Recall that a sequence $S_1, S_2, ..., S_N$ is said to be associated if for every pair of component-wise non-decreasing functions $g_1 : \mathbb{R}^N \to \mathbb{R}$ and $g_2 : \mathbb{R}^N \to \mathbb{R}$, we have

$$cov(g_1(\mathbf{S}), g_2(\mathbf{S})) \geq 0$$

where $\mathbf{S} = (S_1, S_2, ..., S_N)$. An infinite family $\{S_N, N \geq 1\}$ of random variables (r.v's) is said to be associated if every finite sub-family of r.v's is associated. This definition was introduced by Esary et al. [4] in the context of reliability studies.
In the complete associated data case, there is a vast literature devoted to the study of the non parametric estimation and numerous are the papers dealing with survival function and density estimation. To cite only a few of them, Bagai and Prakasa Rao [1] proposed an estimator of the survival function and established its consistency. Roussas [10] established its asymptotic normality. A general method of density estimation for associated random variables has been proposed by Dewan and Prakasa Rao [3].
In the incomplete data case, there are no much works dealing with this kind of model under association condition.Recall that among the different forms in

which incomplete data appear, censoring or/and truncation are two common ones.

Under random right censoring, Cai and Roussas [2] established uniform strong consistency and asymptotic normality for the Kaplan-Meier estimator, while Ferrani et al. [5] established strong consistency rates of kernel density and mode estimates.

Under random left truncated model, Guessoum et al. [7] established the strong uniform convergence with a rate of the product limit estimator, the so-called Lynden-Bell estimator. However, these two types of incomplete data may occur simultaneously in a study and then, the model we deal with is known as the left truncated and right censored (LTRC) one. More specifically, let Y denote the r.v of interest (lifetime) with a continuous distribution function (d.f.) F and a bounded density f. Let T and X be two absolute continuous r.v's having d.f's G and L, representing the random left truncation and the random right censoring times, respectively. In the sequel, it will be assumed that Y, T and X are independent each of others. Let $\{Y_i;\ i = 1, \ldots, N\}$, $\{T_i;\ i = 1, \ldots, N\}$ and $\{X_i;\ i = 1, \ldots, N\}$ be N copies of Y, T and X, defined on a probability space $(\Omega, F, \mathbb{P})$, where the sample size N is fixed but unknown.

In LTRC model, the variable of interest Y may not always be observable, instead one gets only $Z = Y \wedge X := \min(Y, X)$ and the censoring indicator $\delta = \mathbf{1}_{\{Y \leq X\}}$ if $Z \geq T$ and nothing is observable otherwise. Set $\alpha = \mathbb{P}(Z \geq T)$, we shall assume that $\alpha > 0$ to have at disposal at least one observation.

As a consequence of truncation, the size $n := \sum_{i=1}^{N} \mathbf{1}_{\{Z \geq T\}}$ of the actually observed sample is random. Then without possible confusion, we still denote $\{(Z_i, T_i, \delta_i);\ i = 1, \ldots, n\}$, the observed sample. Throughout this study, all probability statements are to be interpreted as conditional probability statements, that is $\mathbf{P}(\cdot) = \mathbb{P}(\cdot | Z \geq T)$. Likewise $\mathbf{E}$ and $\mathbb{E}$ will denote the expectation operators related to $\mathbf{P}$ and $\mathbb{P}$.

Note that as the original sequence of interest is associated, then by Lemma 2.2 of Cai and Roussas [2], the r.v's $(Z_i; i = 1, \ldots, n)$ are associated. Hence by property $(P1)$ in Esary et al.[4], the observed sequence remains associated. Furthermore the sequence of truncation $(T_i; i = 1, \ldots, n)$ is still i.i.d. by Proposition 2.1 in Lemdani and Ould Said [8].

Our goal is to extend to associated case some asymptotic results for the cumulative hazard function and the PLE stated in the i.i.d. case by Tsai et al.[11]. Then, as an application, we derive a strong uniform consistency rate for an estimator of the hazard rate function proposed and studied in the i.i.d. case by Uzunoğullari and Wang [12]. It is of interest to recall that the conditional version of the PLE was investigated by Liang et al. [9] in the α-mixing case.

The rest of the paper is organized as follows: In the next section we introduce some notations and the estimators. In Section 3 we present our main results with the assumptions. Section 4 contains some simulations that support our results. In section 5 we give an application to hazard rate function estimation.

2 Estimations and notations

Let $H(y) = \mathbb{P}(Z \leq y)$ be the distribution function of Z, then from the independence of Y and X, we have $1 - H(y) = (1 - F(y))(1 - L(y))$. Conditionally on n, all estimation results are stated considering $n \to \infty$ which hold true with respect to the probability $\mathbb{P}$ since $n \leq N$ and the distributions of Y, T, X, and Z become

$$\mathbf{F}(y) = \mathbf{P}(Y \leq y) = \mathbb{P}(Y \leq y \mid Z \geq T), \;\; \mathbf{G}(y) = \mathbf{P}(T \leq y) = \mathbb{P}(T \leq y \mid Z \geq T),$$
$$\mathbf{L}(y) = \mathbf{P}(X \leq y) = \mathbb{P}(X \leq y \mid Z \geq T), \;\; \mathbf{H}(y) = \mathbf{P}(Z \leq y) = \mathbb{P}(Z \leq y \mid Z \geq T).$$

For $k = 0, 1$, the sub-distributions of Z are

$$H_k(y) := \mathbb{P}(Z \leq y, \delta = k) \text{ and } \mathbf{H}_k(y) = \mathbf{P}(Z \leq y, \delta = k) = \mathbb{P}(Z \leq y, \delta = k \mid Z \geq T).$$

Then $H(y) = H_1(y) + H_0(y)$ and $\mathbf{H}(y) = \mathbf{H}_1(y) + \mathbf{H}_0(y)$.

It is straightforward to show that

$$\mathbf{H}_k(y) = \frac{1}{\alpha} \int_0^y G(z) \left[1 - kL(z) - (1-k)F(z)\right] d\left[kF(z) + (1-k)L(z)\right],$$

which gives

$$d\mathbf{H}_k(y) = \frac{G(y)}{\alpha} \left[1 - kL(y) - (1-k)F(y)\right] d\left[kF(y) + (1-k)L(y)\right]. \qquad (1)$$

And, let us define

$$C(y) = \mathbb{P}(T \leq y \leq Z \mid Z \geq T) = \mathbf{G}(y) - \mathbf{H}(y). \qquad (2)$$

From (2) one may show that

$$C(y) = \frac{G(y)}{\alpha}(1 - H(y)) = \frac{G(y)}{\alpha}(1 - F(y))(1 - L(y)). \qquad (3)$$

It is easily seen that $\mathbf{F}, \mathbf{G}, \mathbf{L}, \mathbf{H}, \mathbf{H}_0$, $\mathbf{H}_1$ and C are readily estimable through their empirical estimates

$$\mathbf{F}_n(y) = \frac{1}{n} \sum_{i=1}^{n} \mathbb{I}_{\{Y_i \leq y\}}, \;\; \mathbf{G}_n(y) = \frac{1}{n} \sum_{i=1}^{n} \mathbb{I}_{\{T_i \leq y\}}, \;\; \mathbf{L}_n(y) = \frac{1}{n} \sum_{i=1}^{n} \mathbb{I}_{\{X_i \leq y\}}$$

$$\mathbf{H}_n(y) = \frac{1}{n} \sum_{i=1}^{n} \mathbb{I}_{\{Z_i \leq y\}}, \;\; \mathbf{H}_{k,n}(y) = \frac{1}{n} \sum_{i=1}^{n} \mathbb{I}_{\{Z_i \leq y, \delta_i = k\}}; \; k = 0, 1$$

and

$$C_n(y) = \mathbf{G}_n(y) - \mathbf{H}_n(y). \qquad (4)$$

The nonparametric maximum likelihood estimator of F based on the data (Z_i, T_i, δ_i); $i = 1, \ldots, n$ is the product limit estimate (PLE) $\hat{F}_n$, defined in Tsai et al. [11] by

$$1 - \hat{F}_n(y) = \prod_{i:Z_i \leq y} \left(1 - \frac{1}{nC_n(Z_i)}\right)^{\delta_i}. \tag{5}$$

For any df W, let us define $a_W = \inf\{u : W(u) > 0\}$ and $b_W = \sup\{u : W(u) < 1\}$, as the endpoints of the W support. As pointed out in Woodroofe [13], in the case of left truncated model, the df's F and G can be completely estimated only if $a_G \leq a_F, b_G \leq b_F$ and $\int_{a_F}^{\infty} G^{-1} dF < \infty$. In our current setting, these conditions are replaced by $a_G < a_H,\ b_G < b_H$ and $\int_{a_H}^{\infty} G^{-1} dH < \infty$ (see, Gijbels and Wang [6]. The goal of this paper is to state the strong uniform consistency with a rate of the cumulative hazard function estimate and the PLE in the case of association. For this purpose, recall that the cumulative hazard function of the interested variable is defined by

$$\Lambda(y) = \int_{a_H}^{y} \frac{dF(z)}{1 - F(z^-)} = \int_{a_H}^{y} \frac{d\mathbf{H}_1(z)}{C(z)}, .$$

which can be estimated by

$$\Lambda_n(y) = \int_{a_H}^{y} \frac{d\mathbf{H}_{1,n}(z)}{C_n(z)} = \frac{1}{n} \sum_{i=1}^{n} \frac{1_{\{Z_i \leq y, \delta_i = 1\}}}{C_n(Z_i)}, \tag{6}$$

where the sum in the latter formula is taken over the i's such that $C_n(Z_i) \neq 0$.

3 Assumptions and main results

Let a and b be real numbers satisfying $a_G < a_H \leq a < b < b_H$. In the sequel, $D := [a, b]$ and c will denote respectively, a compact set and a generic positive constant which may take different value for each appearance. The conditions needed to establish our results are the following:

A1. $\displaystyle\int \frac{dH(y)}{G(y)} < \infty,$

A2. $\displaystyle\sum_{j \geq n+1} |cov(Y_1, Y_j)|^{1/3} = O(n^{-\frac{r-2}{2}})$ for any constant $r > 2$.

Proposition 1 *Under assumptions A1 and A2, we have as* $n \to \infty$

$$\sup_{y \in D} |\mathbb{H}_{k,n}(y) - \mathbb{H}_k(y)| = O(n^{-\theta}) \ a.s., \quad k = 0, 1.$$

where $0 < \theta < (r-2)/(2r + \zeta + 2)$ for any real $\zeta > 0$.

Theorem 1 *Under assumptions A1-A2 we have*

$$\sup_{y \in D} |\Lambda_n(y) - \Lambda(y)| = O\left(n^{-\theta} + \sqrt{\frac{\log\log n}{n}}\right) \ a.s., \ as \ n \to \infty$$

Theorem 2 *Under assumptions A1-A2 we have*

$$\sup_{y\in D}\left|\hat{F}_n(y)-F(y)\right| = O\left(n^{-\theta}+\sqrt{\frac{\log\log n}{n}}\right) \ a.s., \ as \ n\to\infty$$

4 Simulations

4.1 The model

- The interest variable Y: Generate the associated sequence $\{Y_i, i=1,\cdots,N\}$ by $Y_i = \exp\left[\frac{1}{2}\left(W_{i-1}+W_{i-2}\right)\right]$, where $\{W_t;\ t=-1,0,\cdots,N-1\}$ are $(N+1)$ i.i.d. $\mathcal{N}(0,1)$ rv's, then Y_i has a stationary log-normal density with $\mu=0$ and $\sigma^2=1/2$ (see Chaubey et al 2011).
- The censoring variable C: Generate N i.i.d. rv's $\{C_i;\ i=1,\cdots,N\}$ with distribution $\mathcal{E}(\lambda)$.
- The truncated variable T: Generate independently the i.i.d. rv's $\{T_i;\ i=1,\cdots,N\}$ with distribution $\mathcal{E}(\mu)$. (μ and λ are adapted in order to control the rates of truncation and censoring,).
- The observed data:
  - Let $Z_i = Y_i \wedge C_i$.
  - The indicator of (no)censoring: $\delta_i = \mathbb{I}_{\{Y_i\le C_i\}}$.
  - We keep the n observations $\{(Z_i,T_i,\delta_i)\ i=1,\cdots,n\}$ satisfying the condition $Z_i\ge T_i$, $(n\le N)$.

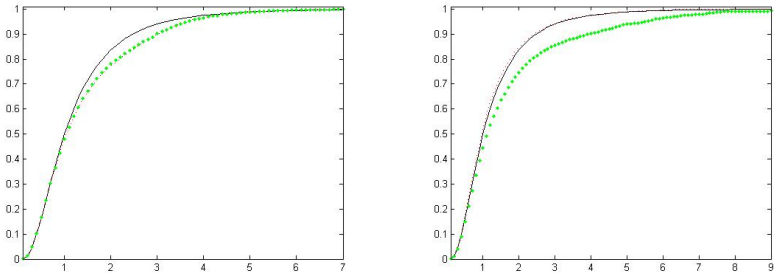

Log-normal distribution and estimated distribution for $n=50$ with 10% and 30% Trunc. and Perc.Cens. = 5% (left), with 5% and 25% Perc.Cens. and Trunc. = 10% (right)

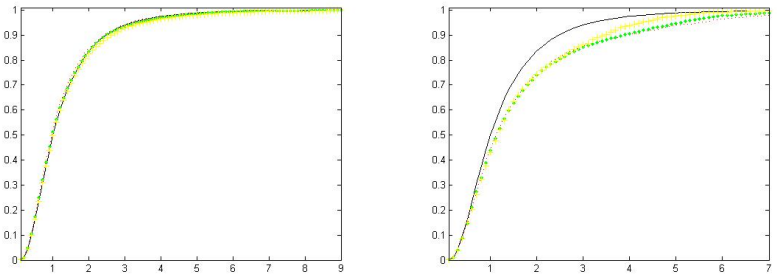

Log-normal distribution and estimated distribution for $n = 50$, $n = 200$ and $n = 500$ with Trunc. $= 10\%$ and Perc.Cens. $= 5\%$ (left), and Perc.Cens. $= 25\%$ (right)

4.2 The Generalized Mean Square Error (GMSE)

		n					
		50		200		500	
	$(no)Trunc.$	90%	70%	90%	70%	90%	70%
Perc.Cens.							
5%	(10^{-6})	3,88	5,91	2,67	3,13	0,88	1,17
25%	(10^{-5})	5,03	9,48	4,95	5,72	2,63	2,41

Table 1. Table of GMSE

Discussion
We note through the graphs and Table 1 that the more the percentage of censoring is low the best the estimation curve is. The truncation has virtually no impact or very few.

5 Application to hazard rate estimation

The hazard function $\lambda(y)$, say, can be defined through its cumulative hazard function $\Lambda(y)$ and then from (6) we have

$$\lambda(z)dz = \frac{d\mathbf{H}_1(z)}{C(z)}.$$

Likewise, proceeding as for the estimator in (6), we define an estimator for $\lambda(y)$ by convolving $K_{h_n}(y) := \frac{1}{h_n}K(\frac{y}{h_n})$ with $\Lambda_n(y)$, namely

$$\hat{\lambda}_n(y) = \int K_{h_n}(y-z)d\Lambda_n(z) = \frac{1}{nh_n}\sum_{i=1}^{n}\frac{\delta_i}{C_n(Z_i)}K\left(\frac{y-Z_i}{h_n}\right), \qquad (7)$$

where K is a kernel function and h_n is a sequence of positive bandwidths tending to zero as $n \longrightarrow \infty$.
The following additional assumptions are needed to state asymptotic results for the hazard rate function estimator defined in (7).

H1. K is a Lipschitz continuous p.d.f. and compactly supported, satisfying $\int uK(u)du = 0$, $\int u^2K(u)du < \infty$ and $\int uK^2(u)du < \infty$.
H2. λ is twice continuously differentiable on D and $\sup_{y\in D}\left|\lambda^{(p)}(y)\right| < \infty$ for $p = 1, 2$.
H3. The bandwidth h_n satisfies: $h_n \to 0$, $nh_n \to \infty$ and $\frac{\log^5 n}{nh_n} \to 0$ as $n \to +\infty$.
H4. The covariance term defined by $\rho(s) := \sup_{|i-j|\geq s} cov(Y_i, Y_j)$ for $s > 0$, satisfies $\rho(s) \leq \gamma_0 e^{-\gamma s}$ for some positive constants γ_0 and γ,
H5. The conditional joint density $\mathbf{f}_{i,j}$ of (Y_i, Y_j) exists and $\sup_{y_1,y_2\in D} |\mathbf{f}_{i,j}(y_1, y_2)| < \infty$.

Theorem 3 *Under assumptions A1, H1-H5, we have as* $n \to +\infty$

$$\sup_{y\in D}\left|\hat{\lambda}_n(y) - \lambda(y)\right| = O\left(n^{-\theta} + \sqrt{\frac{\log n}{nh_n}} + h_n^2\right) \ a.s.$$

where $0 < \theta < \gamma/(2\gamma + \beta + 9)$ for any real $\beta > 0$ and γ is that in H4.

Remark 1 *we pointed out that if we set* $r = \frac{2\gamma}{3} + 2$ *in condition A2, then H4 implies this last one.*

Remark 2 *It is well known that the hazard function* $\lambda(y)$ *can be written as* $\lambda(y) = \frac{f(y)}{1-F(y)}$. *Then by using (5) and (7), an estimate of the density function* f *is defined as* $\hat{f}_n(y) = \hat{\lambda}_n(y)(1 - \hat{F}_n(y))$. *So, the result in Corollary 1 below, follows immediately from Theorem 2 and Theorem 3.*

Corollary 1 *Under assumptions A1, H1-H5, we have as* $n \to +\infty$

$$\sup_{y\in D}\left|\hat{f}_n(y) - f(y)\right| = O\left(n^{-\theta} + \sqrt{\frac{\log n}{nh_n}} + h_n^2\right) \ a.s.$$

References

1. Bagai I, Prakasa Rao BLS. Kernel-type density and failure rate estimation for associated sequences, *Ann. Inst. Stat. Math*, 47:253–266, 1995.
2. Cai Z, Roussas GG. Kaplan-Meier estimator under association, *J. Multivariate Anal*, 67:318–348, 1998.
3. Dewan I, Prakasa Rao BLS. A general method of density estimation for associated random variables, *J. Nonparametric Stat.* 10:405–420, 1999.
4. Esary J, Proschan F, Walkup D. Association of random variables with applications, *Ann. Math. Stat.*, 38:1466–1476, 1967.

5. Ferrani Y, Ould Sad E, Tatachak A. On kernel density and mode estimates for associated and censored data, *Communications in Statistics - Theory and Methods*, 45:1853–1862, 2016.
6. Gijbels I, Wang JL. Strong representations of the survival function estimator for truncated and censored data with applications, *J. Multivar. Anal*, 47:210–229, 1993.
7. Guessoum Z, Ould Sad E, Sadki O, Tatachak A. A note on the Lynden-Bell estimator under association, *Statist. Probab. lett*, 82:1994–2000, 2012.
8. Lemdani M, Ould Sad E. Asymptotic Behavior of the Hazard Rate Kernel Estimator Under Truncated and Censored Data, *Communications in Statistics - Theory and Methods*, 36:155–173, 2007.
9. Liang HY, de na-lvarez J, Iglesias-Prez MdC. Asymptotic properties of conditional distribution estimator with truncated, censored and dependent data, *Test*, 21:790-810, 2012.
10. Roussas G. Asymptotic normality of the kernel estimate of a probability density function under association, *Stat. Probab. Lett*, 50:1–12, 2000.
11. Tsai WY, Jewell NP, Wang MC. A note on the product-limit estimator under right censoring and left truncation, *Biometrika*, 74:883–886, 1987.
12. Uzunoḡullari , Wang JL. A comparison of hazard rate estimators for left truncated and right censored data, *Biometrika*, 79:297–310, 1992.
13. Woodroofe M. Estimating a distribution function with truncated data, *Ann. Statist*, 13:163–177, 1985.

Modelling spread limitations of oil spills at sea

Sambor Guze[1], Krzysztof Koowrocki[2], and Jolanta Mazurek[3]

[1] Department of Mathematics. Faculty of Navigation, Gdynia Maritime University, 83rd Morska Str. 81-225, Gdynia, Poland
(E-mail: s.guze@wn.am.gdynia.pl)
[2] Department of Mathematics. Faculty of Navigation, Gdynia Maritime University, 83rd Morska Str. 81-225, Gdynia, Poland
(E-mail: k.kolowrocki@wn.am.gdynia.pl)
[3] Department of Mathematics. Faculty of Navigation, Gdynia Maritime University, 83rd Morska Str. 81-225, Gdynia, Poland
(E-mail: j.mazurek@wn.am.gdynia.pl)

Abstract. To describe the oil spill central point position a two-dimensional stochastic process is used and its drift trend curve is determined. The oil spill domain movement general model for various hydro-meteorological conditions is constructed and the method of this model unknown parameters estimation is proposed. These methods are used to predict the spill domain movement and to prevent and to mitigate the oil spill consequences by constructing the algorithm for oil spill spread limitations. An exemplary application of this procedure is given.
Keywords: Drift trend, Oil spill domain, Spread limitations, Stochastic model.

1 Introduction

Nowadays, approximately 60% of the world's oil is transported by sea. Thus, the important thing is to maintain the highest level of the safety during the oil extraction, handling, and storing. Especially, it is very important aspect for closed seas such as the Baltic Sea or the Mediterranean Sea, because even small pollution gives very high impact for environment. Unfortunately, despite all efforts, sometimes a smaller or larger leakage of oil occurs. In that situation, the most important thing is time to react and take appropriate actions to minimize the negative effects. There are functioning a lot of models of the spill. Some of them simulate only the advective processes (Al-Rabeh [1], Huang [6], Reed et. al. [12], Spaulding [14]) and some also take into account the spreading processes (Fay [3], Guze et. al. [5], Huang [6], NOAA [10], Reed et.al [12]).
The improvement of the methods of the oil spill domain determination is one of real possibilities leading to the maritime environment protection and chermical pollution reduction. Therefore it seems to be necessary to start with the new and better methods of oil spill domains at sea determination for different hydro-

meteorological conditions and different kinds of oil spills. The most important criterion of new methods should be the attainment time minimising of the reaction to oil spills. One of the essential factors that could ensure these criteria fulfilment is the accuracy of methods of oil spills domain determination. Those methods are a basic part of the integral problem of oil spill and pollution-fighting at the sea directed to the elaboration of a complete information system assisting national maritime environment protection administration to reduce the consequences the oil spills at the sea.
Thus, the main aim of the paper is to propose a probabilistic approach to determination of oil spills domains. It is presented in 5 succeeded subsections, where oil spill trend and drift domain for different hydro-meteorological conditions and oil spill kinds, the pollution-fighting time distribution, and the oil spill random position distribution are determined. Furthermore, the oil spill drift trend and position distribution parameters statistical identification procedure is presented with accordance to the least squares method (Kołowrocki [7], Kołowrocki and Soszyńska-Budny [8], Rice [13]). Finally, the algorithm for oil spill spread limitations is proposed as the possible stochastic oil spill model application. The exemplary results of computer simulation based on introduced model and algorithm are showed.
The suggested probabilistic approach to oil spill domains determination can improve the efficiency of pollution combat at the sea.

2 Oil spill basic characteristics

According to the "Trajectory Analysis Handbook" NOAA [11] the parameters affecting oil spill movement are as follows:

a) weather conditions (wind, temperature, and rainfall),
b) ocean conditions (tides and currents),
c) physical parameters of the materials which could be spilled, i.e.:
   - specific gravity (or density);
   - evaporation rate;
   - boiling range;
   - viscosity;
   - pour point;
   - emulsification ability;
   - water solubility.

Some of these factors are related. For example, the evaporation rate is dependent on weather conditions (especially wind) and the boiling range of the material. Similarly, the spread rate depends on weather, viscosity, and the pour point. Emulsification is a very complex parameter since both oil-in-water and water-in-oil emulsions can be involved and wind and wave conditions are usually controlling NOAA [11].
In the other hand, there are following characteristics of spills NPC [9]:

- maximum area of spread [m^2],
- maximum radius of a circular slick [m],
- time to reach maximum radius [min],

- spill volume [gallons],
- spreading coefficient [dynes/cm].

According to results of Fay [3], estimates of initial spill volume and a spreading equation are required to determine the spreading radius of a hypothetical spill as a function of time. Wind speed and direction, local tidal currents, and the general circulation along the coast are required to determine the trajectory of the slick, and estimates of the general circulation of the water body are needed to predict the fate of that fraction of the spill which may mix downward into the water column.

3 Stochastic Model of Oil Spill

In this section, the stochastic model of oil spill is proposed. This tool gives the possibility to determine the drift trend and the domain of the oil spill. This model adapts and transforms the approach and the results concerned with the survivor search domain at the sea restricted areas determination considered in Blokus and Kołowrocki [2] in the way presented in next five subsections.

3.1 Oil Spill Drift Trend Determination

For each fixed state c_k, $k = 1,2,\ldots,w$, of the climate-weather process $C\text{-}W(t)$ we define a two-dimensional stochastic process

$$(X^k(t), Y^k(t)),\ t \in \langle 0,T\rangle, \tag{1}$$

such that

$$(X^k, Y^k) : \langle 0,T\rangle \to R^2, \tag{2}$$

where $X^k(t)$, $Y^k(t)$ respectively are an abscissa and an ordinate of the plane Oxy point, in which the central point of the oil spill is placed at the moment t while the climate-weather process $C\text{-}W(t)$ is at the state c_k, $k = 1,2,\ldots,w$. The point in which an accident has happened and an oil spill was placed in the water we assume as the origin $O(0,0)$ of the co-ordinate system Oxy. The value of a parameter t at the moment of the accident we assume equal to 0. It means that the process $(X^k(t), Y^k(t))$, is a random two-dimensional co-ordinate (a random position) of the oil spill central point after the time t from the accident moment and that at the accident moment $t = 0$ the oil spill is at the point $O(0,0)$, i.e. $(X^k(0), Y^k(0)) = (0,0)$. After some time, the oil spill starts his drift along a curve called a drift curve. In further analysis we assume that processes

$$(X^k(t), Y^k(t)),\ t \in \langle 0,T\rangle,\ k = 1,2,\ldots,m,$$

are two-dimensional normal processes

$$N(m_X^k(t), m_Y^k(t), \rho_{XY}^k(t), \sigma_X^k(t), \sigma_Y^k(t)), \ t \in <0,T>, \tag{3}$$

with varying in time expected values

$$m_X^k(t) = E[X^k(t)], \quad m_Y^k(t) = E[Y^k(t)], \tag{4}$$

standard deviations

$$\sigma_X^k(t), \quad \sigma_Y^k(t)$$

and correlation coefficients

$$\rho_{XY}^k(t),$$

i.e. with the joint density functions

$$\varphi_t^k(x,y) = \frac{1}{2\pi\sigma_X^k(t)\sigma_Y^k(t)\sqrt{1-(\rho_{XY}^k(t))^2}} \exp\{-\frac{1}{2(1-(\rho_{XY}{}^k(t))^2)}[\frac{(x-m_X{}^k(t))^2}{(\sigma_X{}^k(t))^2}$$
$$-2\rho_{XY}{}^k(t)\frac{(x-m_X{}^k(t))(y-m_Y{}^k(t))}{\sigma_X{}^k(t)\sigma_Y{}^k(t)} + \frac{(y-m_Y{}^k(t))^2}{(\sigma_Y{}^k(t))^2}]\}, \tag{5}$$

where $(x,y) \in R^2$, $t \in <0,T>$.

Then, the points $(m_X^k(t), m_Y^k(t))$, $t \in <0,T>$, create a curve K^k which may be described in the following parametric form

$$K^k : \begin{cases} x^k = x^k(t) \\ y^k = y^k(t), t \in <0,T>. \end{cases} \tag{6}$$

called an oil spill drift trend and presented in Figure 1.

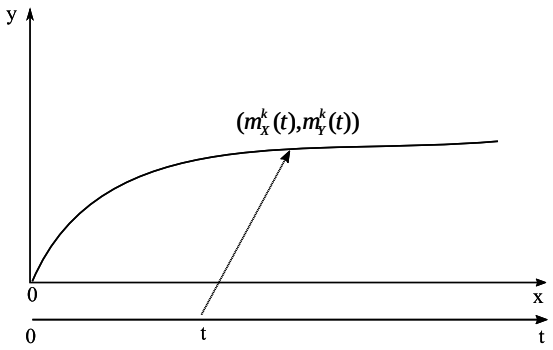

Fig. 1. The oil spill drift trend

3.2 Oil Spill Drift Domain Determination

We are interested in finding the domain $D^k(t)$ such that the oil spill is placed within it with a fixed probability *p*. More exactly, we are looking for *p* such that

$$P((X^k(t), Y^k(t)) \in D^k(t)) = \iint_{D^{(k)}(t)} \varphi_t^k(x,y)dxdy = p, \tag{7}$$

where

$$D^k(t) = \{(x,y): \frac{1}{1-(\rho_{XY}^k(t))^2}[\frac{(x-m_X^k(t))^2}{(\sigma_X^k(t))^2} - 2\rho_{XY}^k(t)\frac{(x-m_X^k(t))(y-m_Y^k(t))}{\sigma_X^k(t)\sigma_Y^k(t)} + \frac{(y-m_Y^k(t))^2}{(\sigma_Y^k(t))^2}] \le c^2\} \tag{8}$$

is the domain bounded by an ellipse being the projection on the plane $0xy$ of the curve rising as the result of intersection of the density function surface

$$\pi_1^k = \{(x,y,z): z = \varphi_t^k(x,y), (x,y) \in R^2\} \tag{9}$$

and the plane

$$\pi_2^k = \{(x,y,z): \ z = \frac{1}{2\pi\sigma_X^k\sigma_Y^k\sqrt{1-(\rho_{XY}^k(t))^2}}\exp[-\frac{1}{2}c^2], (x,y) \in R^2\}. \tag{10}$$

The graph of the domain $D^k(t)$ is given in Figure 2.

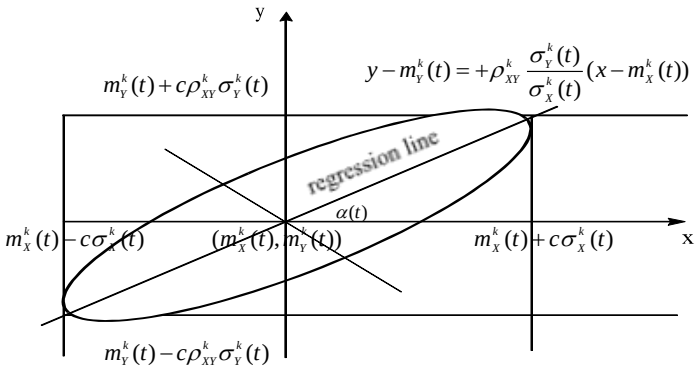

Fig. 2. Domain of integration $D^k(t)$

Since

$$P((X^k(t),Y^k(t))\in D^k(t))=1-\exp[-\frac{1}{2}c^2], \tag{11}$$

then for a fixed probability p, the equality

$$p=P((X^k(t),Y^k(t))\in D^k) \tag{12}$$

holds if $c^2=-2\ln(1-p)$. Thus, the domain in which at the moment t the oil spill is placed with the fixed probability p is given by

$$D^k(t)=\{(x,y):\frac{1}{1-(\rho_{XY}^k(t))^2}[\frac{(x-m_X^k(t))^2}{(\sigma_X^k(t))^2}-2\rho_{XY}^k(t)\frac{(x-m_X^k(t))(y-m_Y^k(t))}{\sigma_X^k(t)\sigma_Y^k(t)}$$
$$+\frac{(y-m_Y^k(t))^2}{(\sigma_Y^k(t))^2}]\le -2\ln(1-p)\}. \tag{13}$$

3.3 Oil Spill Domain for Fixed Climate-Weather Conditions

We suppose that the climate-weather process $C-W(t)$ is in a fixed state c_k, $k=1,2,\ldots,w$. Assuming a time step Δt and a number of steps s, $s\ge 1$, such that

$$(s-1)\Delta t<E[\theta_k]\le s\Delta t,$$

where $E[\theta_k]$ is the expected value of the process $C-W(t)$ sojourn time at the state c_k, $k=1,2,\ldots,w$, we receive the following sequence of domains (Figure 3)

$D^k(\Delta t), D^k(2\Delta t),\ldots,D^k(s\Delta t),$ in which at the moments $\Delta t, 2\Delta t, \ldots, s\Delta t,$ the oil spill is placed with probability p.

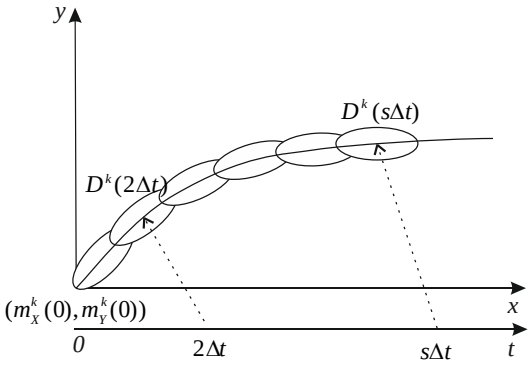

Fig. 3. Sequence of oil spill domains

Then the oil spill domain is described by the sum of selected domains (Figure 4)

$$D^k(v\Delta t) \cup D^k((v+1)\Delta t) \cup \quad . \quad . \quad . \quad \cup D^k(w\Delta t),$$

where v is such that

$$v\Delta t < m_U^k + m_V^k \le (v+1)\Delta t, \tag{14}$$

while w is such that

$$(w-1)\Delta t < m_U^k + m_V^k + m_T^k \le w\Delta t,$$

and

$$m_U^k = E[U^k], \quad m_V^k = E[V^k], \quad m_T^k = E[T^k],$$

are the expected values of the pollution-fighting unit activation time U^k, the time necessary to reach the oil spill domain by the pollution-fighting unit V^k and the unit pollution fighting time T^k, which are determined in the paper Section 3.4.

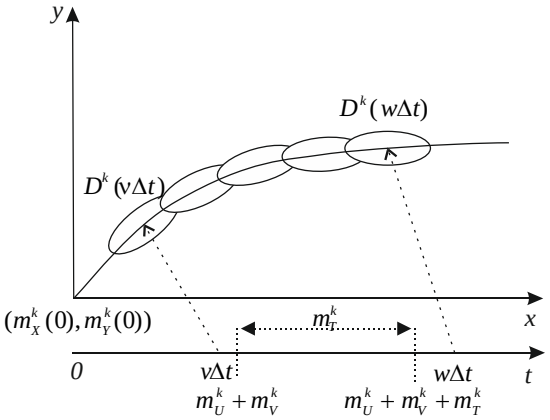

Fig. 4. Oil spill domain for fixed hydro-meteorological conditions

3.4 Oil Spill Domain for Varying Climate-Weather Conditions

We assume that the process of hydro-meteorological conditions changing in succession takes the states $c_{k_1}, c_{k_2}, \ldots, \; k_i \in \{1, 2, \ldots, w\}$. For a time step Δt we determine the oil spill domain as the sum of the domains (Figure 5)

$$\bigcup_{i=1}^{n}[D^{k_i}(v_i\Delta t) \cup D^{k_i}((v_i+1)\Delta t) \cup \quad . \quad . \quad . \quad \cup D^{k_i}(w_i\Delta t)], \tag{15}$$

where v_i is such that

$$v_i\Delta t < \overline{U}^{k_1} + \overline{V}^{k_1} + \sum_{j=1}^{i-1}\overline{\theta}_{k_j k_{j+1}} \le (v_i+1)\Delta t, \quad i = 1,2,\ldots,n,$$

while w_i is such that

$$w_i\Delta t < \overline{U}^{k_1} + \overline{V}^{k_1} + \sum_{j=1}^{i}\overline{\theta}_{k_j k_{j+1}} \le (w_i+1)\Delta t, \quad i = 1,2,\ldots,n, \text{ and } \; \overline{U}^{k_1}, \quad \overline{V}^{k_1}, \quad \overline{\theta}_{k_j k_{j+1}},$$

are the realisations of the pollution-fighting unit activation time U^{k_1}, the time necessary to reach the oil spill domain by the pollution-fighting unit V^{k_1} and the process $A(t)$ sojourn time $\theta_{k_j k_{j+1}}$ in the state k_j while the next transition will be done to the state k_{j+1} respectively and n is such that

$$\overline{U}^{k_1} + \overline{V}^{k_1} + \sum_{j=1}^{n-1}\overline{\theta}_{k_j k_{j+1}} < \max_{1\le j\le n}\{E(T^{k_j})\} \le \quad \overline{U}^{k_1} + \overline{V}^{k_1} + \sum_{j=1}^{n}\overline{\theta}_{k_j k_{j+1}}. \tag{16}$$

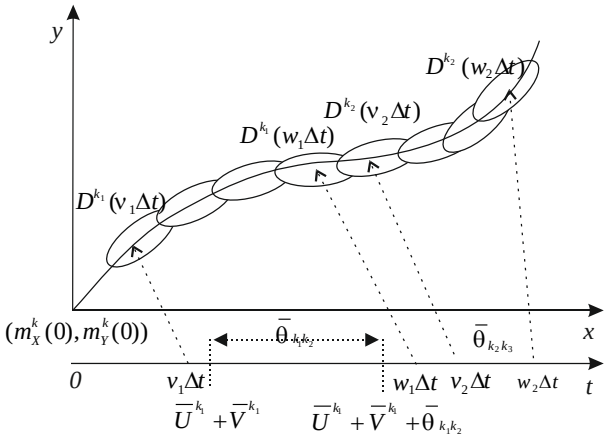

Fig. 5. Oil spill domain for changing hydro-meteorological conditions

3.5 Oil Spill Drift Trend and Position Distribution Parameters Statistical Identification

To determine the evaluations of oil spill drift trend and parameters of joint density function $\varphi_t^k(x,y)$ it is necessary to perform the following steps:

- to fix the number N^k and the moments of observations $t_1, t_2, \ldots, t_{N^k}$, in which the oil spill positions are determined,
- to fix the numbers of the process $(X^k(t), Y^k(t))$ realisations $n^k(1)$, $n^k(2)$, $\cdots$, $n^k(N^k)$ at the moments $t_1, t_2, \ldots, t_{N^k}$,
- to fix the oil spill positions $(x'^k_1(t_\nu), y'^k_1(t_\nu))$, $(x'^k_2(t_\nu), y'^k_2(t_\nu))$, $\ldots$, $(x'^k_{n^k(\nu)}(t_\nu), y'^k_{n^k(\nu)}(t_\nu))$, at each moment $t_\nu, \nu = 1,2,\ldots,N^k$,
- to calculate mean oil spill positions according to the formulae

$$m'_X{}^k(t_\nu) = \frac{1}{n^k(\nu)} \sum_{\nu=1}^{n^k(\nu)} x'^k_\nu(t_\nu), \quad m'_Y{}^k(t_\nu) = \frac{1}{n^k(\nu)} \sum_{\nu=1}^{n^k(\nu)} y'^k_\nu(t_\nu), \quad \nu = 1.2,\ldots,N^k,$$

- to calculate oil spill position standard deviations according to the formulae

$$\sigma'_X{}^k(t_\nu) = \sqrt{\frac{1}{n^k(\nu)} \sum_{\nu=1}^{n^k(\nu)} [x'^k_\nu(t_\nu)]^2 - [m_X{}^k(t_\nu)]^2},$$

$$\sigma'_Y{}^k(t_\nu) = \sqrt{\frac{1}{n^k(\nu)} \sum_{\nu=1}^{n^k(\nu)} [y'^k(t_\nu)]^2 - [m_Y{}^k(t_\nu)]^2}, \quad \nu = 1.2,\ldots,N^k,$$

- to calculate oil spill position correlation coefficients according to the formula

$$\rho'_{XY}{}^{k}(t_\nu) = \frac{\frac{1}{n^k(\nu)}\sum_{\nu=1}^{n^k(\nu)} x'^{k}_{\nu}(t_\nu)\,y'^{k}_{\nu}(t_\nu) - m_X{}^{k}(t_\nu)\,m_Y{}^{k}(t)}{\sigma_{Xi}{}^{k}(t_\nu)\,\sigma_{Yi}{}^{k}(t_\nu)},\ \nu = 1,2,\ldots,N^k,$$

- to find parametric forms of the oil spill drift trend and remaining parameters of oil spill position distribution according to the least squares method (Kołowrocki [7], Kołowrocki and Soszyńska-Budny [8], Rice [13]).

4 Oil spills spread limitations algorithm

In this Section, the algorithm for oil spills spread limitations is introduced as the possible application of the oil spill stochastic model introduced in Section 3. It is done on the basis of the customizing discrete-time oil spill control model which was introduced in Guze et. al [5].

To simplify the considered problem, the water area affected by oil spill is represented by the Cartesian grid graph $G = (V, E)$, where the $V(G) = \{v_1, v_2, \ldots\}$ is a grid vertex set and $E(G) = \{e_1, e_2, \ldots\}$ is an edge set. According to this assumption, the water area is divided into equal-size squares and the vertex $v \in E(G)$ is in central of them. Furthermore, if $v_i, v_j \in E(G)$, $i, j = 1,2,\ldots$, then we call v_i and v_j adjacent vertices. In Cartesian grid graphs every vertex is adjacent to four other vertices.

The possible states of the vertex in algorithm are: “empty”, “oil-affected”, and “barrier-filled”. Moreover, there are two modes of barriers: “attack” and “defence”. The both barriers are performed simultaneously with assumption, that the barrier in attack mode is use in vertices located on the oil spill drift trend and vertices in defence mode in opposite direction. In the algorithm of the oil spill spread limitation, the barriers may be set on the “empty” vertices only, because a vertex state already “oil-affected” or “barrier-filled” cannot be changed.

First step to introduce the oil spills spread limitations algorithm, it is necessary to build the oil spill spread model. In this paper, the discrete-time oil spill spread model converts the results mentioned in Section 3.2 without the impact of the hydro-meteorological conditions is showed. This model uses the cycles as the measure of the time. It is built according to following steps:

- Oil spill appears on the water area in cycle 0.
- First vertex changes its state from “empty” to “oil-affected” is the oil spill source.
- The oil spill source designates the grid centre as the central vertex $(0,0)$. Additionally, it divides the grid into four quarters and sets the system of coordinates.

- In each subsequent cycle, the oil spill spreads from the "oil-affected" vertices to every adjacent "empty" vertex.

The exemplary results of the oil slick in cycle 3, 7, 11 received on the basis of the above procedure are presented in the Fig. 6.

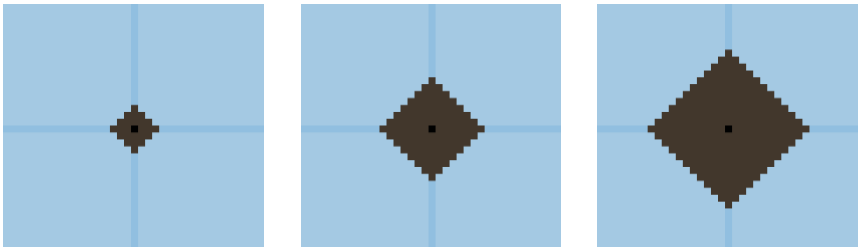

(A) (B) (C)

Fig. 6. The spreading of the oil spill in cycles: N=3 (A), N=7 (B), N=11 (C)

After introducing the all necessary notations, procedures and assumptions the proposed algorithm is as follows:

Algorithm for oil spills spread limitations

Input: The water area affected by oil spill and represents by the Cartesian grid graph $G = (V, E)$.

Steps:

1. To find, on the beginning and in the end of the oil spill drift, the empty vertices adjacent to "oil-affected" ones and to put the barriers in defence mode and next to, simultaneously, the barriers in attack mode, according to general assumption about their location.
2. To change the state of the selected vertices on "barrier-filled".
3. For every empty vertex, adjacent to "oil-affected", and while oil spill is not encircled do:
    a. If empty vertex is on the way of the oil spill drift trend
        i. to put:
            - the barrier in attack mode;
            - and simultaneously the barrier in defence mode in opposite direction;
        ii. to change the vertex state on "barrier-filled";
    b. else
        i. to put:
            - the barrier in defence mode;
            - and simultaneously the barrier in attack mode in opposite direction;
        ii. to change the vertex state on "barrier-filled".

Results: A series of barriers surrounds the oil-affected area and an oil slick without possibility to spread further.

The surrounding of the oil spill is performed according to above algorithm built on the basis of "firefighter algorithm" (Fogarty[4]). According to this approach if the action of surrounding the oil spill starts in cycle $N+1$ and 2 barriers are available in each cycle on the Cartesian grid graphs the number of cycles needed to go around the oil slick is equal $32N+1$ and the number of square of a spill area is equal $318N^2+14N+1$ (Fogarty [4]).
The exemplary simulation results given in Fig. 7 represents an oil slick on the Cartesian grid graph (oil spill source marked with black).

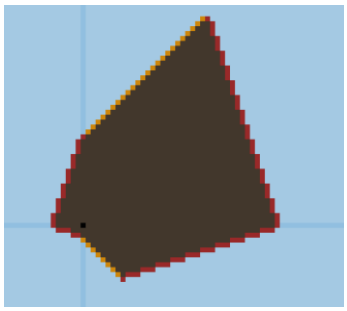

Fig. 7. The resulting Cartesian grid graph model. The red squares represent barriers in attack mode and the yellow squares represent barriers in defense mode

The action started in cycle 3 and lasted for 65 cycles. The number of 130 barriers is used. Oil spill spreads to 1301 vertices. On the Cartesian grid graph 2 barriers in each cycle are minimum number of barriers allowing to surround the oil spill.

Conclusions

In the paper the oil spill domains have been determined for different hydro-meteorological conditions and oil spill kinds by the oil spill drift trend, the pollution-fighting time distribution and the oil spill random position distribution.
Furthermore, the oil spills spread limitations algorithm has been introduced. The exemplary results of proposed algorithm have been presented according to the time-discrete oil spill control model. It has been used to present the possible application of proposed stochastic model.
In practically point of view a weak point of the presented method is large cost of the experiment necessary to perform at the sea in order to identify particular components of the model.
In the other side, a strong point of this method is the fact that the experiments for a restricted sea region should be done only once and the model may be used for all pollution combat actions at this sea region.

The suggested probabilistic approach to oil spill domains determination would surely improve the efficiency of pollution combat at the sea.

Acknowledgements

The paper presents the results developed in the scope of the HAZARD project titled "Mitigating the Effects of Emergencies in Baltic Sea Region Ports" that has received funding from the Interreg Baltic Sea Region Programme 2014-2020 under grant agreement No #R023. https://blogit.utu.fi/hazard/

References

1. A.H. Al-Rabeh, H.M. Cekirge, N. Gunay. A stochastic simulation model of oil spill fate and transport Applied Mathematical Modelling, pp. 322-329, 1989.
2. A. Blokus and K. Kołowrocki. On determination of survivor search domain at sea restricted areas. Risk Decision and Policy, 8, 81-89, 2003.
3. J. A. Fay. Physical Processes in the Spread of Oil on a Water Surface. Proceedings of Joint Conference on Prevention and Control of Oil Spills, sponsored by American Petroleum Industry, Environmental Protection Agency, and United States Coast Guard, 1971.
4. P. Fogarty. Catching the Fire on Grids, Master of Science Thesis, University of Vermont, 2003.
5. S. Guze, J. Mazurek and L. Smolarek. Use of random walk in two-dimensional lattice graphs to describe influence of wind and sea currents on oil slick movement. Journal of KONES Powertrain and Transport, Vol. 23, No. 2, 2016.
6. J. C. Huang. A review of the state-of-the-art of oil spill fate/behavior models. International Oil Spill Conference Proceedings: February 1983, Vol. 1983, No. 1, pp. 313-322, 1983.
7. K. Kołowrocki. Reliability of Large and Complex Systems, Amsterdam, Boston, Heidelberd, London, New York, Oxford, Paris, San Diego, San Francisco, Singapore, Sidney, Tokyo, Elsevier, 2014.
8. K. Kołowrocki and J. Soszyńska-Budny. Reliability and Safety of Complex Technical Systems and Processes: Modeling - Identification - Prediction - Optimization, London, Dordrecht, Heildeberg, New York, Springer, 2011
9. National Petroleum Council. Committee on Environmental Conservation. Environmental Conservation: The Oil and Gas Industries. Vol. 2. 1972.
10. NOAA. Oil Spill Case Histories 1967-1991; Summaries of Significant U.S. and International Spills. Hazardous Material Response and Assessment Division Report HMRAD 92-11. Seattle, WA. September 1992.
11. NOAA. Trajectory Analysis Handbook. NOAA Hazardous Material Response Division. Seattle, WA, undated (see http://www.response.restoration.noaa.gov/ for further information).

12. M. Reed, Ø. Johansen, P. J. Brandvik, P. Daling, A. Lewis, R. Fiocco, D. Mackay, R. Prentki. Oil Spill Modeling towards the Close of the 20th Century: Overview of the State of the Art. Spill Science & Technology Bulletin, 1999, pp. 3-16, 1999.
13. J. A. Rice. Mathematical statistics and data analysis. Duxbury. Thomson Brooks/Cole. University of California. Berkeley, 2007.
14. M. L. Spaulding. A state-of-the-art review of oil spill trajectory and fate modeling, Oil and Chemical Pollution, Volume 4, Issue 1, pp. 39-55, 1988.

Cluster validation by measurement of clustering characteristics relevant to the user

Christian Hennig[1]

Department of Statistical Science, University College London, Gower Street, London WC1E 6BT, United Kingdom
(Email: c.hennig@ucl.ac.uk)

Abstract. There are many cluster analysis methods that can produce quite different clusterings on the same dataset. Cluster validation is about the evaluation of the quality of a clustering; "relative cluster validation" is about using such criteria to compare clusterings. This can be used to select one of a set of clusterings from different methods, or from the same method ran with different parameters such as different numbers of clusters.

There are many cluster validation indexes in the literature. Most of them attempt to measure the overall quality of a clustering by a single number, but this can be inappropriate. There are various different characteristics of a clustering that can be relevant in practice, depending on the aim of clustering, such as low within-cluster distances and high between-cluster separation.

In this paper, a number of validation criteria will be introduced that refer to different desirable characteristics of a clustering, and that characterise a clustering in a multidimensional way. In specific applications the user may be interested in some of these criteria rather than others. A focus of the paper is on methodology to standardise the different characteristics so that users can aggregate them in a suitable way specifying weights for the various criteria that are relevant in the clustering application at hand.
Keywords: Number of clusters, separation, homogeneity, density mode, random clustering.

1 Introduction

The aim of the present paper is to present a range of cluster validation indexes that provide a multivariate assessment covering different complementary aspects of cluster validity. Here I focus on "internal" validation criteria that measure the quality of a clustering without reference to external information such as a known "true" clustering. Furthermore I am mostly interested in comparing different clusterings on the same data, which is often referred to as "relative" cluster validation. This can be used to select one of a set of clusterings from different methods, or from the same method ran with different parameters such as different numbers of clusters.

In the literature (for an overview see Halkidi *et al.*[6]) many cluster validation indexes are proposed. Usually these are advertised as measures of global cluster validation in a univariate way, often under the implicit or explicit assumption that for any given dataset there is only a single best clustering. Mostly these indexes are based on contrasting a measure of within-cluster

17th *ASMDA Conference Proceedings, 6 - 9 June 2017, London, UK*

homogeneity and a measure of between-clusters heterogeneity such as the famous index proposed by Calinski and Harabasz[2], which is a standardised ratio of the traces of the pooled within-cluster covariance matrix and the covariance matrix of between-cluster means.

In Hennig[10] (see also Hennig[9]) I have argued that depending on the subject-matter background and the clustering aim different clusterings can be optimal on the same dataset. For example, clustering can be used for data compression and information reduction, in which case it is important that all data are optimally represented by the cluster centroids; or clustering can be used for recognition of meaningful patterns, which are often characterised by clear separating gaps between them. In the former situation, large within-cluster distances are not desirable, whereas in the latter situation large within-cluster distances may not be problematic as long as data objects occur with high density and without gap between the objects between which the distance is large. See Figure 1 for two different clusterings on an artificial dataset with 3 clusters that may be preferable for these two different clustering aims.

Given a multivariate characterisation of the validity of a clustering, for a given application a user can select weights for the different characteristics depending on the clustering aim and the relevance of the different criteria. A weighted average can then be used to choose a clustering that is suitable for the specific application. This requires that the criteria measuring different aspects of cluster validity and normalised in such a way that their values are comparable when doing the aggregation. Although it is easy in most cases to define criteria in such a way that their value range is $[0, 1]$, this is not necessarily enough to make their values comparable, because within this range the criteria may have very different variation. The idea here is that the expected variation of the criteria can be explored using resampled random clusterings ("stupid K-centroids", "stupid nearest neighbour clustering") on the same dataset, and this can be used for normalisation and comparison.

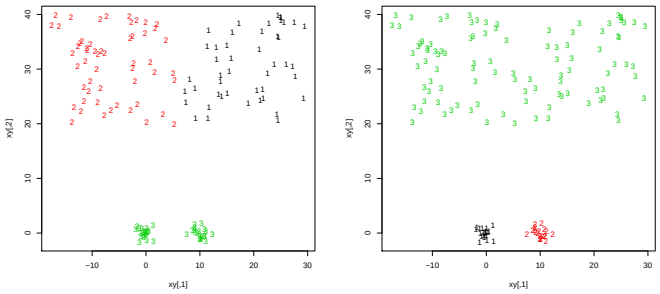

Fig. 1. Artificial dataset. Left side: Clustering by 3-means. Right side: clustering by Single Linkage with 3 clusters.

The approach presented here can also be used for benchmarking cluster analysis methods. Particularly, it does not only allow to show that methods

are better or worse on certain datasets, it also allows to characterise the specific strength and weaknesses of clustering algorithms in terms of the properties of the found clusters.

Section 2 introduces the general setup and defines notation. In Section 3, all the indexes measuring different relevant aspects of a clustering are presented. Section 4 defines an aggregated index that can be adapted to practical needs. The indexes cannot be suitably aggregated in their raw form, and Section 5 introduces a calibration scheme using randmly generated clusterings. Section 6 applies the methodology to two datasets, one illustrative artificial one and a real dataset regarding species delimitation. Section 7 concludes the paper.

2 General notation

Generally, cluster analysis is about finding groups in a set of objects $\mathcal{D} = \{x_1, \ldots, x_n\}$. There is much literature in which the objects $x_1, \ldots, x_n$ are assumed to be from Euclidean space $\mathbb{R}^p$, but in principle the could be from any space $\mathcal{X}$.

A clustering is a set $\mathcal{C} = \{C_1, \ldots, C_K\}$ with $C_j \subseteq \mathcal{D},\ j = 1, \ldots, K$. The number of clusters K may be fixed in advance or not. For $j = 1, \ldots, K$, let $n_j = |C_j|$ be the number of objects in C_j. Obviously not every such $\mathcal{C}$ qualifies as a "good" or "useful" clustering, but what is demanded of $\mathcal{C}$ differs in the different approaches of cluster analysis. Here $\mathcal{C}$ is required to be a partition, e.g., $j \neq k \Rightarrow C_j \cap C_k = \emptyset$ and $\bigcup_{j=1}^{K} C_j = \mathcal{D}$. For partitions, let $\gamma : \{1, \ldots, n\} \mapsto \{1, \ldots, K\}$ be the assignment function, i.e., $\gamma(i) = j$ if $x_i \in C_j$. Some of the indexes introduced below could also by applied to clusterings that are not partitions (particularly objects that are not a member of any cluster could just be ignored), but this is not treated here to keep things simple. Clusters are here also assumed to be crisp rather than fuzzy, i.e., an object is either a full member of a cluster or not a member of this cluster at all. In case of probabilistic clusterings, which give as output probabilities p_{ij} for object i to be member of cluster j, it is assumed that objects are assigned to the cluster j maximising p_{ij}; in case of hierarchical clusterings it is assumed that the hierarchy is cut at a certain number of clusters K to obtain a partition.

Most of the methods introduced here are based on dissimilarity data. A dissimilarity is a function $d : \mathcal{X}^2 \mapsto \mathbb{R}_0^+$ so that $d(x, y) = d(y, x) \geq 0$ and $d(x, x) = 0$ for $x, y \in \mathcal{X}$. Many dissimilarities are distances, i.e., they also fulfil the triangle inequality, but this is not necessarily required here. Dissimilarities are extremely flexible, they can be defined for all kinds of data, such as functions, time series, categorical data, image data, text data etc. If data are Euclidean, obviously the Euclidean distance can be used. See Hennig[10] for a more general overview of dissimilarity measures used in cluster analysis.

3 Aspects of cluster validity

In this Section I introduce measurements for various aspects of cluster validity.

3.1 Small within-cluster dissimilarities

A major aim in most cluster analysis applications is to find homogeneous clusters. This often means that all the objects in a cluster should be very similar to each other, although it can in principle also have different meanings, e.g., that a homogeneous probability model (such as the Gaussian distribution, potentially with large variance) can account for all observations in a cluster.

The most straightforward way to formalise that all objects within a cluster should be similar to each other is the average within-cluster distance:

$$I_{withindis}(\mathcal{C}) = \frac{2}{\sum_{j=1}^{K} n_j(n_j-1)} \sum_{j=1}^{K} \sum_{x \neq y \in C_j} d(x,y).$$

Smaller values are better. Knowing the data but not the clustering, the minimum possible value of $I_{withindis}$ is zero and the maximum is $d_{max} = \max_{x,y\in\mathcal{D}} d(x,y)$, so $I^*_{withindis}(\mathcal{C}) = 1 - \frac{I_{withindis}(\mathcal{C})}{d_{max}} \in [0,1]$ is a normalised version. When different criteria are aggregated (see Section 4), it is useful to define them in such a way that they point in the same direction; I will define all normalised indexes so that larger values are better. For this reason $\frac{I_{withindis}(\mathcal{C})}{d_{max}}$ is subtracted from 1.

There are alternative ways of measuring whether within-cluster dissimilarities are overall small. All of these operationalise cluster homogeneity in slightly different ways. The objective function of K-means clustering can be written down as a constant times the average of all squared within-cluster Euclidean distances (or more general dissimilarities), which is an alternative measure, giving more emphasis to the biggest within-cluster dissimilarities. Most radically, one could use the maximum within-cluster dissimilarity. On the other hand one could use quantiles or trimmed means in order to make the index less sensitive to large within-cluster dissimilarities, although I believe that in most applications in which within-cluster similarity is important, these should be avoided and the index should therefore be sensitive against them.

3.2 Between-cluster separation

Apart from within-cluster homogeneity, the separation between clusters is most often taken into account in the literature on cluster validation (most univariate indexes balance separation against homogeneity in various ways). Separation as it is usually understood cannot be measured by averaging all between-cluster dissimilarities, because it refers to what goes on "between" the clusters, i.e., the smallest between-cluster dissimilarities, whereas the dissimilarities between pairs of farthest objects from different clusters should not contribute to this.

The most naive way to measure separation is to use the minimum between-cluster dissimilarity. This has the disadvantage that with more than two clusters it only looks at the two closest clusters, and also in many applications there may be an inclination to tolerate the odd very small distance between clusters if by and large the closest points of the clusters are well separated.

I propose here an index that takes into account a portion p, say $p = 0.1$, of objects in each cluster that are closest to another cluster.

For every object $x_i \in C_j$, $i = 1, \ldots, n$, $j \in \{1, \ldots, K\}$ let $d_{j:i} = \min_{y \notin C_j} d(x_i, y)$. Let $d_{j:(i)} \leq \ldots \leq d_{j:(n_j)}$ be the values of $d_{j:i}$ for $x_i \in C_j$ ordered from the smallest to the largest, and let $\lfloor pn_j \rfloor$ be the largest integer $\leq pn_j$. Then the p-separation index is defined as

$$I_{p-sep}(\mathcal{C}) = \frac{1}{\sum_{j=1}^{K} \lfloor pn_j \rfloor} \sum_{j=1}^{K} \sum_{i=1}^{\lfloor pn_j \rfloor} d_{j:(i)}.$$

Obviously, $I_{p-sep}(\mathcal{C}) \in [0, d_{max}]$ and large values are good, therefore $I^*_{p-sep}(\mathcal{C}) = \frac{I_{p-sep}(\mathcal{C})}{d_{max}} \in [0, 1]$ is a suitable normalisation.

3.3 Representation of objects by centroids

In some applications clusters are used for information reduction, and one way of doing this is to use the cluster centroids for further analysis rather than the full dataset. It is then relevant to measure how well the observations in a cluster are represented by the cluster centroid. The most straightforward method to measure this is to average the dissimilarities of all objects to the centroid of the cluster they're assigned to. Let $c_1, \ldots, c_K$ be the centroids of clusters $C_1, \ldots, C_K$. Then,

$$I_{centroid}(\mathcal{C}) = \frac{1}{n} \sum_{i=1}^{n} d(x_i, c_{\gamma(i)}).$$

Some clustering methods such as K-means and Partitioning Around Medoids (PAM, Kaufman and Rousseeuw[14]) are centroid-based, i.e., they compute the cluster centroids along with the clusters. Centroids can also be defined for the output of non-centroid-based methods, most easily as

$$c_j = \arg\min_{x \in C_j} \sum_{\gamma(i)=j} d(x_i, x),$$

which corresponds to the definition of PAM. Again, there are possible variations. K-means uses squared Euclidean distances, and in case of Euclidean data the cluster centroids do not necessarily have to be members of $\mathcal{D}$, they could also be mean vectors of the observations in the clusters.

Again, by definition, $I_{centroid}(\mathcal{C}) \in [0, d_{max}]$. Small values are better, and therefore $I^*_{centroid}(\mathcal{C}) = 1 - \frac{I_{centroid}(\mathcal{C})}{d_{max}} \in [0, 1]$.

3.4 Representation of dissimilarity structure by clustering

Another way in which the clustering can be used for information reduction is that the clustering can be seen as a more simple summary or representation of the dissimilarity structure. This can be measured by correlating the vector of pairwise dissimilarities $\mathbf{d} = \text{vec}\left([d(x_i, x_j)]_{i<j}\right)$ with the vector of a "clustering

induced dissimilarity" $\mathbf{c} = \text{vec}([c_{ij}]_{i<j})$, where $c_{ij} = 1(\gamma(i) \neq \gamma(j))$, and $1(\bullet)$ denotes the indicator function. With r denoting the sample Pearson correlation,

$$I_{PearsonΓ}(\mathcal{C}) = r(\mathbf{d}, \mathbf{c}).$$

This index goes back to Hubert and Schultz[13], see also Halkidi *et al.*[6] for alternative versions. $I_{PearsonΓ} \in [-1, 1]$, and large values are good, so it can be normalised by $I^*_{PearsonΓ} = \frac{I_{PearsonΓ}+1}{2} \in [0, 1]$.

3.5 Small within-cluster gaps

The idea that a cluster should be homogeneous can mean that there are no "gaps" within a cluster, and that the cluster is well connected. A gap can be characterised as a split of a cluster into two subclusters so that the minimum dissimilarity between the two subclusters is large. The corresponding index measures the "length" (dissimilarity) of the widest within-cluster gap (an alternative would be to average widest gaps over clusters):

$$I_{widestgap}(\mathcal{C}) = \max_{C\in\mathcal{C}, D, E:\ C=D\cup E} \min_{x\in D, y\in E} d(x, y).$$

$I_{widestgap} \in [0, d_{max}]$ and low values are good, so it is normalised as $I^*_{widestgap} = 1 - \frac{I_{widestgap}}{d_{max}} \in [0, 1]$.

A version of this taking into account density values is defined in Section 3.6. Widest gaps can be found computationally by constructing the within-cluster minimum spanning trees; the widest distance occurring there is the widest gap.

3.6 Density modes and valleys

A very popular idea of a cluster is that it corresponds to a density mode, and that the density within a cluster goes down from the cluster mode to the outer regions of the cluster. Correspondingly, there should be density valleys between different clusters.

The definition of indexes that measure such a behaviour is based on a density function h that assigns a density value $h(x)$ to every observation. For Euclidean data, standard density estimators such as kernel density estimators can be used. For general dissimilarities, I here propose a simple kernel density estimator. Let $q_{d,p}$ be the p-quantile of the vector of dissimilarities $\mathbf{d}$, e.g., for $p = 0.1$, the 10% smallest dissimilarities are $\leq q_{d,0,1}$. Define the kernel and density as

$$k(d) = \left(1 - \frac{1}{q_{d,p}} d\right) 1(d \leq q_{d,p}), \qquad h(x) = \sum_{i=1}^{n} k(d(x, x_i)).$$

These can be normalised to take a maximum of 1:

$$h^*(x) = \frac{h(x)}{\max_{y\in\mathcal{D}} h(y)}.$$

Alternatively, $h_{k-nn}(x) = \frac{1}{d^k(x)}$ with $d^k(x)$ being the dissimilarity to the kth nearest neighbour would be another simple dissimilarity-based density estimator, although this has no trivial upper bound (h, even before normalising by its within-cluster maximum, is bounded by n). One could also standardise h by the within-cluster maxima if clusters with generally lower densities should have the same weight as high density clusters, but lower density values rely on fewer observations and are therefore less reliable.

Three different aspects of density-based clustering are measured by three different indexes:

1. The density should decrease within a cluster from the density mode to the "outskirts" of the cluster ($I_{densdec}$).
2. Cluster boundaries should run through density "valleys", i.e., high density points should not be close to many points from other clusters ($I_{densbound}$).
3. There should not be a big gap between high density regions within a cluster ($I_{highdgap}$; gaps as measured by $I_{widestgap}$ may be fine in the low density outskirts of a cluster).

The idea for $I_{densdec}$ is as follows. For every cluster, starting from the cluster mode, i.e., the observation with the highest density, construct a growing sequence of observations that eventually covers the whole cluster by always adding the closest observation that is not yet included. Optimally, in this process, the within-cluster density of newly included points should always decrease. Whenever actually the density goes up, a penalty of the squared difference of the densities is incurred. The index $I_{densdec}$ aggregates these penalties. The following algorithm computes this, and it also constructs a set T that collects information about high dissimilarities between high density observations and is used for the definition of $I_{highdgap}$ below:

Initialisation $I_{d1} = 0$, $T = \emptyset$. For $j = 1, \ldots, K$:
Step 1 $S_j = \{x\}$, where $x = \arg\max_{y \in C_j} h^*(y)$.
Step 2 Let $R_j = C_j \setminus S_j$. If $R_j = \emptyset$: $j = j + 1$, if $j \leq K$ go to Step 1, if $j + K = 1$ then go to Step 5. Otherwise:
Step 3 Find $(x, y) = \arg\min_{(z_1,z_2): z_1 \in R_j, z_2 \in S_j} d(z_1, z_2)$. $S_j = S_j \cup \{x\}$, $T = T \cup \{\max_{z \in R_j} h^*(z) d(x, y)\}$.
Step 4 If $h^*(x) > h^*(y)$: $I_{d1} = I_{d1} + (h^*(x) - h^*(y))^2$, back to Step 2.
Step 5 $I_{densdec}(\mathcal{C}) = \sqrt{\frac{I_{d1}}{n}}$.

$I_{densdec}$ collects the penalties from increases of the within-cluster densities during this process.

The definition of $I_{densdec}$ does not take into account whether the neighbouring observations that produce high density values $h^*(x)$ for x are in the same cluster as x. But this is important, because it would otherwise be easy to achieve a good value of $I_{densdec}$ by cutting through high density areas and distributing a single high density area to several clusters.

A second index can be defined that penalises a high contribution of points from different clusters to the density values in a cluster (measured by h_o below),

because this means that the cluster border cuts through a high density region.

$$\text{For } x_i,\ i = 1, \ldots, n: \ h_o(x_i) = \sum_{k=1}^{n} k(d(x_i, x_k)) 1(\gamma(k) \neq \gamma(i)).$$

Normalising:

$$h_o^*(x) = \frac{h_o(x)}{\max_{y \in \mathcal{D}} h(y)}.$$

A penalty is incurred if for observations with a large density $h^*(x)$ there is a large contribution $h_o^*(x)$ to that density from other clusters:

$$I_{densbound}(\mathcal{C}) = \frac{1}{n} \sum_{j=1}^{K} \sum_{x \in C_j} h^*(x) h_o^*(x).$$

Both $I_{densdec}$ and $I_{densbound}$ are by definition ≥ 0. Also, the maximum contribution of any observation to any of $I_{densdec}$ and $I_{densbound}$ is $\frac{1}{n}$, because the normalised h^*-values are ≤ 1. These are penalties, so low values are good, and normalised versions are defined as

$$I_{densdec}^*(\mathcal{C}) = 1 - I_{densdec}(\mathcal{C}),\ I_{densbound}^*(\mathcal{C}) = 1 - I_{densbound}(\mathcal{C}).$$

An issue with $I_{densdec}$ is that it is possible that there is a large gap between two observations with high density, which does not incur penalties if there are no low-density observations in between. This can be picked up by a version of $I_{widestgap}$ based on the density-weighted gap information collected in T above. This is suggested instead of $I_{widestgap}$ if a density-based cluster concept is of interest:

$$I_{highdgap}(\mathcal{C}) = \max T.$$

$I_{highdgap}(\mathcal{C}) \in [0, d_{max}]$ and low values are good, so it is normalised as $I_{highdgap}^*(\mathcal{C}) = 1 - \frac{I_{highdgap}(\mathcal{C})}{d_{max}} \in [0, 1]$.

3.7 Uniform within-cluster density

Sometimes different clusters should not (only) be characterised by gaps between them; overlapping regions in data space may be seen as different clusters if they have different within-cluster density levels, which in some applications could point to different data generating mechanisms behind the different clusters, which the researcher would like to discover. Such a cluster concept would require that densities within clusters are more or less uniform.

This can be characterised by the coefficient of variation CV of either the within-cluster density values or the dissimilarities to the kth nearest within-cluster neighbour $d_w^k(x)$ (say $k = 4$). The latter is preferred here because as opposed to the density values, $d_w^k(x)$ is clean from the influence of observations from the other clusters. Define for $j = 1, \ldots, k$, assuming $n_j > k$:

$$m(C_j; k) = \frac{1}{n_j} \sum_{x \in C_j} d_w^k(x), \qquad \text{CV}(C_j) = \frac{\sqrt{\frac{1}{n_j - 1} \sum_{x \in C_j} (d_w^k(x) - m(C_j; k))^2}}{m(C_j; k)}.$$

Using this,

$$I_{cvdens}(\mathcal{C}) = \frac{\sum_{j=1}^{K} n_j \mathrm{CV}(C_j) 1(n_j > k)}{\sum_{j=1}^{K} n_j 1(n_j > k)}.$$

Low values are good. The maximum value of the coefficient of variation based on n observations is $\sqrt{n}$ (Katsnelson and Kotz[15]), so a normalised version is $I^*_{cvdens}(\mathcal{C}) = 1 - \frac{I_{cvdens}(\mathcal{C})}{\sqrt{n}}$.

3.8 Entropy

In some clustering applications, particularly where clustering is done for "organisational" reasons such as information compression, it is useful to have clusters that are roughly of the same size. This can be measured by the entropy:

$$I_{entropy}(\mathcal{C}) = -\sum_{j=1}^{K} \frac{n_j}{n} \log\left(\frac{n_j}{n}\right).$$

Large values are good. The entropy is maximised for fixed K by $e_{max}(K) = -\log\left(\frac{1}{K}\right)$, so it can be normalised by $I^*_{entropy}(\mathcal{C}) = \frac{I_{entropy}(\mathcal{C})}{e_{max}(K)}$.

3.9 Parsimony

In case that there is a preference for a lower number of clusters, one could simply define

$$I^*_{parsimony} = 1 - \frac{K}{K_{max}},$$

(already normalised) with K_{max} the maximum number of clusters of interest. If in a given application there is a known nonlinear loss connected to the number of clusters, this can obviously be used instead, and the principle can be applied also to other free parameters of a clustering method, if desired.

3.10 Similarity to homogeneous distributional shapes

Sometimes the meaning of "homogeneity" for a cluster is defined by a homogeneous probability model, e.g., Gaussian mixture model-based clustering models all clusters by Gaussian distributions with different parameters, requiring Euclidean data. Historically, due to the Central Limit Theorem and Quetelet's "elementary error hypothesis", measurement errors were widely believed to be normally/Gaussian distributed (see Stigler[17]). Under such a hypothesis it makes sense in some situations to regard Gaussian distributed observations as homogeneous, and as pointing to the same underlying mechanism; this could also motivate to cluster observations together that look like being generated from the same (approximate) Gaussian distribution. Indexes that measure cluster-wise Gaussianity can be defined, see, e.g., Lago-Fernandez and Corbacho[16]. One possible principle is to compare a one-dimensional function of the observations within a cluster to its theoretical distribution under the

data distribution of interest; e.g., Coretto and Hennig[3] compare the Mahalanobis distances of observations to their cluster centre with their theoretical χ^2-distribution using the Kolmogorow-distance. This is also possible for other distributions of interest.

3.11 Stability

Clusterings are often interpreted as meaningful in the sense that they can be generalised as substantive patterns. This at least implicitly requires that they are stable. Stability in cluster analysis can be explored using resampling techniques such as bootstrap and splitting the dataset, and clustering from different resampled datasets can be compared. This requires to run the clustering method again on the resampled datasets and I will not treat this here in detail, but useful indexes have been defined using this principle, see, e.g., Tibshirani and Walther[18] and Fang and Wang[4].

3.12 Further Aspects

Hennig[10] lists further potentially desirable characteristics of a clustering, for which further indexes could be defined:

- Areas in data space corresponding to clusters should have certain characteristics such as being linear or convex.
- It should be possible to characterise clusters using a small number of variables.
- Clusters should correspond well to an externally given partition or values of an external variable (this could for example imply that clusters of regions should be spatially connected).
- Variables should be approximately independent within clusters.

4 Aggregation of indexes

The required cluster concept and therefore the way the validation indexes can be used depends on the specific clustering application. The users need to specify what characteristics of the clustering are desired in the application. The corresponding indexes can then be aggregated to form a single criterion that can be used to compare different clustering methods, different numbers of clusters and other possible parameter choices of the clustering.

The most straightforward aggregation is to compute a weighted mean of s selected indexes $I_1, \ldots, I_s$ with weights $w_1, \ldots, w_s > 0$ expressing the relative importance of the different methods:

$$A(\mathcal{C}) = \sum_{k=1}^{s} w_k I_k. \tag{1}$$

Assuming that large values are desirable for all of $I_1, \ldots, I_s$, the best clustering for the application in question can be found by maximising A. This can be

done by comparing different clusterings from conventional clustering methods, but in principle it would also be an option to try to optimise A directly.

The weights can only be chosen to directly reflect the relative importance of the various aspects of a clustering if the values (or, more precisely, their variations) of the indexes $I_1, \ldots, I_s$ are comparable, and give the indexes equal influence on A if all weights are equal. In Section 3 I proposed tentative normalisations of all indexes, which give all indexes the same value range $[0, 1]$. Unfortunately this is not good enough to ensure comparability; on many datasets some of these indexes will cover almost the whole value range whereas other indexes may be larger than 0.9 for all clusterings that any clustering method would come up with. Therefore, Section 5 will introduce a new computational method to standardise the variation of the different criteria.

Another issue is that some indexes by their very nature favour large numbers of clusters K (obviously large within-cluster dissimilarities can be more easily avoided for large K), whereas others favour small values of K (separation is more difficult to achieve with many small clusters). The method introduced in Section 5 will allow to assess the extent to which the indexes deliver systematically larger or smaller values for larger K. Note that this can also be an issue for univariate "global" validation indexes from the literature, see Hennig and Lin[11].

If the indexes should be used to find an optimal value of K, the indexes in A should be chosen in such a way that indexes that systematically favour larger K and indexes that systematically favour smaller K are balanced.

The user needs to take into account that the proposed indexes are not independent. For example, good representation of objects by centroids will normally be correlated with having generally small within-cluster dissimilarities. Including both indexes will assign extra weight to the information that the two indexes have in common (which may sometimes but not always be desired).

There are alternative ways to aggregate the information from the different indexes. For example, one could use some indexes as side conditions rather than involving them in the definition of A. For example, rather than giving entropy a weight for aggregation as part of A, one may specify a certain minimum entropy value below which clusterings are not accepted, but not use the entropy value to distinguish between clusterings that fulfil the minimum entropy requirement. Multiplicative aggregation is another option.

5 Random clusterings for calibrating indexes

As explained above, the normalisation in Section 3 does not provide a proper calibration of the validation indexes. Here is an idea for doing this in a more appropriate way. The idea is that random clusterings are generated on $\mathcal{D}$ and index values are computed, in order to explore what range of index values can be expected on $\mathcal{D}$, so that the clusterings of interest can be compared to these. So in this Section, as opposed to conventional probability modelling, the dataset is considered as fixed but a distribution of index values is generated from various random partitions.

Completely random clusterings (i.e., assigning every observation independently to a cluster) are not suitable for this, because it can be expected that indexes formalising desirable characteristics of a clustering will normally give much worse values for them than for clusters that were generated by a clustering method. Therefore I propose two methods for random clusterings that are meant to generate clusterings that make some sense, at least by being connected in data space. The methods are called "stupid K-centroids" and "stupid nearest neighbours"; "stupid" because they are versions of popular clustering methods (centroid-based clustering like K-means or PAM, and Single Linkage/Nearest Neighbour) that replace optimisation by random decisions and are meant to be computable very quickly. Centroid-based clustering normally produces somewhat compact clusters, whereas Single Linkage is notorious for prioritising cluster separation totally over within-cluster homogeneity, and therefore one should expect these two approaches to explore in a certain sense opposite ways of clustering the data.

5.1 Stupid K-centroids clustering

Stupid K-centroids works as follows. For fixed number of cluster K draw a set of K cluster centroids $Q = \{q_1, \ldots, q_K\}$ from $\mathcal{D}$ so that every subset of size K has the same probability of being drawn. $\mathcal{C}_{K-stupidcent}(Q) = \{C_1, \ldots, C_k\}$ is defined by assigning every observation to the closest centroid:

$$\gamma(i) = \underset{j \in \{1,\ldots,K\}}{\arg\min}\ d(x_i, q_j),\ i = 1, \ldots, n.$$

5.2 Stupid nearest neighbours clustering

Again, for fixed number of cluster K draw a set of K cluster initialisation points $Q = \{q_1, \ldots, q_K\}$ from $\mathcal{D}$ so that every subset of size K has the same probability of being drawn. $\mathcal{C}_{K-stupidnn}(Q) = \{C_1, \ldots, C_k\}$ is defined by successively adding the not yet assigned observation closest to any cluster to that cluster until all observations are clustered:

Initialisation Let $Q^* = Q$. Let

$$\mathcal{C}^*(Q) = \mathcal{C}^*(Q^*) = \{C_1^*, \ldots, C_L^*\} = \{\{q_1\}, \ldots, \{q_K\}\}.$$

Step 1 Let $R^* = \mathcal{D} \setminus Q^*$. If $R^* \neq \emptyset$, find $(x, y) = \underset{(z,q): z \in R^*, q \in Q^*}{\arg\min}\ d(z, q)$, otherwise stop.

Step 2 Let $Q^* = Q^* \cup \{x\}$. For the $C^* \in \mathcal{C}^*(Q^*)$ with $y \in C^*$, let $C^* = C^* \cup \{x\}$, updating $\mathcal{C}^*(Q^*)$ accordingly. Go back to Step 1.

At the end, $\mathcal{C}_{K-stupidnn}(Q) = \mathcal{C}^*(Q^*)$.

5.3 Calibration

The random clusterings can be used in various ways to calibrate the indexes. For any value K of interest, $2B$ clusterings $\mathcal{C}_{K-collection} = (\mathcal{C}_{K:1}, \ldots, \mathcal{C}_{K:2B}) =$

$$(\mathcal{C}_{K-stupidcent}(Q_1), \ldots, \mathcal{C}_{K-stupidcent}(Q_B), \mathcal{C}_{K-stupidnn}(Q_1), \ldots, \mathcal{C}_{K-stupidnn}(Q_B))$$

on $\mathcal{D}$ are generated, say $B = 100$.

As mentioned before, indexes may systematically change over K and therefore may show a preference for either large or small K. In order to account for this, it is possible to calibrate the indexes using stupid clusterings for the same K, i.e., for a clustering $\mathcal{C}$ with $|\mathcal{C}| = K$. Consider an index I^* of interest (the normalised version is used here because this means that large values are good for all indexes). Then,

$$I^{cK}(\mathcal{C}) = \frac{I^*(\mathcal{C}) - m^*(\mathcal{C}_{K-collection})}{\sqrt{\frac{1}{2B-1}\sum_{j=1}^{2B}\left(I^*(\mathcal{C}_{K:j}) - m^*(\mathcal{C}_{K-collection})\right)^2}}, \tag{2}$$

where $m^*(\mathcal{C}_{K-collection}) = \frac{1}{2B}\sum_{j=1}^{2B} I^*(\mathcal{C}_{K:j})$. A desired set of calibrated indexes can then be used for aggregation in (1).

An important alternative to (2) is calibration by using random clusterings for all values of K together. Let $\mathcal{K} = \{2, \ldots, K_{max}\}$ be the numbers of clusters of interest (most indexes will not work for $K = 1$), $\mathcal{C}_{collection} = \{C_{K:j} : K \in \mathcal{K},\ j = 1, \ldots, 2B\}$, $m^*(\mathcal{C}_{collection}) = \frac{1}{2B(K_{max}-1)}\sum_{K=2}^{K_{max}}\sum_{j=1}^{2B} I^*(\mathcal{C}_{K:j})$. With this,

$$I^c(\mathcal{C}) = \frac{I^*(\mathcal{C}) - m^*(\mathcal{C}_{collection})}{\sqrt{\frac{1}{2B(K_{max}-1)-1}\sum_{K=2}^{K_{max}}\sum_{j=1}^{2B}\left(I^*(\mathcal{C}_{K:j}) - m^*(\mathcal{C}_{collection})\right)^2}}. \tag{3}$$

I^c does not correct for potential systematic tendencies of the indexes over $\mathcal{K}$, but this is not a problem if the user is happy to use the uncalibrated indexes directly for comparing different values of K; a potential bias toward large or small values of K in this case needs to be addressed by choosing the indexes to be aggregated in (1) in a balanced way. This can be checked by computing the aggregated index A also for the random clusterings and check how these change over the different values of K.

Another alternative is to calibrate indexes by using their rank value in the set of clusterings (random clusterings and clusterings to compare) rather than a mean/standard deviation-based standardisation. This is probably more robust but comes with some loss of information.

6 Examples

6.1 Artificial dataset

The first example is the artificial dataset shown in Figure 1. Four clusterings are compared (actually many more clusterings with K between 2 and 5

were compared on these data, but the selected clusterings illustrate the most interesting issues).

The clusterings were computed by K-means with $K = 2$ and $K = 3$, Single Linkage cut at $K = 3$ and PAM with $K = 5$. The K-means clustering with $K = 3$ and the Single Linkage clustering are shown in Figure 1. The K-means clustering with $K = 2$ puts the uniformly distributed widespread point cloud on top together in a single cluster, and the two smaller populations are the second cluster. This is the most intuitive clustering for these data for $K = 2$ and also delivered by most other clustering methods. PAM does not separate the two smaller (actually Gaussian) populations for $K = 2$, but it does so for $K = 5$, along with splitting the uniform point cloud into three parts.

	kmeans-2	kmeans-3	Single Linkage-3	PAM-5
$I^*_{withindis}$	0.654	0.799	0.643	0.836
$I^*_{0.1-sep}$	0.400	0.164	0.330	0.080
$I^*_{centroid}$	0.766	0.850	0.790	0.896
$I^*_{PearsonΓ}$	0.830	0.900	0.781	0.837
$I^*_{widestgap}$	0.873	0.873	0.901	0.901
$I^*_{densdec}$	0.977	0.981	0.981	0.985
$I^*_{densbound}$	1.000	0.999	1.000	0.997
$I^*_{highdgap}$	0.879	0.879	0.960	0.964
I^*_{cvdens}	0.961	0.960	0.961	0.959
$I^*_{entropy}$	0.863	0.993	0.725	0.967

Table 1. Normalised index values for four clusterings on artificial data.

Table 1 shows the normalised index values for these clusterings. Particularly comparing 3-means and Single Linkage, the different virtues of these clusterings are clear to see. 3-means is particularly better for the homogeneity-driven $I^*_{withindis}$ and $I^*_{centroid}$, whereas Single Linkage wins regarding the separation-oriented $I^*_{0.1-sep}$ and $I^*_{widestgap}$, with 3-means ignoring the gap between the two Gaussian populations. $I^*_{PearsonΓ}$ tends toward 3-means, too, which was perhaps less obvious, because it does not like too big distances within clusters. It is also preferred by $I^*_{entropy}$ because of joining two subpopulations that are rather small. The values for the indexes, $I^*_{densdec}$, $I^*_{densbound}$, $I^*_{highdgap}$, and I^*_{cvdens} illustrate that that the naive normalisation is not quite suitable for making the value ranges of the indexes comparable. For the density-based indexes, many involved terms are far away from the maximum used for normalisation, so the index values can be close to 0 (close to 1 after normalisation). This is amended by calibration.

Considering the clusterings with $K = 2$ and $K = 5$, it can be seen that with $K = 5$ it is easier to achieve within-cluster homogeneity ($I^*_{withindis}$, $I^*_{centroid}$), whereas with $K = 2$ it is easier to achieve separation ($I^*_{0.1-sep}$).

Table 2 shows the index values I^{cK} calibrated against random clustering with the same K. This is meant to account for the fact that some indexes differ systematically over different values of K. Indeed, using this calibration,

	kmeans-2	kmeans-3	Single Linkage-3	PAM-5
$I^{cK}_{withindis}$	0.906	1.837	-0.482	0.915
$I^{cK}_{0.1-sep}$	1.567	0.646	3.170	-0.514
$I^{cK}_{centroid}$	1.167	1.599	0.248	1.199
$I^{cK}_{Pearson\Gamma}$	1.083	1.506	0.099	0.470
$I^{cK}_{widestgap}$	1.573	1.156	1.364	0.718
$I^{cK}_{densdec}$	1.080	1.191	1.005	1.103
$I^{cK}_{densbound}$	0.452	0.449	0.519	0.647
$I^{cK}_{highdgap}$	1.317	0.428	2.043	1.496
I^{cK}_{cvdens}	1.153	0.836	0.891	0.286
$I^{cK}_{entropy}$	0.246	1.071	-0.620	0.986

Table 2. Calibrated index values (using random clusterings with same K) for four clusterings on artificial data.

PAM with $K = 5$ is no longer best for $I^{cK}_{centroid}$ and $I^{cK}_{withindis}$, and 2-means is no longer best for $I^{cK}_{0.1-sep}$. It can now be seen that 3-means is better than Single Linkage for $I^{cK}_{densdec}$. This is because density values show much more variation in the widely spread uniform subpopulation than in the two small Gaussian ones, so splitting up the uniform subpopulation is better for creating densities decreasing from the modes, despite the gap between the two Gaussian subpopulations. On the other hand, 3-means has to cut through the uniform population, which gives Single Linkage, which only cuts through clear gaps, an advantage regarding $I^{cK}_{densbound}$, and particularly 3-means incurs a large distance between the two Gaussian high density subsets within one of its clusters, which makes Single Linkage much better regarding $I^{cK}_{highdgap}$. Ultimately, the user needs to decide here whether small within-cluster dissimilarities and short dissimilarities to centroids are more important than separation and the absence of within-cluster gaps. The $K = 5$-solution does not look very attractive regarding most criteria (although calibration with the same K makes it look good regarding $I^{cK}_{densbound}$); the $K = 2$-solution only looks good regarding two criteria that may not be seen as the most important ones here.

Table 3 shows the index values I^{cK} calibrated against all random clusterings. Not much changes regarding the comparison of 3-means and Single Linkage, whereas a user who is interested in small within-cluster dissimilarities and centroid representation in absolute terms is now drawn toward PAM with $K = 5$ or even much larger K, indicating that these indexes should not be used without some kind of counterbalance, either from separation-based criteria ($I^{c}_{0.1-sep}$ and $I^{c}_{densbound}$) or taking into account parsimony. A high density gap within a cluster is most easily avoided with large K, too, whereas $K = 2$ achieves the best separation, unsurprisingly.

As this is an artificial dataset and there is no subject-matter information that could be used to prefer certain indexes, I do not present specific aggregation weights here.

	kmeans-2	kmeans-3	Single Linkage-3	PAM-5
$I^c_{withindis}$	-0.483	1.256	-0.607	1.694
$I^c_{0.1-sep}$	2.944	0.401	2.189	-0.512
$I^c_{centroid}$	-0.449	0.944	-0.059	1.712
$I^c_{PearsonΓ}$	0.658	1.515	0.058	0.743
$I^c_{widestgap}$	0.939	0.939	1.145	1.145
$I^c_{densdec}$	-0.279	0.832	0.697	1.892
$I^c_{densbound}$	0.614	0.551	0.609	0.417
$I^c_{highdgap}$	0.464	0.464	1.954	2.025
I^c_{cvdens}	0.761	0.692	0.748	0.615
$I^c_{entropy}$	0.208	1.079	-0.720	0.904

Table 3. Calibrated index values (using all random clusterings) for four clusterings on artificial data.

6.2 Tetragonula bees data

Franck *et al.*[5] published a data set giving genetic information about 236 Australasian tetragonula bees, in which it is of interest to determine the number of species. The data set is incorporated in the package "fpc" of the software system R (`www.r-project.org`) and is available on the IFCS Cluster Benchmark Data Repository `http://ifcs.boku.ac.at/repository`. Bowcock *et al.*[1] defined the "shared allele dissimilarity" formalising genetic dissimilarity appropriately for species delimitation, which is used for the present data set. It yields values in $[0, 1]$. See also Hausdorf and Hennig[7] and Hennig[8] for earlier analyses of this dataset including a discussion of the number of clusters problem. Franck *et al.*[5] provide 9 "true" species for these data, although this manual classification (using morphological information besides genetics) comes with its own problems and may not be 100% reliable.

In order to select indexes and to find weights, some knowledge about species delimitation is required, which was provided by Bernhard Hausdorf, Museum of Zoology, University of Hamburg. The biological species concept requires that there is no (or almost no) genetic exchange between different species, so that separation is a key feature for clusters that are to be interpreted as species. For the same reason, large within-cluster gaps can hardly be tolerated (regardless of the density values associated to them); in such a case one would consider the subpopulations on two sides of a gap separate species, unless a case can be made that potentially existing connecting individuals could not be sampled. Gaps may also occur in regionally separated subspecies, but this cannot be detected from the data without regional information. On the other hand, species should be reasonably homogeneous; it would be against biological intuition to have strongly different genetic patterns within the same species. This points to the indexes $I_{withindis}$, $I_{0.1-sep}$, and $I_{widestgap}$. On the other hand, the shape of the within-cluster density is not a concern here, and neither are representation of clusters by centroids, entropy, and constant within-cluster variation. The index $I_{PearsonΓ}$ is added to the set of relevant indexes, because one can interpret the species concept as a representation of genetic exchange as formalised by the shared allele dissimilarity, and $I_{PearsonΓ}$ measures the quality

of this representation. All these four indexes are used in (1) with weight 1 (one could be interested in stability as well, which is not taken into account here).

	AL-5	AL-9	AL-10	AL-12	PAM-5	PAM-9	PAM-10	PAM-12
$I^{cK}_{withindis}$	0.68	-0.04	1.70	1.60	1.83	2.45	2.03	1.80
$I^{cK}_{0.1-sep}$	1.79	2.35	2.00	2.42	0.43	1.59	2.12	0.94
$I^{cK}_{Pearson\Gamma}$	1.86	2.05	1.92	2.28	1.43	1.84	1.75	0.61
$I^{cK}_{widestgap}$	0.45	4.73	4.90	4.86	-1.03	0.41	0.42	-0.09
$A(\mathcal{C})$	4.78	9.09	10.51	11.13	2.66	6.30	6.32	3.30
ARI	0.53	0.60	0.95	0.94	0.68	0.84	0.85	0.64

Table 4. Calibrated index values (using random clusterings with same K) for eight clusterings on Tetragonula bees data with aggregated index and adjusted Rand index.

Again I present a subset of the clusterings that were actually compared for illustrating the use of the approach presented in this paper. Typically clusterings below $K = 9$ were substantially different from the ones with $K \geq 9$; clusterings with $K = 10$ and $K = 11$ from the same method were often rather similar to each other, and I present clusterings from Average Linkage and PAM with $K = 5, 9, 10$, and 12. Table 4 shows the four relevant index values I^{cK} calibrated against random clustering with the same K along with the aggregated index $A(\mathcal{C})$. Furthermore, the adjusted Rand index (ARI; Hubert and Arabie[12]) comparing the clusterings from the method with the "true" species is given (this takes values between -1 and 1 with 0 expected for random clusterings and 1 for perfect agreement). Note that despite $K = 9$ being the number of "true" species, clusterings with $K = 10$ and $K = 12$ yield higher ARI-values than those with $K = 9$, so these clusterings are preferable (it does not help much to estimate the number of species correctly if the species are badly composed). Some "true" species in the original dataset are widely regionally dispersed with hardly any similarity between subspecies.

The aggregated index $A(\mathcal{C})$ is fairly well related to the ARI (over all 55 clusterings that were compared the correlation between $A(\mathcal{C})$ and ARI is about 0.85). The two clusterings that are closest to the "true" one also have the highest values of $A(\mathcal{C})$. The within-cluster gap criterion plays a key role here, preferring Average Linkage with 9-12 clusters clearly over the other clusterings. $A(\mathcal{C})$ assigns its highest value to AL-12, whereas the ARI for AL-10 is very slightly higher. PAM delivers better clusterings regarding small within-cluster dissimilarities, but this advantage is dwarfed by the advantage of Average Linkage regarding separation and within-cluster gaps.

Table 5 shows the corresponding results with calibration using all random clusterings. This does not result in a different ranking of the clusterings, so this dataset does not give a clear hint which of the two calibration methods is more suitable, or, in other words, the results do not depend on which one is chosen.

	AL-5	AL-9	AL-10	AL-12	PAM-5	PAM-9	PAM-10	PAM-12
$I^c_{withindis}$	0.10	0.59	1.95	2.00	0.83	2.13	2.17	2.16
$I^c_{0.1-sep}$	1.98	1.54	1.05	1.02	0.53	1.01	1.13	0.21
$I^c_{Pearson\Gamma}$	1.79	1.87	1.86	1.87	1.38	1.71	1.73	0.72
$I^c_{widestgap}$	0.39	5.08	5.08	5.08	-1.12	0.39	0.39	-0.08
$A(\mathcal{C})$	4.26	9.08	9.93	9.97	1.62	5.24	5.41	3.01
ARI	0.53	0.60	0.95	0.94	0.68	0.84	0.85	0.64

Table 5. Calibrated index values (using all random clusterings) for eight clusterings on Tetragonula bees data with aggregated index and adjusted Rand index.

7 Conclusion

The multivariate array of cluster validation indexes presented here provides the user with a detailed characterisation of various relevant aspects of a clustering. The user can aggregate the indexes in a suitable way to find a useful clustering for the clustering aim at hand.

The indexes can also be used to provide a more detailed comparison of different clustering methods in benchmark studies, and a better understanding of their characteristics.

The methodology is currently partly implemented in the "fpc"-package of the statistical software system R and will soon be fully implemented there.

Most indexes require $K \geq 2$ and the approach can therefore not directly be used for deciding whether the dataset is homogeneous as a whole ($K = 1$). The individual indexes as well as the aggregated index could be used in a parametric bootstrap scheme as proposed by Hennig and Lin[11] to test the homogeneity null hypothesis against a clustering alternative.

Research is still required in order to compare the different calibration methods and some alternative versions of indexes. A theoretical characterisation of the indexes is of interest as well as a study exploring the strength of the information overlap between some of the indexes, looking at, e.g., correlations over various clusterings and datasets. Random clustering calibration may also be used together with traditional univariate validation indexes. Further methods for random clustering could be developed and it could be explored what collection of random clusterings is most suitable for calibration (some work in this direction is currently done by my PhD student Serhat Akhanli).

Acknowledgement

This work was supported by EPSRC Grant EP/K033972/1.

References

1. A. M. Bowcock, A. Ruiz-Linares, J. Tomfohrde, E. Minch, J. R. Kidd, and L. L. Cavalli-Sforza. High resolution of human evolutionary trees with polymorphic microsatellites. *Nature*, 368, 455–457, 1994.

2. T. Calinski and J. Harabasz. A dendrite method for cluster analysis. *Communications in Statistics* 3, 1-27, 1974.
3. P. Coretto and C. Hennig. Robust improper maximum likelihood: tuning, computation, and a comparison with other methods for robust Gaussian clustering. *Journal of the American Statistical Association* 111, 1648–1659, 2016.
4. Y. Fang and J. Wang. Selection of the number of clusters via the bootstrap method. *Computational Statistics and Data Analysis*, 56, 468-477, 2012.
5. P. Franck, E. Cameron, G. Good, J.-Y. Rasplus and B. P. Oldroyd. Nest architecture and genetic differentiation in a species complex of Australian stingless bees. *Molecular Ecology*, 13, 2317–2331, 2004.
6. M. Halkidi, M. Vazirgiannis and C. Hennig. Method-Independent Indices for Cluster Validation and Estimating the Number of Clusters. In *Handbook of Cluster Analysis*, C. Hennig, M. Meila, F. Murtagh, R. Rocci (eds.), CRC/Chapman & Hall, Boca Raton, 703–730, 2016.
7. B. Hausdorf and C. Hennig. Species Delimitation Using Dominant and Codominant Multilocus Markers. *Systematic Biology*, 59, 491–503, 2010.
8. C. Hennig. How many bee species? A case study in determining the number of clusters. In *Data Analysis, Machine Learning and Knowledge Discovery*, M. Spiliopoulou, L. Schmidt-Thieme, R. Janning (eds.), Springer, Berlin, 41–49, 2013.
9. C. Hennig. What are the true clusters? *Pattern Recognition Letters* 64, 53–62, 2015.
10. C. Hennig. Clustering Strategy and Method Selection. In *Handbook of Cluster Analysis*, C. Hennig, M. Meila, F. Murtagh, R. Rocci (eds.), CRC/Chapman & Hall, Boca Raton, 703–730, 2016.
11. C. Hennig and C.-J. Lin. Flexible parametric bootstrap for testing homogeneity against clustering and assessing the number of clusters. *Statistics and Computing* 25, 821–833, 2015.
12. L. J. Hubert and P. Arabie. Comparing Partitions. *Journal of Classification*, 2, 193–218, 1985.
13. L. J. Hubert and J. Schultz. Quadratic assignment as a general data analysis strategy. *British Journal of Mathematical and Statistical Psychology* 29, 190-241, 1976.
14. L. Kaufman and P. J. Rousseeuw. *Finding Groups in Data*, Wiley, New York, 1990.
15. J. Katsnelson and S. Kotz. On the upper limits of some measures of variability. *Archiv für Meteorologie, Geophysik und Bioklimatologie, Series B* 8, 103-107, 1957.
16. L. F. Lago-Fernandez and F. Corbacho. Normality-based validation for crisp clustering. *Pattern Recognition* 43, 782-795, 2010.
17. S. Stigler. *The History of Statistics: The Measurement of Uncertainty before 1900*. Harvard University Press, Cambridge, 1986.
18. R. Tibshirani and G. Walther. Cluster Validation by Prediction Strength. *Journal of Computational and Graphical Statistics*, 14, 511–528, 2005.

Monitoring the compliance of countries on emissions mitigation, using dissimilarity indices

Eleni Ketzaki[1], Stavros Rallakis[2], Nikolaos Farmakis[1], and Eftichios Sartzetakis[3]

[1] Department of Mathematics, Aristotle University of Thessaloniki, University Campus, 54124, Thessaloniki, Greece
(E-mail: eketzaki@yahoo.gr), (E-mail:farmakis@math.auth.gr)
[2] Department of Business Administration, University of Macedonia, Egnatia 156, 54636, Thessaloniki, Greece
(E-mail:srallakis@yahoo.gr)
[3] Department of Economics, University of Macedonia, Egnatia 156, 54636, Thessaloniki, Greece
(E-mail:esartz@uom.edu.gr)

Abstract. The gaseous pollutant emissions are considered as one of the major environmental problems. The countries' collective action on greenhouse gas emission mitigation, is of crucial importance for the climate sustainability. A climate agreement in order to be effective, has to inspire fairness and equity to its members. This sense of fairness is often suspended by the existing inequalities of carbon emissions between countries. The measurement of inequality of carbon emissions using dissimilarity indices is extensively studied in literature. The current paper contributes to the related literature by proposing a method for monitoring the compliance of countries on emission mitigation, using dissimilarity indices. That method will not only examine the effective measurement of emissions' dissimilarity among members, but it will also contribute to the identification of the "free rider" problem in climate coalitions.
Keywords: climate agreements, dissimilarity indices, inequality measures, Gini index, CO_2 emissions.

1 Introduction

Climate change is the greatest environmental threat that humanity has ever faced. It is caused by the build up of the greenhouse gases (GHGs) from burning fossil fuels. Greenhouse gases are the gases that trap heat into the atmosphere. Carbon dioxide holds the largest proportion of greenhouse gases. Thus it is imperative need for all countries to take collective action in the direction of carbon emission mitigation, in order to moderate the consequences of the climate change. Collective action could be taken through voluntary climate agreements. Climate agreements must ensure fairness and equity among its members, in order to be ratified by both the developed and the developing countries [1]. Therefore, the environmental inequality in terms of emissions mitigation is urgently needed to be treated. According to Boyce (2016)[2], environmental inequality has also some social welfare implications. It is intrinsic, that is every person has the right to a healthful environment. Moreover, it can have impacts on equal opportunities and on other economic outcomes for individual and countries.

The main contribution of this paper is the proposal of a method, related to the measurement of environmental inequality, by monitoring the compliance of countries to carbon emission mitigation. The measurement of the reduction of environmental inequality on carbon emissions is important for policy makers, in order to promote global cooperation. The first attempt for an agreement that set targets on carbon emissions, was made in 1997, with the Kyoto Protocol. Therefore, we apply our method in this agreement. Although, Kyoto protocol didn't manage to ensure the required number of members in order to come into force, it would be useful to see the mitigation policies of the member states, throughout that after-signature period. Some of the country members which eventually didn't ratify the protocol, withdrew from its ratification process close to the first control target emissions' period. The main reason that led to that withdrawal was probably the failure to reach their mitigation targets on time.

The effort for the emission mitigation can be accelerated by the reduction of inequality of the emissions mitigation between the member states. An increase of the inequality of the emission mitigation during a period or an unchanged inequality while there are sensible emissions mitigations from some countries, indicates that a "free rider" problem occurs. "Free riding" exists for two main reasons. The countries act in the direction of maximizing their individual welfare, that is they have incentives to produce more, while saving the mitigation costs. Also, the countries outside the coalition benefit form the coallition's collective emission mitigation, while they continue to derive benefits from their emissions, receiving this way a competitive advantage. In the climate coaliton formation literature this is called the "carbon leakage" problem [3].

Dissimilarity indices, that are commonly used in measuring economic inequality, have been also suggested as an appropriate measure for environmental inequality in terms of per capita emissions [4],[5],[6],[7],[8],[9]. In this paper we propose a method for measuring environmental inequality between countries related to their mitigation on carbon emissions. Moreover, the proposed method is extended for grouped countries. Through our proposal, it can be identified the "free rider" problem, in terms of environmental inequality between countries.

2 The Proposed Method

It is commonly known that the sense of fairness and equity, that a climate agreement must have, can be well expressed by the way in which countries mitigate their GHG emissions. A climate agreement may not be easily succeeded since the industrialised countries cannot directly alter their production process and the developing countries are trying to improve their financial position. A key issue is the confidence and the will for cooperation between its members. The necessary condition to promote the cooperation between countries is to decrease the observed inequality regarding the emissions mitigation. In order to measure the compliance of countries on their emission targets, Gini index is applied on the differences between the emissions of the base year and the target year, of each country, as it was agreed by the Kyoto protocol. Initially it

is described the method considering the countries as individual cases and then considering that countries are grouped by a specific characteristic.

Let us denote: e_i be the CO_2 emissions of gaseous pollutants in kilotons (kt) of country i at a given time, e_{ti} the CO_2 emissions of gaseous pollutants in kilotons that the country i aims to achieve according to its target, e_{bi} the CO_2 emissions in kilotons recorded for the base year, as it was defined for the i country from the Kyoto protocol and p_i the projected rate of quantified mitigation on carbon emissions. It can be easily derived that the target emissions are the product of the base year emissions and the projected rate of quantified mitigation,

$$e_{ti} = e_{bi} \cdot p_i. \tag{1}$$

Denoting y_i the difference between the current emissions and the target emissions, of a country i at a given time,

$$y_i = e_i - e_{ti}. \tag{2}$$

2.1 Description of method for individual data

We examine whether there is a dissimilarity in the differences that the countries have from their target emissions. The value of the Gini index for n countries derives from the following expression,

$$I_G = \frac{1}{(2n^2\mu)} \sum_{i=1}^{n} \sum_{j=1}^{n} |y_i - y_j|, \tag{3}$$

where μ, is the mean value of the differences y_i [11]. The Gini index is commonly used as a measure of income inequality. The data used for its computation are positive, since the income data refer to real values. The differences in the measurement of emission mitigation might also have negative values, when a country manages to fulfil its obligation at a time before the target year but it continues to mitigate its emissions well below the target. Therefore, we compute two expressions of the Gini index, in order to take into account the cases where the differences become negative.

In the first case we compute the Gini index, for positive values. To achieve that, we set $y_i = 0$ for negative differences. That happens when a country achieves its unilateral emission target. In the second case, we consider that a country could contribute to the aggregate emission target, taking into account the negative values as well. Therefore, we propose the Gini index, to be calculated by the following expression [12],

$$G_p = \frac{\Delta}{2\mu_y^p}, \tag{4}$$

where the Δ and μ_y^p are given by the following relations,

$$\begin{aligned} \Delta &= \frac{1}{n^2} \sum_{i=1}^{n} \sum_{j=1}^{n} |y_i - y_j|, \\ \mu_y^p &= \frac{1}{2} \Delta_p, \end{aligned} \tag{5}$$

where,
$\Delta_p = 2[\frac{(n-1)}{n^2}](T^+ + T^-)$, $T^+ = \sum_{i=1}^{n} max(0, y_i)$, $T^- = |\sum_{i=1}^{n} min(0, y_i)|$.

2.2 Description of method for grouped data

Denotes n_h, while $i = 1, 2, ..., m$, the number of individuals that belong to the group h, it is already known [13] that Gini index is given from the following expression,

$$I_G = e^{'} G S \tag{6}$$

where,

$$e^{'} = \left(e^{'}(n_1)\ e^{'}(n_2)\ ...\ e^{'}(n_m)\right),$$

$$S = \begin{pmatrix} s(n_1) \\ s(n_2) \\ \vdots \\ s(n_m) \end{pmatrix},$$

$$G = \begin{pmatrix} G(n_1,n_1) & G(n_1,n_2) & \cdots & G(n_1,n_m) \\ G(n_2,n_1) & G(n_2,n_2) & \cdots & G(n_2,n_m) \\ \vdots & \vdots & \ddots & \vdots \\ G(n_m,n_1) & G(n_m,n_2) & \cdots & G(n_m,n_m) \end{pmatrix}.$$

Denoting $e(n_h)$ the column vectors of n_h elements which are equal to $1/n$. $G(n_\kappa, n_\lambda)$ are the n_κ by n_λ matrices while $\kappa, \lambda = 1, 2, \cdots, m$. If $\kappa = \lambda$, then the n_κ by n_λ $G(n_\kappa, n_\lambda)$ matrices have 0 on their diagonals $(-1)'s$ in their upper right triangle and $(+1)'s$ in their lower left triangle. The n_κ by n_λ $G(n_\kappa, n_\lambda)$ matrices where the $\kappa < \lambda$ have all their elements equal to -1 and the n_κ by n_λ $G(n_\kappa, n_\lambda)$ matrices where the $\kappa > \lambda$ have all their elements equal to 1. $S(n_h)$ is the column vector of the n_h elements $s(i,h)$, where $s(i,h)$ is the share of the individual i belonging to class h in total income.

Expression (6) can be written as a sum of two components, I_w and I_B, that corresponds to the within classes inequality and between classes inequality. Thus we take the expression,

$$\begin{aligned} I_G = e^{'} G S &= \sum_{p=1}^{m} [\sum_{q=1}^{m} e^{'}(n_p) \cdot G(n_p, n_q) \cdot S(n_p)] = \\ &= \sum_{p=1}^{m} e^{'}(n_p) \cdot G(n_p, n_p) \cdot S(n_p) + \sum_{p=1}^{m} [\sum_{q \neq p}^{m} e^{'}(n_p) \cdot G(n_p, n_q) \cdot S(n_p)] = \\ &= I_W + I_B \end{aligned} \tag{7}$$

3 Application of the method

Let us consider the 39 countries, that participated in the negotiations for the signature of the Kyoto protocol (Annex I countries), presented in Table 3 (Appendix). Moreover, Table 3 contains the mitigation's percentage target of each country, the base year and the recorder carbon emissions of the base year.

In this section, it is described an application of the proposed method for The Annex I countries. The data correspond to the CO_2 emissions of each country from the year 2005 to the year 2012. We will distinguish the two cases in our application.

3.1 Application of the method for individual data

Initially, we measure the inequality considering countries as individuals. Our objective in this case is twofold. First we calculate the dissimilarity for each year and then compare it through years. Secondly we detect whether the choice of expression (3) or (4) of the Gini index affects the results.

Year	2005	2006	2007	2008	2009	2010	2011	2012
Only positive values	0.87	0.87	0.88	0.88	0.88	0.88	0.90	0.90
Positive and negative values	0.91	0.90	0.91	0.91	0.90	0.90	0.90	0.90

Table 1. Dissimilarity measurement for individual countries

According to Table 1, the values of the Gini index are close to upper limit. This indicates that there is a big inequality in the differences of the mitigation policy. Studying the data we can easily derive that by 2005, the 1/3 of the examined member states had already managed to achieve their mitigation targets. 2005 was the formal starting period for the Kyoto protocol. Until 2012, which was the target year, only 22/39 members, had managed to reach their targets. Some of the Kyoto members had shown selfish behaviour. The countries with the biggest differences from their targets by 2012, were: Canada (120464.64 kt), Japan (200128.96 kt) and USA (632002.9 kt). Moreover, we derive from Fig 1, that there is no significant difference on the results, by the use of either the restricted to positive values expression (3) or the expression calculating Gini with both positive and negative values (4). That means that our assumption setting $y_i = 0$ for the negative values in the first case, doesn't affect the results.

3.2 Application of the method for grouped data

In this part of the section we separate the countries into four groups. These groups have a geographical orientation. We chose the 15 countries of the European Community, to be the first group. These countries had signed and ratified the Kyoto protocol, as members of the premature European Union. They also set a collective target of mitigation. We chose the other group, to be the countries which they belong geographically in the European continent, but at 1997 they were not yet considered as members of the European Union. The third regional group, constitutes by the countries of the North American continent, which in our case are USA and Canada. These two countries, are the bigger emitters which have signed in the Kyoto protocol. But their policies were always mistrust in the Protocol. As a consequence was the non-ratification of the

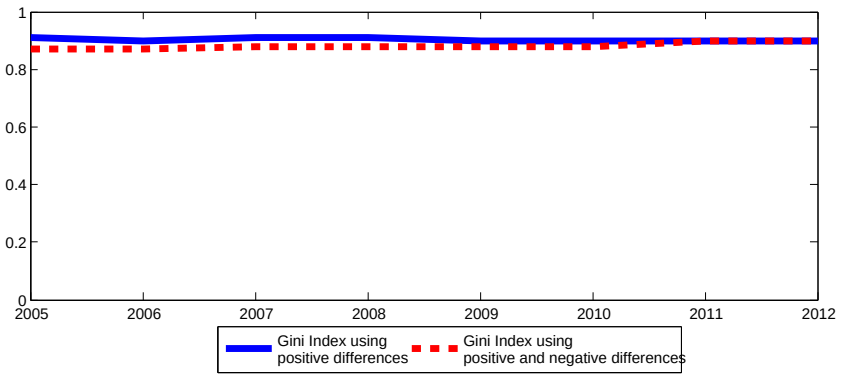

Fig. 1. Comparing methods for inequality measurement of Annex I countries, 2005-2012 period on individual data

Protocol by the USA and the withdrawal of Canada from the coalition, in 2011. The fourth regional group, are the countries of East Asia and Pacific, which includes Australia, New Zealand and Japan. Table 2, shows the values of the Gini index calculated for both between groups and within groups. Calculating the between groups Gini index, it is derived that the index takes the similar high values, across the years. That means that the inequality between groups remain the same despite the effort made by countries on emission mitigation. The same results are obtained for inequality measured within groups.

Year	2005	2006	2007	2008	2009	2010	2011	2012
B.G.G.I.	0.7915	0.7891	0.8026	0.8037	0.8113	0.8205	0.8386	0.8294
W.G.G.I.	0.0707	0.0679	0.0663	0.0666	0.0645	0.0568	0.0538	0.0566

Table 2. Dissimilarity measurement for grouped countries

In this section applying the proposed method we derive that either calculating the Gini index considering the countries as individuals or considering them as groups, the inequality remains high over the examined period of years. This means that some of the country members act as "free riders" throughout the time period and exploit the benefits from mitigation of the other countries. Thus, the proposed method is capable of detecting "free riding", in existed climate coalitions.

Regional grouping follows the World Bank documentation (`http://databank.worldbank.org/data/reports.aspx?Code=NY.GDP.MKTP.CD&id=1ff4a498&report_name=Popular-Indicators&populartype=series&ispopular=y`)

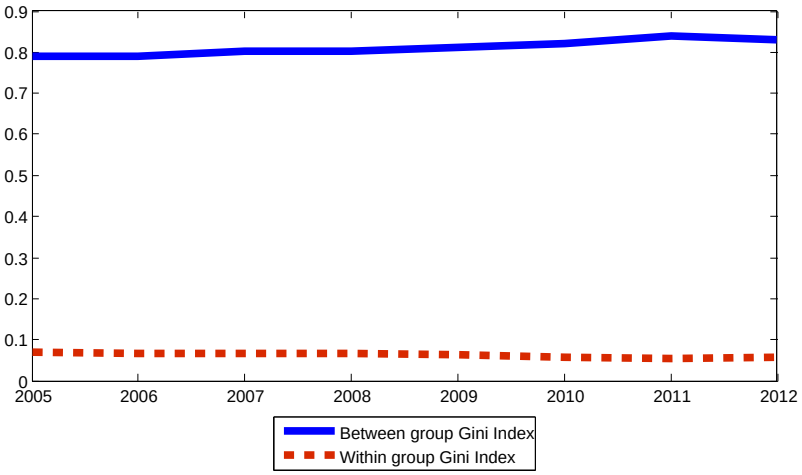

Fig. 2. Between and within group inequality measurement of Annex I countries, 2005-2012 period, on grouped data

4 Conclusions

The dissimilarity in GHG emissions mitigation is an obstacle that undercuts the countries from reaching a significant environmental agreement. This study proposes a method of calculating environmental inequality. The measurement of environmental inequality is a major issue, as it is directly linked to the impacts of climate change. The climate change burdens not only the natural environment but also the budgets of the countries. Applying the method, using different expressions of the Gini index, we reached in some interesting results. First of all, the use of either of the two different expressions of the Gini index, does not significant affect the results. It is also noticed that the values of the Gini index remain high through the time period. This indicates that there is not any difference in emission mitigation, although that some countries claimed that they have mitigate their emissions in this period. Thus, we found that the "free riding" is strongly implied in both cases, either applying the expression which uses positive and negative differences or the expression which uses only the positive ones. Furthermore, when applying the method for grouped data we find out that the Gini index, between groups remain high but it is extremely low within a group, indicating that the environmental policy is affected by the relationships that countries hold to each others.

References

1. M.T. Heil, Q.T. Wodon. Future inequality in CO_2 emissions and the impact of abatement proposals. *Environmental and Resource Economics*, 17, 2, 163–181, 2000.
2. J.K. Boyce,K. Zwickl and M. Ash. Measuring environmental inequality. *Ecological Economics*, 124, 14–123, 2016.

3. M. Heugues. International environmental cooperation: a new eye on the greenhouse gas emissions control. *Annals of Operations Research*, 220, 1, 239–262, 2014.
4. J.A. Duro. On the automatic application of inequality indexes in the analysis of the international distribution of environmental indicators. *Ecological Economics*, 76, 1–7, 2012.
5. M. T. Heil, and Q. T. Wodon. Inequality in CO2 emissions between poor and rich countries. *The Journal of Environment & Development*, 6(4), 426–452. 1997.
6. J.A. Duro and E. Padilla. International inequalities in per capita CO 2 emissions: a decomposition methodology by Kaya factors. *Energy Economics*, 28, 2, 170–187, 2006.
7. E. Padilla, and J. Duro. Explanatory factors of CO 2 per capita emission inequality in the European Union. *Energy Policy*, 62, 1320–1328, 2013.
8. J. A. Duro. Intercountry inequality on greenhouse gas emissions and world levels: An integrated analysis through general distributive sustainability indexes. *Ecological Indicators*, 66, 173–179. 2016.
9. J. A. Duro Moreno, J. Teixid-Figueras, and E. Padilla. Empirics of the international inequality in CO2 emissions intensity. 2013.
10. L. Chancel, and T. Piketty. Carbon and Inequality from Kyoto to Paris: Trends in the global inequality of carbon emissions (1998-2013) and prospects for an equitable adaptation fund. *PSE*, 2015.
11. A. SEN. *On economic inequality*, Oxford University Press, 1973.
12. E. Raffinetti, E. Siletti, and A. Vernizzi. On the Gini coefficient normalization when attributes with negative values are considered. *Statistical Methods & Applications*, 24, 3, 507–521, 2015.
13. J. Silber. Factor components, population subgroups and the computation of the Gini index of inequality. *The Review of Economics & Statistics*, 107-115. 1989

5 Appendix

Annex I countries	Percent of quantified emission mitigation p_i	Base year emissions e_{bi}	Base year
Australia	1.08	277802.53	1990
Austria *	0.92	61932.64	1990
Belgium *	0.92	118684.50	1990
Bulgaria	0.92	98815.11	1988
Canada	0.94	457534.00	1990
Croatia	0.95	23080.45	1990
Czech Republic	0.92	163864.20	1990
Denmark *	0.92	53342.45	1990
Estonia	0.92	37677,86	1990
Finland *	0.92	56767.66	1990
France *	0.92	392627.00	1990
Germany *	0.92	1032776.20	1990
Greece *	0.92	84313.57	1990
Hungary	0.94	85795.50	(1987-1985)/3
Iceland	1.10	2158.64	1990
Ireland *	0.92	32559.50	1990
Italy *	0.92	434781.95	1990
Japan	0.94	1144129.51	1990
Latvia	0.92	18622.93	1990
Lichtenstein	0.92	203.06	1990
Lithuania	0.92	36168.80	1990
Luxembourg *	0.92	12219.20	1990
Monaco	0.92	105.37	1990
Netherlands *	0.92	159389.50	1990
New Zealand	1.00	25462.57	1990
Norway	1.01	34766.97	1990
Poland	0.94	469143.82	1988
Portugal *	0.92	40261.95	1990
Romania	0.92	192407.79	1989
Russian Federation	1.00	2500352.09	1990
Slovakia	0.92	6022.70	1990
Slovenia	0.92	16281.84	1986
Spain *	0.92	228511.44	1990
Sweden *	0.92	56301.08	1990
Switzerland	0.92	44553.30	1990
Ukraine	1.00	714310.07	1990
United Kingdom *	0,92	590319.32	1990
United States of America	0.93	5100000.00	1990

Table 3. Kyoto Annex I countries' quantified emissions targets. Countries with (*) are members of the 1997's European Community.

Operating environment threats influence on critical infrastructure safety – the numerical approach

Krzysztof Kołowrocki[1] Ewa Kuligowska[2] and Joanna Soszyńska-Budny[3]

[1] Gdynia Maritime University, Gdynia, Poland
(E-mail: k.kolowrocki@wn.am.gdynia.pl)
[2] Gdynia Maritime University, Gdynia, Poland
(E-mail: e.kuligowska @wn.am.gdynia.pl)
[3] Gdynia Maritime University, Gdynia, Poland
(E-mail: joannas@am.gdynia.pl)

Abstract. The procedure for numerical approach allowing finding the main practically important safety characteristics of the critical infrastructures at the variable operation conditions including operating environment threats is applied to the safety evaluation of the port oil piping transportation system. It is assumed that the conditional safety functions are different at various operation states and have the exponential forms. Using the procedure and the program written in Mathematica, the considered port oil piping transportation system main characteristics including: the conditional and the unconditional expected values and standard deviations of the system lifetimes, the unconditional safety function and the risk function are determined.
Keywords: safety, operating environment threat, port oil piping transportation system.

1 Introduction

The critical infrastructure safety and operation process analysis is of the vital importance for industrial practice. The convenient tools for analyzing this problem are given in [1-10]. Moreover, there are many internal or external factors that the systems are exposed to. The outside-system dependencies include operating environment threats, which are the unnatural events that may change the critical infrastructure operation activity in the unsafe way or even cause the critical infrastructure damage [9].
The main objective of the paper is to present a general procedure for numerical approach applied to determine safety characteristics of the port oil piping transportation system and its components, related to its operation process including operating environment threats. The procedure is based on the model given in [5]. On the basis of the proposed procedure, the computer calculations in Mathematica environment determining these characteristics are performed.

17th *ASMDA Conference Proceedings, 6 - 9 June 2017, London, UK*

2 System operation at variable conditions including operating environment threats

We assume as in [2, 11], that the system during its operation process is taking v', $v \in N$, different operation states $z'_1,z'_2,...,z'_{v'}$. Further, we define the critical infrastructure new operation process $Z'(t)$, $t \in <0,+\infty)$ related to the critical infrastructure operating environment threats with discrete operation states from the set $\{z'_1,z'_2,...,z'_{v'}\}$. Moreover, we assume that the critical infrastructure operation process $Z'(t)$ related to its operating environment threats is a semi-Markov process with the conditional sojourn times θ'_{bl} at the operation states z'_b when its next operation state is z'_l, $b,l = 1,2,...,v'$, $b \neq l$. Under these assumptions, the critical infrastructure operation process may be described by [2]:
- the vector $[p'_b(0)]_{1\times v'}$ of the initial probabilities $p'_b(0) = P(Z'(0) = z'_b)$, $b = 1,2,...,v'$, of the system operation process $Z'(t)$ staying at particular operation states at the moment $t = 0$;
- the matrix $[p'_{bl}]_{v'\times v'}$ of probabilities p'_{bl}, $b,l = 1,2,...,v'$, $b \neq l$, of the system operation process $Z'(t)$ transitions between the operation states z'_b and z'_l;
- the matrix $[H'_{bl}(t)]_{v'\times v'}$ of conditional distribution functions $H'_{bl}(t) = P(\theta'_{bl} < t)$, $t \in <0,+\infty)$, $b,l = 1,2,...,v'$, $b \neq l$, of the system operation process $Z'(t)$ conditional sojourn times θ'_{bl} at the operation states.

2 Port oil piping transportation system operation process related to operating environment threats

The oil piping transportation system is composed of three subsystems: S_1, S_2 and S_3 linked series [1]. The system scheme is shown in Figure 1.

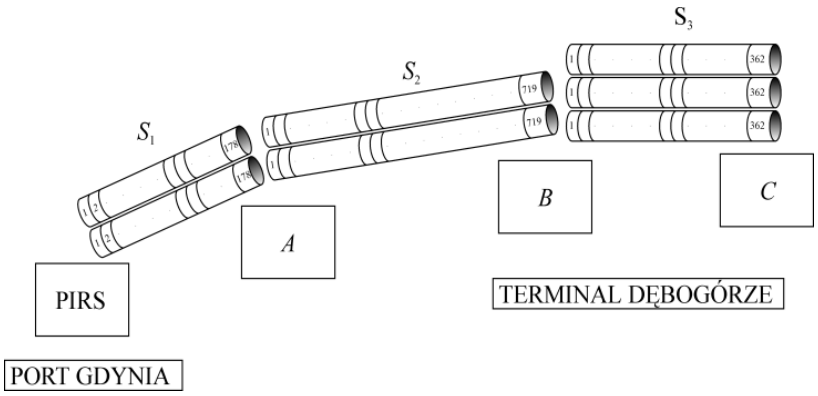

Fig. 1. The scheme of a port oil transportation system

The subsystem S_1 consists of two identical pipelines, each composed of 178 components. The subsystem S_2 consists of two identical pipelines, each composed of 719 components. The subsystem S_3 consists of three, pipelines,

two identical pipelines of the first type and one of the second type, each of them composed of 362 components.
In this report, we assume that the port oil piping transportation system operation process and safety may depend on its operating environment threats and we distinguish the following 3 unnatural threats:

- ut_1 – a human error,
- ut_2 – a terrorist attack,
- ut_3 – an act of vandalizm and/or theft.

Taking into account expert opinions on the operation process without of separation the operating environment threats of the considered piping system, in [1, 11], there were distinguished seven operation states. Taking into account expert opinions on the varying in time operation process $Z'(t)$ of the considered piping system and assuming that the threats are disjoint, according to [2], we distinguish the following as its 28 operation states, respectively marked by:

$$z'_b = z_1, \text{ for } b = 1,\ z'_b = z_2, \text{ for } b = 5,...,\ z'_b = z_7, \text{ for } b = 25; \tag{1}$$

where z'_b, $b = 1,5,...,25$, are the operation states without including operating environment threats ut_1, ut_2, ut_3 and

$$z'_b, \text{ for } b = 2,3,4,\ 6,7,8,...,\ 26,27,28. \tag{2}$$

are the operation states including state z_b, $b = 1,2,...,7$, and successively the threats ut_1, ut_2, ut_3.
The influence of the above system operation states changing on the changes of the pipeline system safety structure is similar to that described in [1].
For the new operation states numeration), we have the following system structures:

- at the system operation states z'_b, $b = 1,2,3,4,9,10,...,28$, the system is composed of two series-parallel subsystems S_1, S_2 and one series-"2 out of 3" subsystem S_3;
- at the system operation states z'_b, $b = 5,6,7,8$, the system is composed of two series-parallel subsystems S_1, S_2 and one series-parallel subsystem S_3.

Considering expert opinions coming from Baltic Oil Terminal in Dębogórze that at all operation states z_b, $b = 1,2,\ldots,7$, of the port oil piping system, the probability of a human error, a terrorist attack and an act of vandalism and/or theft can be approximately and respectively evaluated as [2, 11]

$$P_b(ut_1) = P(ut_1) = 1/1158\text{h} = 0.00086,\quad P_b(ut_2) = P(ut_2) = 0,$$
$$P_b(ut_3) = P(ut_3) = 1/13100\text{h} = 0.000076. \tag{3}$$

According to [2], it was possible to predict the limit transient probabilities of the port oil piping transportation system operation process $Z'(t)$ including operating environment threats at particular states:

$$p'_1 = 0.394064,\quad p'_2 = 0.00086,\quad p'_3 = 0,\quad p'_4 = 0.000076,$$

$p'_5 = 0.059064$, $p'_6 = 0.00086$, $p'_7 = 0$, $p'_8 = 0.000076$,
$p'_9 = 0.002064$, $p'_{10} = 0.00086$, $p'_{11} = 0$, $p'_{12} = 0.000076$,
$p'_{13} = 0.001064$, $p'_{14} = 0.00086$, $p'_{15} = 0$, $p'_{16} = 0.000076$,
$p'_{17} = 0.199064$, $p'_{18} = 0.00086$, $p'_{19} = 0$, $p'_{20} = 0.000076$,
$p'_{21} = 0.057064$, $p'_{22} = 0.00086$, $p'_{23} = 0$, $p'_{24} = 0.000076$,
$p'_{25} = 0.281064$, $p'_{26} = 0.00086$, $p'_{27} = 0$, $p'_{28} = 0.000076$. (4)

3 Safety of port oil piping transportation system related to its operating process including operating environment threats

3.1 Port oil piping transportation system safety parameters

After considering the comments and opinions coming from experts, taking into account the effectiveness and safety aspects of the operation of the oil pipeline transportation system, we fix the number of pipeline system safety states 3 ($z = 2$) and we distinguish the following three safety states:

- a safety state 2 – piping operation is fully safe,
- a safety state 1 – piping operation is less safe and more dangerous because of the possibility of environment pollution,
- a safety state 0 – piping is destroyed.

Moreover, by the expert opinions, we assume that there are possible the transitions between the components safety states only from better to worse ones.
Considering the assumptions and agreements from Section 3, we assume that the components of the subsystem S_υ, $\upsilon = 1,2,3$, at the system operation states z'_b, $b = 1,2,...,28$, have the exponential safety functions, i.e. the coordinates of the vector (1) given in [9] are determined in *Mathematica* using the formula [11]

$$S[lambda\_]:=\text{Exp}[-lambda*t],\ t \in \langle 0,\infty) \tag{5}$$

where *lambda* is the ageing intensity of the port oil piping transportation system component at the system operation process state z'_b, $b = 1,2,...,28$.
According to expert opinions, changing the port oil piping transportation system operation process states including operating environment threats have influence on changing the system safety structures and its selected components‘ safety parameters as well. For this system, the intensities of components departure from the safety states subset {1,2}, {2}, without of operation impact (the input data for *Mathematica*), are given as follows:

- for subsystem S_1:

$lambda_{S1u} = \{0.00002, 0.00002, 0.00005\}$, for $u = 1$,
$lambda_{S1u} = \{0.00003, 0.00003, 0.00006\}$, for $u = 2$; (6)

- for subsystem S_2:

$lambda_{S2u} = \{0.00002, 0.00002, 0.00005\}$, for $u = 1$,
$lambda_{S2u} = \{0.00003, 0.00003, 0.00006\}$, for $u = 2$; (7)

- for subsystem S_3 (both piping types)

$lambda_{S3u_{\mathrm{I}}}$ = {0.00002, 0.00005}, for u = 1,
$lambda_{S3u_{\mathrm{II}}}$ = {0.000024, 0.00005}, for u = 2,
$lambda_{S3u_{\mathrm{I}}}$ = {0.000025, 0.00006}, for u = 1,
$lambda_{S3u_{\mathrm{II}}}$ = {0.000027, 0.00006}, for u = 2. (8)

The coefficients related to the operation process impact in addition with the operating environment threats influence on the port oil piping transportation system safety are given as follows:

- If[b==1||b==5||b==25,{ro_{S1}={1,1,1}; ro_{S2}={1,1,1}; ro_{S3}={1.2,1.2};}];
- If[b==9||b==17,{ro_{S1}={1.2,1.2,1.2}; ro_{S2}={1.2,1.2,1.2}; ro_{S3}={1,1};}];
- If[b==13||b==21,{ro_{S1}={1.2,1.2,1.2}; ro_{S2}={1.2,1.2,1.2}; ro_{S3}={1.2,1.2};}];
- If[b==2||b==3||b==6||b==7||b==26||b==27,{ro_{S1}={1,1,1} * {1,100,1}; ro_{S2}={1,1,1} * {1,100,1}; ro_{S3}={1.2,1.2};}];
- If[b==10||b==11||b==18||b==19,{ro_{S1}={1.2,1.2,1.2} * {1,100,1}; ro_{S2}={1.2,1.2,1.2} * {1,100,1}; ro_{S3}={1,1};}];
- If[b==14||b==15||b==22||b==23,{ro_{S1}={1.2,1.2,1.2} * {1,100,1}; ro_{S2}={1.2,1.2,1.2} * {1,100,1}; ro_{S3}={1.2,1.2};}];
- If[b==4||b==8||b==28,{ro_{S1}={1,1,1} * {1,1.1,1}; ro_{S2}={1,1,1} * {1,1.1,1}; ro_{S3}={1.2,1.2};}];
- If[b==12||b==20,{ro_{S1}={1.2,1.2,1.2} * {1,1.1,1}; ro_{S2}={1.2,1.2,1.2} * {1,1.1,1}; ro_{S3}={1,1};}];
- If[b==16||b==24,{ro_{S1}={1.2,1.2,1.2} * {1,1.1,1}; ro_{S2}={1.2,1.2,1.2} * {1,1.1,1}; ro_{S3}={1.2,1.2};}];

The new intensities of components departure from the safety states subset {1,2}, {2} with the operation impact and also the operating environment threats impact on port oil piping transportation system safety are calculated as a multiplication of the intensities (6)-(8) and the coefficients ro_{S1}, ro_{S2} and ro_{S3} for the particular operation states using the formulae:

- for subsystem S_1:
  $newlambda_{S1u} = lambda_{S1u} * ro_{S1}$, for u = 1,2,

- for subsystem S_2:
  $newlambda_{S2u} = lambda_{S2u} * ro_{S2}$, for u = 1,2,

- for subsystem S_3:
  $newlambda_{S3u_{\mathrm{I}}} = lambda_{S3u_{\mathrm{I}}} * ro_{S3}$, for u = 1,2,
  $newlambda_{S3u_{\mathrm{II}}} = lambda_{S3u_{\mathrm{II}}} * ro_{S3}$, for u = 1,2. (9)

Considering the agreements and assumptions from Section 2, the port oil piping transportation system is composed of subsystems S_1 and S_2, which components form a series-parallel structure and a subsystem S_3, which components form a series-"2 out of 3" structure or a series-parallel structure. Thus, the following procedures determining the system safety functions coordinates considering (5) are constructed:

- for the series-parallel structure (n = 2):

$$S_{s-p} = 1 - ((1 - S[newlambda_{S1u}[[1]] * 174 + newlambda_{S1u}[[2]] * 2 + newlambda_{S1u}[[3]] * 2])\text{^}n), \text{ for subsystem } S_1,\ u = 1,2,$$

$$S_{s-p} = 1 - ((1 - S[newlambda_{S2u}[[1]] * 716 + newlambda_{S2u}[[2]] * 1 + newlambda_{S2u}[[3]] * 2])\text{^}n), \text{ for subsystem } S_2,\ u = 1,2,$$

  where [[x]] gives the x's element of the appropriate list (6)-(7);

- for the series-parallel structure (n = 3):

$$S_{s-p} = 1 - ((1 - S[newlambda_{S3u_I}[[1]] * 360 + newlambda_{S3u_I}[[2]] * 2])\text{^}2 * (1 - S[newlambda_{S3u_{II}}[[1]] * 360 + newlambda_{S3u_{II}}[[2]] * 2])),$$

  for subsystem S_3, u = 1,2, where [[x]] gives the x's element of the appropriate list (8);

- for the series-"m out of k" (m = 2, k = 3) structure:

$$\begin{aligned} S_{m,k} = {} & (S[newlambda_{S3u_I}[[1]] * 360 + newlambda_{S3u_I}[[2]] * 2])\text{^}2 \\ & * (1 - S[newlambda_{S3u_{II}}[[1]] * 360 + newlambda_{S3u_{II}}[[2]] * 2]) \\ & + 2 * S[newlambda_{S3u_I}[[1]] * 360 + newlambda_{S3u_I}[[2]] * 2] \\ & \quad * (1 - S[newlambda_{S3u_I}[[1]] * 360 + newlambda_{S3u_I}[[2]] * 2]) \\ & \quad * S[newlambda_{S3u_{II}}[[1]] * 360 + newlambda_{S3u_{II}}[[2]] * 2] \\ & + (S[newlambda_{S3u_I}[[1]] * 360 + newlambda_{S3u_I}[[2]] * 2])\text{^}2 \\ & \quad * S[newlambda_{S3u_{II}}[[1]] * 360 + newlambda_{S3u_{II}}[[2]] * 2], \end{aligned}$$

  for subsystem S_3, u = 1,2,

where $newlambda_{S1u}$, $newlambda_{S2u}$, $newlambda_{S3u_I}$, $newlambda_{S3u_{II}}$, are the intensities of components departure from the safety states subset $\{u,u + 1,...,z\}$, u = 1,2, with the operation impact and also the climate-weather impact for the particular subsystem, given by (9).

3.2 Port oil piping transportation system safety characteristics

In [8], it is fixed that the port oil piping transportation system safety structure and its subsystems and components safety depend on its changing in time operation states. The influence of the system operation states changing on the changes of the system safety structure and its components safety functions is given in [2, 5]. Thus, in the case when the operation time is large enough [7, 11], the port oil transportation system unconditional safety function is given by the vector

$$\boldsymbol{S}'(t,\cdot) = [1, \boldsymbol{S}'(t,1), \boldsymbol{S}'(t,2)],\ t \in \langle 0,+\infty), \tag{10}$$

where according to (7) and considering the pipeline system operation process transient probabilities at the operation states given by (11), the vector coordinates are given respectively by

$$\begin{aligned}\boldsymbol{S}'(t,u) = {} & 0.394064\,[\boldsymbol{S}'(t,u)]^{(1)} + 0.00086\,[\boldsymbol{S}'(t,u)]^{(2)} + 0.000076\,[\boldsymbol{S}'(t,u)]^{(4)} \\ & + 0.059064\,[\boldsymbol{S}'(t,u)]^{(5)} + 0.00086\,[\boldsymbol{S}'(t,u)]^{(6)} + 0.000076\,[\boldsymbol{S}'(t,u)]^{(8)} \\ & + 0.002064\,[\boldsymbol{S}'(t,u)]^{(9)} + 0.00086\,[\boldsymbol{S}'(t,u)]^{(10)} + 0.000076\,[\boldsymbol{S}'(t,u)]^{(12)} \\ & + 0.001064\,[\boldsymbol{S}'(t,u)]^{(13)} + 0.00086\,[\boldsymbol{S}'(t,u)]^{(14)} + 0.000076\,[\boldsymbol{S}'(t,u)]^{(16)} \\ & + 0.199064\,[\boldsymbol{S}'(t,u)]^{(17)} + 0.00086\,[\boldsymbol{S}'(t,u)]^{(18)} + 0.000076\,[\boldsymbol{S}'(t,u)]^{(20)} \\ & + 0.057064\,[\boldsymbol{S}'(t,u)]^{(21)} + 0.00086\,[\boldsymbol{S}'(t,u)]^{(22)} + 0.000076\,[\boldsymbol{S}'(t,u)]^{(24)} \\ & + 0.281064\,[\boldsymbol{S}'(t,u)]^{(25)} + 0.00086\,[\boldsymbol{S}'(t,u)]^{(26)} + 0.000076\,[\boldsymbol{S}'(t,u)]^{(28)}, \\ t \in \langle 0,+\infty),\ u = 1,2, \end{aligned} \tag{11}$$

where $[\boldsymbol{S}'(t,u)]^{(b)}$, $u = 1,2$, $b = 1,2,...,28$, are given in [5].
The graph of the three-state port oil piping transportation system safety function is presented in Figure 1.

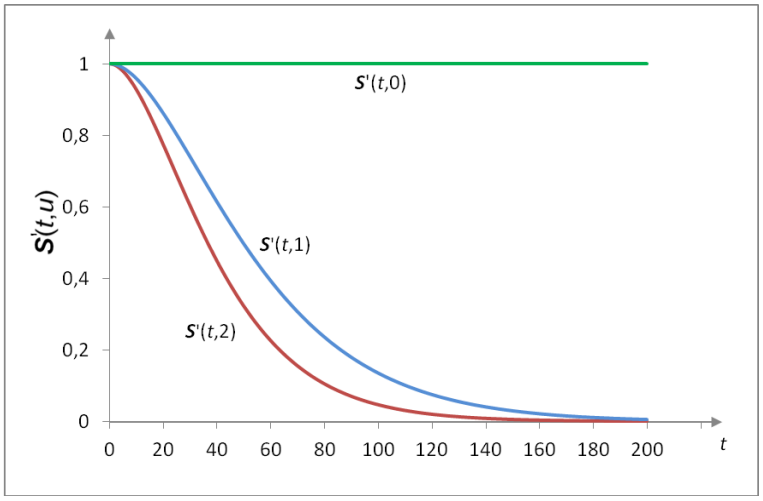

Fig. 1. The graph of the pipeline system safety function $\boldsymbol{S}'(t,\cdot)$ coordinates [11]

The expected values and standard deviations (in years) of the system unconditional lifetimes in the safety state subsets {1,2}, {2}, calculated from the above results given by (11), respectively are:

$$\mu'(1) \cong 58.23,\ \sigma'(1) \cong 39.49,\ \mu'(2) \cong 42.74,\ \sigma'(2) \cong 28.95, \tag{12}$$

and further, considering (12), the mean values (in years) of the unconditional lifetimes in the particular safety states 1, 2, respectively are:

$$\bar{\mu}'(1) = \mu'(1) - \mu'(2) = 15.49, \quad \bar{\mu}'(2) = \mu'(2) = 42.74. \tag{13}$$

Since the critical safety state is $r = 1$, then the system risk function is given by

$$\boldsymbol{r}'(t) = 1 - \boldsymbol{S}'(t,1), \text{ for } t \in \langle 0,+\infty), \tag{14}$$

where $\boldsymbol{S}'(t,1)$ is given by (11). Hence, the moment when the system risk function exceeds a permitted level, for instance $\delta = 0.05$, is

$$\tau = \boldsymbol{r}'^{-1}(\delta) \cong 11.19 \text{ year}. \tag{15}$$

The graph (the fragility curve) of the port oil piping transportation system risk function $r'(t)$ is presented in Figure 2.

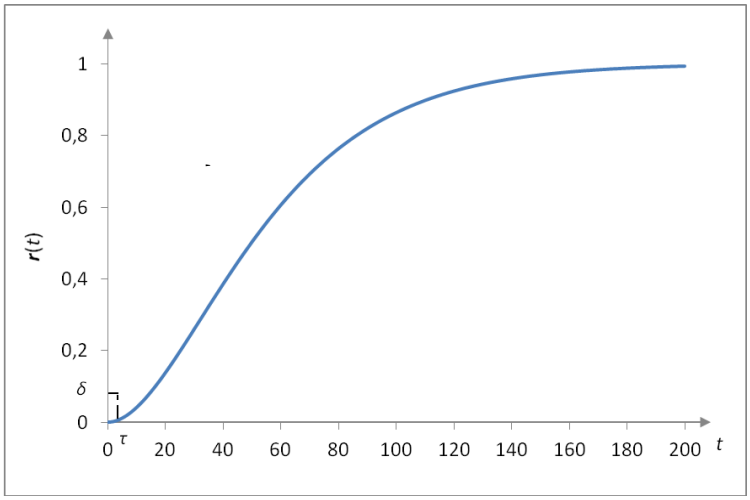

Fig. 2. The graph of the pipeline system risk function $\boldsymbol{r}'(t)$ [11]

Conclusions

The integrated general model of critical infrastructure is applied to the port oil piping transportation system safety evaluation. The predicted safety characteristics of this system operating at the variable conditions including

operating environment threats are different from those determined for the considered system without of considering the impact of operating environment threats on the system safety. This fact justifies the sensibility of considering real systems at the variable operation conditions that is appearing out in a natural way from practice.

Acknowledgments

The paper presents the results developed in the scope of the EU-CIRCLE project titled "A pan – European framework for strengthening Critical Infrastructure resilience to climate change" that has received funding from the European Union's Horizon 2020 research and innovation programme under grant agreement No 653824. *http://www.eu-circle.eu/*.

References

1. EU-CIRCLE Report D3.3-GMU3-CIOP Model1: Critical Infrastructure Operation Process (CIOP), 2016.
2. EU-CIRCLE Report D3.3-GMU3-CIOP Model2: Critical Infrastructure Operation Process (CIOP) Including Operating Environment Threats, 2016.
3. EU-CIRCLE Report D3.3-GMU3-CISM Model0: Critical Infrastructure Safety Model (CISM) Multistate Ageing Approach Independent and Dependent Components And Subsystems, 2016.
4. EU-CIRCLE Report D3.3-GMU3-IMCIS Model1: Integrated Model of Critical Infrastructure Safety (IMCIS) Related To Its Operation Process, 2016.
5. EU-CIRCLE Report D3.3-GMU3-IMCIS Model2: Integrated Model of Critical Infrastructure Safety (IMCIS) Related To Its Operation Process Including Operating Environment Threats (OET), 2016.
6. F. Grabski. Semi-Markov Processes: Applications in System Reliability and Maintenance, 1st Edition, Elsevier Science & Technology, 2014.
7. K. Kołowrocki. Reliability of Large and Complex Systems. Elsevier, 2014.
8. K. Kołowrocki and J. Soszyńska-Budny. Reliability and Safety of Complex Technical Systems and Processes: Modeling-Identification-Prediction-Optimization. Springer, 2011.
9. K. Kołowrocki and J. Soszyńska-Budny. Modelling critical infrastructure operation process including operating environment threats. Journal of Polish Safety and Reliability Association, Summer Safety and Reliability Seminars 7, 3, 81{88, 2016.
10. K. Kołowrocki, E. Kuligowska and J. Soszyńska-Budny. Integrated model of maritime ferry safety related to its operation process including operating environment threats, ESREL Proceedings Paper, 2017, in prep.
11. K. Kołowrocki, E. Kuligowska and J. Soszyńska-Budny. Integrated model of port oil piping transportation system safety including operating environment threats, Journal of KONBiN, 2017, to appear.

Safety prediction of critical infrastructure impacted by climate-weather change process

Krzysztof Kolowrocki[1], Joanna Soszynska-Budny[2,], and MateuszTorbicki

[1] Gdynia Maritime University, Gdynia, Poland
(E-mail: katmatkk@am.gdynia.pl)
[2] Gdynia Maritime University, Gdynia, Poland
(E-mail: joannas@am.gdynia.pl)
[3] Gdynia Maritime University, Gdynia, Poland
(E-mail: m.torbicki@wn.am.gdynia.pl)

Abstract. The paper is devoted to the climate influence on the safety of a critical infrastructure defined as a complex system in its operating environment that in the case of its degradation have significant destructive influence on the health, safety and security, economics and social conditions of large human communities and territory areas. The method based on the joint model linking a multistate approach to critical infrastructure safety with a semi-Markov modelling of the climate-weather change process at the critical infrastructure operation area is proposed to the safety analysis and prediction of critical infrastructures impacted by the climate hazards.

Keywords: critical infrastructure, climate change, safety, climate impact, safety indicator, prediction, oil piping transport

1 Introduction

Most real critical infrastructures are strongly influenced by changing in time the climate-weather conditions at their operating area that increasing their degradation/ageing. The time dependent interactions between the climate-weather states varying at the critical infrastructure operating area and the critical infrastructure components/assets safety states changing are evident features of most real technical critical infrastructures [1]. The common analysis of critical infrastructures safety and the climate-weather change at their operating area is of great value in the industrial practice. The convenient tools for analyzing this problem are the critical infrastructure multistate safety modelling [2], [3], [4]-[7] commonly used with the semi-Markov modelling [8], [9], [10], [3] the climate-weather change process at the critical infrastructure operating area, leading to the construction of the joint general safety model of the critical infrastructure related to climate-weather change process at its operating area

[11]-[13]. In everyday practice, there are needed the tools that could be applied to evaluating the climate-weather hazards influence on the safety characteristics of a critical infrastructure defined as a complex system in its operating environment that significant features are inside-system dependencies and outside-system dependencies, that in the case of its degradation have significant destructive influence on the health, safety and security, economics and social conditions of large human communities and territory areas [1], [14]. In the safety analysis of the critical infrastructure impacted by climate hazards, the determination of its safety function and its risk function which graph corresponds to the fragility curve [15] are crucial indicators/indices for safety practitioners. Other practically significant critical infrastructure safety indices defined in the paper are its mean lifetime up to the exceeding a critical safety state, the moment when its risk function value exceeds the acceptable safety level, the critical infrastructure intensity of ageing/degradation, the coefficient of climate-weather change process impact on critical infrastructure intensities of ageing and the coefficient of critical infrastructure resilience to climate-weather change process impact. The knowledge of these critical infrastructure safety indicators is of great value in the industrial practice. Thus, there are needed the tools for finding the critical infrastructure safety and resilience indicators and the procedures allowing for changing the critical infrastructure features, leading to the strengthening its resilience to climate change [11].
In the paper, to satisfy those needs, the simplified procedures based on the authors' theoretical results [2], [3] developments are proposed directly to users dealing with, and assuring critical infrastructure safety in everyday practice. The procedures are applied to safety analysis and safety indicators prediction for the port oil piping transportation system, the part of the Baltic oil pipeline critical infrastructure network.

2 Multistate system safety analysis

Multistate approach to safety analysis is presented in [16].

3 Critical infrastructure safety indicators

We assume that the changes of the climate-weather change process $C(t)$ states at the critical infrastructure operating area have an influence on its multistate components/assets E_i, $i=1,2,\ldots,n$, safety. Consequently, we denote the system multistate component E_i, $i=1,2,\ldots,n$, conditional lifetime in the safety state subset $\{u,u+1,\ldots,z\}$ while the climate-weather change process $C(t)$ at the system operating area is at the state c_b, $b=1,2,...,w$, by $T''^{(b)}_i(u)$ and its conditional safety function by the vector

$$[S''_i(t,\cdot)]^{(b)} = [1,\ [S''_i(t,1)]^{(b)},\ldots,\ [S''_i(t,z)]^{(b)}],\ t\in<0,\infty),\ b=1,2,\ldots,w,\ i=1,2,\ldots,n, \quad (1)$$

with the coordinates defined by

$$[S''_i(t,u)]^{(b)} = P(T''^{(b)}_i(u) > t \,|\, C(t) = c_b)$$

for $t \in <0,\infty)$, $u = 1,2,...,z$, $b = 1,2,...,w$.

The safety function $[S''_i(t,u)]^{(b)}$ is the conditional probability that the component E_i lifetime $T''^{(b)}_i(u)$ in the safety state subset $\{u, u+1,...,z\}$ is greater than *t*, while the climate-weather change process $C(t)$ at the system operating area is at the state c_b, $b = 1,2,...,w$.

In the case, the system components E_i, $i = 1,2,...,n$, at the climate-weather change process $C(t)$ at the system operating area states c_b, $b = 1,2,...,w$, have the exponential safety functions, the coordinates of the vector (1) are given by

$$[S''_i(t,u)]^{(b)} = P(T''^{(b)}_i(u) > t \,|\, C(t) = c_b) = \exp[-[\lambda''_i(u)]^{(b)} t], \quad t \in <0,\infty), \quad (2)$$

$b = 1,2,...,w$, $i = 1,2,...,n$.

Existing in (2) the intensities of ageing of the system components E_i, $i = 1,2,...,n$, (the intensities of the system components E_i, $i = 1,2,...,n$, departure from the safety state subset $\{u, u+1,...,z\}$) at the climate-weather change process $C(t)$ at the system operating area states c_b, $b = 1,2,...,w$, i.e. the coordinates of the vector

$$[\lambda''_i(\cdot)]^{(b)} = [0, [\lambda''_i(1)]^{(b)}, \ldots, [\lambda''_i(z)]^{(b)}], \quad t \in <0,+\infty), \quad b = 1,2,...,w, \quad (3)$$

$i = 1,2,...,n$,

are given by

$$[\lambda''_i(u)]^{(b)} = \rho''^{(b)}_i(u) \cdot \lambda_i(u), \quad u = 1,2,...,z, \quad b = 1,2,...,w, \quad i = 1,2,...,n, \quad (4)$$

where $\lambda_i(u)$ are the intensities of ageing of the system components E_i, $i = 1,2,...,n$, (the intensities of the system components E_i, $i = 1,2,...,n$, departure from the safety state subset $\{u, u+1,...,z\}$) without climate-weather change impact, i.e. the coordinate of the vector

$$\lambda_i(\cdot) = [0, \lambda_i(1), \ldots, [\lambda_i(z)], \quad i = 1,2,...,n,$$

and

$$[\rho''_i(u)]^{(b)}, \quad u = 1,2,...,z, \quad b = 1,2,...,w, \quad i = 1,2,...,n,$$

are the coefficients of climate-weather impact on the system components E_i, i = 1,2,...,n, intensities of ageing (the coefficients of climate-weather impact on critical infrastructure component E, i = 1,2,...,n, intensities of departure from the safety state subset $\{u, u+1,\ldots,z\}$) at the climate-weather change process operating area states c_b, $b = 1,2,\ldots,w$, i.e. the coordinate of the vector

$$[\rho_i''(\cdot)]^{(b)} = [0, [\rho_i''(1)]^{(b)}, \ldots, [\rho_i''(z)]^{(b)}], \quad b = 1,2,\ldots,w, \quad i = 1,2,\ldots,n. \tag{5}$$

The system component safety function (1), the system components intensities of ageing (3) and the coefficients of the climate-weather impact on the system components intensities of ageing (5) are main system component safety indices.
Further, we denote the critical infrastructure conditional lifetime in the safety state subset $\{u, u+1,\ldots,z\}$ while the climate-weather change process $C(t)$ at the critical infrastructure operating area is at the climate-weather state c_b, $b = 1,2,\ldots,w$, by $T''^{(b)}(u)$ and the conditional safety function (SI1) of the critical infrastructure by the vector [3]

$$[\boldsymbol{S}''(t,\cdot)]^{(b)} = [1, [\boldsymbol{S}''(t,1)]^{(b)}, \ldots, [\boldsymbol{S}''(t,z)]^{(b)}],$$

with the coordinates defined by

$$[\boldsymbol{S}''(t,u)]^{(b)} = P(T''^{(b)}(u) > t | C(t) = c_b)$$

for $t \in <0,\infty)$, $u = 1,2,\ldots,z$, $b = 1,2,\ldots,w$.

The safety function $[\boldsymbol{S}''(t,u)]^{(b)}$ is the conditional probability that the critical infrastructure lifetime $T''^{(b)}(u)$ in the safety state subset $\{u, u+1,\ldots,z\}$ is greater than t, while the climate-weather change process $C(t)$ is at the climate-weather state c_b, $b = 1,2,\ldots,w$.
Further, we assume that the critical infrastructure has the exponential conditional safety function (SI1), i.e.

$$[\boldsymbol{S}''(t,u)]^{(b)} = \exp[-[\boldsymbol{\lambda}''(u)]^{(b)} t], \quad t \in <0,+\infty), \quad [\boldsymbol{\lambda}''(u)]^{(b)} \geq 0,$$
u = 1,2,…,z.

Under this assumption, the mean lifetime of the critical infrastructure in the safety state subset $\{u, u+1,\ldots,z\}$, is given by

$$\mu''_b(u) = \frac{1}{[\boldsymbol{\lambda}''(u)]^{(b)}}, \quad u = 1,2,\ldots,z, \quad b = 1,2,\ldots,v''. \tag{6}$$

We denote the critical infrastructure unconditional lifetime in the safety state subset $\{u, u+1,...,z\}$ by $T''(u)$ and the unconditional safety function of the critical infrastructure (SI1) by the vector

$$\boldsymbol{S''}(t,\cdot) = [1,\ \boldsymbol{S''}(t,1),...,\ \boldsymbol{S''}(t,z)\ ], \tag{7}$$

with the coordinates defined by

$$\boldsymbol{S''}(t,u) = P(T''(u) > t) \text{ for } t \in <0,\infty),\ \ u = 1,2,...,z. \tag{8}$$

In the case when the critical infrastructure operation time C is large enough, the coordinates (8) of the unconditional safety function (SI1) of the critical infrastructure defined by (7) are given by

$$\boldsymbol{S''}(t,u) \cong \sum_{b=1}^{w} q_b \exp[-[\lambda''(u)]^{(b)} t] \text{ for } t \geq 0,\ u = 1,2,...,z, \tag{9}$$

where q_b, $b = 1,2,...,w,$ are the climate-weather change process $C(t)$ limit transient probabilities (C-WCPC1) defined in [12].

The mean value of the critical infrastructure unconditional lifetime $T''(u)$ in the safety state subset $\{u, u+1,...,z\}$ is given by [3], [13]

$$\mu''(u) \cong \sum_{b=1}^{w} q_b \mu''_b(u),\ \ u = 1,2,...,z, \tag{10}$$

where $\mu''_b(u)$ are the mean values of the critical infrastructure conditional lifetimes $T''^{(b)}(u)$ in the safety state subset $\{u, u+1,...,z\}$ at the climate-weather state c_b, $b = 1,2,...,w,$ given by (10) and q_b are defined in [13].

Moreover, according to [3], if r is the critical safety state, then the critical infrastructure risk function (SI2)

$$\boldsymbol{r''}(t) = P(S''(t) < r \mid S''(0) = z) = P(T''(r) \leq t),\ t \in <0,\infty),$$

defined as a probability that the critical infrastructure is in the subset of safety states worse than the critical safety state r, $r \in \{1,...,z\}$ while it was in the safety state z at the moment $t = 0$ is given by [3] , [13]

$$\boldsymbol{r''}(t) = 1 - \sum_{b=1}^{w} q_b \exp[-[\lambda''(r)]^{(b)} t],\ t \in <0,\infty). \tag{11}$$

The critical infrastructure safety function (SI1), the critical infrastructure risk function (SI2) and its graph called the critical infrastructure fragility curve (SI3) are main critical infrastructure safety indicators (SI).

Other practically useful critical infrastructure safety factors are:

- the mean value of the unconditional critical infrastructure lifetime $T''(r)$ up to the exceeding the critical safety state r (SI4) given by

$$\mu''(r) \cong \sum_{b=1}^{w} q_b \mu''_b(r), \tag{22}$$

where $\mu''_b(r)$ are the mean values of the critical infrastructure conditional lifetimes $T''^{(b)}(r)$ in the safety state subset $\{r, r+1, ..., z\}$ at the climate-weather state c_b, $b = 1,2,..w,$ according to (6), given by

$$\mu''_b(r) = \frac{1}{[\boldsymbol{\lambda}''(r)]^{(b)}} \quad b = 1,2,...,w, \tag{13}$$

and q_b are defined in [22];

- the standard deviation of the critical infrastructure lifetime $T''(r)$ up to the exceeding the critical safety state r (SI5) given by

$$\sigma''(r) = \sqrt{n''(r) - [\mu''(r)]^2},$$

(14)

where

$$n''(r) = 2\int_0^{\infty} t\, \boldsymbol{S}''(t,r)dt, \tag{15}$$

where $\boldsymbol{S}''(t,r)$ is given by (9) for $u = r$ and $\mu''(r)$ is given by (12);

- the moment τ'' when the critical infrastructure risk function exceeds a permitted level δ (SI6) given by

$$\tau'' = \boldsymbol{r}''^{-1}(\delta),$$

where $\boldsymbol{r}''^{-1}(t)$, is the inverse function of the risk function $\boldsymbol{r}''(t)$ given by (11).

Other critical infrastructure safety indices are:

- the intensities of ageing (degradation) of the critical infrastructure impacted by the climate-weather change process /the intensities of critical infrastructure departure from the safety state subset $\{u, u+1, ..., z\}$ impaced by the climate-weather change process (SI7), i.e. the coordinates of the vector

$$\boldsymbol{\lambda}''(t,\cdot) = [0, \boldsymbol{\lambda}''(t,1), ..., \boldsymbol{\lambda}''(t,z)], \; t \in <0,+\infty),$$

where

$$\boldsymbol{\lambda}''(t,u) = [\sum_{b=1}^{w}[q_b[\boldsymbol{\lambda}''(u)]^{(b)} \exp[-[\boldsymbol{\lambda}''(u)]^{(b)} t]]/$$

$$[\sum_{b=1}^{w} q_b \exp[-[\boldsymbol{\lambda}''(u)]^{(b)} t]], t \in <0,+\infty), \ u = 1,2,...,z; \quad (16)$$

- the coefficients of the climate-weather change process impact on the critical infrastructure intensities of ageing /the coefficients of the climate-weather change process impact on critical infrastructure intensities of departure from the safety state subset $\{u, u+1,...,z\}$) (SI8), i.e. the coordinates of the vector

$$\boldsymbol{\rho}''(t,\cdot) = [0, \ \boldsymbol{\rho}''(t,1), \ ..., \boldsymbol{\rho}''(t,z) \ ], \ t \in <0,+\infty),$$

where

$$\boldsymbol{\lambda}''(t,u) = \boldsymbol{\rho}''(t,u) \cdot \boldsymbol{\lambda}^0(t,u), \ t \in <0,+\infty), \ t \in <0,+\infty), \ u = 1,2,...,z, \quad (17)$$

and $\boldsymbol{\lambda}^0(t,u)$ are the intensities of ageing of the critical infrastructure (the intensities of the critical infrastructure departure from the safety state subset $\{u, u+1,...,z\}$) without of climate-weather change process impact, i.e. the coordinate of the vector

$$\boldsymbol{\lambda}^0(t,\cdot) = [0, \ \boldsymbol{\lambda}^0(t,1), , ..., \ \boldsymbol{\lambda}^0(t,z)], \ t \in <0,+\infty).$$

Additionally, we define the critical infrastructure resilence indicaator (RI), i.e. the coefficient of critical infrastructure resilience to climate-weather change process impact

$$RI(t) = 1/\boldsymbol{\rho}''(t,r), \ t \in <0,+\infty), \quad (18)$$

where $\boldsymbol{\rho}''(t,r)$ is the coefficients of the climate-weather change process impact on the critical infrastructure intensity of ageing $\boldsymbol{\lambda}''(t,r)$, i.e. the coefficients of the climate-weather change process impact on critical infrastructure intensities of departure from the safety state subset $\{r, r+1,...,z\}$ of states not worse than the critical safety state r.

4 Safety and risk prediction of port oil piping transportation system

4.1 Port oil piping transportation system description

The considered oil piping transportation system operating at one of the Baltic Oil Terminals and is describe in [16].

4.2 Safety parameters of port oil piping transportation system

After considering the comments and opinions coming from experts [17], [18], taking into account the effectiveness and safety aspects of the operation of the oil pipeline transportation system, we fix:

- the number of pipeline system safety states

$$z = 2,$$

and we distinguish the following three safety states:

- a safety state 2 - piping operation is fully safe,
- a safety state 1 - piping operation is less safe and more dangerous because of the possibility of environment pollution,
- a safety state 0 - piping is destroyed,

and, we assume that:

- there are possible the transitions between the components safety states only from better to worse ones,
- the critical safety state of the system is

$$r = 1,$$

- the system risk permitted level

$$\delta = 0.05;$$

- the number of the port oil piping transportation subsystems:

$$n = 3;$$

- the mean values of the port oil piping transportation subsystems lifetimes in the safety state subsets $\{1,2\}$, $\{2\}$, are as follows:

- subsystem S_1
  - for safety state subset $\{1,2\}$

$$\mu(1) = 400 \text{ years}, \quad (19)$$

  - for safety state subset $\{2\}$

$$\mu(2) = 300 \text{ years}. \quad (20)$$

- subsystem S_2
  - for safety state subset $\{1,2\}$

$$\mu(1) = 140 \text{ years}, \quad (21)$$

  - for safety state subset $\{2\}$

$$\mu(2) = 100 \text{ years}. \quad (22)$$

- subsystem S_3
  - for safety state subset $\{1,2\}$

$$\mu(1) = 160 \text{ years}, \tag{23}$$

  - for safety state subset $\{2\}$

$$\mu(2) = 120 \text{ years}. \tag{24}$$

From (19)-(24), it follows that the intensities of the subsystems departure from the safety states subset $\{1,2\}$, $\{2\}$, are:

- subsystem S_1
  - for safety state subset $\{1,2\}$

$$\lambda^{(1)}(1) = 0.002500, \tag{25}$$

  - for safety state subset $\{2\}$

$$\lambda^{(1)}(2) = 0.003333; \tag{26}$$

- subsystem S_2
  - for safety state subset $\{1,2\}$

$$\lambda^{(2)}(1) = 0.007143, \tag{27}$$

  - for safety state subset $\{2\}$

$$\lambda^{(2)}(2) = 0.010000; \tag{28}$$

- subsystem S_3
  - for safety state subset $\{1,2\}$

$$\lambda^{(3)}(1) = 0.006250, \tag{29}$$

  - for safety state subset $\{2\}$

$$\lambda^{(3)}(2) = 0.008333. \tag{30}$$

4.3 Parameters and characteristics of climate-weather change process at port oil piping transportation system operating area

On the basis of the statistical data collected in February during 5 years [19], it is

possible to evaluate the following unknown basic parameters of the climate-weather change process in this month [12]:

- subsystem S_1 operating area

– the number of climate-weather states (C-WCPP1)

$w = 6$

and the climate-weather states:
the climate-weather state c_1 – the wave height from 0 up to 2 m and the wind speed from 0 m/s up to 17 m/s,
the climate-weather state c_2 – the wave height from 2 m up to 5 m and the wind speed from 0 m/s up to 17 m/s,
the climate-weather state c_3 – the wave height from 5 m up to 14 m and the wind speed from 0 m/s up to 17 m/s,
the climate-weather state c_4 – the wave height from 0 up to 2 m and the wind speed from 17 m/s up to 33 m/s,
the climate-weather state c_5 – the wave height from 2 m up to 5 m and the wind speed from 17 m/s up to 33 m/s.
the climate-weather state c_6 – the wave height from 5 m up to 14 m and the wind speed from 17 m/s up to 33 m/s;

- subsystems S_2 and S_3 operating areas

– the number of climate-weather states (C-WCPP1)

$w = 16$

and the climate-weather states:
the climate-weather state c_1 – the air temperature from -25°C up to -15°C and the soil temperature from -30°C up to -5°C,
the climate-weather state c_2 – the air temperature from -15°C up to 5°C and the soil temperature from -30°C up to -5°C,
the climate-weather state c_3 – the air temperature from 5°C up to 25°C and the soil temperature from -30°C up to -5°C,
the climate-weather state c_4 – the air temperature from 25°C up to 35°C and the soil temperature from -30°C up to -5°C,
the climate-weather state c_5 – the air temperature from -25°C up to -15°C and the soil temperature from -5°C up to 5°C,
the climate-weather state c_6 – the air temperature from -15°C up to 5°C and the soil temperature from -5°C up to 5°C,
the climate-weather state c_7 – the air temperature from 5°C up to 25°C and the soil temperature from -5°C up to 5°C,
the climate-weather state c_8 – the air temperature from 25°C up to 35°C and the soil temperature from -5°C up to 5°C,
the climate-weather state c_9 – the air temperature from -25°C up to -15°C and the soil temperature from 5°C up to 20°C,
the climate-weather state c_{10} – the air temperature from -15°C up to 5°C and the soil temperature from 5°C up to 20°C,
the climate-weather state c_{11} – the air temperature from 5°C up to 25°C and the soil temperature from 5°C up to 20°C,

the climate-weather state c_{12} – the air temperature from 25°C up to 35°C and the soil temperature from 5°C up to 20°C,
the climate-weather state c_{13} – the air temperature from -25°C up to -15°C and the soil temperature from 20°C up to 37°C,
the climate-weather state c_{14} – the air temperature from -15°C up to 5°C and the soil temperature from 20°C up to 37°C,
the climate-weather state c_{15} – the air temperature from 5°C up to 25°C and the soil temperature from 20°C up to 37°C,
the climate-weather state c_{16} – the air temperature from 25°C up to 35°C and the soil temperature from 20°C up to 37°C;
The calculated climate-weather change process characteristics are [12]:

- for subsystem S_1 operating area

- the vector of the limit values of transient probabilities (C-WCPC1) of the climate-weather change process $C(t)$ at the particular states c_b

$[q_1]_{1x6} = [q_1, q_2, q_3, q_4, q_5, q_6]$,
where

$q_1 \cong 0.839,\ q_2 \cong 0.137,\ q_3 \cong 0.005,\ q_4 \cong 0,\ q_5 \cong 0.009,\ q_6 \cong 0.010.$

- subsystems S_2 and S_3 operating areas

- the vector of the limit values of transient probabilities (C-WCPC1**)** of the climate-weather change process $C(t)$ at the particular operation states c_b

$[q_1]_{1x6} = [q_1, q_2, \ldots, q_{16}]$,

where

$q_1 \cong 0.001,\ q_2 \cong 0.038,\ q_3 \cong 0,\ q_4 \cong 0,\ q_5 \cong 0,\ q_6 \cong 0.867,\ q_7 \cong 0.031,$
$q_8 \cong 0,\ q_9 \cong 0,\ q_{10} \cong 0.011,\ q_{11} \cong 0.052,\ q_{12} \cong 0,\ q_{13} \cong 0,\ q_{14} \cong 0,\ q_{15} \cong 0,$
$q_{16} \cong 0.$

4.4 Parameters of climate-weather change process impact on port oil piping transportation system safety

The coefficients of the climate-weather impact on the port oil piping transportation subsystems S_υ, $\upsilon = 1,2,3,$ intensities of ageing / the coefficients of the climate-weather impact on the port oil piping transportation subsystems S_υ, $\upsilon = 1,2,3,$ intensities of departure from the safety state subset $\{1,2\}$, $\{2\}$ at the climate-weather change process operating area states c_b, $b = 1,2,\ldots,w,$ are as follows:

- subsystem S_1:

$[\rho''^{(1)}(1)]^{(b)} = 1.30,\ [\rho''^{(1)}(2)]^{(b)} = 1.30,\ b = 3,4,5,6,$

$[\rho''^{(1)}(1)]^{(b)} = 1,\ [\rho''^{(1)}(2)]^{(b)} = 1,\ b = 1,2,$ (31)

- subsystem S_2:

$[\rho''^{(2)}(1)]^{(b)} = 1.10,\ [\rho''^{(2)}(2)]^{(b)} = 1.10,\ b = 1,2,3,4,5,8,9,12,13,14,15,16,$

$[\rho''^{(2)}(1)]^{(b)} = 1,\ [\rho''^{(2)}(2)]^{(b)} = 1,\ b = 6,7,10,11,$ (32)

- subsystem S_3:

$[\rho''^{(3)}(1)]^{(b)} = 1,\ [\rho''^{(3)}(2)]^{(b)} = 1,\ b = 1,2,...,16.$ (33)

4.5 Prediction of Safety Indicators of Port Oil Piping Transportation System

We assume that the subsystems $S_i,\ i = 1,2,3,$ of the port oil piping transportation system at the climate-weather change process $C(t)$ states $c_b,\ b = 1,2,...,16,$ conditional safety functions (1) are exponential with the coordinates $[S_i(t,u)]^{(b)},\ t \in <0,\infty),\ u = 1,2,\ b = 1,2,...,16,\ i = 1,2,3,$ given by (2). Whereas, the intensities of ageing $[\lambda_i(u)]^{(b)},\ u = 1,2,\ b = 1,2,...,16,\ i = 1,2,3,$ for the subsystems $S_i,\ i = 1,2,3,$ of the port oil piping transportation system at the climate-weather change process $C(t)$ states $c_b,\ b = 1,2,...,16,$ existing in (2) are given by (4), where $\lambda_i(u),\ u = 1,2,\ i = 1,2,3,$ are the intensities of ageing of the port oil piping transportation system subsystems $S_i,\ i = 1,2,3,$ without operation process impact and $[\rho_i(u)]^{(b)},\ u = 1,2,\ b = 1,2,...,16,\ i = 1,2,3,$ are the coefficients of climate-weather impact on the port oil piping transportation system subsystems $S_i,\ i = 1,2,3,$ intensities of ageing at the climate-weather change process $C(t)$ states $c_b,\ b = 1,2,...,16$.
After that, from (4), considering (25)-(30) and (31)-(33), it follows that the intensities of subsystems departure from the safety states subset $\{1,2\},\ \{2\},$ with the climate-weather impact on their safety are:
- subsystem S_1:

$[\lambda''^{(1)}(1)]^{(b)} = 0.003250,\ [\lambda''^{(1)}(2)]^{(b)} = 0.004333,\ b = 3,4,5,6,$

$[\lambda''^{(1)}(1)]^{(b)} = 0.002500,\ [\lambda''^{(1)}(2)]^{(b)} = 0.003333,\ i = 1,2,\ b = 1,2,$ (34)

- subsystem S_2:

$$[\lambda''^{(2)}(1)]^{(b)} = 0.007857,\ [\lambda''^{(2)}(2)]^{(b)} = 0.011000,$$
$$b = 1,2,3,4,5,8,9,12,13,14,15,16,$$
$$[\lambda''^{(2)}(1)]^{(b)} = 0.007143,\ [\lambda''^{(2)}(2)]^{(b)} = 0.010000,\ b = 6,7,10,11, \quad (35)$$

- subsystem S_3:

$$[\lambda''^{(3)}(1)]^{(b)} = 0.006250,\ [\lambda''^{(3)}(2)]^{(b)} = 0.008333,\ b = 1,2,\ldots,16. \quad (37)$$

Considering (34)-(36), as the pipeline system is a three-state (z = 2) series system [3], then its safety function (SI1) is given by [13]

$$\boldsymbol{S}''(t,\cdot) = [1, \boldsymbol{S}''(t,1)\ \boldsymbol{S}''(t,2)],\ t \geq 0,$$

where

$$\begin{aligned}\boldsymbol{S}''(t,1) &= \{0.976\exp[-0.002500t] + 0.024\exp[-0.003250t]\}\\ &\quad \{0.961\exp[-0.007143t] + 0.039\exp[-0.0092859t]\}\\ &\quad \{0.961\exp[-0.006250t] + 0.039\exp[-0.008125t]\}\\ &= 0.9013565\exp[-0.015893t] + 0.0365795\exp[-0.017768t]\\ &+ 0.0365795\exp[-0.0180359t] + 0.0014844\exp[-0.0199109t]\\ &+ 0.0221645\exp[-0.016643t] + 0.0008994\exp[-0.018518t]\\ &+ 0.0008994\exp[-0.0187859t] + 0.0000365\exp[-0.0206609t], \quad (37)\end{aligned}$$

$$\begin{aligned}\boldsymbol{S}''(t,2) &= \{0.976\exp[-0.003333t] + 0.024\exp[-0.0043329t]\}\\ &\quad \{0.961\exp[-0.01000t] + 0.039\exp[-0.013t]\}\\ &\quad \{0.961\exp[-0.008333t] + 0.039\exp[-0.010829t]\}\\ &= 0.9013565\exp[-0.021666t] + 0.0365795\exp[-0.024162t]\\ &+ 0.0365795\exp[-0.024666t] + 0.0014844\exp[-0.027162t]\\ &+ 0.0221645\exp[-0.0226659t] + 0.0008994\exp[-0.0251619t]\\ &+ 0.0008994\exp[-0.0281619t] + 0.0000365\exp[-0.0281619t], \quad (38)\end{aligned}$$

The graph of the three-state port oil piping transportation system safety function is shown in Figure 1.

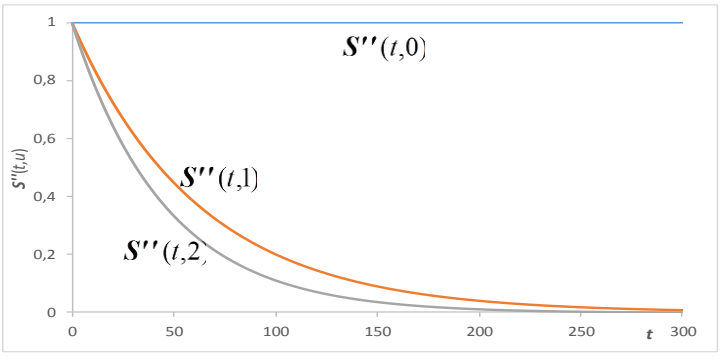

Fig. 1. The graph of the port oil piping transportation system safety function $\boldsymbol{S''}(t,\cdot)$ coordinates

Applying (10), (12)-(15) and (37)-(38), the expected values and standard deviations of the pipeline system lifetimes in the safety state subsets {1,2}, {2}, respectively are:

$$\mu''(1) \cong 62.31,\ \mu''(2) \cong 45.70 \text{ years,} \tag{39}$$

$$\sigma''(1) \cong 62.36,\ \sigma''(2) \cong 45.73 \text{ years,} \tag{40}$$

and further, it follows that the mean values of the pipeline lifetimes in the particular safety states are [17]:

$\overline{\mu}''(1) \cong 16.61$, $\overline{\mu}''(2) \cong 45.70$ year.

As the critical safety state is r =1, then by (11) and (37), the pipeline system risk function (SI2), is given by

$$\begin{aligned}\boldsymbol{r''}(t) &= 1-\boldsymbol{S''}(t,1)\\ &= 1- [0.9013565\exp[-0.015893t] + 0.0365795\exp[-0.017768t]\\ &+ 0.0365795\exp[-0.0180359t] + 0.0014844\exp[-0.0199109t]\\ &+ 0.0221645\exp[-0.016643t] + 0.0008994\exp[-0.018518t]\\ &+ 0.0008994\exp[-0.0187859t] + 0.0000365\exp[-0.0206609t]],\ t \geq 0. \end{aligned} \tag{41}$$

The graph of the risk function $\boldsymbol{r''}(t)$ of the pipeline system, the fragility curve (SI3), is shown in Figure 2.

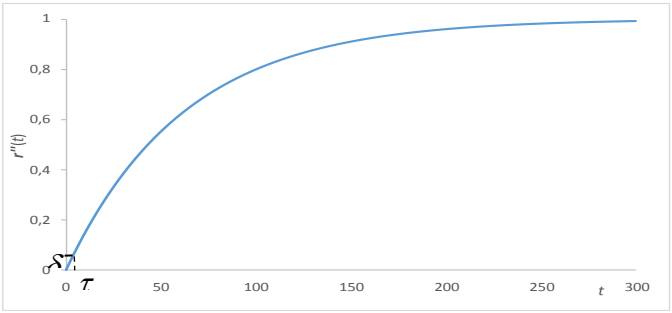

Fig. 2.. The graph of the risk function $\boldsymbol{r''}(t)$ (the fragility curve) of the port oil piping transportation system

By (39) and (40), the pipeline system mean lifetime up to exceeding critical safety state r = 1 (SI4) is

$\mu''(1) \cong 62.31$ years,

and the standard deviation of the pipeline system lifetime up to exceeding critical safety state r = 1 (SI5) is

$\sigma''(1) \cong 62.36$,

From (41), the moment when the pipeline system risk function exceeds a permitted level $\delta = 0.05$ (SI6), is

$\tau = \boldsymbol{r}''^{-1}(\delta) \cong 3.19$ years.

According to (16) and (37)-(38), the pipeline system intensities of ageing (SI7) are:

$$\begin{aligned}\boldsymbol{\lambda}''(t,1) = {} & \{0.015893 \cdot 0.9013565\exp[-0.015893t] \\ & + 0.017768 \cdot 0.0365795\exp[-0.017768t] \\ & + 0.0180359 \cdot 0.0365795\exp[-0.0180359t] \\ & + 0,0199109 \cdot 0.0014844\exp[-0.0199109t] \\ & + 0.016643 \cdot 0.0221645\exp[-0.016643t] \\ & + 0.018518 \cdot 0.0008994\exp[-0.018518t] \\ & + 0.0187859 \cdot 0.0008994\exp[-0.0187859t] \\ & + 0.0206609 \cdot 0.0000365\exp[-0.0206609t]\} \\ & /\{0.9013565\exp[-0.015893t] + 0.0365795\exp[-0.017768t] \\ & + 0.0365795\exp[-0.0180359t] + 0.0014844\exp[-0.0199109t] \\ & + 0.0221645\exp[-0.016643t] + 0.0008994\exp[-0.018518t] \\ & + 0.0008994\exp[-0.0187859t] + 0.0000365\exp[-0.0206609t]\} \\ \cong {} & 0.0160487, \end{aligned} \tag{42}$$

$$\begin{aligned}\boldsymbol{\lambda}''(t,1) = {} & \{0.021666 \cdot 0.9013565\exp[-0.021666t] \\ & + 0.024162 \cdot 0.0365795\exp[-0.024162t] \\ & + 0.024666 \cdot 0.0365795\exp[-0.024666t] \\ & + 0.027162 \cdot 0.0014844\exp[-0.027162t] \\ & + 0.0226659 \cdot 0.0221645\exp[-0.0226659t] \\ & + 0.0251619 \cdot 0.0008994\exp[-0.0251619t] \\ & + 0.0281619 \cdot 0.0008994\exp[-0.0281619t] \\ & + 0.0251619 \cdot 0.0000365\exp[-0.0281619t]\} \\ & /\{0.9013565\exp[-0.021666t] + 0.0365795\exp[-0.024162t] \\ & + 0.0365795\exp[-0.024666t] + 0.0014844\exp[-0.027162t] \\ & + 0.0221645\exp[-0.0226659t] + 0.0008994\exp[-0.0251619t] \\ & + 0.0008994\exp[-0.0281619t] + 0.0000365\exp[-0.0281619t]\} \\ \cong {} & 0.0218818. \end{aligned} \tag{43}$$

Considering (25)-(30) and (42)-(43) and applying (17), the coefficients of the climate-weather impact on the port oil piping transportation system (SI8) are:

$$\rho''(t,1) = \frac{\lambda''(t,1)}{\lambda^0(t,1)} \cong \frac{0.0160487}{0.0158932} \cong 1.01, \tag{44}$$

$$\rho''(t,2) = \frac{\lambda''(t,2)}{\lambda^0(t,2)} \cong \frac{0.0218818}{0.0216638} \cong 1.01.$$

Finally, by (18) and (44), the port oil terminal critical infrastructure resilence indicator (RI), i.e. the coefficient of the port oil terminal critical infrastructure resilience to climate-weather change process impact, is

$$RI(t) = 1/\rho(t,1) \cdot \cong 0.99 = 99\%.$$

Conclusions

The paper delivers procedures that allow to find the main an practically important safety characteristics of the critical infrastructures impacted by the climate-weather change process at their operation area. The safety characteristics of the port oil piping transportation system, using these procedures, are different from that obtained without considering the climate-weather impacts. This fact justifies the sensibility of analysing the technical critical infrastructures safety related to the climate-weather change process that improve the accuracy of their safety evaluation. Presented tools can be useful in safety evaluation of a very wide class of real technical critical infrastructures impacted by climate hazards at their operating areas that have an influence on changing their components safety parameters. The results can be interesting for safety practitioners from various industrial sectors.

Acknowledgments

The paper presents the results developed in the scope of the EU-CIRCLE project titled “A pan – European framework for strengthening Critical Infrastructure resilience to climate change” that has received funding from the European Union’s Horizon 2020 research and innovation programme under grant agreement No 653824. http://www.eu-circle.eu/.

References

1. EU-CIRCLE Taxonomy, EU-CIRCLE Project Report D1.1, 2015.
2. K. Kołowrocki. Reliability of Large and Complex Systems, Amsterdam, Boston, Heidelberd, London, New York, Oxford, Paris, San Diego, San Francisco, Singapore, Sidney, Tokyo, Elsevier, 2014.
3. K. Kołowrocki and J. Soszyńska-Budny. Reliability and Safety of Complex Technical Systems and Processes: Modelling - Identification - Prediction - Optimization, London, Dordrecht, Heildeberg, New York, Springer, 2011.

4. A. Lisnianski, G and Levitin. Multi-State System Reliability. Assessment, Optimization and Applications, World Scientific Publishing Co. Pte. Ltd., 2003.
5. J. Xue. On multi-state system analysis. IEEE Transactions on Reliability, 34, 329{337, 1985.
6. J. Xue and K. Yang. Dynamic reliability analysis of coherent multi-state systems. IEEE Transactions on Reliability, 4, 44, 683{688, 1995a.
7. J. Xue and K. Yang. Symmetric relations in multi-state systems. IEEE Transactions on Reliability, 4, 44, 689{693, 1995b.
8. T. Aven. Reliability evaluation of multistate systems with multistate components. IEEE Transactions on Reliability, 34, 473{479, 1985.
9. F. Grabski. Semi-Markov Processes: Application in System Reliability and Maintenance, Amsterdam, Boston, Heidelberd, London, New York, Oxford, Paris, San Diego, San Francisco, Singapore, Sidney, Tokyo, Elsevier, 2014.
10. D. Klabjan and D. Adelman. Existence of optimal policies for semi-Markov decision processes using duality for infinite linear programming, Siam *J Contr Optim* 44(6), 2104-2122, 2006.
11. K. Kołowrocki and J. Soszyńska-Budny. How to model and to analyse operation threats and climate-weather hazards influence on critical infrastructure safety – An overall approach, EU-CIRCLE Report D3.3-GMU0, 2016.
12. K. Kołowrocki, J. Soszyńska-Budny and M. Torbicki. Critical Infrastructure Operating Area Climate-Weather Change Process (C-WCP) Including Extreme Weather Hazards (EWH), C-WCP Model 3, EU-CIRCLE Report D3.3-GMU0, 2016.
13. K. Kołowrocki, J. Soszyńska-Budny and M. Torbicki. Integrated Model of Critical Infrastructure Safety (IMCIS) Related to Climate-Weather Change Process, IMCIS Model 3, EU-CIRCLE Report D3.3-GMU0, 2016.
14. K. Kołowrocki and J. Soszyńska-Budny. Introduction to safety analysis of critical infrastructures, Journal of Polish Safety and Reliability Association, Summer Safety and Reliability Seminars 3, 73{88, 2012.
15. P. Ben, B.P. Gouldby, M.T. Schultz, J.D. Simm and J.L. Wibowo. Beyond the Factor of Safety: Developing Fragility Curves to Characterize System Reliability, Report in Water Resources Infrastructure Program ERDC SR-10-1, Prepared for Headquarters, U.S. Army Corps of Engineers, Washington, 2010.
16. K. Kołowrocki and J. Soszyńska-Budny. Port oil transport critical infrastructure safety approximate evaluation. Proc. *of 17rd ASMDA Conference,..., 2017.*
17. M. Drzazga, P. Dziula, K. Kołowrocki and M. Reszko. Expert Opinions on Piping and Ferry and Their Components Safety Parameters and Their Exposure to Operating Environment Threats and Climate-Weather Impacts, EU-CIRCLE Report D3.3-GMU0, 2016.
18. S. Helvacioglu and M. Insel. Expert system applications in marine technologies. Ocean Engineering, 35, 11,12, 1067{1074, 2008.

19. E. Jakusik. Climate Change Related Data Collection for Port Oil Piping Transportation System and Maritime Ferry Operating at Baltic Sea Areas, EU-CIRCLE Report D2.2-GMU5, 2016.

Port oil transport critical infrastructure safety approximate evaluation

Krzysztof Kolowrocki[1], and Joanna Soszynska-Budny[2]

[1] Gdynia Maritime University, Gdynia, Poland
(E-mail: katmatkk@am.gdynia.pl)
[2] Gdynia Maritime University, Gdynia, Poland
(E-mail: joannas@am.gdynia.pl)

Abstract. The method based on the multistate approach to critical infrastructure safety modelling is proposed and practically useful critical infrastructure safety indicators are created. The proposed method is applied to the safety analysis of the port oil piping transportation system. Safety indicators of this critical infrastructure are approximately evaluated on the basis of data coming from experts.

Keywords: critical infrastructure, safety, safety indicator, prediction, port oil transport

1 Introduction

Most real complex technical systems are strongly influenced by changing in time their operation conditions that initiate their degradation/ageing. The time dependent interactions between the critical infrastructure safety structure and its components/assets safety states changing concerned with their processes of aging are evident features of most real technical critical infrastructures [1], [2]. The convenient tool for analysing this problem is the critical infrastructure multistate safety modelling [3], [4]-[8], [9]-[12]. In everyday practice, there are needed the tools that could be applied to analyse and evaluation of the safety characteristics of critical infrastructure defined as a complex system in its operating environment that significant features are inside-system dependencies and outside-system dependencies, that in the case of its degradation have significant destructive influence on the health, safety and security, economics and social conditions of large human communities and territory areas. In the critical infrastructure safety analysis, the determination of its safety function and its risk function which graph corresponds to the fragility curve [13] defined in the paper are crucial indicators/indices for safety practitioners. Other practically

17th ASMDA Conference Proceedings, 6-9 June 2017, London, UK

significant critical infrastructure safety indices are its mean lifetime up to the exceeding a critical safety state, the moment when its risk function value exceeds the acceptable safety level and the critical infrastructure intensity of ageing/degradation. The knowledge of these critical infrastructure safety indicators is of great value in the industrial practice. In the paper, simplified procedures of finding those all safety indexes based on the authors' theoretical results, mainly given in [7], are proposed directly to operators dealing with and ensuring safety of critical infrastructures in everyday practice. The procedures are applied to safety analysis and safety indicators determination for the port oil piping transportation system, the part of the Baltic oil pipeline critical infrastructure network.

2 Theoretical backgrounds

2.1 Multistate approach

In the multistate safety analysis to define the system with degrading components, we assume that:

- all components and a system under consideration have the safety state set $\{0,1,...,z\}$, $z \geq 1$,
- the safety states are ordered, the safety state 0 is the worst and the safety state z is the best,
- $T(u)$ is a random variable representing the lifetime of a system in the safety state subset $\{u,u+1,...,z\}$ while it was in the safety state z at the moment $t = 0$,
- the system states degrades with time t,
- $s(t)$ is a system S safety state at the moment t, $t \in <0,\infty)$, given that it was in the safety state z at the moment $t = 0$.

The above assumptions mean that the safety states of the system with degrading components may be changed in time only from better to worse [5], [7], [15], [9]-[12]. The way in which the components and the system safety states change is illustrated in Figures 1 and 2.

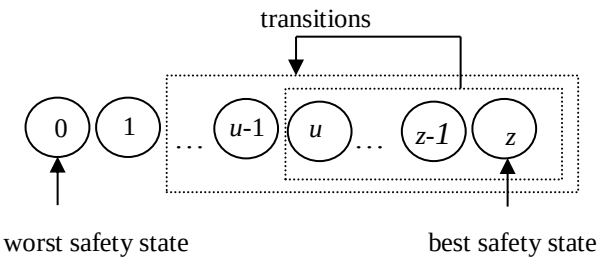

Fig. 1. Illustration of a system safety states changing

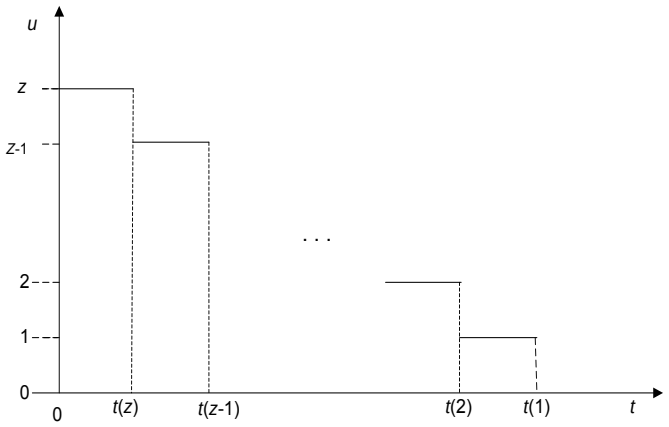

Fig. 2. The relationship between the realizations $t(u)$, $u = 1, 2, \ldots, z$, of the critical infrastructure lifetime $T(u)$, $u = 1, 2, \ldots, z$, in the safety state subsets $\{u, u+1, \ldots, z\}$, $u = 1, 2, \ldots, z$

2.2 Critical infrastructure safety indicators

We denote the critical infrastructure unconditional lifetime in the safety state subset $\{u, u+1, \ldots, z\}$ by $T(u)$ and define the critical infrastructure safety function (SI1) by the vector [7]

$$\boldsymbol{S}(t,\cdot) = [1,\ \boldsymbol{S}(t,1),\ \ldots,\ \boldsymbol{S}(t,z)],$$

with the coordinates defined by

$$\boldsymbol{S}(t,u) = P(T(u) > t) \text{ for } t \in <0,\infty),\ u = 1,2,\ldots,z.$$

The safety function coordinate $\boldsymbol{S}(t,u)$, $u = 1,2,\ldots,z$, is the probability that the system lifetime $T(u)$ in the safety state subset $\{u, u+1, \ldots, z\}$ is greater than t, $t \in <0,\infty)$.

Further, we assume that the critical infrastructure has the exponential safety function (SI1), i.e.

$$\boldsymbol{S}(t,u) = \exp[-\boldsymbol{\lambda}(u)t],\ t \in <0,+\infty),\ \boldsymbol{\lambda}(u) \geq 0,\ u = 1,2,\ldots,z.$$

Under this assumption, the mean lifetime of the system in the safety state subset $\{u, u+1, \ldots, z\}$, is given by

$$\mu(u) = \frac{1}{\boldsymbol{\lambda}(u)}, \; u = 1,2,...,z.$$

The exemplary graph of a five-state ($z = 4$) critical infrastructure safety function

$$\boldsymbol{S}(t,\cdot) = [1, \boldsymbol{S}(t,1), \boldsymbol{S}(t,2), \boldsymbol{S}(t,3), \boldsymbol{S}(t,4)]$$
$$= [1, \exp[-\boldsymbol{\lambda}(1)t], \exp[-\boldsymbol{\lambda}(2)t], \exp[-\boldsymbol{\lambda}(3)t], \exp[-\boldsymbol{\lambda}(4)t], \; t \in <0,\infty),$$

is shown in Figure 3.

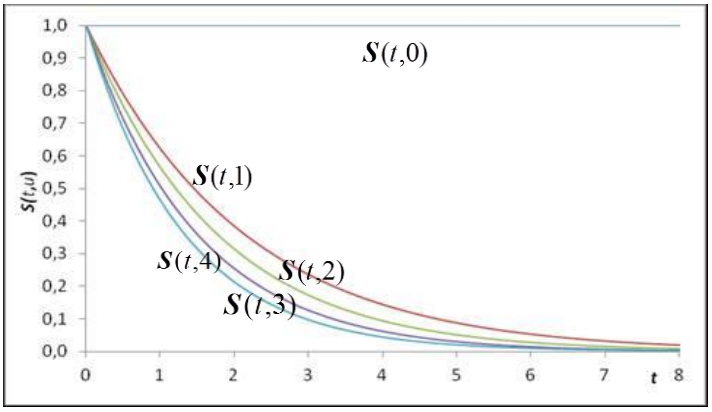

Fig. 3. The graphs of a four-state critical infrastructure safety function $\boldsymbol{S}(t,\cdot)$ coordinates

Moreover, if r is the critical safety state, then the critical infrastructure risk function (SI2)

$$\boldsymbol{r}(t) = P(S(t) < r \mid S(0) = z) = P(T(r) \le t), \; t \in <0,\infty),$$

is defined as a probability that the critical infrastructure in the subset of safety states worse than the critical safety state r, $r \in \{1,...,z\}$ while it was in the best safety state z at the moment $t = 0$ and given by [7]

$$\boldsymbol{r}(t) = 1 - \exp[-\boldsymbol{\lambda}(r)t], \;\; t \in <0,\infty). \tag{1}$$

The graph of the system risk function presented in Figure 4 is called the critical infrastructure fragility curve (SI3).

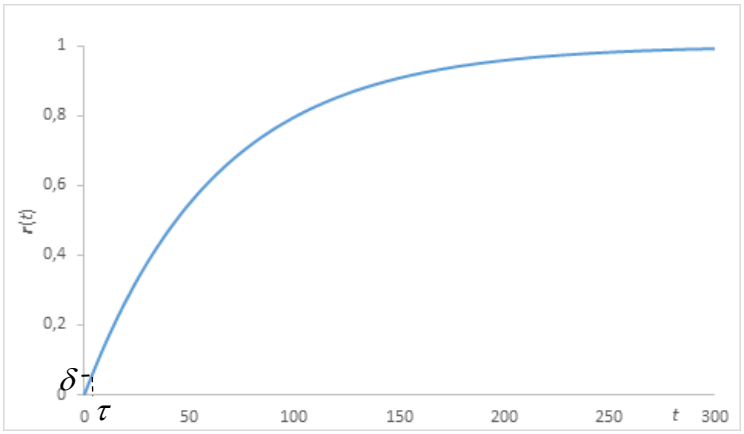

Fig. 4. The graph (The fragility curve) of a system risk function $\boldsymbol{r}(t)$

The critical infrastructure safety function (SI1), the critical infrastructure risk function (SI2) and the critical infrastructure fragility curve (SI3) are proposed as main critical infrastructure safety indicators (SI).
Other practically useful critical infrastructure safety factors are:
- the critical Infrastructure mean lifetime $T(r)$ up to exceeding critical safety state r (SI4) given by

$$\mu(r) = \frac{1}{\boldsymbol{\lambda}(r)}; \tag{2}$$

- the standard deviation of the critical infrastructure lifetime $T(r)$ up to the exceeding the critical safety state r (SI5) given by

$$\sigma(r) = \frac{1}{\boldsymbol{\lambda}(r)}; \tag{3}$$

- the moment τ of exceeding acceptable value of critical infrastructure risk function level δ (SI6) given by

$$\tau = -\frac{1}{\boldsymbol{\lambda}(r)}\ln(1-\delta) \tag{4}$$

- the intensities of ageing (degradation) of the critical infrastructure / the intensities of critical infrastructure departure from the safety state subset $\{u, u+1, ..., z\}$ (SI7), i.e. the coordinates of the vector

$$\boldsymbol{\lambda}(\cdot) = [0,\ \boldsymbol{\lambda}(1),\ \ldots,\ \boldsymbol{\lambda}(z)\ ],$$

where according to (2)

$$\boldsymbol{\lambda}(u) = \frac{1}{\mu(u)},\ u = 1,2,...,z. \tag{5}$$

4 Safety and risk prediction of port oil piping transportation system

4.1 Port oil piping transportation system description

The considered oil piping transportation system is operating at one of the Baltic Oil Terminals that is designated for the reception from ships, the storage and sending by carriages or cars the oil products. It is also designated for receiving from carriages or cars, the storage and loading the tankers with oil products such like petrol and oil. The considered terminal is composed of three parts *A*, *B* and *C*, linked by the piping transportation system with the pier. The scheme of this terminal is presented in Figure 5 [7], [16].

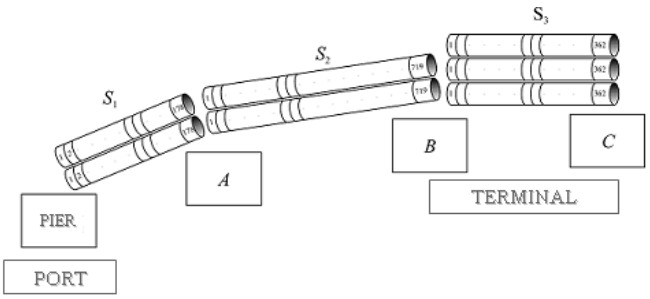

Fig. 5. The scheme of the port oil piping transportation system

Thus, the port oil pipeline transportation system consists of three subsystems:
- the subsystem S_1 composed of two pipelines, each composed of 176 pipe segments and 2 valves,
- the subsystem S_2 composed of two pipelines, each composed of 717 pipe segments and 2 valves,
- the subsystem S_3 composed of three pipelines, each composed of 360 pipe segments and 2 valves.

The subsystems S_1, S_2, S_3, indicated in Figure 9.1 are forming a general series port oil pipeline system safety structure presented in Figure 6.

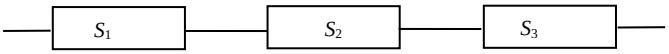

Fig. 6. General scheme of the port oil pipeline system safety structure

4.2 Parameters of port oil piping transportation system safety model

After considering the comments and opinions coming from experts, taking into account the effectiveness and safety aspects of the operation of the oil pipeline transportation system, we fix [14]:

- the number of pipeline system safety states

$$z = 2,$$

and we distinguish the following three safety states:

- a safety state 2 - piping operation is fully safe,
- a safety state 1 - piping operation is less safe and more dangerous because of the possibility of environment pollution,
- a safety state 0 - piping is destroyed,

and, we assume that:

- there are possible the transitions between the components safety states only from better to worse ones,
- the critical safety state of the system is

$$r = 1,$$

- the system risk permitted level

$$\delta = 0.05;$$

- the number of the port oil transportation system subsystems

$$n = 3;$$

- the mean values of the port oil piping transportation subsystems lifetimes in the safety state subsets $\{1,2\}$, $\{2\}$, are as follows:

- subsystem S_1

- for safety state subset $\{1,2\}$

$$\mu(1) = 400 \text{ years},$$

- for safety state subset $\{2\}$

$\mu(2)$ = 300 years.

- subsystem S_2
  - for safety state subset $\{1,2\}$

    $\mu(1)$ = 140 years,

  - for safety state subset $\{2\}$

    $\mu(2)$ = 100 years.

- subsystem S_3
  - for safety state subset $\{1,2\}$

    $\mu(1)$ = 160 years,

  - for safety state subset $\{2\}$

    $\mu(2)$ = 120 years.

4.3 Prediction of port oil piping transportation system safety indicators

Considering that the pipeline system is a three-state (z = 2) series system, its safety function (SI1) is given by [7], [16]

$$\boldsymbol{S}(t,\cdot) = [1,\ \boldsymbol{S}(t,1)\ \ \boldsymbol{S}(t,2)],\ \ t \geq 0,$$

where

$$\begin{aligned}\boldsymbol{S}(t,1) &= \exp[-0.002500t]\exp[-0.007143t]\exp[-0.006250t] \\ &= \exp[-0.015893t],\end{aligned}$$

$$\begin{aligned}\boldsymbol{S}(t,2) &= \exp[-0.003333t]\exp[-0.01000t]\exp[-0.008333t] \\ &= \exp[-0.021666t].\end{aligned}$$

The graph of the three-state pipeline system safety function is shown in Figure 7.

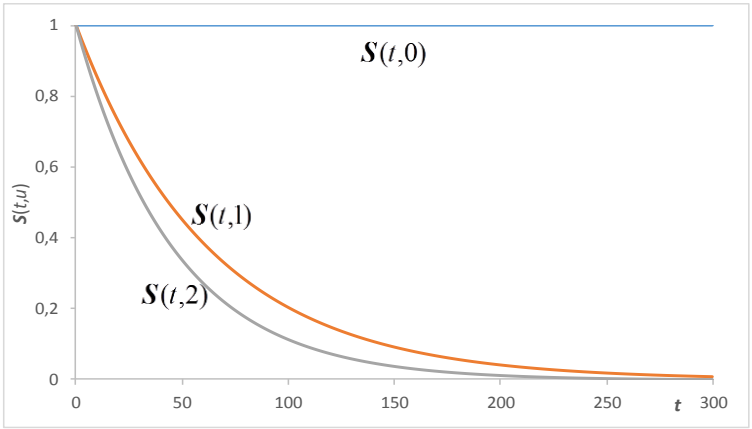

Fig. 7. The graph of the port oil piping transportation system safety function $\boldsymbol{S}(t,\cdot)$ coordinates

The expected values and standard deviations of the pipeline system lifetimes in the safety state subsets $\{1,2\}$, $\{2\}$, according (2)-(3), respectively are [16]:

$\mu(1) \cong 62.92,\ \mu(2) \cong 46.16$ years,

$\sigma(1) \cong 62.92,\ \sigma(2) \cong 46.16$ years,

and further, it follows that the mean values of the pipeline lifetimes in the particular safety states are [7]:

$\overline{\mu}(1) \cong 16.76,\ \overline{\mu}(2) \cong 46.16$ years.

As the critical safety state is r =1, then by (1), the pipeline system risk function (SI2), is given by

$\boldsymbol{r}(t) = 1 - \boldsymbol{S}(t,1)$

$= 1 - \exp[-0.015893t]$ for $t \geq 0$.

The graph of the risk function $\boldsymbol{r}(t)$ of the pipeline system, the fragility curve (SI3), is shown in Figure 8.

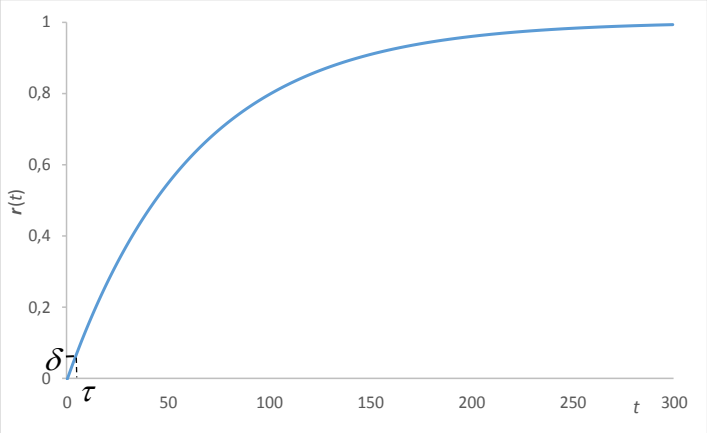

Fig. 8. The graph of the risk function $\boldsymbol{r}(t)$ (the fragility curve) of the port oil piping transportation system

By (2) and (3), the pipeline system mean lifetime up to exceeding critical safety state $r = 1$ (SI4) is

$\mu(1) \cong 62.92$ years,

and the standard deviation of the pipeline system lifetime up to exceeding critical safety state $r = 1$ (SI5) is

$\sigma(1) \cong 62.92$ years.

From (9), the moment when the pipeline system risk function exceeds a permitted level $\delta = 0.05$ (SI6), is

$$\tau = -\frac{1}{0.015893}\ln(1-0.05) \cong 3.23 \text{ years.}$$

The pipeline system intensities of ageing (SI7) are

$$\lambda(t,1) = \lambda(1) = 0.015893,$$

$$\lambda(t,2) = \lambda(2) = 0.021666.$$

The graphs of the intensities of ageing of the port oil piping transportation system are given in Figure 9.

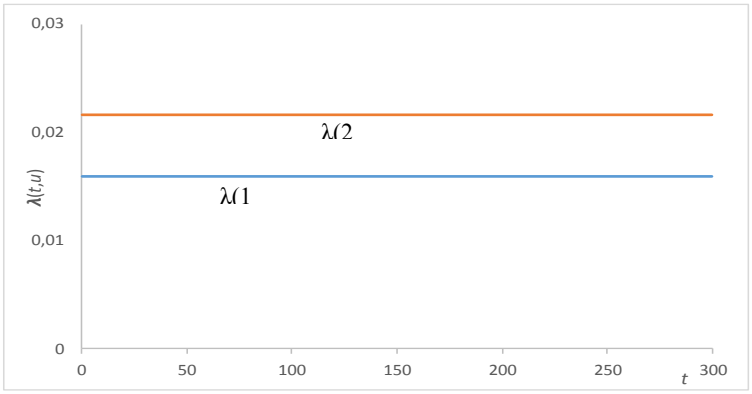

Fig. 9. The graphs of the intensities of ageing of the port oil piping transportation system

Conclusions

The paper delivers the simplified procedures that allow to find the main an practically important safety characteristics of the critical infrastructures. The safety indicators of the port oil transport critical infrastructure are predicted on the basis of data coming from experts. Although the results are approximate, they justify the sensibility of the performed analysis and evaluation of the port oil transport critical infrastructure safety indicators as their knowledge can help in ensuring and improving its safety and making its operation safer. Presented in this paper tool can be useful in safety and operation prediction of a very wide class of real technical critical infrastructures. The results can be interesting for safety practitioners from various industrial sectors.

Acknowledgments

The paper presents the results developed in the scope of the EU-CIRCLE project titled “A pan – European framework for strengthening Critical Infrastructure resilience to climate change” that has received funding from the European Union’s Horizon 2020 research and innovation programme under grant agreement No 653824. http://www.eu-circle.eu/.

References

1. EU-CIRCLE Taxonomy, EU-CIRCLE Project Report D1.1, 2015.
2. A. Lauge, J. Hernantes and J.M. Sarriegi. Critical infrastructure dependencies: A holistic, dynamic and quantitative approach. International Journal of Critical Infrastructure Protection, Vol. 8, 6{23, 2015.
3. T. Aven. Reliability evaluation of multistate systems with multistate components. IEEE Transactions on Reliability, 34, 473{479, 1985.
4. K. Kołowrocki. Safety of critical infrastructures. Journal of Polish Safety and Reliability Association, Summer Safety and Reliability Seminars, Vol. 4, No 1, 51{72, 2013.
5. K. Kołowrocki. Reliability of Large and Complex Systems, Amsterdam, Boston, Heidelberd, London, New York, Oxford, Paris, San Diego, San Francisco, Singapore, Sidney, Tokyo, Elsevier, 2014.
6. K. Kołowrocki. Modeling Reliability of Critical Infrastructures with Application to Port Oil Piping Transportation System, Advances Materials Research, Vols. 891-892, 1565{1570, 2014.
7. K. Kołowrocki and J. Soszyńska-Budny. Reliability and Safety of Complex Technical Systems and Processes: Modelling - Identification - Prediction - Optimization, London, Dordrecht, Heildeberg, New York, Springer, 2011.
8. K. Kołowrocki and J. Soszyńska-Budny. Introduction to safety analysis of critical infrastructures, Journal of Polish Safety and Reliability Association, Summer Safety and Reliability Seminars 3, 73{88, 2012.
9. J. Xue. On multi-state system analysis. IEEE Transactions on Reliability, 34, 329{337, 1985.
10. J. Xue and K. Yang. Dynamic reliability analysis of coherent multi-state systems. IEEE Transactions on Reliability, 4, 44, 683{688, 1995a.
11. J. Xue and K. Yang. Symmetric relations in multi-state systems. IEEE Transactions on Reliability, 4, 44, 689{693, 1995b.
12. K. Yu, I. Koren and Y. Guo. Generalized multistate monotone coherent systems. IEEE Transactions on Reliability, 43, 242{250, 1994.
13. P. Ben, B.P. Gouldby, M.T. Schultz, J.D. Simm and J.L. Wibowo. Beyond the Factor of Safety: Developing Fragility Curves to Characterize System Reliability, Report in Water Resources Infrastructure Program ERDC SR-10-1, Prepared for Headquarters, U.S. Army Corps of Engineers, Washington, 2010.
14. M. Drzazga, P. Dziula, K. Kołowrocki and M. Reszko. Expert Opinions on Piping and Ferry and Their Components Safety Parameters and Their Exposure to Operating Environment Threats and Climate-Weather Impacts, EU-CIRCLE Report D3.3-GMU0, 2016.
15. A. Lisnianski, G and Levitin. Multi-State System Reliability. Assessment, Optimization and Applications, World Scientific Publishing Co. Pte. Ltd., 2003.
16. K. Kołowrocki and J. Soszyńska-Budny. How to model and to analyse operation threats and climate-weather hazards influence on critical

infrastructure safety – An overall approach, EU-CIRCLE Report D3.3-GMU0, 2016.

Simplified approach to safety prediction of port oil transport critical infrastructure related to operation process

Krzysztof Kolowrocki[1], and Joanna Soszynska-Budny[2]

[1] Gdynia Maritime University, Gdynia, Poland
(E-mail: katmatkk@am.gdynia.pl)
[2] Gdynia Maritime University, Gdynia, Poland
(E-mail: joannas@am.gdynia.pl)

Abstract. The method based on the joint model linking a multistate approach to critical infrastructure safety with a semi-Markov modelling of the critical infrastructure operation process is proposed to the safety prediction of critical infrastructures changing in time their structure and their components safety. The proposed method is applied to the safety indicators approximate evaluation of the port oil transport critical infrastructure changing its safety structure and its components safety parameters at variable operation conditions.

Keywords: critical infrastructure, operation, safety, operation influence, safety indicator, prediction, port oil transport

1 Introduction

The critical infrastructures operating at a fixed area may be vulnerable to damage caused by external threats and on the other hand, they may cause threats to other critical infrastructures [1]. This fact should be considered to construct a global network of interconnected and interdependent critical infrastructure networks existing at this operating area what is highly reasonable as usually the critical infrastructures are not isolated and they create a system of interconnected and interdependent critical infrastructures. The proposed approach, taking into account threats associated with critical infrastructures and their components/assets operation [1]-[3], [4]-[5] can help to indicate which of critical infrastructures can be affected by and which ones can affect other critical infrastructures in their operating area. In this context, the safety analysis and prediction of a single critical infrastructure composed of a number of assets impacted by its operation process is very important [4]-[11]. Therefore, in the paper, the method of a single critical infrastructure related to its operation process safety prediction is proposed.
Most real critical infrastructures are strongly influenced by changing in time their operation conditions that initiate their degradation/ageing. The time

17th ASMDA Conference Proceedings, 6-9 June 2017, London, UK

dependent interactions between the operation process states varying at the critical infrastructure operating area and the critical infrastructure safety structure and its components/assets safety states changing are evident features of most real technical systems including critical infrastructures [1]-[2]. The common safety and operation analysis of critical infrastructures is of great value in the industrial practice. The convenient tools for analyzing this problem are the critical infrastructure multistate safety modelling [12]-[13], [4]-[11], [14]-18], commonly used with the semi-Markov modelling [5], [7], [13] the critical infrastructures operation processes, leading to the construction the joint general safety model of the critical infrastructure related to its operation process [13], [19]. Especially, in everyday practice, there are needed the tools that could be applied to evaluate approximately the safety characteristics of critical infrastructures defined as a complex system in its operating environment that significant features are inside-system dependencies and outside-system dependencies, that in the case of its degradation have significant destructive influence on the health, safety and security, economics and social conditions of large human communities and territory areas. In the critical infrastructure safety analysis, the determination of its safety function and its risk function which graph corresponds to the fragility curve [20] are crucial indicators/indices for safety practitioners. Other practically significant critical infrastructure safety indices defined in the paper are its mean lifetime up to the exceeding a critical safety state, the moment when its risk function value exceeds the acceptable safety level, the critical infrastructure intensity of ageing/degradation, the coefficient of operation process impact on critical infrastructure intensities of ageing and the coefficient of critical infrastructure resilience to operation process impact. These critical infrastructure safety indicators evaluation is of great value in the industrial practice. Thus, there are needed the tools for finding the critical infrastructure safety and resilience indicators and the procedures of their practical usage [4]-[5].

In the paper, to satisfy those needs, the simplified procedures based on the authors' theoretical results [7], [10] developments are proposed directly to users dealing with, assuring critical infrastructure safety in everyday practice. The procedures are applied to operation and safety analysis and safety indicators prediction for the port oil terminal critical infrastructure, the part of the Baltic oil pipeline critical infrastructure network [3], [9].

2 Multistate approach to critical infrastructure safety

Multistate approach to safety analysis is presented in [21].

3 Critical infrastructure safety indicators

We denote the critical infrastructure conditional lifetime in the safety state subset $\{u, u+1, \ldots, z\}$ while the critical infrastructure is at the operation process

$Z(t)$ state z_b, $b = 1,2,...,\nu$, by $T'^{(b)}(u)$ and the conditional safety function (SI1) of the system by the vector [4]-[5]

$$[\boldsymbol{S}(t,\cdot)]^{(b)} = [1, [\boldsymbol{S}(t,1)]^{(b)}, ..., [\boldsymbol{S}(t,z)]^{(b)}],$$

with the coordinates defined by

$$[\boldsymbol{S}(t,u)]^{(b)} = P(T'^{(b)}(u) > t | Z(t) = z_b) \text{ for } t \in < 0, \infty),$$
$$u = 1,2,...,z, \; b = 1,2,...,\nu.$$

The safety function coordinate $[\boldsymbol{S}(t,u)]^{(b)}$ is the conditional probability that the critical infrastructure lifetime $T'^{(b)}(u)$ in the safety state subset $\{u, u+1, ..., z\}$ is greater than t, while the critical infrastructure operation process $Z(t)$ is at the operation state z_b.

Further, we assume that the critical infrastructure has the exponential conditional safety function (SI1), i.e.

$$[\boldsymbol{S}(t,u)]^{(b)} = \exp[-[\boldsymbol{\lambda}(u)]^{(b)} t], \; t \in < 0, +\infty), \; [\boldsymbol{\lambda}(u)]^{(b)} \geq 0, \; u = 1,2,\ldots,z.$$

Under this assumption, the mean lifetime of the critical infrastructure in the safety state subset $\{u, u+1, ..., z\}$, is given by

$$\mu_b(u) = \frac{1}{[\boldsymbol{\lambda}(u)]^{(b)}}, \; u = 1,2,...,z, \; b = 1,2,\ldots,\nu. \tag{1}$$

We denote the critical infrastructure unconditional lifetime in the safety state subset $\{u, u+1, ..., z\}$ by $T'(u)$ and the unconditional safety function of the critical infrastructure (SI1) by the vector

$$\boldsymbol{S}(t,\cdot) = [1, \boldsymbol{S}(t,1), ..., \boldsymbol{S}(t,z)],$$

with the coordinates defined by

$$\boldsymbol{S}(t,u) = P(T(u) > t) \quad \text{for} \quad t \in < 0, \infty), \quad u = 1,2,...,z. \tag{2}$$

In the case when the critical infrastructure operation time θ is large enough, the coordinates of the unconditional safety function (SI1) of the critical infrastructure defined by (2) are given by

$$\boldsymbol{S}(t,u) \cong \sum_{b=1}^{\nu} p_b \exp[-[\boldsymbol{\lambda}(u)]^{(b)} t] \text{ for } t \geq 0, \; u = 1,2,...,z, \tag{3}$$

where p_b, $b=1,2,...,\nu$, are the critical infrastructure operation process limit transient probabilities (OPC1) defined in [5].
The mean value of the critical infrastructure unconditional lifetime $T'(u)$ in the safety state subset $\{u,u+1,...,z\}$ is given by [10]

$$\mu(u) \cong \sum_{b=1}^{\nu} p_b \mu_b(u), \quad u=1,2,...,z, \tag{8}$$

where $\mu_b(u)$ are the mean values of the critical infrastructure conditional lifetimes $T'^{(b)}(u)$ in the safety state subset $\{u,u+1,...,z\}$ at the operation state z_b, $b=1,2,...,\nu$, given by (1) and p_b are the transient probabilities at these operation states [15].
Moreover, according to [8], if r is the critical safety state, then the critical infrastructure risk function (SI2)

$$\boldsymbol{r}(t) = P(S(t) < r \mid S(0) = z) = P(T(r) \le t), \; t \in <0,\infty),$$

is defined as a probability that the critical infrastructure is in the subset of safety states worse than the critical safety state r, $r \in \{1,...,z\}$ while it was in the safety state z at the moment $t = 0$ is given by [10]

$$\boldsymbol{r}(t) = 1 - \sum_{b=1}^{\nu} p_b \exp[-[\boldsymbol{\lambda}(r)]^{(b)} t], \; t \in <0,\infty). \tag{4}$$

The critical infrastructure unconditional safety function (SI1), the critical infrastructure risk function (SI2) and its graph called the critical infrastructure fragility curve (SI3) are main critical infrastructure safety indictors (SI).
Other practically useful critical infrastructure safety factors are:
- the mean value of the unconditional critical infrastructure lifetime $T(r)$ up to the exceeding the critical safety state r (SI4) given by

$$\mu(r) \cong \sum_{b=1}^{\nu} p_b \mu_b(r), \quad u=1,2,...,z, \tag{5}$$

where $\mu_b(r)$ are the mean values of the critical infrastructure conditional lifetimes $T'^{(b)}(u)$ in the safety state subset $\{u,u+1,...,z\}$ at the operation state z_b, $b=1,2,...,\nu$, according to (1), given by

$$\mu_b(r) = \frac{1}{[\boldsymbol{\lambda}(r)]^{(b)}}, \; b=1,2,...,\nu, \tag{6}$$

and p_b are the transient probabilities at these operation states [5];

- the standard deviation of the critical infrastructure lifetime $T'(r)$ up to the exceeding the critical safety state r (SI5) given by

$$\sigma(r) = \sqrt{n(r) - [\mu(r)]^2} \ ,$$

(7)

where $n(r) = 2\int_0^{\infty} t\, \boldsymbol{S}(t,r)dt,$

and $\boldsymbol{S}(t,r)$ is given by (3) for $u = r$ and $\mu(r)$ is given by (5);

- the moment τ when the critical infrastructure risk function exceeds a permitted level δ (SI6) given by

$$\tau = \boldsymbol{r}^{-1}(\delta),$$

where $\boldsymbol{r}^{-1}(t)$, is the inverse function of the risk function $\boldsymbol{r}(t)$ given by (4).

Other critical infrastructure safety indices are:

- the intensities of ageing (degradation) of the critical infrastructure impacted by the operation process /the intensities of critical infrastructure departure from the safety state subset $\{u, u+1,\ldots,z\}$) impacted by the operation process (SI7), i.e. the coordinates of the vector

$$\boldsymbol{\lambda}(t,\cdot) = [0,\ \boldsymbol{\lambda}(t,1)\ ,\ \ldots,\ \boldsymbol{\lambda}(t,z)\ ],\ t \in <0,+\infty), \tag{8}$$

where

$$\boldsymbol{\lambda}(t,u) = [\sum_{b=1}^{v} [p_b [\lambda(u)]^{(b)} \exp[-[\lambda(u)]^{(b)} t]\,]/[\sum_{b=1}^{v} p_b \exp[-[\boldsymbol{\lambda}(u)]^{(b)} t]], \tag{9}$$

$t \in <0,+\infty),\ \ u = 1,2,\ldots,z;$

- the coefficients of the operation process impact on the critical infrastructure intensities of ageing /the coefficients of operation process impact on critical infrastructure intensities of departure from the safety state subset $\{u, u+1,\ldots,z\}$ (SI8), i.e. the coordinates of the vector

$$\boldsymbol{\rho}(t,\cdot) = [0,\ \boldsymbol{\rho}(t,1)\ ,\ \ldots,\ \boldsymbol{\rho}(t,z)\ ],\ t \in <0,+\infty),$$

where

$$\boldsymbol{\lambda}(t,u) = \boldsymbol{\rho}(t,u) \cdot \boldsymbol{\lambda}^{\mathbf{0}}(t,u),\ \ t \in <0,+\infty),\ \ u = 1,2,\ldots,z, \tag{10}$$

and $\boldsymbol{\lambda}^{\mathbf{0}}(t,u)$ are the intensities of ageing of the critical infrastructure (the intensities of the critical infrastructure departure from the safety state subset $\{u, u+1,\ldots,z\}$) without of operation impact, i.e. the coordinate of the vector

$$\boldsymbol{\lambda}^{\mathbf{0}}(t,\cdot) = [0,\ \boldsymbol{\lambda}^{\mathbf{0}}(t,1),\ ,\ \ldots,\ \boldsymbol{\lambda}^{\mathbf{0}}(t,z)\,],\ t \in <0,+\infty).$$

Additionally, we define the critical infrastructure resilence indicaator (RI1), i.e. the coefficient of critical infrastructure resilience to operation process impact

$$RI(t) = 1/\rho(t,r), \quad t \in <0,+\infty), \tag{11}$$

where $\rho(t,r)$ is the coefficients of the operation process impact on the critical infrastructure intensity of ageing $\lambda(t,r)$, i.e. the coefficients of operation process impact on critical infrastructure intensities of departure from the safety state subset $\{r, r+1,...,z\}$ of states not worse than the critical safety state r.

4 Safety and risk prediction of port oil piping transportation system

4.1 Port oil piping transportation system description

The considered oil piping transportation system operating at one of the Baltic Oil Terminals and is describe in [21].

4.2 Parameters of port oil piping transportation system safety

After considering the comments and opinions coming from experts, taking into account the effectiveness and safety aspects of the operation of the oil pipeline transportation system, we fix [2]:

- the number of pipeline system safety states

$z = 2$,

and we distinguish the following three safety states:

- a safety state 2 - piping operation is fully safe,
- a safety state 1 - piping operation is less safe and more dangerous because of the possibility of environment pollution,
- a safety state 0 - piping is destroyed,

and, we assume that:

- there are possible the transitions between the components safety states only from better to worse ones,
- the critical safety state of the system is

  $r = 1$,

- the system risk permitted level

  $\delta = 0.05$;

- the mean values of the port oil piping transportation system lifetimes in the safety state subsets $\{1,2\}$, $\{2\}$, are as follows:

- for safety state subset {1,2}

$\mu(1)$ = 63 years, (12)

- for safety state subset {2}

$\mu(2)$ = 46 years. (13)

4.3 Parameters and characteristics of port oil piping transportation system operation process

On the basis of the statistical data and expert opinions [2], it is possible to evaluate the following unknown basic parameters of the port oil piping transportation system operation process [4]-[5]:
– the number of operation process states (OPP1)

$\nu = 7$

and the operation process states:
the operation state z_1 – transport of one kind of medium from the terminal part B to part C using two out of three pipelines of the subsystem S_3,
the operation state z_2 – transport of one kind of medium from the terminal part C to part B using one out of three pipelines of the subsystem S_3,
the operation state z_3 – transport of one kind of medium from the terminal part B through part A to pier using one out of two pipelines of the subsystem S_1 and one out of two pipelines of the subsystem S_2,
the operation state z_4 – transport of one kind of medium from the pier through parts A and B to part C using one out of two pipelines of the subsystem S_1, one out of two pipelines in subsystem S_2 and two out of three pipelines of the subsystem S_3,
the operation state z_5 – transport of one kind of medium from the pier through part A to B using one out of two pipelines of the subsystem S_1 and one out of two pipelines of the subsystem S_2,
the operation state z_6 – transport of one kind of medium from the terminal part B to C using two out of three pipelines of the subsystem S_3, and simultaneously transport one kind of medium from the pier through part A to B using one out of two pipelines of the subsystem S_1 and one out of two pipelines of the subsystem S_2,

the operation state z_7 – transport of one kind of medium from the terminal part B to C using one out of three pipelines of the subsystem S_3, and simultaneously transport second kind of medium from the terminal part C to B using one out of three pipelines of the subsystem S_3.

Calculated operation process characteristics are [4]-[5]:
- the vector of the limit values of transient probabilities (OPC1) of the port oil ping transportation system operation process $Z(t)$ at the particular operation states z_b

$[p_b]_{1X7} = [p_1, p_2, \ldots, p_7]$,

where

$p_1 = 0.395,\ \ p_2 = 0.060,\ \ p_3 = 0.003,\ \ p_4 = 0.002,\ \ p_5 = 0.20,$
$p_6 = 0.058,\ \ p_7 = 0.282.$

4.4 Parameters of operation process impact on port oil piping transportation system safety

The coefficients of the operation process impact on the port oil piping transportation system intensities of ageing / the coefficients of the operation process impact on the port oil piping transportation system intensities of departure from the safety state subset {1,2}, {2} at the operation states z_b, $b = 1,2,...,\nu,$ are as follows:

$[\rho(1)]^{(b)} = 1.10,\ [\rho(2)]^{(b)} = 1.10,\ b = 1,2,7$

$[\rho(1)]^{(b)} = 1.20,\ [\rho(2)]^{(b)} = 1.20,\ b = 3,5,$

$[\rho(1)]^{(b)} = 1.30,\ [\rho(2)]^{(b)} = 1.30,\ b = 4,6.$

4.5 Prediction of safety indicators of port oil piping transportation system

Considering that the pipeline system is a three-state (z = 2) system, its safety function (**SI1**) is given by [4]-[5]

$\boldsymbol{S}(t,\cdot) = [1, \boldsymbol{S}(t,1)\ \ \boldsymbol{S}(t,2)],\ \ t \geq 0,$

where

$$\begin{aligned}\boldsymbol{S}(t,1) &= 0.395\exp[-0.017460t] + 0.060\exp[-0.017460t] + 0.003\exp[-0.019048t] \\ &\quad + 0.002\exp[-0.020635t] + 0.200\exp[-0.019048t] + 0.058\exp[-0.020635t] \\ &\quad + 0.282\exp[-0.017460t] \\ &= 0.737\exp[-0.017460t] + 0.203\exp[-0.019048t] \\ &\quad + 0.060\exp[-0.020635t],\end{aligned}$$

$$\boldsymbol{S}(t,2) = 0.395\exp[-0.023913t] + 0.060\exp[-0.023913t] + 0.003\exp[-0.026087t]$$
$$+ 0.002\exp[-0.028261t] + 0.200\exp[-0.026087t]$$
$$+ 0.058\exp[-0.028261t] + 0.282\exp[-0.023913t]$$
$$= 0.737\exp[-0.023913t] + 0.203\exp[-0.026087t]$$
$$+ 0.060\exp[-0.028261t].$$

The expected values and standard deviations of the pipeline system lifetimes in the safety state subsets $\{1,2\}$, $\{2\}$, according (5)-(7), respectively are [4]-[5]:

$$\mu(1) \cong 55.78,\ \mu(2) \cong 40.72 \text{ years,} \tag{14}$$

$$\sigma(1) \cong 55.90,\ \sigma(2) \cong 40.82 \text{ years,} \tag{15}$$

and further, it follows that the mean values of the pipeline lifetimes in the particular safety states are:

$$\bar{\mu}(1) \cong 15.06\ ,\ \bar{\mu}(2) \cong 40.72 \text{ years.}$$

As the critical safety state is r =1, then the pipeline system risk function (SI2) by (4), is given by

$$\boldsymbol{r}(t) = 1 - \boldsymbol{S}(t,1)$$
$$= 1 - [0.737\exp[-0.017460t] + 0.203\exp[-0.019048t]$$
$$+ 0.060\exp[-0.020635t]] \text{for } t \geq 0. \tag{16}$$

The graph of the risk function $\boldsymbol{r}(t)$ of the pipeline system, the fragility curve (SI3), is shown in Figure 2.

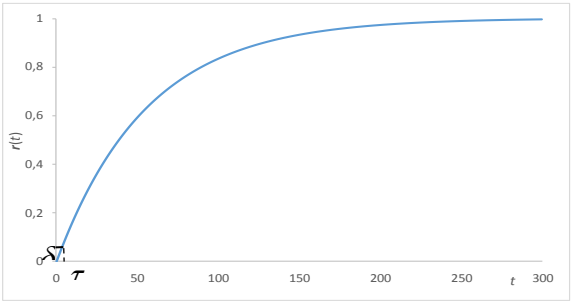

Fig. 2. The graph of the risk function $\boldsymbol{r}(t)$ (the fragility curve) of the port oil piping transportation system

By (14) and (15), the pipeline system mean lifetime up to exceeding critical safety state r = 1 (SI4) is

$$\mu(1) \cong 55.78 \text{ years,}$$

and the standard deviation of the pipeline system lifetime up to exceeding critical safety state $r = 1$ (SI5) is

$$\sigma(1) \cong 55.90,$$

From (16), the moment when the pipeline system risk function exceeds a permitted level $\delta = 0.05$ (SI6), is

$$\tau = \boldsymbol{r}^{-1}(\delta) \cong 2.85 \text{ years.}$$

The pipeline system intensities of ageing (SI7) by (8)-(9) are:

$$\begin{aligned}\boldsymbol{\lambda}(t,1) = {} & \{0.017460 \cdot 0.737\exp[-0.017460t] + 0.019048 \cdot 0.203\exp[-0.019048t] \\ & + 0.020635 \cdot 0.060\exp[-0.020635t]\}/\{0.737\exp[-0.017460t] \\ & + 0.203\exp[-0.019048t] + 0.060\exp[-0.020635t]\} \\ & \cong 0.017928, \end{aligned} \quad (17)$$

$$\begin{aligned}\boldsymbol{\lambda}(t,2) = {} & \{0.023913 \cdot 0.737\exp[-0.023913t] + 0.026087 \cdot 0.203\exp[-0.026087t] \\ & + 0.028261 \cdot 0.060\exp[-0.028261t]\}/\{0.737\exp[-0.023913t] \\ & + 0.203\exp[-0.026087t] + 0.060\exp[-0.028261t]\} \\ & \cong 0.024558. \end{aligned} \quad (18)$$

Considering (12)-(13) and (17)-(18) and applying (10), the coefficients of the operation process impact on the port oil piping transportation system intensities of ageing (SI8) are:

$$\boldsymbol{\rho}(t,1) = \frac{\boldsymbol{\lambda}(t,1)}{\boldsymbol{\lambda}^{\mathbf{0}}(t,1)} \cong \frac{1/55.78}{1/63} \cong 1.13, \quad (19)$$

$$\boldsymbol{\rho}(t,2) = \frac{\boldsymbol{\lambda}(t,2)}{\boldsymbol{\lambda}^{\mathbf{0}}(t,2)} \cong \frac{1/40.72}{1/46} \cong 1.13.$$

Finally, by (11) and (19), the port oil terminal critical infrastructure resilence indicator (RI1), i.e. the coefficient of the port oil terminal critical infrastructure resilience to operation process impact, is

$$RI(t) = 1/\boldsymbol{\rho}(t,1) \cong 0.885 = 88.5\%. \quad t \in <0,+\infty),$$

Conclusions

The paper delivers procedures that allow to find the main an practically important safety characteristics of the critical infrastructures impacted by their operation processes. The safety characteristics of the port oil terminal critical infrastructure predicted in this paper using this procedures are different from that obtained without considering the operation impact. This fact justifies the sensibility of analysing the technical critical infrastructures related to the operation processes. Presented in this paper tools can be useful in safety analysis

and prediction of a very wide class of real technical critical infrastructures operating at the varying conditions that have an influence on changing their safety structures and their components safety parameters. The results can be interesting for safety practitioners from various industrial sectors.

Acknowledgments


The paper presents the results developed in the scope of the EU-CIRCLE project titled "A pan – European framework for strengthening Critical Infrastructure resilience to climate change" that has received funding from the European Union's Horizon 2020 research and innovation programme under grant agreement No 653824. *http://www.eu-circle.eu/*.

References

1. A. Lauge, J. Hernantes and J.M. Sarriegi. Critical infrastructure dependencies: A holistic, dynamic and quantitative approach. International Journal of Critical Infrastructure Protection, Vol. 8, 6{23, 2015.
2. M. Drzazga, P. Dziula, K. Kołowrocki and M. Reszko. Expert Opinions on Piping and Ferry and Their Components Safety Parameters and Their Exposure to Operating Environment Threats and Climate-Weather Impacts, EU-CIRCLE Report D3.3-GMU0, 2016.
3. EU-CIRCLE Taxonomy, EU-CIRCLE Project Report D1.1, 2015.
4. K. Kołowrocki and J. Soszyńska-Budny. How to model and to analyse operation threats and climate-weather hazards influence on critical infrastructure safety – An overall approach, EU-CIRCLE Report D3.3-GMU0, 2016.
5. K. Kołowrocki and J. Soszyńska-Budny. Integrated Model of Critical Infrastructure Safety (IMCIS) Related to Its Operation Process, IMCIS Model 1, EU-CIRCLE Report D3.3-GMU0, 2016.
6. K. Kołowrocki. Safety of critical infrastructures. Journal of Polish Safety and Reliability Association, Summer Safety and Reliability Seminars, Vol. 4, No 1, 51{72, 2013.
7. K. Kołowrocki. Reliability of Large and Complex Systems, Amsterdam, Boston, Heidelberd, London, New York, Oxford, Paris, San Diego, San Francisco, Singapore, Sidney, Tokyo, Elsevier, 2014.
8. K. Kołowrocki. Modeling Reliability of Critical Infrastructures with Application to Port Oil Piping Transportation System, Advances Materials Research, Vols. 891-892, 1565{1570, 2014.
9. K. Kołowrocki et al. Identification of Existing Critical Infrastructures at The Baltic Sea Area and Its Seaside, Their Scopes, Parameters and Accidents in Terms of Climate Change Impacts, EU-CIRCLE Report D1.2-GMU1, 2015.
10. K. Kołowrocki and J. Soszyńska-Budny. Reliability and Safety of Complex Technical Systems and Processes: Modelling - Identification - Prediction - Optimization, London, Dordrecht, Heildeberg, New York, Springer, 2011.

11. K. Kołowrocki and J. Soszyńska-Budny. Introduction to safety analysis of critical infrastructures, Journal of Polish Safety and Reliability Association, Summer Safety and Reliability Seminars 3, 73{88, 2012.
12. T. Aven. Reliability evaluation of multistate systems with multistate components. IEEE Transactions on Reliability, 34, 473{479, 1985.
13. D. Klabjan and D. Adelman. Existence of optimal policies for semi-Markov decision processes using duality for infinite linear programming, Siam *J Contr Optim* 44(6), 2104{2122, 2006.
14. A. Lisnianski, G and Levitin. Multi-State System Reliability. Assessment, Optimization and Applications, World Scientific Publishing Co. Pte. Ltd., 2003.
15. J. Xue. On multi-state system analysis. IEEE Transactions on Reliability, 34, 329{337, 1985.
16. J. Xue and K. Yang. Dynamic reliability analysis of coherent multi-state systems. IEEE Transactions on Reliability, 4, 44, 683{688, 1995a.
17. J. Xue and K. Yang. Symmetric relations in multi-state systems. IEEE Transactions on Reliability, 4, 44, 689{693, 1995b.
18. K. Yu, I. Koren and Y. Guo. Generalized multistate monotone coherent systems. IEEE Transactions on Reliability, 43, 242{250, 1994.
19. F. Grabski. Semi-Markov Processes: Application in System Reliability and Maintenance, Amsterdam, Boston, Heidelberd, London, New York, Oxford, Paris, San Diego, San Francisco, Singapore, Sidney, Tokyo, Elsevier, 2014.
20. P. Ben, B.P. Gouldby, M.T. Schultz, J.D. Simm and J.L. Wibowo. Beyond the Factor of Safety: Developing Fragility Curves to Characterize System Reliability, Report in Water Resources Infrastructure Program ERDC SR-10-1, Prepared for Headquarters, U.S. Army Corps of Engineers, Washington, 2010.
21. K. Kołowrocki and J. Soszyńska-Budny. Port oil transport critical infrastructure safety approximate evaluation. Proc. *of 17rd ASMDA Conference,..., 2017.*

Analysis of Dependencies between Growth Rates of GDP of V4 Countries Using 4–dimensional Vine Copulas

Jozef Komorník[1], Magda Komorníková[2], and Tomáš Bacigál[2]

[1] Faculty of Management, Comenius University, Odbojárov 10, P.O.BOX 95, 820 05 Bratislava, Slovakia
(E-mail: Jozef.Komornik@fm.uniba.sk)
[2] Faculty of Civil Engineering, Slovak University of Technology, Radlinského 11, 810 05 Bratislava, Slovakia
(E-mail: Magdalena.Komornikova,Tomas.Bacigal@stuba.sk)

Abstract. We analyzed seasonally adjusted quarterly data for the V4 countries Czech Republic (Cz), Hungary (Hu), Poland (Pl) and Slovakia (Sk) for the period 1995/Q1 – 2016/ Q3. We investigated parallel changes of GDP of these countries using 4–dimensional Vine copula models. We applied ARIMA – GARCH filters to logarithms of the above countries' data. The obtained residuals have pairwise Kendall's correlation coefficients in the interval (0.1, 0.2) (the maximal value was achieved for the couple (Cz, Sk)). Subsequently, we applied to those residuals (country specific) linear transformations in order to map them in the unit interval. The results served as inputs to calculations of 4–dimensional Vine copulas. The optimal Vine copulas help to obtain more insight in the detailed development of the investigated GDPs.
Keywords: GDP, Correlation, ARIMA-GARCH filter, Vine copula.

1 Introduction

We analyzed seasonally adjusted quarterly data (provided by EUROSTAT) for the V4 countries Czech Republic (Cz), Hungary (Hu), Poland (Pl) and Slovakia (Sk) (that underwent similar historical and economic development during the last 70 years) for the period 1995/Q1 – 2016/ Q3. We investigated parallel changes of GDP of these countries using 4–dimensional Vine copula models. We applied ARIMA – GARCH filters to logarithms of the above countries data. The obtained residuals have pairwise Kendall's correlation coefficients in the interval (0.1, 0.2) (the maximal value was achieved for the couple (Cz, Sk)). Subsequently, we applied to those residuals (country specific) linear transformations in order to map them in the unit interval. Results served as inputs to calculation of 4–dimensional Vine copulas. The computations were performed in R with the help of package VineCopula.

The paper is organized as follows. The second section is devoted to a brief overview of the theory of Vine copulas and methodology of copula fitting to multi–dimensional time series. The third section contains application to real data modeling. Finally, some conclusions are presented.

17th *ASMDA Conference Proceedings, 6 - 9 June 2017, London, UK*

2 Theory

Copulas are fundamental tools for modeling dependence between/among random variables leaving alone their marginal distributions. Due to Sklar [13]

$$F(x_1, ..., x_n) = C\left[F_1(x_1), ..., F_n(x_n)\right],$$

where F is joint cumulative distribution function of random vector $(X_1, ..., X_n)$, F_i is marginal cumulative distribution function of X_i, and $C : [0,1]^n \to [0,1]$ is a copula which is a n-increasing function with 1 as neutral element and 0 as annihilator, see e.g. monograph Nelsen (2006) [9]. Besides three fundamental copulas

$$M(x_1, ..., x_n) = \min(x_1, ..., x_n), \quad W(x_1, x_2) = \max(x_1 + x_2 - 1, 0),$$

$$\Pi(x_1, ..., x_n) = \prod_{i=1}^{n} x_i,$$

which model perfect positive dependence, perfect negative dependence (not applicable for $n > 2$) and independence, respectively, there exist numerous parametric classes, such as Archimedean, Extreme-Value and elliptical copulas. Within the last one there belong such important parametric families as *Gaussian* copulas

$$C_G(x_1, ..., x_n) = \Phi\left[\Phi_1^{-1}(x_1), ..., \Phi_n^{-1}(x_n)\right]$$

and *Student* t-copulas

$$C_t(x_1, ..., x_n) = t\left[t_1^{-1}(x_1), ..., t_n^{-1}(x_n)\right],$$

(where Φ and t are joint distribution functions of multivariate normal and Student t distributions, similarly Φ_i^{-1} and t_i^{-1}, $i = 1, ..., n$ are univariate quantile functions related to X_i), able to flexibly describe dependence in multidimensional random vector.

An n–dimensional regular vine tree structure $\mathcal{S} = \{T_1, ..., T_n\}$ is a sequence of $n-1$ linked trees with properties (see [2,3]):

- Tree T_1 is a tree on nodes 1 to n;
- Tree T_j has $n + 1 - j$ nodes and $d - j$ edges;
- Edges in tree T_j become nodes in tree T_{j+1};
- Two nodes in tree T_{j+1} can be joined by an edge only if the corresponding edges in tree T_j share a node.

Except for 2–dimensional product, Gaussian and Student copulas we utilized numerous 2–dimensional families of copulas (Clayton, Gumbel, Frank, Joe, BB1, BB6, BB7, BB8, Tawn [8,15] and their rotations) as building block of Vine copulas [1,12] and [3]. Vine copulas are constructed as lego using bivariate copulas as construction blocks picked by default for stronger correlated

random variable pairs, the estimated model structure can be visualized and interpreted. We outline the construction of three-dimensional probability density function f

$$\begin{aligned} f(x_1,x_2,x_3) &= f_1(x_1)\cdot f_{2|1}(x_1,x_2)\cdot f_{3|12}(x_1,x_2,x_3) = \\ &= f_1(x_1)\cdot c_{12}\left[F_1(x_1),F_2(x_2)\right]\cdot f_2(x_2)\cdot \\ &\cdot c_{31|2}\left[F_{x_3|x_2}(x_2,x_3),F_{x_1|x_2}(x_1,x_2)\right]\cdot c_{23}\left[F_2(x_2),F_3(x_3)\right]\cdot f_3(x_3) \end{aligned} \tag{1}$$

where f_i is a (marginal) probability density function of $X_i,\ i=1,2,3$,

$$f_{i|j}(x_i,x_j)=\frac{f(x_i,x_j)}{f_j(x_j)}$$

is conditional density function of X_i given X_j. A copula density c_{ij} couples X_i and X_j while $c_{ij|k}$ couples bivariate conditional distributions of $X_i|X_k$ and $X_j|X_k, i,j,k\in\{1,2,3\}, i\neq j\neq k\neq i$. Finally,

$$F_{x_i|x_j}=\frac{\partial C_{ij}\left[F_i(x_i),F_j(x_j)\right]}{\partial F_j(x_j)}$$

is a conditional cumulative distribution function of X_i given X_j.

The construction (1) represented by Figure 2 is one of the three possible pair–copula decompositions, which, graphically, are both [4] (see Figure 1)

- canonical (C–) vine trees: each tree has a unique node connected to $d-j$ edges (use only star like tree - useful for ordering by importance);
- drawable (D–) vine trees: no node is connected to more than 2 edges (use only path like trees - useful for temporal ordering of variables);

In more than three dimensions, C–vines and D–vines are just small subsets of a more general class - regular vines.

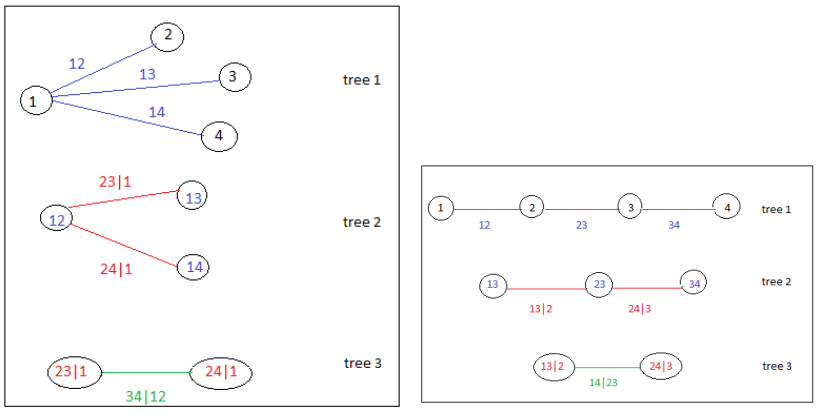

Fig. 1. C-Vine tree (left) and D-Vine tree (right) [4]

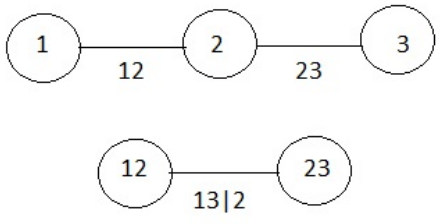

Fig. 2. Vine tree corresponding to construction (1) with the 2^{nd} variable as a root node

The construction (1) has been naturally generalized for larger dimensions (see [3]).

Within the above mentioned classes of 2–dimensional copulas, the optimal models were selected using the Maximum likelihood estimation (MLE) method. Recall that for given m observations $\{X_{j,i}\}_{i=1,...,m}$ of j-th random variable X_j, $j = 1, ..., 4$, the parameters θ of all copulas under consideration were estimated by maximizing the likelihood function

$$L(\theta) = \sum_{i=1}^{m} \log \left[c_\theta(U_{1,i}, U_{2,i}, U_{3,i}, U_{4,i}) \right], \tag{2}$$

where c_θ denotes density of a parametric copula family C_θ, and

$$U_{j,i} = \frac{1}{m+1} \sum_{k=1}^{m} \mathbf{1}(X_{j,k} \leq X_{j,i}), \quad i = 1, ..., m,$$

are so-called pseudo-observations. Goodness-of-fit was performed by a test proposed by Genest et al. [6] and based on empirical copula process using Cramer-von Misses test statistic

$$S_{CM} = \sum_{i=1}^{m} \left[C_\theta(U_{1,i}, U_{2,i}, U_{3,i}, U_{4,i}) - C_m(U_{1,i}, U_{2,i}, U_{3,i}, U_{4,i}) \right]^2 \tag{3}$$

with empirical copula $C_m(\mathbf{x}) = \frac{1}{m} \sum_{i=1}^{m} \prod_{j=1}^{4} \mathbf{1}(X_{j,i} \leq x_j)$ and indicator function $\mathbf{1}(A) = 1$ whenever A is true, otherwise $\mathbf{1}(A) = 0$.

All calculations were done in R [10], some with the help of package VineCopula [11]. Besides the usual parametric families of Archimedean class such as Gumbel, Clayton, Frank, Joe, BB1, BB6, BB7, BB8, Tawn copulas (see e.g. [7–9]) in bivariate case we used also their rotations C_α by angle α defined

$$C_{90}(x_1, x_2) = x_2 - C(1 - x_1, x_2),$$

$$C_{180}(x_1, x_2) = x_1 + x_2 - 1 + C(1 - x_1, 1 - x_2) \quad \text{survival copula},$$

$$C_{270}(x_1, x_2) = x_1 - C(x_1, 1 - x_2),$$

that are implemented in the package VineCopula.

Comparisons of optimal models between different 4–dimensional classes of Vine copulas were based on the *BIC criterion* ([11,14])

$$BIC = -2 * L(\theta) + \log(m) * npar,$$

where *npar* represents the number of parameters in the fitted model and m being the number of observations.

As a preliminary analysis of dependence between random variables, we employ classical measures of dependence such as Pearson's and Kendall's correlation coefficients, moreover to inspect the conditional (in)dependence (which is further investigated parametrically with Vines) the partial correlation matrix comes handy. Given a Pearson's correlation matrix Σ, the partial correlation between variables X_i, X_j conditional on all the other variables in vector $(X_1, \ldots, X_n)$ can be computed

$$\rho_{ij|-ij} = \frac{-p_{ij}}{\sqrt{p_{ii}p_{jj}}}$$

where p_{ij} $(i, j = 1, \ldots, n)$ are elements of the matrix $P = \Sigma^{-1}$. Recall that partial correlation is a measure of the strength and direction of a linear relationship between two continuous random variables that takes into account (removes) the influence of some other continuous random variables. Conditional correlations are important, e.g., a) when building (gaussian) graphical models, where insignificant connections are removed to obtain more parsimonious model, as well as b) to better understand the structure of estimated Vine copula.

3 Results

We analyzed seasonally and calendar adjusted quarterly GDP data (provided by EUROSTAT) for the V4 countries Czech Republic (Cz), Hungary (Hu), Poland (Pl) and Slovakia (Sk) (that underwent similar historical and economic development during the last 70 years) for the period 1995/Q1 – 2016/ Q3 (see Figure 3). We investigated parallel changes of GDP of these countries using 4–dimensional Vine copula models. First we applied ARIMA – GARCH filters ([5]) to logarithms of the above countries data:

$$(1-\varphi_1 B-\varphi_2 B^2-...-\varphi_P B^P)\,(1-B)^d\, X_t = c_0+(1+\theta_1 B+\theta_2 B^2+...+\theta_Q B^Q)e_t,$$

$$e_t = h_t \eta_t,$$

$$h_t^2 = \omega_0 + \sum_{i=1}^{q} \alpha_{0,i} e_{t-i}^2 + \sum_{j=1}^{p} \beta_{0,j} h_{t-j}^2,$$

where B is the shift operator, $X_1, ..., X_m$ are the observations, $c_0 = E[X_t]$, $t = 1, ..., m$, φ_i, $i = 1, ..., P$ are the AR coefficients, θ_j, $j = 1, ..., Q$ are the MA coefficients, $d \geq 1$ is the degree of a polynomial trend, (η_t) is a sequence of

Table 1. ARIMA–GARCH filters

	P	Q	q	p	d	c_0	φ_1	θ_j	ω_0	$\alpha_{0,1}$	$\beta_{0,1}$
Cz	1	2	1	1	1	0.025	-0.509	(1.027, 0.494)	0.004	0.156	0.118
Hu	0	2	1	1	1	0.014	-	(0.302, -0.149)	0.001	0.274	0.010
Pl	0	1	1	1	1	0.016	-	0.195	0.001	0.356	0.002
Sk	1	0	1	1	1	0.016	0.210	-	0.004	0.250	0.095

independent and identically distributed (i.i.d.) random variables such that $E[\eta_t] = 0, E[\eta_t^2] = 1$, $\omega_0 > 0$, $\alpha_{0,i} \geq 0$, $i = 1, ..., q$ and $\beta_{0,j} \geq 0$, $j = 1, ..., p$.

The obtained residuals have pairwise Pearson correlation coefficients in the interval (0.028, 0.601) (the maximal value was achieved for the couple (Pl, Hu), see Table 2) and Kendall correlation coefficients in the interval (0.1, 0.2) (the maximal value was achieved for the couple (Sk, Cz), see Table 3).

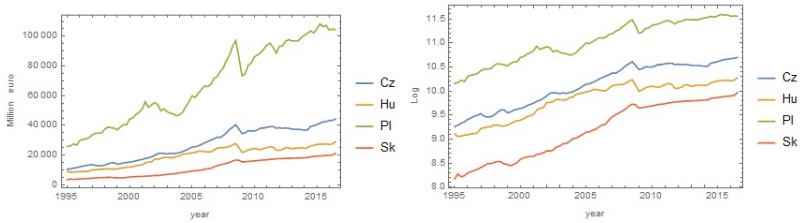

Fig. 3. Seasonally and calendar adjusted quarterly data for the V4 countries (left) and their logarithms (right)

Table 2. Pearson's correlation coefficients for the residuals

	Cz	Hu	Pl	Sk
Cz	1	0.495	0.493	0.028
Hu	0.495	1	0.601	0.298
Pl	0.493	0.601	1	0.270
Sk	0.028	0.298	0.270	1

Figure 5 reveals conditional correlations, showing that the relations Cz-Hu, Sk-Hu and Cz-Pl can be probably explained (and modeled) by other relations.

Subsequently, we applied to those residuals (country specific) linear transformations in order to map them in the unit interval (see Figure 4). Results served as inputs to calculations of 4–dimensional Vine copulas.

The best 4–dimensional Vine copula (based on the BIC information criterion) is summarized in Table 4. We observe that at the lowest tree there reveal

Table 3. Kendall's correlation coefficients for the residuals

	Cz	Hu	Pl	Sk
Cz	1	0.119	0.106	0.193
Hu	0.1195	1	0.157	0.112
Pl	0.106	0.157	1	0.178
Sk	0.193	0.112	0.178	1

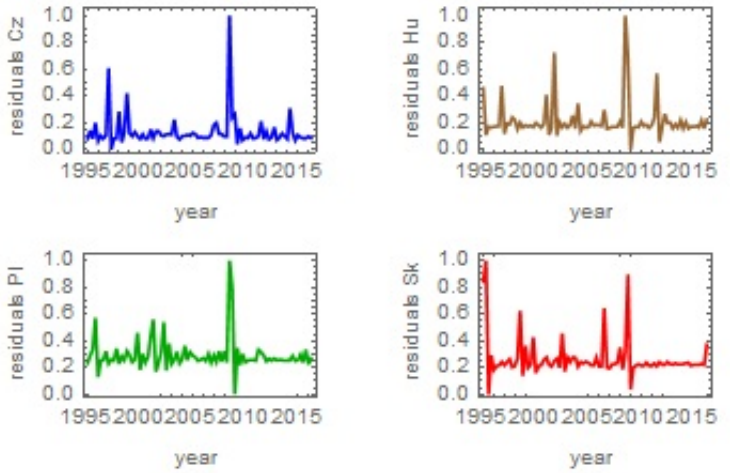

Fig. 4. Residuals transformed to the unit interval

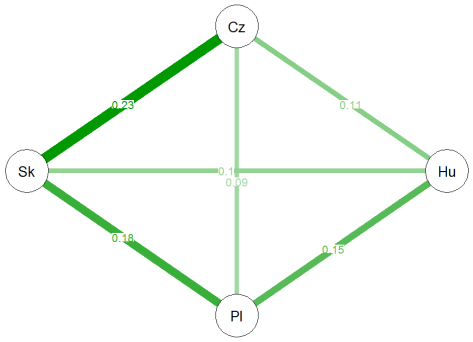

Fig. 5. Partial correlation coefficients for the residuals

stronger links between Slovak and Polish, Slovak and Czech and Polish and Hungarian GDP. The middle trees represent weak or no dependence between Slovak and Hungarian GDP, conditioned on Polish GDP and between Czech and Polish GDP, conditioned on Slovak GDP. The top level tree represents weak or no dependence between Czech and Hungarian GDP when conditioning

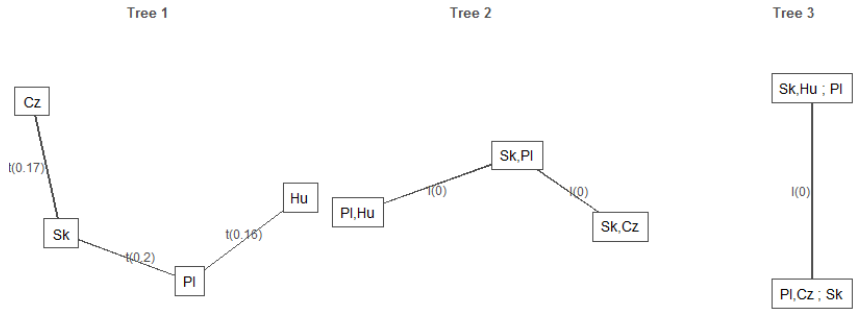

Fig. 6. The tree structure of the optimal Vine copula with pair copula family and Kendall's correlation indicated on edges.

on Slovak and Polish GDP. This is to say that the relations within V4 fellowship is mainly bipolar when adapting national economies to changes.

The graphical visualization of the optimal Vine copula in terms of trees is presented on Figure 6 while the densities of the copula building blocks are depicted on Figure 7 as contour plot, supplemented by an undirected graph encoding independence in Gaussian graphical model.

Table 4. The summary of the best 4–dimensional Vine copula

tree	edge	family	par_1	par_2	τ	λ_U	λ_L
1	Pl - Hu	t	0.25	2.00	0.16	0.27	0.27
	Sk - Cz	t	0.27	2.10	0.17	0.27	0.27
	Sk - Pl	t	0.31	2.00	0.20	0.30	0.30
2	Sk - Hu; Pl	I	-	-	0	0	0
	Pl - Cz; Sk	I	-	-	0	0	0
3	Cz - Hu; Sk - Pl	I	-	-	0	0	0

type: D-vine logLik: 27.04 AIC: -42.07 BIC: -27.35

The above analysis shows that the relations between GDP shocks are faint, yet significant. Graphical structure of dependence does not follow geographical relationship of the countries (D-vine is preferred instead of a C-vine, that would have Sk as root node). Further, relationships co-moves entirely if Sk is involved suggesting tighter touch of Slovak economic with that of western and northern neighbors.

4 Conclusion and future work

We analyzed seasonally and calendar adjusted quarterly data for the V4 countries for the period 1995/Q1 – 2016/ Q3. We have seen that in the optimal

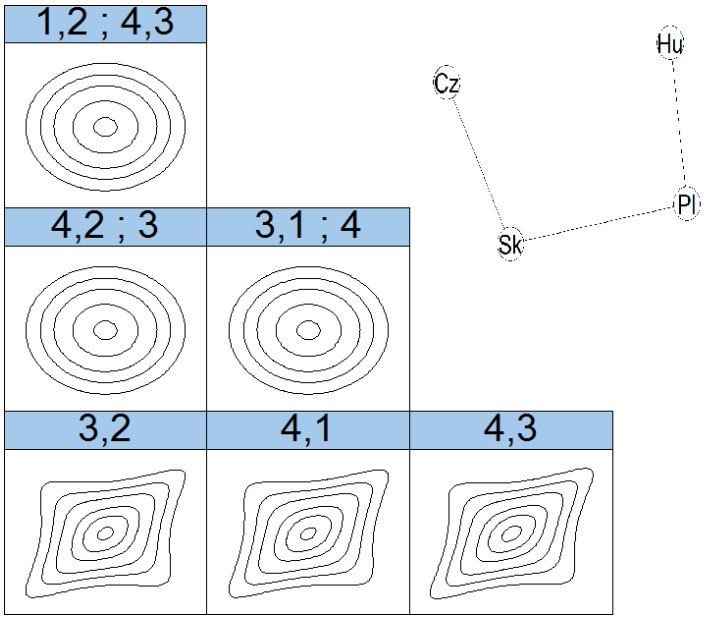

Fig. 7. Contour plots of the optimal Vine copula and a corresponding Gaussian graphical model.

Vine copula model, the Student type copulas dominate at the lowest tree, while the independence copulas prevail at the upper levels.

We also started to analyze local models for the system of subsequent time subintervals with durations of 5 years (20 quarters) and overlaps 2.5 years (10 quarters) between neighboring intervals. We can conclude that the optimal local Vine copulas provide (except for the neighborhood of the crisis years 2008, 2009) comparable levels of Goodness of fit with the local 4–dimensional Student class models. However, the structure of Vine copula models is more interesting to investigate and interpret (since they contain several non-classical partial copulas).

Acknowledgement The support of the grants APVV-0013-14 and VEGA 1/0420/15 is kindly announced.

References

1. Aas, K., Czado, C., Frigessi, A., and Bakken, H.: *Pair-copula constructions of multiple dependence. Tech. Rep. AMBA/24/06, Oslo, Norway: Norwegian Computing Center (2006)*
2. *Bedford, T., and Cooke, R. M.: Vines: A new graphical model for dependent random variables.* The Annals of Statistics **30(4)** (2002), 1031-1068
3. Czado, C.: Pair-copula constructions of multivariate copulas. *Copula theory and its applications (2010), 93–109, Springer Berlin Heidelberg*
4. *Czado, C.: Vine copulas and their applications to financial data. AFMathConf 2013, Brussels, Technische Universität München (2013)*

5. *Franses, P. H., Dijk, D.:* Non-linear time series models in empirical finance. Cambridge University Press (2000)
6. Genest, C., Rémillard, B., and Beaudoin, D.: Goodness-of-fit tests for copulas: A review and a power study. *Insurance: Mathematics and economics* ***44(2)*** *(2009), 199–213*
7. *Joe, H.:* Families of m-Variate Distributions with Given Margins and m(m-1)/2 Bivariate Dependence Parameters. In: Rűschendorf, L., Schweitzer, B., Taylor, M.D. (eds.) Distributions with Fixed Marginals and Related Topics, pp. 120-141, Institute of Mathematical Statistics, Beachwood (1996)
8. Mendes, B., de Melo, E., Nelsen, R.: Communication in Statistics–Simulation and Computation, 36 (2007), 997–1017.
9. Nelsen,R.B.: *An introduction to copulas. Second Edition. Springer Series in Statistics, Springer-Verlag, New York (2006)*
10. *R Core Team. R:* A language and environment for statistical computing. R Foundation for Statistical Computing, Vienna, Austria. URL https://www.R-project.org/ (2015)
11. Schepsmeier, U., Stoeber, J., Brechmann, E. C., Graeler, B., Nagler, T., Erhardt, T.: *VineCopula: Statistical Inference of Vine Copulas. R package version 1.6–1. http://CRAN.R-project.org/package=VineCopula (2015)*
12. *Schirmacher, D., & Schirmacher, E.:* Multivariate dependence modeling using pair-copulas. Technical report, pp. 14–16, (2008)
13. Sklar, A.: Fonctions de répartition a n dimensions et leurs marges. *Publ. Inst. Statist. Univ. Paris* ***8*** *(1959), 229–231*
14. *Schwarz, G. E.: Estimating the dimension of a model. Annals of Statistics 6 (2) (1978), 461–464.*
15. *Tawn, J. A.: Bivariate extreme value theory: models and estimation. Biometrika, 75 (1988), 397–415.*

Monte-Carlo Accuracy Evaluation of a Pintograph-based Laser Cutting Machine

Samuel Kosolapov[1]

[1]ORT Braude Academic College of Engineering, Karmiel, Israel, ksamuel@braude.ac.il

Abstract. Known since the 19th century, the Pintograph has recently become popular due to its simple mechanical implementation that uses inexpensive servo motors controlled by an inexpensive microcontroller. Despite the simplicity of the mechanical design, the mathematical model of the real-life Pintograph contains a large number of mechanical and electronic parameters. Hence, to evaluate the accuracy of the Pintograph, the Monte-Carlo software simulator was created. Relevant math equations were created and solved using MAPLE symbolic software. The simulator takes into account rod length, joint tolerance, and servo motor accuracy. The simulator operation results are the drawing zone map and in the accuracy map in the drawing zone. Simulator runs reveal that for the "4-rod" design with unit length of 100 mm xy, an accuracy of 0.3 mm can be achieved in the center of the drawing zone, which is good enough for an inexpensive laser cutting do-it-yourself (DIY) machine. Modified sizes and tolerances of the Pintograph elements can be input into the simulation to evaluate the drawing zone and the cutting accuracy.
Keywords: Monte-Carlo simulator, Harmonograph, Pintograph, MAPLE, Laser cutting

1 Introduction

A Harmonograph is a mechanical device that operates pendulums to create a geometric image (Doan [1]). A Pintograph is a lateral (2D) implementation of the Harmonograph; it uses a number of rods to move a pen or another instrument relative to a flat drawing surface (Pinterest [2]). Fig. 1 compares the operation of the 2D robotic arm with the operation of a Pintograph.

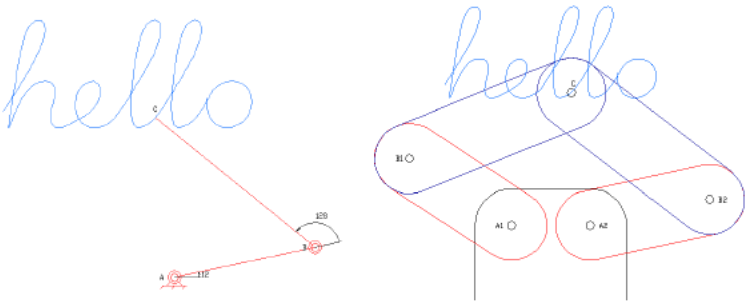

Fig. 1. Pintograph (right) as an alternative tool to a 2D robotic arm (left).

Compared to a 2D robotic arm, the mechanical design of the Pintograph has an advantage; Motor #1 of the 2D robotic arm must move rods, instruments (pen, laser, etc.) and heavy Motor #2; whereas the motors of a Pintograph must move only lightweight rods and the instrument.
The Pintograph is known since the 19th century, and recently became popular because of its simple mechanical implementation that uses inexpensive actuators (servo motors) controlled by an inexpensive microcontroller (Joostens [3]).

2 Mathematical Model of a Pintograph

Mechanical design and parameters of a Pintograph are used to create its mathematical model presented in Fig. 2. Two motors (marked "M#1" and "M#2") are positioned on the axis "X". The distance of Motor #1 from the origin {0,0} is marked as "L1", so that absolute coordinates of the Motor #1 shaft (axis) are {L1, 0}. The distance between Motor #1 and Motor #2 is marked as "L2", so that absolute coordinates of the Motor #2 shaft are {(L1+L2), 0}.

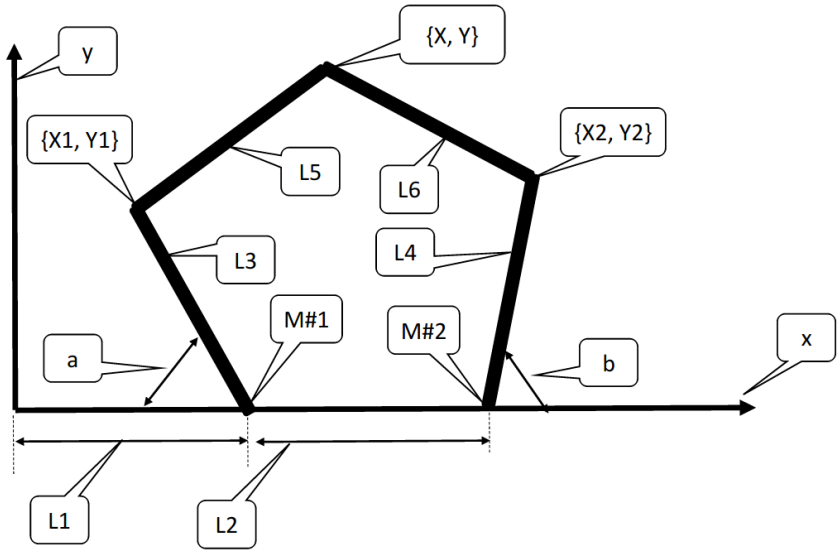

Fig. 2. Mechanical design and parameters of a Pintograph.

The Pintograph contains four rigid rods that are assumed to have equal length. However, to take assembly errors into account, slack (luft) in the motor shafts and joint rod lengths are marked as "L3", "L4", "L5", and "L6".
The bottom left rod is connected to the shaft of the Motor #1, so that the angle between axis "X" and the bottom left rod is marked as "a", whereas the bottom right rod is connected to the Motor #2, so that the angle between axis "X" and the bottom right rod is marked as "b".

Coordinates of the left joint are marked as {X1, Y1}, whereas coordinates of the right joint are marked as {X2, Y2}. Coordinates of the top joint are marked as {X, Y}. We assume that the instrument (for example, a laser) is positioned at this point (the top joint). Considering the mechanical design presented in Fig. 1, angles "a" and "b" define the position of the instrument {X, Y}, so controlled rotating motors shafts can position the instrument{X, Y} in a predictable manner.

The mathematical model of a Pintograph must be able to calculate {X, Y} by {a, b} and vice versa. {L1,L6} are model parameters. Unfortunately, the current design has an inherited mathematical ambiguity; for the same angles {a, b}, two possible sets of {X, Y} exist, as can be seen in Fig. 3: "upper" position {X, Y} and "bottom" position {$\underline{X}$, $\underline{Y}$}. To prevent this ambiguity, the mathematical model of a Pintograph enforces use of the "upper" configuration only.

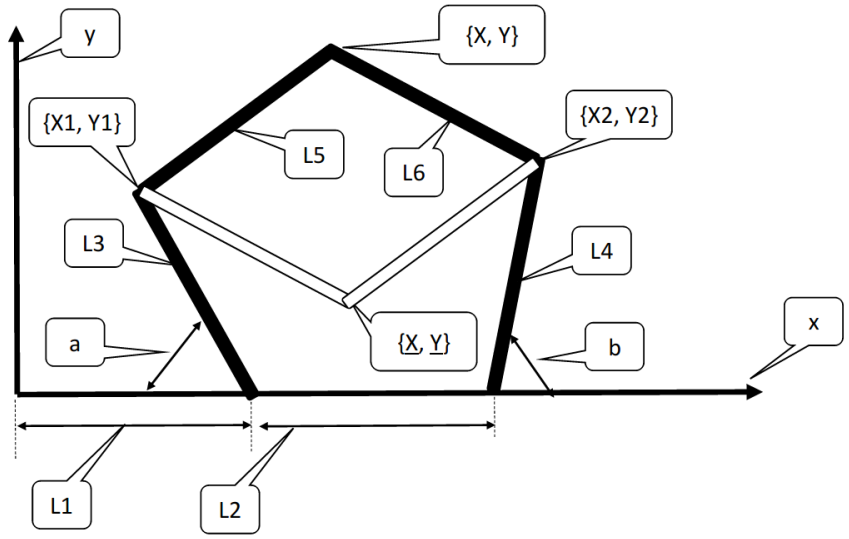

Fig. 3. Ambiguity in {X, Y}.

Fig. 4 specifies the basic Pintograph equations derived from Fig. 2.

$$Term1 := (x - X1)^2 + (y - Y1)^2 - L5^2;$$

$$Term2 := (x - X2)^2 + (y - Y2)^2 - L6^2;$$

Fig. 4. Basic Pintograph equations.

Considering that the derived mathematical model of a Pintograph is to be used in computer microcontroller software, MAPLE symbolic software was used to solve and rearrange relevant mathematical equations and convert derived

formulae to C or C# code. For example, {x,y} were found using MAPLE software. (See Fig. 5 for "X" and Fig. 6 for "Y").

$$x = -\frac{1}{2}\,\frac{L5^2 - L6^2 - XI^2 + X2^2 - YI^2 + 2\,YI\,y + Y2^2 - 2\,Y2\,y}{XI - X2}$$

Fig. 5. Formula for "X". "Y" from Fig. 6 must be substituted into this formula.

As stated before, the mechanical design used here has a mathematical ambiguity. To eliminate this ambiguity, MAPLE was instructed to use a solution with a plus (+) sign before the square root, as shown in the formula presented in Fig 6.

$$y := \frac{1}{2}\,\frac{1}{\frac{1}{4}\,\frac{(2\,YI - 2\,Y2)^2}{(XI - X2)^2} + 1}\left(\frac{1}{XI - X2}\left(\left(-\frac{1}{2}\,\frac{L5^2 - L6^2 - XI^2 + X2^2 - YI^2 + Y2^2}{XI - X2} - XI\right)(2\,YI - 2\,Y2)\right) + 2\,YI + \left(\left(-\frac{\left(-\frac{1}{2}\,\frac{L5^2 - L6^2 - XI^2 + X2^2 - YI^2 + Y2^2}{XI - X2} - XI\right)(2\,YI - 2\,Y2)}{XI - X2} - 2\,YI\right)^2 - 4\left(\frac{1}{4}\,\frac{(2\,YI - 2\,Y2)^2}{(XI - X2)^2} + 1\right)\left(\left(-\frac{1}{2}\,\frac{L5^2 - L6^2 - XI^2 + X2^2 - YI^2 + Y2^2}{XI - X2} - XI\right)^2 + YI^2 - L5^2\right)\right)^{1/2}\right)$$

Fig. 6. Formula for "Y".

Geometry formulae were used (see Fig. 7) to get dependency between {X,Y} and {a,b}. Then, MAPLE was instructed to derive positions of the instrument's "X" and "Y" as functions of the shaft's angles: "a" for Motor #1 and "b" for Motor #2.

Finally, C# code was generated using the CSharp function from the MAPLE software. Because the computer code for the derived formulae is very long (for example, C# code of the mathematical model of Pintograph contains more than one hundred lines), it is not presented here.

$$X1 := L1 - L3\cos(a)$$

$$Y1 := L3\sin(a)$$

$$X2 := L1 + L2 + L4\cos(b)$$

$$Y2 := L4\sin(b)$$

Fig. 7. Geometry formulae in accordance with Fig. 1.

Despite the simple mechanical design of a Pintograph, the resultant mathematical model of the real-life Pintograph is not trivial. Additionally, the real-life model has to take into account the fact that a number of mechanical and electronic parameters have pseudo-random tolerance. The mathematical model of a Pintograph design, presented in Fig. 2, has eight parameters to consider: six lengths {L1..L6} and two angles "a" and "b". A preferable (and inexpensive) implementation of a Pintograph utilizes two servo motors that can change the shaft angles in the range $\{0,180^{o}\}$. However, possible angles of the servo motor shaft, controlled by a microcontroller, can only be set to a limited number of values. These angles have some tolerance, which have to be considered in the real-life model of a Pintograph in addition to tolerances of {L1..L6}. As a result, the actual position {X,Y} of the instrument differs from the position calculated on the basis of the Pintograph model described above.

3 Monte-Carlo Simulator

The operation of a real-life Pintograph was simulated with a software simulator designed for this purpose using the mathematical model described in the previous section. The simulator was implemented using Visual Studio 2015 as a C# .NET desktop application. The simulator considers rod length, joint tolerance, and servo motor accuracy. Joint tolerance was simulated as changes in rod length. Using inexpensive and simple-to-operate servo motors is generally considered a preferable option. However, the digital control of the servo motor results in a discrete number of possible angles. Considering that angles {a, b} in the mathematical model are arguments of nonlinear functions, the simulator operation results are a non-trivial map of the points that can be reached by the instrument. Additionally, not all the points on the XY plane can be reached by the instrument, so that "points that can be reached" effectively creates a "drawing zone", which is a function of the selected {L1..L6}. Considering that variations of the model parameters have a pseudo-random character, simulations utilize the Monte-Carlo approach by running a predefined number of times, while changing the parameter values for every run in a pseudo-random way within the predefined ranges. For simplicity, flat distributions of the tolerances in the predefined ranges were used in the Monte-Carlo loop.

4 Simulation Results

Some exemplary simulation results for a different parameters of a Pintograph are presented in Fig. 8, Fig. 9, Fig. 10, and Fig. 11.

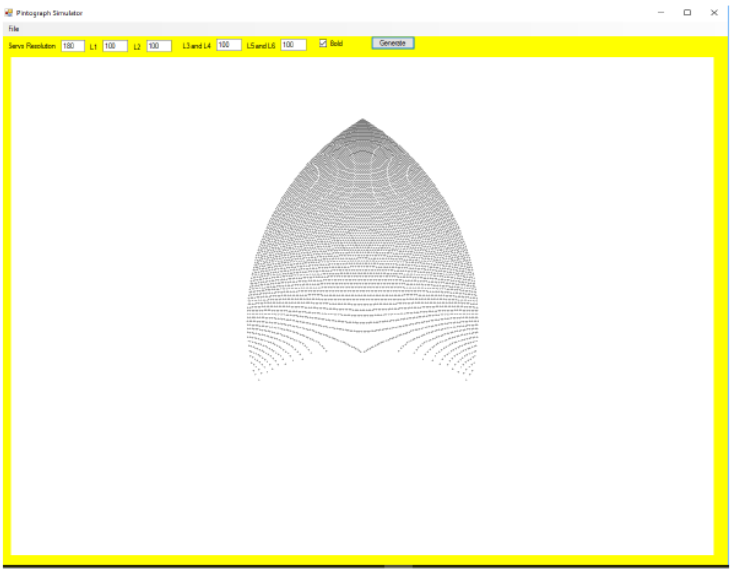

Fig. 8. Drawing map for L1=L2=L3=L4=L5=L6=100 mm

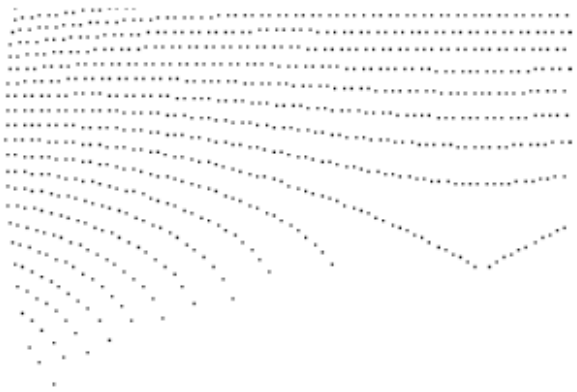

Fig. 9. Zoom in to the bottom portion of the drawing map presented in Fig.8.

Fig. 8 presents a “symmetrical design” where all rod lengths are equal to 100 mm and the distance between motors (L2) also equals 100 mm. The drawing zone is clearly seen, and the obvious conclusion is that the Pintograph’s

instrument cannot reach points that are outside this drawing zone. Additionally, it can be seen that even inside the drawing zone not all the points can be reached by the instrument. This effect (discrete nature of the drawing maps attributed to the digital nature of the servo motors control) is better seen in Fig. 9. The average "distance" between points can be used as an estimation of the accuracy of drawing/engraving/cutting. When planning even the simplest route of the instrument—i.e., a straight cutting line—it must be taken into account that resulting line will be jagged. The Monte-Carlo simulator can predict ranges of the cutting line depending on the selected accuracy of the servo motors, so that the customer can decide if the expected accuracy of the real laser cutting machine is adequate.

Symmetrical design (according to which all rods of the Pintograph and the distance between motors are equal) is not the only possible option. Shortening the distance between motors (L2=10mm) significantly increases the drawing zone of a Pintograph (see Fig. 10). This can be useful in some specific cutting cases.

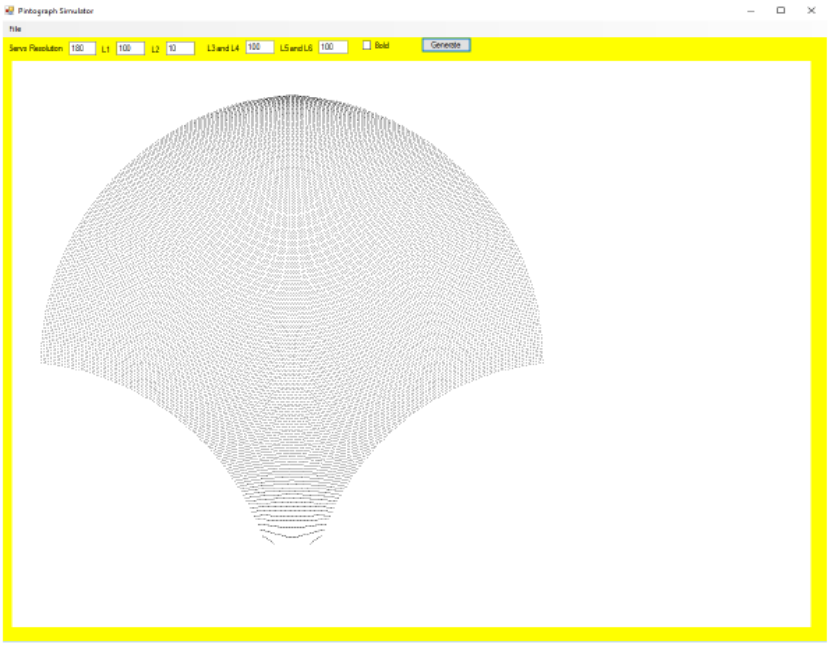

Fig. 10. Drawing map for the modified distance between motors (L2=10mm; L1=L3=L4=L5=L6=100 mm).

By modifying parameters of the Pintograph (modifying the values in the simulator's toolbox) one can select optimal customization for the specific task requirements and evaluate the expected drawing zone and accuracy of the resulting Pintograph.

5 Conclusions

The software developed for the Monte-Carlo simulator enables evaluation of the drawing zone and drawing accuracy of the 4-rod Pintograph for the selected set of parameters. Simulator runs reveal that the 4-rod Pintograph with unit length of 100 mm achieves accuracy of 0.3 mm in the center of the drawing zone, which is good enough for an inexpensive DIY laser cutting machine or laser engraving machine. When better accuracy is required, designs with the customer's selected sizes and tolerances of Pintograph elements can be tested.

Acknowledgments

This study was supported by a grant from the ORT Braude College Research Committee under grant number 5000.838.3.3-58.

References

1. R. Doan. The Harmonograph as a project in high school physics. School Science and Mathematics. Vol 12/5, 1923.
2. Pinterest – The world's catalog of ideas. https://www.pinterest.com/pin/216032113350089616/, 2017.
3. I. Joostens and P. S'heeren. Sand Clock. Elektor. January & February 2017, pp. 33-39.

Order statistics for samples of random size: new results and applications

Vasileios M. Koutras and Markos V. Koutras[1]
Department of Statistics and Insurance Science,
School of Finance and Statistics, University of Piraeus, Greece

Abstract

In the present work we develop some new results for the distribution of order statistics coming from a sample of random variables, with random sample size. Let N be a non-negative integer valued random variable and denote by $X_1, X_2, \ldots$ an infinite sequence of independent and identically distributed random variables, independent of N. Our interest focuses on the distribution of the r-th order statistic $X_{r:N}$ of a random sample $X_1, X_2, \ldots, X_N$ whose length N is a random variable. Besides some new results pertaining to the exact distribution of $X_{r:N}$, several interesting outcomes are developed when N belongs to wide class of discrete distributions such as the family of power series distributions and the Panjer Family. Finally, we illustrate how the stochastic model under study can be exploited for modeling problems arising in the monitoring of non-performing loans, a procedure of crucial importance in financial risk management.

Keywords: Non-performing loans; Panjer family; power series distributions; random order statistics; risk management; samples of random size.

1. Introduction

The motivation of the model studied in the present article stems from several applications of order statistics in numerous areas of applied science such as financial risk management, actuarial science, quality control, reliability, data mining, engineering etc; to mention a few

a. in financial risk management and actuarial science one may be interested in the minimum and maximum loss generated by a portfolio of loans, securities, insurance contracts etc.
b. in outlier and anomaly detection, one would naturally be interested in answering the question what is the probability that the largest observation or the $r-$larger observations of a randomly collected sample are as large as the suspiciously large value he/she has observed;
c. in engineering reliability, the life of the k out of n system is clearly associated to the $k-th$ largest or $k-th$ smallest of the component lifetimes.

[1] vkoutras@icloud.com, mkoutras@unipi.gr

d. in Statistical Quality Control, two popular classes of control charts are the $\bar{X} - R$ chart and the median$-R$ chart which are making use of the smallest, largest and the median observation of a sample

For a more detailed list of theory and applications of order statistics, the interested reader may refer to Arnold *et al.* (1992)), Balakrishnan and Rao (1998a), (1998b) and David and Nagaraja (2003).

In many biological, mechanical engineering, agricultural and quality control problems some observations may get lost, for a variety of reasons, and therefore the sample size is not fixed. In another setup, the sample size may depend on the occurrence of some random events, which makes the sample size random.

The probabilistic framework for this case can be described as follows. Let N be a non-negative integer valued random variable and denote by $X_1, X_2, \ldots$ a (infinite) sequence of independent and identically distributed random variables, independent of N. Our interest focuses on the distribution of the *r*-th order statistic $X_{r:N}$ of a random sample $X_1, X_2, \ldots, X_N$ whose length N is a random variable. For $r = 1$ we have the smallest observation in the sample, while $r = N$ produces the largest one.

As an example let us consider the following experiment described by Consul (1984). A sample of animals is exposed to a dose of radiation and the interest then focuses on the times that the first and the last die. Since the animals that we observe after the radiation is not the whole population but a random number of them (assume for example, that we mark-up the radiated animals and after some time we recapture *N* of them), we are in fact looking at the maximum and minimum of a sample with a random size. The time till the first and the last animal dies is described is $\min(X_1, X_2, \ldots, X_N)$ and $\max(X_1, X_2, \ldots, X_N)$ respectively, while the time till *r* of the recaptured animals die equals $X_{r:N}$.

Under another setting, in a transportation problem (see Shaked and Wong (1997a), (1997b)) $\min(X_1, X_2, \ldots, X_N)$ describes the accident-free distance of a shipment of explosives, with *N* of them being defective (*N* is a random variable); each of the defective items may explode and cause an accident after $X_1, X_2, \ldots X_N$ miles, respectively.

A third example comes from the area of biostatistics, and refers to the so-called cure rate models, see e.g. the recent article of Koutras and Milienos (2007) and references therein. Let *N* denote the number of clonogens (carcinogenic cells) left active after a cancer treatment, and assume that *N* follows a specific discrete distribution. A non-negative random variable X_i is assigned to each surviving clonogen, denoting the time for the $i-$th clonogenic cell to produce a detectable cancer mass. Then, $\min(X_0, X_2, \ldots, X_N)$ accounts for the population time-to-event. Note that under this scenario, adopting the convention $X_0 = 1$ almost surely,

the probability of tumor cure is defined as the probability of the event $N = 0$, i.e. no clonogens survived by the end of the treatment.

Random minima, maxima and more generally order statistics arise also in the study of floods, droughts, and breaking strength experiments as well as in financial risk management, actuarial science, biostatistics, educational psychology, statistical quality control, reliability, etc. In Section 4 we describe in detail some problems encountered in financial risk management which call for the study of random order statistics and illustrate how the results developed in the present MS can be fruitfully used to handle them.

An early study of order statistics associated with a sample of random size was provided by Epstein (1949); his study was focused in the case when the random sample size *N* follows a Poisson distribution. His work was motivated from the need to study particles that are distributed over unit areas in such a way that the number of particles to be found in each areas is a random variable following the Poisson law; the particles themselves are assumed to vary in magnitude according to a prespecified size distribution (independently of the particular unit area chosen) and the problem is to find the distribution of the smallest, largest, or more generally the i −th smallest or $i - th$ largest particle in a randomly chosen unit area.

Raghunandanan and Patil (1972) presented some results for the distribution function of the $i -$ order statistic when the sample size *N* has a binomial or a negative binomial distribution, while Consul (1984) and Gupta and Gupta (1984) considered the case when *N* follows a generalized negative binomial distribution, generalized Poisson and generalized logarithmic series distribution,. For more general results, see Rohatgi (1987).

Berman (1962), Barndorff-Nielsen (1964), Silvestrov and Teugels (1998), Barakat and El-Shandidy (1990) and Voorn (1989) studied the limiting distributions of the maximum of a random number of dependent and independent random variables. Ahsanullah (1988), Grudzien and Szynal (1998) and Voorn (1987) used order statistics from a sample with random size for characterization of distributions.

Recently, many researchers have studied stochastic comparisons of order statistics associated to random sample sizes; see Nanda *et. al* (2005), Nanda and Shaked (2008) and references therein.

The present paper is organized as follows. In Section 2, we introduce some definitions and notations and present a few preliminary results on the distribution of a random order statistic, namely the *r*-th order statistic $X_{r:N}$ of a random sample $X_1, X_2, \dots, X_N$ whose length N is a random variable. Section 2 provides some new general results for the cumulative distribution function and probability mass function of random order statistics while Section 3 presents several interesting outcomes when N belongs to classical discrete distributions or wide classes of discrete distributions such as the power series and the Panjer family. Finally, in Section 4 we illustrate how the stochastic model under study can be exploited for modeling problems

arising in financial risk management, and more specifically in the study of non-performing loans.

2. Definitions and Preliminaries

In this section we shall present the notations that will be used in the MS and some preliminary results on the distribution of order statistics coming from a sample with random size.

To fix our notations, assume that $X_1, X_2, \ldots$ is a sequence of positive valued iid random variables and denote by $F(x) = P(X \leq x)$ their common cumulative distribution function (cdf) and by $f(x)$ the respective probability mass function (pmf). Let also N be a discrete random variable independent of $X_1, X_2, \ldots$ with support $S_N = \{0,1,2, \ldots\}$ or a subset of S_N and denote by $P_N(z) = E(z^N) = \sum_{n=0}^{\infty} P(N = n) z^n$ the probability generating function (pgf) of *N*. The random variable of interest in the present article is defined as follows

$$T = \begin{cases} 0, & \text{if } N < r \\ X_{r:n}, & \text{if } N = n \geq r; \end{cases}$$

that is, we are looking at the *r*-th order statistic of a random sample $X_1, X_2, \ldots, X_N$ of random length, under the assumption that, when the number of observed values in the random sample are not sufficient to compute the *r*-th order statistic ($N < r$) we conventionally set the value of T to be zero.

Since $P(T = 0) = P(N < r) > 0$, the random variable *T* has a **mixed-type distribution** with support $S = [0, \infty)$. More specifically, a part of the distribution of *T* is concentrated at the discrete set $S_1 = \{0\}$ and the rest of it is continuously spread over the interval $S_2 = (0, \infty)$.

Denoting by $F_r(t) = P(T \leq t)$ the cdf of *T* (see Figure 1) and by $f_r(t)$ the respective pmf, we shall have $f_r(0) = P(T = 0) = P(N < r)$ and $f_r(t) = F_r'(t)$ for all $t \in (0, +\infty)$.

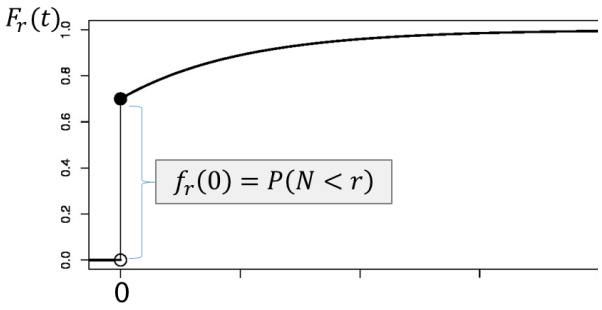

Figure 1. The pdf $F_r(t)$ of the random variable *T*.

Needless to say, if the support of *N* is a subset of $\{r, r+1, \ldots\}$ then $f_r(0) = P(N < r) = 0$ and the distribution of *T* reduces to a classical continuous distribution.

In this case, the cdf of *T* can be expressed in terms of the cdf of the order statistic $X_{r:n}$ (see e.g. Arnold *et al.* (1992) or David and Nagaraja (2003))

$$F_{X_{r:n}}(t) = \frac{n!}{(r-1)!\,(n-r)!} \int_0^{F(t)} y^{r-1}(1-y)^{n-r} dy = B_{F(t)}(r, n-r+1)$$

as follows

$$F_r(t) = \sum_{n=r}^{\infty} P(X_{r:n} \le t | N = n) P(N = n)$$

$$= \sum_{n=r}^{\infty} F_{X_{r:n}}(t) P(N = n) = \sum_{n=r}^{\infty} B_{F(t)}(r, n - r + 1)\, P(N = n)$$

where $B_x(p, q)$ denotes the incomplete Beta ratio function with parameters p, q (see also Nanda *et al.* (2005)). Apparently, if the support of N is $S_N = \{0,1, \ldots\}$ then we may write $F(t|N = n) = P(X_{n:r} \le t | N = n) = \frac{1}{P(N=n)} F_{X_{n:r}}(t)$ for all $n \in S_N$ and $t > 0$.

3 Main Results

In the present section we shall present some results pertaining to the evaluation of the cdf and pmf of the random variable T.

Proposition 1. The cdf of *T* is given as follows

$$F_r(t) = \begin{cases} P(N < r) & \text{for } t = 0 \\ P(N < r) + \sum_{k=r}^{\infty} \frac{1}{k!} P_N^{(k)}\big(1 - F(t)\big) F^k(t) & \text{for } t > 0. \end{cases}$$

Proof. Manifestly $F_r(0) = P(T = 0) = P(N < r)$. Assume next that $t > 0$. Conditioning on the value of the random variable N we may write

$$F_r(t) = \sum_{n=0}^{r-1} P(T \le t | N = n) P(N = n) + \sum_{n=r}^{\infty} P(T \le t | N = n) P(N = n)$$

and taking into account that

$$P(T \le t | N = n) = \begin{cases} 1, & \text{for } n \le r - 1 \\ P(X_{r:n} \le t), & \text{for } n \ge r \end{cases}$$

we may easily arrive at the expression

$$F_r(t) = P(N < r) + \sum_{n=r}^{\infty} P(X_{r:n} \le t) P(N = n).$$

Substituting the well-known expression for the cdf of the *r*-th order statistic in a fixed length sample (see e.g. Arnold *et al.* (1992) or David and Nagaraja (2003))

$$P(X_{r:n} \le t) = \sum_{k=r}^{\infty} \binom{n}{k} F^k(t)\big(1 - F(t)\big)^{n-k}$$

we obtain

$$F_r(t) = P(N < r) + \sum_{n=r}^{\infty} \sum_{k=r}^{n} \binom{n}{k} F^k(t)\big(1 - F(t)\big)^{n-k} P(N = n).$$

and interchanging the order of summation we deduce the expression

$$F_r(t) = P(N < r) + \sum_{k=r}^{\infty} \left(\sum_{n=k}^{\infty} \binom{n}{k} \big(1 - F(t)\big)^{n-k} (t) P(N = n) \right) F^k(t). \qquad (1)$$

Note next that, by differentiating k times the formula $P_N(z) = E(z^N) = \sum_{n=0}^{\infty} z^n P(N = n)$ we obtain

$$P_N^{(k)}(z) = \sum_{n=k}^{\infty} (n)_k z^{n-k} P(N = n)$$

and therefore

$$\frac{1}{k!} P_N^{(k)}\big(1 - F(t)\big) = \sum_{n=k}^{\infty} \binom{n}{k} \big(1 - F(t)\big)^{n-k} P(N = n).$$

Thus formula (1) may be rewritten in the equivalent form

$$F_r(t) = P(N < r) + \sum_{k=r}^{\infty} \frac{1}{k!} P_N^{(k)}\big(1 - F(t)\big) F^k(t)\,. \qquad \blacksquare$$

It is worth noting that the infinite sum appearing in the formula of Proposition 1 may be evaluated easier through a finite sum, since

$$\sum_{k=0}^{r-1} \frac{1}{k!} P_N^{(k)}\big(1 - F(t)\big) F^k(t) + \sum_{k=r}^{\infty} \frac{1}{k!} P_N^{(k)}\big(1 - F(t)\big) F^k(t) = P_N(1) = 1.$$

Note also that, as expected since we are dealing with a mixed-type distribution with positive mass at 0, the cdf $F_r(t)$ is not continuous at $t = 0$. Manifestly $\lim_{t \to 0^+} F_r(t) = P(N < r) = F_r(0)$ while $\lim_{t \to 0^-} F_r(t) = 0$. Needless to say, if the support of the discrete random variable N is $\{r, r+1, \dots\}$ or a subset of that set, then the distribution of T becomes absolutely continuous.

The next Corollary follows immediately from Proposition 1, after some elementary algebra.

Corollary 1. The cdf of *T* obeys the next recurrence

$$F_{r+1}(t) = F_r(t) + P(N = r) - \frac{1}{r!} P_N^{(r)}\big(1 - F(t)\big) F^r(t)$$

with initial condition

$$F_1(t) = \begin{cases} P(N = 0), & for\ t = 0 \\ P_N\big(1 - F(t)\big), & for\ t > 0. \end{cases}$$

In the next Proposition we provide a closed formula for the pmf of T.

Proposition 2. The pmf of *T* is given as follows:

$$f_r(t) = \begin{cases} P(N < r) & \text{for } t = 0 \\ \dfrac{1}{(r-1)!} P_N^{(r)}\big(1 - F(t)\big) F^{r-1}(t) f(t) & \text{for } t > 0 \end{cases}$$

Proof. The first part of the formula is obvious (results from the definition of T). In order to get an expression for $t > 0$ we recall the result stated after the proof of Proposition 1, to write $F_r(t)$ as

$$F_r(t) = P(N < r) + 1 - \sum_{k=1}^{r-1} \frac{1}{k!} P_N^{(k)}\big(1 - F(t)\big)F^k(t) - P_N(1 - F(t))$$

and then differentiate this expression to get

$$f_r(t) = F_r'(t) = \frac{d}{dt}\left(-P_N(1 - F(t)) - \sum_{k=1}^{r-1} \frac{1}{k!} P_N^{(k)}\big(1 - F(t)\big)F^k(t)\right).$$

Therefore

$$f_r(t) = P_N'\big(1 - F(t)\big)f(t) + \sum_{k=1}^{r-1} \frac{1}{k!}[P_N^{(k+1)}\big(1 - F(t)\big)f(t)F^k(t) - P_N^{(k)}\big(1 - F(t)\big)kF^{k-1}(t)f(t)]\,. \quad (2)$$

Note next that

$$\sum_{k=1}^{r-1} \frac{1}{k!} P_N^{(k)}\big(1 - F(t)\big)kF^{k-1}(t)f(t) = P_N'\big(1 - F(t)\big)f(t) + \sum_{k=1}^{r-2} \frac{1}{k!} P_N^{(k+1)}\big(1 - F(t)\big)F^k(t))f(t)$$

a fact that leads to the cancelation of all the terms of the sum appearing in (2), apart from the last term $\frac{1}{(r-1)!} P_N^{(r)}\big(1 - F(t)\big)f(t)F^{r-1}(t)$. This concludes the proof. ■

The formula given in Proposition 2 for $t > 0$ is closely related to the expression provided by Rohatgi (1987) for the conditional distribution of T given that $N \geq r$.

3. Families of random order statistics distributions

In this section we shall present some results pertaining to the evaluation of the probability mass function of T for some well known families of distributions. Let us consider first the cases where N follows the Poisson, Binomial and Negative binomial distributions.

a. *Poisson distribution*

If N follows a Poisson distribution with parameter λ, i.e.

$$P(N = n) = \exp(-\lambda)\frac{\lambda^n}{n!}, \quad n = 0,1,2, \ldots$$

then the pgf of N will be given by the formula $P_N(z) = E(z^N) = \exp(-\lambda(1 - z))$ and it is not difficult to verify that

$$P_N^{(r)}(z) = \lambda^r \exp\big(-\lambda(1 - z)\big).$$

Applying Proposition 2 we get

$$f_r(t) = \frac{1}{\Gamma(r)}\lambda^r \exp\big(-\lambda F(t)\big)F^{r-1}(t)f(t)$$

or equivalently

$$f_r(t) = f_G\big(F(t)\big)f(t)$$

where $f_G(.)$ denotes the pmf of a Gamma distribution with parameters r and λ.

In the special case where T follows the power distribution with cdf $F(t) = t^a, 0 < t < 1$, the pmf of T takes on the form

$$f_r(t) = \frac{a\lambda^r}{\Gamma(r)}t^{ar-1}\exp(-\lambda t^a), \qquad 0 < t < 1.$$

It is of interest to note that, the continuous part of the mixed distribution that has been produced, is proportional to the pmf of Stacy's (1962) generalized gamma distribution. The new distribution, however, has its support limited in the interval [0,1) with a positive mass placed at $t = 0$.

Note alos that, for $a = 1$ (in which case the random variable T follows a uniform distribution in the interval (0, 1)), the pmf of T, for $0 < t < 1$ becomes proportional to the pmf of the typical gamma distribution.

b. *Binomial distribution*

If N follows a binomial distribution with pmf

$$P(N = n) = \binom{m}{n}p^n(1-p)^{m-n}, n = 0,1,\dots,m$$

then the pgf of N is given by the formula $P_N(z) = E(z^N) = (pz + q)^m$ where $q = 1 - p$ and it's r −th derivative reads

$$P_N^{(r)}(z) = (m)_r(pz + q)^{m-r}p^r \quad \text{for } k \le m.$$

Applying Proposition 2 we arrive at the formula

$$f_r(t) = r\binom{m}{r}\big(1 - pF(t)\big)^{m-r}F^{r-1}(t)f(t)$$

In the special case where T follows the power distribution with cdf $F(t) = t^a, 0 < t < 1$, the pmf of T takes on the form

$$f_r(t) = ar\binom{m}{r}(1 - pt^a)^{m-r}t^{ar-1}, \qquad 0 < t < 1.$$

It is worth noting that, in this case, the distribution of pT^a has a continuous part that is proportional to the continuous part of the beta distribution with parameters $m - r + 1$ and r. For a similar result pertaining to a conditional distribution see Raghunandanan and Patil (1972).

c. *Negative Binomial distribution*

If N follows a Negative Binomial distribution with pmf

$$P(N=n)=\frac{\Gamma(m+n)}{n!\,\Gamma(m)}p^m(1-p)^n, n=0,1,\ldots$$

then the pgf of N will be given by the formula $P_N(z)=E(z^N)=\left(\frac{p}{1-qz}\right)^m$ and it is easy to verify that

$$P_N^{(r)}(z)=\frac{\Gamma(m+n)}{\Gamma(m)}\frac{p^m\,q^r}{(1-qz)^{m+r}}.$$

Applying Proposition 2 we get

$$f_r(t)=\frac{\Gamma(m+r)}{\Gamma(r)\Gamma(m)}\frac{p^m q^r}{\big(p+qF(t)\big)^{m+r}}F^{r-1}(t)f(t).$$

In the special case where T follows the power distribution with cdf $F(t)=t^a, 0<t<1$, the pmf of T takes on the form

$$f_r(t)=\frac{a\Gamma(m+r)}{\Gamma(r)\Gamma(m)}\frac{p^m q^r t^{ar-1}}{(p+qt^a)^{m+r}}, 0<t<1.$$

Before closing this section we shall provide some general results for two families that contain all three distributions mentioned above, more specifically the family of Power series distributions and the Panjer family.

Suppose that $c_n, n=0,1,2,\ldots$ is a sequence of nonnegative real numbers such that the series $C(\theta)=\sum_{n=0}^{\infty}c_n\theta^n$ converges for all $\theta\in[0,\theta_0)$. A discrete random variable N has the power series distribution associated with the function $C(\theta)$ (or equivalently with the sequence $c_n, n=0,1,2,\ldots$) if it has pmf of the form

$$P(N=n)=\frac{c_n\theta^n}{C(\theta)},\ \ n=0,1,\ldots$$

(see Johnson *et al.* (2005)). In this case, the pgf of N takes on the form

$$P_N(z)=\frac{C(\theta z)}{C(\theta)}$$

and differentiating it n times we obtain

$$P_N^{(r)}(z)=\frac{\theta^r C^{(r)}(\theta z)}{C(\theta)}.$$

It is now easy to verify that the pmf of T is given by the formula

$$f_r(t)=\frac{\theta^r}{(r-1)!\,C(\theta)}\ C^{(r)}\big(1-F(t)\big)F^{r-1}(t)f(t)$$

(compare to a similar formula provided by Rohatgi (1987) for the conditional distribution of T given that $N \geq r$). Since the Poisson, Binomial and Negative Binomial distributions are members of the family of Power Series distributions, it is not difficult to check that the formulae provided above for the pmf of T, can be obtained as well by a direct application of the last expression.

Another wide family of discete distributions, with many applications in the Actuarial Science is the celebrated Panjer family (see e.g. Panjer (1981) or Bowers *et al.* (1997)). A discrete random variable *N* is a member of the Panjer family, otherwise known as the $(a, b, 0)$ class of distributions ($N \sim P(a, b, 0)$), if the pmf $p_n = P(N = n), n = 0,1, \ldots$ of *N* satisfies the recurrence relation

$$p_n = \left(a + \frac{b}{n}\right) p_{n-1} \text{ for } n = 1,2, \ldots .$$

with initial condition $p_0 = P(N = 0)$.

The Panjer family $P(a, b, 0)$ includes as special cases many classical discrete distributions; see next table where the values of the parameters a, b as well as the initial condition are provided for the three distributions mentioned earlier.

Distribution	$\boldsymbol{p_n = P(N = n)}$	$\boldsymbol{a}$	$\boldsymbol{b}$	$\boldsymbol{p_0}$
Binomial	$\binom{m}{n} p^n (1-p)^{m-n}$	$-\frac{p}{1-p}$	$\frac{p(m+1)}{1-p}$	$(1-p)^m$
Poisson	$e^{\lambda} \frac{\lambda^n}{n!}$	0	λ	$e^{-\lambda}$
Negative binomial	$\frac{\Gamma(m+n)}{n!\,\Gamma(m)} p^m (1-p)^n$	$1-p$	$(m-1)(1-p)$	p^m

Table 1. *Classical discrete distributions as special cases of the Panjer Family.*

Hess et al. (2002) proved that the pgf of $N \sim P(a, b, 0)$ satisfies the differential equation $(1 - az)P_N'(z) = (a + b)P_N(z)$. One may easily verify by induction that $P_N^{(r)}(z)$ can be expressed in terms of $P_N^{(r-1)}(z)$ by the formula

$$(1 - az)P_N^{(r)}(z) = (ar + b)P_N^{(r-1)}(z).$$

A direct application of Proposition 2 yields the next result.

Proposition 3. If $N \sim P(a, b, 0)$ then the pmf $f_r(t), t > 0$ of *T* satisfies the next recurrence relation

$$f_r(t) = \frac{ar + b}{r - 1} \frac{F(t)}{1 - a\big(1 - F(t)\big)} f_{r-1}(t) \text{ for } r = 2,3, \ \ldots$$

with initial condition

$$f_1(t) = \frac{a+b}{1-a(1-F(t))} P_N(t)$$

A repeated application of Proposition 3, leads to the following closed formula for the pmf of $f_r(t)$.

Proposition 4. If $N \sim P(a,b,0)$ then the pmf $f_r(t), t > 0$ can be expressed as

$$f_r(t) = \frac{\prod_{k=1}^{r}(ak+b)}{(r-1)!} \frac{F^{r-1}(t)}{\left(1-a\left(1-F(t)\right)\right)^r} P_N\left(1-F(t)\right) f(t) \quad \text{for } r = 1,2,3, \ \ldots$$

Needless to say, by applying the formula of Proposition 4 for the special case of a Poisson, Binomial and Negative Binomial distribution (Table 1 provides the appropriate values of the parameters a, b for each case), we may reproduce again the results obtained earlier for the three classical discrete distributions.

4. An application to financial risk management

The European Banking Authority (EBA, http://www.eba.europa.eu/), established on January 1st, 2011 as part of the European System of Financial Supervision (ESFS), is an independent EU Authority which works to ensure effective and consistent prudential regulation and supervision across the European banking sector. Its overall objectives are to maintain financial stability in the EU and to safeguard the integrity, efficiency and orderly functioning of the banking sector. The main task of the EBA is to contribute to the creation of the European Single Rulebook in banking whose objective is to provide a single set of harmonised prudential rules for financial institutions throughout the EU. The Authority also plays an important role in promoting convergence of supervisory practices and is mandated to assess risks and vulnerabilities in the EU banking sector.

One of the major activities of EBA is to set rules and supervise the actions of the European banking sector for the "non-performing exposures" (NPE's). According to paragraph 145 of Annex V of the EBA FINAL draft Implementing Technical Standards on Supervisory reporting on forbearance and non-performing exposures under article 99(4) of Regulation EU575/2013, non-performing exposures are those that satisfy either or both of the following criteria:

a. material exposures which are more than 90 days past-due;
b. the debtor is assessed as unlikely to pay its credit obligations in full without realization of collateral, regardless of the existence of any past-due amount or of the number of days past due. Therefore, the definition of NPE's is based on the "past-due" criterion and the "unlikely-to-pay" criterion.

Let us next set up a probabilistic model associated with the monitoring of the "health" a portfolio of non-performing loans (NPL's). At the start of the monitoring period we have at our disposal a portfolio of performing loans. At a specific time point in the future, a number N of the loans will have transitioned to a non-performing status. Apparently N is a discrete random variable. After restructuring each one of the *N* NPL's, the stochastic behavior of the portfolio is associated to the following variables:

X_i: time elapsed until the *i*-th restructured loan returns to a Non-Performing status (becomes again an NPL)

W_i: loss incurred by the *i*-th restructured loan that returned to a Non-Performing status.

Apparently, a monetary financial institution will be primarily interested in the stochastic behavior of the following random variables:

- $\min_{1\le i\le N} X_i$: the minimum time elapsed until a restructured loan of the portfolio returns to a Non-Performing status.
- $\max_{1\le i\le N} X_i$: the time until all portfolio restructured loans return to a Non-Performing status.
- $\min_{1\le i\le N} W_i$: the minimum loss incurred by a restructured loan, that returned to a Non-Performing status.
- $\max_{1\le i\le N} W_i$: the maximum loss incurred by a restructured loan, that returned to a Non-Performing status.

Under a more general setup, one may look at the $r-$th smallest or the $r-$th largest of the random variables X_i, W_i.

Manifestly the simplest scenario for the problem described above, is to assume that at the start of the monitoring period we have at our disposal a portfolio of m performing loans and each of them has a fixed probability p to transition to a non-performing status at a specific time point in the future. Under these assumptions, the number N of the loans that will have transitioned to a non-performing status by the time we are focusing on, will follow a Binomial distribution with pmf

$$P(N=n)=\binom{m}{n}p^n(1-p)^{m-n},\qquad n=0,1,\dots,m.$$

Taking into account Proposition 1 and the analysis carried out for the Binomial model in Section 3, we may state that the cdf of the random variable describing the time till the $r-th$ worst restructured loan has transitioned again to non-performing status, is given by the following formula

$$F_r(t)=P(N<r)+\sum_{k=r}^{m}\binom{m}{k}(1-pF(t))^{m-k}p^kF^k(t),\qquad t>0$$

or equivalently

$$F_r(t) = 1 - \sum_{k=r}^{m} \binom{m}{k} \left[p^k (1-p)^{m-k} - \left(1 - pF(t)\right)^{m-k} \left(pF(t)\right)^k \right] \qquad t > 0.$$

Therefore, should we have an estimate of the cdf $F(t)$ of the time X_i until a restructured loan returns to non-performing status (e.g. through the empirical cdf calculated by the use of past data), it is easy to compute the future behavior of the portfolio for all time instances t.

The same analysis can be repeated by exploiting the random variable W_i describing the loss incurred by the *i*-th restructured loan that returned to a Non-Performing status instead of the time X_i elapsed until the *i*-th restructured loan returns to a Non-Performing status. By this approach we shall create a model describing the stochastic behavior of the minimum, maximum or, more generally, the $r-$th smallest loss incurred by the restructured loan portfolio.

In closing we mention that if the probability p to have a transition to a non-performing status is very small (this is a plausible assumption in some banking activities, e.g. in Project financing), one may use the Poisson model instead of the Binomial model for the random variable N. In this case the cdf of the random variable describing the time till the $r-th$ worst restructured project loan has transitioned again to non-performing status, will be given by the formula

$$F_r(t) = P(N < r) + \exp(-\lambda F(t)) \sum_{k=r}^{\infty} \frac{\left(\lambda F(t)\right)^k}{k!}$$

for $t > 0$, or equivalently

$$F_r(t) = \exp(-\lambda) \sum_{k=0}^{r-1} \frac{\lambda^k}{k!} + \exp(-\lambda F(t)) \sum_{k=r}^{\infty} \frac{\left(\lambda F(t)\right)^k}{k!}.$$

Acknowledgment

Work funded by National Matching Funds 2014-2016 of the Greek Government, and more specifically by the General Secretariat for Research and Technology (GSRT), related to EU project "ISMPH: Inference for a Semi-Markov Process" (GA No 329128).

References

Ahsanullah, M. (1988). Characteristic properties of order statistics based on random sample size from an exponential distribution. *Statistica Neerlandica*, **42**,193–197.

Arnold, B., Balakrishnan, N., Nagaraja, H. (1992). *A First Course in Order Statistics*. New York, John Wiley & Sons.

Balakrishnan, N., Rao, C. R. (1998a). *Handbook of Statistics* 16 – *Order Statistics, Theory and Methods*. Amsterdam, Elsevier Science B. V.

Balakrishnan, N., Rao, C. R. (1998b). *Handbook of Statistics* 17 – *Order Statistics, Applications*. Amsterdam, Elsevier Science B. V.

Barakat, H. M. and El-Shandidy, M. A. (1990). On the limit distribution of the extremes of a random number of independent random variables. *Journal of Statistical Planning and Inference*, **26**, 353-361.

Barndorff-Nielsen, O. (1964). On the limiting distribution of the maximum of a random number of independent random variables. *Acta Mathematica Academiae Scientiarum Hungaricae*, **15**,399–403.

Berman, S. M. (1962). Limiting distribution of the maximum term in sequences of dependent random variables. *Annals of Mathematical Statistics*, **33**,894–908.

Bowers, N. L., Hickman, J. C., Gerber, H. U., Nesbitt, C. J. and Jones D. A. (1997). *Actuarial Mathematics* (2nd Edition). Society of Actuaries.

Consul, P. C. (1984). On the distributions of order statistics for a random sample size. *Statistica Neerlandica*, **38**,249–256.

David, H. A., Nagaraja, H. (2003). *Order Statistics* (3rd edition). John Wiley & Sons, Hoboken, NJ.

Epstein, B. (1949). A modified extreme value problem. *Annals of Mathematical Statistics*, **20**, 99–103.

Grudzien, Z., Szynal, D. (1998). On characterizations of continuous distributions in terms of moments of order statistics when the sample size is random. *Journal of Mathematical Science*, **92**, 4017–4022.

Gupta, D., Gupta, R. C. (1984). On the distribution of order statistics for a random sample size. *Statistica Neerlandica*, **38**, 13–19.

Johnson, N. L., Kotz, S. and Kemp, A. W. (2005). *Univariate Discrete Distributions*. John Wiley & Sons, N. Y.

Koutras, M.V., Milienos, F.S. (2017). A flexible family of transformation cure rate models. *Statistics in Medicine*, **36**, 2559-2575.

Nanda, A. K., Misra, N., Paul, P. , Singh, H. (2005). Some properties of order statistics when the sample size is random. *Communications in Statistics-Theory and Methods*, **34**, 2105-2113.

Nanda, A. K., Shaked, M. (2008). Partial ordering and aging properties of order statistics when the sample size is random: A brief review. *Communications in Statistics-Theory and Methods*, **38**, 1710- 1720.

Panjer, H. H. (1981). Recursive evaluation of a family of compound distributions. *ASTIN* Bulletin, **12**, 22–26.

Raghunandanan, K., Patil, S. A. (1972). On order statistics for random sample size. *Statistica Neerlandica*, **26**, 121–126.

Rohatgi, V. K. (1987). Distribution of order statistics with random sample size. *Communications in Statistics-Theory and Methods*, **16**, 3739–3743.

Shaked, M., Wong, T. (1997a). Stochastic orders based on ratios of Laplace transforms. *Journal of Applied Probability*, **34**, 404–419.

Shaked, M., Wong, T. (1997b). Stochastic comparisons of random minima and maxima. *Journal of Applied Probability* , **34**, 420–425.

Silvestrov, D. S., Teugels, J. L. (1998). Limit theorems for extremes with random sample size. *Advances in Applied Probability*, **30**, 777–806.

Stacy, E. W. (1962). A Generalization of the Gamma Distribution. *The Annals of Mathematical Statistics*, **33**, 1187-1192.

Voorn, W. J. (1987). Characterization of the logistic and loglogistic distributions by extreme value related stability with random sample size. *Journal of Applied Probability*, **24**,838–851.

Voorn, W. J. (1989). Stability of extremes with random sample size. *Journal of Applied Probability*, **26**,734–743.

Climate-weather change process realizations uniformity testing for maritime ferry operating area

Ewa Kuligowska[1] and Mateusz Torbicki[2]

[1] Gdynia Maritime University, Gdynia, Poland
(E-mail: e.kuligowska@wn.am.gdynia.pl)
[2] Gdynia Maritime University, Gdynia, Poland
(E-mail: m.torbicki@wn.am.gdynia.pl)

Abstract. The paper is concerned with a method for statistical data uniformity testing applied to the realizations of the climate-weather change process empirical conditional sojourn times coming from different measurement points for maritime ferry operating at Baltic Sea open waters. The collected empirical data sets during Februaries of the years 1988-1993 at the four measurement points are under consideration. Assuming that the statistical data sets are separate, the verification of the non-parametric hypotheses on the basis of Kolmogorov-Smirnov test and Wald-Wolfowitz runs test is prepared. In the case when the null hypothesis about the uniformity data sets for two measurement points is not rejected, corresponding to each other statistical data sets of realisations are joined. After using this approach, the climate-weather change process at the fixed area is better described.
Keywords: climate-weather change process, uniformity testing, maritime ferry.

1 Introduction

The model of the climate-weather change processes is proposed in [2]. The statistical data for estimating the unknown parameters of the climate-weather change process very often come from different experiments of the same climate-weather change process and are collected into separate data sets. Furthermore, these data sets may be collected at different measurement points of the critical infrastructure operating area with some of the points located close to each other. Thus, before the climate-weather change process identification, the investigation of these empirical data uniformity is necessary. In this paper, the uniformity test is described in general and applied to the data sets including climate-weather change process realisations coming from four measurement points at maritime ferry operating area.

2 Modeling of climate-weather change process

We assume, as in [2], that the climate-weather change process for the critical infrastructure operating area is taking w, $w \in N$, different climate-weather states $c_1, c_2, ..., c_w$. Next, we mark by $C(t)$, $t \in <0,+\infty)$, the climate-weather change

process, that is a function of a continuous variable t, taking discrete values in the set $\{c_1, c_2, ..., c_w\}$ of the climate-weather states. We assume a semi-Markov model [1,4-9] of the climate-weather change process $C(t)$ and we mark by C_{bl} its random conditional sojourn times at the climate-weather states c_b, when its next climate-weather state is c_l, $b,l \in 1,2,\ldots,w$, $b \neq l$.
Consequently, the climate-weather change process may be described by the following parameters [3]:

- the vector $[q_b(0)]_{1\times w}$ of the initial probabilities of the climate-weather change process $C(t)$ staying at the particular climate-weather states c_b, $b = 1,2,\ldots,w$, at the moment $t = 0$;
- the matrix $[q_{bl}(t)]_{w\times w}$ of the probabilities of the climate-weather change process transitions between the climate-weather states c_b and c_l, $b,l = 1,2,\ldots,w$, $b \neq l$;
- the matrix $[C_{bl}(t)]_{w\times w}$ of the distribution functions of the climate-weather change process conditional sojourn times C_{bl} at the climate-weather states, $b,l = 1,2,\ldots,w$, $b \neq l$.

3 Procedure of statistical data uniformity analysis

3.1 Uniformity analysis of two realizations samples

We consider Kolmogorov-Smirnov test and Wald-Wolfowitz runs test [3] that can be used for testing whether two independent samples of realizations of the conditional sojourn times at the climate-weather states of the climate-weather change process are drawn from the population with the same distribution. We assume as in [7], that we have two independent samples of non-decreasing ordered realizations

$$C_{bl}^{1k},\ \ k = 1,2,\ldots,n_{bl}^{1},\ \text{and}\ C_{bl}^{2k},\ \ k = 1,2,\ldots,n_{bl}^{2}, \tag{1}$$

of the sojourn times C_{bl}^{1} and C_{bl}^{2}, $b,l \in \{1,2,...,w\}$, $b \neq l$, respectively composed of n_{bl}^{1} and n_{bl}^{2} realizations and we mark their empirical distribution functions by

$$C_{bl}^{1}(t) = \frac{1}{n_{bl}^{1}} \#\{k : C_{bl}^{1k} < t,\ k \in \{1,2,\ldots,n_{bl}^{1}\}\},\ \ t \geq 0, \tag{2}$$

and

$$C_{bl}^{2}(t) = \frac{1}{n_{bl}^{2}} \#\{k : C_{bl}^{2k} < t,\ k \in \{1,2,\ldots,n_{bl}^{2}\}\}.\ \ t \geq 0. \tag{3}$$

3.1.1 Kolmogorov-Smirnov test for homogeneity

The Kolmogorov-Smirnov test for two independent samples is used to check whether the maximum absolute difference between two distribution functions is significant. According to Kolmogorov-Smirnov theorem, we can use the test, if both sample sizes are large, i.e., we assume that each statistical data set contains at least 30 realizations.
The sequence of distribution functions given by the equation [7]

$$Q_{n_1 n_2}(\lambda) = P(D_{n_1 n_2} < \frac{\lambda}{\sqrt{n}}) \tag{4}$$

defined for $\lambda > 0,$ where

$$n_1 = n_{bl}^1, \;\; n_2 = n_{bl}^2, \;\; n = \frac{n_1 n_2}{n_1 + n_2}, \tag{5}$$

and

$$D_{n_1 n_2} = \max_{-\infty < t < +\infty} \left| C_{bl}^1(t) - C_{bl}^2(t) \right|, \tag{6}$$

is convergent, as $n \to \infty,$ to the limit distribution function

$$Q(\lambda) = \sum_{k=-\infty}^{+\infty} (-1)^k e^{-2k^2\lambda^2}, \;\; \lambda > 0. \tag{7}$$

The distribution function $Q(\lambda)$ given by (7) is called λ distribution and its tables of values are available.
The convergence of the sequence $Q_{n_1 n_2}(\lambda)$ to the λ distribution $Q(\lambda)$ means that for sufficiently large n_1 and n_2 we may use the following approximate formula

$$Q_{n_1 n_2}(\lambda) \cong Q(\lambda). \tag{8}$$

Hence, it follows that if we define the statistic

$$U_n = D_{n_1 n_2} \sqrt{n}, \tag{9}$$

where $D_{n_1n_2}$ is defined by (6), then by (7) and (8), we have

$$P(U_n < u) = P(D_{n_1n_2}\sqrt{n} < u) = P(D_{n_1n_2} < \frac{u}{\sqrt{n}}) = Q_{n_1n_2}(u) \cong Q(u), \text{ for } u > 0. \quad (10)$$

This result means that in order to formulate and next to verify the hypothesis that the two independent samples of the realizations of the climate-weather change process conditional sojourn times C_{bl}^1 and C_{bl}^2, $b,l \in \{1,2,...,w\}$, $b \neq l$, at the climate-weather state c_b, when the next transition is to the climate-weather state c_l, $b,l \in \{1,2,\ldots,w\}$, $b \neq l$, are coming from the population with the same distribution, it is necessary to proceed according to the following scheme:

- to fix the numbers of realizations n_{bl}^1 and n_{bl}^2 in the samples;
- to collect the realizations (1) of the conditional sojourn times C_{bl}^1 and C_{bl}^2 of the climate-weather change process in the samples;
- to find the realization of the empirical distribution functions $C_{bl}^1(t)$ and $C_{bl}^2(t)$ defined by (2) and (3) respectively, in the following forms:

$$C_{bl}^1(t) = \begin{cases} \frac{n_{bl}^{11}}{n_{bl}^1} = 0, & t \le C_{bl}^{11} \\ \frac{n_{bl}^{12}}{n_{bl}^1}, & C_{bl}^{11} < t \le C_{bl}^{12} \\ \frac{n_{bl}^{13}}{n_{bl}^1}, & C_{bl}^{12} < t \le C_{bl}^{13} \\ \cdot \ \cdot \ \cdot & \\ \frac{n_{bl}^{1k}}{n_{bl}^1}, & C_{bl}^{1k-1} < t \le C_{bl}^{1k} \\ \cdot \ \cdot \ \cdot & \\ \frac{n_{bl}^{1n_{bl}^1}}{n_{bl}^1}, & C_{bl}^{1n_{bl}^1-1} < t \le C_{bl}^{1n_{bl}^1} \\ \frac{n_{bl}^{1n_{bl}^1+1}}{n_{bl}^1} = 1, & t \ge C_{bl}^{1n_{bl}^1}, \end{cases} \qquad C_{bl}^2(t) = \begin{cases} \frac{n_{bl}^{21}}{n_{bl}^2} = 0, & t \le C_{bl}^{21} \\ \frac{n_{bl}^{22}}{n_{bl}^2}, & C_{bl}^{21} < t \le C_{bl}^{22} \\ \frac{n_{bl}^{23}}{n_{bl}^2}, & C_{bl}^{22} < t \le C_{bl}^{23} \\ \cdot \ \cdot \ \cdot & \\ \frac{n_{bl}^{2k}}{n_{bl}^2}, & C_{bl}^{2k-1} < t \le C_{bl}^{2k} \\ \cdot \ \cdot \ \cdot & \\ \frac{n_{bl}^{2n_{bl}^2}}{n_{bl}^2}, & C_{bl}^{2n_{bl}^2-1} < t \le C_{bl}^{2n_{bl}^1} \\ \frac{n_{bl}^{2n_{bl}^2+1}}{n_{bl}^2} = 1, & t \ge C_{bl}^{2n_{bl}^2}, \end{cases}$$

(11)

where

$$n_{bl}^{11} = 0\ ,\ n_{bl}^{1n_{bl}^1+1} = n_{bl}^1, \quad (12)$$

and

$$n_{bl}^{1k} = \#\{j : C_{bl}^{1j} < C_{bl}^{1k},\ j \in \{1,2,\ldots,n_{bl}^{1}\}\},\quad k = 2,3,\ldots,n_{bl}^{1}, \tag{13}$$

is the number of the sojourn time C_{bl}^{1} realizations less than its realization C_{bl}^{1k}, $k = 2,3,\ldots,n_{bl}^{1}$, and respectively

$$n_{bl}^{21} = 0,\ n_{bl}^{2\,n_{bl}^{2}+1} = n_{bl}^{2}, \tag{14}$$

and

$$n_{bl}^{2k} = \#\{j : C_{bl}^{2j} < C_{bl}^{2k},\ j \in \{1,2,\ldots,n_{bl}^{2}\}\},\ k = 2,3,\ldots,n_{bl}^{2}, \tag{15}$$

is the number of the sojourn time C_{bl}^{2} realizations less than its realization C_{bl}^{2k}, $k = 2,3,\ldots,n_{bl}^{2}$;

- to calculate the realization of the statistic u_n defined by (9) according to the formula

$$u_n = d_{n_{bl}^{1}n_{bl}^{2}}\sqrt{n},\ = \max\{\, d^{1}_{n_{bl}^{1}n_{bl}^{2}},\ d^{2}_{n_{bl}^{1}n_{bl}^{2}}\}\sqrt{n},\quad n = \frac{n_{bl}^{1}n_{bl}^{2}}{n_{bl}^{1}+n_{bl}^{2}}; \tag{16}$$

where

$$d^{1}_{n_{bl}^{1}n_{bl}^{2}} = \max\{\left|C_{bl}^{1}(C_{bl}^{1k}) - C_{bl}^{2}(C_{bl}^{1k})\right|, k \in \{1,2,\ldots,n_{bl}^{1}\}\}, \tag{17}$$

$$d^{2}_{n_{bl}^{1}n_{bl}^{2}} = \max\{\left|C_{bl}^{1}(C_{bl}^{2k}) - C_{bl}^{2}(C_{bl}^{2k})\right|, k \in \{1,2,\ldots,n_{bl}^{2}\}\}, \tag{18}$$

- to formulate the null hypothesis H_0: The samples of realizations (1) are coming from the populations with the same distributions. In the case when the null hypothesis H_0 is not rejected we may join the statistical data from the considered two separate sets into one new set of data.

3.1.1 Wald–Wolfowitz runs test for homogeneity

The Wald–Wolfowitz test utilizes a runs approach to examine the similarity between two statistical data sets in the case, when one or both samples contain more than 4 and less than 30 realisations [3].

We consider two separate sets of independent random variables of the sojourn times C_{bl}^1 and C_{bl}^2, $b,l \in \{1,2,\ldots,w\}$, $b \neq l$, coming from two different experiments, respectively composed of n_{bl}^1 and n_{bl}^2 realizations [3]. A run of a sequence is a non-empty segment of the sequence consisting of adjacently ranked realisations. Assuming the continuous probability distributions of the sojourn times C_{bl}^1 and C_{bl}^2 given by (11), a unique ordering is always possible, since the ties do not exist [3].

We define the test statistics U_n as the total number of runs in the combined ordered arrangement of n_{bl}^1 realisations of the climate-weather change process conditional sojourn time C_{bl}^1 and n_{bl}^2 realisations of the climate-weather change process conditional sojourn time C_{bl}^2.

If $n_{bl}^1 \geq 20$ and $n_{bl}^2 \geq 20$, then the distribution of U_n can be approximated to normal distribution with the mean $\frac{2n_{bl}^1 n_{bl}^2}{n_{bl}} + 1$ and variance $\frac{2n_{bl}^1 n_{bl}^2 (2n_{bl}^1 n_{bl}^2 - n_{bl})}{(n_{bl})^2 (n_{bl} - 1)}$ and then the test statistic is defined as follows:

$$U_n = \frac{r_{n_{bl}^1, n_{bl}^2} - \left(\frac{2n_{bl}^1 n_{bl}^2}{n_{bl}} + 1 \right) - \frac{1}{2}}{\sqrt{\frac{2n_{bl}^1 n_{bl}^2 (2n_{bl}^1 n_{bl}^2 - n_{bl})}{(n_{bl})^2 (n_{bl} - 1)}}}, \tag{19}$$

where $r_{n_{bl}^1, n_{bl}^2}$ is the total number of runs in the combined ordered arrangement, n_{bl}^1 and n_{bl}^2 are the numbers of realisations in the samples and n_{bl} is the total number of runs in the combined ascending ordered arrangement, i.e. $n_{bl} = n_{bl}^1 + n_{bl}^2$.

In order to formulate and next to verify the hypothesis that the two independent samples of the realizations of the climate-weather change process conditional sojourn times C_{bl}^1 and C_{bl}^2, $b,l \in \{1,2,\ldots,w\}$, $b \neq l$, at the climate-weather state c_b when the next transition is to the climate-weather state c_l are coming from the population with the same distribution, it is necessary to proceed according to the following scheme:

- to fix the numbers of realizations n_{bl}^1 and n_{bl}^2 in the samples,
- to collect the realizations (11) of the conditional sojourn times C_{bl}^1 and C_{bl}^2 of the climate-weather change process in the samples,

- to combine two samples of realisations into a single ascending ordered sequence, keeping track of which realisations correspond to the conditional sojourn time C_{bl}^1 and which to the conditional sojourn time C_{bl}^2,

- if both samples contain different realisations, rank the combined sample realisations and compute the number $r_{n_{bl}^1, n_{bl}^2}$ of runs,

- if the same value occur in both samples, arrange the realisations twice: first, to yield the fewest runs and again to yield the most runs, rank both combined sample realisations and compute the number $r_{n_{bl}^1, n_{bl}^2}$ of runs as an average of the most and the fewest runs,

- to calculate the realization of the statistic $u_n = r_{n_{bl}^1, n_{bl}^2}$,

- to formulate the null hypothesis H_0: The samples of realizations (11) are coming from the populations with the same distributions. To verify the hypothesis, we use the tables of standard normal distribution values, if $n_{bl}^1 \geq 20$ and $n_{bl}^2 \geq 20$ or we use the tables of critical values for the Runs Test, if $n_{bl}^1 \geq 4$, $n_{bl}^2 \geq 4$ and $n_{bl}^1 < 20$ or $n_{bl}^2 < 20$. In the case when the null hypothesis H_0 is not rejected, we may join the statistical data from the considered two separate sets into one new set of data.

3.2 Uniformity analysis of data from two and more different measurement points

Using Kolmogorov-Smirnov test or Wald-Wolfowitz runs test, we check the homogeneity of each pair of samples containing at least 4 realisations. Otherwise, because of the lack of sufficient numbers of realizations of the climate-weather change process conditional sojourn times at the climate-weather states, it is not possible to identify statistically their distributions and perform the procedure of statistical data uniformity analysis. Thus, if there are no other sets of statistical data from two different measurement points or one of the samples contains less than 4 realisations, we assume the distributions' homogeneity and we can join the corresponding sojourn times realisations from the considered measurement points into new sets of data.

To perform the procedure for three different measurement points containing the independent realisations samples, we consider the new joined data sets coming from the two successful uniformity tested measurement points and the data sets coming from the third measurement point. In the case when the all possible null hypotheses for all the climate-weather change process conditional sojourn times realisations are not rejected, we may join the corresponding statistical data sets into new sets of data. If there are more different measurement points, we repeat the steps presented above.

4 Climate-weather change process realisations uniformity testing for maritime ferry operating area

The empirical data sets during Februaries of the years 1988-1993 at the four different measurement points at Baltic Sea open waters (Figure 1) were collected [2].

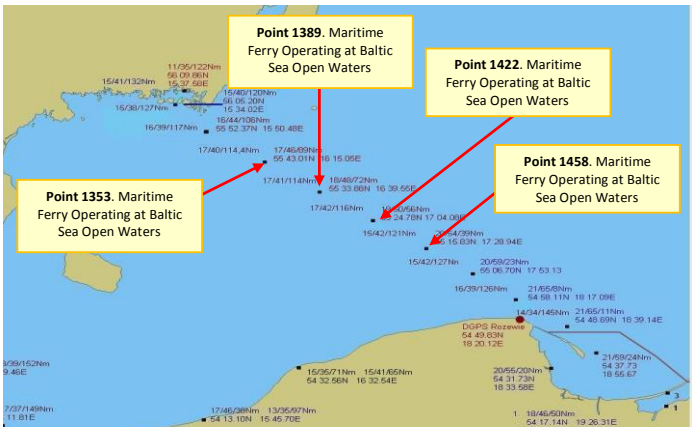

Fig. 1. Maritime ferry operating area between Karlskrona and Gdynia ports

The procedure of statistical data sets uniformity testing will be applied to the empirical realizations of sojourn times at climate-weather states coming from realizations of a maritime ferry climate-weather change process collected in four different measurement points.

The statistical data for the conditional sojourn times C_{bl} at the climate-weather states c_b when the next climate-weather state is c_l, $b,l \in \{1,2,...,8\}$, $b \neq l$, are as follows:

- <u>point 1353</u>

- the realizations C_{12}: 6, 6, 15, 6, 21, 15, 123, 117, 93, 69, 45, 21, 93, 81, 57, 33, 9, 51, 48, 24, 15, 3, 30, 27, 3, 96, 90, 15, 84, 69, 45, 21, 9, 30, 15, 21, 3, 69, 51, 27, 3, 45, 27, 3, 261, 48, 27, 3, 3, 33, 9, 6, 3, 165, 141, 117, 93, 69, 45, 21, 6, 6, 3, 78, 54, 30, 6, 45, 30, 6, 6, 18, 12, 81, 72, 48, 24, 69, 51, 27, 3, 30, 15, 51, 27, 3, 42, 24, 69, 63, 12, 24, 21, 66, 63, 39, 15, 45, 39, 15, 57, 48, 24, 9, 6, 114, 105, 81, 57, 33, 9, 12, 144, 129, 105, 81, 57, 48, 24, 264, 258, 234, 210, 186, 162, 138, 114, 90, 66, 42, 18, 42, 21, 30, 18, 15, 12, 57, 54, 30, 6, 498, 483, 459, 435, 411;
- the realizations C_{15}: 6, 6;
- the realizations C_{21}: 75, 57, 33, 9, 24, 15, 39, 18, 51, 42, 18, 15, 12, 12, 12, 42, 21, 15, 9, 15, 9, 39, 36, 12, 30, 27, 3, 12, 9, 57, 54, 30, 6, 3, 3, 3, 3, 12, 6, 36, 24, 33, 18, 24, 21, 30, 27, 3, 6, 12, 3, 18, 60, 42, 18, 3, 30, 6, 6, 33, 24, 51, 30, 6, 18, 9, 48, 45, 21, 27, 18, 24, 15, 36, 12, 12, 9, 24, 15, 3, 18, 9, 9, 9, 3, 15, 12, 3, 9, 3;
- the realizations C_{25}: 15, 27, 3, 36, 18, 9, 6, 15, 9, 21, 12, 6, 15, 12, 27, 18, 9, 3, 15, 3, 3, 9, 51, 27, 3;

- the realizations C_{52}: 6, 3, 3, 27, 21, 36, 18, 9, 12, 9, 6, 9, 3, 9, 3, 3, 3, 12, 3, 6, 30, 24, 6;
- the realizations C_{56}: 9, 9, 9;
- the realizations C_{62}: 6;
- the realizations C_{65}: 24, 24, 15;

- point 1389
- the realizations C_{12}: 6, 9, 18, 6, 21, 15, 129, 117, 93, 69, 45, 21, 93, 81, 57, 33, 9, 78, 75, 51, 27, 3, 30, 27, 3, 99, 93, 9, 84, 69, 45, 21, 9, 27, 15, 93, 75, 51, 27, 3, 45, 27, 3, 261, 45, 24, 3, 6, 33, 9, 6, 6, 165, 141, 117, 93, 69, 45, 21, 6, 6, 3, 126, 102, 78, 54, 30, 6, 9, 105, 96, 72, 48, 24, 63, 48, 24, 24, 12, 51, 27, 3, 12, 21, 18, 162, 159, 12, 18, 15, 33, 12, 45, 39, 15, 51, 45, 21, 3, 3, 114, 105, 81, 57, 33, 9, 9, 141, 129, 105, 81, 57, 48, 24, 261, 258, 234, 210, 186, 162, 138, 114, 90, 66, 42, 18, 39, 18, 15, 3, 9, 12, 42, 18, 6, 3, 498, 483, 459, 435, 411;
- the realizations C_{15}: 6;
- the realizations C_{21}: 75, 57, 33, 9, 18, 12, 39, 18, 45, 36, 12, 15, 12, 12, 42, 21, 15, 12, 15, 9, 42, 39, 15, 18, 3, 15, 12, 57, 54, 30, 6, 3, 3, 3, 15, 6, 36, 24, 33, 18, 24, 18, 30, 27, 3, 6, 12, 18, 54, 39, 15, 21, 9, 12, 36, 24, 36, 30, 6, 3, 27, 21, 12, 54, 48, 24, 12, 3, 30, 18, 27, 18, 42, 39, 15, 18, 12, 24, 15, 6, 21, 12, 12, 9, 3, 18, 12, 6, 6, 12, 3, 6;
- the realizations C_{25}: 15, 30, 27, 3, 36, 18, 9, 6, 6, 18, 12, 3, 24, 15, 3, 6, 45, 42, 18, 9, 15, 3, 3, 3, 3, 12, 12, 51, 27, 3;
- the realizations C_{52}: 6, 3, 3, 27, 21, 36, 18, 3, 9, 3, 3, 6, 3, 9, 9, 3, 9, 12, 3, 6, 3, 3, 3, 6, 6;
- the realizations C_{56}: 12, 3, 6, 12, 9, 12, 9;
- the realizations C_{62}: 3;
- the realizations C_{65}: 6, 9, 24, 15, 9.

- point 1422
- the realizations C_{12}: 6, 9, 21, 6, 21, 15, 132, 120, 96, 72, 48, 24, 93, 81, 57, 33, 9, 78, 75, 51, 27, 3, 33, 30, 6, 99, 96, 9, 84, 69, 45, 21, 9, 27, 15, 459, 441, 417, 393, 369, 345, 321, 45, 24, 3, 33, 9, 6, 6, 168, 165, 141, 117, 93, 69, 45, 21, 9, 6, 3, 123, 99, 75, 51, 27, 3, 6, 63, 54, 30, 6, 39, 24, 63, 48, 24, 21, 12, 51, 27, 3, 9, 15, 183, 180, 12, 15, 6, 30, 12, 45, 39, 15, 51, 45, 21, 3, 114, 105, 81, 57, 33, 9, 12, 138, 129, 105, 81, 57, 48, 24, 261, 258, 234, 210, 186, 162, 138, 114, 90, 66, 42, 18, 42, 21, 15, 3, 9, 12, 39, 18, 6, 3, 498, 483, 459, 435, 411;
- the realizations C_{15}: 3, 6;
- the realizations C_{21}: 75, 57, 33, 9, 15, 9, 42, 18, 45, 36, 12, 12, 12, 42, 21, 15, 12, 15, 9, 42, 39, 15, 21, 6, 15, 12, 57, 54, 30, 6, 3, 15, 6, 36, 24, 33, 18, 24, 15, 27, 24, 6, 12, 21, 57, 39, 15, 3, 21, 9, 15, 36, 24, 36, 30, 6, 9, 30, 21, 15, 3, 60, 54, 30, 6, 18, 6, 30, 18, 27, 18, 63, 60, 36, 12, 24, 15, 6, 21, 15, 12, 9, 3, 15, 12, 6, 6, 15, 3, 3, 6;

- the realizations C_{25}: 15, 30, 27, 3, 39, 21, 9, 6, 6, 24, 18, 24, 15, 6, 45, 42, 18, 9, 3, 15, 3, 3, 3, 9, 12, 54, 30, 6;
- the realizations C_{52}: 3, 3, 12, 36, 18, 3, 9, 3, 6, 6, 6, 9, 3, 3, 3, 3, 3, 6, 3, 3;
- the realizations C_{56}: 9, 6, 9, 9, 9, 12, 9, 9, 6;
- the realizations C_{62}: 6, 3;
- the realizations C_{65}: 3, 27, 3, 30, 21, 15;

- point 1458
- the realizations C_{12}: 9, 48, 33, 9, 30, 15, 132, 120, 96, 72, 48, 24, 93, 81, 57, 33, 9, 75, 51, 27, 3, 36, 30, 6, 138, 135, 12, 84, 69, 45, 21, 9, 3, 30, 18, 462, 444, 420, 396, 372, 348, 324, 48, 24, 6, 33, 9, 9, 3, 6, 171, 165, 141, 117, 93, 69, 45, 21, 3, 12, 6, 3, 123, 99, 75, 51, 27, 3, 6, 63, 54, 30, 6, 39, 24, 63, 48, 24, 21, 12, 57, 51, 27, 3, 12, 15, 201, 12, 18, 6, 30, 12, 45, 39, 15, 54, 48, 24, 6, 18, 12, 90, 81, 57, 33, 9, 9, 138, 129, 105, 81, 57, 48, 24, 264, 261, 237, 213, 189, 165, 141, 117, 93, 69, 45, 21, 42, 21, 18, 3, 12, 15, 39, 18, 507, 483, 459, 435, 411;
- the realizations C_{14}: 6;
- the realizations C_{21}: 72, 57, 33, 9, 48, 33, 9, 45, 36, 12, 12, 15, 39, 18, 15, 12, 15, 9, 42, 39, 15, 21, 6, 15, 12, 60, 54, 30, 6, 15, 3, 36, 24, 33, 18, 21, 12, 36, 33, 9, 27, 24, 6, 9, 21, 57, 39, 15, 3, 21, 9, 15, 30, 18, 36, 30, 6, 6, 33, 24, 15, 3, 57, 54, 30, 6, 18, 6, 30, 18, 27, 18, 60, 36, 12, 24, 18, 3, 9, 21, 15, 69, 45, 21, 6, 3, 12, 9, 6, 3, 12, 3, 6;
- the realizations C_{25}: 69, 45, 21, 9, 6, 6, 3, 24, 18, 21, 15, 6, 6, 12, 12, 3, 3, 3, 12, 12;
- the realizations C_{32}: 3;
- the realizations C_{45}: 3;
- the realizations C_{52}: 3, 15, 3, 6, 3, 3, 3, 3, 3, 3, 3, 3;
- the realizations C_{53}: 9, 3;
- the realizations C_{56}: 6, 3, 12, 6, 9, 9, 9, 6;
- the realizations C_{62}: 6, 48, 39, 15, 18;
- the realizations C_{65}: 15, 9, 3, 33, 30, 6.

4.1 Uniformity testing for two measurement points

We verify the hypotheses that the conditional sojourn times C_{bl}, $b,l \in \{1,2,...,8\}$, $b \neq l$, realizations of the maritime ferry climate-weather change process at the climate-weather states for the points 1353 and 1389 are from the populations with the same distribution. We use the two-sample λ test for the conditional sojourn times C_{12} and C_{21} realisations (n_{12}^1 = 146, n_{12}^2 = 141, n_{21}^1 = 90, n_{21}^2 = 92) and the Wald–Wolfowitz runs test for the conditional sojourn times C_{25}, and C_{52} realisations (n_{25}^1 = 25, n_{25}^2 = 30, n_{52}^1 = 23, n_{52}^2 = 25). To illustrate the application of the procedure of testing the data uniformity described in

section 3, we perform it for the conditional sojourn time C_{21}. The conditional sojourn times C_{21}^1 and C_{21}^2 have the empirical distribution functions

$$C_{21}^1(t)=\begin{cases}0, & t\le 3,\\ 12/90, & 3<t\le 6,\\ 18/90, & 6<t\le 9,\\ 28/90, & 9<t\le 12,\\ 38/90, & 12<t\le 15,\\ 45/90, & 15<t\le 18,\\ 53/90, & 18<t\le 21,\\ 56/90, & 21<t\le 24,\\ 62/90, & 24<t\le 27,\\ 65/90, & 27<t\le 30,\\ 70/90, & 30<t\le 33,\\ 73/90, & 33<t\le 36,\\ 76/90, & 36<t\le 39,\\ 78/90, & 39<t\le 42,\\ 81/90, & 42<t\le 45,\\ 82/90, & 45<t\le 48,\\ 83/90, & 48<t\le 51,\\ 85/90, & 51<t\le 54,\\ 86/90, & 54<t\le 57,\\ 88/90, & 57<t\le 60,\\ 89/90, & 60<t\le 75,\\ 90/90, & t>75;\end{cases}\qquad C_{21}^2(t)=\begin{cases}0, & t\le 3,\\ 9/92, & 3<t\le 6,\\ 17/92, & 6<t\le 9,\\ 21/92, & 9<t\le 12,\\ 36/92, & 12<t\le 15,\\ 45/92, & 15<t\le 18,\\ 55/92, & 18<t\le 21,\\ 59/92, & 21<t\le 24,\\ 64/92, & 24<t\le 27,\\ 67/92, & 27<t\le 30,\\ 71/92, & 30<t\le 33,\\ 73/92, & 33<t\le 36,\\ 77/92, & 36<t\le 39,\\ 81/92, & 39<t\le 42,\\ 84/92, & 42<t\le 45,\\ 85/92, & 45<t\le 48,\\ 86/92, & 48<t\le 51,\\ 89/92, & 51<t\le 54,\\ 91/92, & 54<t\le 57,\\ 92/92, & 57<t\le 60,\\ 0, & 60<t\le 75,\\ 9/92, & t>75.\end{cases} \tag{20}$$

The null hypothesis H_0: The samples of conditional sojourn times C_{21}^1 and C_{21}^2 realizations are coming from the population with the same distribution. To verify this hypothesis we will apply the two-sample λ test at the significance level $\alpha=0.05$. Using the above empirical distributions (20), we form a common Table 1 composed of all their values. In Table 1, the values t_k are joint together all realizations C_{21}^{1k}, $k=1,2,\ldots,n_{21}^1$, and C_{21}^{2k}, $k=1,2,\ldots,n_{21}^2$, of the conditional sojourn times C_{21}^1 and C_{21}^2, i.e. they are all discontinuity points of the empirical distribution function $C_{21}^1(t)$ and $C_{21}^2(t)$ were they have jumps in their values $C_{21}^1(t_k)$ and $C_{21}^2(t_k)$.

Next, according to (16) and from Table 1, we get

$$d_{9092} = \max_{t_k} \left| C_{21}^{1}(t_k) - C_{21}^{2}(t_k) \right| \cong 0.083,$$

$$n_{21} = \frac{90 \cdot 92}{90 + 92} \cong 45.49 .$$

Table 1. Joint empirical distribution function

$t_k = C_{21}^{1k} \vee C_{21}^{2k}$	$C_{21}^{1}(t_k)$	$C_{21}^{2}(t_k)$	$\lvert C_{21}^{1}(t_k) - C_{21}^{2}(t_k) \rvert$
3	0	0	0
6	12/90	9/92	0.036
9	18/90	17/92	0.015
12	28/90	21/92	**0.083**
15	38/90	36/92	0.031
18	45/90	45/92	0.011
21	53/90	55/92	0.009
24	56/90	59/92	0.019
27	62/90	64/92	0.007
30	65/90	67/92	0.006
33	70/90	71/92	0.006
36	73/90	73/92	0.018
39	76/90	77/92	0.007
42	78/90	81/92	0.014
45	81/90	84/92	0.013
48	82/90	85/92	0.013
51	83/90	86/92	0.013
54	85/90	86/92	0.01
57	86/90	89/92	0.012
60	88/90	91/92	0.011
75	89/90	91/92	0
>75	90/90	92/92	0

Thus, the realization u_n of the statistics (9) is

$$u_n = d_{9092}\sqrt{n_{21}} = 0.083\sqrt{45.49} \cong 0.560.$$

From the table of the λ distribution for the significance level $\alpha = 0.05$, we get the critical value $\lambda_0 = u \cong 1.442$. Since $u_n \cong 0.560 < u = 1.442$, then we do not reject the null hypothesis H_0.

After proceeding in an analogous way with data in the remaining climate-weather states we can obtain the same conclusions that the data sets composed of the conditional sojourn times C_{12}^{1} and C_{12}^{2} realizations are from the

populations with the identical distributions. To verify the hypotheses for the conditional sojourn times C_{25}, and C_{52} realisations, we use the Wald–Wolfowitz runs test, described in section 3. Unless the numbers of realisations in the samples are greater than 20, the distribution of U_n can be approximated to normal distribution, according to (19).
It is not possible to verify the uniformity hypothesis for the conditional sojourn times C_{15}, C_{56}, C_{62} and C_{65} realizations because of the lack of sufficient numbers of those realizations.
In the case when the all possible null hypotheses for all the climate-weather change process conditional sojourn times realisations are not rejected, we may join the corresponding statistical data sets into new sets of data. Finally, we obtain that for the points 1353 and 1389 the each considered pair of the conditional sojourn times realizations at the climate-weather states are from the populations with the same distribution.

4.2 Uniformity testing for three measurement points

We verify the hypotheses that the conditional sojourn times C_{bl}, $b,l \in \{1,2,...,8\}$, $b \neq l$, realizations of the maritime ferry climate weather change process at the climate-weather states for the joined samples (points 1353 and 1389) and the point 1422 are from the populations with the same distribution. We use the Kolmogorov-Smirnov test for the conditional sojourn times C_{12} and C_{21} realisations ($n_{12}^1 = 287$, $n_{12}^2 = 138$, $n_{21}^1 = 182$, $n_{21}^2 = 91$) and the Wald–Wolfowitz runs test for the conditional sojourn times C_{25}, C_{52}, C_{56} and C_{65} realisations ($n_{25}^1 = 55$, $n_{25}^2 = 28$, $n_{52}^1 = 48$, $n_{52}^2 = 20$, $n_{56}^1 = 10$, $n_{56}^2 = 9$, $n_{65}^1 = 8$, $n_{65}^2 = 6$), according to the procedure described in section 3. The remaining conditional sojourn times at the particular climate-weather states have less than 4 realisations, thus, we cannot verify the hypotheses.
In the case when the all possible null hypotheses for all the climate-weather change process conditional sojourn times realisations are not rejected, we may join the corresponding statistical data sets into new sets of data. Finally, we obtain that for the joined samples (points 1353 and 1389) and the point 1422 the each considered pair of the conditional sojourn times realizations at the climate-weather states are from the populations with the same distribution.

4.3 Uniformity testing for four measurement points

We verify the hypotheses that the conditional sojourn times C_{bl}, $b,l \in \{1,2,...,8\}$, $b \neq l$, realizations of the maritime ferry at the climate-weather states for the joined samples (points 1353, 1389 and 1422) and the point 1458 are from the populations with the same distribution. We use the Kolmogorov-Smirnov test for the conditional sojourn times C_{12} and C_{21} realisations ($n_{12}^1 = 425$, $n_{12}^2 = 139$, $n_{21}^1 = 273$, $n_{21}^2 = 93$) and the Wald–Wolfowitz runs test for the conditional

sojourn times C_{25}, C_{52}, C_{56} and C_{65} realisations (n^1_{25} = 83, n^2_{25} = 20, n^1_{52} = 68, n^2_{52} = 12, n^1_{56} = 19, n^2_{56} = 8, n^1_{62} = 4, n^2_{62} = 5, n^1_{65} = 14, n^2_{65} = 6), according to the procedure described in section 3. The remaining conditional sojourn times at the particular climate-weather states have less than 4 realisations, thus, we cannot verify the hypotheses.

In the case when the all possible null hypotheses for all the climate-weather change process conditional sojourn times realisations are not rejected, we may join the corresponding statistical data sets into new sets of data. Finally, we obtain that for the joined samples (points 1353, 1389 and 1422) and the point 1458 the each considered pair of the conditional sojourn times realizations at the climate-weather states are from the populations with the same distribution.

Conclusions

The procedure of the uniformity testing of statistical data coming from different sets of realizations of the same climate-weather change process before joining them into one common set of data was practically applied for four different measurement points of the maritime ferry operating area. The results of this application to the climate-weather change process' empirical data uniformity testing justifies the proposed procedures practical importance in everyday practice. Considering the new joined data sets uniformly tested, we may improve the accuracy of the climate-weather change processes identification and prediction.

Acknowledgments

The paper presents the results developed in the scope of the EU-CIRCLE project titled “A pan – European framework for strengthening Critical Infrastructure resilience to climate change” that has received funding from the European Union’s Horizon 2020 research and innovation programme under grant agreement No 653824. *http://www.eu-circle.eu/*.

References

1. V. Barbu and N. Limnios, Empirical estimation for discrete-time semi-Markov processes with applications in reliability. Journal of Nonparametric Statistics, 18, 7-8, 483{498, 2006.
2. EU-CIRCLE Report D2.1-GMU3, Modelling Climate-Weather Change Process Including Extreme Weather Hazards, 2016.
3. EU-CIRCLE ReportD6.4-GMU1-12, Identification Methods and Procedures of Climate-Weather Change Process Including Extreme Weather Hazards, 2017.
4. F. Ferreira and A. Pacheco. Comparison of level-crossing times for Markov and semi-Markov processes. Stat & Probab Lett vol. 77, 2, 151{157, 2007.
5. F. Grabski. Semi-Markov Processes: Applications in System Reliability and Maintenance, 1st Edition, Elsevier Science & Technology, 2014.
6. K. Kołowrocki. Reliability of Large and Complex Systems. Elsevier, 2014.

7. K. Kołowrocki and J. Soszyńska-Budny. Complex system operation process realizations uniformity testing. 16th ASMDA Conference Proceedings, Applied Stochastic Models and Data Analysis 2015, Pireus, Greece, 2015.
8. K. Kołowrocki and J. Soszyńska-Budny. Reliability and Safety of Complex Technical Systems and Processes: Modeling-Identification-Prediction-Optimization. Springer, 2011.
9. N. Limnios and G. Oprisan. Semi-Markov Processes and Reliability. Birkhauser, Boston, 2005.

Identification and prediction of climate-weather change processes for port oil piping transportation system and maritime ferry operation areas after their realisations successful uniformity testing

Ewa Kuligowska[1] and Mateusz Torbicki[2]

[1] Gdynia Maritime University, Gdynia, Poland
(E-mail: e.kuligowska@wn.am.gdynia.pl)
[2] Gdynia Maritime University, Gdynia, Poland
(E-mail: m.torbicki@wn.am.gdynia.pl)

Abstract. The paper is concerned with unknown climate-weather change process parameters identification after successful uniformity testing of data sets including its realisations coming from different measurement points. The data coming from points at port oil piping transportation system operating area and at the maritime ferry operating the area are under consideration. Finally, those identified climate-weather change processes are applied to their characteristics prediction.
Keywords: climate-weather change process, port oil piping transportation system, maritime ferry.

1 Introduction

The general joint model linking the critical infrastructure safety model with the model of climate-weather change process at its operating area is constructed in [1]. To apply this model practically to the evaluation and prediction of the real critical infrastructure safety it is necessary to elaborate the statistical methods concerned to determining the unknown parameters of the climate-weather change process [4-8]. In the case when the statistical data are coming from different experiments or the data sets may be collected at different, but close to each other measurement points at the critical infrastructure operating area, before the identification of parameters, the investigation of these data uniformity is necessary. The uniformity testing procedure for the climate-weather change process data including its realisations from different experiments or the data sets is presented in [7,10]. Moreover, the methods of estimating the probabilities of the initial climate-weather states, the probabilities of transitions between the climate-weather states and the distributions of the sojourn times of the climate-weather change process at the particular climate-weather states should be proposed. Fortunately, after successful uniformity testing and joining realisations of conditional sojourn times from different

17th *ASMDA Conference Proceedings, 6 - 9 June 2017, London, UK*

experiments or the data sets into new sets of data, we can apply similar methods of investigations unknown parameters from [3].

2 Theoretical Background

We assume that the climate-weather change process $C(t)$, $t \in <0,+\infty)$, is a semi-Markov process and for the critical infrastructure operating area takes w, $w \in N$, different climate-weather states $c_1, c_2, ..., c_w$. We mark by C_{bl} its random conditional sojourn times at the climate-weather states c_b, when its next climate-weather state is c_l, $b,l \in 1,2,\ldots,w$, $b \neq l$.

Under those assumptions, the climate-weather change process can be described by the following unknown parameters: the vector $[q_b(0)]_{1\times w}$ of probabilities of the climate-weather change process staying at the particular climate-weather states at the initial moment $t = 0$, the matrix $[q_{bl}(t)]_{w\times w}$ of the probabilities of the climate-weather change process transitions between the climate-weather states and the matrix $[C_{bl}(t)]_{w\times w}$ of the distribution functions of the conditional sojourn times C_{bl} of the climate-weather change process at the climate-weather states, $b,l = 1,2,\ldots,w$, $b \neq l$.

Moreover, we assume that the statistical data for estimating the above parameters of the climate-weather change process $C(t)$ is coming from κ, $\kappa \in N$, different, but located close to each other, measurement points of the critical infrastructure operating area and the uniformity testing for the realisations of conditional sojourn times C_{bl}^{i}, $i = 1,..., \kappa$, $b,l \in \{1,...,w\}$, $b \neq l$, coming from considered points, presented in [9-10], is successful.

Then, to identify the climate-weather change process $C(t)$ parameters, we have to perform the following steps:

- to join the realisations of conditional sojourn times C_{bl}^{i}, $i = 1,..., \kappa$, $b,l \in \{1,...,w\}$, $b \neq l$, from measurement points into new sets of data C_{bl};
- to evaluate vectors of the realizations $n_b^i(0)$, $i = 1,..., \kappa$, $b = 1,...,w$, of the numbers of staying of the climate-weather change process $C(t)$, respectively at the climate-weather states $c_1, c_2, ..., c_w$, at the initial moment $t = 0$ of $n^i(0)$, $i = 1,..., \kappa$, observed realizations of the climate-weather change process

$$[\, n_b^i(0) \,] = [\, n_1^i(0) \,,\, n_2^i(0) \,,\, \ldots,\, n_w^i(0) \,],\ i = 1,..., \kappa, \tag{1}$$

where

$$n_1^i(0) \ + \ n_2^i(0) + \ldots + \ n_w^i(0) \ = n^i(0),\ i = 1,..., \kappa; \tag{2}$$

- to determinate the vector of the realizations of the probabilities $q_b(0)$, $b = 1,2,...,w$, of the climate-weather change process staying at the climate-weather states $c_1, c_2, ..., c_w$, at the initial moment $t = 0$, according to the formula

$$[q_b(0)]_{1\times w} = [q_1(0), q_2(0), \ldots, q_w(0)], \tag{3}$$

where

$$q_b(0) = \frac{n_b^1(0) + \ldots + n_b^\kappa(0)}{n^1(0) + \ldots + n^\kappa(0)},\ b = 1,...,w; \tag{4}$$

- to determinate the matrix $[q_{bl}(t)]_{w\times w}$ of the probabilities of the climate-weather change process transitions between the climate-weather states and the matrix $[C_{bl}(t)]_{w\times w}$ of the distribution functions of the conditional sojourn times C_{bl} of the climate-weather change process at the climate-weather states, $b,l = 1,2,\ldots,w$, $b \neq l$, using the proposed procedures given in [3].
After that, we can predicted the limit values q_b, $b = 1,\ldots,w$, of the climate-weather change process at critical infrastructure operating area transient probabilities at the states c_b, and the mean values $\hat{N}_b$ of the climate-weather change process total sojourn times at the particular operation states during θ days.

3 Climate weather change process at port oil piping transportation system operation area

In the following subsections, we will analyze the climate-weather change process for the port oil piping transportation system operating at underwater Baltic Sea area. The statistical climate-weather data sets were collected during Februaries of the years 1988-1993 at three different measurement points [9].

3.1 Statistical identification of climate-weather change process for piping operation area

To identify all parameters of the considered climate-weather change process [3] for the port oil piping transportation system area the statistical data coming from this process is needed. The joined statistical data sets are:
- the number of the climate-weather change process states $w = 6$;
- the climate-weather change process observation time $\Theta = 6$ years (1988-1993);
- the number of the climate-weather change process realizations $n(0) = 510$;
- the vectors of realizations of the numbers $n_b^i(0)$, $i = 1,..., 3$, $b = 1,...,6$, of the climate-weather change process staying at the climate-weather states c_b at the initial moment $t = 0$

$[\, n_b^1(0)\,]_{1\times 6} = [120, 40, 1, 0, 4, 5]$;

$[\, n_b^2(0)\,]_{1\times 6} = [124, 36, 1, 0, 6, 3]$;

$$[\, n_b^3(0)\,]_{1\times 6} = [122, 39, 0, 0, 8, 1]; \tag{5}$$

- the matrix of realizations n_{bl} of the numbers of the climate-weather change process $C(t)$ transitions from the state c_b into the state c_l during the observation time $\Theta = 6$ years

$$[n_{bl}]_{6\times 6} = \begin{bmatrix} 0 & 466 & 0 & 0 & 7 & 0 \\ 205 & 0 & 0 & 1 & 43 & 0 \\ 0 & 9 & 0 & 0 & 0 & 2 \\ 0 & 0 & 0 & 0 & 1 & 0 \\ 1 & 32 & 4 & 0 & 0 & 12 \\ 0 & 2 & 14 & 0 & 4 & 0 \end{bmatrix}; \tag{6}$$

- the vector of realizations of the total numbers of the climate-weather change process transitions from the climate-weather state c_b during the observation time $\Theta = 6$ years

$$[n_b]_{6\times 1} = [473, 249, 11, 1, 49, 20]^{\mathrm{T}}. \tag{7}$$

On the basis of the above statistical data it is possible to evaluate
- after applying (3)-(4) and using (5), the vector of realizations

$$[q_b(0)] = [0.718, 0.225, 0.004, 0, 0.035, 0.018], \tag{8}$$

of the initial probabilities $q_b(0)$, $b = 1,2,\ldots,6$, of the climate-weather change process transitions at the climate-weather states c_b at the moment $t = 0$
- the matrix of realizations

$$[q_{bl}] = \begin{bmatrix} 0 & 0.99 & 0 & 0 & 0.01 & 0 \\ 0.83 & 0 & 0 & 0 & 0.17 & 0 \\ 0 & 0.82 & 0 & 0 & 0 & 0.18 \\ 0 & 0 & 0 & 0 & 1 & 0 \\ 0.02 & 0.66 & 0.08 & 0 & 0 & 0.24 \\ 0 & 0.1 & 0.7 & 0 & 0.2 & 0 \end{bmatrix}. \tag{9}$$

of the transition probabilities q_{bl}, $b,l = 1,2,\ldots,6$, of the climate-weather change process $C(t)$ from the climate-weather state c_b into the climate-weather state c_l.
The statistical data allow that applying the same methods as in [3], we may verify the hypotheses about the conditional distribution functions $C_{bl}(t)$ of the climate-weather change process sojourn times C_{12}, C_{15}, C_{21}, C_{24}, C_{25}, C_{32}, C_{36}, C_{45}, C_{51}, C_{52}, C_{53}, C_{56}, C_{62}, C_{63}, C_{65}, on the base of their joint realizations. For

instance, the conditional sojourn time C_{25} has an exponential distribution with the density function

$$c_{25}(t) = 0.067 \exp[-0.067t], \text{ for } t > 0, \tag{10}$$

the conditional sojourn time C_{52} has a chimney distribution with the density function

$$c_{52}(t) = \begin{cases} 0.875, & 0 \le t < 15.6 \\ 0.125, & 15.6 \le t < 46.8. \end{cases} \tag{11}$$

Next for the verified distributions, the matrix of the mean values $N_{bl} = E[C_{bl}]$, $b,l = 1,2,\ldots,6$, $b \neq l$, of the system operation process $C(t)$ conditional sojourn times at the climate-weather states can be determined:

$$[N_{bl}] = \begin{bmatrix} 0 & 255.35 & 0 & 0 & 12.86 & 0 \\ 21.51 & 0 & 0 & 3 & 14.93 & 0 \\ 0 & 3.67 & 0 & 0 & 0 & 6 \\ 0 & 0 & 0 & 0 & 3 & 0 \\ 3 & 10.72 & 6 & 0 & 0 & 10 \\ 0 & 6 & 14.57 & 0 & 7.5 & 0 \end{bmatrix}. \tag{12}$$

3.2 Prediction of climate-weather change process for piping operation area

After applying (5.11) from [2] and the results (8), (12), the unconditional mean sojourn times of the climate-weather change process at the particular climate-weather states are given in the matrix:

$$[N_b] = [252.93, 20.39, 4.09, 3, 10.02, 12.3] \tag{13}$$

Considering (8) in the system of equations (5.13) from [2], we get its following solution

$$\pi_1 \cong 0.391, \pi_2 \cong 0.469, \pi_3 \cong 0.025, \pi_4 \cong 0, \pi_5 \cong 0.089, \pi_6 \cong 0.026. \tag{14}$$

Hence and from (13), after applying (5.12) form [2], it follows that the limit values of the climate-weather change process transient probabilities at the climate-weather states c_b, $b = 1,2,\ldots,6$, are:

$$q_1 = 0.901, q_2 = 0.087, q_3 = 0.001, q_4 = 0, q_5 = 0.008, q_6 = 0.003. \tag{15}$$

The expected values of the total sojourn times of the climate-weather change process $C(t)$ at the particular climate-weather states c_b, $b = 1,2,\ldots,6$, during the fixed operation time $C = 1$ month (February) = 29 days, are given in the vector (its coordinates are measured in days):

$$[\hat{N}_b]_{1x6} = [E[\hat{C}_b]]_{1x6} \cong [26.129, 2.523, 0.029, 0, 0.232, 0.087]. \quad (16)$$

4 Climate weather change process for maritime ferry operation area

In the following subsections, we will analyze the climate-weather change process for the maritime ferry technical system operating at Baltic Sea open waters area. The statistical climate-weather data sets were collected during Februaries of the years 1988-1993 at four different measurement points [10].

4.1 Statistical identification of climate-weather change process for maritime ferry operation area

To identify all parameters of the considered climate-weather change process [3] for the port oil piping transportation system area the statistical data coming from this process is needed. The joined statistical data sets are:
- the number of the climate-weather change process states $w = 6$;
- the climate-weather change process observation time $\Theta = 6$ years (1988-1993);
- the number of the climate-weather change process realizations $n(0) = 680$;
- the vectors of realizations of the numbers $n_b^i(0)$, $i = 1,\ldots, 4$, $b = 1,\ldots,6$, of the climate-weather change process staying at the climate-weather states c_b at the initial moment $t = 0$

$$[\, n_b^1(0)\,]_{1\times 6} = [103, 57, 0, 0, 8, 2];$$
$$[\, n_b^2(0)\,]_{1\times 6} = [101, 59, 0, 0, 9, 1];$$
$$[\, n_b^3(0)\,]_{1\times 6} = [99, 62, 0, 0, 6, 3];$$
$$[\, n_b^4(0)\,]_{1\times 6} = [102, 59, 0, 0, 4, 5]; \quad (17)$$

- the matrix of realizations n_{bl} of the numbers of the climate-weather change process $C(t)$ transitions from the state c_b into the state c_l during the observation time $\Theta = 6$ years

$$[n_{bl}]_{6\times 6} = \begin{bmatrix} 0 & 564 & 0 & 1 & 5 & 0 \\ 366 & 0 & 0 & 0 & 103 & 0 \\ 0 & 1 & 0 & 0 & 0 & 0 \\ 0 & 0 & 0 & 0 & 1 & 0 \\ 0 & 80 & 2 & 0 & 0 & 27 \\ 0 & 9 & 0 & 0 & 20 & 0 \end{bmatrix}; \tag{18}$$

- the vector of realizations of the total numbers of the climate-weather change process transitions from the climate-weather state c_b during the observation time $\Theta = 6$ years

$$[n_b]_{6\times 1} = [570, 469, 1, 1, 109, 29]^{T}. \tag{19}$$

On the basis of the above statistical data it is possible to evaluate
- after applying (3)-(4) and using (17), the vector of realizations

$$[q_b(0)] = [0.595, 0.349, 0, 0, 0.04, 0.016], \tag{20}$$

of the initial probabilities $q_b(0)$, $b = 1,2,\ldots,6$, of the climate-weather change process transitions at the climate-weather states c_b at the moment $t = 0$
- the matrix of realizations

$$[q_{bl}] = \begin{bmatrix} 0 & 0.99 & 0 & 0 & 0.01 & 0 \\ 0.78 & 0 & 0 & 0 & 0.22 & 0 \\ 0 & 1 & 0 & 0 & 0 & 0 \\ 0 & 0 & 0 & 0 & 1 & 0 \\ 0 & 0.73 & 0.02 & 0 & 0 & 0.25 \\ 0 & 0.31 & 0 & 0 & 0.69 & 0 \end{bmatrix} \tag{21}$$

of the transition probabilities q_{bl}, $b,l = 1,2,\ldots,6$, of the climate-weather change process $C(t)$ from the climate-weather state c_b into the climate-weather state c_l.
The statistical data allow that applying the same methods as in [3], we may verify the hypotheses about the conditional distribution functions $C_{bl}(t)$ of the climate-weather change process sojourn times C_{12}, C_{14}, C_{15}, C_{21}, C_{25}, C_{32}, C_{45}, C_{52}, C_{53}, C_{56}, C_{62}, C_{65}, on the base of their joint realizations. For instance, the conditional sojourn time C_{15} has an empirical distribution function

$$C_{15}(t) = \begin{cases} 0, & t \le 3 \\ 0.2, & 3 < t \le 6 \\ 1, & t > 6. \end{cases} \tag{22}$$

the conditional sojourn time C_{25} has a gamma distribution with the density function

$$c_{25}(t) = 0.039t^{0.357} \cdot \exp(-0.085\,t),\ t \geq 0. \tag{23}$$

Next for the verified distributions, the matrix of the mean values $N_{bl} = E[C_{bl}]$, $b,l = 1,2,\ldots,6,\ b \neq l,$ of the system operation process $C(t)$ conditional sojourn times at the climate-weather states can be determined:

$$[N_{bl}] = \begin{bmatrix} 0 & 151.53 & 0 & 6 & 5.4 & 0 \\ 30.56 & 0 & 0 & 0 & 16.02 & 0 \\ 0 & 3 & 0 & 0 & 0 & 0 \\ 0 & 0 & 0 & 0 & 3 & 0 \\ 0 & 9.01 & 6 & 0 & 0 & 8.44 \\ 0 & 16 & 0 & 0 & 16.05 & 0 \end{bmatrix}. \tag{24}$$

4.2 Prediction of climate-weather change process for maritime ferry operation area

After applying (5.11) from [2] and the results (21), (24), the unconditional mean sojourn times of the climate-weather change process at the particular climate-weather states are given in the matrix:

$$[N_b] = [150.07,\ 27.36,\ 3,\ 3,\ 8.81,\ 16.03] \tag{25}$$

Considering (21) in the system of equations (5.13) from [2], we get its following solution

$$\pi_1 \cong 0.366,\ \pi_2 \cong 0.47,\ \pi_3 \cong 0.003,\ \pi_4 \cong 0,\ \pi_5 \cong 0.129,\ \pi_6 \cong 0.032. \tag{26}$$

Hence and from (25), after applying (5.12) from [2], it follows that the limit values of the climate-weather change process transient probabilities at the climate-weather states c_b, $b = 1,2,\ldots,6$, are:

$$q_1 = 0.792,\ q_2 = 0.185,\ q_3 = 0,\ q_4 = 0,\ q_5 = 0.016,\ q_6 = 0.007. \tag{27}$$

The expected values of the total sojourn times of the climate-weather change process $C(t)$ at the particular climate-weather states c_b, $b = 1,2,\ldots,6$, during the fixed operation time C = 1 month (February) = 29 days, are given in the vector (its coordinates are measured in days):

$$[\hat{N}_b]_{1x6} = [E[\hat{C}_b]]_{1x6} \cong [22.968,\ 5.365,\ 0,\ 0,\ 0.464,\ 0.203]. \tag{28}$$

Conclusions

The statistical identification methods of the unknown parameters of the climate-weather change process was practically applied for the statistical climate-weather data coming from different measurement points after their realisations successful uniformity testing at the port oil piping transportation system operating area and at the maritime ferry operating area.
The results allow us for further practical applications in evaluation real complex critical infrastructures safety. After using this approach, the climate-weather change process at the fixed area is better described.

Acknowledgments

The paper presents the results developed in the scope of the EU-CIRCLE project titled "A pan – European framework for strengthening Critical Infrastructure resilience to climate change" that has received funding from the European Union's Horizon 2020 research and innovation programme under grant agreement No 653824. *http://www.eu-circle.eu/*.

References

1. EU-CIRCLE ReportD3.3-GMU3, Integrated Model Of Critical Infrastructure Safety (IMCIS) Related To Climate-Weather Change Process Including Extreme Weather Hazards (EWH) – Model 3, 2017.
2. EU-CIRCLE ReportD3.3-GMU3-C-WCP-MODEL-V1.0, Critical Infrastructure Operating Area Climate-Weather Change Process (C-WCP) Including Extreme Weather Hazards (EWH) - C-WCP Model, 2017.
3. EU-CIRCLE ReportD6.4-GMU1-12-Part0, Identification Methods And Procedures Of Climate-Weather Change Process Including Extreme Weather Hazards - Part 0 - Theoretical Backgrounds, 2017.
4. EU-CIRCLE ReportD6.4-GMU1-12, Identification Methods and Procedures of Climate-Weather Change Process Including Extreme Weather Hazards, 2017.
5. F. Ferreira and A. Pacheco. Comparison of level-crossing times for Markov and semi-Markov processes. Stat & Probab Lett vol. 77, 2, 151-157, 2007.
6. F. Grabski. Semi-Markov Processes: Applications in System Reliability and Maintenance, 1st Edition, Elsevier Science & Technology, 2014.
7. K. Kołowrocki. Reliability of Large and Complex Systems. Elsevier, 2014.
8. K. Kołowrocki and J. Soszyńska-Budny. Complex system operation process realizations uniformity testing. 16th ASMDA Conference Proceedings, Applied Stochastic Models and Data Analysis 2015, Pireus, Greece, 2015.
9. K. Kołowrocki and J. Soszyńska-Budny. Reliability and Safety of Complex Technical Systems and Processes: Modeling-Identification-Prediction-Optimization. Springer, 2011.
10. E. Kuligowska and M. Torbicki. Climate-weather change process realizations uniformity testing for port oil piping transportation system operating area. 17th ASMDA Conference Proceedings, Applied Stochastic Models and Data Analysis 2017, London, United Kingdom, 2017.

11. E. Kuligowska and M. Torbicki. Climate-weather change process realizations uniformity testing for maritime ferry operating area. 17th ASMDA Conference Proceedings, Applied Stochastic Models and Data Analysis 2017, London, United Kingdom, 2017.

Climate-weather change process realizations uniformity testing for port oil piping transportation system operating area

Ewa Kuligowska[1] and Mateusz Torbicki[2]

[1] Gdynia Maritime University, Gdynia, Poland
(E-mail: e.kuligowska@wn.am.gdynia.pl)
[2] Gdynia Maritime University, Gdynia, Poland
(E-mail: m.torbicki@wn.am.gdynia.pl)

Abstract. The paper is concerned with a method for statistical data uniformity testing applied to the realizations of the climate-weather change process empirical conditional sojourn times coming from different measurement points for port oil piping transportation system operating under Baltic Sea waters area. The collected empirical data sets during Februaries of the years 1988-1993 at the three different measurement points are under consideration. Assuming that the statistical data sets are separate, the verification of the non-parametric hypotheses on the basis of Kolmogorov-Smirnov test and Wald-Wolfowitz runs test is prepared. In the case when the null hypothesis about the uniformity data sets for two measurement points is not rejected, corresponding to each other statistical data sets of realisations are joined. After using this approach, the climate-weather change process at the fixed area is better described.
Keywords: climate-weather change process, uniformity testing, port oil piping transportation system.

1 Introduction

The model of the climate-weather change processes is proposed in [2]. The statistical data for estimating the unknown parameters of the climate-weather change process very often come from different experiments of the same climate-weather change process and are collected into separate data sets. Furthermore, these data sets may be collected at different measurement points of the critical infrastructure operating area with some of the points located close to each other. Thus, before the climate-weather change process identification, the investigation of these empirical data uniformity is necessary. In this paper, the uniformity test is applied to the data sets including climate-weather change process realisations coming from three measurement points at port oil piping transportation system operating area.

17th *ASMDA Conference Proceedings, 6 - 9 June 2017, London, UK*

2 Modeling of climate-weather change process

The climate-weather change process for port oil piping transportation system operating under Baltic Sea waters area is modeled in [2]. It is taking 6 different climate-weather states c_1, c_2, ..., c_6, and is marked by process $C(t)$, $t \in \langle 0,+\infty)$, taking discrete values in the set $\{c_1, c_2, ..., c_6\}$ of the climate-weather states. We assume a semi-Markov model [1, 4-10] of the climate-weather change process $C(t)$ and we mark by C_{bl} its random conditional sojourn times at the climate-weather states c_b, when its next climate-weather state is c_l, $b,l \in 1,2,\ldots,6$, $b \neq l$. Under these assumptions, the climate-weather change process may be described by the vector $[q_b(0)]_{1\times 6}$ of probabilities of the climate-weather change process staying at the particular climate-weather states at the initial moment $t = 0$, the matrix $[q_{bl}(t)]_{6\times 6}$ of the probabilities of the climate-weather change process transitions between the climate-weather states and the matrix $[C_{bl}(t)]_{6\times 6}$ of the distribution functions of the conditional sojourn times C_{bl} of the climate-weather change process at the climate-weather states, $b,l = 1,2,\ldots, 6$, $b \neq l$.

3 Climate-weather change process realisations uniformity testing for port oil piping transportation system operating area

The empirical data sets during Februaries of the years 1988-1993 at the three different measurement points at under water Baltic Sea area (Figure 1) were collected [2].

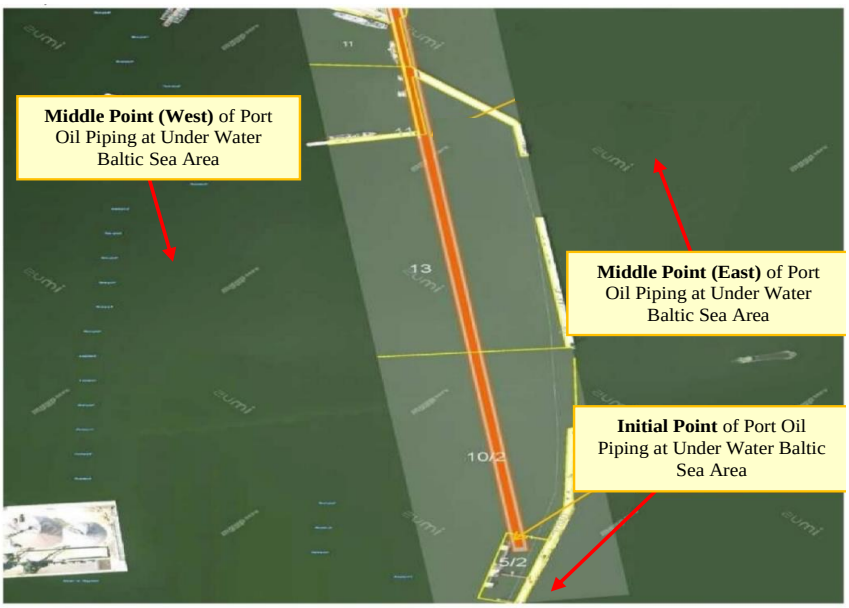

Fig. 1. The port oil piping transportation system alignment in the Gdynia Port

The procedure of statistical data sets uniformity testing will be applied to the empirical realizations of sojourn times at climate-weather states coming from realizations of a port oil piping transportation system climate-weather change process collected in three different measurement points.

The statistical data for the conditional sojourn times C_{bl} at the climate-weather states c_b when the next climate-weather state is c_l, $b,l \in \{1,2,...,6\}$, $b \neq l$, are as follows:

- initial point

- the realizations C_{12}: 60, 36, 12, 60, 42, 18, 336, 324, 300, 276, 252, 228, 204, 180, 156, 132, 108, 84, 60, 36, 12, 84, 81, 57, 33, 9, 486, 477, 453, 429, 24, 12, 81, 69, 45, 21, 18, 6, 6, 3, 6, 45, 33, 9, 3, 474, 456, 432, 408, 384, 360, 336, 54, 30, 6, 36, 33, 9, 225, 219, 195, 171, 147, 123, 99, 75, 51, 27, 3, 6, 18, 15, 9, 6, 192, 168, 144, 120, 96, 72, 48, 24, 114, 96, 72, 48, 24, 60, 48, 24, 18, 12, 63, 54, 30, 6, 15, 12, 495, 15, 24, 3, 33, 18, 51, 45, 21, 63, 54, 30, 6, 9, 12, 39, 21, 84, 60, 36, 12, 18, 6, 153, 138, 114, 90, 66, 54, 30, 6, 6, 6, 345, 342, 318, 294, 270, 246, 222, 198, 174, 150, 126, 102, 78, 54, 30, 6, 33, 21, 594, 576, 552, 528, 504, 480, 456;
- the realizations C_{15}: 21, 9;
- the realizations C_{21}: 18, 6, 18, 12, 9, 30, 15, 12, 33, 12, 39, 36, 12, 3, 6, 6, 42, 36, 12, 24, 9, 42, 30, 6, 6, 33, 21, 33, 18, 30, 9, 36, 21, 3, 6, 6, 15, 12, 18, 27, 15, 48, 30, 6, 3, 36, 24, 9, 57, 33, 9, 21, 9, 24, 18, 18, 15, 27, 9, 15, 9, 9, 6, 3, 6, 3, 3, 12, 3, 36, 21, 6, 9, 6;
- the realizations C_{25}: 60, 48, 24, 9, 6, 6, 3, 6, 3, 9, 3, 6, 3, 12;
- the realizations C_{32}: 3, 3, 3, 6, 6, 3;
- the realizations C_{36}: 3, 9;
- the realizations C_{52}: 3, 3, 3, 6, 3;
- the realizations C_{53}: 3, 12, 6, 3;
- the realizations C_{56}: 6, 9, 9, 6, 9, 6;
- the realizations C_{62}: 3;
- the realizations C_{63}: 3, 30, 6, 30, 24, 3, 21, 3;
- the realizations C_{65}: 3, 6;

- west point

- the realizations C_{12}: 15, 27, 15, 51, 36, 12, 81, 66, 42, 18, 249, 228, 204, 180, 156, 132, 108, 84, 60, 36, 12, 156, 153, 129, 105, 81, 57, 33, 9, 441, 432, 42, 18, 84, 72, 48, 24, 3, 24, 12, 6, 6, 30, 21, 6, 480, 459, 435, 411, 387, 363, 339, 54, 30, 6, 12, 39, 33, 9, 12, 6, 207, 195, 171, 147, 123, 99, 75, 51, 27, 3, 6, 24, 18, 312, 288, 264, 240, 216, 192, 168, 144, 120, 96, 72, 48, 24, 60, 51, 27, 3, 108, 105, 81, 57, 33, 9, 30, 12, 501, 51, 27, 3, 3, 33, 21, 57, 48, 24, 69, 60, 36, 12, 6, 15, 42, 21, 87, 63, 39, 15, 174, 162, 138, 114, 90, 66, 87, 63, 39, 15, 9, 3, 990, 987, 963, 939, 915, 891, 867, 843, 819, 795, 771, 747, 723, 699, 675, 651, 627, 603, 579, 555, 531, 507, 483, 459;
- the realizations C_{15}: 6;

- the realizations C_{21}: 21, 12, 18, 9, 21, 9, 9, 3, 9, 6, 33, 12, 3, 30, 12, 6, 6, 45, 39, 15, 36, 33, 9, 36, 27, 3, 6, 3, 27, 18, 36, 18, 6, 30, 9, 36, 18, 15, 18, 15, 18, 45, 30, 6, 36, 24, 54, 33, 9, 24, 12, 18, 15, 15, 24, 12, 15, 9, 3, 3, 6, 3, 18;
- the realizations C_{25}: 54, 48, 24, 3, 21, 15, 3, 6, 9, 6, 30, 12, 6, 6, 9;
- the realizations C_{32}: 3, 3, 3;
- the realizations C_{52}: 9, 6, 12, 3, 3, 6, 6, 6, 3;
- the realizations C_{56}: 24, 15, 9, 6, 12;
- the realizations C_{62}: 9;
- the realizations C_{63}: 12, 3, 27, 24, 15, 3;

- <u>east point</u>
- the realizations C_{12}: 60, 36, 12, 60, 42, 18, 339, 324, 300, 276, 252, 228, 204, 180, 156, 132, 108, 84, 60, 36, 12, 84, 81, 57, 33, 9, 486, 477, 453, 429, 33, 15, 90, 75, 51, 27, 3, 6, 6, 45, 33, 9, 6, 477, 456, 432, 408, 384, 360, 336, 51, 27, 3, 42, 36, 12, 225, 219, 195, 171, 147, 123, 99, 75, 51, 27, 3, 9, 21, 15, 9, 6, 177, 153, 129, 105, 81, 57, 33, 9, 114, 96, 72, 48, 24, 63, 48, 24, 33, 24, 72, 54, 30, 6, 30, 12, 495, 15, 21, 9, 33, 18, 57, 45, 21, 66, 54, 30, 6, 9, 15, 126, 108, 84, 60, 36, 12, 174, 159, 135, 111, 87, 63, 54, 30, 6, 6, 9, 6, 384, 378, 354, 330, 306, 282, 258, 234, 210, 186, 162, 138, 114, 90, 66, 42, 18, 597, 579, 555, 531, 507, 483, 459;
- the realizations C_{15}: 18, 6, 21, 9;
- the realizations C_{21}: 18, 6, 15, 9, 9, 30, 15, 6, 30, 9, 33, 12, 15, 6, 42, 36, 12, 21, 6, 39, 27, 3, 9, 30, 18, 33, 18, 27, 6, 39, 18, 9, 9, 21, 6, 18, 9, 15, 6, 48, 30, 6, 36, 24, 9, 57, 54, 30, 6, 18, 9, 18, 12, 15, 12, 27, 9, 12, 6, 9, 6, 9, 3, 9, 9, 18, 12, 6;
- the realizations C_{24}: 3;
- the realizations C_{25}: 57, 48, 24, 3, 12, 6, 6, 3, 3, 3, 9, 3, 3, 12;
- the realizations C_{45}: 3;
- the realizations C_{51}: 3;
- the realizations C_{52}: 9, 6, 3, 12, 3, 3, 3, 42, 33, 9, 9, 3, 12, 18, 3, 9, 12, 24;
- the realizations C_{56}: 9;
- the realizations C_{65}: 12, 9.

Using Kolmogorov-Smirnov test or Wald-Wolfowitz runs test, we check the homogeneity of each pair of samples containing at least 4 realisations. Otherwise, because of the lack of sufficient numbers of realizations of the climate-weather change process conditional sojourn times at the climate-weather states, it is not possible to identify statistically their distributions and perform the procedure of statistical data uniformity analysis. Thus, if there are no other sets of statistical data from two different measurement points or one of the samples contains less than 4 realisations, we assume the distributions' homogeneity and we can join the corresponding sojourn times realisations from the considered measurement points into new sets of data.

3.1 Uniformity testing for two measurement points

We verify the hypotheses that the conditional sojourn times C_{bl}, $b,l \in \{1,2,...,6\}$, $b \neq l$, realizations of the port oil piping transportation system climate-weather change process at the climate-weather states for the initial point and west point are from the populations with the same distribution. We use the two-sample Kolmogorov-Smirnov test for the conditional sojourn times C_{12} and C_{21} realisations (n_{12}^1 = 156, n_{12}^2 = 157, n_{21}^1 = 74, n_{21}^2 = 63) and the Wald–Wolfowitz runs test for the conditional sojourn times C_{25}, C_{52}, C_{56} and C_{63} realisations (n_{25}^1 = 14, n_{25}^2 = 15, n_{52}^1 = 5, n_{52}^2 = 9, n_{56}^1 = 6, n_{56}^2 = 5, n_{63}^1 = 8, n_{63}^2 = 6). To illustrate the application of the procedure of testing the data uniformity described in [8], we perform it for the conditional sojourn time C_{25}. The sorted conditional sojourn times C_{25}^1 and C_{25}^2 realisations are given as follows:

- the realizations C_{25}^1: **3**, **3**, **3**, **3**, **6**, **6**, **6**, **6**, **9**, **9**, **12**, **24**, **48**, **60**;
- the realizations C_{25}^2: 3, 3, 6, 6, 6, 6, 9, 9, 12, 15, 21, 24, 30, 48, 54.

The null hypothesis H_0 is formulated as follows: the samples of conditional sojourn times C_{25}^1 and C_{25}^2 realizations are coming from the population with the same distribution. To verify this hypothesis we will apply the Wald–Wolfowitz runs test at the significance level $\alpha = 0.05$.

We mark by *a* the realisations which correspond to the conditional sojourn time C_{25}^1 and we mark by *b* the realisations which correspond to the conditional sojourn time C_{25}^2. Further, we have to combine two samples of realisations into a single ascending ordered sequence. There is more than one the same realisation occurring in both samples (i.e. 3, 6, 9, 12, 24, 48), thus, we arrange and rank the combined sample realisations to yield the fewest runs

3, 3, **3**, 3, **3**, **3**, **6**, 6, **6**, 6, **6**, 6, **6**, 6, **9**, **9**, 9, **9**, **12**, 12, 15, 21, 24, **24**, 30, 48, **48**, 54, **60**,
a b a b aaa b a b a b a bb a b aa bbbb a bb a b a

and again to yield the most runs

3, 3, **3**, 3, **3**, **3**, **6**, 6, **6**, 6, **6**, 6, **6**, 6, **9**, **9**, 9, **9**, 12, **12**, 15, 21, **24**, 24, 30, **48**, 48, 54, **60.**
a b a b aa b a b a b a b a b a b a b a bb a bb a bb a

Then we compute the number of runs for each combined sample

<u>*a*</u>, <u>*b*</u>, <u>*a*</u>, <u>*b*</u>, <u>*a, a, a*</u>, <u>*b*</u>, <u>*a*</u>, <u>*b*</u>, <u>*a*</u>, <u>*b*</u>, <u>*a*</u>, <u>*b, b*</u>, <u>*a*</u>, <u>*b*</u>, <u>*a, a*</u>, <u>*b, b, b, b*</u>, <u>*a*</u>, <u>*b, b*</u>, <u>*a*</u>, <u>*b*</u>, <u>*a*</u>
r_1 r_2 r_3 r_4 r_5 r_6 r_7 r_8 r_9 r_{10} r_{11} r_{12} r_{13} r_{14} r_{15} r_{16} r_{17} r_{18} r_{19} r_{20} r_{21}

<u>*a*</u>, <u>*b*</u>, <u>*a*</u>, <u>*b*</u>, <u>*a, a*</u>, <u>*b*</u>, <u>*a*</u>, <u>*b*</u>, <u>*a*</u>, <u>*b*</u>, <u>*a*</u>, <u>*b*</u>, <u>*a*</u>, <u>*b*</u>, <u>*a*</u>, <u>*b*</u>, <u>*a*</u>, <u>*b*</u>, <u>*a*</u>, <u>*b, b*</u>, <u>*a*</u>, <u>*b, b*</u>, <u>*a*</u>

r_1 r_2 r_3 r_4 r_5 r_6 r_7 r_8 r_9 r_{10} r_{11} r_{12} r_{13} r_{14} r_{15} r_{16} r_{17} r_{18} r_{19} r_{20} r_{21} r_{22} r_{23}

and the number of runs is an average of the most and the fewest runs

$$\bar{n}_{14,15} = \frac{21+25}{2} = 23.$$

From the tables of critical values for the runs test, the get the value $r_\alpha = u = 11$. Since $u_n = 23 > u = 11$, then we do not reject the null hypothesis H_0.

After proceeding in an analogous way with data in the remaining climate-weather states we can obtain the same conclusions that the data sets composed of the corresponding pairs of conditional sojourn times C_{52}, C_{56} and C_{63} realizations are from the populations with the identical distributions. To verify the hypotheses for the conditional sojourn times C_{12}, and C_{21} realisations, we use the Kolmogorov-Smirnov test, described in [8, 9].

It is not possible to verify the uniformity hypothesis for the conditional sojourn times C_{15}, C_{32}, C_{36}, C_{53}, C_{62}, and C_{65} realizations because of the lack of sufficient numbers of those realizations.

Finally, we obtain that for the initial point and the west point the each considered pair of the conditional sojourn times realizations at the climate-weather states are from the populations with the same distribution.

3.2 Uniformity testing for three measurement points

To perform the procedure for three different measurement points containing the independent realisations samples, we consider the new joined statistical data sets for the conditional sojourn times C_{bl} at the climate-weather states c_b when the next climate-weather state is c_l, $b,l \in \{1,2,...,6\}$, $b \neq l$, from section 3.1 and the data sets coming from the third measurement point.

The new joined statistical data sets are as follows:

- the realizations C_{12}: 60, 36, 12, 60, 42, 18, 336, 324, 300, 276, 252, 228, 204, 180, 156, 132, 108, 84, 60, 36, 12, 84, 81, 57, 33, 9, 486, 477, 453, 429, 24, 12, 81, 69, 45, 21, 18, 6, 6, 3, 6, 45, 33, 9, 3, 474, 456, 432, 408, 384, 360, 336, 54, 30, 6, 36, 33, 9, 225, 219, 195, 171, 147, 123, 99, 75, 51, 27, 3, 6, 18, 15, 9, 6, 192, 168, 144, 120, 96, 72, 48, 24, 114, 96, 72, 48, 24, 60, 48, 24, 18, 12, 63, 54, 30, 6, 15, 12, 495, 15, 24, 3, 33, 18, 51, 45, 21, 63, 54, 30, 6, 9, 12, 39, 21, 84, 60, 36, 12, 18, 6, 153, 138, 114, 90, 66, 54, 30, 6, 6, 6, 345, 342, 318, 294, 270, 246, 222, 198, 174, 150, 126, 102, 78, 54, 30, 6, 33, 21, 594, 576, 552, 528, 504, 480, 456, 15, 27, 15, 51, 36, 12, 81, 66, 42, 18, 249, 228, 204, 180, 156, 132, 108, 84, 60, 36, 12, 156, 153, 129, 105, 81, 57, 33, 9, 441, 432, 42, 18, 84, 72, 48, 24, 3, 24, 12, 6, 6, 30, 21, 6, 480, 459, 435, 411, 387, 363, 339, 54, 30, 6, 12, 39, 33, 9, 12, 6, 207, 195, 171, 147, 123, 99, 75, 51, 27, 3, 6, 24, 18, 312, 288, 264, 240, 216, 192, 168, 144, 120, 96, 72, 48, 24, 60, 51, 27, 3, 108, 105, 81, 57, 33, 9, 30, 12, 501, 51, 27, 3, 3, 33, 21, 57, 48, 24, 69, 60, 36, 12, 6, 15, 42, 21, 87, 63, 39, 15, 174, 162, 138, 114, 90, 66, 87,

63, 39, 15, 9, 3, 990, 987, 963, 939, 915, 891, 867, 843, 819, 795, 771, 747, 723, 699, 675, 651, 627, 603, 579, 555, 531, 507, 483, 459;

- the realizations C_{15}: 21, 9, 6;
- the realizations C_{21}: 18, 6, 18, 12, 9, 30, 15, 12, 33, 12, 39, 36, 12, 3, 6, 6, 42, 36, 12, 24, 9, 42, 30, 6, 6, 33, 21, 33, 18, 30, 9, 36, 21, 3, 6, 6, 15, 12, 18, 27, 15, 48, 30, 6, 3, 36, 24, 9, 57, 33, 9, 21, 9, 24, 18, 18, 15, 27, 9, 15, 9, 9, 6, 3, 6, 3, 3, 12, 3, 36, 21, 6, 9, 6, 21, 12, 18, 9, 21, 9, 9, 3, 9, 6, 33, 12, 3, 30, 12, 6, 6, 45, 39, 15, 36, 33, 9, 36, 27, 3, 6, 3, 27, 18, 36, 18, 6, 30, 9, 36, 18, 15, 18, 15, 18, 45, 30, 6, 36, 24, 54, 33, 9, 24, 12, 18, 15, 15, 24, 12, 15, 9, 3, 3, 6, 3, 18;
- the realizations C_{25}: 60, 48, 24, 9, 6, 6, 3, 6, 3, 9, 3, 6, 3, 12, 54, 48, 24, 3, 21, 15, 3, 6, 9, 6, 30, 12, 6, 6, 9;
- the realizations C_{32}: 3, 3, 3, 6, 6, 3, 3, 3, 3;
- the realizations C_{36}: 3, 9, 9, 6, 12, 3, 3, 6, 6, 6, 3;
- the realizations C_{52}: 3, 3, 3, 6, 3;
- the realizations C_{53}: 3, 12, 6, 3;
- the realizations C_{56}: 6, 9, 9, 6, 9, 6, 24, 15, 9, 6, 12;
- the realizations C_{62}: 3, 9;
- the realizations C_{63}: 3, 30, 6, 30, 24, 3, 21, 3, 12, 3, 27, 24, 15, 3;
- the realizations C_{65}: 3, 6;

We verify the hypotheses that the conditional sojourn times C_{bl}, $b,l \in \{1,2,...,6\}$, $b \neq l$, realizations of the port oil piping transportation system climate weather change process at the climate-weather states for the joined samples (initial point and west point) and the east point are from the populations with the same distribution. We use the Kolmogorov-Smirnov test for the conditional sojourn times C_{12} and C_{21} realisations ($n_{12}^1 = 313$, $n_{12}^2 = 153$, $n_{21}^1 = 137$, $n_{21}^2 = 68$) and the Wald–Wolfowitz runs test for the conditional sojourn times C_{25} and C_{52} realisations ($n_{25}^1 = 29$, $n_{25}^2 = 14$, $n_{52}^1 = 14$, $n_{52}^2 = 18$), according to the procedure described in [8, 9]. The remaining conditional sojourn times at the particular climate-weather states have less than 4 realisations, thus, we cannot verify the hypotheses.

The new sorted data sets containing conditional sojourn times C_{25}^1 (initial point and west point) and the data sets containing conditional sojourn times C_{25}^2 realisations (east point) are given as follows:

- the realizations C_{25}^1: **3**, **3**, **3**, **3**, **3**, **3**, **6**, **6**, **6**, **6**, **6**, **6**, **6**, **9**, **9**, **9**, **9**, **12**, **12**, **15**, **21**, **24**, **24**, **30**, **48**, **48**, **54**, **60**;
- the realizations C_{25}^2: 3, 3, 3, 3, 3, 3, 6, 6, 9, 12, 12, 24, 48, 57.

The null hypothesis H_0 is formulated as follows: the samples of conditional sojourn times C_{25}^1 and C_{25}^2 realizations are coming from the population with

the same distribution. To verify this hypothesis we will apply the Wald–Wolfowitz runs test at the significance level $\alpha = 0.05$.

We mark by *a* the realisations which correspond to the conditional sojourn time C_{25}^1 and we mark by *b* the realisations which correspond to the conditional sojourn time C_{25}^2. Further, we have to combine two new samples of realisations into a single ascending ordered sequence. There is more than one the same realisation occurring in both samples (i.e. 3, 6, 9, 12, 24, 48), thus, we arrange and rank the combined sample realisations to yield the fewest runs

3, 3, **3**, 3, **3**, 3, **3**, 3, **3**, 3, **3**, 3, **6**, 6, **6**, **6**, **6**, **6**, **6**, **6**, **6**, **9**, 9, **9**, **9**, **9**, **12**, 12, **12**, 12,
a b a b a b a b a b a bb a b aaaaaaaa b aaaa b a b

15, **21**, **24**, 24, **24**, **30**, **48**, 48, **48**, **54**, 57, **60**,
aaa b aaa b aa b a

and again to yield the most runs

3, 3, **3**, 3, **3**, 3, **3**, 3, **3**, 3, **3**, 3, **6**, 6, **6**, 6, **6**, **6**, **6**, **6**, **6**, 9, **9**, **9**, **9**, **9**, 12, **12**, 12,
a b a b a b a b a b a b a b a b aaaaaa b aaaa b a b

12, **15**, **21**, 24, **24**, **24**, **30**, 48, **48**, **48**, **54**, 57, **60**.
aaa b aaa b aaa b a

Then we compute the number of runs for each combined sample

$\underline{a}, \underline{b}, \underline{a}, \underline{b}, \underline{a}, \underline{b}, \underline{a}, \underline{b}, \underline{a}, \underline{b}, \underline{a}, \underline{b, b}, \underline{a}, \underline{b}, \underline{a, a, a, a, a, a, a, a}, \underline{b}, \underline{a, a, a, a}, \underline{b}, \underline{a}, \underline{b},$
$r_1\ r_2\ r_3\ r_4\ r_5\ r_6\ r_7\ r_8\ r_9\ r_{10}\ r_{11}\ r_{12}\ r_{13}\ r_{14}\ r_{15}\ r_{16}\ r_{17}\ r_{18}\ r_{19}\ r_{20}$

$\underline{a, a, a}, \underline{b}, \underline{a, a, a}, \underline{b}, \underline{a}, \underline{a}, \underline{b}, \underline{a},$
$r_{21}\ r_{22}\ r_{23}\ r_{24}\ r_{25}\ r_{26}\ r_{27}$

and

$\underline{a}, \underline{b}, \underline{a}, \underline{b}, \underline{a}, \underline{b}, \underline{a}, \underline{b}, \underline{a}, \underline{b}, \underline{a}, \underline{b}, \underline{a}, \underline{b}, \underline{a}, \underline{b}, \underline{a, a, a, a, a, a}, \underline{b}, \underline{a, a, a, a}, \underline{b}, \underline{a}, \underline{b},$
$r_1\ r_2\ r_3\ r_4\ r_5\ r_6\ r_7\ r_8\ r_9\ r_{10}\ r_{11}\ r_{12}\ r_{13}\ r_{14}\ r_{15}\ r_{16}\ r_{17}\ r_{18}\ r_{19}\ r_{20}\ r_{21}\ r_{22}$

$\underline{a, a, a}, \underline{b}, \underline{a, a, a}, \underline{b}, \underline{a, a, a}, \underline{b}, \underline{b}, \underline{a}.$
$r_{23}\ r_{24}\ r_{25}\ r_{26}\ r_{27}\ r_{28}\ r_{29}$

The number of runs is an average of the most and the fewest runs

$$\bar{r}_{29,14} = \frac{27+29}{2} = 28.$$

From the tables of critical values for the runs test, the get the value $r_\alpha = u = 11$. Since $u_n = 28 > u = 15$, then we do not reject the null hypothesis H_0.

If the numbers of realisations in the samples n_{bl}^1 and n_{bl}^2 are greater or equal to 20, then, according to [9], the distribution of U_n can be approximated to normal distribution with the mean $\frac{2n_{bl}^1 n_{bl}^2}{n_{bl}}+1$ and variance $\frac{2n_{bl}^1 n_{bl}^2(2n_{bl}^1 n_{bl}^2 - n_{bl})}{(n_{bl})^2(n_{bl}-1)}$.
However, that choice for a boundary is a rule of thumb. Thus, to make the procedure familiar to the reader, we perform it for the conditional sojourn time C_{25}.
We compute the total number of runs in the combined ascending ordered arrangement

$$n_{25} = n_{25}^1 + n_{25}^2 = 29 + 14 = 43,$$

the mean and the variance of the approximate normal distribution

$$m = \frac{2n_{25}^1 n_{25}^2}{n_{25}}+1 = \frac{2\cdot 29\cdot 14}{43}+1 \cong 19.884$$

$$s^2 = \frac{2n_{25}^1 n_{25}^2(2n_{25}^1 n_{25}^2 - n_{25})}{(n_{25})^2(n_{25}-1)} .= \frac{2\cdot 29\cdot 14(2\cdot 29\cdot 14-43)}{43^2(43-1)} \cong 8.041.$$

Thus, the realisation of the statistic U_n is given as follows

$$u_n = \frac{r_{n_{25}^1, n_{25}^2} - m - \frac{1}{2}}{\sqrt{s^2}} = \frac{28-19.884-\frac{1}{2}}{\sqrt{8.041}} \cong 2.686. \qquad (19)$$

From the tables of standard normal distribution, the get the critical value $u = -1.645$. Since $u_n = 2.686 > u = -1.645$, then we do not reject the null hypothesis H_0.
In the case when the all possible null hypotheses for all the climate-weather change process conditional sojourn times realisations are not rejected, we may join the corresponding statistical data sets into new sets of data.
Finally, we obtain that for the joined samples (initial point and west point) and the east point, the each considered pair of the conditional sojourn times realizations at the climate-weather states are from the populations with the same distribution.

Conclusions

The procedure of the uniformity testing of statistical data coming from different sets of realizations of the same climate-weather change process before joining them into one common set of data was practically applied for three different measurement points of the port oil piping transportation system operating area. The results of this application to the climate-weather change process' empirical

data uniformity testing justifies the proposed procedures practical importance in everyday practice. Considering the new joined data sets uniformly tested, we may improve the accuracy of the climate-weather change processes identification and prediction.

Acknowledgments

The paper presents the results developed in the scope of the EU-CIRCLE project titled "A pan – European framework for strengthening Critical Infrastructure resilience to climate change" that has received funding from the European Union's Horizon 2020 research and innovation programme under grant agreement No 653824. *http://www.eu-circle.eu/*.

References

1. V. Barbu and N. Limnios, Empirical estimation for discrete-time semi-Markov processes with applications in reliability. Journal of Nonparametric Statistics, 18, 7-8, 483{498, 2006.
2. EU-CIRCLE Report D2.1-GMU3, Modelling Climate-Weather Change Process Including Extreme Weather Hazards, 2016.
3. EU-CIRCLE ReportD6.4-GMU1-12, Identification Methods and Procedures of Climate-Weather Change Process Including Extreme Weather Hazards, 2017.
4. F. Ferreira and A. Pacheco. Comparison of level-crossing times for Markov and semi-Markov processes. Stat & Probab Lett vol. 77, 2, 151{157, 2007.
5. F. Grabski. Semi-Markov Processes: Applications in System Reliability and Maintenance, 1st Edition, Elsevier Science & Technology, 2014.
6. K. Kołowrocki. Reliability of Large and Complex Systems. Elsevier, 2014.
7. K. Kołowrocki and J. Soszyńska-Budny. Complex system operation process realizations uniformity testing. 16th ASMDA Conference Proceedings, Applied Stochastic Models and Data Analysis 2015, Pireus, Greece, 2015.
8. K. Kołowrocki and J. Soszyńska-Budny. Reliability and Safety of Complex Technical Systems and Processes: Modeling-Identification-Prediction-Optimization. Springer, 2011.
9. E. Kuligowska and M. Torbicki. Climate-weather change process realizations uniformity testing for maritime ferry operating area. 17th ASMDA Conference Proceedings, Applied Stochastic Models and Data Analysis 2017, London, United Kingdom, 2017.
10. N. Limnios and G. Oprisan. Semi-Markov Processes and Reliability. Birkhauser, Boston, 2005.

Bilaplacian on a Riemannian Manifold and Levi-Civita Connection

Rémi Léandre

Laboratoire de Mathématiques. Université de Bourgogne-Franche-Comté. Route de Gray. 25030. Besançon. France
(E-mail: remi.leandre@univ-fcomte.fr)

Abstract. We generalize to the case of a Bilaplacian on a Riemannian manifold the classical relation in stochastic analysis between the Brownian motion on a Riemannian manifold and its horizontal lift.
Keywords: Horizontal lift. Bilaplacian.

1 Introduction

It is classical in stochastic analysis that the horizontal lift of a diffusion is useful in order to construct canonically the Brownian motion on a Riemannian manifold ([1], [2]). We extend in this note this classical relation on the Brownian motion and the (degenerated) process associated to the horizontal Laplacian to the case of a Bilaplacian. See [7] in the subelliptic case.

We consider a compact Riemannian oriented manifold M endowed with its normalized Riemannian measure dx. x is the generic element of M which is of dimension m. We consider the special orthonormal frame bundle $SO(M)$ endowed with the Levi-Civita connection with canonical projection π on M. u is the generic element of $SO(M)$. We consider the canonical vector fields X_i on $SO(M)$ and the associated horizontal Laplacian

$$L = \sum_{i=1}^{m} X_i^2 \tag{1}$$

Δ is the Laplace-Beltrami operator on M and Δ^2 the associated Bilaplacian. The Bilaplacian is elliptic, symmetric on $L^2(dx)$ and by elliptic theory ([5], [6])generates a unique contraction semi group P_t^{Δ} on $L^2(dx)$ with generic element f: $\frac{\partial}{\partial t} P_t^{\Delta} = -\Delta^2 P_t$.

We can glue on the fiber the normalized "Haar" measures (See appendix for the details) such that we get a probability measure du on $SO(M)$. L^2 is symmetric, densely defined on $L^2(du)$ and therefore admits a self-adjoint extension which generates a contraction semi-group P_t^L on $L^2(du)$:$\frac{\partial}{\partial t} P_t^L = -L^2 P_t$.

Theorem 1. *If f is a smooth function on M, we have if $\pi u = x$*

$$P_t^{\Delta}[f](x) = P_t^L[f \circ \pi](u) \tag{2}$$

This theorem enters in our general program to extend stochastic analysis tools to the general theory of linear semi-group (See [8] and [9] for reviews).

17th *ASMDA Conference Proceedings, 6 - 9 June 2017, London, UK*

2 Proof of the theorem

If g_0 belongs to $SO(\mathbb{R}^m)$ we get clearly

$$P_t^L[f \circ \pi](ug_0) = P_t^L[f \circ \pi(.g_0)](u) = P_t^L[f \circ \pi](u) \tag{3}$$

Therefore, $u \to P_t^L[f \circ \pi](u)$ defines a function on M. This function when t is moving defines a semi-group. Namely

$$P_{t+s}^L[f \circ \pi](u) = P_t^L[P_s^L[f \circ \pi]](u) = P_t^L[P_s^L[f \circ \pi] \circ \pi](u) \tag{4}$$

where is the right-hand side $P_s^L[f \circ \pi]$ is seen as a function on M.

We are therefore in presence of two semi-groups on $L^2(dx)$. But

$$L(f \circ \pi) = (\Delta f) \circ \pi \tag{5}$$

such that

$$L^2(f \circ \pi) = (\Delta^2 f) \circ \pi \tag{6}$$

Since there is only one semi-group generated by Δ^2, the result holds.

$\diamondsuit$

Remark: It is possible to extend this theorem when we replace Δ^2 by $Q(\Delta)$ where $Q(\Delta) = \sum_{i=0}^n a_i \Delta^i$, $a_n > 0$ and L^2 by $Q(L)^2$.

3 Appendix: A brief review on Riemannian geometry

Let M be the compact oriented manifold of dimension m. It is homeomorphic locally to $\mathbb{R}^m$ and the change of charts are local diffeomrphism. When we will write the formulas in local coordinates, we won't write the change of formulas coming for a change of chart. A smooth function function on M is called f. A vector field Y is a smooth derivation acting on smooth functions:

$$X(fg) = gX(f) + fX(g) \tag{7}$$

and is linear in f. In local coordinates x_i $X = \sum_{i=0}^m a_i(x) \frac{\partial}{\partial x_i}$. Therefore X can be a smooth function of the tangent bundle $T(M)$ of$M$: each fibers $T_x(M)$ are transformed as X when we do a change of charts. A Riemannian metric can be seen as a smooth section of $T^*(M) \otimes T^*(M)$, where $T^*(M)$ is the bundle of 1-form. This section is assume definite positive. In local coordinates, we we can write

$$< ., . > (x) = \sum_{i,j} g_{i,j}(x) dx^i \otimes dx^j \tag{8}$$

From the metric, we deduce naturally a positive measure which is unique modulo a constant. It is called the Riemannian measure dx.

A connection is a map ∇ such that:

-)$\nabla_X Y$ is a smooth vector field if X and Y are smooth vector fields.

-)If X, Y_1, Y_2 are smooth vector fields

$$\nabla_X(Y_1 + Y_2) = \nabla_X Y_1 + \nabla_X Y_2 \tag{9}$$

-)If X, Y are smooth vector fields and f is a smooth function

$$\nabla_X(fY) = f\nabla_X Y + X(f)Y \tag{10}$$

-)$X \to \nabla_X Y$ is linear in X.

A connection is said to be without torsion if

$$\nabla_X Y - \nabla_Y X = [X, Y] \tag{11}$$

where $[X, Y]$ is the Lie bracket of the two vector fields X and Y (which is still a vector field).

A connection is said metric if

$$X < Y, Z >=< \nabla_X Y, Z > + < Y, \nabla_X Z > \tag{12}$$

for any vector fields X, Y, Z.

The main theorem of Riemannian geometry is that there exists a **unique** metric connection without torsion on a Riemannian manifold called the Levi-Civita connection ∇^0.

If ω is a one-form (a 1-form forn $T_x M$ which depends smoothly on x or equivalently a smooth section of the cotangent bundle $T^*(M)$), we can define its covariant derivative with respect of the connection ∇ by

$$X\omega(Y) = \omega(\nabla_X Y) + (\nabla_X \omega)(Y) \tag{13}$$

If f is a smooth function, df is a 1-form. The Laplace-Beltrami operator Δ is defined by

$$\Delta f = Tr(\nabla^0)^2 f = \sum_{i=1}^{m} \nabla_{Y_i} \nabla_{Y_i} f - \sum_{i=1}^{m} \nabla_{\nabla_{Y_i} Y_i} f \tag{14}$$

where Y_i is a local smooth orthonormal basis of the tangent bundle. The problem is that there is no **canonical** orthonormal basis of the tangent bundle.

The price to pay is to consider the restricted frame bundle $SO(M)$. It is constituted of the space of directl isometries u of $\mathbb{R}^m$ oriented into $T_x(M)$ oriented. $SO(M)$ is a principal bundle: $SO(\mathbb{R}^m)$ acts on $SO(M)$ on the right.π is the projection from $SO(M)$ onto M. From this action, we deduce a subbundle of $TSO(M)$ called the vertical bundle. We can splitt the tangent space $T_u(S0(M)$ into the vertical bundle and a lift of $T_{\pi u}(M)$ compatible with the right action of $SO(\mathbb{R}^m)$ called the horizontal subspace compatible with the Levi-Civita connection.

Let be $Y_i(x)$ be a direct orthonormal basis of $t_x(M)$ in a neighborhood O of M. The matrix $< Y_j, \nabla^0_X Y_i >$ is an antisymmetrix matrix called $S^{Y_\cdot}_{\cdot}$ which depends tensorially from the vector field X. We remark that $Y_i = u_x e_i$ where e_i is the direct orthonormal basis of $\mathbb{R}^m$. $x \to u_x$ is called a local gauge of $SO(M)$. A system of local coordinates of $SO(M)$ is given by $(x, g) \to (x, u_x g)$ where (x, g) belongs to $O \times SO(\mathbb{R}^m)$. In this gauge, the horizontal lift of the vector field X is given by $(X, -S^{Y_\cdot}_X(x)g)$.

From the oriented standard basis e_i of $\mathbb{R}^m$, we deduce a direct orthonormal basis of $T_{\pi u}(M)$. We consider its horizontal lift and we get the canonical vector

fields X_i of $SO(M)$. If $S^{Y_\cdot}(\pi x)$ is equal to zero in x for some gauge, we will deduce that

$$F(f \circ \pi) = (\Delta f) \circ \pi \tag{15}$$

We consider the Riemannian distance between x and y:

$$d^2(x,y) = \inf_{h(0)=x;h(1)=y} \int_0^1 < h's), h'(s) >_{h(s)} ds \tag{16}$$

where $s \to h(s)$ is a smooth curve joining x to y. In a small open neighborhood of x, there is only one curve $h(y)$ joining x and y satisfying (16) defined by its speed $h'(y)$. The map $h'(y)$ defined a local system of coordinates, called normal coordinates. We consider the horizontal lift of the speed $h'(y)_s$ and the dynamical system associated $u(y)_s = (h(y)_s, \tau(y)_s))$. The parallel transport $\overline{Y}_\cdot(y) = \tau(y)_1(.)$ between x and y along the curve satisfies our requirement.

Moreover the vector fields X_i commute with the right action of $SO(\mathbb{R}^m)$. Therefore L does the same, and therefore P_t^L does the same.

In a local gauge, we can consider the Haar measure in the fiber of $SO(M)$. When we change of gauge, the measure does not change.

References

1. K.D. Elworthy, *Stochastic differential equations on manifolds*. LMS Lectures Notes 70. Cambridge-University Press, Cambridge, 1982.
2. N. Ikeda and S.Watanabe, *Stochastic differential equations and diffusion processes*Sec. Edi. North-Holland, Amsterdam,1989.
3. S. Kobayashi and N. Nomizu, *Foundations of differential geometry I*, Interscience, New-York, 1963.
4. S.Kobayashi and N. Nomizu, *Foundations of differential geometry II*, Interscience, New-York, , 1969.
5. L. Hoermander, *The analysis of linear partial operators III*, Springer, Berlin, 1984.
6. L. Hoermander, *The analysis of linear partial operators IV*, Springer, Berlin, 1984.
7. R. Léandre, A geometrical hypoelliptic diffusion, In *Differential geometry and its applications*.J. Bures and al eds. matfyzpress, Prague,2004, 517-523.
8. R. Léandre, Malliavin Calculus of Bismut type in semi-group theory, *Far-East. J. Math. Sci*, 30, 1-26, 2008.
9. R. Léandre, Stochastic analysis for a non-markovian generator: an introduction, *Russian Journal of Mathematical Physics*, 22, 39–52, 2015.

Using Child, Adult, and Old-age Mortality to Establish a Developing Countries Mortality Database (DMD)

Nan Li[1], Hong Mi[2], and Patrick Gerland[1]

1. Population Division, Department of Economic and Social Affairs, United Nations, 2 UN Plaza, 233 East 44th Street, Room DC2-1938, 1934, New York, NY 10017, USA (Email: li32@un.org, gerland@un.org). The views expressed in this paper are those of the author and do not necessarily reflect those of the United Nations.

2. Corresponding author， School of Public Affairs, Zhejiang University, Room 265#, Mengminwei Building, Zijin'gang Campus, Hangzhou, Zhejiang, P. R. China. (E-mail: spsswork@163.com). The work on this paper was supported by the Nature Science Foundation of China (NSFC) project (NO.71490732), NSFC project (NO.71490733) , Zhejiang Social Science Planning Project Key Program(NO.17NDJC029Z), and Nature Science Foundation of Zhejiang project(NO.LZ13G030001)

Keywords: Life table, Database, Developing countries

Abstract. Life-table databases have been established for developed countries and effectively used for various purposes. For developing countries of which the deaths counted 78% that of the world in 2010-2015, however, reliable life tables can hardly be found. Indirect estimates of life tables using empirical data on child and adult mortality are available for developing countries. But more than half of all deaths already occurred at age 60 and higher in developing countries in 2010-2015, which leads to the irony that worldwide the number of deaths at old-ages is the biggest, and also the least reliable. This reality indicates that improving the estimates of old-age mortality for individual developing countries is not enough, and that establishing a life-table database for all developing countries, which utilizes the improved estimations of old-age mortality, is necessary. To fulfill this task, we introduce two methods: (1) the Census Method that uses populations enumerated from census to estimate old-age mortality, and (2) the three-input model life table that utilizes child, adult, and old-age mortality to calculate life tables. Compared to using only child and adult mortality, applying the two methods to the data from the Human Mortality Database after 1950, the errors of fitting old-age mortality are reduced for more than 70% of all the countries. For the three non-European-origin populations in the Human Mortality Database the errors are reduced by 17% for Chile, 48% for Japan, and 17% for Taiwan, which is more relevant for developing countries. These results indicate that the methodology is adequate and empirical data are available to establish a mortality database for developing countries.

1 Introduction

Empirical data used in estimating life tables are collected from three types of source: (1) death registration that counts deaths by sex and age in a certain period, usually a calendar year; (2) census that enumerates the numbers of population by age and sex at a certain time point, and sometimes also death by age and sex during a period before the census time; and (3) sample survey that, in principle, could collect data on both death and population but cover only a small portion of the population in a country. Censuses are conducted in almost all the countries of the world. Besides providing middle-year populations to compute death rates for countries with reliable death registration, some developing countries rely also on census to obtain life tables directly. Since census interviewers must visit every household in a country to enumerate the number of residents at a certain time point, they could also ask just one more question about whether there was a death, or were deaths, in the household in past year; and if yes what is the gender and age of the death, or the genders and ages of the deaths (United Nations Statistics Division (UNSD), 2008). Furthermore, using population data of two successive censuses, some mortality indicators of the period between the two censuses could be estimated, especially for old ages at which the effect of migration is negligible (Li and Gerland, 2013). For many countries, census data on population by age and sex can be found from the United

Nations Demographic Yearbook (e.g., UNSD, 2013a). Occasionally, surveys using large sample size could also provide life tables.

Typical sample surveys often collect information only from a small portion of the population. Subsequently, they cannot produce life tables. This is because death rates at some ages, for example 10-20 years, could be very low, and hence require a large population to be estimated reliably. Nonetheless, sample surveys could provide reliable indicators of mortality for certain age groups when death is not a rare event or when the age group is wide enough. The most commonly sampled mortality indicator is child mortality, which is the probability of dying between birth and age 5, and is often denoted as ${}_5q_0$. The United Nations Children's Fund (UNICEF) as part of the United Nations Inter-agency Group for Child Mortality Estimation (IGME) has been regularly collecting, analyzing, and publishing child mortality for most of the countries back to the 1970s or earlier (see United Nations Children's Fund, 2013; http://www.childmortality.org). Based on the same principles used to estimate child mortality using birth histories, surveys such as the Demographic and Health Surveys (DHS, http://www.measuredhs.com/) have been collecting sibling histories since the 1990s to measure adult mortality, allowing to derive the probability of dying between age 15 and 50 or 60 years, namely ${}_{35}q_{15}$ or ${}_{45}q_{15}$, respectively, for an increasing number of developing countries (Timæus, 2013). Combining data of surveys and other sources, Wang and colleagues (2012) at the Institute for Heath Metrics and Evaluation (IHME) estimated adult mortality for 187 countries from 1970 to 2010.

Life-table databases have been established for developed countries (e.g., Human Mortality Database (HMD), 2016) and effectively used for various purposes. For developing countries of which the deaths counted 78% that of the world in 2010-2015 (United Nations Population Division (UNPD), 2015), however, reliable life tables can hardly be found. Indirect estimates of life tables have been provided by the UNPD (2015) and IHME (Wang and colleagues, 2012) for developing countries, using empirical data on child mortality (${}_5q_0$) and adult mortality (${}_{45}q_{15}$). But more than half of all deaths already occurred at age 60 and higher in developing countries in 2010-2015. Thus, estimating old-age mortality (${}_{15}q_{60}$), and using it together with the ${}_5q_0$ and ${}_{45}q_{15}$ estimated by the UNICEF and IHME mentioned above, to establish a life-table database for developing countries is a relevant and urgent task. To fulfil this task, this paper introduces two methods: (1) the Census Method that uses populations enumerated in census to estimate ${}_{15}q_{60}$, and (2) the three-input model life table that utilizes ${}_5q_0$, ${}_{45}q_{15}$, and ${}_{15}q_{60}$ to calculate life tables. Compared to using only child and adult mortality, applying the two methods to the data of HMD after 1950, the errors of fitting old-age mortality are reduced for more than 70% of all the countries. To be more specific to developing countries, the errors are reduced by 17% for Chile, 48% for Japan, and 17% for Taiwan, for two sexes combined, which are the three non-European-origin populations in Human Mortality Database. These results indicate that, in order to establish a life-table database for developing countries, the methodology is adequate and the empirical data are available.

2 Methods

The methods include the Census Method and the three-input model life table (three-input MLT).

2.1 The Census Method

The Census Method utilizes populations enumerated from census to estimate ${}_{15}q_{60}$, and includes two models. The first is the Census Method with variable-r model (Bennett.andHoriuchi,1981;Li and Gerland, 2013), which is more suitable when the period between the two successive censuses is not close to 10 years; and the second is the Census Method with survival model, which should work better when the period is close to 10 years.

2.1.1 The Census Method with variable-r model

The variable-r model (Bennett.andHoriuchi,1981) assumes zero migration and evenly distributed enumeration errors over age. Let *p(x, t)* be the observed number of population in age group *[x,x+5)* enumerated from a census conducted at time *t*, where *x*=60, 65, 70. The growth rates at age *x* are computed as

$$r(x) = Log[\frac{p(x,t_2)}{p(x,t_1)}]/(t_2 - t_1), \quad x = 60,65,70, \qquad (1)$$

where t_1 and t_2 represent the date of the first and second census, respectively. And the accumulated growth rates are

$$\begin{aligned} s(60) &= 2.5r(60), \\ s(65) &= 5r(60) + 2.5r(65), \\ s(70) &= 5[r(60) + r(65)] + 2.5r(70). \end{aligned} \qquad (2)$$

Further, the middle-point population in age group *[x,x+5), N(x),* are estimated as

$$N(x) = \sqrt{p(x,t_1)p(x,t_2)}, \quad x = 60,65,70. \qquad (3)$$

Furthermore, the person-years lived in 5-year age group *[x,x+5),* L_x, in the underlying stationary population, are obtained as (Bennett And Horiuchi, 1981)

$$L_x = N(x)\exp[s(x)], x = 60,65,70. \qquad (4)$$

At old ages such as 60 and over, migrants are negligible comparing to deaths. Thus, the zero-migration assumption is naturally satisfied. In developing countries, however, the errors in enumerating population often occur unevenly across age. A typical example is age heaping. When such errors are severe, the L_x resulted from (4), would show implausible patterns of increasing with age, which cannot occur in a stationary population. When such implausible situations occur, adjusting L_x is necessary. Li and Gerland (2013) proposed such an adjustment as is shown in the appendix A, which provides the adjusted $\hat{L}_x$. After adjusting the age-reporting errors, the number of survivors at age x, l_x, can be estimated using nonlinear optimization and a Gompertz model (Li and Gerland, 2013), or it can be estimated locally linearly as below:

$$\begin{aligned} l_{65} &= \frac{\hat{L}_{60} + \hat{L}_{65}}{2.5} \frac{\hat{L}_{65}}{(\hat{L}_{60} + 2\hat{L}_{65} + \hat{L}_{70})}, \\ l_{70} &= \frac{\hat{L}_{65} + \hat{L}_{70}}{2.5} \frac{\hat{L}_{65}}{(\hat{L}_{60} + 2\hat{L}_{65} + \hat{L}_{70})}, \\ l_{60} &= \frac{\hat{L}_{60}}{2.5} - l_{65}, \\ l_{75} &= \frac{\hat{L}_{70}}{2.5} - l_{70}. \end{aligned} \qquad (5)$$

In (5), the $\frac{\hat{L}_{60}+\hat{L}_{65}}{2.5}$ and $\frac{\hat{L}_{65}+\hat{L}_{70}}{2.5}$ are the first-step estimates of l_{65} and l_{70}, which are linear interpolations between $\hat{L}_{60}$, $\hat{L}_{65}$ and $\hat{L}_{70}$. The $\frac{\hat{L}_{65}}{(\hat{L}_{60}+2\hat{L}_{65}+\hat{L}_{70})}$ is an adjustment that makes $2.5\cdot(l_{60}+l_{65})=\hat{L}_{65}$. The last two lines in (5) are linear formulas of calculating $\hat{L}_{60}$ and $\hat{L}_{70}$.

Finally, after estimating l_x, ${}_{15}q_{60}$ is obtained as

$$ {}_{15}q_{60}=1-\frac{l_{75}}{l_{60}} \tag{6}$$

2.1.2 The Census Method with survival model

When the period between the two successive censuses is close to 10 years, the populations between the period of exactly 10 years can be reliably estimated assuming over-time constant growth rates and using (1). Consequently, the 10-year survival ratio of the stationary population is estimated as

$$ S=\frac{L_{70}}{L_{60}}=\frac{p(70-74,t_2)}{p(60-64,t_1)}. \tag{7}$$

Assuming that the over-age survival ratio is constant, the 1-year and 15-year survival ratios are therefore $S^{\frac{1}{10}}$ and $S^{\frac{15}{10}}$, respectively. Subsequently, the 15-year probability of death between age 60 and 75 can be estimated as

$$ q=1-S^{\frac{15}{10}}. \tag{8}$$

The assumption of constant over-age survival ratio can be adjusted using the United Nations general model life table (UNPD, 1982), which leads to a more accurate estimate of old-age mortality as

$$ {}_{15}q_{60}=\begin{cases} q\cdot(1.021-0.0002\cdot q+0.0002\cdot q^2), & R^2=0.999, \quad female, \\ q\cdot(1.0153-0.0003\cdot q+0.0002\cdot q^2), & R^2=0.999, \quad male. \end{cases} \tag{9}$$

2.2 The three-input model life table

The three-input model life table is an augmentation of the flexible two-dimensional model life table (two-input MLT, Wilmoth et al, 2012), which is expressed as

$$ \log(m_x)=a_x+b_x\cdot\log({}_5q_0)+c_x\cdot[\log({}_5q_0)]^2+v_x\cdot k, \tag{10}$$

where m_x stands for the five-year age-specific death rates with *x=0,1,5,10,…*; coefficient vectors a_x, b_x, c_x, and v_x are obtained from fitting mortality data of the Human Mortality Database; and parameter *k* is flexible, which can

be solved to fit an additional ${}_{45}q_{15}$. Obviously, the two-input MLT can be used to produce a life table when ${}_5q_0$ and ${}_{45}q_{15}$ are used as two inputs.

How to utilize the estimated old-age mortality (${}_{15}\hat{q}_{60}$)? A simple answer (Li, 2014) can be found by following the logic of the Logit transformation: $\log[{}_x\hat{q}_0/(1-{}_x\hat{q}_0)] = \alpha + \beta\log[{}_xq_0/(1-{}_xq_0)]$, in which the standard ${}_xq_0$ is naturally that of the two-input MLT, and level α and pattern β can be chosen to fit some function of observed probability of death (${}_x\hat{q}_0$). When there is only ${}_{15}\hat{q}_{60}$, a customary is to set $\beta = 1$ and solve α to fit ${}_{15}\hat{q}_{60}$(see Preston, Heuveline and Guillot, 2001; p.200). The rationale for using the Logit transformation is that $\log[{}_xq_0/(1-{}_xq_0)]$ would be close to linear at all the ages. It is worth noting that, at old ages, $\log(\hat{m}_x)$ would be close to linear according to the Gompertz law. Thus, at old ages, the linear relationship of the Logit transformation can be simplified as:

$$\log(\hat{m}_x) = \alpha + \log(m_x). \tag{11}$$

Because

$${}_{15}\hat{q}_{60} \approx 1 - \exp[-5\cdot(\hat{m}_{60} + \hat{m}_{65} + \hat{m}_{70})], \tag{12}$$

α is solved by inserting (11) to (12):

$$\alpha \approx \log[\frac{\log(1-{}_{15}\hat{q}_{60})}{\log(1-{}_{15}q_{60})}] \tag{13}$$

where ${}_{15}q_{60}$ is the old-age mortality of the two-input MLT. Subsequently, (10) is augmented to the three-input MLT:

$$\log(m_x) = \hat{a}_x + b_x\cdot\log({}_5q_0) + c_x\cdot[\log({}_5q_0)]^2 + v_x\cdot k, \tag{14}$$

$$\hat{a}_x = \begin{cases} a_x, & x < 60, \\ a_x + \log[\frac{\log(1-{}_{15}\hat{q}_{60})}{\log(1-{}_{15}q_{60})}], & x \geq 60, \end{cases} \tag{15}$$

which will exactly fit the three inputs: child, adult, and old-age mortality.

3 Validations

We use the data of HMD to test whether or not the three-input MLT (with ${}_5q_0$, ${}_{45}q_{15}$, and ${}_{15}q_{60}$) can improve the performance of the two-input MLT with only ${}_5q_0$ and ${}_{45}q_{15}$. We choose the periods after 1950 to avoid the irregular effect of World War II, and all the countries or areas except Israel, for which the Census Method could not work because of territory change. In HMD, all 'census' dates are adjusted to January first. Consequently, periods 1950-1959, 1960-1969, …, and 2000-2009, and the Census Method with survival model, are chosen to carry

out the validations. In real census, there are undercounts. Nonetheless, these undercounts tend to cancel each other in causing the errors of estimating mortality level, as is indicated in appendix B.

We first choose the observed ${}_5q_0$ and ${}_{45}q_{15}$ of a certain population in a certain period as the inputs of two-input MLT, which will produce a life table that includes an estimated ${}_{15}\tilde{q}_{60}$. This ${}_{15}\tilde{q}_{60}$ will differ from the observed old-age mortality, ${}_{15}q_{60}$. We then use the 'census' populations at the two ends of each period to estimate the values of old-age mortality, and use an exponential model to smooth them. The results are denoted as ${}_{15}\hat{q}_{60}$.

The purpose of two-input MLT is to use the ${}_5q_0$ and ${}_{45}q_{15}$ to best describe the corresponding life table, including particularly the ${}_{15}q_{60}$, using the mortality patterns of the HMD populations. Thus, ${}_{15}\tilde{q}_{60}$ is the best estimated ${}_{15}q_{60}$ that the two-input MLT could provide. We believe that for developing countries ${}_{15}\tilde{q}_{60}$ should also be reasonable to some extent. Therefore, we use

$$ {}_{15}\bar{q}_{60} = [w \cdot {}_{15}\hat{q}_{60} + (1-w) \cdot {}_{15}\tilde{q}_{60}] \qquad (16) $$

as the estimated old-age mortality of the three-input MLT, where the w stands for the weight that can be determined flexibly, and is taken as 0.5 in all the validations here. The values of ${}_{15}\bar{q}_{60}$ are input to the three-input model life tables, which will have the same ${}_5q_0$ and ${}_{45}q_{15}$ as that of two-input MLT. But the values of old-age mortality of these life tables are ${}_{15}\bar{q}_{60}$, which will differ from the observed ${}_{15}q_{60}$.

For a given population, we use the root-mean-squared error (RMSE) to measure errors. More specifically, we use $RMSE_2$ to indicate the difference between ${}_{15}\tilde{q}_{60}$ and ${}_{15}q_{60}$, and $RMSE_3$ to show the distance between ${}_{15}\bar{q}_{60}$ and ${}_{15}q_{60}$. Let the ith estimates be ${}_{15}\tilde{q}_{60}(i)$ and ${}_{15}q_{60}(i)$, and the total number of periods be n, there are

$$ \begin{aligned} RMSE_2 &= \sqrt{\sum_{i=1}^{n} [{}_{15}\tilde{q}_{60}(i) - {}_{15}q_{60}(i)]^2 / n}, \\ RMSE_3 &= \sqrt{\sum_{i=1}^{n} [{}_{15}\bar{q}_{60}(i) - {}_{15}q_{60}(i)]^2 / n}. \end{aligned} \qquad (17) $$

If $RMSE_3 < RMSE_2$ for a given population, we conclude that the three-input MLT fits this population better than does the two-input MLT, and vice versa.

The validations use HMD data. If reliable life tables for developing countries were not rare, we would choose them to carry out the validation. For the 37 (excluding Israel) countries' 74 populations by sex in HMD, the results of validation are summarized in figure 1, in which the position of a population is marked by its $RMSE_2$ on the horizontal axis and $RMSE_3$ on the vertical axis. When the three-input MLT improves the performance of two-input MLT for a given population, the position of this population is below the equal line, and vice versa.

Figure 1. Root-mean-squared errors in predicting ${}_{15}q_{60}$ for the 74 populations by sex in HMD

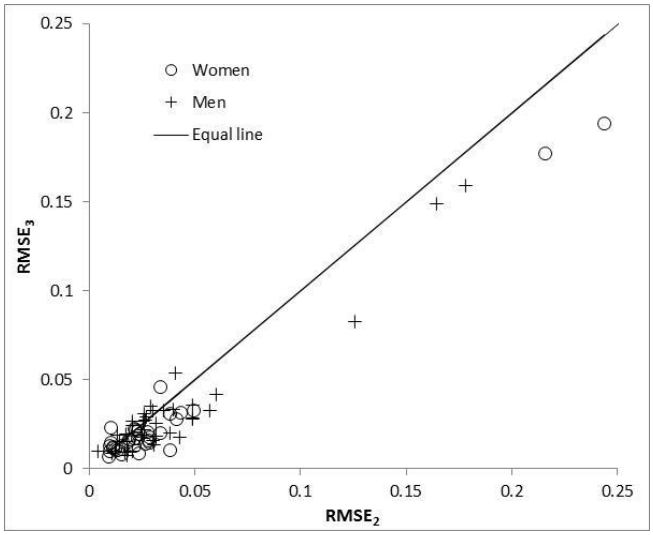

We see that the three-input MLT improved the performance of the two-input MLT for most of the populations. To be more specific, the three-input MLT improved the performance of the two-input MLT for 55 of the 74 populations. We also see from figure 1 that the chance for the improvement to occur is bigger when the $RMSE_2$ is larger. Since the two-input MLT is based on the data of HMD of which the populations are almost exclusively of European origin, we expect that for non-European-origin populations the error of two-input MLT are more likely to be larger and therefore improvements are more likely to occur. This expectation turned to be true within the HMD populations. The errors are reduced by 17% for Chile, 48% for Japan, and 17% for Taiwan, which are the three non-European-origin populations in HMD. Furthermore, since developing countries are all non-European origin, we expect that the three-input should provide greater improvements than that in the validations.

To see more details of the improvement, we choose Japanese women as an example, and show the fittings of old-age mortality in figure 2. We see that the three-input MLT performed slightly worse than did the two-input MLT for years before 1980, but remarkably better later. Overall, the three-input MLT reduced the errors of the two-input MLT by 49% (48% for both men and women).

Figure 2. Old-age mortality (${}_{15}q_{60}$) of Japanese women

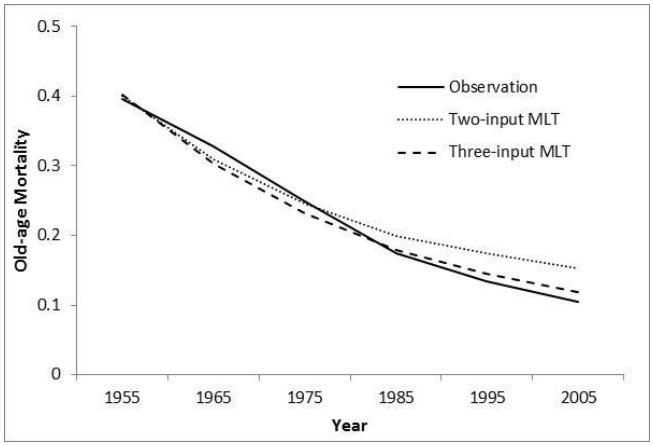

Our final target is not only to better fit ${}_{15}q_{60}$, but to improve the estimates of life tables at old ages. To see how this target is reached, we choose Japanese women in 2000-2009 as an example, and show the result in figure 3. We see that the three-input MLT remarkably improved the estimates of age-specific death rate at old ages.

Figure 3. Age-specific death rates of Japanese women, 2000-2009

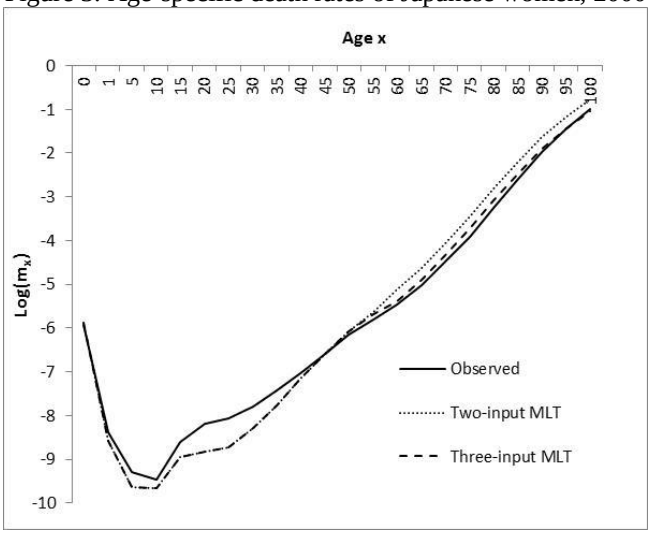

4Summary

In 2010-2015, for example, the deaths at age 60 and older already reached 60% of all deaths worldwide (UNPD, 2015). Compared to the numbers of deaths at child and adult ages, the number of deaths at old ages is the biggest and, ironically, also the least reliable. This is because, for most developing countries, the numbers of old-age deaths are not estimated on the basis of empirical data. They are extrapolations of mortality at younger ages. This reality indicates that improving the estimates of old-age mortality for individual developing countries is not enough, and that establishing a life-table database for all developing countries, which utilizes the improved estimations of old-age mortality, is necessary.

At old ages, migrants are rare comparing to deaths. Thus, census data on population by age and sex could be used to estimate old-age mortality; and such data are available for almost all the countries of the world. For example, among the 233 countries and areas (UNPD, 2015), 220 have conducted the 2010-round census between 2005 and 2014 (United Nations Statistics Division, 2013b). Moreover, some developing countries had surveys or censuses that collected information on old-age mortality, which can be used as supplementary data to more reliably estimate old-age mortality.

In recent years, new methodological developments have been made to use census population to estimate old-age mortality, and extend one-input model life tables to better utilize existing information. Furthermore, these methods are improved to work better for old ages in recent years. In this paper, we described and organized these methods as the three-input MLT; and we validated performance of the three-input MLT using the HMD data. We found that the three-input MLT could improve the performance of the previous methods for 55 of the 74 populations in HMD, and that the average improvement is 14%. To be more relevant to developing countries that are non-European-origin populations, confirm this suggestion, improvements are observed for all the non-European-origin populations in HMD, which are 17% for Chile, 48% for Japan, and 17% for Taiwan.

This paper indicated that establishing a life-table database for developing countries is necessary, that the methodology is adequate, and that the empirical data are available.

References

Bennett, N.G.and S. Horiuchi.1981. Estimating the Completeness of Death Registration in a Closed Population.*Population Index* 47(2):207-221.

Haman Mortality Database, 2016. University of California, Berkeley (USA), and Max Planck Institute for Demographic Research (Germany). Available at www.mortality.org or www.humanmortality.de.

Li, N., 2014. Estimating Life Tables for Developing Countries. Technical paper of the United Nations Population Devision 2014/4. Available at http://www.un.org/en/development/desa/population/publications/pdf/technical/TP2014-4.pdf.

Li, N. and P. Gerland. 2013. Using census data to estimate old-age mortality for developing countries. Paper prepared for Session 17-05: Indirect methods of mortality and fertility estimation: new techniques for new realities, in *XXVII IUSSP International Population Conference*. Busan, Korea. http://iussp.org/en/event/17/programme/paper/1959

Preston, S. H., P. Heuveline and M. Guillot (2001). *Demography, Measuring and Modeling Population Process*. Oxford, United Kingdom: Blackwell Publishers Ltd.

Timæus I.M. 2013. Estimation of adult mortality from sibling histories. In Moultrie T.A., R.E. Dorrington, A.G. Hill, K. Hill, I.M. Timæus and B. Zaba (eds). *Tools for Demographic Estimation*. Paris: International Union for the Scientific Study of Population. http://demographicestimation.iussp.org/content/sibling-histories

United Nations Population Division. 2015. *World Population Prospects: The 2015 Revision*. United Nations, New York.

United NationsPopulation Division. 1982. *Model life tables for developing countries*. New York: United Nations.

United Nations Statistics Division. 2008.*Principles and Recommendations for Population and Housing Censuses, Revision 2,Statistical papers Series M,* Rev. 2 ed., New York, NY:United Nations. http://unstats.un.org/unsd/demographic/sources/census/census3.htm

United Nations Statistics Division. 2013a. *Demographic Yearbook 2012, Sixty-third issue*. New York: United Nations. https://unstats.un.org/unsd/demographic/products/dyb/2010_round_latest.htm

United Nations Statistics Division. 2013b. Availablehttp://unstats.un.org/unsd/demographic/sources/census/2010_PHC/censusclockmore.htm

Wang H., L. Dwyer-Lindgren, K.T. Lofgren, J.K. Rajaratnam, J.R. Marcus, A. Levin-Rector, C. Levitz, A.D. Lopez, C.J.L. Murray. 2012. Age-specific and sex-specific mortality in 187 countries, 1970–2010: a systematic analysis for the Global Burden of Disease Study 2010. *The Lancet*. 2012 Dec 13; 380: 2071–2094.

Wilmoth, J., S. Zureick, V. Canudas-Romo, V. Inoue, and C. Sawyer, 2012. A flexible two-dimensional mortality model for use in indirect estimation. *Population Studies*, (66). 1-28.

Appendix A. Adjusting age reporting errors

It is hard to find a proper basis to adjust enumerating errors in a real population, which is affected by historical fertility, mortality and migration. But a stationary population is determined only by mortality. Thus, it is possible to find a proper basis to adjust age errors for stationary populations. According to the United Nations general model life table (United Nations Population Division, 1982), there is a common relationship between the survival ratios $S_{60} = \frac{L_{65}}{L_{60}}$ and $S_{65} = \frac{L_{70}}{L_{65}}$ among model life tables, which is

$$S_{65} = -0.29 + 1.27 \cdot S_{60}, \quad R^2 = 0.998. \tag{A.1}$$

This relationship is called the model line. When the observed survival-ratio point, (S_{60}, S_{65}), is above the model line, or when the survival ratio is abnormally rising with age, the difference between the survival-ratio point and the model line is caused mainly by age heaping. Accordingly, assuming that the heaping ratio at age 60 equals to that at age 70, the adjustment is

$$\begin{aligned} \hat{L}_{60} &= L_{60} - \frac{L_{60}}{L_{70}}\Delta, \\ \hat{L}_{65} &= L_{65} + \Delta, \\ \hat{L}_{70} &= L_{70} - \Delta, \end{aligned} \tag{A.2}$$

where

$$\begin{aligned} \Delta &= \frac{-B + \sqrt{B^2 - 4AC}}{2A}, \\ A &= b - a\frac{L_{60}}{L_{70}} - \frac{L_{60}}{L_{70}}, \\ B &= a(L_{60} - \frac{L_{60}}{L_{70}}L_{65}) + 2bL_{65} + L_{60} + \frac{L_{60}}{L_{70}}L_{70}, \\ C &= L_{65}(aL_{60} + bL_{65}) - L_{60}L_{70}, \\ a &= -0.29, \quad b = 1.27. \end{aligned} \tag{A.3}$$

On the other hand, when the survival-ratio point is below the model line, the difference between the survival-ratio point and the model line is caused by nonspecific errors. Accordingly, the adjustment is to move the survival ratio point into the model line through minimal distance as

$$\begin{aligned} \hat{S}_{60} &= \frac{-ab + S_{60} + bS_{65}}{1 + b^2}, \\ \hat{S}_{65} &= a + b\hat{S}_{60}. \end{aligned} \tag{A.4}$$

$$\begin{aligned} \hat{L}_{60} &= w\frac{L_{60} + \hat{S}_{60}L_{65} + \hat{S}_{60}\hat{S}_{65}L_{70}}{1 + \hat{S}_{60}^2 + \hat{S}_{60}^2\hat{S}_{65}^2} + (1-w)L_{60}, \\ \hat{L}_{65} &= w\hat{S}_{60}\frac{L_{60} + \hat{S}_{60}L_{65} + \hat{S}_{60}\hat{S}_{65}L_{70}}{1 + \hat{S}_{60}^2 + \hat{S}_{60}^2\hat{S}_{65}^2} + (1-w)L_{65}, \\ \hat{L}_{70} &= w\hat{S}_{65}\hat{S}_{60}\frac{L_{60} + \hat{S}_{60}L_{65} + \hat{S}_{60}\hat{S}_{65}L_{70}}{1 + \hat{S}_{60}^2 + \hat{S}_{60}^2\hat{S}_{65}^2} + (1-w)L_{70}, \end{aligned} \tag{A.5}$$

where $0 \le w \le 1$ is the weight, and is used as 0.5.

Appendix B. The errors of estimating survival ratio using census population

Let the net undercounting rates be u_1 and u_2 for the first and second censuses, respectively. Neglecting intercensal migration, the estimated survival ratio (*Se*) is:

$$Se = \frac{p(70-74, t_2)\cdot(1-u_2)}{p(60-64, t_1)\cdot(1-u_1)} = S\frac{(1-u_2)}{(1-u_1)}. \quad \text{(b.1)}$$

Subsequently, the relative error in estimating survival ratio is:

$$E(u_1, u_2) = \frac{Se-S}{S} = \frac{1-u_2}{1-u_1} - 1 = \frac{u_1-u_2}{1-u_1}. \quad \text{(b.2)}$$

It can be seen that the estimating error of survival ratio is determined only by census undercounts. In addition, census undercounts tend to cancel each other in causing the errors of estimating survival ratio, which would therefore be small in general.

Moments of the forward recurrence time in a renewal process

Sotirios Losidis[1] and Konstadinos Politis[2]

[1] Department of Statistics and Insurance Science
University of Piraeus 80 Karaoli & Demetriou Str,Piraeus 18534,GREECE (E-mail: losidis_sotiris@hotmail.com)
[2] Department of Statistics and Insurance Science
University of Piraeus 80 Karaoli & Demetriou Str,Piraeus 18534,GREECE
(E-mail: kpolitis@unipi.gr)

Abstract. We study the moments of the forward recurrence times in a renewal process. We discuss in particular the monotonicity of the variance for these recurrence times. Finally we study the covariance between the forward recurrence time at t and the number of renewals over $[0, t]$.
Keywords: renewal function; renewal density; forward recurrence time; IMRL; HNBUE; HNWUE..

1 Introduction

One of the key quantities of interest in renewal theory is the forward recurrence time (also known as the overhshoot or the excess lifetime), that is the time between an arbitrary time point and the occurrence of the next renewal. Many of the numerous applications of this quantity and the basic setting of renewal theory can be found e.g. in the books by Feller [5] or Tijms [10]. The aim of the present note is to give some results about the (higher) moments of forward recurrence times, while we also give a result concerning the covariance between the forward recurrence time at time t and the number of renewals in $[0, t]$.

Let $X_1, X_2, \ldots$, be a sequence of independent, identically distributed (i.i.d.) nonnegative random variables with distribution function (d.f.) F. Define $S_0 = 0$ and, for $n = 1, 2, \ldots$, let $S_n = X_1 + X_2 + \ldots + X_n$. Renewal theory is concerned with the study of the counting process $\{N(t) : t \geq 0\}$, where $N(t) = \sup\{n : S_n \leq t\}$, so that $N(t)$ represents the number of partial sums (renewal epochs) S_n which are less than or equal to t. A primary quantity of interest is the *renewal function* $M(t) = E[N(t)]$, while the forward recurrence time, denoted by γ_t, is defined by $\gamma_t = S_{N(t)+1} - t$.

In the present paper we consider the case where the distribution F has a monotone mean residual life; more explicitly, for a nonnegative random variable X with d.f. F, the mean residual life function is defined by $c(t) = E(X - t|X > t)$. We say that F is an increasing (resp. decreasing) residual life distribution function (IMRL, resp. DMRL) if $E(X) < \infty$, $F(0) < 1$ and $c(t)$ is increasing (decreasing) in t. The term increasing (decreasing) is used throughout for non-decreasing (non-increasing). We write $\mu_k = \int_0^\infty x^k dF(x)$ for the moments of F; for simplicity, we write μ rather than μ_1 for the first moment. Further, the equilibrium distribution associated with F, denoted by F_e, is defined as $F_e(t) = \mu^{-1} \int_0^t \overline{F}(y)dy$, where $\overline{F} = 1 - F$.

The elementary renewal theorem states that $M(t) \sim t/\mu$. For $t \geq 0$, we define $L(t)$ as the difference between $M(t)$ and t/μ; that is,

$$L(t) = M(t) - \frac{t}{\mu}.$$

We assume throughout that the interarrival distribution F is absolutely continuous; in that case, M is also absolutely continuous with a density m, the *renewal density* and it holds that $M^{'}(t) = m(t)$ almost everywhere. An important quantity in what follows is the derivative of the function $L(t)$, which we denote by l; namely,

$$l(t) = m(t) - \frac{1}{\mu}. \tag{1}$$

In the first part of the paper we present a formula for the forward recurrence time based on the equilibrium distribution F_e associated with the distribution F of the inter-arrival times. In the second part we discuss the variance of the forward recurrence times and we show that this is increasing if F is an IMRL distribution. In the final section we give a result for the sign of the covariance between the forward recurrence time and the number of renewals up to time t, as t tends to infinity.

2 Moments of the forward recurrence time

An expression for the moments of the forward recurrence time in a renewal process has been given by Coleman [4], who showed that for $r = 1, 2, \cdots$,

$$E(\gamma_t^r) = E(X-t)^r + \mu_r M(t) - r\int_0^t \left(E(X+z-t)^{r-1} - (z-t)^{r-1}\right) M(z)dz. \tag{2}$$

In this section we will present an alternative way to calculate the r-th moment of the forward recurrence time which is based on the equilibrium distribution F_e and the function $l(t)$ defined in the previous section.

First, we note that the survival function of the forward recurrence time is given by the following formula

$$P(\gamma_t > y) = \overline{F}(t+y) + \int_0^t \overline{F}(u+y)m(t-u)du, \qquad y \geq 0, \tag{3}$$

see, e.g. Gakis and Sivazlian [6]. For convenience, we define a function $\phi(y;t)$ as follows:

$$\phi(y;t) = \int_0^y \overline{F}(z)l(t+y-z)dz. \tag{4}$$

Proposition 1. *The survival function of the forward recurrence times is given by the formula*

$$P(\gamma_t > y) = \overline{F}_e(y) - \phi(y;t). \tag{5}$$

Proof Inserting equation (1) into (3) we have

$$\begin{aligned} P(\gamma_t > y) &= \overline{F}(t+y) + \int_0^t \overline{F}(u+y)\left(l(t-u) + \frac{1}{\mu}\right)du \\ &= \overline{F}(t+y) + \overline{F}_e(y) - \overline{F}_e(t+y) + \int_0^t \overline{F}(u+y)l(t-u)du. \end{aligned} \tag{6}$$

The last integral can be written as

$$\begin{aligned} \int_0^t \overline{F}(u+y)l(t-u)du &= \int_y^{t+y} \overline{F}(z)l(t+y-z)dz \\ &= \int_0^{t+y} \overline{F}(z)l(t+y-z)dz - \int_0^y \overline{F}(z)l(t+y-z)dz. \end{aligned}$$

Next, it is known [Chen [3], Losidis and Politis [7]] that

$$\int_0^t \overline{F}(z)l(t-z)dz = \overline{F}_e(t) - \overline{F}(t).$$

From the last two expressions we get

$$\int_0^t \overline{F}(u+y)l(t-u)du = \overline{F}_e(t+y) - \overline{F}(t+y) - \int_0^y \overline{F}(z)l(t+y-z)dz.$$

The proof follows by substituting the last result and equation (4) into (6). □

Equation (5) permits a straightforward comparison between the survival function of the forward recurrence time in an ordinary renewal process and a stationary renewal process. More explicitly, in a stationary renewal process the distribution of the first inter-arrival time is F_e, while all the other inter-arrivals have a distribution F [see, e.g. Serfozo [8] for details]. We denote the forward recurrence time in a stationary renewal process by $\overline{\gamma_t}$. The right tail of this recurrence time is given by

$$P(\overline{\gamma_t} > y) = \overline{F}_e(y), \qquad t, y \geq 0, \tag{7}$$

see, e.g. Serfozo [8]. It is now obvious that $P(\gamma_t > y) \geq (\leq) P(\overline{\gamma_t} > y)$ if the function $L(t)$ (or the renewal function $M(t)$) is concave (convex). In other words, the forward recurrence time in an ordinary renewal process is *stochastically larger* (*smaller*) that the same quantity in a stationary process, if $M(t)$) is concave (convex). Conditions for concavity (convexity) of the renewal function have been given by Shaked and Zhu [9].

Equation (5) will also help us to calculate the r-moment of the forward recurrence time. Coleman [4] proved that, when $\mu_{r+1} < \infty$, then it holds that

$$\lim_{t\to\infty} E(\gamma_t^r) = \frac{\mu_{r+1}}{(r+1)\mu}.$$

Put now

$$S_r(t) = E(\gamma_t^r) - \frac{\mu_{r+1}}{(r+1)\mu}. \tag{8}$$

Then we have the following.

Lemma 1. *For $r = 1, 2, \ldots$, it holds that*

$$S_r(t) = -r \int_0^\infty y^{r-1}\phi(y;t)dy. \tag{9}$$

Proof Multiplying equation (5) with ry^{r-1} and integrating with respect to y on (0,∞) we have

$$r\int_0^\infty y^{r-1}P(\gamma_t > y)dy = r\int_0^\infty y^{r-1}\overline{F}_e(y)dy - r\int_0^\infty \int_0^y y^{r-1}\overline{F}(z)l(t+y-z)dzdy.$$

The integral on the left equals $E({\gamma_t}^r)$, see, e.g. Feller [5],(p. 150). It is easy to see that the first integral on the right is equal to $\mu_{r+1}/(\mu(r+1))$. Therefore, substituting (4) in the second integral on the right yields

$$E({\gamma_t}^r) = \frac{\mu_{r+1}}{\mu(r+1)} - r\int_0^\infty y^{r-1}\phi(y;t)dy,$$

which, in view of (8), is the desired result. □

It is easy to deduce from Lemma 1 that, if the renewal function $M(t)$ is a concave (convex) function, then $E({\gamma_t}^r)$ is an increasing (decreasing) function of t. This last result can also be inferred from Theorem 4 in Shaked and Zhu [9]. Further, we see from (4) that, if $l(t) \leq (\geq)0$, then we have $\phi(y;t) \leq (\geq)0$ for all t, y and, by an appeal to Lemma 1, we obtain the following.

Corollary 1. *If $L(t)$ is a decreasing (increasing) function of t, then we have that $S_r(t) \geq (\leq)0$.*

A well-known sufficient condition for $L(t)$ to be an increasing function, obtained by Brown [1], is that the interarrival distribution function F is IMRL. Brown [1] also proved that, when the distribution of the inter-arrival times is IMRL, then

$$M(t) \leq \frac{t}{\mu} + \frac{\mu_2}{2\mu^2} - 1. \tag{10}$$

Let now

$$Q(t) = M(t) - \frac{t}{\mu} + 1 - \frac{\mu_2}{2\mu^2}. \tag{11}$$

Both an upper and a lower bound for $Q(t)$ have been given recently by Losidis and Politis [7]. Note that, by Wald's identity, the mean forward recurrence time is given by $E(\gamma_t) = \mu(1 + M(t)) - t$, so that the last expression gives

$$E(\gamma_t) = \frac{\mu_2}{2\mu} + \mu Q(t). \tag{12}$$

On the other hand, equation (9) for $r = 1$ gives $E(\gamma_t) = \mu_2/(2\mu) - \int_0^\infty \phi(y;t)dy$. Thus, another formula for the "remainder term" $Q(t)$ is

$$Q(t) = -\frac{1}{\mu}\int_0^\infty \phi(y;t)dy.$$

3 The variance of the forward recurrence time

Here we consider the variance of the forward recurrence time. First, using equation (9) we obtain the following formula

$$Var(\gamma_t) = \frac{\mu_3}{3\mu} - 2\int_0^\infty y\phi(y;t)dy - \left(\frac{\mu_2}{2\mu} - \int_0^\infty \phi(y;t)dy\right)^2.$$

Next, Tijms [10] gave the following expression for the second moment of γ_t,

$$E({\gamma_t}^2) = \mu_2\,(1 + M(t)) - 2\mu\left(t + \int_0^t M(x)dx\right) + t^2. \tag{13}$$

Using this and the results of the previous section we now show that, under the IMRL assumption for F, both the second moment and the variance of the forward recurrence time are increasing functions of t.

Lemma 2. *The second moment of the forward recurrence time is given by the following formula*

$$E({\gamma_t}^2) = \frac{{\mu_2}^2}{2\mu^2} + \mu_2 Q(t) - 2\left(\mu\int_0^t Q(x)dx\right) \tag{14}$$

If, in addition, the d.f of the inter-arrival times is IMRL, then this is an increasing function of t.

Proof Equation (14) is proved by inserting (11) into (13) and some simple algebra. Further, the derivative of the second moment of the forward recurrence time is

$$\frac{d}{dt}E({\gamma_t}^2) = \mu_2 l(t) + 2\frac{d}{dt}\left(-\mu\int_0^t Q(x)dx\right) = \mu_2 l(t) - 2\mu Q(t),$$

and this is nonnegative under the IMRL assumption. □

We note that the second part of the lemma can also be inferred from Theorem 2 in Brown [2], who gave a more general result.

Proposition 2. *The variance of the forward recurrence time in an ordinary renewal process is given by the following formula*

$$Var(\gamma_t) = \frac{\mu_2^2}{4\mu^2} - 2\mu\int_0^t Q(x)dx - \mu^2 Q(t)^2.$$

If the d.f of the inter-arrival times is IMRL, then this is an increasing function of t.

Proof Since $Var(\gamma_t) = E({\gamma_t}^2) - E(\gamma_t)^2$, from (12) and (14) we obtain

$$\begin{aligned} Var(\gamma_t) &= \frac{{\mu_2}^2}{2\mu^2} + \mu_2 Q(t) - 2\left(\mu\int_0^t Q(x)dx\right) - \left(\frac{\mu_2}{2\mu} + \mu Q(t)\right)^2 \\ &= \frac{\mu_2^2}{4\mu^2} - 2\mu\int_0^t Q(x)dx - \mu^2 Q(t)^2. \end{aligned}$$

In the IMRL case, a simple differentiation yields

$$\frac{d}{dt}Var(\gamma_t) = -2\mu Q(t) - 2\mu^2 Q(t),$$

and the fact that $Q(t) \leq 0$ implies now that $Var(\gamma_t)$ is increasing. □

4 The covariance between the forward recurrence time and the number of renewals as $t \to \infty$

Here we study the behaviour of the covariance between the forward recurrence time and the number of renewals up to time t, $N(t)$, in an ordinary renewal process as $t \to \infty$. To begin with, Coleman [4] showed that, if $\mu_3 < \infty$, then

$$\lim_{t\to\infty} Cov(\gamma_t, N(t)) = \frac{{\mu_2}^2}{4\mu^3} - \frac{\mu_3}{6\mu^2}. \tag{15}$$

It is also known (Tijms [10]) that

$$\lim_{t\to\infty}\left(\int_0^t M(x)dx - \left(\frac{t^2}{2\mu} + \left(\frac{\mu_2}{2\mu^2} - 1\right)t\right)\right) = \frac{{\mu_2}^2}{4\mu^3} - \frac{\mu_3}{6\mu^2}.$$

The left-hand side of this can be written as follows:

$$\begin{aligned} \lim_{t\to\infty}\left(\int_0^t M(x)dx - \left(\frac{t^2}{2\mu} + \left(\frac{\mu_2}{2\mu^2} - 1\right)t\right)\right) &= \lim_{t\to\infty}\int_0^t \left(M(x) - \left(\frac{x}{\mu} + \frac{\mu_2}{2\mu^2} - 1\right)\right)dx \\ &= \int_0^\infty Q(x)dx, \end{aligned}$$

using the definition of the function Q in (11). We therefore see that the asymptotic covariance between the forward recurrence time and the number of renewals $N(t)$ is given by the following formula

$$\lim_{t\to\infty} Cov(\gamma_t, N(t)) = \int_0^\infty Q(x)dx.$$

This implies in particular that, if F is IMRL, the asymptotic covariance is less than or equal to zero, since in that case $Q(x) \leq 0$ for all x. The next result is much stronger, however, as it applies to a class of distributions which is considerably larger than the IMRL class. More explicitly, we recall the following definition. A distribution F supported on $[0,\infty)$ is HNWUE (HNBUE), we call this as 'harmonic new worse (better) than used in expectation', if for all $x \geq 0$,

$$\int_x^\infty \overline{F}(t)\, dt \geq (\leq)\mu\, e^{-x/\mu},$$

where μ is the first moment of F.

The HNWUE (HNBUE) classes seem to be the largest among the commonly used ageing classes of distributions. In particular, if a distribution F is IMRL, then both F and the associated equilibrium distribution F_e are also HNWUE.

Proposition 3. *If, in a renewal process, the equilibrium distribution F_e is HNBUE (HNWUE), then*

$$\lim_{t\to\infty} Cov(\gamma_t, N(t)) \geq (\leq)0.$$

Proof From the definition of the HNBUE (HNWUE) classes above, it is easy to see that if the equilibrium distribution is in the HNBUE (HNWUE) class, then

$$\int_t^\infty \overline{F}_e(z)dx \leq (\geq)\frac{\mu_2}{2\mu} e^{\frac{-2\mu}{\mu_2}t}.$$

Integrating both sides of this over $(0,\infty)$ we get

$$\int_0^\infty \int_t^\infty \overline{F}_e(z)dzdt \leq (\geq)\frac{\mu_2}{2\mu}\int_0^\infty e^{\frac{-2\mu}{\mu_2}t}dt \tag{16}$$

The right-hand side of the above inequality is equal to

$$\frac{\mu_2}{2\mu}\int_0^\infty e^{\frac{-2\mu}{\mu_2}t}dt = \frac{\mu_2^2}{4\mu^2},$$

while for the left-hand side we get

$$\begin{aligned}\int_0^\infty \int_t^\infty \overline{F}_e(z)dzdt &= \mu^{-1}\int_0^\infty \int_t^\infty \int_z^\infty \overline{F}(y)dydzdt = \mu^{-1}\int_0^\infty \int_t^\infty \int_t^y \overline{F}(z)dzdydt \\ &= \mu^{-1}\int_0^\infty \int_t^\infty (z-t)\overline{F}(z)dzdt = \frac{1}{\mu}\int_0^\infty \int_0^z x\overline{F}(z)dxdz \\ &= \frac{1}{2\mu}\int_0^\infty z^2\overline{F}(z)dz = \frac{\mu_3}{6\mu}.\end{aligned}$$

By inserting the last two expressions into (16) we obtain that, if F_e is a HNBUE (HNWUE) distribution, then

$$\frac{\mu_3}{6\mu} - \frac{{\mu_2}^2}{4\mu^2} \leq (\geq)0$$

and the result follows in view of (15). □

Acknowledgement : This work has been partly supported by the University of Piraeus Research Center.

References

1. Brown, M. Bounds, Inequalities, and Monotonicity Properties for Some Specialized Renewal Processes. *Ann. Prob.*, **8**, 227-240, 1980.
2. Brown, M. Further Monotonicity Properties for Specialized Renewal Processes. *Ann. Prob.*, **9**(5), 891–895, 1981.
3. Chen, Y-H. Classes of life distributions and renewal counting processes. *J. Appl. Prob.*, **31**, 1110–1115, 1994.
4. Coleman, Moments of the forward recurrence time. *Eur. J. Oper. Research*, **9**(2), 181–183, 1982.
5. Feller, W. *An Introduction to Probability Theory and Its Applications.* Vol. II, 2nd edition. Wiley, New York, 1971.
6. Gakis, K.G , Sivazlian, B.D The correlation of the backward and forward recurrence times in a renewal process. *Stochastic Analysis and Applications*, **12**(5), 543–549, 1994.
7. Losidis, S. and Politis, K. A two-sided bound for the renewal function when the interarrival distribution is IMRL. *Stat. Prob. Letters*, **125**, 164–170, 2017.
8. Serfozo, R. *Basics of Applied Stochastic Processes.* Springer-Verlag. Berlin, Heidelberg, 2009.
9. Shaked, M. and Zhu, H. Some results on block replacement policies and renewal theory. *J. Appl. Prob.*, **29**, 932–946, 1992.
10. Tijms, H. *A First Course in Stochastic Models.* 2nd edition. Wiley, New York, 2003.

Extremes in Random Graphs Models of Complex Networks

Natalia Markovich[1]

V.A.Trapeznikov Institute of Control Sciences, Russian Academy of Sciences, Profsoyuznaya 65, 117997 Moscow, Russia,
Moscow Institute of Physics and Technology State University, Kerchenskaya 1, 117303 Moscow, Russia,
(E-mail: nat.markovich@gmail.com)

Abstract. Regarding the analysis of Web communication, social and complex networks the fast finding of most influential nodes in a network graph constitutes an important research problem. We use two indices of the influence of those nodes, namely, PageRank and a Max-linear model. We consider the PageRank as an autoregressive process with a random number of random coefficients that depend on ranks of incoming nodes and their out-degrees and assume that the coefficients are independent and distributed with regularly varying tail and with the same tail index. Then it is proved that the tail index and the extremal index are the same for both PageRank and the Max-linear model and the values of these indices are found. The achievements are based on the study of random sequences of a random length and the comparison of the distribution of their maxima and linear combinations.
Keywords: Extremal Index, PageRank, Max-Linear Model, Branching Process, Autoregressive Process, Complex Networks.

1 Introduction

Regarding the analysis of Web communication, social and complex networks the fast finding of most influential nodes in a network graph constitutes an important research problem. PageRank remains the most popular characteristic of such influence. We aim to find an extremal index of PageRank whose reciprocal value determines the first hitting time, i.e. a minimal time to reach the first influential node by means of a PageRank random walk. The extremal index $\theta \in [0,1]$ has many other interpretations and plays a significant role in the theory of extreme values. Particularly, the limit distribution of maxima of stationary random variables (r.v.s) depends on θ. For independent r.v.s $\theta = 1$ holds.
θ has a connection to the tail index that shows the heaviness of the tail of a stationary distribution of an underlying process.
Google's PageRank defines the rank $R(X_i)$ of the Web page X_i as

$$R(X_i) = c \sum_{X_j \in N(X_i)} \frac{R(X_j)}{D_j} + (1-c)q_i, \qquad i = 1, ..., n, \tag{1}$$

where $N(X_i)$ is the set of pages that link to X_i (in-degree), D_j is the number of outgoing links of page X_j (out-degree), $c \in (0,1)$ is a damping factor, $q =$

$(q_1, q_2, ..., q_n)$ is a personalization probability vector or user preference such that $q_i \geq 0$ and $\sum_{i=1}^{n} q_i = 1$, and n is the total number of pages, [11]. We omit in (1) the term with dangling nodes for simplicity.
PageRank of a randomly selected page (a node in the graph) with random in- and out-degrees may be considered as a branching process (Cf. [4], [5], [14])

$$R_i = \sum_{j=1}^{N_i} A_j R_i^{(j)} + Q_i, \quad i = 1, ..., n, \tag{2}$$

denoting $R_i = R(X_i)$, $A_j =^d c/D_j$, $Q_i = (1-c)q_i$, [14]. $R_i^{(j)}$ are ranks of descendants of node i, i.e. nodes with incoming links to node i. The r.v. N_i determines an in-degree, i.e. a number of directed edges to the ith node, and a number of nodes in the first generation of descendants belonging to the ith node as a parent, $\{Q_i\}$ is a sequence of i.i.d. r.v.s.
Starting from the initial page (node) X_0, a PageRank random walk determines a regenerative process or Harris recurrent process $\{X_t\}$, letting it visits pages-followers of the underlying node with probability c and it restarts with probability $1-c$ by jumping to a random independent node.
A Max-linear model can be considered as an alternative characteristic of the node influence. This model is obtained by a substitution of sums in Google's definition of PageRank by maxima, i.e.

$$R_i = \bigvee_{j=1}^{N_i} A_j R_i^{(j)} \vee Q_i, \quad i = 1, ..., n, \tag{3}$$

is proposed in [6].
Formally, (2) can be considered as an autoregressive process with the random number N_i of random coefficients and the independent random term Q_i. The extremal index of $AR(1)$ processes with regularly varying stationary distribution and its relation to the tail index were considered in [9]. The extremal index of $AR(q)$, $q \geq 1$ processes with q random coefficients was obtained in [10] in a form which is not convenient for calculations. In [7] the results by [9] were extended to multivariate regularly varying distributed random sequences and the extremal and tail indices of sum and maxima of such sequences with $l \geq 1$ r.v.s were derived.
Our achievements extend and adapt the results by [7] to PageRank and Max-linear processes. The problem concerns the finding of the extremal index of a random graph that models a real network where incoming nodes of the root node may be linked and, hence, be dependent. Such a random graph is called a Thorny Branching Tree (TBT) since any node may have outbound stubs (teleportations) to arbitrary nodes of the network, [4]. In this respect, such a graph cannot be considered as a pure Galton-Watson branching process where descendants of any node are mutually independent and teleportations are impossible.
The paper is organized as follows. In Section 2 we recall necessary results regarding the relation between the tail and extremal indices obtained in [7] for

multivariate random sequences which are regularly varying distributed (Theorems 1 and 2). Linear combinations and maxima of the random sequences of a fixed length are considered and it is derived that they have the same tail and extremal indices. In Section 3 we extend Theorem 2 to the case of unequal tail indices assuming r.v.s of a random sequence (Theorem 3). In Section 4 we consider sequences of random lengths and obtain the tail and extremal indices of their linear combinations and maxima (Theorem 4). We further discuss how these results can be applied to PageRank and the Max-linear processes in Section 5.

2 Related Work

Let $\{R_j\}$ be a stationary sequence with distribution function $F(x)$ and maxima $M_n = \max_{1\le j\le n} R_j$. We shall interpret $\{R_j\}$ as PageRanks of Web pages.

Definition 1. A stationary sequence $\{R_n\}_{n\ge 1}$ is said to have extremal index $\theta \in [0,1]$ if for each $0 < \tau < \infty$ there is a sequence of real numbers $u_n = u_n(\tau)$ such that

$$\lim_{n\to\infty} n(1 - F(u_n)) = \tau \qquad \text{and} \tag{4}$$

$$\lim_{n\to\infty} P\{M_n \le u_n\} = e^{-\tau\theta} \tag{5}$$

hold ([12], p.53).

In [7] the following theorems are proved which we will use to find the extremal and tail indices of PageRank and a Max-linear model. Let $Y_n^{(1)}, Y_n^{(2)}, ..., Y_n^{(l)}$, $n \ge 1$, $l \ge 1$ be sequences of r.v.s having stationary distributions with tail indices $k_1, ..., k_l$ and extremal indices $\theta_1, ..., \theta_l$, respectively, i.e.

$$P\{Y_n^{(i)} > x\} \sim c^{(i)} x^{-k_i} \qquad \text{as} \qquad x \to \infty,$$

where $c^{(i)}$ are some real positive constants.
Let us consider the weighted sum

$$Y_n(z) = z_1 Y_n^{(1)} + z_2 Y_n^{(2)} + ... + z_l Y_n^{(l)}, \qquad z_1, ..., z_l > 0 \tag{6}$$

and denote its tail index by $k(z)$ and extremal index by $\theta(z)$. Supposing that there is a minimal tail index among $k_1, ..., k_l$, the following theorem states the corresponding $k(z)$ and $\theta(z)$.

Theorem 1. *([7]) Let $k_1 < k_i$, $i = 2, ..., l$ hold. Then $Y_n(z)$ has the tail index $k(z) = k_1$ and the extremal index $\theta(z) = \theta_1$.*

In the next theorem it is assumed that sequences $Y_n^{(1)}, Y_n^{(2)}, ..., Y_n^{(l)}$ are mutually independent with equal tail indices $k_1 = ... = k_l = k$. We denote

$$Y_n^*(z) = \max\left(z_1 Y_n^{(1)}, z_2 Y_n^{(2)}, ..., z_l Y_n^{(l)}\right). \tag{7}$$

Theorem 2. *([7]) The sequences $Y_n^*(z)$ and $Y_n(z)$ have the same tail index k and the same extremal index equal to*

$$\theta(z) = \frac{c^{(1)} z_1^k}{c^{(1)} z_1^k + ... + c^{(l)} z_l^k}\theta_1 + ... + \frac{c^{(l)} z_l^k}{c^{(1)} z_1^k + ... + c^{(l)} z_l^k}\theta_l.$$

3 Generalization of Theorem 2

Theorem 3 is a generalization of Theorem 2 to the case of unequal tail indices.

Theorem 3. *Let $\{Y_n^{(j)}\}$, $n \geq 1$, $j = 1, ..., l$ be mutually independent regularly varying r.v.s with tail indices $k_1, ..., k_l$, respectively. Let $k_m < k_i$, $i = 1, ..., l$, $i \neq m$ hold. Then r.v.s $Y_n^*(z)$ and $Y_n(z)$ have the same tail index $k(z) = k_m$ and the same extremal index $\theta(z) = \theta_m$.*

Proof. First we show that

$$P\{Y_n^*(z) > x\} \sim c(z)x^{-k_m}, \qquad x \to \infty, \tag{8}$$

where $c(z) = \sum_{i=1}^{l} c^{(i)} z_i^{k_i} \mathbf{1}\{k_i = k_m\}$. Similar to [7] and as

$$P\{z_i Y_n^{(i)} > x\} \sim c^{(i)} z_i^{k_i} x^{-k_i} \tag{9}$$

holds, we have

$$\begin{aligned}
&P\{Y_n^*(z) > x\} = P\{\max(z_1 Y_n^{(1)}, .., z_l Y_n^{(l)}) > x\} \\
&= 1 - P\{\max(z_1 Y_n^{(1)} \leq x\} \cdot ... \cdot P\{z_l Y_n^{(l)}) \leq x\} \\
&= \sum_{i=1}^{l} P\{z_i Y_n^{(i)} > x\} \\
&+ \sum_{k=2}^{l} (-1)^{k-1} \sum_{i_1 < i_2 < ... < i_k; i_1, i_2, ..., i_k = 1}^{l} P\{z_{i_1} Y_n^{(i_1)} > x\} \cdot ... \cdot P\{z_{i_k} Y_n^{(i_k)} > x\} \\
&\sim \sum_{i=1}^{l} c^{(i)} z_i^{k_i} x^{-k_i} \\
&+ \sum_{k=2}^{l} (-1)^{k-1} \sum_{i_1 < i_2 < ... < i_k; i_1, i_2, ..., i_k = 1}^{l} c^{(i_1)} z_{i_1}^{k_{i_1}} x^{-k_{i_1}} \cdot ... \cdot c^{(i_k)} z_{i_k}^{k_{i_k}} x^{-k_{i_k}} \\
&\sim c(z)x^{-k_m} + o(x^{-k_m}), \qquad x \to \infty.
\end{aligned} \tag{10}$$

Thus, $P\{Y_n(z) > x\} \sim c(z)x^{-k_m}$ follows from Theorem 1.
Now we show that $Y_n^*(z)$ and $Y_n(z)$ have the same extremal index $\theta(z) = \theta_m$. We use the same notations as in [7]

$$\begin{aligned}
M_n^{(i)} &= \max\{Y_1^{(i)}, Y_2^{(i)}, ..., Y_n^{(i)}\}, \ i = 1, .., l; \\
M_n(z) &= \max\{Y_1(z), Y_2(z), ..., Y_n(z)\}, \\
M_n^*(z) &= \max\{Y_1^*(z), Y_2^*(z), ..., Y_n^*(z)\}, \ n \geq 1.
\end{aligned}$$

By (7) it holds

$$\begin{aligned}
M_n^*(z) &= \max\{z_1 Y_1^{(1)}, ..., z_1 Y_n^{(1)}, ..., z_l Y_1^{(l)}, ..., z_l Y_n^{(l)}\} \\
&= \max\{z_1 M_n^{(1)}, ..., z_l M_n^{(l)}\}.
\end{aligned}$$

Then we get

$$P\{M_n^*(z)n^{-1/k} \le x\} = P\{z_1 M_n^{(1)} n^{-1/k} \le x, ..., z_l M_n^{(l)} n^{-1/k} \le x\} \quad (11)$$

Since k_m is the minimal tail index we have

$$P\{z_i M_n^{(i)} n^{-1/k_m} \le x\} = P\{z_i M_n^{(i)} n^{-1/k_i} \le x n^{1/k_m - 1/k_i}\}.$$

It implies

$$z_i M_n^{(i)} n^{-1/k_m} \to^P 0, \quad i = 1, ..., l, \quad i \ne m \ \text{ as } \ n \to \infty \quad (12)$$

since $\lim_{n\to\infty} P\{z_i M_n^{(i)} n^{-1/k_i} \le x\} = \exp(-c^{(i)}\theta_i z_i^{k_i} x^{-k_i})$. By (11) it holds

$$P\{M_n^*(z)n^{-1/k_m} \le x\} \to \exp(-c^{(m)} z_m^{k_m} \theta_m x^{-k_m}), \qquad n \to \infty.$$

Now we have to show that $P\{M_n^*(z)n^{-1/k_m} \le x\} \sim P\{M_n(z)n^{-1/k_m} \le x\}$. Let us denote $u_n = xn^{1/k_m}$. Note that the event $\{M_n^*(z) \le u_n\}$ follows from $\{M_n(z) \le u_n\}$. Then, as in [7], we obtain

$$\begin{aligned} & 0 \le P\{M_n^*(z) \le u_n\} - P\{M_n(z) \le u_n\} \quad (13) \\ &= P\{M_n^*(z) \le u_n\} - P\{M_n^*(z) \le u_n, M_n(z) \le u_n\} \\ &= P\{M_n^*(z) \le u_n, M_n(z) > u_n\} \le \sum_{k=1}^{n} P\{M_n^*(z) \le u_n, Y_k(z) > u_n\} \\ &\le \sum_{k=1}^{n} P\{Y_k^*(z) \le u_n, Y_k(z) > u_n\} = nP\{Y_n^*(z) \le u_n, Y_n(z) > u_n\} \end{aligned}$$

due to the stationarity of the sequences $Y_n^*(z)$ and $Y_n(z)$. Lemma 1 in [7] states that

$$P\{Y_n^*(z) \le u_n | Y_n(z) > u_n\} \to 0, \qquad n \to \infty, \quad (14)$$

for i.i.d. regularly varying $\{Y_n^{(j)}\}$ with equal tail index. This can be extended to the case of unequal $k_1, ..., k_l$. Since

$$nP\{Y_n(z) > u_n\} \to c(z)x^{-k_m}, \qquad n \to \infty, \quad (15)$$

and (14) hold, it follows

$$\lim_{n\to\infty} (P\{M_n^*(z) \le u_n\} - P\{M_n(z) \le u_n\}) = 0.$$

4 Extremal Index of PageRank and the Max-Linear Processes

We denote in (2) R_i as $Y_i(z)$ and $A_j R_i^{(j)} = cR_i^{(j)}/D_j$, $j = 1, ..., N_i$ as $z_j Y_i^{(j)}$. Then we can represent (2) in the form (6) as

$$Y_i(z) = \sum_{j=1}^{N_i} z_j Y_i^{(j)} + Q_i, \qquad i = 1, ..., n, \quad (16)$$

where N_i is a nonnegative integer-valued r.v.. In the context of PageRank $z_j = c$, $j = 1, 2, ..., N_i$, $Q_i = z^* q_i$ with $z^* = 1 - c$ and N_i represents the node in-degree. It is realistic to assume that N_i is a power law distributed r.v. with parameter $\alpha > 0$, i.e.

$$P\{N_i = \ell\} \sim \ell^{-\alpha} \tag{17}$$

and N_i is bounded by a total number of nodes in the network.
The distribution of N_i is in the domain of attraction of the Fréchet distribution with shape parameter $\alpha > 0$ and $P\{N_i > x\} = x^{-\alpha}\ell(x)$, $\forall x > 0$, where $\ell(x)$ is a slowly varying function, since it satisfies a sufficient condition for this property, i.e. the von Mises type condition $\lim_{n\to\infty} nP\{N_i = n\}/P\{N_i > n\} = \alpha$, [1].
Theorem 4 is an extension of Theorems 2 and 3 to maxima and sums of multivariate random sequences of random lengths, that can be applied to PageRank and the Max-linear processes. Let us turn to (16) and denote

$$Y^*_{N_n}(z) = \max(z_1 Y_n^{(1)}, .., z_{N_n} Y_n^{(N_n)}, Q_n),$$
$$Y_{N_n}(z) = z_1 Y_n^{(1)} + .. + z_{N_n} Y_n^{(N_n)} + Q_n.$$

Theorem 4. *Let $\{Y_n^{(j)}\}$, $n \geq 1$, $j = 1, ..., N_n$ and $q_n = Q_n/z^*$ be mutually independent regularly varying i.i.d. r.v.s with tail indices $k > 0$ and $\beta > 0$, respectively, and N_n be regularly varying r.v. with tail index $\alpha > 0$. Let $Y_n^{(1)}$,.., $Y_n^{(N_n)}$ have extremal indices $\theta_1, ..., \theta_{N_n}$, respectively. Then r.v.s $Y^*_{N_n}(z)$ and $Y_{N_n}(z)$ are regularly varying distributed with the same tail index $k(z) = \min(k, \alpha, \beta)$ and the same extremal index $\theta(z)$ such that*

$$\theta(z) = (z^*)^\beta, \quad \textit{if} \;\; k \geq \beta,$$
$$\theta(z) = \sum_{i=1}^{\infty} c^{(i)} \theta_i z_i^k / c(z), \quad \textit{if} \;\; k < \beta, \tag{18}$$

where $c(z) = \sum_{i=1}^{\infty} c^{(i)} z_i^k$ holds.

Proof. We shall show first that

$$P\{Y^*_{N_n}(z) > x\} \sim P\{Y_{N_n}(z) > x\} \sim x^{-\min(k,\alpha,\beta)}. \tag{19}$$

Since r.v.s $\{Y_n^{(j)}\}_{j\geq 1}$ are subexponential and i.i.d. it holds

$$P\{z_1 Y_n^{(1)} + .. + z_{\lfloor x \rfloor} Y_n^{(\lfloor x \rfloor)} > x\} \sim P\{\max(z_1 Y_n^{(1)}, .., z_{\lfloor x \rfloor} Y_n^{(\lfloor x \rfloor)}) > x\}$$
$$\sim xP\{z_1 Y_n^{(1)} > x\}, \qquad x \to \infty, \tag{20}$$

[8]. Due to mutual independence of Q_n and $\{Y_n^{(j)}\}$ and similar to (10) we get

$$P\{Y^*_{N_n}(z) > x\} = P\{Y^*_{N_n}(z) > x, N_n \leq x\} + P\{Y^*_{N_n}(z) > x, N_n > x\}$$
$$\leq P\{Y^*_{\lfloor x \rfloor}(z) > x\} + P\{N_n > x\}$$
$$= 1 - P\{\max(z_1 Y_n^{(1)}, .., z_{\lfloor x \rfloor} Y_n^{(\lfloor x \rfloor)}) \leq x\} P\{Q_n \leq x\} + P\{N_n > x\}$$
$$\sim c_N x^{-\alpha} + c_q (z^*)^\beta x^{-\beta} + c(z) x^{-k} \sim x^{-\min\{k,\alpha,\beta\}}, \tag{21}$$

as $x \to \infty$, where $c_N, c_q > 0$, $c(z) = \sum_{i=1}^{\infty} c^{(i)} z_i^k$. On the other hand,

$$\begin{aligned} & P\{Y^*_{N_n}(z) > x\} \geq 0 + P\{Y^*_{N_n}(z) > x, N_n > x\} \\ & \geq P\{Y^*_{\lceil x \rceil}(z) > x\} + P\{N_n > x\} + P\{Y^*_{\lceil x \rceil}(z) \leq x, N_n \leq x\} - 1 \\ & \sim x^{-\min\{k,\alpha,\beta\}} \end{aligned} \tag{22}$$

holds, since $P\{Y^*_{\lceil x \rceil}(z) \leq x, N_n \leq x\} \to 1$ as $x \to \infty$. Due to (21) and (22) we obtain

$$P\{Y^*_{N_n}(z) > x\} \sim x^{-\min\{k,\alpha,\beta\}}.$$

The same is valid for $Y_{N_n}(z)$ by substitution of the maximum by the sum due to (20). Hence, (19) follows.
Let us prove that $Y^*_{N_n}(z)$ and $Y_{N_n}(z)$ have the same extremal index $\theta(z)$. Let us denote

$$\begin{aligned} & M^*_{N_n}(z) = \max\{Y^*_{N_1}(z), Y^*_{N_2}(z), ..., Y^*_{N_n}(z)\} \\ & = \max\{z_1 Y_1^{(1)}, ..., z_{N_1} Y_1^{(N_1)}, Q_1, ..., z_1 Y_n^{(1)}, ..., z_{N_n} Y_n^{(N_n)}, Q_n\} \end{aligned} \tag{23}$$

and

$$\begin{aligned} M_{N_n}(z) &= \max\{Y_{N_1}(z), Y_{N_2}(z), ..., Y_{N_n}(z)\} \\ &= \max\{z_1 Y_1^{(1)} + ... + z_{N_1} Y_1^{(N_1)} + Q_1, ..., z_1 Y_n^{(1)} + ... + z_{N_n} Y_n^{(N_n)} + Q_n\}. \end{aligned}$$

Without loss of generality we may assume that $N_n = \max\{N_1, ..., N_n\}$. Then we can complete vectors $(z_1 Y_i^{(1)}, ..., z_{N_i} Y_i^{(N_i)})$, $i = 1, 2, ..., n$ by zeros up to the dimension N_n and separate the vector $(Q_1, ..., Q_n)$. We rewrite (23) as

$$\begin{aligned} & M^*_{N_n}(z) = \max\{z_1 Y_1^{(1)}, ..., z_1 Y_n^{(1)}, ..., z_{N_n} \cdot 0, ..., z_{N_n} \cdot 0, ..., z_{N_n} Y_n^{(N_n)}, \\ & Q_1, ..., Q_n\} \\ & = \max(z_1 M_n^{(1)}, z_2 M_n^{(2)}, ..., z_{N_n} M_n^{(N_n)}, M_n^{(Q)}). \end{aligned}$$

Here, $M_n^{(Q)} = \max\{Q_1, ..., Q_n\}$ relates to the second term in the rhs of (16) corresponding to the user preference term Q_i in (2). Following the same arguments as after (11) in Section 3 the statement follows. Really, denoting $k^* = \min\{k, \beta\}$ and $u_n = x n^{1/k^*}$, $x > 0$, we get

$$\begin{aligned} & P\{M^*_{N_n}(z) > u_n\} \\ & = P\{M^*_{N_n}(z) > u_n, N_n > u_n\} + P\{M^*_{N_n}(z) > u_n, N_n \leq u_n\} \\ & \leq P\{M^*_{\lceil u_n \rceil}(z) > u_n\} + P\{N_n > u_n\}. \end{aligned}$$

On the other hand,

$$\begin{aligned} & P\{M^*_{N_n}(z) > u_n\} \geq P\{M^*_{\lceil u_n \rceil}(z) > u_n, N_n > u_n\} \\ & = P\{N_n > u_n\} + P\{M^*_{\lceil u_n \rceil}(z) > u_n\} + P\{M^*_{\lceil u_n \rceil}(z) \leq u_n, N_n \leq u_n\} - 1. \end{aligned}$$

Note that $P\{M^*_{\lceil u_n \rceil}(z) \le u_n, N_n \le u_n\} - 1$ tends to zero as $n \to \infty$. Hence, it holds

$$P\{M^*_{N_n}(z) > u_n\} \sim P\{M^*_{\lceil u_n \rceil}(z) > u_n\} + P\{N_n > u_n\}, \quad n \to \infty. \quad (24)$$

If $k < \beta$ holds, then $M_n^{(Q)} \cdot n^{-1/k^*} \to^P 0$ as $n \to \infty$ since $P\{z_i M_n^{(i)} n^{-1/k} \le x\} \to \exp(-c^{(i)}\theta_i z_i^k x^{-k})$, $i = 1, 2, ...$ Since $P\{N_n > u_n\} \sim u_n^{-\alpha} \to 0$ as $n \to \infty$ holds, then by (24) it follows

$$\lim_{n\to\infty} P\{M^*_{N_n}(z) n^{-1/k^*} \le x\} = \exp\{-c(z)\theta^*(z)x^{-k}\}, \quad (25)$$

where $\theta^*(z) = \sum_{i=1}^{\infty} c^{(i)}\theta_i z_i^k / c(z)$ and $c(z) = \sum_{i=1}^{\infty} c^{(i)} z_i^k$.
If $k \ge \beta$ holds, then $z_i M_n^{(i)} \cdot n^{-1/k^*} \to^P 0$, $i = 1, 2, ...$ follows since $P\{M_n^{(Q)} n^{-1/\beta} \le x\} \to \exp(-c_q (z^*)^\beta x^{-\beta})$ as $n \to \infty$. Thus, we obtain

$$\lim_{n\to\infty} P\{M^*_{N_n}(z) n^{-1/k^*} \le x\} = \exp(-c_q (z^*)^\beta x^{-\beta}). \quad (26)$$

Since $\{q_i\}$ are i.i.d., its extremal index is equal to one. Then by (25) and (26) the extremal index of $Y^*_{N_n}(z)$ satisfies (18) irrespectively of α.
It remains to show that $Y^*_{N_n}(z)$ and $Y_{N_n}(z)$ have the same extremal index. Similarly to [7], we have to derive that

$$\lim_{n\to\infty} P\{M_{N_n}(z) n^{-1/k^*} \le x\} = \lim_{n\to\infty} P\{M^*_{N_n}(z) n^{-1/k^*} \le x\}. \quad (27)$$

Since from the event $\{M_{N_n}(z) \le u_n\}$ it follows $\{M^*_{N_n}(z) \le u_n\}$, and $P\{M_{N_n}(z) \le u_n\} \le P\{M^*_{N_n}(z) \le u_n\}$ holds, we obtain similarly to (13)

$$\begin{aligned}
0 &\le P\{M^*_{N_n}(z) \le u_n\} - P\{M_{N_n}(z) \le u_n\} \\
&= P\{M^*_{N_n}(z) \le u_n\} - P\{M^*_{N_n}(z) \le u_n, M_{N_n}(z) \le u_n\} \\
&= P\{M^*_{N_n}(z) \le u_n, M_{N_n}(z) > u_n\} \\
&= P\{M^*_{N_n}(z) \le u_n, M_{N_n}(z) > u_n, N_n > u_n\} \\
&+ P\{M^*_{N_n}(z) \le u_n, M_{N_n}(z) > u_n, N_n \le u_n\} \\
&\le P\{N_n > u_n\} + P\{M^*_{N_n}(z) \le u_n, M_{\lfloor u_n \rfloor}(z) > u_n, N_n \le u_n\} \\
&\le P\{N_n > u_n\} + \sum_{k=1}^{\lfloor u_n \rfloor} P\{Y_k^*(z) \le u_n, Y_k(z) > u_n\} \\
&= P\{N_n > u_n\} + \lfloor u_n \rfloor P\{Y_k^*(z) \le u_n, Y_k(z) > u_n\} \quad (28)
\end{aligned}$$

due to the stationarity of $\{Y_k^*(z)\}$ and $\{Y_k(z)\}$.
Completing vectors $(z_1 Y_k^{(1)}, ..., z_{N_k} Y_k^{(N_k)})$ by zeroes up to the maximal dimension $\lfloor u_n \rfloor$, we get

$$\begin{aligned}
P\{Y_k^*(z) \le u_n, Y_k(z) > u_n\} = P\{&\max(z_1 Y_k^{(1)}, ..., z_{\lfloor u_n \rfloor} Y_k^{(\lfloor u_n \rfloor)}, Q_k) \le u_n, \\
&z_1 Y_k^{(1)} + ... + z_{\lfloor u_n \rfloor} Y_k^{(\lfloor u_n \rfloor)} + Q_k > u_n\}
\end{aligned}$$

Then (27) follows from (14) and (15) since in (28)

$$P\{Y_k^*(z) \le u_n, Y_k(z) > u_n\} = P\{Y_k(z) > u_n\} P\{Y_k^*(z) \le u_n | Y_k(z) > u_n\}$$

holds.

5 Application to Indices of Complex Networks

Theorem 4 can be applied to PageRank and the Max-linear processes. These processes then have the same tail index and the same extremal index. Theorem 4 is in the agreement with statements in [5] and [14], namely, that the stationary distribution of PageRank $R =^d \sum_{j=1}^{N_i} A_j R_i^{(j)} + Q_i$ is regularly varying and its tail index is determined by a most heavy-tailed distributed term in the triple $(N_i, Q_i, A_i R_i^{(j)})$. This is derived if all terms in the triple are mutually independent. In contrast, Theorem 4 is valid for an arbitrary dependence structure between N_n and $\{Y_n^{(j)}\}$ as well as N_n and Q_n, and $\{N_i\}$ are not necessarily independent. The novelty of Theorem 4 is that the extremal index of both PageRank and the Max-linear processes is the same and it depends on the tail indices in the couple $(Q_i, A_i R_i^{(j)})$, irrespective of the tail index of N_i. The assumptions of both Theorem 4 and the statements in [5] and [14] do not reflect properly the complicated dependence between node ranks due to the entanglement of links in a real network. For better understanding let us consider the matrix

$$\begin{pmatrix} z_1 Y_1^{(1)} & z_2 Y_1^{(2)} & ... z_{N_1} Y_1^{(N_1)} & 0 & 0 & Q_1 \\ z_1 Y_2^{(1)} & z_2 Y_2^{(2)} & ... z_{N_1} Y_2^{(N_1)} & ... z_{N_2} Y_2^{(N_2)} & 0 & Q_2 \\ ... & ... & ... & ... & ... & ... \\ z_1 Y_n^{(1)} & z_2 Y_n^{(2)} & ... z_{N_1} Y_n^{(N_1)} & ... z_{N_2} Y_n^{(N_2)} & ... z_{N_n} Y_n^{(N_n)} & Q_n \end{pmatrix}$$

$$\big((k, \theta_1)\ (k, \theta_2)\ ... (k, \theta_{N_1})\ ... (k, \theta_{N_2})\ ..... (k, \theta_{N_n})\ ... (\beta, (z^*)^\beta) \big)$$

corresponding to (16) and completed by zeros up to the maximal dimension, let's say N_n. Strings of the matrix correspond to generations of descendants of nodes with numbers $1, 2, ..., n$. Each column may contain descendants of different nodes having the same extremal index θ_i, $i = 1, 2, ..., N_n$. All columns apart of the last one are identically regularly varying distributed with the same tail index k. The columns are mutually independent.

In terms of some network, the conditions of Theorem 4 imply that ranks of all nodes with incoming links to a root node (i.e. its followers) are mutually independent, but followers of different nodes may be dependent and, thus, they are combined into clusters. The reciprocal of the extremal index approximates the mean cluster size, [12].

The statement (18) implies that the extremal index of PageRank is equal to $\theta(z) = (1 - c)^\beta$ if the user preference dominates (i.e. its distribution tail is heavier than the tail of ranks of followers). If the damping factor c is close to one, then $\theta(z)$ is close to zero. The latter means the huge-sized cluster of nodes around a root-node in the presence of rare teleportations. If c is close to zero, then $\theta(z)$ is close to one due to the independence of frequent teleportations. If $k < \beta$ holds, then roughly, the mean size of the cluster is determined by the consolidation of all clusters related to the followers of the underlying root.

In practice, the followers of a node may be linked and their ranks can therefore be dependent. The future work will focus on the extremal index of PageRank process when the terms $\{Y_i^{(j)}\}$ in (16) are mutually dependent.

References

1. C.W. Anderson. Local limit theorems for the maxima of discrete random variables. *Mathematical Proceedings of the Cambridge Philosophical Society*, 88, 161–166, 1980.
2. K. Avrachenkov, N. M. Markovich and J.K. Sreedharan. Distribution and Dependence of Extremes in Network Sampling Processes. *Computational Social Networks*, 2, 12, 1–21, 2015.
3. G.L. O'Brien. Extreme values for stationary and Markov sequences. *The Annals of Probability*, 15, 1, 281–291, 1987.
4. N. Chen, N. Litvak and M. Olvera-Cravioto. PageRank in Scale-Free Random Graphs. *WAW 2014, LNCS 8882, ed. A. Bonato et al.*, Springer, Switzerland, 120–131, 2014.
5. P. R. Jelenkovic and M. Olvera-Cravioto. Information ranking and power laws on trees. *Advances in Applied Probability*, 42(4), 1057–1093, 2010.
6. N. Gissibl and C. Klüppelberg. Max-linear models on directed acyclic graphs. *arXiv:1512.07522v1[math.PR]*, 1–33, 2015.
7. A.A. Goldaeva Indices of multivariate recurrent stochastic sequences. *In book ed. Shiryaev A. N.: Modern problem of mathematics and mechanics*, Vol. VIII. Issue 3, 42–51, 2013, Moscow state university ISBN 9785211056527 (In russian)
8. C.M. Goldie and C. Klüppelberg. Subexponential Distributions, A Practical Guide to Heavy Tails, eds R. Adler, R. Feldman and M.S. Taqqu, Birkhäuser, Boston, MA, 435–459, 1998
9. L. de Haan, S. Resnick, H. Rootzén and G. de Vries. Extremal behaviour of solutions to a stochastic difference equation with applications to ARCH processes. *Stochastic Processes and Applications*, 32, 213–224, 1989.
10. C. Klüppelberg and S. Pergamenchtchikov. Extremal behaviour of models with multivariate random recurrence representation. *Stochastic Processes and their Applications*, 117, 432-456, 2007.
11. A. N. Langville and C. D. Meyer. *Google's PageRank and Beyond: The Science of Search Engine Rankings*, Princeton University Press, 2006.
12. M.R. Leadbetter, G. Lingren and H. Rootzén. *Extremes and Related Properties of Random Sequence and Processes*, ch.3, Springer, New York, 1983.
13. H. Rootzén. Maxima and exceedances of stationary markov chains. *Advances in Applied Probability*, 20, 371–390, 1988.
14. Y.V. Volkovich and N. Litvak. Asymptotic analysis for personalized web search. *Advances in Applied Probability*, 42(2), 577–604, 2010.

Comparing the computational complexity of different matrix exponential algorithms in R

Meabh G. McCurdy, Adele H. Marshall, and Karen J. Cairns

Mathematical Science Research Centre, School of Mathematics and Physics, Queens University Belfast, Northern Ireland
(E-mail: mmccurdy01@qub.ac.uk)

Abstract. The calculation of the exponential of a matrix is arguably the most widely used and widely studied matrix function. This is due to the key role it plays in finding solutions to differential equations. The major issue with this matrix operator is the computational time, which gets progressively worse as the dimensions of the matrix increase. Scaling and squaring combined with a Padé approximation is the most commonly used approach within software such as R and Matlab. However this approach becomes problematic when the matrix is large and sparse in nature. Krylov subspace methods are the latest efficient emerging approach used for calculating the matrix exponential. This paper aims at comparing the different algorithms used to calculate both the exponential of a matrix in isolation and with the product of a vector. A comparison study is carried out to determine the most efficient technique resulting in the fastest computational time.
Keywords: Matrix, Exponential, Computational, Efficient, Krylov.

1 Introduction

This paper will focus on the matrix exponential operator, with a particular interest in the computational complexity. The exponential of a matrix can be calculated in numerous ways, most of which when looking at issues such as efficiency and computational stability are of very little practical use, Moler and Van Loan [1]. This paper will provide a brief introduction to the theory behind this matrix operator and look at one of the most popular methods in more detail, the scaling and squaring method combined with the Padé approximation. Details of the implementation of this method in R will also be discussed. Krylov subspace methods will be introduced, which are seen as a new emerging technique used to compute the matrix exponential, Moler and Van Loan [2]. The theory of these methods along with the software that implements them will be discussed. Such methods are aimed at reducing the computational challenge with the matrix exponential. Results of a simulation study interested in the comparison of computational timing between the current existing methods within software such as R and the new Krylov subspace techniques will also be provided and further discussed.

2 Matrix Exponential

The calculation of the matrix exponential is arguably the most commonly used and most widely studied matrix function, Higham [3]. The main interest in

this matrix operator is a result of the key role it plays in finding solutions to ordinary differential equations (ODE) within many different application areas. If $\mathbf{A}$ is a fixed, real or complex $n \times n$ matrix, this leads to the following ODE.

$$\dot{\mathbf{x}}(t) = \mathbf{A}\mathbf{x}(t) \tag{1}$$

Solving equation (1) requires the matrix exponential to be computed. The solution to this ODE must satisfy the initial condition, $\mathbf{x}(0) = \mathbf{x}_0$ and is therefore given by $\mathbf{x}(t) = e^{\mathbf{A}t}\mathbf{x}_0$ where $e^{\mathbf{A}t}$ can be defined using the power series, which is one of the nineteen methods examined in Moler and Van Loan [1].

$$e^{\mathbf{A}t} = I + \mathbf{A}t + \frac{\mathbf{A}^2t^2}{2!} + \frac{\mathbf{A}^3t^3}{3!} + ... \tag{2}$$

The importance of equation (1), although difficult to compute, has resulted in a growing interest in the matrix exponential operator along with an increased number of methods available. Many of these methods can be found in both of Moler and van Loan's review papers 'Nineteen dubious ways to compute the exponential of a matrix' [1, 2], where the second publication is an updated version of the first, twenty-five years later. In both of their review papers Moler and Van Loan categorised each of the nineteen methods into one of five categories: matrix decomposition methods, polynomial methods, series methods, differential equation methods and splitting methods. A lot of these methods are of very little practical use, hence why many would agree with Moler and Van Loan's classification of these methods as 'dubious'.

For problems that require the calculation of $e^{\mathbf{A}t}$ repeatedly where $\mathbf{A}$ is large, the most efficient matrix decomposition methods are those that are centred around the decomposition or factorisation of matrix $\mathbf{A}$. However one of the drawbacks associated with these methods is that of stability. Polynomial methods are limited to a certain type of problem. This is due to most of these methods requiring the calculation of a characteristic polynomial. Other types of polynomial methods have stability issues, similar to those of matrix decomposition methods but are much less efficient. Ordinary differential equation methods while easy to use, are very computational expensive.

Originally Moler and Van Loan highlighted the fact that due to a lack of research into using splitting methods to compute the matrix exponential led to the conclusion that these methods are both speculative and untried. However twenty-five years later these methods have been linked to numerical partial differential equation problems, Celledoni and Iserles [4]. From the three series methods, Moler and Loan originally suggested that the only competitive approach was the scaling and squaring method which was still the case twenty-five years later, commenting that this method continues to attract more attention in relation to the other eighteen methods. This method was introduced by Al-Mohy and Higham [5] and incorporates an already established method, the Padé approximation in between the scaling and squaring operations.

3 Padé Approximation

Padé approximations can be derived by expanding a function as a ratio of two power series, Deb *et al* [6]. Given $\mathbf{A}$ is an $n \times n$ matrix, the (k, m) Padé approximation for calculating the exponential of $\mathbf{A}$ is given by r_{km}, Moler and Van Loan [1].

$$r_{km}(\mathbf{A}) = \frac{p_{km}(\mathbf{A})}{q_{km}(\mathbf{A})} \tag{3}$$

where

$$p_{km}(\mathbf{A}) = \sum_{j=0}^{k} \frac{(k+m-j)!k!}{(k+m)!j!(k-j)!}\mathbf{A}^j \tag{4}$$

$$q_{km}(\mathbf{A}) = \sum_{j=0}^{k} \frac{(k+m-j)!m!}{(k+m)!j!(m-j)!}(-\mathbf{A})^j \tag{5}$$

It was suggested by Moler and Van Loan to use the Padé diagonal approximations, meaning $k = m$. One reason for this suggestion is that supposing one had $k \neq m$, say $k > m$. The calculation of r_{km} (defined in equation (1)), has order $k + m$ which takes the same computational time as the calculation of r_{mm}. However this approximation has order $2m > k + m$.

Throughout the literature it is known that Padé approximations are favourable when calculating the matrix exponential of small dense matrices. One of the major drawbacks with the Padé approximation method, along with the computational costs, is that they are only accurate when near the origin, Stewart [7]. When the eigenvalues of $\mathbf{A}$ are widely spread this results in computing $r_{km}(\mathbf{A})$ involving an ill-conditioned linear system. This issue can be resolved by performing a scaling operation and is one of the major benefits for using the Padé approximation combined with the scaling and squaring method.

4 Scaling and Squaring

The scaling and squaring method is arguably the most widely used method for computing the exponential of a matrix, Higham [8]. The round-off errors that occur when implementing the Taylor series and the computational costs of the Padé approximants both increase as $t\|\mathbf{A}\|$ increases. However when implementing the scaling and squaring method both these issues can be controlled by exploiting the relation $e^{\mathbf{A}} = (e^{\mathbf{A}/\sigma})^{\sigma}$, for $\mathbf{A} \in \mathbb{C}^{n\times n}$ and $\sigma \in \mathbb{C}$. This relation can be combined with the fact that the Padé approximant for $e^{\mathbf{A}}$ when $\|\mathbf{A}\|$ is small, is good when it is near the origin. The scaling and squaring method has many different implementations, which is a direct result of the variation in the order of the error analysis in the algorithm.

This method is as follows: firstly reduce the norm of matrix $\mathbf{A}$ to order 1. To ensure this norm of $\mathbf{A}/\sigma$ is achieved, σ is chosen to be an integral power of 2, therefore $\sigma = 2^s$. A Padé approximant to the scaled matrix exponential, $e^{\mathbf{A}/2^s}$, is then obtained using a $[k/m]$ Padé approximant of the exponential.

$$e^{\mathbf{A}/2^s} \approx r_{km}(\mathbf{A}/2^s) \tag{6}$$

To obtain the exponential of the original matrix $\mathbf{A}$, the Padé approximant is squared s times, where the value of s is equal to the s used to obtain σ. Therefore squaring the Padé approximant s times will undo any effects the scaling process may have had on the matrix.

$$e^{\mathbf{A}} \approx r_{km}(\mathbf{A}/2^s)^{2^s} \tag{7}$$

One of the advantages of using this method is that all the possible $[k/m]$ Padé approximants $r_{km} = p_{km}(\mathbf{A})/q_{km}(\mathbf{A})$ for the exponential function are known for all values of k and m. This $r_{km}(\mathbf{A})$ equation therefore satisfies the definition of the Padé approximant.

The Taylor series method can also be used in some cases to compute the matrix exponential of the scaled matrix in place of the Padé approximation, Sastre *et al* [9]. However as previously mentioned the scaling and squaring method combined with a Padé approximation has become the most widely used method, with it being the default method in both Matlab and R.

In the initial scaling stage, $\mathbf{A} \to \mathbf{A}/2^s$, the main aim is to choose s, such that the matrix computation is completed with minimal cost while at the same time producing a backward error that is restricted by a unit round-off. While Golub and Van Loan [10] suggested that $\|\mathbf{A}\| \leq 1/2$, Higham [8] agreed that there were good motives behind this assumption, however went on to adapt these ideas to obtain a bound that makes no prior assumptions on $\|\mathbf{A}\|$.

In Moler and Van Loan's second review paper [2], new emerging methods and algorithms were added to the original nineteen. One of these additional methods was the Krylov subspace methods.

5 Krylov Subspace Methods

Many problems within scientific computing that involve large sparse matrices can now be solved with the use of Krylov subspace methods, Philippe and Reichel [11]. These methods can be applied to various problems such as solving large systems of linear equations or for finding eigenvalues of large sparse matrices and more recently for calculating the exponential of matrices. However this was not the initial intention of Krylov subspace methods. These methods were

motivated by an application involving the analysis of oscillations of mechanical systems, Liesen and Strakos [12]. The origins for the Krylov subspace can be traced back to the Cayley-Hamilton theorem, which states that every square matrix satisfies it's own characteristic equation, Bellman [13]. Given matrix $\mathbf{A}$ with dimensions $n \times n$ the associated characteristic polynomial is defined as:

$$p(\lambda) = det(\lambda \mathbf{I} - \mathbf{A}) \tag{8}$$

One of the major advantages of using Krylov subspace methods are that they avoid performing matrix-matrix operations and instead perform matrix-vector operations. This is seen as beneficial particularly when reducing the computational time required to calculate the matrix exponential. Another attractive quality with Krylov methods are that they allow the computation of the matrix exponential with the product of a vector without explicitly having to calculate the matrix exponential in full, Sidje and Stewart [14].

Consider a large linear system given by

$$\mathbf{Ax} = \mathbf{b} \tag{9}$$

where $\mathbf{A}$ is a non-singular $n \times n$ matrix and $\mathbf{b}$ is an n-vector, where n is large. Krylov subspaces can be beneficial when n is large and one cannot afford to solve the system using Gaussian elimination by performing n^3 operations or even when one does not have direct access to the full matrix but only the product of $\mathbf{Av}$, where $\mathbf{v}$ is an n-vector.

The Krylov subspace generated by $\mathbf{A}$ and $\mathbf{b}$ is the subspace spanned by the vectors of the Krylov sequence, Krylov and Stewart [15]:

$$\mathcal{K}_m = \text{span}\{\mathbf{b}, \mathbf{Ab}, \mathbf{A}^2\mathbf{b}, ..., \mathbf{A}^{m-1}\mathbf{b}\} \tag{10}$$

This method seeks to find an approximate solution $\mathbf{x_m}$ from a subspace $\mathbf{x_0}+\mathcal{K}_m$ of dimension m which is achieved by imposing the Petrov-Galerkin condition, where $\mathcal{L}_m$ is a subspace of dimension m.

$$\mathbf{b} - \mathbf{Ax_m} \perp \mathcal{L}_m \tag{11}$$

In order to achieve a desired solution a Krylov method starts with an initial guess, $\mathbf{x_0}$, then bootstraps its way up to a more accurate approximation $\mathbf{x_k}$. One approach to finding $\mathbf{x}$ is to firstly compute the initial residual, $\mathbf{r_0}$.

$$\mathbf{r_0} = \mathbf{b} - \mathbf{A}\mathbf{x_0} \tag{12}$$

A Krylov method is one in which the subspace $\mathcal{K}_m$ is given by the Krylov subspace

$$\mathcal{K}_m(\mathbf{A}, \mathbf{r_0}) \equiv \text{span}\{\mathbf{r_0}, \mathbf{A}\mathbf{r_0}, ..., \mathbf{A}^{m-1}\mathbf{r_0}\}$$

It is also assumed in this Krylov subspace that the positive integer m is much smaller than n. This m-th Krylov subspace associated with $\mathbf{A}$ and $\mathbf{r_0}$ is denoted by $\mathcal{K}_m(\mathbf{A}, \mathbf{r_0})$, Saad [16].

5.1 Matrix Exponential

The exponential of a matrix, as previously mentioned, is a complex operation and often computationally expensive to implement. However many application areas only need the product $e^{\mathbf{A}}\mathbf{v}$, for some vector $\mathbf{v}$ rather than the exponential of the matrix $e^{\mathbf{A}}$. This can be seen when solving the initial value problem.

$$\dot{\mathbf{x}} = \mathbf{A}\mathbf{x}, \quad \mathbf{x}(0) = \mathbf{x_0} \tag{13}$$

Where the solution for equation (13) is given by $\mathbf{x}(t) = e^{\mathbf{A}t}\mathbf{v}$.

The theory behind using Krylov subspace methods to compute $e^{\mathbf{A}}\mathbf{v}$ is to approximately project $e^{\mathbf{A}}$ onto a small Krylov subspace. Considering the calculation $e^{\mathbf{A}}\mathbf{v}$, one has the following approximation.

$$e^{\mathbf{A}}\mathbf{v} \approx p_{m-1}(\mathbf{A})\mathbf{v} \tag{14}$$

Where p_{m-1} is a polynomial of degree $m-1$. One can write the approximation to $\mathbf{x} = e^{\mathbf{A}}\mathbf{v}$ as $\mathbf{x_m} = \mathbf{V_m}\mathbf{y}$, where $\mathbf{y}$ is an m-vector. Gallopoulos and Saad [17] suggested the choice for $\mathbf{y}$ should be $\mathbf{y} = \beta e^{\mathbf{H_m}}\mathbf{e_1}$, which resulted in the following formula:

$$e^{\mathbf{A}}\mathbf{v} \approx \beta \mathbf{V_m} e^{\mathbf{H_m}}\mathbf{e_1} \tag{15}$$

The $\mathbf{H_m}$ matrix in equation (15) is the Hessenberg matrix produced as a result of implementing the Arnoldi iteration [18]. The structure and properties of matrix $\mathbf{A}$ are crucial when deciding on the appropriate Krylov subspace method to utilise. If matrix $\mathbf{A}$ was Hermitian this would result in $\mathbf{H_m} \equiv \mathbf{T_m}$, where $\mathbf{T_m}$ is a tridiagonal matrix. The process for dealing with these types of matrices is known as the Lanczos iteration [19].

5.2 Iterations

There are different types of Krylov subspace methods which is a result of the different choices for the subspace $\mathcal{L}_m$, seen in equation (11). The Arnoldi iteration was first introduced as a direct algorithm for reducing a general matrix into upper Hessenberg form. However it was then discovered that this algorithm was a good approach for approximating eigenvalues of large sparse, non-Hermitian matrices. The Arnoldi iteration is a type of Krylov subspace method used when the matrix involved is non-Hermitian or unsymmetric. The Lanczos iteration can be thought of as a simplification of the Arnoldi iteration, where matrix $\mathbf{A}$ is symmetric. This algorithm can be applied to the eigenvalue problem, $\mathbf{Ax} = \lambda\mathbf{x}$, where $\mathbf{A}$ is a Hermitian, or when dealing with the real case a symmetric, matrix.

6 Software

Computing the exponential of a matrix can be efficiently obtained using various software environments. This degree of efficiency is heavily dependent on both the algorithm being implemented and within what software environment. This issue of efficiency will be later explored through results obtained from a comparison study. As a result of the rise in interest into this matrix research area, well established software environments such as Matlab and R have their own inbuilt functions to calculate this matrix exponential operator.

In Matlab the function expm can be used to calculate the matrix exponential. This function implements Al-Mohy and Higham's [20] scaling and squaring algorithm. The Matlab directory also contains three older functions for matrix exponentials; expodemo1, expodemo2 and expodemo3. These methods implement an older version of the scaling and squaring method, Golub and Van Loan [21], the Taylor series and a matrix decomposition method using eigenvectors respectively. Another software environment that can be utilised to compute the matrix exponential is R. This software has specific packages designed to compute this matrix operator, one being the expm package, Goulet *et al* [22]. This package includes functions to compute both $e^{\mathbf{A}}$ and $e^{\mathbf{A}t}v$ given by expm and expAtv respectively. The expm function has various different algorithms available with the default method being Higham08.b which is Higham's scaling and squaring method with balancing [8]. The expAtv function implements a Krylov routine also found within the Expokit software.

Another additional update added to Moler and Van Loan's second review paper on matrix exponential methods along with Krylov subspace methods was the software Expokit, Sidje [23]. This package computes the exponential of both real and complex matrices. The usage of Expokit is not as mainstream as Matlab and R, however has the advantage of being able to efficiently handle small dense matrices and large sparse matrices. The small dense matrices are computed using either the Padé approximation or Chebyshev approximation. Krylov subspace methods play an important role in the routines implemented

to deal with large sparse matrices. The Expokit at the time of release was not available in R, only Matlab and Fortran, however these Krylov subspace methods can now be implemented within an R environment through the utilisation of the R package Rexpokit.

The creation of the R package Rexpokit by Matzke and Sidje [25] enables the Expokit code to be implemented in R. This package includes wrappers that call in the original Fortan code. This R package similar to Expokit has routines to deal with both small dense and large sparse matrices.

7 Comparison

A study of the current methods available in R for the product of the matrix exponential with a vector $e^{\mathbf{A}t}$, has been carried out. This study is conducted to identify which method is the most efficient when interested in computational time. There were three functions included in the study. The first was the expm function which implemented the Higham08.b algorithm. The second was the expAtv function which implemented a Krylov routine written in R code and the third was the expokit_dgexpv_Qmat function within the Rexpokit package which also implemented a Krylov routine called in from fortran. In order to accurately compare these methods, matrices of varying dimensions are simulated from a linear birth-death Markov process with immigration, Sidje and Hansen [26].

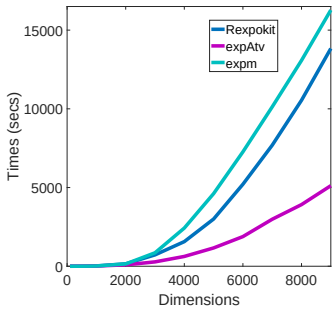

Fig. 1. Computational times for functions in Rexpokit and expm

From Fig.1 one can see that the current expAtv function in the expm package is the most efficient while the expm function is the least efficient. This result is not surprising as the expAtv function is designed to specifically calculate the product of the matrix exponential with a vector. The Rexpokit method in Fig.1 appears to be quite inefficient, with a computational time over twice as long for that of expAtv. This study was carried out for a second time but with the addition of a new function kexpmv, which is essentially a different method for running the Expokit code within an R environment.

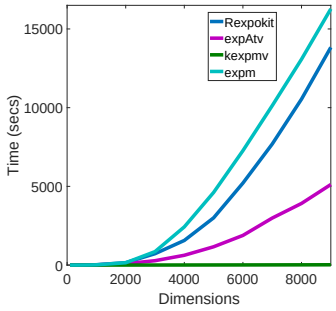

Fig. 2. Computational times for four different functions.

From Fig.2 one can see that the kexpmv method is now the most efficient method for computing the product of the matrix exponential with a vector. Due to the computational performance of kexpmv being a lot faster in comparison to the other three methods, the kexpmv times are plotted in isolation in Fig.3. This is to show how this method performs when the dimension of the matrix increases.

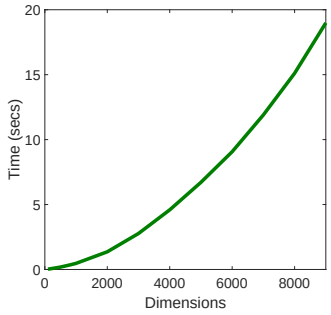

Fig. 3. Computational times for KEXPMV.

In conclusion, as previously mentioned the matrix exponential operator is the most widely used and widely studied matrix function, which is reflected in the vast number of methods available to compute this matrix operator. The majority of these methods as recorded within the literature are of little practical use when looking at issues such as computational time and efficiency. Krylov methods are the latest emerging technique used to compute the matrix exponential and as seen from Fig.2 when implementing the Expokit code within an R environment, paying particular attention to the computational time, the kexpmv method is the most efficient method.

From the simulation study one can conclude that the size of the matrix will affect the computational complexity of the calculation as expected. However

an interesting investigation would be to look into the structure and density of the matrix and determine if these factors also have an impact on the computational complexity. Therefore mathematically defining the term 'small dense' and 'large sparse' matrices. An important issue when looking at sparsity and the algorithms used to compute the exponential of sparse matrices is how they store the matrix. This will have a major impact on the computational time if not stored efficiently.

References

1. C. Moler and C. Van Loan. Nineteen dubious ways to compute the exponential of a matrix. *SIAM review*, 20(4), 801-836, 1978.
2. C. Moler and C. Van Loan. Nineteen dubious ways to compute the exponential of a matrix, twenty-five years later. *SIAM review*, 45(1), 3-49, 2003.
3. N.J. Higham. Functions of matrices: theory and computation. *SIAM*, 2008.
4. E. Celledoni and A. Iserles. Methods for the approximation of the matrix-exponential in a Lie-algebraic setting. *IMA J. Numer. Anal.*, 21, pp. 463-488, 2001.
5. A.H Al-Mohy and N.J. Higham. A new scaling and squaring algorithm for the matrix exponential. *SIAM journal on Matrix Analysis and Applications*, 31(3), 970-9893, 2009.
6. A. Deb, S. Roychoudhury and G. Sarkar. Analysis and Identification of Time-Invariant Systems, Time-Varying Systems, and Multi-Delay Systems using Orthogonal Hybrid Functions: Theory and Algorithms with MATLAB ®. *Springer*, Vol. 46, 2016.
7. W.J. Stewart. Probability, Markov chains, queues, and simulation: the mathematical basis of performance modeling. *Princeton University Press*.
8. N.J. Higham. The Scaling and Squaring Method for the Matrix Exponential Revisited. *SIAM Journal on Matrix Analysis and Applications*, 26(4), 1179-1193, 2005.
9. J. Sastre, J. Ibánez, E.Defez and P. Ruiz. New scaling-squaring taylor algorithms for computing the matrix exponential. *SIAM Journal on Scientific Computing*, 37(1), A439-A455, 2015.
10. G.H. Golub and C.F Van Loan. Matrix computations *The John Hopkins University Press, Baltimore, MD*, 374-426, 1996.
11. B. Philippe and L. Reichel. On the generation of Krylov subspace bases *Applied Numerical Mathematics*, 62(9), 1171-1186, 2012.
12. J. Liesen and Z. Strakos. Krylov subspace methods: principles and analysis *Oxford University Press*, 2012.
13. R. Bellman. Introduction to matrix analysis *Society for Industrial and Applied Mathematics*, 1997.
14. R.B Sidje and W.J. Stewart. A numerical study of large sparse matrix exponentials arising in Markov chains *Computational statistics & data analysis*, 29(3), 345-368, 1999.
15. A.N. Krylov and W.J. Stewart. On the numerical solution of the equation by which the frequency of small oscillations is determined in technical problems *Izv. Akad. Nauk SSSR Ser. Fiz.-Mat 4*, 491-539, 1931.
16. Y. Saad. Overview of Krylov subspace methods with applications to control problems , 1989.
17. E. Gallopoulos and Y. Saad. On the parallel solution of parabolic equations *Proceedings of the 3rd international conference on Supercomputing*, ACM, 1989.

18. W.E. Arnoldi. The principle of minimized iterations in the solution of the matrix eigenvalue problem *Quarterly of Applied Mathematics*, 9(1), 17-29, 1951.
19. C. Lanczos. An iteration method for the solution of the eigenvalue problem of linear differential and integral operators *Los Angeles, CA: United States Governm. Press Office*, 1950.
20. A.H. Al-Mohy and N.J. Higham. A new scaling and squaring algorithm for the matrix exponential *SIAM Journal on Matrix Analysis and Applications*, 26(4), 1179-1193, 2009.
21. G.H. Golub and C.F Van Loan. Matrix computations *JHU Press*, Vol. 3, 2012.
22. V. Goulet, C. Dutang, M. Maechler, D. Firth, M. Shapira and M. Stadelmann. expm: Matrix exponential, R package version 0.99-0, 2013.
23. R.B. Sidje. Expokit software, http://www.maths.uq.edu.au/expokit.
24. R.B. Sidje. Expokit: Software Package for Computing Matrix Exponentials *ACM Transactions on Mathematical Software (TOMS)*, 24(1), 130-156, 1998.
25. N.J. Matzke and R.B. Sidje. Package rexpokit, 2003.
26. R.B. Sidje and N.R Hansen. Package expoRkit, 2012.

Data Analysis and Nanoliquid Thin Film Flow over an Unsteady Stretching Sheet in Presence of Magnetic Field

Prashant G Metri[1] and Sergei Silvestrov[1]

Division of Applied Mathematics, UKK, Mälardalen University, Västerås, Sweden.
(E-mail: prashant.g.metri@mdh.se, sergei.silvestrov@mdh.se)

Abstract. This paper presents a mathematical analysis of nanoliquid thin film flow over an unsteady stretching sheet in presence of magnetic field. The flow of thin fluid film and subsequent heat transfer from stretching surface is investigated with the aid of similarity transformations. The resulting non-linear ordinary differential equations are solved numerically using Runge-Kutta-Fehlberg and Newton-Raphson schemes based shooting technique. A relationship between film thickness β and the unsteadiness parameter S is found. Besides, the effect of unsteadiness parameter S, the solid volume fraction of nanoliquid ϕ, Prandtl number Pr and the magnetic field parameter M on the temperature distributions are presented and discussed in detail. Present analysis shows the combined effect of magnetic field and viscous dissipation is to enhance the thermal boundary layer thickness.
Keywords: Boundary layer flow, Nanoliquid, Magnetic field, Similarity transformation, Thin film, Unsteady stretching sheet.

1 Introduction

The study of heat transfer phenomena within a thin liquid film due to a stretching of a sheet has several applications in many industrial processes. The main application of such flows in a coating processes such as in wire and fiber coatings. All the coating processes demand a smooth glossy surface to meet the requirements for the best appearance and optimum service properties such as low friction transparency, strength etc. In a melt spinning process, the extrudate from the die is generally drawn and simultaneously stretched into a filament or sheet, which is then solidified through rapid quenching or gradual cooling by direct contact with water or chilled metal rolls. In fact, stretching imparts a unidirectional orientation to the extrudate, thereby improving its mechanical properties as the quality of the final product greatly depends on the rate of cooling. Essentially, the cooling procedure should be effectively controlled to obtain the desired quality of the final product, and the cooling rate is significantly influenced by the fluid flow and heat transfer mechanism.

In view of these applications, the boundary layer equation is considered and the boundary conditions are prescribed at the sheet and at infinity. [4] initiated the study of hydrodynamics of thin liquid film over a stretching sheet by reducing the unsteady Navier–Stokes equations to non-linear ordinary differential equations by means of similarity transformations and solved the resulting differential equations using a multiple shooting method. Santra et al. [5] analyzed

the thermocapillary effects on unsteady thin film flow over a heated horizontal stretching sheet. The effect of thermocapillary in the temperature distrubution in stretching direction decreases at higher values of Prandtl number and Biot number.

All the above investigations were restricted to the laminar flow of Newtonian fluids. However, in the recent past, nanofluids have attracted the attention of the science and engineering community because of their possible applications in industries. Nanotechnology is an emerging science that is extensive use in industry due to the unique chemical and physical properties that nano-sized materials possess. These fluids are colloidal suspensions, typically metals, oxides, carbides, or carbon nanotubes in a base fluid, etc. Common base fluids include water and ethylene glycol. Nanofluids have properties that make them potentially useful in many heat transfer processes including microelectronics, fuel cells, pharmaceutical processes and hybrid powered engines. They exhibit enhanced thermal conductivities and heat transfer coefficients compared to the base fluids. For this reason nanofluids can often be preferred to conventional coolants like oil, water and ethylene glycol mixtures [6]. Mahesha et al. [7] studied the laminar flow of a thin film of a nanoliquid over an unsteady stretching sheet is considered. An effective medium theory (EMT) based model is used for the thermal conductivity of the nanoliquid. A parametric study that deals with the effect of the unsteadiness parameter and the nanoparticle volume fraction on the dynamics of the liquid film. Maity et al. [8] investigated two-dimensional flow of a thin nanoliquid film over an unsteady stretching sheet is studied under the assumption of planar film thickness when the sheet is heated/cooled along the stretching direction. It is observed that there exists a boundary demarcating the region of heat transfer within the film. One side of this boundary heat is transported into the film, while on the other side heat is transported out of the film. Depending on the nanomaterials, this delineated boundary is either squeezed or enlarged. Metri.et.al. [9] investigated the effect of convective boundary condition on heat and mass transfer on nano particle volume fraction profile over a stretching surface in nanofluid in presence of viscous dissipation. Metri.et.al. [10] studied the mathematical analysis of magnetohydrodynamic flow and heat transfer charecteristics of laminar liquid film over an unsteady stretching sheet with thermal radiation. The effect of thermal radiation produces a significant increase in the thickness of the thermal boundary layer of the liquid film. Metri.et.al. [11] studied the effect of viscous dissipation and non-uniform heat source/sink on magnetohydrodynamic mixed convective viscoelastic fluid flow and heat transfer over a permeable stretching sheet. Metri.et.al. [12] examined the hydromagnetic boundary layer flow and heat transfer of a laminar nanoliquid film over an unsteady stretching sheet, and he also studied the analytical steady solution of nano liquid film over an unsteady stretching sheet. Narayana.et.al. [13] analyzed the thermocapillary flow of carboxymethyl cellulose (CMC) water based nanoliquid film over an unsteady stretching sheet. Maity. [14] studied the flow and development of thin nanoliquid film over a rotating disk. The thermal conductivity of the nanoliquid was modeled based on the effective medium theory. We have also assumed that the initially deposited liquid film over the rotating disk is planar and re-

main planar throughout film thinning process. Metri et al. [15,16] investigated the MHD boundry layer flow due to stretching sheet. Jawali et al. [17,18] studied the maxwell fluid nanofluid flow in a saturated porous layer subjected to time-periodic temperature modulations and vertical double passage channel in presence of first order chemical reaction.

The purpose of present study is to give to numerical analysis of boundary layer flow of a thin nanoliquid film over an unsteady stretching sheet in presence of magnetic field and viscous dissipation with uniform film thickness. In this study we considered three different tyepes of nano liquid, namely aluminium oxide(Al_2O_3), silver (Ag) and titanium oxide (TiO_2). The governing equations are transformed into highly non-linear ordinary differential equations and then solved numerically by using Runge-Kutta-Fehlberg and newton-Raphason schemes based on shooting technique. Numerical computation has been carried out for thermal boundary layer for various values of flow parameters.

2 Mathematical formulation

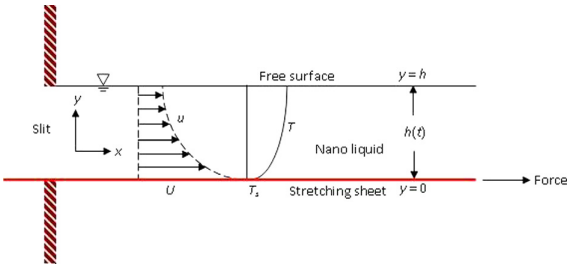

Fig. 1. Schematic representation of a nanoliquid film on an elastic sheet

Let us consider a nanoliquid thin film flow and heat transfer in the vicinity of thin elastic sheet which emerges from a narrow slit at the origin of a Cartesian coordinate system for investigations as shown schematically in Fig. 1. The continuous sheet at $y = 0$ is parallel with the x-axis and moves in its own plane with the velocity.

$$U(x,t) = \frac{bx}{1-\alpha t}, \tag{1}$$

where b and α are both positive constants with dimension per time. The surface temperature T_s of the stretching sheet is assumed to vary with the distance x from the slit as

$$T_s(x,t) = T_0 - T_{ref}\left[\frac{bx^2}{2\nu}\right](1-\alpha t)^{-\frac{3}{2}}, \tag{2}$$

where T_0 is the temperature at the slit and T_{ref} can be taken as a constant reference temperature such that $0 \leq T_{ref} \leq T_0$. The term $\frac{bx^2}{\nu(1-\alpha t)}$ can be

recognized as the local Reynolds number based on the surface velocity U. The expression (1) for the velocity of the sheet $U(x,t)$ reflects that the elastic sheet which is fixed at the origin is stretched by applying a force in the positive x-direction and the effective stretching rate $\frac{b}{(1-\alpha t)}$ increase with time as $0 \leq \alpha < 1$. With the same analogy the expression for the surface temperature $T_s(x,t)$ given by expression (2) represents a situation in which the sheet temperature decreases from T_0 at the slit in proportion to x^2 and such that the amount of temperature reduction along the sheet increases with time. The applied magnetic field is assumed to be of variable kind and is chosen in its special form as

$$B(x,t) = B_0(1-\alpha t)^{-\frac{1}{2}}. \tag{3}$$

The particular form of the expressions for $U(x,t)$, $T_s(x,t)$ and $B(x,t)$ are chosen so as to facilitate the construction of a new similarity transformation which enables in transforming the governing partial differential equations of momentum and heat transport into a set of non-linear ordinary differential equations.

The thermo-physical properties of the nanoliquid (homogeneous mixture of base liquid and nanoparticle) are given in Table 1.

A nanoliquid is an engineered colloidal suspension of nanoparticles in a base liquid and exhibits a significant enhancement in thermal conductivity at modest nanoparticle concentrations. The mechanism leading to this anomalous increase in the thermal performance is still under scrutiny, but recently, several authors proposed two different models of nanoliquids to resolve this issue. The first model consolidates the effects of Brownian motion and thermophoresis (see [6]), in the energy equation. Another model is based on effective medium theory (EMT) like the Maxwell-Garnett theory for the electrical conductivity and dielectric constant of the medium. In this model the macroscopic properties of the nanoliquid such as density, heat capacity, thermal conductivity and so on are expressed in terms of the properties and relative fractions of its components, namely, base liquid and the suspended nanoparticles. In this study we make use of the latter model for the proposed problem along with the following assumptions;

- The flow is laminar and the nanoliquid is incompressible.
- The nanoliquid is non-volatile so that the effect of latent heat due to evaporation is negligible.
- The buoyancy effect is negligible due to the relativity thin liquid film, but it is not so thin that intermolecular forces come into play.
- The influence of surface tension on the flow is negligible.

The standard boundary layer approximation, based on the scale of analysis, we can write the governing equations

$$\frac{\partial u}{\partial x} + \frac{\partial v}{\partial y} = 0 \tag{4}$$

	$\rho(kg/m^3)$	$C_p(J/kgK)$	$k(W/mK)$
Pure water	997.1	4179	0.613
Aluminium oxide(Al_2O_3)	3790	765	40
Silver(Ag)	10500	235	429
Titanium oxide(TiO_2)	4250	686.2	8.9538

Table 1. Thermo-physical properties of liquid and nanoparticle

$$\frac{\partial u}{\partial t} + u\frac{\partial u}{\partial x} + v\frac{\partial u}{\partial y} = \frac{\mu_{nf}}{\rho_{nf}}\frac{\partial^2 u}{\partial y^2} - \frac{\sigma B_0^2}{\rho_{nf}}u \tag{5}$$

$$\frac{\partial T}{\partial t} + u\frac{\partial T}{\partial x} + v\frac{\partial T}{\partial y} = \frac{K_{nf}}{(\rho Cp)_{nf}}\frac{\partial^2 T}{\partial y^2} + \frac{\mu_{nf}}{(\rho C_p)_{nf}}\left(\frac{\partial u}{\partial y}\right)^2 \tag{6}$$

where u and v are the velocity components along the x and y axes respectively. T is temperature.
The physical properties characterizing the base liquid and the nanoparticles, namely, density, dynamic viscosity, thermal conductivity, thermal diffusivity and heat capacitance are assumed to be constants while those of the nanoliquid are assumed to be functions of the volume fraction ϕ. The effective density of the nanoliquid is given by

$$\rho_{nf} = (1-\phi)\rho_f + \phi\rho_s \tag{7}$$

Although the use of the above thermal conductivity model is restricted to nanoparticles of spherical shape it is found to be very appropriate for studying heat transfer enhancement using nanoliquids. The effective viscosity of the nanoliquid as given by Brinkman is

$$\mu_{nf} = \frac{\mu_f}{(1-\phi)^{2.5}} \tag{8}$$

The effective thermal conductivity of the nanoliquid is approximated by the Maxwell-Garnett model as

$$K_{nf} = K_f\left[\frac{K_s + 2K_f - 2\phi(K_f - K_s)}{K_s + 2K_f + \phi(K_f - K_s)}\right] \tag{9}$$

The heat capacitance of the nanoliquid is expressed as (see [1]).

$$(\rho C_p)_{nf} = (1-\phi)(\rho C_p)_{nf} + (\rho C_p)_s \tag{10}$$

The associated boundary conditions for Eqs. (4)-(6) are

$$u = U, v = 0, T = T_w \quad at \quad y = 0 \tag{11}$$

$$\frac{\partial u}{\partial y} = \frac{\partial T}{\partial y} = 0 \quad at \quad y = h \tag{12}$$

$$v = \frac{\partial h}{\partial t} \quad at \quad y = h \tag{13}$$

We introduce the following similarity variables

$$\psi(x, y, t) = \left(\frac{\nu_f b}{1 - \alpha t}\right)^{1/2} x f(\eta) \tag{14}$$

$$T(x, y, t) = T_0 - T_{ref}\left[\frac{bx^2}{2\nu_f}\right](1 - \alpha t)^{-3/2}\theta(\eta) \tag{15}$$

$$\eta = \left[\frac{b}{\nu_f(1 - \alpha t)}\right]^{1/2} y \tag{16}$$

The velocity components u and v in terms of the Stream function $\psi(x, y, t)$ are given by

$$u = \frac{\partial \psi}{\partial y} = \left(\frac{bx}{1 - \alpha t}\right) f'(\eta) \tag{17}$$

$$v = -\frac{\partial \psi}{\partial x} = -\left(\frac{\nu_f b}{1 - \alpha t}\right)^{1/2} f(\eta) \tag{18}$$

Assuming $\eta = \beta$ at free the free surface and using Eq.16

$$\beta = \sqrt{\frac{b}{\nu_f}}(1 - \alpha t)^{-1/2} h \tag{19}$$

which gives

$$\frac{dh}{dt} = -\frac{\alpha\beta}{2}\sqrt{\frac{\nu_f}{b}}(1 - \alpha t)^{-1/2} \tag{20}$$

Substituting similarity variable (14)-(16) into Eqs.(4)-(6), the continuity equation (3) automatically satisfied and the momentum and the energy equations are reduced to

$$f''' + \phi_1\left[ff'' - (f')^2 - S\left(\frac{\eta}{2}f'' + f'\right) + \frac{1}{\phi_2}Mf'\right] = 0 \tag{21}$$

$$\theta'' + Pr\left(\frac{K_{nf}}{K_f}\right)\phi_3\left[f\theta' - 2f'\theta - \frac{S}{2}(3\theta + \eta\theta) + \frac{1}{\phi_4}Ec(f'')^2\right] = 0 \tag{22}$$

subject to the boundary conditions

$$f(0) = 0, f'(0) = \theta(0) = 1, \tag{23}$$

$$f''(\beta) = \theta'(\beta) = 0, \tag{24}$$

$$f(\beta) = \frac{S\beta}{2} \tag{25}$$

Where, The constants $\phi_1, \phi_2, \phi_3, \phi_4$ that depend on the volume fractions are respectively given by,

$$\phi_1 = (1-\phi)^{2.5}[(1-\phi) + \phi\left(\frac{\rho_s}{\rho_f}\right) \tag{26}$$

$$\phi_2 = 1 - \phi + \phi\left(\frac{\rho_s}{\rho_f}\right) \tag{27}$$

$$\phi_3 = 1 - \phi + \phi\left(\frac{(\rho C_p)_s}{(\rho C_p)_f}\right) \tag{28}$$

$$\phi_4 = (1-\phi)^{2.5}\left[1 - \phi + \phi\frac{(\rho C_p)_s}{(\rho C_p)_f}\right] \tag{29}$$

3 Numerical solution

The system of non-linear differential equations Eq.(21) and (22) subjected to the boundary conditions Eq. (23)-(25) are solved numerically, using Runge-Kutta-Fehlberg and Newton-Raphson schemes based shooting method. (see [2]). In this method, non-linear ordinary differential equation Eq. (21) and (22) have been reduced to first order differential equations as follows:

$$\frac{df_0}{d\eta} = f_1, \tag{30}$$

$$\frac{df_1}{d\eta} = f_2, \tag{31}$$

$$\frac{df_2}{d\eta} = \phi_1\left[S\left(f_1 + \frac{\eta}{2}f_2\right) + (f_1)^2 - f_0 f_2 + \frac{1}{\phi_2}Mf_1\right], \tag{32}$$

$$\frac{d\theta_0}{d\eta} = \theta_1, \tag{33}$$

$$\frac{d\theta_1}{d\eta} = \phi_3 Pr\left(\frac{K_f}{K_{nf}}\right)$$
$$\left[\frac{S}{2}(3\theta_0 + \eta\theta_1) + 2f_1\theta_0 - \theta_1 f_0 - \frac{1}{\phi_4}Ecf_2^2\right], \tag{34}$$

Corresponding boundary conditions take the form,

$$f_1(0) = 1, \quad f_0(0) = 0, \quad \theta_0(0) = 1, \tag{35}$$

$$f_2(\beta) = 0, \quad \theta_1(\beta) = 0, \tag{36}$$

$$f_0(\beta) = \frac{S\beta}{2}. \tag{37}$$

Here $f_0(\eta) = f(\eta)$ and $\theta_0(\eta) = \theta(\eta)$. The above boundary value problem is first converted into an initial value problem by appropriately guessing the missing slopes $f_2(0)$ and $\theta_1(0)$. The resulting IVP is solved by shooting method for a set of parameters appearing in the governing equations and a known value of S. The value of β is so adjusted that condition Eq. (37) holds. This is done on the trial and error basis. The value for which condition Eq. (37) holds is taken as the appropriate film thickness and the IVP is finally solved using this value of β. The step length of $h = 0.01$ is employed for the computation purpose. The convergence criterion largely depends on fairly good guesses of the initial conditions in the shooting technique. The iterative process is terminated until the relative difference between the current and the previous iterative values of $f(\beta)$ matches with the value of $\frac{S\beta}{2}$ up to a tolerance of 10^{-6}. Once the convergence in achieved we employed shooting technique with the Runge-Kutta-Fehlberg and Newton-Raphason schemes to determine the unknown in order to convert the boundary value problem to initial value problem. Once all initial conditions are determined, the resulting differential equations were integrated using initial value solver. For this purpose Runge-Kutta-Fehlberg scheme was used.

4 Results and Discussion

The problem of laminar flow of nanoliquid thin film flow over an unsteady stretching sheet in presence of viscous dissipation and magnetic field has been analyzed. The thermo-physical properties of the nanoliquid were assumed to be functions of the volume fraction and the thermal conductivity was modeled based on the effective medium theory. A suitable similarity transformation was used to transform the governing partial differential equations into ordinary ones. The numerical solution obtained by shooting method together with Runge-Kutta-Fehlberg and Newton-Raphson schemes.

The parameters that affect the flow and heat transfer are the unsteady parameter S, film thickness β and the nanoparticle volume fraction ϕ. Hence, the numerical solution of the problem is explored in the two parameter space (S, ϕ) for three different types of nanoliquids namely aluminium oxide(Al_2O_3), silver (Ag) and titanium oxide (TiO_2). The Prandtl number Pr for the base liquid water is usually around 7. Using the definition of Prandtl number and the thermo-physical properties of water as listed in Table 1 along with $\mu_f = 1\times10^{-3}$ Pas at 20^0C the Prandtl number of water is calculated to be $Pr = 6.8173$. This value has been used throughout our computations.

It is note worthy to mention that the solution exists only for small value of unsteadiness parameter $0 \leq S \leq 2$. Moreover, when $S \to 0$ the solution approaches to the analytical solution obtained by Crane [3] with infinitely thick layer of fluid ($\beta \to \infty$). The other limiting solution corresponding to $S \to 2$ represents a liquid film of infinitesimal thickness ($\beta \to 0$). The numerical results are obtained for $0 \leq S \leq 2$ and $0 \leq \phi \leq 0.5$. The effects of the unsteadiness parameter S, magnetic field M and nanoparticle volume fraction ϕ on the flow and heat transfer are shown in Figs. 2- 6.

The effect of nanoparticle volume fraction ϕ on the thin film thickness β for three different nanoliquids are plotted in Fig. 2, respectively. It is shown in the figure that ϕ plays important role on variation of β. For the all the three nanoliquid, β decreases gradually as ϕ increases from 0.0 to 0.2 and then enlarges evenly as ϕ continuously increases. On the other hand Eqs. 26- 29, it is readily to know that the film thickness β is depend on the density of the nanoparticles ρ_s as well. For the prescribed value of ϕ, the larger density of nanoparticles ρ_s, the smaller is the value of β. We further notice that ρ_s has influence on ϕ, which increases with enlargement of ρ_s. This can be explained that the greater density of the nanoliquid helps to reduce the thickness of the film.

The effect of the nanoparticle volume fraction on the temperature profiles $\theta(\eta)$ are predicted for different values of S, in Fig. 3 - 4 for all the three nanoliquid. We note here that the inclusion of nano-sized particles in water like cooling liquids greatly enhances their thermal conductivity thereby resulting in increased heat transfer rates. Increasing the values of the volume fraction results in thickening of the thermal boundary layer for any given value of the unsteadiness parameter. We observe the significant variation of temperature profiles against volume fraction in case of all the three nanoliquid. The unsteadiness parameter has a decreasing effect on $\theta(\eta)$ profiles in case of all the three nanoliquids.

The effect of magnetic field on temperature profile for different values of unsteadiness parameter S in Fig. 5- 6 in case of all the three nanoliquid. The dimensionless temperature is higher at the surface and it decreases with the magnetic field distance inside the thermal boundary layer (as shown in figs 5- 6). Due to a decrease in the dimensionless film thickness, the dimensionless temperature increases with the increase in the magnetic field each value of unsteadiness parameter and results the thermal boundary layer thickness increases. On the otherhand , the effect of the unsteadiness parameter S on $-\theta'(0)$ is presented in Table 2. It is found that this quantity decreases dramatically as S enlarges for all the three nanoliquids, its value can reduce, when S increases from 0.3 to 1.8 for each nanofluid. For any a given value of S, it is found from the table that the value of $-\theta'(0)$ decreases monotonously with ϕ increasing. In Table 3 it is found that this quantity increases as S enlarges for in all the three nano liquids.

5 Conclusion

The laminar flow of a thin nanoliquid film over an unsteady stretching surface in presence of magnetic field and viscous dissipation has been analyzed using a shooting method that involves Runge-Kutta-Fehlberg and Newton-Raphson schemes. The thermo-physical properties of the nanoliquid were assumed to be functions of properties of the components and their volume fraction. A similarity solution that depends on the unsteadiness parameter S and the nanoparticle volume fraction ϕ was presented. Some of the important findings of the investigation are listed as follows:

Types of nanoliquids	S	$\phi = 0.0$	$\phi = 0.1$	$\phi = 0.2$
Al_2O_3	0.3	9.49448354	8.21914135	7.21097505
	0.4	7.43387372	6.45050017	5.67767995
	0.5	6.17754466	4.89066055	4.7379221
	0.6	5.3202505	4.62984045	4.09403367
	0.7	4.69013197	4.0857758	3.62021146
	0.8	4.20204733	3.66443282	3.25418206
	0.9	3.80795479	3.32538133	2.96068799
	1.0	3.47841537	3.0426417	2.71735362
	1.1	3.193028	2.79876989	2.50815207
	1.2	2.93677954	2.57982615	2.32059187
	1.3	2.69701155	2.37440384	2.14392328
	1.4	2.46244915	2.17186814	1.96777728
	1.5	2.22126221	1.96091387	1.78149254
	1.6	1.95946528	1.72841567	1.57256247
	1.7	1.65788047	1.45685925	1.32451277
	1.8	1.28527789	1.11922258	1.0131573
Ag	0.3	9.49448603	6.30230848	4.10734857
	0.4	7.43386589	4.97229202	3.2904248
	0.5	6.17755012	4.15418981	3.2904248
	0.6	5.32025334	3.59206778	2.78357437
	0.7	4.69013197	3.17798981	2.4335424
	0.8	4.20205044	2.85841842	1.98116188
	0.9	3.80795805	2.60300927	1.82747319
	1.0	3.47841537	2.39190109	1.70284863
	1.1	3.1930316	2.21094727	1.59709454
	1.2	2.93677576	1.50505682	1.50134514
	1.3	2.69701155	1.89492528	1.40773409
	1.4	2.46244915	1.74026218	1.30816606
	1.5	2.2212578	1.57471104	1.19441778
	1.6	1.9594699	1.38671868	1.05718896
	1.7	1.65786618	1.1619417	0.88561394
	1.8	0.34672556	0.8803575	0.66593056
TiO_2	0.3	9.49449848	8.20801037	7.159999524
	0.4	7.43387111	6.44379944	5.64262252
	0.5	6.17755012	5.36483054	4.71227601
	0.6	5.32025619	4.62674367	4.07443904
	0.7	4.69013197	4.08360774	3.60509909
	0.8	4.20205044	3.66336489	3.24338102
	0.9	3.80795805	3.32535221	2.9539648
	1.0	3.47840853	3.04392686	2.71467343
	1.1	3.193028	2.80147178	2.50985349
	1.2	2.93677197	2.58406144	2.32662729
	1.3	2.69700357	2.38036502	2.15421021
	1.4	2.46244915	2.17939247	1.98220149
	1.5	2.2212578	1.96989346	1.79957274
	1.6	1.95946528	1.73858599	1.59344372
	1.7	1.65786142	1.46763901	1.34538524
	1.8	1.28528742	1.12952079	1.03448954

Table 2. Nussuelt number $-\theta'(0)$ for various values of S and ϕ with $Pr = 6.8173$ and $M = 2$

Types of nanoliquids	S	$\phi = 0.0$	$\phi = 0.1$	$\phi = 0.2$
Al_2O_3	0.3	6.84816095	6.88304732	6.91315758
	0.4	5.17426572	5.20680572	5.23517367
	0.5	4.15650729	3.84576906	4.20993448
	0.6	3.45850852	3.48258561	4.09403367
	0.7	2.93846813	2.95772743	2.97386683
	0.8	2.52682104	2.54193072	2.55434233
	0.9	2.18602431	2.1975325	2.20681297
	1.0	1.89401639	1.90255485	1.90941679
	1.1	1.63692196	1.64313584	1.6480675
	1.2	1.40566658	1.41003553	1.41344975
	1.3	1.19386341	1.19689219	1.19916633
	1.4	0.99721776	0.99918194	1.00069674
	1.5	0.81243729	0.81364587	0.81459189
	1.6	0.63713612	0.63781773	0.63836062
	1.7	0.46949382	0.46984265	0.47012957
	1.8	0.30812787	0.30826542	0.09508691
Ag	0.3	6.84816274	6.95034032	7.02005426
	0.4	5.17426027	5.26896816	5.33148109
	0.5	4.15651096	4.2388321	4.29128574
	0.6	3.45851038	3.59206778	3.56818154
	0.7	2.93846813	2.9924374	3.02431103
	0.8	2.52682291	2.56837495	2.5922538
	0.9	2.18602618	2.21731976	2.23477096
	1.0	1.89401639	1.91705272	1.92952395
	1.1	1.6369238	1.65347101	1.66223297
	1.2	1.40566477	1.41717457	1.42320739
	1.3	1.19386341	1.19702606	1.2057395
	1.4	0.99721776	1.00235811	1.00493195
	1.5	0.81243568	0.81561332	0.81717883
	1.6	0.63713763	0.63894738	0.63983612
	1.7	0.46948977	0.47040902	0.47083759
	1.8	0.30812787	0.308484	0.30864766
TiO_2	0.3	6.84817172	6.88833479	6.92259184
	0.4	5.1742639	5.21172427	5.24364232
	0.5	4.15651096	4.1894603	4.21718571
	0.6	3.45851223	3.48628381	4.21718571
	0.7	2.93846813	2.9606241	2.97867719
	0.8	2.52682291	2.54418466	2.55790862
	0.9	2.18602618	2.19917861	2.20947964
	1.0	1.89401267	1.90379801	1.91138923
	1.1	1.63692196	1.164404822	1.649456
	1.2	1.40566296	1.41064122	1.41440369
	1.3	1.19385988	1.1973072	1.19985069
	1.4	0.99721776	0.99945833	1.00113355
	1.5	0.81243568	0.81380491	0.81486948
	1.6	0.63713612	0.63791451	0.63854435
	1.7	0.46948842	0.46992054	0.46936435
	1.8	0.30813015	0.30828994	0.30839695

Table 3. Skin friction coefficient $-f''(0)$ for various values of S and ϕ with $Pr = 6.8173$ and $M = 2$

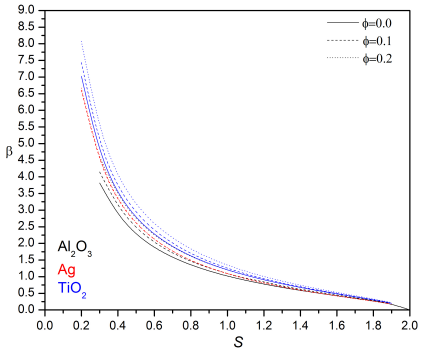

Fig. 2. Variation of diemensionaless film thickness β with S for different values of ϕ

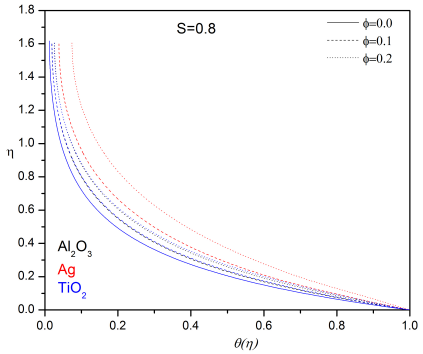

Fig. 3. Effect of ϕ on temperature profile $\theta(\eta)$ with $S = 0.8$

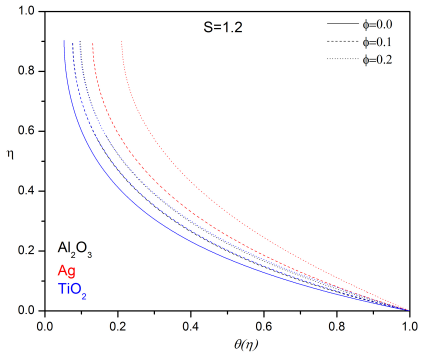

Fig. 4. Effect of ϕ on temperature profile $\theta(\eta)$ for with $S = 1.2$

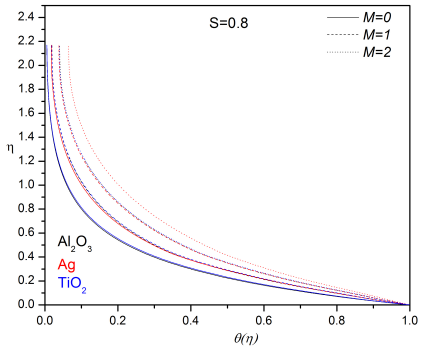

Fig. 5. Effect of magnetic field M on temperature profile $\theta(\eta)$ with $S = 0.8$

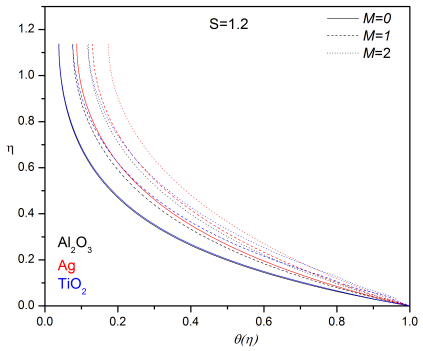

Fig. 6. Effect of magnetic field M on temperature profile $\theta(\eta)$ with $S = 1.2$

1. The film thickness β can be affected seriously by S, that is to say, β decreases dramatically with increasing S. We further notice that there is a linear relationship between the film thickness β and the unsteadiness parameter S. With this relation, the film thickness for other type of nanofluids can be evaluated accurately.
2. The film thinning rate decreases with the increase of the nanoparticle volume fraction.
3. Viscous dissipation enhances the thermal boundary layer thickness.
4. The wall temperature gradient(Nusselt number) $-\theta'(0)$ is a decreasing function of in all the considered nanoliquids while the opposite is true for skin friction $-f''(0)$.

References

1. K. Khanafer, K. Vafai and M. Lightstone. Buoyancy-driven heat transfer enhancement in a two-diemensional enclosure utilizing nanofluids, I. J. of Heat and Mass

trans. 46, 3639–3653, 2003.
2. S. D. Conte and C. De Boor. Elementary Numerical Analysis. McGraw-Hill. New York 1972.
3. L. J. Crane. Flow past a stretching plate, Z. Angrew. Math. Phys. 21, 645–647, 1970.
4. C.Y. Wang. Liquid film on an unsteady stretching surface. Quart. Appl. Math. 48, 601–610, 1990.
5. B. Santra and B. S. Dandpat. Unsteady thin film flow over a heated stretching sheet, Int. J. H. and M. Tra. 52, 1965–1970, 2009.
6. J. Buongiorno. Convective transport in Nanofluids, ASME J. Heat Transfer 128, 240–250, 2006.
7. M. Narayana and P. Sibanda. Laminar flow of a nanoliquid film over an unsteady stretching sheet, International Journal of Heat and Mass Transfer, 55, 7552–7560, 2012.
8. S. Maity, Y. Ghatani and B. S. Dandpat. Thermocapillary Flow of a Thin Nanoliquid Film Over an Unsteady Stretching Sheet, J. of heat transfer(ASME) 138, DOI: 10.1115/1.4032146, 2016.
9. P.G. Metri, M. S. Abel and S. Silvestrov. Heat and mass transfer in MHD boundary layer flow over a nonlinear stretching sheet in a nanoliquid with convective boundary condition and viscous dissipation, Springer Proceedings in Mathematics and Statistics, 178, 203–219, 2016.
10. P. G. Metri, S. Abel, J. Tawade and P. G. Metri. "Fluid flow and radiative nonlinear heat transfer in a liquid film over an unsteady stretching sheet," IEEE Con. Proc. doi: 10.1109/ICMAE.2016.7549513, 2016.
11. P. G. Metri, P. G. Metri, M. S. Abel and S. Silvestrov. "Heat transfer in MHD mixed convection viscoelastic fluid flow over a stretching sheet embedded in a porous medium with viscous dissipation and non-uniform heat source/sink" Procedia Engineering, 157, 309–316, doi: 10.1016/j.proeng.2016.08.371, 2016.
12. P.G. Metri, M. Narayana and S. Silvestrov. Hypergeometric steady solution of hydromagnetic nano liquid film flow over an unsteady stretching sheet, AIP Conference Proceedings, 1798, 020097; doi: 10.1063/1.4972689, 2017.
13. M. Nayarana, P.G. Metri and S. Silvestrov. Thermocapillary flow of a non-Newtonian nanoliquid film over an unsteady stretching sheet, AIP Conf. Proc., 1798, 020109; doi:10.1063/1.4972701, 2017.
14. S. Maity. Thermocapillary flow of thin Cu-water nanoliquid film during spin coating process. Int. Nano.Lett. DOI 10.1007/s40089-016-0196-5, 2017.
15. P.G. Metri, E. Guariglia, S. Silvestrov.*Lie Group Analysis for MHD Boundary Layer Flow and Heat Transfer over a Stretching Sheet in presence of Viscous Dissipation and Uniform Heat Source/Sink*, AIP conf. Proc. 1798. 020096; doi:10.1063/1.4972688 2017.
16. P.G. Metri, V. Bablad, P.G. Metri, , M. S. Abel, S, Silvestrov. *Mixed Convection Heat Transfer in MHD Non–Darcian Flow Due to an Exponential Stretching Sheet Embedded in a Porous Medium in Presence of Non-uniform Heat Source/Sink*, in Engineering Mathematics I: Springer Proceedings in Mathematics & Statistics 178, 187–201, 2016.
17. U. Jawali, K. Vajravelu, P. G. Metri, , S, Silvestrov. *Effect of Time-Periodic Boundary Temperature Modulations on the Onset of Convection in a Maxwell Fluid-Nanofluid Saturated Porous Layer*, in Engineering Mathematics I: Springer Proceedings in Mathematics & Statistics 178, 221–245, 2016.
18. P. Jada, U. Jawali, P.G.Metri, S. Silvestrov. *Effect of First Order Chemical Reaction on Magneto Convection in a Verticle Double Passage Channel*, in Engineering Mathematics I: Springer Proceedings in Mathematics & Statistics 178, 247–279, 2016.

The Flexible Beta Regression Model

Sonia Migliorati[1], Agnese M. Di Brisco[2], and Andrea Ongaro[3]

[1] Department of Economics, Management and Statistics - University of Milano-Bicocca, 20126 Milan, Italy
(E-mail: sonia.migliorati@unimib.it)
[2] Department of Economics, Management and Statistics - University of Milano-Bicocca, 20126 Milan, Italy
(E-mail: agnese.dibrisco@unimib.it)
[3] Department of Economics, Management and Statistics - University of Milano-Bicocca, 20126 Milan, Italy
(E-mail: andrea.ongaro@unimib.it)

Abstract. A relevant problem in applied statistics concerns modelling rates, proportions or, more generally, continuous variables restricted to the interval (0,1). Aim of this contribution is to study the performances of a new regression model for continuous variables with bounded support that extends the well-known Beta regression model (Ferrari and Cribari-Neto, 2004, Journal of Applied Statistics). Under our new regression model, the response variable is assumed to have a Flexible Beta (FB) distribution, a special mixture of two Beta distributions that can be interpreted as the univariate version of the Flexible Dirichlet distribution (Ongaro and Migliorati, 2013, Journal of Multivariate Analysis). In many respects, the FB can be considered as the counterpart on (0,1) to the well-established mixture of normal distributions sharing a common variance. The FB guarantees a greater flexibility than the Beta distribution for modelling bounded responses, especially in terms of bimodality, asymmetry and heavy tails. The peculiar mixture structure of the FB makes it identifiable in a strong sense and guarantees a bounded likelihood and a finite global maximum on the assumed parameter space. In the light of these good theoretical properties, the new model results to be very tractable from a computational perspective, in particular with respect to posterior computation. Therefore, we provide a Bayesian approach to inference and, in order to estimate its parameters, we propose a new mean-precision parametrization of the FB that guarantees a variation independent parametric space. Interestingly, the FB regression model can be understood itself as a mixture of regression models. The strength of our new FB regression model is illustrated by means of application to a real dataset. To simulate values from the posterior distribution we implement the Gibbs sampling algorithm through the BUGS software.
Keywords: beta regression, flexible Dirichlet, mixture models, proportions, MCMC.

1 Introduction

To implement standard linear regression models for continuous variables restricted to the interval $(0, 1)$, one has to transform the response variable so that its support becomes the real line. Despite having been the preferred method for a long time, such an approach has two relevant drawbacks: first, the difficulty in interpreting the estimated parameters with respect to the original response variable [7]; and second, the failure of the assumptions of normality (proportions typically show asymmetric distributions) and homoscedasticity [21].

To overcome these drawbacks, many researchers have developed regression models assuming a beta distributed response variable on the original restricted space [7]. Since the beta distribution is not a dispersion-exponential family [16], inference requires an ad hoc maximum likelihood estimation approach [7] or alternatively a Bayesian approach [4].

The beta distribution can show very different shapes (unimodal, monotone and U-shaped) but it does not provide enough flexibility to model a wide range of phenomena, including heavy tailed responses with a bounded support [3,10] and bimodality. A first attempt to handle greater flexibility is due to [13] who introduced the beta rectangular (BR) distribution which is defined as a mixture of a uniform and a beta distribution. Later, [3] defined a BR regression model for both mean and dispersion parameters by considering a Bayesian approach. The authors showed that the model enables heavier tails and is robust in the presence of outliers. With the purpose of achieving even greater flexibility, we may consider a generic mixture of beta distributions. Nevertheless, despite mixture distributions provide accurate data fit and robustness [15,12], a generic beta mixture may be hard to treat because of its lack of invariance under relabelling of the mixture components. Such an issue, well-known as the label switching problem, determines undesirable effects on posterior distributions, especially in case of overlapping components. To handle the trade-off between flexibility and tractability, we propose a new regression model based on a special mixture of beta distributions. To this end, we introduce the flexible beta (FB) distribution (univariate version of the flexible Dirichlet distribution [20]), which is a special mixture of two beta distributions with arbitrary means and common variance. The FB distribution enables a great variety of density shapes in terms of tail behavior, asymmetry and multimodality. Nevertheless, its peculiar mixture structure avoids the label switching problem, making the FB very tractable from a computational perspective, for example with respect to posterior computation in Bayesian inference.

The rest of the paper is organized as follows. In Section 2 we introduce the FB distribution and we propose a re parametrization which is designed for this regression context and enables a very clear interpretation of the new parameters. In Section 3 we define the FB regression model and we also interpret it as mixture of regression models [9]. In Section 4 we provide details concerning Bayesian inference and the Gibbs sampling algorithm specifically designed for mixture models. In order to evaluate the performance of the FB regression model and compare it with the BR and beta regression ones, we perform an illustrative application on a real dataset (Section 5).

2 The Flexible Beta Distribution

2.1 The Beta Distribution

The beta is the preferred distribution for modeling a continuous response variable bounded on $(0, 1)$. Let us define a random variable beta distributed $Y \sim Beta(\mu\phi, (1-\mu)\phi)$, according to the mean-precision parametrization (see

[7] for details) i.e. with a probability density function (pdf):

$$f_B^*(y;\mu,\phi) = \frac{\Gamma(\phi)}{\Gamma(\mu\phi)\Gamma((1-\mu)\phi)} y^{\mu\phi-1}(1-y)^{(1-\mu)\phi-1} \qquad 0<y<1 \qquad (1)$$

where $0<\mu<1$ and $\phi>0$. The parameter μ identifies the mean of Y, while the parameter ϕ is interpreted as a *precision* parameter being:

$$Var[Y] = \frac{\mu(1-\mu)}{\phi+1}.$$

2.2 The Flexible Beta Distribution

The FB distribution is the univariate version of the flexible Dirichlet one, firstly proposed by [20] as a generalization of the Dirichlet distribution. While the latter has been shown to be inadequate to model compositional data because of its rigid structure, the flexible Dirichlet distribution allows for considerably greater flexibility still preserving a remarkable tractability (see [20] and [18] for a detailed analysis of its properties and statistical potential).

The FB distribution is defined as a special mixture of two beta distributions with a common precision parameter ϕ and arbitrary (but distinct) means $\lambda_1 > \lambda_2$. Its pdf for $0<y<1$ results equal to:

$$f_{FB}^*(y;\lambda_1,\lambda_2,\phi,p) = pf_B^*(y;\lambda_1,\phi) + (1-p)f_B^*(y;\lambda_2,\phi) \qquad (2)$$

where $0<\lambda_2<\lambda_2<1$, $\phi>0$, $0<p<1$ and f_B^* is the mean-precision parametrized beta (1). The first two moments of the FB are equal to:

$$\mathbb{E}(Y) = p\lambda_1 + (1-p)\lambda_2$$

$$Var(Y) = \frac{\mathbb{E}(Y)(1-\mathbb{E}(Y)) + \tau^2 p(1-p)/\phi}{\phi+1} \qquad (3)$$

The special mixture structure of the FB distribution greatly extends the variety of shapes of the beta mainly in terms of bimodality, asymmetry and tail behavior, as illustrated in Figure 1. In addition, it ensures that each component is distinguishable, avoiding the label switching problem. Interestingly, this property makes the FB distribution computationally very tractable, as we will point out in Section 4.

2.3 Reparametrization of the Flexible Beta

With the we aim of defining a regression model with a FB distributed response variable, we propose a reparametrization which explicitly includes the mean, complemented with other three clearly interpretable parameters:

$$\begin{cases} \mu = \mathbb{E}(Y) = p\lambda_1 + (1-p)\lambda_2 \\ \phi = \phi \\ \tilde{w} = \lambda_1 - \lambda_2 \\ p = p \end{cases} \qquad (4)$$

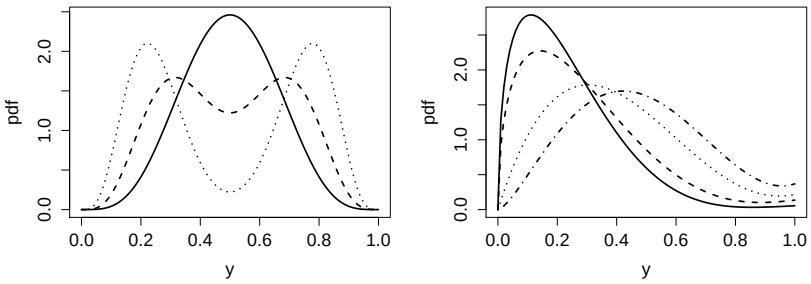

Fig. 1. Some examples of FB distributions. Left panel: $\alpha_1 = 5$, $\alpha_2 = 5$, $p = 0.5$ and τ={1 (solid line), 5 (dashed line), 10 (dotted line)}. Right panel: α_2 is fixed at 1, while $\alpha_1 = 1.5$, $\tau = 4$, $p = 0.01$ (solid line), $\alpha_1 = 1.5$, $\tau = 3$, $p = 0.03$ (dashed line), $\alpha_1 = 2$, $\tau = 2.3$, $p = 0.05$ (dotted line) and $\alpha_1 = 2.5$, $\tau = 2.1$, $p = 0.08$ (dashed-dotted line)

where μ is the mean parameter, $\tilde{w}$ is a measure of distance between the two mixture components, p is the mixing proportion, and ϕ plays the role of a precision parameter since $Var(Y)$ is a decreasing function of ϕ.

In the parametric space so far defined, ϕ is free to move in $\mathbb{R}^+$ while μ, p and $\tilde{w}$ are linked by some constraints. We then decide to require a variation-independent parametric space, first to properly adopt a Bayesian approach to inference through Gibbs sampling [2], as illustrated in Section 4, second to separately model any parameter as a function of covariates.

To this purpose, we chose to leave μ and p free to assume values in (0,1), and to properly normalize $\tilde{w}$ to make it free to move on the range (0,1) as well. Having fixed μ and p, the constraints $0 < \lambda_2 < \lambda_1 < 1$ imply that $\tilde{w}$ takes values between 0 and $\min\left\{\frac{\mu}{p}, \frac{1-\mu}{1-p}\right\}$.

Therefore, we normalize $\tilde{w}$ accordingly:

$$w = \frac{\tilde{w}}{\min\left\{\frac{\mu}{p}, \frac{1-\mu}{1-p}\right\}}. \tag{5}$$

The chosen reparametrization guarantees a variation independent parameter space where p, μ and w vary in $(0, 1)$ and $\phi > 0$ without penalizing the interpretability of the parameters.

3 The Flexible Beta Regression Model

Given a vector of independent responses $\mathbf{Y}^T = (Y_1, \ldots, Y_i, \ldots, Y_n)$ which assume values in the unit interval $(0, 1)$, in accordance to the GLM methodology [16], a regression model for the mean can be defined as

$$g(\mu_i) = \mathbf{x}_i^T \boldsymbol{\beta} \qquad i = 1, \ldots, n \tag{6}$$

where μ_i is the mean of Y_i, $\mathbf{x}_i^T = (x_{i0}, x_{i1}, \ldots, x_{ik})$ is a vector of covariates, $\boldsymbol{\beta}^T = (\beta_0, \beta_1, \ldots, \beta_k)$ is a vector of regression parameters and $g(\cdot)$ is an adequate link function, strictly monotone and twice differentiable. The most

popular link function is the logit, $logit(\mu_i) = \log(\mu_i/(1-\mu_i))$, which allows to interpret the regression coefficients in terms of odds ratios.

If Y_i is assumed to follow a beta distribution, then the beta regression model is obtained [7]. If the response variable is assumed to follow a BR distribution, having $Y \sim BR(\mu, \phi, \alpha)$ where $\mu = E(Y)$, $\alpha = p/(1- \mid 2\mu - 1 \mid)$ and ϕ is the precision parameter of the beta component, then the BR regression model is achieved (see [3] for further details).

Here we define the FB regression (FBR) model by assuming that each Y_i is independently distributed as a flexible beta under the parametrization given in Section 2.3: $Y_i \sim FB(\mu_i, \phi, w, p)$.

Note that none of the above distributions belongs to the dispersion-exponential family [16] and therefore none of the above models is of the GLM type.

Though the regression model (6) concerns only the mean parameters, it naturally induces a form of heteroscedasticity since the response variances are functions of the corresponding means (see formula (3)). However, in some cases, it may be desirable to independently model the variance as a function of covariates. Many authors have proposed extensions in this direction [21,25,8]. This can be easily achieved in the FB regression too, as the parameters μ and ϕ do not share any constraint. The regression for the dispersion can be defined as

$$h(\phi_i) = \mathbf{z}_i^T \boldsymbol{\delta} \tag{7}$$

where $h(\cdot)$ is an appropriate link function, $\mathbf{z}_i^T = (z_{i0}, z_{i1}, \ldots, z_{il})$ is a vector of covariates and $\boldsymbol{\delta}^T = (\delta_0, \delta_1, \ldots, \delta_l)$ is a vector of regression parameters. In [21] it is proposed the logarithm as a proper link function (strictly monotone and double differentiable) since $\phi > 0$.

As a further extension, a regression function can be defined also for the remaining parameters of the FB distribution, namely w and p, since the parametric space is variation independent.

It is of interest to observe that the FBR model can be easily understood as a mixture of regression models [9]. In these models, the regression function is not fixed over all realizations, but different groups of observations may display different dependencies of the means on covariates. In this respect, the FBR is a special mixture of two beta regression models, with common precision and means given by

$$\begin{cases} \lambda_{1i} = \mu_i + (1-p)\tilde{w}_i \\ \lambda_{2i} = \mu_i - p\tilde{w}_i \end{cases} \tag{8}$$

where $\tilde{w}_i = w \min\left\{\frac{\mu_i}{p}, \frac{1-\mu_i}{1-p}\right\}$. Note that such means are piecewise increasing linear functions of μ_i, varying from 0 to 1. The underlying assumption here is that there are two groups, one of which displays a greater mean than the other, for any given value of covariates. The parameter w retains the meaning of distance between the regression functions of the two groups. Thus the FBR structure can also be usefully employed to model two distinct groups which have special regression function patterns.

4 Bayesian Inference

Given a sample of n independent observations $\mathbf{y}^T = (y_1, \ldots, y_i, \ldots, y_n)$, the likelihood function for the FBR model (6) results equal to:

$$L(\boldsymbol{\eta}|\mathbf{y}) = \prod_{i=1}^{n} f^*_{FB}(y_i|\mu_i, \phi, w, p) \tag{9}$$

where $\boldsymbol{\eta} = (\boldsymbol{\beta}, \phi, w, p)$, $\mu_i = g^{-1}(\mathbf{x}_i^T\boldsymbol{\beta})$, and $f^*_{FB}(y|\mu, \phi, w, p)$ is given by (2) with

$$\begin{cases} \lambda_1 = \mu + (1-p)\tilde{w} \\ \lambda_2 = \mu - p\tilde{w} \end{cases} \tag{10}$$

where $\tilde{w} = w \min\left\{\frac{\mu}{p}, \frac{1-\mu}{1-p}\right\}$.

A mixture model can be seen as an incomplete data problem [6] since the allocation of each i^{th} observation to one of the mixture components is unknown. Since no explicit solution to the estimation problem exists, we propose here to adopt MCMC techniques such as data augmentation [27] and Gibbs sampling [11] which are well suited to cope with incomplete data.

Formally, let us define a n-dimensional vector of latent variables $\mathbf{v}$, such that $v_i = 1$ if the i^{th} observation belongs to the first mixture component and $v_i = 0$ otherwise. Having identified these latent variables as missing data, we define a Gibbs sampling algorithm which is split into two steps: one for the parameter simulation conditional on $\mathbf{v}$, and the other for the classification of the observations (i.e. updating $\mathbf{v}$) conditional on knowing the parameter. The posterior distribution $\pi(\boldsymbol{\eta}|\mathbf{y})$ is computed by marginalizing the "complete-data" posterior distribution $\pi(\boldsymbol{\eta}, \mathbf{v}|\mathbf{y})$. To compute the "complete-data" posterior distribution, the complete-data likelihood $L_{CD}(\boldsymbol{\eta}|\mathbf{y}, \mathbf{v})$ is needed, i.e. the likelihood based on both observed ($\mathbf{y}$) and missing ($\mathbf{v}$) data. More precisely:

$$\pi(\boldsymbol{\eta}, \mathbf{v}|\mathbf{y}) \propto L_{CD}(\boldsymbol{\eta}|\mathbf{y}, \mathbf{v})\pi(\boldsymbol{\eta}) \tag{11}$$

with

$$L_{CD}(\boldsymbol{\eta}|\mathbf{y}, \mathbf{v}) = \prod_{i=1}^{n} [p f^*_B(y_i; \lambda_{1i}, \phi)]^{\{v_i\}} [(1-p) f^*_B(y_i; \lambda_{2i}, \phi)]^{\{1-v_i\}} \tag{12}$$

where λ_{1i} and λ_{2i} are given by (8), f^*_B is defined by (1), and $\pi(\boldsymbol{\eta})$ is an appropriate prior distribution. With respect to the prior distribution, we assumed a priori independence, which is a usual choice when no prior information is available. Since the parametric space is variation independent, the joint prior distribution can be factorized as:

$$\pi(\boldsymbol{\eta}) = \pi(\boldsymbol{\beta})\pi(\phi)\pi(w)\pi(p).$$

Moreover, we decided to adopt flat priors, so as to generate the minimum impact on the posteriors (see e.g. [2]). Specifically, we selected the usual multivariate normal prior $\boldsymbol{\beta} \sim N_{k+1}(\mathbf{a}, \mathbf{B})$ for the regression parameters with

$\mathbf{a} = \mathbf{0}$ for the mean, and a diagonal covariance matrix with "large" values for the variances in $\mathbf{B}$. For the remaining parameters we chose a gamma distribution $Ga(g, g)$ for ϕ, which is a rather standard choice for precision parameters (see e.g. [4]), and we selected non-informative uniform priors for the remaining parameters $w \sim U(0, 1)$ and $p \sim U(0, 1)$. The estimation procedure described above can be easily extended to deal with cases in which the precision parameter is modeled as a function of the covariates (see (7)). It is enough to replace the prior for ϕ with a convenient multivariate normal prior for the regression coefficients $\boldsymbol{\delta} \sim N_{l+1}(\mathbf{c}, \mathbf{D})$. Analogous considerations hold for the parameters w and p. We implemented the Gibbs sampling algorithm through the BUGS software [28,14] in order to generate a finite set of values from the posterior distribution, and further analysed the results through the R software [23]. We iterated the algorithm until convergence by burning-in the first B simulated values (for different values of B in the various contexts), to avoid the influence of the chains' initial values. Furthermore, to properly treat autocorrelations, we also set a thinning interval, say L, such that only the first generated values in every batch of L iterations were kept. Finally, we checked for convergence of the algorithm through several statistical tests, with a focus on diagnostic tests for stationarity (Geweke and Heidel diagnostics) and for the level of autocorrelation (Raftery diagnostic) [17,19].

To the purpose of comparing the FBR model with other competing models, we take into consideration some comparison criteria. Typically these criteria favour models with a better fit while simultaneously penalize more complex models. To quantify the lack of fit of a model, we shall consider the deviance which is defined as a function of the likelihood, $L(\boldsymbol{\eta}|\mathbf{y})$ (see (9) for the FBR model), and can be interpreted as the residual information in data, given the parameters:

$$D(\boldsymbol{\eta}) = -2log[L(\boldsymbol{\eta}|\mathbf{y})].$$

Given the MCMC output, the deviance can simply be estimated by taking the posterior mean of the deviance $\overline{D}$, i.e. the mean of the deviances of the MC sample.

To evaluate model complexity we may consider different measures. By way of example, the deviance information criterion (DIC) [26]:

$$DIC = \overline{D} + p_D$$

penalizes the complexity of the model via:

$$p_D = \overline{D} - D(\bar{\boldsymbol{\eta}}),$$

where $\bar{\boldsymbol{\eta}}$ is the vector of posterior means of the parameters. Alternatively, one can penalize model complexity the same way as is done by the well-known AIC [1] and BIC [24] criteria, thus obtaining the corresponding Bayesian counterparts EAIC and EBIC [5], i.e.:

$$EAIC = \overline{D} + 2p$$

$$EBIC = \overline{D} + p\log(n)$$

where p is the number of the model parameters and n is the sample size.

Clearly, the smaller the values of DIC, EAIC and EBIC, the better the model.

When dealing with mixture models, the values of such criteria are not implemented by default in BUGS. Nevertheless, they can be easily computed from the MCMC output.

5 Illustrative Application

In this Section, we show how the FBR can be successfully applied, comparing it with the two competing models, namely the BR and the beta ones.

We consider a dataset about the gasoline yield data [22] (the dataset *GasolineYield* is included in the R library *betareg*). The proportion of crude oil converted to gasoline after distillation and fractionation, naturally quantified on $(0, 1)$, is defined as the dependent variable of the regression model.

The FBR model for the proportion of converted crude oil, $Y_i \sim FB(\mu_i, \phi, p, w)$ for $i = 1, \ldots, n$ is defined as:

$$logit(\mu_i) = \beta_0 + \beta_1 X_{i1}, \quad i = 1, \ldots, n.$$

where X_1 is a quantitative covariate about the standardized temperature (originally in degrees Fahrenheit) at which all gasoline has vaporized and β_0, β_1 are unknown regression parameters. The response variances, being functions of the corresponding means (see formula (3)), will also vary with the covariates, thus inducing a preliminary form of heteroscedasticity.

However, to further improve the fit of the FBR model one can let also the parameter ϕ depend directly on the same covariate rather then being constant for all observations

$$log(\phi_i) = \delta_0 + \delta_1 X_{i1}, \quad i = 1, \ldots, n$$

where δ_0, δ_1 are unknown regression parameters. To compare the FBR model with the beta and with the BR regression ones, we simulated MCMCs of length 10000, discarded the first half values, and used a thinning interval set equal to 3 for the beta model, to 1 for the BR model and to 10 for FB model. These values satisfy the various diagnostic tests mentioned in Section 4.

The results are shown in Tables 1 and 2, and in Figure 2.

Parameter	β_0	β_1	δ_0	δ_1	p	w	α
FB	-1.4848	0.5300	-3.4124	0.1626	0.5866	0.2659	
BR	-1.4132	0.5140	-3.2077	0.1604			0.0984
Beta	-1.4853	0.5318	-3.1811	0.1755			

Table 1. Posterior means of the parameters under the three models

We may observe that we get similar estimates for the four regression parameters under the competing models. Indeed, in Figure 2 we plotted the three

Model	DIC	EAIC	EBIC
FB	-86.9641	-71.59964	-62.80523
BR	-71.93797	-65.75476	-58.42608
Beta	-72.39978	-68.42512	-62.56218

Table 2. Model comparison criteria for the FB, the BR and the beta regression models.

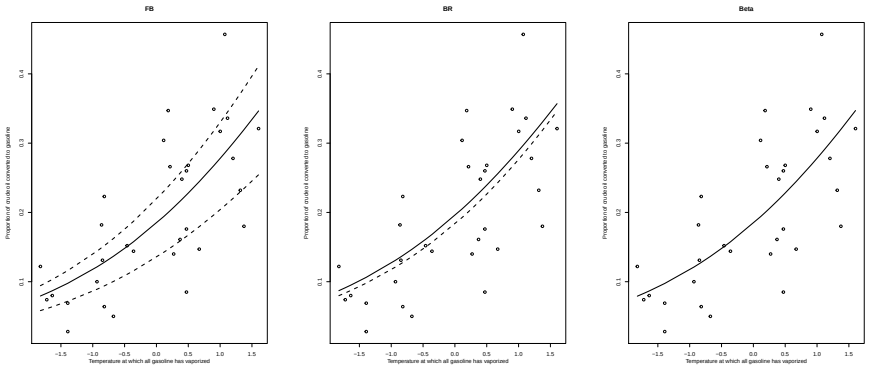

Fig. 2. From the left: fitted regression curve for the FB mean model (solid) and for the components λ_{1i} and λ_{2i} (dashed); fitted regression curve for the BR mean model (solid) and for the group means (dashed, the uniform component 1/2 lies out of the plot); fitted regression curve for the Beta mean model (solid).

fitted regression curves into three different plots to avoid overlapping. The FBR exhibits a better fit than the other two models, especially with respect to DIC, whereas the BR displays the worst one.

To better grasp the behavior of the models, the left panel in Figure 2 reports the group regression means of the FBR. The FB and the beta display a nearly identical behavior in terms of mean regression model. In fact, the better fit of the FBR is due to its ability to locate and accurately describe two groups with a different rate curve. Thus, the FBR efficiently exploits its greater flexibility. On the contrary, the flexibility of the BR model does not seem to provide a better fit since the uniform component, equal to 1/2, lies completely outside the observed scatter plot.

6 Concluding remarks

The FB proves to be a good compromise between tractability and flexibility, when modeling continuous responses bounded to the unit interval. Although in the paper we consider only response variables restricted to the interval $(0, 1)$, the model we propose can be easily extended via an obvious linear transformation of the response to deal with variables taking values on a generic bounded interval.

Our preliminary results show that the FB greatly expands the modeling potential of the beta, without demanding the theoretical and computational

intricacy of a general beta mixture. In particular, the special mixture structure defining the FB ensures good theoretical properties which lead to computational tractability in terms of posterior computation.

At the same time, the FB regression model displays easiness of interpretation. More specifically, the FB directly models the overall regression mean μ as an arbitrary suitably chosen function of the covariates. This mean can be interpreted as weighted average of the two group regression means (one of which lies above the other for any value of the covariates), whose difference is represented by a further parameter w. The mixing weight p and a precision parameter ϕ complete its description. Interestingly, the model incorporates a form of heteroscedasticity natural for this type of data, since the response variance not only depends on ϕ, but also on μ.

From an applicative viewpoint, the illustrative example shows that the FB regression model outperforms the beta and BR regression models even when no clear evidence of bimodality is present. Though further analysis is required, this seems to be an indication of a broad applicability of the model.

Finally, it seems also worthwhile to stress the possibility that some of the parameters ϕ, p, and w of the FB model may depend on covariates too. This greatly further expands its flexibility, enabling it to model fairly complex data patterns.

References

1. H. Akaike. Information theory and an extension of the maximum likelihood principle. In *Selected Papers of Hirotugu Akaike*, pages 199–213. Springer, 1998.
2. J. Albert. *Bayesian computation with R*. Springer Science & Business Media, 2009.
3. C. L. Bayes, J. L. Bazn, and C. Garca. A new robust regression model for proportions. *Bayesian Analysis*, 7(4):841–866, 2012.
4. A. J. Branscum, W. O. Johnson, and M. C. Thurmond. Bayesian beta regression: Applications to household expenditure data and genetic distance between foot-and-mouth disease viruses. *Australian & New Zealand Journal of Statistics*, 49(3):287–301, 2007.
5. S. Brooks. Discussion on the paper by spiegelhalter, best, carlin and van der linde, 2002.
6. A. P. Dempster, N. M. Laird, and D. B. Rubin. Maximum likelihood from incomplete data via the em algorithm. *Journal of the Royal Statistical Society. Series B*, 39:1–38, 1977.
7. S. Ferrari and F. Cribari-Neto. Beta regression for modelling rates and proportions. *Journal of Applied Statistics*, 31(7):799–815, 2004.
8. S. L. Ferrari, P. L. Espinheira, and F. Cribari-Neto. Diagnostic tools in beta regression with varying dispersion. *Statistica Neerlandica*, 65(3):337–351, 2011.
9. S. Frühwirth-Schnatter. *Finite mixture and Markov switching models*. Springer Science & Business Media, 2006.
10. C. García, J. G. Pérez, and J. R. van Dorp. Modeling heavy-tailed, skewed and peaked uncertainty phenomena with bounded support. *Statistical Methods & Applications*, 20(4):463–486, 2011.
11. A. E. Gelfand and A. F. Smith. Sampling-based approaches to calculating marginal densities. *Journal of the American Statistical Association*, 85(410):398–409, 1990.

12. A. Gelman, J. B. Carlin, H. S. Stern, and D. B. Rubin. *Bayesian data analysis*, volume 2. Taylor & Francis, 2014.
13. E. D. Hahn. Mixture densities for project management activity times: A robust approach to {PERT}. *European Journal of Operational Research*, 188(2):450 – 459, 2008.
14. D. J. Lunn, A. Thomas, N. Best, and D. Spiegelhalter. Winbugs-a bayesian modelling framework: concepts, structure, and extensibility. *Statistics and Computing*, 10(4):325–337, 2000.
15. M. Markatou. Mixture models, robustness, and the weighted likelihood methodology. *Biometrics*, 56:483–486, 2000.
16. P. McCullagh and J. A. Nelder. *Generalized linear models*, volume 37. CRC press, 1989.
17. K. L. Mengersen, C. P. Robert, and C. Guihenneuc-Jouyaux. Mcmc convergence diagnostics: a review. *Bayesian Statistics*, 6:415–440, 1999.
18. S. Migliorati, A. Ongaro, and G. S. Monti. A structured dirichlet mixture model for compositional data: inferential and applicative issues. *Statistics and Computing*, 27(4):963–983, 2017.
19. I. Ntzoufras. *Bayesian modeling using WinBUGS*, volume 698. John Wiley & Sons, 2011.
20. A. Ongaro and S. Migliorati. A generalization of the dirichlet distribution. *Journal of Multivariate Analysis*, 114:412–426, 2013.
21. P. Paolino. Maximum likelihood estimation of models with beta-distributed dependent variables. *Political Analysis*, 9(4):325–346, 2001.
22. N. Prater. Estimate gasoline yields from crudes. *Petroleum Refiner*, 35(5):236–238, 1956.
23. R Core Team. *R: A Language and Environment for Statistical Computing*. R Foundation for Statistical Computing, Vienna, Austria, 2016. ISBN 3-900051-07-0.
24. G. Schwarz. Estimating the dimension of a model. *The Annals of Statistics*, 6(2):461–464, 1978.
25. M. Smithson and J. Verkuilen. A better lemon squeezer? maximum-likelihood regression with beta-distributed dependent variables. *Psychological Methods*, 11(1):54, 2006.
26. D. J. Spiegelhalter, N. G. Best, B. P. Carlin, and A. Van Der Linde. Bayesian measures of model complexity and fit (with discussion). *Journal of the Royal Statistical Society: Series B*, 64(4):583–639, 2002.
27. M. A. Tanner and W. H. Wong. The calculation of posterior distributions by data augmentation. *Journal of the American Statistical Association*, 82(398):528–540, 1987.
28. A. Thomas. Bugs: A statistical modelling package. *RTA/BCS Modular Languages Newsletter*, 2:36–38, 1994.

Bayesian Multidimensional Item Response Theory Modeling Using Working Variables

Alvaro Montenegro[1] and Luisa Parra[1]

Departamento de Estadistica, Universidad Nacional de Colombia, Sede Bogotá
(E-mail: ammontenegrod@unal.edu.co, lfparraar@unal.edu.co)

Abstract. We propose a hybrid Metropolis-Hastings within Gibbs type algorithm with independent proposal distributions to the latent traits and the item parameters in order to fit classical Multidimensional Item Response Theory Models. The independent proposals are all multivariate normal distributions based on the working variables approach applied to the latent traits and the item parameters. The covariance matrix of the latent traits is estimated using an inverse Wishart distribution. The results show that the algorithm is very efficient, effective, and yields to high acceptation rates. The algorithm is applied to real data from a large-scale test applied in Universidad Nacional de Colombia.
Keywords: Multidimensional Item Response Theory, working variables, Bayesian Modeling, Large scale tests.

1 Introduction

The multidimensional item response theory (MIRT) models are based on the assumption that people require more than one basic ability to response correctly to an item on a test. There are two major types of MIRT models, the compensatory model, Reckase [12], [13] and the non-compensatory or partial compensatory model. In this paper we only refer to the compensatory MIRT model, which it will be called simply MIRT model.

Bayesian solutions based on MCMC algorithms are due to Albert [1], Patz [10], and other authors. Kim and Bolt [6] showed how to implement 2pl Bayesian UIRT models using *WinBUGS* which is a free software to implement general Bayesian models.

Full Bayesian inference methods for MIRT models have been proposed by several authors. Patz[10] proposed a framework of Bayesian inference for IRT models. After that work Glas and Beguin [5], Patz [11], Montenegro et al. [8], and other authors have proposed Bayesian implementations of a different kind of IRT models. Classical prior distributions are proposed in those implementations, which led to Gibbs, Metropolis-Hastings, and hybrid algorithms. None of them use independent priors. Specifically for the MIRT models, [5] implemented the three-parameter normal ogive (3PNO) model, by using a Gibbs sampler algorithm based on augmented variables. They included the cases of multiple groups and incomplete data. Patz [11] proposed a classical M-H algorithm for the 3pl MIRT model of simple structure. In that kind of models only one of the slopes in each vector of slopes is different from zero. Bold [2] compared some implementation of Bayesian MIRT models and showed how to carry out them using *WinBUGS*.

In this work, we propose a hybrid Metropolis-Hastings(M-H) within Gibbs algorithm, based on the technique of working variables, Gamerman [3], Gutierrez [4]. At each iteration an iterative weighted least squares (IWLS) step is included to move the chains toward the mode of the full conditional posterior densities. The IWLS step is based on the algorithm proposed by Nelder and Wedderburn [9] in the framework of the generalized linear (GLM) models. Bayesian algorithms based on that technique are M-H within Gibbs hybrid algorithms with independent proposals. Those algortihms usually have high acceptance rates and does not require tunning parameters.

The paper is organized as follows. In section 2 we introduce the 2PL MIRT model and in section 3 we discuss the problem of identifiability of the model and introduce a special parameterization to have an identifiable model. Section 4 presents the complete and full conditioned posterior distributions. The gradient vectors and the information matrices of MIRT models are derived in section 5. Section 6 presents the details of the proposed Bayesian algorithm. In section 7 we exhibit the results of fitting a set of real data from an admission test. Finally, section 8 is the discussion of the paper.

2 Specification of the 2PL MIRT Model

In the dichotomous multidimensional item response theory (MIRT) models, the data is organized in a $N \times p$ matrix $\boldsymbol{y}$. The ijth element represents the response of person i to item j. It is assumed that the value y_{ij} is the realization of a binary random variable $Y_{ij} \sim Ber(\pi_{ij})$. The value 1 is assigned to a correct response and 0 otherwise. The latent trait of person i is denoted $\boldsymbol{\theta}_i$ and it is assumed to be an independent realization of a random d-vector $\boldsymbol{\Theta}$, where $\boldsymbol{\Theta}$ has some multivariate distribution as $N_m(\mathbf{0}, \boldsymbol{\Sigma})$. The probability π_{ij} is given byIn the dichotomous multidimensional item response theory (MIRT) models, the data is organized in a $N \times p$ matrix $\boldsymbol{y}$. The ijth element represents the response of the person i to the item j. It is assumed that the value y_{ij} is the realization of a binary random variable $Y_{ij} \sim Ber(\pi_{ij})$. The value 1 is assigned to a correct response and 0 otherwise. The latent trait of person i is denoted $\boldsymbol{\theta}_i$ and it is assumed to be an independent realization of a random d-vector $\boldsymbol{\Theta}$, where $\boldsymbol{\Theta}$ has some multivariate distribution as $N_m(\mathbf{0}, \boldsymbol{\Sigma})$. The probability π_{ij} is given by

$$\pi_{ij} = \frac{1}{1 + e^{-\eta_{ij}}}, \tag{1}$$

where $\eta_{ij} = \boldsymbol{a}_j^t \boldsymbol{\theta}_i + d_j = a_{j1}\theta_{i1} + \cdots + a_{jm}\theta_{im} + d_j, \quad a_{jk}, \theta_{ik} \in \Re$. It is common to assume that $a_{jk} > 0$ to guarantee that π_{ij} is a monotonic function of $\boldsymbol{\theta}$. Nevertheless, that assumption is not strictly necessary. In this work, we assume that $-\infty < a_{jk} < \infty$, for all j, k. However, in practical applications where it is required that $a_{jk} > 0$, a logarithmic reparameterization can be introduced to these parameters such that $\log a_{jk} = a^*_{jk}$ and $-\infty < a^*_{jk} < \infty$.

The set of item parameters of the test is denoted by $\boldsymbol{\beta}$. Thus, $\boldsymbol{\beta}$ is a $p \times (m + 1)$ matrix. The set of latent traits of the sample is represented

by $\boldsymbol{\theta}$. Then $\boldsymbol{\theta}$ is a $N \times m$ matrix. The following notation is adopted. Let $\boldsymbol{\beta}_j = (\boldsymbol{a}_j^t, d_j)^t$. $\boldsymbol{\beta}_j$ will be called the latent regression parameter of the item j.

Let $\alpha_j = (a_{j1}^2 + \ldots + a_{jm})^{1/2}$ be the Euclidean norm of the vector $\boldsymbol{a}_j$. The value α_j is called the multidimensional item discrimination (MDISC) of item j. The vector $\boldsymbol{\nu}_j = \boldsymbol{a}_j/\alpha_j$ is the direction of the item j and $b_j = -d_j/\alpha_j$ is called the multidimensional item difficulty (MDIFF) of item j. For details see Reckase [12], [13].

3 Identifiability of the 2PL MIRT Model

It is known that the MIRT models are non-identifiable. In fact, if $\boldsymbol{B}$ is a non singular matrix, then $\boldsymbol{a}_j^t\boldsymbol{\theta}_i = (\boldsymbol{B}^t\boldsymbol{a}_j)^t(\boldsymbol{B}^{-1}\boldsymbol{\theta}_i)$. Our solution to have an identifiable model is partially based on the parameterization proposed by [14] in the framework of the nonlinear factor analysis models and Montenegro [7] and Montenegro et al. [8] in the framework of MIRT models.

1. The random d-vector $\boldsymbol{\Theta}$ has a multivariate normal distribution $N_m(\mathbf{0}, \boldsymbol{\Sigma})$, where $\boldsymbol{\Sigma}$ is a hyperparameter that must be estimated.
2. We fix the parameters of m items. Yalcin and Amemiya [14] proposed to fix these parameters in a way such that if the items are reorder, the matrix of the selected $\boldsymbol{a}_j$'s is the identity matrix $\boldsymbol{I}_m$ and the corresponding intercept parameters conform the m-vector $\mathbf{0}_m$.

In the unidimensional case ($m = 1$), it is common to assume that $\boldsymbol{\Theta} \sim N(0, 1)$. This solution is not sufficient if $m > 1$. If we assume that $\boldsymbol{\Theta}$ has standard multivariate normal distribution $N_m(\mathbf{0}, \boldsymbol{I}_m)$ and $\boldsymbol{B}$ is an orthogonal matrix, thus $\boldsymbol{B}^{-1}\boldsymbol{\Theta} \sim N_m(\mathbf{0}, \boldsymbol{I}_m)$. This is an indeterminacy of the model by rotations and reflexions. The proposed parameterization overcomes this problem.

4 Posterior density and full conditional marginals

To build the likelihood it is necessary to state the following assumptions.

1. The response patterns among the people are independent.
2. Given the latent trait $\boldsymbol{\theta}_i$, the responses $Y_{ij}, j = 1, \ldots, p$ are independent (local independence).

The probability function of each variable Y_{ij} is given by $f(y_{ij}|\pi_{ij}) = \pi_{ij}^{y_{ij}}(1 - \pi_{ij})^{1-y_{ij}}$. Let us suppose that $p(\boldsymbol{\theta}_i)$ is a prior density for the latent trait of person i and $p(\boldsymbol{\beta}_j)$ is a prior density for the parameter of the item j. Let $\boldsymbol{y}_{i\cdot} = (y_{i1}, \ldots, y_{ip})^t$ be the response pattern of individual i and $\boldsymbol{y}_{\cdot j} = (y_{1j}, \ldots, y_{Nj})^t$ the complete vector of responses to item j. Thus the posterior joint density is specified by

$$p(\boldsymbol{\theta}, \boldsymbol{\beta}|\boldsymbol{y}) \propto \prod_{i=1}^{N}\prod_{j=1}^{p} \pi_{ij}^{y_{ij}}(1 - \pi_{ij})^{1-y_{ij}} p(\boldsymbol{\theta}_i)p(\boldsymbol{\beta}_j). \tag{2}$$

The full conditional marginals are specified by

$$p(\boldsymbol{\theta}, \boldsymbol{\beta}|\boldsymbol{y}) \propto \prod_{i=1}^{N}\prod_{j=1}^{p} \pi_{ij}^{y_{ij}}(1-\pi_{ij})^{1-y_{ij}} p(\boldsymbol{\theta}_i)p(\boldsymbol{\beta}_j). \tag{3}$$

The full conditional marginals are specified by

$$p(\boldsymbol{\theta}_i|\boldsymbol{y}_{i.}, \boldsymbol{\beta}) \propto \prod_{j=1}^{p} \pi_{ij}^{y_{ij}}(1-\pi_{ij})^{1-y_{ij}} p(\boldsymbol{\theta}_i) \tag{4}$$

$$p(\boldsymbol{\beta}_j|\boldsymbol{y}_{.j}, \boldsymbol{\theta}) \propto \prod_{i=1}^{N} \pi_{ij}^{y_{ij}}(1-\pi_{ij})^{1-y_{ij}} p(\boldsymbol{\beta}_j). \tag{5}$$

Since all the parameters are real numbers we propose priors based on multivariate normal distributions. For the latent trait vector $\boldsymbol{\theta}_i$ we propose priors $N_m(\boldsymbol{\mu}_{i0}, \boldsymbol{\Sigma}_{\boldsymbol{\theta}})$ and for the item vector parameter $\boldsymbol{\beta}_j$ we propose priors $N_{(m+1)}(\boldsymbol{\beta}_{j0}, \boldsymbol{\Sigma}_{\boldsymbol{\beta}})$. In the next section, we derive normal approximations of the full conditional marginals. Such approximations will be used as independent proposals in the proposed algorithm.

5 Gradient and Information Matrices

It is easy to see that

$$\frac{\partial l_{ij}}{\partial \boldsymbol{\theta}_i} = \frac{\partial l_{ij}}{\partial \pi_{ij}}\frac{\partial \pi_{ij}}{\partial \eta_{ij}}\frac{\partial \eta_{ij}}{\partial \boldsymbol{\theta}_i} = (y_{ij}-\pi_{ij})\boldsymbol{a}_j, \tag{6}$$

$$\frac{\partial l_{ij}}{\partial \boldsymbol{\beta}_j} = \frac{\partial l_{ij}}{\partial \pi_{ij}}\frac{\partial \pi_{ij}}{\partial \eta_{ij}}\frac{\partial \eta_{ij}}{\partial \boldsymbol{\beta}_j} = (y_{ij}-\pi_{ij})\begin{bmatrix}\boldsymbol{\theta}_i \\ 1\end{bmatrix}. \tag{7}$$

We have that $\nabla_{\boldsymbol{\theta}_i} = \frac{\partial L}{\partial \boldsymbol{\theta}_i} = \sum_{j=1}^{P} \frac{\partial l_{ij}}{\partial \boldsymbol{\theta}_i}$ and $\nabla_{\boldsymbol{\beta}_j} = \frac{\partial L}{\partial \boldsymbol{\beta}_j} = \sum_{i=1}^{N} \frac{\partial l_{ij}}{\partial \boldsymbol{\beta}_i}$.

5.1 Information Matrices

Tra matrices information are given by

$$\mathfrak{I}_{\boldsymbol{\theta}_i} = E\left[\frac{\partial L}{\partial \boldsymbol{\theta}_i}\frac{\partial L}{\partial \boldsymbol{\theta}_i^t}\right] = \sum_{j=1}^{p}\pi_{ij}(1-\pi_{ij})\boldsymbol{a}_j\boldsymbol{a}_j^t, \tag{8}$$

$$\mathfrak{I}_{\boldsymbol{\beta}_j} = E\left[\frac{\partial L}{\partial \boldsymbol{\beta}_j}\frac{\partial L}{\partial \boldsymbol{\beta}_j^t}\right] = \sum_{i=1}^{N}\pi_{ij}(1-\pi_{ij})\begin{bmatrix}\boldsymbol{\theta}_i \\ 1\end{bmatrix}\begin{bmatrix}\boldsymbol{\theta}_i \\ 1\end{bmatrix}^t. \tag{9}$$

Let $w_{ij} = \pi_{ij}(1-\pi_{ij})$, $\boldsymbol{W}_{i.} = \text{diag}(w_{ij}, \ldots, wip)$, $\boldsymbol{W}_{.j} = \text{diag}(w_{1j}, \ldots, w_{Nj})$, $i = 1, \ldots, N$, $j = 1, \ldots, p$. Thus we have that,

$$\mathfrak{I}_{\boldsymbol{\theta}_i} = \boldsymbol{A}^t \boldsymbol{W}_{i.} \boldsymbol{A} \tag{10}$$

$$\mathfrak{I}_{\boldsymbol{\beta}_j} = [\boldsymbol{\theta}|\mathbf{1}_N]^t \boldsymbol{W}_{.j} [\boldsymbol{\theta}|\mathbf{1}_N]. \tag{11}$$

For the unidimensional case the matrix $\boldsymbol{A}$ reduces to the p-vector, whose jth component is a_j and $\boldsymbol{\Theta}$ is the N-vector whose ith component is θ_i.

6 Proposed Bayesian Algorithm

The algorithm proposed in this section is based directly on the Bayesian IWLS algorithm. At each iteration a IWLS step is introduced to improve the approximation, by searching a point closer to the mode of the full conditional distribution than the current position.

6.1 Prior distributions

For the $\boldsymbol{\beta}_j$ vector parameters we propose a prior distribution given by the normal $N(\widetilde{\boldsymbol{\pi}}_\beta, \widetilde{\boldsymbol{\Sigma}}_\beta)$, where $\widetilde{\boldsymbol{\pi}}_\beta = \left(\frac{1}{\sqrt{m}}\mathbf{1}_m^t, 0\right)^t$ and $\widetilde{\boldsymbol{\Sigma}}_\beta = \boldsymbol{I}_{m+1}$. For the latent traits we propose the normal distribution $N(\widetilde{\boldsymbol{\pi}}_\theta, \widetilde{\boldsymbol{\Sigma}}_\theta)$. where $\widetilde{\boldsymbol{\pi}}_\theta = \mathbf{0}_m$, and $\widetilde{\boldsymbol{\Sigma}}_\theta$ is a correlation matrix, with 1s on the diagonal and correlation σ_{st} between $\boldsymbol{\theta}_s$ and $\boldsymbol{\theta}_t$, $s \neq t$. To model $\widetilde{\boldsymbol{\Sigma}}_\theta$ it was introduced an unconstraint covariance matrix $\boldsymbol{R}$, where $\boldsymbol{R} = [\rho_{st}]$ and such that the constrained covariance matrix $\widetilde{\boldsymbol{\Sigma}}_\theta$ can be obtained from $\boldsymbol{R}$ using

$$\sigma_{st} = \frac{\rho_{st}}{\sqrt{\rho_{ss}\rho_{tt}}}, \quad s \neq t. \tag{12}$$

A non informative prior that can be assumed for $\boldsymbol{R}$ is the Jeffreys' prior given by $p(\theta) \propto |I(\theta)|^{\frac{1}{2}}$, where $I(w)$ is the expected Fisher information matrix of w. In this work, it was used the Jeffreys' prior given by $p(\boldsymbol{R}) \propto |\boldsymbol{R}|^{-(m+1)/2}$. According to [7], the posterior distribution for $\boldsymbol{R}$ is given by the inverse Wishart distribution $IW_m(S, N)$, where $S = \sum_{i=1}^N \boldsymbol{\theta}_i \boldsymbol{\theta}_i^t$.

6.2 The Algorithm

In this section we use the following notation. For a matrix $\boldsymbol{S}$, $\boldsymbol{S}_{i.}$ represents the ith row of $\boldsymbol{S}$, and $\boldsymbol{S}_{.j}$ is its jth column. The symbol $\dot{\boldsymbol{S}}_{i.}$ represents the diagonal matrix whose diagonal $\boldsymbol{S}_{i.}$, and $\dot{\boldsymbol{S}}_{.j}$ is the diagonal matrix whose diagonal is $\boldsymbol{S}_{.j}$. The symbol $\odot$ represents the Hadamard product between matrices or vectors, $\mathbf{1}_k$ is the k vector of ones, and $\boldsymbol{J}_{Np}$ is the $N \times p$ matrix whose elements are all equal to 1. The proposed Bayesian IWLS algorithm for 2PL-MIRT models is as follows.

1. Step 1. Obtain Initial values for both, the item parameters $\boldsymbol{\beta}^*$ and the latent traits $\boldsymbol{\theta}^*$. Set $\boldsymbol{\beta}_j^{(1)} = \boldsymbol{\beta}_j^*$, $j = 1, \ldots, p$ and $\boldsymbol{\theta}_i^{(1)} = \boldsymbol{\theta}_i^*$, $i = 1, \ldots, N$. Let $\widetilde{\boldsymbol{\Sigma}}_\theta^{(1)} = \boldsymbol{I}_m$.

2. Step $k+1$, $k \geq 1$. Block $\boldsymbol{\beta}$. IWLS step.
   (a) $\boldsymbol{\eta}^{(k)} = [\boldsymbol{\theta}^{(k)}|\mathbf{1}_N]\boldsymbol{\beta}^{t(k)}$
   (b) $\boldsymbol{\pi}^{(k)} = h^{-1}(\boldsymbol{\eta}^{(k)})$
   (c) $\boldsymbol{z}^{(k)} = \boldsymbol{\eta}^{(k)} + h'(\boldsymbol{\pi}^{(k)}) \odot (\boldsymbol{y} - \boldsymbol{\pi}^{(k)})$
   (d) $\boldsymbol{W}^{(k)} = \boldsymbol{\pi}^{(k)} \odot (\boldsymbol{J}_{Np} - \boldsymbol{\pi}^{(k)}))$
   (e) $\widetilde{\boldsymbol{\beta}}_j^{(k)} = \left([\boldsymbol{\theta}^{(k)}|\mathbf{1}_N]^t \dot{\boldsymbol{W}}_{.j}[\boldsymbol{\theta}^{(k)}|\mathbf{1}_N]\right)^{-1} [\boldsymbol{\theta}^{(k)}|\mathbf{1}_N]^t \dot{\boldsymbol{W}}_{.j}\boldsymbol{z}^{(k)}$, $j = 1, \ldots, p$; (except the fixed item parameters). Let $\widetilde{\boldsymbol{\beta}}^{(k)}$ be the matrix whose rows are $\widetilde{\boldsymbol{\beta}}_j$.
3. Step $k+1$, $k \geq 1$. Block $\boldsymbol{\beta}$. Sampling step
   (a) $\boldsymbol{\eta}^{(k)} = [\boldsymbol{\theta}^{(k)}|\mathbf{1}_N]\widetilde{\boldsymbol{\beta}}^{t(k)}$
   (b) $\boldsymbol{\pi}^{(k)} = h^{-1}(\boldsymbol{\eta}^{(k)})$
   (c) $\boldsymbol{z}^{(k)} = \boldsymbol{\eta}^{(k)} + h'(\boldsymbol{\pi}^{(k)}) \odot (\boldsymbol{y} - \boldsymbol{\pi}^{(k)})$
   (d) $\boldsymbol{W}^{(k)} = \boldsymbol{\pi}^{(k)} \odot (\boldsymbol{J}_{Np} - \boldsymbol{\pi}^{(k)}))$
   (e) For $j = 1, \ldots, p$; (except the fixed item parameters) do
      e.1 $\mathfrak{I}_{\beta_j}^{(k)} = [\boldsymbol{\theta}^{(k)}|\mathbf{1}_N]^t \dot{\boldsymbol{W}}_{.j}^{(k)}[\boldsymbol{\theta}^{(k)}|\mathbf{1}_N]$
      e.2 $\boldsymbol{\Sigma}_{\beta_j}^{(k)} = \left[\widetilde{\boldsymbol{\Sigma}}_{\boldsymbol{\beta}}^{-1} + \mathfrak{I}_{\beta_j}^{(k)}\right]^{-1}$
      e.3 $\boldsymbol{\pi}_{\beta_j}^{(k)} = \boldsymbol{\Sigma}_{\beta_j}^{(k)} \left[\widetilde{\boldsymbol{\Sigma}}_{\beta}^{-1}\widetilde{\boldsymbol{\pi}}_{\beta} + [\boldsymbol{\theta}^{(k)}|\mathbf{1}_N]^t \dot{\boldsymbol{W}}_{.j}^{(k)}\boldsymbol{z}_{.j}^{(k)}\right]$
      e.4 Obtain a candidate sample $\boldsymbol{\beta}_j^*$ from $N(\boldsymbol{\pi}_{\beta_j}^{(k)}, \boldsymbol{\Sigma}_{\beta_j}^{(k)})$.
      e.5 Acceptation rule. Let $q_{\beta_j}(\boldsymbol{\beta}_j|\cdot)$ denote the kernel of the density of $N(\boldsymbol{\pi}_{\beta_j}^{(k)}, \boldsymbol{\Sigma}_{\beta_j}^{(k)})$, and $p(\boldsymbol{\beta}_j|\cdot)$ the posterior density of $\boldsymbol{\beta}_j$. Define

$$\alpha_{\beta_j} = \frac{p(\boldsymbol{\beta}_j^*|\boldsymbol{y}_{.j}, \boldsymbol{\theta}^{(k)})/q_{\beta_j}(\boldsymbol{\beta}_j^*|\boldsymbol{\pi}_{\beta_j}^{(k)}, \boldsymbol{\Sigma}_{\beta_j}^{(k)})}{p(\boldsymbol{\beta}_j^{(k)}|\boldsymbol{y}_{.j}, \boldsymbol{\theta}^{(k)})/q_{\beta_j}(\boldsymbol{\beta}_j^{(k)}|\boldsymbol{\pi}_{\beta_j}^{(k)}, \boldsymbol{\Sigma}_{\beta_j}^{(k)})} \tag{13}$$

      If $\alpha_{\beta_j} \geq 1$ accept $\boldsymbol{\beta}_j$. If $\alpha_{\beta_j} < 1$ accept $\boldsymbol{\beta}_j$ with probability α_{β_j}. That is, generate a random value $u \sim U(0,1)$. If $\alpha_{\beta_j} > u$ accept $\boldsymbol{\beta}_j$. If accept $\boldsymbol{\beta}_j$, set $\boldsymbol{\beta}_j^{(k+1)} = \boldsymbol{\beta}_j^*$. Otherwise $\boldsymbol{\beta}_j^{(k+1)} = \boldsymbol{\beta}_j^{(k)}$.
4. Step $k+1, k \geq 1$. Block $\boldsymbol{\Theta}$. IWLS step.
   (a) $\boldsymbol{\eta}^{(k)} = [\boldsymbol{\theta}^{(k)}|\mathbf{1}_N]\boldsymbol{\beta}^{t(k+1)}$
   (b) $\boldsymbol{\pi}^{(k)} = h^{-1}(\boldsymbol{\eta}^{(k)})$
   (c) $\boldsymbol{z}^{(k)} = \boldsymbol{\eta}^{(k)} + h'(\boldsymbol{\pi}^{(k)}) \odot (\boldsymbol{y} - \boldsymbol{\pi}^{(k)})$
   (d) $\boldsymbol{W}^{(k)} = \boldsymbol{\pi}^{(k)} \odot (\boldsymbol{J}_{Np} - \boldsymbol{\pi}^{(k)}))$
   (e) $\widetilde{\boldsymbol{\theta}}_i^{(k)} = \left(\boldsymbol{A}^{t(k)}\dot{\boldsymbol{W}}_{i.}^{(k)}\boldsymbol{A}^{(k)}\right)^{-1} \boldsymbol{A}^{t(k)}\dot{\boldsymbol{W}}_{i.}^{(k)}\boldsymbol{z}^{(k)}$, $i = 1, \ldots, N$. Let $\widetilde{\boldsymbol{\theta}}^{(k)}$ be the matrix whose rows are $\widetilde{\boldsymbol{\theta}}_i$.
5. Step $k+1, k \geq 1$. Block $\boldsymbol{\Theta}$. Sampling step.
   (a) $\boldsymbol{\eta}^{(k)} = [\widetilde{\boldsymbol{\theta}}^{(k)}|\mathbf{1}_N]\boldsymbol{\beta}^{t(k+1)}$
   (b) $\boldsymbol{\pi}^{(k)} = h^{-1}(\boldsymbol{\eta}^{(k)})$
   (c) $\boldsymbol{z}^{(k)} = \boldsymbol{\eta}^{(k)} + h'(\boldsymbol{\pi}^{(k)}) \odot (\boldsymbol{y} - \boldsymbol{\pi}^{(k)})$
   (d) $\boldsymbol{W}^{(k)} = \boldsymbol{\pi}^{(k)} \odot (\boldsymbol{J}_{Np} - \boldsymbol{\pi}^{(k)}))$
   (e) For $i = 1, \ldots, N$; do
      e.1 $\mathfrak{I}_{\theta_i}^{(k)} = \boldsymbol{A}^{t(k+1)}\dot{\boldsymbol{W}}_{i.}^{(k)}\boldsymbol{A}^{(k+1)}$

e.2 $\boldsymbol{\Sigma}_{\theta_i}^{(k)} = \left[\left(\widetilde{\boldsymbol{\Sigma}}_{\theta}^{(k)} \right)^{-1} + \mathfrak{I}_{\theta_i}^{(k)} \right]^{-1}$

e.3 $\boldsymbol{\pi}_{\theta_i}^{(k)} = \boldsymbol{\Sigma}_{\theta_i}^{(k)} \left[\left(\widetilde{\boldsymbol{\Sigma}}_{\theta}^{(k)} \right)^{-1} \widetilde{\boldsymbol{\pi}}_{\theta} + \boldsymbol{A}^{t(k)} \dot{\boldsymbol{W}}_{i.}^{(k)} \boldsymbol{z}_{i.}^{(k)} \right]$

e.4 Obtain a candidate sample $\boldsymbol{\theta}_i^*$ from $N(\boldsymbol{\pi}_{\theta_i}^{(k)}, \boldsymbol{\Sigma}_{\theta_i}^{(k)})$.

e.5 Acceptation rule. Let $q_{\theta_i}(\boldsymbol{\theta}_i|\cdot)$ denote the density of $N(\boldsymbol{\pi}_{\theta_i}^{(k)}, \boldsymbol{\Sigma}_{\theta_i}^{(k)})$, and $p(\boldsymbol{\theta}_i|\cdot)$ the posterior density of $\boldsymbol{\theta}_i$. Define

$$\alpha_{\theta_i} = \frac{p(\boldsymbol{\theta}_i^*|\boldsymbol{y}_{i.}, \boldsymbol{\beta}^{(k+1)})/q_{\theta_i}(\boldsymbol{\theta}_i^*|\boldsymbol{\pi}_{\theta_i}^{(k)}, \boldsymbol{\Sigma}_{\theta_i}^{(k)})}{p(\boldsymbol{\theta}_i^{(k)}|\boldsymbol{y}_{i.}, \boldsymbol{\beta}^{(k+1)})/q_{\theta_i}(\boldsymbol{\theta}_i^{(k)}|\boldsymbol{\pi}_{\theta_i}^{(k)}, \boldsymbol{\Sigma}_{\theta_i}^{(k)})} \tag{14}$$

If $\alpha_{\theta_i} \geq 1$ accept $\boldsymbol{\theta}_i$. If $\alpha_{\theta_i} < 1$ accept $\boldsymbol{\theta}_i$ with probability α_{θ_i}. That is, generate a random value $u \sim U(0,1)$. If $\alpha_{\theta_i} > u$ accept $\boldsymbol{\theta}_i$. If accept $\boldsymbol{\theta}_i$, set $\boldsymbol{\theta}_i^{(k+1)} = \boldsymbol{\theta}_i^*$. Otherwise $\boldsymbol{\theta}_i^{(k+1)} = \boldsymbol{\theta}_i^{(k)}$.

6. Step $k+1$. Block $\boldsymbol{\Sigma}$.
   (a) Obtain a sample $\boldsymbol{R}$ from $IW_m(S^{(k)}, N)$, where $S^{(k)} = \sum_{i=1}^{N} \boldsymbol{\theta}_i^{(k)} (\boldsymbol{\theta}_i^{(k)})^t$.
   (b) Obtain $\widetilde{\boldsymbol{\Sigma}}_{\theta}^{(k+1)}$ from $\boldsymbol{R}$ by using equation (12).

An implementation of the algorithm in R, with scripts for simulation data and real data can be obtianed by request to the authors.

7 Real data

The data are from the admission test at the Universidad Nacional de Colombia, applied in the second semester of 2009. We took a sample size of N=1449. The test was taken by more than 35,000 people. There were seven forms of the test, but the only difference between them was the order of the questions. The data correspond to a sample from one form. The test size was $p = 95$ with 5 subtests. The subtests were: mathematics (Math) with $p_1 = 20$ items, natural sciences (Science) with $p_2 = 25$ items, social sciences (Social) with $p_3 = 26$, textual analysis (Textual) with $p_4 = 15$ items, and image analysis (Image) with $p_5 = 9$ items. The items 10, 21, 55, 75, 95 were fixed. The results are based on 6000 iterations after a burn-in period of 2500 iterations. Table 1 shows a summary of the acceptance rates for both, the item parameters and the latent traits. The sampling chains passed the Heidelberger-Welch stationarity test for almost all the cases.

	Min.	1st Qu.	Median	Mean	3rd Qu.	Max.
latent traits	0.10	0.4678	0.5692	0.5478	0.6518	0.8352
item parameters	0.8662	0.9364	0.9517	0.9467	0.9615	0.9758

Table 1. Summary of the acceptation rates. Real data.

Table 2 shows a summary of the item parameters estimated by the Bayesian algorithm. Some of the discrimination parameters are negative, but they are

small. We did not do any special treatment with those values. However, it is easy to include the logarithm transformation in the model to obtain only positive values.

	$\boldsymbol{a}_1$	$\boldsymbol{a}_2$	$\boldsymbol{a}_3$	$\boldsymbol{a}_4$	$\boldsymbol{a}_5$	d
Min.	-0.20658	-0.1728	-0.228664	-0.1487	-0.19353	-2.3188
1st Qu.	0.00973	0.1352	-0.002583	0.1383	0.02684	-0.9227
Median	0.16772	0.2357	0.132120	0.2248	0.14929	-0.3533
Mean	0.20694	0.2504	0.161899	0.2882	0.18663	-0.1765
3rd Qu.	0.34229	0.3513	0.256368	0.4058	0.27698	0.4400
Max.	2.22373	1.0544	1.700400	1.3903	1.51406	2.1505

Table 2. Summary of the item parameters. Real data.

Finally, table 3 shows the main statistics of the latent traits estimated by the Bayesian algorithm.

	$\boldsymbol{\theta}_1$	$\boldsymbol{\theta}_2$	$\boldsymbol{\theta}_3$	$\boldsymbol{\theta}_4$	$\boldsymbol{\theta}_5$
Min.	-1.88994	-2.084656	-1.96438	-2.45430	-2.09705
1st Qu.	-0.55483	-0.423623	-0.52520	-0.46252	-0.47362
Median	-0.17325	-0.005061	-0.08354	0.01508	0.02279
Mean	-0.04458	0.006222	-0.02150	0.01428	0.01376
3rd Qu.	0.38927	0.417533	0.48706	0.52226	0.53826
Max.	2.73310	2.358814	2.21566	2.10364	2.02972

Table 3. Summary of the latent traits. Real data.

8 Discussion

We have introduced a IWLS Bayesian algorithm to fit a 2PL MIRT model. The proposed algorithm is a hybrid MH within Gibbs sampler with independent proposals for the latent traits and the item parameters. The algorithm has several characteristics that promise a very good performance in other IRT models. The first important issue is that the proposal densities are normal distributions derived from a linear approximation of the link function at the observations and around their expect values. This is the basis of the working variables technique. Even though the MIRT models can be considered mixed models with repeated observations, we did not use that fact. Instead we treated both, the latent traits and the item parameters in a symmetrical way. In the β block we fixed the latent traits and obtained the normal approximation of the posterior densities of the item parameters, introducing the corresponding working variables. In the θ block we fixed the item parameters and obtained the normal approximation of the posterior densities of latent traits introducing the corresponding working variables and considering the covariance matrix obtained in the previouos step for the prior densities.

References

1. J. Albert. Bayesian Estimation of Normal Item Response Curves Using Gibbs Sampling. *Journal of Educational Statistics*, 17,3,251-269, 1992
2. D. Bold and V.F. Lall. Estimation of Compensatory and non-compensatory multidimensional Item Response Theory Models Using Markov Chain Monte Carlo. *Applied Psychological Measurement*, 27,6, 395-414, 2003.
3. D. Gamerman. Sampling from the posterior distribution in generalized linear mixed models. Statistics and Computing, 7, 57-68, 1997.
4. A. Gutierrez, The Use of Working Variables in the Bayesian Modeling of Mean and Dispersion Parameters in Generalized Nonlinear Models with Random Effects, *Communications in Statistics-Simulation and Computation*, 44, 1, 168-195, 2015.
5. C.A. Glas and A. Béguin. MCMC Estimation and some model-fit analysis of multidimensional IRT models. *Psychometrika*, 66, 4, 21., 2001.
6. J. Kim, D. and Bolt. Estimating Item Response Theory Models Using Markov Chain Monte Carlo Methods. *Educational Measurement: Issues and Practice*,26, 38-51, 2007.
7. Multidimensional Item Response Theory Models where the Ability has a Linear Latent Structure, PhD dissertation, Univesidad Nacional e Colombia, 2010.
8. A. Montenegro, L. Parra, E. Berdugo. A MIRT Model for Tests with Multiple Subtests. *IOSR-JRME*, 6,6 7-20,2016.
9. J. Nelder, and R, Wedderburn. Generalized Linear Models. *Journal of the Royal statistical society: Series A*, 135, 370-384,1972.
10. A Straighforward Approach to Markov Chain Monte Carlo Methods for item Response Models. *Journal of Educational and Behavioral Statistics*, 24, 2 , 146-178, 1999.
11. J. De la Torre and R. Patz. Making the most of what we have: a practical application of multidimensional item response theory in test scoring. *Journal of Educational and Behavioral Statistics*, 30, 3, 295-311, 2005
12. M. Reckase. The difficulty of test items that measure more than one ability. *Applied Psycological Measurement*, 9, 9, 401-412, 1985.
13. M. Reckase, *Multidimensional Item Response Theory*, Springer, 2009.
14. I. Yalcin and Y. Amemiya, Nonlinear Factor Analysis as a Statistical Method. *Statistical Science*, 16,3,275-294, 2001.

Lie Symmetries of the Black–Scholes Type Equations in Financial Mathematics

Asaph Keikara Muhumuza[1], Anatoliy Malyarenko[2], and Sergei Silvestrov[3]

[1] Division of Applied Mathematics, Mälardalen University, Box 883, Högskoleplan 1, SE 721 23 Västerås, Sweden
(E-mail: asaph.keikara.muhumuza@mdh.se)
[2] Division of Applied Mathematics, Mälardalen University, Box 883, Högskoleplan 1, SE 721 23 Västerås, Sweden
(E-mail: anatoliy.malyarenko@mdh.se)
[3] Division of Applied Mathematics, Mälardalen University, Box 883, Högskoleplan 1, SE 721 23 Västerås, Sweden
(E-mail: sergei.silvestrov@mdh.se)

Abstract. In this paper, we consider a two-dimensional Black–Scholes model of financial mathematics. Using Lie theory, we determine the generators of the symmetry group of the corresponding Feynman–Kac partial differential equation.
Keywords: Lie theory, Black–Scholes model, Feynman–Kac equation.

1 Introduction

This article presents the method of symmetry analysis of the Black–Scholes type equation in financial mathematics. Itô's formula for Brownian motion is an important ingredient in the derivation of the Black–Scholes type equations in financial mathematics (i.e., Black and Scholes [5]). Let $x(t)$ be a function of t which satisfies the stochastic differential equation

$$dx = a(x,t)dt + b(x,t)dz,$$

where $a(x,t)$ and $b(x,t)$ are deterministic functions of x and t, and z represents the standard Brownian motion. Also, let $f(x,t) \in C^2$ be a twice continuously differentiable function of x and t. Then,

$$df(x,t) = \left(f_t + a(x,t)f_x + \frac{1}{2}b^2 f_{xx} \right) dt + b(x,t)f_x dz.$$

This was a basis of the work of Black and Scholes [5] and Merton [35] that opened a new era in mathematical modelling of problems in finance. Originally, the models were formulated in terms of stochastic differential equations. Under certain restrictive assumptions, these models can be written as linear evolutionary partial equations with variable coefficients.

The widely used one-dimensional model (or one state variable plus time) known as the Black–Scholes model for European option, is described by the equation

$$u_t + \frac{1}{2}(\sigma x)^2 u_{xx} + rxu_x - ru = 0, \tag{1}$$

where $u(x,t)$ is the value of option with defined payoff, $x \in [0,\infty)$ is the price of the underlying asset, $t \in [0,\infty)$ is the time, the constant coefficient σ^2 is the volatility of the underlying asset (annual volatility of the asset price) and r is the constant risk-free interest rate. σ^2 and r are referred to as the parameters of the model. Black and Scholes reduced it to the classical heat equation and used this relation for solving Cauchy's problem with special initial data.

Assuming now the European call options of two assets x and y both with constant risk-free interest rate r, volatility σ_i^2, $i = 1, 2$ and correlation coefficient ρ. We assume that x and y are governed by stochastic processes of the form:

$$dx = rxdt + \sigma_1 x dw^1, \qquad dy = rydt + \sigma_1 y dw^2, quad\rho = d(w^1, w^2).$$

Along with Equation (1), more complex models aimed at explaining additional effects are discussed in current literature (see, e.g., Sharp [15]). The option $u(x,y,t)$ with payoff $u_T(x,y)$ at maturity T satisfies a two-dimension Black–Scholes partial differential equation in $\mathbb{R}^2_+[0,T]$ as stated in Koh et al. [53] and Jeong et al. [3]

$$u_t + \frac{1}{2}(\sigma_1 x)^2 x^2 u_{xx} + \frac{1}{2}(\sigma_2 y)^2 x^2 u_{yy} + \sigma_1\sigma_2\rho xy u_{xy} + rxu_x + ryu_y - ru = 0. \quad (2)$$

An analytical study of solutions of this equation as well as of other complex models of financial mathematics presents a challenge for mathematicians. This is due to the fact that, as a rule, these models unlike the Black–Scholes equation (1), cannot be reduced to simple equations with known solutions. In this article, we demonstrated this fact for the *Black–Scholes equation* (2) by using methods of Lie group analysis.

The *Lie group analysis* is a mathematical theory that synthesises symmetry of differential equations. The founder of this theory, Sophus Lie [45,46] was the first who classified differential equations in terms of their symmetry groups, thereby identifying the set of equations which could be integrated or reduced to lower-order equations by group-theoretic algorithms. In particular, Lie [41,44] gave the group classification of linear second-order partial differential equations with two independent variables and developed methods of their integration. According to his classification all parabolic equations admitting the symmetry group of the highest order reduce to the heat conduction equation. These and a wide variety of other results in group analysis of differential equations are to be found in Ibragimov [23–25], Ibragimov et al [27], Ovsyannikov [19], Olver [28–31], Olver and Sosenaul [32], Bluman and Cole [6], Bluman et al [7,8], Bluman and Kumei [9], Kumei and Blueman [40], Leray [14], Dickson [18], Peter [4], Hadamard [12] and many others.

A symmetry group of a (system of) differential equations is a group which transforms solutions of the system to other solutions. The group elements are geometric transformations on the space of independent and dependent variables for the system. Acting on solutions, they transform their graphs.

Differential equations occurring in sciences as mathematical models, often involve undetermined parameters an or arbitrary function of certain variables.

Usually, these arbitrary elements (parameter function) are found experimentally or chosen from a "simplicity criterion". Lie group theory provides a regular procedure for determining arbitrary element from symmetry point of view. This direction of study is known today as *Lie group classification of differential equations*. For detailed presentations of methods used in Lie group classification of differential equations the reader is referred to the first foundation paper on this topic i.e., Lie [46] dealing with the classification of linear second-order partial differential equation with two independent variables.

Lie group classification of differential equations provides a mathematical background for what can be called a *group theoretic modelling*(see e.g., Ibragimov [23], Ovsyannikov [19], Olver [28], Bluman and Cole [6]). In this approach the differential equations admitting more symmetries are considered to be "preferable".

In this way, one often arrives at the equation possessing remarkable physical properties. Given a family of differential equations, the procedure of Lie group classification begins with determining the so-called *principal Lie group* of this family of equations. This i s the group admitted by any equation of the family of question. The Lie algebra of the principal Lie group is called the *principal Lie algebra* of the equation and is denoted by L_p (see, e.g., [23]). It may happen that for particular choice of arbitrary element of this family the corresponding equation admits, along with the principal Lie group, additional symmetry transformations. Determination of all distinctly different particular cases when an extension of $L_\wp$ occurs is the problem of the group classification.

This paper is aimed at Lie group analysis (symmetries, classification and invariant solutions) of the two dimensional Black–Scholes (1) and (2) models for European options. In Section 2 we give a brief outline of the method of symmetry analysis of differential equations and in Section 3 we calculate the symmetries of a special case of the Black–Scholes model also referred to as the Feynman–Kac partial differential equation in financial mathematics.

2 Brief Outline of the Method for Calculation of Infinitesimal Symmetries

Consider a one-dependent variable and three-independent variables evolutionary partial differential equations of the second order (e.g., see Ibragimov [25], Olver [30], and Bluman *et al.* [7], Ovsyannikov [19]):

$$u_t - F(t, x, y, u, u_{(1)}, u_{(2)}) = 0, \tag{3}$$

where u is a function of independent variable t and $x = (x^1, dots, x^n)$, $y = (y^1, \ldots, y^n)$ and $u_{(1)}$, $u_{(2)}$ are the sets of its first and second-order partial derivatives

$$u_{(1)} = (u_{x^1}, u_{y^1}, \ldots, u_{x^n}, u_{y^n}),$$
$$u_{(2)} = (u_{x^1x^1}, u_{y^1y^1}, u_{x^1x^2}, u_{y^1y^2}, \ldots, u_{x^nx^n}, u_{y^ny^n}).$$

Recalling that an invertible transformation of the variable t, x, y, u,

$$\begin{aligned} \bar{t} = \ & f(t,x,y,u,\epsilon), \qquad \bar{x}^i = g^i(t,x,y,u,\epsilon), \\ \bar{y}^j = \ & g^j(t,x,y,u,\epsilon), \qquad \bar{u} = h(t,x,y,u,\epsilon), \quad i = 1,\ldots,n \end{aligned} \tag{4}$$

depending on a parameter ϵ are said to be *symmetry transformation of Equation* (3), if Equation (3) has the same form in the new variables $\bar{t}, \bar{x}, \bar{y}, \bar{u}$. The set G of such transformation is a *continuous group*, i.e., G contains the identity transformation

$$\bar{t} = t, \qquad \bar{x}^i = x^i, \qquad \bar{y}^j = y^j, \qquad \bar{u} = u,$$

the inverse to any transformation from G and the composition of any transformations from G. The symmetry group G is also known as the group *admitted* by equation (3).

According to the Lie theory, the symmetry group G is equivalent to determination of its *infinitesimal transformations:*

$$\begin{aligned} \bar{t} \approx \ & t + \epsilon\tau(t,x,y,u), \qquad \bar{x}^i \approx x^i + \epsilon\xi^i(t,x,y,u), \\ \bar{y}^j \approx \ & y^j + \epsilon\eta^j(t,x,y,u), \qquad \bar{u} \approx u + \epsilon\phi(t,x,y,u). \end{aligned} \tag{5}$$

It is convenient to introduce the *symbol* (after Lie) of the infinitesimal transformation (5), i.e., the operator

$$X = \tau(t,x,y,u)\frac{\partial}{\partial t} + \xi^i(t,x,y,u)\frac{\partial}{\partial x^i} + \eta^j(t,x,y,u)\frac{\partial}{\partial y^j} + \phi(t,x,y,u)\frac{\partial}{\partial u.} \tag{6}$$

The operator (6) is also known in the literature as the *infinitesimal operator or generator of the group G.* The symbol X of the group *admitted by* equation (3) is called an operator admitted by Equation (3).

The group transformation (4) corresponding to the infinitesimal transformation with the symbol (6) are found by solving the *Lie equation*

$$\begin{aligned} \frac{d\bar{t}}{d\epsilon} = \ & \tau(\bar{t},\bar{x},\bar{y},\bar{u}), \qquad \frac{d\bar{u}}{d\epsilon} = \xi^i(\bar{t},\bar{x},\bar{y},\bar{u}), \\ \frac{d\bar{u}}{d\epsilon} = \ & \eta^j(\bar{t},\bar{x},\bar{y},\bar{u}), \qquad \frac{d\bar{u}}{d\epsilon} = \phi(\bar{t},\bar{x},\bar{y},\bar{u}) \end{aligned} \tag{7}$$

with the initial conditions:

$$\bar{t}|_{\epsilon=0} = t, \qquad \bar{x}^i|_{\epsilon=0} = x, \qquad \bar{y}^j|_{\epsilon=0} = y, \qquad \bar{u}|_{\epsilon=0} = u.$$

By definition, the transformation (4) from a symmetry group of Equation (3) if the function $\bar{u} = \bar{u}(\bar{t},\bar{x},\bar{y})$ satisfy the equation.

$$\bar{u}_{\bar{t}} - F(\bar{t},\bar{x},\bar{y},\bar{u},\bar{u}_{(1)},\bar{u}_{(2)}) = 0 \tag{8}$$

whenever the function $u = u(t,x,y)$ satisfies equation (3). Here $\bar{u}_{\bar{t}}$, $\bar{u}_{(1)}, \bar{u}_{(2)}$ are obtained from Equation (4) according to the usual formulas of change of

variables in derivatives. The infinitesimal form of these formulae are written as:

$$\begin{aligned}
\bar{u}_{\bar{t}} &\approx u_t + \epsilon\phi^t(\bar{t},\bar{x},\bar{y},\bar{u},\bar{u}_{(t)},\bar{u}_{(1)}),\\
\bar{u}_{\bar{x}^i} &\approx u_{x^i} + \epsilon\phi^i(\bar{t},\bar{x},\bar{y},\bar{u},\bar{u}_{(t)},\bar{u}_{(1)}),\\
\bar{u}_{\bar{y}^j} &\approx u_{y^j} + \epsilon\phi^j(\bar{t},\bar{x},\bar{y},\bar{u},\bar{u}_{(t)},\bar{u}_{(1)}),\\
\bar{u}_{\bar{x}^i\bar{x}^k} &\approx u_{x^ix^k} + \epsilon\phi^{ik}(\bar{t},\bar{x},\bar{y},\bar{u},\bar{u}_{(t)},\bar{u}_{(1)},\bar{u}_{tx^k},\bar{u}_{(2)}),\\
\bar{u}_{\bar{x}^i\bar{y}^j} &\approx u_{x^iy^j} + \epsilon\phi^{ij}(\bar{t},\bar{x},\bar{y},\bar{u},\bar{u}_{(t)},\bar{u}_{(1)},\bar{u}_{x^ky^k},\bar{u}_{(2)}),\\
\bar{u}_{\bar{y}^j\bar{y}^k} &\approx u_{y^jy^k} + \epsilon\phi^{jk}(\bar{t},\bar{x},\bar{y},\bar{u},\bar{u}_{(t)},\bar{u}_{(1)},\bar{u}_{ty^k},\bar{u}_{(2)}),
\end{aligned} \tag{9}$$

where the function $\phi_t, \phi_x, \phi_y, \phi_{ij}$ are obtained by differentiation of $\tau, \xi^i, \eta^i, \phi$ and are given by the *prolongation formulas:*

$$\begin{aligned}
&\phi^t = D_t(\phi) - u_tD_t(\tau) - u_{x^i}D_t(\xi^i) - u_{y^i}D_t(\eta^i),\\
&\phi^i = D_i(\phi) - u_tD_i(\tau) - u_{x^k}D_i(\xi^k) - u_{y^k}D_i(\eta^k),\\
&\phi^j = D_j(\phi) - u_tD_j(\tau) - u_{x^k}D_j(\eta^k) - u_{y^k}D_j(\xi^k),\\
&\phi^{ij} = D_j(\phi_i) - u_{x^ix^k}D_j(\xi^i) - u_{y^jy^k}D_j(\eta^j) - u_{yx^i}D_j(\eta^j) - u_{tx^i}D_j(\tau).
\end{aligned} \tag{10}$$

Here D_t, D_i and D_j denotes the total differentiations with respect to t and x^i:

$$\begin{aligned}
D_t &= \tfrac{\partial}{\partial t} + u_t\tfrac{\partial}{\partial u} + u_{tt}\tfrac{\partial}{\partial u_t} + u_{tx^k}\tfrac{\partial}{\partial u_{x^k}} + u_{ty^k}\tfrac{\partial}{\partial u_{y^k}} + \ldots,\\
D_i &= \tfrac{\partial}{\partial x^i} + u_{x^i}\tfrac{\partial}{\partial u} + u_{tx^i}\tfrac{\partial}{\partial u_t} + u_{yx^i}\tfrac{\partial}{\partial u_y} + u_{x^ix^k}\tfrac{\partial}{\partial u_{x^k}} + \ldots,\\
D_j &= \tfrac{\partial}{\partial y^j} + u_{y^j}\tfrac{\partial}{\partial u} + u_{ty^j}\tfrac{\partial}{\partial u_t} + u_{xy^j}\tfrac{\partial}{\partial u_x} + u_{y^jy^k}\tfrac{\partial}{\partial u_{y^k}} + \ldots
\end{aligned}$$

Substitution of Equation (5) and (9) into the left-hand side of Equation (8) yields:

$$\begin{aligned}
&\bar{u}_{\bar{t}} - F(\bar{t},\bar{x},\bar{u},\bar{u}_{(1)},\bar{u}_{(2)}) \approx u_t - F(t,x,u,u_{(1)},u_{(2)})\\
&+\epsilon\left(\phi^t - \tfrac{\partial F}{\partial u_{x^ix^k}}\phi^{ik} - \tfrac{\partial F}{\partial u_{y^jy^k}}\phi^{jk} - \tfrac{\partial F}{\partial u_{x^i}}\phi^i - \tfrac{\partial F}{\partial u_{y^j}}\phi^j - \tfrac{\partial F}{\partial u}\phi - \tfrac{\partial F}{\partial u_{x^i}}\xi^i - \tfrac{\partial F}{\partial u_{y^j}}\eta^j - \tfrac{\partial F}{\partial t}\tau\right)
\end{aligned}$$

Therefore, by virtue of equation (2), Equation (8) yields

$$\phi^t - \frac{\partial F}{\partial u_{x^ix^k}}\phi^{ik} - \frac{\partial F}{\partial u_{y^jy^k}}\phi^{jk} - \frac{\partial F}{\partial u_{x^i}}\phi^i - \frac{\partial F}{\partial u_{y^j}}\phi^j - \frac{\partial F}{\partial u}\phi - \frac{\partial F}{\partial u_{x^i}}\xi^i - \frac{\partial F}{\partial u_{y^j}}\eta^j - \frac{\partial F}{\partial t}\tau = 0, \tag{11}$$

where u_t is replaced by $F(t,x,y,u,u_{(1)},u_{(2)})$ in $\phi, \phi^i, \phi^j, \phi^{ik}, \phi^{jk}$.

Equation (11) defines all infinitesimal symmetries of Equation (3) and, therefore, it is called the *determining equation.* Conventionally, it is written in the compact form

$$X(u_t - F(t,x,y,u,u_{(1)},u_{(2)}))\,|_{(3)} = 0. \tag{12}$$

Here X denotes the *prolongation* of the operator (6) to the first and second-order derivatives:

$$\begin{aligned}
X = {} & \tau(t,x,y,u)\frac{\partial}{\partial t} + \xi(t,x,y,u)\frac{\partial}{\partial x^i} + \eta^j(t,x,y,u)\frac{\partial}{\partial u}\\
&+ \phi^t\frac{\partial}{\partial u_t} + \phi^i\frac{\partial}{\partial u_{x^i}} + \phi^j\frac{\partial}{\partial u_{y^j}} + \phi^{ik}\frac{\partial}{\partial u_{x^ix^k}} + \phi^{ij}\frac{\partial}{\partial u_{x^iy^j}} + \phi^{jk}\frac{\partial}{\partial u_{y^jx^k}},
\end{aligned}$$

and the notation $|_3$ means evaluated on Equation (3).

The determining equation (11) (or its equivalent, Equation (12)) is a linear homogeneous partial differential equation of the second order for unknown functions $\tau(t,x,y,u)$, $\xi^i(t,x,y,u)$, $\eta^j(t,x,y,u)$ of the 'independent variables t,x,y,u. At the first glance, this equation seems to be complexity. Indeed, the left-hand side of the determining equation involves the derivatives u_t, u_{x^i}, u_{y^j}, $u_{x^ix^k}$, $u_{x^iy^j}$, $u_{y^iy^k}$, along with the variable t,v x, y, u and the functions τ, ξ^i, η^j, ϕ of these variables. Since Equation (11) is valid identically with respect to all the variable involved, the variables u_t, u_{x^i}, u_{y^j}, $u_{x^ix^k}$, $u_{x^iy^j}$, $u_{y^iy^k}$ are treated as "independent" ones. It follows that determining equation decomposes into a system of several equations. As a rule, this is an over determined system (it contains more equations than $n+2$ of the unknown functions τ, ξ^i, η^j, ϕ). Therefore, in practical applications, the determining equation can be solved analytically, unlike the original differential equation (3).

All the above concepts can be summarised by this important theorem as stated by Olver [30] for the case of one variable.

Theorem 1. *Let*

$$X=\sum_{i=1}^{n}\xi^i(x,y,t,u)\frac{\partial}{\partial x^i}+\sum_{\alpha=1}^{q}\phi_\alpha(x,y,t,u)\frac{\partial}{\partial u^\alpha}$$

be a vector field of an open subset. The nth prolongation of X is the vector

$$X^{(n)}=X+\sum_{\alpha=1}^{q}\sum_{J}\phi_\alpha^J\left(x,y,t,u^n\right)\frac{\partial}{\partial u_J^\alpha}$$

defined on the corresponding jet space $M^{(n)}\subset U^{(n)}$, the second summation being over all (unordered) multi-indices $J=(j_1,\cdots,j_k)$, with $1\le j_k\le p, 1\le k\le n$. The coefficient functions ϕ_α^J are given by the following formula:

$$\phi_\alpha^J(x,u^{(n)})=D_J\left(\phi_\alpha\sum_{i=1}^{p}\xi^iu_i^\alpha\right)+\sum_{i=1}^{p}\xi^iu_{J,i}^\alpha$$

where $u_i^\alpha=\frac{\partial u^\alpha}{\partial x^i}$, $u_{J,i}^\alpha=\frac{\partial_J^\alpha}{\partial x^i}$ and D_J is the total differential operator.

2.1 Exact Solutions Provided by Symmetry Groups

Group analysis provide two basic ways for construction of exact solution: group transformations of known solution and construction of *invariant solutions.*

Group Transformation of Known Solutions The first way is based on the fact that a symmetry group transformations any solutions the equation in question into solution of the same equation. let (4) be a symmetry transformation group of equation (3), and let a function

$$u=\phi(t,x,y). \tag{13}$$

Solve equation (3)). since (4) is a symmetry transformation, the solution (13) can be also written using the new variables:

$$\bar{u} = \phi(\bar{t}, \bar{x}, \bar{y}). \tag{14}$$

Replacing here, $\bar{u}, \bar{t}, \bar{x}, \bar{y}$ from equation (4), we get

$$h(t, x, y, u, \epsilon) = \phi(f(t, x, y, u, \epsilon), g(t, x, y, u, \epsilon))$$

Having solved this equation with respect to u, we arrive at the following one-parameter family (with the parameter a) of new solutions of Equation (3):

$$\bar{u} = \phi_\epsilon(\bar{t}, \bar{x}, \bar{y}) \tag{15}$$

Consequently, any known solution is a source of a multi-parameter class of new solutions provided that the differential equation considered admitted a multi-parameter symmetry group.

2.2 Invariant Solution

If a group transformation maps a solution into itself, we arrive at what is called a *self-similar or group invariant solution* The search of this kind of solution reduces the number if independent variables of the equation in question. Namely, the invariance with respect to one-parameter group reduces the number of variables by one. The further reduction can be achieved by considering an invariance under symmetry group with two or more parameters.

The construction of invariant solutions under one-parameter group is is widely known in the literature as studied by Gazizov and Ibragimov [36], Ibragimov [23–25], Ibragimov et al [27], Ovsyannikov [19], [28–31], Olver and Sosenaul [32], Bluman and Cole [6], Bluman et al [7,8], Bluman and Kumei [9], Kumei and Blueman [40].

3 The Symmetry Analysis of the Black–Scholes Models

3.1 The Basic One Parameter Black–Scholes Equation

For mathematical modelling stock option pricing, Black and Scholes [5] proposed the partial differential equation

$$u_t + \frac{1}{2}\sigma^2 x^2 u_{xx} + rxu_x - ru = 0 \tag{1}$$

with constant coefficient σ, r (parameter of the model). It is shown in [5] that Equation (1) is transformable into the classical heat equation

$$\nu_\tau = \nu_{zz}, \tag{16}$$

provided that $A \neq 0, \mathcal{D} \equiv r - \sigma^2/2 \neq 0$. Using the connection between Equation (1) and (16), they given an explicit formula for the solution, defined in the

interval $-\infty < t < t^*$, of the Cauchy problem with a special initial data at $t = t^*$.

The Lie symmetries for this a one parameter Black–Scholes model (1) have been derived by Gazizov and Ibragimov [36] and the infinitesimal symmetries of Equation (1) spanned by following operators:

$$\begin{aligned}
X_1 =&\ \frac{\partial}{\partial t}, \qquad X_2 = X\frac{\partial}{\partial x},\\
X_3 =&\ 2tx\frac{\partial}{\partial x} + (\ln x + \mathcal{D}t)x\frac{\partial}{\partial x} + 2rtu\frac{\partial}{\partial u},\\
X_4 =&\ \sigma^2t^2x\frac{\partial}{\partial\partial x} + (\ln x - \mathcal{D}t)u\frac{\partial}{\partial u},\\
X_5 =&\ 2\sigma^2t^2\frac{\partial}{\partial t} + 2\sigma^2tx\ln x\frac{\partial}{\partial x} + \left((\ln x - \mathcal{D}t)^2 + 2\sigma^2t(rt-1)\right)u\frac{\partial}{\partial u},
\end{aligned} \tag{17}$$

and

$$X_6 = u\tfrac{\partial}{\partial t}, \qquad X_\alpha = \phi(t,x)\tfrac{\partial}{\partial u}, \tag{18}$$

where $\mathcal{D} \equiv r - \sigma^2/2$ and $\alpha(t,x)$ is an arbitrary solution of Equation (1).

The finite symmetry transformations (4),

$$\bar t = f(t,x,u,\epsilon), \qquad \bar x = g(t,x,u,\epsilon), \qquad \bar u = h(t,x,u,\epsilon),$$

corresponding to the basic generators (17) and (18) are obtained by solving the *Lie equation* (7). The result is as follows:

$$\begin{aligned}
X_1:&\quad \bar t = t+\epsilon_1, \quad \bar x = x \quad \bar u = u;\\
X_2:&\quad \bar t = t, \quad \bar x = x\epsilon_2 \quad \bar u = u, \quad \epsilon_2 \neq 0;\\
X_3:&\quad \bar t = t\epsilon_3^2, \quad \bar x = x^{\epsilon_2}e^{\mathcal{D}(\epsilon_3^2-\epsilon_3)t}, \quad \bar u = u^{r(\epsilon_3^2-1)t}, \quad \epsilon_3 \neq 0;\\
X_4:&\quad \bar t = t, \quad \bar x = xe^{\sigma^2t\epsilon_4}, \quad \bar u = ux^{\epsilon_4}e^{((1/2)\sigma^2\epsilon_4^2-\mathcal{D}a_4)t};\\
X_5:&\quad \bar t = \frac{t}{1-2\sigma^2\epsilon_5 t}, \quad \bar x = x^{t/(1-2\sigma^2\epsilon_5 t)},\\
&\quad \bar u = u\sqrt{1-2\sigma^2\epsilon_5 t}\exp\left(\frac{[(\ln x - \mathcal{D}t)^2 + 2\sigma^2t^2]\epsilon_5}{1-2\sigma^2\epsilon_5 t}\right),
\end{aligned}$$

and

$$\begin{aligned}
X_6:&\quad \bar t = t, \quad \bar x = x \quad \bar u = u\epsilon_6; \quad \epsilon_6 \neq 0;\\
X_\phi:&\quad \bar t = t, \quad \bar x = x, \quad \bar u = u + \phi(t,x).
\end{aligned}$$

Here, $\epsilon_1, \ldots, \epsilon_6$ the parameter of one parameter groups generated by $X_1, \ldots, X_6$, respectively and $\phi(t,x)$ is an arbitrary solution of Equation (1). Consequently the operator $X_1, \ldots, X_6$ are generate a six-parameter group and X_ϕ generates an infinite-dimensional group. The general symmetry group is the composition of the above transformations.

3.2 The Feynman–Kac Partial Differential Equation

In financial engineering, the fair price of a financial instrument may be found by solving a boundary value problem for a Feynman–Kac partial differential equation. Calculating the symmetry group of the above equation goes back to Gazizov and Ibragimov [36] who found the symmetry group of the Black–Scholes equation as outline in Subsection 3.1 above. This line of research have been extended by Naicker et al [49], Leach et al [33], Sinkala et al [50,51], Sophocleous et al [1,2], Ivanova et al [26], Dimas et al [39], Sinkala [52], Edelstein and Govinder [38], Caister et al [22], Okeola et al [21], Wang et al [47], Liu and Wang [55], Liu [10], Bordag and Mikaelyan [17], Motsepa et al [48], Lekalakala et al [43], among others.

In this paper, we find the symmetry group of a two-asset variant of the Black–Scholes equation considered by Jeong et al [3], see also classical books by Hull [13] and Kwok [54]. Let $S_0(t)$ be the price of the risk-free asset described by a boundary value problem for an ordinary differential equation

$$\mathrm{d}S_0(t) = r\,\mathrm{d}t, \qquad S_0(0) = 1,$$

and let $S_1(t)$ and $S_2(t)$ be the prices of two risky assets described by a boundary value problem for the following system of stochastic differential equations

$$\mathrm{d}S_i(t) = \mu_i S_i(t)\,\mathrm{d}t + \sigma_i S_i(t)\,\mathrm{d}W_i(t), \qquad S_i(0) = S_i^0$$

with $\mathrm{d}W_1\,\mathrm{d}W_2 = \rho_{12}\,\mathrm{d}t$. The Feynman–Kac theorem leads to the following model:

$$u_t = \frac{1}{2}(\sigma_1 x)^2\frac{\partial^2 u}{\partial x^2} + \frac{1}{2}(\sigma_2 y)^2\frac{\partial^2 u}{\partial y^2} + \sigma_1\sigma_2\rho xy\frac{\partial^2 u}{\partial x\partial y} + rx\frac{\partial u}{\partial x} + ry\frac{\partial u}{\partial y} - ru, \quad (19)$$

where $u = u(x, y, t)$ and all the other terms have the same meaning as for the case of Equation (2).

To determine the symmetries of (19) we let F represent the homogeneous linear partial differential equation as in (2) where

$$F : \mathbb{R}^3_{x,y,t} \times \mathbb{R}_u \times \mathbb{R}^3_{u_x,u_y,u_t} \times \mathbb{R}^6_{u_{xx},u_{xy},u_{xt},u_{yy},u_{yt},u_{tt}} \longrightarrow \mathbb{R}$$

is such that

$$\begin{aligned} &F(x, y, t, u, u_x, u_y, u_t, u_{xx}, u_{xy}, u_{xt}, u_{yy}, u_{yt}, u_{tt}) \\ &\quad = u_t - Au_{xx} - Bu_{yy} - Cu_{xy} - Du_x - Eu_y + Fu, \end{aligned} \quad (20)$$

where $A = \frac{1}{2}(\sigma_1 x)^2, B = \frac{1}{2}(\sigma_2 y)^2, C = \sigma_1\sigma_2\rho xy, D = rx, E = ry, F = r$.

According to Theorem 1, the determining vector for (19) is defined by:

$$\mathbf{X} = \xi\frac{\partial}{\partial x} + \eta\frac{\partial}{\partial y} + \tau\frac{\partial}{\partial t} + \phi\frac{\partial}{\partial u} \quad (21)$$

and its prolongation becomes

$$\begin{aligned} X^{(2)} = \xi\frac{\partial}{\partial x} + \eta\frac{\partial}{\partial y} + \tau\frac{\partial}{\partial t} + \phi\frac{\partial}{\partial u} + \phi^x\frac{\partial}{\partial u_x} + \phi^y\frac{\partial}{\partial u_y} + \phi^t\frac{\partial}{\partial u_t} + \phi^{xx}\frac{\partial}{\partial u_{xx}} \\ +\phi^{xy}\frac{\partial}{\partial u_{xy}} + \phi^{xt}\frac{\partial}{\partial u_{xt}} + \phi^{yy}\frac{\partial}{\partial u_{yy}} + \phi^{yt}\frac{\partial}{\partial u_{yt}} + \phi^{tt}\frac{\partial}{\partial u_{tt}} \end{aligned} \quad (22)$$

Then, the characteristic equation for X is defined by

$$\phi - \xi u_x - \eta u_y - \tau u_t$$

This helps in computing $\phi^1 = \phi^x, \phi^2 = \phi^y, \phi^t, \phi^{11} = \phi^{xx}, \phi^{12} = \phi^{xy}$, noting that $(\phi^{xt} = \phi^{yy} = \phi^{yt} = \phi^{tt} = 0)$, we proceed on as follows:

$$\begin{aligned}
\phi^x &= D_x(\phi - \xi u_x - \eta u_y - \tau u_t) + \xi u_{xx} + \eta u_{xy} + \tau u_{xt} \\
&= D_x\phi - (\xi D_x u_x + u_x D_x \xi) - (\eta D_x u_y + u_y D_x \eta) - (\tau D_x u_t + u_t D_x \tau) + \xi u_{xx} + \eta u_{xy} + \tau u_{xt} \\
&= D_x\phi - \underline{\xi u_{xx}} - u_x D_x \xi - \underline{\eta u_{xy}} - u_y D_x \eta - \underline{\tau u_{xt}} - u_t D_x \tau + \underline{\xi u_{xx}} + \underline{\eta u_{xy}} + \underline{\tau u_{xt}} \\
&= D_x\phi - u_x D_x \xi - u_y D_x \eta - u_t D_x \tau
\end{aligned}$$

But $D_x = \frac{\partial}{\partial x} + u_x \frac{\partial}{\partial u}$. Thus

$$\begin{aligned}
\phi^x &= \left(\frac{\partial \phi}{\partial x} + u_x \frac{\partial \phi}{\partial u}\right) - u_x \left(\frac{\partial \xi}{\partial x} + u_x \frac{\partial \xi}{\partial u}\right) - u_y \left(\frac{\partial \eta}{\partial x} + u_x \frac{\partial \eta}{\partial u}\right) - u_t \left(\frac{\partial \tau}{\partial x} + u_x \frac{\partial \tau}{\partial u}\right) \\
&= \phi_x + u_x \phi_u - \xi_x u_x - u_x^2 \xi_u - \eta_x u_y - \eta_u u_x u_y - \tau_x u_t - \tau_u u_x u_t \\
\implies \phi^x &= \phi_x + (\phi_u - \xi_x) u_x - \eta_x u_y - \tau_x u_t - \xi_u u_x^2 - \eta_u u_x u_y - \tau_u u_x u_t \qquad (23)
\end{aligned}$$

Following the same steps as for ϕ^x we compute ϕ^y and ϕ^t such that

$$\phi^y = \phi_y - \xi_y u_x + (\phi_u - \eta_y) u_y - \tau_y u_t - \xi_u u_x u_y - \eta_u u_y^2 - \tau_u u_y u_t \qquad (24)$$

and

$$\phi^t = \phi_t - \xi_t u_x - \eta_t u_y + (\phi_u - \tau_t) u_t - \xi_u u_x u_t - \eta_u u_y u_t - \tau_u u_t^2 \qquad (25)$$

We proceed on to compute ϕ^{xx}, ϕ^{yy} and ϕ^{xy}:

$$\begin{aligned}
\phi^{xx} &= D_x(\phi^x - \xi u_{xx} - \eta u_{xy} - \tau u_{xt}) + \xi u_{xxx} + \eta u_{xxy} + \tau u_{xxt} \\
&= D_x\phi^x - (\xi D_x u_{xx} + u_{xx} D_x \xi) - (\eta D_x u_{xy} + u_{xy} D_x \eta) - (\tau D_x u_{xt} + u_{xt} D_x \tau) \\
&\quad + \xi u_{xxx} + \eta u_{xxy} + \tau u_{xxt} \\
&= D_x\phi^x - \underline{\xi u_{xxx}} - u_{xx} D_x \xi - \underline{\eta u_{xxy}} - u_{xy} D_x \eta - \underline{\tau u_{xxt}} - u_{xt} D_x \tau + \underline{\xi u_{xxx}} + \underline{\eta u_{xxy}} + \underline{\tau u_{xxt}} \\
&= D_x\phi^x - u_{xx} D_x \xi - u_{xy} D_x \eta - u_{xt} D_x \tau
\end{aligned}$$

But $D_x = \frac{\partial}{\partial x} + u_x \frac{\partial}{\partial u}$. Thus

$$\begin{aligned}
\phi^{xx} &= \left(\frac{\partial \phi^x}{\partial x} + u_x \frac{\partial \phi^x}{\partial u}\right) - u_{xx} \left(\frac{\partial \xi}{\partial x} + u_x \frac{\partial \xi}{\partial u}\right) - u_{xy} \left(\frac{\partial \eta}{\partial x} + u_x \frac{\partial \eta}{\partial u}\right) - u_{xt} \left(\frac{\partial \tau}{\partial x} + u_x \frac{\partial \tau}{\partial u}\right) \\
&= \phi_x^x + u_x \phi_u^x - \xi_x u_{xx} - u_{xx} u_x \xi_u - \eta_x u_{xy} - \eta_u u_x u_{xy} - \tau_x u_{xt} - \tau_u u_x u_{xt} \\
&= \phi_x^x + \phi_u^x u_x - \xi_x u_{xx} - \eta_x u_{xy} - \tau_x u_{xt} - \xi_u u_x u_{xx} - \eta_u u_x u_{xy} - \tau_u u_x u_{xt}.
\end{aligned}$$

Using (23) where $\phi_x^x = \frac{\partial \phi^x}{\partial x}$ and $\phi_u^x = \frac{\partial \phi^x}{\partial u}$, then

$$\begin{aligned}
\phi^{xx} &= (\phi_{xx} + (\phi_u - \xi_x) u_{xx} + (\phi_{xu} - \xi_{xx}) u_x - \eta_{xx} u_y - \eta_x u_{xy} - \tau_{xx} u_t - \tau_x u_{xt} - \xi_{xu} u_x^2 \\
&\quad - 2\xi_u u_x u_{xx} - \eta_{xu} u_x u_y - \eta_u u_y u_{xx} - \eta_u u_x u_{xy} - \tau_{xu} u_x u_t - \tau_u u_t u_{xt} - \tau_u u_x u_{xt}) \\
&\quad + (\phi_{xu} u_x + \phi_{uu} u_x^2 + \xi_{xu} u_x^2 - \eta_{xu} u_x u_y - \tau_{xu} u_x u_t - \xi_{uu} u_x^3 - \eta_{uu} u_x^2 u_y - \tau_{uu} u_x^2 u_t) \\
&\quad - \xi_x u_{xx} - \eta_x u_{xy} - \tau_x u_{xt} - \xi_u u_x u_{xx} - \eta_u u_x u_{xy} - \tau_u u_x u_{xt}.
\end{aligned}$$

On rearranging and collecting like terms together,

$$\begin{aligned}\phi^{xx} &= \phi_{xx} + (2\phi_{xu} - \xi_{xx})u_x - \eta_{xx}u_y - \tau_{xx}u_t + (\phi_{uu} - 2\xi_{xu})u_x^2 - 2\eta_{xu}u_xu_y \\ &\quad - 2\tau_{xu}u_xu_t + (\phi_u - \xi_x)u_{xx} - 2\eta_x u_{xy} - 2\tau_x u_{xt} - \xi_{uu}u_x^3 - \eta_{uu}u_x^2u_y \\ &\quad - \tau_{uu}u_x^2u_t - 3\xi_u u_x u_{xx} - \eta_u u_y u_{xx} - \tau_u u_t u_{xx} - 2\eta_u u_x u_{xy} - 2\tau_u u_x u_{xt} \quad (26)\end{aligned}$$

Following similar steps we obtain ϕ^{yy}:

$$\begin{aligned}\phi^{yy} &= \phi_{yy} - \eta_{yy}u_x + (2\phi_{yu} - \eta_{yy})u_y - \tau_{yy}u_t - 2\eta_{yu}u_xu_y + (\phi_{uu} - 2\eta_{yu})u_y^2 \\ &\quad - 2\tau_{yu}u_yu_t + (\phi_u - \eta_y)u_{yy} - 2\xi_y u_{xy} - 2\tau_y u_{yt} - \eta_{uu}u_y^3 - \xi_{uu}u_xu_y^2 \\ &\quad - \tau_{uu}u_y^2u_t - 3\eta_u u_y u_{yy} - \xi_u u_x u_{yy} - \tau_u u_t u_{yy} - 2\xi_u u_y u_{xy} - 2\tau_u u_y u_{yt} \quad (27)\end{aligned}$$

Almost in a similar way we compute ϕ^{xy}

$$\begin{aligned}\phi^{xy} &= D_x(\phi^y - \xi u_{xy} - \eta u_{yy} - \tau u_{yt}) + \xi u_{xxy} + \eta u_{xyy} + \tau u_{xyt} \\ &= D_x\phi^y - (\xi D_x u_{xy} + u_{xy}D_x\xi) - (\eta D_x u_{yy} + u_{yy}D_x\eta) - (\tau D_x u_{yt} + u_{yt}D_x\tau) \\ &\quad + \xi u_{xxy} + \eta u_{xyy} + \tau u_{xyt} \\ &= D_x\phi^y - \underline{\xi u_{xxy}} - u_{xy}D_x\xi - \underline{\eta u_{xyy}} - u_{yy}D_x\eta - \underline{\tau u_{xyt}} - u_{yt}D_x\tau + \underline{\xi u_{xxy}} + \underline{\eta u_{xyy}} + \underline{\tau u_{xyt}} \\ &= D_x\phi^y - u_{xy}D_x\xi - u_{yy}D_x\eta - u_{yt}D_x\tau\end{aligned}$$

But $D_x = \frac{\partial}{\partial x} + u_x\frac{\partial}{\partial u}$. Thus

$$\begin{aligned}\phi^{xy} &= \left(\frac{\partial\phi^y}{\partial x} + u_x\frac{\partial\phi^y}{\partial u}\right) - u_{xy}\left(\frac{\partial\xi}{\partial x} + u_x\frac{\partial\xi}{\partial u}\right) - u_{yy}\left(\frac{\partial\eta}{\partial x} + u_x\frac{\partial\eta}{\partial u}\right) - u_{yt}\left(\frac{\partial\tau}{\partial x} + u_x\frac{\partial\tau}{\partial u}\right) \\ &= \phi_x^y + u_x\phi_u^y - \xi_x u_{xy} - u_{xy}u_x\xi_u - \eta_x u_{yy} - \eta_u u_x u_{yy} - \tau_x u_{yt} - \tau_u u_x u_{yt} \\ &= \phi_x^y + \phi_u^y u_x - \xi_x u_{xy} - \eta_x u_{yy} - \tau_x u_{yt} - \xi_u u_x u_{xy} - \eta_u u_x u_{yy} - \tau_u u_x u_{yt}.\end{aligned}$$

Using (24), where $\phi_x^y = \frac{\partial\phi^y}{\partial x}$ and $\phi_u^y = \frac{\partial\phi^y}{\partial u}$, then

$$\begin{aligned}\phi^{xy} &= \phi_{xy} + (\phi_u - \eta_y)u_{xy} + (\phi_{xu} - \eta_{xy})u_y - \xi_{xy}u_x - \xi_y u_{xx} - \tau_{xy}u_t - \tau_y u_{xt} - \eta_{xu}u_y^2 \\ &\quad - 2\eta_u u_y u_{xy} - \xi_{xu}u_x u_y - \xi_u u_x u_{xy} - \xi_u u_y u_{xx} - \tau_{xu}u_y u_t - \tau_u u_t u_{xy} - \tau_u u_y u_{xt}) \\ &\quad + (\phi_{xu}u_x + \phi_{uu}u_x u_y - \eta_{yu}u_x u_y - \xi_{yu}u_x^2 - \tau_{yu}u_x u_t - \xi_{uu}u_x^2 u_y - \eta_{uu}u_x u_y^2 - \tau_{uu}u_x u_y u_t) \\ &\quad - \xi_x u_{xy} - \eta_x u_{yy} - \tau_x u_{yt} - \xi_u u_{xx}u_y - \eta_u u_x u_{yy} - \tau_u u_x u_{yt}.\end{aligned}$$

On rearranging and collecting like terms together,

$$\begin{aligned}\phi^{xy} &= \phi_{xy} + (\phi_{yu} - \xi_{xy})u_x + (\phi_{xu} - \eta_{xy})u_y - \tau_{xy}u_t + (\phi_{uu} - \eta_{yu} - \xi_{xu})u_xu_y \\ &\quad - \tau_{yu}u_xu_t - \tau_{xu}u_yu_t - \xi_{yu}u_x^2 - \eta_{xu}u_y^2 - \xi_y u_{xx} - \eta_x u_{yy} + (\phi_u - \eta_y - \xi_x)u_{xy} \\ &\quad - \tau_y u_{xt} - \tau_x u_{yt} - \xi_u u_x u_{xy} - \xi_u u_{xx}u_y - \eta_u u_x u_{yy} - \eta_{uu}u_x u_y^2 - \tau_u u_x u_{yt} \\ &\quad - 2\eta_u u_y u_{xy} - \tau_u u_y u_{xt} - \xi_u u_{xy}u_t - \tau_{uu}u_x u_y u_t. \quad (28)\end{aligned}$$

Substituting the expressions for $\phi^t = u_t, \phi^x = u_x, \phi^y = u_y, \phi^t = u_t, \phi^{xx} = u_{xx}, \phi^{xy} = u_{xy}, \phi^{yy} = u_{yy}$ into (20) we obtain:
$\phi_t - \xi_t u_x - \eta_t u_y + (\phi_u - \tau_t)u_t - \xi_u u_x u_t - \eta_u u_y u_t - \tau_u u_t^2 =$
$A[\phi_{xx} + (2\phi_{xu} - \xi_{xx})u_x - \eta_{xx}u_y - \tau_{xx}u_t + (\phi_{uu} - 2\xi_{xu})u_x^2 - 2\eta_{xu}u_xu_y - 2\tau_{xu}u_xu_t$

$$
\begin{aligned}
&+(\phi_u-\xi_x)u_{xx}-2\eta_x u_{xy}-2\tau_x u_{xt}-\xi_{uu}u_x^3-\eta_{uu}u_x^2u_y-\tau_{uu}u_x^2u_t-3\xi_u u_x u_{xx}\\
&-\eta_u u_y u_{xx}-\tau_u u_t u_{xx}-2\eta_u u_x u_{xy}-2\tau_u u_x u_{xt}]\\
&+B[\phi_{yy}-\eta_{yy}u_x+(2\phi_{yu}-\eta_{yy})u_y-\tau_{yy}u_t-2\eta_{yu}u_xu_y+(\phi_{uu}-2\eta_{yu})u_y^2-2\tau_{yu}u_yu_t\\
&+(\phi_u-\eta_y)u_{yy}-2\xi_y u_{xy}-2\tau_y u_{yt}-\eta_{uu}u_y^3-\xi_{uu}u_xu_y^2-\tau_{uu}u_y^2u_t-3\eta_u u_y u_{yy}\\
&-\xi_u u_x u_{yy}-\tau_u u_t u_{yy}-2\xi_u u_y u_{xy}-2\tau_u u_y u_{yt}]\\
&+C[\phi_{xy}+(\phi_{yu}-\xi_{xy})u_x+(\phi_{xu}-\eta_{xy})u_y-\tau_{xy}u_t+(\phi_{uu}-\eta_{yu}-\xi_{xu})u_xu_y\\
&-\tau_{yu}u_xu_t-\tau_{xu}u_yu_t-\xi_{yu}u_x^2-\eta_{xu}u_y^2-\xi_y u_{xx}-\eta_x u_{yy}+(\phi_u-\eta_y-\xi_x)u_{xy}\\
&-\tau_y u_{xt}-\tau_x u_{yt}-\xi_u u_x u_{xy}-\xi_u u_{xx}u_y-\eta_u u_x u_{yy}-\eta_{uu}u_xu_y^2-\tau_u u_x u_{yt}\\
&-2\eta_u u_y u_{xy}-\tau_u u_y u_{xt}-\xi_u u_{xy}u_t-\tau_{uu}u_xu_yu_t]\\
&+D[\phi_x+(\phi_u-\xi_x)u_x-\eta_x u_y-\tau_x u_t-\xi_u u_x^2-\eta_u u_x u_y-\tau_u u_x u_t]\\
&+E[\phi_y-\xi_y u_x+(\phi_u-\eta_y)u_y-\tau_y u_t-\xi_u u_x u_y-\eta_u u_y^2-\tau_u u_y u_t]\\
&-F\phi
\end{aligned}
$$

Equating the coefficients in the corresponding terms on the left and right hand side.

Monomial	Coefficients	Reference
$u_xu_yu_t$	$0=-C\tau_{uu}$	(S_1)
u_tu_{xy}	$0=-C\xi_u$	(S_2)
u_yu_{xt}	$0=-C\tau_u$	(S_3)
u_yu_{yt}	$0=-2B\tau_u$	(S_4)
u_xu_{yt}	$0=-C\tau_u$	(S_5)
u_xu_{xt}	$0=-2A\tau_u$	(S_6)
u_yu_{xy}	$0=-2B\xi_u-2C\eta_u$	(S_7)
u_xu_{xy}	$0=-2A\eta_u-2C\xi_u$	(S_8)
u_tu_{yy}	$0=-B\tau_u$	(S_9)
u_tu_{xx}	$0=-A\tau_u$	(S_{10})
u_yu_{xx}	$0=-A\eta_u-C\xi_u$	(S_{11})
u_yu_{yy}	$0=-3B\eta_u$	(S_{12})
u_xu_{yy}	$0=-B\xi_u-C\eta_u$	(S_{13})
u_xu_{xx}	$0=-3A\xi_u$	(S_{14})
$u_y^2u_t$	$0=-B\tau_{uu}$	(S_{15})
$u_x^2u_t$	$0=-A\tau_{uu}$	(S_{16})
$u_x^2u_y$	$0=-A\eta_{uu}-C\xi_{uu}$	(S_{17})
$u_xu_y^2$	$0=-B\xi_{uu}-C\eta_{uu}$	(S_{18})
u_y^3	$0=-B\eta_{uu}$	(S_{19})
u_x^3	$0=-A\xi_{uu}$	(S_{20})
u_{yt}	$0=-B2\tau_y-C\tau_x$	(S_{21})
u_{xt}	$0=-2A\tau_x-C\tau_y$	(S_{22})
u_{xy}	$0=-2A\eta_x-B2\xi_y+C(\phi_u-\eta_y-\xi_y-\xi_x$	(S_{23})
u_{yy}	$0=+B(\phi_u-\eta_y)-C\eta_x$	(S_{24})
u_{xx}	$0=+A(\phi_u-\xi_x)-C\xi_y$	(S_{25})
u_yu_t	$-\eta_u=-B2\tau_{yu}-C\tau_{xu}-E\tau_u$	(S_{26})
u_xu_t	$-\xi_u=-2A\tau_{xu}-C\tau_{yu}-D\tau_u$	(S_{27})
u_xu_y	$0=-2A\eta_{xu}-2B\eta_{yu}+C(\phi_{uu}-\eta_{yu}-\xi_{xu})-D\eta_u-E\xi_u$	(S_{28})
u_y^2	$0=+B(\phi_{uu}-B\eta_{yu})-C\eta_{xu}-E\eta_u$	(S_{29})
u_x^2	$0=+A(\phi_{uu}-2\xi_{xu})-C\xi_{yu}-D\xi_u$	(S_{30})

Table 1: (continued)

Monomial	Coefficients	Reference
u_t^2	$-\tau_u = 0$	(S_{31})
u_t	$+(\phi_u - \tau_t) = -A\tau_{xx} - B\tau_{yy} - C\tau_{xy} - D\tau_x - E\tau_y$	(S_{32})
u_y	$-\eta_t = -A\eta_{xx} + B(2\phi_{yu} - \eta_{yy}) + C(\phi_{xu} - \eta_{xy}) - D\eta_x + E(\phi_u - \eta_y)$	(S_{33})
u_x	$-\xi_t = A(2\phi_{xu} - \xi_{xx}) - B\eta_{yy} + C(\phi_{yu} - \xi_{xy}) + D(\phi_u - \xi_x) - E\xi_y$	(S_{34})
1	$\phi_t = A\phi_{xx} + B\phi_{yy} + C\phi_{xy} + D\phi_x + E\phi_y - F\phi)$	(S_{35})

Table 1: Table for the corresponding coefficients in the equation

The main goal is to determine the unknown functions τ, ξ, η and ϕ that are necessary to find the Lie-algebra of the infinitesimal symmetries, thereafter the symmetry groups and finally given that u is a solution, we be able to determine other solutions.

Considering conditions $S_1, S_3, S_1, S_4, S_6, S_9, S_{10}, S_{15}, S_{16}, S_{31}$, it should be noted that $\tau_u = \tau_{uu} = 0$. It implies that τ is necessarily a function of t only. Thus from conditions $S_{21}, S_{22}, S_{26}, S_{27}$ it follows that $\tau_x = \tau_y = \tau_{xu} = \tau_{yu} = 0$. This eliminates the same conditions with no further computations.
Also conditions $S_2, S_7, S_8, S_{11}, S_{12}, S_{13}, S_{14}, S_{17}, S_{18}, S_{19}, S_{20}$, require that ξ, η cannot be functions of u implying that $\xi_u = \eta_u = \xi_{uu} = \eta_{uu} = 0$. And basing on the fact that ξ, η, τ cannot be functions of u, then from conditions $S_{28}, S_{29}, S_{30}, S_{32}$ will imply that $\phi_u = \tau_t$ and $\phi_{uu} = 0$. This reduces the conditions in Table 1 to the following system differential equations to be solved for τ, ξ, η, ϕ.

$$\phi_u = \tau_t \tag{29}$$
$$\phi_{uu} = 0 \tag{30}$$
$$0 = -2A\eta_x - 2B\xi_y + C(\phi_u - \eta_y - \xi_y - \xi_x) \tag{31}$$
$$0 = +A(\phi_u - \xi_x) - C\xi_y \tag{32}$$
$$0 = +B(\phi_u - B\eta_y) - C\eta_x \tag{33}$$
$$-\eta_t = -(A\eta_{xx} + B\eta_{yy} + C\eta_{xy} + D\eta_x + E\eta_y) + (2B\phi_{yu} + C\phi_{xu} + E\phi_u) \tag{34}$$
$$-\xi_t = -(A\xi_{xx} + B\xi_{yy} + C\xi_{xy} + D\xi_x + E\xi_y) + (2A\phi_{xu} + C\phi_{yu} + D\phi_u) \tag{35}$$
$$\phi_t = A\phi_{xx} + B\phi_{yy} + C\phi_{xy} + D\phi_x + E\phi_y - F\phi \tag{36}$$

It should be noted that Equation (36) is exactly similar to Equation (19) which we are expected to solve. This suggests that indeed $\phi(x, y, t, u)$ is indeed as solution to (19). And from Equation (30), $\phi_{uu} = 0$, it suggest that $\phi(x, y, t, u)$ can only be of the form

$$\phi(x, y, t, u) = \beta(x, y, t)u + \alpha(x, y, t). \tag{37}$$

and it follows that
$\phi_u(x, y, t, u) = \beta(x, y, t), \phi_{xu}(x, y, t, u) = \beta_x(x, y, t), \phi_{yu}(x, y, t, u) = \beta_y(x, y, t)$.

With the help of Maple computing software we solve the the above system leads to the following solutions leading to the following results for $\tau(t), \xi(x,y,t), \phi(x,y,t,u)$ where $\phi(x,y,t,u) = \beta(x,y,t)u + \alpha(x,y,t)$.

$$\tau(t) = C_4\left[\frac{1}{2}t^2 + t\right] + C_0 \tag{38}$$

$$\xi(x,y,t) = C_5\left[\frac{1}{2}\frac{\sigma_1}{\rho\sigma_2}x\ln y + \frac{1}{2}xt\ln x\right] + C_1 \tag{39}$$

$$\eta(x,y,t) = C_6\left[\frac{1}{2}\frac{1}{\sigma_1\rho}y\left(2\sigma_1\rho\ln y - \sigma_2\ln x\right) + \frac{1}{2}yt\ln y\right] + C_2 \tag{40}$$

$$\begin{aligned}\phi(x,y,t,u) = {} & \frac{C_5u}{16\rho\sigma_1^2\sigma_2^2(\rho^2-1)}\left[\left(-\frac{1}{2}\sigma_2^2\ln x + \sigma_1\sigma_2\rho\ln y\right)\ln(x)+\right] \\ & \frac{C_5u}{16\rho\sigma_1^2\sigma_2^2(\rho^2-1)}\left[t(1-\rho)\left(\frac{1}{2}\sigma_1^2\sigma_2^2 + \rho\sigma_1\sigma_2(\frac{1}{2}\sigma_2^2 - r) - r\sigma_2^2\right)\ln x+\right] \\ & \frac{C_6u}{16\rho\sigma_1^2\sigma_2^2(\rho^2-1)}\left[\left(-\frac{1}{2}\sigma_1^2\ln y + (\sigma_1^3\sigma_2(\frac{1}{2}\rho t + \rho^2 - \frac{1}{2})\right)\ln y+\right] \\ & \frac{C_6u}{16\rho\sigma_1^2\sigma_2^2(\rho^2-1)}\left[\left(\sigma_1^2(\frac{1}{2}\sigma_2^2 - r)(t-\rho) + \sigma_1\sigma_2 r(\rho t + 2\rho^2 - 1)\right)\ln y+\right] \\ & \frac{C_4u}{16\rho\sigma_1^2\sigma_2^2(\rho^2-1)}\left[t(t+2\rho)[-\frac{1}{8}\sigma_1^4\sigma_2^2 - \frac{1}{2}\rho\sigma_1^3\sigma_2(-\frac{1}{2}\sigma_2^2 + r)+\right] \\ & \frac{C_4u}{16\rho\sigma_1^2\sigma_2^2(\rho^2-1)}\left[(-\frac{1}{8}\sigma_2^4 + \sigma_1^2\sigma_2^2(\rho^2 + r - 1)) - \frac{1}{2}\sigma_1^2r^2 + \sigma_1^2\sigma_2^2t(1-\rho^2)+\right] \\ & \frac{C_4u}{16\rho\sigma_1^2\sigma_2^2(\rho^2-1)}\left[\rho\sigma_1\sigma_2 r(-\frac{1}{2}\sigma_2^2 + r) - \frac{1}{2}\sigma_2^2r^2]\right] + C_3u + C_\alpha\alpha(x,y,t)\end{aligned} \tag{41}$$

The Lie symmetry infinitesimal dimensional basis for (18) is spanned by the arbitrary constants. For instance to find this successively we set each constant equal to 1 and the rest equal to 0, i.e., $C_0 = 1$ and $C_1, \cdots, C_6, C_\alpha = 0$. This

will generate the required symmetry vector field.

$$X_0 = \frac{\partial}{\partial t}, \quad X_1 = \frac{\partial}{\partial x}, \quad X_2 = \frac{\partial}{\partial y}, \quad X_3 = u\frac{\partial}{\partial u},$$

$$\begin{aligned}
X_4 = &\left[\frac{1}{2}t^2 + t\right]\frac{\partial}{\partial t} + \frac{t(t+2\rho)}{16\rho\sigma_1^2\sigma_2^2(\rho^2-1)}\left[-\frac{1}{8}\sigma_1^4\sigma_2^2 - \frac{1}{2}\rho\sigma_1^3\sigma_2(-\frac{1}{2}\sigma_2^2 + r)\right]u\frac{\partial}{\partial u} \\
&+\frac{1}{16\rho\sigma_1^2\sigma_2^2(\rho^2-1)}\left[\left(-\frac{1}{8}\sigma_2^4 + \sigma_1^2\sigma_2^2(\rho^2 + r - 1)\right) - \frac{1}{2}\sigma_1^2 r^2 + \sigma_1^2\sigma_2^2 t(1-\rho^2)\right]u\frac{\partial}{\partial u} \\
&+\frac{1}{16\rho\sigma_1^2\sigma_2^2(\rho^2-1)}\left[\rho\sigma_1\sigma_2 r(-\frac{1}{2}\sigma_2^2 + r) - \frac{1}{2}\sigma_2^2 r^2\right]u\frac{\partial}{\partial u}, \\
X_5 = &\left[\frac{1}{2}\frac{\sigma_1}{\rho\sigma_2}x\ln y + \frac{1}{2}xt\ln x\right]\frac{\partial}{\partial x} \\
&+\frac{t(1-\rho)}{16\rho\sigma_1^2\sigma_2^2(\rho^2-1)}\left[\left(\frac{1}{2}\sigma_1^2\sigma_2^2 + \rho\sigma_1\sigma_2(\frac{1}{2}\sigma_2^2 - r) - r\sigma_2^2\right)\ln x\right]u\frac{\partial}{\partial u}, \\
X_6 = &\left[\frac{1}{2}\frac{1}{\sigma_1\rho}y\left(2\sigma_1\rho\ln y - \sigma_2\ln x\right) + \frac{1}{2}yt\ln y\right]\frac{\partial}{\partial y} \\
&+\frac{1}{16\rho\sigma_1^2\sigma_2^2(\rho^2-1)}\left[\left(-\frac{1}{2}\sigma_1^2\ln y + (\sigma_1^3\sigma_2(\frac{1}{2}\rho t + \rho^2 - \frac{1}{2})\right)\ln y\right]u\frac{\partial}{\partial u} \\
&+\frac{1}{16\rho\sigma_1^2\sigma_2^2(\rho^2-1)}\left[\left(\sigma_1^2(\frac{1}{2}\sigma_2^2 - r)(t-\rho) + \sigma_1\sigma_2 r(\rho t + 2\rho^2 - 1)\right)\ln y +\right]u\frac{\partial}{\partial u}, \\
X_\alpha = &\,\alpha(x,y,t)\frac{\partial}{\partial u}.
\end{aligned}$$

4 Conclusion

In this paper we applied the Lie Symmetry group analysis to the Black-Scholes type equation also famously known as the Feynman-Kac model. The aim was to generate a wide class of analytic solutions to this type of stochastic partial differential equation in finance. We were able to compute the infinitesimal vectors that for a basis to generate the possible Lie symmetry groups, the exact solutions and the invariant solutions of this equation.

In our next work we are continuing these generated results to characterize all the possible symmetry groups, use the invariance principle to construct the fundamental solutions that can be used for general analysis of an arbitrary initial value problem. And for this same equation, Feynman-Kac model, we shall present the group classification which shows that the dimension of the symmetry Lie algebra essentially depends only on the parameters of the model.

Acknowledgement
We acknowledge the financial support for this research by the Swedish International Development Agency, (Sida), Grant No.316, International Science Program, (ISP) in Mathematical Sciences, (IPMS). We are also grateful to the Division of Mathematics and Applied Mathematics, Mlardalen University for providing an excellent and inspiring environment for research education and research.

References

1. C. Sophocleous, P. G. L. Leach, and K. Andriopoulos. Algebraic properties of evolution partial differential equations modelling prices of commodities. *Mathematical Methods in the Applied Sciences*, 31(6):679–694, 2008.
2. C. Sophocleous, J. G. O'Hara, and P. G. L. Leach. Symmetry analysis of a model of stochastic volatility with time-dependent parameters. *Journal of Computational and Applied Mathematics*, 235(14):4158–4164, 2011.
3. D. Jeong, J. Kim and I.-S. Wee, An accurate and efficient numerical method for Black-Scholes equations. *Journal of the Korean Mathematical Society*, Science Publications, **24**, 4, 617–628, 2009.
4. E.H. Peter. Symmetry Methods for Differential Equations. Cambridge University Press, 2000.
5. F. Black and M. Scholes. The pricing of option and corporate liabilities. *Journal of political Economy*, **81**, 637–654, 1973.
6. G.W. Bluman and J. Cole. General similarity solution of the heat equation. *Journal of Applied Mathematics and Mechanics*, **18**, 1025–1042, 1968.
7. G.W. Bluman, A.F. Cheviakov and S.C. Anco. Application of Lie symmetry methods to partial differential equations. *Journal of Applied Mathematical Sciences*. Vol. 168, Springer, New York, 2000.
8. G.W. Bluman, S. Kumei and G. Reid. New classes of symmetries for partial differential equations. *Journal of Mathematical Physics* **29**, 806–811, 1988.
9. G.W. Bluman and S. Kumei. Use of group analysis in solving overdetermined systems of ordinary differential equations. *Journal of Mathematical Analysis and Applications* **138**, 1989.
10. H. Liu. Symmetry analysis and exact solutions to the space-dependent coefficient PDEs in finance. Abstract and *Applied Analysis*, pages Art.ID 156965, 10, 2013.
11. H. Stephan. Differential equations: symmetries and solution methods. *Spektrum Akad*, Verlag, 1994.
12. J. Hadamard. Lectures on cauchy's Problem in Linear in partial Differential Equations. Yale University Press, New Haven, 1923. (Reprinted by dover publicatins, New York, 1952).
13. J. Hull. Options, Futures and Other Derivatives. Pearson/Prentice Hall, Ninth edition, 2015.
14. J. Leray. Hyperbolic differential equations. Mimeographed, The Institute for Advanced Study, Princeton, 1953. Prublished in Russian translation by N.H., Ibragimov, Moscow: Nauka, 1984.
15. K.P. Sharp. Stochastic differential equations in finance. *Applied mathematics and Computation*, 38, 207–413, 1990.
16. L.A. Bordag. On option-valuation in illiquid markets: invariant solutions to a nonlinear model. *Mathematical control theory and finance*, Springer, Berlin, 71-94, 2008.
17. L.A. Bordag and A. Mikaelyan. Models of self-financing hedging strategies in illiquid markets: symmetry reductions and exact solutions. *Letter of Mathematical Physics*, 96(1-3): 191–207, 2011.
18. L.E. Dickson. Differential equations from the group standpoint. *Annals of Mathematics*, **25**, 287–378, 1924.
19. L.V. Ovsyannikov. Group properties of differential Equations. USSR Academy of Sciences, Siberian Branch, Novosibirsk, 1962 [in Russian].
20. M. Abramowitz and I.A. Stegun. Handbook of mathematical functions with formulas, graphs, and mathematical tables. *National Bureau of Standards Applied Mathematics Series-55, For sale by the Superintendent of Documents, US.*, U.S. Government Printing Office, Washington, D.C., 1964.

21. M. O. Okelola, K. S. Govinder, and J. G. O'Hara. Solving a partial differential equation associated with the pricing of power options with time-dependent parameters. *Mathematical Methods in the Applied Sciences*, 38(14):2901–2910, 2015.
22. N. C. Caister, K. S. Govinder, and J. G. O'Hara. Optimal system of Lie group invariant solutions for the Asian option PDE. *Mathematical Methods in the Applied Sciences*, 34(11):1353–1365, 2011.
23. N.H. Ibragimov. CRC Handbook of lie Group Analysis of Differential Equations. (ed) Vol.1, 1994, Vol. 2, 1995; Vol.3, 1996, CRC Press, Boca Raton, FL.
24. N.H. Ibragimov. Primer on group analysis. Moscow: Znanie, No. **8**, 1989 (in Russian)
25. N.H. Ibragimov. Elementary Lie group analysis and ordinary differential equations. Chichester: John Wiley and Sons, 1999.
26. N. M. Ivanova, C. Sophocleous, and P. G. L. Leach. Group classification of a class of equations arising in financial mathematics. *Journal of Mathematical Analysis and Applications*, 372(1):273–286, 2010.
27. N.H. Ibragimov, M. Torris and A. Valenti. Modern Group Analysis: Advance analyitical and computational methods in mathematical physics. *Proceedings of the International Workshop,* Acireale, Cantania, Italy, October 27–31, 1992.
28. P.J. Olver. Equivalence, Invariants and Symmetry. Cambridge University Press, UK, 1995.
29. P.J. Olver. Application of Lie groups to differential equations. Second Edition, Springer-Verlag New York, Inc., 1993.
30. P.J. Olver. Symmetry groups and group invariant solutions of partial differential equations. *Journal of Differential Geometry*, **14**, 497–542, 1979.
31. P.J. Olver Symmetry Groups of Partial Differential Equations, Thesis, Harvard University, 1976.
32. P.J. Olver and P. Rosenau. Construction of special solutions to partial differential equations. Physics Letter. **114A**, 107–112, 1986.
33. P. G. L. Leach, J. G. O'Hara, and W. Sinkala. Symmetry-based solution of a model for a combination of a risky investment and a riskless investment. *Journal of Mathematical Analysis and Applications*, 334(1):368–381, 2007.
34. R. Courant and D. Hilbert. Methods of Mathematical Physics. Vol. II, Interscience Publishers, New York, 1962.
35. R.C. Merton. Optimum consumption and portfolio rules in a continuous time model. *Journal of Economics Thoery*, **3**, 4, 79–93, 1971.
36. R.K. Gazizov and N.H. Ibragimov. Lie symmetry analysis of differential equations in finance. *Nonlinear Dynamics*, Kluwer Academic Publishers, Netherlands, **17**, 4 387–407. 1998.
37. R.L. Jacobs and R.A. Jones. A two factor latent variable model of the term structure of interest rates. Economics Department, Simon Fraser, Burnaby, B.C., Canada, 1986.
38. R.M. Edelstein and K. S. Govinder. Conservation laws for the Black-Scholes equation. *Journal of Nonlinear Analysis: Real World Applications*, Elsevier, 10(6):3372–3380, 2009.
39. S. Dimas, K. Andriopoulos, D. Tsoubelis, and P. G. L. Leach. Complete specification of some partial diferential equations that arise in financial mathematics. *Journal of Nonlinear Mathematical Physics*, 16(suppl.1):73–92, 2009.
40. S. Kumei and G.W. Bluman. When nonlinear differential equations are equivalent to linear differential equations, *SIAMS: Journal of Applied Mathematics* **42**, 1157-1173, 1982.

41. S. Lie. *Gesammelte Abhandlungen. Band 3.* Johnson Reprint Corp., New York-London, german edition, 1973. Herausgegeben von Friedrich Engel und Poul Heegaard, Abhandlungen zur Theorie der Differential-gleichungen. Erste Abteilung, Herausgegeben von Friedrich Engel.
42. S.L. Heston. A closed-form solution for options with stochastic volatility with applications to bond and currency options. *Review of financial studies*, **6**, 327–343, 1993.
43. S.L. Lekalakala, T. Motsepa, and C.M. Khalique. Lie symmetry reductions and exact solutions of an option-pricing equation for large agents. *Mediterranean Journal of Mathematics*-Springer, 13(4):1753–1763, 2016.
44. S. Lie. *Gesammelte Abhandlungen. Band 4.* Johnson Reprint Corp., New York-London, german edition, 1973. Herausgegeben von Friedrich Engel und Poul Heegaard, Abhandlungen zur Theorie der Differential- gleichungen. Abteilung 2, Herausgegeben von Friedrich Engel.
45. S. Lie. On integration of a class of linear partial differential equations by means of definite integral. *Archive for mathematik og naturvidenskab* 6, 3, 328–368, 1881 [in German]. reprinted in S., Lie *Collected Works*, Vol.6, paper III, 139-223.
46. S. Lie. General Studies on differential equations admitting finite continuous groups. *Mathematische Annalen,* **25**, 1, 71–151, 1885 [in German]. reprinted in S. Lie. Gesammelte Abhandlundgen, Vol.3, paper XXXV. (English translation published in N. H., Ibragimov (ed), CRC Handbook of lie Group Analysis of Differential Equations, Vol.2, 1995, CRC Press, Boca Raton, FL.)
47. T.-H. Wang, P. Laurence, and S.-L. Wang. Generalized uncorrelated SABR models with a high degree of symmetry. *Journal of Quantitative Finance*, 10(6):663–679, 2010.
48. T. Motsepa. C.M. Khalique and M. Molati. Group classification of a general bond-option pricing equation of mathematical finance. *Abstract and Applied Analysis*, 709–871, 2014.
49. V. Naicker, K. Andriopoulos, and P.G.L. Leach. Symmetry reductions of a Hamilton-Jacobi-Bellman equation arising in financial mathematics. *Journal of Nonlinear Mathematical Physics*, **12**, 268-283, 2005.
50. W. Sinkala, P.G.L Leache and J.G. O'Hara. Invariance properties of general bond-pricing equation. *Journal of Differential Equations*, **244**, 2820–2835, 2008.
51. W. Sinkala, P. G. L. Leach, and J. G. O'Hara. Zero-coupon bond prices in the Vasicek and CIR models: their computation as group-invariant solutions. *Mathematical Methods in the Applied Sciences*, 31(6):665–678, 2008.
52. W. Sinkala. On the generation of arbitrage-free stock price models using Lie symmetry analysis. *Computer and Mathematics with Applications*, **72**, 1386–1393, 2016.
53. W.S. Koh, J. Sulaiman and R. Mail, Numerical solution for 2D European option pricing using quarter-sweep modified Guass-Seidel method. *Journal of Mathematics and Statistics*, Science Publications, **8**, 1, 129–135, 2012.
54. Y.-K. Kwok. Mathematical models of financial derivatives. Springer Finance. Springer, Berlin, second edition, 2008.
55. Y. Liu and D.-S. Wang. Symmetry analysis of the option pricing model with dividend yield from financial markets. *Applied Mathematics Letters-Journal*-Letter, 24(4):481–486, 2011.

Context-specific independence in innovation study

Federica Nicolussi and Manuela Cazzaro

Department of Statistics and Quantitative Methods, via Bicocca degli Arcimboldi 8, University of Milano Bicocca, Milano, Italy
(E-mail: federica.nicolussi@unimib.it; manuela.cazzaro@unimib.it)

Abstract. The study of (in)dependence relationships among a set of categorical variables collected in a contingency table is an amply topic. In this work we want to focus on the so called context-specific independence where the conditional independence holds only in a subspace of the outcome space. The main aspects that we introduce concern the definition in the same model of marginal, conditional and context-specific independencies, through the marginal models. Furthermore, we investigate how it is possible to test these context-specific independencies when there are ordinal variables. Finally, we propose a graphical representation of all the considered independencies taking advantages from the chain graph model. We show the results on an application on "The Italian Innovation Survey" of Istat (2012).
Keywords: Context-specific independence, ordinal variables, graphical models, innovation.

1 Introduction

In the field of the categorical variables, with the term context-specific (CS) independence we refer to the particular conditional independence that holds only for some modalities of the variable(s) in the conditioning set, but not for all. That is, given three variables X_1, X_2 and X_3 we describe this situation as $X_1 \perp X_2 | X_3 = c_3$, where c_3 is a subset of all possible values of X_3. Among other, Højsgaard (2004) [11] and Nyman (2016), [10] deepen this topic. In this paper we want to improve the main results of these works by dealing with CS independencies concerning subsets of all the considered (also ordinal) variables. At this aim we use the Hierarchical Multinomial Marginal Models (HMMMs), see Bartolucci, Colombi and Forcina, 2007 [1]; Cazzaro and Colombi, 2014 [3]. The need of this parametrization chases the will of consider a model where we want to test simultaneously marginal and conditional independencies. In addition, it uses also local logits evaluated on different marginal contingency tables in order to consider the ordered modalities of the CS conditioning variables.
The paper is organized as follows. In Section 2 we introduce the constraints to impose on the HMMM in order to represent also CS independencies. The proposed model is also represented through a Stratified Chain Graph Model (SCGM), an extension of Stratified Graphical Model proposed by Nyman (2016) [10], that uses a Chain Graph Model (CGM) to represent the classical conditional independencies and labelled arcs in the graph to denote CS independencies. The details are explained in Section 3.
Finally we analyze a real dataset, "The Italian Innovation Survey" of Istat

(2012) [5], in order to investigate the effect of the innovation in different aspects of small and medium Italian enterprises on the grown in revenue terms. The procedure and the results are showed in Section 4. In Section 5, we summarize the main results of this work and future research.

2 Parametrization for context specific independencies

Let us consider q categorical variables $(X_1, \ldots, X_q)$ taking values $(i_1, \ldots, i_q)$ in the contingency table $\mathcal{I} = (n_1 \times \cdots \times n_q)$, where the modalities of the generic variable X_j, i_j takes value in $\mathcal{I}_j$. A parametrization of a model able to capture marginal and conditional independencies among non ordinal variables comes through the marginal model, see Bergsma and Rudas, 2002 [2], which defines the classical log-linear parameters on marginal distributions by respecting certain properties of completeness and hierarchy. The marginal parameters are $\eta_{\mathcal{L}}^{\mathcal{M}}(i_{\mathcal{L}})$ where $\mathcal{M}$ refers to the marginal set, $\mathcal{L}$ denotes the subset of variables which the parameter pertains and $i_{\mathcal{L}}$, in parenthesis, the modalities of the variable selected in $\mathcal{L}$ (when the parenthesis are omitted means that the parameters refer to each $i_{\mathcal{L}} \in \mathcal{I}_{\mathcal{L}}$). The following example shows how to define the marginal parameters in order to describe a conditional independence.

Example 1 Let us consider a set of four variables, say X_1, X_2, X_3 and X_4 and suppose we are interested in describing the independence $X_1 \perp X_2 | X_3$. At this aim, we have to define the marginal sets $\{(1,2,3),(1,2,3,4)\}$ where $(1,2,3,4)$ is a shortcut for $(X_1X_2X_3X_4)$. Then, we define the classical log-linear parameters on the contingency table $\mathcal{I}_{1,2,3}$ restricted to $(1,2,3)$ and the remaining parameters on the unrestricted contingency table $\mathcal{I}$. Finally, we have to constrain to zero the parameters associated to the statement of independence $\eta_{1,2}^{1,2,3}$ and $\eta_{1,2,3}^{1,2,3}$.

Now, let us collect 4 subsets of variables, supposing A, B, C and D. As we mentioned, our aim is to find a parametrization able to describe, beyond the classical statements of conditional independencies, the following statement of CS independence, formally:

$$A \perp B | (C = i_C, D), \qquad i_C \in \mathcal{K} \tag{1}$$

where i_c is the vector of certain modalities of variables in C which take values in $\mathcal{K}$ that is a subset of the modalities of C ($\mathcal{I}_C$) for which the conditional independence holds.

Theorem 1. *The independence in formula (1) holds if and only if the marginal log-linear parameters satisfy the following constraints*

$$\sum_{\substack{v \in \mathcal{V} \\ c \in \mathcal{P}(C)}} \eta_{vc}^{\mathcal{M}}(i_v i_c) = 0 \qquad i_v \in \mathcal{I}_v \quad i_c \in \mathcal{K} \tag{2}$$

where $\mathcal{P}(\cdot)$ denotes the power set, $\mathcal{V} = \{(\mathcal{P}(A) \setminus \emptyset) \cup (\mathcal{P}(B) \setminus \emptyset) \cup \mathcal{P}(D)\}$ and $\mathcal{K}$ is a subset of the modalities of C ($\mathcal{I}_C$) for which the CS independence holds.

The proof is close to the one of Theorem 1, page 1497, [10], for log-linear parameters defined on the joint distribution.

Example 2 (recall Example 1) Let suppose that we want to define through marginal model the CS independence $X_1 \perp X_2 | X_3 X_4 = i_4$, with $i_4 \in \mathcal{K}$ where $\mathcal{K} \subseteq I_4$ is a subset of the modalities i_4 of X_4 for which the conditional independence holds. The constraints on the marginal parameters will be in this case

$$\eta_{1,2}^{1,2,3,4}(i_1 i_2) + \eta_{1,2,3}^{1,2,3,4}(i_1 i_2 i_3) + \eta_{1,2,4}^{1,2,3,4}(i_1 i_2 i_4) + \eta_{1,2,3,4}^{1,2,3,4}(i_1 i_2 i_3 i_4) = 0$$
$$i_1 \in \mathcal{I}_1, \quad i_2 \in \mathcal{I}_2, \quad i_3 \in \mathcal{I}_3, \quad i_4 \in \mathcal{K}.$$

Now, we consider the case where we have at least an ordinal variable. In this unexplored case we move in the HMMM framework, see Bartolucci, Colombi and Forcina, 2007 [1] and Cazzaro and Colombi, 2014 [3]. In the HMMMs, beyond the baseline parameters, we can use parameters η coded with different criteria in order to consider the possible proper order of the modalities. In this work we take advantage from the local logits that compare the probability of a cell π_i with the previous one, for instance, referring to variable X_1 we have $\eta_1^1(i_1) = log(\frac{\pi_{i_1}}{\pi_{i_1-1}})$.

Theorem 2. *The independence in formula (1) holds if and only if the parameters of HMMM coded with local logits, satisfy the following constraints*

$$\sum_{\substack{v \in \mathcal{V} \\ c \in \mathcal{P}(C)}} \sum_{i_c^* \leq i_c} \eta^{vc}(i_v i_c) = 0 \qquad i_v \in \mathcal{I}_v \quad i_c \in \mathcal{K} \tag{3}$$

where $\mathcal{P}(\cdot)$ denotes the power set, $\mathcal{V} = \{(\mathcal{P}(A) \setminus \emptyset) \cup (\mathcal{P}(B) \setminus \emptyset) \cup \mathcal{P}(D)\}$ and $\mathcal{K}$ is a subset of the modalities of C ($\mathcal{I}_C$) for which the CS independence holds.

Proof. Let us call the baseline parameters η_b and the local parameters η_l. Between these two types of parameters the following relationship exists:

$$\eta_{b\mathcal{L}}^{\mathcal{M}}(i_{\mathcal{L}}) = \sum_{i_{\mathcal{L}}^* \leq i_{\mathcal{L}}} \eta_{l\mathcal{L}}^{\mathcal{M}}(i_{\mathcal{L}}^*) \tag{4}$$

The statement follows replacing the baseline parameters in formula 2 with the corresponding local parameters.

Example 3 By considering the CS independence in Example 2, by adopting local logit for coding the conditioning variable, the constraints in formula (3) become

$$\eta_{1,2}^{1,2,3,4}(i_1, i_2) + \eta_{1,2,3}^{1,2,3,4}(i_1 i_2 i_3) +$$
$$+ \textstyle\sum_{i_4^*=1}^{i_4} \eta_{1,2,4}^{1,2,3,4}(i_1 i_2 i_4^*) + \sum_{i_4^*=1}^{i_4} \eta_{1,2,3,4}^{1,2,3,4}(i_1 i_2 i_3 i_4^*) = 0 \tag{5}$$

with $i_1 \in \mathcal{I}_1$, $i_2 \in \mathcal{I}_2$, $i_3 \in \mathcal{I}_3$ and $i_4 \in \mathcal{K}$. It is worthwhile to note that the constraints in formula (3), when we deal with local logit, correspond to the CS independence $X_1 \perp X_2 | X_3 X_4 \leq i_4$, $i_4 \in \mathcal{K}$.

3 Stratified Chain Graph models

A *Chain Graph* is a graph with both directed and undirected arcs and without any directed or semi-directed cycle. The vertices of a chain graph are decomposable in so-called *Chain Components*, denoted by $T_1, ..., T_s$. Within these chain components there are only undirected arcs and between vertices belonging to different components there are only directed arcs, all head toward the same direction. Trivially, the Chain Graph Models (CGM) are graphical models which take advantages from chain graphs to describe a system of independencies. There are different types of CGM, see Drton, 2009 [4], that interpret in different way the presence/absence of directed/indirected arcs. In this work we use the CGM of type I, see Lauritzen and Wermuth, 1989 [7] and Frydenberg, 1990, [6], as natural generalization of classical graphical models. CGMs are used when the variables to analyze are of different nature, such that they can be naturally collected in different components. Furthermore, it is reasonable to suppose that between variables within the same component there is a kind of dependence relationship that differs from the relationship between variables collected in different components. Therefore, it is possible to define an explicative order between the variables collected in different components.
As it is shown in Rudas, Bergsma and Németh, 2010, [12] and in Nicolussi, 2013, [9], the marginal log-linear models and the HMMMs give a suitable parameterization for the CGM of type I. Now, the improvement in CGMs necessary to represent the CS independencies closely follows the Nyman's approach (Nyman, 2016 [10]) for undirected graphs. Thus we introduce the Stratified Chain Graph Models (SCGM) as extension of stratified graphical models, [10]. A stratified chain graph has, in addition to the previous graphs, labeled arcs. These identify the "stratum" of the models, that is the modality(ies) of the variable(s) in the conditional set according to the context-specific independence.

Example 4 Let us consider 5 variables X_1, X_2, X_3, X_4 and X_5. Suppose that, according to the nature of the variables we can split them in two components such that variables X_1 and X_2 can be considered explicative for X_3, X_4 and X_5. The SCGM represented by the graph in Figure 1 is one possible situation that can occur. In this case we have the conditional independencies $X_3 \perp X_2|X_1$ and $X_5 \perp X_1X_2|(X_3, X_4)$ and the CS independence $X_3 \perp X_4|(X_1 = i_1^*, X_2, X_5 = i_5^*)$.

4 Application on real data

In this section we investigate the potential of a model that simultaneously, consider marginal, conditional and CS indpendencies on a set of (ordinal) categorical variables. Our aim is to study the effect of innovation in small and medium Italian enterprises, during the 2009-2012, in the revenue growth. With the term "innovation" we refer to any improvement in product, services, productive line, logistic system, organization and investment in Research and Development (R&D) area. We used the "Italian innovation survey on SM enterprises" [5].

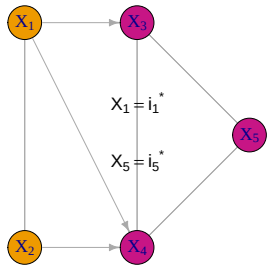

Fig. 1. SCGM with the labelled arc $X_3 - X_4$ referring to modality i_1^* of X_1 and modality i_5^* of X_5.

Thus we considered the *revenue growth in 2012*, **G** (Yes, No) henceforth denoted as variable **1**, as the pure response variable. Then, we took into account the innovation through three dichotomous variables referring to the period 2009-2012: *innovation in products or services or production line or investment in R&D*, **IPSP** (Yes, No), *innovation in organization system*, **IORG** (Yes, No) and *innovation in marketing strategies*, **IMAR** (Yes, No), henceforth denoted as variables **2, 3** and **4** respectively. Finally, other variables concerning the firm's featuring in 2009-2012 were collected: the *main market (in revenue terms)*, **MARK** (A= Regional, B= National, C= International), the *percentage of graduate employers*, **DEG** (1= 0% $\vdash$ 10%, 2= 10% $\vdash$ 50%, 3=50% $\vdash$ 100%) and the *enterprise size*, **TYP** (1= Small, 2= Medium), henceforth denoted as variables **5, 6** and **7** respectively.
In order to analyze this dataset, we build a chain graph with three components according to the nature of the variables, so in the first component we collect the firm's features (**MARK 5**, **DEG 6**, **TYP 7**), in the second component the innovations variables (**IPSP 2**, **IORG 3**, **IMAR 4**) and in the third component the revenue growth **G 1**. Then, starting from the complete chain graph, where there are all possible edges, corresponding to the saturated HMMM, we tested all chain graph models of type I with only one missing edge, in order to investigate, one by one, which pairwise relationship is plausible. The test was lead with the maximum likelihood ratio test, by comparing the likelihood of unconstrained HMMM, with the likelihood of the corresponding constrained model. In the HMMM, the parameters of dummy variables were codified with baseline logits while the parameters referring to the ordinal **MARK** and **DEG** were codified with local logits.
We removed from the complete chain graph all the edges which given positive results in the previous tests, obtained in this way a reduced CGM. Subsequently, we test the reduced CGM adding one by one all the edges previously removed. Table 1 shows the statistic test, the degree of freedom and the p-value of the HMMM for the main significant models. The numbers involved in the

independencies represent the variables in the order of presentation. The CGMs associated to these three HMMMs were depicted in Figure 2.

Name	Independencies	GSQ	df	p-value
A	$1 \perp 4 \mid 2,3,5,6,7$ $3 \perp 5 \mid 2,4,6,7$	100.88	84	0.1012
B	$1 \perp 4 \mid 2,3,5,6,7$ $4 \perp 7 \mid 2,3,5,6$	91.87	81	0.1921
C	$1 \perp 4 \mid 2,3,5,6,7$ $3 \perp 5 \mid 2,4,6,7$ $4 \perp 7 \mid 2,3,5,6$	112.02	93	0.0872

Table 1. Values of statistics test of HMMM associated to CG models.

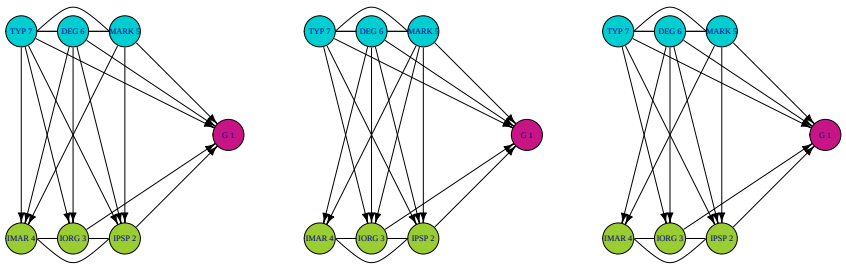

(a) (b) (c)

Fig. 2. CG models.

It is clear (i.e. it is common to all models), that the growth (**1**) is independent by the innovation in the marketing strategies (**4**) given by the remaining variables (**2, 3, 5, 6, 7**). In model A we have that the innovation in the organization system (**3**) is independent on the market where the enterprise works (**5**) given the other variables concerning the innovation and the firm's features (**2, 4, 6, 7**). On the contrary, in model B we have that the innovation in marketing strategies (**4**) is independent on the enterprise's size (**7**) given the other variables concerning the innovation and the firm's features (**2, 3, 5, 6**). Model C is the union of the independencies in model A and in model B. As we can see from Table 1 by choosing a reference level of the first type error α equal to 0.1 we reject the null hypothesis, thus we have no enough evidence to choose the model C. Thus, we considered the three independencies characterizing model C like CS independencies and we test all possible alternatives. The more interesting models were reported in Table 2. The preferable model, according to the parsimonious principle, is C4. The difference between models C and C4 is the independence concerning the organization system (**3**) and the

market where the enterprise works (**5**). In fact, in C4 this independence holds only when the conditioning variable percentage of graduated employers (**6**) is lower than 10% or greater than 50% that we can assume as indicator of unspecialized or high specialized firms. This means that only when the percentage of graduated employers is between $10\% - 50\%$ the market affects the innovation in the organization system.

Name	Independencies	GSQ	df	p-value
C1	$1 \perp 4 \mid 2,3,5,6,7$ $3 \perp 5 \mid 2,4,(6=1),7$ $4 \perp 7 \mid 2,3,5,6$	94.75	85	0.22002
C2	$1 \perp 4 \mid 2,3,5,6,7$ $3 \perp 5 \mid 2,4,(6=2),7$ $4 \perp 7 \mid 2,3,5,6$	102.77	85	0.09205
C3	$1 \perp 4 \mid 2,3,5,6,7$ $3 \perp 5 \mid 2,4,(6=3),7$ $4 \perp 7 \mid 2,3,5,6$	101.08	85	0.1125
C4	$1 \perp 4 \mid 2,3,5,6,7$ $3 \perp 5 \mid 2,4,(6=1,3),7$ $4 \perp 7 \mid 2,3,5,6$	105.09	89	0.1171

Table 2. Values of statistics test of HMMM

The stratified chain graph associated to the model C4 is depicted in Figure 3. In this graph the labeled arc between the node **MARK** and **IORG** reports the modalities of the variables **DEG** according to the arc is removed. That is, only when the variable **DEG** assume the first or the third modality, there is **MARK** independent by **IORG** given by **ISPS**, **IMAR**, **DEG** and **TYP**.

Finally, in Table 3 we report the values of the second order marginal log-linear parameters (referring to paired variables) of model C4. At first we remind that these are defined in the first marginal distribution where they occur. In this case, the marginal subsets associated to the CG models in Figure 2 and to the SCG model in Figure 3 are $\{(5,6,7),(2,3,4,5,6,7),(1,2,3,4,5,6,7)\}$. Furthermore, we remind that in order to define the conditional (marginal) independencies in model C4 we have to constraint to zero the parameter $\eta_{1,4}^{1,2,3,4,5,6,7}$ and all the higher order parameters, defined in the marginal set $(1,2,3,4,5,6,7)$, containing the paired variables $(1,4)$ and also the parameter $\eta_{4,7}^{2,3,4,5,6,7}$ and all the higher order parameters, defined in the marginal set $(2,3,4,5,6,7)$, containing the paired variables $(4,7)$. Finally, in order to define the CS independence, according to the formula (3), we have to constrain to zero the sum of parameters $\eta_{3,5}^{2,3,4,5,6,7}$ and all the higher order parameters, defined in the marginal $(2,3,4,5,6,7)$, containing the paired variables $(3,5)$ but where the variable 6 assumes value 1 or 3. Note that in Table 3, the parameters $\eta_{3,5}^{2,3,4,5,6,7}$ are free and assume value zero. This reveals the lack of relationship between the variables **MARK** and **IORG** at least concerning the parameters of third or higher order.

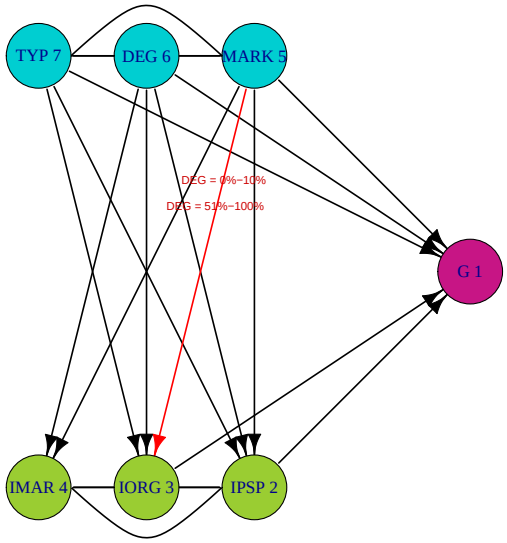

Fig. 3. SCG model C4.

Variable	Modalities	G 1 *Yes*	IPSP 2 *Yes*	IORG 3 *Yes*	IMAR 4 *Yes*	MARK 5 *National*	MARK 5 *Internat.*	DEG 6 *10%-50%*	DEG 6 *≥ 50%*
ISPS 2	*Yes*	0.1927							
		(0.0793)							
IORG 3	*Yes*	0.1023	1.8221						
		(0.0709)	(0.0827)						
IMAR 4	*Yes*	0	1.4848	1.9967					
		(0.0000)	(0.0907)	(0.0764)					
MARK 5	*National*	0.0980	0.6378	0	0.3005				
		(0.0688)	(0.0960)	(0.0000)	(0.0928)				
	Internat.	0.4668	0.1517	0	-0.2096				
		(0.1486)	(0.1815)	(0.0000)	(0.1912)				
DEG 6	*10%-50%*	0.0332	0.5020	0.4372	0.4323	0.6902	0.2547		
		(0.0821)	(0.10400)	(0.0988)	(0.0927)	(0.0567)	(0.0856)		
	≥50%	-0.1333	-0.0422	0.5048	0.3451	0.1758	-0.1186		
		(0.1436)	(0.2070)	(0.1624)	(0.1746)	(0.1024)	(0.1493)		
TYP 7	*Medium*	0.3700	0.6447	0.5687	0	0.9878	0.7591	1.1702	-0.3302
		(0.0790)	(0.1064)	(0.0868)	(0.0000)	(0.0497)	(0.0775)	(0.0543)	(0.0899)

Table 3. Second order marginal log-linear parameters.

From Table 3 we can see that between the three innovation variables there is a strong (positive) second order association: (**IPSP**, **IORG**) with log odds ratio of 1.82, (**IPSP**, **IMAR**) with log odds ratio of 1.49 and (**IMAR**, **IORG**) with log odds ratio of 2. In the graph they correspond to the undirected arcs between the nodes **2** and **3**. This means that is more likely to have firms that

improve innovations in different levels. Another strong association is between the firm's dimension and the main market. In particular it seems, reasonably, that bigger is the firm bigger is the market where it works. It is also worthwhile to focus on the parameters concerning the variable **DEG**, which discriminates between a conditional and a CS independence in model C4. In particular from Table 3 it came to light that there is a reverse direction between the parameters (all positive) referring to the $10\% - 50\%$ modality and the one referring to the $\geq 50\%$ which are more than half negative. This means that moving from the unspecialized firm (less than 10% graduate) to a medium specialized firm ($10\% - 50\%$ graduate), we have a positive association with all the other variables. On the other hand, by considering the highly specialized firm ($\geq 50\%$ graduate) with respect to the medium specialized firm, we can see that there is a negative trend with the revenue growth. The same trend occurs also with the innovation in product, services, product line and R&D (**IPSP**), the main market (**MARK**) and the firm's size (**TYP**). This change probably would been unobserved by codifying the parameters with baseline logits. Furthermore, by accepting the conditional independence $3 \perp 5|2, 4, 6, 7$ we would not focus on the variable 6.

5 Conclusion

In this work we showed how to represent CS independencies in HMMMs when we treat with ordinal variable and we are interested in representing also marginal and conditional independencies. We also provide a graphical representation based on chain graph in order to give visual simplification of the relationships among the variables.
The final SCGM have been chosen following a two steps procedure to identify the best CGM and then by watching the problem at hand to find the "strata" of the graph, but further research will be dedicated to implement the procedure able to test all possible models (testing all hypothesis of independence). Furthermore, other research involves the definition of constraints for parameters coded with "global" or "continuation" logits. It should be interenting also to study the definition of SCGM by considering the Chain Graph Models of type 4, see Drton (2009) [4], with the parameterization explained by Marchetti and Lupparelli (2011) [8].

References

1. Bartolucci, F., Colombi, R., and Forcina, A. An extended class of marginal link functions for modelling contingency tables by equality and inequality constraints. *Statistica Sinica*, **17**, 691 – 711, 2007.
2. Bergsma, W. P., and Rudas, T. Marginal models for categorical data. *Annals of Statistics*, **30(1)**, 140 – 159, 2002.
3. Cazzaro, M., and Colombi, R. Marginal nested interactions for contingency tables. *Communications in Statistics - Theory and Methods*, **43(13)**, 2799 – 2814, 2014.
4. Drton, M. Discrete chain graph models. *Bernoulli*, **15(3)**, 736 – 753, 2009.
5. Istat. Italian innovation survey on SM enterprises, 2012.

6. Frydenberg, M. The chain graph Markov property. *Scandinavian Journal of Statistics*, **17(4)**, 333-353, 1990.
7. Lauritzen, S. L., and Wermuth, N.. Graphical models for associations between variables, some of which are qualitative and some quantitative. *The Annals of Statistics*, **17(1)**, 31-57, 1989.
8. Marchetti, G. M., and Lupparelli, M. Chain graph models of multivariate regression type for categorical data. *Bernoulli*, **17(3)**, 827 – 844, 2011.
9. Nicolussi, F. Marginal parameterizations for conditional independence models and graphical models for categorical data. *PhD Thesis*. University of Milano Bicocca. 2013.
10. Nyman, H., Pensar, J., Koski, T., and Corander, J. Context-specific independence in graphical log-linear models. *Computational Statistics*, **31(4)**, 1493 – 1512, 2016.
11. Højsgaaard, S. Statistical inference in context specific interaction models for contingency tables. *Scandinavian journal of statistics*, **31(1)**, 143-158, 2004.
12. Rudas, T., Bergsma, W. P., and Németh, R.. Marginal log-linear parameterization of conditional independence models. *Biometrika*, **97(4)**, 1006-1012, (2010).

PROBABILISTIC MODELING OF HYDRAULIC CONDITIONS OF PIPELINE NETWORKS UNDER RANDOM COMPOSITION OF BOUNDARY CONDITIONS AT NODES

Nikolay N.Novitsky[1], Olga V.Vanteyeva[1]

[1] Melentiev Energy Systems Institute of Siberian Branch of the Russian Academy of Sciences , 130 Lermontov str., Irkutsk, Russia, 664033 (e-mail: pipenet@isem.irk.ru, vanteeva@isem.irk.ru)

Abstract. The paper is concerned with the problem of probabilistic analysis of hydraulic conditions in pipeline networks, which occur under the impacts of external environment. These impacts are taken into account to specify boundary conditions for nodal flow rates or pressures in a probabilistic form. The research reveals practical value of such a statement which arises at the stages of design and operation of pipeline networks in the analysis of their transmission capacities and feasibility of operating conditions. A mathematical statement and a general scheme for solving the problems are presented. The final relationships are obtained to calculate the mean value and covariance matrices of the sought state variables. The relationships provide analytical representation of the model of probabilistic flow distribution. A numerical example is presented to illustrate high computational efficiency of the proposed method for probabilistic analysis of operating conditions and its advantages over the traditional deterministic models and methods for such an analysis.

Keywords: Pipeline systems, probabilistic modeling, flow distribution, hydraulic circuits, statistical parameters.

Introduction. The problems of calculation of hydraulic conditions represent the fundamental problems in the analysis of operating conditions of the pipeline networks in their design, operation and dispatching control. In practice the calculations of hydraulic conditions of the pipeline networks pursue two goals: 1) to assess transmission capacity of pipeline networks under specified (normally maximum) loads of consumers; 2) to assess the extent to which the consumers are provided with water at given characteristics of consumption systems. The first (main) type of calculations is based on the models with lumped loads of consumers and is applied at the stages of pipeline network design, development and reconstruction. It is also applied to calculate the main operating parameters of the networks. The second (check) type of calculations is based on the models with non-fixed loads and is applied at the stages of pipeline network operation to calculate and analyze off-design conditions, for example emergency ones.

In both cases traditionally the deterministic models of flow distribution are involved. However, the actual conditions of the pipeline network depend on the random impacts of external environment (load of consumers, pressure at sources, etc.). This is why solving the problem of probabilistic modeling of steady state hydraulic conditions to obtain the calculation results in the form that allows their probabilistic interpretation is topical.

The present paper is concerned with the problem of probabilistic modeling of steady state hydraulic conditions of a pipeline network. The problem is based on the models with lumped loads, but pressures can be specified at a random number of nodes (for example, at the working fluid entrance points). Thus, the nodal boundary conditions are specified, when either pressure or flow rate is specified for each node, and pressure should be specified for no less than one node. Such a statement of the

problem is refinement of more general ones [1-3]. From the viewpoint of applied significance, however, it should be considered independently.

Statement of a problem of probabilistic calculation of hydraulic conditions

The probabilistic description of an individual condition is reduced to the distribution density function to be denoted by $p(R,\phi_R)$, where R – the value of random vector of state variables (pressures, flow rates, etc.); ϕ_R –distribution parameters. In most of the practical cases it is possible to assume a hypothesis about normal distribution of R. Then $\phi_R = \{\bar{R}, C_R\}$ and probabilistic description of the conditions are reduced to the indication of mean value ($\bar{R}$) and covariance matrix (CM) (C_R) for the magnitude R.

Not any combination of R components is admissible, since they should meet the equations of the flow distribution model $U(R) = 0$ (where U – nonlinear vector function). These equations follow from the general physical laws of conservation and, hence, should be deterministic.

The traditional deterministic model of steady-state hydraulic conditions in pipeline network as hydraulic circuit with lumped parameters can be represented as [4]

$$U(R) = U(G,Y) = U(x,Q,P) = \begin{pmatrix} Ax - Q \\ A^{\mathrm{T}}P - y \\ y = f(x) \end{pmatrix} = 0. \qquad (1)$$

Where: the first subsystem of equations represents conditions of mass balance at the nodes for the calculated scheme of a pipeline network (equations of the first law of Kirchhoff); the second - the equations of the second law of Kirchhoff in a nodal form; G – boundary conditions (BC); Y – unknown state variables; T – transposition symbol; A – $m \times n$-dimensional incidence matrix of nodes and branches of the calculated scheme with elements $a_{ji} = 1(-1)$, if node j is initial (final) for branch i, $a_{ji} = 0$, if branch i is not incident to node j; m, n – number of nodes and branches in the calculated scheme; x – n-dimensional vector of flow rates in branches, P, Q – m-dimensional vectors of nodal flow rates and pressures; y – n-dimensional vector of pressure losses in branches; $f(x)$ – n-dimensional vector-function with elements $f_i(x_i)$, that reflect the laws of hydraulic flow for branches, for example, $f_i(x_i) = s_i x_i |x_i| - H_i$, where x_i – flow rate in the i-th branch; s_i – hydraulic resistance of the branch; $H_i > 0$ – increase in the pressure in the case of active branch (for example, the one modeling a pumping station); $H_i = 0$ in the case of a passive branch (for example, the one modeling a pipeline section). Assuming that in (1) all parameters s_i, H_i, $i = \overline{1,n}$ are specified deterministically, we obtain $R = (x^{\mathrm{T}}, \bar{Q}^{\mathrm{T}}, \bar{P}^{\mathrm{T}})^{\mathrm{T}}$.

Thus, the probabilistic model of steady-state flow distribution can be represented as $U(R) = 0$, $R \sim N_r(\bar{R}, C_R)$, where N_r – r – dimensional normal distribution of probabilities; r – dimension of vector R. In the case of normal

distribution of G, the nonlinear distortion of distribution $p[Y(G), \phi_{Y(G)}]$ (where $Y(G)$ – implicit function specified by equations of flow distribution) is neglected, and the problem is reduced to the determination of $\varphi_R = \{\bar{R}, C_R\}$ at a given value $\varphi_G = \{\bar{G}, C_G\}$ and condition $U(R) = U(G,Y) = 0$. In this case the composition of G should provide solvability of equations $U(G,Y) = 0$ with respect to G, i.e. $\dim(G) = \dim(U) = \mathrm{rank}(\partial U / \partial Y)$, where $\partial U / \partial Y$ – Jacobi matrix (of partial derivatives) at fixed boundary conditions G^* in the vicinity of a point of solution Y^*, $\dim(\cdot)$ – dimension of vector, $\mathrm{rank}(\cdot)$ – matrix rank.

Methodological approach. Let $\xi_G = (G - \bar{G})$ be a random deviation of possible realization of boundary conditions from its mean $\bar{G}$. By linearizing function $Y(G)$ in the vicinity of $\bar{G}$, we obtain $Y \approx Y(\bar{G}) + (\partial Y / \partial G)\xi_G$, where $\partial Y / \partial G$ – matrix of derivatives at point $\bar{G}$. Since $E(Y) = \bar{Y}$ and $E(\xi_G) = 0$, where E – operation of mean, then $\bar{Y} = Y(\bar{G})$. Thus, the mean of unknown state variables ($\bar{Y}$) is a function of flow distribution equations at a specified mean of boundary conditions ($\bar{G}$). Since $\xi_Y = (Y - \bar{Y})$, then $\xi_Y \approx \dfrac{\partial Y}{\partial G}\xi_G$. Accordingly,

$$\bar{R} = \begin{pmatrix} \bar{G} \\ \bar{Y} \end{pmatrix} = \begin{pmatrix} \bar{G} \\ Y(\bar{G}) \end{pmatrix} \text{ and } C_R = E\left[\begin{pmatrix} \xi_G \\ \xi_Y \end{pmatrix}\begin{pmatrix} \xi_G \\ \xi_Y \end{pmatrix}^{\mathrm{T}}\right] = \left[\begin{array}{c:c} C_G & C_{GY} \\ \hdashline C_{YG} & C_Y \end{array}\right],$$

where $C_Y = E\left[\xi_Y \xi_Y^{\mathrm{T}}\right] \approx E\left[\dfrac{\partial Y}{\partial G}\xi_G \xi_G^{\mathrm{T}}\left(\dfrac{\partial Y}{\partial G}\right)^{\mathrm{T}}\right] = \dfrac{\partial Y}{\partial G} C_G \left(\dfrac{\partial Y}{\partial G}\right)^{\mathrm{T}}$,

$$C_{GY} = C_{YG}^{\mathrm{T}} = E(\xi_G \xi_Y^{\mathrm{T}}) \approx E\left(\xi_G \xi_G^{\mathrm{T}}\left(\frac{\partial Y}{\partial G}\right)^{\mathrm{T}}\right) = C_G\left(\frac{\partial Y}{\partial G}\right)^{\mathrm{T}}.$$

Thus, the general scheme of solving the problem of probabilistic modeling of operating conditions is reduced to the following: 1) to obtain vector $\bar{Y}$ by traditional methods of flow distribution calculation on the basis of input data of $\bar{G}$; 2) to determine matrix C_R, by using the known matrix C_G and matrix of derivatives $\partial Y / \partial G$ at point $\bar{G}$.

In this case a question arises what the final form of the relationship for the resultant covariance matrices is at $G = (Q_G^{\mathrm{T}}, P_G^{\mathrm{T}})^{\mathrm{T}}$, since in the traditional methods for flow distribution calculation the derivatives $\partial Y / \partial G$ in an explicit form are not calculated, which represents an independent problem.

Relationships for covariance matrices of state variables. Let $J = \{1, 2, ..., m\}$ – be a set of indices of all nodes of the calculated scheme. We will divide it into two subsets: J_Q – a set of nodes with specified flow rates; J_P – a set of nodes with specified pressures, so that $J = J_Q \bigcup J_P$, $J_Q \bigcap J_P = \varnothing$, $m_Q = |J_Q|$, $m_P = |J_P|$, $m_Q + m_P = m$. In the case, if either pressure or flow rate are specified as deterministic boundary conditions, their variances and all covariances with other

parameters, at this node are equated to zero. A typical case of deterministic boundary conditions is zero flow rates at simple nodes without load. Thus, the presence of deterministic boundary conditions will be a special case of the technique considered below.

Taking into account the introduced sets, the model of flow distribution with lumped loads (1) can be represented in the form:

$$A_Q x - Q_G = 0,$$
$$A_P x - Q_Y = 0,$$
$$A_Q^{\mathrm{T}} P_Y + A_P^{\mathrm{T}} P_G - y = 0,$$
$$y = f(x,s).$$

where A_Q – an $(m_Q \times n)$-dimensional incidence matrix of nodes of set J_Q and branches of the scheme; A_P – an $(m_P \times n)$-dimensional incidence matrix of nodes of set J_P and branches of the scheme; Q_G, P_Y – m_Q-dimensional vectors of flow rates and pressures at nodes of set J_Q; P_G, Q_Y – m_P-dimensional vectors of flow rates and pressures at nodes of set J_P.

We linearize this flow distribution model at the point of mean value of boundary conditions $G = (Q_G^{\mathrm{T}}, P_G^{\mathrm{T}})^{\mathrm{T}}$, which provides interrelation between the deviations of these conditions and deviations of sought parameters of flow distribution:

$$A_Q \xi_x - \xi_{QG} = 0 \quad (2)$$
$$A_P \xi_x - \xi_{QY} = 0, \quad (3)$$
$$A_Q^{\mathrm{T}} \xi_{PY} + A_P^{\mathrm{T}} \xi_{PG} - \xi_y = 0, \quad (4)$$
$$\xi_y = f_x' \xi_x. \quad (5)$$

Here: ξ_{QG}, ξ_{PG} – deviations of nodal flow rates and pressures included in the boundary conditions; ξ_{QY}, ξ_{PY} – deviations of unknown nodal flow rates and pressures, ξ_x, ξ_y – deviations of unknown flow rates and pressure losses in branches, f_x' – an $n \times n$ - dimensional diagonal matrix with elements $\partial f_i / \partial x_i$ on the diagonal.

To obtain an explicit relationship between the deviations of sought state variables and deviations in the initial data $\xi_Y \approx \dfrac{\partial Y}{\partial G} \xi_G$ we will perform the following transformations.

Substitute expression (5) for ξ_y to (4) and express ξ_x as

$$\xi_x = (f_x')^{-1} A_Q^{\mathrm{T}} \xi_{PY} + (f_x')^{-1} A_P^{\mathrm{T}} \xi_{PG} \ . \quad (6)$$

By using the obtained expression (6) exclude ξ_x from (2) and (3)

$$\frac{\partial Q_G}{\partial P_Y} \xi_{PY} + \frac{\partial Q_G}{\partial P_G} \xi_{PG} - \xi_{QG} = 0, \quad (7)$$
$$\frac{\partial Q_Y}{\partial P_Y} \xi_{PY} + \frac{\partial Q_Y}{\partial P_G} \xi_{PG} - \xi_{QY} = 0, \quad (8)$$

where $\frac{\partial Q_G}{\partial P_Y} = A_Q (f_x')^{-1} A_Q^{\mathrm{T}}$, $\frac{\partial Q_G}{\partial P_G} = A_Q (f_x')^{-1} A_P^{\mathrm{T}}$, $\frac{\partial Q_Y}{\partial P_Y} = A_P (f_x')^{-1} A_Q^{\mathrm{T}}$, $\frac{\partial Q_Y}{\partial P_G} = A_P (f_x')^{-1} A_P^{\mathrm{T}}$.

From (7) we obtain an expression for ξ_{PY}, with its right-hand side depending only on the deviations in boundary conditions

$$\xi_{PY} = \frac{\partial P_Y}{\partial Q_G} \xi_{QG} + \frac{\partial P_Y}{\partial P_G} \xi_{PG}, \tag{9}$$

since $\frac{\partial P_Y}{\partial Q_G} = \left(\frac{\partial Q_G}{\partial P_Y} \right)^{-1}$, $\frac{\partial P_Y}{\partial P_G} = -\left(\frac{\partial Q_G}{\partial P_Y} \right)^{-1} \frac{\partial Q_G}{\partial P_G}$.

We use back substitution to substitute expression for ξ_{PY} in (8), from which

$$\xi_{QY} = \frac{\partial Q_Y}{\partial Q_G} \xi_{QG}, \tag{10}$$

and by substituting it to (6) we will obtain expression for ξ_x

$$\xi_x = \frac{\partial x}{\partial Q_G} \xi_{QG} + \frac{\partial x}{\partial P_G} \xi_{PG}, \tag{11}$$

where $\frac{\partial x}{\partial Q_G} = (f_x')^{-1} A_Q^{\mathrm{T}} \frac{\partial P_Y}{\partial Q_G}$, $\frac{\partial x}{\partial P_G} = (f_x')^{-1} A_Q^{\mathrm{T}} \frac{\partial P_Y}{\partial P_G} + (f_x')^{-1} A_P^{\mathrm{T}}$.

And eventually by substituting ξ_x from (11) to (5) we obtain

$$\xi_y = f_x' \frac{\partial x}{\partial Q_G} \xi_{QG} + f_x' \frac{\partial x}{\partial P_G} \xi_{PG}, \tag{12}$$

In the end. we have an explicit relationship between the deviations of sought state variables and deviations in boundary conditions

$$\begin{pmatrix} \xi_{PY} \\ \xi_x \\ \xi_{QY} \\ \xi_y \end{pmatrix} = \left[\begin{array}{c:c} \frac{\partial P_Y}{\partial P_G} & \frac{\partial P_Y}{\partial Q_G} \\ \hdashline \frac{\partial x}{\partial P_G} & \frac{\partial x}{\partial Q_G} \\ \hdashline 0 & \frac{\partial Q_Y}{\partial Q_G} \\ \hdashline f_x' \frac{\partial x}{\partial P_G} & f_x' \frac{\partial x}{\partial Q_G} \end{array} \right] \left[\begin{array}{c} \xi_{PG} \\ \hdashline \xi_{QG} \end{array} \right] \tag{13}$$

From (13) we can obtain final relationships for the covariance matrix of: unknown nodal pressures

$$C_{PY} = \mathrm{E}[\xi_{PY}\xi_{PY}^{T}] \approx \frac{\partial P_Y}{\partial P_G} C_{PG} \left(\frac{\partial P_Y}{\partial P_G}\right)^{\mathrm{T}} + \frac{\partial P_Y}{\partial Q_G} C_{QG} \left(\frac{\partial P_Y}{\partial Q_G}\right)^{\mathrm{T}};$$

flow rates in branches

$$C_x = \mathrm{E}[\xi_x \xi_x^{T}] \approx \frac{\partial x}{\partial Q_G} C_{QG} \left(\frac{\partial x}{\partial Q_G}\right)^{\mathrm{T}} + \frac{\partial x}{\partial P_G} C_{PG} \left(\frac{\partial x}{\partial P_G}\right)^{\mathrm{T}};$$

unknown nodal flow rates

$$C_{QY} = \mathrm{E}\left[\xi_{QY}, \xi_{QY}^{\mathrm{T}}\right] \approx \frac{\partial Q_Y}{\partial Q_G} C_{QG} \left(\frac{\partial Q_Y}{\partial Q_G}\right)^{\mathrm{T}};$$

unknown pressure losses

$$C_y = \mathrm{E}\left[\xi_y, \xi_y^{\mathrm{T}}\right] \approx f_x' \frac{\partial x}{\partial Q_G} C_{QG} \left(\frac{\partial x}{\partial Q_G}\right)^{\mathrm{T}} f_x' + f_x' \frac{\partial x}{\partial P_G} C_{PG} \left(\frac{\partial x}{\partial P_G}\right)^{\mathrm{T}} f_x' \approx f_x' C_x f_x'.$$

These equations consider that $f_x' = (f_x')^{\mathrm{T}}$.

A numerical example. We will illustrate the capabilities of the proposed approach on a conventional scheme of pipeline network with parameters $m = 16$, $n = 22$ (Fig.1). Also, the Figure shows 2 nodes with pressures given in a probabilistic form and 14 nodes with flow rates, and their mean values and standard deviations.

According to the condition of obtaining the required amount of water at the hour of maximum water consumption in this study case an identical value (18 m of water column) of the minimum admissible pressure ($P_j^{\min}$) was given at nodes 1-14 [5]. The calculations were performed by the proposed method and traditional Monte-Carlo method. Tables 1 and 2 present the results of the probabilistic calculation of hydraulic conditions for branches and nodes, respectively.

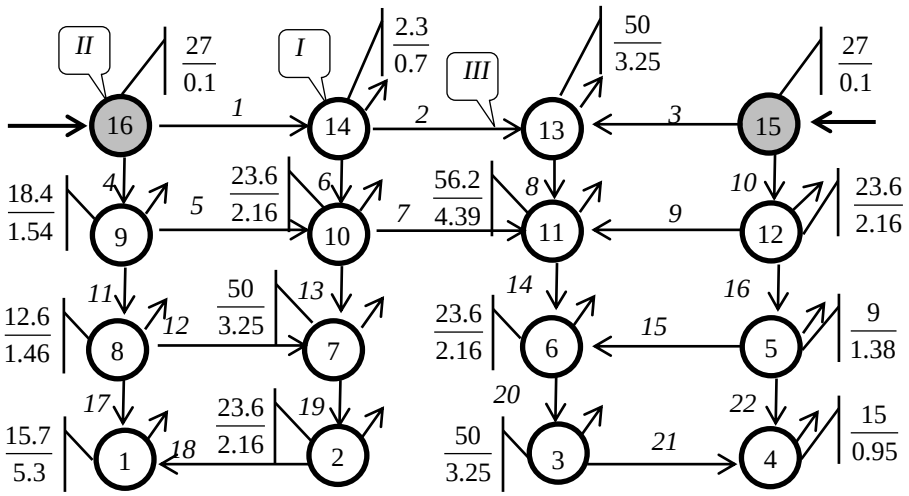

Fig. 1. Calculated scheme and initial data by node

I – node with specified flow rate (mean value/standard deviation); *II* – node with specified pressure (mean value/ standard deviation); *III* – branch - pipeline.

Table 1.

Initial data and results of probabilistic hydraulic calculation by branch

Branch, *i*	Initial data	Calculation results by Monte Carlo method(5000 realizations)		Calculation results by proposed method		Relative error	
	Resistance of branch *i*					Mean value	Standard deviation
		$\bar{x}_i^{\text{MMK}}$	$\sigma_{x,i}^{\text{MMK}}$	$\bar{x}_i$	$\sigma_{x,i}$	$\delta_{\bar{x},i}$	$\delta_{\sigma x,i}$
1	0.000025	235.0	6.5	235.1	6.5	0.00	0.01
2	0.000054	148.5	5.1	148.6	5.1	0.00	0.01
3	0.005751	21.4	0.7	21.4	0.8	0.00	0.03
4	0.000750	60.1	2.7	61.0	2.6	0.02	0.04
5	0.002273	14.9	1.0	14.9	0.9	0.00	0.06
6	0.000263	84.2	4.7	84.2	4.6	0.00	0.01
7	1.146865	1.4	0.1	1.4	0.1	0.00	0.00
8	0.000193	119.9	4.8	120.0	4.7	0.00	0.02
9	0.002253	9.1	1.8	9.1	1.8	0.00	0.02
10	0.001670	56.0	1.8	56.0	1.8	0.00	0.00
11	0.004145	27.7	2.3	27.8	2.1	0.00	0.08
12	0.085265	0.7	1.7	0.6	1.8	0.09	0.08
13	0.000496	74.0	4.6	74.1	4.7	0.00	0.01
14	0.000229	74.0	3.5	74.3	3.4	0.00	0.03
15	0.458178	1.0	0.2	1.0	0.1	0.01	0.07
16	0.001766	23.3	1.3	23.3	1.3	0.00	0.01
17	0.009992	14.8	3.6	14.5	3.4	0.02	0.04
18	0.199824	1.2	1.8	1.2	1.9	0.04	0.08
19	0.002935	24.4	2.6	24.8	2.6	0.02	0.01
20	0.000517	51.5	2.9	51.7	2.8	0.00	0.04
21	0.012947	1.7	0.9	1.7	1.0	0.01	0.02
22	0.010800	13.3	0.7	13.3	0.7	0.00	0.05

where $\delta_{\bar{x},i} = \dfrac{\left|\bar{x}_i^{\text{MMK}} - \bar{x}_i\right|}{\bar{x}_i^{\text{MMK}}}$, $\delta_{\sigma x,i} = \dfrac{\left|\sigma_{x,i}^{\text{MMK}} - \sigma_{x,i}\right|}{\sigma_{x,i}^{\text{MMK}}}$.

Table 2.

Results of probabilistic hydraulic calculation by node

Node, j	Calculation results by Monte Carlo method		Calculation results by proposed method		Relative error	
					Mean value	Standard deviation
	$\bar{P}_j$	$\sigma_{P,j}$	$\bar{P}_j$	$\sigma_{P,j}$	$\delta_{\bar{P},j}$	$\delta_{\sigma P,j}$
1	18.7	1.7	18.9	1.7	0.02	0.00
2	19.2	0.9	19.2	0.9	0.00	0.00
3	18.9	0.6	18.9	0.5	0.00	0.00
4	19.9	0.5	18.9	0.5	0.00	0.00
5	20.8	0.4	20.8	0.4	0.00	0.00
6	20.3	0.4	20.3	0.4	0.00	0.00
7	21.0	0.6	21.0	0.6	0.00	0.00
8	21.0	0.8	21.0	0.7	0.00	0.00
9	24.2	0.3	24.2	0.3	0.00	0.00
10	23.7	0.3	23.7	0.3	0.00	0.00
11	21.6	0.4	21.8	0.4	0.01	0.00
12	21.8	0.3	21.4	0.3	0.04	0.00
13	24.4	0.2	24.4	0.2	0.00	0.00
14	25.6	0.1	25.6	0.1	0.00	0.00

The Tables show that the differences in the calculation results obtained by different methods are negligibly small. However, the calculation time (in the Maple environment) made up 97.5 minutes for Monte Carlo method (5000 realizations); 18 minutes for Monte Carlo method (10000 realizations), and 5 seconds for the proposed method, which demonstrates fast operation of the latter.

Calculation of probabilistic indices of pipeline network operation

The proposed approach to the calculation of statistical parameters of the pipeline network operating conditions enables us to obtain probabilistic estimates of virtually any pipeline network state variable by known formulas of probability theory [6,7]. Thus, the estimate of probability that the *j*-th state variable belongs to a specified range [$R_j^{\min}$, $R_j^{\max}$] is calculated by the equation

$$p_{Rj} = \frac{1}{\sigma_{Rj}\sqrt{2\pi}} \int_{R_j^{\min}}^{R_j^{\max}} \exp\left\{-\frac{\left(R_j - \bar{R}_j\right)^2}{2\sigma_{Rj}^2}\right\} dR_j , \qquad (14)$$

where R_j – random realization of state variable; $\bar{R}_j$ – mean value; R_j; σ_{Rj} – standard deviation R_j; p_{Rj} – realization probability of R_j in a specified range; $R_j^{\max}$, $R_j^{\min}$ – upper and lower boundaries of this range, which can take infinite values.

Table 3 presents the values of redundant pressures calculated as $P_j^{\text{over}} = \bar{P}_j - P_j^{\min}$, and the probabilities of violations of lower boundaries of the admissible pressure at nodes, calculated by equation (14).

Table 3.

Calculated violations of admissible boundaries by nodal pressure

Node, j	$\overline{P}_j$	$P_j^{\min}$	P_j^{over}	$p(P_j < P_j^{\min})$
1	18.9	18	0.9	0.3
2	19.2	18	1.2	0.1
3	18.9	18	0.9	0.0
4	18.9	18	0.9	0.0
5	20.8	18	2.8	0.0
6	20.3	18	2.3	0.0
7	21.0	18	3.0	0.0
8	21.0	18	3.0	0.0
9	24.2	18	6.2	0.0
10	23.7	18	5.7	0.0
11	21.8	18	3.8	0.0
12	21.4	18	3.4	0.0
13	24.4	18	6.4	0.0
14	25.6	18	7.6	0.0

One of the main indices of sufficient transmission capacity of the network in the analysis of conditions by deterministic methods is $P_j > P_j^{\min}$ for all $j \in J_Q$. Table 3 shows that at the point of mean value this condition is met, however, the probability of its violation at different nodes is different. For example, under the same value of redundant pressures at nodes 1,3 and 4 we have the value $p(P_1 < P_1^{\min}) = 0.3$. This illustrates the limitedness of the deterministic analysis compared to the probabilistic one.

Instead of equation (14) for conditional probability that an admissible boundary is violated by one parameter (when the rest of them remain in the vicinity of mean value) it is sensible to determine joined probability that the conditions belong to the feasibility region. Such a probability is calculated by the equation [6,7]

$$p_R = \frac{1}{\sqrt{(2\pi)^n |C_R|}} \int_{R_r^{\min}}^{R_r^{\max}} \dots \int_{R_1^{\min}}^{R_1^{\max}} \exp\left\{-\frac{1}{2}\left(R-\overline{R}\right)^{\mathrm{T}} \mathrm{C}_R^{-1}\left(R-\overline{R}\right)\right\} dR_1 \dots dR_n \qquad (15)$$

where $\overline{R}$ – an r-dimensional vector of mean value R; C_R – an $(r \times r)$-dimensional covariance matrix for R; p_R – probability that R belongs to a specified range $[R^{\min}, R^{\max}]$; $R^{\max} = [R_1^{\max}, \dots, R_r^{\max}]^{\mathrm{T}}$, and $R^{\min} = [R_1^{\min}, \dots, R_r^{\min}]^{\mathrm{T}}$, – vectors of upper and lower boundaries of an admissible range for R components.

Equation (15) can also be used to estimate feasibility of the operating conditions of any subset of the pipeline network components by one or several parameters (pressure, flow rates, etc.). In this case matrix C_R is formed from a complete covariance matrix of state variables by crossing out unnecessary rows and

columns. For the conditions of the study case the probability of violating the lower boundaries of admissible pressure for all nodes will equal 0.03.

Conclusions

1. The paper reveals the applied value of special consideration and development of analytical methods for probabilistic modeling of pipeline network hydraulic conditions when boundary conditions are represented by nodal flow rates or pressures.
2. Mathematical statement of the problem and general scheme of solving it are presented. The final relationships for covariance matrices of sought state variables for this case of boundary conditions are derived. They enable an analytical representation of the model of probabilistic flow distribution as a whole.
3. A numerical example is used to show high computational efficiency of the proposed method compared to the traditional Monte Carlo methods, which is achieved virtually without loss of adequacy of the obtained results.
4. The advantages of the probabilistic methods over the deterministic methods for the analysis of transmission capacity of pipeline networks and feasibility of their operating conditions are shown. A procedure for calculating the conditional and joint probabilities that operating conditions of any subset of pipeline network components belong to the admissible region by one or several parameters is demonstrated.
5. The proposed method will provide a qualitatively new level of reliability of the analysis and quantitative substantiation of solutions on operating conditions of pipeline networks at their design and operation.

References

1. Novitsky N.N., Vanteyeva O.V. Problems and methods for probabilistic modeling of hydraulic conditions of pipeline networks// // St. Petersburg State Polytechnic University Journal. – 2008. – No. 1. – P.68–75.
2. Novitsky N.N.,Vanteyeva O.V. Modeling of flow distribution stochastics in the hydraulic circuits //Proceedings of RAS. Power Engineering. – 2011. – No. № 2. – P.145-154.
3. Novitsky N.N., Vanteyeva O.V. Modeling of stochastic hydraulic conditions of pipeline systems // Chaotic Modeling and Simulation (CMSIM). – 2014. – No.1. – P. 95-108.
4. Merenkov A.P., Khasilev V.Y. Theory of hydraulic circuits. – M.: Nauka, 1985. – 280 p.
5. Water supply. Design of systems and structures: in 3 vol. V.3 Systems of water distribution and supply/ Methodological leadership and general editing by Dr.Sc., Prof. Zhurba M.G. Vologda-Moscow: VoSTU, 2001. –188 p.
6. Ventsel E.S.Theory of probabilities. – M.: Publ. H. "Vysshaya Shkola", 2001.– 575 p.
7. Ventsel E.S., Ovcharov L.A. Problems and exercises on theory of probabilities. – Textbook for Higher Educational Institutions. Ster. ed.3. – M.: Publ. H. "Vysshaya Shkola", 2000. – 366 p.

Perspectives on coverage of deaths in Brazil

Neir Antunes Paes[1], and Alisson dos Santos Silva[2]

[1](Postgraduate Program in Decision Modelling and Health of the Department of Statistics of the Federal University of Paraíba, Cidade Universitária, João Pessoa, Brazil (E-mail: antunes@de.ufpb.br)
[2] Postgraduate in Mathematical and Computational Modeling, Federal University of Paraíba, Brazil (E-mail: allisonpb22@hotmail.com)

Abstract. Vital statistics reflect the health status of a population, which are widely used in the formulation of important demographic indicators. The evolution of vital records in Brazil is marked by political factors and administrative instabilities that have compromised its quality and utility. Due to this commitment, the two main sources of vital records, the Brazilian Institute of Geography and Statistics and the Ministry of Health do not capture all of these records, mainly in less developed regions such as the Northeast of Brazil with a population of 56 million inhabitants in 2016. Although there have been gradual advances in coverage of deaths in Brazil, the Northeast region has not yet reached full coverage of deaths (100%). Among the nine States that compose this region, coverage of deaths in 2011 ranged from 79-94%. In order to estimate the year in which the States of the Northeast will reach the full coverage of death records projections were performed on coverage of deaths for each state. The annual series of death coverage estimated by the Ministry of Health from 1991 to 2011 were used. The projections were made through the mathematical methods of projections: Logistic, Gompertz and Holt's Exponential Smoothing Model. The model of Holt, in general, was the best fit to the pattern of the series of coverage of deaths. The States were classified in three intervals of years when they reached 100% of coverage, which varied from 2019 to 2028. It is estimated that for the Northeast the full coverage of deaths will be reached between 2021-2005. It is expected that these scenarios can contribute to the planning strategies and to the evaluation of managers regarding the actions and policies to be implemented on the performance of death statistics in the Northeast and Brazil.

Keywords: Vital Statistics, Mortality, Death Coverage, Projections, Brazil.

1 Introduction

Mortality projections are an essential input for projections of population, and also the financial development of pension schemes. Governments and insurance companies all over the world rely on mortality projections for counting its population and for efficient administration of their pension commitments. They also need to have some idea about how patterns of death (mortality) are likely to change so that they can plan for the future.

Mortality forecast in Brazil is officially produced by the Brazilian government [1], which every single year has the commitment to review such statistics. According to the government in 2042, the number of deaths in Brazil (more than 2.2 million) will exceed for the first time the number of births (2.1 million), and the population (then of 228 million) will decrease. However, the forecasting of mortality and its patterns of deaths for the less developed regions are usually very hard to calculate

because the uncertainties regarding the coverage of deaths in these regions. This is especially true for the Northeast region with a population of around 57 million in 2016, where little has been known about the coverage of deaths, particularly in the future.

The demographic models used in projecting mortality are usually based on statistical modeling of historical data. But before doing projections an important question to be answered is, is it the coverage of deaths complete, and if not, what do demographers need to do to estimate the coverage in the future? In another words, when the coverage of deaths will be complete in the case to be incomplete?

This last question was the motivation for doing this work for the Northeast region of Brazil. In this way is hoped to give a contribution using some mathematical methods which can be applied for any region or Country which death coverage is not complete.

2 Study Data and Methods

This study has an ecological time-trend design, which geographical unites are the 9 States (provinces) belonging to the Brazilian northeast region and the region as whole. A longitudinal dataset for the years from 1991 to was created. The data used in this study refers to the coverage of deaths for both sexes estimated by RIPSA [2], vinculated to the Ministry of Health. This longitudinal dataset is the only one available.

Two types of nonlinear modeling were used to estimate the year of full coverage of deaths for Northeast States: Logistic Growth Model and Gompertz function. In addition, the Holt Exponential Smoothing Model was used, which presupposes linear growth trend of a series of data.

Logistic function [3]

$$Y = \frac{\alpha}{1 + e^{-\gamma(x-\beta)}}$$

where:

Y = coverage of deaths;

e = the natural logarithm base;

x = time in years of coverage of deaths;

α = the curve's maximum value (indicating the stabilization value of the dependent variable in relation to time);

β = the x-value of the sigmoid's midpoin (location parameter); and

γ = the steepness of the curve (curve growth rate measure).

α, β e γ are parameters, where $\alpha > 0$ e $\gamma > 0$.

Gompertz function [4]

$$Y = \alpha e^{-e^{\gamma(x-\beta)}}$$

Where, the meaning of each variable and parameter of the Gompertz function is the same, as specified for the Logistic function.

Holt Exponential Smoothing Model [5]

Holt (1957) extended simple exponential smoothing to allow forecasting of data with a trend. This method involves a forecast equation considering the level, trend and residual with zero mean and constant variance:

$Z_t = \mu_t + T_t + a_t, \qquad t = 1, \ldots, N,$

where:

μ_t denotes an estimate of the level of the series at time t;

T_t denotes an estimate of the trend of the series at time t;

a_t denotes the random error at time t.

The level and trend values of the series were estimated by

$\bar{Z}_t = AZ_t + (1 - A)(\hat{Z}_{t-1} + \hat{T}_{t-1}),\ 0 < A < 1,\ t = 2, \ldots, N,$

$\hat{T}_t = C(\bar{Z}_t - \bar{Z}_{t-1}) + (1 - C)\hat{T}_{t-1},\ 0 < C < 1,\ t = 2, \ldots, N,$

A and C are the smoothing constants. The prediction of future series values for this procedure is given by:

$\bar{Z}_t(h) = \bar{Z}_t + h\hat{T}_t, \forall h > 0$

That is, the forecast is made by adding to the basic value ($\bar{Z}_t$) the multiplicative trend by the number of steps ahead that one wishes to predict (h).

Diagnostic and residual measures

In non-linear regression, the analysis of the residuals of a model is done to check the plausibility of the assumptions involved [6]. The Shapiro-Wilk statistical test was used to verify the normality assumption. To measure the heteroscedasticity of the residues, the Breusch-Pagan test and the graphic inspection of the residues were used against the estimated values to examine whether the error variances are constant. The Durbin-Watson test was used to verify the existence of first order autocorrelation.

The Mean Square Error (MSE) was proposed as criterion for selecting the best model. The MSE is defined by the sum of the squares of the differences between estimated/predicted results and the observations [7].

The diagnostic measures were used for residue analysis, detection of outliers, influential points, and colinearity. In addition, tests based on statistical hypotheses were carried out to verify the suitability of the Logistic and Gompertz model adjustments [3,4].

In order to obtain the estimates from the application of the prediction methods and the error measures, the R-3.3.1 free-access software was

used.

Criteria for selection of full coverage of deaths

The year of optimal coverage was chosen for the first year whose estimate was greater than or equal to 99% or when the maximum inflection point of the model curve was reached.

Then, the criteria for selecting the range of forecast of full coverage of deaths were:

1 - When the estimates between the models did not exceed four years a range of forecast of full coverage using both values was adopted;

2 - In case the difference between forecasts was greater than four years, a four-year forecast interval was considered based on the model with the lowest MSE;

3 - The model with estimated full coverage below 2019 was discarded. In this case, a two year interval was considered based on the selected coverage.

3 Results and Discussion

Among the nine States that compose this region, coverage of deaths in 2011 ranged from 79 to 94%. In the beginning of the series, in 1991, the coverage ranged from 25 to 70%. According to Table 1 the deviations between the coverages with the use of the EQM showed that the Holt model had the best performance for five States and the Northeast as a whole.

Table 1: Mean Square Error of estimates with full coverage of deaths, according to the models by Brazilian Northeast States.

State/Region	Mean Square Error (MSE)		
	Logistic	Gompertz	Holt
Maranhão	52,28	58,44	29,37
Piauí	70,01	80,20	56,85
Ceará	17,82	19,91	16,49
Rio G. Norte	14,38	15,01	15,61
Paraíba	37,00	38,24	37,70
Pernambuco	17,53	18,01	13,14
Alagoas	41,97	43,48	46,04
Sergipe	10,38	11,01	29,03
Bahia	7,38	7,69	4,84
Nordeste	21,72	22,92	15,16

Note: The model with the lowest MSE is highlighted.

The Logistic model presented the smallest errors for three States. These States are highlighted.

The standardized residuals versus the adjusted values for the Northeast and all States indicated homogeneity of the variances that can be confirmed by the estimates of the Breusch-Pagan statistic test. In it, the null hypothesis that the residues were homocedastic was not rejected. Verifying the normality assumption the Shapiro-Wilk test with p-values $\geq$ 0.05 for the Logistic Model and the Gompertz model did not reject the null hypothesis, indicating that the residues followed a normal distribution.

The Durbin-Watson test indicated that the residues were independent as desired. According to the estimates of the p-value of the Dickey-Fuller Test, the time series discussed were stationary over time with a significance level of 5%. The Wilcoxon test pointed to the presence of increasing trend and almost stationary behavior in the series of data for all the regions, satisfying the requirements for the applicability of the Holt model.

Figure 1 shows the time series of observed and estimated death coverage for the Northeast and the adjustment curves for each model adopted.

There is no technique of correction of the coverage of deaths free of assumptions, which are hardly fulfilled for any region of the world, and Brazil. In this way, errors are allowed in any estimate. The greatest errors in RIPSA's estimates [2] are related to the period from 1991 to 1999 that made use of the projections of deaths which are part of the population projections elaborated by IBGE [1]. From 2000 onwards, the correction factors of the Active Search Project from the Ministry of Health[8] were used which are considered more accurate. However, the change in coverage levels from 1999 to 2000 was not only due to a change in methodology in its estimates, but also to other factors.

The evolution of coverage levels indicates that the year 2000 can be considered as a milestone in time, after which an unprecedented rate of increase in the history of death coverage in the Brazilian Northeast was triggered. The poor quality of coverage before 2000 may be due to the enormous political and economic crisis that directly affected investments in health and basic care in Brazil [9] reinforced by the precarious training of health professionals regarding data collection and manipulation, and non-standardization of these tasks, which led to poor quality and unreliability of information [10,11,12].

The main factors that contributed to the great increase in coverage in the Northeastern States since the year 2000 are the technological development of information, which has enabled a considerable leap in quality in the collection and processing of data.

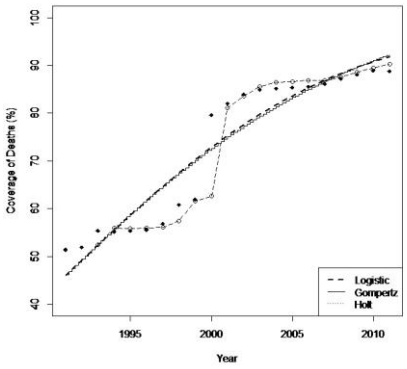

Figure 1: Modeling of death coverage according to the models, Northeast of Brazil

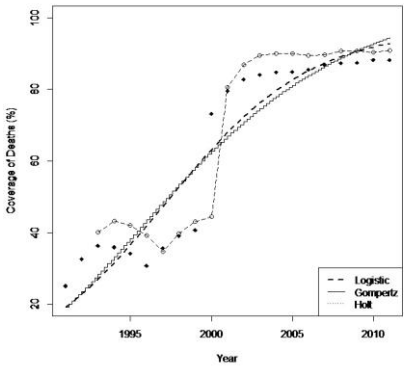

Figure 2: Modeling of death coverage according to the models State of Piauí

These actions were reinforced by the expansion of coverage of health services through programs such as the Family Health Strategy, and monitoring of the Death Verification System (SVO), and increased awareness, supervision and vigilance by physicians. The significant improvement in the quality of death records from the Mortality Information System of the Ministry of Health can be further credited to the addition of the hospitals in the collection of data, previously collected only in civil registries offices [12,13].

According to Figure 1 a better smoothing is observed for the Holt model, since the Logistic model and the Gompertz model did not show any differences in plotting the curve. This pattern of models for the Northeast was practically the same observed for States, with small variations in the pace for some States (not shown).

Estimates of Northeast coverage up to the year 1999 showed a steady but fluctuating increase, with a sharp fall in the pace between 1999 and 2000. Then, the rate of increase continues, but in a slower way reaching almost constant behavior at the end of the series. Two trends are evident, before and after this break. Prior to 2000, the pace of increase was lower than the second, for almost all States, and the Northeast as a whole.

Because the Gompertz model had a very similar behavior to the Logistic model (Figure 1) and provided the worst accuracy errors for most States (Table 1), it was discarded as a predictive model.

Table 2 shows the projections of the years when the full coverage of deaths for the Northeast and States will be reached, using the Logistic and Holt's model. The final estimates are presented in forecast intervals, according to the established criteria.

Table 2: Interval of prediction of the year with full coverage of deaths by models, according to Brazilian Northeast States.

State/ Region	Model		Model w/lowest MSE	Criteria	Interval of prediction
	Logistic	Holt			
Maranhão	2030*	2028	Holt	1	2028-2030
Piauí	2032*	2016	Holt	**	2022-2026
Ceará	2024*	2023	Holt	1	2023-2024
Rio G. Norte	2025*	2021	Logístico	1	2021-2025
Paraíba	2017	2020	Logístico	3	2020-2022
Pernambuco	2020	2023	Holt	1	2020-2023
Alagoas	2019	2018	Logístico	3	2019-2021
Sergipe	2026*	2022	Logístico	1	2022-2026
Bahia	2030	2023	Holt	2	2023-2027
Northeast	2035	2021	Holt	2	2021-2025

* Inflection point of the curve below 100%.
** An interval of two years for plus and minus was considered based on the mean of the two predictions models (2024).

It was considered that maximum amplitude of four years in the forecast of the full coverage to be reached by Northeast States is a reasonable variation in the results generated by the models.

Attention is drawn to the fact that the models captured the behavior of the coverage of deaths of a historical series, and that they are mathematical. Although the coverage of deaths in the past is a reflection of the conditions of life in general [10,11,12] one may not be assured that living conditions will be maintained in the future, and that they reproduce a pace of evolution of the past. Thus, the forecast interval seeks to cover non-measurable constraints, not captured by a mathematical model.

4 Conclusions

In view of the established criteria, in general, the Holt model performed better (less deviations in the coverage series) by adhering more to the behavior of the past coverage series.

Obviously, the results should be viewed with caution, since the errors inherent in any prediction must be taken into account. It should be noted that in order to verify the suitability of the models, it is necessary to comply with certain assumptions. One of them referred to the number of points (years) available in the time series, restricted to 21 points. But they are the only ones available in the literature. This restriction may have prevented full use of the application of the models, which should be considered as indicators of the evolution of death coverage.

The final estimates showed three different groups regarding the universalization of coverage of deaths: Alagoas, Paraíba and Pernambuco (2019-2023); these States would be the first to reach full coverage of deaths regarding data quality. In a more distant position were Maranhão and Bahia (2023-2030). And, in an intermediate position, Ceará, Rio Grande do Norte, Sergipe and Piauí (2021-2026). It is estimated that for the Northeast the full coverage of deaths will be reached around 2021-2025.

However, it must be acknowledged that, like any scenario, this outline reflects a possibility considered plausible and that only the future can confirm these scenarios. Nevertheless, it is expected that these scenarios may contribute to the planning strategies, and to the evaluation of managers regarding the actions and policies to be implemented on the performance of death statistics in the Northeast and in the Country.

References

1. IBGE. Diretoria de Pesquisas (DPE). Coordenação de População e Indicadores Sociais (COPIS). Projections of population of Brazil, large regions and units of Federation, by sex and age, for the period 1991-2030. Rio de Janeiro 2005.
2. Rede Interagencial de Informações para a Saúde no Brasil. Ripsa IDB 2012. Available at: http://tabnet.datasus.gov.br/cgi/idb2012/a1801b.htm. Accessed in: Jun 25, 2016).
3. Bezerra J. Population Ecology: The logistic curve and population growth. NEPAM - UNICAMP, Campinas, SP, 2008. p. 1-18.
4. Souza VJ, Martinez EZ, Nunes AA. Gompertz Growth Curves for the Follow-up of High-Risk Children. Rev Bras. Biom. 2010; 28:39-58.
5. Moretin PA, Toloi CMC. Time series analysis. 2nd ed. São Paulo: Blucher; 2006.
6. Thode HC. Testing for normality. New York: Marcel Dekker; 2002.
7. Keyfitz N. The limits of populations forecasting. Population and Development Review 1981; 8:579-93.
8. Szwarcwald CL, Neto OLM, Frias PG, Junior PRBS, Escalante JC, Lima RB e Viola RC. Active search for deaths and births in the Northeast and in the Legal Amazon: Estimation of coverage of SIM and SINASC in Brazilian municipalities. In: Ministry of Health, organizer. Health Brazil 2010: an analysis of the health situation and selected evidence of impact of health surveillance actions.Brasília: Ministério da Saúde; 2011. p. 79-98.
9. Polignano MV. History of health policies in Brazil - a short review. Ministry of Health of Mato Grosso. 2004. p. 1-35. Available at: http://www.saude.mt.gov.br/ces/arquivo/2165/books (accessed Jan 25, 2016).
10. Paes NA. Quality of death statistics for unknown causes in Brazilian States. Rev Saúde Pública 2007; 41: 436-45.
11. Mello Jorge MHP, Laurenti R, Gotlieb SLD. An analysis of the quality of Brazilian vital statistics: the experience of SIM and SINASC implementation. Cienc Saúde Coletiva 2007; 12: 643-54.
12. Mello Jorge MHP, Laurenti R, Gotlieb SLD. Evaluation of health information systems in Brazil. Cad Saúde Coletiva 2010; 18: 07-18.
13. Lima, EMC, Queiroz BL. The evolution of the mortality registry system in Brazil: changes in the mortality profile, coverage of the death registry and the ill-defined causes of death. Cad Saúde Pública 2014; 30: 1721-30.

ESTIMATION OF A TWO-VARIABLE SECOND DEGREE POLYNOMIAL VIA SAMPLING

Papatsouma Ioanna, Farmakis Nikolaos, Ketzaki Eleni

Department of Mathematics

Aristotle University of Thessaloniki

54124, Thessaloniki, Greece

ioannapapatsouma@gmail.com, farmakis@math.auth.gr, eketzaki@yahoo.gr

ABSTRACT

In various fields of environmental and agriculture sciences the estimation of a two-variable second degree polynomial coefficients via sampling is of major importance, as it gives very useful information. In this paper, we propose a very simple and very low budget systematic sampling plan for the estimation of the coefficients A, B, C, D, E and H of the polynomial $f(x,y) = (Ax^2 + By^2 + Cxy + Dx + Ey + H)^{-1}$, which is sometimes found to be a probability density function. The above polynomial is defined on a domain $D = [a, b]$ x $[c, d]$, which can be represented by the domain $D = [0, 1]$ x $[0,1]$ for convenience. Numerical methods, such as Simpson's rule, are applied. The comparison between means of both estimated and theoretic functions is used to confirm the accuracy of the results. The stability of the numerical methods allows us to get results with very good accuracy for small sample sizes. Illustrative examples are given.

Keywords: systematic sampling, polynomial, coefficients, Simpson

MSC2010 Classification*:* 62D05, 62E17

1. Introduction

All across the world, people are facing a wealth of environmental problems everyday. Point-source pollutants have a major impact on environmental concentrations on a local scale and also contribute to the concentrations on a larger regional scale [1]. In accordance with the U.S. Environmental Protection Agency (EPA), point-source pollution is defined as "any single identifiable source of pollution from which pollutants are discharged, such as a pipe, ditch, ship or factory smokestack" [2]. Environmental authorities are concerned with locating and punishing violations of environmental protection regulations, but even if laws are followed, these types of practices occurred in the past before the laws were enacted and the pollutants are still around [3].

From the mathematical point of view, these sources are called point-sources because, in mathematical modeling, they can be approximated as a mathematical point to simplify analysis.

Let us consider the bivariate function:

$$f(x,y)=\left(Ax^2+By^2+Cxy+Dx+Ey+H\right)^{-1} \quad (1)$$

defined on a domain $D = [a, b] \times [c, d]$. The coefficient H is equal to the inverse value of the function f when both x and y are zero, $H^{-1} = f(0,0)$, and the rest coefficients are estimated as described in Section 2.

2. Proposed Method

We will describe a method to estimate the coefficients A, B, C, D and E of the function given in (1), where the studied area is $D = [0, 1] \times [0, 1]$. The proposed method consists of the following steps:

Step 1. We conduct systematic sampling [4] by taking samples of linear subspaces of R^2.

Step 2. In each sampling space (Step 1), we integrate the function given in (1) with respect to x or y, for x or y between 0 and 1.

Step 3. We apply the Simpson's rule of Integration [5] to three points which are equally spaced in the interval $[0, 1]$, $0, 0.5$ and 1.

Step 4. We equate each integration result (Step 2) with its approximation (Step 3).

Step 5. We solve the system derived from Step 4.

2.1 First Restriction

Let us consider that $y = 0$:

$$f_1(x)=f(x,0)=\left(Ax^2+Dx+H\right)^{-1} \quad (2)$$

or

$$Ax^2+Dx+H=1/f_1(x) \quad (3)$$

The sampling is done on the x-axis of the given field D (Figure 1a). We integrate the equation (3) with respect to x, for x between 0 and 1 and we get:

$$I_1=\left(2A+3D+6H\right)/6 \quad (4)$$

By applying Simpson's rule of Integration to the three points which are equally spaced in the interval $[0,1]$ $x = 0, 0.5$ and 1 we get:

$$I_1=\left(1/f_1(0)+4/f_1(0.5)+1/f_1(1)\right)/6=1/6\left(\sum 1/f_1\right) \quad (5)$$

If we then equate (4) and (5), we get the so-called $\tilde{g}_1$ estimator:

$$6I_1 = 2A + 3D + 6H = \tilde{g}_1 = 1/f_1(0) + 4/f_1(0.5) + 1/f_1(1) = \sum 1/f_1 \quad (6)$$

2.2 Second Restriction

Let us consider that $x = 0$:

$$f_2(y) = f(0,y) = \left(By^2 + Ey + H\right)^{-1} \quad (7)$$

or

$$By^2 + Ey + H = 1/f_2(y) \quad (8)$$

The sampling is done on the y-axis of the given field D (Figure 1b). We integrate the equation (8) with respect to y, for y between 0 and 1 and we get:

$$I_2 = (2B + 3E + 6H)/6 \quad (9)$$

By applying Simpson's rule of Integration to the three points which are equally spaced in the interval [0,1] we get:

$$I_2 = \left(1/f_2(0) + 4/f_2(0.5) + 1/f_2(1)\right)/6 = 1/6\left(\sum 1/f_2\right) \quad (10)$$

If we then equate (9) and (10), we get the so-called $\tilde{g}_2$ estimator:

$$6I_2 = 2B + 3E + 6H = \tilde{g}_2 = 1/f_2(0) + 4/f_2(0.5) + 1/f_2(1) = \sum 1/f_2 \quad (11)$$

2.3 Third Restriction

Let us consider that $x = y$:

$$f_3(x) = f(x,x) = \left((A + B + C)x^2 + (D + E)x + H\right)^{-1} \quad (12)$$

or

$$(A + B + C)x^2 + (D + E)x + H = 1/f_3(x) \quad (13)$$

The sampling is done on the diagonal line $y = x$ of the given field D (Figure 1c). We integrate the equation (13) with respect to x, for x between 0 and 1, and we get:

$$I_3 = \left(2(A + B + C) + 3(D + E) + 6H\right)/6 \quad (14)$$

By applying Simpson's rule of Integration to the three points which are equally spaced in the interval [0,1] we get:

$$I_3 = \left(1/f_3(0) + 4/f_3(0.5) + 1/f_3(1)\right)/6 = 1/6\left(\sum 1/f_3\right) \quad (15)$$

If we then equate (14) and (15), we get the so-called $\tilde{g}_3$ estimator:

$$6I_3 = 2(A + B + C) + 3(D + E) + 6H = \tilde{g}_3 = 1/f_3(0) + 4/f_3(0.5) + 1/f_3(1) = \sum 1/f_3 \quad (16)$$

2.4 Fourth Restriction

Let us consider that $y = x/2$:

$$f_4(x) = f(x, x/2) = \left((A + B/4 + C/2)x^2 + (D + E/2)x + H\right)^{-1} \quad (17)$$

or

$$(A + B/4 + C/2)x^2 + (D + E/2)x + H = 1/f_4(x) \quad (18)$$

The sampling is done on the diagonal line $y = x/2$ of the given field D (Figure 1d). We integrate the equation (18) with respect to x, for x between 0 and 1, and we get:

$$I_4 = (4A + B + 2C + 6D + 3E + 12H)/12 \quad (19)$$

By applying Simpson's rule of Integration to the three points which are equally spaced in the interval $[0,1]$ we get:

$$I_4 = \left(1/f_4(0) + 4/f_4(0.5) + 1/f_4(1)\right)/6 = 1/6\left(\sum 1/f_4\right) \quad (20)$$

If we then equate (19) and (20), we get the so-called $\tilde{g}_4$ estimator multiplied by 2:

$$12I_4 = 4A + B + 2C + 6D + 3E + 12H = 2\tilde{g}_4 = 2/f_4(0) + 8/f_4(0.5) + 2/f_4(1) = \sum 1/f_4 \quad (21)$$

2.5 Fifth Restriction

Let us consider that $x = y/2$:

$$f_5(y) = f(y/2, y) = \left((A/4 + B + C/2)y^2 + (D/2 + E)y + H\right)^{-1} \quad (22)$$

or

$$(A/4 + B + C/2)y^2 + (D/2 + E)y + H = 1/f_5(y) \quad (23)$$

The sampling is done on the line $y = 2x$ of the given field D (Figure 1e). We integrate the equation (23) with respect to y, for y between 0 and 1, and we get:

$$I_5 = (A + 4B + 2C + 3D + 6E + 12H)/12 \quad (24)$$

By applying Simpson's rule of Integration to the three points which are equally spaced in the interval $[0,1]$ we get:

$$I_5 = \left(1/f_5(0) + 4/f_5(0.5) + 1/f_5(1)\right)/6 = 1/6\left(\sum 1/f_5\right) \quad (25)$$

If we then equate (24) and (25), we get the so-called $\tilde{g}_5$ estimator multiplied by 2:

$$12I_5 = A + 4B + 2C + 3D + 6E + 12H = 2\tilde{g}_5 = 2/f_5(0) + 8/f_5(0.5) + 2/f_5(1) = \sum 1/f_5 \quad (26)$$

2.6 Coefficient Estimates

The following figure illustrates the restrictions on the use of the proposed method and summarizes the sampling spaces (**bold line**) using systematic sampling.

Figure 1. Restrictions on the use of the proposed method

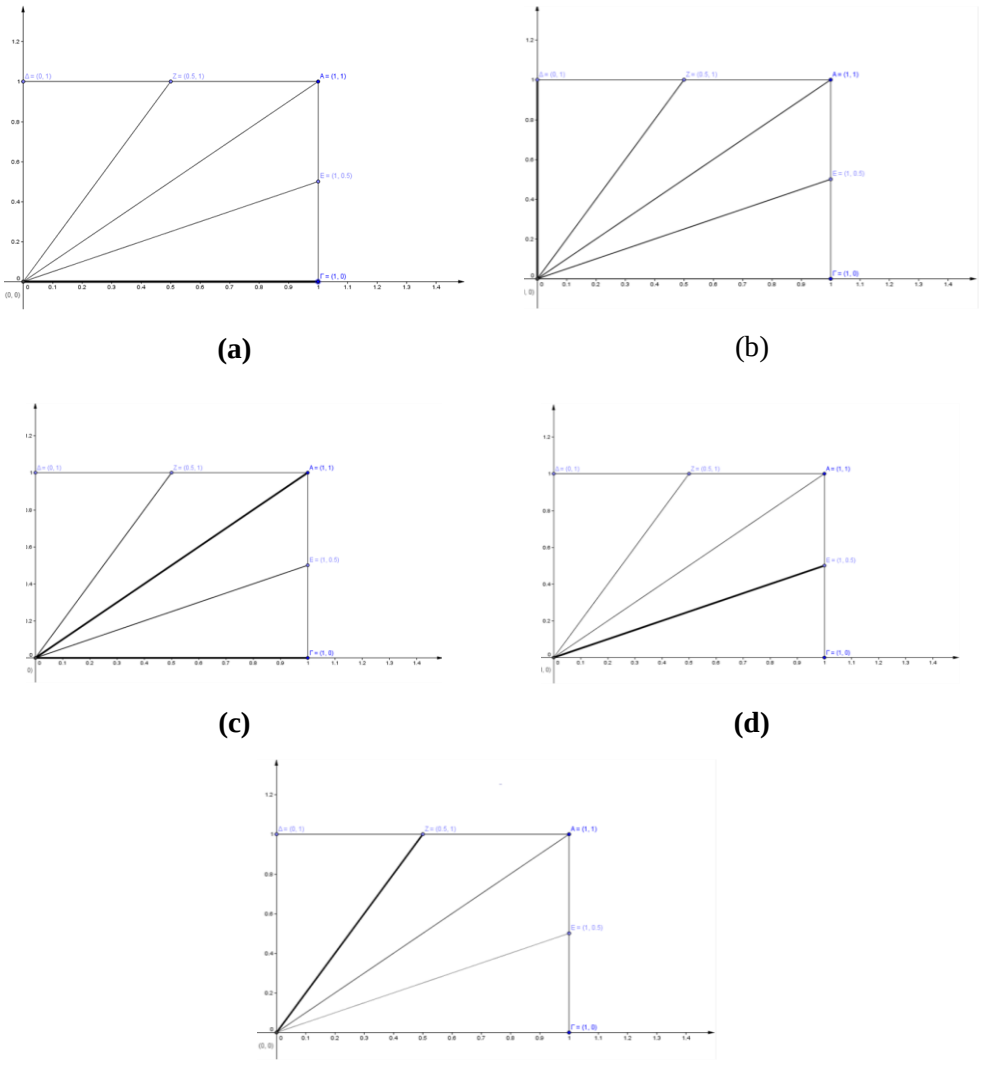

(a) (b)

(c) **(d)**

(e)

By solving the following system derived from (6), (11), (16), (21) and (26):

$$\begin{bmatrix} 2 & 0 & 0 & 3 & 0 & 6 \\ 0 & 2 & 0 & 0 & 3 & 6 \\ 2 & 2 & 2 & 3 & 3 & 6 \\ 4 & 1 & 2 & 6 & 3 & 12 \\ 1 & 4 & 2 & 3 & 6 & 12 \end{bmatrix} \cdot \begin{bmatrix} A \\ B \\ C \\ D \\ E \\ H \end{bmatrix} = \begin{bmatrix} \tilde{g}_1 \\ \tilde{g}_2 \\ \tilde{g}_3 \\ 2\tilde{g}_4 \\ 2\tilde{g}_5 \end{bmatrix} \tag{27}$$

we estimate the coefficients of the bivariate function as follows:

$$
\begin{aligned}
A &= \tilde{g}_2 + \tilde{g}_3 - 2\tilde{g}_5 \\
B &= \tilde{g}_1 + \tilde{g}_3 - 2\tilde{g}_4 \\
C &= 3H + \left(\tilde{g}_3 - \tilde{g}_2 - \tilde{g}_1\right)/2 \\
D &= -2H + \left(\tilde{g}_1 - 2\tilde{g}_2 - 2\tilde{g}_3 + 4\tilde{g}_5\right)/3 \\
E &= -2H - \left(2\tilde{g}_1 - \tilde{g}_2 + 2\tilde{g}_3 - 4\tilde{g}_4\right)/3
\end{aligned}
\tag{28}
$$

where $H = f^{-1}(0,0)$, and the formula for the $\tilde{g}_i$ estimators is given by:

$$
\tilde{g}_i = \begin{cases} \sum 1/f_i, & if\ i = 1,2,3 \\ (\sum 1/f_i)/2, & if\ i = 4,5 \end{cases}
\tag{29}
$$

3. Experimental Approaches

3.1 Experiment A

Five different three-point measurements of pollutant concentration over a field have been recorded. The inverse values of a function measuring pollutant concentration obeying the five restrictions described are presented in the Table 1.

The last column includes the $\tilde{g}_i$ estimators, $i = 1,2,3,4,5$ derived from the experimental measurements.

Table 1. Pollutant concentration

Points			$\tilde{g}$
0	**0.5**	**1**	
18	16.75	17	102
18	18.25	22	113
18	17.5	23	111
18	16.6875	18.25	103
18	17.6875	21.75	110.5

It can be easily observed that the coefficient H is equal to 18. The rest coefficients are estimated as follows:

$$
\begin{aligned}
A &= \tilde{g}_2 + \tilde{g}_3 - 2\tilde{g}_5 = 113 + 111 - 221 = 3 \\
B &= \tilde{g}_1 + \tilde{g}_3 - 2\tilde{g}_4 = 102 + 111 - 206 = 7 \\
C &= 3H + \left(\tilde{g}_3 - \tilde{g}_2 - \tilde{g}_1\right)/2 = 54 + \left(111 - 113 - 102\right)/2 = 2 \\
D &= -2H + \left(\tilde{g}_1 - 2\tilde{g}_2 - 2\tilde{g}_3 + 4\tilde{g}_5\right)/3 = -36 + \left(102 - 226 - 222 + 442\right)/3 = -4 \\
E &= -2H - \left(2\tilde{g}_1 - \tilde{g}_2 + 2\tilde{g}_3 - 4\tilde{g}_4\right)/3 = -36 - \left(204 - 113 + 222 - 412\right)/3 = -3
\end{aligned}
\tag{30}
$$

The requested function is:

$$f(x,y)=\left(3x^2+7y^2+2xy-4x-3y+18\right)^{-1} \tag{31}$$

We use statistical software to investigate the above function's local extrema. The denominator of the function has a local minimum at point $(5/8, 1/8)$, which equals to $265/16 = 16.5625$. This implies that the pollutant concentration function reaches its maximum value at the same point, which equals to $f(5/8, 1/8) = 16/265 = 0.0604$ (accurate to four decimal places). The following figure confirms our analysis.

Figure 2. Point-source pollutant

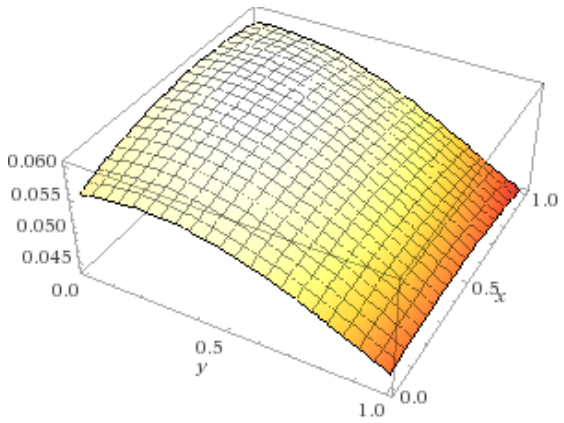

3.2 Experiment B

Five different three-point measurements of intensity of radiation at a height of 3 meters over a field have been recorded. The inverse values of a function measuring the intensity of radiation obeying the five restrictions described are presented in Table 2.

The last column includes the $\tilde{g}_i$ estimators, $i = 1, 2, 3, 4, 5$ derived from the experimental measurements.

Table 2. Intensity of radiation

Points			$\tilde{g}$
0	**0.5**	**1**	
11	10	11	62
11	10.75	12	66
11	9	9	56
11	9.3125	9.25	57.5
11	9.625	9.5	59

It can be easily observed that the coefficient H is equal to 11. The rest coefficients are estimated as follows:

$$
\begin{aligned}
A &= \tilde{g}_2 + \tilde{g}_3 - 2\tilde{g}_5 = 113 + 111 - 221 = 3 \\
B &= \tilde{g}_1 + \tilde{g}_3 - 2\tilde{g}_4 = 102 + 111 - 206 = 7 \\
C &= 3H + \left(\tilde{g}_3 - \tilde{g}_2 - \tilde{g}_1\right)/2 = 33 + \left(111 - 113 - 102\right)/2 = 2 \\
D &= -2H + \left(\tilde{g}_1 - 2\tilde{g}_2 - 2\tilde{g}_3 + 4\tilde{g}_5\right)/3 = -36 + \left(102 - 226 - 222 + 442\right)/3 = -4 \\
E &= -2H - \left(2\tilde{g}_1 - \tilde{g}_2 + 2\tilde{g}_3 - 4\tilde{g}_4\right)/3 = -36 - \left(204 - 113 + 222 - 412\right)/3 = -3
\end{aligned}
\tag{32}
$$

The requested function is:

$$
f\left(x,y\right) = \left(3x^2 + 7y^2 + 2xy - 4x - 3y + 11\right)^{-1} \tag{33}
$$

We use statistical software to investigate the above function's local extrema. The denominator of the function has a local minimum at point $(30/39, 28/39)$, which equals to $341/39 = 8.7436$. In other words, the pollutant concentration function, given in (33), reaches its maximum value at the same point, which equals to $f(30/39, 28/39) = 39/341 = 0.1144$ (accurate to four decimal places). The following figure confirms our analysis.

Figure 3. Point-source of radiation

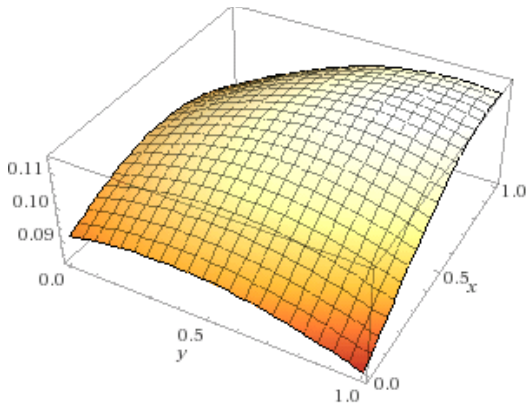

4. Conclusions

In this paper, we have proposed a simple and easy-to-remember method to estimate the coefficients of a two variable second degree polynomial via sampling. We have used the systematic sampling to define the areas of sampling and the Simpson's rule of Integration to approximate definite integrals on the domain $D = [0,1]$x$[0,1]$. The proposed method can be characterized as a low-budget sampling, because of the small sample size. It is advantageous because it can be applied to detect point-source pollutants and point-source of radiation and thus determine risk assessment in public health. Finally, the stability of the numerical methods allows us to get accurate results.

REFERENCES

[1] van Leeuwen, C.J. (2010). *Risk Assessment of Chemicals: An Introduction*, 2nd Ed., Dordrecht, The Netherlands: Springer.

[2] Hill, M.S. (1997). *Understanding Environmental Pollution*. Cambridge, UK: Cambridge University Press.

[3] Osborne, F.H. *Kean University Continuing Education. Implementing the Science Standards K-4. Point Source and Non-Point-Source Pollution.* Retrieved from http://www.kean.edu/~fosborne/resources/ex12j.htm (last assessed on July 20, 2017)

[4] Farmakis, N. (2016). *Introduction to Sampling*, Kyriakidis Bros - Publications SA (in Greek).

[5] Davis, P.J., Rabinowitz, P. (2007). *Methods of Numerical Integration*, 2nd Ed., Dover Publications.

Air pollution variability within an alpine Italian province

Giuliana Passamani[1], Matteo Tomaselli[2]

[1] Department of Economics and Management, Via Inama 5, University of Trento, Trento, Italy
(E-mail: giuliana.passamani@unitn.it)
[2] PhD in Economics and Management, School of Social Sciences, Via Verdi 26, University of Trento, Trento, Italy
(E-mail: matteo.tomaselli.1@unitn.it)

Abstract. This paper aims to analyse intra e inter-annual variability in air pollution concentrations in the Italian Province of Trento, once taking into account meteorological conditions. The main purpose is the proposal of an analytical procedure that, moving from the statistical properties of the observed time-series for each of the seven monitoring sites, controls for that part of air pollution that is explained by the meteorological variables, and then moves to analyse the unexplained part mainly due to human behaviour.
Keywords: Air pollution, Principal component factor analysis, Panel data models.

1 Introduction

As it is generally acknowledged that greenhouse gases and atmospheric aerosols represent a major causal force of climate change and that they may interact physically and chemically in the atmosphere and make it much more difficult to forecast the future variations in climate and in global warming, we can understand the importance of empirical modelling the time-series data measuring their levels. The question is, therefore, to understand the temporal evolution of the gaseous and aerosol pollutants, how they interact among themselves and with atmospheric factors. Air pollution undoubtedly affects also human health, especially in large cities, and a vast specialized literature has primary focused on this issue (see for instance Jerrett *et al.*[6], and Heines *et al.*[5]). From both these perspectives, a better comprehension of the dynamics of air pollutants and of the impact of meteorological variables have on them, possibly using stochastic models that can then be used for simulation, can surely help in deciding future policy interventions aiming to reduce the pollution levels and to improve the quality of air.
This work analyses pollution at local level by also considering meteorological factors such as temperature, wind and rain. In particular, our data set is made up of daily time series observations on the main pollutants and meteorological variables of seven monitoring sites within the alpine province of Trento. It is an Italian province located in the North-eastern part of Italy, not far from Austria. Mainly rural, it is a mountainous area characterised by valleys, rivers and lakes of different dimensions. It is also intersected by two important roads of

communication: the Brenner motorway, that crosses the province from North to South in the direction of Austria, and the Valsugana highway, that links Trento to the Eastern part of Italy. The largest towns are located along the Brenner motorway and in the Valsugana valley. Though the air quality of the province may be considered overall enough good, it is indeed affected by important sources of pollution, above all in the valleys, where much of the population lives[1]. Therefore, pollution has a direct impact on the lives of the majority of the inhabitants of the area. Understanding pollution behaviour may thus be the first step towards the adoption of appropriate policy measures to limit pollution and its negative consequences on health.

The rest of the paper is organised as follows. First, we describe our data set and the air pollution levels for each monitoring site. Second, for each of them we compute the pollution factor, on which we then base our empirical analysis. The latter is divided into two parts: in the first, using an estimated panel data model, we remove the part explained by the weather variables from the pollution factors, while in the second part we study how the three main pollutants affect the unexplained part of the pollution factors. On this component, in fact, policy makers should focus.

2 Data set description and qualitative analysis

Our analysis is based on the data on air pollutants and meteorological variables collected and provided by the Trentino Environmental Protection Agency (APPA). Due to the availability of data, only two years, 2014 and 2015, and seven monitoring sites within the province of Trento are considered. Two sites, Trento PSC (Trento 1 henceforth) and Rovereto, are located in the two largest cities and are thus referred to as urban and residential areas. The two sub-urban sites of Borgo Valsugana and Riva del Garda are located in two middle-size towns, but the climates are quite different as the latter is mitigated by the influence of the Garda Lake, the largest Italian lake. Moreover, it should be noticed that Borgo Valsugana is not far from a highway characterized by heavy traffic levels. On the other hand, the two monitoring sites of Monte Gaza and Piana Rotaliana are both referred to as rural areas: in particular, the former is a mountain site located 1601 meters above the sea level, far from any air pollution source, whose data are used as a comparative measure for the other sites, while the latter is located in the countryside. Finally, the monitoring site of Trento VBZ (Trento 2 henceforth) is an urban area situated near a heavy traffic road in the commercial area of Trento, and is specifically devoted to monitor car traffic.

The diversity of the locations of the seven monitoring sites directly reflects into the distributions of the three pollutants that we consider: PM_{10}, NO_x, and O_3, whose distributions are synthetized in Fig. 1 and Table 1. The first picture refers

[1]In 2014, approximately 82% of the population lived below 750 meters on the sea level. See: https://www.ufficiostampa.provincia.tn.it/Comunicati/CONOSCERE-IL-TRENTINO-DISPONIBILE-LA-TERZA-EDIZIONE-DELLA-PUBBLICAZIONE-DEL-SERVIZIO-STATISTICA

to PM_{10}, the particles with a diameter between 2.5 and 10 micrometres, which are produced by cars engines and other combustion processes. As can be seen from Table 1, according to expectations, the lowest average level is observed for Monte Gaza, the mountain area, and the highest average level is observed for Trento 2, the heavy traffic area. However, an average level as high as Trento 2 is also observed for Borgo Valsugana. The other monitoring sites show intermediate comparable levels of PM_{10}. Therefore, it is straightforward to derive a raw relationship between the locations and the PM_{10} levels: the higher the traffic levels, the higher the PM_{10} levels.

As can also be seen in Fig. 1, the differences in the distributions are more pronounced for NO_x (nitrogen oxides, given by the combination of NO and NO_2), mainly originated by combustion processes. The most polluted area is Trento 2 and, as before, the least polluted is Monte Gaza. Low average levels of NO_x are also registered for Piana Rotaliana, Rovereto, and Riva del Garda, while Trento 1 and Borgo Valsugana show slightly higher levels.

Finally, we consider O_3 (ozone), a pollutant that is originated by the action of daylight UV rays on the other pollutants, especially those produced during combustion processes. The pertaining boxplots show comparable distributions between the monitoring sites[2], with the only exception of Monte Gaza: this site is characterized by somewhat higher levels of O_3. This finding may appear surprising, but in fact the position of this site implies high solar radiation levels throughout the year, which are the primary responsible for the generation of the ozone and hence for the unusual O_3 levels (for more details, see the Air Quality Reports, APPA[1], [2]). A similar reasoning can also explain the higher levels observed for Riva del Garda and Piana Rotaliana.

An analysis[3] using the inverse distance weight spatial interpolations for the three pollutants and depicting them in a spatial form where darker colors indicate relatively higher pollution levels, confirms the results emerged from the boxplots. Since Monte Gaza's observations are clear outliers with respect to the observations of the other sites, the spatial interpolation was repeated by excluding it: the new spatial interpolations show that, for what concern PM_{10} and NO_x, the rural and sub-urban areas are effectively less polluted than the traffic and urban areas (with the already recognized exception of Borgo Valsugana for the PM_{10} levels), while for the O_3 level the exposure to solar radiation is far more relevant than the distinction between urban or rural location: the rural area of Piana Rotaliana and the suburban area of Riva del Garda are more polluted than the urban area of Trento 1.

Finally, Fig. 2 shows the dynamics of the time series and their trend[4] for each monitoring sites. Beyond the three air pollutants, we depicted the dynamics of the daily average weather variables that we will consider below: temperature (°C), rain (mm), solar radiation (W/m^2), humidity (%), dew point (°C), wind

[2] O_3 data are not available for Trento 2.

[3] The results and the graphs of the analysis are available upon request.

[4] The trend was obtained by applying the Hodrick and Prescott filter to each time series.

run[5] (km), and atmospheric pressure (bar). With the understandable exception of rain, that depends on local atmosphere phenomena above all in summer, all the variables exhibit comparable seasonal dynamics. Moreover, as expected, O_3 shows a behaviour that follows the dynamics of the temperature and of the solar radiation, in contrast with the behaviour of PM_{10} and NO_x.
With these time series, we constructed a slightly unbalanced panel data set including the daily average data for each monitoring site in which the periods of few missing observations were filled through linear interpolation (longer periods of missing data were left blank). We also excluded the last five days of observations for 2015 since data were not available for all the monitoring sites. This data set represents the starting point of the following econometric analysis.

3 Unobserved air pollution factors

3.1 Methodology: PCFA

In order to compare pollution levels across the different monitoring sites using panel data analysis, we need a variable that summarizes the three pollutants in an indicator. To this purpose it is possible to adopt a methodology called Principal Component Factor Analysis (PCFA). The PCFA extracts meaningful linear combinations by decomposing the correlation matrix of a set of observed variables that may jointly explain a certain phenomenon, and provides the so-called *common factors* and the corresponding *factor loadings.* The common factors are thus latent variables which are described through their relationship with the variables of interest, while the factor loadings show the weight of each variable in explaining the factors. In details, given the observation on the *j*-th variable relative to the *i*-th unit, y_{ij}, the common factors z_{iq} relative to the same *i*-th unit contribute to explain it through the following relationship:

(1) $$y_{ij} = z_{i1}\lambda_{1j} + z_{i2}\lambda_{2j} + \ldots + z_{iq}\lambda_{qj} + u_{ij}$$

where λ_{ij} is the factor loading, and u_{ij} is a unique factor proper of the *j*-th variable.
The appropriate number q of unobserved factors, smaller than the number of observed variables, depends on their observed correlations, and can be chosen either on the basis of the eigenvalues obtained from the decomposition of the correlation matrix, or on the basis of the percentage of explained variance.

3.2 Pollution factors

To avoid misleading results determined by "extreme" locations, two monitoring sites were excluded from the analysis: Monte Gaza and Trento 2, the first because located in a mountainous position, and the second because it is devoted to the study of traffic pollution and of the specific pollutant CO which is not recorded at the other sites. For the remaining sites, the three considered air

[5] Wind speed (km/h) has been excluded because it is strongly correlated with wind run.

pollutants display well determined patterns (see Section 2) and strong correlations coefficients. PM_{10} and NO_X are strongly and positively correlated for all the sites, as NO_X and O_3 are strongly but negatively correlated. PM_{10} and O_3 are also negatively correlated for each site, but the magnitude of the coefficient is lower (Table 2).
Given the small number of observed pollutants and their correlation structure, it is reasonable to study pollution as a single latent variable, and thus we estimate one factor z_{it} and consider it as an indicator of pollution level for each monitoring site as suggested by Passamani and Masotti[7]. By employing the PCFA discussed above, the indicator "summarises a complex situation in a single variable whose evolution can be compared in time and in space" (Passamani and Masotti[7], p. 787)[6]. The dynamics of the *pollution factor*, or *PF*, for each site is shown in Fig. 3.

4 First step: panel data analysis

The following two-steps analysis aims, first, to study the impact of the weather variables, and second, to analyse the part of these factors that remains "unexplained".
A first aspect characterising our data is seasonality, which affects both the pollution factors and the meteorological variables. Seasonality directly implies heteroskedasticity. From Fig. 2 and Fig. 3 it is evident that the winter season is characterised by higher volatility than the summer season. The heating systems and the higher usage of cars in cold days are probably the primary responsible for this phenomenon.
Another aspect that should be included into the analysis is the intrinsic intertemporal nature of pollution: today's levels pollutant levels directly affect tomorrow's levels and are determined by yesterday's levels. Therefore, a dynamic approach is essential to study the evolution of the pollution factor.
Finally, a last aspect that affects our data set and that has already emerged above is undoubtedly heterogeneity. The monitoring sites are remarkably different in terms of location, and this is responsible for the different levels observed throughout the period of analysis. This fact clearly emerges if we scatterplot each pollution factor versus each meteorological variable, showing the different slopes for the partial relationships between them[7]. All these elements are taken into consideration by the adopted panel estimation technique: the Dynamic Common Correlated Effects (DCCE) [8].

4.1 Methodology: DCCE

The first step of our analysis adopts a panel time series data approach, in

[6] In fact, Passamani and Masotti[7] suggests a dynamic approach, whereas for the purposes of this work we adopt a static principal component factor approach.
[7] The graphs are available upon request.
[8] Stata package xtdcce2, see Ditzen[4].

particular the Dynamic Common Correlated Effects estimator (DCCE) proposed by Pesaran[8] which deals with all the aspects described in the previous section. This estimator is implemented in Stata 13 by the command *xtdcce2* and it allows:

- a dynamic approach.
- heterogeneous slopes, thus fully considering the intrinsic heterogeneity behind the monitoring sites.
- it could control for cross-section dependence, an aspect that we do not consider here.

Given the dependent variable z_{it} and the vector of explanatory variables x_{it}, the stochastic model is:

(2) $$z_{it} = \lambda_i z_{it-1} + \beta'_i x_{it} + \varepsilon_{it}$$
$$\varepsilon_{it} = \gamma_i f_t + e_{it}$$

where β_i is a vector of heterogeneous panel coefficient, f_t is an unobserved common factor and γ_i is a heterogeneous factor loading. Model (2) is estimated through:

(3) $$z_{it} = \lambda_i z_{it-1} + \beta'_i x_{it} + \sum_{k=0}^{p} \delta'_{i,k} \bar{w}_{t-k} + \varepsilon_{it}$$
$$\bar{w}_t = (\bar{z}_t, \bar{z}_{t-1}, \bar{x}_t)$$

where the bar indicates the cross-section means and $p = \sqrt[3]{T}$, as suggested by Chudik and Pesaran[3]. The mean-group panel estimations are then computed as a simple mean of the heterogenous estimations:

(4) $$\hat{\pi}_{MG} = \frac{1}{N} \sum_{i=1}^{N} \hat{\pi}_i$$

where $\hat{\pi}_i = (\hat{\lambda}_i, \hat{\beta}_i)$.

4.2 Estimation

In order to study the general within-province relationship between air pollution and atmospheric variables including all the data provided by the monitoring sites, we make use of DCCE technique discussed in the previous section. This approach estimates a coefficient for each monitoring site, then it provides the panel mean group estimates.

Estimation results of equation (3) are shown in Table 3. As explanatory variables we included the meteorological variables that are commonly assumed to influence air pollution (temperature (*TOut*), wind run (*WRun*), rain (*R*), solar radiation (*SR*), humidity (*Hum*) and atmospheric pressure (*Press*)), the square of temperature, wind run and rain to capture the non-linear relationship emerged from analysing the aforementioned scatterplots, and three seasonal dummies to capture the seasonal impact of winter (S1), spring (S2) and autumn (S3). We checked the correlations between all these weather variables to avoid problems of multicollinearity in the estimation. The strongest correlation is between *Hum* and *Dew* and is equal to 0.77, whereas the other values are lower in absolute value. Therefore, by excluding *Dew*, it is plausible to exclude the problem of multicollinearity.

Aggregate mean estimates show significant values for each variable with the only exception of the seasonal dummies. Therefore, the level of the pollution

factor depends positively on the previous-day level (while the second lag was not significant) and, as expected, it is negatively but not linearly affected by wind and rain, that directly reduce air pollution, while humidity and pressure have both a positive effect. This sign is, however, less easy to interpret. Finally, the temperature and the solar radiation are also negatively linked to the pollution level, since higher values may represent favourable conditions to avoid using cars and heating systems.
The next section aims to study the component of the pollution factor that is unexplained by the atmospheric variables, namely the residuals of the panel model in Table 3.

5 Second step: analysis of the residuals

Given the estimated residuals $\hat{\varepsilon}_{it}$, which can be considered as that part of pollution due mainly to human behaviour, the question is: "How can we reduce pollution by reducing the pollutant levels?".
As can be seen in Fig. 4, the variability of the residuals differs from site to site, is not homoskedastic and it can be analysed in order to understand how it can be explained and controlled. To this purpose, for each site we regress the panel residuals obtained in the previous section, on three main pollutants, as follows:

(5) $\hat{\varepsilon}_t = \alpha' y_t + e_t$

obtaining the results showed in Table 4.
As expected, the coefficients associated to the pollutants are positive and significant and they are much higher where the levels of the pollutants are lower, which means that reducing by a certain amount the single pollutant the effect on reducing the level of pollution is larger for the sites with lower levels of the same pollutant, keeping the other pollutants constant. These results could be used for simulating the effects on air pollution of adopting policies imposing any reduction in the limits of pollutant emissions.

6 Conclusions

This paper has been developed, first, to estimate a model able to describe the intertemporal relationship between air pollution and the available meteorological variables within the alpine province of Trento, and second, to better understand the unexplained part of this relationship, which represents that part of the overall air pollution due to human behaviour.
The province of Trento is characterised by heterogeneous landscapes, with a majority of rural areas and a relevant minority of urban and traffic areas. As expected, the panel data analysis show that rain and the strength of wind are the main responsible of a (non-linear) decline in the air pollution levels, as well as the temperature, that probably affect pollution through human behaviours (i.e. a lower usage of cars and heating systems). The impact of humidity and solar radiation is, instead, less clear and probably reflects a seasonal effect.

For what concerns the component of the air pollution unexplained by the atmospheric variables, the empirical analysis shows the effects on improving ambient air quality that can be obtained of reducing the levels of the pollutants by policy decisions.

Appendix

Fig. 1. Single air pollutant distributions: boxplots with outliers.

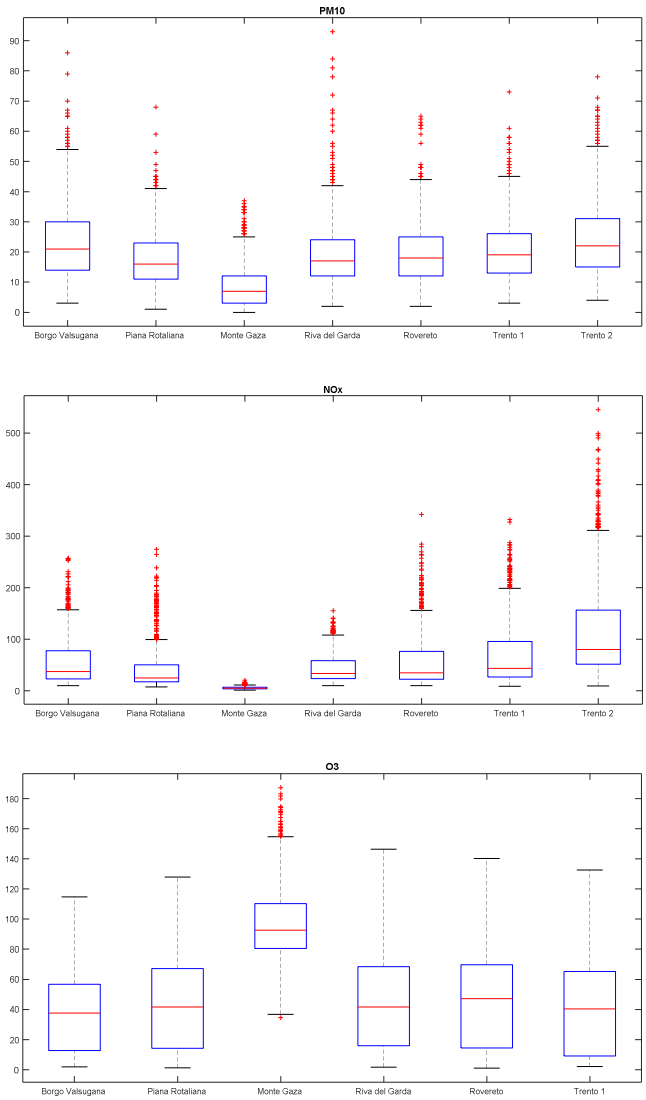

Table 1. Air pollutants: means and standard deviations.

	PM_{10}		NO_x		O_3	
	Mean	*SD*	*Mean*	*SD*	*Mean*	*SD*
Borgo	23.7643	12.8861	57.4694	48.7014	37.6219	25.7096
Piana Rotaliana	18.097	9.42676	43.1551	43.7226	43.612	30.7884
Monte Gaza	8.75994	7.212855	5.744358	2.674718	97.74003	24.5914
Riva del Garda	19.6321	11.6479	44.2184	27.6082	45.8782	32.6563
Rovereto	19.5082	10.1885	58.7943	54.7562	46.6496	33.2752
Trento 1	20.4828	10.1521	71.3097	63.417	41.3936	31.9458
Trento 2	24.1767	12.7727	119.625	96.8155	-	-

Fig. 2. Pollutants and meteorological variables:
temporal dynamics and trend for each monitoring site.

a) Borgo

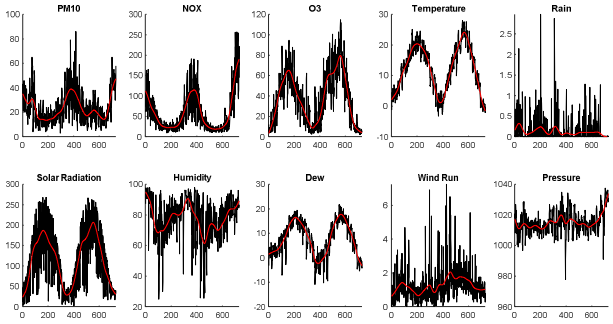

b) Piana Rotaliana

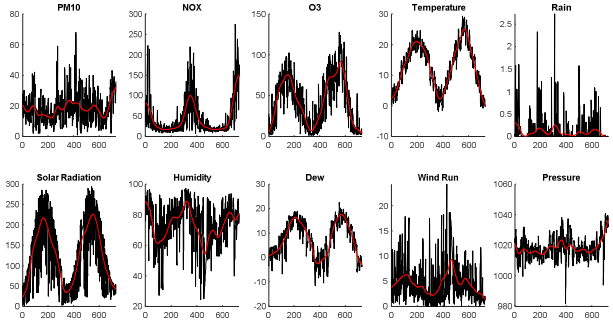

c) Monte Gaza

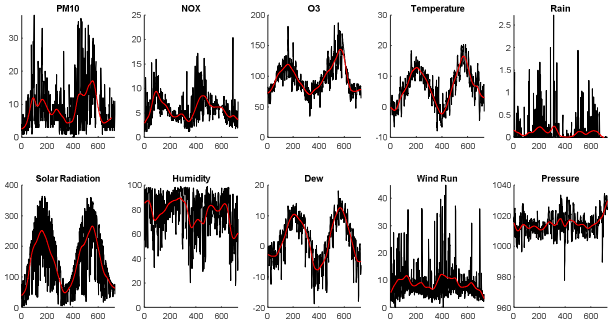

d) Riva del Garda

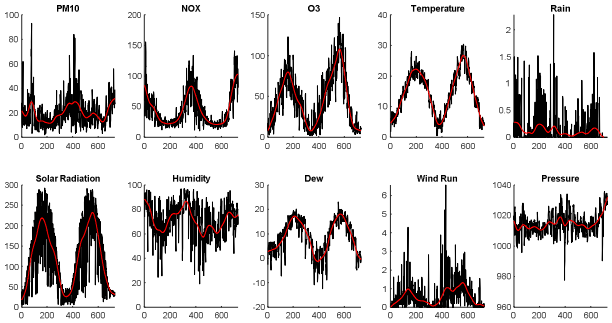

e) Rovereto

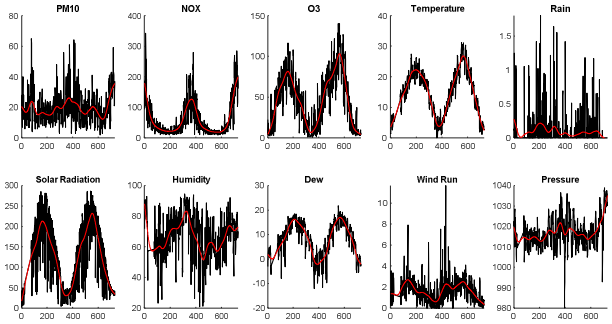

f) Trento 1

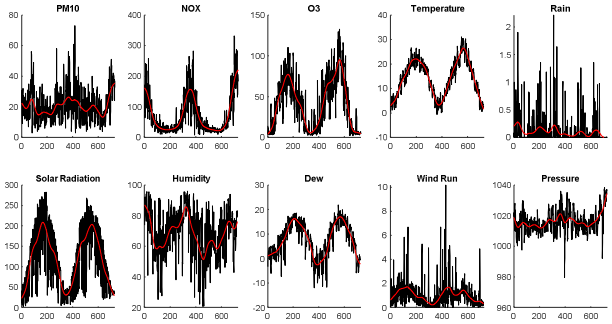

g) Trento 2 (O_3 not available)

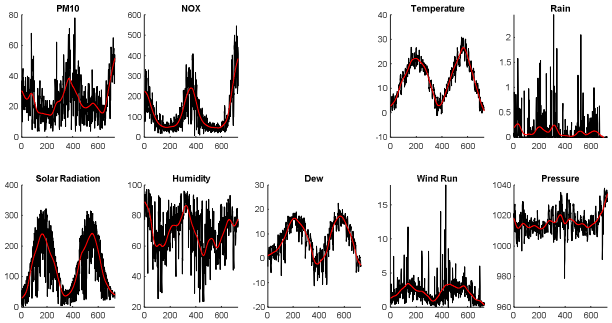

Fig. 3. Pollution factors (*PF*): dynamics.

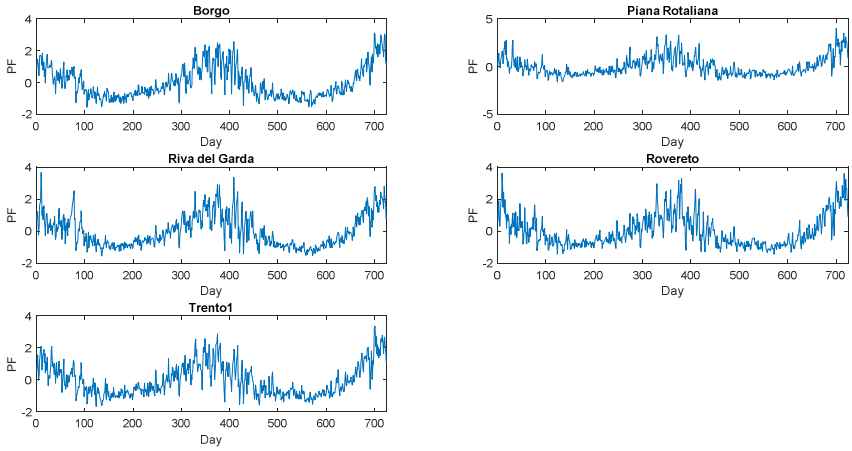

Table 2. Air pollutants, correlations.

	PM_{10}, NO_X	PM_{10}, O_3	O_3, NO_X
Borgo	0.6646	-0.3962	-0.6995
Piana	0.51	-0.1579	-0.654
Riva	0.5478	-0.2238	-0.701
Rovereto	0.5488	-0.2246	-0.7058
Trento 1	0.5116	-0.2309	-0.72

Table 3. Panel estimation (robust standard errors in parentheses; ***, ** and * indicate statistical significance at 1%, 5% and 10% level).

Dep. Var.	**PF**
PF(-1)	0.4670***
	(0.0106)
TOut	-0.0803***
	(0.0043)
Tout^2	0.0018***
	(0.0002)
WRun	-0.2510***
	(0.0470)
WRun^2	0.0134***
	(0.0048)
R	-0.4055***
	(0.1281)
R^2	0.1564**
	(0.0620)
SR	-0.0012***
	(0.0003)
Hum	0.0039***
	(0.0009)
Press	0.0134***
	(0.0009)
S1	-0.0333
	(0.0552)
S2	-0.0271
	(0.0223)
S3	0.0453
	(0.0373)
Cons.	-12.7663***
	(1.0864)
N = 3620	**Adj. R^2** = 0.86

Fig. 4. Residuals from panel model.

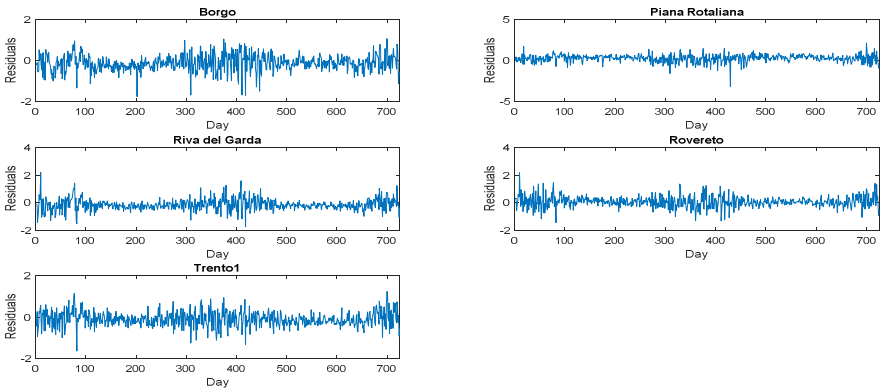

Table 4. Analysis of the residuals (robust standard errors in parentheses; ***, ** and * indicate statistical significance at 1%, 5% and 10% level).

.

	Borgo	**Piana Rotaliana**	**Riva del Garda**	**Rovereto**	**Trento 1**
Dep. Var.	**Residuals**	**Residuals**	**Residuals**	**Residuals**	**Residuals**
PM_{10}	0.0091*** (0.0015)	0.0122*** (0.0024)	0.0162*** (0.0015)	0.0160*** (0.0017)	0.0150*** (0.0015)
NO_X	0.0029*** (0.0005)	0.0031*** (0.0007)	0.0051*** (0.0008)	0.0023*** (0.0005)	0.0016*** (0.0003)
O_3	0.0030*** (0.0006)	0.0046*** (0.0007)	0.0017*** (0.0005)	0.0025*** (0.0006)	0.0011** (0.0005)
Cons.	-0.6068*** (0.0418)	-0.2535*** (0.0480)	-0.7704*** (0.0495)	-0.4909*** (0.0464)	-0.5545*** (0.0396)
N	724	724	724	724	724
Adj. R^2	0.2483	0.1869	0.4299	0.3247	0.3237

References

1. APPA Trento (2014). Air Quality Report 2014. URL: http://www.appa.provincia.tn.it/binary/pat_appa_restyle/rapporti_annuali_aria/Rapporto_QA_2014.1475227470.pdf
2. APPA Trento (2015). Air Quality Report 2015. URL: http://www.appa.provincia.tn.it/binary/pat_appa_restyle/rapporti_annuali_aria/Rapporto_QA_2015.1475227283.pdf
3. Chudik, A., & Pesaran, M. H. (2015). Common correlated effects estimation of heterogeneous dynamic panel data models with weakly exogenous regressors. Journal of Econometrics, 188, 2, 393-420.
4. Ditzen, J. (2016), xtdcce2: Estimating Dynamic Common Correlated Effects in Stata, Heriot Watt University. (http://repec.org/usug2016/ditzen_uksug16.pdf).
5. Haines A., Kovats R.S., Campbell-Lendrum D., Corvalan C. (2006). Climate change and human health: Impacts, vulnerability and public health. Public Health 120, 7, 585-596.
6. Jerrett M., Burnett R.T., Ma R., Arden Pop, C., Krewski D., Newbold K.B., Thurston G., Shi Y., Finkelstein N., Calle E.E., Thun M.J. (2005). Spatial Analysis of Air Pollution and Mortality in Los Angeles. Epidemiology 16, 727–736.
7. Passamani, G., Masotti, P. (2016). Local Atmospheric Pollution Evolution through Time Series Analysis. Journal of Mathematics and Statistical Science 2, 12, 781-788.
8. Pesaran, M. H. (2004). General diagnostic tests for cross section dependence in panels. CESifo Working Paper Series No. 1229.

STOCHASTIC FORECAST MODEL OF SEVERE STORM WIND OVER THE TERRITORY OF NORTH EUROPE AND ENGLAND

Elvira Perekhodtseva

Moscow technological university (perekhod@mecom.ru)

Abstract. The results of the development of the hydrodynamic-statistical models of the automated forecast of severe squalls and tornadoes are submitted in this paper. The submitted forecast methods are based on different recognition statistical models and use the prognostic production of hydrodynamic models. These methods were tested successfully in the operative synoptic practice and were recommended to use. The independent automated verification of these phenomena forecast was provided together with different hydrodynamic forecasts in the Hydrometeorological Center of Russia. The result of the comparative analysis and the examples of the hydrodynamic-statistical forecast of squalls and tornadoes over the northern regions of Russia and Europe are presented. The forecast examples of severe storm wind over England are also provided.

Introduction

The development of a successful method for the automated statistical well-in-advance forecast (from 12 hours to two days) of dangerous summer winds, including severe squalls and tornadoes, could allow taking proper measures against destruction of buildings, protecting people and mitigating losses. The prediction of these phenomena is a very difficult problem for the synoptic till recently. The synoptic forecast of these phenomena using the existing graphic and calculation methods still depends on the subjective decision of an operator. A meteorologist usually gives the storm warning of this dangerous phenomenon (the velocity of V>24 m/s) only 3 hours ahead. Nowadays in Russia there is no successful hydrodynamic model for the forecast of wind of such velocity, hence the main tools for the objective forecast development are the methods that use the statistical model for these phenomena recognition.

The statistical model for the alternative forecast of dangerous summer wind

The meteorological situation involved such dangerous phenomena as squalls, tornadoes, and wind with the velocity V=>20 m/s, is presented as the vector $\mathbf{X}(A)=(x_1(A), x_2(A), \ldots x_n(A))$ where *n* is the quantity of the empiric potential atmospheric parameters (predictors).

The values of these predictors for the dates and towns where these phenomena occurred, were accumulated in the set {**X**(A)}; this is the learning sample of the phenomena A presence. The learning sample of the phenomena A absence or the phenomena B presence ({**X**(B)}) was obtained for the towns where the atmosphere was instable and thunderstorms and rainfalls were observed, but wind velocity values were not high (V<8 m/s). The recognition model of the sets {**X**(A)} and {**X**(B)} was constructed with the Bayesian approach [1, 3].

At the beginning, it is necessary to solve the problem of the compressing the predictors space without information losses in order to choose the informative vector-predictor and to calculate the decisive rules for the recognition of the sets {**X**(A)} and {**X**(B)}. It was done using the transmutation algorithm of the columns and lines of the sample mean correlation matrix **R**. As a result, we get the matrix **R** with diagonal blocks. The method of the diagonalization of matrix **R** is described in [3]. The informative predictors, i.e. representatives from each of blocks, and two independent predictors have composed the vector-predictor of the dimension k=6 (from n=26 potential predictors) [3]. For this purpose we have estimated the most informative predictors using the Mahalanobis distance criterion Δ^2 [1, 3]: $\Delta^2 = (m_i(A)-m_i(B))\uparrow 2/\sigma^2$.

Here $m_i(A)$ and $m_i(B)$ are the components of **M**(A) and **M**(B), that is, of the vectors of the empiric expectation of A presence and A absence, respectively; σ^2_i is the mean variance of *i*-th predictor. Also the criterion of the entropy minimum by Vapnik-Chervonenkis H_{min} was used for the assessment of the information value of predictors [2, 3]. As a result, the informative vector-predictor of the most informative and weakly dependent predictors composed from six atmospheric parameters after this selection [3, 4]:

$$(V_{700},\ H_{0,}\ (T\text{-}T')_{500},\ dT/dn_{ea}\ ,\ T_{ea\ ,}\ Td_{ea}\ ),\ \text{where}$$

V_{700} is the value of the mean wind velocity at the 700 hPa level, m/s; H_0 is the level of the isotherm of 0°C, hPa; $(T'\text{-}T)_{500}$ is the difference between the values of the stratification curve and the moist adiabatic at the 500 hPa level, °C; dT/dn_{ea} is the maximum difference between the temperatures over the front on the surface level near the forecast point, °C; T_{ea} is the maximum temperature on the surface level, °C; Td_{ea} is the maximum dew point temperature on the surface level, °C.

The independent tests of the statistical forecast of severe wind for the north-west of Russia including Karelia and St.-Petersburg have shown very good results. The Pierce–Obukhov

criterion was T=0,68. The forecast of dangerous wind, including tornado, was successful in Ivanovo on June 9, 1984. The tornado was very strong there. This method is objective but not fully automated.

The automated hydrodynamic-statistical forecast of storm wind, squalls, and tornadoes based on the hemispheric model

The successful development of hydrodynamic models for short-term forecasts and improvement of two-three-day forecasts of pressure, temperature, and others parameters allowed us to use the prognostic fields of hydrodynamic models for the calculation of the values of discriminant functions $F_1(\mathbf{X})$ (for the wind velocity V>19 m/s) and $F_2(\mathbf{X})$ (for the wind velocity V>24 m/s) in the nodes of the grid and the values of the probability of dangerous winds of two classes $P_1(\mathbf{X})$ and $P_2(\mathbf{X})$, including squalls and tornadoes:

$P_1(\mathbf{X})=100/(1+\exp(-F_1(\mathbf{X}))$;

$P_2(\mathbf{X})=100/(1+\exp(-F_2(\mathbf{X}))$.

As a result we get the fully automated forecast of these phenomena. The statistical decisive rules $F_1(\mathbf{X})$ and $F_2(\mathbf{X})$ for the automated alternative and probability forecasts were obtained in accordance with the conception PP of “the perfect prognosis” using the objective analysis data. For this purpose the new learning samples were automatically arranged that include the values of n=38 physically substantiated potential predictors [8]. We obtained the informative vectors-predictors of each class (k=8) by the same empirical-statistical selection method [3]. The discriminant functions $F_1(\mathbf{X})$ and $F_2(\mathbf{X})$ and the probabilities of the phenomena $P_1(\mathbf{X})$ and $P_2(\mathbf{X})$ [5] were calculated by using the values of the prognostic fields of the first short-term hydrodynamic hemispherical model of Hydrometeorological Center (the author is L.V. Berkovich) in the nodes of the rectangular grid of 150x150 km:

The author proposes the empirical threshold values $\mathbf{P}_{thr}$ specified for each phenomena and the lead time of 12–24–36 hours in order to get the alternative forecast of these phenomena. The tornadoes in Moscow in 1998 and in 2001 were predicted to 24 hours ahead. The forecast of severe wind, dangerous squalls and tornadoes over the European part of Russia was tested successfully and was recommended for synoptic practice for the lead time of 12–36 hours [5, 8]. The independent results were also better for the Northern Europe. The forecast assessments of severe summer wind with the velocity V>24 m/s over the northern Russia were very high. So, this method was recommended as the best for synoptic practice (the Pierce–Obukhov criterion value T was 0,78 [6], the warning W=92%).

The model of the hydrodynamic-statistical forecast of severe squalls and tornadoes based on the regional model output data. Forecast examples.

The values of the prognostic fields of the regional hydrodynamic model of the short-term forecast (the author is V. M. Losev) are calculated in the nodes of the grid 75x75 km into the operative system of Hydrometcenter twice a day. Nowadays we use the values of these prognostic fields in the same discriminant functions $F_1(\mathbf{X})$ and $F_2(\mathbf{X})$ for the forecast of squalls, tornadoes and severe wind of two classes. Also the new values of the probabilities $P_1(\mathbf{X})$ and $P_2(\mathbf{X})$ are calculated in the nodes of the grid 75x75 km in percents with the same formulae. The new threshold probability **P** gives the forecast areal of severe wind on the map.

The examples of the automated hydrodynamic-statistical forecast of severe squalls and tornadoes over the European part of Russia and Europe base on the regional model and are submitted in the paper [8]. There is an example of severe storm wind called "St. Jude storm" that passed over Northern Europe and England in October, 2013 (Fig. 1) [9]. The area of storm wind is bounded by the isoline P=65%–90%. Next day this storm wind came to St.-Petersburg.

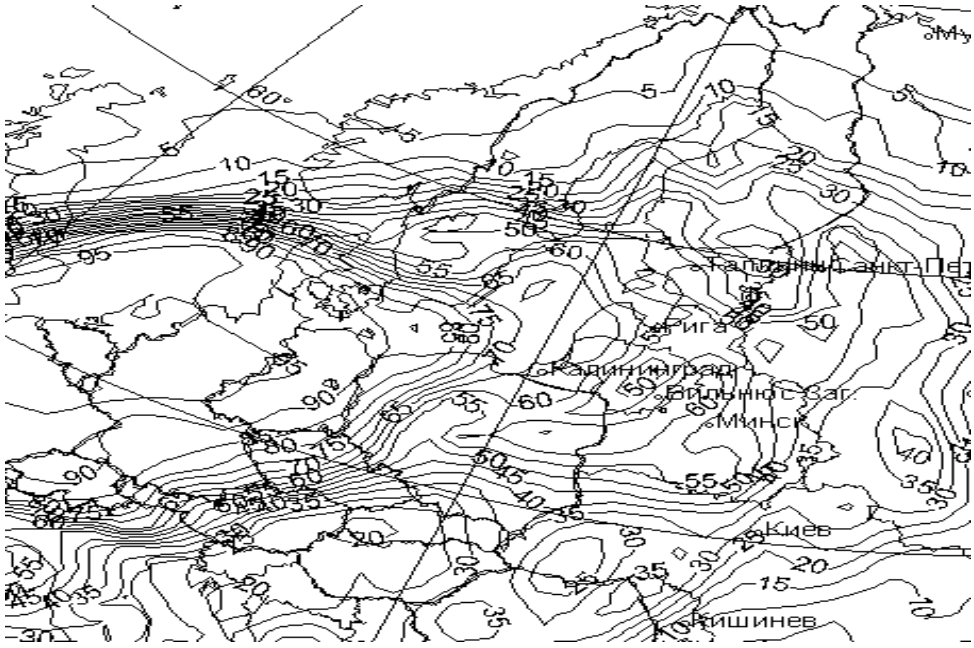

Fig. 1. The forecast area (on the left) is bounded with the isoline P=65%–95%
The storm wind velocity was observed in Germany, in France and in England too.

Our new technology allows us to send forecast maps to different regions of Russia and Europe including England. We have many examples of the storm wind forecast for the Northern Europe and England. too. These forecasts are calculated in operative system of Hydrometeorological Center. There the maps are formed and are sent to server. All of meteorologists can take these maps and use then as a help in your synoptic practice. The lead time of forecasts is 12, 24, 36, 48h.

The very dangerous wind with the velocity 30m/s was observed at Moscow on 29.05.2017. The forecast area over Moscow (fig.2) shows us the velocity 31-33m/s. This day the dangerous and storm wind were observed in the areas of Smolensk, Bryansk, Tver and in Northern Europe. These prognostic areas are seen very well at the fig.3. (the forecast area with the lead time 24h and the time of the calculation is 15h of the Moscow time on 28.05.2017) and at the fig.4. (the forecast area with the lead time 36h).

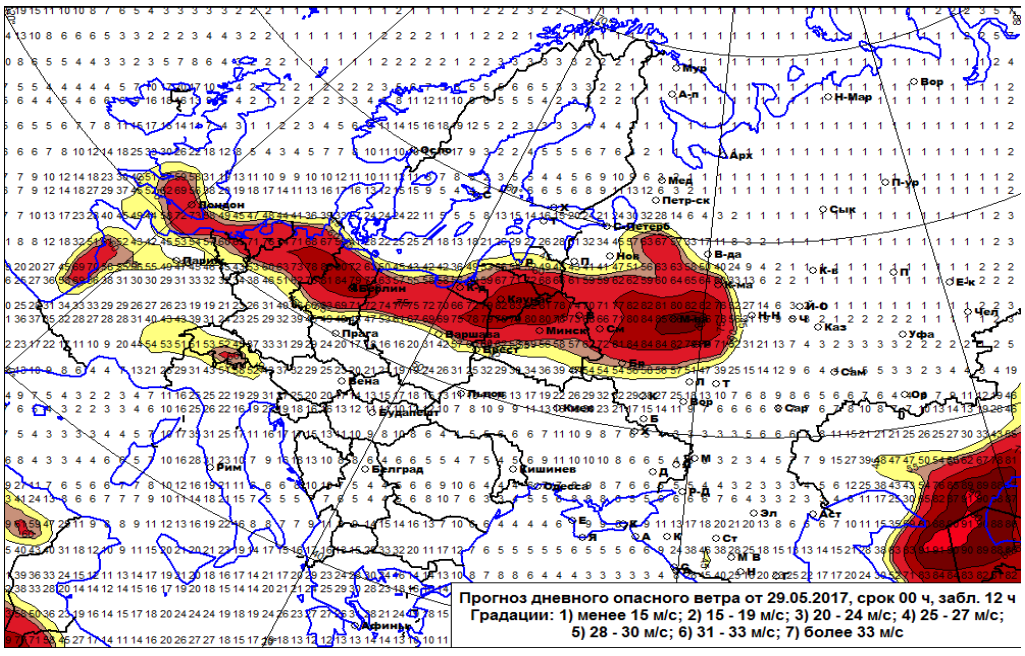

Fig. 2. The forecast of dangerous wind velocity for the date of 29.05.2017. with the lead time 12h. The gradations 1) below 15 m/s; 2) 15-19 m/s; 3) 20-24 m/s; 4) 25-27m/s ; 5) 28-30 m/s; 6) 31-33 m/s; 7) over 33 m/s

The forecast area of dangerous and storm wind came to Germany and other northern countries to the next day 30.05.2017 (fig.5). It's really, the wind velocity of 25m/s was observed in Berlin this day. We submit also several interesting examples of storm wind

forecast over the territory of England: the prognostic areas to 14.05.2017: with the lead time 12h and 48h (fig.6, 7) and also the prognostic area of storm wind to the date 6.06.2017. (fig, 8).

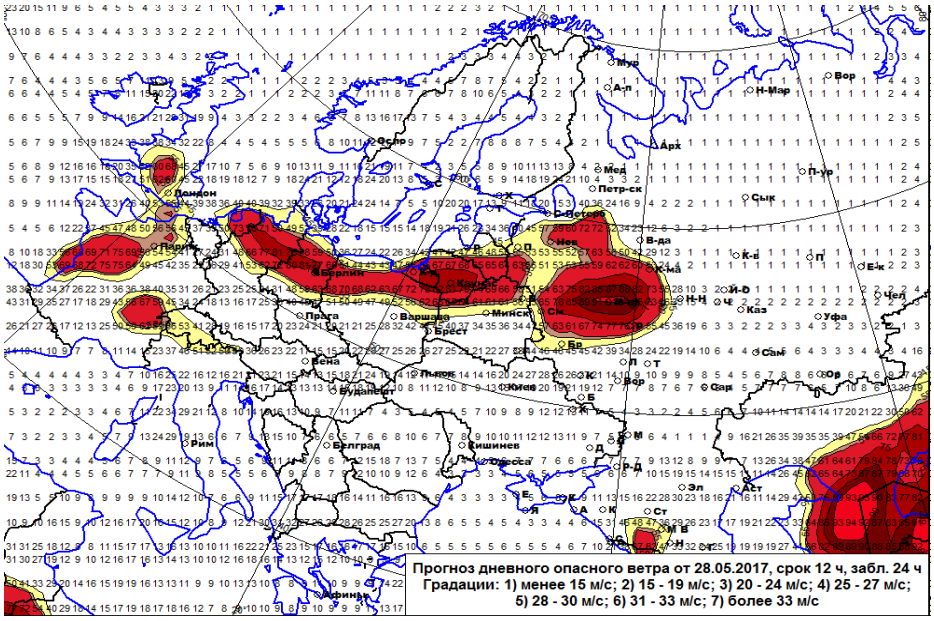

Fig. 3. The forecast of dangerous wind velocity for the date of 28.05.2017., the lead-time 24h. The gradations 1) less 15 m/s 2) 15-19 m/s 3) 20-24 m/s 4) 25-27m/s ; 5) 28-30 m/s 6) 31-33 m/s 7) over 33 m/s

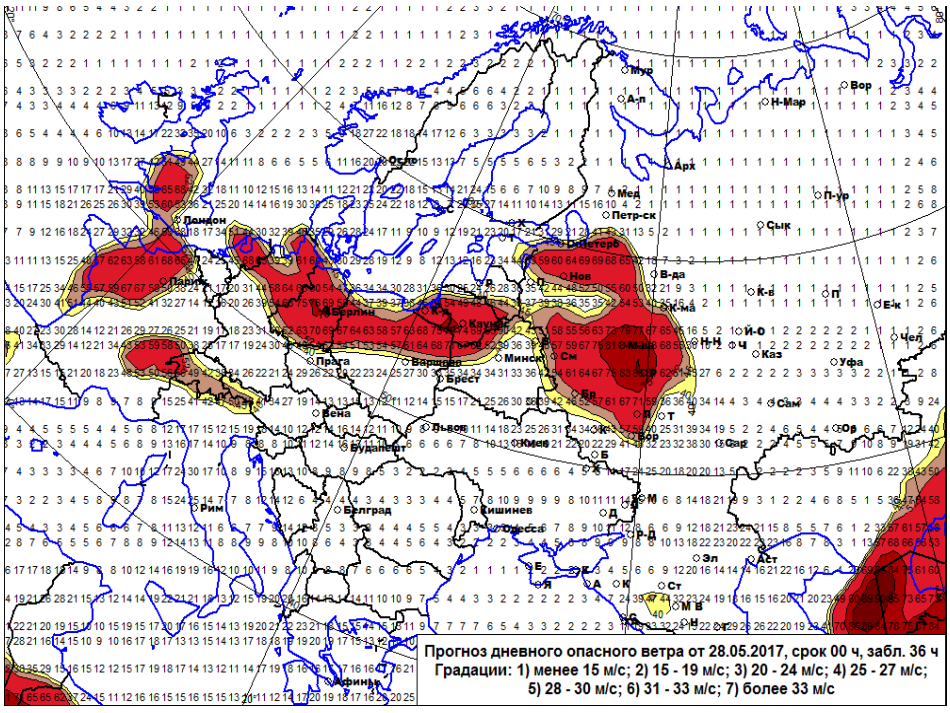

Fig. 4. The forecast of dangerous wind velocity for the date of 28.05.2017., the lead-time 36h. The gradations 1) less 15 m/s 2) 15-19 m/s 3) 20-24 m/s 4) 25-27m/s ; 5) 28-30 m/s 6) 31-33 m/s 7) over 33 m/s

Is shown at the fig.4, that the prognostic area (which was calculated on 28.05.2017 with lead time 36h) of the velocity V=28m/s-30m/s is located over Moscow and Moscow region.

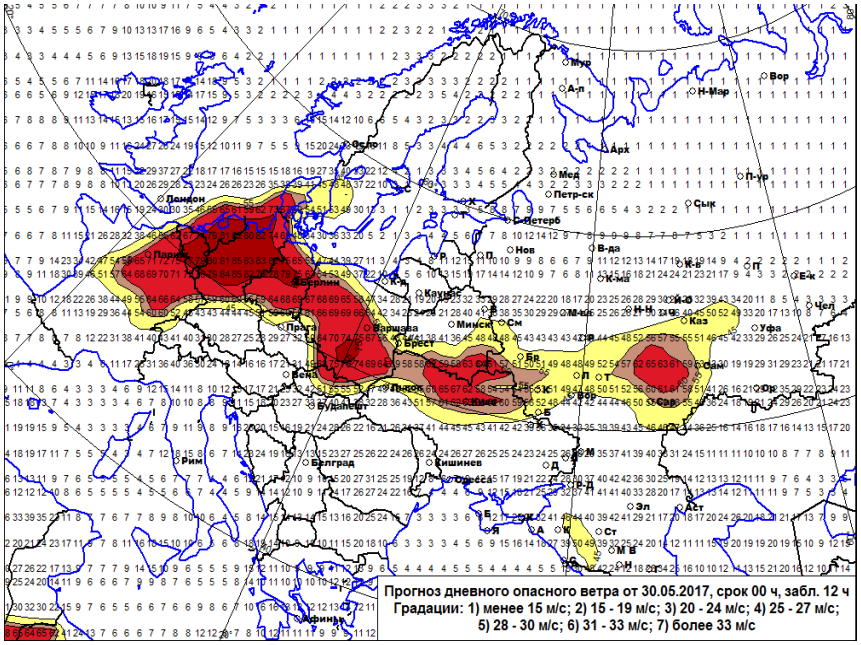

Fig.5. The forecast of dangerous wind velocity for the date of 30.05.2017.
The gradations 1) less 15 m/s 2) 15-19 m/s 3) 20-24 m/s 4) 25-27m/s ; 5) 28-30 m/s
6) 31-33 m/s 7) over 33 m/s

Very strong storm winds were observed over the territory of England during the month of May. The example of such forecast with the lead time 12h and 48h to the day of 14.05.2017 is shown at the fig.6 and fig.7 below.

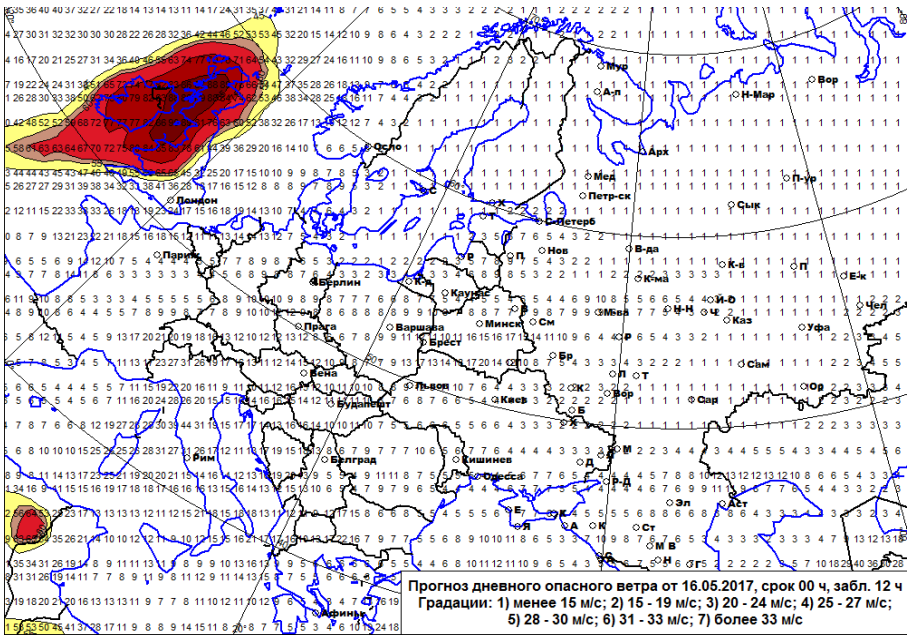

Fig. 6 The forecast of dangerous wind velocity for the date of 16.05.2017., the lead-time 12h.
The gradations 1) below 15 m/s 2) 15-19 m/s 3) 20-24 m/s 4) 25-27m/s ; 5) 28-30 m/s
6) 31-33 m/s 7) over 33 m/s

The weather was very nasty in the day of the opening of conference ASMDA-2017.

This day London city was located in the center of the cyclone. Our operative prognostic scheme issued the forecast of heavy rainfalls and storm winds on this day (fig. 8). Really, this day the quantity Q of the factice precipitation was equal Q=30mm/12h, the mean velocity of wind amounted V=12-15m/s, and maximal velocity was equal 20m/s.

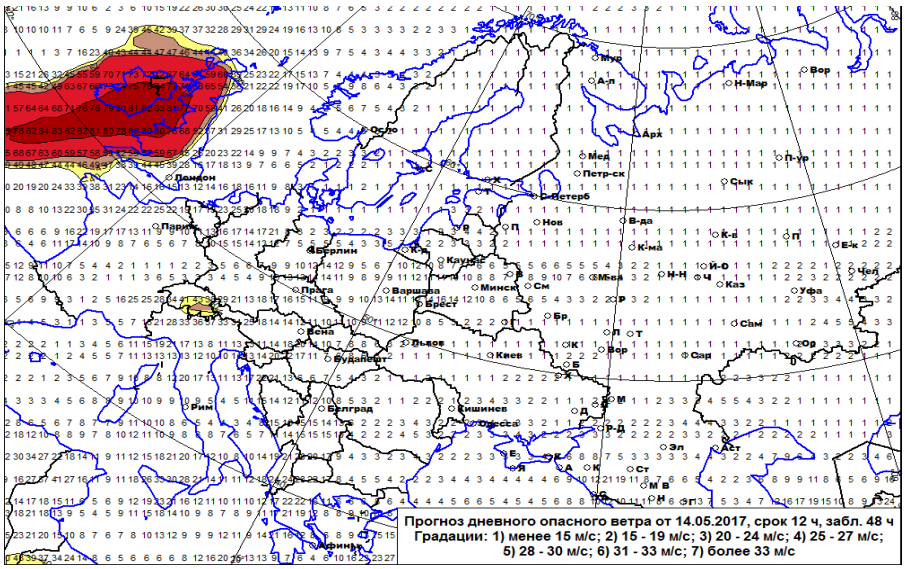

Fig. 7 The forecast of dangerous wind velocity for the date of 16.05.2017., the lead-time 48h. The gradations 1) below 15 m/s 2) 15-19 m/s 3) 20-24 m/s 4) 25-27m/s ; 5) 28-30 m/s 6) 31-33 m/s 7) over 33 m/s

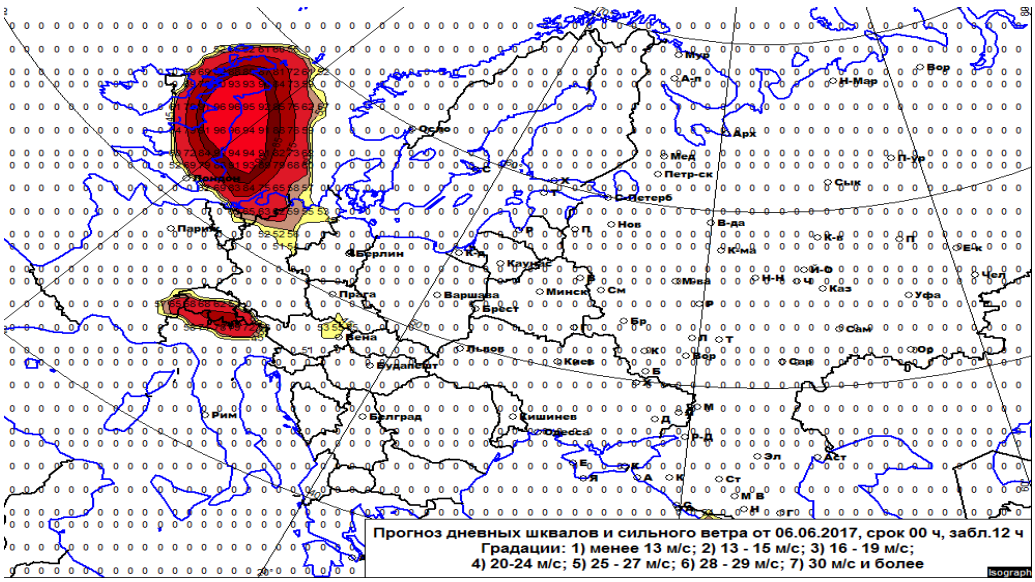

Fig. 8 The forecast of storm wind velocity for the date of 06.06.2017., the lead time 12h. The gradations 1) below 13 m/s 2) 13-15 m/s 3) 16-19 m/s 4) 20-24m/s ; 5) 25-27 m/s 6) 28-29 m/s 7) over 29 m/s

Conclusions

The assessments of the new hydrodynamic-statistical method for the forecast of very strong squalls and tornadoes with the velocity V>24m/s over the territory of Russia were successful, the criterion of Pirsy-Obukhov was equal T=0,42 [10]. They have also shown the stability of the statistical model for the forecast of squalls, tornadoes and dangerous wind over the territory of Russia using the output production of successful hydrodynamic models (hemispheric and regional models). In future we are going to develop our stochastic model for the dangerous and storm wind forecast till 72 hours ahead using the output production of the global model of Hydrometeorological Center of Russia (the author is M. A. Tolstykh).

References

1. T. Anderson, *An Introduction to the Multivariate Statistical Analysis* (Moscow, Fizmatgiz, 1963) [Transl. from English], 500 p.

2. V. N. Vapnik, Reconstruction of the Dependents with the Help of the Empiric Data (Moscow, Science, 1979) [in Russian].

3. E. V. Perekhodtseva, "The Forecast of Squalls by Statistical Methods of Classification on the Base of Diagnostic and Prognostic connections," Proceedings of Hydrometcenter of the USSR, **271** (1985), p. 37–60 [in Russian].

4. E.V. Perekhodtseva, *The Objective Physical-statistical Forecast Method of Squalls (V=20 m/s and More) for the Current Day for the European Territory of Russia. The Method Recommendations* (Moscow, 1992), 10 p [in Russian].

5. E.V. Perekhodtseva, "The Hydrodynamic-statistical Model of the Forecast to 36 Hours Ahead of Dangerous Convective Daytime and Nighttime Phenomena – Squalls, Tornadoes and Rainfalls," Research Activities in Atmospheric and Oceanic Modeling, Report 32 (2003).

6. E.V. Perekhodtseva, "The Hydrodynamic-statistical Model of Operative Forecast to 12–36 Hours Ahead of Storm Winds Including Squalls and Tornadoes at the Territory of Siberia. Research Activities in Atmospheric and Oceanic Modeling, Report 48 (2006).

7. E.V. Perekhodtseva and L. V. Zolin, “Hydrodynamic-statistical Forecast and the Expert System of the Tornado Forecast over the European Part of Russia,” Proceedings of Hydrometcenter of Russia, **342** (2008), p. 45–54 [in Russian].

8. E.V. Perekhodtseva, “The Forecast of Severe Squalls and Tornadoes in the Summer of 2009 on the Base of Statistical Models,” Proceedings of Hydrometcenter of Russia, **344** (2010), p.265-280 [in Russian].

9. E.V. Perekhodtseva, “Operative Hydrodynamic-statistical Forecast of St. Jude Storm and Other Dangerous Storm Winds over the Territory of Russia and Europe on the Base of the Regional Model of Russia,” Research Activities in Atmospheric and Oceanic Modeling, Report 53 (2014).

10. E.V. Perekhodtseva. “Hydrodynamic-statistical Forecast of Squalls and Very Strong Wind in the Gradation of Dangerous Phenomena at the Summer Season with the Lead Time 12-36h on the Output Data of Regional Model for European Part of Russia”. Proceedings of Information of HMC, **40** (2013**)**, p.170-180 [in Russian].

AR Dynamic Evolving Neuro-Fuzzy Inference System for Mortality Data

Gabriella Piscopo[1]

[1] Department of Economics, University of Genoa, Via Vivaldi 16,16126 Genova (Italy)
(E-mail: piscopo@economia.unige.it)

Abstract. In this paper we implement an integrated autoregressive Dynamic Evolving Neuro-Fuzzy Inference System in the context of mortality projections and compare the results with the classical Lee Carter model. DENFIS is an adaptive intelligent system suitable for dynamic time series prediction, where the learning process is driven by an Evolving Cluster Method. The typical fuzzy rules of the neuro- fuzzy systems are updated during the learning process and adjusted according to the features of the data. This makes possible to capture the historical changes in the mortality evolution.

Keywords: AR, DENFIS, ECM, Lee Carter model, mortality projections.

1 Introduction

In the last century the improvements in standards of living, the progress in medicine and the economic enhancements have driven human population to live better and longer. From an actuarial point of view, the decreasing trends in global mortality represent risk for insurers, which price their products on the basis of the historical mortality tables, and for governments, which have to plan health and pension policies. In this context, the so called longevity risk derives from improvements in mortality trend with systematic deviations of the number of the deaths from its expected values. In order to capture this trend and produce accurate mortality forecasts, stochastic models have been introduced. The most used is the Lee-Carter (LC) model [6], whose main statistical tools are the least square estimation through the Singular Value Decomposition of the matrix of the log age specific mortality rate and the Box and Jenkins modelling and forecasting for time series. The LC is fitted to historic data and used to forecast long term mortality. However, strong structural changes have occurred in mortality patterns and several extensions have been proposed to overcome the limits of the model due to extrapolation based on the past data. Recently, Neural network (NN) and fuzzy inference system (FIS) have been introduced in the context of mortality data by Atsalaki et. al [1]. They implement an Adaptive Neuro-Fuzzy Inference System (ANFIS) model based on a first order Takagi Sugeno (TS) type FIS [8]. They predict the yearly mortality in a one step ahead

17th *ASMDA Conference Proceedings, 6 - 9 June 2017, London, UK*

prediction scheme and use the method of trial and error to select the type of membership function that describe better the model. The least-squares and the backpropagation gradient descent methods are used for training the parameters of the FIS. They show that the ANFIS produces better results than the AR and ARIMA models for mortality projections. D'Amato et al. [2] produce a comparative analysis between classical stochastic models and ANFIS implementing them on the Italian mortality dataset. Piscopo [7] proposes an Integrated Dynamic Evolving Neuro-Fuzzy Inference System (DENFIS) for longevity predictions. DENFIS is introduced by Kasabov et al [5] for adaptive learning of dynamic time series predictions. It is an adaptive intelligent system where the learning process is updated thanks to a preliminary clusterization of the training data. The Evolving Clustering Method (ECM) is used to subdivide the input set and determine the position of each data in the input set. [5] show that DENFIS effectively describes complex data and outperforms some existing methods. In this paper we use an integrated AR-DENFIS model to produce mortality forecasts with an application to the Italian population and compare the results with the classical LC . The paper is organized as follows: in Section 2 we present the dynamic evolving neuro fuzzy procedure; in Section 3 we briefly describe the LC; in Section 4 we show a comparative application to Italian mortality dataset; final remarks are offered in Section 5.

2 The Dynamic Evolving Neuro Fuzzy System

The Dynamic Evolving Neuro Fuzzy System is an adaptive learning fuzzy system for dynamic time series prediction. It differs from the ANFIS because the fuzzy rules and parameters are dynamically updated as new informations come in the system; both use a TS architecture to implement learning and adaptation. Jang [4] introduce the ANFIS: the procedure learn information from the data and Fuzzy Logic computes the membership function parameters that best allow the associated fuzzy inference system to track the given input/output data. A first order TS architecture is described in Figure 1.

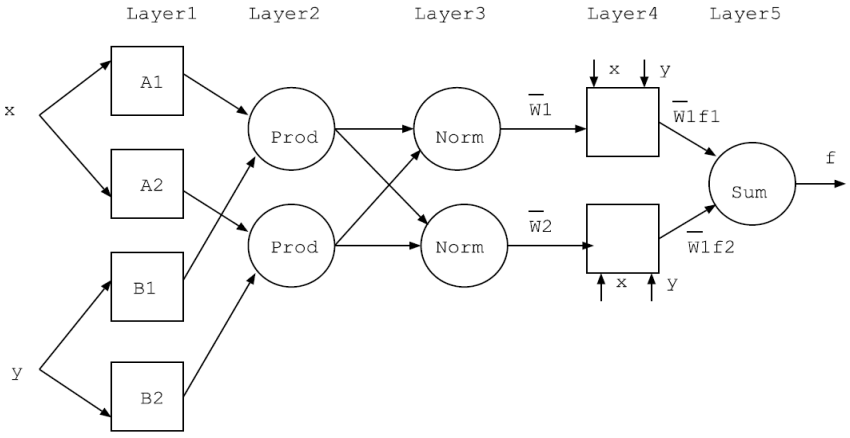

Fig1: Takagi- Sugeno Architecture

Let us assume that the FIS has two input *x* and *y* and one output z. A first order TS fuzzy model has the following rules:
Rule 1: if *x* is A_1 and *y* is B_1 then $f_1=p_1x+q_1y+r_1$
Rule 2: if *x* is A_2 and *y* is B_2 then $f_2=p_2x+q_2y+r_2$
The procedure follows the steps:
Let $O_{i,l}$ be the output of the node *i* in the layer *l*

1. Layer 1: Every node in this layer is an adaptive one with a node function

$$O_{1,i} = \mu_{A_i}(x) \text{ for } i = 1,2, \text{ or}$$
$$O_{1,i} = \mu_{B_{i-2}}(x) \text{ for } i = 3,4 \quad (1)$$

where the typical membership functions depend on the premise parameters a_i,b_i,c_i.

2. Layer 2: The output of each node is the product of all the incoming signals:

$$O_{2,i} = w_i = \mu_{A_i}(x) \cdot \mu_{B_i}(y), \quad i = 1,2 \quad (3)$$

3. Layer 3: the outputs of this layer are the normalization of the incoming signals:

$$O_{3,i} = \overline{w}_i = \frac{w_i}{w_1+w_2}, \quad i = 1,2 \quad (4)$$

4. Layer 4: each node in this layer is an adaptive node with a node function

$$O_{4,1} = \overline{w}_i f_i = \overline{w}_i(p_x + q_i y + r_i) \quad (5)$$

p_i,q_i,r_i are the consequent parameters.

5. Layer 5: the i^{th} output of this layer is computed as the summation of the all incoming signals $\sum_i \overline{w}_i f_i$

In the hybrid learning algorithm the consequent parameters are identified by the least square estimation while the premise parameters are updated by gradient descent.
The DENFIS uses TS model where the fuzzy rules are created dynamically and the learning process is driven by the ECM procedure. The ECM is introduced to create a partition of the input space. Once a threshold value Dthr is set, a first cluster of inputs from the training data is extracted and its radius is set equal to zero. Another sample is extracted: if the distance between its centre and that of the existing cluster is less than the value of the parameter Dthr then the vector extracted is incorporated in the first cluster and the centre is updated and the radius increased; otherwise another cluster is created. A cluster will not be

modified anymore when its radius becomes equal to Dthr. We refer to [5] for a detailed description of the ECM algorithm.
Once the clusters are created, the fuzzy rules of DENFIS are generated and updated within the partitioned input space using a TS model. The steps of the DENFIS are the following:

1. Define the training data set

2. Apply the ECM to the training data set

3. For each cluster create the fuzzy rule through the triangular membership function

   $$\mu(x) = mf(x, a, b, c) = \max(\min((x-a)/(b-a),(c-x)/c-b)),0) \quad (6)$$

   where x is the input vector, b is the cluster centre, $a=b-d\times Dthr$, $c=b+d\times Dthr$, d is a parameter of the width of the triangular function.

4. The consequent parameters of the TS procedure are calculated through a weighted least square estimation. In particular, the weighs are represented by $1-d_j$ where d_j is the distance between the j-th sample and the corresponding cluster centre.

5. The fuzzy rules and the parameters are updated when a new cluster is created or the existing clusters are modified. When the ECM stops, the output of the system is generated according to the TS procedure.

3. The Lee Carter Model

In order to model the mortality separately for each i population without considering dependence between groups, the widely used Lee Carter Model (LC) describes the mortality rates at age x and time t as follows:

$$m_{xt,i} = \exp(\alpha_{x,i} + \beta_{x,i}k_{t,i} + u_{xt,i}) \quad (7)$$

where $m_{xt,i}$ is the sum of an age specific parameter independent of time $\alpha_{x,i}$ and a component given by the product of a time-varying parameter $k_{t,i}$, reflecting the general level of mortality and the parameter $\beta_{x,i}$, representing how rapidly or slowly mortality at each age varies when the general level of mortality changes. The model is fitted to historical data through the Singular Value Decomposition of the matrix of the observed mortality rates. The estimated time varying parameter is modelled as a stochastic process; standard Box and Jenkins

methodology are used to identify an appropriate ARIMA model according which $k_{t,i}$ are projected.

4. An Application to Mortality Dataset

In this work we apply AR-DENFIS to mortality forecasts and compare the results with the LC.

In order to define the number of inputs of the DENFIS in the mortality dataset, we firstly apply an AR scheme; then we compare the results of mortality forecasts obtained by the LC and AR-DENFIS. The data used are taken from the Human Mortality Database [3]. We work on the mortality rates m_t for the Italian males aged 50, collected from t=1940 up to t=2012. The data, considered by single calendar year, are split into training dataset from 1940 up to 1993 and test dataset from 1994 up to 2012. The AR is fitted to the whole time serie and the order equal to 2 is chosen minimizing the Akaike Information Criterion; consequently, in our DENFIS we introduce two input variable x_1 and x_2 (mortality one and two years before) and one output y (mortality one step ahead).

Firstly, we implement the DENFIS on the training dataset, setting the value of Dthr equal to 0.1, the maximum number of iteration equal to 10, the parameter d equal to 2, the step size of the gradient descent equal to 0.01. Once the DENFIS is created, the mortality rate is projected on the testing period and the results are compared with the realized mortality.

In the second step of our application, we implement the LC. We fit the model on the male population aged between 0 and 100, considering years between 1940 and 1993; the parameter kt is derived and shown in Figure 2; a random walk model is fitted on the serie of kt and is projected from 1994 up 2012 through a Monte Carlo simulation with n=1000 paths. Finally the value of projected mortality rates for male aged 50 are derived using eq. (7).

The MSE of the LC and DENFIS are compared. The results are shown in Tables 1 and 2.

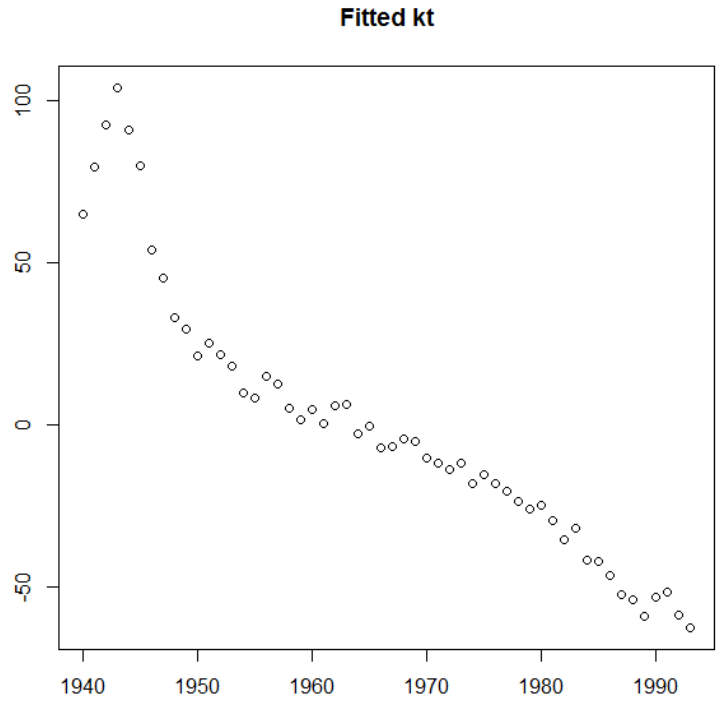

Fig2: The fitted parameter kt of the LC

T	Realized	DENFIS	LC
1994	0.00461	0.004458675	0.005083814
1995	0.00413	0.004593811	0.005004209
1996	0.00409	0.004354364	0.004934666
1997	0.00388	0.004143083	0.004868312
1998	0.00390	0.004003856	0.004802357
1999	0.00371	0.003933489	0.004728343
2000	0.00359	0.003829500	0.004659374
2001	0.00359	0.003684567	0.004591524
2002	0.00316	0.003637632	0.004525431
2003	0.00334	0.003384584	0.004462271
2004	0.00312	0.002780000	0.004403274
2005	0.00305	0.002780000	0.004347287

2006	0.00297	0.002780000	0.004286747
2007	0.00304	0.002780000	0.004222623
2008	0.00294	0.002780000	0.004164231
2009	0.00292	0.002780000	0.004100000
2010	0.00278	0.002780000	0.004049956
2011	0.00288	0.002780000	0.003990748
2012	0.00286	0.002780000	0.003937622

TABLE 1: THE MORTALITY RATES REALIZED VS PROJECTED THROUGH LC AND DENFIS

	LC	**DENFIS**
MSE	1.219046e-06	5.726724e-08

TABLE 2: RMSE IN THE LC AND DENFIS

5. Final Remarks

In this paper we have applied an integrated AR-DENFIS procedure to forecasts mortality and have compared the results with the standard LC. The backtesting procedure highlights the improvements in mortality forecasts moving from LC to DENFIS: the mean square error decreases and the projected mortality trend appears more similar to the realized trend. In particular, the DENFIS catches the improvements in mortality realized in the last years better than the LC. This feature makes it attractive to handle with the longevity risk.

REFERENCES

[1] Atsalakis G., Nezis D., Matalliotakis G., Ucenic C.I., Skiadas C., *Forecasting Mortality Rate using a Neural Network with Fuzzy Inference System*. No 0806,2008, Working Papers, University of Crete, Department of Economics, http://EconPapers.repec.org/RePEc:crt:wpaper:080

[2] D'Amato V., Piscopo G., Russolillo M., Adaptive Neuro-Fuzzy Inference System vs Stochastic Models for mortality data, in *Smart Innovation, Systems and Technologies*,Springer,26, 2014, 251-258

[3] *Human Mortality Database*. University of California, Berkeley (USA), and Max Planck Institute for Demographic Research (Germany). www.mortality.org

[4] Jang J.S.R., ANFIS: Adaptive-Network-based Fuzzy Inference Systems, *IEEE Transaction on Systems, Man and Cybernetics*, 23, 1993, 665-685

[5] Kasabov N.K., Song Q., DENFIS:dynamic Evolving neuro-fuzzy inference system and its application for time series-prediction, *IEEE Transaction on Fuzzy System, 10(2),* 2002
[6] Lee R.D., Carter L.R., Modelling and Forecasting U.S. Mortality,*Journal of American Statistical Association, 87,* 1992, 659-671
[7] Piscopo G., Dynamic Evolving Neuro Fuzzy Inference System for mortality Prediction, *Int. Journal of Engineering Research and Application, 2017*
[8] Takagi T., Sugeno M., Fuzzy identification of systems and its application to modelling and control, *IEEE Transactions on Systems, Man and Cybernetics, 15 (1),* 1985, 116 - 132.
[9] Wei L.Y., Cheng C.H., Wu H.H., Fusion ANFIS Model based on AR for forecasting EPS of leading industries, *International Journal of Innovative Computing, Information and Control, 7(9),* 2011, 5445-5458

TRIBAL DEATH CLUSTERING IN CENTRAL AND EASTERN INDIAN STATES

Mukesh Ranjan

International Institute for Population Sciences (IIPS)
Mumbai, Maharashtra
India

Introduction

The infant mortality rate has been regarded as a highly sensitive (proxy) measure of population health. This reflects the apparent association between the causes of infant mortality and other factors that are likely to influence the health status of whole populations such as their economic development, general living conditions, social wellbeing, rates of illness, and the quality of the environment (Whitehouse, 1982). There were 4.6 million deaths (74 percent of all under-five deaths) occurred within the first year of life (WHO, 2011). Globally, the infant mortality rate has decreased from an estimated rate of 63 deaths per 1000 live births in 1990 to 34 deaths per 1000 live births in 2013 (Unicef,2014) but still India is experiencing high IMR than global average.

As we are approaching towards the end of the year 2015, the year of deadlines to achieve the Millennium Development Goals- 4th target to reduce Under Five Mortality (U5MR) by two-third from 1990 levels. The year has come now, but still we are lagging far behind the MDG goals (UN Millennium Project, 2006).

India's Under Five Mortality (U5MR) declined from 125 per 1,000 live births in 1990 to 74.6 per 1,000 live births in 2005-06. According to the latest figure of World Bank, the U5MR and IMR for India in 2013, is 53 and 42 per 1,000 live births respectively (World Bank, 2015).

This means India would still fall short of the target of 42 per 1,000 live births for U5MR and of 28 per 1,000 live births for IMR. In view of these statistics, child survival in India needs sharper focus. This includes better managing neonatal and childhood illnesses, improving child survival, particularly among vulnerable communities and we need a different approach to tackle the IMR & U5MR. Survival risk remains a key challenge for the disadvantaged who have little access to reproductive and child health services. Major states in the heartland of India are likely to fall significantly short of these targets, by more than 20 points.

In the backdrop of high mortality situation prevailing in the developing nations across the world including India, the situation of high mortality is not only an issue of concern in itself but it also have a strong linkages with the intra-family clustering of deaths in a particular region. In other words, there may be a situation when there is a high mortality in the region but deaths are not randomly distributed in the entire exposed families of the area rather there are certain High- risk families which only experiences deaths frequently and other families in the nearby in spite of sharing the similar socio-cultural environment do not experience frequent child loss. This situation is known widely among researcher as death clustering. This phenomena was first highlighted in 1990 by Monica Dasgupta in her paper entitled "Death clustering, mothers' education and the determinants of child mortality in rural Punjab, India.". Since then it is on the research agenda while

studying infant mortality and also a new dimension of familial component got added and entire research community has seen this phenomena as another important approach for studying infant and child mortality.

Accordingly, the present research was undertaken to investigate the clustering of infant deaths by family in central and eastern states of India. We have considered tribal population for our study. These tribes are varied in terms of their socio-economic and political development. The term "Scheduled Tribes" refers to specific indigenous peoples whose status is acknowledged by the Constitution of India. The tribal population in India, according to the 2011 census, was 87 million and it constitutes around 8.2 percent of the total Indian population. Around 80 percent of them found in central India and a large part of the rest in the north-eastern states. The maximum share of tribal population is contributed by Madhya Pradesh (14.7 percent), followed by Odisha (9.2 percent), Jharkhand (8.3 percent) and Chhattisgarh (7.5 percent) to the India's population (in central and eastern states). The majority of tribal population living in these states are the Particularly Vulnerable Tribal Groups (PVTGs) (Ministry of Tribal Affairs, 2015). They are socially as well as economically very backward in the sense that they have little access to the resources for their development, low rate of literacy, relatively small population size, dwindling in numbers and some of the groups are at the verge of extinction. They are distributed in various ecological zones beyond the state boundaries with immense variation in subsistence pattern, technological development, ways of living and contact with outside world as well as with different worldviews in respect with neighbourhood- so called mainstream population. Lots of problems are faced by them and in most of the areas they are unable to cope the situations.

Among various social groups, it has been found that on an average, an Indian child has 25 percent lower likelihood of dying under age five as compared to an Adivasi or Tribal child (Das, Kapoor, & Nikitin, 2010). As per NFHS-3,(2005-06), estimates, the under-five mortality rate and the child Mortality rate are much higher for STs than any other social group/ castes at all childhood ages (95.7 and 35.8 respectively). However, it is found that STs have a lower infant mortality rate (62.1) than SCs (66.4) but higher than OBCs (56.6). Further, According to Census 2001, the IMR and the U5MR for STs is highest in Madhya Pradesh (110 and 169 respectively per 1,000 live births).

Materials and Methods

In order to examine the family level infant death clustering bivariate analysis was carried out and for capturing the linkages between survival prospects of siblings and mother specific unobserved heterogeneity, the dynamic panel data model or mixed effect model with random intercept was applied. This model has the advantage of simultaneously capturing unobserved heterogeneity and the causal positive or negative scarring mechanisms at the same time in the model. The model also accounted for the endogeneity factor which arose due to the inclusion of previous sibling-survival status in the model, thus avoiding the potential bias in previous studies.

The potential problem which has been found in the empirical specification of the earlier models include the problem of left truncation & endogeneity, measurement error and time inconsistency(Bolstad & Manda, 2001; Sian L Curtis et al., 1993; Guo, 1993; Sastry, 1997). It would be very important to understand these unaddressed problems of the earlier models. First, Left truncation problem is the problem associated with retrospective data. It means an age cut-off is used to select the interviewees. The interviewees may be a representative sample at survey date, but they will not be so for earlier years (Rindfuss, Palmore, & Bumpass, 1982).This non-representativeness of the sample over the years along with the recall bias, a common practice in previous research has been to discard information on children who were born before an arbitrarily selected date, such as 10 or 15 years before the date of the survey (Bhargava, 2003; Bolstad & Manda, 2001; Sian L Curtis et al., 1993; Guo, 1993; Madise & Diamond, 1995; Sastry, 1997). This left truncation of the data by calendar time occurs at the different points in the birth history, creating additional complications.

Many studies have even discarded the first-born child in every family. This will result in a severe loss of information. Moreover, left truncation of the data, whether by calendar time or by birth order of child, will lead to the problem that the start of the sample does not coincide with the start of the stochastic process under study. The next problem is of measurement error as can be seen in the previous models. Infant death is on both side of the equation because the index child mortality risk is a function of the preceding child's survival status. Positively correlated measurement error in these variables will tend to create an upward bias in the scarring coefficient. This potential problem is addressed as follows in the present model. The dependent variable and the survival status of the preceding child were both coded as binary variables i.e. 1 if the child dies before the age of 12 months and 0 otherwise. The other problem related was with time inconsistency which has been sorted out in the present model. It is usually seen that data in retrospective surveys with regard to child, year of birth and death is available for the larger number of years. In our case, information was available for more than 35 years before the survey date. These surveys typically gather information on variables such as household assets, toilet facilities, electricity or access to piped water at the date of the survey. The time inconsistency problem is that, in such cases, data that pertain to the survey date are less informative. It means the information of certain predictors which are though important one are not available for all the children under study. In the present analysis, where the entire birth history of each tribal mother was used, the problem was even more severe. We, therefore, did not include any currently dated variables as explanatory variables in the model.

If we do not consider these potential problems, bias will be created because previous child's survival status and its correlation with survival status of index child will confound the causal interpretation of previous death in the family. In order to avoid these biases, modelling of the initial condition (mortality risk for first-born children) jointly with the dynamic mortality process for the second and higher-order births need to be applied (Arulampalam & Bhalotra, 2006, 2008; Heckman, 1987; Manski & McFadden, 1981; Oettinger, 2000; Wooldridge, 2010) .Present study used the dynamic panel data model along with the initial condition which will be discussed in the statistical modelling part , avoided such type of problems. Model with such initial condition will estimate the scarring effect without bias and shows the true picture of the impact of survival status of previous death of sibling in a tribal household on the survival status of the index child.

Data source

The data used in the study is from National Family health Survey-3 which was conducted in 2005-06. It interviewed 124385 ever married women aged 15-49 at the time of the survey. It has a complete retrospective history of births together with a record of child deaths for each mother, for a period spanning more than 35 years (1968-2006). Thus, it would give sufficient number of cases for analysis as well as we would be able to construct (unbalanced) panel data for mothers. Further full retrospective birth history has been used for all the statistical analysis in the study.

The empirical model

The dependent variable i.e. infant death and the survival status of the preceding child (i.e. lagged variable) were both coded as binary variables -one if a child died before the age of 12 months and zero otherwise. By taking child specific and mother specific covariates along with preceding child (lagged variable), the mixed effect model was applied. Children who were younger than 12 months at the time of the survey were dropped from the sample because they had not 12 months of exposure to mortality risk. When the index child was not singleton but instead twins they were also dropped from the model so that siblings should be identified properly.

Choice of Independent Variables:

The predictors (or factors) like, sex of the child, birth order, place of residence, mother's education, religion, caste, exposure to mass media, availability of toilet facility, type of fuel used for cooking and standard of living, mother receiving tetanus immunization during pregnancy, preceding birth interval were considered as the main determinants of infant and child mortality in all the Indian states (Pandey & Tiwary, 1993). Apart from the above factors, the tribal children, in fact, face certain adverse realities like insufficient food intake, frequent infections, and lack of access to health services. They also have the lack of awareness about environmental sanitation and personal hygienic practices, proper child rearing, breastfeeding and weaning practices (Pandey & Tiwary, 1993; Reddy, 2008). Women's autonomy, social class, mother's education and quality care received by the children has been cited as some of the reasons for clustering(Madise & Diamond, 1995).Causal factors that determine equality levels in the distribution of mortality risks for children between families or between mothers may conveniently be divided into two factors: Bio-demographic differentials and differentials in other socioeconomic characteristics of the families (and/or the mother) (Zaba & David, 1996). Bio-demographic factors include mother's age, fertility levels, and birth-spacing patterns, as well as inherited genetic disorders and the mother's medical condition and disease profile. Socioeconomic differentials includes characteristics of the families like income, occupation, and social class, and level of education, as well as factors relating to the wider environment of the child, such as the community, the neighbourhood, and the family's ecological and disease environment. The socioeconomic category also contains the much-discussed "maternal competence" factor (breastfeeding behaviour and behaviours or attitudes that affect the child health). Other authors have likewise stressed the connections among clustered mortality, family size, and fertility patterns(Ronsmans, 1995). Arulampalam have argued that deaths may cluster in the families not only because of unobserved heterogeneity—because siblings share certain traits—but also as a result of a causal process driven by the scarring effects. Heuristically, taking the idea that the death of one child 'scars' the family, making the next child in that family more vulnerable (Arulampalam & Bhalotra, 2006).The older studies often attribute death clustering to socio-demographic covariates: either a causal scarring effect (the previous sibling's survival status being included as a covariate) or unobserved heterogeneity (with family or community-specific effects) not both of them (Reddy, 2008).Some studies included both, but without accounting for the (bias induced by) potential correlation between the unobserved heterogeneity term and the previous child's survival-status dummy(Bolstad & Manda, 2001; Sian L Curtis et al., 1993; Ronsmans, 1995; Sastry, 1997).The present study is using econometric dynamic panel data model which at the same time capture both the unobserved heterogeneity and the causal positive or negative scarring mechanisms. This model has also been used in few of the earlier studies (also referred to as 'state dependence' if panel data are used (Arulampalam & Bhalotra, 2006, 2008; J. J. Heckman, 1987; Manski & McFadden, 1981; Wooldridge, 2010) . The model used in the study accounts for the endogeneity of previous sibling-survival status, thus avoiding the potential bias in previous studies.

Child specific factors in the model: Birth order, Sex of the child, Survival status of the previous sibling

Mother specific factors in the model: Her educational attainment and her partner's educational attainment, Year of birth of mother.

Birth order has been categorized into 5 categories viz. '1-2', 3, 4, 5 and 6+ birth order. The educational attainment of respondent's partner has been categorized into two categories viz. literate and illiterate. Respondent year of birth has been categorized into 3 categories those women who were born between 1956-1969, 1970-79 and after 1980.

Information on household assets, immunization, prenatal care, access to piped water, and relevant community-level variables were not used because they are time inconsistent (Rosenzweig & Wolpin, 1986).The same holds for breastfeeding. Covariates that have often been used in previous research which are time inconsistent (or endogenous) were avoided. The only potential endogenous

variable in the model is Yij-1, addressing this potential problem is an important part of the statistical approach that is taken here.

The purpose of the mother-level random effect, which was included in the model, was to control for the time-invariant component of these omitted variables, for example, for the fact that some mothers are more prone to breastfeed than others. Mother's age at birth and her cohort (year of birth) tends to capture trends in these omitted variables.

Statistical Model:

The dynamic panel data model applied was:

$$Y_{ij}^{*} = X_{ij}^{*}\beta + \gamma Y_{ij-1} + \alpha_i + u_{ij} \quad \ldots\ldots\ldots\ldots\ldots\ldots (1)$$

Let there be ni children of mother *i*. For child *j (j=1,2…,n_i)* of mother *i (i=1,2,…,N),*the unobservable propensity to experience an infant death, Y_{ij} * is specified in equation (1).Where *X* is a vector of strictly exogeneous observable child-specific and mother-specific characteristics and β is the vector of coefficients associated with *X* . The dynamic panel data model of equation (1) has the panel consisting of a naturally time ordered sequence of siblings within mothers. A child is observed to die when his or her propensity for death crosses a threshold; in this case $Y_{ij}^{*} > 0$ .The model has a random intercept α_i, to account for time-invariant mother specific unobserved characteristics. This picks up any correlation of death risks among siblings arising,for example, from shared genetic characteristics or from innate ability of their mother.

The model also includes the observed survival status of the previous siblings, Y_{ij-1}, the coefficient on which picks up scarring. The null of no scarring implies 0 .The estimated parameter γ should be interpreted as the 'average' effect of scarring over the time period considered. In models of this sort, the previous sibling's survival status, Y_{ij-1} is necessarily correlated with unobserved heterogeneity,α_i. In order to identify a causal effect, we need to take account of this correlation in the estimation. This is referred to as the 'initial conditions' problem [22-23]. We are thus able to model the initial condition of the process as a natural extension of the model given in (1). We specify the equation for the first-born child of each mother as

$$Y^{*}i1 = Zi'\lambda + \theta\,\alpha i + ui1 \quad \ldots\ldots\ldots (2)\ i = 1\ldots N \text{ and } j = 1$$

has a probability mass of 0.5 at zero and 0.5.

Where, Z_i is a vector of strictly exogenous covariates. In general, equation (2) allows the vector of covariates *Z* to differ from *X* in (1). However, we set the two vectors of covariates to be the same given that we observe the process from the start. Equations (1) and (2) together specify a complete model for the infant survival process. In this way, the endogeneity of the 'lagged dependent variable', that is, the previous child's survival status is taken into account. We assume that u_{ij} is independently distributed as a logistic distribution, and that the mother specific unobservable, α_i, are independent and identically distributed as normal. Marginalizing the likelihood function with respect to α_i, gives for mother *i*. Previous analyses of dynamic models with unobserved heterogeneity have shown the potential sensitivity of the estimates to the assumption made about the distributional form for unobserved heterogeneity, α_i (J. Heckman & Singer, 1984)**.** A weakness of the normality assumption is that it may not be flexible enough to account for the fact that some families never experience any child deaths and that, in some families, all children die (the mover-stayer problem). Our sample does not contain any families in which all children die in infancy. However, there are many families that experience no infant deaths, and this is accommodated by allowing for a single (empirically determined) mass at minus infinity: a very large negative value for α_i gives a very

small value for Y_{ij}^{*}, and hence a very small probability of observing death of the index child (Narendranathan & Elias, 1993). A test of $H_0 : \sigma_\alpha^2 = 0$ is a test that there are no unobservable characteristics of the mother in the model.

This can be tested by using a likelihood ratio test (or a standard normal test) but the test statistic will not have a standard chi-square (or a standard normal) distribution since the parameter under the null hypothesis is on the boundary of the parameter space. The standard likelihood ratio (normal) test statistic $0.5\ \chi^2(1)$ ($0.5N(0, 1)$) for positive values.

In addition to mother-specific unobserved heterogeneity, community level random effects were included in the model to account for the sampling design, which involved clustering at the community level. Failure to allow for community level unobserved heterogeneity in the likelihood maximization would provide consistent parameter estimators but inconsistent standard errors (Deaton, 1997). Although the model is multilevel, we have chosen to treat the community level effect as a nuisance parameter. This is because we cannot interpret a time invariant community level effect in any meaningful manner. To the extent that families migrate or the infrastructure of different communities develops at different rates, the assumption of a time invariant community effect is restrictive: we expect that children of the same mother, who are born at different dates, may experience different community level effects. In any case, in this paper, the focus is not on estimation of the variance that is associated with mothers versus communities but, rather, on robust estimation of the scarring effect, which is captured in the parameter γ.

Result

Sample characteristics of the study population

The sample characteristics of the tribal population in selected states of central and eastern India is shown in table no. 1. There are 12,534 families of which 20 percent belongs to STs. The distribution of samples shows that, over one-third of the tribal families' lives in Madhya Pradesh and nearly 20 percent are in Chhattisgarh. The children ever born to them is 9,069 of which 1,632 children were died at different ages in a period spanning more than 35 years from 1970 to 2006. Among these deaths nearly two-third children were died in their infancies. About experiencing an infant death by a family, there are about 70 percent families in the sample those who never had an infant death, but there are about 712 families that has experienced at least one infant death in their family. Further, the clustering of infant death in the present study is viewed among those families where two or more infant deaths had happened. Accordingly, we have 218 families for cluster analysis that has experienced at least two or more infant deaths. Out of total infant deaths nearly 55 percent are males and 45 percent are females. Preceding birth interval among these deaths represents, 60 percent of babies are born with less than 24 months interval. The effect of scarring is viewed for both the categories of preceding birth intervals, which are; firstly among those families which experienced two infant deaths and secondly among those families which experienced exactly one infant death assuming that this died infant was not the first child. The religious composition portrays, the majority of families belongs to Hindus (90 percent), followed by others and Christians. Further, parental educational attainment is also extremely poor among tribal population. Nearly 80 percent of mothers and 55 percent of fathers have no formal schooling and are illiterate. Merely 10 percent of mothers and 30 percent of fathers are secondary and above educated.

Clustering of infant deaths among families across different caste groups can be seen in table no. 2. Although, it is clearly evident from the table that majority of infant deaths comes from the OBC families i.e., 1446 infant deaths but percentage contribution of infant death per family is highest among tribal families. It has been recorded over 40 percent among STs, followed by SCs (35 percent), OBCs (30 percent) and is noted lowest among Other caste group. Further, it has been observed that over half of the infant death in SCs and STs were concentrated among those families,

which have experienced two or more infant deaths in their family, it is only 7 percent and 9 percent respectively. Therefore, maximum clustering is existed for tribal families and is least among Others. Overall the clustering of infant death in this region is 47 percent from just 6 percent of the families.

Clustering of infant deaths across different caste groups in central and eastern India

It is apparent from the table no. 3. that there is substantial amount of clustering of infant deaths by families across different caste as well. Nearly 95 percent of children belongs to families that contribute two or more children to the sample. Families with five or more children account for 15 percent of the families, but contribute nearly 40 percent of the total number of children in the sample. The mean number of children per family is 3.2. Further, about 10 percent of infant deaths were observed in the sample from 40,517 total birth. The magnitude of the family effect in the model is determined primarily by the number of deaths per family, since children in family in which there are a large number of deaths face higher mortality risks. Nearly 50 percent of the deaths in the sample comes from the 6 percent of families with two or more deaths. It is noteworthy to mention that, merely 1.6 percent of the families in the sample contribute three or more deaths; together these families account for almost 20 percent of the total number of deaths. Clustering of infant deaths within tribal families is presented in table no. 4. The sample have total 1,024 infant deaths among 2,494 tribal families. More than 95 percent of the children belong to families that contribute two or more children to the sample. Families with five or more children account for 17 percent of the families, but contribute over 50 percent of the total number of children in the sample. The mean number of children per tribal family is 3.6. It is clearly evident table that over half of the deaths in the sample come from the 9 percent of the families with two or more deaths. It's worth mentioning that, only 2.5 percent of the families in the sample contributes three or more deaths; together these families account for approximately one-fourth of the total infant deaths. Largely, we can conclude that the tribal women have high parity, as half of the tribal families have three or more children. It makes mothers and their child at a greater risk of death.

The probability of infant death using raw data is shown in column 1 of table 5. The raw data probabilities illustrates, the IMR is fairly high among tribal families. It is highest in Madhya Pradesh (124) followed by Chhattisgarh, Odisha (111) and is recorded lowest in Jharkhand (103). The high mortality in all four states indicate vulnerability of frequent infant deaths. There is not much differences in socio-economic and demographic indicators among families from different states. In column no. 2nd & 3rd, we have raw data probabilities for infant deaths based on survival status of the previous sibling to that of index child. Further, the difference between the two is calculated in column no. 4. It indicates the probability of extent of death clustering within a family. In view of that, we find the maximum probabilities of infant deaths clustering is existed in Chhattisgarh with 0.213. Although it is nearly two and half times lower in Jharkhand as compared to Chhattisgarh. It is interesting to note that the probability of death for index child is highest among the families of Chhattisgarh followed by Madhya Pradesh, when there is a prior infant death in the family, but on contrary the probabilities of death is observed highest among the families of Madhya Pradesh instead of Chhattisgarh which have prior survived infant in the family. The probability of extent of death clustering is maximum in Chhattisgarh and minimum in Jharkhand, shown in column 4. Column no. 5th shows an alternate representation of data in terms of relative odds. The relative odds ratio of infant death based on previous sibling's death varies from 2.33 to 5.24. Here, the relative risk shows that the effect of previous infant death in a family on the risk of death of the index child. The relative odds ratio in Chhattisgarh is 5.24 which means that a newborn in a tribal family will have five times more likely to risk of death, if one of his earlier sibling died as an infant as compared to those families where none of the earlier siblings had died as an infant. The relative odds

results based on the model is also quite close to what we have tried to capture from raw data and it is highly statistically significant ($p<0.01$) for all four states.

Overall, the data demonstrates high degree of death clustering in tribes from Central and Eastern India. These are the observed tendencies in the data. However, without any further analysis, it would be impossible to draw inferences about whether the reflected scarring was actually contributed in intra- family infant death concentration or it merely reflected the risks that are common to siblings on account of shared family characteristics (heterogeneity). Estimation of the statistical model allowed us to disentangle clustering effects into correlated risks amongst sibling and, conditional upon this, a causal effect of the death of one sibling on the risk of death of next sibling.

Model based clustering analysis: Scarring

Column 1 of Table 6 records the probability of extent of death clustering persistence in the raw data that was first displayed in Table 5. Estimates of scarring from the model that ignored unobserved heterogeneity are in Panel 1 and these were compared with estimates from the preferred model that allowed for it in Panel 2 of Table 6. The marginal effect associated with the estimated γ, the coefficient on the previous child's survival status, is computed as the difference between the sample averages of the probability of death predicted by estimated model when Yij-1=0 and when Yij-1=1.These were approximately equivalent to the first partial derivative of the conditional probability of infant death Yij=1 with respect to Yij-1. The scarring effect observed from the above explained model, is prominent among tribal families in all four states, after controlling exogenous factors at individual and family level for all unobserved differences between families. Further result shows that the death in infancy of a previous sibling in the family raises the probability of death for the index child during his infancy in the every state.

It is evident from the column 2 and 5 of that irrespective of the fact whether we consider mother level heterogeneity or not, we observe that the marginal effect of scarring is statistically significant for all four states in both the panels. The maximum effect of scarring is observed in Chhattisgarh in both panels. There is nearly two hundred infant deaths per thousand live birth that is clustered due to scarring in Chhattisgarh in Panel 1. If we look at the Panel 2, which allows unobserved heterogeneity in the model, we will find the effect of scarring related to clustering of infant deaths in family is notifiable in all states. The scarring associated infant death cluster in the family ranges from 73 infant deaths per thousand live births in Jharkhand ($p<0.01$) to a maximum of 182 infant deaths in Chhattisgarh ($p<0.01$).

If we did not take into account the survival status of previous sibling the estimate for infant mortality would be underestimated. The underestimation of mortality varied between 9 percent (Jharkhand) to 25 percent (Chhattisgarh) as shown in column 4 of table 6. A similar pattern can be observed in column no. 7 but the reduction is lesser. It implies that the unobserved or hidden factors can be responsible for clustering of infant deaths in the family to some extent. Scarring obtained from the model without controlling for unobserved heterogeneity explained 95 percent part of the raw data clustering in case of Chhattisgarh as shown in column [3]. Thus, Scarring is putting maximum impact in Chhattisgarh and it was a leading cause for explaining the clustering of infant deaths. The least was for Orissa where scarring explains only 82 percent part of the probability of death clustering.

Column [6] shows the percentage of raw clustering explained by scarring in the model which accommodated the unobserved factors. The part of scarring effect explained by the model of the raw data varied between 75 percent (Orissa) to 89 percent (Madhya Pradesh). We notice that, in column [3], the contribution of scarring explaining raw clustering of mortality in these two polar cases inflated to 82 percent and 90 percent respectively. The maximum inflation was there for Chhattisgarh. It was nearly 86 percent in column [6] and which increased to 96 percent in column [3]. Thus a model that fails to allow for unobserved heterogeneity overestimated the level of scarring

in every state, but it is also under-estimated the differences in scarring across the states. The estimates flowing from the model with no unobserved heterogeneity were, unsurprisingly, larger (Column [4]) than the same where unobserved heterogeneity factor is included in the model (Column [7]). For all states it was less than 3 per cent (column [7]) while the same for without unobserved heterogeneity, the reduction in infant mortality went up to 25 percent. It means once we controlled the heterogeneity factor on the risk of infant deaths between families residing in a particular region, the infant mortality reduction within a family due to scarring was very less. In other words, it would be wrong to neglect the familial and other components (unobserved factors) while estimating infant mortality.

Unobserved heterogeneity

Column 8 and 9 of Table 6 presented the estimated variance of the unobserved heterogeneity term and the proportion of total error variance attributed to this.

It showed that even after controlling for scarring effect, mother and child level specific explanatory variables in the model, there was heterogeneity in the risk of mother experiencing the infant deaths (either due to genetic or some other community level and other unobservable factors) in Jharkhand and M.P as estimated variance is coming significant at 1 percent as shown in column 8 of Table 6. It also showed that in these two states, familial and other components cannot be neglected while explain the clustering of infant deaths. The percentage of error variance, attributable to unobserved heterogeneity is shown in Column 9. It is lowest for Jharkhand as well as Madhya Pradesh and is highest for Chhattisgarh. The model shows error variance attributable to unobserved factor is statistically insignificant in Chhattisgarh and Odisha. Hence, in these two states scarring performs the vital role in defining clustering of infant deaths among tribal families. Demographers interpreted mother level effects in mortality equations as a measure of the importance of genetic traits [4] or, occasionally, other variables like maternal ability [5]. These results further shows that though various mother in the region contribute independently in clustering of deaths. It explains that irrespective of mother-specific factors inclusion in the model was not sufficient enough to explain variation in mother level variation in these two states. May be some other factors like community level factor are acting as troubling parameter (captured in the error term of the model).

Discussion & Policy Implications

The clustering of sibling infant deaths by family in demographic survey data provides researchers with an opportunity to estimate measure of familial association. Accordingly, we have tried to cluster infant deaths at family level for aboriginal's (tribal population) living in the forested hill tracts of peninsular India in four states.

Most of these tribes are the Particularly Vulnerable Tribal Groups. The challenge of inaccessibility to health services and their health care seeking behaviour seem to dominate the discourse in tribal health (Balgir, 2006).

Here in this research article, our discussion is primarily based on few specific findings from the study. We started examining the level of infant death clustering based on our observation from table no. 2. Here, we have estimated the extent of death clustering among various caste groups by family. The scheduled tribes have the highest number of families with at least two infant deaths (9 percent), whereas among Other caste group it is merely 3 percent. Further, among the total tribal infant deaths of 1,024, more than fifty percent of the index child (died infant) comes from the families having prior infant death. In, 1990 a study done by Monica Das Gupta on twentieth-century rural Punjab, demonstrated that families who had already experienced the loss of other children stood an increased chance of losing further children (Das Gupta, 1990). This relationship applied to a child's survival

chances at all stages of childhood following the neonatal period. It is understandable that, siblings share a large number of highly relevant demographic characteristics of the mother, such as the mother's age;her breastfeeding patterns; and her level of fecundity, which strongly correlates with length of birth interval. These factors are already well documented in previous studies on infant and child mortality(Hobcraft, McDonald, & Rutstein, 1983) .Parity, however or, more broadly, fertility patterns is an underestimated but highly important variable that is also relevant in itself, disregarding the related influence of mother's age or duration of marriage. Zaba and David (1996) have clearly demonstrated the causal relationship between high-parity women and high-risk mothers. In our results as well (table. No. 4) it is apparent that, nearly 80 percent of the infant deaths are attributed by families having four or more child. In other words, we can conclude that, the contribution of high parity women to infant deaths is extremely high as compared to mothers with low parity (less than four births). This phenomena can be explained in two ways; first, women who experience one or more child deaths are more likely than other women to progress to higher parities through either voluntary or physiological replacement mechanisms. Second, children born to high-parity mothers may suffer higher mortality risks than other children because of increased infection hazards, sibling competition, or the depletion of maternal resources as a result of short birth intervals and high numbers of births(Zaba & David, 1996). Earlier Miller et al. had also suggested that both selection effects and maternal depletion played a prominent role in the risk polarization among high-parity mothers (Miller, Trussell, Pebley, & Vaughan, 1992).

We have limited studies on death clustering, in which both scarring and unobserved heterogeneity were used simultaneously in a single model to assess the extent of death clustering. Wiji Arulampalam and Sonia Bhalotra in the year 2006 & 2008 have tried to capture Sibling Death Clustering in India, by using 2nd round of NFHS data, conducted in the year 1998-99. They have considered general population to capture the extent of death clustering irrespective of their caste composition. Whereas, we have restricted ourselves mainly on tribal families residing in the central and eastern states of India. In other words, there was heterogeneity in their samples and homogeneity in ours. Meanwhile between the two rounds of NFHS surveys (2nd & 3rd round), there were state divisions in year 2001. These states were carve out as Jharkhand and Chhattisgarh from Bihar and Madhya Pradesh. The newly formed states on which we did our analysis are mainly constituted by tribal population (over 25 percent).After observing voluminous amount of death clustering among tribal families in all the states, subsequently,we also tried to capture the effect of scarring under two different models (in Panel 1st & 2nd of table no. 6) by observing unobserved heterogeneity.

The scarring effect (both positive as well as negative) has played a deliberate role in intra-family death clustering in all states. It's a consequential finding from our study because, if we control the risk of death for the children of first and second order, then the experience gained by mother in rearing of these two children would automatically help in reducing the risk of infant death of the next child and this would reduce infant deaths significantly. The findings of scarring effects suggest a higher pay-off to interventions designed to reduce mortality than previously recognized. Manski called this as the activation of a social multiplier(Manski, 1999).This is because reducing the risk of death of a child automatically implies reducing the risk of death of his or her succeeding siblings. We found that, when we eliminate the scarring effect from the model, it would also underestimate the mortality levels up to certain extent. The mortality is underestimated in both the conditions, either we consider unobserved heterogeneity in the model or not. If we remove the scarring effect the underestimation of infant mortality is more in panel 1 than in panel 2. Further it shows that, when we include unobserved heterogeneity into the model and remove scarring from the model, the level of infant mortality remains almost same for all the states. Arulampalam and Bhalotra (2006) in their research have argued that deaths may cluster in families not only because of unobserved heterogeneity - because of siblings share certain traits - but also as a result of a causal process driven by the scarring effects on mothers and families from an earlier child death, making the next child in

the family more vulnerable. One of the ways in which interfamilial scarring occurs is when a mother quickly conceives again after the death of an infant through either resumed fecundity or the wish to replace the child that was lost. In addition, scarring may occur when an infant death causes the mother to become depressed, which may also have serious deleterious health effects on the next infant, either after its birth or in the womb. The authors demonstrate that the full impact of scarring can only be estimated by including the previous infant's survival status as a regressor while excluding the variable indicating the length of the previous birth interval. In their research on populations in three states in contemporary India, the authors do indeed find significant scarring effects, with the proportion of clustering explained by scarring varying from 14 percent to as much as 40 percent.

In Jharkhand and Madhya Pradesh, the estimated error variance attributable to mother specific unobserved heterogeneity is found to be very less though it is highly significant when we adjust it by parental educational (both mother and father) and by the maternal age at birth. This may be because of maternal characteristics and their behaviour are quite similar within the region or may be it is getting influenced by the community level factors or biological factors (both are treated as nuisance parameter or error term in our model) making every women at the equal risk of experiencing infant death. Although some unobservable factors are putting impact on family but inter family variation in risk of infant death is very less. Arulampalam and Bhalotra (2008) in their similar type of study found that the estimated variance of the mother specific unobservable was also significant in both the states but there was an inter-mother variation but our result is though significant but shows no mother level variation. So this could be a new finding that among tribes of Jharkhand and MP all mothers are equally vulnerable to face frequent child loss. This may be due the fact that in our study, the sample are of tribal families which are sharing similar type of characteristics throughout the region. Our finding contradicts in some way Arulampalam and Bhalotra (2008) findings. These differences may be due to the fact that they have taken entire population irrespective of their social class, which are in most cases are heterogeneous in their characteristics so the variation in their study due to mother specific unobservable is quite obvious. There is significantly unexplained no variations in the infant death risk, among the tribal families of Madhya Pradesh and Jharkhand. It may because of the unavailability of quality health care infrastructure, or it may be due to some genetic factor associated with mothers. In addition to the above factors, there may be the possibility that community level factors or other factors are also impacting on frequent infant deaths by the tribal mother. The mother level, insignificant unexplained variation in Chhattisgarh and Orissa can be attributed to homogeneity in culture, poverty and hazardous environmental factors in the entire state. Income, occupation, "Maternal competence" factor(which concerns the mother's breastfeeding behaviour or other attitudes and behaviours that affect her children's health), inherited genetic disorders and the mother's medical condition and disease profile may be other factors which explain the significant but no inter-family unobserved heterogeneity in two out of all the four central and eastern Indian states. Some of the previous studies too found that the unexplained variation between families or mothers cannot always be found, or, in some cases, it appears to be very modest (Das Gupta, 1990; Guo, 1993).Guo conducted his study in Guatemala, a Latin American country which is also a poor country found the similar result. Within contemporary Guatemala, for instance,(Guo, 1993)concluded that the variation between mothers was only slight once family income level and mother's educational attainment were controlled for. Guo attributed the lack of residual or unexplained variation to the fact that in developing countries such as Guatemala, mortality resulting from poverty and environmental factors is still high. Under these conditions, only genes favourable to early survival are passed on as a result of a process of natural selection. This argument highlights the importance of historical research into death clustering, as these studies almost invariably concern societies with high-mortality regimes. Given the low residual variation

between mothers, Guo also dismissed differences in the quality of maternal care as a major source of unexplained death clustering. Sastry too found inter-family heterogeneity to be small and unimportant in his study on Brazilian population, but only after controlling for heterogeneity at the community level. Sastry, therefore, argued, much in line with Guo that shared environmental conditions were more important determinants of shared frailty than either parental competence or genetic and biological factors. There is a whole range of other well-known socioeconomic determinants that might cause deaths to be clustered within certain families, all of which need to be considered when examining the determinants of clustering. We have ignored these factors, which include urban-rural differences, cultural differences between regions, ethnic differences, and other factors that have their expression in intercommunity mortality differentials. As has been argued, these shared "environmental" conditions are more crucial determinants of mortality hazards in both past and present societies than that of maternal competence, genetic factors, or biological determinants. Present study on tribes is an attempt to capture the death clustering behaviour giving due importance to cultural and ethnic differences.

Scarring involves responsive behaviour which may be amenable to policy because this shows there is some causal process whereby frequent infant death in the family is affected by the previous sibling's death in the family. If the causal process works through the fecundity mechanism, then policies that improve the uptake of contraception are likely to reduce death clustering among the tribes. More specific policy insight depends on identifying the mechanism underlying scarring. While unobserved heterogeneity involves largely untreatable factors like genes or fixed behaviour and unalterable family specific traits is central to the nature-nurture debate(Pinker, 2003). The studies cited here underlined the need for systematic and comparative research into the varying levels and shaping of the familial component of children's mortality hazards in different communities and time periods, as well as the conditions that determine this hazard's appearance or disappearance. Heterogeneity can have considerable implications for reproductive health and child survival programmes. In India, as in many other countries, health services are made available largely in response to demand. If child deaths are heavily concentrated in some families, this would suggest that substantial improvements in child mortality could be achieved by adopting the more cost-effective techniques of focusing healthcare resources specifically on the sub-group of families with a high risk of child death.

Scarring is of considerable theoretical interest, contributing to understanding the interrelations of family behaviour, fertility and mortality. It is also clearly of interest to policy making. It can also be useful in targeting interventions at the most vulnerable households. The government needs to not only try to reduce scarring mechanism among tribes, but it should also promote education, awareness among tribes about modern health facilities and infrastructure development in tribal areas. The policy initiatives should be pro tribe culture and it should be encouraging. Mass media based should information about government policies should be promoted in those areas.

Table 1: The sample characteristics of tribal population in selected states, India, 1970- 2006

Background Characteristics	**JH**	**OR**	**CG**	**MP**	**n**
Caste					
Schedule Caste	11.4	29.7	18.1	40.8	2020
Schedule Tribe	**17.8**	**22.3**	**26.0**	**34.0**	**2494**
Other Backward Class	20.5	16.7	24.7	38.1	4920
Other	13.7	38.6	10.1	37.5	3100
Characteristics of Schedule Tribes					
	JH	**OD**	**CH**	**MP**	**n**
Total births	18.2	22.4	27.1	32.3	9,069
Total deaths among total births	15.4	20.0	24.3	40.4	1,632
Under 5 deaths	15.7	20.0	24.0	40.3	1,493
Infant deaths	15.9	19.3	24.7	40.1	1,024
Families with at least					
One infant death	17.5	20.7	23.1	38.7	712
Two infant deaths	15.1	16.4	24.5	44.0	218
Children born in families with at least					
One infant death	16.9	21.6	27.1	34.5	1024
Two infant deaths	14.3	18.7	29.4	37.5	530
Preceding birth interval					
< 24 months	11.9	15.4	24.9	47.9	369
> = 24 months	18.1	21.5	23.2	37.2	290
Sex of child					
Male	16.4	19.8	27.2	36.5	570
Female	15.2	18.7	21.6	44.5	454
Religion					
Hindu	10.3	23.6	28.4	37.7	2,226
Muslim	66.4	22.1	11.5	0.0	89
Others	94.1	5.4	0.6	0.0	179
Mother's education					
Illiterate	17.1	22.9	24.7	35.3	1,969
Primary	13.6	20.4	29.8	36.3	235
Secondary	25.1	20.5	32.3	22.0	274
Higher and above	47.3	3.7	29.4	19.5	16
Father's education					
Illiterate	16.4	23.8	22.9	36.9	1321
Primary	8.8	23.5	31.2	36.5	466
Secondary	26.9	18.6	27.7	26.7	626
Higher and above	27.3	15.7	36.8	20.3	76

Note: Sample characteristics are based on complete retrospective birth history of the women between 1970- 2006, ased on 3rd round of NFHS (2005-2006) All 'n' values are unweighted; *Abbr*., JH- Jharkhand, OR- Odisha, CG- Chhattisgarh, MP- Madhya Pradesh

Table 2: Distribution of infant deaths among families of various caste group in selected states, India 1970- 2006

Families with infant deaths	Number of infant deaths

Infant deaths	SC*	ST**	OBC	Others	Total
0	1,535	1,782	3,856	2,644	9817
1	345	494	786	364	1,989
2	92	152	206	65	515
3	31	44	51	20	146
4	12	17	14	3	46
5	3	4	4	2	13
6	0	1	2	1	4
7	2	0	1	1	4
Total	2,020	2,494	4,920	3,100	12,534

SC*	ST**	OBC	Others	Total
0	0	0	0	0
345	494	786	364	1989
184	304	412	130	1030
93	132	153	60	438
48	68	56	12	184
15	20	20	10	65
0	6	12	6	24
14	0	7	7	28
699	1024	1446	589	3758

	Families with at least 2 infant death	Families with at least 2 infant death	Families with at least 2 infant death	Families with at least 2 infant death	Families with at least 2 infant death
Extent of infant death clustering	6.9	8.7	5.6	3	5.8

At least 2 infant death	At least 2 infant death	At least 2 infant death	At least 2 infant death	At least 2 infant death
50.64	51.75	45.64	38.2	47.07

Table: 3 Distribution of families according to number of children per family and number of child deaths per family in selected states, India, 1970-2006.

(General Population)	Infant deaths per family												
Children per family	**0**	**1**	**2**	**3**	**4**	**5**	**6**	**7**	Families	Total Children	Percent of Children	Total Infant death	Percent of Infant death
1	1,952	101	0	0	0	0	0	0	2,053	2,053	5.1	101	2.7
2	2,818	231	20	0	0	0	0	0	3,069	6,138	15.2	271	7.2
3	2,399	355	40	4	0	0	0	0	2,798	8,394	20.7	447	11.9
4	1,386	487	72	11	1	0	0	0	1,957	7,828	19.3	668	17.8
5	707	396	118	25	8	1	0	0	1,255	6,275	15.5	744	19.8
6	335	200	115	35	7	1	0	0	693	4,158	10.3	568	15.1
7	143	111	68	27	9	3	0	0	361	2,527	6.2	379	10.1
8	45	52	36	23	14	3	1	0	174	1,392	3.4	270	7.2
9	25	39	22	11	4	0	1	1	103	927	2.3	145	3.9
10	11	11	15	8	1	3	1	2	52	520	1.3	104	2.8
11	2	6	5	2	2	1	1	0	19	209	0.5	41	1.1
12	0	2	4	0	0	1	0	1	8	96	0.2	22	0.6
Total:	9,823	1,991	515	146	46	13	4	4	**12,542**	40,517	100.0	3760	100.0
Percent of children:	68.1	21.0	7.3	2.4	0.8	0.3	0.1	0.1	100.0	-	-	-	-
Percent of infant death:	0.0	53.0	27.4	11.7	4.9	1.7	0.6	0.7	100.0	-	-	-	-

Source: Author's tabulation of all singleton births in selected states for the period 1970-2006 based on the 3rd round of NFHS (2005-06), India

Table: 4 Distribution of families according to number of children per family and number of child deaths per family in selected states, India 1970-2006

Source: Author's tabulation of all singleton births in selected states for the period 1970-2006 based on the 3rd round of NFHS (2005-06), India

(Tribal Population)	No. of infant deaths per tribal family											
Children per family	**0**	**1**	**2**	**3**	**4**	**5**	**6**	Families	Total children	Percent Children	Total Infant death	Percent Infant death
1	335	30	0	0	0	0	0	365	365	4.0	30	2.9
2	403	58	7	0	0	0	0	468	936	10.3	72	7.0
3	417	72	12	2	0	0	0	503	1509	16.6	102	10.0
4	285	95	24	5	0	0	0	409	1636	18.0	158	15.4
5	176	94	31	7	3	0	0	311	1555	17.1	189	18.5
6	97	68	33	8	0	0	0	206	1236	13.6	158	15.4
7	47	36	16	6	6	2	0	113	791	8.7	120	11.7
8	11	20	14	6	4	0	0	55	440	4.9	82	8.0
9	7	16	9	7	4	0	0	43	387	4.3	71	6.9
10	4	4	4	3	0	2	1	18	180	2.0	37	3.6
11	0	1	1	0	0	0	0	2	22	0.2	3	0.3
12	0	0	1	0	0	0	0	1	12	0.1	2	0.2
Total:	1,782	494	152	44	17	4	1	2,494	9,069	100	1024	100
Percent of children:	60.8	24.6	9.6	3.2	1.4	0.4	0.1	100.0	-	-	-	-
Percent of infant death:	0.0	48.2	29.7	12.9	6.6	2.0	0.6	100.0	-	-	-	-

Table- 5: Raw data based probabilities of tribal infant deaths in selected states, India, 1970-2006

	Raw Data					Estimated Model
State	Probability of death **[1]**	Probability of death given previous sibling's infant death **[2]**	Probability of death given previous sibling's survival **[3]**	Death Clustering **[4]= [2]-[3]**	Relative Odds Ratio **[5]***	Relative Odds Ratio [p- value] **[6]****
Jharkhand:	0.103	0.157	0.075	0.083	2.330	2.27 [0.002]
Odisha:	0.111	0.179	0.080	0.099	2.500	2.22 [0.004]
Chhattisgarh:	0.111	0.283	0.070	0.213	5.240	4.90 [0.000]
Madhya Pradesh:	0.124	0.249	0.092	0.157	3.280	3.33 [0.000]

Note:*The relative odds ratio is calculated as the ratio of Column [2]/ (1- column [2]) to Column [3]/ (1- Column [3]).This is the exponential of the estimated scarring coefficient in a simple logit model that includes an intercept and the survival status of the previous sibling.

**Column [6] reports the equivalent numbers from the estimated model which control for the effects of other covariates and for unobserved mother- specific effects. These are exponentials of the estimated scarring coefficients γ. The p-values refer to those associated with the estimated γ.

Table 6: Effect of scarring on the clustering of infant mortality within the tribal families in selected states, India, 1970- 2006. Results are based on random effect of logit regression[1].

Panel 1: Model without unobserved heterogeneity (Col. 1 to 4)					Panel 2: Model with unobserved heterogeneity (Col. 5 to 9)				
State	**Raw data death clustering2**	**Estimated marginal effects3**	**Raw clustering explained by scarring (%)**	**Reduction in infant mortality if no scarring**	**Estimated marginal effects3**	**Raw clustering explained by scarring (%)**	**Reduction in infant mortality if no scarring**	**Estimated variance of the mother specific unobservable**	**Estimated intra-mother correlation coefficient**
	[1]	**[2]**	**[3]=[2]/[1]**	**(%)⁵ [4]**	**[5]**	**[6]=[5]/[1]**	**(%)⁵ [7]**	**[p-value][8]**	**[9]**
Jharkhand	0.083	0.0739 [0.002]	89.15	9.37	0.0737 [0.002]	88.86	1.02	0.00 [0.000]	0.000
Orissa	0.099	0.0806 [0.003]	81.51	12.6	0.0746 [0.004]	75.39	1.2	0.11 [0.170]	0.034
Chhattisgarh	0.213	0.2036 [0.000]	95.6	25.12	0.1823 [0.000]	85.77	2.8	0.15 [0.570]	0.046
Madhya Pradesh	0.157	0.1407 [0.000]	89.64	15.28	0.1398 [0.000]	89.05	2.1	0.00 [0.000]	0.000

Note: 1- The equation is estimated with the initial condition of the process. It means start of the process same as sample start. The marginal effect associated with scarring is significant at the 1 per cent level in all states. The p-values calculated to test whether the variance attributable to unobserved mother-specific heterogeneity is zero are computed accounting for the fact that the parameter under the null hypothesis is on boundary.

2.This is column [4] of Table 13.

3. The marginal effect is computed as the difference between the sample averages of the probability of death predicted by the estimated model when Yij-1=0 and when Yij-1=1(excluding the first born).This is approximately equivalent to the partial derivative of the conditional probability of death of the index child with respect to the covariate, Yij-1.

4.This is calculated as the difference between the predicted probability of death from the estimated model and predicted probability of death from the model when $\gamma=0$ is imposed after estimation, and excluding first-born children.

5.This is equal to column [8] as a proportion of estimated total variance

Source: National Family Health Survey III, 1970-2006

References

Arulampalam, W., & Bhalotra, S. (2006). Sibling death clustering in India: state dependence versus unobserved heterogeneity. Journal of the Royal Statistical Society: Series A (Statistics in Society), 169(4), 829-848.

Arulampalam, W., & Bhalotra, S. (2008). The linked survival prospects of siblings: evidence for the Indian states. Population studies, 62(2), 171-190.

Balgir, R. (2006). Tribal health problems, disease burden and ameliorative challenges in tribal communities with special emphasis on tribes of Orissa. Paper presented at the Proceedings of National Symposium on "Tribal Health" 19th-20th October.

Bhargava, A. (2003). Family planning, gender differences and infant mortality: evidence from Uttar Pradesh, India. Journal of Econometrics, 112(1), 225-240.

Bolstad, W. M., & Manda, S. O. (2001). Investigating child mortality in Malawi using family and community random effects: A Bayesian analysis. Journal of the American Statistical Association, 96(453), 12-19.

Bongaarts, J., & Potter, R. E. (2013). Fertility, biology, and behavior: An analysis of the proximate determinants: Academic Press.

Caldwell, J. C. (1986). Routes to low mortality in poor countries. Population and development review, 171-220.

Claeson, M., Bos, E. R., Mawji, T., & Pathmanathan, I. (2000). Reducing child mortality in India in the new millennium. Bulletin of the World Health Organization, 78(10), 1192-1199.

Cleland, J. G., & Sathar, Z. A. (1984). The effect of birth spacing on childhood mortality in Pakistan. Population studies, 38(3), 401-418.

Curtis, S. L., Diamond, I., & McDonald, J. W. (1993). Birth interval and family effects on postneonatal mortality in Brazil. Demography, 30(1), 33-43.

Curtis, S. L., & Steele, F. (1996). Variations in familial neonatal mortality risks in four countries. Journal of Biosocial Science, 28(02), 141-159.

Das Gupta, M. (1990). Death clustering, mothers' education and the determinants of child mortality in rural Punjab, India. Population studies, 44(3), 489-505.

Das, M. B., Kapoor, S., & Nikitin, D. (2010). A closer look at child mortality among Adivasis in India. World Bank Policy Research Working Paper Series.

Dyson, T., & Moore, M. (1983). On kinship structure, female autonomy, and demographic behavior in India. Population and development review, 35-60.

Gazdar, H., & Dreze, J. (1996). Uttar Pradesh: The burden of inertia. Indian development: Selected regional perspectives, 33-128.

Guo, G. (1993). Use of sibling data to estimate family mortality effects in Guatemala. Demography, 15-32.

Gupta, M. D. (1997). Socio-economic status and clustering of child deaths in rural Punjab. Population studies, 51(2), 191-202.

Heckman, J., & Singer, B. (1984). A method for minimizing the impact of distributional assumptions in econometric models for duration data. Econometrica: Journal of the Econometric Society, 271-320.

Heckman, J. J. (1987). The incidental parameters problem and the problem of initial conditions in estimating a discrete time-discrete data stochastic process and some Monte Carlo evidence: University of Chicago Center for Mathematical studies in Business and Economics.

Hill, K., & Pebley, A. R. (1989). Child mortality in the developing world. Population and development review, 657-687.

Hobcraft, J., McDonald, J. W., & Rutstein, S. (1983). Child-spacing effects on infant and early child mortality. Population Index, 585-618.

Kennedy, K. I., & Visness, C. M. (1992). Contraceptive efficacy of lactational amenorrhoea. The Lancet, 339(8787), 227-230.

Levels & Trends in Child Mortality, Report 2014, UNICEF. Retrieved from http://www.unicef.org/media/files/Levels_and_Trends_in_Child_Mortality_2014.pdf

Lynch, K. A., & Greenhouse, J. B. (1994). Risk factors for infant mortality in nineteenth-century Sweden. Population studies, 48(1), 117-133.

Madise, N. J., & Diamond, I. (1995). Determinants of infant mortality in Malawi: an analysis to control for death clustering within families. Journal of Biosocial Science, 27(01), 95-106.

Maharatna, A. (1998). On tribal fertility in late nineteenth and early twentieth century India. Harvard Center for Population and Development Studies, Harvard University: Cambridge, MA, USA.

Maharatna, A. (2000). Fertility, mortality and gender bias among tribal population: an Indian perspective. Social Science & Medicine, 50(10), 1333-1351.

Maharatna, A. (2005). Demographic perspectives on India's tribes: Oxford University Press.

Manski, C. F. (1999). Identification problems in the social sciences: Harvard University Press.

Manski, C. F., & McFadden, D. (1981). Structural analysis of discrete data with econometric applications: Mit Press Cambridge, MA.

Ministry of Tribal affairs. (2015). Retrieved from http://tribal.nic.in/

Miller, J. E., Trussell, J., Pebley, A. R., & Vaughan, B. (1992). Birth spacing and child mortality in Bangladesh and the Philippines. Demography, 29(2), 305-318.

Mosley, W. H., & Chen, L. C. (1984). An analytical framework for the study of child survival in developing countries. Population and development review, 10, 25-45.

Murthi, M., Guio, A.-C., & Dreze, J. (1995). Mortality, fertility, and gender bias in India: A district-level analysis. Population and development review, 745-782.

Narendranathan, W., & Elias, P. (1993). INFLUENCES OF PAST HISTORY ON THE INCIDENCE OF YOUTH UNEMPLOYMENT: EMPIRICAL FINDINGS FOR THE UK†. Oxford Bulletin of Economics and Statistics, 55(2), 161-185.

Oettinger, G. S. (2000). Sibling similarity in high school graduation outcomes: Causal interdependency or unobserved heterogeneity? Southern Economic Journal, 631-648.

Pandey, G., & Tiwary, R. (1993). Demographic characteristics in a tribal block of Madhya Pradesh. Social Change, 23(2/3), 124-131.

Pinker, S. (2003). The blank slate: The modern denial of human nature: Penguin.

Preston, S. H. (1985). Mortality in childhood: lessons from WFS.

Rahman, A., Iqbal, Z., Bunn, J., Lovel, H., & Harrington, R. (2004). Impact of maternal depression on infant nutritional status and illness: a cohort study. Archives of general psychiatry, 61(9), 946-952.

Rawlings, J. S., Rawlings, V. B., & Read, J. A. (1995). Prevalence of low birth weight and preterm delivery in relation to the interval between pregnancies among white and black women. New England Journal of Medicine, 332(2), 69-74.

Reddy, S. (2008). Health of Tribal Women and Children: An Interdisciplinary Approach. Indian Anthropologist, 61-74.

Rindfuss, R. R., Palmore, J. A., & Bumpass, L. L. (1982). Selectivity and the analysis of birth intervals from survey data. Paper presented at the Asian and Pacific Census Forum.

Ronsmans, C. (1995). Patterns of clustering of child mortality in a rural area of Senegal. Population studies, 49(3), 443-461.

Rosenzweig, M. R., & Wolpin, K. I. (1986). Evaluating the effects of optimally distributed public programs: Child health and family planning interventions. The American Economic Review, 76(3), 470-482.

Sastry, N. (1997). Family-level clustering of childhood mortality risk in Northeast Brazil. Population studies, 51(3), 245-261.

Steer, R. A., Scholl, T. O., Hediger, M. L., & Fischer, R. L. (1992). Self-reported depression and negative pregnancy outcomes. Journal of clinical epidemiology, 45(10), 1093-1099.

Stephansson, O., Dickman, P. W., & Cnattingius, S. (2003). The influence of interpregnancy interval on the subsequent risk of stillbirth and early neonatal death. Obstetrics & gynecology, 102(1), 101-108.

THE WORLD BANK. (2015 July 23). Retrieved from http://data.worldbank.org/indicator/SP.DYN.IMRT.IN

UN Millennium Project 2002-2006, UNDP Retrieved from http://www.unmillenniumproject.org/goals/gti.htm

Whitehouse, C. (1982). THE HEALTH OF CHILDREN. A REVIEW OF RESEARCH ON THE PLACE OF HEALTH IN CYCLES OF DISADVANTAGE: British Journal of General Practice.

World Health Organization. (2011). Global health observatory data repository. 2011. See http://apps. who. int/ghodata.

Wooldridge, J. M. (2010). Econometric analysis of cross section and panel data: MIT press.

Zaba, B., & David, P. H. (1996). Fertility and the distribution of child mortality risk among women: an illustrative analysis. Population studies, 50(2), 263-278.

Zenger, E. (1993). Siblings' neonatal mortality risks and birth spacing in Bangladesh. Demography, 30(3), 477-488.

Assessment of clustering of deaths among families with declining levels of mortality in India, 1992-2006

Mukesh Ranjan
International Institute for Population Sciences (IIPS)
Mumbai, Maharashtra
India

Abstract

In the changing socio-economic environment in the country in the post liberalization period, the mortality levels have been declined substantially but we found that the pace of reduction in mortality is much faster than the pace in reduction of clustered deaths in families. Though the high risk families have declined but now almost similar level of clustered death is experienced by lower number of families. Utilizing the pooled retrospective birth history data of the three rounds of National Family Health Survey data (1992-2006) in random effect logit model, we found that after adjusting the socio-bio demographic factors in Model 2, the odds of infant deaths for interaction of time with previous death in the family has increased but the Infant mortality has declined substantially as captured by the time factor and constant. Nearly 10 percent variation (intraclass correlation) in infant mortality is explained by the mother level unobserved factors.

Introduction

Many prior research have been conducted on the levels, trends and correlates of infant mortality but the familial clustering of infant death still requires attention as a major contributor of infant mortality is proportion of clustered deaths in high risk families. This phenomena is occurring in both developed as well as developing countries, India is no exception to it. It has been observed in Punjab (Das Gupta 1990, Gupta 1997),Orissa(Pradhan and Arokiasamy 2005),some selected states in India (Arulampalam and Bhalotra 2006, Arulampalam and Bhalotra 2008), Guatemala (Guo and Rodriguez 1992, Guo 1993), Brazil (Curtis, Diamond et al. 1993), Bangladesh (Zenger 1993), Senegal (Ronsmans 1995), and Kenya (Zaba and David 1996; (Omariba, Rajulton et al. 2008). Each of these studies specifically points to their observation that the survival chances of children in the same family are more alike than those of children born in different families.

This phenomenon of clustered distribution of infant deaths within families was first identified in 1990s by Monica Dasgupta in her study entitled "Death clustering, mothers' education and the determinants of child mortality in rural Punjab, India" and she called this phenomena as death clustering. Since then this issue of death clustering has been on research agenda when infant or child mortality were talked off. It is so because right from its definition to its methodology, there is not much unanimity among the scholars about how to capture such a complex phenomenon .On the basis of **v**arious research papers, scholars have added many dimensions to it. Mostly it has been defined consistently as:

i). Counting the number of women who have experienced more than one child loss and extent of deaths concentrated in such families (Das Gupta 1990, Curtis, Diamond et al. 1993, Guo 1993, Curtis and Steele 1996).

ii).Whether the number of women with the different number of child deaths exceeds which would be expected if the risks were constant for all women and their children (Ronsmans 1995, Zaba and David 1996).

Two main aspects of death clustering which make it an important issue in the analysis of mortality: first aspect is the methodological one in the sense that observations are not independent since siblings living in the same family have shared similar environment and they share the same genetic pool and socioeconomic position and second aspect is clustering in itself (Arulampalam and Bhalotra 2006).

Present study have tried to address the changing nature of clustered deaths in families when there is a declining trends in almost all mortality indicators. The issue is also relevant because the study period of 1992-2006 is also a period of post liberalization in India where the income, opportunity and choices for availing various services among the people have increased exponentially. The government spending in various sectors including health, infrastructure, Information technology, e-governance etc. has also led to the drastic change in socio-economic set up in the country.

Data source and Methodology

We have done all our analysis on pooled the complete birth history data of three rounds of National Family Health Survey (NFHS) (NFHS-1(1992-93), NFHS-2 (1998-99) & NFHS-3(2005-06)) in order to see that over the three time periods how the clustered deaths in families has changed. Bivariate analysis was performed to get the familial clustering of infant deaths. Random effect logit model was applied to see the change in clustering of infant deaths within families. Dependent variable was infant deaths which coded as 0 “no infant deaths” and 1 “infant deaths”. Similarly, previous deaths in families (refers to mothers) was included as one of the covariates which was captured through a lagged variable coded as 0 “no previous infant deaths” 1 “previous infant death ”.This variable was considered as the proxy for capturing clustering of infant death clustering at family level.After pooling the three period data and we have generated a time variable for capturing the three surveys and made its dummy. These time dummies along with the interaction of time and previous death was included in the model as predictors. We have captured the change in clustering of deaths at family level through this interaction term but the change in infant mortality was captured through time dummies as well as constant term. Other covariates are included in the model based on literatures and their relevance.

Results:

Table 1, 2, 3 and 4 clearly reflects that Neonatal mortality, Infant mortality and U5 child mortality has reduced a lot in a period of 15 years .In the same time period clustering of deaths in families has also reduced but the pace of reduction in neonatal, infant and U5 child mortality is substantially much faster than the reduction of clustering of deaths in families. If we see tables 3 & table 4, it can be concluded that though there occurred a huge reduction in families which experienced two or more deaths but the level of clustered deaths in families remained at almost similar level. In other words, now the same number of deaths is concentrated in smaller number of families.

If we see the table5, after adjusting the socio-economic and bio demographic factors in model 2 we found that previous death, time variable and their interactions are all statistically significant. If we see the interaction for change in clustering over time we conclude that the odds of having infant deaths is 10 percent higher ($p<0.01$) if there is previous death in NFHS-2 in comparison to previous death in NFHS-1.Similarly,the the odds of having infant deaths is again 10 percent higher ($p<0.01$) if there is previous death in NFHS-3 in comparison to previous death in NFHS-1.If we see the constant term as well as time factor in both Model1 and Model2 the odds of having infant death has been reduced over the survey periods. This led to very contrasting results that on one hand our bivariate analysis shows clustering of deaths among families are reducing at lesser pace than reduction in infant mortality but our multivariate result shows that over the three survey periods infant mortality has declined significantly but the clustering of deaths among families has increased significantly over the years. Out of total unexplained variation in infant mortality, mother level unobserved variation has contributed 10 percent ($p<0.01$) as measured by intra class correlation coefficient.

Conclusion

It is very important to understand that the 15 year period between 1992-2006 is also the period of liberalization and globalization of Indian market and there is a huge increase in income sources and opportunities among the population. In that scenario of changing socio-economic environment in India mortality indicators have improved and but still it seems that the clustering of deaths in families have not reduced like mortality indicators. Still there exists families who had not been affected by the social and economic change and they are contributing a higher number of neonatal and infant deaths. In this context our study is more relevant that why the development has not improved the condition of the households where these high risk families are located.

Table1: Trends of NMR, IMR and U5MR in India.

	Neonatal mortality (NMR)	Infant mortality (IMR)	U5 child mortality (U5MR)
NFHS-1	48.6	78.5	109.3
NFHS-2	43.4	67.6	94.9
NFHS-3	39.00	57.0	74.3

Table2: Relative change from NFHS-1 in NMR, IMR and U5 mortality in India.

	Relative change NMR	Relative change IMR	Relative change U5MR
NFHS-1	Reference	Reference	Reference
NFHS-2	-10.70	-13.89	-13.17
NFHS-3	-19.75	-27.39	-32.02

Table 3: Trends of clustering of deaths in India.

	Percent Families	Percent Neonatal deaths concentration	Percent Families	Percent Infant deaths concentration	Percent Families	Percent U5Child deaths concentration
NFHS-1	3.2	41.4	6.4	50.9	1.7	36.2
NFHS-2	2.9	41.3	5.2	47.8	1.3	32.2
NFHS-3	2.2	37.8	3.8	43.6	0.76	27.7

Table 4: Relative change from NFHS-1 survey of clustering deaths among families in India.

	Families	Clustering of Neonatal deaths	Families	Clustering of Infant deaths	Families	Clustering of U5MR deaths
NFHS-1	Reference	Reference	Reference	Reference	Reference	Reference
NFHS-2	-8.4	-0.3	-18.5	-6.2	-23.0	-10.9
NFHS-3	-24.5	-8.4	-27.1	-8.8	-43.3	-14.0

Table 5: Random effect logit model result.

Infant death	Model1 (OR)		Model2 (OR)	
	Pooled estimates	P-value	Pooled estimates	P-value
Previous infant death				
No	1		1	
Yes	1.80 (0.042)	0.000	2.08(0.049)	0.000
Time*previous infant death				
NFHS-1*previous infant death	1		1	
NFHS-2*Previous infant death	1.05(0.032)	0.090	1.10(0.035)	0.002
NFHS-3*Previous infant death	1.07(0.035)	0.032	1.10(0.038)	0.005
Age				
13-20			1	
20-34			1.04 (0.082)	0.656
35+			1.26 (0.099)	0.003
Place of residence				
Urban			1	
rural			1.21(0.018)	0.000
Child sex				
Female			1	
male			1.02(0.011)	0.047
Birth order				
3 or less			1	
births_3plus			0.98 (0.012)	0.058
Birth interval				
less than 12 months			1	
12-24 months			0.54(0.012)	0.000
more than 24 months			0.27(0.006)	0.000
Religion				
Hindu			1	
Muslims			0.81(0.015)	0.000
Other_religion			0.66(0.016)	0.000
Caste				
SC			1	
ST			0.92(0.020)	0.000
Other_caste			0.95(0.015)	0.003
Partner's education				
Higher			1	
Illiterate			1.35 (0.040)	0.000
Primary			1.25 (0.037)	0.000
Secondary			1.10(0.031)	0.000
Partner working				
Yes			1	
No			0.95 (0.032)	0.096
Respondent working				
Yes			1	
No			0.98(0.012)	0.108
Respondent Education				
Higher			1	
Illiterate			2.40(0.143)	0.000
Primary			1.88 (0.113)	0.000
Secondary			1.46(0.087)	0.000
Time				
Nfhs-1 (1992-93)	1		1	
Nfhs-2 (1998-99)	0.86 (0.010)	0.000	0.89 (0.013)	0.000

Nfhs-3 (2005-06)	0.73(0.009)	0.000	0.79(0.013)	0.000
Constant	0.068(0.001)	0.000	0.01(0.001)	0.000
Mother level unobservable(sigma_u)	0.76(0.011)		0.61 (0.014)	
Intraclass correlation	0.15 (0.004)		0.10(0.004)	
Wald statistic	2075.16		13427.32	
Loglikelihood	-209202.45		-131956.64	
Chi sq	0.000		0.00	

References

Arulampalam, W. and S. Bhalotra (2006). "Sibling death clustering in India: state dependence versus unobserved heterogeneity." Journal of the Royal Statistical Society: Series A (Statistics in Society) 169(4): 829-848.

Arulampalam, W. and S. Bhalotra (2008). "The linked survival prospects of siblings: evidence for the Indian states." Population Studies 62(2): 171-190.

Guo, G. and G. Rodriguez (1992). "Estimating a multivariate proportional hazards model for clustered data using the EM algorithm, with an application to child survival in Guatemala." Journal of the American Statistical Association 87(420): 969-976.

Das Gupta, M. (1990). Death clustering, mothers' education and the determinants of child mortality in rural Punjab, India. Population studies, 44(3), 489-505.

Gupta, M. D. (1997). Socio-economic status and clustering of child deaths in rural Punjab. Population studies, 51(2), 191-202.

Guo, G. (1993). "Use of sibling data to estimate family mortality effects in Guatemala." Demography: 15-32.

Pradhan, J. and P. Arokiasamy (2005). "High Infant and Child Mortality In Orissa: An Assessment of Possible Reasons." Population, Space and Place.

Compound Run Length Distribution: Properties and Applications

Athanasios C. Rakitzis[1] and Markos V. Koutras[2]

[1] Department of Mathematics, University of Aegean, 83200 Karlovasi, Samos, Greece
(E-mail: arakitz@unipi.gr)
[2] Department of Statistics and Insurance Science, University of Piraeus, 18354 Piraeus, Greece
(E-mail: mkoutras@unipi.gr)

Abstract. In the present work we study a compound run length distribution of runs-rules based control charts, by exploiting the fact that the distribution of the run length L is a discrete Phase-type one. The term compound run length distribution refers to the distribution of the random sum $S_L = \sum_{t=1}^{L} Y_t$, where $Y_1, Y_2, \ldots$, is a sequence of independent and identically distributed, positive valued random variables, independent of L. The suggested framework, provides a more realistic scenario, as compared to the classical control chart setup. Finally, an extensive numerical study illustrates how the performance of compound control charts, suitable for monitoring Poisson observations, can be evaluated in terms of the distribution of S_L.
Keywords: Control charts, geometric distribution, runs rules, phase-type distributions, Poisson distribution, time between inspections, statistical quality control.

1 Introduction

Control charts are considered as one of the most important tools of statistical process monitoring (SPM). Practitioners use them for monitoring a process and identifying possible changes in it. Traditionally, control charts have been developed for the monitoring of continuous characteristics. The most popular schemes are the $\bar{X}$, the S and the R charts; See Montgomery[18] for more details.

The usual approach when implementing a control chart is to collect samples from the process, determine the value of a charting statistic (e.g., sample mean) and plot this value on the chart, against one or more control limits. Important information for the performance of a control chart, is conveyed by the respective run length (RL) distribution, that is the distribution of the number L of points plotted on the chart until an out-of-control (OOC) signal is initiated. A comprehensive summary of the performance of a control chart is provided by the mean and the standard deviation of the run length distribution, i.e., the so-called average run length (ARL) and standard deviation run length ($SDRL$). Percentiles of the run length distribution, such as the median run length (MRL) may also be used for additional or complementary information of the control chart performance.

In the classical setup, the time between the collection of successive samples is not taken into account. However, for specific applications, this time may be

of special importance; moreover in many cases this time may have a stochastic nature, therefore it should be described by an appropriate (positive) random variable (r.v.). Under this scenario, instead of focusing on the number of points plotted on the chart until an OOC signal is generated, a more realistic statistic to be considered is the total time (in appropriate time units, e.g., hours, days etc) until the OOC signal. Thus, the control chart's performance in that case is associated to the *time to signal* (TS) and its distribution.

Let us consider the r.v. $S_L = \sum_{t=1}^{L} Y_t$ where $Y_1, Y_2, \ldots$ is a sequence of independent and identically distributed (IID) positive valued r.v.'s, independent of L. We denote by L the RL of a control chart while the Y_t's denote the times between successive samplings. Then, the compound r.v. S_L describes the TS of a surveillance/monitoring procedure (i.e., a control chart), under a particular sampling policy with intermediate times between successive samples $Y_1, Y_2, \ldots$. More specifically, let us consider the following example: An external inspector, or examiner, performs inspections of (identical) units at random times, so that the manufacturer under inspection cannot figure out the exact time that the process will be evaluated. Let Y_1 be the time when the first inspection occurs; the number of defects on the inspection unit is also assumed to be a r.v., say X_1. Thus, the first inspection (or the collection of the first sample) takes place after Y_1 time units, yielding X_1 defects on the unit (or on the sample). In a similar manner, let Y_t be interarrival time between the $(t-1)^{th}$ and t^{th} inspection, and X_t be the respective number of defects at the t^{th} inspection, $t \geq 2$. The inspector uses only the X_t values in order to declare a process as OOC but the total time until an OOC signal is triggered equals $\sum_{t=1}^{L} Y_t$.

One can easily come up with many alternative frameworks of applied nature where the aforementioned setup may be practiced. Let us consider the case where lots of items are subject to inspection under an acceptance sampling scheme. Instead of inspecting every lot (e.g., due to cost reasons), only a fraction of them is inspected. We assume that each lot is inspected with probability θ, so the number Y_t of produced lots between the $(t-1)^{th}$ and the t^{th} inspected lot is a r.v. After the inspection of the t^{th} lot, the number of defects X_t found in it is recorded. Under this scenario the r.v. S_L denotes the total number of the produced lots until the end of inspection or a change in the inspection level.

In this work, we study the distribution of the compound run length S_L, in the case of upper one-sided control charts that are suitable for monitoring Poisson observations. The most common approach is to use the classical Poisson-based c-chart, (Montgomery[18]) either with or without supplementary runs rules. For the time between inspections, we assume that it is described by a geometric r.v. with parameter θ, i.e., $Y_t \sim Ge(\theta)$, $t \geq 1$. Next, we consider both the ordinary upper one-sided c-chart and an upper one-sided runs-rules based c-chart. An important role in our analysis plays the fact that in both cases, L is a discrete phase-type r.v. Thus, the distribution of S_L can be studied by using the methodology of Koutras and Eryilmaz[14] and Koutras et al.[16].

The structure of the paper is as follows. In Section 2 we describe the operation of the upper one-sided Poisson control charts we shall analyse, while in Section 3 we provide the necessary general results for the study of the run

length distribution L as well as for any compound r.v. of the form $S_L = \sum_{t=1}^{L} Y_t$, where L is a discrete phase-type r.v. Section 4, contains the results of an extensive numerical study along with a discussion on the practical use of these results. Finally, in Section 5 we state the concluding remarks.

2 Control Charts for Poisson Observations

Assume that a process produces identical units and each unit is inspected with probability θ $(0 < \theta < 1)$. When a unit is selected for inspection, the number X of defects on it is recorded. The number of defects registered during the inspection process will be denoted by $X_1, X_2, \ldots$, whereas the intermediate times between the inspections by $Y_1, Y_2, \ldots$ (Y_1 denotes the time until the first inspection). Clearly, Y_1 is a geometric r.v. with parameter θ, i.e., $Y_1 \sim Ge(\theta)$. Let us also assume that the number X_1 of defects recorded at first inspection follows a Poisson distribution with parameter μ, i.e., $X_1 \sim P(\mu)$. In a similar manner, the time Y_t between the $(t-1)^{th}$ and the t^{th} inspected unit, $t \geq 2$, is a geometric r.v. with parameter θ, i.e., $Y_t \sim Ge(\theta)$, whereas the number X_t of defects recorded at this point will be considered as a Poisson r.v. with parameter μ, i.e., $X_t \sim P(\mu)$.

We denote by μ_0 the in-control (IC) value of μ and assume that when the process shifts out-of-control, the value of μ increases, i.e., for an OOC process we have $\mu = \mu_1 > \mu_0$. Clearly, when the number of defects exceeds an upper threshold x_0, an indication is provided for a possible increase on the average number of defects (process deterioration). Should this situation occur, an OOC signal should be initiated. Usually, the threshold x_0 is used as an upper control limit of the chart. Obviously, one would wish to identify situations like this, as soon as possible. The control charts that can be used in order to do so, are described in the subsequent Sections. In this work we also assume that μ_0 is known or has been accurately estimated from a sufficiently large, Phase I in-control sample.

2.1 The Upper One-Sided *c*-Chart

The natural approach to monitor the process and detect an upward shift in μ_0, is to define an upper control limit UCL for the upper one-sided c-chart (a Shewhart-type chart) and plot the successive values X_t, $t \geq 1$, on it until a point exceeds the UCL for first time. Let $X_1, X_2, \ldots$ be independent $P(\mu_1)$ r.v.'s, where $\mu_1 = \delta\mu_0$ is the OOC parameter value for μ ($\delta > 1$ is a constant reflecting the shift in μ_0 while for $\delta = 1$, the value of μ_0 remains unchanged). Thus, the probability $\beta = P(X_t > UCL)$ that the number X_t of non-conformities exceeds the UCL, equals

$$\beta = 1 - F_P(UCL|\mu_1),$$

where $F_P(x\,|\mu)$ is the c.d.f. of the Poisson distribution with parameter μ.

Let L be the number of points plotted on the chart, until it gives an OOC signal for the first time, i.e.,

$$L = \inf\{\ell \geq 1 : X_\ell > UCL\}.$$

Clearly, L is the run length of the upper one-sided c-chart, which is a geometric r.v. with parameter β, i.e., the p.m.f. and the c.d.f. of L are given by $f_L(\ell) = \beta(1-\beta)^{\ell-1}$ and $F_L(\ell) = 1-(1-\beta)^{\ell}$, respectively, for $\ell = 1, 2, \ldots$. Consequently, the ARL and $SDRL$ of the upper one-sided c-chart read

$$ARL = \frac{1}{\beta}, \;\; SDRL = \frac{\sqrt{1-\beta}}{\beta},$$

while the γ-percentile point L_γ of L, $\gamma \in (0,1)$, satisfies the inequality $P(L \leq L_\gamma) \geq \gamma$ and it is equal to

$$L_\gamma = \lceil \frac{\ln(1-\gamma)}{\ln(1-\beta)} \rceil.$$

2.2 The Upper One-Sided r-of-m c-Chart

It is known that, in general, Shewhart-type control charts are rather insensitive in detecting small and moderate shifts in the parameters of a process. The use of runs-rules based schemes is a simple approach for solving this problem.

Consequently, due to their easy practical implementation and interpretation, runs-rules based schemes have been studied by several researchers (see, for example, Acosta-Mejia[1], Bersimis et al.[4], Castagliola et al.[6], Khoo[12], Klein[13], Lucas et al.[17], Rakitzis and Antzoulakos[20], Riaz et al.[22] and Wu et al.[24]). We refer to Koutras et al.[15] for an up-to-date review on control charts with supplementary runs rules.

Motivated by the aforementioned works, we consider next several control schemes with runs rules in order to improve the capability of the ordinary upper one-sided c-chart to detect an increase in μ_0. More specifically, we consider a scheme which gives an OOC signal if r-out-of-m consecutive points ($2 \leq r \leq m$), are plotted above an appropriate upper control limit UCL. The UCL is determined so as to achieve the desired IC performance. Next, we will only focus on the 2-out-of-3, 3-out-of-4 and 4-out-of-5 runs rules, i.e., $(r,m) \in \{(2,3),(3,4),(4,5)\}$, to be denoted as $c : 2/3$, $c : 3/4$ and $c : 4/5$, respectively. These rules are simple modifications of the usual rules proposed by the Western Electric Company[23]. Moreover, they are also termed as *pure runs rules* (see Castagliola et al.[6]) in the sense that they are not used as supplements to the ordinary 1/1 rule along with warning limits. Note also that the upper one-sided c-chart, described in Section 2.1, is equivalent to the runs rule $c : 1/1$ scheme.

It is worth stressing that the term *runs rule* is used to describe either a rule of type r-out-of-r consecutive points (i.e., a rule based on pure runs of length r, $m = r$) or a rule of type r-out-of-m consecutive points (i.e., a rule based on a scan statistic, $m > r$). Since the rules we consider here are associated either to pure runs or to scans with $m = r + 1$, which have also been termed as almost perfect runs, we have chosen to refer to both of them with the single name *runs rules*. For more details, see Balakrishnan and Koutras[3].

Let L be the number of points plotted on the $c : r/m$ chart, until it gives an OOC signal for the first time, i.e.,

$$L = \inf \left\{ \ell : \sum_{t=\max(\ell-m+1,1)}^{\ell} I_{(UCL,\infty)}(X_t) \geq r \right\},$$

where $I_A(x)$ equals 1 if $x \in A$ and 0 otherwise. Clearly, L is the run length of the upper one-sided $c : r/m$-chart.

When runs-rules based criteria are applied to a control chart to indicate an OOC signal, the computation of the run length distribution is much more involved. In such cases, the Markov chain technique may facilitate the derivation of the run length properties (p.m.f., c.d.f., ARL, $SDRL$). In this work, the Markov chain technique originally proposed by Brook and Evans[5] has been employed. Further details can be also found in Champ and Woodall[7], Fu and Lou[10] and Antzoulakos and Rakitzis[2].

3 The Compound Run Length

In the following subsections we present the necessary theoretical results for the study of the run length distribution L (Subsection 3.1) as well as the distribution of the compound r.v. S_L (Subsection 3.2).

3.1 The Run Length Distribution

It is not difficult to verify that, for the charts described in Subsections 2.1-2.2, the respective run length distribution is a discrete phase-type distribution of order, say, d. We recall that a phase-type distribution describes the time to absorption in a finite discrete time Markov chain with d transient states and one absorbing state (Neuts[19], He[11]).

Let us assume that we have a discrete-time Markov chain with $d+1$ states, where states $0, 1, ..., d-1$ are transient and state d is an absorbing one. The transition probability matrix $\mathbf{P}$ of this discrete-time Markov chain is of the form

$$\mathbf{P} = \begin{pmatrix} \mathbf{Q} & \mathbf{r} \\ \mathbf{0}' & 1 \end{pmatrix} = \begin{pmatrix} q_{00} & q_{01} & \cdots & q_{0,d-1} & r_0 \\ q_{10} & q_{11} & \cdots & q_{1,d-1} & r_1 \\ \vdots & \vdots & \ddots & \vdots & \vdots \\ q_{d-1,0} & q_{d-1,1} & \cdots & q_{d-1,d-1} & r_d \\ 0 & 0 & \cdots & 0 & 1 \end{pmatrix},$$

where $\mathbf{Q}$ is the $d \times d$ matrix of transient probabilities, $\mathbf{0} = (0, 0, ..., 0)'$ and the $d \times 1$ vector $\mathbf{r}$ satisfies $\mathbf{r} = \mathbf{1} - \mathbf{Q1}$ with $\mathbf{1} = (1, 1, ..., 1)'$. Let $\mathbf{q}$ be the $d \times 1$ vector of initial probabilities associated with the d transient states, i.e., $\mathbf{q} = (q_0, q_1, ..., q_{d-1})'$. Then, the p.m.f. of the discrete phase-type r.v. L is given by

$$f_L(\ell) = P(L = \ell) = \mathbf{q}'\mathbf{Q}^{\ell-1}(\mathbf{I}_d - \mathbf{Q})\mathbf{1}, \quad \ell = 1, 2, \ldots \tag{1}$$

where $\mathbf{I}_d$ is the $d \times d$ identity matrix and $\mathbf{1}$ is the $1 \times d$ vector with 1 in all of its entries. Thus, the r.v. L with p.m.f. given in (1) is a discrete phase-type r.v. of order d with parameters $\mathbf{q}$ and $\mathbf{Q}$, i.e., $L \sim PH_d(\mathbf{q}, \mathbf{Q})$ (see, for example, Neuts[19] and He[11]). In addition, the c.d.f. $F_L(\ell)$, the mean $\mathbb{E}(L)$ and the standard deviation $\sqrt{\mathbb{V}(L)}$ of r.v. L may be expressed as

$$F_L\left(\ell \,|\mathbf{Q}, \mathbf{q}\right) = 1 - \mathbf{q}'\mathbf{Q}^{\ell}\mathbf{1}, \tag{2}$$

$$\mathbb{E}(L) = \mathbf{q}'(\mathbf{I}_d - \mathbf{Q})^{-1}\mathbf{1}, \tag{3}$$

$$\sqrt{\mathbb{V}(L)} = \sqrt{2\mathbf{q}'(\mathbf{I}_d - \mathbf{Q})^{-2}\mathbf{Q}\mathbf{1} - \mathbb{E}(L)^2 + \mathbb{E}(L)}. \tag{4}$$

Therefore, in order to evaluate the entire run length distribution for the control charts described in Subsection 2.2, we need to know the elements of matrix $\mathbf{Q}$ and vector $\mathbf{q}$; this is explained later in the paper.

3.2 The Distribution of S_L

Let L be a r.v. having a discrete phase-type distribution. In this subsection, we present all the necessary results for the study of the distribution of the compound r.v. $S_L = \sum_{t=1}^{L} Y_t$.

Denote by

$$P_{S_L}(z) = \mathbb{E}(z^{S_L}) = \sum_{t=1}^{\infty} f_{S_L}(t) z^t = \sum_{t=1}^{\infty} P(S_L = t) z^t,$$

$$P_L(z) = \mathbb{E}(z^L) = \sum_{\ell=1}^{\infty} P(L = \ell) z^{\ell},$$

the probability generating functions (p.g.f.) of S_L and L (respectively) and by

$$P_Y(z) = \mathbb{E}(z^Y) = \sum_{y=1}^{\infty} P(Y = y) z^y,$$

the common p.g.f. of Y_t's, $t \geq 1$. Recalling the well known formula for the p.g.f. of a random sum of i.i.d. r.v. (see Feller[9]), the p.g.f. of S_L equals

$$P_{S_L}(z) = P_L\left(P_Y(z)\right), \tag{5}$$

while the mean and the variance of S_L, are given by

$$\mathbb{E}(S_L) = \mathbb{E}\left(\sum_{t=1}^{L} Y_t\right) = \mathbb{E}(L)\mathbb{E}(Y_t),$$

$$\mathbb{V}(S_L) = \mathbb{V}\left(\sum_{t=1}^{L} Y_t\right) = \mathbb{E}(L)\mathbb{V}(Y_t) + (\mathbb{E}(Y_t))^2\mathbb{V}(L).$$

Once the p.g.f. $P_{S_L}(z)$ is available, by using the well known formula

$$f_{S_L}(t) = P(S_L = t) = \frac{1}{t!}\frac{d^t}{dz^t}(\mathbb{E}(z^{S_L}))\Big|_{z=0},$$

we can numerically determine the probability mass function (p.m.f.) of S_L, for given values of the parameters. In practice, this can be easily accomplished by the use of appropriate mathematical software (e.g. by using the function `SeriesCoefficient` of Wolfram Mathematica).

Apart from the above mentioned approach, Eisele[8] obtained recursive schemes for the p.m.f. of the r.v. S_L when $Y_1, Y_2, \ldots$ is a sequence of positive valued IID r.v. (discrete or continuous) with common p.m.f. $f_Y(t)$ and L is a discrete r.v. having a phase-type distribution of order d, i.e., $L \sim PH_d(\mathbf{q}, \mathbf{Q})$. The recurrence schemes of Eisele[8] are making use of two sets of coefficients that are computed from the $d \times d$ matrix $\mathbf{Q}$. The first set $\{b_1, b_2, \ldots, b_d\}$ is simply the set of coefficients of the characteristic polynomial of $\mathbf{Q}$, i.e.,

$$\det(x\mathbf{I}_d - \mathbf{Q}) = x^d + \sum_{i=1}^{d} b_i x^{d-i},$$

while the second sequence $\{a_1, a_2, \ldots, a_d\}$ can be computed through $\{b_1, b_2, \ldots, b_d\}$ and the p.m.f. $f_L(\ell) = P(L = \ell)$ of r.v. L, via the following formulas

$$a_1 = P(L = 1), \quad a_\ell = P(L = \ell) + \sum_{i=1}^{\ell-1} b_i P(L = \ell - i), \ \ \ell \in \{2, \ldots, d\}.$$

For more details, see also Koutras and Eryilmaz[14] and Koutras et al.[16]. As Eisele[8] indicated, having at hand the sets of coefficients $\{a_1, a_2, \ldots, a_d\}$ and $\{b_1, b_2, \ldots, b_d\}$, the p.m.f. of the r.v. $S_L = \sum_{t=1}^{L} Y_t$, where $L \sim PH_d(\mathbf{q}, \mathbf{Q})$ and $Y_1, Y_2, \ldots$ is a sequence of positive valued IID r.v. independent of L, can be easily reproduced through the recursive scheme

$$f_{S_L}(t) = P(S_L = t) = \sum_{j=1}^{\min(d,t)} a_j f_Y^{*j}(t) - \sum_{j=1}^{\min(d,t-1)} b_j \left(\sum_{u=1}^{t-1} P(S_L = u) f_Y^{*j}(t-u) \right),$$

for $t \geq 1$. The notation $f_Y^{*j}(t)$ is used for the p.m.f. of the j-th convolution of $Y_1.Y_2, \ldots, Y_j$, i.e.,

$$f_Y^{*j}(t) = P\left(\sum_{i=1}^{j} Y_i = t \right), \ \ j = 1, 2, \ldots.$$

Finally, when the r.v. $Y_1, Y_2, \ldots$ follow a phase-type distribution of order c, i.e., $Y_t \sim PH_c(\boldsymbol{\rho}, \mathbf{M})$, the p.m.f. $f_L(\ell)$, can alternatively be evaluated by the aid of the exact formula

$$f_{S_L}(t) = P(S_L = t) = \boldsymbol{\sigma}' \boldsymbol{\Sigma}^{t-1} (\mathbf{I}_{cd} - \boldsymbol{\Sigma}) \mathbf{1}, \tag{6}$$

where

$$\boldsymbol{\sigma} = \boldsymbol{\rho} \otimes \mathbf{q}(\mathbf{I}_d - \alpha\mathbf{Q})^{-1},$$

$$\boldsymbol{\Sigma} = \mathbf{M} \otimes \mathbf{I}_d + \mathbf{r}_c \cdot \boldsymbol{\rho}' \otimes (\mathbf{I}_d - \alpha\mathbf{Q})^{-1}\mathbf{Q},$$

and $\alpha = 1 - \boldsymbol{\rho}'\mathbf{1}$, $\mathbf{r}_c = (\mathbf{I}_c - \mathbf{M})\mathbf{1}$ (the notation $A \otimes B$ represents the Kronecker product of two matrices A and B). Especially, for the case of IID geometric r.v. $Y_1, Y_2, \ldots$, formula (6) reduces to (see Koutras and Eryilmaz[14])

$$f_{S_L}(t) = P(S_L = t) = \theta \mathbf{e}_1' \boldsymbol{\Sigma}^{t-1}(\mathbf{I}_d - \mathbf{Q})\mathbf{1},$$

since the geometric distribution is a discrete phase-type distribution of order $c = 1$.

Clearly, combining the results in the present subsection with the ones in Subsection 3.1 we can deduce the exact compound run length distribution of the compound r.v. $S_L = \sum_{t=1}^{L} Y_t$, for the Poisson charts described earlier in Subsections 2.1-2.2. For the case of the $c : 1/1$ chart, when $Y_t \sim Ge(\theta)$, it is not difficult to see that $S_L \sim Ge(\theta\beta)$, since the p.g.f.'s of Y and L are $P_Y(z) = \theta z/(1-(1-\theta)z)$, $P_L(z) = \beta z/(1-(1-\beta)z)$ respectively and taking advantage of Equation (5), we may readily verify that $P_{S_L}(z) = \theta\beta z/(1-(1-\theta\beta)z)$.

Also, let us consider for illustrative purposes the case of the upper one-sided $c : 3/4$ chart. Its run length properties are obtained by using, along with Equations (1)-(4), the following transition probability matrix $\mathbf{P}$

$$\mathbf{P} = \begin{pmatrix} \mathbf{Q} & \mathbf{r} \\ \mathbf{0}' & 1 \end{pmatrix} = \left(\begin{array}{cccccc|c} 1-p & p & 0 & 0 & 0 & 0 & 0 \\ 0 & 0 & p & 1-p & 0 & 0 & 0 \\ 0 & 0 & 0 & 0 & 0 & 1-p & p \\ 1-p & 0 & 0 & 0 & p & 0 & 0 \\ 0 & 0 & 0 & 1-p & 0 & 0 & p \\ 1-p & 0 & 0 & 0 & 0 & 0 & p \\ \hline 0 & 0 & 0 & 0 & 0 & 0 & 1 \end{array}\right),$$

where p is the probability that a single point falls above UCL. Thus, for $\mu = \mu_1$, we have

$$p = P(X_i > UCL) = 1 - F_P(UCL\,|\mu_1\,).$$

The entries of $\mathbf{P}$ are obtained by directly applying the Markov chain technique of Brook and Evans[5] (see also Rakitzis et al.[21])

In the above notation, $\mathbf{Q}_{(6\times6)}$ is the matrix of the transition probabilities between the transient states of the chain, vector $\mathbf{r}_{(6\times1)}$ equals $\mathbf{r} = \mathbf{1} - \mathbf{Q}\mathbf{1}$ with $\mathbf{1}_{(6\times1)} = (1,1,1,1,1,1)'$, whereas $\mathbf{q}_{(6\times1)} = (1,0,0,0,0,0)'$ is the vector of initial probabilities associated with the transient states of the Markov chain. The initial state of the Markov chain is state 1.

Next, it is not difficult to verify that the Eisele's coefficients associated with the run length r.v. L of the $c : 3/4$ chart are given by

$$b_1 = p-1,\ \ b_2 = p(p-1),\ \ b_3 = 0,\ \ b_4 = -p^2(1-p)^2,\ \ b_5 = 0,\ \ b_6 = -p^3(p-1)^3,$$

and

$$\alpha_1 = 0,\ \ \alpha_2 = 0,\ \ \alpha_3 = p^3,\ \ \alpha_4 = 2p^3(1-p),\ \ \alpha_5 = p^4(p-1),\ \ \alpha_6 = -p^4(1-p)^2.$$

Thus, the p.m.f. of S_L for the $c:3/4$ chart may be obtained by the aid of the following recursive scheme for $t \geq 7$:

$$f_{S_L}(t) = p^3 f_Y^{*3}(t) + 2p^3(1-p) f_Y^{*4}(t) + p^4(p-1) f_Y^{*5}(t) - p^4(1-p)^2 f_Y^{*6}(t)$$
$$-(p-1)\left(\sum_{u=1}^{t-1} f_{S_L}(u) f_Y^{*1}(t-u)\right) - p(p-1)\left(\sum_{u=1}^{t-1} f_{S_L}(u) f_Y^{*2}(t-u)\right)$$
$$+p^2(1-p)^2\left(\sum_{u=1}^{t-1} f_{S_L}(u) f_Y^{*4}(t-u)\right) + p^3(p-1)^3\left(\sum_{u=1}^{t-1} f_{S_L}(u) f_Y^{*6}(t-u)\right)$$

where

$$f_Y^{*j}(y) = \binom{y-1}{j-1}\theta^j(1-\theta)^{y-j}, \;\; y = 0, 1, \ldots.$$

The initial conditions needed to launch the scheme are the following ones:

$$f_{S_L}(0) = f_{S_L}(1) = f_{S_L}(2) = 0,$$

$$f_{S_L}(3) = \theta^3 p^3, \; f_{S_L}(4) = 3(1-\theta)\theta^3 p^3 + 3(1-p)p^3\theta^4,$$

$$f_{S_L}(5) = 3\theta^3 p^3(2 - 4\theta p - (1 - p(p+2))\theta^2),$$

$$f_{S_L}(6) = \theta^3 p^3(10 - 30\theta p - 15\theta^2(1 - p(p+2)) + (8 - p(7 + p(p+10)))\theta^3).$$

The distribution of S_L for the $c:2/3$ and $c:4/5$ charts can be similarly derived. It is worth mentioning that for the $c:2/3$ chart, the distribution of S_L has also been studied by Koutras et al.[16] while the form of matrix $\mathbf{Q}$ in case of the $c:4/5$ chart can be found in Bersimis et al.[4]. Further details are left to te reader. Generally speaking, given the values of r and m, one can write down the form of matrix $\mathbf{Q}$ (by applying the Markov chain techique) and with the aid of appropriate software (e.g., Wolfram Mathematica) can numerically evaluate the theoretical properties of the S_L distribution, by using either the recurrsive formulas or the matrix representation.

4 Numerical Results

In the present section we evaluate the performance of the control charts introduced in Subsections 2.1-2.2 under various IC scenarios. We consider as IC mean $\mu_0 \in \{5, 10, 15\}$ while $\theta \in \{0.25, 0.50, 0.75, 1.0\}$. The case $\theta = 1$ is in fact describing the case when the time between the successive inspections is very short and can be ignored.

For the statistical design of the charts, we determine the appropriate UCL value in order to have the desired IC performance, in terms of the expected value $\mathbb{E}(S_L)$ for $\mu = \mu_0$. This expected value is the average time to signal (ATS), i.e., $ATS = \mathbb{E}(S_L)$. For an IC (resp. OOC) process, we will denote it as ATS_0 (resp. ATS_1). Thus, we want to have a prespecified ATS_0 value. For illustrative purposes, we considered for all the control charts, the desired ATS_0 value to be around 500, i.e., $ATS_0 \approx 500$. Any other value can be used.

μ_0	θ	UCL	5%	10%	25%	50%	75%	90%	95%	ATS	$SDTS$
5	0.25	10	15	31	84	203	405	672	874	292.07	291.57
	0.50	11	19	39	106	254	508	844	1098	366.76	366.26
	0.75	12	34	70	190	458	915	1520	1978	660.44	659.94
	1.00	12	26	53	143	343	686	1140	1463	495.33	494.83
10	0.25	18	29	59	160	386	771	1281	1666	556.60	556.10
	0.50	19	30	61	167	401	802	1332	1733	578.98	578.48
	0.75	19	20	41	111	268	535	888	1155	385.99	385.49
	1.00	20	33	67	181	437	873	1449	1885	629.62	629.12
15	0.25	24	19	38	103	248	496	824	1072	358.27	357.77
	0.50	26	31	64	174	419	837	1390	1808	603.88	603.38
	0.75	26	21	43	116	279	558	926	1205	402.59	402.09
	1.00	27	30	62	168	404	808	1341	1745	582.82	582.32

Table 1. The IC distribution of the Time to Signal for the $c : 1/1$ chart

In the following Tables 1-4, we present the IC statistical design of the $c : 1/1$ chart (Table 1), the $c : 2/3$ chart (Table 2), the $c : 3/4$ chart (Table 3) and the $c : 4/5$ chart (Table 4). Also, we provide the percentile points $100f\%$, $f \in \{0.05, 0.10, 0.25, 0.50, 0.75, 0.90, 0.95\}$ (in the respective columns) as well as the IC mean and standard deviation for the distribution of the time to signal S_L in the columns entitled "ATS" and "$SDTS$", respectively. It is worth mentioning that due to the discrete nature of the process, it is not always possible to achieve the desired ATS_0 value. Therefore, in Tables 1-4, the actual IC ATS value is *as close as possible* to 500.

From Tables 1-4 we notice that for some cases the IC ATS is above the

μ_0	θ	UCL	5%	10%	25%	50%	75%	90%	95%	ATS	$SDTS$
5	0.25	8	31	58	150	352	698	1156	1502	505.28	872.15
	0.50	8	16	29	75	176	349	578	751	252.64	436.07
	0.75	9	39	77	206	493	984	1633	2124	710.63	1229.76
	1.00	9	29	58	155	370	738	1225	1593	532.97	531.06
10	0.25	14	23	42	104	243	480	793	1030	347.57	599.06
	0.50	15	27	53	138	328	654	1084	1409	472.49	816.81
	0.75	15	18	35	92	219	436	722	939	314.99	544.54
	1.00	16	39	79	211	507	1011	1679	2183	730.11	728.19
15	0.25	20	23	42	105	245	485	802	1041	351.31	605.53
	0.50	21	24	45	118	280	556	921	1198	401.91	694.56
	0.75	22	37	73	195	467	932	1546	2011	672.85	1164.33
	1.00	22	28	55	147	350	699	1159	1508	504.64	502.73

Table 2. The IC distribution of the Time to Signal for the $c : 2/3$ chart

desired value, while for the rest is below. This fact is attributed to the discrete nature of the process. Thus, no specific trends can be identified. Also, as it was expected, the distribution of the S_L in all the examined cases is very skewed. Therefore, the additional use of other performance measures (e.g., percentile points) is necessary. From the comparison with the case $\theta = 1$ it is

μ_0	θ	UCL	5%	10%	25%	50%	75%	90%	95%	ATS	$SDTS$
5	0.25	7	49	91	231	543	1076	1780	2313	778.72	1343.44
	0.50	7	25	46	113	271	538	890	1156	389.36	671.72
	0.75	7	17	31	77	181	358	593	770	259.57	447.81
	1.00	7	13	23	58	136	269	445	578	194.68	191.85
10	0.25	13	48	87	222	520	1030	1705	2215	746.03	1286.84
	0.50	13	24	44	111	260	515	852	1107	373.02	643.42
	0.75	13	16	29	74	173	343	568	738	248.68	428.95
	1.00	14	39	77	204	487	972	1612	2096	701.67	698.72
15	0.25	18	27	46	108	248	486	801	1039	353.18	606.67
	0.50	19	29	54	138	324	643	1065	1384	465.35	803.32
	0.75	19	19	36	92	216	429	710	922	310.23	535.54
	1.00	20	39	78	207	495	988	1638	2131	710.30	713.25

Table 3. The IC distribution of the Time to Signal for the $c : 3/4$ chart

μ_0	θ	UCL	5%	10%	25%	50%	75%	90%	95%	ATS	$SDTS$
5	0.25	6	42	72	174	401	789	1301	1689	572.43	984.29
	0.50	6	21	36	87	200	394	650	844	286.22	492.14
	0.75	6	14	24	58	134	263	433	562	190.81	328.10
	1.00	6	11	18	44	100	197	325	421	143.11	139.46
10	0.25	11	25	39	84	184	356	583	755	260.39	444.27
	0.50	12	30	53	134	312	617	1021	1326	447.20	770.88
	0.75	12	20	36	89	208	411	680	884	298.13	513.92
	1.00	12	15	27	67	156	309	510	662	223.60	219.88
15	0.25	17	37	62	147	335	657	1083	1405	477.70	820.30
	0.50	18	45	84	217	513	1019	1687	2193	736.83	1272.43
	0.75	18	30	56	145	342	679	1125	1462	491.22	848.29
	1.00	18	22	42	109	257	509	843	1096	368.42	364.62

Table 4. The IC distribution of the Time to Signal for the $c : 4/5$ chart

not difficult to see that a smaller value for the UCL is necessary, in order to have (approximatelly) the same ATS_0 value. This fact also reveals that if someone uses the UCL value obtained in case $\theta = 1$ when the intermediate times cannot be ignored (i.e., when $\theta \in (0, 1)$) then the actual time until an OOC signal will be longer while the two distributions will be much more different, as well. This can be confirmed from the values of the percentile points. Consider, for example, the case $\mu_0 = 5$ for the $c : 3/4$ and $c : 4/5$ charts. Also, it is not difficult to verify that for the same values of the design parameters, the ATS for $\theta \neq 1$ is $1/\theta$ times the ATS for $0 < \theta < 1$ or, equivalently, $\mathbb{E}(S_L) = \mathbb{E}(L)/\theta$.

Note also that the $SDTS$ is much larger than the ATS when $0 < \theta < 1$, because considering geometrically distributed times between consecutive samples adds variability to the TS. Practitioners should have in mind that when adopting a chart with a larger IC (resp. OOC) $SDTS$, there will be larger probabilities of large deviations from the large (resp. small) IC (resp. OOC) ATS, thus increasing the probability of having observations beyond UCL much sooner or much later than expected. Therefore, in that case percentile points

δ	1/1	2/3	3/4	4/5
1.0	385.99, 385.49	314.94, 544.54	248.68, 428.95	298.13, 513.92
	268, 1155	219, 939	173, 738	208, 884
1.1	143.53, 143.03	95.91, 165.16	72.77, 124.43	79.95, 136.25
	100, 429	67, 283	51, 211	57, 231
1.2	62.66, 62.16	38.43, 65.69	30.00, 50.51	32.10, 53.60
	44, 187	27, 111	22, 84	23, 88
1.3	31.25, 30.74	19.17, 32.41	15.99, 26.39	17.26, 28.10
	22, 93	14, 54	12, 42	13, 44
1.5	10.69, 10.17	7.65, 12.60	7.54, 11.98	8.64, 13.43
	8, 31	6, 19	6, 17	7, 18
1.7	5.06, 4.53	4.58, 7.39	5.28, 8.18	6.44, 9.77
	4, 14	4, 10	5, 10	6, 11
2.0	2.52, 1.95	3.20, 5.08	4.31, 6.59	5.57, 8.36
	2, 6	3, 6	4, 7	5, 8
UCL	19	15	13	12

Table 5. Performance measures for runs rules charts for $\mu_0 = 10$, $\theta = 0.75$

must be used in order to have a more clear picture of control chart's performance in terms of S_L.

Numerical comparisons between the schemes we studied are given in Tables 5 and 6. In order to have a fair comparison, the IC ATS values of all schemes were chosen to be as close as possible to the IC ATS value of the $c : 1/1$ chart. However, due to the discrete nature of the data, this was not feasible for all the competitive charts and thus, the results should be interpreted with caution. Note also that the desired ATS_0 is no longer ≈ 500 but the UCL values were re-determined (where necessary) in order to have a similar IC performance for the most of the Poisson charts. For a shift $\delta \in \{1.0, 1.1, 1.2, 1.3, 1.5, 1.7, 2.0\}$ we provide the ATS, $SDTS$ values (first row) as well as the median and the 95^{th} percentile point (second row) of the time to signal distribution, in two different cases: For $\theta = 0.75$, $\mu_0 = 10$ (Table 5) and $\theta = 0.25$, $\mu_0 = 15$ (Table 6).

For larger shifts (i.e. $\delta > 1.5$), either the $c : 2/3$ or the $c : 1/1$ chart attain the lowest ATS value. Also, the $c : r/m$ charts outperform the $c : 1/1$ charts for small shifts (i.e. $\delta \leq 1.5$). Also, as δ increases, the ATS value tends to the value r/θ (for the $c : r/m$ charts).

5 Conclusions

In this work, we studied the compound run length distribution of various Poisson control charts. By using the fact that the exact run length distribution L of each chart is a discrete phase-type distribution, we illustrated how one can compute the exact distribution of the compound r.v. $S_L = \sum_{t=1}^{L} Y_t$, where $Y_1, Y_2, \ldots$ are IID geometric r.v. with parameter θ. The statistical design of the examined schemes was given under various IC scenarios, while comparisons between the different control charts were given, as well. Moreover, the differences between the proposed and the classical setup, i.e., when the intermediate times are not taken into account, were also highlighted.

δ	1/1	2/3	3/4	4/5
1.0	385.27, 357.77 248, 1072	351.31, 605.53 245, 1041	353.18, 606.67 248, 1039	477.70, 820.30 335, 1405
1.1	131.38, 130.88 91, 393	108.17, 184.74 77, 314	102.76, 173.56 74, 291	123.88, 208.37 90, 348
1.2	58.60, 58.10 41, 175	46.73, 78.66 34, 131	45.59, 75.10 34, 121	53.13, 86.60 40, 138
1.3	30.69, 30.19 21, 91	25.95, 42.93 20, 69	27.02, 43.37 21, 66	31.73, 50.11 26, 75
1.5	12.26, 11.75 9, 36	13.10, 21.09 11, 32	15.88, 24.59 14, 34	19.66, 29.85 18, 38
1.7	7.07, 6.55 5, 20	9.66, 15.34 8, 22	13.11, 20.07 12, 26	16.95, 25.46 16, 31
2.0	4.75, 4.22 3, 13	8.30, 13.12 7, 18	12.16, 18.58 11, 24	16.12, 24.18 15, 29
UCL	24	20	18	17

Table 6. Performance measures for runs rules charts for $\mu_0 = 15$, $\theta = 0.25$

Finally, it goes without saying that this setup can be used when the r.v. X has any other discrete distribution or when the r.v. Y has a negative binomial distribution or any other discrete probability model, suitable for describing intermediate times. It should be stressed that the distribution of S_L can be derived in a similar manner, for any control chart for which its exact run length distribution is a discrete-phase type one (e.g. a CUSUM one).

Acknowledgments

M. V. Koutras has been partially funded by the National Matching Funds 2014-2016 of the Greek Governement, and more specifically by the General Secretariat for Research and Technology (GSRT), related to EU project "IS MPH: Inference for a Semi-Markov Process" (GA No 329128)

References

1. C.A. Acosta-Mejia. Two sets of runs rules for the chart. *Quality Engineering*, 19, 2, 129–136, 2007.
2. D.L. Antzoulakos and A.C. Rakitzis. The modified r out of m control chart. *Communications in Statistics-Simulation and Computation*, 37, 396–408, 2008.
3. N. Balakrishnan and M.V. Koutras. *Runs and Scans with Applications*, John Wiley & Sons, 2002.
4. S. Bersimis, M.V. Koutras and G.K. Papadopoulos. Waiting time for an almost perfect run and applications in statistical process control. *Methodology and Computing in Applied Probability*, 16, 1, 207–222, 2014.
5. D. Brook and D.A. Evans. An approach to the probability distribution of CUSUM run length. *Biometrika*, 59, 539–549, 1972.

6. P. Castagliola, A. Achouri, H. Taleb, G. Celano and S. Psarakis. Monitoring the coefficient of variation using control charts with run rules. *Quality Technology and Quantitative Management*, 10, 75–94, 2013.
7. C.W. Champ and W.H. Woodall. Exact results for Shewhart control charts with supplementary runs rules. *Technometrics*, 29, 393–399, 1987.
8. K.-T. Eisele. Recursions for compound phase distributions. *Insurance: Mathematics and Economics*, 38, 149–156, 2006.
9. W. Feller. *An Introduction to Probability Theory and its Applications, Vol. I*, 3rd edn, John Wiley & Sons, New York, USA, 1968.
10. J.C Fu and W.W.Y. Lou. *Distribution Theory of Runs and Patterns and Its Applications*, Singapore: World Scientic, 2003.
11. Q.-M. He. *Fundamentals of Matrix-Analytic Methods*, Springer, 2014.
12. M.B.C. Khoo. Design of runs rules schemes. *Quality Engineering*, 16, 1, 27–43, 2003.
13. M. Klein. Two alternatives to the Shewhart $\bar{X}$ control chart. *Journal of Quality Technology*, 32, 427–431, 2000.
14. M.V Koutras and S. Eryilmaz. Compound geometric distribution of order k. *Methodology and Computing in Applied Probability*, 19, 377–393, 2017.
15. M.V. Koutras, S. Bersimis and P.E. Maravelakis. Statistical process control using Shewhart control charts with supplementary runs rules. *Methodology and Computing in Applied Probability*, 9, 207–224, 2007.
16. V.M. Koutras, M.V. Koutras and F. Yalcin. A simple compound scan statistic useful for modeling insurance and risk management problems. *Insurance:Mathematics and Economics*, 69, 202-209, 2016.
17. J.M. Lucas, D.J. Davis and E.M. Saniga. Detecting improvement using Shewhart attribute control charts when the lower control limit is zero. *IIE Transactions*, 38, 699–709, 2006.
18. D.C. Montgomery. *Introduction to Statistical Quality Control*, 6th edn, John Wiley & Sons, Inc., New York, USA, 2009.
19. M.F. Neuts. *Matrix-Geometric Solutions in Stochastic Models: An Algorithmic Approach*, Dover Publications Inc, 1981.
20. A.C. Rakitzis and D.L. Antzoulakos. On the improvement of one-sided S control charts. *Journal of Applied Statistics*, 38, 12, 2839-2858, 2011.
21. A.C. Rakitzis, P. Castagliola and P.E. Maravelakis. On the modelling and monitoring of general inflated Poisson processes. *Quality and Reliability Engineering International*, 32, 1837-1851, 2016.
22. M. Riaz, R. Mehmood and R.J.M.M. Does. On the performance of different control charting rules. *Quality and Reliability Engineering International*, 27, 1059–1067, 2011.
23. Western Electric Company. *Statistical Quality Control Handbook*, Indianapolis, IN, 1956.
24. S. Wu, P. Castagliola and M.B.C. Khoo. Run rules based phase II c and np charts when process parameters are unknown. *Communications in Statistics - Theory and Methods*, 45, 4, 1182-1197, 2016.

Analysis of the determinants and outputs of innovation in the Nordic countries

Cátia Rosário[1], António Augusto Costa[2] and Ana Lorga da Silva[3]

[1] Centro de Pesquisa e Estudos Sociais, Escola de Ciências Económicas e das Organizações; Universidade Lusófona de Humanidades e Tecnologias, Campo Grande 376, 1749-024 Lisboa – Portugal
(E-mail: rosario.catia@hotmail.com),
[2] Escola de Ciências Económicas e das Organizações; Universidade Lusófona de Humani-dades e Tecnologias, Campo Grande 376, 1749-024 Lisboa – Portugal
(E-mail: aaugusto@ulusofona.pt)
[3] Centro de Pesquisa e Estudos Sociais, ECEO and FCSEA, Universidade Lusófona de Humanidades e Tecnologias, Campo Grande 376, 1749-024 Lisboa – Portugal
(E-mail: ana.lorga@ulusofona.pt)

Abstract
This study was applied to the European Nordic countries (Denmark, Finland, Iceland, Norway and Sweden) which are referred by the European Commission as countries with high innovation performance.
The analysed panel data concern the period between 1999 and 2014 and it was studied how different inputs of innovation affect the different outputs.
The "innovation" variable was constructed using factor analysis, given that the Organisation for Economic Co-operation and Development considers that innovation is the result of a set of macro measures common to different countries. The factor obtained through the exploratory factor analysis represents the results of innovative activity and economic performance.
It was analysed how the quality of human capital, the research and development efforts carried out by different economic agents affect the results of innovation. It was possible to conclude that countries with a higher proportion of applied research and more cooperation between researches carried out by companies, universities and the government lead to better economic results and to higher outcomes of intellectual property.

Keywords: Innovation, Panel Data, Regression Models, Factorial analysis.

1 Introduction

Innovation is a central theme in current literature and the recognition of its importance has increased over the last few decades. As Porter [19] has pointed out innovation has become the challenge that defines global competitiveness.

Panel data refers to a sectional and temporal sample, merging an approach of

time series with a cross-section approach Baltagi [1]. The use of panel data analysis allows us to analyse several individuals, in this case the Nordic countries.

The choice of these countries is related with the fact that they are references in the field of innovation European Commission [10]. European Innovation Scoreboard (EIS) and the Global Innovation Index (GII) group different information for the construction of a single indicator of innovation. Therefore, Factor Analysis was used to construct a representative factor that can be considered as the output of the innovative activity.

The main purpose of this investigation is to determine how different sources and approaches of research, as well as the quality of human capital, contribute to the outputs of innovation.

2 Innovation

Joseph Schumpeter mentioned the importance of innovation as a form of "creative destruction" that leads to value creation. Schumpeter [23] pointed out that this "weed" goes beyond the simple idea of creating something new, since it can also lead to the creation of new markets.

According to the Oslo Manual 2005 [16] innovation is the implementation of a new or significantly improved product (good or service), process or method of marketing, or a new organizational method in business practices, workplace and external relations. Cunha *et al* [6] specify organizational innovation as being a way of establishing new agreements with clients or suppliers, new ways of providing after-sales service, new modus operandi for the relationship with customers, among other practices.

Related to innovation are the concepts of change, invention and creativity Drucker [7]. And as said by Schumpeter [23] it is possible to distinguish: invention, innovation and diffusion. Teixeira [25] points out that innovation is a process, composed by three phases: Invention (creation of something new that results from the creation or acquisition of knowledge); Innovation (transformation or application of new knowledge) and Diffusion (acceptance and adoption of innovation, recognizing its economic utility).

Innovation is a complex process, and it is also due to the many ways in which it is represented. As mentioned by Sarkar [22] it is a process that affects the different organizational areas. Depending on the degree of novelty of the results,

innovation can be classified as: Incremental (associated with gradual improvements), Radical (referring to the creation of something new) and Disruptive (it can originate a new industry or create a symbiosis between unrelated technologies until then).

Innovation can have different degrees of novelty, it can also be differentiated through its "object" and as mentioned in the Oslo Manual [16] there are four types of innovation: product, process, organizational and marketing.

As mentioned there are different forms and types of innovation. This is a process that affects several organizational areas, so there is an evolution in the way that this process can be developed.

Table 1: Description of innovation models

Innovation models		Description
1st Generation (1950 to 1960)	Technology push	Sequential and linear process in which the market functions as a receiver of research results developed in universities, considering that basic research is sufficient.
2nd Generation (1960 to 1970)	Market Pull	Sequential and linear process where needs are opportunities to explore, initiating the process of creating ideas, directing R&D efforts.
3rd Generation (1970 to 1980)	Coupling model	Continuous sequential process with interconnected steps that relate different sectors of the company to the scientific community and to other economic agents.
4th Generation (1980 to 1990)	Integrated business processes	Parallel process, with integrated development where production and sales are integrated to work simultaneously in the development of products / services.
5th Generation (after 1990)	System integration & networking	Process with vertical and horizontal integration within companies, broadening the horizons of collaborative research.

Source: adapted from Campos & Valadares [3], Rothwell [21] and Teixeira [25]

According to the Oslo Manual [16] innovation goes beyond technological development; however, this remains the feature that has the greatest impact on organizations as well as on society. These models show the importance of research for innovation success and, per Castilho, Borges and Pereira [4], research is the development of a research based on a set of procedures that seek solutions to certain problems. This is a generic concept; however, it is sure that innovation influences and is influenced by two types of research: basic (fundamental) and applied.

As referred by the World Intellectual Property Organization (WIPO) [5],

measures of innovation can be ambiguous, given that research is essential for innovative activity results. That is, the efforts employed essentially involve R&D, and research is the cornerstone of such efforts.

Basic research is mostly performed at universities and their contribution is mainly to the scientific knowledge, while applied research is concerned on solving concrete "problems". In this way, applied research responds more effectively to the purpose of innovation Campos & Valadares [3]. According to the European Commission [17], research has increasingly and significantly contributed to results of the innovative activity, it is required to invest in R&D and this can be done by different agents: Companies, Universities and Government.

The cooperation of different agents enable the creation of synergies, leveraging the sharing of information, technology and results as we can read in the Oslo Manual [16]. This systemic view of innovation was approached by Etzkowitz & Leydesdorf [12] by the Triple Helix model that considers the coordination between the different mechanisms and institutions to be fundamental, as shown in the following figure.

Fig. 1: Triple Helix Model

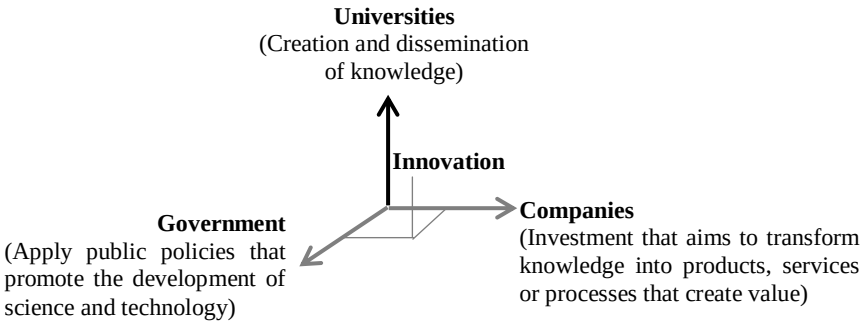

Source: adapted from Leydesdorff & Ivanova [13]

As shown in figure 1, this relationship is considered by Etzkowitz [9] through three dimensions: relationship between each axis in function of the economic mission, mutual influence between them and creation of a new layer of organizations that result from the interaction of these three agents. Therefore, the investment in R&D programs carried out by each one of them must consider the research that is carried out by the others.

Since innovation is so important, it is necessary to find the best way to evaluate it, to take measures to promote it in a sustainable way. Referred to by the OECD, the collection of data on scientific and technological capacities at national level has become a priority. In 1963 the OECD developed a manual - Frascati Manual - which established a set of procedures for collecting data on human resources and R&D expenditures, so that it would be possible to assess and compare innovation between countries.

In 1999, the OECD had 45 innovation indicators and currently has about 200 innovation references to analyse scientific and technological practice, such as: international mobility of researchers and scientists; growth of the information economy; innovation by regions and industries; innovation strategies; among other things OECD [17]

The European Union uses a set of tools to collect information on innovation:

- Community Innovation Survey (CIS) - required for the EU member States, based on the conceptual framework set out in the Oslo Manual, as well as Eurostat methodological recommendations.

- European Innovation Scoreboard (EIS) - the European Innovation Scoreboard was developed at the European Summit in Lisbon in 2000. Its purpose is to measure the innovation performance of EU countries and their comparison with other countries.

As mentioned by Godinho [11] and Lhuillety, Raffo & Hamdars-Livramento [14] there are many ways in which innovation can be measured and there is no single indicator or measure that can reflect the full potential and innovative outcome of a country. In this way, the challenge is even greater because it is necessary to articulate correctly the different measures of innovation.

Similarly, Roszko-Wojtowicz & Biateck [20], using multidimensional statistics, concluded that the set of 25 indicators used by the EIS can be effectively reduced. However, they draw attention to the fact that it includes inputs and outpost of innovation, which makes it difficult to analyse which inputs contribute the most to innovation success. In the same sense, other authors such as Lhuillery, Raffo & Hamdan-Livramento [14] point out the importance of distinguishing these two components of innovation. In the same way, Sarkar [22] reinforces the idea of a systemic approach that distinguishes input, process and output, allowing a better understanding not only of the innovation process but also of the determinants of its success.

3 Methodology

The data collected (1999 to 2014) refers to the main Northern European countries, namely the Nordic countries: Denmark, Finland, Iceland, Norway and Sweden. The variables used were collected through the World Bank and the OECD.

Using the Exploratory Factor Analysis (EFA), a single factor was obtained, considered representative of the results of the innovation efforts. The construction of this factor included the following variables: Registration of patents (PR) and trademarks (TR) made by residents, Exports of high technology in the pharmaceutical industry (EHTFI) and in the aerospace industry (EHTAI).

The relational structure of the considered variables was evaluated by the EFA on the matrix of correlations, with extraction of the factors by the method of principal components. The retained factor had an eigenvalue greater than 1, in agreement with Screen Plot and the percentage of variance retained. The use of the different criteria allows a higher robustness in the retention of factors.

To evaluate the validity of EFA, the KMO criterion was used, with a KMO=0,729 and the Bartlett Equilibrium test has a p-value very close to 0, one can concludes that AFE is adequate and that the variables are significantly correlated.

Henson & Roberts [8] sustain that there is no consensus regarding the minimum cumulative variance acceptable for all the research areas. As mentioned by Taherdoost, Sahibuddin & Jalaliyoon [24] in natural sciences the admissible values are higher to 95%, while in humanities, values between 50% and 60% are already acceptable. It was considered that the 72% obtained are acceptable to proceed with the analysis.

The obtained factor was:

$$\hat{INNOV} = 0,296PR + 0,331TR + 0,253EHTFI + 0,295EHTAI$$

For each econometric model presented was made a panel diagnosis, to determine the most suitable model. Through the results of F-Statistic, the Breusch-Pagan test and the Hausman test, it was found that, in all cases, the fixed effects model is the most adequate Pesaran [18].

The fixed effects models obtained:

$$y_{it} = \beta_0 + \beta_1 x_{it1} + ... + \beta_k x_{itk} + a_i + u_{it}$$

$i = 1,...,5$ - countries

$t = 1,...,16$ - years

$k = 8$ - explanatory variables

a_i - fixed effect of each country

u_{it} - error term

The presented models and analysed in section 4 aim to answer the main question of this study: how do different sources of innovation contribute to the entrepreneurial and commercial outputs of innovation?

The variables used can be grouped as follows:

- Business and commercial results of innovation: Patent registration (PR) and trademarks (TR) made by residents and exports of high technology goods/services in the pharmaceutical industry (EHTFI) and aerospace (EHTAI). This set of variables refers to the factor created using AFE and which is representative of the business and commercial outputs of innovation Roszko-Wojtowicz & Biateck [20]

- Human capital: higher education in engineering (HEE), higher education in business, law sciences (HEBL) and vocational programs (VP). This set of variables relates to the quality of human capital Valente [26]

- Research and Development: R&D expenditure by companies (BERD), universities (HERD) and government (GOVERD), number of researchers (RES) and scientific publications (SP). These variables reflect innovation efforts European Commission [10]

4 Results

The results of the econometric models obtained are analysed here. Their analysis is complemented with descriptive statistics of some of the considered variables, comparing the countries under study. In the model (1), R&D investments made by companies contribute positively to innovation, contrary to the investments made by the universities and the government, which, although not statistically significant, show a negative sign. Another research perspective (researchers and

scientific production), show that not all types of research appear to have a positive impact on innovation outputs. About human capital, the contribution of training in business and law sciences has a positive impact in achieving business and commercial results of innovation. The analysis to the model (1), not being conclusive, raises the interest to try to verify if the contribution of the explanatory variables is different through the different innovation outputs considered.

Dependent variables: Model (1) - INNOV: Factor obtained through EFA; Model (2) - PR: Number of patent registrations submitted by national applicants through the Patent Cooperation Treaty procedure or with a national patent office; Model (3) - TR: Number of trademark applications made by national applicants in a particular national intellectual property office; Model (4) - EHTFI: Volume of exports in the pharmaceutical industry, in millions of USD; Model (5) - EHTAI: Volume of exports in the aerospace industry, in millions of USD.

Explanatory variables: BERD, HERD and GOEVRD: Expenditures made by firms, universities and government in R&D, as% of GDP; HEE: Proportion of people with higher education in Engineering and Industry and HEBL: Proportion of people with higher education in Business and Law Sciences (relative to total of people with higher education); VP: Percentage of vocational training programs in secondary and post-secondary (non-tertiary) education based on programs geared specifically to a given class of professions or trades; RES: Number of researchers per 1000 persons employed; SP: Number of publications in scientific journals, per million dollars of GDP, corresponding, according to the Policy Platform for Innovation developed by the OECD and World Bank, a measure of the quality of scientific publications.

	(1) INNOV	**(2)** PR	**(3)** TR	**(4)** EHTFI	**(5)** EHTAI
BERD	0,564057***	411,014**	433,115	−57,6046	518,667***
	(0,168618)	(193,269)	(685,198)	(948,616)	(188,557)
HERD	−0,487268	−1690,37***	−1211,57	9654,62***	−632,148*
	(0,328954)	(378,529)	(1336,74)	(1857,92)	(369,301)
GOVERD	−0,536596	−504,28	5456,20***	−2206,12	−1198,35**
	(0,490689)	(555,119)	(1993,97)	(2724,68)	(541,587)
HEE	−0,209773	2964,19**	−10884,10**	−15313,5**	1658,23
	(1,04808)	(1195,02)	(4258,98)	(5865,50)	(1165,89)
HEBL	3,13243***	−27,3018	15305,0***	559,692	1546,51
	(1,01792)	(1152,79)	(4136,45)	(5658,20)	(1124,69)
VP	0,0110596*	−13,0432*	73,9348***	74,6904*	1,22994
	(0,0065235)	(7,50171)	(26,5092)	(36,8204)	(7,31883)
RES	0,00318607	9,32919	−79,5665	348,854**	−16,5242
	(0,0243858)	(27,5731)	(99,0943)	(135,336)	(26,9010)
SP	−6,85333	9146,21*	−56188,5***	−23028,8	−1675,69
	(4,46935)	(5115,01)	(18161,7)	(25105,8)	(4990,31)
cons	−1,83473**	1718,95*	−997,705	−6861,26	−337,428
	(0,788494)	(904,877)	(3204,13)	(4441,38)	(882,818)

INNOV: F(12,33) = 254,26*** , PR: F(12,34) = 128,37*** , TR: F(12,33) = 140,56***
EHTFI: F(12,34) = 136,70*** , EHTAI: F(12,34) = 27,82***
Number of observations: INNOV = 46 , PR = 47 , TR = 46 , EHTFI = 47 , EHTAI = 47
INNOV: R^2=0,9893, INNOV: $\bar{R}^2$=0,9870, PR: R^2=0,9784, PR: $\bar{R}^2$=0,9739, TR: R^2=0,9808, TR: $\bar{R}^2$=0,9766
EHTFI: R^2=0,9797, EHTFI: $\bar{R}^2$=0,9751, EHTAI: R^2 =0,9076, EHTAI: $\bar{R}^2$=0,8881
(Standard errors in parenthesis)
*** p<0.01, ** p<0.05, * p<0.1

Models (2) and (3) are related to intellectual property, with patents (2) being more associated with technological development, while trademark registration (3) has a greater link with the commercial component developed by Companies.

Analysing the variables associated with R&D, the expenses of companies in R&D programs contribute positively in both models, being statistically significant when it comes to patent registration (2). Contrary, the impact of university spending is negative in both models. This can be justified by the fact that essentially applied research is carried out in companies seeking to create / improve products, services or processes (2) and to improve the competitive position in current or new markets (3). In the universities, the research done is mainly of the basic research, and can contribute to intellectual property, but not directly, as referred by the National Science Board (NSC) [15].

According to the EIS [10], R&D expenditures made by the Government aim to promote the innovative activity by the private sector and its contribution to innovation outputs may not be direct. Therefore, the negative coefficient of the GOVER variable of model (2) was expected. However, when it comes to trademark registration, Government expenditures have a positive impact that may be associated with its contribution to promote entrepreneurship and the registration of trademarks is encouraged both nationally and internationally - through the European Trademarks and Designs Network - a European global network of trademarks and designs.

To complement the analysis of the impact of research on innovation outputs, there are two explanatory variables to consider: RES (researchers) and SP (scientific publications). In this case, the coefficients associated to these two variables are positive in the model (2) and negative in the model (3), which means that research done in the Nordic countries seeks to promote technological development. In other words, there is a higher balance between fundamental and applied research, which leads to positive results in the field of technological development Bentley, Gulbrandsen & Gulbrandsen [2]. These results would be expected, given that the Nordic countries have been leaders in the innovative activity over the last 13 years EIS [10].

Regarding the quality of human capital, the proportion of people with higher education in engineering (HEE) make a positive contribution to patent registration (2). This observation it is in harmony with the authors Bentley, Gulbrandsen & Gulbrandsen [2] who emphasized engineering as being the academic area whose proportion of applied research is higher. It was verified the

opposite on Trademark registration (TR), since the contribution of the variable HEE is negative. However, the impact of the proportion of people with higher education in business and law (HEBL) is positive, which can be justified by the fact that trademark registration is closely associated with commercial aspects. The variable VP has a negative coefficient in model (2) and a positive one on the model (3), which shows that vocational programs are more appropriate to certain business activities as the commercial area.

Models (4) and (5) are related to commercial results of the innovative activity EIS [10]. Were selected two sectors of activity as a way of comparing the different contributions of the explanatory variables considered.

It is important to highlight the impact of R&D expenditures thru the universities that presents a positive coefficient on the contribution of export of goods in the pharmaceutical industry sector (4). It is possible to reaffirm the high performance of the selected countries, which appear to have an adequate cooperation between applied and basic research. In the same sense, Bentley, Gulbrandsen & Gulbrandsen [2] had identified Norway and Finland as being among the 5 countries where the balance on these two types of research is higher.

In both models (4 and 5), the scientific publications (SP) have a negative impact, which may be related to the areas that these publications respect. In the same sense, we have the variable RES that presents a different contribution to the outputs of innovation, through the areas to which these researchers are affected.

As for the contribution of human capital, the proportion of people with a background in engineering (HEE) have a negative impact on the model (4) and a positive impact on the model (5). The proportion of people with a background in business and law sciences (HEBL) have a positive impact in both models, demonstrating once again that the quality of human capital influence differently the outputs of innovation. That is, the needs of human capital are distinguished by sector of activity NSC [15].

It is considered important to combine the analysis performed with a brief comparison between the selected countries. These 5 countries are considered leaders of innovation and strong innovators, both by the European Commission [10] and the Global Innovation Index [5], however there are differences among themselves. To make a comparison about the outputs of innovation, were used the dependent variables of the econometric models, having been converted per

the GDP (in millions de USD).
Chart 1: Outputs of innovation per million GDP (USD)

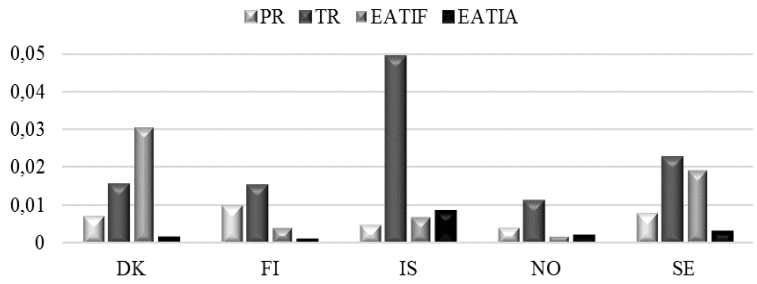

Analysing each of the dependent variables and establishing a comparison with the average values of the explanatory variables considered relevant in each case and for each country, the following conclusions are obtained:

- Concerning the patent registration (PR), Finland (FI) and Sweden (SE) stand out. Based on the analysis of the model (2), company's investments (BERD) are essential and these countries present averages of 2.37% and 2.45% (%of GDP) for Finland and Sweden. These countries are also the most outstanding in the proportion of people with higher education in engineering, with 0.26 (Finland) and 0.25 (Sweden). It should be noted that the number of researchers in Finland is significantly higher (around 16 researchers), while in the rest of the countries this figure is between 9 and 13.

- In relation to trade mark registration (TR), Iceland (IS) stands out and as seen in model (3), the investments made by the government and higher education in business sciences and law are those who present the best contribution to this output of innovation. The variable GOVERD presents an average value of 0.52 for Iceland, followed by Finland with 0.32. Likewise, it has been found that the HESBL is superior in this Iceland (0.41). Which shows its advantage in the trademark registration.

- Pharmaceutical exports (EHTFI) shows that, Denmark (DK) is the country with the highest proportion of exports in relation to GDP, followed by Sweden. In the model (4), the variable HERD stands out and in this case the average R&D expenses made by the universities (HERD) is 0.70 and 0.80 in Denmark and Sweden respectively, being ahead of the other countries.

- Regarding exports in the aerospace industry (EHTAI), the country that stands out is Iceland and, as mentioned in the analysis of the model (5), BERD, HEE

and HEBL are the variables that contribute most to the positive evolution of this variable. Not being the country that stands out with the most for investments made by companies in R&D (1.37% of GDP) or higher education in the areas of engineering and business sciences (0,49), appears to have a higher quality in the adequacy and channelling of the expenses incurred in innovation.

Conclusion

Having chosen the Nordic countries as examples in the appropriate investment and results of innovation, it was possible to verify that the innovation inputs contribute in different ways depending on the type of outputs of innovation.

R&D investment made by companies are fundamental to the success of innovation and it was verified that the way these expenses are channelled should be done depending on the results that are intended to be achieved. However, it is possible to affirm that the applied research (made fundamentally by companies) leads to higher results.

The number of researchers as well as the scientific publications are essential for the development of innovation, affecting differently the different outputs. In the same sense, human capital is crucial for innovation and its quality (here studied through higher education in engineering, business sciences and vocational programs) contributes in different ways to the results of innovation.

Comparing the innovative performance of the Nordic countries, it was possible to verify that Sweden and Finland take a prominent position both in the results of the innovation and in the factors, that determine them. These countries are those that invest seriously in R&D made by companies, universities and the Government (creating synergies with companies).

As for the number of researchers and scientific publications, the results, although favourable to innovation performance, were not conclusive, which reveals the need to study these variables but grouped by areas of research.

In terms of human capital, Finland and Sweden are the countries with the highest proportions of people with higher education in engineering and business sciences. Nevertheless, it should be pointed out that the different areas of specialization contribute in different ways to innovation.

References

1. Baltagi, B. H. (2013). Econometric Analysis of Panel Data, 5th Edition, Willey.

2. Bentley, P. J., Gulbrandsen, M. & Kyvik, S. (2015). The relationship between basic and applied research in universities. *High Educ in Springerlink*. (pp. 689-709).
3. Campos, I. M. & Valadares, E. C. (2008). Inovação tecnológica e desenvolvimento económico. (Consultado a 20 de março de 2016). Disponível em http://www.schwartzman.org.br/simon/blog/inovacaomg.pdf.
4. Castilho, A.P., Borges, N.R. & Pereira, V.T. (2014). Manual de Metodologia Científica. ULBRA.
5. Cornell University, INSEAD & WIPO (2016). The Global Innovation Index 2016: Winning with Global Innovation, Ithaca, Fontainebleu and Geneva.
6. Cunha, M. P., Rego, A., Cunha, R. C., Cabral-Cardoso, C. & Neves, P. (2016). Manual de Comportamento Organizacional e Gestão, 8ª Edição, Rh Editora.
7. Drucker, P. F. (1997). Inovação e Gestão, 4ª Edição, Editorial Presença.
8. Henson, R. K., & Roberts, J. K. (2006). Use of exploratory factor analysis in published research. *Educational and Psychological Measurement*. (vol.66, pp.393-416).
9. Etzkowitz, H. (2002). The Triple Helix of University - Industry - Government Implications for Policy and Evaluation. Science Policy Institute, SiSTER.
10. European Commission (2016). European Innovation Scoreboard 2016, European Union, Belgium.
11. Godinho, M. M. (2007). Indicadores de C&T, inovação e conhecimento: onde estamos? Para onde vamos? *Análise Social, ISEG* (Vol. 42. Pp. 239-274)
12. Leydesdorff, L. & Etzkowitz, H. (1998). The Triple Helix as a Model for Innovation Studies. *Science & Public Policy*. (Vol. 25, pp. 195-203)
13. Leydesdorf, L. & Ivanova, I. (2016). "Open innovation" and "Triple Helix" models of innovation: can synergy in innovation systems be measured?. Journal of Open Innovation.
14. Lhuillery, S., Raffo, J. & Hamdan-Livramento, I. (2016). Measuring Creativity: Learning from Innovation Measurement. Economics & Statistics Series, WIPO
15. National Science Board (NSB). (2012). Reserach & Development, Innovation and the Science and Engineering workforce. National Science Foundation.
16. OECD (2005). Oslo Manual: Guidelines for collecting and interpreting innovation data, 3th Edition, OECD and Eurostat.
17. OECD (2015). OECD Science, Technology and Industry Scoreboard 2015: Innovation for Growth and Society, OECD Publishing, Paris.
18. Pesaran, M. H. (2015). Time series and panel data econometrics, 1th Edition, Oxford University Press.
19. Porter, M. E. (2007). Estratégi e Vantagem Competitiva, Planeta Dagostini Editora.
20. Roszko-Wójtowicz, E. & Biatek, J. (2016). A multivariate approach in measuring innovation performance. *Journal of Economics and Business of Rijeka Faculty of Economics*. (Vol. 2, pp. 443-479).
21. Rothwell, P. (1994). Five generations of innovation models. *International Marketing Review*. (Vol.11, pp. 7-31). (Consultado a 15 de janeiro de 2017). Disponível em http://www.emeraldinsight.com/doi/abs/10.1108/02651339410057491.
22. Sarkar, S. (2014). Empreendedorismo e Inovação, 3ª Edição, Escolar Editora.
23. Schumpeter, J. A. (1939), Business Cycles: A Theoretical, Historical and Statistical Analysis of the Capitalist Process, New York: McGraw-Hill
24. Taherdoost, H., Sahibuddin, S. & Jalaliyoon, D. (2014). Exploratory Factor Analysis; Concepts and Theory. *Advances in Applied and Pure Mathematics* (pp. 375-382).
25. Teixeira, S. (2011). Gestão Estratégica, Escolar Editora.
26. Valente, A. C. (2014). Inovação, Educação e Trabalho n Economia Europeia, 1ª Edição, Princípia Editora.

Risk-adjusted control charts with emphasis on multivariate risk-adjusted survival time CUSUM and EWMA control charts

Athanasios Sachlas[1,2], Stelios Psarakis[2], and Sotiris Bersimis[3]

[1] Department of Statistics and Insurance Science, University of Piraeus, Piraeus, Greece
(E-mail: asachlas@unipi.gr)
[2] Department of Statistics & Laboratory of Statistical Methodology, Athens University of Economics and Business, Athens, Greece
(E-mail: psarakis@aueb.gr)
[3] Department of Statistics and Insurance Science, University of Piraeus, Piraeus, Greece
(E-mail: sbersim@unipi.gr)

Abstract. In the last two decades, a modification of standard and advanced control charts appeared in the bibliography to improve the monitoring mainly of medical processes. This is the risk-adjusted control charts, which take into consideration the varying health conditions of the patients. Biswas and Kalbfleisch (2008) outlined a risk-adjusted CUSUM procedure based on the Cox model for a failure time outcome while Sego et al. (2009) proposed a risk-adjusted survival time CUSUM chart for monitoring a continuous, time-to-event variable that may be right-censored. In this paper we have tried to present all the risk-adjusted control charts presented in the literature. The risk-adjusted charts have been grouped into four categories: control charts for continuous variables, control charts for attributes, time-weighted control charts, and multivariate control charts. Finally, we present some preliminary results on multivariate risk-adjusted survival time CUSUM and EWMA control charts.
Keywords: Control charts, Risk-adjustment, Statistical process monitoring.

1 Introduction

According to Hart et al. (2003) risk adjustment (RA) is a statistical technique for reducing the effects of confounding factors that a patient may bring to a health care encounter. There are broadly three categories of RA approaches including randomization, stratification, and multiple regression models.

Benneyan and Borgman (2003) briefly discussed risk-adjusted sequential probability ratio tests and longitudinal surveillance methods. Koetsier et al. (2012) conducted a simulation study to evaluate the performance of risk-adjusted control charts to monitor in-hospital mortality of intensive care unit patients.

Winkel and Zhang (2007) devoted the second part of their book on RA and especially the sixth section on the presentation of several risk-adjusted control charts. In a same context, Zeng (2016) reviewed the main developments concerning the two basic problems involved in RA monitoring establishing RA models, which includes identifying the appropriate performance measures to monitor and associated patient risk factors, constructing statistical models that

characterize the dependency of the performance measures on the risk factors, and change detection based on the established models, which includes estimating baseline parameters of the RA models and detecting deviations from them.

Cook et al. (2008) reviewed several RA techniques such as standardised mortality ratios, risk-adjusted p chart, observed minus expected outcome (VLAD), risk-adjusted cumulative sum (RA CUSUM), risk-adjusted sequential probability ratio test (RA SPRT), and risk-adjusted exponentially weighted moving average (RA EWMA) charts. This overview is an introduction to the use of RA methods to track mortality rates.

Grigg and Farewell (2004a) provided an overview of risk-adjusted charts (the RA CUSUM, the resetting SPRT, the sets method and Shewhart chart), with examples based on two data sets: the first consisting of outcomes following cardiac surgery and patient factors contributing to the Parsonnet score; the second being agesex-adjusted death-rates per year under a single general practitioner.

Steward and Rigdon (2016) addressed the problem of risk-adjusted monitoring as a change-point problem with several possible change-point models. For p risk variables, there are 2^{p+1} possible change-point models, because each of the slope parameters or the intercept in the logistic regression model can change. Their approach generalizes previous risk-adjusted charts in that they look for changes in any of the parameters. They adopted a Bayesian approach and found the posterior distribution for the model (i.e., which coefficients changed), the time of the change, and the values of the parameters for those that changed. All three tasks are accomplished in the context of a single model.

The paper is organized as follows: Section 2 deals with risk-adjusted control charts for continuous variables while Section 3 deals with risk-adjusted control charts for attributes. Section 4 presents time-weighted risk-adjusted control charts while Section 5 discusses multivariate risk-adjusted control charts. The last section discusses several open problems on the field of risk-adjusted process monitoring.

2 Risk-adjusted variable control charts

Alemi et al. (1996) presented a methodology for adjusting a health care organization's control charts to reflect their patient population's severity of illness during different time intervals. They demonstrated that risk-adjusting expected patient outcomes can change the assessments of the relative quality of care offered by a health care organization in different time periods. According to the authors, to risk-adjust control chart data you have to follow four steps. Firstly, you determine the number of expected deaths after RA in each of the time periods. Secondly, you calculate the expected mortality rate for each time period, while then you calculate the standard deviation of the expected mortality rate for each time period. Finally, you calculate the risk-adjusted UCL and LCL values for each time period. More specifically, to predict outcomes for each patient a regression model which includes all the patient data is used. Once the cases are assessed, their predictions are summed by time period to yield the

expected number of deaths that should occur in each of the eight time periods. Since the model only uses severity of illness variables to predict the number of patients not discharged alive in each of the time periods, this model in effect produces a risk-adjusted estimate of the number of deaths that should have occurred in each time period.

Now that the number of risk-adjusted deaths has been calculated for each time period, the next steps are to calculate the risk-adjusted expected mortality rates

$$\hat{P}_i = \frac{\sum_{j=1}^{n_i} P_{ij}}{n_i}$$

and the risk-adjusted standard deviations

$$\hat{S}_i = \frac{\sqrt{\sum_{j=1}^{n_i} (\hat{P}_{ij}(1 - \hat{P}_{ij}))}}{n_i}$$

for these same time periods as well as their risk-adjusted lower control limit

$$LCL_i = \hat{P}_i - t_{a/2}\hat{S}_i$$

and upper control limit

$$UCL_i = \hat{P}_i + t_{a/2}\hat{S}_i.$$

In these equations, $\sum_{j=1}^{n_i} P_{ij}$ is the expected number of deaths for a time period and n_i, is the number of cases for a time period. Here, $\hat{P}_{ij}$ is the probability that patient i in time period j dies. The risk-adjusted control limits are called the Expected Upper Control Limit and the Expected Lower Control Limit, respectively.

Alemi and Sullivan (2001) presented a tutorial on risk adjusted X-bar charts and their applications to measurement of diabetes control, involving nine steps.

Hart et al. (2004) discussed the use of 3-sigma $\bar{X}$ and S control charts for continuous data that are often skewed. The key feature of these charts is their application of risk-adjusted data in addition to actual performance data. The resulting charts should decrease the occurrence of both type I and type II errors as compared to the unadjusted control charts.

Zhang et al. (2012) developed a phase I risk-adjusted Shewhart control chart for monitoring surgical performances. The risk-adjusted statistic used is shown to be a likelihood ratio test statistic. The false alarm rate can be set as

$$\alpha_L = maximum\left\{0.00135, \frac{k_L}{\text{Number of negative's } w_t\text{'s}}\right\}$$

and

$$\alpha_U = maximum\left\{0.00135, \frac{k_U}{\text{Number of positive's } w_t\text{'s}}\right\}$$

for the lower- and the upper-sided chart, respectively. k_L is the number of operation cases (from the set of patients who survived) that can be reviewed/checked within constraints, following the idea of economic quality control while k_U is the number of operation cases (from the set of patients who

died) that can be reviewed/checked within constraints. The value 0.00135 comes from the traditional 3-sigma Shewhart control charts. Using the maximum of the two numbers is to ensure that the checking rate is not less than 0.135%.

The lower control limit can then be set at

$$LCL \approx \alpha_L - \text{th sample quantile of } \{w_t | w_t \leq 0, \text{ for } t = 1, 2, \ldots, N\}$$

while the upper control limit can then be set at

$$UCL \approx (1 - \alpha_U) - \text{th sample quantile of } \{w_t | w_t > 0, \text{ for } t = 1, 2, \ldots, N\}$$

and can be both obtained by using the bootstrap method.

Asadayyoobi and Niaki (2016) proposed a general Phase-I accelerated failure time-based risk-adjusted control chart for monitoring continuous surgical outcomes based on a likelihood-ratio test derived from a change-point model. Let T_i be a random variable denoting the failure time of the subject i, and $x_{i1}, \ldots, x_{ip}$ be the values of covariates for the same subject. The AFT model is then

$$logT_i = \beta_0 + \beta_1 x_{i1} + \beta_2 x_{i2} + \ldots + \beta_p x_{ip} + \sigma\epsilon_i,$$

where ϵ_i is the random disturbance term. Note that the only differences between the AFT model and the usual linear regression models are that there is a σ before ϵ_i and that the dependent variable is logged. Define $\psi^{(sl)}$ as the parameter vector of the RA model for observations $s+1$ to l. Suppose an assignable cause occurs at an unknown time τ, which leads to the change of the parameter vector from $\boldsymbol{\psi}^{(0l)} = \boldsymbol{\beta}_0^T = (\gamma_{01}^T, \gamma_{02}^T, \ldots, \gamma_{0K}^T, \beta_0^T)^T$, (in-control vector), to $\boldsymbol{\psi}^{(\tau l)} = \boldsymbol{\beta}_1^T = (\gamma_{11}^T, \gamma_{12}^T, \ldots, \gamma_{1K}^T, \beta_1^T)^T$ (out-of-control vector). If all the data follow an identical distribution, i.e. $\psi^{(0l)} = \psi^{(\tau m)}$ for all $\tau = u, u+1, \ldots, m-u$, then the process is in-control, where u ($u >$ the number of coefficients) is the minimum required sample size to estimate the parameters of the RA model. The value of u is chosen so that at least one outcome with value 0 and one outcome with value 1 exist among the sampled data from 1 to u and also from $m-u+1$ to m. Then, the aim here is to evaluate the following hypotheses

$$H_0 : \boldsymbol{\psi}^{(0\tau)} = \boldsymbol{\psi}^{(\tau m)} - H_1 : \boldsymbol{\psi}^{(0\tau)} \neq \boldsymbol{\psi}^{(\tau m)}, \tau = u, u+1, \ldots, m-u.$$

$\boldsymbol{\psi}^{(0\tau)}$ or $\boldsymbol{\beta}_0^T$ is the parameter vector of the RA model for observations 1 to τ (before the change) and $\boldsymbol{\psi}^{(\tau m)}$ or $\boldsymbol{\beta}_1^T$ corresponds to the parameter vector after the change.

3 Risk-adjusted control charts for attributes

Alemi and Oliver (2001) presented a step by step tutorial on the construction of a p-chart taking into account the severity of the patients' illness. In this chart, both the observed and the expected rates are plotted. The expected rate of falls is calculated by averaging the expectations regarding individual patients, through the formula

$$E_i = \frac{1}{N} \sum_{i=1}^{N_i} E_{ij},$$

where E_{ij} is the expected fall rate of case j in time period i. The expected fall rate can be calculated using the expected probability of falls for each patient.

Albers (2011) presented the way that information about category membership can be used to adjust the basic negative binomial charts to the actual risk incurred.

Hart et al. (2003) proposed a new class of control charts for attribute data. The charts are either additive or multiplicative models depending on how observed and risk-adjusted data are combined. These models have distinct properties and are different from standard Shewhart control charts in many aspects. Risk-adjusted rates are obtained using multivariate logistic regression models.

The comparison of each patient's demographic and clinical history with a large reference population, the RA process estimates the a priori probability of occurrence of some event for each patient. Month i will have n_i of these estimates, with their sum being the expected number of occurrences for the month E_i. Because of the averaging methods of RA, the month-to-month variation of the monthly E_i values tends to be much lower than that of the observed O_i values; the expected monthly counts are not binomially distributed. To avoid any possible confusion between the distributional properties of the observed monthly mortality count and the monthly expected mortality count the monthly expected mortality rate (not proportion) is referred to here as $E_i/n_i = r_{E_i}$ (where r_{E_i} is the expected rate).

Additive models work with the difference between the p_{O_i} and the r_{E_i}, i.e. $r_{D_i} = p_{O_i} r_{E_i}$. Because the difference in rates alone can be misleading because its significance should be assessed in relation to the size of expected rate, a multiplicative model should be considered. The multiplicative method the authors considered was based on the indirect standardization approach. A_i is the "adjusted observed occurrence count" indirectly standardized to the overall expected rate, r_E. The A_i values are the counts that would have occurred if the same standard risks were observed each month and are assumed to be binomially distributed. The risk-adjusted mortality proportion each month is therefore

$$p_{A_i} = \frac{O_i \left(\frac{r_{\bar{E}}}{r_{E_i}} \right)}{n_i}.$$

Because the variation in r_{E_i} is small, as noted previously, the quotients $\frac{r_{\bar{E}}}{r_{E_i}}$ will be close to unity and the variations of the p_{A_i} values will be close to those of p_{O_i}.

Zeng and Zhou (2011) proposed a Bayesian approach to risk-adjusted monitoring for cases where historical data are not available. Detection of change was formulated as a model-selection problem and solved using a popular Bayesian tool for variable selection, the Bayes factor.

Paynabar and Jin (2012) presented a general phase I risk-adjusted control chart for monitoring binary surgical outcomes based on a likelihood-ratio test derived from a change-point model. Different from the existing methods, this paper further shows that the binary surgical outcomes depend on not only the patient conditions described by the Parsonnet scores but also on other categorical operational covariates, such as different surgeons.

Mohammadian et al. (2016) proposed a risk-adjusted geometric control chart for monitoring the number of patients survived at least 30 days after a surgery. In this chart, the patient risk is modeled using a logistic regression. The new scheme is proposed to be used in Phase-I where a likelihood ratio test derived from a change-point model is employed.

4 Time-weighted risk-adjusted control charts

Lovegrove et al. (1997) improved the CUSUM chart that weights death and survival by each patients risk status and provides a display of surgical performance over time. This chart is called variable life-adjusted (VLAD) chart and shows the difference between expected and actual cumulative mortality. Lovegrove et al. (1999) described an alternative approach which takes account of an individual cardiac surgeon's case-mix by explicitly incorporating the inherent risk faced by patients due to a combination of factors relating to their age and the degree of disease they have.

Poloniecki et al. (1998) proposed cumulative plots for the expected mortality counts minus the observed counts that could be applied, for example, to physicians or hospitals.

Steiner et al. (2000) described a new CUSUM procedure that adjusts for each patient's pre-operative risk of surgical failure through the use of likelihood-based scoring method.

Grigg et al. (2003) discussed the use of charts derived from the sequential probability ratio test (SPRT): the CUSUM chart, RSPRT (resetting SPRT), and FIR (fast initial response) CUSUM. They described the theoretical development of the methods and explored some considerations including the approximation of average run lengths (ARLs), the importance of detecting improvements in a process as well as detecting deterioration and estimation of the process parameter following a signal.

Sismanidis et al. (2003) explored the properties of the cumulative risk-adjusted mortality (CRAM) chart, including the number of deaths before a doubling of the death rate is detected.

Grigg and Farewell (2004b) proposed the risk-adjusted version of the Sets method (Chen, 1978) for monitoring adverse medical outcomes and presented the graphical representation of it, called the Grass plot.

Grigg and Spiegelhalter (2007) proposed a simple RA EWMA control chart. The standard EWMA control chart is given by

$$E_i = \gamma s_i + (1-\gamma)E_{i-1},$$

where γ is a smoothing constant, $0 < \gamma < 1$. In the RA context, s_i is a score assigned to patient i and E_0 equals some suitable starting value that is set equal to the (estimated) average patient score before any process change. The functions of γ is the patient weights, e.g. the weight for patient $i-2$ is $\gamma(1-\gamma)^2$. To create the control chart we plot E_i versus time (actually patient number), and the chart signals if $E_i > h_U$ or $E_i < h_L$, where h_U and h_L are pre-specified constants, called the upper and lower control limits, respectively.

The RA EWMA chart is given by

$$E_i^R = \gamma \tilde{s}_i + (1-\gamma)E_{i-1}^R,$$

where $\tilde{s}_i = s_i - (\hat{E}_i^+ - \hat{E}_i)$ and $\hat{E}_i^+ = g^{-1}(g(\hat{E}_i) + \boldsymbol{\beta}^T \boldsymbol{u}_i)$.

Biswas and Kalbfleisch (2008) outlined a RA CUSUM procedure based on the Cox model for a failure time outcome. This work seems to be the first to use survival analysis models for monitoring (Gandy et al., 2010). Gandy et al. (2010) investigated how time to event models may be used for monitoring purposes. They considered monitoring using CUSUMs based on the partial likelihood ratio between an out-of-control state and an in-control state. They also considered both proportional and nonproportional alternatives, as well as a head start. Against proportional alternatives, they present an analytic method of computing the expected number of observed events before stopping or the probability of stopping before a given observed number of events.

Sego et al. (2009) proposed a risk-adjusted survival time CUSUM chart, called RAST CUSUM for monitoring a continuous, time-to-event variable that may be right-censored. RA is accomplished using accelerated failure time (AFT) regression models.

Let X_i represent the survival time for patient i with survival function $P(X_i > x_i) = S(x_i, \boldsymbol{\theta}_i)$ and density $f(x_i, \boldsymbol{\theta}_i)$. The data are observed in pairs (T_i, δ_i) where

$$T_i = min\{X_i, c\} \text{ and } \delta_i = \begin{cases} 1 \text{ if } X_i \leq c \\ 0 \text{ if } X_i > c \end{cases}$$

where c is a fixed censoring time. The likelihood function for a single observation (t_i, δ_i) is given by

$$L(\boldsymbol{\theta}_i | t_i, \delta_i) = [f(t_i, \boldsymbol{\theta}_i)]^{\delta_i} [S(t_i, \boldsymbol{\theta}_i)]^{1-\delta_i}.$$

The AFT model is based on the assumption that the survival function of patient i with observed covariate $\boldsymbol{u}_i$ at time x_i is the same as the baseline survival function, $S_0(x_i, \boldsymbol{\theta})$, evaluated at time $x_i exp\{\boldsymbol{\beta}^T \boldsymbol{u}_i\}$. The AFT model is $S(x_i, \boldsymbol{\theta}_i | \boldsymbol{U}_i = \boldsymbol{u}_i) = S_0(x_i exp\{\boldsymbol{\beta}^T \boldsymbol{u}_i\}, \boldsymbol{\theta})$, where β_i is a vector of regression parameters and $S_0(x_i, \boldsymbol{\theta}) = S(x_i, \boldsymbol{\theta}_i | \boldsymbol{U}_i = 0)$.

Numerous parametric distributions can be used to model survival times with an AFT regression model, and be used in an RAST CUSUM chart.

To detect a shift from λ_0 to $\lambda_1 = \rho_1 \lambda_0$, the log-likelihood score of the RAST CUSUM chart is given by

$$W_i(t_i, \delta_i | \boldsymbol{U}_i = \boldsymbol{u}_i) = log\left(\frac{[f(t_i | \lambda = \rho_1 \lambda_0, \boldsymbol{U}_i = \boldsymbol{u}_i)]^{\delta_i} [S(t_i | \lambda = \rho_1 \lambda_0, \boldsymbol{U}_i = \boldsymbol{u}_i)]^{1-\delta_i}}{[f(t_i | \lambda = \lambda_0, \boldsymbol{U}_i = \boldsymbol{u}_i)]^{\delta_i} [S(t_i | \lambda = \lambda_0, \boldsymbol{U}_i = \boldsymbol{u}_i)]^{1-\delta_i}} \right).$$

With predefined scores, the RAST CUSUM statistic is then calculated using using $Z_i = max(0, Z_{i-1} + W_i)$, $i = 1, 2, \ldots$.

Sego et al. (2009) proposed a risk-adjusted survival time CUSUM chart, called RAST CUSUM for monitoring a continuous, time-to-event variable that may be right-censored. RA is accomplished using accelerated failure time regression models. The general form of the risk-adjusted CUSUM (RA CUSUM)

is given by

$$Z_0 = 0 \tag{1}$$
$$Z_i = max(0, Z_{i-1} + W_i), i = 1, 2, \ldots$$

where Z_i is the CUSUM statistic and W_i is the CUSUM score. The chart gives an alarm if Z_i is larger then a control limit h. The CUSUM score is given by

$$W_i = log\left\{\frac{L(\boldsymbol{\theta}_{i1}|r_i)}{L(\boldsymbol{\theta}_{i0}|r_i)}\right\},$$

where $\boldsymbol{\theta}_{i1}$ is the nominal out-of-control value of the parameter for patient i and r_i is the measured outcome (e.g. mortality status, survival time, or censoring time).

A RA model $\boldsymbol{\theta}_{i0} = g(\boldsymbol{\psi}, \boldsymbol{U}_i)$, where $\boldsymbol{U}_i$ is a vector of covariates that reflect the risk factors for patient i and $\boldsymbol{\psi}$ is a corresponding vector of regression parameters, is used to predict $\boldsymbol{\theta}_{i0}$ for each newly arriving patient.

Steiner and Jones (2010) proposed an updating EWMA (uEWMA) control chart to monitor risk-adjusted survival times. The uEWMA operates in a continuous time; hence, the scores for each patient always reflect the most up-to-date information. The uEWMA is defined as

$$E_t = \gamma s_{it} + \gamma(1-\gamma)s_{i-1,t} + \gamma(1-\gamma)^2 s_{i-2,t} + \gamma(1-\gamma)^3 s_{i-3,t} + \ldots,$$

where s_{it} is the score for patient i (where the index i gives the order of surgery) at time t.

At time t, for patient i, we have at hand $(x_{it}, \delta_{it}, \boldsymbol{u}_i)$, where x_{it} is the minimum of the current time since time zero, the time to death and the follow-up time (or time at occurrence of a competing risk) each minus the time of surgery, $\delta_{it} = 1$ if patient i dies by time t and $\delta_{it} = 0$ otherwise, and $\boldsymbol{u}_i$ is a vector of covariates. The values of the covariates are determined at the time of surgery and are not updated as time passes.

Let, for patient i, denote t as the current time, a_i as the time of surgery, c_i as the time of a competing risk (or follow-up time) and d_i as the time of a death. Then $x_{it} = min\{t, c_i, d_i)\} - a_i$. Note that c_i and d_i represent realizations of random variables only the smaller of which is observed. For patient i there are three possibilities for (x_{it}, δ_{it}):

1. Death: $(x_{it}, 1)$, where $x_{it} = d_i - a_i$ is the time between surgery and death.
2. Success: $(x_{it}, 0)$, where $x_{it} = c_i - a_i$ is the time between surgery and the follow-up time (or some competing risk).
3. At risk: $(x_{it}, 0)$, where $x_{it} = t - a_i$ is the time between surgery and the current time.

The patient scores, s_{it}, are based on $(x_{it}, \delta_{it}, u_i)$; hence, as x_{it} and possibly δ_{it} change for case (3) as time passes, so will (some of) the scores. A patient in case (3) can become case (1) or (2) or remain in case (3) with a larger x_{it}. Note that once a patient is in case (1) or (2) x_{it} and δ_{it} (and thus the patient score) stay the same. The patient scores also depend on the selected survival-time distribution.

Gombay et al. (2011) proposed four sequential curtailed and risk-adjusted charts by using score statistics. They performed Monte Carlo simulations to explore the merits of each of these methods in terms of ARLs as well as in terms of type I probabilities. They also compared the proposed methods to the RA-CUSUM chart. They illustrated the methodologies by using data on monitoring performance of seven surgeons from a cardiac surgery center in the UK.

Assareh et al. (2011) considered estimation of the time when a linear trend disturbance has occurred in an in-control clinical dichotomous process in the presence of variable patient mix. To model the process and change point, they formulated a linear trend in the odds ratio of a Bernoulli process using hierarchical models in a Bayesian framework. The performance of the Bayesian estimator is investigated through simulations and the result shows that precise estimates can be obtained when they are used in conjunction with the risk-adjusted CUSUM and EWMA control charts for different magnitude and direction of change scenarios.

Jones and Steiner (2012) studied the effect of estimation error on risk-adjusted binary CUSUM performance using actual and simulated data on patients undergoing coronary artery bypass surgery and assessed for mortality up to 30 days post-surgery. The effect of estimation error was indicated by the variability of the "true" average run lengths (ARLs) obtained using repeated sampling of the observed data under various realistic scenarios.

Sparks (2016) developed an adaptive EWMA control chart that can be used as either a p chart for monitoring significant departures from in-control non-homogenous probabilities of failure or success or a risk-adjusted control chart for success or failure of an event.

Assareh et al. (2015) developed change point estimation methods through Bayesian hierarchical models for a clinical dichotomous process in the presence of case mix. The performance of the Bayesian estimator is investigated through simulations and the result shows that precise estimates can be obtained when they are used in conjunction with the risk-adjusted CUSUM and EWMA control charts.

Richards et al. (2015) discussed the use of risk-adjusted monitoring nonhomogeneous Poisson processes.

Keefe et al. (2016) proposed a spatially risk-adjusted Bernoulli CUSUM chart for concurrent observations to monitor foreclosure rates.

Ghasemi et al. (2016) applied a Bayesian estimation method to find the time and the size of a change in patients' post-surgery death or survival outcome. The process is monitored in phase I using risk-adjusted log-likelihood ratio test chart, in which the logistic regression model is applied to take into account pre-operation individual risks. Markov Chain Monte Carlo method was applied to obtain the posterior distribution of the change point model including time and size of the change in the Bayesian framework and also to obtain the corresponding credible intervals.

Zhang et al. (2016) investigated the effect of estimation error on the performance of risk-adjusted survival time CUSUM scheme in continuous time with the cardiac surgery data. The impact was studied with the use of the median

run lengths (medRLs) and the standard deviation (SD) of medRLs for different sample sizes, specified in-control median run length, adverse event rate and patient variability.

Zhang and Woodall (2016a) examined the effect of estimation error on the in-control performance of the risk-adjusted Bernoulli CUSUM chart with dynamic probability control limits (DPCLs) while the same authors applied the DPCLs developed for the upper risk-adjusted Bernoulli CUSUM charts to the lower and two-sided charts and examine their in-control performance (Zhang and Woodall, 2016b).

Oliveira et al. (2016) extended the risk-adjusted survival time cumulative sum (RAST CUSUM) control chart to monitor a time-to-event outcome, possibly right censored, by considering a regression model in which the covariates affect the cure fraction. The CUSUM scores are obtained for Weibull and log-logistic promotion time model to monitor a scale parameter for nonimmune individuals.

Recently, Hussein et al. (2017) explored the performance of risk-adjusted CUSUM charts when the assumptions of independence and model correctness are not met. They found out that if autocorrelations are present in the binary series being monitored and such autocorrelations are ignored, the average run lengths of the charts can deviate greatly from their design values. The impact of model misspecification on the run lengths is not severe.

5 Multivariate risk-adjusted control charts

Shojaei and Niaki (2013) extended the RA-CUSUM scheme to monitor multi-attribute medical processes for entities having different levels of risk. In the new chart, called *RA-MCUSUM* there is a vector of weights for each patient ($\boldsymbol{w}_t$) instead of one weight.

Assume that we want to monitor k patients with respect to n attitudes. The elements of the $i \times n$ vector $\boldsymbol{w}_t$ are

$$w_{t,i} = \begin{cases} log\left[K\frac{(1-p_{t,i}+p_{t,i}R_{0i})}{(1-p_{t,i}+p_{t,i}R_{Ai})}\right], & y_t = 0 \\ log\left[K\frac{(1-p_{t,i}+p_{t,i}R_{0i})R_{Ai}}{(1-p_{t,i}+p_{t,i}R_{Ai})R_{0i}}\right], & y_t = 1 \end{cases}$$

for $i = 1, 2, \ldots, n$ and $t = 1, 2, \ldots, k$. $p_{t,i}$ is the risk of patient t and R_{0i} and R_{Ai} are the odds ratios under the null and the alternative hypotheses for the i-th attribute.

Having an initial $i \times n$ zero-vector $\boldsymbol{s}_0$, i.e. a vector with all elements equal to 0, and using the relation

$$\boldsymbol{s}_t = \boldsymbol{s}_{t-1} + \boldsymbol{w}_t,$$

we calculate

$$\boldsymbol{y}_t = \left\{\boldsymbol{s}_t' \boldsymbol{\Sigma}^{-1} \boldsymbol{s}_t\right\}^{1/2}$$

which is the quantity depicted in the control chart. If $\boldsymbol{y}_t$ is greater than a threshold h, then the medical process is diagnosed to be in out of control. $\boldsymbol{\Sigma}$ is

the covariance matrix of the random vector w_t. The authors used simulation to estimate $\boldsymbol{\Sigma}$ and h. The constant parameter K appearing in $w_{t,i}$ is needed to prevent from negative weights.

5.1 Multivariate time-weighted risk-adjusted control charts

Although several authors have dealt with multivariate CUSUM charts and multivariate EWMA charts little or no work has been done to multivariate time-weighted risk-adjusted control charts. In this work, we describe the multivariate extensions of the time-weighted risk-adjusted charts.

Let X_{ji}, represent the j survival time for patient i. The data are observed in pairs (T_{ji}, δ_{ji}) where

$$T_{ji} = min\{X_{ji}, c\} \text{ and } \delta_{ji} = \begin{cases} 1 \text{ if } X_{ji} \leq c \\ 0 \text{ if } X_{ji} > c \end{cases}$$

where c is a fixed censoring time. The likelihood function for a single observation (t_{ji}, δ_{ji}) is given by

$$L(\boldsymbol{\theta}_{ji}|t_{ji}, \delta_{ji}) = [f(t_{ji}, \boldsymbol{\theta}_{ji})]^{\delta_{ji}}[S(t_{ji}, \boldsymbol{\theta}_{ji})]^{1-\delta_{ji}}.$$

To detect a shift from $\boldsymbol{\lambda}_0$ to $\boldsymbol{\lambda}_1 = \rho_1\boldsymbol{\lambda}_0$, the log-likelihood score of the RAST CUSUM chart is given by

$$W_{ji}(t_{ji}, \delta_{ji}|\boldsymbol{U}_{ji} = \boldsymbol{u}_{ji}) = log\left(\frac{[f(t_{ji}|\boldsymbol{\lambda} = \boldsymbol{\lambda}_1, \boldsymbol{U}_{ji} = \boldsymbol{u}_{ji})]^{\delta_{ji}}[S(t_{ji}|\boldsymbol{\lambda} = \boldsymbol{\lambda}_1, \boldsymbol{U}_{ji} = \boldsymbol{u}_{ji})]^{1-\delta_{ji}}}{[f(t_{ji}|\boldsymbol{\lambda} = \boldsymbol{\lambda}_0, \boldsymbol{U}_{ji} = \boldsymbol{u}_{ji})]^{\delta_{ji}}[S(t_{ji}|\boldsymbol{\lambda} = \boldsymbol{\lambda}_0, \boldsymbol{U}_{ji} = \boldsymbol{u}_{ji})]^{1-\delta_{ji}}}\right).$$

The RAST MCUSUM statistic is then calculated using $Z_{ji} = max(0, Z_{ji-1} + W_{ji})$, $i = 1, 2, \ldots$.

Following a similar approach, the RAST MEWMA can be defined as

$$E_{jt} = \gamma s_{jit} + \gamma(1-\gamma)s_{ji-1,t} + \gamma(1-\gamma)^2 s_{ji-2,t} + \gamma(1-\gamma)^3 s_{ji-3,t} + \ldots,$$

where s_{jit} is the j score for patient i (where the index i gives the order of surgery) at time t.

Since we target to monitoring simultaneous more than one survival time, we can use multivariate frailty models such as Gamma frailty.

6 Discussion

In this paper we have tried to present the most of the advances regarding the risk- adjusted control charts presented in the literature. We followed a four groups categorization: control charts for continuous variables, control charts for attributes, time-weighted control charts, and multivariate control charts.

Moreover, we presented some preliminary results regarding multivariate risk-adjusted survival time-weighted control charts. The central idea is to monitor simultaneously more than one survival times. For example, one may be interested in monitoring both the time of wound healing and the time the patient feels pain after a serious open heart surgery. Based on the work of Sego et al. (2009) on risk-adjusted survival time CUSUM charts and of Steiner and Jones (2010) on risk-adjusted survival time EWMA (uEWMA) we outlined the corresponding multivariate control charts.

Bibliography

W. Albers. Risk-adjusted control charts for health care monitoring. International Journal of Mathematics and Mathematical Sciences, Article ID 895273: 16 pages, 2011.

F. Alemi and D.W. Oliver. Tutorial on risk-adjusted p-charts. Quality Management in Healthcare, 10(1):1–9, 2001.

F. Alemi and T. Sullivan. Tutorial on risk adjusted x-bar charts: applications to measurement of diabetes control. Quality Management in Healthcare, 9: 57–65, 2001.

F. Alemi, W. Rom, and E. Eisenstein. Risk-adjusted control charts for health care assessment. Annals of Operations Research, 67:45–60, 1996.

N. Asadayyoobi and S. T. A. Niaki. Monitoring patient survival times in surgical systems using a risk-adjusted aft regression chart. Quality Technology & Quantitative Management, 2016. doi: dx.doi.org/10.1080/16843703.2016.1208932.

H. Assareh, I. Smith, and K. Mengersen. Bayesian estimation of the time of a linear trend in risk-adjusted control charts. IAENG International Journal of Computer Science, 38(4):409–417, 2011.

H. Assareh, I. Smith, and K. Mengersen. Change point detection in risk adjusted control charts. Statistical Methods in Medical Research, 24(6):747–768, 2015.

J.C. Benneyan and A.D. Borgman. Risk-adjusted sequential probability ratio tests and longitudinal surveillance methods. International Journal for Quality in Health Care, 15(1):5–6, 2003.

P. Biswas and J.D. Kalbfleisch. A risk-adjusted cusum in continuous time based on the cox model. Statistics in Medicine, 27:3382–3406, 2008.

R. Chen. A surveillance system for congenital malformations. Journal of the American Statistical Association, 73:323–327, 1978.

D.A. Cook, G. Duke, G.K. Hart, D. Pilcher, and D. Mullany. Review of the application of risk-adjusted charts to analyse mortality outcomes in critical care. Critical Care and Resuscitation, 10:239–251, 2008.

A. Gandy, J. T. Kvaløy, A. Bottle, and F. Zhou. Risk-adjusted monitoring of time to event. Biometrika, 97(2):375–388, 2010.

R. Ghasemi, Y. Samimi, and H. Shahriari. Bayesian estimation of change point in phase one risk adjusted control charts. Journal of Industrial and Systems Engineering, 9(2):20–37, 2016.

E. Gombay, A.A. Hussein, and S.H. Steiner. Monitoring binary outcomes using risk-adjusted charts: a comparative study. Statistics in Medicine, 30:2815–2826, 2011.

O. Grigg and V. Farewell. An overview of risk-adjusted charts. Journal of the Royal Statistical Society: Series A, 167(3):523–539, 2004a.

O. Grigg and V. Farewell. A risk-adjusted sets method for monitoring adverse medical outcomes. Statistics in Medicine, 23:1593–1602, 2004b.

O. Grigg and D. Spiegelhalter. A simple risk-adjusted exponentially weighted moving average. Journal of the American Statistical Association, 102(477): 140–152, 2007.

O. Grigg, V. Farewell, and D.J. Spiegelhalter. Use of risk-adjusted cusum and rsprtcharts for monitoring in medical contexts. StatisticalMethods in Medical Research, 12:147–170, 2003.

M.K. Hart, K.Y. Lee, R.F. Hart, and J.W. Robertson. Application of attribute control charts to risk-adjusted data for monitoring and improving health care performance. Quality Management in Health Care, 12(1):5–19, 2003.

M.K. Hart, J.W. Robertson, R.F. Hart, and K.Y. Lee. Application of variables control charts to risk-adjusted time-ordered healthcare data. Quality Management in Health Care, 13(2):99–119, 2004.

A. Hussein, A. Kasem, S. Nkurunziza, and S. Campostrini. Performance of risk-adjusted cumulative sum charts when some assumptions are notmet. Communications in Statistics - Simulation and Computation, 2017. doi: dx.doi.org/10.1080/03610918.2014.964805.

M.A. Jones and S.H. Steiner. Assessing the effect of estimation error on risk-adjusted cusum chart performance. International Journal for Quality in Health Care, 24(2):176–181, 2012.

M.J. Keefe, C.T. Franck, and W.H. Woodall. Monitoring foreclosure rates with a spatially risk-adjusted bernoulli cusum chart for concurrent observations. Journal of Applied Statistics, 2016. doi: dx.doi.org/10.1080/02664763.2016.1169257.

A. Koetsier, N.F. de Keizer, E. de Jonge, D.A. Cook, and N. Peek. Performance of risk-adjusted control charts to monitor in-hospital mortality of intensive care unit patients: A simulation study. Critical Care Medicine, 40(6):176–181, 2012.

J. Lovegrove, O. Valencia, T. Treasure, C. Sherlaw-Johnson, and S. Gallivan. Monitoring the results of cardiac surgery by variable life-adjusted display. The Lancet, 350:1128–1130, 1997.

J. Lovegrove, C. Sherlaw-Johnson, O. Valencia, T. Treasure, and S. Gallivan. Monitoring the performance of cardiac surgeons. Journal of the Operational Research Society, 50(7):684–689, 1999.

F. Mohammadian, S.T.A. Niaki, and A. Amiri. Phase-i risk-adjusted geometric control charts to monitor health-care systems. Quality and Reliability Engineering International, 32(1):19–28, 2016.

J.W. Oliveira, D.M. Valenca, P.G. Medeiros, and M. Marcula. Risk-adjusted monitoring of time to event in the presence of long-term survivors. Biometrical Journal, 2016. doi: dx.doi.org/10.1002/bimj.201500094.

K. Paynabar and J. Jin. Phase i risk-adjusted control charts for monitoring surgical performance by considering categorical covariates. Journal of Quality Technology, 44(1):39–53, 2012.

J. Poloniecki, O. Valencia, and P. Littlejohns. Cumulative risk adjusted mortality chart for detecting changes in death rate: observational study of heart surgery. Quality and Safety in Health Care, 316:1697–1700, 1998.

S.C. Richards, W.H. Woodall, and G. Purdy. Surveillance of nonhomogeneous poisson processes. Technometrics, 57(3):388–394, 2015.

L.H. Sego, M.R. Reynolds Jr, and W.H. Woodall. Risk-adjusted monitoring of survival times. Statistics in Medicine, 28:1386–1401, 2009.

S.N. Shojaei and S.T.A. Niaki. A risk-adjusted multi-attribute cumulative sum control scheme in health-care systems. In *2013 IEEE International Conference on Industrial Engineering and Engineering Management*, pages 1102–1106, Dec 2013. doi: 10.1109/IEEM.2013.6962581.

C. Sismanidis, M. Bland, and J. Poloniecki. Properties of the cumulative risk-adjusted mortality (cram) chart, including the number of deaths before a doubling of the death rate is detected. Medical Decision Making, 23(3): 242–251, 2003.

R. Sparks. Linking ewma p charts and the risk adjustment control charts. Quality and Reliability Engineering International, 2016. doi: dx.doi.org/10.1002/qre.2045.

S.H. Steiner and M. Jones. Risk-adjusted survival time monitoring with an updating exponentially weighted moving average (ewma) control chart. Statistics in Medicine, 29:444–454, 2010.

S.H. Steiner, R.J. Cook, and V.T. Farewall. Monitoring surgical performance using risk-adjusted cumulative sum charts. Biostatistics, 1:441–452, 2000.

R.M. Steward and S.E. Rigdon. Risk-adjusted monitoring of healthcare quality: Model selection and change-point estimation. Statistics in Medicine, 2016. doi: dx.doi.org/10.1002/qre.2074.

P. Winkel and N.F. Zhang. *Statistical Development of Quality in Medicine*. John Wiley & Sons, Ltd., Chichester, 2007. ISBN 978-0-470-02777-6.

L. Zeng. *Risk-Adjusted Performance Monitoring in Healthcare Quality Control*, pages 27–45. Springer London, London, 2016. ISBN 978-1-4471-6778-5. doi: 10.1007/978-1-4471-6778-5_2.

L. Zeng and S. Zhou. A bayesian approach to risk-adjusted outcome monitoring in healthcare. Statistics in Medicine, 30:3431–3446, 2011.

L. Zhang, F.F. Gan, and C.K. Loke. Phase i study of surgical performances with risk-adjusted shewhart control charts. Quality Technology & Quantitative Management, 9(4):375–382, 2012.

M. Zhang and W.H. Woodall. Dynamic probability control limits for lower and two-sided risk-adjusted bernoulli cusum charts. Quality and Reliability Engineering International, 2016a. doi: dx.doi.org/10.1002/qre.2044.

M. Zhang and W.H. Woodall. Reduction of the effect of estimation error on in-control performance for risk-adjusted bernoulli cusum chart with dynamic probability control limits. Quality and Reliability Engineering International, 2016b. doi: dx.doi.org/10.1002/qre.2014.

M. Zhang, Y. Xu, Z. He, and X. Hou. The effect of estimation error on risk-adjusted survival time cusum chart performance. Quality and Reliability Engineering International, 2016. doi: dx.doi.org/10.1002/qre.1849.

Realized *p*-Variation Random Functions As Statistical Diagnostics for Itô Semimartingales

Lino Sant [1]

[1] Department of Statistics and Operations Research, Faculty of Science, University of Malta, Msida, Malta
(E-mail: lino.sant@um.edu.mt)

Abstract. The stochastic properties of the *p*-variation of semimatingales, and recently the statistical properties of realized *p*-variation, have played important and crucial roles in the study of semimartingales and their applications. Realized *p*-variation can help solve problems involving hypothesis testing, diagnostic checking and parameter estimation for stochastic processes.
In this paper random functions are constructed out of suitably normalized sums of *p*'th power of increments obtained from sample path readings for suitable values of *p*. Some properties are studied within a Banach space setting wherein stochastic equicontinuity ensures uniform convergence. These random functions are being proposed as general purpose diagnostics for investigating the nature of the generating process under study using path sample values. Statistical results and simulation runs are proposed and discussed.

Keywords: Itô semimartingales, realized *p*-variation, variationgram.

.

1 Introduction

Needs to provide a suitably sophisticated theory of stochastic processes for modeling purposes have grown widely within many fields. The establishment of stochastic calculus set the stage for major advances in modeling complex phenomena. From Brownian Motion the passage to processes with jumps, effected quite a while ago through Lèvy processes, blossomed into many applications in various physical, engineering, biological and earth sciences. Finance entered the scene with vigour slightly later. But with its deep pockets it soon became a major stakeholder. This very active background serves to render fertile interfaces between mathematical theory and applications beyond what many practitioners in the two subfields seem to be aware of.

Theoretical frameworks have been devised to offer scope and latitude wherein the complexity of systems under study can be addressed. Deep structural results from stochastic analysis have, and are still, being put into service for heavy duty work within stochastic modelling. Once mathematical contexts are in place, theory is developed to show how properties possessed by models correspond to features existing within systems under study and are reflected in available data. Inferring from data up to the system producing it is a crucial modelling task. Statistics provides the support to translate inductive undertakings into useful

algorithms for understanding and controlling stochastically evolving dynamical systems. This could serve as a mission statement for Stochastics.

Stochastic processes have paths as possible realizations. Path properties are thus distinguishing features about which no decent theory should fail to provide results. One such property which goes beyond the continuity property is the existence or otherwise of the *p*-variation of a given path.

The smallest value of p for which the *p*-variation exists in the data-generating-mechanism one is studying is a key question in many areas. However unless a continuous trace is available, data comes as lists of readings sampled over time. Observations are usually "sparse". Values in between adjacent actual readings are not available and we have to work with realized *p*-variation. Statistics has to come to the rescue. It provides estimation techniques, hypotheses formulations and testing routines for various inferences needed by researchers and practitioners.

Why Semimartingales?

We shall work with semimartingales. Semimartingales occupy an important, high place in the hierarchy of stochastic process. From the theoretical point of view their importance derives from stochastic analysis. In a precise sense, they are the farthest we can go in defining properly stochastic integration.

From the applications point of view it was financial mathematics which brought semimartingales back strongly into the limelight. They offer an elegant and theoretically fertile background for dealing with arbitrage and they are well suited to include stochastic volatility models. In many research circles Lèvy processes shot to great prominence quite a few decades ago are still much in vogue. Nevertheless, they are after all special cases of semimartingales, which offer wider generality and a better theoretical platform to understand how things work and where they fail.

We take $(\Omega, \mathcal{F}, \mathbb{P})$ to be a a probability space with increasing, right-continuous family of sub-σ-algebras $\mathcal{F}_t : t \geq 0$ forming a complete filtration. The real-valued stochastic process X_t is a semimartingale if it is adapted, has a right-continuous modification with left-hand limits and can be decomposed as the sum of a local martingale and a process of finite variation : $X_t = M_t + A_t$.

The local martingale part is in fact locally square integrable, that is a process which when stopped along some suitable stopping time sequence it yields a square integrable martingale. The finite variation part can have both a continuous component and jumps. It generates a product jump measure μ on $\Omega \times \mathbb{R}_+$. Paths can be purely continuous, that is they are made up of pure jumps or be a mixture of continuous trajectories and jumps.

Semimartingales can be characterized by triplets of the form (B, C, ν) where B is the drift, C is the quadratic variation process associated with X^c and ν is

the compensator of the jump random measure μ taking all processes concerned to be predictable.

p-Variation of Paths

For a given process , X_t with paths $s \to X_s(\omega)$ corresponding to each $\omega \in \Omega$, subdivisions of the type $0 = t_0 < t_1 < ... < t_n = t$ give us partition $\mathcal{P}_n$ of $[0,t]$, with corresponding variation given by $\sum_{i=1}^{n} \left| X_{t_i} - X_{t_{i-1}} \right|$. As we let partitions vary we get a net of values generated by sums as above and the supremum of this net is declared to be the total variation : $\sup_{\mathcal{P}_n \in \mathcal{P}} \sum_{i=1}^{n} \left| X_{t_i} - X_{t_{i-1}} \right|$ where $\mathcal{P}$ is the set of all partitions. There are two problems with this measure of path behaviour.
Firstly paths with finite variation form probabilistically a rather meagre collection within the context of stochastic processes. Secondly the set of all finite partitions offers too many fine selections possible as to allow one to pick up path oscillations and stretch them out to infinity.

For most interesting and useful stochastic processes the total variation of paths is almost surely infinite. In Brownian motion if we change our focus to quadratic variation, $\sum_{i=1}^{n} \left| X_{t_i} - X_{t_{i-1}} \right|^2$, we just about avoid drifting off to infinite by choosing partitions suitably "inattentive" to oscillations at a local level. They are partitions of time intervals with mesh size going to 0.

Quadratic variation deserves special attention. Results involving it date back to Paul Lèvy and it figured prominently in early works on martingales and eventually semimartingales by P.A. Meyer[9] and D. Lepingle[8]. Renewed recent interest in the study of the empirical counterpart of quadratic variation, realized quadratic variation especially in mathematical finance, feeds a relatively new stream of research. Seminal papers by Andersen, Bollerslev, Aït Sahhalia[1], Barndorff-Nielsen , Shephard[2] , Mancini and more recently Jacod[5],[6], [7] have produced a large amount of important results with useful empirical repercussions.

A cardinal property for semimartingales is that they all have finite **quadratic** variation. The martingale component can have a continuous part as well as a part with jumps. The continuous martingale component will have unbounded variation with the increasing process $\left\langle X_t^c, X_t^c \right\rangle$ as compensator for the martingale part squared. The jumps might not be summable and so they also might need a compensator for us to write them meaningfully. This compensator forms part of A_t in the decomposition above.

The quadratic variation process corresponding to semimartingale X_t was in fact shown to be given by the increasing process $\left[X_t^c, X_t^c \right] = \left\langle X_t^c, X_t^c \right\rangle + \sum_{s \le t} \Delta X_s^2$.

We would also like to consider different values of the power *p*. When $p > 2$ for paths $s \to X_s(\omega)$ corresponding to each $\omega \in \Omega$ the *p*-variation process, whenever it exists, is given by: $S_t^p(X) = \sum_{s \le t} \left| X_s - X_{s-} \right|^p$. We note that this quantity is a process in its own right and does not derive from sample paths.

We also saw that the choice of partitions needs to be restrained. In effect partitions should be chosen to correspond to sampling schemes from the empirical point of view. From the theoretical point of view one has to be especially careful to distinguish between the high frequency and the low frequency type of sampling schemes. The asymptotics are different.

To make our context more manageable, we limit partitions of $[0,t]$ to have *n* equally spaced intervals, $t_i = it/n$ and sums of the type $V_t^n(p, X) = \sum_{i=1}^{n} \left| X_{t_i} - X_{t_{i-1}} \right|^p$.

Thus we formulate the statistical problem with sample path values from some stochastic process as follows : As the mesh size of partitions decreases, do sums of the type above converge in some sense to $S_t^p(X)$ say?

The asymptotic behaviour of the realized variation $V_t^n(p, X)$ was studied in depth in the late 1970's. Convergence in probability gives a decent theory with useful results , notably those of Lepingle[8] and Meyer[9].
In particular it was shown that:

- For $p > 2$ processes of bounded *p*-variation $V_t^n(p, X)$ tend to $S_t^p(X)$ $\mathbb{P}$-almost surely for each $t \in \mathbb{R}_+$.
- $V_t^n(2, X)$ tends to $\left[X_t^c, X_t^c \right]$ in probability.
- For $1 < p < 2$ there is convergence to $S_t^p(X)$ only if the continuous part of the semimartingale is zero and $S_t^p(X) < \infty$.

The smallest *p* for which *p*-variation of a process exists is known as the Bloomenthal-Getoor index. Values of this minimal *p* less than 1 are not exciting because continuous components do not exist and jumps have to stick to being of finite variation. The level of activity is indeed low and nothing exotic takes place. In fact a continuous component forces the minimal *p* to be 2.
For the more interesting semimartingales, $V_t^n(p, X)$ diverges to infinity for small values of *p*. However, with our partitions, equally spaced for which the mesh is given by t/n if we normalize as follows:

$$U_t^n(p,X)=\left(\frac{t}{n}\right)^{1-p/2}\sum_{i=1}^{n}\left|X_{t_i}-X_{t_{i-1}}\right|^p=\begin{cases}\left(\frac{t}{n}\right)^{1-p/2}V_t^n(p,X) & \text{if } 0\le p\le 2\\ V_t^n(p,X) & \text{if } p>2\end{cases}$$

convergence results do in fact materialize.

The map $\omega\to\{p\to U_t^n(p,X)(\omega)\}$ defines a statistical random function on which we shall apply a number of results, obtained fairly recently. However, we need to restrict further the class of semimartingales for which these results hold.

Itô Semimartingales

Itô semimartingales are semimartingales whose predictable characteristics (B,C,ν) are absolutely continuous with respect to Lebesgue measure. There are a number of representations of these processes. We give the following Grigelionis form:

$X_t=X_0+\int_0^t b_s ds+\int_0^t \sigma_s dW_s+\kappa'(\delta)*\mu_t+\kappa(\delta)*(\nu-\mu)_t$ where W_s is a Brownian Motion, $B_t=\int_0^t b_s ds$, $C_t=\int_0^t \sigma_s^2 ds$, $\kappa(x)=x1_{\{|x|<\varepsilon\}}$ is a truncation function with $\kappa'(x)=x-\kappa(x)$, μ is a Poisson random measure, δ a predictable process on $\Omega\times\mathbb{R}_+\times\mathbb{R}$ which satisfies $\int_A \delta(\omega,t,x)dsdx=\int_0^t\int_A \nu(\omega,ds,x)dx$

The truncation function takes care of jumps with size decreasing to 0.

We take b_t and the process corresponding to δ to be predictable, locally bounded processes with the latter also square summable. σ_t is adapted and cadlag. We propose the convergence of $U_t^n(p,X)$ in probability to a specific limit as an established result:

Theorem 1 (Jacod)

Let X_t be an Itô semimartingale. For $0<p<2$, as the size of the partition mesh tends to 0, as $n\to\infty$, $U_t^n(p,X)$ converges in probability, uniformly over $[0,t]$ to $U_t(p,X)=\sqrt{\frac{2^p}{\pi}}\Gamma\left(\frac{p+1}{2}\right)\int_0^t\sigma_s^p ds$, that is:

$$\mathbb{P}-\lim_{n\to\infty}\left|U_s^n(p,X)-U_s(p,X)\right|=0$$

Proof of this theorem can be found in Jacod[6]

Results for $p=2$ as well as for $p>2$ have been known in detail for

semimartingales in general since Lepingle[8]. For $p > 2$ we have in fact stronger results because convergence occurs $\mathbb{P}$-almost surely. These results allow us to extend a limit function $U_t(p, X)$ over the whole of $\mathbb{R}_+$ as follows:

$$U_t(p,X) = \begin{cases} t & \text{for } p = 0 \\ \sqrt{\dfrac{2^p}{\pi}}\Gamma\left(\frac{p+1}{2}\right)\displaystyle\int_0^t \sigma_s^p ds & \text{for } 0 < p < 2 \\ \displaystyle\int_0^t \sigma_s^2 ds + S_t^2(X) & \text{for } p = 2 \\ S_t^p(X) & \text{for } p > 2 \end{cases}$$

We note the potential jump at $p = 2$ and call $U_t(p, X)$ the **variationgram** because it gives an important graphical tool to characterize the nature of a semimartingale using the *p*-variation of a process.

Four examples of variationgrams are next given (figures 1 to 4) showing typical plots for limit functionals $U_t(p, X)$, two for processes without jumps but with different Brownian components and two for processes with processes having jumps of different sizes. Processes being sums of the two types would be expected to have superimposed variationgrams.

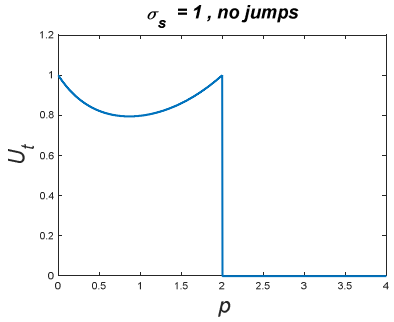

Fig. 1

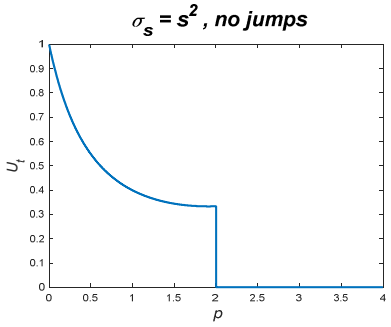

Fig.2

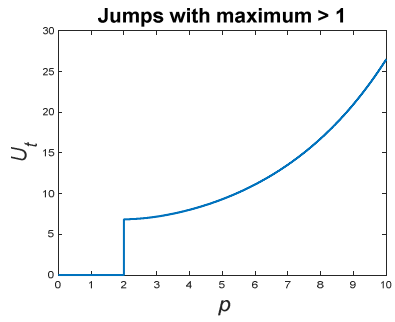

Fig. 3

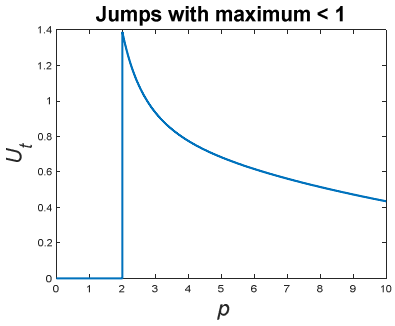

Fig.4

The major theoretical difference between variationgrams for purely continuous and for pure jump processes is that their supports are disjoint. Other intuitions gathered from the plots and validated by theorems above can be summarized as:
i. The limit functionals make very strong distinctions between processes which are continuous, others which are pure jump processes and processes which are composed of continuous components and jumps.
ii. features of the shape of the two curves (symmetry or lack of it in the first, and whether the curve is increasing or decreasing in the second) give some indications as to the nature of the underlying stochastic process.

In practice we do not have these limiting functions, but we have sample path readings which yield statistical random functions. The relevant statistical question we can ask is how close and fast does the estimator $U_t^n(p,X)$, the **sample variationgram**, converges in probability to $U_t(p,X)$ again uniformly over $[0,t]$ for $p>0$. There are a number of theorems in the literature for whom the authors claim a "Central Limit Theorem" status designed for this context. Going through the conditions given for the corresponding proofs to carry through, one can see that the situation for general semimartingales is complex. Therefore we shall make a number of assumptions which allow us to make use of asymptotic results later on. In practice these assumptions do not limit much the range of processes in common use.

Condition 1.

The diffusion (volatility) term takes the form of an Itô semimartingale:

$\sigma_t = \sigma_0 + \int_0^t \mu_s ds + \int_0^t \eta_s dW_s + \int_0^t \tilde{\eta}_s d\tilde{W}_s$ with $\tilde{W}_s$ an independent Brownian motion of W_t, and μ_t, η_t, $\tilde{\eta}_t$ adapted, left continuous and with right hand limits.

Condition *s*

For $0 \le s \le 2$ The distribution function for the jump size satisfies the inequality:

$\int_0^1 |x|^s \delta(\omega,t,x)dx + \int_1^\infty \delta(\omega,t,x)dx < \infty$

We quote a result from Jacod[6].

Theorem 2 (Jacod)

Let X_t be an Itô semimartingale which satisfies Conditions 1 and *s* in addition to the earlier ones above. Letting $0 < p < 2$

i. For $0 \le s \le 1$ and fixed $t \in \mathbb{R}_+$ the random variable $\sqrt{\frac{n}{t}}\left[U_t^n(p,X) - U_t(p,X)\right]$ converges stably in distribution to: $\sqrt{\frac{2^p}{\pi}\left[\sqrt{\pi}\Gamma\left(p+\frac{1}{2}\right) - \Gamma\left(\frac{p+1}{2}\right)^2\right]}\int_0^t \sigma^p d\tilde{W}_s$ where $\tilde{W}_t$ is a standard Brownian motion defined on an auxiliary probability space.

ii. For $s>1$ and fixed $t\in\mathbb{R}_+$ the random variable $\frac{t}{n}\left[U_t^n(p,X)-U_t(p,X)\right]$ converges in probability to 0.

Proofs of these results can be found in Jacod[6]

The Sample Variationgram

The idea which we are pushing is that of looking at $U_t^n(p,X)$ as a sequence of stochastic processes, generated by different path sample readings from some semimartingale, with values in an appropriately chosen Banach space of piecewise continuous functions. Actually all our random functions stay within the closed, positive cone of this Banach space. For each $t\in\mathbb{R}_+$, the original process has its own distinctive, deterministic function $p\to U_t(p,X)$. These functions can have at most just one jump and moreover they serve as limits to sample-derived random functions $p\to U_t^n(p,X)$ in the corresponding sense. We would like to include $[2,K]$ as domain of our functions because the contrast between what happens here and on $[0,2]$ can tells us a lot about the nature of the original stochastic process.

For our Banach space we could take the product of two spaces of continuous functions, $\mathcal{C}([0,2-\varepsilon])\times\mathcal{C}([2+\varepsilon,K])$ for suitable small $\varepsilon>0$ and K larger than 2 with the supremum norm. This formulation takes care of the jump at $p=2$ whenever it arises for processes with continuous Brownian components. Sample variationgrams enforce continuity at 2, but not differentiability. One could thus investigate what happens on $(2-\varepsilon,2+\varepsilon)$ as there are different rates on the two sides of 2, but we shall refrain. For the sake of clarity we shall display graphs with domains $[0,2-\varepsilon]\cup[2+\varepsilon,K]$

What we shall procede to prove our main result: convergence in probability of $U_t^n(p,X)$ is uniform in $\boldsymbol{p}$.

Lemma 3

Let X_t be an Itô semimartingale. For each $t\in\mathbb{R}_+$, and fixed $\omega\in\Omega$ the collection of random functions indexed by $n\in\mathbb{N}$,

$$\{p\to U_t^n(p,X)(\omega):0\le p\le 2-\varepsilon\}$$

is stochastically equicontinuous in *p*.

Note that $U_t^n(0,X)(\omega)=t$ for all *n*.

$\{p\to U_t^n(p,X)(\omega):2+\varepsilon\le p\le K,n\in\mathbb{N}\}$ is stochastically equicontinuous in *p*.

Proof

Given $0 \le p, p' < 2$, we have

$$\left|U_t^n(p,X) - U_t^n(p',X)\right| =$$

$$\left|U_t^n(p,X) - U_t(p,X) + U_t(p,X) - U_t(p',X) - (U_t^n(p',X) - U_t(p',X))\right|$$

$$\le \left|U_t^n(p,X) - U_t(p,X)\right| + \left|U_t(p,X) - U_t(p',X)\right| + \left|U_t^n(p',X) - U_t(p',X)\right| = A_n$$

where we call the last random variable on the RHS of the above inequality A_n

For fixed ω, $U_t(p,X)$ is clearly continuous **with respect to *p*** on the compact set we are restraining it to. So $U_t(p,X)$ is uniformly continuous.

With *p* fixed, given any $\varepsilon > 0$ there exists $\delta > 0$ such that:

$\left|p - p'\right| < \delta \Rightarrow \left|U_t(p,X) - U_t(p',X)\right| < \varepsilon/2$.

Now

$$\mathbb{P}\left[\left|U_t^n(p,X) - U_t(p,X)\right| + \left|U_t^n(p',X) - U_t(p',X)\right| > \varepsilon/2\right] \le$$

$$\mathbb{P}\left[\left|U_t^n(p,X) - U_t(p,X)\right| > \varepsilon/4\right] + \mathbb{P}\left[\left|U_t^n(p',X) - U_t(p',X)\right| > \varepsilon/4\right]$$

But both $U_t^n(p,X)$ and $U_t^n(p',X)$ converge in probability to their respective limits. So given $\eta > 0$ we can take *N* large enough such that for all $n > N$:

$$\mathbb{P}\left[\left|U_t^n(p,X) - U_t(p,X)\right| > \varepsilon/4\right] < \eta/2 \;\&\; \mathbb{P}\left[\left|U_t^n(p',X) - U_t(p',X)\right| > \varepsilon/4\right] < \eta/2$$

With these choices we see that $\sup_{|p-p'|<\delta} \left|U_t^n(p,X) - U_t^n(p',X)\right| \le A_n(\varepsilon,\eta)$ which for $n > N$ gives us convergence of $A_n(\varepsilon,\eta)$ to 0 in probability.

$$\mathbb{P}\left[A_n(\varepsilon,\eta) > \varepsilon\right] \le \mathbb{P}\left[\left|U_t^n(p,X) - U_t(p,X)\right| > \varepsilon/4\right] + \mathbb{P}\left[\left|U_t^n(p',X) - U_t(p',X)\right| > \varepsilon/4\right] < \eta$$

But this gives us precisely the result that $U_t^n(p,X)$ is stochastically equi-continuous.

For the second result we can follow the scheme above, actually in a stronger manner, because convergence here is $\mathbb{P}$-almost surely, and a fortiori in probability.

■

Theorem 4

The statistical functional $U_t^n(p,X)$ (resp $\tilde{U}_t^n(p,X)$) converges stably in probability to the random function $U_t(p,X)$ uniformly in p on $[0, 2-\varepsilon]$ and in $0 \le s \le t$: $\sup_{0 \le p \le 2-\varepsilon} |U_t^n(p,X) - U_t(p,X)| = o_{\mathbb{P}}(1)$

Convergence occurs almost surely to $U_t(p,X)$ uniformly in p on $[2+\varepsilon, K]$ and in $0 \le s \le t$: $\sup_{2+\varepsilon \le p \le K} |U_t^n(p,X) - U_t(p,X)| = o(1)$ $\mathbb{P}$-almost surely.

Therefore $U_t^n(p,X)$ can be considered to be an asymptotically unbiased and consistent estimator of $U_t(p,X)$.

Proof:

Knowing that $U_t^n(p,X)-U_t(p,X)$ converges pointwise in probability to 0 on a compact set, with $U_t(p,X)$ having no dependence on *n*, since we have established stochastic equicontinuity, we can conclude the result stated in the theorem using for example Theorem 2.1 Newey[10].

■

These results allow us to investigate the convergence properties of sums of functions of Itô semimartingales increments on partitions of decreasing mesh.

Corollary 5

The statistical random functions :

$$p \to \sum_{i=1}^{n}\left(\log\left(\left|X_{t_i}-X_{t_{i-1}}\right|\right)-\frac{1}{2}\log\left(\frac{t}{n}\right)\right)\left(\frac{t}{n}\right)^{1-p/2}\left|X_{t_i}-X_{t_{i-1}}\right|^p$$

are uniformly bounded in probability uniformly over *p* with the same range restrictions as for Theorem 4.

Proof

Using the mean value theorem for function $f(p)=a^{1-p/2}|b|^p$, given p' we know there exists a *q* where $p \le q \le p'$ and

$$\left|U_t^n(p,X)-U_t^n(p',X)\right|=\left|\sum_{i=1}^{n}\left(\frac{t}{n}\right)^{1-p/2}\left|X_{t_i}-X_{t_{i-1}}\right|^p-\left(\frac{t}{n}\right)^{1-p'/2}\left|X_{t_i}-X_{t_{i-1}}\right|^{p'}\right|=$$

$$|p-p'|\left|\sum_{i=1}^{n}\left(\log\left(\left|X_{t_i}-X_{t_{i-1}}\right|\right)-\frac{1}{2}\log\left(\frac{t}{n}\right)\right)\left(\frac{t}{n}\right)^{1-q/2}\left|X_{t_i}-X_{t_{i-1}}\right|^q\right|$$

For the LHS stochastic equicontinuity was established and that shows that the RHS must be asymptotically bounded in probability.

■

It is worthwhile to study functions of the type $\varphi(n,x,p)=\sum_{i=1}^{n}\frac{t}{n}^{1-p/2}\left|x\right|^p$ we are using in dealing with our variationgram and related ones. In particular, we consider the derivative wrt *p* which the previous corollary showed us has to be quite well-behaved. This can allow us to deduce interesting repercussions. The functions within the summation in the derivative have the form $(\log x+a)\,x^p$. This function has contrasting behavior for different values of *p*. We note that special values of *a* and *p* interest us because we are interested in asymptotic behaviour. Thus we may assume $a>0$.

For $x \ge 1$, $(\log x+a)\,x^p$ starts from 0 and increases indefinitely always below *x* but eventually exceeding any x^p but never reaching x^{p+1}.

For $0 \le x \le 1$ $(\log x + a)\, x^p$ starts from 0 goes down to a minimal negative value at $x = e^{-(a+1/p)}$ and then grows to a. Thus $g(x) = |\log x + a|\ x^p$ starts from 0 grows for an initial stage achieving a maximum of $e^{-(1+a/p)} / p$ at $x = e^{-(a+1/p)}$ and goes down to 0 at $x = 1$. This indicates that the statistical random function $\sum_{i=1}^{n} \left(\log\left(\left| X_{t_i} - X_{t_{i-1}} \right| \right) - \frac{1}{2} \log\left(\frac{t}{n} \right) \right) \left(\frac{t}{n} \right)^{1-q/2} \left| X_{t_i} - X_{t_{i-1}} \right|^p$ has its very own virtues in giving more importance to certain brackets of low values in absolute value of the increments. A graph of the corresponding sample-derived random function could also help in inferences about the original data generating process.

Simulations and Application

To test the usefulness of the results above in practice we have run a huge number of simulations from which we pick a few. These should be indicative of how the statistical random functions discussed above work on familiar processes. We have generated 1024 readings equally spaced in time s, so that $0 \le s \le 1$ with $t = 1$. We have generated 10 samples from each of the following 4 processes : Brownian motion, Compound Poisson, Cauchy and a sum of BM and Cauchy processes. The plots $U_t^n = U_1^{1024}$ against p were superimposed for each process and the graphs are displayed in figures 5 to 8.

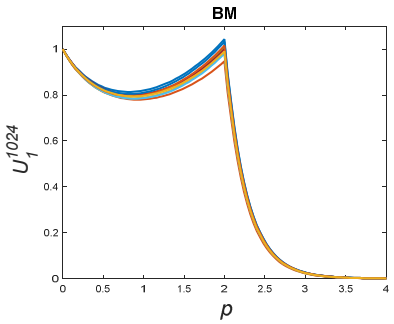

Fig. 5

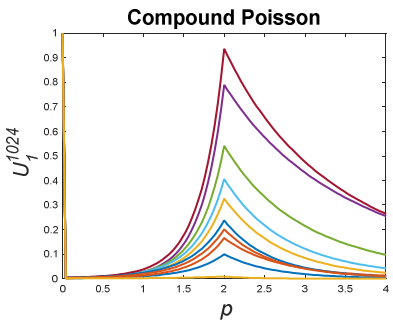

Fig.6

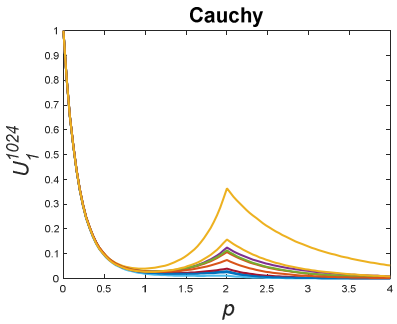

Fig. 7

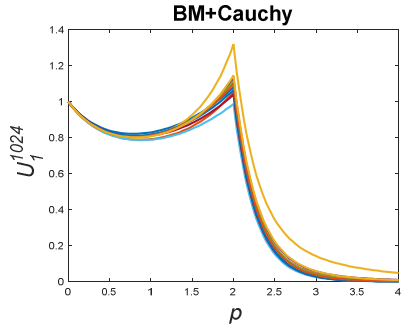

Fig.8

We notice again a number of features which in practice would be helpful to indicate which theoretical process would most likely be able to give samples with variationgrams obtained from real samples.

We also ran an experiment with real data. 3763 Readings of values labelled by NASDAQ as “market close” covering just over a week’s readings were analysed. The actual period they were registered started on 28th March 2016 at 9:30 and ended on 8th Apr 2016 at 16:00.

The sample variationgrams were computed and graphed for different frequencies: at the frequency supplied, every 10’th reading, every 50’th reading and every 100’th reading. The graphs are displayed in figures 9-12.

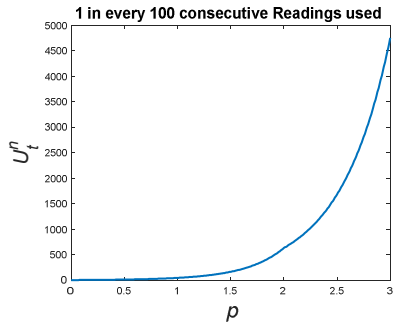

Fig. 9

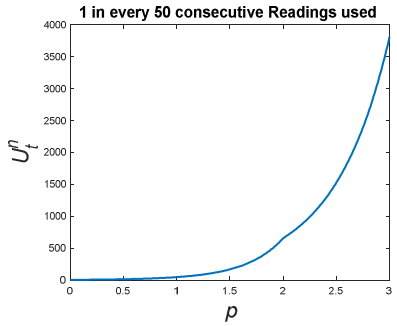

Fig.10

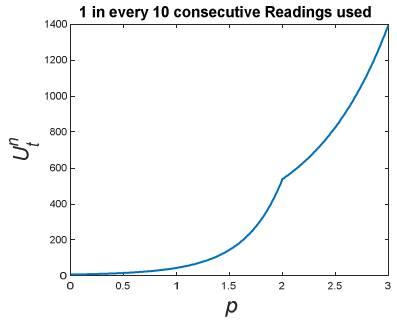

Fig. 11

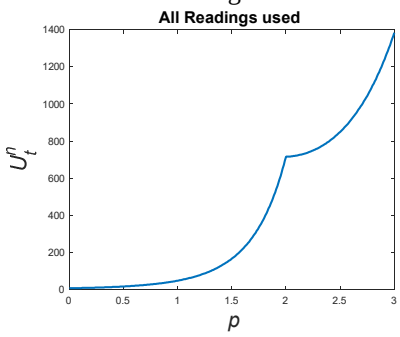

Fig.12

From these figures it is clear that a number of features should be very important to modelers who are trying to obtain a decent process to mimic the data generating mechanism. As the frequency of available readings increases we see that the mixed nature of the underlying mechanism (continuous process plus purely discontinuous one) becomes more evident. Also we can see how the quadratic variation increases.

Conclusion

Having shown asymptotic unbiasedness and consistency the statistical random functions can now be used safely for various statistical inference tasks. We mention a few obvious ones :

- Characterizing graphically specific types of processes as well as some of their properties
- Constructing tests for deciding whether a set of readings is more likely to come from one dgm rather than from another
- Test whether it is more likely that the paths of the dgm have jumps or not
- Estimate the relative contributions of the drift plus compensation and the jumps to the dynamics of a given process

There are other results about these functions related to rates of convergence and confidence intervals which refer us back to Theorem 2 and which would do with some more development in future work along this direction.

References

1. Y. Aït Sahhalia and J. Jacod. Semimartingale: Itö or not?, preprint , 2016.
2. O.E. Barndorff-Nielsen and N. Shephard. Econometric analysis of realised volatility and its use in estimating stochastic volatility models. Jour. of Roy. Stat. Soc., Series B64, 253-280, 2002.
3. O.E. Barndorff-Nielsen, S.E., Graversen and J. Jacod. A central limit theorem for realised power and bipower variations of continuous semimartingales. From "Stochastic Analysis to Mathematical Finance, Festschrift for Albert Shiryaev", Springer, 2006.
4. A. Diop , J. Jacod and V.Todorov. Central Limit Theorems for approximate quadratic variations of pure jump Itö semimartingales. Stochastic Processes and their Applications 123(2012) 839-886 . 2013
5. J. Jacod and A.N. Shiryaev. Limit Theorems for Stochastic Processes, Springer Verlag. 2003.
6. J. Jacod. Asymptotic properties of realized power variations and related functionals of semimartingales, Stochastic Processes and their Applications 118(2008) 517-559., 2008.
7. J. Jacod and P.E. Protter. Discretization of Processes, Springer, 2012
8. D. Lepingle. La variation d' ordre *p* des semi-martingales, Zeitschrift fűr Wahr., Springer-Verlag, 1976.
9. P.A. Meyer. Un cours sur les intégrales stochastiques, Strasbourg, Springer, 1975.
10. W. K. Newey. Uniform Convergence in Probability and Stochastic Equicontinuity, Econometrica, Vol. 59. No 4 (1991) 1161-1167.

Choosing tuning instruments for Generalized Rubin-Tucker Lévy Measure Estimators

Lino Sant[1] and Mark Anthony Caruana[2]

[1] Department of Statistics and Operations Research, Faculty of Science, University of Malta, Msida, Malta.
(E-mail: lino.sant@um.edu.mt)
2 Department of Statistics and Operations Research, Faculty of Science, University of Malta, Msida, Malta.
(E-mail: mark. Caruana@um.edu.mt)

Abstract. Estimation of the Lévy measure through the increments of a Lévy process is a problem which attracted much attention over recent decades. The first such estimator comes much earlier from Rubin and Tucker but it has not been much in use. Its performance is not satisfactory and researchers have tried alternatives. Various issues surround this statistical problem, most notably the behavior of the Lévy measure at the origin. Even increments from BM yield poor estimates. But Rubin-Tucker type estimators, that is distribution function estimators constructed out of increments X_{ik} coming from sample path values proposed in the more general form:

$$\hat{G}(u) = \frac{1}{N}\sum_{i=1}^{N} n^b \sum_{k=1}^{n} \frac{|X_{ik}|^{\psi(X_{ik})}}{1+|X_{ik}|^{\psi(X_{ik})}} 1_{\{|X_{ik}|<u\}}$$

can improve the performance.
In this paper the authors study this estimator and look for suitable choices of the tuning parameter b and the function ψ to improve estimator quality and convergence rates. Various classical and other recent results are put into use to obtain an estimator for an equivalent Lévy measure distribution function suitably transformed. The choice of the function ψ was guided by convergence results, in particular, the choice $\psi(x) = 2 - x^{\beta}$ for $-1 \le x \le 1$, with β close to 0 on the positive side, is shown to have special benefits which are studied in this paper.
Keywords: Lévy measure, Lévy process, convergence rates, distribution function.

1 Introduction

The nonparametric estimation problem concerning Lévy processes has attracted much attention in the past decades. This was mainly fueled by the fact that Lévy processes have and still are being used heavily in various fields of study, most notably in Finance. The link between infinitely divisible distributions and Lévy process is well understood. This allows us to express the characteristic function $\varphi(t)$ corresponding to the distribution of the increments of such processes via the so-called Lévy-Khitchine representation (or its

variants). In particular, throughout this paper we shall mainly concentrate on the Lévy-Khitchine canonical representation which is expressed as follows:

$$\varphi(t) = \exp\left(i\lambda t + \int_{\mathbb{R}} \left(\exp(itu) - 1 - \frac{itu}{1+u^2} \right) \frac{1+u^2}{u^2} dH(u) \right). \qquad (1.1)$$

In equation (1.1), λ is the drift term while H is a non-decreasing function of bounded variation such that $H(-\infty) = 0$. Moreover, *H* might have a jump at 0, this jump is equal in size to σ^2 which in turn is the variance of the Brownian motion component, if it exists. λ and *H* together completely determine the infinitely divisible distribution and thus allow us to uniquely determine the law of any Lévy process.

Rubin and Tucker[5] provide two nonparametric estimators for the function *H*. In particular, we focus on the first estimator which fits within the so-called high-frequency setting and which was inspired by the concepts illustrated in chapter 2, section 24 of Gendenko and Kolmogorov[4]. The primary concern of the latter authors was to find necessary and sufficient conditions for the existence of sums of independent infinitesimal random variables. To obtain useful results they used the function $f(x) = x^2/(1+x^2)$ which squares small values and at the same time truncates large values to 1. This function clearly also features in the Rubin and Tucker estimator which can be defined as follows:

$$\hat{H}(u) = \frac{1}{N} \sum_{i=1}^{N} \sum_{k=1}^{n} \frac{X_{ik}^2}{1+X_{ik}^2} 1_{\{X_{ik} < u\}}$$

where X_{ik} represents the k^{th} increment within the i^{th} unit time interval of a Lévy process L_t which is observed over N unit time intervals. For simplicity in this paper we assume that $N \in \mathbb{N}$. Moreover, in each unit time interval we have *n* increments. Hence all the increments X_{ik} share the same distribution with $L_{1/n}$. Rubin and Tucker show that this estimator converges P-a.s. to *H* at all points of continuity. However the authors do not comment about the rate of convergence nor about the asymptotic distribution of this estimator.

Though the Rubin and Tucker estimator is considered as one of the earliest attempts to estimate the function *H* nonparametrically, it has rarely been used or discussed. Gegler and Stadmüller[1] consider an altered version of the above estimator by avoiding completely the interval close to 0. On the other hand, Caruana and Sant[2] study the behaviour of this estimator on intervals close to and including 0. In particular the authors also explore the idea of altering the above estimator by of using some fixed power of X_{ik} that is closer to 0 than 2. Furthermore Caruana and Sant[2] show that for the Brownian motion case, under certain conditions, their proposed estimator converges faster than the original Rubin and Tucker estimator over a unit time interval. Asymptotic normality of the estimator is also discussed.

In this paper we propose to alter the power of X_{ik} in such a way that this is a function involving X_{ik}: $\hat{G}(u) = \frac{1}{N} \sum_{i=1}^{N} n^b \sum_{k=1}^{n} \frac{|X_{ik}|^{\psi(X_{ik})}}{1+|X_{ik}|^{\psi(X_{ik})}} 1_{\{X_{ik} < u\}}$

where $\psi(x) = 2 - |x|^{\beta}$ for β a tuning parameter greater to but close to 0, and *b* a suitable chosen normalizing factor is to be discussed later. We study the behaviour of $\hat{G}(u)$, which

is an estimator of a function G on an interval close to 0. As we shall see in section 2, when suitably transformed, the function G is equal to H.

In the above estimator, we require the function $\psi(x)$ to be in such a way that $\lim_{x\to 0}\left(1-\cos(x)/|x|^{\psi(x)}\right)=C<\infty$. $\psi(x)$ cannot take value less than 2 at $x=0$ because if this were the case, the above requirement would not be satisfied. The validity of these statements will be used in the proof of theorem 2.1. We note that for other values of x convergence of the estimator is recovered by inserting n^b in $\hat{G}$.

When we compare the function $|x|^{2-|x|^\beta}/1+|x|^{2-|x|^\beta}$ with $x^2/1+x^2$, we observe that both functions are bounded below by 0 and above by 1. However the former goes to 0 as $x\to\pm\infty$ while the latter goes to 1. Hence these functions and therefore the estimators defined earlier, operate on the set of incremetns of the Lévy process in different ways. The property which we just mentioned of the former function will be quite useful in the course of sections 3 and 4 as it will be exploited in certain sections of the proofs.

The rest of the paper is organised as follows: in the next section we state and prove a modified version of the theorem concerning the canonical representation of the characteristic function of infinitely divisible distribtuions. This theorem gives us an alternative way of expressing the characteristic function of infinitely divisible distirbutions. We define the function G and discuss the relation between the G and H. In section 3 we state and prove a number of theorems which are related to the limits of sums of infinitesimal random variables. These theorems, in particular theorem 3.3, will lay the theoretical foundation securing the validity of *G*. In section 4 we discuss some of its properties. Section 5 contains a number of simulation results. These results corroborate our statements regarding properties of $\hat{G}$. Section 6 contains some concluding remarks.

2 Modified version of the Canonical Representation

The function $f(x)=x^2/(1+x^2)$ plays a key role in the proof of the canonical representation, which features in section 18 of Gnedenko and Kolmogorov[4]. As we shall see in this section, the theorem still holds if the power of *x* in the function $f(x)$ is altered. However, not any power of *x* which is less than 2 will do at $x=0$. In fact we show that if the power of *x* is changed from 2 to $2-|x|^\beta$ for $\beta>0$ but close to 0, then the theorem still holds. However, in so doing we shall have to replace the function *H* by another function *G* that is shown to be of bounded variation.

2.1 Theorem

$\varphi(t)$ is the characteristic function of an infinitely divisible distribution, if and only if its logarithm can be expressed as follows:

$$\log(\varphi(t))=i\gamma t+\int\left(e^{itu}-1-\frac{itu}{1+|u|^{2-|u|^\beta}}\right)\frac{1+|u|^{2-|u|^\beta}}{|u|^{2-|u|^\beta}}dG(u)$$

for $\beta>0$. $\gamma\in\mathbb{R}$ and G a non-decreasing function of bounded variation. At $u=0$ the integrand is well-defined taking its value to be its limit as $u\to 0$.

Proof

Only the necessity part of the proof is relevant to this paper.

If $\varphi(t)$ is the characteristic function of an infinitely divisible distribution F, then for $n \in \mathbb{N}$, $\varphi_n(t) = [\varphi(t)]^{1/n}$ gives a sequence of characteristic functions with corresponding distribution function F_n. We next define $G_n(u) = n\int_{-\infty}^{u} \frac{|x|^{2-|x|^\beta}}{n^{\frac{|x|^\beta}{2}}\left(1+|x|^{2-|x|^\beta}\right)} dF_n(x)$ and

$I_n(t) = \int \left(\exp(itu)-1\right) \frac{\left(1+|u|^{2-|u|^\beta}\right)}{|u|^{2-|u|^\beta}} n^{\frac{|u|^\beta}{2}} dG_n(u)$.

The existence of each $I_n(t)$ is guaranteed by the existence of $\int \left(\exp(itx)-1\right) dF_n(x)$.

The corresponding sequence of functions converges pointwise to $\log\left(\varphi(t)\right)$ since $\lim_{n\to\infty} n[\varphi_n(t)-1] = \log\left(\varphi(t)\right)$.

Next we consider $\Re\left(I_n(t)\right) = \int \left(\cos(tu)-1\right) \frac{\left(1+|u|^{2-|u|^\beta}\right)}{|u|^{2-|u|^\beta}} n^{\frac{|u|^\beta}{2}} dG_n(u)$

.

We use the above to prove that G_n which is an increasing function, is bounded.

Let $A_n = \int_{|u|\le 1} dG_n(u)$ and $B_n = \int_{|u|\ge 1} dG_n(u)$ and $C_n = A_n + B_n = \int dG_n(u)$.

For every $\epsilon > 0$ we have that for *n* sufficiently large

$$-\log\left|\varphi(t)\right| + \epsilon \ge \int_{|u|\le 1} \left(1-\cos(tu)\right) \frac{\left(1+|u|^{2-|u|^\beta}\right)}{|u|^{2-|u|^\beta}} n^{\frac{|u|^\beta}{2}} dG_n(u)$$

$$\ge \int_{|u|\le 1} \left(1-\cos(tu)\right) \frac{1}{|u|^{2-|u|^\beta}} dG_n(u)$$

Hence: $-\log|f(1)| + \epsilon \ge \int_{|u|\le 1} \left(1-\cos(u)\right) \frac{1}{|u|^{2-|u|^\beta}} dG_n(u)$

The function $\left(1-\cos(u)\right)\frac{1}{|u|^{2-|u|^\beta}}$, for $\beta > 0$ has a minimum at $\pm u_\beta$, which values we denote by $C_\beta = \left(1-\cos(u_\beta)\right)\frac{1}{|u_\beta|^{2-|u_\beta|^\beta}}$. (Clearly the same value hold for $-u_\beta$).

It can be shown that $|u|^{|u|^\beta} > |u|$ for all $\beta > 0$ and hence for all $\beta > 0$

$$\left(1-\cos(u)\right)\frac{1}{\left|u\right|^{2-|u|^{\beta}}} \geq \frac{|u|^{|u|^{\beta}}}{3} > \frac{|u|}{3}$$

This implies that for $|u| \leq 1$, $\left(1-\cos(u)\right)\frac{1}{\left|u\right|^{2-|u|^{\beta}}} > 0$ and hence $C_{\beta} > 0$. Thus,

$$-\frac{\log|f(1)|+\epsilon}{C_{\beta}} \geq \int_{|u|\leq 1} dG_n(u) = A_n$$

Next, if we integrate the LHS and the RHS of the inequality:

$$-\log\left|f(t)\right| + \epsilon \geq \int_{|u|\geq 1} \left(1-\cos(tu)\right) dG_n(u)$$

on the interval $0 \leq t \leq 2$ we obtain:

$$-\frac{1}{2}\int_0^2 \log|f(t)|\,dt + \epsilon \geq \int_{|u|\geq 1}\left(1-\frac{\sin(2u)}{2u}\right) dG_n(u) \geq \frac{1}{2}B_n$$

Hence from the above we have that G_n is bounded.

Moreover following the proof of theorem 1 in section 18 of Gnedenko and Kolmogorov[4] in our case also $\int_{|u|>T} dG_n(u) \to 0$ as $T \to \infty$ uniformly with respect to *n*. Using these results together with Theorem 3 bis in section 9 of Gnedenko and Kolmogorov[4] we can choose a subsequence from $G_n(u)$, which we denote by $G_{n_k}(u)$, which converges pointwise at all points of continuity to a function G which is non decreasing function of bounded variation.

We next put $\gamma_{n_k} = \int \frac{|u|^{|u|^{\beta}}}{|u|} n_k^{\frac{|u|^{\beta}}{2}} dG_{n_k}(u)$, so that

$$I_{n_k}(t) = \int\left(e^{itu} - 1 - \frac{itu}{1+|u|^{2-|u|^{\beta}}}\right)\frac{1+|u|^{2-|u|^{\beta}}}{|u|^{2-|u|^{\beta}}} n_k^{\frac{|u|^{\beta}}{2}} dG_{n_k}(u) + it\gamma_{n_k}$$

By what we discussed in the previous pages, as $k \to \infty$, the integral on the right hand side of this equation, converges to

$$i\gamma t + \int\left(e^{itu} - 1 - \frac{itu}{1+\left|u\right|^{2-|u|^{\beta}}}\right)\frac{1+\left|u\right|^{2-|u|^{\beta}}}{\left|u\right|^{2-|u|^{\beta}}} dG(u)$$

Indeed since $I_n(t) \to \log\left(f(t)\right)$ then γ_{n_k} must converge to some constant γ. This completes the necessity part of the proof.

■

At zero, the functions *H* and *G* both can experience a jump. However, for the latter the size of this jump is not equal to σ^2 (as is for the former function). Indeed for the Brownian motion case the jump is of size $\lim_{n\to\infty}\mathbb{E}\left(\frac{|L_{1/n}|^{2-|L_{1/n}|^{\beta}}}{n^{|x|^{\beta}/2-1}\left(1+|L_{1/n}|^{2-|L_{1/n}|^{\beta}}\right)} 1_{\{L_{1/n}<u\}}\right)$.

Furthermore, for pure jump processes, the function *G* cannot experience a jump at zero. In literature (1.1) is not the most widely used representation for the characteristic function of infintely divisble distributions. Indeed the Lévy Khintchine representation is the most frequently used. In the latter representation an infinitely divisible distribution (and hence the corresponding Lévy process) is fully determined via three parameters $\left(\mu, \sigma^2, v(.)\right)$. This is the so-called Lévy triple were ν is the Lévy measure. The relation between *H* in (1.1) and ν is given through the equation: $\nu(dx) = \frac{1+x^2}{x^2} H(dx)$. Similarly $\nu(dx) = \frac{1+|x|^{2-|x|^\beta}}{|x|^{2-|x|^\beta}} G(dx)$.

3 Limit Theorems of Sums of Infinitesimal Random Variables

The estimator proposed by Rubin and Tucker[5] is based on a remark present in page 121 in Gnedenko and Kolmogorov[4] which is based on Theorem 1 of section 24. The theoretical foundation of the estimator which we propose in this paper will be based on a reformulation of this remark as presented in remark 3.4 below. Moreover, this remark is based on theorem 3.3 which is a reformulation of Theorem 1 in section 24 of Gnedenko and Kolmogorov[4].

The proof of theorem 3.3 is based on a number of results, some of which can easily be adapted from theorems found in sections 22 and 23 in Gnedenko and Kolmogorov[4]. They are not included in this paper. It is important to note that the said authors were finding generic conditions under which sums of infinitesimal random variables converge.

In the framework of this paper, from the i^{th} unit time interval each X_{ik}, has a distribution function which we denote by $F_k(x)$ and corresponding characteristic function $\varphi_k(t)$. So in the first unit time interval we have: $X_{11} + \ldots + X_{1n} = L_1$ where $X_{1k} = L_{k/n} - L_{(k-1)/n}$ for $k = 1, 2, \ldots, n$ and likewise with X_{ik} for the *i*'th unit interval. Hence, the distribution of L_1, like that of any L_i, is the limit law of the distribution of this sequence of sums.

Although we are primarily interested in the behavior of the estimator $\hat{G}$ in an interval close to 0, which we arbitrarily take to be $[-1,1]$, in this section we shall consider a number of results that are true for any $u \in \mathbb{R}$. As a result, the estimator of *G*, which we define in the next section, will be valid for $u \in \mathbb{R}$. Moreover, for simplicity, in this section (and parts of the next section) we shall be working within the first unit time interval. Hence one of the indices of X_{ik} will be fixed at 1. This will not stop us from going more general at the end of section 4 when the estimator is defined and its properties discussed.

We start off by proving the following the following lemma which will play a key role in a number of subsequent proofs.

3.1 Lemma

For any $x, y \in [-1,1]$ we have that $|x-y|^{2-|x-y|^\beta} \leq |x|^{2-|x|^\beta} + K_\beta |y|$ for all $0 < \beta < \infty$, where K_β is some constant that depends on β.

Proof:

We start by showing that the derivative of the function $|x|^{2-|x|^\beta}$ is bounded for $\beta > 0$. The first derivative of x^{2-x^β} is given by $x^{1-x^\beta}\left[2 - x^\beta\left(1+\beta\log(x)\right)\right]$. As $x \to 0$ this function tends continuously to 0 on the compact interval $[-1,1]$. Hence it must be bounded by some constant K_β which depends on β. But then the function $|x|^{2-|x|^\beta}$ is Lipschitz and for any $a, b \in [-1,1]$ we have that:

$$|a|^{2-|a|^\beta} - |b|^{2-|b|^\beta} \le K_\beta |a-b|$$

Taking $a = x - y$ and $b = x$ we get the result.

■

3.2 Theorem

Let $X_{11},\ldots,X_{1n}$ be a sequence of independent, infinitesimal, random variables. If the distribution of the sums $X_{11}+\ldots+X_{1n}-A_n$ converges to a limit as $n \to \infty$ for a sequence of real numbers A_n, then there exists $C \in \mathbb{R}$, such that,

$$\sum_{k=1}^{n}\int \frac{x^{2-|x|^\beta}}{1+x^{2-|x|^\beta}} dF_k\left(x+\alpha_k\right) < C \text{ where } \alpha_k = \int_{|x|<\tau} x\, dF_k(x), \text{ where } \tau \in \mathbb{R}^+ .$$

Proof:

We note that if X_{1k} is an infinitesimal random variable which has a median, which we denoted by m_k, then $\sup|m_k| \to 0$ and $\sup|\alpha_k| \to 0$. We refer the reader to Gnedenko and Kolmogorov[4], section 23, pg 111 for further details concerning these two properties of infinitesimal random variables.

We start by considering a sequence δ_n such that $0 < \delta_n \le 1$, $\delta_n \to 0$ as $n \to \infty$. Then:

$$\sum_{k=1}^{n}\int_{-\infty}^{\infty} \frac{|x|^{2-|x|^\beta}}{1+x^{2-|x|^\beta}} dF_k\left(x+\alpha_k\right) \le \sum_{k=1}^{n}\int_{-\delta_n}^{\delta_n} \frac{|x|^{2-|x|^\beta}}{1+x^{2-|x|^\beta}} dF_k\left(x+\alpha_k\right) + \sum_{k=1}^{n}\int_{|x|>\delta_n} \frac{|x|^{2-|x|^\beta}}{1+|x|^{2-|x|^\beta}} dF_k\left(x+\alpha_k\right)$$

We consider the terms in each summation on the right hand side separately.

$$\begin{aligned}\sum_{k=1}^{n}\int_{-\delta_n}^{\delta_n} \frac{|x|^{2-|x|^\beta}}{1+|x|^{2-|x|^\beta}} dF_k\left(x+\alpha_k\right) &\le \sum_{k=1}^{n}\int_{-\delta_n}^{\delta_n} \frac{{\delta_n}^{2-{\delta_n}^\beta}}{1+{\delta_n}^{2-{\delta_n}^\beta}} dF_k\left(x+\alpha_k\right) \\ &\le \sum_{k=1}^{n}\int_{-\delta_n}^{\delta_n} \delta_n dF_k\left(x+\alpha_k\right) \\ &\le n\delta_n \\ &\to 0\end{aligned}$$

if we choose say, $\delta_n = \frac{1}{n^a}$ for $a > 1$.

In the second summation, we have that:

$$\sum_{k=1}^{n}\int_{|x|\geq\delta_n}\frac{x^{2-|x|^{\beta}}}{1+x^{2-|x|^{\beta}}}dF_k(x+\alpha_k)=\sum_{k=1}^{n}\int_{\delta_n\leq|x+m_k-\alpha_k|<1}\frac{|x+m_k-\alpha_k|^{2-|x+m_k-\alpha_k|^{\beta}}}{1+|x+m_k-\alpha_k|^{2-|x+m_k-\alpha_k|^{\beta}}}dF_k(x+m_k)$$

$$+\sum_{k=1}^{n}\int_{|x+m_k-\alpha_k|\geq1}\frac{|x+m_k-\alpha_k|^{2-|x+m_k-\alpha_k|^{\beta}}}{1+|x+m_k-\alpha_k|^{2-|x+m_k-\alpha_k|^{\beta}}}dF_k(x+m_k)$$

$$\leq\sum_{k=1}^{n}\int_{\delta_n\leq|x+m_k-\alpha_k|<1}\frac{|x+m_k-\alpha_k|^{2-|x+m_k-\alpha_k|^{\beta}}}{1+|x+m_k-\alpha_k|^{2-|x+m_k-\alpha_k|^{\beta}}}dF_k(x+m_k)+\sum_{k=1}^{n}\int_{|x+m_k-\alpha_k|\geq1}1dF_k(x+m_k)$$

$\sum_{k=1}^{n}\int_{|x+m_k-\alpha_k|\geq1}1dF_k(x+m_k)\leq\sum_{k=1}^{n}\int_{|x|\geq1/2}1dF_k(x+m_k)\to0$ as $n\to\infty$ by a result which features in Gnedenko and Kolmogorov[4], page 105.

Next we consider:

$$\sum_{k=1}^{n}\int_{\delta_n\leq|x+m_k-\alpha_k|<1}\frac{|x+m_k-\alpha_k|^{2-|x+m_k-\alpha_k|^{\beta}}}{1+|x+m_k-\alpha_k|^{2-|x+m_k-\alpha_k|^{\beta}}}dF_k(x+m_k)\leq\sum_{k=1}^{n}\int_{\delta_n\leq|x+m_k-\alpha_k|<1}|x+m_k-\alpha_k|^{2-|x+m_k-\alpha_k|^{\beta}}dF_k(x+m_k)\ .$$

The function $x^{-x^{\beta}}$ has a maximum turning point when $x=\exp(-1/\beta)$. Yielding a maximum value of $\exp(1/\beta e^{1})$.

Hence, it follows that $x^{2-x^{\beta}}\leq x^{2}\exp(1/\beta e^{1})$ for any $x\geq0$ provided that $\beta>0$. Thus,

$$\sum_{k=1}^{n}\int_{\delta_n\leq|x+m_k-\alpha_k|<1}|x+m_k-\alpha_k|^{2-|x+m_k-\alpha_k|^{\beta}}dF_k(x+m_k)\leq\exp(1/\beta e^{1})\left(\sum_{k=1}^{n}\int_{\delta_n\leq|x+m_k-\alpha_k|<1}2x^{2}dF_k(x+m_k)+2\sum_{k=1}^{n}\int_{\delta_n\leq|x+m_k-\alpha_k|<1}(m_k-\alpha_k)^{2}dF_k(x+m_k)\right)$$

$$\leq\exp(1/\beta e^{1})\left(\sum_{k=1}^{n}\int_{\delta_n\leq|x+m_k-\alpha_k|<1}2x^{2}dF_k(x+m_k)+2\sum_{k=1}^{n}(m_k-\alpha_k)^{2}\right)$$

Next we need to show that the summations in the RHS go to zero as $n\to\infty$.

$$\sum_{k=1}^{n}\int_{\delta_n\leq|x+m_k-\alpha_k|<1}2x^{2}dF_k(x+m_k)\leq\sum_{k=1}^{n}\int_{|x+m_k-\alpha_k|<1}2x^{2}dF_k(x+m_k)\leq\sum_{k=1}^{n}\int_{|x|<2}2x^{2}dF_k(x+m_k)\to0$$

by a result which features in Gnedenko and Kolmogorov[4], page 105.

$\lim_{n\to\infty}\sum_{k=1}^{n}(m_k-\alpha_k)^{2}=0$ by a result which features in Gnedenko and Kolmogorov[4], page 111-112.

■

Theorem 3.3

Let $X_{11},\ldots,X_{1n}$ be a sequence of independent and infinitesimal random variables. The distribution function of the sums

$$\zeta_n=X_{11}+\ldots+X_{1n}-A_n \tag{1.2}$$

converges to a limit for some suitable chosen A_n, if and only if the infinitely divisible laws converge and are such that the logarithm of their corresponding characteristic functions is given by the formula:

$$\Psi_n(t)=-iA_nt+\sum_{k=1}^{n}\left(it\alpha_k+\int e^{itx-1}dF_k(x+\alpha_k)\right). \tag{1.3}$$

The limit of the distribution functions for the two sequences coincide.

Proof

As before, we only need to prove the necessity part of the proof.

We start by setting $F'_k(x) = F_k(x+\alpha_k)$, then the sum in (1.2) will converge if and only if

$$\varphi_n(t) = e^{-iA_n t}\prod_{k=1}^{n}\varphi_k(t) = e^{-iA_n t + it\sum_{k=1}^{n}\alpha_k}\prod_{k=1}^{n}\varphi'_k(t) \to \varphi(t)\cdot$$

We set $\varphi'_k(t) - 1 = \beta_k$. Since X_{1k} are infinitesimal then $\lim_{n\to\infty}\left(\sup_{1\le k\le n}|\beta_k|\right) = 0$.

Moreover it can also be shown that for sufficiently large *n*,

$$\left|\sum_{k=1}^{n}\log(\varphi'_k(t) - \beta_k\right| \le \sup_{1\le k\le k_n}|\beta_k|\sum_{k=1}^{n}|\beta_k|\,.$$

We next show that $\sum_{k=1}^{n}|\beta_k|$ is bounded.

We start by considering $\left|\exp(itx) - 1 - it|x|^{2-|x|^\beta}\right|$:

$$\begin{aligned}\left|\exp(itx) - 1 - it|x|^{2-|x|^\beta}\right| &= \sqrt{2 - 2cos(tx) - 2\sin(tx)t|x|^{2-|x|^\beta} + t^2|x|^{4-2|x|^\beta}}\\ &\le \sqrt{(tx)^2 + 2t^2|x|^{3-|x|^\beta} + t^2|x|^{4-2|x|^\beta}}\\ &\le 2|t||x|\end{aligned}$$

Hence by letting $0 < \tau < 1$,

$$|B_k| = \left|\int_{|x|<\tau}\left(\exp(itx) - 1 - it|x|^{2-|x|^\beta}\right)dF'_k(x) + \int_{|x|\ge\tau}\left(\exp(itx) - 1\right)dF'_k(x) + it\int_{|x|<\tau}|x|^{2-|x|^\beta}\,dF'_k(x)\right|$$

$$\le 2|t|\int_{|x|<\tau}|x|\,dF'_k(x) + 2\int_{|x|\ge\tau}dF'_k(x) + |t|\left|\int_{|x|<\tau}|x|^{2-|x|^\beta}\,dF'_k(x)\right|$$

We next consider each term in the RHS above.

Using an argument similar to Gnedenko and Kolmogorov, pg113-114, it can be shown that that for *n* sufficiently large (such that $|\alpha_k| \le \tau/2$) we have that:

$$\int_{|x|<\tau}|x|\,dF'_k(x) \le 2\tau\int_{|x|\ge\tau/2}dF'_k(x)$$

Hence, by theorem 2 in pg 111 which features in Gnedenko and Kolmogorov, it follows that,

$$\sum_{k=1}^{n}\int_{|x|\le\tau}|x|\,dF'_k(x) \le \frac{2\tau(1+\tau_*^2)}{\tau_*^2}\sum_{k=1}^{n}\int_{|x|>\tau_*}\frac{x^2}{1+x^2}dF'_k \le \frac{2\tau C(1+\tau_*^2)}{\tau_*^2}$$

where $\tau_* = \tau/2$.

Next, $\int_{|x|<\tau}|x|^{2-|x|^\beta}\,dF'_k(x) \le (1+\tau^{2-\tau^\beta})\int_{|x|<\tau}\frac{|x|^{2-|x|^\beta}}{1+|x|^{2-|x|^\beta}}dF'_k(x)$.

Moreover, using theorem 3.2 and the fact that $\beta > 0$ but close to zero, then:

$$\sum_{k=1}^{n}\int_{|x|<\tau}|x|^{2-|x|^\beta}\,dF'_k(x) \le 2(1+\tau^{2-\tau^\beta})\sum_{k=1}^{n}\int_{|x|<\tau}\frac{|x|^{2-|x|^\beta}}{1+|x|^{2-|x|^\beta}}dF'_k(x) \le 2C(1+\tau^{2-\tau^\beta})$$

Finally,

$$\sum_{k=1}^{n}\int_{|x|\geq\tau} dF'_k(x) \leq \frac{(1+\tau^2)}{\tau^2}\sum_{k=1}^{n}\int_{|x|>\tau}\frac{x^2}{1+x^2}dF'_k \leq \frac{C(1+\tau^2)}{\tau^2}$$

Hence we have that:

$$\sum_{k=1}^{n}|B_k| \leq \left(|t|\frac{4\tau C(1+\tau_*^2)}{\tau_*^2}+2\frac{C(1+\tau^2)}{\tau^2}+|t|C\tau(1+\tau^{2-\tau^\beta})\right).$$

Hence $\left|\log(\varphi_n(t))-\Psi_n(t)\right| = \left|\sum_{k=1}^{n}\log(\varphi'_k(t)-\beta_k\right| \leq \sup_{1\leq k\leq k_n}|\beta_k|\sum_{k=1}^{n}|\beta_k| \to 0$

Since $e^{\Psi_n(t)}$ is a characteristic function, then its modulus cannot exceed one. Hence, $\lim_{n\to\infty}\varphi_n(t)=\varphi(t)$. This proves the necessity part of the proof.

■

3.4 Remark

Theorem 1 in section 19 in Gnedenko and Kolmogorov together with theorem 3.3 above allow us to state the conditions for the existence of a limit law for the sums in (1.2) as follows:

There exists a sequence of real numbers A_n guaranteeing convergence of the distribution laws of the sums in (1.2) of infinitesimal summands to a limit law if and only if there exists a non-decreasing function $G(u)$ of bounded variation such that:

$$\lim_{n\to\infty}\sum_{k=1}^{n}\int_{-\infty}^{u}\frac{n^{-\frac{|x|^\beta}{2}}|x|^{2-|x|^\beta}}{1+|x|^{2-|x|^\beta}}dF_k(x+\alpha_k)=G(u)$$

We denote the sum on the LHS by $G_n(u)$. Moreover, the function on the RHS is identical to the function G present in theorem 2.1 above. Furthermore, since the power of *x* in the above is smaller than 2, then the term $n^{-\frac{|x|^\beta}{2}}$ ensures convergence of the sum $\sum_{k=1}^{n}\frac{n^{-\frac{|X_{ik}|^\beta}{2}}|X_{1k}|^{2-|X_{1k}|^\beta}}{1+|X_{1k}|^{2-|X_{1k}|^\beta}}1_{\{X_{ik}\leq u\}}$ by the Marcinkiewicz-Zygmund strong law of large numbers in Chow and Teicher[3]. This previously mentioned term also featured in Caruana and Sant[2] and is still required here.

4 Modification of the Rubin and Tucker Estimator

The method which we shall use to estimate G, is based entirely on remark 3.4. Indeed if we manage to remove, as we actually do, the need for α_k in the above remark then we can define an estimator of G. Since the random variables X_{ik} are iid then we set $\alpha_n=\alpha_k$ for $1\leq k\leq n$ and similarly we set $F_n = F_k$. Here we leave *n* in the subscript to show that the distribution indeed depends on *n*. Moreover, $G_n(u)$ may be re-written as follows:

$$G_n(u)=\int_{-\infty}^{u}\frac{n^{1-\frac{|x|^\beta}{2}}|x|^{2-|x|^\beta}}{1+|x|^{2-|x|^\beta}}dF_n(x+\alpha_n)$$

We next show that we can eliminate the need for α_n.

Let $\widehat{G}_n(u) = \int_{-\infty}^{u} \frac{n^{1-\frac{|x|^\beta}{2}} \mid x \mid^{2-|x|^\beta}}{1+\mid x \mid^{2-|x|^\beta}} dF_n(x)$, for which we show that $\lim_{n\to\infty} \widehat{G}_n(u) = G(u)$. To help us do that, let $G_n^*(u) = \int_{-\infty}^{u} \frac{n^{1-\frac{|x-\alpha_n|^\beta}{2}} \mid x-\alpha_n \mid^{2-|x-\alpha_n|^\beta}}{1+\mid x-\alpha_n \mid^{2-|x-\alpha_n|^\beta}} dF_n(x)$ and, by adapting the proof of lemma 2.11 and lemma 2.12 in Rubin and Tucker[5] it is easy to show that $\lim_{n\to\infty} G_n^*(u) = G(u)$ and $\lim_{n\to\infty} \widehat{G}_n(u) = G(u)$ provided that u is a point of continuity of the function G provided that $u < 0$. It remains to show that this result is also true for $u > 0$.

Theorem 4.1

If $u > 0$ is a point of continuity of the function G then $\lim_{n\to\infty} \widehat{G}_n(u) = G(u)$.

Proof

The function $|x|^{2-|x|^\beta}$ and $|x|^{2-|x|^\beta} \Big/ \left(1+|x|^{2-|x|^\beta}\right)$ are both monotonitcally decreasing on the interval $(-1,0)$ and monotonically increasing on the interval $(0,1)$. Hence, if we let $0 < \tau < 1$, and take n sufficiently large such that $|\, a_n \,| < \tau/2$, then this ensures that the function $|x-\alpha_n|^{2-|x-\alpha_n|^\beta}$ and $|x-\alpha_n|^{2-|x-\alpha_n|^\beta} \Big/ \left(1+|x-\alpha_n|^{2-|x-\alpha_n|^\beta}\right)$ still behave in a similar manner (as discussed above) in the intervals $\left(-\tau/2, \alpha_n\right)$ and $(\alpha_n, \tau/2)$. This in turn ensures that the inequality in (1.6) and (1.8) below is true.

Using lemma 3.1 we have that:

$$\int_{-\tau/2}^{\tau/2} \frac{n^{1-\frac{|x|^\beta}{2}} |x|^{2-|x|^\beta}}{1+|x|^{2-|x|^\beta}} dF_n(x) \le \int_{-\tau/2}^{\tau/2} n^{1-\frac{|x|^\beta}{2}} |x|^{2-|x|^\beta} dF_n(x) \tag{1.4}$$

$$\le \int_{-\tau/2}^{\tau/2} n^{1-\frac{|x|^\beta}{2}} \left(\mid x-\alpha_n \mid^{2-|x-\alpha_n|^\beta} + K_\beta \mid \alpha_n \mid \right) dF_n(x) \tag{1.5}$$

$$\le \left(1+\mid \tau/2+\alpha_n \mid^{2-|\tau/2+|\alpha_n||^\beta}\right) \int_{-\tau/2}^{\tau/2} n^{1-\frac{|x|^\beta}{2}} \left(\frac{\mid x-\alpha_n \mid^{2-|x-\alpha_n|^\beta}}{1+\mid x-\alpha_n \mid^{2-|x-\alpha_n|^\beta}} + K_\beta \mid \alpha_n \mid \right) dF_n(x) \tag{1.6}$$

Hence,

$$\int_{-\tau/2}^{\tau/2} \frac{n^{1-\frac{|x|^\beta}{2}} |x|^{2-|x|^\beta}}{1+|x|^{2-|x|^\beta}} dF_n(x) - K_\beta n \mid \alpha_n \mid \left(1+(\tau/2+\mid \alpha_n \mid)^{2-|\tau+|\alpha_n||^\beta}\right)\left(F_n(\tau/2) - F_n(-\tau/2)\right)$$

$$\le \left(1+(\tau/2+\mid \alpha_n \mid)^{2-|\tau+|\alpha_n||^\beta}\right) \int_{-\tau/2}^{\tau/2} n^{1-\frac{|x|^\beta}{2}} \left(\frac{\mid x-\alpha_n \mid^{2-|x-\alpha_n|^\beta}}{1+\mid x-\alpha_n \mid^{2-|x-\alpha_n|^\beta}} \right) dF_n(x) \tag{1.7}$$

We next continue modifying the RHS of the inequality in (1.7):

$$\left(1+(\tfrac{\tau}{2}+|\alpha_n|)^{2-|\frac{\tau}{2}+|\alpha_n||^\beta}\right)\int_{-\tau/2}^{\tau/2} n^{1-\frac{|x|^\beta}{2}}\left(\frac{|x-\alpha_n|^{2-|x-\alpha_n|^\beta}}{1+|x-\alpha_n|^{2-|x-\alpha_n|^\beta}}\right)dF_n(x)$$

$$\le\left(1+(\tfrac{\tau}{2}+|\alpha_n|)^{2-|\frac{\tau}{2}+|\alpha_n||^\beta}\right)\int_{-\tau/2}^{\tau/2} n^{1-\frac{|x|^\beta}{2}}\left(|x-\alpha_n|^{2-|x-\alpha_n|^\beta}+K_\beta|\alpha_n|\right)dF_n(x) \quad (1.8)$$

$$\le\left(1+(\tfrac{\tau}{2}+|\alpha_n|)^{2-|\frac{\tau}{2}+|\alpha_n||^\beta}\right)\int_{-\tau/2}^{\tau/2} n^{1-\frac{|x|^\beta}{2}}\left(|x|^{2-|x|^\beta}+K_\beta|\alpha_n|\right)dF_n(x) \quad (1.9)$$

$$\le(1+\tfrac{\tau}{2}^{2-\frac{\tau}{2}^\beta})\left(1+(\tfrac{\tau}{2}+|\alpha_n|)^{2-|\frac{\tau}{2}+|\alpha_n||^\beta}\right)\int_{-\tau/2}^{\tau/2} n^{1-\frac{|x|^\beta}{2}}\left(\frac{|x|^{2-|x|^\beta}}{1+|x|^{2-|x|^\beta}}+K_\beta|\alpha_n|\right)dF_n(x) \quad (2.0)$$

$$\le(1+\tfrac{\tau}{2}^{2-\frac{\tau}{2}^\beta})\left(1+(\tfrac{\tau}{2}+|\alpha_n|)^{2-|\frac{\tau}{2}+|\alpha_n||^\beta}\right)\left(\int_{-\tau/2}^{\tau/2} n^{1-\frac{|x|^\beta}{2}}\left(\frac{|x|^{2-|x|^\beta}}{1+|x|^{2-|x|^\beta}}\right)dF_n(x)+\int_{-\tau/2}^{\tau/2} K_\beta n|\alpha_n|dF_n(x)\right) \quad (2.1)$$

$$\le(1+\tfrac{\tau}{2}^{2-\frac{\tau}{2}^\beta})\left(1+(\tfrac{\tau}{2}+|\alpha_n|)^{2-|\frac{\tau}{2}+|\alpha_n||^\beta}\right)\left(\int_{-\tau/2}^{\tau/2} n^{1-\frac{|x|^\beta}{2}}\left(\frac{|x|^{2-|x|^\beta}}{1+|x|^{2-|x|^\beta}}\right)dF_n(x)+K_\beta n|\alpha_n|\left(F_n(\tau/2)-F_n(-\tau/2)\right)\right) \quad (2.2)$$

Furthermore $\lim_{n\to\infty}\alpha_n=0$.

Hence using the above inequalities we have that,

$$\limsup_{n\to\infty}\left(\int_{-\tau/2}^{\tau/2}\frac{n^{1-\frac{|x|^\beta}{2}}|x|^{2-|x|^\beta}}{1+|x|^{2-|x|^\beta}}dF_n(x)-\left(1+(\tau/2+|\alpha_n|)^{2-|\frac{\tau}{2}+|\alpha_n||^\beta}\right)2K_\beta n|\alpha_n|\left(F_n(\tfrac{\tau}{2})-F_n(-\tfrac{\tau}{2})\right)\right)$$

$$\le(1+\tfrac{\tau}{2}^{2-\frac{\tau}{2}^\beta})\left(G(\tfrac{\tau}{2})-G(-\tfrac{\tau}{2})\right)$$

$$\le(1+\tfrac{\tau}{2}^{2-\frac{\tau}{2}^2})^2\liminf_{n\to\infty}\left(\int_{-\tau/2}^{\tau/2}\frac{n^{1-\frac{|x|^\beta}{2}}|x|^{2-|x|^\beta}}{1+|x|^{2-|x|^\beta}}dF_n(x)+2K_\beta n|\alpha_n|\left(F_n(\tfrac{\tau}{2})-F_n(-\tfrac{\tau}{2})\right)\right)$$

From the first line to the second line we used (1.7). Furthermore from the second to the third line we used (2.2).

Next let $0<\tau/2<u$ then:

$$\liminf_{n\to\infty}\int_{-\infty}^{u}\frac{n^{1-\frac{|x|^\beta}{2}}|x|^{2-|x|^\beta}}{1+|x|^{2-|x|^\beta}}dF_n(x)-2K_\beta n|\alpha_n|\left(F_n(\tau/2)-F_n(-\tau/2)\right)=$$

$$\liminf_{n\to\infty}\int_{-\infty}^{-\tau/2}\frac{n^{1-\frac{|x|^\beta}{2}}|x|^{2-|x|^\beta}}{1+|x|^{2-|x|^\beta}}dF_n(x)+\left(\int_{-\tau/2}^{\tau/2}\frac{n^{1-\frac{|x|^\beta}{2}}|x|^{2-|x|^\beta}}{1+|x|^{2-|x|^\beta}}dF_n(x)-2K_\beta n|\alpha_n|\left(F_n(\tau/2)-F_n(-\tau/2)\right)\right)+\int_{\tau/2}^{u}\frac{n^{1-\frac{|x|^\beta}{2}}|x|^{2-|x|^\beta}}{1+|x|^{2-|x|^\beta}}dF_n(x)$$

$$\ge G(-\tau/2)+\frac{G(\tau/2)-G(-\tau/2)}{1+\tfrac{\tau}{2}^{2-\frac{\tau}{2}^\beta}}+G(u)-G(\tfrac{\tau}{2})$$

Finally allowing $\tau\to 0$ we get:

$$\liminf_{n\to\infty}\int_{-\infty}^{u}\frac{n^{1-\frac{|x|^\beta}{2}}|x|^{2-|x|^\beta}}{1+|x|^{2-|x|^\beta}}dF_n(x)\ge G(u)$$

In a similar way it can be shown that $\limsup_{n\to\infty}\int_{-\infty}^{u}\frac{n^{1-\frac{|x|^\beta}{2}}|x|^{2-|x|^\beta}}{1+|x|^{2-|x|^\beta}}dF_n(x)\le G(u)$

Hence the theorem is proved.

■

Using theorem 4.1 together with remark 3.4 we can defined the following estimator for *G*:

$$\hat{G}(u) = \frac{1}{N}\sum_{i=1}^{N}\sum_{k=1}^{n} \frac{n^{-\frac{|X_{ik}|^{\beta}}{2}} \mid X_{ik} \mid^{2-|X_{ik}|^{\beta}}}{1+\mid X_{ik} \mid^{2-|X_{ik}|^{\beta}}} 1_{\{X_{ik} \le u\}} .$$

The inner sum converges by the Marcinkiewicz-Zygmund strong law of large numbers. The outer average uses the usual strong law of large numbers to give us:

$$\mathbb{P}[\lim_{N\to\infty} \hat{G}(u) = \widehat{G}_{n}(u)] = 1,$$

for any fixed *n*. Moreover combining this result with theorem 4.1 we conclude that:

$$\mathbb{P}[\lim_{N\to\infty}\lim_{n\to\infty} \hat{G}(u) = G(u)] = 1,$$

provided that u is point of continuity of the function *G*.

5 Simulation Results

Lévy processes have two components: the continuous and the pure jump part. In Caruana and Sant[2] the continuous part has already been considered and an improved estimator over the Rubin and Tucker estimator was obtained, therefore in the simulations below, we consider more general Lévy processes. In particular, we consider a jump-diffusion process and the Cauchy process, the latter being a pure jump Lévy process of unbounded variation. These simulations were conducted to compare $\hat{G}(u)$ with $G(u)$ and $H(u)$. The Cauchy process was chosen with location and scale parameters both equal to 1, while the jump diffusion process $X_t = B_t + \sum_{i=1}^{N_t} Y_i$ was chosen with B_t denoting Brownian motion such that $B_t - B_{t-1} \sim N(0,1)$, N_t is a Poisson process with $\lambda = 50$ and Y_i are Gamma distributed with shape and scale parameters being 5 and 2 respectively. Hence this is a Lévy process having a continuous part as well as a pure jump part with finite activity. The results of the simulations are illustrated in the diagrams below:

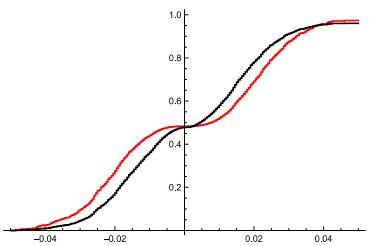

Fig. 1. Jump Diffusion Process

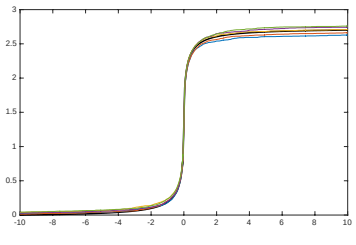

Fig. 2. Cauchy Process

In all cases, the parameter β was chosen to be 0.001. In the figure 1, the red curve represents the Rubin and Tucker estimator $\hat{H}$ while the black curve represents the estimator $\hat{G}$ which has been suitably transformed in such a way that it can be compared with $\hat{H}$. It is known that for the Brownian motion case, $H(u)=0$ for $u<0$ and $H(u)=\sigma^2=1$ for $u\geq 0$. Similarly, for the above mentioned jump diffusion process, H still experiences a jump of size σ^2 when $u=0$. Furthermore since $Y_i's$ are gamma distributed then $H(u)=0$ for $u<0$ and $H(u)\approx\sigma^2$ for values of *u* that are greater but close to zero. In line with many other simulation conducted, evidence has been obtained that $\hat{G}$ is considerably superior to $\hat{H}$ when a continuous component is present. Furthermore the parameter β can be tuned to give sharper estimates. For the Cauchy process, neither the function *H* nor *G* experience a jump at 0. Hence in Figure 2, we compare the function $G(.)$ (which is represented by the dark bold line) with the other five curves which represent $\hat{G}(u)$, one for each simulation, each of which consists of 500 time increments with 1000 observations in each time increment). This shows that the estimator proposed does not introduce any irrelevant and misleading features even when a continuous component is missing.

6. Conclusion

In this paper we discussed in detail a modification of the so-called Lévy Khintchine canonical representation of infinitely divisible distributions. The main alteration was the change of power of the variable *x* present in the function $f(x)=x^2/(1+x^2)$. As shown in this paper no power less than 2 will do. Indeed the power of *x* was carefully selected. Furthermore the link between the modified canonical representation, the original canonical representation and other representations was also discussed.

From this modified canonical representation we also derived an estimator for the function *G*. The estimator $\hat{G}(u)$ was shown to have useful properties which can be used for statistical purposes and is superior to $\hat{H}(u)$. Furthermore this estimator was compared not only with $G(u)$ but also with *H*(u).

References

1. A. Gegler and U. Stadmüller. Estimation of the characteristics of a Lévy process. Journal of Statistical Planning and Inference, 140,1481{1496, 2010.
2. M.A. Caruana and L. Sant, An analysis of Rubin and Tucker Estimator, SMTDA conference proceedings, 2016.
3. Y.S. Chow and H. Teicher, Probability Theory, Springer-Verlag, 2003.
4. B.V. Gnedenko and A. N. Kolmogorov, Limit Distributions for Sums of Independent Random Variables. Addison-Wesley Publishing Company, 1968.
5. H. Rubin and H.G. Tucker. Estimating the Parameters of a Differential Process. Ann. Math. Statist. 30,641{658, 1959.

Estimation of the healthy life expectancy in Italy through a simple model based on mortality rate

Christos Skiadas[1] and Maria Felice Arezzo[2]

[1]*ManLab, Technical University of Crete, Greece*
[2]*Università di Roma "La Sapienza", Italy*

Abstract: We use an advanced methodology based on the mortality rate of a population to explore the healthy life expectancy (HALE) estimates of the World Health Organization (WHO) from the Global Burden of Disease Study. First we calculate the loss of healthy life year estimator (LHLY) and then the healthy life expectancy (HLE). We use the full life tables from the Human Mortality Database (HMD). Our estimates are compared with the HALE estimates for Italy and other countries. Another direct estimation based on the *mx* and *qx* quantities provided from the Life Tables is also introduced and tested.
Analysis of the health situation in Italy males and females is presented along with the healthy life expectancy estimates.

Keywords: Healthy life expectancy, World Health Organization, Global burden of disease study, Life tables, Healthy life expectancy in Italy, Healthy life years lost, WHO, HALE.

1 Introduction

The debate in Europe is currently paying considerable attention on healthy life expectancy (HALE), focusing on some important subpopulations like those of the elderly and/or those of the females and males. Following the approach of the World Health Organization (WHO), health should be considered as having a dynamic nature, and should be taken into consideration in the context of life, as the ability to fulfill actions or to carry out a certain role in society. This is the so-called functional approach, taken by the WHO in the elaboration of the international frame of reference on the matter.

17th *ASMDA Conference Proceedings, 6 - 9 June 2017, London, UK*

The most suitable indicator to measure the state of health of a population is health expectancy, which measures the length of life spent in different states of health.
There are several methods to estimate health expectancies. Among them the most commonly used are the Sullivan and the multi-state, respectively based on classical life table and longitudinal data.
The first method was pioneered by Wolfbein on the length of "working life" (Wolfbein 1949) and is described in details in Sullivan (1971); as it is well known, it combines the prevalence of disability obtained through a cross-sectional survey and a period life table.
The second method, named multi-state tables, was pioneered by Rogers (1975) and Willekens for migration and marital status (Willekens 1979; Hoem and Fong 1976) for the multi-state table of working life and Brouard for the introduction of the period prevalence of labor participation (Brouard 1980; Cambois et al. 1999, Giudici et al 2013). Multi-state models are based on the analysis of the transitions between states in competition with the probabilities of dying from each state.
The information necessary for this type of analysis derives from longitudinal surveys. The result, in this case, is the so called period (or stable) prevalence and can be interpreted analogously to the stationary population of a period life table, as the proportion of the disabled amongst the survivors of successive fictitious cohorts, subject to the flows of entry on disability, recovery and death observed in the period under examination.
Thus, the period health expectancy is the expected number of years to be spent in the healthy state by this fictitious cohort.
In the classical life table analysis, the survivors of any age are supposed to be at the same risk of dying. When taking heterogeneity into account, the simplest model consists in considering two states (healthy vs unhealthy, enabled vs disabled), but assuming that the population in each state is homogeneous over time, i.e at each age they are at the same risks of changing their status. This corresponds to the common Markov hypothesis.
Starting from the late 80's a Global Burden of Disease (GBD) study was applied in many countries reflecting the optimistic views of many researchers and policy makers worldwide to quantify the health state of a population or a group of persons. In the time course they succeeded in establishing an international network collecting and providing adequate information to calculate health measures under terms as Loss of Healthy Life Years (LHLY) or Healthy Life Expectancy (HALE).
So far the process followed was towards statistical measures including surveys and data collection using questionnaires and disability and epidemiological data as well (McDowell, 2006).

However, a serious scientific part is missing or it is not very much explored that is to find the model underlying the health state measures. Observing the health state measures by country from 1990 until nowadays it is clear that the observed and estimated health parameters follow a rather systematic way. The lessons learned during the last centuries were towards the introduction of models in the analysis of health and mortality. The classical examples are Edmund Halley for Life Tables and Benjamin Gompertz for the law of mortality and may others. Today our ability to use mass storage tools as the computers and the extensive application of surveys and polls to many political, social and economic activities directed the main health state studies. In other words we give much attention to opinions of the people for their health status followed by extensive health data collection. However, it remains a serious question: can we validate the health status results? As it is the standard procedure in science a systematic study as the Global Burden of Disease should be validated by one or more models. Especially as these studies are today the main tool for the health programs of many countries the need of verification is more important.

2 Estimation with a model

We test a simple model proposed by Skiadas (2015) and Skiadas and Skiadas (2017), which we briefly describe in the following, using Italian data and compare the results with those provided by the Italian National Institute of Statistics (ISTAT) and by the GBD.
The model is based on two parameters, b and T, and it is:

$$\mu_x = \left(\frac{x}{T}\right)^b$$

T represents the age at which μ_x=1 and b is a crucial health state parameter expressing the curvature of μx. As the health state is improved b gets higher values.
Figure 1 represents a mortality diagram and illustrates the idea behind the methods proposed.

Fig 1. – Mortality diagram

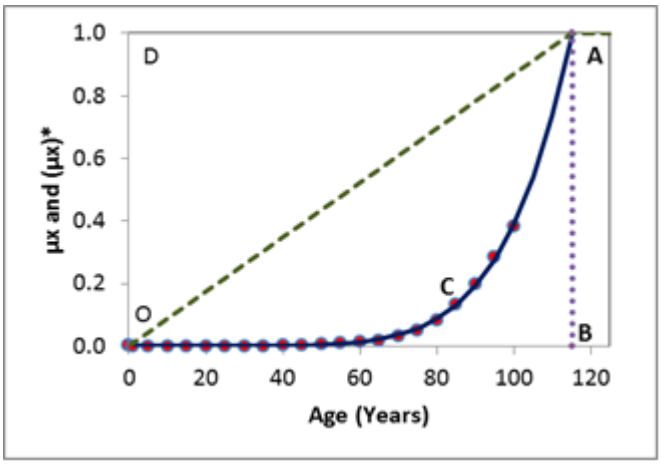

The main task is to find the area *Ex* under the curve OCABO in the mortality diagram (see Figure 1) which is a measure of the mortality effect. This is done by estimating the following integral:

$$E_x = \int_0^T \left(\frac{x}{T}\right)^b dx = \frac{T}{b+1}\left(\frac{x}{T}\right)^b$$

The resulting value for Ex in the interval [0, T] is given by the simple form:

$$E_{mortality} = \frac{T}{b+1}$$

The total information for the mortality is the area provided under the curve μx and the horizontal axis. The total area *Etotal* of the healthy and mortality part of the life span is nothing else but the area included into the rectangle of length T and height 1 that is *Etotal*=*T*. The health area is given by:

$$E_{health} = T - E_{mortality} = \frac{bT}{b+1}$$

It then follows that:

$$b = \frac{E_{health}}{E_{mortality}}$$

This is the simplest indicator for the loss of health status of a population. Another interesting and closely related estimator is in the form:

$$b + 1 = \frac{E_{total}}{E_{mortality}}$$

This indicator is more appropriate for the severe and moderate disability causes. It provides larger values for the disability measures as the *Etotal* is larger or the *Emortality* area is smaller by means that as we live longer the disability period becomes larger.

This method suggests a simple but yet interesting tool for estimating the loss of healthy life years (LHLY). A correction multiplier λ should be added for specific situations so that the estimator is in the form:

$$LHLY = \frac{E_{total}}{E_{mortality}} = \lambda(b + 1)$$

3 Estimation without a model (Direct estimation)

As the needed data sets in the form of mx or qx data are provided from the life tables, we have developed a method of direct estimation of the loss of healthy life year estimators directly from the life table by expanding the life table to the right.

$$b = \frac{E_{total}}{E_{mortality}} = \frac{xm_x}{\sum_0^x m_x}$$

The only need is to estimate the above fraction from the life table data. A similar indicator results by selecting the *qx* data from the life table and using the:

$$b = \frac{E_{total}}{E_{mortality}} = \frac{xq_x}{\sum_0^x q_x}$$

In both cases the results are similar. The estimates from *mx* are slightly larger than from *qx*. In both cases the *b* estimators growth to a maximum at old ages and then decline. The selected *b* indicator for the life years lost from birth is that of the maximum value. A smoothing technique is used to avoid sharp fluctuations in the maximum range area. Both the estimation of the *b* indicator by this direct method and the method by using a model give similar results.

4 Applications

Our preliminary results for the Italian data are encouraging as shown in figures 2a and 2b. For both cases we have estimated the Healthy Life Expectancy (HLE) by the Direct Method (without a model) and by the Fit Method (with the simple model). Both methods provide close estimates and mainly for the males case. The HALE estimates (Salomon, et al. 2012, Murray et al. 2016 and WHO 2001, 2002, 2013, 2014) are also close to ours especially for the latest years.
Three of the nearby countries with Italy are also studied in Figure 3. For all countries, Switzerland, France and Austria, the estimates are close to the related HALE figures.
It should be noted that our methods based on the Life Table data sets are easy to apply even for time periods when health and disease estimates are not collected. Even more the needed second method to straighten the HALE estimates is proposed and applied along with a third one to support the previous (Skiadas 2015, 2016). Another three parallel methods based on Gompertz, Weibull and a Stochastic model (Skiadas & Skiadas 2010, 2014, 2015) provide similar and supporting estimates.

Fig 2 HLE estimates and HALE estimates and confidence intervals for Italian males (left) and females (right)

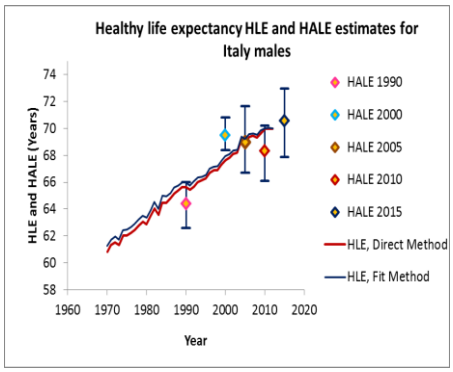

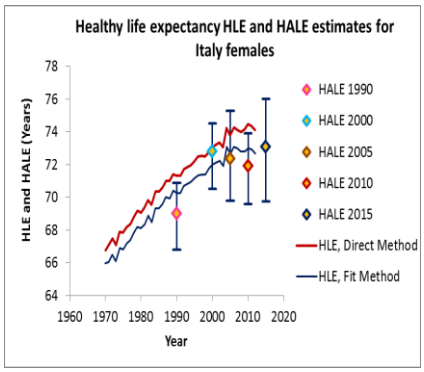

Fig 3 HLE estimates and HALE estimates and confidence intervals for Switzerland, France and Austria males (left) and females (right).

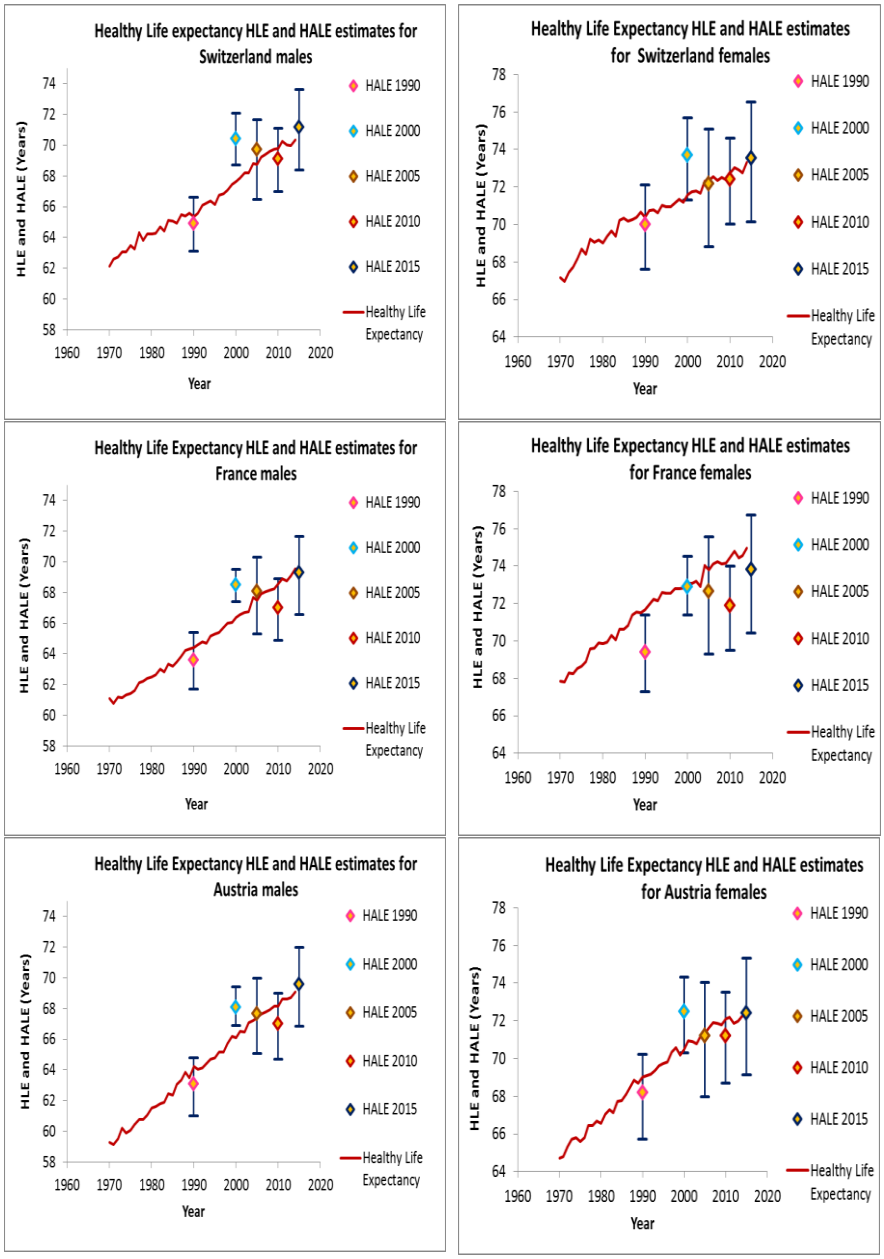

References

1. Brouard N (1980) Espérance de vie active, reprises d'activité féminine: un modèle. Revue économique 31:1260–1287.

2. Cambois E, Robine JM, Brouard N (1999) Life expectancies applied to specific statuses. A history of the indicators and methods of calculation. Popul Engl Sel 11:7–34.

3. Giudici, C., Arezzo, M.F. & Brouard, N. (2013). Estimating health expectancy in presence of missing data: an application using HID survey. Stat Methods Appl 22: 517.

4. Hoem J, Fong M (1976) A Markov chain model of working life tables. Working paper 2 Laboratory of Actuarial Mathematics, University of Copenhagen.

5. McDowell, I. (2006). Measuring Health: A Guide to Rating Scales and Questionnaires, Third Edition, Oxford University Press.

6. Rogers A (1975) Introduction to multi regional mathematical demography. Wiley, England.

7. Murray, C. J. L., et al. Global, regional, and national disability-adjusted life-years (DALYs) for 315 diseases and injuries and healthy life expectancy (HALE), 1990–2015: a systematic analysis for the Global Burden of Disease Study 2015, Lancet 388: 1603–58, 2016.

8. Salomon, et al. (2012) Healthy life expectancy for 187 countries, 1990–2010: a systematic analysis for the Global Burden Disease Study 2010, Lancet 380: 2144–62.

9. Skiadas, C. and Skiadas, C. H. Development, Simulation and Application of First Exit Time Densities to Life Table Data, Communications in Statistics - Theory and Methods, 39, 3, 444-451, 2010.

10. Skiadas, C. H. and Skiadas, C. The First Exit Time Theory applied to Life Table Data: the Health State Function of a Population and other Characteristics, Communications in Statistics-Theory and Methods, 34, 1585-1600, 2014.

11. Skiadas, C. H. and Skiadas, C. Exploring the State of a Stochastic System via Stochastic Simulations: An Interesting Inversion Problem and the Health State Function, Methodology and Computing in Applied Probability, 17, 973-982, 2015.

12. Skiadas, C. H. Verifying the Global Burden of Disease Study: Quantitative Methods Proposed, ArXiv.org, October 2015. http://arxiv.org/abs/1510.07346

13. Skiadas, C. H. Exploring the HALE Estimates of the Global Burden of Disease Study by a Simple, Gompertz, Weibull and an advanced IM model, 28th REVES Conference, Wien, Austria, 8-10 June 2016.

14. Skiadas, C. H. and Skiadas, C. (2017). Exploring the Health State of a Population by Dynamic Modeling Methods. The Springer Series on Demographic Methods and Population Analysis book series (PSDE, volume 45), Springer. (DOI 10.1007/978-3-319-65142-2) https://link.springer.com/book/10.1007/978-3-319-65142-2 .

15. Sullivan D (1971) A single index of mortality and morbidity. HSMHA Heal Rep 86(4):347–354.

16. WHO. Department of Health Statistics and Information system. "WHO methods and data sources for the global burden of disease estimates 2000-2011". Global Health Estimates Technical Paper WHO/HIS/HSI/GHE/2013.4. November, 2013.http://www.who.int/healthinfo/statistics/GlobalDALYmethods_2000_2011.pdf

17. WHO. "WHO methods for life expectancy and healthy life expectancy". Global Health Estimates Technical Paper WHO/HIS/HSI/GHE/2014.5. March, 2014. http://www.who.int/healthinfo/statistics/LT_method.pdf.

18. WHO, The World Health Report 2001, Statistical Annex, Annex Table 4 Healthy life expectancy (HALE) in all Member States, estimates for 2000. annex4_en_HALE_2000.pdf.

19. WHO. The World 132 Health Report 2004, Statistical Annex, Annex Table 4 Healthy life expectancy (HALE) in all WHO Member States, estimates for 2002. annex_4_en_2002.pdf.

20. WHO. The World Health Report 2002, Statistical Annex, Annex Table 4 Healthy life expectancy (HALE) in all Member States, estimates for 2000 and 2001. whr2002_annex4_2001.pdf.

21. WHO. WHO methods for life expectancy and healthy life expectancy, Global Health Estimates Technical Paper WHO/HIS/HSI/GHE/2014.5, March 2014.

22. Willekens F (1979) Computer program for increment-decrement (multistate) life table analysis: a user's manual to lifeindec. Working papers of the international institute for applied systems analysis.

23. Wolfbein S (1949) The length of working life. Popul Stud 3:286–294.

Recurrent Algorithms for Mixed Power-Exponential Moments of Hitting Times for Semi-Markov Processes

Dmitrii Silvestrov[1] and Raimondo Manca[2]

13 January, 2016

Abstract. New algorithms for computing exponential and mixed power-exponential moments of hitting times and accumulated rewards of hitting type for semi-Markov processes are presented. The algorithms are based on special techniques of sequential phase space reduction and recurrence relations connecting exponential moments of rewards.

Key words: Semi-Markov process, Hitting time, Accumulated reward, Exponential moment, Power-exponential moment, Phase space reduction, Recurrent algorithm.

AMS Mathematical Subject Classification 2010. Primary: 60J10, 60J22, 60J27, 60K15; Secondary: 65C40.

1. Introduction

In this paper, we study recurrent relations for exponential and mixed power-exponential moments of hitting times and accumulated rewards of hitting type for semi-Markov processes and present effective algorithms for computing these moments. These algorithms are based on procedures of sequential of phase space reduction for semi-Markov processes. The present paper continue research study results presented in this paper results given in the paper Silvestrov and Manca (2015), where analogous results have been obtained for more simple power moments of hitting times and accumulated rewards of hitting type for semi-Markov process. In the above paper, readers can also find a survey of works in the area.

The paper includes five sections. In Section 2, we introduce Markov renewal processes, semi-Markov processes and define hitting times and accumulated rewards of hitting type. We also present basic stochastic relations

[1]Department of Mathematics, Stockholm University, 106 91, Stockholm, Sweden, E-mail: silvestrov@math.su.se

[2]Department of Methods and Models for Economics, Territory and Finance, University "La Sapienza", 00161 Rome, Italy, E-mail: raimondo.manca@uniroma1.it

17th *ASMDA Conference Proceedings, 6 - 9 June 2017, London, UK*

and systems of linear equations for exponential and mixed power-exponential moments of these random functionals. In Section 3, we describe a procedure of phase space reduction for semi-Markov processes and formulas for computing transition characteristics for reduced semi-Markov processes. We also prove invariance of hitting times and their exponential and mixed power-exponential moments with respect to the above procedure of phase space reduction. In Section 4, we describe a procedure of sequential phase space reduction for semi-Markov process and derive recurrent formulas for computing exponential and mixed power-exponential moments of hitting times for semi-Markov processes. In Section 5, we present a numerical example for the corresponding recurrent algorithm for computing exponential moments of hitting times for semi-Markov processes.

2. Semi-Markov processes and hitting times

In this section, we introduce Markov renewal processes and semi-Markov processes. We define also hitting times and hitting accumulated rewards, and give basic recurrent system of linear equations for their exponential moments, which are the main objects of our studies. We refer to books by Silvestrov (1980) and Janssen and Manca (2006, 2007), where one can find basic facts about semi-Markov processes and hitting times and accumulated rewards.

2.1. Markov renewal processes and semi-Markov processes. Let $\mathbb{X} = \{0, \ldots, m\}$ and $(J_n, X_n), n = 0, 1, \ldots$ be a Markov renewal process, i.e., a homogeneous Markov chain with the phase space $\mathbb{X} \times [0, \infty)$, an initial distribution $\bar{p} = \langle p_i = \mathsf{P}\{J_0 = i, X_0 = 0\} = \mathsf{P}\{J_0 = i\}, i \in \mathbb{X}\rangle$ and transition probabilities,

$$Q_{ij}(t) = \mathsf{P}\{J_1 = j, X_1 \leq t / J_0 = i, X_0 = s\},\ (i, s), (j, t) \in \mathbb{X} \times [0, \infty). \quad (1)$$

In this case, the random sequence η_n is also a homogeneous (embedded) Markov chain with the phase space $\mathbb{X}$ and the transition probabilities,

$$p_{ij} = \mathsf{P}\{J_1 = j / J_0 = i\} = Q_{ij}(\infty),\ i, j \in \mathbb{X}. \quad (2)$$

As far as random variable X_n is concerned, it can be interpreted as sojourn time in state J_{n-1} or as a transition time from state J_{n-1} to state J_n, for $n = 1, 2, \ldots$.

We assume that the following communication conditions hold:

A: $\mathbb{X}$ is a communicative class of states for the embedded Markov chain J_n.

We also assume that the following condition excluding instant transitions holds:

B: $Q_{ij}(0) = 0, i, j \in \mathbb{X}$.

Let us now introduce a semi-Markov process,

$$J(t) = J_{N(t)},\ t \geq 0, \tag{3}$$

where $N(t) = \max(n \geq 0 : T_n \leq t)$ is a number of jumps in the time interval $[0, t]$, for $t \geq 0$, and $T_n = X_1 + \cdots + X_n,\ n = 0, 1, \ldots$, are sequential moments of jumps, for the semi-Markov process $J(t)$.

This process has the phase space $\mathbb{X}$, the initial distribution $\bar{p} = \langle p_i = \mathsf{P}\{J(0) = i\}, i \in \mathbb{X}\rangle$ and semi-Markov transition probabilities $Q_{ij}(t)$, $t \geq 0$, $i, j \in \mathbb{X}$.

2.2. Hitting times and accumulated rewards of hitting type. Let us also introduce moments of sojourn times, for $\rho \geq 0$ and $i, j \in \mathbb{X}$,

$$\phi_{ij}(\rho) = \mathsf{E}_i e^{\rho X_1} I(J_1 = j) = \int_0^\infty e^{\rho t} Q_{ij}(dt). \tag{4}$$

Here and henceforth, notations P_i and E_i are used for conditional probabilities and expectations under condition $J(0) = i$.

Note that, $\phi_{ij}(0) = p_{ij},\ i, j \in \mathbb{X}$.

We assume that the following condition holds, for some real $\rho > 0$:

C$_\rho$: $\phi_{ij}(\rho) < \infty$, $i, j \in \mathbb{X}$.

Note that conditions **B** imply that $\phi_{ij}(\rho) > 0$, if $p_{ij} > 0$, while $\phi_{ij}(\rho) = 0$, if $p_{ij} = 0$.

The first hitting time to state 0 for the semi-Markov process $J(t)$ can be defined as,

$$W_0 = \inf(t \geq X_1 : J(t) = 0) = \sum_{n=1}^{U_0} X_n, \tag{5}$$

where $U_0 = \min(n \geq 1 : J_n = 0)$ is the first hitting time to state 0 for the Markov chain J_n.

The random variable W_0 can also be interpreted as a reward accumulated on trajectories of Markov chain J_n up to its first hitting to state 0.

The main object of our studies are power moments for the first hitting times,

$$\Phi_{i0}(\rho) = \mathsf{E}_i e^{\rho W_0},\ \rho \geq 0,\ i \in \mathbb{X}. \tag{6}$$

Note that, $\Phi_{i0}(0) = 1$, $i \in \mathbb{X}$.

Conditions **A** and **C**$_\rho$ imply that there exists $\rho_0 \in (0, \rho]$ such that, for $\varrho \in [0, \rho_0]$ and $i \in \mathbb{X}$,

$$\Phi_{i0}(\varrho) < \infty. \tag{7}$$

Indeed, let us introduce conditional exponential moments, for $i, j \in \mathbb{X}$,

$$\psi_{ij}(\rho) = \begin{cases} \phi_{ij}(\rho)/p_{ij} & \text{if } p_{ij} > 0, \\ 1 & \text{if } p_{ij} = 0. \end{cases} \tag{8}$$

and define, for $\varrho \in [0, \rho]$, the following function,

$$\psi(\varrho) = \max_{i,j \in \mathbb{X}} \phi_{ij}(\varrho) \tag{9}$$

If conditions **A** and $\mathbf{C}_\rho$ hold, then function $\psi(\varrho) \in [1, \infty)$, for $\varrho \in [0, \rho]$ and it is continuous nondecreasing function in this interval such that $\psi(\varrho) \to 1$ as $\varrho \to 0$.

The following relation takes place, for $\varrho \in [0, \rho]$ and $i \in \mathbb{X}$,

$$\begin{aligned} \Phi_{i0}(\varrho) &= \sum_{n=1}^{\infty} \sum_{i_0=i, i_1, \ldots, i_{n-1} \neq 0, i_n = 0} \prod_{k=1}^{n} \psi_{i_{k-1}, i_k}(\varrho) p_{i_{k-1}, i_k} \\ &\leq \sum_{n=1}^{\infty} \psi(\varrho)^n \sum_{i_0=i, i_1, \ldots, i_{n-1} \neq 0, i_n = 0} \prod_{k=1}^{n} p_{i_{k-1}, i_k} \\ &= \sum_{n=0}^{\infty} \psi(\varrho)^n \mathsf{P}_i\{U_0 = n\}. \end{aligned} \tag{10}$$

Condition **A** implies that $\mathsf{P}_i\{U_0 \geq n\} \to 0$ as $n \to \infty$, for $i \in \mathbb{X}$. Thus, for any $0 < \theta < 1$, there exists integer $n_\theta \geq 1$ such that, for $i \in \mathbb{X}$,

$$\mathsf{P}_i\{U_0 \geq n_\theta\} \leq \theta. \tag{11}$$

This inequality implies that, for every $i \in \mathbb{X}$ and $k \geq 1$,

$$\begin{aligned} \mathsf{P}_i\{U_0 \geq k n_\theta\} &= \sum_{j \neq 0} \mathsf{P}_i\{U_0 \geq (k-1) n_\theta, J_{(k-1)n_\theta} = j\} \mathsf{P}_j\{U_0 \geq n_\theta\} \\ &\leq \theta \mathsf{P}_i\{U_0 \geq (k-1) n_\theta\} \leq \cdots \leq \theta^k. \end{aligned} \tag{12}$$

Inequalities (13) imply in an obvious way that, for for every $i \in \mathbb{X}$ and $n \geq 1$,

$$\mathsf{P}_i\{U_0 \geq n\} \leq \theta^{[\frac{n}{n_\theta}]} \leq L_\theta \theta^{\frac{n}{n_\theta}} \tag{13}$$

where $L_\theta = \theta^{-n_\theta}$.

Finally, relations (10) and (13) imply that the following inequality holds, for $\rho_0 \in [0, \rho]$ such that $\psi(\rho_0)\theta^{\frac{1}{n_\theta}} < 1$, and $i \in \mathbb{X}$,

$$\Phi_{i0}(\rho_0) \leq \sum_{n=0}^{\infty} L_\theta (\psi(\rho_0)\theta^{\frac{1}{n_\theta}})^n < \infty. \tag{14}$$

However, it should be noted that conditions **A** and $\mathbf{C}_\rho$ do not guarantee that the exponential moments $\Phi_{i0}(\rho) < \infty$. The corresponding example is given below.

In what follows, symbol $Y \stackrel{d}{=} Z$ is used to denote that random variables or vectors Y and Z have the same distribution.

The Markov property of the Markov renewal process (J_n, X_n) implies that following system of stochastic equalities takes place for hitting times,

$$\begin{cases} W_{i,0} \stackrel{d}{=} X_{i,1} I(J_{i,1} = 0) + \sum_{j \neq 0} (X_{i,1} + W_{j,0}) I(J_{i,1} = j), \\ i \in \mathbb{X}, \end{cases} \tag{15}$$

where: (a) $W_{i,0}$ is a random variable which has distribution $\mathsf{P}\{W_{i,0} \leq t\} = \mathsf{P}_i\{W_0 \leq t\}, t \geq 0$, for every $i \in \mathbb{X}$; (b) $(J_{i,1}, X_{i,1})$ is a random vector, which takes values in space $\mathbb{X} \times [0, \infty)$ and has the distribution $P\{J_{i,1} = j, X_{i,1} \leq t\} = Q_{ij}(t), j \in \mathbb{X}, t \geq 0$, for every $i \in \mathbb{X}$; (c) the random variables $W_{j,0}$ and the random vector $(J_{i,1}, X_{i,1})$ are independent, for every $i, j \in \mathbb{X}$.

By computing exponential moments in stochastic relations (15) we get, for every $0 \leq \varrho \leq \rho$, the following system of linear equations for moments $\Phi_{i0}(\varrho), i \in \mathbb{X}$,

$$\begin{cases} \Phi_{i0}(\varrho) = \phi_{i0}(\varrho) + \sum_{j \in \mathbb{X}, j \neq 0} \phi_{ij}(\varrho) \Phi_{j0}(\varrho), \\ i \in \mathbb{X}. \end{cases} \tag{16}$$

Note that it is possible that the moment $\phi_{ij}(\varrho)$ equals to 0, while the moment $\Phi_{j0}(\varrho)$ equal to $+\infty$ in relation (16). In such cases, one should set the product $0 \cdot \infty$ to be 0 when calculating the products at the right-hand side of equality (16).

Let consider the simplest semi-Markov process with the two-point phase space $\mathbb{X} = \{0, 1\}$ and, also, assume that all probabilities $p_{ij} > 0, i, j = 0, 1$, and, the exponential moments $\phi_{ij}(\rho) \in (0, \infty), i, j = 0, 1$.

In this case system of equations (16) takes the form,

$$\begin{cases} \Phi_{00}(\rho) = \phi_{00}(\rho) + \phi_{01}(\rho) \Phi_{10}(\rho), \\ \Phi_{10}(\rho) = \phi_{10}(\rho) + \phi_{11}(\rho) \Phi_{10}(\rho). \end{cases} \tag{17}$$

If $\phi_{11}(\rho) \geq 1$, then $\Phi_{00}(\rho), \Phi_{10}(\rho) = \infty$ as follows from relations (17).

If $\phi_{11}(\rho) < 1$, then $\Phi_{00}(\rho), \Phi_{10}(\rho) < \infty$ and these moments are given by formulas,

$$\Phi_{10}(\rho) = \frac{\phi_{10}(\rho)}{1 - \phi_{11}(\rho)}, \ \Phi_{00}(\rho) = \phi_{00}(\rho) + \frac{\phi_{01}(\rho)\phi_{10}(\rho)}{1 - \phi_{11}(\rho)}. \tag{18}$$

It should be noted that the finiteness of the exponential moment for return time $\Phi_{00}(\rho)$ does not guarantee the finiteness of the exponential moment $\Phi_{11}(\rho)$. Indeed, according the above remarks, the exponential moments $\Phi_{11}(\rho), \Phi_{01}(\rho) = \infty$ if $\phi_{00}(\rho) \geq 1$.

Necessary and sufficient conditions of finiteness for exponential moments of hitting times are given in terms of so-called test-functions in Silvestrov (2004) and Gyllenberg and Silvestrov (2008).

We refer to functions $v(i), i \in \mathbb{X}$ defined on the space $\mathbb{X}$ and taking value in the interval $[0, \infty)$ as test-functions.

Let us introduce condition:

$\mathbf{D}_\rho$: There exists a test-function $v_\rho(i), i \in \mathbb{X}$ such that the following test inequalities hold,

$$v_\rho(i) \geq \phi_{i0}(\rho) + \sum_{j \in \mathbb{X}, j \neq 0} \phi_{ij}(\rho) v_\rho(j), \ i \in \mathbb{X}.$$

The following lemma gives the pointed above conditions finiteness for exponential moments of hitting times.

Lemma 1. *Let conditions* $\mathbf{A}$, $\mathbf{B}$ *and* $\mathbf{C}_\rho$, *for some* $\rho > 0$, *hold. Then, exponential moments* $\Phi_{i0}(\rho) < \infty, i \in \mathbb{X}$ *if and only if condition* $\mathbf{D}_\rho$ *holds. In this case, inequalities* $\Phi_{i0}(\rho) \leq v_\rho(i), \ i \in \mathbb{X}$ *hold and the exponential moments* $\Phi_{i0}(\rho), i \in \mathbb{X}$ *are the unique solution of the system of linear equations* (16).

It is useful to note that, in the above example with two-state semi-Markov process, this is impossible to find a test function $v_\rho(i), i = 0, 1$ such that the test inequalities penetrating condition $\mathbf{D}_\rho$ holds, if $\phi_{11}(\rho) \geq 1$.

Indeed, the second test inequality, which takes the form, $v_\rho(1) \geq \phi_{10}(\rho) + \phi_{11}(\rho) v_\rho(1)$, can not hold in this case, since $\phi_{10}(\rho) > 0$.

Condition $\mathbf{D}_\rho$, however, holds if $\phi_{11}(\rho) < 1$.

Indeed, the test inequality penetrating this condition holds for test-functions $v_\rho(1) = \frac{\phi_{10}(\rho)}{1 - \phi_{11}(\rho)}$ and $v_\rho(0) = \phi_{00}(\rho) + \phi_{01}(\rho) v_\rho(1)$ in the form of equalities.

The system of linear equation given in (16) has, for every $0 \leq \varrho \leq \rho$, the matrix of coefficients $\mathbf{I} - {}_0\mathbf{P}(\varrho)$, where $\mathbf{I} = \|I(i = j)\|$ is the unit matrix and matrix ${}_0\mathbf{P}(\varrho) = \|\phi_{ij}(\varrho) I(j \neq 0)\|$. Under conditions of Lemma 1, there exists the inverse matrix,

$$[\mathbf{I} - {}_0\mathbf{P}(\varrho)]^{-1} = \|g_{i0j}(\varrho)\|. \tag{19}$$

The elements of this matrix have the following probabilistic sense,

$$g_{i0j}(\varrho) = \sum_{n=1}^{\infty} \mathsf{E}_i e^{\varrho T_{n-1}} I(U_0 > n-1, J_{n-1} = j), \ i, j \in \mathbb{X}. \tag{20}$$

Thus, the formula for moments $\Phi_{i0}(\varrho), i \in \mathbb{X}$ has the following form,

$$\Phi_{i0}(\varrho) = \sum_{j \in \mathbb{X}} g_{i0j}(\varrho)\phi_{j0}(\rho), \ i \in \mathbb{X}. \tag{21}$$

This is useful to note that the above remarks imply that condition **A** can be replaced by simpler hitting condition:

$\mathbf{A_0}$: $\mathsf{P}_i\{U_0 < \infty\} = 1$, $i \in \mathbb{X}$.

In this paper, we propose an alternative method, which can be considered as a stochastic analogue of Gauss elimination method for finding exponential moments $\Phi_{i0}(\rho), i \in \mathbb{X}$.

2.3. Mixed power-exponentional moments. Let us introduce mixed power-exponential moments, for $\rho \geq 0, r = 0, 1, \ldots, i, j \in \mathbb{X}$,

$$\phi_{ij}(r, \rho) = \mathsf{E}_i X_1^r e^{\rho X_1} I(J_1 = j) = \int_0^\infty t^r e^{\rho t} Q_{ij}(dt). \tag{22}$$

,

Note that $\phi_{ij}(0, \rho) = \phi_{ij}(\rho), \rho \geq 0, i \in \mathbb{X}$.

It is easily seen that condition $\mathbf{C}_\rho$ implies that, $\phi_{ij}(r, \varrho) < \infty$, for any $0 \leq \varrho < \rho, r = 0, 1, \ldots, i, j \in \mathbb{X}$.

It is easily seen that for every $0 \leq \varrho < \rho, r = 1, \ldots, i, j \in \mathbb{X}$, function $\phi_{ij}(\varrho)$ has a derivative of order r, and it is the function $\phi_{ij}(r, \rho)$.

Let us also introduce mixed power-exponential moments, for $\rho \geq 0$, $r = 0, 1, \ldots, i \in \mathbb{X}$,

$$\Phi_{i0}(r, \rho) = \mathsf{E}_i W_0^r e^{\rho W_0}. \tag{23}$$

Note that $\Phi_{i0}(0, \rho) = \Phi_{i0}(\rho), \rho \geq 0, i \in \mathbb{X}$.

Condition $\mathbf{D}_\rho$ implies that $\Phi_{ij}(r, \varrho) < \infty$, for every $0 \leq \varrho < \rho$ and $r = 0, 1, \ldots, i, j \in \mathbb{X}$.

Moreover, it is easily seen that for every $0 \leq \varrho < \rho, r = 1, \ldots, i, j \in \mathbb{X}$, function $\Phi_{ij}(\varrho)$ has a derivative of order n, and it is the function $\Phi_{ij}(r, \rho)$.

Therefore, we can differentiate equations (16) and get the following system of linear equation for every $0 \leq \varrho < \rho$ and $r = 0, 1, \ldots,$

$$\begin{cases} \Phi_{i0}(r, \varrho) = \lambda_{i0}(r, \varrho) + \sum_{j \in \mathbb{X}, j \neq 0} \phi_{ij}(\varrho)\Phi_{ij}(r, \varrho), \\ i \in \mathbb{X}, \end{cases} \tag{24}$$

where

$$\lambda_{i0}(r, \varrho) = \phi_{i0}(r, \varrho) + \sum_{j \in X, j \neq 0} \sum_{l=1}^{r} \binom{r}{l} \phi_{ij}(r - l, \varrho)\Phi_{j0}(l, \varrho). \tag{25}$$

Note that $\lambda_{ij}(0,\varrho)=\phi_{ij}(\varrho), i,j\in\mathbb{X}$.

In the case $r=0$, system (24) coincides with system (16).

Systems (24) have the same coefficient matrix ${}_0\mathbf{P}(\varrho)$ but different free terms $\lambda_{i0}(r,\varrho)$, for $r=0,1,\ldots$. These systems should be solved recursively.

First, the system (24) should be solved for $r=0$, where, as was mentioned above, it coincides with the system of linear equation (16).

Second, we solve system (24) for $r=1$. Note that expressions for the free terms $\lambda_{i0}(1,\varrho)=\phi_{i0}(1,\varrho)+\sum_{j\in\mathbb{X},j\neq 0}\phi_{ij}(1,\varrho)\Phi_{j0}(0,\varrho), i\in\mathbb{X}$ include the solutions $\Phi_{i0}(0,\varrho), i\in\mathbb{X}$, of systems (24), for $r=0$.

This recursive procedure can be repeated for $r=1,2,\ldots$. The expressions for the free terms $\lambda_{i0}(r,\varrho)$ given in (25) include the solutions $\Phi_{i0}(l,\varrho), i\in\mathbb{X}$, of systems (24) for $l=0,1,\ldots,r-1$.

3. Semi-Markov processes with reduced phase spaces

In this section, we describe an one-step algorithm for reduction of a phase space for a semi-Markov process. We also give recurrent systems of linear equations for power moments of hitting times for a reduced semi-Markov process.

3.1. Reduced semi-Markov processes. Let us choose some state $k\in\mathbb{X}$ and consider the reduced phase space ${}_k\mathbb{X}=\mathbb{X}\setminus\{k\}$, with the state k excluded from the phase space $\mathbb{X}$.

Let us define the sequential moments of hitting the reduced space ${}_k\mathbb{X}$ by the embedded Markov chain J_n,

$$ {}_kV_n=\min(r>{}_kV_{n-1},\ J_r\in{}_k\mathbb{X}),\ n=1,2,\ldots,\ {}_kV_0=0. \tag{26}$$

Now, let us define the random sequence,

$$ ({}_kJ_n,\ {}_kX_n)=\begin{cases}(J_0,0) & \text{for } n=0,\\ (J_{{}_kV_n},\sum_{r={}_kV_{n-1}+1}^{{}_kV_n}X_r) & \text{for } n=1,2,\ldots.\end{cases} \tag{27}$$

This sequence is also a Markov renewal process with phase space $\mathbb{X}\times[0,\infty)$, the initial distribution $\bar{p}=\langle p_i=\mathsf{P}\{J_0=i,X_0=0\}=\mathsf{P}\{J_0=i\}, i\in\mathbb{X}\rangle$ and transition probabilities,

$$\begin{aligned}{}_kQ_{ij}(t)&=\mathsf{P}\{{}_kJ_1=j,\ {}_kX_1\le t/\,{}_kJ_0=i,\ {}_kX_0=s\}\\&=Q_{ij}(t)+\sum_{n=0}^{\infty}Q_{ik}(t)*Q_{kk}^{(*n)}(t)*Q_{kj}(t),\ t\ge 0,\ i,j\in\mathbb{X}.\end{aligned} \tag{28}$$

Here, symbol $*$ is used to denote the convolution of distribution functions (possibly improper), and $Q_{kk}^{(*n)}(t)$ is the n times convolution of the distribution function $Q_{kk}(t)$.

In this case, the Markov chain ${}_kJ_n$ has the transition probabilities,

$$
\begin{aligned}
{}_kp_{ij} = {}_kQ_{ij}(\infty) &= \mathsf{P}\{\, {}_kJ_1 = j, / \, {}_kJ_0 = i\} \\
&= p_{ij} + \sum_{n=0}^{\infty} p_{ik} p_{kk}^n p_{kj} = p_{ij} + p_{ik} \frac{p_{kj}}{1 - p_{kk}},\ i, j \in \mathbb{X}. \qquad (29)
\end{aligned}
$$

Note that condition **A** implies that probabilities $p_{kk} \in [0, 1)$, $k \in \mathbb{X}$.

The transition distributions for the Markov chain ${}_kJ_n$ are concentrated on the reduced phase space ${}_k\mathbb{X}$, i.e., for every $i \in \mathbb{X}$,

$$
\begin{aligned}
\sum_{j \in {}_k\mathbb{X}} {}_kp_{ij} &= \sum_{j \in {}_k\mathbb{X}} p_{ij} + p_{ik} \sum_{j \in {}_k\mathbb{X}} \frac{p_{kj}}{1 - p_{kk}} \\
&= \sum_{j \in {}_k\mathbb{X}} p_{ij} + p_{ik} = 1. \qquad (30)
\end{aligned}
$$

If the initial distribution $\bar{p}$ is concentrated on the phase space ${}_k\mathbb{X}$, i.e., $p_k = 0$, then the random sequence $({}_kJ_n,\ {}_kX_n), n = 0, 1, \ldots$ can be considered as a Markov renewal process with the reduced phase ${}_k\mathbb{X} \times [0, \infty)$, the initial distribution ${}_k\bar{p} = \langle\, p_i = \mathsf{P}\{{}_kJ_0 = i,\ {}_kX_0 = 0\} = \mathsf{P}\{{}_kJ_0 = i\}, i \in {}_k\mathbb{X}\rangle$ and transition probabilities ${}_kQ_{ij}(t), t \geq 0, i, j \in {}_k\mathbb{X}$.

If the initial distribution $\bar{p}$ is not concentrated on the phase space ${}_k\mathbb{X}$, i.e., $p_k > 0$, then the random sequence $({}_kJ_n,\ {}_kX_n), n = 0, 1, \ldots$ can be interpreted as a Markov renewal process with so-called transition period.

Let us now introduce the semi-Markov process,

$$
{}_kJ(t) = {}_kJ_{{}_kN(t)},\ t \geq 0, \qquad (31)
$$

where ${}_kN(t) = \max(n \geq 0 :\ {}_kT_n \leq t)$ is a number of jumps at time interval $[0, t]$, for $t \geq 0$, and ${}_kT_n = {}_kX_1 + \cdots + {}_kX_n,\ n = 0, 1, \ldots$ are sequential moments of jumps, for the semi-Markov process ${}_kJ(t)$.

As follows from the above remarks, the semi-Markov process ${}_kJ(t), t \geq 0$ has transition probabilities ${}_kQ_{ij}(t), t \geq 0, i, j \in \mathbb{X}$ concentrated on the reduced phase space ${}_k\mathbb{X}$, which can be interpreted as the actual "reduced" phase space of this semi-Markov process ${}_kJ(t)$.

If the initial distribution $\bar{p}$ is concentrated on the phase space ${}_k\mathbb{X}$, then process ${}_kJ(t), t \geq 0$ can be considered as the semi-Markov process with the reduced phase ${}_k\mathbb{X}$, the initial distribution ${}_k\bar{p} = \langle\, {}_kp_i = \mathsf{P}\{{}_kJ_1(0) = i\}, i \in {}_k\mathbb{X}\rangle$ and transition probabilities ${}_kQ_{ij}(t), t \geq 0, i, j \in {}_k\mathbb{X}$.

According to the above remarks, we can refer to the process ${}_kJ(t)$ as a reduced semi-Markov process.

If the initial distribution $\bar{p}$ is not concentrated on the phase space ${}_k\mathbb{X}$, then the process ${}_kJ(t), t \geq 0$ can be interpreted as a reduced semi-Markov process with transition period.

3.2. Transition characteristics for reduced semi-Markov processes. Relation (29) implies the following formulas, for probabilities ${}_kp_{kj}$ and ${}_kp_{ij}$, $i, j \in {}_k\mathbb{X}$,

$$\begin{cases} {}_kp_{kj} &= \frac{p_{kj}}{1-p_{kk}}, \\ {}_kp_{ij} &= p_{ij} + p_{ik}\,{}_kp_{kj} = p_{ij} + \frac{p_{ik}p_{kj}}{1-p_{kk}}. \end{cases} \tag{32}$$

It is useful to note that the second formula in relation (32) reduces to the first one, if to assign $i = k$ in this formula.

Taking into account that ${}_kV_1$ is Markov time for the Markov renewal process (J_n, X_n), we can write down the following system of stochastic equalities, for every $i, j \in {}_k\mathbb{X}$,

$$\begin{cases} {}_kX_{i,1}I({}_kJ_{i,1} = j) &\stackrel{d}{=} X_{i,1}I(J_{i,1} = j) \\ &\quad + (X_{i,1} + {}_kX_{k,1})I(J_{i,1} = k)I({}_kJ_{k,1} = j), \\ {}_kX_{k,1}I({}_kJ_{k,1} = j) &\stackrel{d}{=} X_{k,1}I(J_{k,1} = j) \\ &\quad + (X_{k,1} + {}_kX_{k,1})I(J_{k,1} = k)I({}_kJ_{k,1} = j), \end{cases} \tag{33}$$

where: (a) $(J_{i,1}, X_{i,1})$ is a random vector, which takes values in space $\mathbb{X} \times [0, \infty)$ and has the distribution $P\{J_{i,1} = j, X_{i,1} \le t\} = Q_{ij}(t)$, $j \in \mathbb{X}$, $t \ge 0$, for every $i \in \mathbb{X}$; (b) $({}_kJ_{i,1},\ {}_kX_{i,1})$ is a random vector which takes values in the space ${}_k\mathbb{X} \times [0, \infty)$ and has distribution $\mathsf{P}\{{}_kJ_{i,1} = j,\ {}_kX_{i,1} \le t\} = \mathsf{P}_i\{{}_kJ_1 = j,\ {}_kX_1 \le t\} = {}_kQ_{ij}(t)$, $j \in {}_k\mathbb{X}$, $t \ge 0$, for every $i \in \mathbb{X}$; (c) $(J_{i,1}, X_{i,1})$ and $({}_kJ_{k,1},\ {}_kX_{k,1})$ are independent random vectors, for every $i, k \in \mathbb{X}$.

Let us denote, for $\rho \ge 0,\ i, k \in \mathbb{X}, j \in {}_k\mathbb{X}$,

$${}_k\phi_{ij}(\rho) = \int_0^\infty e^{\rho t}\,{}_kQ_{ij}(dt). \tag{34}$$

Note that ${}_k\phi_{ij}(0) = {}_kp_{ij},\ i, k \in \mathbb{X}, j \in {}_k\mathbb{X}$.

By computing exponential moments in stochastic relations (33) we get, for every $i, j \in {}_k\mathbb{X}$, the following system of linear equations for the moments ${}_k\phi_{kj}(\rho)$, ${}_k\phi_{ij}(\rho)$,

$$\begin{cases} {}_k\phi_{kj}(\rho) = \phi_{kj}(\rho) + \phi_{kk}(\rho)\,{}_k\phi_{kj}(\rho), \\ {}_k\phi_{ij}(\rho) = \phi_{ij}(\rho) + \phi_{ik}(\rho)\,{}_k\phi_{kj}(\rho). \end{cases} \tag{35}$$

Relation (35) yields the following formulas for moments ${}_k\phi_{kj}(\rho)$ and ${}_k\phi_{ij}(\rho)$, which should be used, for every $i, j \in {}_k\mathbb{X}, k \in \mathbb{X}$,

$$\begin{cases} {}_k\phi_{kj}(\rho) &= \frac{\phi_{kj}(\rho)}{1-\phi_{kk}(\rho)}, \\ {}_k\phi_{ij}(\rho) &= \phi_{ij}(\rho) + \frac{\phi_{ik}(\rho)\phi_{kj}(\rho)}{1-\phi_{kk}(\rho)}. \end{cases} \tag{36}$$

It is useful to note that the second formula in relation (36) reduces to the first one, if to assign $i = k$ in this formula.

Relation (36) imply that, under conditions **A**, **B** and $\mathbf{C}_\rho$, the following condition is necessary and sufficient for finiteness of exponential moments ${}_k\phi_{kj}(\rho)$, ${}_k\phi_{ij}(\rho), i, j \in {}_k\mathbb{X}$,

$\mathbf{E}^{(1)}_{k,\rho}$: $\phi_{kk}(\rho) < 1$.

Let us introduce mixed power-exponential moments, for $\rho \geq 0, r = 0, 1, \ldots,\ i, k \in \mathbb{X}, j \in {}_k\mathbb{X}$,

$$ {}_k\phi_{ij}(r, \rho) = \int_0^\infty t^r e^{\rho t}\, {}_kQ_{ij}(dt). \tag{37}$$

Note that ${}_k\phi_{ij}(0, \rho) = {}_k\phi_{ij}(\rho)$, for $\rho \geq 0,\ i, k \in \mathbb{X}, j \in {}_k\mathbb{X}$.

Condition $\mathbf{E}^{(1)}_{k,\rho}$ implies that ${}_k\phi_{ij}(r, \varrho) < \infty$, for every $0 \leq \varrho < \rho, r = 0, 1, \ldots,\ i, k \in \mathbb{X}, j \in {}_k\mathbb{X}$.

Moreover, it is easily seen that for every $0 \leq \varrho < \rho, r = 1, \ldots, i, j \in \mathbb{X}$, function ${}_k\phi_{ij}(\varrho)$ has a derivative of order n, and it is the function ${}_k\phi_{ij}(r, \rho)$.

Therefore, we can differentiate equations (35) and get the following system of linear equation, for every $0 \leq \varrho < \rho, r = 0, 1, \ldots, i, j \in {}_k\mathbb{X}, k \in \mathbb{X}$,

$$ \begin{cases} {}_k\phi_{kj}(r, \rho) = {}_k\lambda_{kj}(r, \rho) + \phi_{kk}(\rho)\, {}_k\phi_{kj}(r, \rho), \\ {}_k\phi_{ij}(r, \rho) = {}_k\lambda_{ij}(r, \rho) + \phi_{ik}(\rho)\, {}_k\phi_{kj}(r, \rho). \end{cases} \tag{38}$$

where, for $0 \leq \varrho < \rho, r = 0, 1, \ldots, i, k \in \mathbb{X}, j \in {}_k\mathbb{X}$,

$$ {}_k\lambda_{ij}(r, \varrho) = \phi_{ij}(r, \varrho) + \sum_{l=1}^{r} \binom{r}{l} \phi_{ik}(r - l, \varrho)\, {}_k\phi_{kj}(l, \varrho). \tag{39}$$

Note that ${}_k\lambda_{ij}(0, \varrho) = {}_k\phi_{ij}(\varrho)$, for $i, k \in \mathbb{X}, j \in {}_k\mathbb{X}$.

Relation (38) yields the following formulas for moments ${}_k\phi_{kj}(r, \varrho)$ and ${}_k\phi_{ij}(r, \varrho)$, which should be used, for every $0 \leq \varrho < \rho, r = 0, 1, \ldots, i, j \in {}_k\mathbb{X}, k \in \mathbb{X}$,

$$ \begin{cases} {}_k\phi_{kj}(r, \varrho) &= \frac{{}_k\lambda_{kj}(r, \varrho)}{1 - \phi_{kk}(\varrho)}, \\ {}_k\phi_{ij}(r, \varrho) &= {}_k\lambda_{ij}(r, \varrho) + \frac{\phi_{ik}(\varrho)\, {}_k\lambda_{kj}(r, \varrho)}{1 - \phi_{kk}(\varrho)}. \end{cases} \tag{40}$$

Formulas (40) have recurrent character since expressions for functions ${}_k\lambda_{kj}(r, \varrho)$, ${}_k\lambda_{ij}(r, \varrho)$ includes functions ${}_k\phi_{kj}(l, \varrho), l = 0, 1, \ldots, r - 1$.

For $r = 0$, formulas (40) reduce to formulas (36).

3.3. Exponential and mixed power-exponential moments for hitting times of reduced semi-Markov processes. Let us assume that

$k \neq 0$ and introduce the first hitting time to state 0 for the reduced semi-Markov process ${}_kJ(t)$,

$$ {}_kW_0 = \inf(t \geq {}_kX_1 : {}_kJ(t) = 0) = \sum_{n=1}^{{}_kU_0} {}_kX_n, \tag{41} $$

where ${}_kU_0 = \min(n \geq 1 : {}_kJ_n = 0)$ is the first hitting time to state 0 by the reduced Markov chain ${}_kJ_n$.

Let also introduce, for $\rho \geq 0, i \in \mathbb{X}$, exponential moments,

$$ {}_k\Phi_{i0}(\rho) = \mathsf{E}_i e^{\rho\, {}_kW_0}, \tag{42} $$

and, for $\rho \geq 0$, $n = 0, 1, \ldots, i \in \mathbb{X}$, mixed power-exponential moments,

$$ {}_k\Phi_{i0}(n, \rho) = \mathsf{E}_i\, {}_kW_0^n e^{\rho\, {}_kW_0}, \tag{43} $$

Note that, ${}_k\Phi_{i0}(0, \rho) = {}_k\Phi_{i0}(\rho)$, for $\rho \geq 0$, $n = 0, 1, \ldots, i, k \in \mathbb{X}$ and ${}_k\Phi_{i0}(0) = 1$, for $i, k \in \mathbb{X}$.

The following theorem plays the key role in what follows.

Theorem 2. *The hitting times W_0 and ${}_kW_0$ to the state 0, respectively, for semi-Markov processes $J(t)$ and ${}_kJ(t)$, coincide, for every $k \neq 0$ and, thus, for every $\rho \geq 0, r = 0, 1, \ldots, i \in \mathbb{X}, k \neq 0$,*

$$ \Phi_{i0}(r, \rho) = \mathsf{E}_i W_0^r e^{\rho W_0} = {}_k\Phi_{i0}(r, \rho) = \mathsf{E}_i\, W_0^r e^{\rho\, {}_kW_0}. \tag{44} $$

Proof. The first hitting times to a state 0 are connected for Markov chains J_n and ${}_kJ_n$ by the following relation,

$$ U_0 = \min(n \geq 1 : J_n = 0) = \min({}_kV_n \geq 1 : {}_kJ_n = j) = {}_kV_{{}_kU_0}, \tag{45} $$

where ${}_kU_0 = \min(n \geq 1 : {}_kJ_n = 0)$.

The above relations imply that the following relation holds for the first hitting times to state 0, for the semi-Markov processes $J(t)$ and ${}_kJ(t)$,

$$ W_0 = \sum_{n=1}^{U_0} X_n = \sum_{n=1}^{{}_kV_{{}_kU_0}} X_n = \sum_{n=1}^{{}_kU_0} {}_kX_n = {}_kW_0. \tag{46} $$

The equality for mixed power-exponential moments of hitting times is an obvious corollary of relation (46). $\square$

Lemma 2. *Let $\rho \geq 0$ and conditions* **A**, **B**, $\mathbf{C}_\rho$ *and* $\mathbf{D}_\rho$ *hold for the semi-Markov process $J(t)$. Then, these conditions also hold for the reduced semi-Markov process ${}_kJ(t)$, for any state $k \neq 0$.*

Proof. Holding of conditions **A** and **B** for the semi-Markov process ${}_kJ(t)$ is obvious. Holding of condition $\mathbf{C}_\rho$ for the semi-Markov process ${}_kJ(t)$ follows from relation (36). Holding of condition $\mathbf{D}_\rho$ for the semi-Markov process ${}_kJ(t)$ follows from Lemma 1. $\square$

4. Algorithms of sequential phase space reduction

In this section, we present a multi-step algorithm for sequential reduction of phase space for semi-Markov processes. We also present the recurrent algorithm for computing exponential moments of hitting times for semi-Markov processes, which is based on the above algorithm of sequential reduction of the phase space.

4.1. Sequential reduction of phases space for semi-Markov processes. In what follows, let $i \in \{1, \ldots, m\}$ and let $\bar{k}_{i,m} = \langle k_{i,1}, \ldots, k_{i,m} \rangle = \langle k_{i,1}, \ldots, k_{i,m-1}, i \rangle$ be a permutation of the sequence $\langle 1, \ldots, m \rangle$ such that $k_{i,m} = i$, and let $\bar{k}_{i,n} = \langle k_{i,1}, \ldots, k_{i,n} \rangle$, $n = 1, \ldots, m$ be the corresponding chain of growing sequences of states from space $\mathbb{X}$.

Let us assume that $p_0 + p_i = 1$. Denote as ${}_{\bar{k}_{i,0}}J(t) = J(t)$, the initial semi-Markov process. Let us exclude state $k_{i,1}$ from the phase space ${}_{\bar{k}_{i,0}}\mathbb{X} = \mathbb{X}$ of semi-Markov process ${}_{\bar{k}_{i,0}}J(t)$ using the time-space screening procedure described in Section 3. Let ${}_{\bar{k}_{i,1}}J(t)$ be the corresponding reduced semi-Markov process. The above procedure can be repeated. The state $k_{i,2}$ can be excluded from the phase space of the semi-Markov process ${}_{\bar{k}_{i,1}}J(t)$. Let ${}_{\bar{k}_{i,2}}J(t)$ be the corresponding reduced semi-Markov process. By continuing the above procedure for states $k_{i,3}, \ldots, k_{i,n}$, we construct the reduced semi-Markov process ${}_{\bar{k}_{i,n}}J(t)$.

The process ${}_{\bar{k}_{i,n}}J(t)$ has, for every $n = 1, \ldots, m$, the actual "reduced" phase space,

$$
{}_{\bar{k}_{i,n}}\mathbb{X} = {}_{\bar{k}_{i,n-1}}\mathbb{X} \setminus \{k_{i,n}\} = \mathbb{X} \setminus \{k_{i,1}, k_{i,2}, \ldots, k_{i,n}\}. \tag{47}
$$

The transition probabilities ${}_{\bar{k}_{i,n}}p_{k_{i,n},j'}$, ${}_{\bar{k}_{i,n}}p_{i'j'}$, $i', j' \in {}_{\bar{k}_n}\mathbb{X}$, and the exponential moments ${}_{\bar{k}_{i,n}}\phi_{k_{i,n},j'}(\rho)$, ${}_{\bar{k}_{i,n}}\phi_{i'j'}(\rho)$, $i', j' \in {}_{\bar{k}_{i,n}}\mathbb{X}$ are determined for the semi-Markov process ${}_{\bar{k}_{i,n}}J(t)$ by the transition probabilities and the expectations of sojourn times for the semi-Markov process ${}_{\bar{k}_{i,n-1}}J(t)$, respectively, via relations (32) and (36), which take the following recurrent forms, for $i', j' \in {}_{\bar{k}_{i,n}}\mathbb{X}$ and $n = 1, \ldots, m$,

$$
\begin{cases}
{}_{\bar{k}_{i,n}}p_{k_{i,n},j'} &= \frac{{}_{\bar{k}_{i,n-1}}p_{k_{i,n},j'}}{1 - {}_{\bar{k}_{i,n-1}}p_{k_{i,n},k_{i,n}}}, \\
{}_{\bar{k}_{i,n}}p_{i'j'} &= {}_{\bar{k}_{i,n-1}}p_{i'j'} + \frac{{}_{\bar{k}_{i,n-1}}p_{i'k_{i,n}} \, {}_{\bar{k}_{i,n-1}}p_{k_{i,n},j'}}{1 - {}_{\bar{k}_{i,n-1}}p_{k_{i,n},k_{i,n},}},
\end{cases} \tag{48}
$$

and

$$\begin{cases} {}_{\bar{k}_{i,n}}\phi_{k_{i,n},j'}(\rho) &= \frac{{}_{\bar{k}_{i,n-1}}\phi_{k_{i,n},j'}(\rho)}{1-{}_{\bar{k}_{i,n-1}}\phi_{k_{i,n},k_{i,n}}(\rho)}, \\ {}_{\bar{k}_{i,n}}\phi_{i'j'}(\rho) &= {}_{\bar{k}_{i,n-1}}\phi_{i'j'}(\rho) + \frac{{}_{\bar{k}_{i,n-1}}\phi_{i'k_{i,n}}(\rho)\,{}_{\bar{k}_{i,n-1}}\phi_{k_{i,n},j'}(\rho)}{1-{}_{\bar{k}_{i,n-1}}\phi_{k_{i,n},k_{i,n}}(\rho)}, \end{cases} \tag{49}$$

Relation (49) implies that, under conditions **A**, **B** and $\mathbf{C}_\rho$, the following condition is necessary and sufficient for finiteness of exponential moments ${}_{\bar{k}_{i,n'}}\phi_{k_{i,n'},j'}(\rho)$, ${}_{\bar{k}_{i,n'}}\phi_{i'j'}(\rho)$, $i', j' \in {}_{\bar{k}_{i,n'}}\mathbb{X}$, $n' = 1, \ldots, n$:

$\mathbf{E}^{(n)}_{\bar{k}_{i,n},\rho}$: ${}_{\bar{k}_{i,n'-1}}\phi_{k_{i,n'},k_{i,n'}}(\rho) < 1, n' = 1, \ldots, n.$

Also, mixed power-exponential moments ${}_{\bar{k}_{i,n}}\phi_{k_{i,n},j'}(n,\rho)$, ${}_{\bar{k}_{i,n}}\phi_{i'j'}(n,\rho)$, i', $j' \in {}_{\bar{k}_{i,n}}\mathbb{X}$ are determined for every $0 \le \varrho < \rho, r = 0, 1, \ldots$ by the following recurrent relations,

$$\begin{cases} {}_{\bar{k}_{i,n}}\phi_{k_{i,n},j'}(r,\varrho) &= \frac{{}_{\bar{k}_{i,n-1}}\lambda_{k_{i,n},j'}(r,\varrho)}{1-{}_{\bar{k}_{i,n-1}}\phi_{k_{i,n},k_{i,n}}(\varrho)}, \\ {}_{\bar{k}_{i,n}}\phi_{i'j'}(r,\varrho) &= {}_{\bar{k}_{i,n-1}}\lambda_{i'j'}(r,\varrho) + \frac{{}_{\bar{k}_{i,n-1}}\phi_{i'k_{i,n}}(\varrho)\,{}_{\bar{k}_{i,n-1}}\lambda_{k_{i,n},j'}(r,\varrho)}{1-{}_{\bar{k}_{i,n-1}}\phi_{k_{i,n},k_{i,n}}(\varrho)}, \end{cases} \tag{50}$$

where, for $0 \le \varrho < \rho, r = 0, 1, \ldots, i', k_{i,n} \in {}_{\bar{k}_{i,n-1}}\mathbb{X}, j' \in {}_{\bar{k}_{i,n}}\mathbb{X}$,

$$\begin{aligned} {}_{\bar{k}_{i,n-1}}\lambda_{i'j'}(r,\varrho) = {}& {}_{\bar{k}_{i,n-1}}\phi_{i'j'}(r,\varrho) \\ & + \sum_{l=1}^{r}\binom{r}{l}\,{}_{\bar{k}_{i,n-1}}\phi_{i'k_{i,n}}(r-l,\varrho)\,{}_{\bar{k}_{i,n}}\phi_{k_{i,n}j'}(l,\varrho). \end{aligned} \tag{51}$$

Note that ${}_{\bar{k}_{i,n}}\phi_{k_{i,n},j'}(0,\varrho) = {}_{\bar{k}_{i,n}}\phi_{k_{i,n},j'}(r,\varrho)$ and ${}_{\bar{k}_{i,n}}\phi_{i'j'}(0,\varrho) = {}_{\bar{k}_{i,n}}\phi_{i'j'}(\varrho)$ for $i', j' \in {}_{\bar{k}_{i,n}}\mathbb{X}$.

Relations (50) and (51) should be used recurrently, for $r = 1, 2, \ldots$, since expressions for functions ${}_{\bar{k}_{i,n-1}}\lambda_{k_{i,n}j'}(r,\varrho)$ and ${}_{\bar{k}_{i,n-1}}\lambda_{i'j'}(r,\varrho)$ include functions ${}_{k_{i,n}}\phi_{k_{i,n}j}(l,\varrho), j' \in {}_{\bar{k}_{i,n}}\mathbb{X}, l = 0, 1, \ldots, r-1$.

4.2. Recurrent algorithms for computing of moments of hitting times. Let us ${}_{\bar{k}_{i,n}}W_0$ be the first hitting time to state 0 for the reduced semi-Markov process ${}_{\bar{k}_{i,n}}J(t)$ and ${}_{\bar{k}_{i,n}}\Phi_{i'0}(\rho) = \mathsf{E}_{i'}e^{\rho\,{}_{\bar{k}_{i,n}}W_0}, i' \in {}_{\bar{k}_{i,n}}\mathbb{X}$ be the exponential moments for these random variables.

By Theorem 1, the above exponential moments of hitting time coincide for the semi-Markov processes ${}_{\bar{k}_{i,0}}J(t)$, ${}_{\bar{k}_{i,1}}J(t), \ldots,$ ${}_{\bar{k}_{i,n}}J(t)$, i.e., for $n' = 0, \ldots, n$,

$${}_{\bar{k}_{j,n'}}\Phi_{k_{i,n'}0}(\rho) = \Phi_{k_{i,n'}0}(\rho),\ {}_{\bar{k}_{j,n'}}\Phi_{i'0}(\rho) = \Phi_{i'0}(\rho),\ i' \in {}_{\bar{k}_{i,n}}\mathbb{X}. \tag{52}$$

Moreover, exponential moments of hitting times ${}_{\bar{k}_{j,n}}\Phi_{k_{i,n}0}(\rho)$, ${}_{\bar{k}_{i,n}}\Phi_{i'0}(\rho)$, $i' \in {}_{\bar{k}_{i,n}}\mathbb{X}$, resulted by the recurrent algorithm of sequential phase space

reduction described above, are invariant with respect to any permutation $\bar{k}'_{i,n} = \langle k'_{i,1}, \ldots, k'_{i,n} \rangle$ of sequence $\bar{k}_{i,n} = \langle k_{i,1}, \ldots, k_{i,n} \rangle$.

Indeed, for every permutation $\bar{k}'_{i,n}$ of sequence $\bar{k}_{i,n}$, the corresponding reduced semi-Markov process ${}_{\bar{k}'_{i,n}}J(t)$ is constructed as the sequence of states for the initial semi-Markov process $J(t)$ at sequential moment of its hitting into the same reduced phase space ${}_{\bar{k}'_{i,n}}\mathbb{X} = \mathbb{X} \setminus \{k'_{i,1}, \ldots, k'_{i,n}\} = {}_{\bar{k}_{i,n}}\mathbb{X} = \mathbb{X} \setminus \{k_{i,1}, \ldots, k_{i,n}\}$. The times between sequential jumps of the reduced semi-Markov process ${}_{\bar{k}'_{i,n}}J(t)$ are the times between sequential hitting of the above reduced phase space by the initial semi-Markov process $J(t)$.

This implies that the transition probabilities ${}_{\bar{k}_{i,n}}p_{k_{i,n}j'}$, ${}_{\bar{k}_{i,n}}p_{i'j'}, i', j' \in {}_{\bar{k}_{i,n}}\mathbb{X}$ and the exponential moments ${}_{\bar{k}_{i,n}}\phi_{k_{i,n}j'}(\rho)$, ${}_{\bar{k}_{i,n}}\phi_{i'j'}(\rho), i', j' \in {}_{\bar{k}_{i,n}}\mathbb{X}$ and, in sequel, exponential moments ${}_{\bar{k}_{i,n}}\Phi_{k_{i,n}0}(\rho)$, ${}_{\bar{k}_{i,n}}\Phi_{i'0}(\rho), i' \in {}_{\bar{k}_{i,n}}\mathbb{X}$ are, for every $n = 1, \ldots, m$, invariant with respect to any permutation $\bar{k}'_{i,n}$ of the sequence $\bar{k}_{i,n}$.

Let us now choose $n = m$. In this case, the reduced semi-Markov process ${}_{\bar{k}_{i,m}}J(t)$ has the one-state phase space ${}_{\bar{k}_{i,m}}\mathbb{X} = \{0\}$ and state $k_{i,m} = i$.

In this case, the reduced semi-Markov process ${}_{\bar{k}_{i,m}}J(t)$ return to state 0 after every jump and hitting time to state 0 coincides with the sojourn time in state ${}_{\bar{k}_{i,m}}J(0)$.

Thus, the transition probabilities,

$$ {}_{\bar{k}_{i,m}}p_{i0} = {}_{\bar{k}_{i,m}}p_{00} = 1. \tag{53} $$

Also, by Theorem 1, moments,

$$ \Phi_{i0}(\rho) = {}_{\bar{k}_{i,m}}\Phi_{i0}(\rho) = {}_{\bar{k}_{i,m}}\phi_{i0}(\rho), \tag{54} $$

and

$$ \Phi_{00}(\rho) = {}_{\bar{k}_{i,m}}\Phi_{00}(\rho) = {}_{\bar{k}_{i,m}}\phi_{00}(\rho). \tag{55} $$

Relations (54) and (55) imply that, under conditions **A**, **B** and $\mathbf{C}_\rho$, the following condition is necessary and sufficient for finiteness of exponential moments $\Phi_{i0}(\rho), i \neq 0, \Phi_{00}(\rho)$:

$\mathbf{E}^{(m)}_{\bar{k}_{i,m},\rho}$: ${}_{\bar{k}_{i,n-1}}\phi_{k_{i,n},k_{i,n}}(\rho) < 1, n = 1, \ldots, m.$

In fact, if condition $\mathbf{E}^{(m)}_{\bar{k}_{i,m},\rho}$ holds for some permutation $\bar{k}_{i,m} = \langle k_{i,1}, \ldots, k_{i,m-1}, i \rangle$ of the sequence $\langle 1, \ldots, m \rangle$, it also holds for any other permutation $\bar{k}'_{i',m} = \langle k'_{i',1}, \ldots, k'_{i',m-1}, i' \rangle$ of the sequence $\langle 1, \ldots, m \rangle$.

Thus, condition $\mathbf{E}^{(m)}_{\bar{k}_{i,m},\rho}$ is an alternative to condition $\mathbf{D}_\rho$.

The above remarks can be summarized in the following theorem, which presents the recurrent algorithm for computing of power moments for hitting times.

Theorem 2. *Let $\rho \geq 0$ and conditions* **A**, **B**, $\mathbf{C}_\rho$ *and* $\mathbf{D}_\rho$ *hold for the semi-Markov process $J(t)$. Exponential moments $\Phi_{i0}(\rho)$ and $\Phi_{00}(\rho)$ are given, for every $i = 1, \ldots, m$, by formulas* (54) *and* (55)*, where the exponential moments ${}_{\bar{k}_{i,n}}\phi_{k_{i,n},j'}(\rho)$, ${}_{\bar{k}_{i,n}}\phi_{i'j'}(\rho)$, $i', j' \in {}_{\bar{k}_{i,n}}\mathbb{X}$ are determined, for $n = 1, \ldots, m$, by recurrent formulas* (49)*. The moments $\Phi_{i0}(\rho)$ and $\Phi_{00}(\rho)$ are invariant with respect to any permutation $\bar{k}_{i,m}$ of sequence $\langle 1, \ldots, m \rangle$ used in the above recurrent algorithm.*

In analogous way, we can get, for every $0 \leq \varrho < \rho, r = 0, 1, \ldots$, the following relations,

$$\Phi_{i0}(r, \varrho) = {}_{\bar{k}_{i,m}}\Phi_{i0}(r, \varrho) = {}_{\bar{k}_{i,m}}\phi_{i0}(r, \varrho), \tag{56}$$

and

$$\Phi_{00}(r, \varrho) = {}_{\bar{k}_{i,m}}\Phi_{00}(r, \varrho) = {}_{\bar{k}_{i,m}}\phi_{00}(r, \varrho). \tag{57}$$

and prove the following theorem.

Theorem 3. *Let $\rho \geq 0$ and conditions* **A**, **B**, $\mathbf{C}_\rho$ *and* $\mathbf{D}_\rho$ *hold for the semi-Markov process $J(t)$. Mixed power-exponential moments $\Phi_{i0}(r, \varrho)$ and $\Phi_{00}(r, \varrho)$ are given, for every $i = 1, \ldots, m$ and $0 \leq \varrho < \rho$, $r = 0$, $1, \ldots$, by formulas* (56) *and* (57)*, where the mixed power-exponential moments ${}_{\bar{k}_{i,n}}\phi_{k_{i,n},j'}(r, \varrho)$, ${}_{\bar{k}_{i,n}}\phi_{i'j'}(r, \rho)$, $i', j' \in {}_{\bar{k}_{i,n}}\mathbb{X}$ are determined, for $n = 1, \ldots, m$, by recurrent formulas* (50) *and* (51)*. The moments $\Phi_{i0}(r, \varrho)$ and $\Phi_{00}(r, \varrho)$ are invariant with respect to any permutation $\bar{k}_{i,m}$ of sequence $\langle 1, \ldots, m \rangle$ used in the above recurrent algorithm.*

5. An example.

Let us consider a numerical example illustrating the recurrent algorithm for computing power moment of hitting times and accumulated rewards of hitting times for semi-Markov processes, based on sequential reduction of their phase spaces.

Let $J(t)$ be a semi-Markov process with the phase space $\mathbb{X} = \{0, 1, 2, 3\}$, and the 4×4 matrix of transition probabilities, $\|Q_{ij}(t)\|$, which has the following form, for $t \geq 0$,

$$\left\| \begin{array}{cccc} \frac{1}{2}I(t \geq \ln\frac{10}{9}) & 0 & 0 & \frac{1}{2}I(t \geq \ln\frac{10}{9}) \\ \frac{1}{2}(1 - e^{-9t}) & \frac{1}{6}(1 - e^{-9t}) & \frac{1}{6}(1 - e^{-9t}) & \frac{1}{6}(1 - e^{-9t}) \\ 0 & \frac{1}{2}(1 - e^{-10t}) & \frac{1}{4}(1 - e^{-10t}) & \frac{1}{4}(1 - e^{-10t}) \\ 0 & \frac{1}{2}I(t \geq \ln\frac{9}{8}) & \frac{1}{4}I(t \geq \ln\frac{9}{8}) & \frac{1}{4}I(t \geq \ln\frac{9}{8}) \end{array} \right\|. \tag{58}$$

Let us compute the exponential moments of hitting times $\Phi_{00}(\rho)$ and $\Phi_{10}(\rho)$, for $\rho = 1$, using the recurrent algorithm described in Sections 3 – 5.

Note that we chosed parameters of semi-Markov transition probabilities and the value of ρ in the way simplifying the corresponding numerical calculations.

The 4×4 matrices of transition probabilities $\|p_{ij}\|$, for the embedded Markov chain J_n and exponential moments $\|\phi_{ij}(1)\|$ of transition times, for the semi-Markov process $J(t)$, have the following forms,

$$\left\| \begin{matrix} \frac{1}{2} & 0 & 0 & \frac{1}{2} \\ \frac{1}{2} & \frac{1}{6} & \frac{1}{6} & \frac{1}{6} \\ 0 & \frac{1}{2} & \frac{1}{4} & \frac{1}{4} \\ 0 & \frac{1}{2} & \frac{1}{4} & \frac{1}{4} \end{matrix} \right\| \text{ and } \left\| \begin{matrix} \frac{5}{9} & 0 & 0 & \frac{5}{9} \\ \frac{9}{16} & \frac{3}{16} & \frac{3}{16} & \frac{3}{16} \\ 0 & \frac{5}{9} & \frac{5}{18} & \frac{5}{18} \\ 0 & \frac{9}{16} & \frac{9}{32} & \frac{9}{32} \end{matrix} \right\|. \tag{59}$$

Let us first exclude state 3 from the phase space $\mathbb{X} = \{0, 1, 2, 3\}$ of the semi-Markov process $J(t)$. The corresponding reduced semi-Markov process ${}_{\langle 3 \rangle}J(t)$ has the phase space ${}_{\langle 3 \rangle}\mathbb{X} = \{0, 1, 2\}$.

The recurrent formulas (48), for transition probabilities of the embedded Markov chain ${}_{\langle 3 \rangle}J_n$, and (49), for exponential moments ${}_{\langle 3 \rangle}\phi_{ij}(1)$ of sojourn times for the semi-Markov process ${}_{\langle 3 \rangle}J(t)$, have the following forms, respectively, ${}_{\langle 3 \rangle}p_{ij} = p_{ij} + \frac{p_{i3}p_{3j}}{1-p_{33}}$ and ${}_{\langle 3 \rangle}\phi_{ij}(1) = \phi_{ij}(1) + \frac{\phi_{i3}(1)\phi_{3j}(1)}{1-\phi_{33}(1)}$, for $i = 0, 1, 2, 3$, $j = 0, 1, 2$.

The 4×3 matrices of transition probabilities $\|{}_{\langle 3 \rangle}p_{ij}\|$ exponential moments $\|{}_{\langle 3 \rangle}\phi_{ij}(1)\|$, computed according the above recurrent formulas, take the following forms,

$$\left\| \begin{matrix} \frac{1}{2} & \frac{1}{3} & \frac{1}{6} \\ \frac{1}{2} & \frac{5}{18} & \frac{2}{9} \\ 0 & \frac{2}{3} & \frac{1}{3} \\ 0 & \frac{2}{3} & \frac{1}{3} \end{matrix} \right\| \text{ and } \left\| \begin{matrix} \frac{5}{9} & \frac{10}{23} & \frac{5}{23} \\ \frac{9}{16} & \frac{123}{368} & \frac{6}{23} \\ 0 & \frac{160}{207} & \frac{15}{46} \\ 0 & \frac{160}{207} & \frac{15}{46} \end{matrix} \right\|. \tag{60}$$

Let us now exclude state 2 from the phase space ${}_{\langle 3 \rangle}\mathbb{X} = \{0, 1, 2\}$ of the semi-Markov process ${}_{\langle 3 \rangle}J(t)$. The corresponding reduced semi-Markov process ${}_{\langle 3,2 \rangle}J(t)$ has the phase space ${}_{\langle 3,2 \rangle}\mathbb{X} = \{0, 1\}$.

The recurrent formulas (48), for transition probabilities ${}_{\langle 3,2 \rangle}p_{ij}$ of the embedded Markov chain ${}_{\langle 3,2 \rangle}J_n$, and (49), for exponential moments ${}_{\langle 3,2 \rangle}\phi_{ij}(1)$ of sojourn times for the semi-Markov process ${}_{\langle 3,2 \rangle}J(t)$, have the following forms, respectively, ${}_{\langle 3,2 \rangle}p_{ij} = {}_{\langle 3 \rangle}p_{ij} + \frac{{}_{\langle 3 \rangle}p_{i2}\,{}_{\langle 3 \rangle}p_{2j}}{1-{}_{\langle 3 \rangle}p_{22}}$ and ${}_{\langle 3,2 \rangle}\phi_{ij}(1) = {}_{\langle 3 \rangle}\phi_{ij}(1) + \frac{{}_{\langle 3 \rangle}\phi_{i2}(1)\,{}_{\langle 3 \rangle}\phi_{2j}(1)}{1-{}_{\langle 3 \rangle}\phi_{22}(1)}$, for $i = 0, 1, 2$, $j = 0, 1$.

The 3×2 matrices of transition probabilities $\|{}_{\langle 3,2 \rangle}p_{ij}\|$ and exponential moments $\|{}_{\langle 3,2 \rangle}\phi_{ij}(\rho)\|$, computed according the above recurrent formulas,

take the following forms,

$$\left\| \begin{array}{cc} \frac{1}{2} & \frac{1}{2} \\ \frac{1}{2} & \frac{1}{2} \\ 0 & 1 \end{array} \right\| \text{ and } \left\| \begin{array}{cc} \frac{5}{9} & \frac{3490}{4347} \\ \frac{9}{16} & \frac{65037}{102672} \\ 0 & \frac{320}{189} \end{array} \right\|. \tag{61}$$

Finally, let us exclude state 1 from the phase space ${}_{\langle 3,2\rangle}\mathbb{X} = \{0,1\}$ of the semi-Markov process ${}_{\langle 3,2\rangle}J(t)$. The corresponding reduced semi-Markov process ${}_{\langle 3,2,1\rangle}J(t)$ has the phase space ${}_{\langle 3,2,1\rangle}\mathbb{X} = \{0\}$.

The recurrent formulas (48) and (49) for transition probabilities of the embedded Markov chain ${}_{\langle 3,2,1\rangle}J_n$, expectations of sojourn times and second moments of sojourn times for the semi-Markov process ${}_{\langle 3,2,1\rangle}J(t)$ have the following forms, respectively, ${}_{\langle 3,2,1\rangle}p_{i0} = {}_{\langle 3,2\rangle}p_{i0} + \frac{{}_{\langle 3,2\rangle}p_{i1}\,{}_{\langle 3,2\rangle}p_{10}}{1-{}_{\langle 3,2\rangle}p_{11}} = 1$ and ${}_{\langle 3,2,1\rangle}\phi_{i0}(1) = {}_{\langle 3,2\rangle}\phi_{i0}(1) + \frac{{}_{\langle 3,2\rangle}\phi_{i1}(1)\,{}_{\langle 3,2\rangle}\phi_{10}(1)}{1-{}_{\langle 3,2\rangle}\phi_{11}(1)}$, for $i = 0, 1$.

The 2×1 matrix of exponential moments $\|\Phi_{i0}(1)\| = \|{}_{\langle 3,2,1\rangle}\phi_{i0}(1)\|$ computed according the above recurrent formulas, take the following forms,

$$\|\Phi_{i0}(1)\| = \left\| \begin{array}{c} \frac{282557}{158067} \\ \frac{57753}{37635} \end{array} \right\|. \tag{62}$$

In conclusion, we would like to note that recurrent algorithms presented in the paper are subjects of effective program realization. These programs let one compute power moments for hitting times and accumulated rewards of hitting times for semi-Markov processes with very large numbers of states. We are going to present such programs and results of large scale experimental studies in future publications.

References

[1] Gyllenberg, M., Silvestrov, D. (2008). Quasi-Stationary Phenomena in Nonlinearly Perturbed Stochastic Systems. De Gruyter Expositions in Mathematics, 44, Walter de Gruyter, Berlin, ix+579 pp.

[2] Janssen, J., Manca, R. (2006). Applied Semi-Markov Processes. Springer, New York, xii+309 pp.

[3] Janssen, J., Manca, R. (2007). Semi-Markov Risk Models for Finance, Insurance and Reliability. Springer, New York, xvii+429 pp.

[4] Silvestrov, D. S. (1980). Semi-Markov Processes with a Discrete State Space. Library for an Engineer in Reliability, Sovetskoe Radio, Moscow, 272 pp.

[5] Silvestrov, D. S. (2004). Upper bounds for exponential moments of hitting times for semi-Markov processes. Comm. Statist. Theory, Methods, 33, no.3, 533–544.

[6] Silvestrov, D., Manca, R. (2015). Reward algorithms for semi-Markov processes. Research Report 2015:16, Department of Mathematics, Stockholm University, 23 pp. and arXiv:1603.05693. (To appear in Method. Comp. Appl. Probab.).

At-Risk-of-Poverty or Social Exclusion Rate – Regional Aspects in the Slovak and Czech Republic and International Comparison

Iveta Stankovičová[1], Jitka Bartošová[2], and Vladislav Bína[2]

[1] Department of Information Systems, Faculty of Management, Comenius University, Odbojárov 10, P.O.BOX 95, 820 05 Bratislava, Slovakia
(E-mail: iveta.stankovicova@fm.uniba.sk)
[2] University of Economics Prague, Faculty of Management, Jarošovská 1117/II, 37701 Jindřichův Hradec, Czech Republic
(E-mail: bartosov@fm.vse.cz; bina@fm.vse.cz)

Abstract. More than 120 million people are at risk of poverty or social exclusion in the EU. EU leaders have pledged to bring at least 20 million people out of poverty and social exclusion by 2020. The fight against poverty and social exclusion is at the heart of the Europe 2020 strategy for smart, sustainable and inclusive growth. Each individual member state will have to adopt one or several national targets.
Presented article examines the aggregate indicator of poverty and social exclusion AROPE in the Slovakia and Czech Republic. Indicator AROPE is the sum of persons who are at-risk-of-poverty or severely materially deprived or living in households with very low work intensity as a share of the total population. Source for calculating of this indicator is harmonized EU SILC statistical survey. We focus on distribution of poverty and social exclusion in the regions of Slovakia and Czech Republic. We describe current trends for aggregate indicator in Slovakia and Czech Republic and compare our values and trends with others EU countries.
Keywords: Europe 2020 Strategy, At-Risk-of-Poverty, Material Deprivation, Low Work Intensity, Region, EU SILC database.

1 Introduction

A strategy for smart, sustainable and inclusive growth, Europe 2020 was proclaimed by European Commission at the beginning of 2010. Primarily, it was a reaction on the impact of last world-wide economic crisis which revealed crucial structural deficiencies in EU economics. The strategy is formulated into five major goals concerning the assurance of general growth of EU [5].
Particularly, in social area the goal was defined in the following way: Reduction of the number of Europeans living below national poverty lines by 25%, lifting 20 million people out of poverty and social exclusion is one of the five headline Europe 2020. Each individual Member State will have to adopt one or several (sub) national targets [7].

Target for Czech Republic: Reduce by 100 000 the number of persons living in poverty or social exclusion (- 100 000 persons).
Target for Slovakia: Reduce to a rate of 17.2 % the number of persons living in poverty or social exclusion (compared to 20.6% in 2008) [8].
The presented paper focuses on a question whether and to what extent were the goals of strategy Europe 2020 in Czech Republic and Slovakia fulfilled in the period 2010 – 2014 and brings a comparison with results in other EU countries. Yet another goal is a decomposition of AROPE indicator into its components and an analysis of income distribution of individuals from particular subgroups endangered by poverty and social exclusion. The last goal elaborated in the paper is an estimation of poverty and social exclusion threat in particular Czech and Slovak regions and detection of significant regional differences.

2 Poverty Measures and Definitions of the Indicators in EU

Analysis of living conditions of individuals and household can be based on measurement of poverty and deprivation. Since the poverty is a complicated issue different approaches for measurement and analysis are used. The most importand possibilities are absolute and relative concepts, in EU a multidimensional relative approach of direct and indirect measurement is used. Among the indirect measures ranks the Foster-Greer-Thorbecke poverty measures defined using concept of generalized entropy [6]. EU employs measures of a*t-risk-of-poverty rate* and *poverty gap*.
Concepts of direct measurement analyse the living standart of inhabitants, e.g., material deprivation related to a reference point [9]. Basic reference in this field is P. Townsend's Poverty in the United Kingdom [14] following the ideas of W. Runciman [10]. EU uses two important indicators: *Severe material deprivation rate* and *Depth of material deprivation*. Yet another possibility to identify endangered individuals is *Low work intensity* indicator. For quantitative evaluation of Europe 2020 goals an aggregated indicator *AROPE* (*At-risk-of-poverty or social exclusion rate*) was defined in the following way.
At-risk-of-poverty or social exclusion rate (AROPE) - The sum of persons who are: at risk of poverty (POV=1) or severely materially deprived (SMD=1) or living in households with very low work intensity (LWI=1) as a share of the total population, expressed in numbers or shares of the population.
At-risk-of-poverty rate (POV=1) - Share of population aged 0+ with an equalised disposable income below 60% of the national equalised median income (after social transfers). The poverty risk rate must always be analysed in conjunction with the at-risk-of-poverty threshold.
The equalised median income is defined as the household's total disposable income divided by its "equivalent size", to take account of the size and composition of the household, and is attributed to each household member (including children). Equalisation is based on the OECD modified scale.
Severe material deprivation rate (SMD=1) – The share of the population lacking at least 4 items among the 9 following items. The household could not afford: 1. to face unexpected expenses; 2. one-week annual holiday away from

home; 3. to pay for arrears (mortgage or rent, utility bills or hire purchase instalments); 4. a meal with meat, chicken or fish every second day; 5. to keep home adequately warm, or could not afford (even if wanted to): 6. a washing machine; 7. a colour TV; 8. a telephone; 9. a personal car.

Whereas the at-risk-of-poverty rate (POV) measures income to identify a lack of resources, the material deprivation rate (SMD) focuses on the ability of households or individuals to afford certain items. The effect of low income might be offset by high savings, access to credit or other sources. By focusing on expenses, the material deprivation rate could take these factors into account. Moreover, by measuring deprivation using a threshold (4 items) of and a list of items that are common to all Member States, the material deprivation is more sensitive to differences in living standards across countries than the poverty risk rate with its nationally defined poverty threshold.

Low work intensity (LWI=1) - People aged 0-59, living in households, where working-age adults (18-59) work less than 20% of their total work potential during the past year. This indicator refers to people living in households with work intensity less than 0.2.

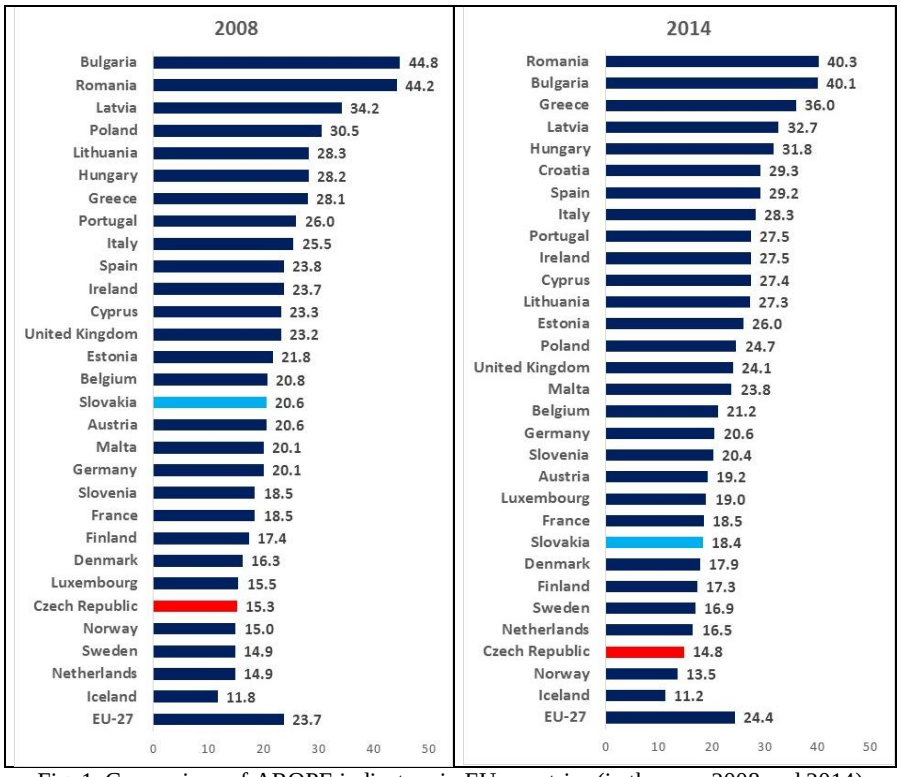

Fig. 1. Comparison of AROPE indicators in EU countries (in the year 2008 and 2014)
Source: Eurostat database, authors' construction

Topicality of the analysed issue can be documented by a wide range of papers dedicated to analyses of poverty and material deprivation and published recently Among the papers concerning situation in the Czech Republic and Slovakia ranks results of Želinský [15], Bartošová and Želinský [3], Bartošová and Bína [4], Stankovičová, Vlačuha and Ivančíková [12] and [13]. The computation of AROPE components are based on data from EU Statistics on Income and Living Conditions (EU-SILC).

3 Comparison of AROPE indicators in EU countries

Based on Fig. 1 it is obvious that in both Slovakia and Czech Republic the values of AROPE indicator shows lower values than average in EU countries (EU27). Situation in the field of poverty and social exclusion in Czech Republic is better than in Slovakia. The proportion of inhabitants suffering from poverty or social exclusion in Czech Republic in 2008 – 2015 was relatively stable. The AROPE indicator shows gentle decrease from 15.3% (2008) to 14.0% (2015), i.e. 1.3 percentage points. In Slovakia we can observe the decrease as well but the values are higher. The AROPE indicator in Slovakia decreased from 20.6% (2008 and 2010) to 18.4% (2015), i.e. by 2.2 percentage points.
In 2008 the Czech Republic was at the 5th place and in 2015 the position was even better (3rd place). Slovakia was in 2008 on the 14th place and in 2014 performed better with 8th position in the ranking of EU countries.

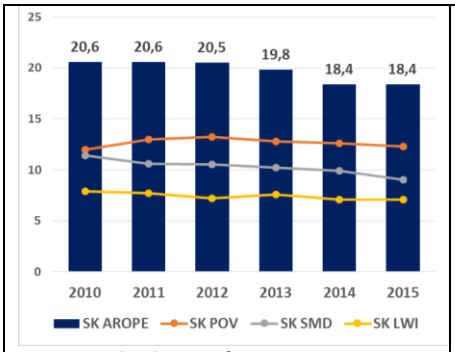

Fig. 2. AROPE and its components in Slovak Republic (2010 – 2015)
Source: Eurostat database

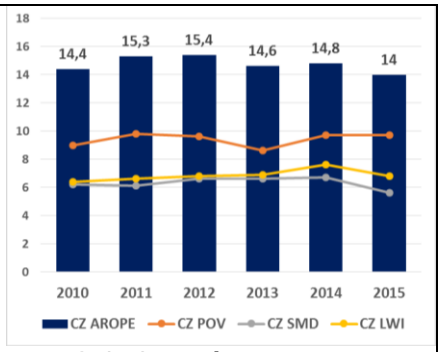

Fig. 3. AROPE and its components in Czech Republic (2010 – 2015)
Source: Eurostat database

4 Trends of AROPE indicator by its components in Slovakia and Czech Republic in the period 2010-2015

The AROPE indicator is composed from three partial indicators (components): POV, SMD and LWI. Each component has different subject and meaning and it is important to consider the development of particular components as well. The following table and graphs (Table 1, Fig. 2 - Fig. 3) show the change of AROPE indicator and its components in range from 2010 to 2015 Slovakia and Czech

Republic. It is obvious that in case of Slovakia we observe in the considered period decrease of all three partial components, but most significant was the decrease of SMD indicator. In the Czech Republic the change of partial indicators was less fluent, but even in this case all three indicators declined. From Fig. 3 we can observe that in 2013 the partial indicators decreased, particularly the indicator of monetary poverty (POV). In 2014 in the Czech Republic all three components again increased.

indicator	geo\time	2010	2011	2012	2013	2014	2015
AROPE	**EU28**	23.7	24.3	24.7	24.6	24.4	23.7
	CZ	14.4	15.3	15.4	14.6	14.8	14.0
	SK	20.6	20.6	20.5	19.8	18.4	18.4
POV	**EU28**	16.5	16.8	16.8	16.7	17.2	17.3
	CZ	9.0	9.8	9.6	8.6	9.7	9.7
	SK	12.0	13.0	13.2	12.8	12.6	12.3
SMD	**EU28**	8.4	8.8	9.9	9.6	8.9	8.1
	CZ	6.2	6.1	6.6	6.6	6.7	5.6
	SK	11.4	10.6	10.5	10.2	9.9	9.0
LWI	**EU28**	10.3	10.5	10.5	10.9	11.2	10.6
	CZ	6.4	6.6	6.8	6.9	7.6	6.8
	SK	7.9	7.7	7.2	7.6	7.1	7.1

Table 1. AROPE indicator and its components (POV, SMD, LWI) in SK, CZ and average EU28 in the period 2010 – 2015 (as % of total population)
Source: Eurostat database

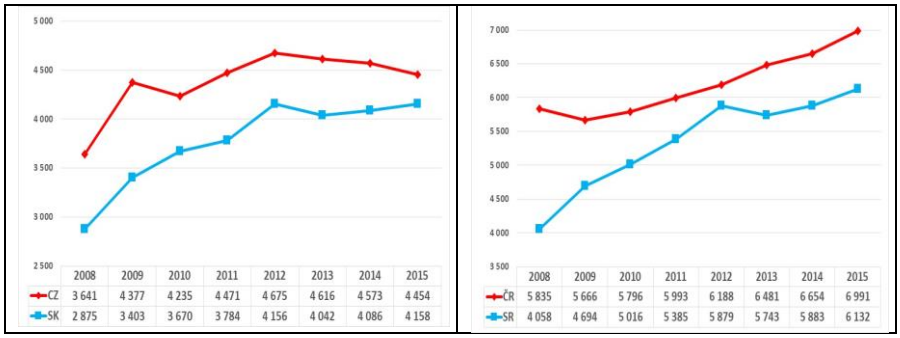

Fig. 4. At-risk-of-poverty thresholds in SK and CZ in the years 2008 – 2015 (left: in EUR; right: in PPS)
Source: Eurostat database, authors' construction in Excel

Values of AROPE indicator are mostly influenced by the partial indicator of the poverty risk rate (POV). The poverty risk rate must always be analysed in conjunction with the at-risk-of-poverty threshold. The progress of at-risk-of-poverty threshold in the Slovakia and Czech Republic (in EUR and in PPS for 2010 – 2015 is depicted on Fig. 4. Values of at-risk-of-poverty threshold in the

Czech Republic (year 2008: 3641 EUR or 5835 PPS; year 2014: 4573 EUR or 6654 PPS) are in all cases higher than in case of Slovakia (year 2008: 2875 EUR or 4058 PPS; year 2014: 4086 EUR and 5883 PPS). In 2008 the difference in poverty thresholds between Slovakia and Czech Republic was as high as 766 EUR (1777 PPS), in 2014 it was 487 EUR (771 PPS) and in 2015 decreased to only 296 EUR but in PPS increased to 859 PPS.

5 Analysis of AROPE indicator by its components in Slovakia and Czech Republic in the year 2014

As we already mentioned, the AROPE indicator is composed from three partial indicators: POV, SMD and LWI. Each component has different subject and meaning and it is important to consider the development of particular components as well. The following tables (Table 2 and 3) show the frequencies of AROPE and its components in 2014 in the Slovakia and Czech Republic.

	SK (2014)		CZ (2014)	
AROPE_B	**Frequency**	**Percent**	**Frequency**	**Percent**
0	4257775	81.6	8783724	85.2
1	**960242**	**18.4**	**1531695**	**14.8**
Total	5218017	100.0	10315419	100.0

Table 2. AROPE indicator in SK and CZ in the year 2014
(numbers of persons in population and as % of total population)
Source: EU-SILC SK and CZ 2014, authors' calculation in SAS Enterprise Guide

			SK		CZ	
AROPE_B	**AROPE (3 digits)**	**AROPE**	**Pearsons**	**%**	**Pearsons**	**%**
AROPE_B = 0	**000**	**0**	4258	81.6	8784	85.2
AROPE_B = 1	**001**	**1**	51	1.0	152	1.5
	010	**10**	240	4.6	335	3.2
	011	**11**	10	0.2	42	0.4
	100	**100**	326	6.2	490	4.7
	101	**101**	70	1.3	195	1.9
	110	**110**	100	1.9	116	1.1
	111	**111**	163	3.1	202	2.0
Total sum of AROPE_B = 1			**960**	**18.4**	**1532**	**14.8**
POV = 1	**1..**	**100+101+110+111**	659	12.6	1002	9.7
SMD = 1	**.1.**	**10+11+110+111**	514	9.9	695	6.7
LWI = 1	**..1**	**1+11+101+111**	294	5.6	591	5.7

Table 3. AROPE indicator and its components in SK and CZ in the year 2014
(numbers of persons (in thousand) in population and as % of total population)
Source: EU-SILC SK and CZ 2014, authors' calculation in SAS Enterprise Guide

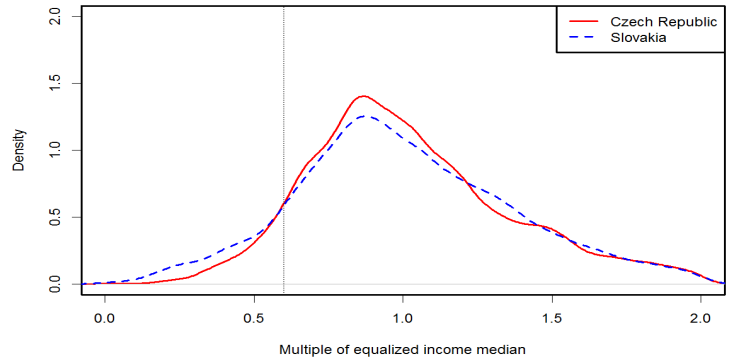

Fig. 5. Kernel estimates of density of equivalised disposable income for hole population (SK and CZ, in year 2014)

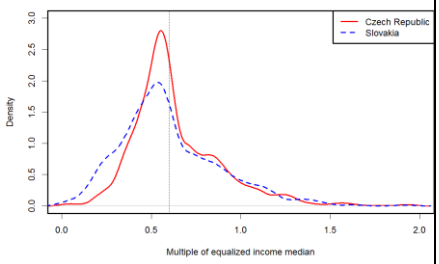

Fig. 6. Kernel estimates of density of equivalised disposable income for population with AROPE_B=1 (SK and CZ, in year 2014)

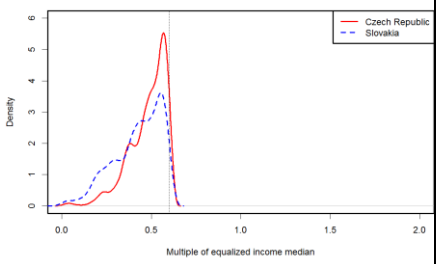

Fig. 7. Kernel estimates of density of equivalised disposable income for population with POV=1 (SK and CZ, in year 2014)

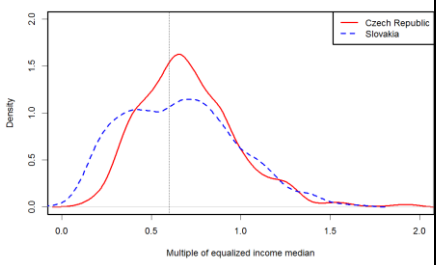

Fig. 8. Kernel estimates of density of equivalised disposable income for population with SMD=1 (SK and CZ, in year 2014)

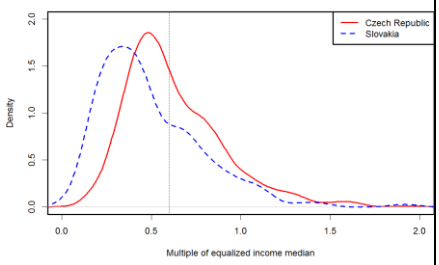

Fig. 9. Kernel estimates of density of equivalised disposable income for population with LWI=1 (SK and CZ, in year 2014)

Source: EU-SILC SK and CZ 2014 database, authors' construction in R

Fig. 5 – 9 present kernel density estimates (see, e.g., [1]) of equalised disposable incomes of the whole population (see Fig. 5), inhabitants endangered by risk of

monetary poverty or social exclusion (AROPE_B = 1), inhabitants at risk of monetary poverty (POV = 1), material deprivation (SMD = 1) and showing low work intensity (LWI = 1).

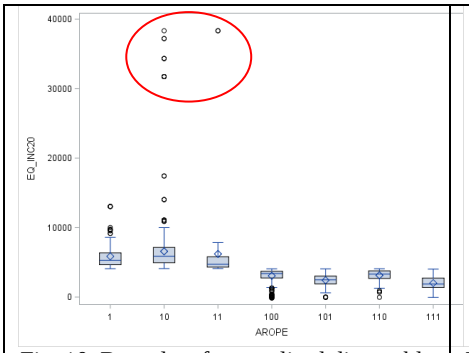

Fig. 10. Box-plots for equalised disposable income in Slovak Republic (AROPE_B = 1)

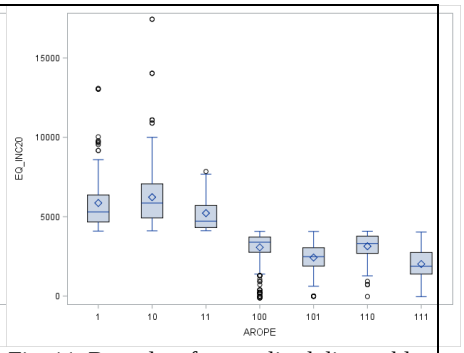

Fig. 11. Box-plots for equalised disposable income in Slovak Republic (AROPE_B = 1 and EQ_INC20 < 20000)

Source: Data EU-SILC SK 2014, authors' construction in SAS Enterprise Guide

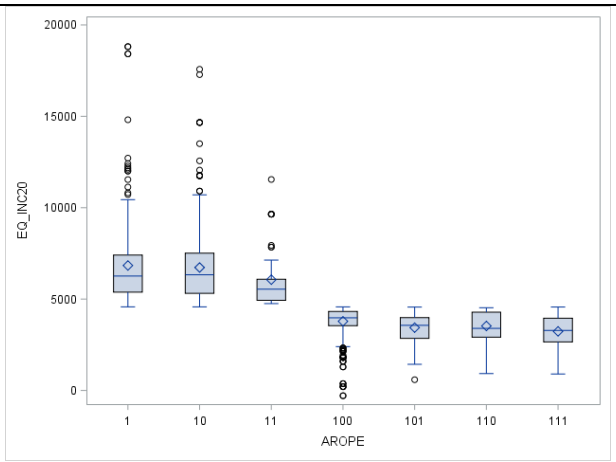

Fig. 12. Box-plots for equalised disposable income in Czech Republic (AROPE_B = 1)

Source: Data EU-SILC CZ 2014, authors' construction in SAS Enterprise Guide

We performed more detailed analysis of equalized disposable income according to the components of AROPE indicator based on the date from sample survey EU-SILC 2014 in Slovakia and Czech Republic (Fig. 10 – 12). The analysis showed that in case of Slovakia in some households occurs extremely high values of equalised disposable incomes per individual in case of individuals only with SMD (AROPE = 10), or SMD together with LWI (AROPE = 11). This effect does not appear in the data from Czech Republic where all values of equalised disposable income are lower than 20 000 EUR.

Box-plots (Fig. 10 – 12) show that the level of equalised disposable incomes in this group is significantly higher, frequently higher than the official poverty threshold in the country. Therefore, such individuals are not endangered by poverty (POV), but perceive subjectively material deprivation (SMD) or live in the household with low work intensity (LWI).

5 Analysis of AROPE indicator by NUTS 2 regions in Slovakia and Czech Republic

The development of AROPE indicator in Slovakia and Czech Republic is favourable. The proportion of individuals suffering from poverty and social exclusion in the population decreases in the long-run (2005 – 2015) and values in both countries are lower than EU27 or EU28 average (Fig. 13). The graphs also present the fact that in particular NUTS 2 regions the values of aggregated AROPE indicator decrease. We can observe that in Slovakia and also in Czech Republic probably significant differences in the values of AROPE indicator appear (according to the NUTS 2 regions). The highest values of indicator in Slovakia appear in case of region SK04 (Eastern Slovakia) and in case of Czech Republic it appears in two regions: CZ04 (North-west) and CZ08 (Moravian-Silesian).

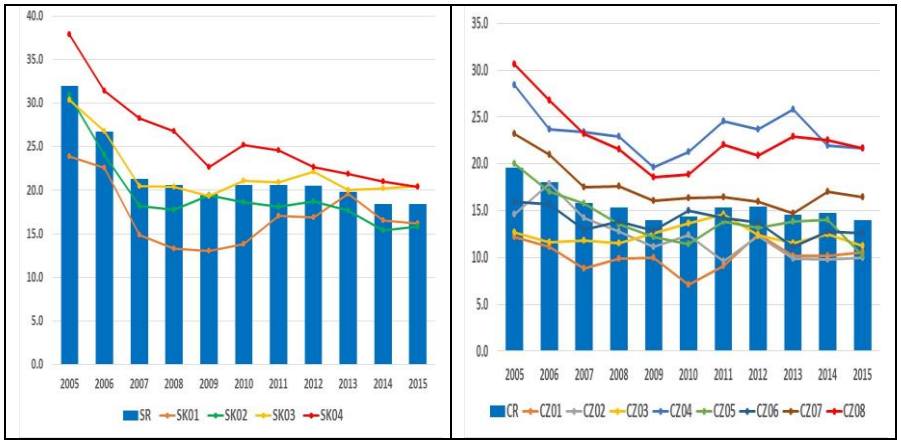

Fig. 13. AROPE by NUTS 2 regions in SK and CZ (in the years 2005 – 2015)
Source: Eurostat database, authors' construction in Excel

Based on the data of EU-SILC for Slovakia and Czech Republic in 2014 we performed more detailed analysis of distribution of population and their equalised disposable incomes in case of at risk poverty or social exclusion subgroup according to NUTS 2 regions. From the results (Table 4 and 5) it is obvious that in both countries persist significant regional differences in poverty or social exclusion (AROPE_B = 1) but also in level and variability of equalised

disposable incomes (EQ_INQ20) of the individuals in considered NUTS 2 regions.
Pearson chi-square was used to test the hypothesis concerning the homogeneity of distribution in case of at risk of poverty or social exclusion according to regions and distribution of population in regions NUTS 2 (DB040). In both countries the test rejected null hypothesis concerning the homogeneity of distributions (p-values were significantly lower than 0.0001 in both countries).

			EQ_INC20 (AROPE_B = 1)		
Region (DB040)	**% of population**	**% of population in AROPE_B = 1**	**Mean**	**Std Dev**	**Median**
SK01	11.5%	10.3%	5677.5	5791.5	4770.1
SK02	33.9%	28.4%	3892.8	1976.3	3597.1
SK03	24.9%	27.4%	3526.4	1736.5	3428.8
SK04	29.7%	33.9%	3691.6	2267.2	3248.7

Table 4. Distribution Slovak population by NUTS 2 regions and descriptive statistics for equalised disposable income (EQ_INC20) for population at risk of poverty rate or social exclusion (AROPE_B = 1) in the year 2014
Source: EU-SILC SK 2014, authors' calculation in SAS Enterprise Guide

			EQ_INC20 (AROPE_B = 1)		
Region (DB040)	**% of population**	**% of population in AROPE_B = 1**	**Mean**	**Std Dev**	**Median**
CZ01	11.7%	8.1%	5077.5	2257.1	4523.7
CZ02	12.3%	8.1%	5099.0	1970.6	4466.6
CZ03	11.5%	9.7%	4490.7	1565.7	4173.3
CZ04	10.6%	15.7%	4376.9	1539.2	4059.5
CZ05	14.4%	13.6%	5044.0	2708.4	4304.6
CZ06	16.0%	13.8%	4783.0	1819.6	4388.0
CZ07	11.7%	13.3%	4590.5	2219.6	3998.0
CZ08	11.7%	17.7%	4258.8	1663.7	4083.9

Table 5. Distribution Czech population by NUTS 2 regions and descriptive statistics for equalised disposable income (EQ_INC20) for population at risk of poverty rate or social exclusion (AROPE_B = 1) in the year 2014
Source: EU-SILC CZ 2014, authors' calculation in SAS Enterprise Guide

In Slovakia (Table 4) lower proportion of individuals at risk poverty or social exclusion appear than the proportion of region in the population in case of two regions, namely SK01 (Bratislava region: 10.3% < 11.5% population) and SK02 (Western Slovakia: 28.4% < 33.9% population). In region SK03 (Central Slovakia: 27.4% > 24.9% population) and SK04 (Eastern Slovakia: 33.9% > 29.7% population) the situation is opposite. There appears higher proportion of persons suffering from poverty and social exclusion than is the corresponding part within population. The worst situation concerning the occurrence of individuals at risk poverty or social exclusion appears in SK04 region.

In the Czech Republic (Table 5) appears the lowest proportion at risk of poverty or social exclusion in regions CZ01 (Praha: 8.1% < 11.7% population) and CZ02 (Central Bohemia: 8.1% < 12.3% population). But also in other 3 regions is lower proportion of inhabitants suffering from the risk of poverty or social exclusion than is the proportion of inhabitants from the regions. Namely regions CZ03, CZ05 a CZ06. High proportion of inhabitants at risk of poverty or social exclusion is particularly in the regions CZ04 (North-west) a CZ08 (Moravian-Silesian).

Together with the appearance of poverty and social exclusion relates also low level of incomes. We analysed the level of equalised disposable income (EQ_INQ20) in NUTS 2 regions in Slovakia and Czech Republic for inhabitants living in household at risk of poverty and social exclusion, i.e. AROPE_B = 1 (Table 4 - 5, Fig. 14 - 15).

The results show that in Slovakia among inhabitants at risk of poverty and social exclusion (AROPE_B = 1) appear also persons (or households) with extremely high equalised disposable incomes, namely incomes over 20 000 EUR (EQ_INC20 > 20000). Such extremely high incomes appear in two Slovak regions, namely in SK01 and SK04. In EU-SILC data from the Czech Republic such extremely high values of equalised disposable income do not appear. It presents the fact that particularly the SMD component of the AROPE indicator where the respondents of EU-SILC answers nine items concerning SMD is strongly loaded by subjective perception of respondent (see Fig. 18 and 19).

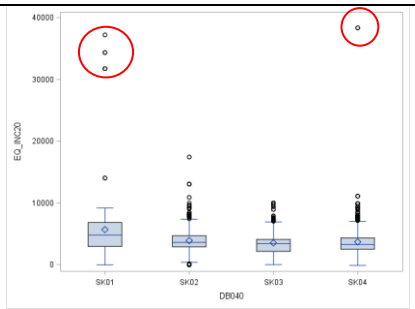

Fig. 14. Box-plots for equalised disposable income in Slovak regions NUTS 2 (2014, AROPE_B = 1)

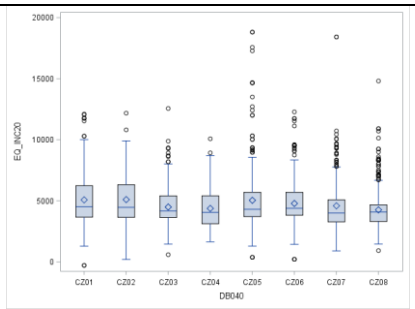

Fig. 15. Box-plots for equalised disposable income in Czech regions NUTS 2 (2014, AROPE_B = 1)

Source: EU-SILC 2014 database, authors' construction in SAS Enterprise Guide

The significance of differences in level of equalised disposable incomes of individuals endangered by poverty or social exclusion (AROPE_B = 1) was tested using Kruskal-Wallis test with Wilcoxon Scores because incomes are highly skewed and their variability is non-homogenous in regions of Slovakia and Czech Republic. For both countries we rejected null hypothesis concerning equality of median scores in NUTS 2 regions (p-values < 0.0001). Therefore, we can claim that the level of equalised disposable incomes in the regions of Slovakia and Czech Republic significantly differs.

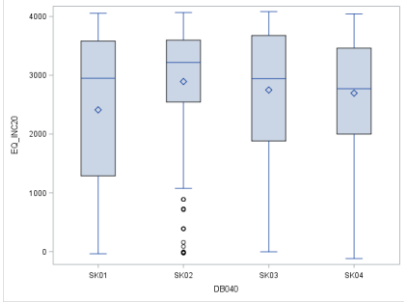

Fig. 16. Box-plots for equalised disposable income in Slovak regions NUTS 2 (POV=1)

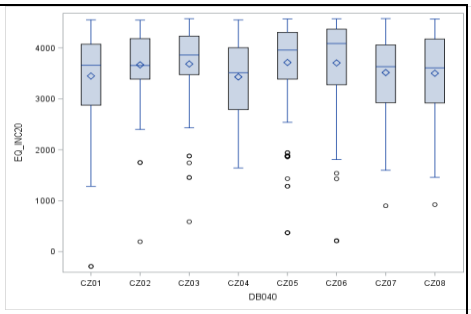

Fig. 17. Box-plots for equalised disposable income in Czech regions NUTS 2 (POV=1)

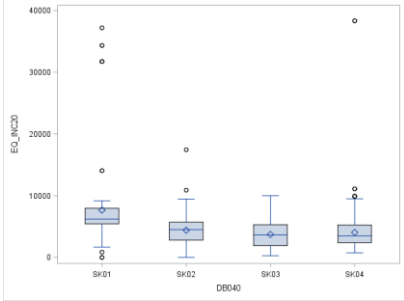

Fig. 18. Box-plots for equalised disposable income in Slovak regions NUTS 2 (SMD=1)

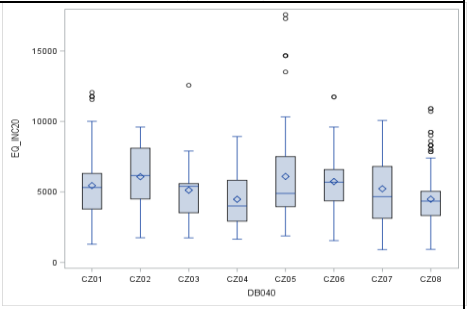

Fig. 19. Box-plots for equalised disposable income in Czech regions NUTS 2 (SMD=1)

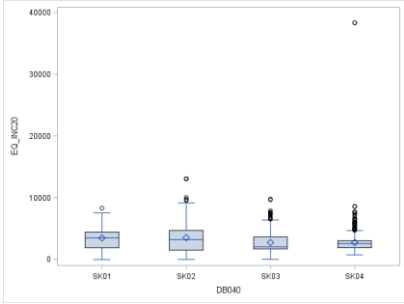

Fig. 20. Box-plots for equalised disposable income in Slovak regions NUTS 2 (LWI=1)

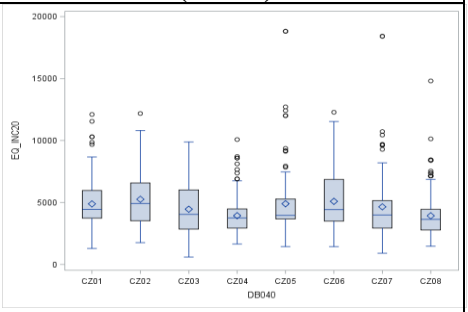

Fig. 21. Box-plots for equalised disposable income in Czech regions NUTS 2 (LWI=1)

Source: EU-SILC SK and CZ 2014 database, authors' construction in SAS EG

On the graphs (Fig. 14 – 21) we can observe distribution of equalised disposable income (EQ_INC20) in particular components of AROPE indicator in Slovak and Czech NUTS 2 regions.

The distribution of equalised disposable incomes for inhabitants at risk of poverty (POV = 1) obviously appears under the poverty threshold (in 2014:

Slovakia 4086 EUR and Czech Republic 4573 EUR, see Fig.4). The distributions in regions are skewed and modus of the distribution is skewed towards the poverty threshold. Variability of incomes in Slovakia differ in regions. The highest variability shows in region SK01 (Bratislava). But the highest mean and median of incomes appears in SK02 (Western Slovakia). In the region CZ04 (North-west) we can observe the lowest values of mean and median incomes in the Czech Republic. The variability of incomes is more uniform in the Czech Republic.

Values of equalised disposable incomes for individuals endangered by material deprivation (SMD = 1) can be higher than the national poverty threshold. The values are influenced by subjective assessment of SMD and therefore it happens that even individuals with quite high level of incomes subjectively perceive that they cannot get some of the 9 items enumerated in the EU-SILC questionnaire. In Slovakia such extreme values of incomes (EQ_INC20 > 20000) appear in 2 regions: in the wealthiest SK01 and in the poorest SK04.

Incomes of inhabitants with low work intensity (LWI = 1) appears in regions of Slovakia significantly lower (under 5000 EUR) than in the Czech Republic. In the region SK04 an extremely high income over 20 000 EUR appeared.

Conclusions

Based on the results of data from Eurostat database we can claim that the proportion of inhabitants at risk of poverty or social exclusion (AROPE) in Slovakia and Czech Republic lies bellow the mean of EU27 (or EU28) and in 2008 – 2015 was further decreasing. Although the ratio of inhabitants under the risk of poverty and social exclusion in the whole EU did not decrease (actually increase of about 1699 thousand persons), but in Slovakia and Czech Republic the decrease took place. In the period 2008 – 2015 in Slovakia the number of inhabitants at risk of poverty and social exclusion decreased about 148 thousand and about 122 thousand in the Czech Republic. Czech Republic thus succeeded in fulfilling the goal (sub-target: reduce by 100 000 the number of persons living in poverty or social exclusion) which was set in this field in the strategy Europa 2020. Slovakia set the goal in a relative way, particularly aims to reduce a rate from 20.6% in 2008 to 17.2 % in 2020. In 2015 Slovakia achieved value of AROPE indicator equal to 18.4% and therefore it is necessary to continue in efforts to reduce the rate further, but the trend is positive.

Based on the results from Slovak and Czech EU-SILC data in 2014 we can state that regional disparities still persist in both Slovakia and Czech Republic. Disparities are present not only in distribution of inhabitants at risk of poverty and social exclusion in particular regions but also in the level and variability of equalised disposable income of those inhabitants in regions of Slovakia and Czech Republic. The most problematic component of AROPE indicator appears to be the SMD component suffering seriously from the subjectivity of respondent perception.

References

1. Antoch, J., Vorlíčková, D. *Vybrané metody statistické analýzy dat*. Praha: Academia, 1992.
2. Atkinson, T., Cantillon, B., Marlier, E., Nolan, B. *Social Indicators: The EU and social inclusion*, Oxford University Press, Oxford, 2002.
3. Bartošová, J., Želinský, T.: Extent of poverty in the Czech and Slovak Republics fifteen years after split. *Post-Communist Economies*, 25(1), 2013, 119-131.
4. Bartošová, J., Bína, V.: Sensitivity of monetary poverty measures on the setting of parameters concerning equalization of household size. In: *Proceedings of 30th International Conference Mathematical Methods in Economics 2012*. Karviná: Silesian University, School of Business Administration, 2012, 25-30. ISBN 978-80-7248-779-0.
5. European Commission. *Europe 2020: A European Strategy for smart, sustainable and inclusive growth*, Communication NO COM (2010) 2020, Brussels: European Commission, 2010.
6. Foster, J., Greer, J., Thorbecke, E.: A Class of Decomposable Poverty Measures. *Econometrica*, 52(3), 1984, 761–766.
7. Frazer, H., Marlier, E., Nicaise, I.: *A Social Inclusion Roadmap for Europe 2020*. Antwerp: Garant, 2010. ISBN 978-90-441-2267-9.
8. Ivančíková, L., Vlačuha, R.: Stratégia EU 2020 a ohrozenie chudobou v regiónoch Slovenska. In.: *Sociálny kapitál, ľudský kapitál a chudoba v regiónoch Slovenska*. Košice: Technical University, 2010, 31-36. ISBN 978-80-553-0573-8.
9. Morrison, D.: Some Notes Toward Theory on Relative Deprivation, Social Movements, and Social Change. The American Behavioral Scientist, 14, (5), 1971, 675–690.
10. Runciman, W. G.: Relative Deprivation and Social Justice. A Study of Attitudes to Social Inequality in Twentieth-Century England. *The British Journal of Sociology*, 17(4), 1966, 430–434.
11. Řezanková, H., Želinský, T. Factors of Material Deprivation Rate in the Czech Republic by Household Type. *Ekonomický časopis*, 62(4), 2014, 394–410.
12. Stankovičová, I., Vlačuha, R., Ivančiková, Ľ.: Trend analysis of monetary poverty measures in the Slovak and Czech republic. In: *International days of statistics and economics*. Slaný Melandrium, 2013, 1334-1343 [online]. ISBN 978-80-86175-87-4.
13. Stankovičová, I., Vlačuha, R., Ivančiková, Ľ.: Revision of the concept of measuring material deprivation in the EU. In: *International days of statistics and economics*. Slaný: Melandrium, 2014, 1441-1449 [online]. ISBN 978-80-87990-02-5. http://msed.vse.cz/msed_2015/article/113-Stankovicova-Iveta-paper.pdf
14. Townsend, P.: Poverty in the United Kingdom: A Survey of Household Resources and Standards of Living. Harmondsworth: Penguin Books, 1979.
15. Želinský, T.: Analýza chudoby na Slovensku založená na koncepte relatívnej deprivácie. *Politická ekonomie*, 58 (4), 2010, 542–565.

A neuro-fuzzy approach to measuring attitudes

Maria Symeonaki[1], Aggeliki Kazani[2] and C. Michalopoulou[3]

[1,2,3] Department of Social Policy, School of Political Sciences, Panteion University of Social and Political Sciences, Athens, Greece
(E-mail: msymeon@panteion.gr, agkazani@gmail.com, kmichalop@panteion.gr)

Abstract. The present paper deals with the application of neuro-fuzzy techniques to the measurements of attitudes. The methodology used is illustrated and evaluated on data drawn from a large-scale survey conducted by the National Centre of Social Research of Greece, in order to investigate opinions, attitudes and stereotypes towards the "other" foreigner. The illustration provides a meaningful way of classifying respondents into xenophobic levels, taking also into account other important socio-demographic characteristics, such as age, education, gender, political beliefs, religion practice and the way each question is answered by the respondent. The methodology provides a way of classifying respondents whose responses are identified as questionable.
Keywords: Likert scales, attitude measurement, neuro-fuzzy systems.

1 Introduction

The present paper develops a neuro-fuzzy technique for measuring an attitude. Many definitions have been provided in the literature as to what constitutes an attitude. For example in Hoog and Vaughan[3] an attitude is defined as 'a relatively enduring organization of beliefs, feelings, and behavioral tendencies towards socially significant objects, groups, events or symbols'. According to Eagly and Chaiken[1] an attitude is 'a psychological tendency that is expressed by evaluating a particular entity with some degree of favor or disfavor'. In psychology, an attitude is a psychological construct, it is a mental and emotional entity that inheres in, or characterizes a person (Perloff [7]). How to measure attitudes has also been an issue of utmost importance in social sciences and numerous rating scales have been suggested in the past for that reason. The most commonly used rating scale is the Likert scale developed in 1932 (Likert[5]) by the American psychologist Rensis Likert. It is composed of third-person items/questions and it rates the respondents by asking them to place themselves on a scale of favor/disfavor with a neutral midpoint. Therefore a respondent is asked to select between several response categories, indicating various strengths of agreement and disagreement. The response categories are assigned scores and the respondents' attitudes are measured by their total score, which is the sum of the scores of the categories the respondents have chosen for each item-question.
When this traditional type of methodology is used the respondent's attitude is assessed by examining the response categories he/she chooses in a number of items/questions. In this study we provide a hybrid expert system that classifies respondents into levels of xenophobia. The focus is on the development of a neuro-fuzzy system that will measure the specific attitude, taking into account a number of important factors such as age, level of education, gender, political

and religion beliefs and finally the way each question is answered by the respondent. The proposed system takes into account the answers for each respondent and distinguishes between questionable and non-questionable answers. The intelligent system put forward in the present paper simulates the respondent's final score when the answers are not questionable and takes into account a number of other crucial factors when the answers are questionable so as to classify the respondents into xenophobic levels, reducing therefore the uncertainty.

This approach is an extension of the methodology suggested in Symeonaki and Kazani[11] and it can be used in every real problem where researchers would like to classify respondents with the aid of Likert scales to different levels of belief, feeling or opinion towards a specific object.

Recently, there have been attempts to combine expert systems with attitude scaling. In Symeonaki *et al.*[10] a fuzzy system based on factor analysis is proposed whereas in Symeonaki and Michalopoulou[9] cluster analysis and fuzzy k-means is used in order to produce a more reliable final scale. Moreover, in Symeonaki *et al.*[12] and in Symeonaki and Kazani [8] a fuzzy system that measures xenophobia in Greece is suggested. In addittion, Lalla *et al.*[4] proposed a fuzzy system to analyze qualitative ordinal data produced by a course-evaluation questionnaire and Gil and Gil[2] provided a guideline to design questionnaires allowing free fuzzy-numbered response format.

The paper has been organized in the following way. Section 2 provides some information concerning the data and the methodology used in the present study and the respective results. The next Section discusses the validation of the proposed neuro-fuzzy approach. Section 4 discusses the results and provides concluding remarks and aspects of future work.

2 Data, Methodology and Results

The Likert scale studied in the following sections is included in the questionnaire of a large-scale survey conducted under the auspices of the National Centre for Social Research[1] that was designed in order to measure xenophobia (Michalopoulou[6]). More specifically, the following questions were given (see Symeonaki *et al*. [12]):

1. Foreigners who live in our country must have equal rights with us.
2. Many of the foreigners who live in our country are responsible for the increase in the crime rate.
3. Foreigners must have lower wages even when they do the same job as we.
4. The foreigners in our country increase unemployment for Greeks.
5. The local authorities must organize events so we get to know the foreigners who live and work here.

[1] www.ekke.gr

6. I would never marry a foreigner.
7. I would never work for a foreigner.
8. We should facilitate foreigners who want to settle in our country.
9. Foreigners who work in our country do harm to our economy.
10. The state must organize programmes of further education to help those foreigners who live in our country.
11. The more foreigners there arrive the lower the wages get.
12. We must create reception departments in our schools for the foreigners' children.
13. Only as tourists should foreigners come.
14. Work permits must be given to foreigners who want to live here.
15. We must close our borders to foreigners who come to work here.

The units had 5 response categories, ranging from total agreement to total disagreement. The sample of the survey was 1200 individuals, aged 18-80 years, residents of Macedonia, Northern Greece, during the time of the fieldwork.

Let us now provide a very brief introduction to the theory of Fuzzy Logic presented by L. A. Zadeh [13] in 1965 and the theory of artificial neural networks.

In fuzzy set theory when A is a fuzzy set and x is a relevant object, the statement, x is a member of A, is not necessarily either true or false, but it may be true only to some degree represented by the membership function of the fuzzy set A, $m_x(A)$. A membership function is a curve that defines how each point in the input space is mapped to a membership value in [0,1]. Fuzzy systems are systems in which variables have as domain fuzzy sets encoding structured, heuristic knowledge in a numerical framework.

The operation of an artificial neural network is based on a recurrent interconnection of simple processing units, called the neurons. Each neuron receives an input, a vector $\mathbf{x}$ and produces an output y (Figure 1) through the equations:

$$U = f(\mathbf{x}, \mathbf{w}) - \theta$$

$$y = a(\mathbf{u})$$

where θ represents the activation threshold and $f(\mathbf{x}, \mathbf{w})$ is called the transfer function that relates the input information $\mathbf{x}$ with the weights $\mathbf{w}$ that are stored in the neuron. In most cases it is of the form:

$$f(\mathbf{x}, \mathbf{w}) = \sum_{i=1}^{m} w_i x_i$$

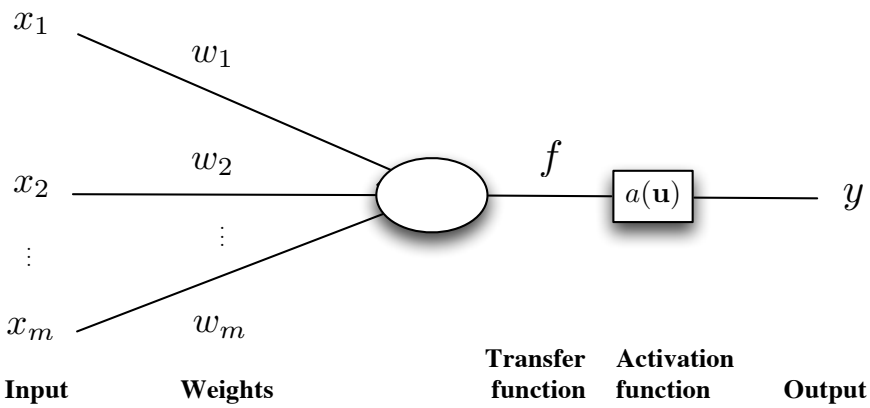

Fig. 1. Typical form of an artificial neuron.

The function α is called the activation function and it generally takes values according to:

$$\alpha(\mathbf{u}) = 1, \text{ if } \mathbf{u}>\mathbf{0} \text{ και } \alpha(\mathbf{u}) = \mathbf{0}, \text{ αν } \mathbf{u}<\mathbf{0}.$$

Neural networks are in fact a mass of interconnected simple units and the way the interconnection is carried out defines the network's structure and therefore the way it operates. In order to describe the structure of a network, the nodes (i.e. the neurons) are assumed to be laying in different layers and the basic architecture consists of three types of neuron layers: input, hidden, and output. The nodes that belong to the same layer are being evaluated simultaneously. Another significant matter of artificial neural network modeling is its ability of learning, its ability of adopting and changing its elements in order to simulate a given behaviour.
Our objective here is to develop a neuro-fuzzy system that classifies respondents into xenophobic levels. We denote by:

- m: the number of questions (here $m=15$)
- Q_j: the j-the question $j=1,2,...,m$
- $q_j(i)$: the answer of the i-th respondent to the Q_j question, i.e, $q_j(i)=1,2,3,4$ or 5, $\forall i=1,2,...,1200$, $\forall j=1,2,...,m$.
- $\mathbf{x}(i)$: the response vector of the i-th respondent to items-questions Q_1, Q_2, ..., Q_m, i.e. $\mathbf{x}(i)=[q_1(i),q_2(i),...,q_m(i)]$.

A first step would be to distinguish between questionable and non-questionable answers. We assume that non-questionable answers are those based on which we can classify the respondent to different levels of xenophobia *without uncertainty*. For example, if the response vector of the *i*-th respondent is $\mathbf{x}(i)=[1,1,....,1]$ then the respondent's score is equal to 15 and he/she is classified into the category denoting a non-xenophobic person, without uncertainty. Let us now examine what could be defined as *questionable answers*. Those answers include a series of responses that lead to a questionable outcome, where the respective respondents cannot be classified to xenophobic levels with certainty. Consider, a respondent that answers that he/she would be willing to marry a foreigner and generally holds a non-xenophobic attitude if one looks at the answers he/she provides, but strongly disagrees with working for a foreigner or believes that only as tourists should foreigners come. His/her response vector would look like $\mathbf{x}=(1,1,1,1,1,1,5,1,1,1,1,1,5,1,1)$ and we could say that there is an ambiguity as to the level of xenophobia that he/she holds. There exist, therefore, certain sets of responses that may lead to an uncertain classification. In those cases there are more factors that need to be taken into account.

Now, for the purpose of this study a statistical analysis was performed on the data with the aid of IBM Statistics SPSS 24.0. The values of all negatively worded items were reversed in order to achieve correspondence between the ordering of the response categories. Summing up the response categories that they have chosen and dividing by the number of the questions estimated the mean scores for each respondent, i.e. $\overline{xen}=\frac{\sum_{i=1}^{m} q_j(i)}{m}$, where m denotes the number of questions.

Definition 2.1 The *i*-th respondent's answer $\mathbf{x}(i)$ is said to be *questionable at level d* if $\exists j: \left|q_j(i)-\overline{xen}\right|\geq d$.

Definition 2.2 The *i*-th respondent's answer $\mathbf{x}(i)$ is said to be *non-questionable at level d* if $\nexists j: \left|q_j(i)-\overline{xen}\right|\geq d$.

We denote questionable answers at level *d* by *QA-d*, whereas *NQA-d* denotes the non-questionable answers at level *d*. For the purpose of this analysis we

consider *QA-3* and *NQA-3* answers. This means that we define questionable answers to be those for which there exists at least one answer (response category chosen by the respondent) whose absolute difference to his/her mean xenophobic score is equal or greater to 3. For example if the *i*-th respondent's response vector is $\mathbf{x}(i)=[5,1,1,...,1]$, then his/her response vector would be identified as questionable since there exists a $j=1: \left|q_1(i)-\overline{xen}\right|=\left|5-1.26\right|=3.73\geq 3$. The sample was split into two categories: respondents providing non-questionable answers $(N=930)$ and respondents providing questionable answers $(N=160)$. The artificial neural network system determines the classification of the respondents in the case of *NQA-3*. For the case of the *QA-3* we develop two fuzzy systems, since there exist several factors that need to be considered and the classification is not ambiguous. The first fuzzy system takes into account a set of rules and determines the *degree of belief (TRUST)* about the xenophobic level of the respondent that will determine the way this answer will be scored. The second fuzzy system determines the *xenophobic level*, considering the *degree of belief (TRUST)*, which is the output of the first fuzzy system and the score of the respondent. Subsequently, a final level is provided for each respondent based on the results (outcomes) of all systems. The neural network that was implemented is a three-layer Back Propagation network (Figure 2). The structure of the proposed intelligent classification system is shown in Figure 3 and a part of the *NQA-3* is revealed in Table 1.

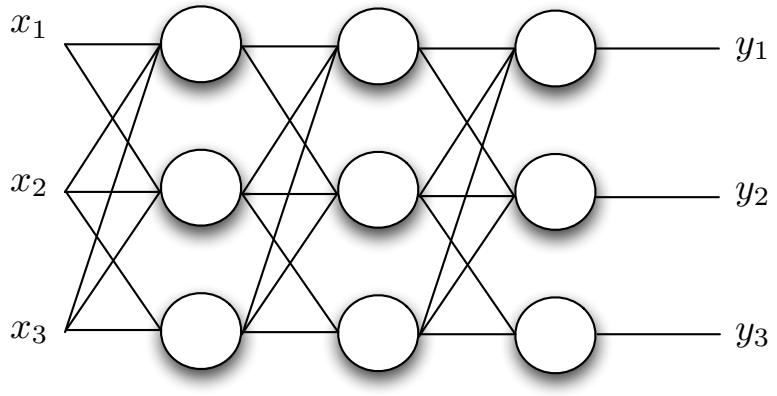

Fig. 2. The structure of the implemented artificial neural network.

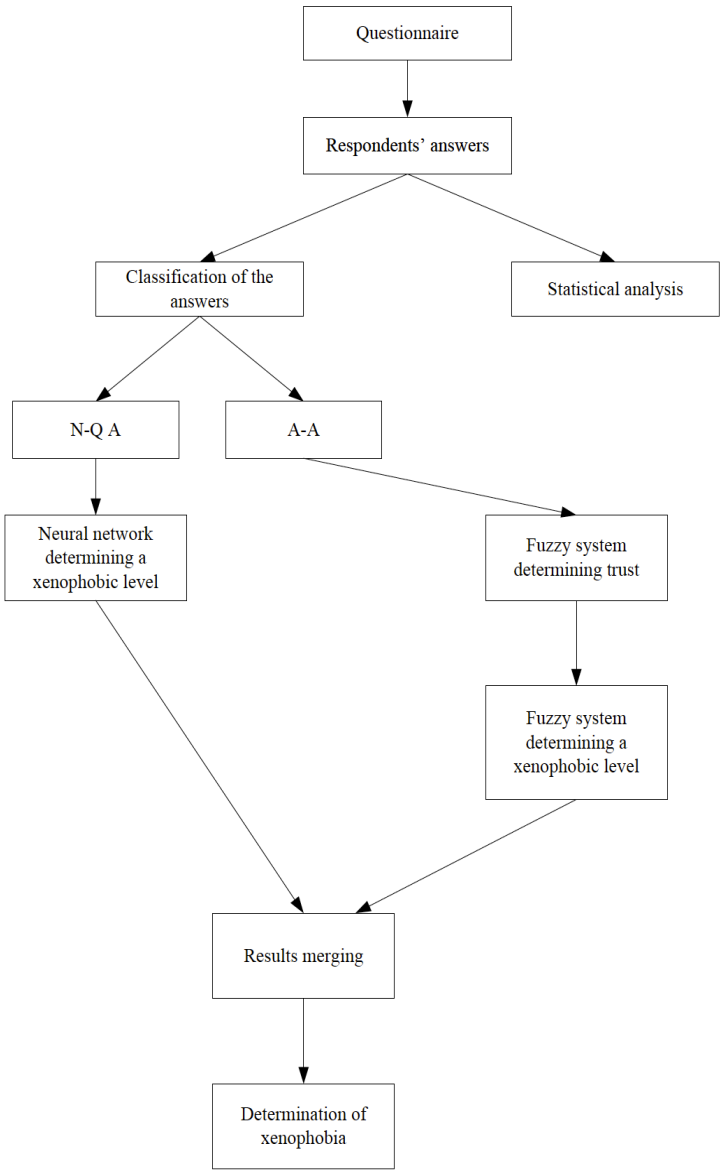

Fig. 3. The structure of the proposed system

Non questionable answers	Level of Xenophobia
$\mathbf{x}=(1,1,\ldots,1)$	1
$\mathbf{x}=(2,1,\ldots,1)$	1
$\mathbf{x}=(2,2,\ldots,2)$	2
$\mathbf{x}=(2,2,\ldots,1)$	2
$\mathbf{x}=(3,3,\ldots,3)$	3
$\mathbf{x}=(2,2,\ldots,3)$	2
$\mathbf{x}=(4,4,\ldots,4)$	4
$\mathbf{x}=(4,4,\ldots,5)$	4
$\mathbf{x}=(5,5,\ldots,5)$	5
$\mathbf{x}=(5,5,\ldots,4)$	5

Table 1. An excerpt of non questionable answers and their classifications to levels of xenophobia

For non-questionable answers the Neural Network Toolbox of MATLAB R2014a was used and the xenophobic levels were determined. For validation the analysis was repeated with the Neural Network analysis provided by IBM Statistics SPSS 24.0 and the same results were given as outcomes with very slight differences.

For the questionable answers we firstly develop the following system that has five inputs and one output. The inputs are factors that determine xenophobia: Age, Education, Sex, Politics and Religious Practice. The output is the degree of belief or trust that the specific respondent is xenophobic. Figure 4 provides the inputs and output of the first system whereas Figure 5 presents the fuzzy partitioning of Age, Education, Sex, Politics and Religious Practice.

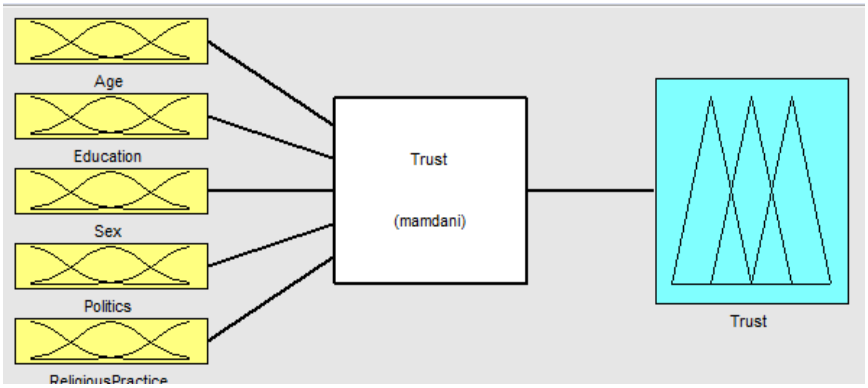

Fig. 4. Input and Output of the fist fuzzy system

Age is measured in years, Education in one of the categories from 1=Illiterate/has left primary school to 7=Postgraduate degree, Gender is either Male (1) or Female (2), Politics is a variable that takes values from 1 (Left wing) to 10 (Right wing) and Religious practice (how often do you go to church) takes values from Every Sunday or more often (1) to Never (5). Therefore, a possible input for the first fuzzy system would be $input = [23,4,1,4,3]$. The fuzzy partition of the output of the first fuzzy system is presented in Figure 6.

An excerpt of the fuzzy rule base for TRUST, which consists of 28 inference rules of the canonical form, i.e. IF-THEN rules, is the following:

1. IF (*Age, Education, Gender, Politics, ReligiousPractice*) IS (Young, High, Male, LeftWing, Rarely), THEN *Trust* IS Low.
2. IF (*Age, Education, Gender, Politics, ReligiousPractice*) IS (Young, High, Female, LeftWing, Rarely), THEN *Trust* IS Low.
3. IF (*Age, Education, Gender, Politics, ReligiousPractice*) IS (Old, Low, Female, RightWing, Frequently), THEN *Trust* IS High, etc.

Table 2 provides an excerpt of the respondents' socio-demographic characteristics (those who provided the questionable answers) and their output (trust in being xenophobic (values from 0 to 1)).

Respondent	Age	Education	Gender	Politics	Religion Practice	Degree of Belief
4	31	4	1	3	3	0.14
15	30	5	1	3	4	0.15
18	60	3	2	3	1	0.48
24	59	4	1	2	4	0.19
34	32	4	1	5	3	0.61
35	43	1	2	5	2	0.65
37	28	3	2	2	4	0.15
60	36	4	2	1	1	0.17
64	78	4	1	5	3	0.48
65	63	3	1	4	1	0.48

Table 2. An excerpt of the respondents' socio-demographic characteristics (*QA-3)* and their output (trust in being xenophobic)

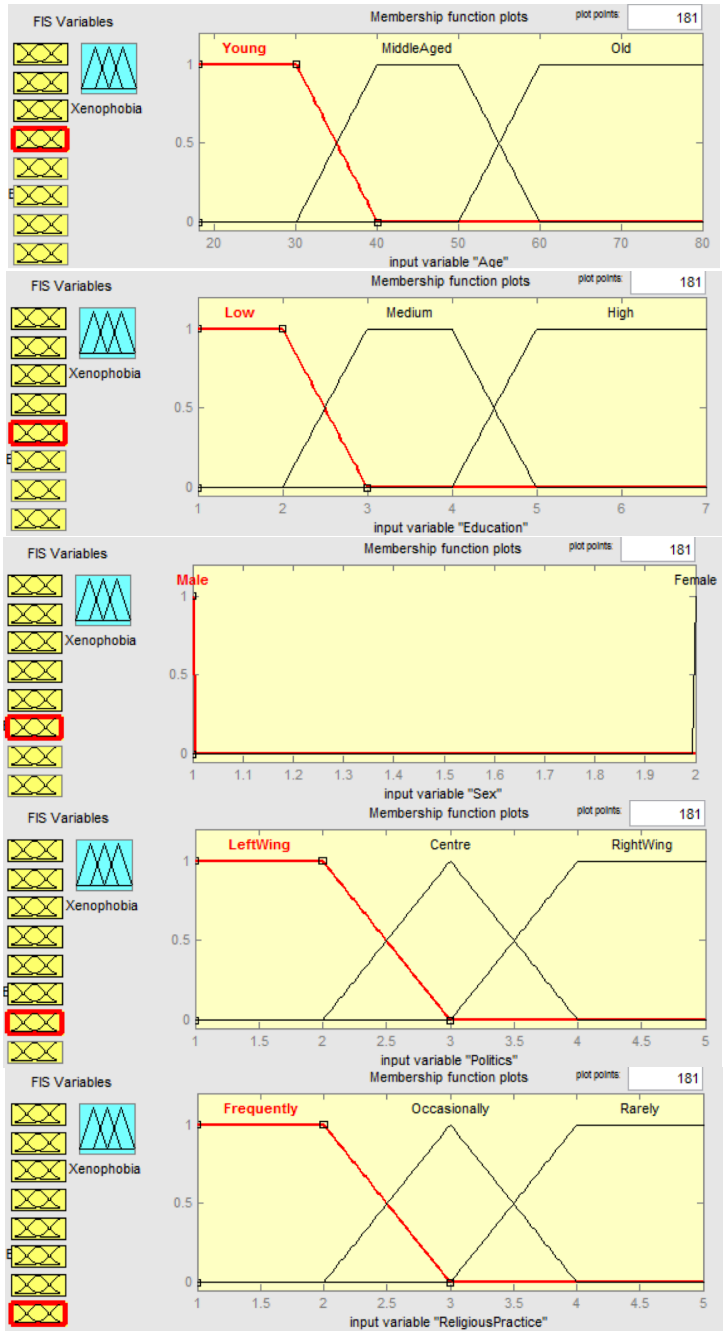

Fig. 5. Fuzzy Partitions of Age, Education, Sex, Politics, Religious Practice

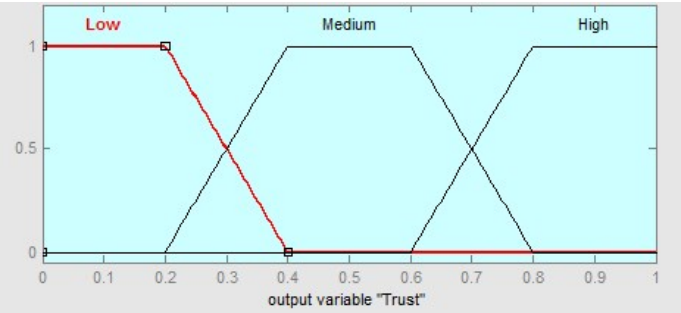

Fig. 6. The fuzzy partition of the variable *Trust*

We then proceed with the development of the second system that has two inputs (the respondent's score (RespondentScore) and the degree of belief (Trust)) and provides as an output the xenophobic level of the respondent (XenophobiaLevel). The inputs and the output of the system are presented in Figure 7.

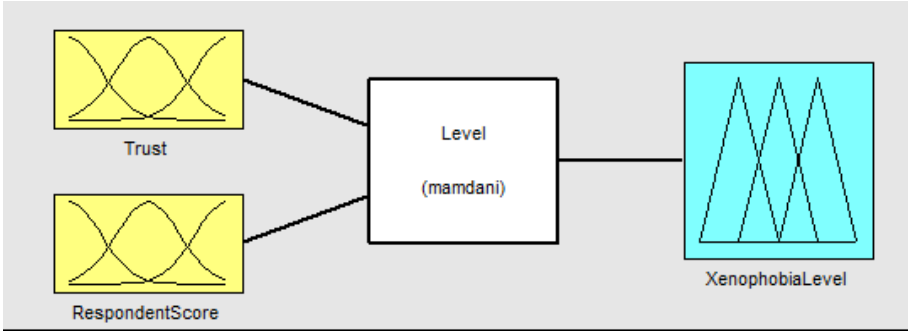

Fig. 7. Input and Output of the second system

A possible input for the first fuzzy system would be $input = [0.52\ 29]$. The fuzzy partition of Trust and RespondentScore can be seen in Figure 8.

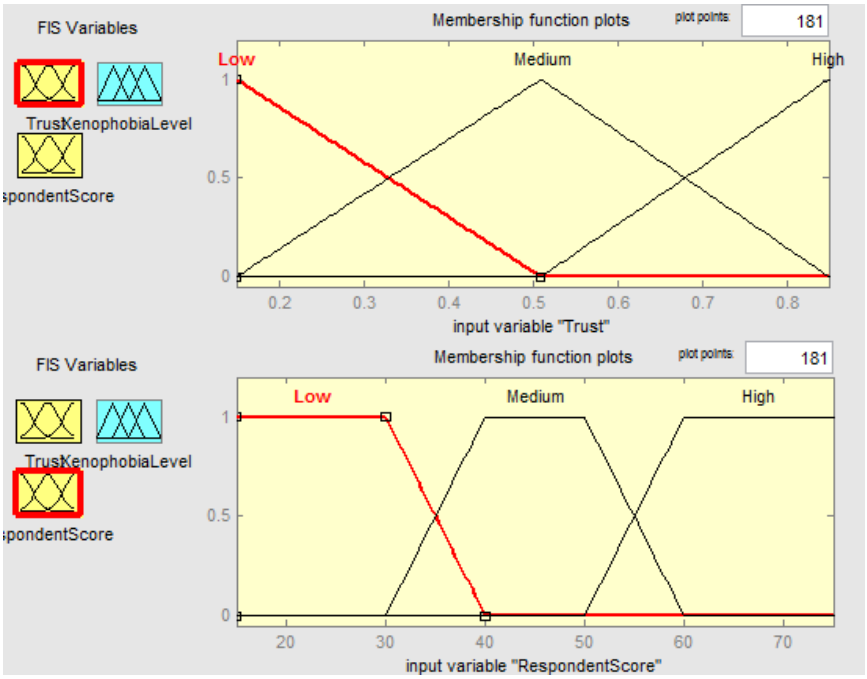

Fig. 8. Fuzzy partition of Trust and RespondentScore

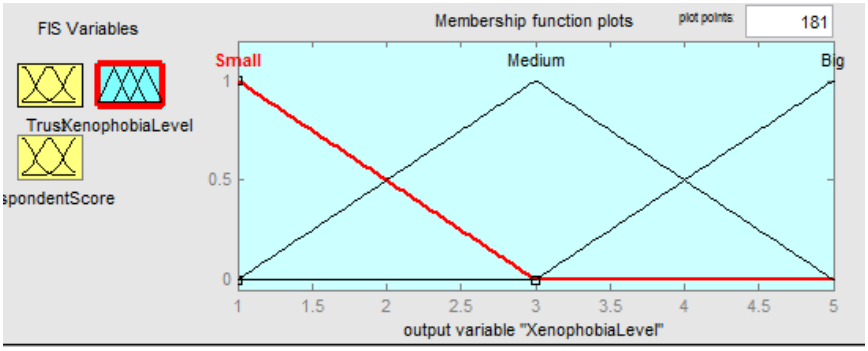

Fig. 9. Fuzzy partition of XenophobiaLevel

An excerpt of the fuzzy rule base for XenophobiaLevel, which consists of IF-THEN inference, is now provided:

1. IF (*Trust, RespondentScore*) IS (Low, Low), THEN *XenophobiaLevel* IS Low.
2. IF (*Trust, RespondentScore*) IS (Medium, Medium), THEN

XenophobiaLevel IS Medium.

3. IF (*Trust, RespondentScore*) IS (High, High), THEN *XenophobiaLevel* IS High, etc.

3 Validation

In order to validate the suggested method, the neuro-fuzzy scores were correlated with five single items that are considered in the literature as indicators of xenophobia (Eurobarometer 1989). The same procedure was used in order to validate the proposed method in Symeonaki et al.[12] where a fuzzy set theory solution to combining Likert items into a single overall scale (or subscales) was presented. A combination of four of these items was used as an indicator of xenophobia (Michalopoulou *et al.*[6]). These indicators measure xenophobia based on the perception of the number of 'others' (of another nationality or religion) and the disturbance caused by their presence. Table 3 provides the reader with the combined results (*QA-3* and *NQA-3)* for the first 67 respondents.

The indicators used are given in Table 4, whereas Table 5 exhibits the correlation analysis results between xenophobia neuro-fuzzy and crisp and all xenophobia indicators. As expected xenophobia crisp and neuro-fuzzy are highly correlated. As shown neuro-fuzzy scores are higher correlated with all xenophobia indicators, thus obviously producing a more accurate measurement of xenophobia (Table 6).

4 Conclusions

Central to attitude measurement in social survey research is Likert scaling theory. The present paper puts forward an intelligent system that simulates the respondent's final score when the answers are not questionable and takes into account a number of other crucial factors when the answers are questionable in order to classify the respondents into xenophobic levels reducing therefore the uncertainty. The proposed methodology is illustrated using raw data of a survey designed to measure xenophobia but it can be applied in Likert scaling in general. The presented methodology, moreover suggests that semantic information, usually available by the experts of the attitude domain, must also be taken into account, together with results of the statistical analysis produced by the current or previous studies and therefore can handle the uncertainty introduced to attitude measurement in social survey research. The findings show that the measurement of xenophobia levels produced is valid and more accurate since correlation analysis revealed that a) xenophobia scores (neuro-fuzzy and crisp) are highly correlated and more importantly, b) neuro-fuzzy scores are higher correlated with a number of xenophobia indicators.

Respondent	Level of Xenophobia C	Level of Xenophobia NF	Respondent	Level of Xenophobia C	Level of Xenophobia NF
1	3	2.73	32	3	3.07
2	3	3.27	33	1	1.07
3	3	3.41	34	5	4.35
4	2	1.78	35	4	4.35
5	2	2.23	36	3	3.14
6	3	3.52	37	1	1.65
7	4	3.77	38	3	3.27
8	4	3.91	40	2	2.24
9	4	3.45	41	2	1.83
10	3	3.28	44	1	1.30
11	3	3.01	45	3	3.03
12	2	2.28	46	1	1.16
13	3	2.55	47	3	2.88
15	2	1.65	49	2	2.43
16	2	2.35	51	2	2.48
18	5	4.12	52	4	3.90
19	3	2.71	54	3	3.33
20	3	3.34	55	2	2.43
21	2	2.16	56	1	1.07
22	2	2.30	57	2	2.40
24	2	1.65	60	2	1.65
25	1	1.28	61	1	1.28
26	3	2.95	62	2	2.23
27	3	3.15	63	3	3.23
28	3	3.36	64	4	4.12
29	3	2.65	65	4	4.12
30	5	4.94	66	2	2.25
31	2	2.48	67	4	3.88

Table 3. Levels of Xenophobia (classical (C) and Neuro-fuzzy approach (NF)) for the first 67 respondents

Indicator	Question
1	During the last years individuals from other countries which are not members of the European Union have come to live and work in Greece. According to your opinion, these foreigners who live today in Greece are too many, many but not too many, not too many.
2	How do you feel about the presence of individuals of another nationality? Disturbing or not disturbing?
3	How do you feel about the presence of individuals of another religion? Disturbing or not disturbing?
4	In your opinion these individuals of another nationality are too many, many but not too many or not too many.
5	In your opinion these individuals of another religion are too many, many but not too many or not too many
6	Combination of Indicators 2-5

Table 4. Indicators of xenophobia

	Xenophobia (NF)	Xenophobia (C)
Xenophobia (NF)		0,924
Xenophobia (C)	0,924	

**Note:* N=1,090, $p<0.001$.

Table 5. Pearson's Correlation Coefficients, Xenophobia (classical (C) and Neuro-fuzzy approach (NF))

Indicator	Xenophobia (NF)	Xenophobia (C)
1	-0,264	-0,246
2	-0,432	-0,422
3	-0,387	-0,360
4	-0,245	-0,217
5	-0,212	-0,192
6	0,451	0,428

**Note:* N=1,090, $p<0.001$.

Table 6. Spearman's rho Correlation Coefficients

References

1. A. Eagly and S. Chaiken, *The psychology of attitudes*, Harcourt Brace Jovanovich College Publishers, 1993.
2. M.A. Gil, M.A. and G.-R. Gil. Fuzzy vs. Likert scale in statistics. *Comb. Exp. Theory Stud. Fuzziness Soft Comput*ing, 271, 407–420, 2012.
3. M. Hogg and G. Vaughan. *Social Pchychology*, Prentice Hall, 2008.
4. M. Lalla, G. Facchinetti and G. Mastroleo. Ordinal scales and fuzzy set systems to measure agreement: An application to the evaluation of teaching activity, *Quality and Quantity*, 38, 577-601, 2005.
5. R. Likert, A technique for the measurement of attitudes. *Arch. Psychol.* 140, 1–55, 1932.
6. A. Michalopoulou, P. Tsartas, M. Giannisopoulou, P. Kafetzis and Eudokia Manologlou. *Macedonia and the Balkans: Xenophobia and Development, National Centre of Social Research*, Alexandria (Abridged English edition), Athens, Greece, 1999.
7. R. M. Perloff. *The Dynamics of Persuasion: Communication and Attitudes in the Twenty-First Century*, Routledge, 2016.
8. M. Symeonaki and A. Kazani. Developing a fuzzy Likert scale for measuring Xenophobia in Greece, ASMDA, Rome, Italy, 7-10 June, 2011.
9. M. Symeonaki and C. Michalopoulou. Measuring Xenophobia in Greece: A Cluster Analysis Approach, ASMDA, Rome, Italy, 7-10 June, 2011.
10. M. Symeonaki, A. Kazani and C. Michalopoulou. Fuzzifying Likert scales with factor analysis techniques, ERCIM, London, UK, 15-17 December, 2011.
11. M. Symeonaki and A. Kazani. Measuring xenophobia in Greece using neural network and fuzzy techniques, SMTDA, Chania, Greece, 5-8 June, 2012.
12. M. Symeonaki, C. Michalopoulou and A. Kazani, A fuzzy set theory solution to combining Likert items into a single overall scale (or subscales), *Quality and Quantity*, 49(2), 739-762, 2015.
13. L. Zadeh. Fuzzy sets, *Information and Control*, 8, **3**, 1965.

On the Measurement of Early Job Insecurity in Europe

Maria Symeonaki[1], Glykeria Stamatopoulou[2] and Maria Karamessini[3]

[1,2,3] Department of Social Policy, School of Political Sciences, Panteion University of Social and Political Sciences, Athens, Greece
(E-mail: msymeon@panteion.gr, gl.stamat@gmail.com, mkarames@panteion.gr)

Abstract. In the present paper[1] the estimation of different indicators that can be used in order to capture the extent and forms of early job insecurity is studied. This specific matter has been receiving increasing research and policy attention throughout the two last decades. The present study proposes a new composite index for measuring the degree of early job insecurity on the basis of the estimation of the transition probabilities between labour market states and school-to-work transitions, with raw data drawn from the European Union's Labour Force Survey (EU- LFS) for the year 2014. This indicator captures the whole spectrum of early job insecurity in a single measurement. Thus, an attempt is made to provide a new index of early job insecurity, connecting it also to school-to-work transition probabilities, that captures the extent of early job insecurity.
Keywords: Early job insecurity, labour market transition probabilities, EU-LFS.

1 Introduction

The measurement of early job insecurity and labour market exclusion is not a straightforward procedure, since 'ideal' indicators for early job insecurity don't actually exist. Different indicators though, such as the unemployment rate, the youth unemployment rate, the youth to adult unemployment ratio, or the NEET indicator can serve as useful tools, when comparing job insecurity in different countries. When one wants to compare early job insecurity (EJI) among different European countries or study the evolution of early job insecurity over

1 This paper has received funding from the European Union's Horizon 2020 research and innovation programme under grant agreement No 649395 (NEGOTIATE – Negotiating early job-insecurity and labour market exclusion in Europe, Horizon 2020, Societal Challenge 6, H2020-YOUNG-SOCIETY-2014, Research and Innovation Action (RIA), Duration: 01 March 2015 – 28 February 2018).

time, it is difficult, if not impossible, to take into account numerous indicators simultaneously. Thus, there is a strong need to provide one single indicator of early job insecurity that takes into account all possible indices connected to EJI for which we have reliable data to depend on. In the present paper we provide a composite index of EJI based on a number of indicators that we measure using raw data drawn from the EU-LFS, in order to estimate and compare early job insecurity among European countries.

When it comes to measuring early job insecurity and patterns of school-to-work transition, several methodological approaches have been proposed. In Karamessini *et al.*[10] and in Dingeldey *et al.*[7] an attempt was made to provide a definition of early job insecurity and to connect early job insecurity with school-to-work transitions. Symeonaki *et al.*[20, 22] studied the transition flows between labour market states for young individuals based on the EU-LFS and the EU-SILC data. In Eurofound[8] the labour market situation of young people in Europe is presented, focusing in particular on the school-to-work transition, in terms of the amount of time it takes to start the first job after education, while also monitoring the more general transition to adulthood, the age at which young people leave the parental home. In Brzinsky-Fay[4] sequences of school-to-work transitions are studied in ten European countries using the exploratory methods of optimal matching and cluster analysis. The process of labour market entry is observed for five years after leaving school by examining monthly labour market statuses. Christodoulakis and Mamatzakis[6] applied a Bayesian approach that employed a Monte Carlo integration procedure to expose the empirical posterior distribution of transition probabilities from full-time employment to part-time employment, temporary employment and unemployment and vice versa, in the EU 15. Additionally, Alvarez et al.[1] study the labour dynamics of the population by fitting a stationary Markov chain to the Argentine official labour survey. On the other hand, Betti et al.[2] describe some aspects of school-to-work transitions by analysing the employment situation of individuals as a function of the time elapsed since the completion of education and training, with a special focus on the patterns in Southern European countries. Ward-Warmedinger and Macchiarelli[24] present information on labour market mobility in 23 European countries, using the Eurostat's Labour Force Survey data over the period 1998-2008, whereas in Flek and Mysíková[9], the labour market flows, i.e. flows between employment, unemployment and inactivity, are analysed using Markov transition systems in order to draw conclusions on unemployment dynamics in Central Europe. Markov system analysis is also used in Symeonaki and Stamatopoulou[23] in order to analyse labour market dynamics in Greece and in Karamessini *et al.*[12] Markov systems are used to estimate the school-to-labour market entry probabilities for a number of European countries with raw data drawn from the EU-LFS datasets for 2013. Bosch and Maloney[3] discuss a set of statistics for examining and comparing labour market dynamics based on the estimation of continuous time Markov transition processes. They then use these to establish stylised facts about dynamic patterns of movement with the aid of panel data

from Argentina, Brazil and Mexico. Moreover, the socio-economic background and the degree to which it affects the transition process has also been studied in the literature, as individuals from poorer households have lower job prospects, while educational background may postpone their first entry in countries with strong family support system. Educational qualification and skills also have a strong effect on transitions from school-to-work, as low educated people hardly escape from spells of unemployment and inactivity, restricted mostly on temporary contracts (Quintini *et. al* [15]). Additionally, Scherer[17] shows that compared to Germany and Great Britain, in Italy the parental educational attainments has a negative effect on young people's speed of entry, as the more educated parents support their offspring in longer searches for better jobs. Gender plays an important role in young people's integration, since young women seem to face more problems relating to their transition than their male counterparts, with higher probabilities of being inactive or in non-standard employment for longer periods of time, while caring responsibilities also delay their entrance on labour market (Sigle-Rushton and Perrons[16]; Plantenga *et. al*[14]). The methods most commonly used to examine school-to-work transitions as a sequence and not as a single event are the optimal matching method and the cluster analysis (McVicar and Anyadike-Danes[13]; Scherer[18]; Schoon[19]). Brzinsky-Fay[5] presents the main advantages and disadvantages of sequence analysis in comparison to event history analysis.

Here, in order to capture the whole spectrum of early job and employment insecurity we use indicators, referring to different aspects of EJI: indicators that refer to labour market outcomes and to quality of job, indicators for employment insecurity and for transition from school-to-work. These indicators, estimated for the 15-24 age group, should be considered as complementary rather than competing and are combined into a single composite indicator of EJI. The results reveal that countries differ when early job insecurity is considered and the values of the proposed index vary between -0.84 for Switzerland (lowest early job insecurity) to 1.01 for Greece (highest early job insecurity).

The paper is onganised in the following way. Section 2 provides the estimations of the early job insecurity indicators for the European countries based on the EU-LFS data of 2014. Section 3 presents the new composite index of EJS and provides the results for these countries, sorting them from countries of low EJI to countries with high EJI. Section 4 provides the reader with the conclusions of the study and aspects of future work.

2 Indicators of early job insecurity

As earlier mentioned, to capture the entire range of early job and employment insecurity we use indicators, referring to distinctive traits of EJI: indicators that refer to labour market outcomes and to quality of job, indicators for employment insecurity and for transition from school-to-work. These indicators are estimated for the 15-24 age group, from raw data drawn from the EU-LFS survey. Table 1

provides the indicators that are measured and their description, thus offering information of how these were actually measured.

Typical indicators used for the measurement of early job insecurity provided in the present analysis are the Youth Participation Rate (Ind1), the Youth Employment Rate (Ind2), the Youth Unemployment Rate (Ind3), the Youth Unemployment Ratio (Ind4), the incidence of long-term unemployment (Ind5) and the NEET (not in Employment, Education or Training) indicator (Ind6).

Indicators, directly linked to the quality of jobs, are the incidence of temporary and part-time employment (Ind7 and Ind8), the incidence of underemployed part-time workers (Ind9) and working intensity measured as the distribution of employees according to usual weekly hours worked (hour bands) (Ind10).

Another important aspect is connected to the transition of young individuals from school (education or training) to work. It is well accepted that young people's pathways from school to sustained work have become more and more rough and irregular and the probability of someone who has completed full-time education to move effectively into full-time occupation decreases, whereas the probability of engaging into part-time or temporary employment increases. Therefore, it is important to highlight useful indicators that fall into the category of measuring school-to-work transitions. In this respect, we estimate the probability of an individual that has concluded education or training to enter each one of the three labour market states: employment (Ind11), unemployment (Ind12) and inactivity (Ind13). This part of analysis will be handled with the aid of Markov system theory.
Two other useful indicators for measuring employment insecurity are the job finding rate and the job separation rate. In the present paper, as is the case with empirical studies (Hobijn and Sahin[10]), we will use the percent of unemployed individuals at time t-1, who are employed at time t as the job finding rate (Ind14) and the percent of employed individuals in time t-1, who are not employed at time t as the separation rate (Ind15).

Moreover, two indicators regarding relative changes in unemployment rates are: the Youth to Adult Unemployment Ratio (Ind16) and the Relative Unemployment Rate of those individuals with low skills to those individuals with high skills (Ind17), as it provides evidence of how education and training influences unemployment.

Table 2 provides the reader with the estimations of all indicators that relate to labour market outcomes (Ind1 – Ind6), for all European countries, for 2014. In an analogous way, Table 3 and 4 present the values of the indicators regarding the job quality for the same year and countries (Ind7 – Ind10). The probabilities that can be used as indicators for school-to-work transition are given in Table 5 (Ind11 – Ind13**)**, followed by Table 6, which reveals the indicators for employment (in)security (Ind14 – Ind15)**.** Finally, Table 7 provides indicators concerning the relative changes in unemployment rates (Ind16 – Ind17).

Table 1 Early job insecurity indicators, Ages: 15 – 24, EU-LFS, 2014

INDICATORS		DESCRIPTION
Ind1	Youth Participation Rate	Number of individuals in the labour force, aged 15 - 24 / Total number of individuals, aged 15 - 24
Ind2	Youth Employment Rate	Number of employed individuals, aged 15-24 / Total Population, aged 15 - 24
Ind3	Youth Unemployment Rate	Number of unemployed individuals, aged 15 - 24 / Number of individuals in the labour force, aged 15 - 24
Ind4	Youth Unemployment Ratio	Number of unemployed individuals, aged 15-24 / Total population, aged 15-24
Ind5	Incidence of long-term unemployment	Young unemployed (12 months or more) as % of all young unemployed
Ind6	NEET rate	The population not in employment, education or training as a percentage of total population 15-24
Ind7	Incidence of temporary employment	As % of all employees
Ind8	Incidence of part-time employment	As % of all employed
Ind9	Underemployed part-time workers	As % of total part-time workers
Ind10	Working time	Distribution of employees according to usual weekly hours worked (hour bands)
Ind11	Probability of entry to employment from education and training	Markov system
Ind12	Probability of entry to unemployment from education and training	Markov systems
Ind13	Probability of entry to inactivity from education and training	Markov systems
Ind14	Job finding rate	Percent of unemployed at time t-1, who are employed at time t
Ind15	Job separation rate	Percent of employed in time t-1, who are not employed at time t
Ind16	Youth to Total Unemployment Ratio	Youth unemployment rate (age: 15-24) / Total unemployment rate (age>15)
Ind17	Relative UR low skills/high skills	UR of those ISCED < 3 (HATLEV = 1 / UR of those ISCED ³ 3 (HATLEV = 2 or 3)

Table 2 Basic labour market indicators, 2014

Country	Ind1	Ind2	Ind3	Ind4	Ind5	Ind6
Austria	67.1	61.1	8.9	5.9	16.4	10.8
Belgium	49.6	41.5	16.4	8.1	40.1	14.9
Bulgaria	45.6	37.4	18.0	8.2	57.1	24.6
Croatia	51.4	34.8	32.3	16.6	51.6	22.3
Cyprus	57.5	42.5	26.2	15.1	37.2	19.7
Czech Republic	51.3	45.8	10.6	5.4	28.0	12.2
Denmark	67.4	59.7	11.4	7.7	11.8	10.3
Estonia	56.6	50.0	11.5	6.5	35.7	14.3
Finland	61.0	51.4	15.7	9.6	7.6	12.5
France	53.5	43.3	19.1	10.2	31.0	17.2
Germany	61.8	57.6	6.8	4.2	26.9	8.9
Greece	49.3	27.1	45.0	22.1	65.3	27.3
Hungary	47.3	40.8	13.9	6.6	35.9	17.2
Ireland	53.2	43.0	19.1	10.1	46.0	18.4
Italy	41.5	28.3	31.6	13.1	59.5	27.3
Latvia	58.7	50.3	14.4	8.4	27.7	15.8
Lithuania	51.8	44.2	14.7	7.6	28.2	13.2
Luxemburg	49.5	43.0	13.0	6.4	-	6.9
Netherlands	74.0	66.0	10.8	8.0	19.6	8.9
Norway	63.7	59.3	6.8	4.3	15.8	8.6
Poland	53.2	44.4	16.5	8.8	35.1	15.8
Portugal	52.3	39.0	25.4	13.3	41.8	16.6
Romania	48.6	41.0	15.6	7.6	38.7	20.0
Slovakia	50.1	39.4	21.3	10.7	60.0	18.3
Slovenia	52.9	42.9	18.9	10.0	-	14.0
Spain	54.6	33.0	39.6	21.7	40.3	22.7
Sweden	65.9	55.0	16.7	11.0	8.4	10.4
Switzerland	75.8	70.1	7.6	5.7	21.9	8.8
UK	66.7	58.4	12.5	8.4	27.5	14.3

Notes: Not reliable results for IS. Small samples for LU, MT, SI.
Sources: EU-LFS, 2014

Table 3 Basic labour market indicators, 2014

Country	Ind7	Ind8	Ind9
Austria	23.7	23.8	29.6
Belgium	22.1	20.2	39.4
Bulgaria	9.3	3.4	-
Croatia	40.1	7.1	62.9
Cyprus	27.1	18.3	75.7
Czech Republic	20.3	7.2	15.5
Denmark	19.3	51.4	17.1
Estonia	7.2	13.0	11.2
Finland	34.9	29.7	28.7
France	39.6	19.0	56.3
Germany	38.4	21.8	21.6
Greece	23.3	16.6	83.4
Hungary	17.9	5.6	46.0
Ireland	21.1	30.7	34.9
Italy	40.6	25.7	23.0
Latvia	5.1	7.1	-
Lithuania	4.9	9.6	27.4
Netherlands	47.3	64.2	25.2
Norway	22.8	42.3	25.4
Poland	53.6	9.7	49.7
Portugal	49.1	14.7	65.0
Romania	3.8	10.5	57.3
Slovakia	17.6	6.3	-
Slovenia	49.7	22.7	-
Spain	54.2	28.3	67.0
Sweden	42.1	36.8	35.7
Switzerland	36.3	27.0	34.7
UK	10.6	27.5	34.5

Sources: EU-LFS, 2014

Table 4 Working time indicators, 2014

Country	Working time				
	1-19	**20-29**	**30-34**	**35-39**	**40+**
Austria	10.7	7.3	4.6	30.8	46.6
Belgium	7.2	10.2	6.7	49.7	26.1
Bulgaria	0.2	2.5	0.7	0.2	96.4
Croatia	0.9	3.0	1.2	0.5	94.5
Cyprus	3.6	7.5	5.1	20.1	63.6
Czech Republic	2.0	4.0	1.7	15.1	77.2
Denmark	41.4	6.9	6.1	41.5	4.0
Estonia	3.5	5.8	2.8	2.3	85.6
Finland	17.1	8.7	7.1	38.0	29.1
France	5.4	8.9	4.2	59.8	21.7
Germany	13.4	5.1	3.6	24.1	53.9
Greece	5.9	11.4	5.5	1.7	75.5
Hungary	0.7	3.4	1.7	0.5	93.8
Ireland	13.3	14.8	5.3	33.0	33.6
Italy	6.7	15.4	6.2	10.1	61.4
Latvia	0.9	4.1	2.1	0.7	92.2
Lithuania	1.3	7.7	1.4	2.2	87.5
Netherlands	41.5	12.7	10.8	13.3	21.7
Norway	28.0	8.0	6.1	51.3	6.6
Poland	2.0	4.9	2.2	1.6	89.3
Portugal	4.5	6.8	2.4	5.6	80.8
Romania	-	0.6	0.3	0.2	98.9
Slovakia	2.1	4.5	0.7	11.4	81.3
Slovenia	6.5	8.5	3.1	1.1	80.7
Spain	11.8	15.0	6.4	9.7	57.1
Sweden	16.1	9.8	10.0	12.7	51.4
Switzerland	12.1	6.3	5.3	4.1	72.2
UK	15.4	9.7	5.4	26.4	43.1

Notes: Not reliable results for IS, LU, MT. Small samples for CY, EE, LV.
Sources: EU-LFS, 2014

Table 5 Indicators for transition from school to work, 2014

Country	School-to-Work Transition	School-to-Unemployment	School-to-Inactivity
AT	0.684	0.157	0.159
BE	0.566	0.257	0.177
BG	0.369	0.358	0.273
CH	0.784	0.079	0.137
CZ	0.657	0.324	0.019
DK	0.663	0.228	0.109
EE	0.600	0.185	0.215
EL	0.194	0.513	0.293
ES	0.224	0.377	0.399
FI	0.582	0.239	0.179
FR	0.583	0.310	0.107
HR	0.297	0.695	0.008
HU	0.500	0.343	0.157
IT	0.274	0.637	0.089
LT	0.643	0.217	0.140
LV	0.608	0.248	0.144
PL	0.535	0.340	0.125
PT	0.443	0.500	0.057
RO	0.358	0.528	0.114
SE	0.619	0.306	0.075

For the countries for which MAINSTAT and WSTAT1Y (or both) are EMPTY the respective transition probabilities cannot be estimated

Sources: Own Calculations, EU-LFS, 2014

Table 6 Indicators for employment (in)security

Country	Job Finding Rate	Job Separation Rate[2]
Austria	44.45	12.5
Belgium	32.05	9.35
Bulgaria	18.20	7.75
Croatia	25.35	12.85
Cyprus	41.80	12.3
Czech Republic	59.65	4.65
Denmark	48.10	13.40
Estonia	46.70	12.15
Finland	32.00	19.50
France	33.6	15.50
Germany	-	-
Greece	14.75	13.50
Hungary	44.10	9.05
Italy	19.60	11.85
Latvia	51.90	14.90
Lithuania	47.35	7.80
Malta	43.75	14.25
Poland	32.65	9.15
Portugal	34.85	15.60
Romania	13.80	6.05
Slovakia	32.80	9.25
Slovenia	27.85	29.00
Spain	27.05	14.10
Sweden	42.80	19.10
Switzerland	53.55	14.6

For the countries for which MAINSTAT and WSTAT1Y (or both) are EMPTY the respective rates cannot be estimated.
Sources: EU-LFS, 2014

[2] In this report, we omit inactivity-unemployment flows and focus only on employment-unemployment flows. See Shimer (2007) and Barnichon (2009) for evidence supporting this choice.

Figure 1 displays the values of Job Finding Rates and Job Separation Rates for the European countries.

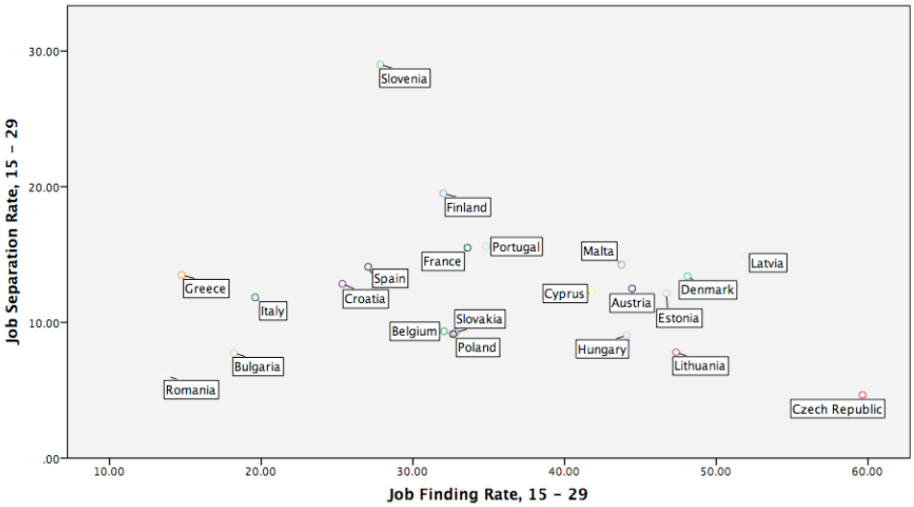

Fig. 1. Job finding rates and job separation rates across European countries,

15 – 29, EU-LFS, 2014

Table 7 Relative changes in unemployment rates

Country	Youth to Total UR	Relative UR, low skills/high skills
Austria	1.58	2.12
Belgium	1.92	2.49
Bulgaria	1.58	2.46
Croatia	1.87	2.01
Cyprus	1.63	1.25
Czech Republic	1.73	3.61
Denmark	1.73	1.55
Estonia	1.57	1.87
Finland	1.82	2.34
France	1.85	2.11
Germany	1.38	2.68
Greece	1.70	1.03
Hungary	1.80	2.59
Ireland	1.69	2.41
Italy	2.49	1.29
Latvia	1.32	2.26
Lithuania	1.37	2.74
Luxemburg	2.15	-
Netherlands	1.45	2.12
Norway	1.95	2.46
Poland	1.84	1.89
Portugal	1.82	1.27
Romania	2.29	1.00
Slovakia	1.61	2.78
Slovenia	1.95	1.47
Spain	1.62	1.54
Sweden	2.09	3.06
Switzerland	1.66	1.41
UK	2.04	2.43

Notes: Not reliable results for LU and CY
Sources: EU-LFS, 2014

3 A composite index of early job insecurity

In the present section we define the composite index of early job insecurity and estimate its values for all European countries for which we have the necessary data (variables).

The composite index is defined as:

$$EJI = \frac{\sum_{i=1}^{d} w_{d_i} \times \frac{\sum_{j=1}^{d_i} w_{ij} \times zInd_{ij}}{\sum_{j=1}^{d_i} w_{ij}}}{\sum_{i=1}^{d} w_{d_i}}, \quad (1)$$

where:

d : the number of dimensions (here d=5)

d_i : the number of indicators in the i-th dimension

w_{ij} : the weight of the j-th indicator in the i-th dimension

w_{d_i} : the weight of the i-th dimension

$zInd_{ij}$: the z-score of the j-th indicator in the i-th dimension.

Using Equation (1) we estimate the values of EJI for the European countries.

The values are presented in Table 8.

Table 8 Early Job Insecurity Indicator, EU-LFS, 2014

	Country	**Early Job Insecurity Index**
1.	Switzerland	-0.84
2.	Denmark	-0.79
3.	Austria	-0.68
4.	Estonia	-0.45
5.	Lithuania	-0.38
6.	Finland	-0.29
7.	Czech Republic	-0.41
8.	Sweden	-0.24
9.	Belgium	-0.14
10.	France	-0.07
11.	Hungary	-0.01
12.	Poland	0.01
13.	Romania	0.16
14.	Portugal	0.25
15.	Croatia	0.60
16.	Italy	0.61
17.	Spain	0.84
18.	Greece	1.01

4 Conclusions

In the present paper we provided a composite index of EJI based on a number of indicators that we measured using raw data drawn from the EU-LFS, in order to estimate and compare early job insecurity among European countries. It is obvious that early job insecurity differs among European countries. Countries with low EJI can be identified (Switzerland, Denmark, Austria for example), whereas countries of high EJI are also recognisable. Croatia, Italy, Spain and Greece are the countries facing worrying EJI. Figure 2 provides the map of early job insecurity for 2014.

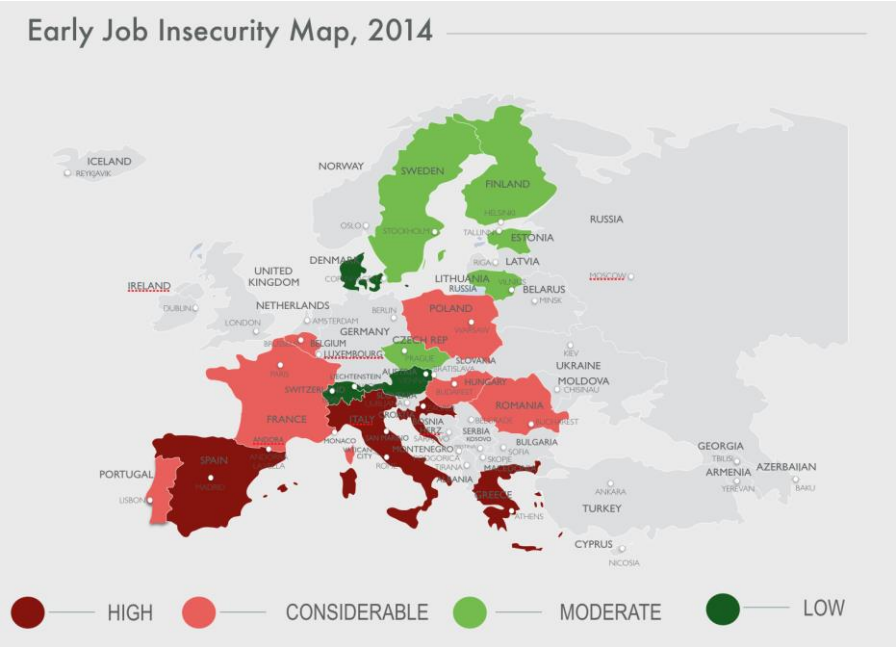

Fig.2. Mapping Early Job Insecurity

Early job insecurity can have multiple consequences: Systematic labour market exclusion of young people at the very beginning of their professional careers, the growing discourses over the 'threat of a lost generation', accompanied by a multi-faceted social malaise that includes among others high risks of poverty, precarity, social exclusion, disaffection, insecurity, scarring, higher propensity towards offence and crime, as well as (mental and physical) health problems, to name but a few. Therefore, it is very important to activate effective policies that can prevent the unfavourable effects of early job insecurity and youth unemployment. In this paper we have provided evidence based on empirical data that early job insecurity exists, it can be measured and it must be tackled since it exhibits worrying trends for a lot of European countries. Further research will be perused with the EU-LFS data for 2015.

References

1. E. Alvarez, F. Ciocchini and K. Konwar. A Locally Stationary Markov Chain Model for Labour Dynamics. *Journal of Data Science*, 7, 27-42, 2008.
2. G. Betti, A. Lemmi and V. Verma. A comparative analysis of school-to-work transitions in the European Union. *Innovation: The European Journal of Social Science Research*, 18 ,4, 419-442, 2007.
3. M. Bosch and W. Maloney. Comparative Analysis of Labor Market Dynamics Using Markov Processes: An Application to Informality. *Discussion Paper Series*, IZA DP, 3038, 2007.

4. C. Brzinsky-Fay. Lost in Transition? Labour Market Entry Sequences of School Leavers in Europe. *European Sociological Review* , 23, 4, 409-422, 2007
5. C. Brzinsky-Fay. The measurement of school-to-work transitions as processes. About Events and Sequences. *European Societies*, 16, 2, 213-232, 2014.
6. G. Christodoulakis and C. Mamatzakis. Labour Market Dynamics in EU: a Bayesian Markov Chain Approach. *Discussion paper series*, Department of Economics, University of Macedonia, no. 2009-07, 2009
7. I. Dingeldey, B. Hvinden, C. Hyggen, J. O'Reilly and M. A. Schøyen. *Understanding the consequences of early job insecurity and labour market exclusion: The interaction of structural conditions, institutions, active agency and capability*, Negotiate working paper, 2015 https://blogg.hioa.no/negotiate/files/2015/04/NEGOTIATE-working-paper-no-D2.1.pdf.
8. Eurofound. *Mapping youth transitions in Europe*, Publications Office of the European Union, Luxembourg, 2014.
9. V. Flek and M. Mysíková. Unemployment Dynamics in Central Europe: A labour flow approach. *Prague Economic Papers , 24*, 1, 73-87, 2015.
10. B. Hobijn and A. Sahin. Job-Finding and Separation Rates in the OECD. *Federal Reserve Bank of New York*, Staff Report, 298, 2007.
11. M. Karamessini, A. Papazachariou, D. Parsanoglou and G. Stamatopoulou. *Indicators and data sources to measure patterns of labour market entry across countries*, Negotiate working papers, 2015, https://blogg.hioa.no/negotiate/files/2015/04/NEGOTIAE-working-paper-no-D3.1.pdf
12. M. Karamessini, M. Symeonaki, G. Stamatopoulou and A. Papazachariou. *The careers of young people in Europe during the economic crisis: Identifying risk factors*. Negotiate working papers, 2016, https://blogg.hioa.no/negotiate/files/2015/04/NEGOTIATE-working-paper-no-D3.2-The-careers-of-young-people-in-Eurpa-during-the-economic-crisis.pdf
13. D. McVicar and M. Anyadike- Danes. Predicting successful and unsuccessful transitions from school to work by using sequence methods. *Journal of the Royal Statistical Society: Series A (Statistics in Society) , 165*, 2, 317-334, 2002.
14. J. Plantenga, C. Remery and M. S. Lodovici. *Starting Fragile: Gender differences in the youth labour market*, European Commission, Luxembourg, 2013
15. G. Quintini, J. Martin and S. Martin. The Changing Nature of the School-to-Work Transition Process in OECD Countries. *IZA Discusion Paper* , 2582, 2007.
16. W. Sigle-Rushton and D. Perrons. Employment transitions over the life cycle: a statistical analysis. *LSE Working Paper Series*, 46, 2013.
17. S. Scherer. Patterns of Labour Market Entry – Long Wait or Career Instability? An Empirical Comparison of Italy, Great Britain and West Germany. *European Sociological Review* , 21, 5, 427-440, 2005.
18. S. Scherer. Early Career Patterns: A comparison of Great Britain and West Germany. *European Sociological Review* , 17, 2, 119-144, 2001.
19. I. M. Schoon. Transitions from school to work in a changing social context. *YOUNG-UPPSALA-*, 9, 4-22, 2001.
20. M. Symeonaki, M. Karamessini and G. Stamatopoulou. Measuring School-to-Work Transition Probabilities in Europe with Evidence from the EU-SILC. *5th Demographics Workshop*, Valletta, Malta, 1-4 June, 2016. Eds Christos Skiadas, Sergei Silvestrov and Teresa Oliveira (Springer).

21. M. Symeonaki. Rate of convergence in fuzzy non-homogeneous Markov systems. *SMTDA*, Valletta, Malta, 1-4 June 2016.
22. M. Symeonaki, M. Karamessini and G. Stamatopoulou, Gender-based differences on the impact of the economic crisis on labour market flows in Southern Europe. *SMTDA*, Valletta, Malta, 1-4 June 2016.
23. M. Symeonaki and G. Stamatopoulou. A Markov system analysis application on labour market dynamics: The case of Greece. *IWPLMS.* Athens, 2015.
24. M. Ward-Warmedinge, E. Melanie and C. Macchiarelli. Transitions in labour market status in the European Union. *LEQS Paper* 69, 2013.

Frost Prediction in Apple Orchards Based Upon Time Series Models

Monika A. Tomkowicz[1] and Armin O. Schmitt[2]

[1] Faculty of Science and Technology, Free University of Bozen/Bolzano, Piazza Università, 1, 39100 Bolzano BZ, Italy
(E-mail: MonikaAgnieszka.Tomkowicz@natec.unibz.it)
[2] Breeding Informatics, Faculty of Agricultural Sciences, Georgia-Augusta-University of Göttingen, Margarethe von Wrangell-Weg 7, 37075 Göttingen, Germany
(E-mail: armin.schmitt@uni-goettingen.de)

Abstract. The scope of this work was to evaluate the autoregressive integrated moving average (ARIMA) model as a frost forecast model for South Tyrol in Italy using weather data of the past 20 years which were recorded by 150 weather stations located in this region. Accurate frost forecasting should provide growers with the opportunity to prepare for frost events in order to avoid frost damage. The radiation frost in South Tyrol occurs during the so-called frost period, i.e. in the months of March, April and May during calm nights between sunset and sunrise. In case of a frost event, the farmers should immediately switch on water sprinklers. The ice cover, which is built on the trees, protects the buds and blossoms from damage. Based on the analysis of time series data, the linear regression and ARIMA models were compared and evaluated. The best result was achieved by the ARIMA model, with the optimal value of 1.0 for recall in case of forecast of 95% confidence intervals. This means that all frost cases could be correctly predicted. Despite the encouraging results for recall, the rate of false positives with a sensivity of 21% is too high, such that further investigations are desirable (e.g., testing VARIMA models, which are a multivariate extension of ARIMA models). The graphical illustration of the 95% confidence intervals of the ARIMA model forecast and the linear models forecast should be helpful in frost prediction and could be integrated in the electronic monitoring system that permits forecasting of frost weather phenomena.
Keywords: Frost Forecast, ARIMA Models, Time Series Prediction Models

1 Introduction

Accurate frost forecasting should provide growers in South Tyrol with the opportunity to prepare for frost events in order to avoid frost damage. The higher the level of forecast accuracy, the lower the risk of frost damage. Damage to apple orchards brought by freezing night temperatures can cause high crop yield losses to the growers. The critical period for frost damage in apple orchards are the months of spring March, April and May. The radiation frost occurs during clear nights with little or no wind after sunset and lasts until after sunrise.

Over-plant conventional sprinklers are widely used in South Tyrol as effective frost protection method for apple orchards. The ice cover prevents the temperature of the protected plant from falling below the freezing point. Sprinkling must start with the onset of the critical temperature and be maintained until the temperature rises above 0° C. This work describes frost prediction in apple orchards based upon a non-seasonal ARIMA model and three different Linear Regression models.
The general autoregressive moving average (ARMA) model was described first in 1951 by Peter Whittle in his thesis "Hypothesis testing in time series analysis". The ARIMA model is a generalization of the ARMA model. Nowadays it is widely used in time series analysis. However, there exists only little literature about frost forecasting with ARIMA.

In Castellanos *et al.* [9] the authors apply the ARIMA model to forecast the minimum monthly absolute temperature and the average monthly minimum temperature following the Box and Jenkins methodology.

Another interesting research project about frost forecasting of minimum temperature in the Alpine area is described by Eccel *et al.*[8]. In this work a simple linear model (LR), a random forest (RF) model and a neural network (NN) model were compared and evaluated. The results achieved by RF were

slightly superior to those of other methods. The linear regression model for frost forecasting was introduced and implemented by Snyder *et al.*[2].

2 Weather database

The weather database holds data from about 150 weather stations, which have been operating since the year 1993. The weather stations are distributed in apple orchards at an elevation between 200-1100 m.a.s.l.

Currently, the database continues to receive data every 5 minutes via radio waves or GPRS. The measurements include atmospheric conditions, air and soil temperature, relative air humidity, soil humidity at a depth of 10, 30 and 50 cm, wind speed and direction, precipitation amounts, and the relative humidity at leaf surfaces. Moreover, the database contains information of the geographic coordinates of each station (latitude, longitude and altitude).

The historical climate patterns of the past 20 years stored in the weather database can serve as indicator of the climate for future time points. Based on the measurements of the past years we calculated the forecast of frost weather phenomena and compared the prediction against the observed temperature in order to evaluate the results.

Measurement	Unit
wet bulb temp (60 cm)	◦C
dry bulb temp (60 cm)	◦C
rel. air humidity	%
air temp (2 m)	◦C
wind speed	m/sec
wind direction	N/S/E/W
leaf surface humidity	%
precipitation	mm
irrigation	ON/OFF
irrigation	mm
soil temp (-25 cm)	◦C
min interval air temp (2 m)	◦C
max interval air temp (2 m)	◦C
min interval rel. air humidity	%
max interval rel. air humidity	%
max interval wind speed	m/sec
soil humidity (-10 cm)	%
soil humidity (-30 cm)	%
soil humidity (-50 cm)	%

Tab. 1. Variables that were recorded by the weather stations.

3 ARIMA forecast model

The autoregressive integrated moving average (ARIMA) models are a widely used approach to time series forecasting based on autocorrelations in the data.

3.1. Stationarity and differencing

ARIMA models as described by Hyndman and Athanasopoulos[7] require that the time series to which they are applied be stationary. A stationary time series is one whose properties like the mean, variance and autocorrelation do not depend on the time point at which the series is observed. A stationary time series has no predictable pattern in the long-term. The time plots show a horizontal pattern with constant variance. A non-stationary time series can be transformed into a stationary one by computing the differences between consecutive observations. This transformation is known as differencing. The first-order differenced series can be written as:

$$y'_t = y_t - y_{t-1} \tag{1.1}$$

If the result of the first-order differencing is still a non-stationary time series, second-order differencing can be applied to obtain a stationary time series (Hyndman and Athanasopoulos[7]):

$$y''_t = y'_t - y'_{t-1} \tag{1.2}$$

One approach to identify non-stationarity is an ACF (autocorrelation function) plot. The ACF plot shows the autocorrelations, which measure the relationship between y_t and y_{t-k} for k (k = 1, 2, 3….) lags. In case of non-stationarity the ACF will slowly decrease.

Further widely used tests are the Kwiatkowski-Phillips-Schmidt-Shin (KPSS) test and the Augmented Dickey-Fuller test (ADF).

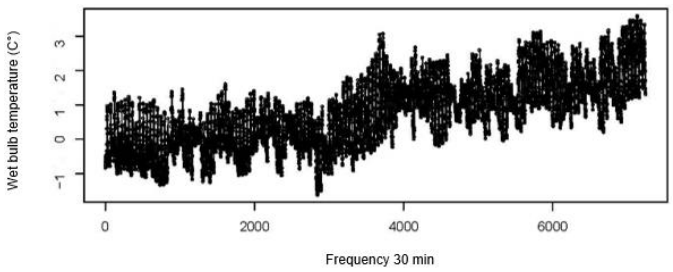

Fig. 1. Non-stationary time series

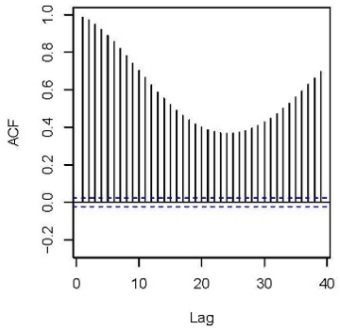

Fig. 2. ACF before differencing

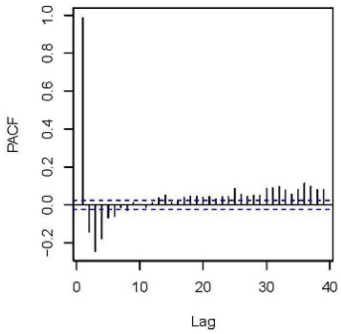

Fig. 3. PACF before differencing

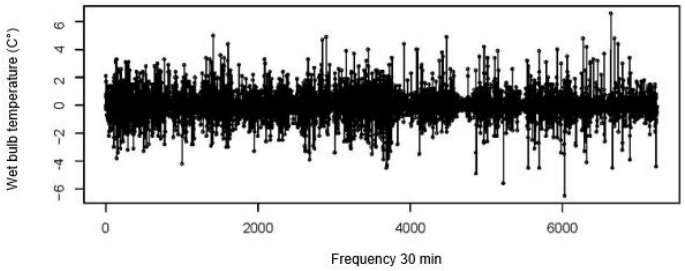

Fig. 4. Differenced time series

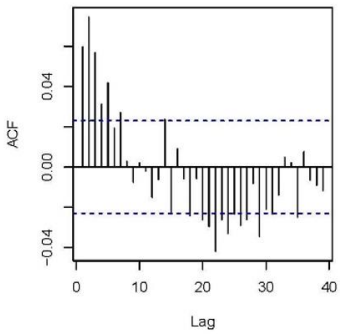

Fig. 5. ACF after differencing

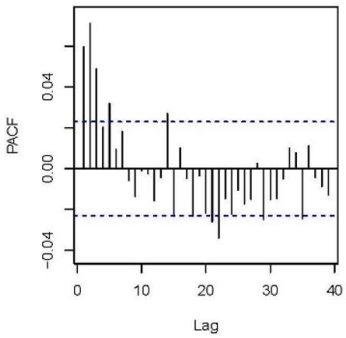

Fig. 6. PACF after differencing

3.2. Non-seasonal ARIMA models

The non-seasonal ARIMA model described by Hyndman and Athanasopoulos[7] is a combination of an AR(p) model, differencing and an MA(q) model and can be written as:

$$y'_t = c + \phi_1 y'_{t-1} + \cdots + \phi_p y'_{t-p} + \cdots + \theta_1 e_{t-1} + \theta_q e_{t-q} + e_t \tag{1.3}$$

where:

y'_t is the differenced series,
e_t is white noise,
c is a constant,
p and q are the order of the AR and the MA model, respectively.

A non-seasonal ARIMA model is written in the form:

$$ARIMA(p, d, q) \tag{1.4}$$

where:
p means order of the autoregressive part $\mathrm{AR}(p)$;
d means degree of first differencing involved;
q stands for order of the moving avarage part $\mathrm{MA}(q)$.

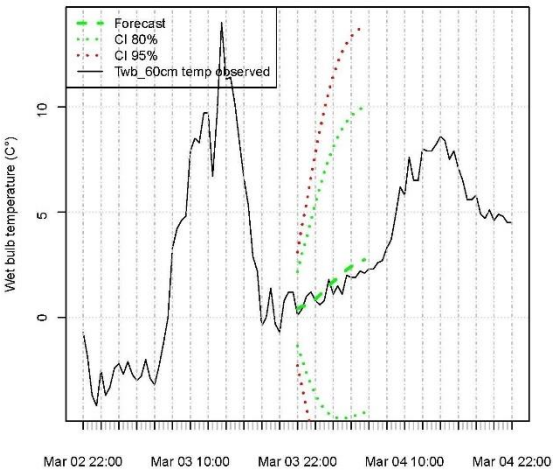

Fig. 7. ARIMA(4,1,4) forecast from 22:00 until sunrise. The observed temperature is shown as full line.

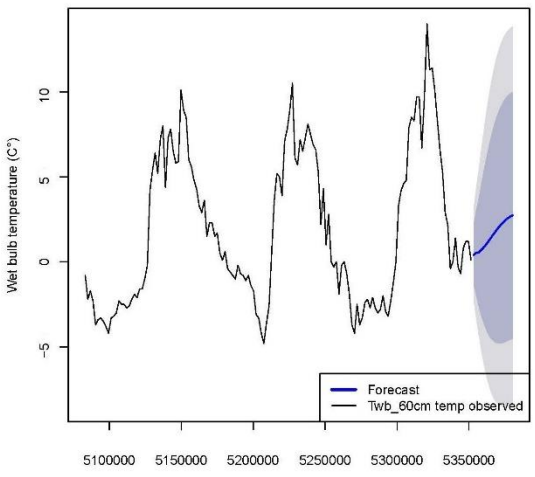

Fig. 8. ARIMA(4,1,4) forecast shown with the temperature of the previous three days.

In Figure 7, a forecast plot for ARIMA(4,1,4) built on the wet bulb temperature time series is shown for the 4th of March 2006 for the station 14 in Terlano as a green dashed line together with the observed data and the confidence intervals. In this example the point forecast suits well the real data. Figure 8 shows the forecast plot (blue line) with blue shadowed confidence intervals together with the observed time series data of the previous three days.

4 Model building

As preliminary step for the analysis we tested ARIMA models for the wet bulb and dry bulb temperature time series. We ran numerous trials in order to optimize the length of time series to be included in the model and the time frequencies. The results were best when the frequency was 30 minutes and the length was approximately equal to the length of the frost period. We compared also the results of the manually created ARIMA models following the steps of the procedure described by Hyndman and Athanasopoulos[7] with those created by the automatic ARIMA function *auto.arima()* from the R package *"forecast"* for "Forecasting Functions for Time Series and Linear Models". Altogether, the results obtained manually and automatically were quite comparable.
For the calculation of the sunrise and sunset time we used the geographic coordinates of the station from the database.

4.1. ARIMA and Linear Regression models

The scope of the first analysis was to compare automatically modelled ARIMA (1.4) for the dry bulb temperature time series and three linear regression (LR) forecast models, which are variations of the model described by Snyder *et al.*[2]:

$$LRmodel1: TdbSunrise \sim TdbSunset + TdpSunset \tag{1.5}$$

$$LRmodel2: TdbSunrise \sim TdbSunset + RHSunset \tag{1.6}$$

$$LRmodel3: TdbSunrise \sim TdbSunset + TwbSunset \tag{1.7}$$

where:
$TdbSunrise$ is the dry bulb temperature at 60 cm above ground at sunrise
$TdbSunset$ is the dry bulb temperature at 60 cm above ground at sunset
$TdpSunset$ stands for the dew point temperature at sunset
$TwbSunset$ is the wet bulb temperature at 60 cm above ground at sunset
$RHSunset$ is relative humidity at sunset

For the test 100 forecasts for each model were calculated and tested on a randomly chosen data set. The point forecast, lower bound of the 80% and the 95 % confidence interval were calculated.

4.2. Binary classification of the frost data

The following test conditions were defined:

- *frost* - positive condition, when the predicted variable, dry bulb temperature at 60 cm above ground falls below 0°C at sunrise.
- *no frost* - negative condition, when the predicted variable, dry bulb temperature at 60 cm above ground does not fall below 0°C at sunrise.

4.2. Training and test set

The data set for the forecast was selected in the following manner:

1. Choose randomly one station from all stations.
2. Choose randomly one year from the range of years.
3. Choose randomly one day for the forecast from the relevant frost period (from March until May).

We selected randomly 47 frost cases and 53 days without frost, altogether 100 days. As training set a 30-days time period before the previously randomly selected day of the forecast was chosen. As a test set served the day of the forecast itself. Next, the following two-step procedure was conducted:

1. Calculate the ARIMA non-seasonal model on the training set.
2. Test the model on the test set.

5 Evaluation

In order to assess the quality of a forecast we considered the following quantities: accuracy, recall and specificity. Accuracy is defined as ratio of all correctly recognized cases to the total number of test cases. The recall is defined as ratio of true positives to all frost cases. The specificity is ratio of true negatives to all no frost cases.

On the basis of the recall value for the point forecast the LR model 3 with recall value equal to 70% could be identified as the best model. The two other LR models and the ARIMA model reached a recall value of about 60%. The specificity values for all models were between 96% and 100%. The accuracy for the point forecast was between 79% (ARIMA) and 85% (LR model 3). The test results for the 80% and 95% confidence intervals for the linear regression models were quite similar. Their recall values reached from 68% to 83%, the specificity from 85% to 91% and the accuracy from 79% and 85%. The model 2 was the best in this group for both confidence intervals. For the test level of the 80% and 95% confidence interval lower bounds, the best model was ARIMA, which reached higher values for recall than the linear regression models. In case of the 95% CI lower bound the optimal value of 1.0 for the recall was achieved. Unfortunately, the payoff of the good results for recall was a low value for specificity of 20% only, which resulted in a low accuracy of 58%.

Point forecast						
Model	Precision	NPV	Specificity	Recall	Accuracy	F_2
db_sr ~ db_st + dp	1.00	0.75	1.00	0.62	0.82	0.67
db_sr ~ db_st + RH	1.00	0.75	1.00	0.62	0.82	0.67
db_sr ~ db_st + wb	0.97	0.79	0.98	0.70	0.85	0.74
ARIMA	0.93	0.73	0.96	0.60	0.79	0.64

80 % CI						
Model	Precision	NPV	Specificity	Recall	Accuracy	F_2
db_sr ~ db_st + dp	0.97	0.76	0.89	0.68	0.79	0.72
db_sr ~ db_st + RH	1.00	0.80	0.91	0.74	0.83	0.78
db_sr ~ db_st + wb	0.95	0.79	0.87	0.74	0.81	0.78
ARIMA	0.66	0.94	0.57	**0.96**	0.75	0.88

95 % CI						
Model	Precision	NPV	Specificity	Recall	Accuracy	F_2
db_sr ~ db_st + dp	0.95	0.81	0.87	0.77	0.82	0.80
db_sr ~ db_st + RH	0.95	0.85	0.87	0.83	0.85	0.85
db_sr ~ db_st + wb	0.93	0.83	0.85	0.81	0.83	0.83
ARIMA	0.53	1.00	0.21	1.00	0.58	0.85

Fig. 9. Evaluation results of ARIMA and linear regression models.

6 ARIMA model selection

The scope of the second analysis was to study, which ARIMA model parameters were selected for the forecast by the automatic model building function *auto.arima*() from the R package "forecast". The forecast was made for 500 selected days. We chose randomly one station from the range of all stations, one year, one day from the frost period and calculated the model for the previous 30 days before the randomly selected day.

The results of the trial showed that there was a wide range of possible model parameter sets. The distribution of p and q values is shown in Figures 10 and 11, respectively. At the same time it is notable that the p and q values are correlated. The higher the p the higher the q value. The correlation between p and q is shown in Figure 12. On the other hand, the p and q values are not correlated when d=0, which confirmed the test for association between paired samples, using Pearson's product moment correlation coefficient. The p-value for the statistical significance was above the conventional threshold of 0.05, so the correlation is not statistically significant.

.

	if d=0	if d=1
p	Count	
0	0	2
1	9	199
2	60	44
3	39	87
4	9	29
5	4	18
∑	121	379

Fig. 10. Count of p

	if d=0	if d=1
q	Count	
0	0	11
1	24	71
2	32	182
3	40	61
4	18	46
5	7	8
∑	121	379

Fig. 11. Count of q

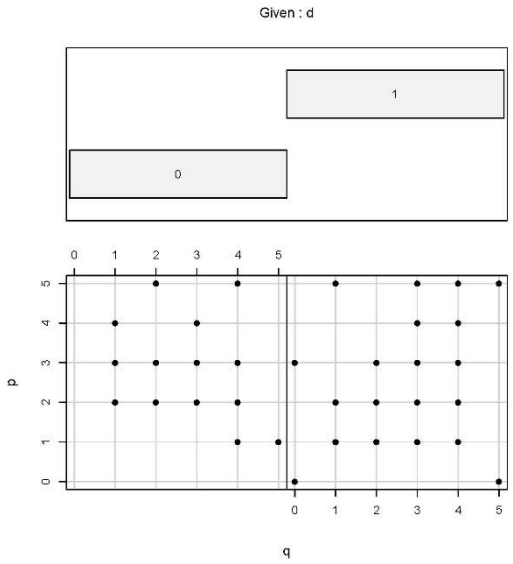

Fig. 12. Conditional plot of p versus q given d.

Conclusions

This work described frost prediction in apple orchards based upon time series models; a non-seasonal ARIMA model and three different Linear Regression models. The model should help in the design of an electronic monitoring system that permits forecasting of frost weather phenomena. Based on analysis of time series data and numerous trials, the proposed models could be compared and evaluated. The following observations regarding temperature forecast for up to twelve hours after sunset were made:

- For the test level of the lower bound of the 80% and 95% confidence intervals, the ARIMA model reached higher values for recall (the ratio of correctly recognized frost cases to all frost cases) than the linear regression models. In case of ARIMA models and the lower bound of the

95% CI, the optimal value of 1.0 for the recall was achieved, which means that all frost cases could be correctly forecast.
- Unfortunately, the payoff of the good results for recall is the low value for the specificity of 20% only. This means risk of frequent false alarms.

Despite the high risk of false alarms, the ARIMA model offers encouraging results worth further investigations. Linear regression models can be further improved as well. Here is a list of several complementary analysis steps, which could be tried out towards more accurate forecasting:

- Vector ARIMA models (VARIMA), which are a multivariate extension of ARIMA models should be tested. The vector of predictors variable in Linear Regression models could be extended by wind speed and soil temperature, which would likely lead to more precise forecast.
- The length of the training data can be still optimized in order to find the optimal fit.
- The orders p and q of the ARIMA model should be studied in order to find out potential correlations with temperature. This would allow to exclude some of the models.
- A similarity study of the forecast coming from different stations should be made. Such similarity information could turn out to be helpful in the ARIMA model selection.

References

1. A. Bootsma, D. Murray. Freeze protection methods for crops. Factsheet, December 1985.
2. R.L Snyder, J.P. de Melo-Abreu, S. Matulich. Frost protection: fundamentals, practice, and economics, volume 1, 2. FAO, 2005.
3. H. Oberhofer. Eine Frostnacht - eine Lehre? Obstbau Weinbau Mitteilungen des Südtiroler Beratungsringes, April 1986.
4. W. Waldner. Was bewirken die Spätfröste Ende März? Obstbau Weinbau Mitteilungen des Südtiroler Beratungsringes, April 1993.
5. H. Oberhofer. Erfahrungen aus den Spätfrösten 1969. Obstbau Weinbau Mitteilungen des Südtiroler Beratungsringes, May 1969.
6. Beratungsring. Leitfaden 2012, Febr, 2012.
7. R.J. Hyndman and G. Athanasopoulos. Forecasting: principles and practice, OTexts 2012.
8. E. Eccel, L. Ghielmi, P. Granitto, R. Barbiero, F. Grazzini, D. Cesari. Techniche di post-elaborazione di previsione di temperatura minima a confronto per un' area alpina, Italian Journal of Agrometeorology 38-44, 2008(3).
9. M. T. Castellanos, A. M. Tarquis, M .C. Morató, A. Saa. Forecast of frost days based on monthly temperatures, Spanish Journal of Agricultural Research 513-524, 2009 7(3).
10. B. L. Bowermann, R. T. O'Connell, A .B. Koehler. Forecasting, Time Series, and Regression, Pacific Grove, CA: Thomson, Brooks/Cole 2005.

Adaptive MCMC Method for Multivariate Stable Distributions

Ingrida Vaiciulyte

Business and Technologies Faculty, Šiauliai State College, Aušros ev. 40, 76241 Šiauliai, Lithuania
(E-mail: i.vaiciulyte@svako.lt)

Abstract. Markov chain Monte Carlo adaptive methods by creating computationally effective algorithms for decision-making of data analysis with the given accuracy are analyzed in this paper. The task for estimation of parameters of the multivariate stable symmetric vector law which is constructed in hierarchical way is described and solved in this paper. To create the adaptive MCMC procedure, the sequential generating method is applied for Monte Carlo samples, introducing rules for statistical termination and for sample size regulation of Markov chains. Statistical task, solved by this method, reveal characteristics of relevant computational problems including MCMC method.
Effectiveness of the MCMC algorithms is analyzed by statistical modeling method, constructed in the paper. Tests made with financial data of enterprises, confirmed that numerical properties of the method correspond to the theoretical model. Tests of algorithms have shown that adaptive MCMC algorithm allows obtaining estimators of examined distribution parameters in lower number of chains, and reducing the volume of calculations approximately two times. The algorithms created in this paper can be used to test the systems of stochastic type and to solve other statistical tasks by MCMC method.
Keywords: Monte Carlo method, EM algorithm, maximum likelihood method, stable distributions, stochastic optimization.

1 Introduction

Stochastic processes can be modelled, estimated and predicted by probabilistic statistical methods, using the data that describes the course of the process. Markov chain Monte Carlo (MCMC) is a computer simulation method, which is widely used in statistics, technology, physics, bioinformatics, etc. (Rubinstein, Kroese[12], Spall[15]). MCMC method is often applied to calculate probabilities or rare events by importance sampling, in data analysis by EM (expectation maximization) algorithm, for practical application of Bayesian method by modeling the posterior distribution and using numerical methods in determining their parameters, etc. (Booth and Hobert[2], Koopman *et al.*[8], Zeger and Karim[17]).
Known MCMC algorithms usually generate some or several chains, determining convergence by empirical method and recording large enough Monte Carlo sample size in all chains (Bradley and Thomas[3]). It is evident that these

procedures are not very effective from the computational viewpoint as generation of chains uses too much computer's time, and in case of empirical termination of chain generation, statistically significant convergence might be not achieved yet. What is more, while applying MCMC, the problem often occurs in deciding what Monte Carlo sample size should be generated for separate chains.

The research object of this paper is adaptive Markov chain Monte Carlo method study, its numerical realization and application in data analysis, regulation techniques of assessment of accuracy of estimators, selection of number of chains, algorithm termination, and Monte Carlo sample size for separate chains.

2 Stable symmetric vector distribution

Zolotarev's expression of stable distribution $S_\alpha(\sigma,\beta,\mu)$ density is used in this paper (Золотарев[18]):

$$\psi(x|\alpha,\sigma,\beta,\mu)=\begin{cases}\textbf{(1)}\\ \textbf{(2)}\end{cases}$$

$$\textbf{(1)}\quad \exp\left\{-|\sigma\cdot\theta|^{\alpha}\cdot\left(1-i\beta\,\mathrm{sgn}(\theta)\tan\left(\frac{\pi\alpha}{2}\right)\right)+i\mu\theta\right\},\ \text{jeigu } \alpha\in(0;1)\cup(1;2], \qquad (1)$$

$$\textbf{(2)}\quad \exp\left\{-|\sigma\cdot\theta|\cdot\left(1+\frac{2i\beta}{\pi}\ln|\theta|\,\mathrm{sgn}(\theta)\right)+i\mu\theta\right\},\quad \text{jeigu } \alpha=1,$$

where $\theta\in\Re$ and $\mathrm{sgn}(\theta)=\begin{cases}1, & \text{jei } \theta>0,\\ 0, & \text{jei } \theta=0,\\ -1, & \text{jei } \theta<0.\end{cases}$

In one-dimension case, it is known that $s=s_1\cdot s_2$, where:

s_1 – random stable variable with skewness parameter $\beta=1$ and shape parameter $\alpha_1<1$;

s_2 – another random stable variable with skewness parameter $\beta=0$ and shape parameter α_2;

s – random stable variable with skewness parameter $\beta=0$ and shape parameter $\alpha=\alpha_1\cdot\alpha_2$ (Rachev and Mittnik[10], Ravishanker and Qiou[11]).

While applying this method, it is usually selected that s_2 would be a random variable, which is normally distributed, i.e., $\alpha_1=\frac{\alpha}{2}$ and $\alpha_2=2$. In this way, the multivariate stable symmetric vector can be expressed through normally distributed random vector, and α-stable variables (Rachev and Mittnik[10],

Ravishanker and Qiou[11]) as $X = \mu + \sqrt{s_1} \cdot s_2$, where s_1 – subordinator with parameter α, random vector $s_2 \sim N(0, \Omega)$ and μ is a random vector of mean.

3 Estimators of maximum likelihood approach

From computational viewpoint, MCMC approach allows us to solve the equations, which include complex multivariate integrals, by constructing Markov chain of Monte Carlo samples. These equations can often be derived as necessary condition of optimality for some stochastic criteria (Polyak[16]). In this paper, likelihood functions that describe these criteria are assumed as continuous and smoothly differentiated, therefore, MCMC method can be interpreted as gradient descent method for this likelihood function. Usually, it is possible to prove that EM algorithm, widely used in statistics, is a separate case of stochastic gradient search.

Let's consider that the sample $X = \left(X^1, X^2, \ldots, X^K\right)$ consists of independent *d*-variate stable vectors. The likelihood function of this sample is (Ravishanker and Qiou[11]):

$$\tilde{L}(X, \mu, \Omega, \alpha) = \frac{\left(\frac{\alpha}{2-\alpha}\right)^K}{(2\pi)^{\frac{K}{2}} \cdot |\Omega|^{\frac{K}{2}}} \cdot \prod_{i=1}^{K} \int_0^{\infty} \int_{-1}^{1} \exp\left[-\left| \frac{t_\alpha(y_i)}{s_i} \right|^{\frac{\alpha}{2-\alpha}} - \right.$$
$$\left. -\frac{1}{2}\left(X^i - \mu\right)^T \frac{\Omega^{-1}}{s_i}\left(X^i - \mu\right) \right] \cdot \left| \frac{t_\alpha(y_i)}{s_i} \right|^{\frac{\alpha}{2-\alpha}} \cdot \frac{1}{s_i^{\frac{d}{2}+1}} dy_i ds_i, \tag{2}$$

where

$$t_\alpha(y) = \frac{\sin\left(\frac{\pi \cdot \alpha \cdot y}{2}\right) \cdot \sin\left(\frac{\pi \cdot (2-\alpha) \cdot y}{2}\right)^{\frac{2-\alpha}{\alpha}}}{(\sin \pi \cdot y)^{\frac{2}{\alpha}} \cdot \left(\cos\frac{\pi \cdot \alpha}{4}\right)^{\frac{2}{\alpha}}}.$$

The log-likelihood function of this sample is:

$$L(X, \mu, \Omega, \alpha) = \frac{K}{2} \ln|\Omega| - \sum_{i=1}^{K} \ln\left(\int_0^{\infty} \int_0^{1} B\left(X^i, y_i, z_i, \mu, \Omega, \alpha\right) \cdot \exp\{-z_i\} dy_i dz_i \right), \tag{3}$$

where

$$z_i = \left| \frac{t_\alpha(y_i)}{s_i} \right|^{\frac{\alpha}{2-\alpha}},$$

$$B\left(X^i, y_i, z_i, \mu, \Omega, \alpha\right) = \exp\left\{ -\frac{z_i^{\frac{2-\alpha}{\alpha}} \left(X^i - \mu\right)^T \Omega^{-1} \left(X^i - \mu\right)}{2 \cdot t_\alpha(y_i)} \right\} \cdot \frac{z_i^{\frac{2-\alpha}{\alpha} \cdot \frac{d}{2}}}{t_\alpha(y_i)^{\frac{d}{2}}}.$$

Estimators of parameters are calculated by fixed-point method (Sakalauskas and Vaiciulyte[14]):

$$\hat{\mu} = \frac{\sum_{i=1}^{K} \frac{X^i \cdot g_i}{f_i}}{\sum_{i=1}^{K} \frac{g_i}{f_i}}, \tag{4}$$

$$\hat{\Omega} = \frac{1}{K} \cdot \sum_{i=1}^{K} \frac{\left(X^i - \hat{\mu}\right)\left(X^i - \hat{\mu}\right)^T g_i}{f_i}, \tag{5}$$

where

$$g\left(X, \hat{\mu}, \hat{\Omega}, \alpha\right) = \int_0^\infty \int_0^1 \frac{z^{\frac{2-\alpha}{\alpha}}}{t_\alpha(y)} \cdot B\left(X, y, z, \hat{\mu}, \hat{\Omega}, \alpha\right) \cdot \exp\{-z\} dy dz, \tag{6}$$

$$f\left(X, \hat{\mu}, \hat{\Omega}, \alpha\right) = \int_0^\infty \int_0^1 B\left(X, y, z, \hat{\mu}, \hat{\Omega}, \alpha\right) \cdot \exp\{-z\} dy dz, \tag{7}$$

EM algorithm can be used to solve the equations (4), (5) after integrals (6) and (7) are calculated by Monte Carlo method. When μ and Ω are fixed, the shape parameter estimate can be obtained by solving the exercise of one variable minimization.

4 Adaptive Markov chain Monte Carlo algorithm

Let's say the initial values $\mu^0, \Omega^0, \alpha^0$ are selected, then k number of Markov chains is generated, and estimates $\mu^k, \Omega^k, \alpha^k$ in each chain are calculated. Let's say

$$\begin{aligned} Y_j &\sim U(0,1), \\ Z_j &\sim -\ln\left(Y_j\right), \end{aligned} \tag{8}$$

where $j = 1, 2, \ldots, N^k$, N^k – is Monte Carlo sample size of the k^{th} chain. Then the sums are calculated:

$$P_i^k = \frac{1}{N^k} \sum_{j=1}^{N^k} B\left(X^i, Y_j, Z_j, \mu^k, \Omega^k, \alpha^k\right), \tag{9}$$

$$PP_i^k = \frac{1}{N^k} \sum_{j=1}^{N^k} \left(B\left(X^i, Y_j, Z_j, \mu^k, \Omega^k, \alpha^k\right)\right)^2, \tag{10}$$

$$V_i^k = \frac{1}{N^k} \sum_{j=1}^{N^k} \frac{Z_j^{\frac{2-\alpha^k}{\alpha^k}}}{t_{\alpha^k}\left(Y_j\right)} B\left(X^i, Y_j, Z_j, \mu^k, \Omega^k, \alpha^k\right), \tag{11}$$

$$VV_i^k = \frac{1}{N^k} \sum_{j=1}^{N^k} \left(\frac{Z_j^{\frac{2-\alpha^k}{\alpha^k}}}{t_{\alpha^k}\left(Y_j\right)} B\left(X^i, Y_j, Z_j, \mu^k, \Omega^k, \alpha^k\right) \right)^2, \tag{12}$$

that are necessary to receive estimators in the next iteration, according to (4) and (5) and EM algorithm:

$$\mu^{k+1} = \frac{\sum_{i=1}^{K} X^i \frac{V_i^k}{P_i^k}}{\sum_{i=1}^{K} \frac{V_i^k}{P_i^k}}, \tag{13}$$

$$\Omega^{k+1} = \frac{1}{K} \sum_{i=1}^{K} \left(X^i - \mu^k\right)\left(X^i - \mu^k\right)^T \frac{V_i^k}{P_i^k}. \tag{14}$$

Then the consistent Monte Carlo estimator of log-likelihood function is obtained:

$$L^k = -\sum_{i=1}^{K} \ln\left(P_i^k\right). \tag{15}$$

The 95% confidence interval for likelihood function is:

$$\left[L^k - \frac{2}{\sqrt{N^k}} \sqrt{N^k \cdot \sum_{i=1}^{K} \frac{PP_i^k}{\left(P_i^k\right)^2} - K}, L^k + \frac{2}{\sqrt{N^k}} \sqrt{N^k \cdot \sum_{i=1}^{K} \frac{PP_i^k}{\left(P_i^k\right)^2} - K} \right]. \qquad (16)$$

Some or several chains are usually generated in the known MCMC algorithms, when fixed and large enough Monte Carlo sample size is detected in all chains and by estimating convergence empirically (Bradley and Thomas[3], Brooks and Roberts[5]). One way of solving the problem of selecting the Markov chain size is to terminate the generation of chain if samples, calculated in adjacent chains, do not differ statistically after applying statistical methods for verification of hypothesis on differences and matches of aforementioned samples (Brooks and Gelman[4], Sakalauskas[13]). Some authors attempted to introduce tests for comparison of two adjacent chains, however, these tests are one dimensional or allow to compare two vectors at best (Gelman and Rubin[7], Brooks and Gelman[4], Flegal *et al.*[6]), while in practical exercises probability distributions are often described by several vectors and several matrixes.

Monte Carlo chains are generated, according to formulas (13), (14) the length of confidence interval (16) becomes lower than chosen value ε, $\varepsilon > 0$, and statistical hypothesis about matching of mean vectors and covariance matrices in two adjacent iterations $H_0 : \mu^{k+1} = \mu^k$, $\Omega^{k+1} = \Omega^k$ is not rejected. To test this hypothesis, the Anderson[1] criterion is used:

$$H^k = \frac{K}{\frac{1}{K}\sum_{i=1}^{K} \frac{VV_i^k}{\left(P_i^k\right)^2}} \times \left(-\ln \frac{\left|\Omega^{k+1}\right|}{\left|\Omega^k\right|} + \left(\mu^{k+1} - \mu^k\right)^T \cdot \left(\Omega^{k+1}\right)^{-1} \cdot \left(\mu^{k+1} - \mu^k\right) + \sum_{i=1}^{d} \left(\Omega^{k+1} \cdot \left(\Omega^k\right)^{-1} \right)_{i,i} - d \right). \qquad (17)$$

Therefore, the statistical hypothesis is rejected according to the criteria (17) if:

$$H^k > \Psi_{\delta,p}, \qquad (18)$$

where $\Psi_{\delta,p}$ – is χ_p^2 distribution quantile with $p = \frac{1}{2} d(d+3)$ degrees of freedom, δ – significance level (Krishnaiah[9]).

Another problem, related to reduction of calculation volume, is regulation of Monte Carlo sample size in separate chains. In fact, there is no need to generate large Monte Carlo samples when constructing first chains of Markov chain because smaller sample sizes are enough for iterative modification of model parameters. Large Monte Carlo samples should be generated only at the end of Markov chain, when statistical criterion is compatible with hypothesis on concurrence of the last chains of probabilistic models. Methods of Monte Carlo

sample size regulation are proposed and simulated by computer in this paper by using statistical criterion about uniformity of Monte Carlo sample distributions in two Markov chains.
To regulate Monte Carlo sample size, the rule, analogical to rule, which is applied in stochastic programming, is introduced (Sakalauskas[13]):

$$N^{k+1} \geq \frac{N^k}{H^k} \cdot \Psi_{\nu,p}, \tag{19}$$

where in separate case ν can be equal to δ. Application of this rule allows to choose the Monte Carlo sample size in Markov chain rationally, also ensures the convergence of sets (13) and (14) into optimal value of likelihood function with probability 1 (Sakalauskas[13]).

5 Computer modeling

The algorithm created was tested with chosen simulated data and share data of 3 telecommunication enterprises: AT&T, BellSouth and CenturyLink. By using MCMC algorithm, described in the paper, $k = 50$ Markov chains were generated. The sample size limit $N^k \geq 500$ was applied to avoid too small or too large values. In this case, termination conditions of the algorithm were satisfied after $k = 28$ iterations.
Fig. 1–4 depict dependences when the length of confidence interval does not exceed $\varepsilon = 0{,}2$. As it might be observed in fig. 8, the log-likelihood function is decreasing until the zone of possible solution is achieved. The presented dependences in fig. 9 show that the confidence interval decreases down to the required value of 0,2. In fig. 10, N real is obtained by terminating sample generation when the length of confidence interval does not exceed the critical value $\varepsilon = 0{,}2$. N predictable is Monte Carlo sample size, calculated according to rule (19). Termination test is depicted in fig. 4, where critical value is the value of 0,999-quantile of χ^2_p distribution with $p = 9$ degrees of freedom (equal to 27,88).

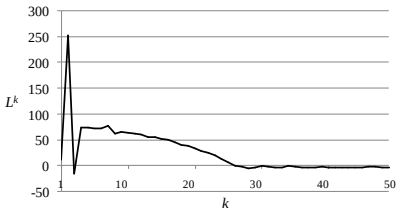

Fig. 1. Likelihood Function L^k

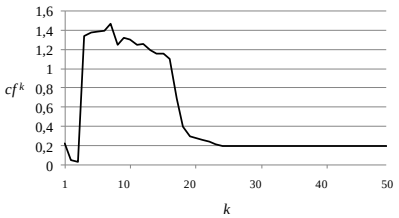

Fig. 2. Confidence interval length cf^k

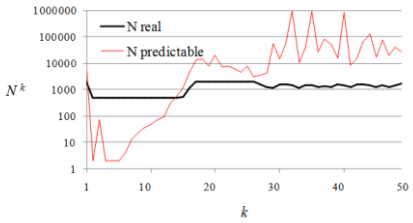

Fig. 3. Sample size N^k

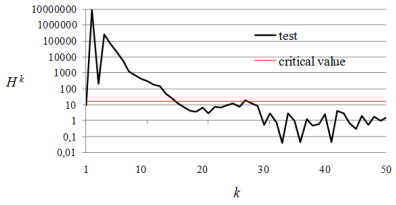

Fig. 4. Termination test H^k

Analogical research of share prices was carried out with the following 5 enterprises: AT&T, Bellsouth, CenturyLink, CBS, and Sprint. In table 2, the fixed and regulated by rule (19) Monte Carlo sample size is presented, required to meet the conditions for algorithm termination.

Table 2. Comparison of standard and adaptive MCMC algorithms of stable symmetric vector distribution

Dimension d	ε	Sample size	k	N^k in the last iteration	Total N
3	0,1	regulated	28	6 478	88 004
		fixed	30	7 000	210 000
	0,2	regulated	28	1 646	32 346
		fixed	29	2 000	58 000
5	0,1	regulated	23	11 724	156 567
		fixed	19	12 000	228 000
	0,2	regulated	12	2 519	16 904
		fixed	19	3 000	57 000

Comparison of created algorithm with a standard MCMC algorithm with fixed sample size has revealed that it allows to obtain the estimators symmetric stable vector law with the necessary accuracy in lower number of chains, and, thus, reducing the volume of calculations by almost two times.

Conclusions

The statistical adaptive MCMC algorithm for researching parameters of the multivariate stable symmetric vector distributions was constructed. It was shown that this method realizes log-likelihood function stochastic gradient search, implementing it with EM algorithm. Methods and algorithms for statistical estimation of Markov chains differences were proposed and analyzed using standard Hoteling and Anderson's criteria. Sample sizes were taken as inversely proportional to the ratio of termination statistic and quantile of

termination criterion. This algorithm was applied for creation of model of share data of telecommunication. Efficiency of MCMC algorithms was tested by statistical modeling. Tests of algorithms behaviour have shown that adaptive MCMC algorithm allows to obtain estimators of examined distribution parameters in lower number of chains, and reducing the volume of calculations approximately two times. Algorithm can be used to test the systems of stochastic type and to solve other statistical tasks by MCMC method.

References

1. T. W. Anderson. An introduction to multivariate statistical analysis. Wiley, New York, 1958.
2. J. G. Booth and J. P. Hobert. Maximizing generalized linear mixed model likelihoods with an automated Monte Carlo EM algorithm. Journal of the Royal Statistical Society, Series B, 61, 1, 265–285, 1999.
3. P. C. Bradley and A. L. Thomas. Bayes and empirical Bayes methods for data analysis. Chapman and Hall, New York, 2000.
4. S. P. Brooks and A. Gelman. General methods for monitoring convergence of iterative simulations. Journal of Computational and Graphical Statistics, 7, 434–455, 1998.
5. S. P. Brooks and G. O. Roberts. Convergence assessment techniques for Markov chain Monte Carlo. Statistics and Computing, 8, 319–335, 1998.
6. J. M. Flegal, M. Haran and G. L. Jones. Markov chain Monte Carlo: can we trust the third significant figure? Statistical Science, 23, 2, 250–260, 2008.
7. A. Gelman and D. B. Rubin. Inference from iterative simulation using multiple sequences. Statistical Science, 7, 457–511, 1992.
8. S. J. Koopman, N. Shephard and D. Creal. Testing the assumptions behind importance sampling. Journal of Econometrics, 149, 1, 2–11, 2009.
9. P. R. Krishnaiah. Handbook of statistics 1: analysis of variance. Elsevier Science & Technology Books, New York, 1984.
10. S. T. Rachev and S. Mittnik. Modeling asset returns with alternative stable distributions. Econometric Reviews, 12, 3, 261– 330, 1993.
11. N. Ravishanker and Z. Qiou. Monte Carlo EM estimation for multivariate stable distributions. Statistics & Probability Letters, 45, 4, 335–340, 1999.
12. R. Y. Rubinstein and D. P. Kroese. Simulation and the Monte Carlo method (2nd ed.). Wiley, New York, 2007.
13. L. Sakalauskas. Nonlinear stochastic optimization by Monte-Carlo estimators. Informatica, 11, 4, 455–468, 2000.
14. L. Sakalauskas and I. Vaiciulyte. Maximum likelihood method for the estimation of multivariate alpha-stable distribution. Journal of Young Scientists, 1, 45, 54-59, 2016.
15. J. C. Spall. Introduction to stochastic search and optimization: estimation, simulation, and control. Wiley, New York, 2003.
16. B. T. Polyak. Introduction to optimization. Optimization Software, New York, 1987.
17. S. L. Zeger and M. R. Karim. Generalized linear models with random effects: a Gibbs sampling approach. Journal of the American Statistical Association, 86, 79–86, 1991.
18. В. М. Золотарев. Одномерные устойчивые распределения. Наука, Москва, 1983.

Bibliometric Variables Determining the Quality of a Dentistry Journal

Pilar Valderrama[1], Manuel Escabias[2], Evaristo Jiménez-Contreras[3], Mariano J. Valderrama[4], Pilar Baca[5]

[1] Department of Statistics and Operations Research, University of Granada, Campus de Cartuja, 18071 Granada, Spain (E-mail: piluvb95@correo.ugr.es)
[2] Department of Statistics and Operations Research, University of Granada, Campus de Cartuja, 18071 Granada, Spain (E-mail: escabias@ugr.es)
[3] Department of Information and Communication, University of Granada, Campus de Cartuja, 18071 Granada, Spain (E-mail: evaristo@ugr.es)
[4] Department of Statistics and Operations Research, University of Granada, Campus de Cartuja, 18071 Granada, Spain (E-mail: valderra@ugr.es)
[5] Department of Dentistry, University of Granada, Campus de Cartuja, 18071 Granada, Spain (E-mail: pbaca@ugr.es)

Abstract. Considering the impact factor by Journal Citation Report as a measurement of the scientific quality of a journal, a logit regression model has been fitted in order to select the most influential bibliometric variables to estimate the forementioned indicator. In particular the study has focused in journals belonging to the field *Dentistry* and the explicative variables have been: H index of the journal, H index of the editor in chief, percentage of papers whose researchs have been supported by external institutions, as well as other factors related to the contents and framework of the journal. Regarding to this criterion, the logit model provides a correct classification rate of 83.3% for a cut-point of 0.5.
Keywords: H-index, journal citation report, logit regression.

1 Introduction

On the last decades several indicators to evaluate the quality of scientific journals have been developed being one the most common and useful the impact factor (IF) provided by the *Journal Citation Reports* (Thomson Reuters), that is a relative quality index obtained by dividing the number of yearly citations received by a journal into the total number of papers published in this journal, both related to the last two years. The IF allows to divide a set of journals of a certain field ordered decreasingly in groups by quantiles such as terciles, quartiles or percentiles.

In order to estimate and forecast the IF several explanatory variables including the H index of the own journal and the one of the editor-in-chief, the percentage of papers

published in this journal whose research received public or private finantial support (Bornmann *et al.*[2]), as well as other qualitative characteristics such as the aim of the journal (including survey papers, theoretical, applicative,...) or diffusion along the world can be considered.

The aim of this paper is to estimate a logit regression model to explain the IF rank from the above mentioned covariables and factors, but studying previously an optimal criterion for dividing the IF in two groups. For that we started from a division of IF in terciles, as is usual in science evaluation in the field of Mathematics and Statistics, and a comparison among the means of the independent quantitaive variables of the model was performed once the Gaussian hypothesis was tested. The essay was achieved with journals of Dentistry, that is a field of increasing interest in bibliometric studies (Lucena *et al.*[3]).

2 Statistical Methodology

The database used has been InCites™ Journal Citation Reports®, edition 2016, with free access for the University of Granada. Dentistry field includes 91 journals and, if they are ordered by decreasing IF, two of them: *Dental Materials Journal* and *Medicina Oral, Patología Oral y Cirugía Bucal* were in the same place 60 with an IF of 1.087. So they can easily divided in terciles. Moreover, a stratified sampling by terciles was performed choosing in a random way 12 journals in each stratum, obtaining in this way a sample size of 36, corresponding to a sampling fraction nearly to 40%. The selected journals are included in Table 1 together the following variables:

- IF rank in the field (*R*)
- H-index of the journal (*H-J*)
- H-index of the editor-in-chief (*H-Ed*)
- Sections (*S*): homogeneous framework (1) or including sections (2)
- Type of journal (T): generalist (1) or specialized (2)
- Percentage of papers with external finantial support (P)
- Anscombe transformation (*AnsP*)

H-J and *H-Ed* were calculated from Scopus® database while information about *S* and *T* was obtained by reading the own journals. With regard to estimate *P* a sample of 100 papers for each one of the 36 sampled journals corresponding to the same time interval of the considered IF's, was looked up. In order to deal with a quantitative continuous variable, *P* was transformed to a Gaussian variable by means of (Anscombe[1]): $arcsin(P/100)^{½}$. All this information is included in Table 1. Journals were divided in three groups by terciles, so that there were twelve in each one.

The preliminary step in the further development was to check the normality of the numeric explanatory variables by means of the *Kolmogorov-Smirnov* test, with *Lilliefors* significance correction for critical values. Once that all the involved variables could be processed as Gaussian, the hypothesis of equality among means of *H-J*, *H-Ed* and *AnsP* by terciles was tested by a simple ANOVA together the Levene's test for checking equality of variances. Furthermore, when ANOVA resulted significant, a *post-hoc* LSD

test (*least significant diference*) was applied in order to look for grouping between terciles. As can be seen in next section, a cluster between second and third tercil was found for the three variables so that, in fact, there were only two categories that will be called *Level*.

Journal	**IF**	**R**	**H-J**	**H-Ed**	**S**	**T**	**P**	**AnsP**
J. Dent. Res.	4.602	2	133	48	1	1	63%	0.91691
Dent. Mater	3.931	5	101	41	1	2	62%	0.90658
J. Clin. Periodontol.	3.915	6	109	55	2	2	56%	0.84554
Clin. Oral Implant. Res.	3.464	7	111	29	1	2	34%	0.62253
J. Dent.	3.109	8	80	17	1	1	43%	0.71517
Mol. Oral Microbiol.	3.061	9	61	39	1	2	83%	1.14581
J. Endod.	2.904	10	103	52	2	2	39%	0.67449
Int. Endod. J.	2.842	12	86	35	2	2	67%	0.95886
J. Oral Facial Pain Headache	2.824	13	55	52	1	1	32%	0.60126
Int. J. Oral Sci.	2.595	15	23	58	1	1	36%	0.64350
Clin. Oral Investig.	2.207	21	50	33	1	2	36%	0.64350
Int. J. Oral Maxillofac. Implants	1.690	25	24	25	1	2	54%	0.82544
J. Oral Maxillofac. Surg.	1.231	32	89	8	2	2	19%	0.45103
J. Adhes. Dent.	1.194	34	51	34	1	2	33%	0.61194
J. Cranio-MaxilloFac. Surg.	1.182	35	56	37	1	2	20%	0.46365
Odontology	1.640	38	8	8	1	1	40%	0.68472
Int. J. Prosthodont.	1.592	40	71	43	1	2	30%	0.57964
J. Evid.-Based Dent. Pract.	1.563	41	15	27	2	1	42%	0.70505
Eur. J. Orthodont.	1.272	42	60	21	1	2	26%	0.53507
Gerodontology	1.262	44	38	29	1	1	30%	0.57964
Dent. Traumatol.	1.237	45	63	26	1	2	21%	0.47603
J. Esthet. Restor. Dent.	1.231	50	42	28	1	2	34%	0.62253
J. Public Health Dent.	1.171	53	48	38	1	2	52%	0.80540
Med. Oral Patol. Oral Cir. Bucal	1.162	60	32	32	2	2	38%	0.66422
Int. J. Periodontics Restor. Dent.	1.154	63	61	34	1	2	23%	0.50018
Implant Dent.	1.117	64	44	8	1	2	31%	0.59050
Brit. Dent. J.	0.844	65	59	3	1	1	20%	0.46365
Int. Dent. J.	0.830	66	47	43	2	1	49%	0.77540
Head Face Med.	0.800	67	10	19	1	1	27%	0.54640
Aust. Endod. J.	0.795	68	24	2	1	2	25%	0.52360
J. Adv. Prosthodont.	0.791	70	12	12	1	2	28%	0.55760
Quintessence Int.	0.789	72	25	25	1	1	14%	0.38350
J. Oral Sci.	0.784	73	1	18	1	1	37%	0.65389
Pediatr. Dent.	0.767	74	50	12	2	1	28%	0.55760
J. Dental Sci.	0.449	75	8	31	1	2	51%	0.79540
Int. J. Dent. Hyg.	0.421	76	23	15	1	2	28%	0.55760

Table 1. Data of IF and of explanatory variables included in the study

The last stage of the analysis was to estimate a *logit* regression equation taking as response the new variable *Level* and as covariates *H-J*, *H-Ed* and *AnsP*, and as factors *S* and *T*.

3 Results

The Kolmogorov-Smirnov test for the variables *H-J*, *H-Ed* and *AnsP* concluded the normality of the three variables as can be seen in Table 2.

K-S test	H-J	H-Ed	AnsP
Z	0.721	0.397	0.735
p-value	0.676	0.998	0.652

Table 2. Normality test for variables *H-J*, *H-Ed* and *AnsP*

An ANOVA test for the above mentioned variables, previous application the Levene's test for homogeneity of variances, concluded significant differences among terciles for the three ones, as shows Table 3.

Variables	Levene	p-value	ANOVA	p-value
H-J	2.857	0.072	9.435	0.001
H-Ed	0.470	0.629	9.681	0.000
AnsP	2.335	0.113	9.387	0.001

Table 3. ANOVA and Levene's tests among terciles for *H-J*, *H-Ed* and *AnsP*

Then the *post-hoc* LSD test provided groupings among terciles so that in all cases the second and third terciles showed a similar behaviour and at the same time different from the first tercil (see Table 4). Their associated 95% confidence intervals are represented in Figure 1. This result allowed to introduce a new classificatory variable for quality of the journals, that will be called *Level*, with two categories: first tercil (1) and second-third tercils (2).

Tercil		Groups for H-J		Groups for H-Ed		Groups for AnsP	
JCR	N	1	2	1	2	1	2
1	12	78.00		40.33		0.79	
2	12		47.75		27.58		0.60
3	12		30.33		18.50		0.58
p-value		1.000	0.126	1.000	0.078	1.000	0.680

Table 4.LSD test associated to ANOVA of terciles for *H-J*, *H-Ed* and *AnsP*

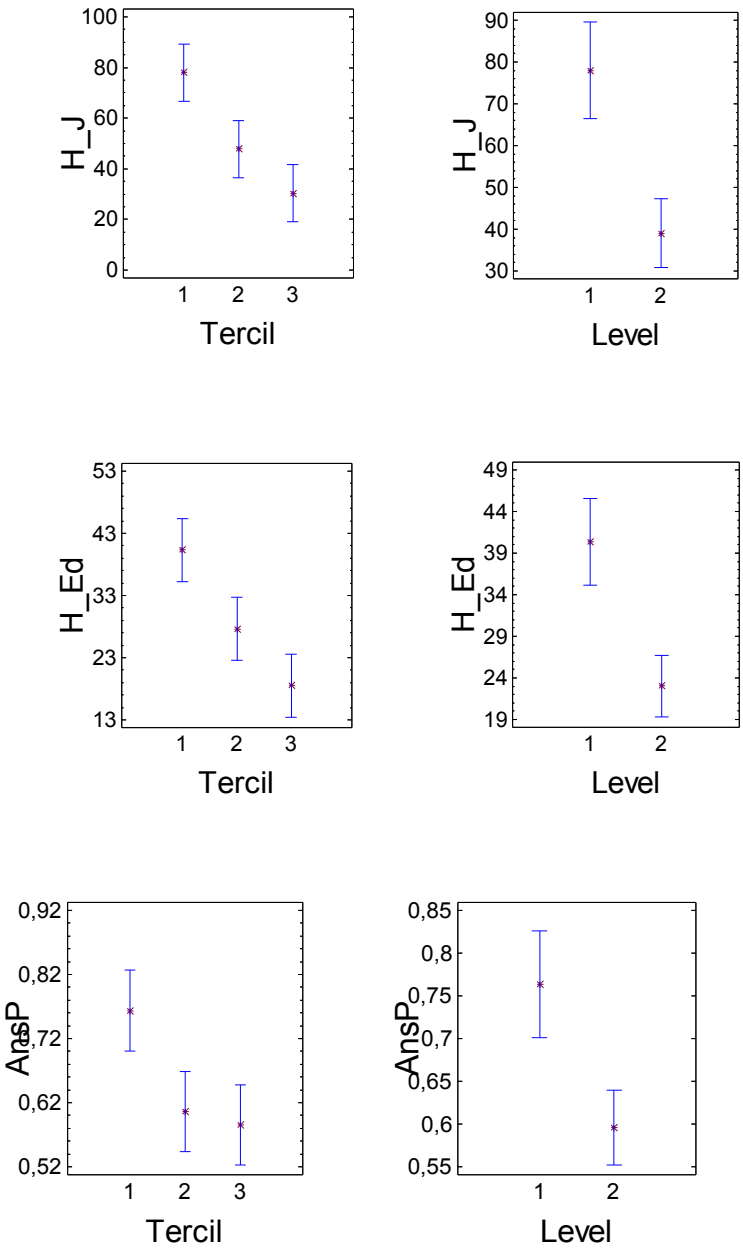

Fig. 1. 95% LSD confidence intervals

Taking as response the binary variable *Level*, a preliminary *logit* regression model with explanatories covariables *H-J*, *H-Ed* and *AnsP* and *S* and *T* as factors was estimated. The corresponding Nagelkerke's pseudo-R^2 coefficient was 0.794 and estimated parameters of the model appear in Table 5.

Variable	Coefficient	p-value
H-J	-0.075	0.037
H-Ed	-0.089	0.168
AnsP	-17.976	0.038
S	-4.135	0.096
T	-1.784	0.287
Constant	23.630	0.014

Table 5. Estimated coefficients of the preliminar *logit* regession

It can be noticed that factors *S* and *T* are not significant al level α=0.05, neither *H-Ed*. Therefore, reestimating the coefficients by means of a stepwise procedure, the final logit model with selected variables appears in Table 6. The Nagelkerke's pseudo-R^2 coefficient was 0.661:

Variable	Coefficient	p-value
H-J	-0.050	0.024
AnsP	-12.435	0.016
Constant	11.579	0.003

Table 6. Estimated coefficients of the final *logit* regession

Stepwise method for selection of variables to be included in the model must be carefully used because, when all the variables are included, predicted variables have low bias but large variance. Moreover, sometimes multicollinearity among variables induces to delete some important ones and prevail some independent variables with difficult interpretation (Steyerberg *et al.*[4]).

The correct classification rate (CCR) of the final model that includes only as independent variables *H-J* and *AnsP*, for a cut-point of 0.7 was 80.6% as figures in Table 7, where the percentage of success for journals of *Level* 2 was 83.3%.

	Estimated Level		
Real Level	1	2	CCR
1	8	4	66.7%
2	2	22	91.7%
		Total	83.3%

Table 7. CCR provided by the *logit* model (cut-point: 0.5)

Conclusions

Once the journals of the field *Dentistry* have been decreasingly ordered according their impact factor (JCR) and grouped by terciles, significant differences were found among these groups for the variables *H-J*, *H-Ed* and *AnsP*, what motivated the introduction of a new quality indicator called *Level* with two categories of journals depending on they belong to the first tercil or to the second and third tercil, on the basis of their behavior. Then a *logit* regression model was estimated taking *Level* as response variable and as independent variables the factors *S* and *T*, and covariates the above mentioned *H-J*, *H-Ed* and *AnsP*. Only *H-J* and *AnsP* were considered in the final model for significance level 0.05. The model was tested with the sampled journals providing a CCR up to 80% taking as cut-point 0.5.

The preliminary model including all the covariates and factors would give a higher CCR, near to 90% but including several non-significant covariates and factors.

Acknowledgement

This research was supported with the grant MTM2013–47929–P of Secretaría de Estado de Investigación, Desarrollo e Innovación, Ministerio de Economía y Competitividad de España.

References

1. F.J. Anscombe. The Validity of Comparative Experiments. Journal of the Royal Statistical Society, Series A. 111 (3), 181-211, 1948.
2. L. Bornmann, R. Mutz, W. Marx, H. Schier and H.D. Daniel. A multilevel modeling approach to investigating the predictive validity of editorial decisions: Do the editors of a high profile journal select manuscripts that are highly cited after publication? Journal of the Royal Statistical Society, Series A, 174 (4), 857-879, 2011.
3. C. Lucena, E.M. Souza, G.C. Voinea, R. Pulgar, M.J. Valderrama and G. De-Deus. A quality assessment of randomized controlled trial reports in Endodontics. International Endodontic Journal, 50 (3), 237-250. 2017.
4. E.W. Steyerberg, M.J. Eijkemans and J.D.F. Habbema. Stepwise selection in small data sets: a simulation study of bias in logistic regression analysis. Journal of Clinical Epidemiology, 52 (10), 935–942. 1999.

LAWS OF LARGE NUMBERS FOR NON-HOMOGENEOUS MARKOV SYSTEMS

P.-C.G. VASSILIOU

Department of Statistical Sciences, University College London.

Abstract. In the present we establish Laws of Large Numbers for Non-Homogeneous Markov Systems and Cyclic Non-homogeneous Markov systems. We start with a theorem, where we establish, that for a NHMS under certain conditions, the fraction of time that a membership is in a certain state, asymptotically converges in mean square to the limit of the relative population structure of memberships in that state. We continue by proving a theorem which provides the conditions under which the mode of covergence is almost surely. We continue by proving under which conditions a Cyclic NHMS is Cesaro strongly ergodic. We then proceed to prove, that for a Cyclic NHMS under certain conditions the fraction of time that a membership is in a certain state, asymptotically converges in mean square to the limit of the relative population structure in the strongly Cesaro sence of memberships in that state. We then proceed to establish a founding Theorem, which provides the conditions under which, the relative population structure asymptotically converges in the strongly Cesaro sense with geometrical rate. This theorem is the basic instrument missing to prove, under what conditions the Law of Large Numbers for a Cycl-NHMS is with almost surely mode of convergence. Finally, we present two applications firstly for geriatric and stroke patients in a hospital and secondly for the population of students in a University system.

1. Introductory notes

One of the most celebrated theorems in probability theory is the Law of Large Numbers (Grimmett and Stirzaker (2001)). The Law of Large Numbers were also studied for finite Markov chains (Kemeny and Snell (1981). The Law of Large Numbers for a regular homogeneous Markov chain states, that if π_j is the limiting probability of being in state j independent of the initial state, then also π_j represents the fraction of time, that the process can be expected to be in state j for a large number of steps. The Law of Large Numbers for Markov chains is also linked with the Martingale Convergence Theorem (Kemeny, Snell and Knapp (1976). Laws of Large Numbers were also studied for non-homogeneous semi-Markov processes by Vadori and Swishchuk (2015). For Markov chains in general state spaces there exists a chapter on Laws of Large Numbers in Meyn and Tweedie (2009), where the theory of martingales is the main instrument for proving various types of LLN. These laws are of value for Markov chains exactly as they are for all stochastic processes: the LLN and CLT, in particular, provide the theoretical basis for many

Date: March 14, 2017; The present was a Keynote Talk at the conference ASMDA2017 London.
2000 *Mathematics Subject Classification.* Primary 60J10,60J20.
Key words and phrases. Non-Homogeneous Markov Systems, Cyclic Non Homogeneous Markov Systems, Laws of Large Numbers.

results in the statistical analysis of chains as they do in related fields. For this and other applications, the reader is referred to Hall and Heyde (1980).

In the present paper we will study the Laws of Large Numbers for Non-Homogeneous Markov Systems and for Cyclic Non-Homogeneous Markov systems. The theory of NHMSs has its roots in the use of Markov models in manpower systems, which started with the work of Young and Almond (1961) and Bartholomew (1963). Young's motive was the application of homogeneous Markov chain models in the British University system. Bartholomew created important multiple renewal theory models for various social processes and his first related book Bartholomew (1967) among other things, provided an important theoretical reference of applied probability style for everyone. The concept of Non-homogeneous Markov systems was first introduced in Vassiliou (1982). From then onwards a vast literature in a great variety of journals was created by many authors, a sample of which could be found in the review papers by Vassiliou (1997) and Ugowgo and McClean (2000). The motive was to provide a more general framework for a number of Non-homogeneous Markov chain models in manpower systems. There is also a great variety of applied probability models, that could be accommodated in this general framework. Let us consider a population (system), which is stratified into classes (states) according to various characteristics. The members of the system could be sections of human societies, parts of the animal kingdom, populations of fisheries, biological microorganisms, particles in a physical phenomenon, various types of machines, various types of cells or viruses of the human body etc. The members of the system are categorized into various states, according to the problem at hand. The set of states are assumed to be exclusive, so that each member of the system may be in one and only one state at a given time. We call population structure, the vector containing the number of members of each state in the system. Members are leaving the system in a stochastic way and also new members are entering the system in a stochastic way. In fact a non-homogeneous Markov chain is a NHMS with one particle as a member, which never leaves the system and in which no other particles enter.

There are a large number of applications of the theory of NHMS and in quite diverse areas, where the present results will have an impact. We will only refer to some of these applications that contribute to the health care of human beings. For example, applications to the evolution of the population of HIV virus within the human of T-cells in Mathiew et. al. (2006), and Foucher et.al. (2005); gene expression sequences in McClean et.al. (2003); in hospital and geriatric patient care McClean et.al. (1998a, 1998b), Taylor et.al. (2000), Faddy and McClean (2005), Garg, McClean et. al. (2010), McClean and Millard (2007), Marshal et.al. (2002), Marshal and McClean (2003,2004).Garg, McClean et. al. (2009), McClean et.al. (2007), McClean et.al. (2009),Lalit et.al. (2010), McClean et.al. (2014) and McClean et.al. (2014b).

The paper is organized as follows: In section 2 we provide basic concepts and useful results for a NHMS, which are known or slightly amended. Also we provide some useful in what follows theorems on the various modes of convergence of random variables in a probability space. The results in this section will be used repeatedly in the sections that follow. In section 3 we first prove a theorem which is a Law of Large Numbers for a NHMS. We prove, that for a NHMS under certain

conditions the fraction of time that a membership is in a certain state, asymptotically converges in mean square to the limit of the relative population structure of membership in that state. In a second theorem in the same section we provide and prove under what conditions the mode of convergence in the previous basic result is almost surely. In section 4 we study the important category of Cyclic NHMS, a concept which was motivated by the work of Gani (1963) on students enrolment at Michigan state University and Bartholomew (1982). We prove in two theorems, under what conditions the relative population structure of a Cycl-NHMS asymptotically converges in the strongly Cesaro sense. In section 5 we first prove a theorem which is a Law of Large Numbers for a Cycl-NHMS. We prove, that for a Cycl- NHMS under certain conditions the fraction of time that a membership is in a certain state, asymptotically converges in mean square to the limit of the relative population structure in the strongly Cesaro sense of membership in that state. We then proceed to establish a founding Theorem, which provides the conditions under which the relative population structure asymptotically converges in the strongly Cesaro sense with geometrical rate. This theorem is the basic instrument missing to prove, under what conditions the Law of Large Numbers for a Cycl-NHMS is with almost surely mode of convergence. In section 6 we provide applications of the present results in section 3 to geriatric and stroke patients. Also, we provide applications of the results in section 4 and 5 for the movements of students in a University system.

2. Basic concepts and useful results for a NHMS in discrete time

We firstly recall the concept of an NHMS and introduce concepts and known results necessary for the study of the Law of Large numbers for NHMSs. Consider a population (system) which is stratified into classes (states) according to various characteristics. Let $S = \{1, 2, ..., k\}$ be the set of states, that are assumed to be exclusive and exhaustive. Let, that we have a discrete time scale $t = 0, 1, 2, ...$ and $\{\mathbf{P}(t)\}_{t=0}^{\infty}$ be the sequence of transition probability matrices between the states. Assume, that we have wastage from the system and denote by ω the state which represents the external environment of the system to which the population members, who leave the system go. Let $\{\mathbf{p}_{\omega}(t)\}_{t=0}^{\infty}$ be the vector of probabilities of wastage from the various states of the system. Let $\{T(t)\}_{t=0}^{\infty}$ be the total number of memberships of the system at time t, which is assumed to be a realization of a known stochastic process. We assume that each member holds a membership, which is left, when the member leaves the system and is taken by new members entering the system to replace leavers or to expand the system. Apparently, $T(t) \geq 0$ and it is assumed that $\Delta T(t) = T(t+1) - T(t) \geq 0$. Let $\{\mathbf{p}_0(t)\}_{t=0}^{\infty}$ be the vector of probabilities of allocation of replacements and new memberships, in the various states of the system, which is being done independently of internal movements. Denote by $\mathbf{Q}(t) = \mathbf{P}(t) + \mathbf{p}_{\omega}^{\top}(t)\,\mathbf{p}_0(t)$; then $\mathbf{Q}(t)$ is a stochastic matrix, and the non-homogeneous Markov chain defined by the sequence $\{\mathbf{Q}(t)\}_{t=0}^{\infty}$ will be called the *imbedded non-homogeneous Markov chain* of the NHMS. Define by $N_i(t)$ the random variable representing the number of memberships in state i at time t; $\mathbf{N}(t) = [N_1(t), N_2(t), ..., N_k(t)]$ the vector of the random variables representing the *population structure* of the NHMS. Let $\mathbf{q}(t) = \mathbf{N}(t)/T(t)$ be the *relative*

population structure. Define by

$$\mathbf{q}(s,t) = [q_1(s,t), q_2(s,t), ..., q_k(s,t)], \tag{2.1}$$

where

$$q_j(s,t) = \mathbb{P}[X_t = j \mid \mathbf{q}(s)], \quad \text{for} \quad s \leq t, \tag{2.2}$$

then from Georgiou and Vassiliou (1992) p.140 we get that

$$\mathbb{E}[\mathbf{q}(t-1,t)] = a(t-1)\,\mathbf{q}(t-1)\,\mathbf{Q}(t-1) + b(t-1)\,\mathbf{p}_0(t-1), \tag{2.3}$$

where

$$a(t-1) = \frac{T(t-1)}{T(t)} \text{ and } b(t-1) = \frac{T(t) - T(t-1)}{T(t)}. \tag{2.4}$$

also we get that

$$\mathbb{E}[\mathbf{q}(0,t)] = a(t-1)\,\mathbb{E}[\mathbf{q}(0,t-1)]\,\mathbf{Q}(t-1) + b(t-1)\,\mathbf{p}_0(t-1), \tag{2.5}$$

from which recursively we get (see Georgiou and Vassiliou (1992) p.149) that

$$\begin{aligned} \mathbb{E}[\mathbf{q}(0,t)] &= \frac{T(0)}{T(t)}\mathbf{q}(0)\,\mathbf{Q}(0,t-1) \\ &\quad + \frac{1}{T(t)}\sum_{\tau=1}^{t} \Delta T(\tau-1)\,\mathbf{p}_0(\tau-1)\,\mathbf{Q}(\tau,t-1), \end{aligned} \tag{2.6}$$

where $\mathbf{Q}(s,t) = \mathbf{Q}(s)\,\mathbf{Q}(s+1)...\mathbf{Q}(t)$ for $s \leq t$. We set $\mathbf{Q}(s,t) = \mathbf{I}$ the identity matrix for $s > t$. Note also that we set $\mathbf{q}(s,t) = \mathbf{0}$ for $s > t$.

We denote by

$$\mathbb{E}[\mathbf{q}(s,t)] = [\mathbb{E}[q_1(s,t)], \mathbb{E}[q_2(s,t)], ..., \mathbb{E}[q_k(s,t)]],$$

and apparently we have

$$\begin{aligned} \mathbb{E}[\mathbf{q}(s,t)] &= \frac{T(s)}{T(t)}\mathbf{q}(s)\,\mathbf{Q}(s,t-1) \\ &\quad + \frac{1}{T(t)}\sum_{\tau=s+1}^{t} \Delta T(\tau-1)\,\mathbf{p}_0(\tau-1)\,\mathbf{Q}(\tau,t-1). \end{aligned}$$

We denote by $\mathbb{E}\left[\mathbf{q}^{(i)}(s,t)\right]$ if it is known that

$$\mathbf{q}(s) = \left[0, 0, ..., \underbrace{1}_{i-th}, ..., 0\right],$$

and the vector $\mathbb{E}\left[\mathbf{q}^{(i)}(s,t)\right]$ is then

$$\mathbb{E}\left[\mathbf{q}^{(i)}(s,t)\right] = \left[\mathbb{E}\left[q_1^{(i)}(s,t)\right], \mathbb{E}\left[q_2^{(i)}(s,t)\right], ..., \mathbb{E}\left[q_k^{(i)}(s,t)\right]\right].$$

Let $\mathcal{M}_{n,m}(\mathbb{R})$ be the vector space of all $n \times m$ real matrices $\mathcal{SM}_{n,n}$; the vector space of all $n \times n$ stochastic matrices. Let $\mathbf{Q} \in \mathcal{SM}_{n,n}$,then it is regular if it's states consist of a single communicating class which is aperiodic or equivalently $\mathbf{Q}$ has 1 as the only eigenvalue with modulus 1 and with geometric multiplicity one. For $\mathbf{A} \in \mathcal{M}_{n,n}(\mathbb{R})$ we define the norm $\|.\|$

$$\|\mathbf{A}\| = \sup_{i \in S} \sum_{j \in S} |a_{ij}|.$$

Now from Vassiliou (1981) we get the following theorem:

Theorem 1. *Let a NHMS and let that*

a) $\lim_{t\to\infty}\|\mathbf{Q}(t)-\mathbf{Q}\|=0$ and $\mathbf{Q}$ a regular stochastic matrix;
b) $\lim_{t\to\infty}\|\mathbf{p}_0(t)-\mathbf{p}_0\|=0$;
c)$\lim_{t\to\infty}[\Delta T(t)/T(t)]=0$,
then

$$\lim_{t\to\infty}\|\mathbb{E}[\mathbf{q}(0,t)]-\mathbf{q}(\infty)\|=0,$$

where $\mathbf{q}(\infty)$ is the row of the stable stochastic matrix $\mathbf{Q}(\infty)=\lim_{t\to\infty}\mathbf{Q}^t$.

From Isaacson and Madsen p.157 and p. 170 we get the following two theorems

Theorem 2. *A non-homogeneous Markov chain with transition matrices* $\{\mathbf{Q}(t)\}_{t=0}^{\infty}$ *is strongly ergodic if and only if there exists a constant matrix* $\mathbf{Q}$ *such that for each* m

$$\lim_{t\to\infty}\|\mathbf{Q}(m,t)-\mathbf{Q}\|=0.$$

Theorem 3. *Let* $\{\mathbf{Q}(t)\}_{t=0}^{\infty}$ *be a sequence of transition matrices corresponding to a non-homogeneous Markov chain. If* $lim_{t\to\infty}\|\mathbf{Q}(t)-\mathbf{Q}\|=0$ *where* $\mathbf{Q}$ *is weakly ergodic, then the chain is strongly ergodic.*

Following the steps of the proof of Theorem 1 in Vassiliou (1981) and using Theorems 2 and 3 we arrive at

Theorem 4. *Let a NHMS and let that*

a) $\lim_{t\to\infty}\|\mathbf{Q}(t)-\mathbf{Q}\|=0$ and $\mathbf{Q}$ a regular stochastic matrix;
b) $\lim_{t\to\infty}\|\mathbf{p}_0(t)-\mathbf{p}_0\|=0$;
c)$\lim_{t\to\infty}[\Delta T(t)/T(t)]=0$,
then

$$\lim_{t\to\infty}\|\mathbb{E}[\mathbf{q}(s,t)]-\mathbf{q}(\infty)\|=0,\text{ for every } s\le t.$$

Let a probability space $(\Omega,\mathcal{F},\mathbb{P})$ and a sequence of random variables $\{X_n\}_{n=0}^{\infty}$ with $X_n:\Omega\to\mathbb{R}$. It is well known that there are various modes of convergence of the sequence $\{X_n\}_{n=0}^{\infty}$ to a random variable $X:\Omega\to\mathbb{R}$. We now provide the formal definition of three of these modes.

Definition 1. *Let a probability space* $(\Omega,\mathcal{F},\mathbb{P})$ *and a sequence of random variables* $\{X_n\}_{n=0}^{\infty}$ *with* $X_n:\Omega\to\mathbb{R}$ *and a random variable* $X:\Omega\to\mathbb{R}$. *We say that the sequence of random variables* $\{X_n\}_{n=0}^{\infty}$ *converge almost surely to the random variable* X *if the event*

$$\{\omega\in\Omega:X_n(\omega)\to X(\omega)\ \text{ as } n\to\infty\},$$

has probability one. We will denote this type of convergence by

$$X_n\overset{a.s.}{\to}X\quad or\quad\lim_{n\to\infty}X_n=X\quad a.s.$$

Definition 2. *Let a probability space* $(\Omega,\mathcal{F},\mathbb{P})$ *and a sequence of random variables* $\{X_n\}_{n=0}^{\infty}$ *with* $X_n:\Omega\to\mathbb{R}$ *and a random variable* $X:\Omega\to\mathbb{R}$. *If* $|X_n|$ *and* $|X|$ *are in* L^p *where* $1\le p\le\infty$, *i.e.,* $\mathbb{E}[|X_n^p|]<\infty$ *for all* n *and* $\mathbb{E}[|X|]<\infty$, *then we say that the sequence of random variables* $\{X_n\}_{n=0}^{\infty}$ *converges to* X *in* p*-th mean and we denote it by*

$$X_n\overset{L^p}{\to}X,$$

if and only if

$$\lim_{n\to\infty} \mathbb{E}\left\{|X_n - X|^p\right\} = 0.$$

One of the most useful modes of convergence is the *mean square,* that is, for $p = 2$ we have

$$X_n \overset{L^2}{\to} X, \quad \text{or} \quad X_n \to X \text{ in mean square, or } X_n \overset{m.s.}{\to} X.$$

Definition 3. *Let a probability space $(\Omega, \mathcal{F}, \mathbb{P})$ and a sequence of random variables $\{X_n\}_{n=0}^{\infty}$ with $X_n : \Omega \to \mathbb{R}$ and a random variable $X : \Omega \to \mathbb{R}$. We say that $X_n \to X$ in probability, and we write $X_n \overset{P}{\to} X$, if*

$$\mathbb{P}\left(|X_n - X| > \epsilon\right) \to 0 \text{ as } n \to \infty \text{ for all } \epsilon > 0.$$

From Grimmett and Stirzaker (2001) p.311 we get the following Theorem.

Theorem 5. *Let a probability space $(\Omega, \mathcal{F}, \mathbb{P})$ and a sequence of random variables $\{X_n\}_{n=0}^{\infty}$ with $X_n : \Omega \to \mathbb{R}$ and a random variable $X : \Omega \to \mathbb{R}$. Then (a) If $r > s \geq 1$ and $X_n \overset{L^r}{\to} X$ then $X_n \overset{L^s}{\to} X$. (b) If $X_n \overset{L^1}{\to} X$ then $X_n \overset{P}{\to} X$. The converse assertions fail in general.*

Note that any sequence $\{X_n\}_{n=0}^{\infty}$ which satisfies $X_n \overset{P}{\to} X$ necessarily contains a subsequence $\{X_{n_i} : 1 \leq i < \infty\}$ which converge almost surely. From Grimmett and Stirzaker (2001) p.314 we get the following Theorem.

Theorem 6. *Let a probability space $(\Omega, \mathcal{F}, \mathbb{P})$ and a sequence of random variables $\{X_n\}_{n=0}^{\infty}$ with $X_n : \Omega \to \mathbb{R}$ and a random variable $X : \Omega \to \mathbb{R}$. If $X_n \overset{P}{\to} X$, there exists a non-random increasing sequence of integers $n_1, n_2, ...$ such that $X_{n_i} \overset{a.s.}{\to} X$ as $i \to \infty$.*

Also from Grimmett and Stirzaker (2001) p.310 we get the following Theorem.

Theorem 7. *Let a probability space $(\Omega, \mathcal{F}, \mathbb{P})$ and a sequence of random variables $\{X_n\}_{n=0}^{\infty}$ with $X_n : \Omega \to \mathbb{R}$ and a random variable $X : \Omega \to \mathbb{R}$. If $P_n(\epsilon) = \mathbb{P}\left(|X_n - X| > \epsilon\right)$ satisfies*

$$\sum_n P_n(\epsilon) < \infty \text{ for all } \epsilon > 0$$

then $X_n \overset{a.s.}{\to} X$.

Theorem 8. *(Chebychov inequality). Let a probability space $(\Omega, \mathcal{F}, \mathbb{P})$ and a random variable $X : \Omega \to \mathbb{R}$. Then*

$$\mathbb{P}\left(|X| \geq a\right) \leq \frac{\mathbb{E}\left(X^2\right)}{a^2} \text{ if } a > 0.$$

From Huang, Isaacson and Vinograde (1976) we amend slightly the basic theorem to get that

Theorem 9. *Let a probability space $(\Omega, \mathcal{F}, \mathbb{P})$ and a non-homogeneous Markov chain defined by the sequence of transition matrices $\{\mathbf{Q}(s,t)\}_{s,t}$. Let $\lim_{t\to\infty} \|\mathbf{Q}(t) - \mathbf{Q}\| = 0$ geometrically fast with $\mathbf{Q}$ a regular stochastic matrix. Then $\|\mathbf{Q}(s,t) - \mathbf{Q}\| = 0$ geometrically fast uniformly in s. That is, for every s there exists constants $c > 0$ and $0 < b < 1$ such that*

$$\|\mathbf{Q}(s,t) - \mathbf{Q}\| \leq cb^{t-s}.$$

From Vassiliou and Georgiou (1990) p. 541 we get the following theorem:

Theorem 10. *Let an NHMS be given with* $\{\mathbf{P}(t)\}_{t=0}^{\infty}$, $\{T(t)\}_{t=0}^{\infty}$, $\{\mathbf{p}_{k+1}(t)\}_{t=0}^{\infty}$, $\{\mathbf{p}_0(t)\}_{t=0}^{\infty}$. *Assume that*

$$a)\ \lim_{t\to\infty}\|\mathbf{P}(t)-\mathbf{P}\|=0,\ b)\ \lim_{t\to\infty}\|\mathbf{p}_{k+1}(t)-\mathbf{p}_{k+1}\|=0,\ c)\ \|\mathbf{p}_0(t)-\mathbf{p}_0\|=0,$$

the rate of convergence is geometric in all cases and $\mathbf{Q}=\mathbf{P}+\mathbf{p}_{\omega}^{\intercal}\mathbf{p}_0$ *is regular. Also,* $T(t)\geq T(t-1)$ *and*

$$\left\{\frac{\Delta T(t)}{T(t)}\right\}_{t=0}^{\infty}\quad \textit{converges to zero geometrically fast.}$$

Then the sequence of relative structures converges to $\mathbf{q}(\infty)=\mathbf{p}_0\mathbf{Q}^{\infty}$ *geometrically fast, where* $\mathbf{Q}^{\infty}=\lim_{t\to\infty}\mathbf{Q}^t$.

3. Laws of Large Numbers for a NHMS

In the present section we will study the Law of Large Numbers for a NHMS. We will start with the mode of mean square convergence and then we will proceed to prove almost sure convergence. Let X_t the random variable representing the state of a membership at time t. Define by

$$u_j(t)=\left\{\begin{matrix}1 & \text{if} & X_t=j\\ 0 & \text{if} & X_t\neq j\end{matrix}\right\}, \tag{3.1}$$

also let $y_j(t)$ be the random variable representing the number of times the membership is in state j up to time t, *i.e.*, $X_s=j$, $1\leq s\leq t$; $\nu_j(t)$ be the random variable representing the fraction of time the membership is in state j up to time t. We have that

$$y_j(t)=\sum_{s=1}^{t}u_j(s)\quad\text{and}\quad\nu_j(t)=\frac{y_j(t)}{t}. \tag{3.2}$$

Denote by

$$\mathbf{u}(t)=[u_1(t),u_2(t),...,u_k(t)]\ ,\ \mathbf{y}(t)=[y_1(t),y_2(t),...,y_k(t)]\ ,$$

and

$$\boldsymbol{\nu}(t)=[\nu_1(t),\nu_2(t),...,\nu_k(t)].$$

We will now provide and prove the following theorem of the Law of Large Numbers for a NHMS

Theorem 11. *Let a probability space* $(\Omega,\mathcal{F},\mathbb{P})$ *and a NHMS as defined in section 2. Assume that a)* $\lim_{t\to\infty}\|\mathbf{Q}(t)-\mathbf{Q}\|=0$ *and* $\mathbf{Q}$ *a regular stochastic matrix; b)* $\lim_{t\to\infty}\|\mathbf{p}_0(t)-\mathbf{p}_0\|=0$*; c)* $\lim_{t\to\infty}[\Delta T(t)/T(t)]=0$. *Then*

$$\boldsymbol{\nu}(t)\overset{L^2}{\to}\mathbf{q}(\infty).$$

Proof. It is equivalent to show that

$$\mathbb{E}\left[(\boldsymbol{\nu}(t)-\mathbf{q}(\infty))^2\right]=0. \tag{3.3}$$

Since the dimension of the vectors is finite it is equivalent to show that

$$\mathbb{E}\left[(\nu_j(t)-q_j(\infty))^2\right]=0\quad\text{for every } j=1,2,...,k. \tag{3.4}$$

We have that

$$\begin{aligned}\mathbb{E}\left[\left(\nu_j(t)-q_j(\infty)\right)^2\right] &= \mathbb{E}\left[\left(\sum_{n=1}^{t}\frac{u_j(n)}{t}-q_j(\infty)\right)^2\right] \\ &= \frac{1}{t^2}\mathbb{E}\left[\left(\sum_{n=1}^{t}\left(u_j(n)-q_j(\infty)\right)\right)^2\right] \\ &= \frac{1}{t^2}\mathbb{E}\left[\left(\sum_{n=1}^{t}\left(u_j(n)-q_j(\infty)\right)\right)\left(\sum_{l=1}^{t}\left(u_j(l)-q_j(\infty)\right)\right)\right].\end{aligned} \tag{3.5}$$

Hence we have that

$$\mathbb{E}\left[\left(\nu_j(t)-q_j(\infty)\right)^2\right]=\frac{1}{t^2}\sum_{n=1}^{t}\sum_{l=1}^{t}\mathbb{E}\left[u_j(n)\,u_j(l)\right] \tag{3.6}$$

$$-\frac{1}{t^2}\sum_{n=1}^{t}\sum_{l=1}^{t}q_j(\infty)\,\mathbb{E}\left[u_j(n)\right] \tag{3.7}$$

$$-\frac{1}{t^2}\sum_{n=1}^{t}\sum_{l=1}^{t}q_j(\infty)\,\mathbb{E}\left[u_j(l)\right] \tag{3.8}$$

$$+\frac{1}{t^2}\sum_{n=1}^{t}\sum_{l=1}^{t}q_j^2(\infty). \tag{3.9}$$

Now we have that

$$\begin{aligned}\lim_{t\to\infty}\left\{-\frac{1}{t^2}\sum_{n=1}^{t}\sum_{l=1}^{t}q_j(\infty)\,\mathbb{E}\left[u_j(n)\right]\right\} &= \lim_{t\to\infty}\left\{-\frac{1}{t^2}\sum_{n=1}^{t}\sum_{l=1}^{t}q_j(\infty)\,\mathbb{E}\left[\mathbb{E}\left[u_j(n)\mid\mathbf{q}(0)\right]\right]\right\} \\ &= \lim_{t\to\infty}\left\{-\frac{1}{t}q_j(\infty)\sum_{n=1}^{t}\mathbb{E}\left[\mathbb{P}\left(X_n=j\mid\mathbf{q}(0)\right)\right]\right\} \\ &= \lim_{t\to\infty}\left\{-q_j(\infty)\,\frac{1}{t}\sum_{n=1}^{t}\mathbb{E}\left[q_j(0,n)\right]\right\} \\ &= \text{(by Theorem 1)} = -q_j^2(\infty).\end{aligned} \tag{3.10}$$

Similarly we get that

$$\lim_{t\to\infty}\left\{-\frac{1}{t^2}\sum_{n=1}^{t}\sum_{l=1}^{t}q_j(\infty)\,\mathbb{E}\left[u_j(l)\right]\right\}=-q_j^2(\infty). \tag{3.11}$$

It is easy to see that

$$\frac{1}{t^2}\sum_{n=1}^{t}\sum_{l=1}^{t}q_j^2(\infty)=q_j^2(\infty). \tag{3.12}$$

Finally it remains to find

$$\begin{aligned}\lim_{t\to\infty}\left\{\frac{1}{t^2}\sum_{n=1}^{t}\sum_{l=1}^{t}\mathbb{E}\left[u_j\left(n\right)u_j\left(l\right)\right]\right\} &= \lim_{t\to\infty}\left\{\frac{1}{t^2}\sum_{n=1}^{t}\sum_{l=1}^{t}\mathbb{E}\left[\mathbb{E}\left[u_j\left(n\right)u_j\left(l\right)\right]\mid\mathbf{q}\left(0\right)\right]\right\}\\ &= \lim_{t\to\infty}\left\{\frac{1}{t^2}\sum_{n=1}^{t}\sum_{l=1}^{t}\mathbb{E}\left[\mathbb{P}\left(X_n=j,X_l=j\mid\mathbf{q}\left(0\right)\right)\right]\right\}\\ &= A. \qquad (3.13)\end{aligned}$$

Define by $n\wedge l=\max\left\{n,l\right\}$ and $n\vee l=\min\left\{n,l\right\}$ then we have that

$$\mathbb{P}\left(X_{n\wedge l}=j,X_{n\vee l}=j\mid\mathbf{q}\left(0\right)\right)=\mathbb{P}\left(X_{n\wedge l}=j\mid X_{n\vee l}=j,\mathbf{q}\left(0\right)\right)\mathbb{P}\left(X_{n\vee l}=j\mid\mathbf{q}\left(0\right)\right)$$

$$=\mathbb{P}\left(X_{n\wedge l}=j\mid q_j(0,n\vee l)=1\right)\mathbb{P}\left(X_{n\vee l}=j\mid\mathbf{q}\left(0\right)\right). \qquad (3.14)$$

Hence from (3.13) and (3.14) we get that

$$\begin{aligned}A &= \lim_{t\to\infty}\left\{\frac{1}{t^2}\sum_{n=1}^{t}\sum_{l=1}^{t}\mathbb{E}\left[\mathbb{P}\left(X_n=j,X_l=j\mid\mathbf{q}\left(0\right)\right)\right]\right\}\\ &= \lim_{t\to\infty}\left\{\frac{1}{t^2}\sum_{n=1}^{t}\sum_{l=1}^{t}\mathbb{E}\left[\mathbb{P}\left(X_{n\wedge l}=j\mid q_j(0,n\vee l)=1\right)\right]\mathbb{E}\left[\mathbb{P}\left(X_{n\vee l}=j\mid\mathbf{q}\left(0\right)\right)\right]\right\}\\ &= \lim_{t\to\infty}\left\{\frac{1}{t^2}\sum_{n=1}^{t}\sum_{l=1}^{t}\mathbb{E}\left[q_j^{(j)}\left(n\vee l,n\wedge l\right)\right]\mathbb{E}\left[q_j\left(0,n\vee l\right)\right]\right\}\\ &= \left(\text{since } q_j^{(j)}\left(s,t\right)=0 \text{ for } s>t\right)\\ &= \lim_{t\to\infty}\left\{\frac{1}{t^2}\sum_{n=1}^{t}\sum_{l=n}^{t}\mathbb{E}\left[q_j^{(j)}\left(n,l\right)\right]\mathbb{E}\left[q_j\left(0,n\right)\right]\right\}\\ &= \lim_{t\to\infty}\left\{\frac{1}{t}\sum_{n=1}^{t}\mathbb{E}\left[q_j\left(0,n\right)\right]\frac{1}{t}\sum_{l=n}^{t}\mathbb{E}\left[q_j^{(j)}\left(n,l\right)\right]\right\}=\text{(by Theorems 1,2 and 3)}\\ &= q_j^2\left(\infty\right). \qquad (3.15)\end{aligned}$$

Hence from $(3.6),(3,7),...,(3.15)$ we get (3.4) which completes the proof. □

Hence, we have actually proved, that under certain conditions the fraction of time the membership of an NHMS stays in a state after a large number of steps, converges in mean square to the limit of the relative population structure in that state. This result constitutes the Weak Law of Large Numbers for a NHMS. We are now going to proceed and prove under which conditions the mode of convergence is almost surely.

Theorem 12. *Let a probability space* $(\Omega,\mathcal{F},\mathbb{P})$ *and an NHMS as defined in section 2. Assume that a)* $\lim_{t\to\infty}\left\|\mathbf{Q}\left(t\right)-\mathbf{Q}\right\|=0$ *geometrically fast and* $\mathbf{Q}$ *a regular stochastic matrix; b)* $\lim_{t\to\infty}\left\|\mathbf{p}_0\left(t\right)-\mathbf{p}_0\right\|=0$ *geometrically fast c)* $\lim_{t\to\infty}\left[\Delta T\left(t\right)/T\left(t\right)\right]=0$ *geometrically fast. Then*

$$\boldsymbol{\nu}\left(t\right)\overset{a.s.}{\to}\mathbf{q}\left(\infty\right).$$

Proof. In Theorem 11 we have actually proved that

$$\nu_j\left(t\right)\overset{L^2}{\to}q_j\left(\infty\right) \text{ as } t\to\infty \text{ for ever } j\in S, \qquad (3.16)$$

or equivalently

$$\frac{1}{t}\sum_{s=1}^{t} u_j(s) \xrightarrow{L^2} q_j(\infty) \text{ as } t \to \infty \text{ for ever } j \in S, \tag{3.17}$$

from Theorem 5 (a) and (3.17) we get that

$$\frac{1}{t}\sum_{s=1}^{t} u_j(s) \xrightarrow{L^1} q_j(\infty) \text{ as } t \to \infty \text{ for ever } j \in S, \tag{3.18}$$

from Theorem 5 (b) and (3.18) we get that

$$\frac{1}{t}\sum_{s=1}^{t} u_j(s) \xrightarrow{P} q_j(\infty) \text{ as } t \to \infty \text{ for ever } j \in S. \tag{3.19}$$

By Theorem 6 there exists a non-random increasing sequence of integers $t_1, t_2, ...$ such that

$$\frac{1}{t_i}\sum_{s=1}^{t_i} u_j(s) \xrightarrow{a.s} q_j(\infty) \text{ as } i \to \infty \text{ for ever } j \in S. \tag{3.20}$$

We will now prove that such a choice of subsequence is $t_i = i^2$ for $i = 1, 2, ...$ In order to do so it is sufficient by Theorem 7 to show that

$$\text{For every } \epsilon > 0 \ \sum_i \mathbb{P}\left(\left|\frac{1}{i^2}\sum_{s=1}^{i^2} u_j(s) - q_j(\infty)\right| > \epsilon\right) < \infty. \tag{3.21}$$

By Theorem 8 , that is, Chebychov inequality we get that

$$\mathbb{P}\left(\left|\frac{1}{i^2}\sum_{s=1}^{i^2} u_j(s) - q_j(\infty)\right| > \epsilon\right) \leq \frac{\mathbb{E}\left[\left(\frac{1}{i^2}\sum_{s=1}^{i^2} u_j(s) - q_j(\infty)\right)^2\right]}{\epsilon^2}. \tag{3.22}$$

Therefore, we should prove that

$$\text{For every } \epsilon > 0 \ B = \frac{1}{\in^2}\sum_i \mathbb{E}\left[\left(\frac{1}{i^2}\sum_{s=1}^{i^2} u_j(s) - q_j(\infty)\right)^2\right] < \infty. \tag{3.23}$$

From (3.10) , (3.11) , (3.12) and (3.15) we get that

$$\begin{aligned} B &= \frac{1}{\in^2}\sum_i \frac{1}{i^4}\{\sum_{n=1}^{i^2}\sum_{l=1}^{i^2}[-q_j(\infty)\,\mathbb{E}[q_j(0,n)] + q_j^2(\infty) - q_j(\infty)\,\mathbb{E}[q_j(0,l)] \\ &\quad + \mathbb{E}\left[q_j^{(j)}(n\vee l, n\wedge l)\right]\mathbb{E}[q_j(0,n\vee l)]]\} \\ &\leq \frac{1}{\in^2}\sum_i \frac{1}{i^4}\sum_{n=1}^{i^2}\sum_{l=1}^{i^2}\{|q_j(\infty) - \mathbb{E}[q_j(0,n)]| + |q_j(\infty) - \mathbb{E}[q_j(0,l)]| \\ &\quad + |\mathbb{E}[q_j(0,n\vee l)] - q_j(\infty)| + \left|\mathbb{E}\left[q_j^{(j)}(n\vee l, n\wedge l)\right] - q_j(\infty)\right|\}. \end{aligned} \tag{3.24}$$

From Theorem 10 we get that there exists constants $c > 0$ and $0 < b < 1$ such that

$$\begin{aligned} |q_j(\infty) - \mathbb{E}[q_j(0,n)]| &\leq cb^n \ ; \ |q_j(\infty) - \mathbb{E}[q_j(0,l)]| \leq cb^l \text{ and } (3.25) \\ |\mathbb{E}[q_j(0, n \vee l)] - q_j(\infty)| &\leq cb^{n \vee l}. \end{aligned}$$

From Theorem 9 we get that there exists constants $c_1 > 0$ and $0 < b_1 < 1$ such that

$$\left| \mathbb{E}\left[q_j^{(j)}(n \vee l, n \wedge l) \right] - q_j(\infty) \right| \leq c_1 b_1^{n \wedge l - n \vee l}. \tag{3.26}$$

From (3.24), (3.25) and (3.26) we get that

$$B \leq \frac{1}{\epsilon^2} \sum_i \frac{1}{i^4} \sum_{n=1}^{i^2} \sum_{l=1}^{i^2} \left[cb^n + cb^l + cb^{n \vee l} + c_1 b_1^{n \wedge l - n \vee l} \right] < \infty.$$

Hence, we have proved that

$$\frac{1}{i^2} \sum_{s=1}^{i^2} u_j(s) \overset{a.s.}{\to} q_j(\infty). \tag{3.27}$$

We have that

$$\sum_{s=1}^{i^2} u_j(s) \text{ is monotonic non-decreasing,} \tag{3.28}$$

therefore

$$\sum_{s=1}^{i^2} u_j(s) \leq \sum_{s=1}^{t} u_j(s) \leq \sum_{s=1}^{(i+1)^2} u_j(s) \quad \text{if } i^2 \leq t \leq (i+1)^2, \tag{3.29}$$

from which we get

$$\frac{1}{(i+1)^2} \sum_{s=1}^{i^2} u_j(s) \leq \frac{1}{t} \sum_{s=1}^{t} u_j(s) \leq \frac{1}{i^2} \sum_{s=1}^{(i+1)^2} u_j(s) \quad \text{if } i^2 \leq t \leq (i+1)^2. \tag{3.30}$$

In (3.30) let $t \to \infty$, use the fact that $\lim_{i \to \infty} \left(i^2 / (i+1)^2 \right) \to 1$, and relation (3.27) to get

$$\frac{1}{t} \sum_{s=1}^{t} u_j(s) \overset{a.s.}{\to} q_j(\infty).$$

□

4. Convergence in the Cesaro sense for Cyclic NHMS

In the present section we study convergence of the relative population structure in the Cesaro sense for an NHMS which undergoes a cyclic behavior. This is a founding step in order to study Laws of Large Numbers in Cyc-NHMS in the next section. The importance of cyclic behavior was firstly stressed in Bartholomew (1982) p.71. The motive was Gani's (1963) study of student enrolment at Michigan state University. A general theorem for the limiting behavior of the expected population structure for a Cyc-NHMS was in given in Vassiliou (1984). Also, the asymptotic variability of nonhomogeneous Markov systems under cyclic behavior was studied in Vassiliou (1986). Georgiou and Tsantas (1996) studied asymptotic

attainability of nonstationary cyclic Markov systems as a natural extension of Cyc-NHMS.

We now provide the definition of a Cyc-NHMS

Definition 4. *Let a probability space* $(\Omega, \mathcal{F}, \mathbb{P})$ *and an NHMS as defined in section 2. We say that the NHMS undergoes a cyclic behavior with period* d *if and only if for all* $m = 1, 2, ...$ *and* $s = 0, 1, ..., d-1$

$$\mathbf{P}(md+s) = \mathbf{P}(s);\ \mathbf{p}_{k+1}^{\top}(md+s) = \mathbf{p}_{k+1}^{\top};\ \mathbf{p}_0(md+s) = \mathbf{p}_0. \tag{4.1}$$

It is apparent that for a Cyc-NHMS with period d we have that for all $m = 1, 2, ...$ and $s = 0, 1, ..., d-1$

$$\mathbf{Q}(md+s) = \mathbf{Q}(s). \tag{4.2}$$

We now define the following stochastic matrices

$$\begin{aligned} \mathbf{Q}_0 &= \mathbf{Q}(0)\mathbf{Q}(1)...\mathbf{Q}(d-1);\ \mathbf{Q}_1 = \mathbf{Q}(1)\mathbf{Q}(2)...\mathbf{Q}(d-1)\mathbf{Q}(0), ..., \\ \mathbf{Q}_{d-1} &= \mathbf{Q}(d-1)\mathbf{Q}(0)...\mathbf{Q}(d-2). \end{aligned} \tag{4.3}$$

It is well known that if $\mathbf{Q}_0$ is a regular stochastic matrix then $\lim_{t\to\infty}\mathbf{Q}_0^t = \mathbf{Q}_0^{\infty}$ a stable matrix or equivalently

$$\lim_{t\to\infty}\left\|\mathbf{Q}_0^t - \mathbf{Q}_0^{\infty}\right\| = 0. \tag{4.4}$$

We will now provide the following Proposition:

Proposition 1. *Let a probability space* $(\Omega, \mathcal{F}, \mathbb{P})$ *and a Cyc-NHMS. If* $\mathbf{Q}_0$ *is a regular stochastic matrix then*

$$\lim_{t\to\infty}\left\|\mathbf{Q}_i^t - \mathbf{Q}_i^{\infty}\right\| = 0, \quad \text{for } i = 1, 2, ..., d-1. \tag{4.5}$$

where

$$\mathbf{Q}_i^{\infty} = \mathbf{Q}_0^{\infty}\left(\prod_{j=0}^{i-1}\mathbf{Q}(j)\right), \quad \text{for } i = 1, 2, ..., d-1. \tag{4.6}$$

Proof. Since $\mathbf{Q}_0^{\infty}$ is a stable stochastic matrix we have that

$$\mathbf{Q}_i^{\infty} = \left(\prod_{j=i}^{d-1}\mathbf{Q}(j)\right)\mathbf{Q}_0^{\infty}\left(\prod_{j=0}^{i-1}\mathbf{Q}(j)\right), \tag{4.7}$$

therefore we have that

$$\begin{aligned} \mathbf{Q}_i^t &= \underbrace{\mathbf{Q}_i\mathbf{Q}_i...\mathbf{Q}_i}_{t\text{-times}} = \\ &= \mathbf{Q}(i)\mathbf{Q}(i+1)...\mathbf{Q}(d-1)\mathbf{Q}(0)\mathbf{Q}(1)...\mathbf{Q}(i-1) \\ &= \mathbf{Q}(i)\mathbf{Q}(i+1)...\mathbf{Q}(d-1)\mathbf{Q}(0)\mathbf{Q}(1)...\mathbf{Q}(i-1) \\ &= ..... \\ &= \mathbf{Q}(i)\mathbf{Q}(i+1)...\mathbf{Q}(d-1)\mathbf{Q}(0)\mathbf{Q}(1)...\mathbf{Q}(i-1) \\ &= \left(\prod_{j=i}^{d-1}\mathbf{Q}(j)\right)\mathbf{Q}_0^{t-1}\left(\prod_{j=0}^{i-1}\mathbf{Q}(j)\right), \end{aligned} \tag{4.8}$$

hence, for every $\epsilon > 0$ there is a t_0 such that for $t \geq t_0$

$$\left\|\mathbf{Q}_i^t - \mathbf{Q}_i^{\infty}\right\| =$$

$$\begin{aligned} & \left\| \left(\prod_{j=i}^{d-1} \mathbf{Q}(j) \right) \mathbf{Q}_0^{t-1} \left(\prod_{j=0}^{i-1} \mathbf{Q}(j) \right) - \left(\prod_{j=i}^{d-1} \mathbf{Q}(j) \right) \mathbf{Q}_0^{\infty} \left(\prod_{j=0}^{i-1} \mathbf{Q}(j) \right) \right\| \\ \leq & \left\| \mathbf{Q}_0^t - \mathbf{Q}_0^{\infty} \right\| < \epsilon. \end{aligned}$$

□

From Vassiliou and Georgiou (1990) p.541 we get the following Lemma

Lemma 1. *Let a probability space $(\Omega, \mathcal{F}, \mathbb{P})$ and an NHMS as defined in section 2. Suppose that the sequence*

$$\left\{ \frac{\Delta T(t)}{T(t)} \right\}_{t=0}^{\infty}$$

converges to zero geometrically fast with $T(t) \geq T(t-1)$. Then $\{T(t)\}_{t=0}^{\infty}$ converges geometrically fast.

Remark 1. *The assumption $lim_{t\to\infty} \frac{\Delta T(t)}{T(t)} = 0$ allows for $lim_{t\to\infty} T(t) = \infty$.*

We will now prove the following theorem

Theorem 13. *Let a probability space $(\Omega, \mathcal{F}, \mathbb{P})$ and a Cyc-NHMS. If (a) $\mathbf{Q}_0 = \mathbf{Q}(0)\mathbf{Q}(1)...\mathbf{Q}(d-1)$ is a regular stochastic matrix; $lim_{t\to\infty} \frac{\Delta T(t)}{T(t)} = 0$ with $\lim_{t\to\infty} T(t) = \infty$ then the sequence $\mathbb{E}[q(0,t)]$ splits into d subsequences with limits*

$$\begin{aligned} \mathbf{q}_s(\infty) &= \sum_{r=0}^{s-1} \mathbf{p}_0(r) s_r \mathbf{Q}_r^{(\infty)} \left(\prod_{j=r}^{s-1} \mathbf{Q}(j) \right) \\ &\quad + \sum_{r=s}^{d-1} \mathbf{p}_0(r) s_r \mathbf{Q}_r^{(\infty)} \left(\prod_{j=r}^{d-1} \mathbf{Q}(j) \right) \left(\prod_{j=0}^{s-1} \mathbf{Q}(j) \right) \\ \text{for } s &= 0, 1, ..., d-1. \end{aligned}$$

(b) $\mathbf{Q}_0 = \mathbf{Q}(0)\mathbf{Q}(1)...\mathbf{Q}(d-1)$ is a regular stochastic matrix; $lim_{t\to\infty} \frac{\Delta T(t)}{T(t)} = 0$ geometrically fast then the sequence $\mathbb{E}[q(0,t)]$ splits into d subsequences with limits

$$\begin{aligned} \mathbf{q}_s(\infty) &= \frac{T(0)}{T} \mathbf{q}(0) \mathbf{Q}_{s-1}^{(\infty)} + \sum_{r=0}^{s-1} \mathbf{p}_0(r) s_r \mathbf{Q}_r^{(\infty)} \left(\prod_{j=r}^{s-1} \mathbf{Q}(j) \right) \\ &\quad + \sum_{r=s}^{d-1} \mathbf{p}_0(r) s_r \mathbf{Q}_r^{(\infty)} \left(\prod_{j=r}^{d-1} \mathbf{Q}(j) \right) \left(\prod_{j=0}^{s-1} \mathbf{Q}(j) \right) \\ \text{for } s &= 0, 1, ..., d-1. \end{aligned}$$

Proof. Without loss of generality assume that $t = md + s$. Due to the fact that we have a Cyc-NHMS we get that

$$\mathbf{Q}(0, md+s-1) = \mathbf{Q}_0^m \left(\prod_{j=0}^{s-1} \mathbf{Q}(j) \right).$$

Since $\mathbf{Q}_0$is a regular stochastic matrix it is easy using (4.6) to see that

$$\lim_{m\to\infty} \left\| \mathbf{Q}(0, md+s-1) - \mathbf{Q}_{s-1}^{\infty} \right\| = 0. \tag{4.9}$$

Denote by

$$\begin{aligned} U(md+s) &= \frac{1}{T(md+s)}\sum_{\tau=1}^{md+s}\Delta T(\tau-1)\,\mathbf{p}_0(\tau-1)\,\mathbf{Q}(\tau,md+s-1) \\ &= \sum_{\tau=0}^{m-1}\sum_{r=0}^{d-1}\frac{\Delta T(\tau d+r)}{T(md+s)}\mathbf{p}_0(\tau d+r)\,\mathbf{Q}(\tau d+r,md+s-1) \quad (4.10) \\ &\quad +\sum_{r=0}^{s-1}\frac{\Delta T(md+r)}{T(md+s)}\mathbf{p}_0(md+r)\,\mathbf{Q}(md+r,md+s-1) \quad (4.11) \end{aligned}$$

From (4.11) we get that

$$\begin{aligned} &\lim_{m\to\infty}\left\|\sum_{r=0}^{s-1}\frac{\Delta T(md+r)}{T(md+s)}\mathbf{p}_0(md+r)\,\mathbf{Q}(md+r,md+s-1)\right\| \\ \leq\ &\lim_{m\to\infty}\sum_{r=0}^{s-1}\frac{\Delta T(md+r)}{T(md+s)}\left\|\mathbf{p}_0(md+r)\right\|\left\|\mathbf{Q}(md+r,md+s-1)\right\| \\ \leq\ &\lim_{m\to\infty}\sum_{r=0}^{s-1}\frac{\Delta T(md+r)}{T(md+s)}=0. \end{aligned} \quad (4.12)$$

Let $r\leq s-1$ then it is not difficult to see that

$$\mathbf{Q}(\tau d+r,md+s-1)=\mathbf{Q}_r^{(m-\tau)}\left(\prod_{j=r}^{s-1}\mathbf{Q}(j)\right). \quad (4.13)$$

On the other hand when $r>s-1$ then

$$\mathbf{Q}(\tau d+r,md+s-1)=\mathbf{Q}^{(m-\tau-1)}\left(\prod_{j=r}^{d-1}\mathbf{Q}(j)\right)\left(\prod_{j=0}^{s-1}\mathbf{Q}(j)\right). \quad (4.14)$$

The expression in (4.10) could be written as

$$\begin{aligned} &\sum_{\tau=0}^{m-1}\sum_{r=0}^{d-1}\frac{\Delta T(\tau d+r)}{T(md+s)}\mathbf{p}_0(\tau d+r)\,\mathbf{Q}(\tau d+r,md+s-1) \\ =\ &\sum_{\tau=0}^{m-1}\sum_{r=0}^{s-1}\frac{\Delta T(\tau d+r)}{T(md+s)}\mathbf{p}_0(\tau d+r)\,\mathbf{Q}(\tau d+r,md+s-1) \\ &+\sum_{\tau=0}^{m-1}\sum_{r=s}^{d-1}\frac{\Delta T(\tau d+r)}{T(md+s)}\mathbf{p}_0(\tau d+r)\,\mathbf{Q}(\tau d+r,md+s-1) \\ =\ &U_1(md+s)+U_2(md+s). \end{aligned} \quad (4.15)$$

We now have that

$$\begin{aligned} &\lim_{m\to\infty}\sum_{\tau=0}^{m-1}\sum_{r=0}^{s-1}\frac{\Delta T(\tau d+r)}{T(md+s)}\mathbf{p}_0(\tau d+r)\,\mathbf{Q}(\tau d+r,md+s-1) \\ =\ &\text{(from the fact that we have a Cyc-NHMS and (4.13))} \\ =\ &\sum_{r=0}^{s-1}\mathbf{p}_0(r)\lim_{m\to\infty}\sum_{\tau=0}^{m-1}\frac{\Delta T(\tau d+r)}{T(md+s)}\mathbf{Q}_r^{(m-\tau)}\left(\prod_{j=r}^{s-1}\mathbf{Q}(j)\right). \end{aligned} \quad (4.16)$$

Now the series

$$\sum_{\tau=0}^{m-1}\frac{\Delta T(\tau d+r)}{T(md+s)} \text{ for } r=0,1,...,d-1, \tag{4.17}$$

is bounded by the series

$$\sum_{\tau=0}^{t}\frac{\Delta T(\tau)}{T(t)}\leq 1,$$

hence

$$\lim_{m\to\infty}\sum_{\tau=0}^{m-1}\frac{\Delta T(\tau d+r)}{T(md+s)}\leq 1, \tag{4.18}$$

since $\{T(t)\}_{t=0}^{\infty}$ is a monotonically increasing function of t, we have $\frac{\Delta T(\tau d+r)}{T(md+s)}\geq 0$ and consequently the series in (4.18) is converging and denote by

$$s_r=\lim_{m\to\infty}\sum_{\tau=0}^{m-1}\frac{\Delta T(\tau d+r)}{T(md+s)} \quad \text{for} \quad r=0,1,...,d-1. \tag{4.19}$$

We now have that

$$\begin{aligned}&\left\|\sum_{\tau=0}^{m-1}\frac{\Delta T(\tau d+r)}{T(md+s)}\mathbf{Q}_r^{(m-\tau)}\left(\prod_{j=r}^{s-1}\mathbf{Q}(j)\right)-\sum_{\tau=0}^{m-1}\frac{\Delta T(\tau d+r)}{T(md+s)}\mathbf{Q}_r^{(\infty)}\left(\prod_{j=r}^{s-1}\mathbf{Q}(j)\right)\right\|\\ \leq &\sum_{\tau=0}^{m-1}\frac{\Delta T(\tau d+r)}{T(md+s)}\left\|\mathbf{Q}_r^{(m-\tau)}-\mathbf{Q}_r^{(\infty)}\right\|.\end{aligned} \tag{4.20}$$

From Proposition 1, (4.16), (4.18) and (4.20) we get that

$$\lim_{m\to\infty}U_1(md+s)=\sum_{r=0}^{s-1}\mathbf{p}_0(r)\,s_r\mathbf{Q}_r^{(\infty)}\left(\prod_{j=r}^{s-1}\mathbf{Q}(j)\right) \quad \text{for} \quad r\leq s-1. \tag{4.21}$$

In a similar way we arrive at

$$\lim_{m\to\infty}U_2(md+s)=\sum_{r=s}^{d-1}\mathbf{p}_0(r)\,s_r\mathbf{Q}_r^{(\infty)}\left(\prod_{j=r}^{d-1}\mathbf{Q}(j)\right)\left(\prod_{j=0}^{s-1}\mathbf{Q}(j)\right). \tag{4.22}$$

Hence, from (4.10), (4.11) and (4.15) we get that

$$\begin{aligned}\lim_{m\to\infty}U(md+s) &= \sum_{r=0}^{s-1}\mathbf{p}_0(r)\,s_r\mathbf{Q}_r^{(\infty)}\left(\prod_{j=r}^{s-1}\mathbf{Q}(j)\right)\\ &\quad+\sum_{r=s}^{d-1}\mathbf{p}_0(r)\,s_r\mathbf{Q}_r^{(\infty)}\left(\prod_{j=r}^{d-1}\mathbf{Q}(j)\right)\left(\prod_{j=0}^{s-1}\mathbf{Q}(j)\right).\end{aligned} \tag{4.23}$$

Now from (2.6) and (4.23) we get that for $\lim_{t\to\infty}\frac{\Delta T(t)}{T(t)}=0$ and $\lim_{t\to\infty}T(t)=\infty$ the sequence $\mathbb{E}[q(0,t)]$ splits into d subsequences with limits

$$\begin{aligned}\mathbf{q}_s(\infty) &= \sum_{r=0}^{s-1}\mathbf{p}_0(r)\,s_r\mathbf{Q}_r^{(\infty)}\left(\prod_{j=r}^{s-1}\mathbf{Q}(j)\right) \\ &\quad+\sum_{r=s}^{d-1}\mathbf{p}_0(r)\,s_r\mathbf{Q}_r^{(\infty)}\left(\prod_{j=r}^{d-1}\mathbf{Q}(j)\right)\left(\prod_{j=0}^{s-1}\mathbf{Q}(j)\right) \\ \text{for } s &= 0,1,...,d-1.\end{aligned} \tag{4.24}$$

If $\lim_{t\to\infty}\frac{\Delta T(t)}{T(t)}=0$ in a geometrical rate then by Lemma 1 $\lim_{t\to\infty}T(t)=T$ and the sequence $\mathbb{E}[q(0,t)]$ splits into d subsequences with limits

$$\begin{aligned}\mathbf{q}_s(\infty) &= \frac{T(0)}{T}\mathbf{q}(0)\,\mathbf{Q}_{s-1}^{(\infty)}+\sum_{r=0}^{s-1}\mathbf{p}_0(r)\,s_r\mathbf{Q}_r^{(\infty)}\left(\prod_{j=r}^{s-1}\mathbf{Q}(j)\right) \\ &\quad+\sum_{r=s}^{d-1}\mathbf{p}_0(r)\,s_r\mathbf{Q}_r^{(\infty)}\left(\prod_{j=r}^{d-1}\mathbf{Q}(j)\right)\left(\prod_{j=0}^{s-1}\mathbf{Q}(j)\right) \\ \text{for } s &= 0,1,...,d-1.\end{aligned} \tag{4.25}$$

□

We will now introduce the concept of Cesaro strongly ergodic for a Cycl-NHMS:

Definition 5. *A Cycl-NHMS is called Cesaro strongly ergodic if there exists a vector* $\mathbf{q}(\infty)$ *such that*

$$\lim_{t\to\infty}\left\|\frac{1}{t}\sum_{n=0}^{t}\mathbb{E}[\mathbf{q}(0,n)]-\mathbf{q}(\infty)\right\|=0.$$

We call the $\mathbf{q}(\infty)$ *the Cyclic strong run distribution for the NHMS.*

We will now provide a basic theorem on the Cesaro convergence for a Cycl-NHMS.

Theorem 14. *Let a Cycl-NHMS and let that:* (a) $\mathbf{Q}_0=\mathbf{Q}(0)\,\mathbf{Q}(1)...\mathbf{Q}(d-1)$ *is a regular stochastic matrix;* (b) $\lim_{t\to\infty}\frac{\Delta T(t)}{T(t)}=0$ *then the Cycl-NHMS is Cesaro strongly ergodic in the sense that*

$$\lim_{t\to\infty}\left\|\frac{1}{t}\sum_{n=0}^{t}\mathbb{E}[\mathbf{q}(0,n)]-\frac{1}{d}\sum_{s=0}^{d-1}\mathbf{q}_s(\infty)\right\|=0,$$

where

$$\begin{aligned}\mathbf{q}_s(\infty) &= \sum_{r=0}^{s-1}\mathbf{p}_0(r)\,s_r\mathbf{Q}_r^{(\infty)}\left(\prod_{j=r}^{s-1}\mathbf{Q}(j)\right) \\ &\quad+\sum_{r=s}^{d-1}\mathbf{p}_0(r)\,s_r\mathbf{Q}_r^{(\infty)}\left(\prod_{j=r}^{d-1}\mathbf{Q}(j)\right)\left(\prod_{j=0}^{s-1}\mathbf{Q}(j)\right).\end{aligned}$$

If (a) $\mathbf{Q}_0 = \mathbf{Q}(0)\mathbf{Q}(1)...\mathbf{Q}(d-1)$ *is a regular stochastic matrix;* $\left(\hat{b}\right)$ $\lim_{t\to\infty}\frac{\Delta T(t)}{T(t)} = 0$ *geometrically fast then the Cycl-NHMS is Cesaro strongly ergodic in the sense that*

$$\lim_{t\to\infty}\left\|\frac{1}{t}\sum_{n=0}^{t}\mathbb{E}\left[\mathbf{q}(0,n)\right] - \frac{1}{d}\sum_{s=0}^{d-1}\mathbf{q}_s(\infty)\right\| = 0,$$

where

$$\begin{aligned}\mathbf{q}_s(\infty) &= \frac{T(0)}{T}\mathbf{q}(0)\mathbf{Q}_{s-1}^{(\infty)} + \sum_{r=0}^{s-1}\mathbf{p}_0(r)\,s_r\mathbf{Q}_r^{(\infty)}\left(\prod_{j=r}^{s-1}\mathbf{Q}(j)\right)\\ &\quad + \sum_{r=s}^{d-1}\mathbf{p}_0(r)\,s_r\mathbf{Q}_r^{(\infty)}\left(\prod_{j=r}^{d-1}\mathbf{Q}(j)\right)\left(\prod_{j=0}^{s-1}\mathbf{Q}(j)\right).\end{aligned}$$

Proof. We start with the first part, that is (a) and (b) hold. Since the Cycl-NHMS is of finite size it is sufficient to show that

$$\lim_{t\to\infty}\frac{1}{t}\sum_{n=0}^{t}\mathbb{E}\left[\mathbf{q}(0,n)\right] = \frac{1}{d}\sum_{s=0}^{d-1}\mathbf{q}_s(\infty). \tag{4.26}$$

Let $\left[\frac{a}{b}\right]$ the integer part of the division then we have that

$$\frac{1}{t}\sum_{n=0}^{t}\mathbb{E}\left[\mathbf{q}(0,n)\right] = \frac{1}{t}\sum_{n=0}^{d[t/d]-1}\mathbb{E}\left[\mathbf{q}(0,n)\right] + \frac{1}{t}\sum_{n=d[t/d]}^{t}\mathbb{E}\left[\mathbf{q}(0,n)\right]. \tag{4.27}$$

Now we have that

$$\begin{aligned}\lim_{t\to\infty}\frac{1}{t}\sum_{n=0}^{d[t/d]-1}\mathbb{E}\left[\mathbf{q}(0,n)\right] &= \lim_{t\to\infty}\frac{1}{t}\sum_{s=0}^{d-1}\sum_{n=0}^{[t/d]-1}\mathbb{E}\left[\mathbf{q}(0,nd+s)\right] \qquad (4.28)\\ &= \sum_{s=0}^{d-1}\lim_{t\to\infty}\frac{[t/d]}{t}\frac{1}{[t/d]}\sum_{n=0}^{[t/d]-1}\mathbb{E}\left[\mathbf{q}(0,nd+s)\right].\end{aligned}$$

From (a), (b), Theorem 13 and the fact that the series is an arithmetic mean we get that

$$\begin{aligned}\lim_{t\to\infty}\frac{1}{[t/d]}\sum_{n=0}^{[t/d]-1}\mathbb{E}\left[\mathbf{q}(0,nd+s)\right] &= \sum_{r=0}^{s-1}\mathbf{p}_0(r)\,s_r\mathbf{Q}_r^{(\infty)}\left(\prod_{j=r}^{s-1}\mathbf{Q}(j)\right) \qquad (4.29)\\ &\quad + \sum_{r=s}^{d-1}\mathbf{p}_0(r)\,s_r\mathbf{Q}_r^{(\infty)}\left(\prod_{j=r}^{d-1}\mathbf{Q}(j)\right)\left(\prod_{j=0}^{s-1}\mathbf{Q}(j)\right)\end{aligned}$$

Also $\lim_{t\to\infty}[t/d]/t = 1/d$ therefore from (4.28) and (4.29) we get that

$$\begin{aligned}\lim_{t\to\infty}\frac{1}{t}\sum_{n=0}^{d[t/d]-1}\mathbb{E}\left[\mathbf{q}(0,n)\right] &= \frac{1}{d}\sum_{s=0}^{d-1}\sum_{r=0}^{s-1}\mathbf{p}_0(r)\,s_r\mathbf{Q}_r^{(\infty)}\left(\prod_{j=r}^{s-1}\mathbf{Q}(j)\right) \qquad (4.30)\\ &\quad + \frac{1}{d}\sum_{s=0}^{d-1}\sum_{r=s}^{d-1}\mathbf{p}_0(r)\,s_r\mathbf{Q}_r^{(\infty)}\left(\prod_{j=r}^{d-1}\mathbf{Q}(j)\right)\left(\prod_{j=0}^{s-1}\mathbf{Q}(j)\right).\end{aligned}$$

Now it is easy to see that

$$\lim_{t\to\infty}\frac{1}{t}\sum_{n=d[t/d]}^{t}\mathbb{E}\left[\mathbf{q}\left(0,n\right)\right]=0. \tag{4.31}$$

The second part of the Theorem is proved in a similar way. □

5. Laws of Large numbers for a Cycl-NHMS

We are now in a position to study the first Law of Large Numbers for a Cycl-NHMS. We will start with the mode of mean square convergence. Let $X_t, u_j\left(t\right), y_j\left(t\right)$ and $\nu_j\left(t\right)$ be defined as in section 3. We will now provide and prove the following theorem of the Law of Large Numbers

Theorem 15. *Let a probability space $(\Omega,\mathcal{F},\mathbb{P})$ and a Cyc-NHMS. If (a) $\mathbf{Q}_0=\mathbf{Q}\left(0\right)\mathbf{Q}\left(1\right)...\mathbf{Q}\left(d-1\right)$ is a regular stochastic matrix and $lim_{t\to\infty}\frac{\Delta T(t)}{T(t)}=0$ then*

$$\boldsymbol{\nu}\left(t\right)\overset{L^2}{\to}\frac{1}{d}\sum_{s=0}^{d-1}\mathbf{q}_s\left(\infty\right),$$

where $\mathbf{q}_s\left(\infty\right)$ is given by (4.24) if in addition $T\left(t\right)\to_{t\to\infty}\infty$; and where $\mathbf{q}_s\left(\infty\right)$ is given by (4.25) if $lim_{t\to\infty}\frac{\Delta T(t)}{T(t)}=0$ geometrically fast.

Proof. It is equivalent to show that

$$\lim_{t\to\infty}\mathbb{E}\left[\left(\boldsymbol{\nu}\left(t\right)-\frac{1}{d}\sum_{s=0}^{d-1}\mathbf{q}_s\left(\infty\right)\right)^2\right]=0. \tag{5.1}$$

Since the dimensions of the vectors are finite it is equivalent to show that

$$\lim_{t\to\infty}\mathbb{E}\left[\left(\nu_j\left(t\right)-\frac{1}{d}\sum_{s=0}^{d-1}q_{sj}\left(\infty\right)\right)^2\right]=0\quad\text{for}\quad j=1,2,...,k. \tag{5.2}$$

We have that

$$\begin{aligned}\mathbb{E}\left[\left(\nu_j\left(t\right)-\frac{1}{d}\sum_{s=0}^{d-1}q_{sj}\left(\infty\right)\right)^2\right] &= \mathbb{E}\left[\left(\sum_{n=1}^{t}\frac{u_j\left(n\right)}{t}-\frac{1}{d}\sum_{s=0}^{d-1}q_{sj}\left(\infty\right)\right)^2\right] \\ &= \frac{1}{t^2}\mathbb{E}\left[\left(\sum_{n=1}^{t}\left(u_j\left(n\right)-\frac{1}{d}\sum_{s=0}^{d-1}q_{sj}\left(\infty\right)\right)\right)^2\right]\end{aligned} \tag{5.3}$$

$$=\frac{1}{t^2}\mathbb{E}\left[\left(\sum_{n=1}^{t}\left(u_j\left(n\right)-\frac{1}{d}\sum_{s=0}^{d-1}q_{sj}\left(\infty\right)\right)\right)\left(\sum_{l=1}^{t}\left(u_j\left(l\right)-\frac{1}{d}\sum_{s=0}^{d-1}q_{sj}\left(\infty\right)\right)\right)\right].$$

Therefore we get that

$$\mathbb{E}\left[\left(\nu_j\left(t\right)-\frac{1}{d}\sum_{s=0}^{d-1}q_{sj}\left(\infty\right)\right)^2\right]=\frac{1}{t^2}\sum_{n=1}^{t}\sum_{l=1}^{t}\mathbb{E}\left[u_j\left(n\right)u_j\left(l\right)\right] \tag{5.4}$$

$$-\frac{1}{t^2d}\sum_{s=0}^{d-1}\sum_{n=1}^{t}\sum_{l=1}^{t}q_{sj}\left(\infty\right)\mathbb{E}\left[u_j\left(n\right)\right] \tag{5.5}$$

$$-\frac{1}{t^2 d}\sum_{s=0}^{d-1}\sum_{n=1}^{t}\sum_{l=1}^{t} q_{sj}(\infty)\,\mathbb{E}\left[u_j(l)\right] \tag{5.6}$$

$$+\frac{1}{t^2}\sum_{n=1}^{t}\sum_{l=1}^{t}\left(\frac{1}{d}\sum_{s=0}^{d-1} q_{sj}(\infty)\right)^2. \tag{5.7}$$

We start with relation (5.5)

$$\begin{aligned}
\lim_{t\to\infty}\left\{-\frac{1}{t^2 d}\sum_{s=0}^{d-1}\sum_{n=1}^{t}\sum_{l=1}^{t} q_{sj}(\infty)\,\mathbb{E}\left[u_j(n)\right]\right\} &= \lim_{t\to\infty}\left\{-\frac{1}{d}\sum_{s=0}^{d-1} q_{sj}(\infty)\,\frac{1}{t}\sum_{n=1}^{t}\mathbb{E}\left[u_j(n)\right]\right\}\\
&= \lim_{t\to\infty}\left\{-\frac{1}{d}\sum_{s=0}^{d-1} q_{sj}(\infty)\,\frac{1}{t}\sum_{n=1}^{t}\mathbb{E}\left[\mathbb{E}\left[u_j(n)\mid \mathbf{q}(0)\right]\right]\right\}\\
&= \lim_{t\to\infty}\left\{-\frac{1}{d}\sum_{s=0}^{d-1} q_{sj}(\infty)\,\frac{1}{t}\sum_{n=1}^{t}\mathbb{E}\left[\mathbb{P}\left(X_n=j\right)\mid \mathbf{q}(0)\right]\right\}\\
&= \lim_{t\to\infty}\left\{-\frac{1}{d}\sum_{s=0}^{d-1} q_{sj}(\infty)\,\frac{1}{t}\sum_{n=1}^{t}\mathbb{E}\left[q_j(0,n)\right]\right\}\\
&= \text{(by Theorem 14)} = -\left(\frac{1}{d}\sum_{s=0}^{d-1} q_{sj}(\infty)\right)^2. \qquad (5.8)
\end{aligned}$$

Similarly we get that

$$-\frac{1}{t^2 d}\sum_{s=0}^{d-1}\sum_{n=1}^{t}\sum_{l=1}^{t} q_{sj}(\infty)\,\mathbb{E}\left[u_j(l)\right] = -\left(\frac{1}{d}\sum_{s=0}^{d-1} q_{sj}(\infty)\right)^2. \tag{5.9}$$

It is easy to see that

$$\frac{1}{t^2}\sum_{n=1}^{t}\sum_{l=1}^{t}\left(\frac{1}{d}\sum_{s=0}^{d-1} q_{sj}(\infty)\right)^2 = \left(\frac{1}{d}\sum_{s=0}^{d-1} q_{sj}(\infty)\right)^2. \tag{5.10}$$

The term (5.4) could be written as

$$\begin{aligned}
\lim_{t\to\infty}\left\{\frac{1}{t^2}\sum_{n=1}^{t}\sum_{l=1}^{t}\mathbb{E}\left[u_j(n)\,u_j(l)\right]\right\} &= \lim_{t\to\infty}\left\{\frac{1}{t^2}\sum_{n=1}^{t}\sum_{l=1}^{t}\mathbb{E}\left[\mathbb{E}\left[u_j(n)\,u_j(l)\mid \mathbf{q}(0)\right]\right]\right\}\\
&= B \qquad (5.11)
\end{aligned}$$

Now from (5.11) and (3.14) we get that

$$\begin{aligned}
B &= \lim_{t\to\infty}\left\{\frac{1}{t^2}\sum_{n=1}^{t}\sum_{l=1}^{t}\mathbb{E}\left[\mathbb{P}\left[u_j\left(n\right)u_j\left(l\right)\mid\mathbf{q}\left(0\right)\right]\right]\right\}\\
&= \text{(from (3.14))}\\
&= \lim_{t\to\infty}\left\{\frac{1}{t^2}\sum_{n=1}^{t}\sum_{l=1}^{t}\mathbb{E}\left[\mathbb{P}\left(X_{n\wedge l}=j\mid q_j\left(0,n\vee l\right)=1\right)\right]\mathbb{E}\left[\mathbb{P}\left[X_{n\vee l}=j\mid\mathbf{q}\left(0\right)\right]\right]\right\}\\
&= \lim_{t\to\infty}\left\{\frac{1}{t^2}\sum_{n=1}^{t}\sum_{l=1}^{t}\mathbb{E}\left[q_j^{(j)}\left(n\vee l,n\wedge l\right)\right]\mathbb{E}\left[q_j\left(0,n\vee l\right)\right]\right\}\\
&= \left(\text{since } q_j^{(j)}\left(s,t\right)\ =0 \text{ for } s>t\right)\\
&= \lim_{t\to\infty}\left\{\frac{1}{t^2}\sum_{n=1}^{t}\sum_{l=n}^{t}\mathbb{E}\left[q_j^{(j)}\left(n,l\right)\right]\mathbb{E}\left[q_j\left(0,n\right)\right]\right\}\\
&= \lim_{t\to\infty}\left\{\frac{1}{t}\sum_{n=1}^{t}\mathbb{E}\left[q_j\left(0,n\right)\right]\frac{1}{t}\sum_{l=n}^{t}\mathbb{E}\left[q_j^{(j)}\left(n,l\right)\right]\right\}\\
&= \text{(by Theorem 14 and 13)}\\
&= \left(\frac{1}{d}\sum_{s=0}^{d-1}q_{sj}\left(\infty\right)\right)\left(\frac{1}{d}\sum_{s=0}^{d-1}q_{sj}\left(\infty\right)\right)=\\
&= \left(\frac{1}{d}\sum_{s=0}^{d-1}q_{sj}\left(\infty\right)\right)^2. \qquad (5.12)
\end{aligned}$$

From $(5.3),(5.4),...,(5.12)$ we get (5.1) and that completes the proof. □

We will now establish under what conditions the L^2 convergence of the Law of Large numbers we proved in Theorem 15 holds for almost sure convergence also. In order to do so we need the following founding Theorem which provides the conditions under which the Cesaro convergence in Theorem 14 is with geometrical rate.

Theorem 16. *Let a probability space $(\Omega,\mathcal{F},\mathbb{P})$ and a Cyc-NHMS. If (a) $\mathbf{Q}_0=\mathbf{Q}\left(0\right)\mathbf{Q}\left(1\right)...\mathbf{Q}\left(d-1\right)$ is a regular stochastic matrix and $lim_{t\to\infty}\frac{\Delta T(t)}{T(t)}=0$ geometrically fast then*

$$\lim_{t\to\infty}\left\|\frac{1}{t}\sum_{n=0}^{t}\mathbb{E}\left[\mathbf{q}\left(0,n\right)\right]-\frac{1}{d}\sum_{s=0}^{d-1}\mathbf{q}_s\left(\infty\right)\right\|=0,$$

in a geometrical rate.

Proof. From the fact that $\mathbf{Q}_0$ is a regular stochastic matrix we know that

$$\text{There exists } c_0>0 \text{ and } 0<b_0<1 \text{ such that } \left\|\mathbf{Q}_0^t-\mathbf{Q}_0^{(\infty)}\right\|\leq c_0b_0^t. \qquad (5.13)$$

From the end of the proof of Proposition 1 we get that

$$\left\|\mathbf{Q}_i^t-\mathbf{Q}_i^{(\infty)}\right\|\leq c_0b_0^{t-1}, \qquad (5.14)$$

hence the convergence is geometric. Now we have

$$\left\| \mathbf{Q}\left(0, md+s-1\right) - \mathbf{Q}_0^{(\infty)} \left(\prod_{j=0}^{s-1} \mathbf{Q}\left(j\right) \right) \right\| \tag{5.15}$$

$$= \left\| \mathbf{Q}_0^m \left(\prod_{j=0}^{s-1} \mathbf{Q}\left(j\right) \right) - \mathbf{Q}_0^{(\infty)} \left(\prod_{j=0}^{s-1} \mathbf{Q}\left(j\right) \right) \right\| \leq \left\| \mathbf{Q}_0^m - \mathbf{Q}_0^{(\infty)} \right\| \leq c_0 b_0^m.$$

From Vassiliou and Georgiou (1990) we know that since $\lim_{t\to\infty} \Delta T\left(t\right)/T\left(t\right) = 0$ geometrically fast, then the sequence $\left\{T\left(t\right)\right\}_{t=0}^{\infty}$ converges geometrically fast to a positive scalar T and so there exists $c_1 > 0$ and $0 < b_1 < 1$ such that

$$\left| \frac{1}{T\left(t\right)} - \frac{1}{T} \right| < c_1 b_1^t \ . \tag{5.16}$$

We start with the first part of the right hand side of equation (2.6) for the case of Cycl-NHMS:

$$\left\| \frac{T\left(0\right)}{T\left(md+s\right)} \mathbf{q}\left(0\right) \mathbf{Q}\left(0, md+s-1\right) - \frac{T\left(0\right)}{T} \mathbf{q}\left(0\right) \mathbf{Q}_{s-1}^{(\infty)} \right\| \tag{5.17}$$

$$\leq \ T\left(0\right) \left\| \mathbf{q}\left(0\right) \right\| \left\| \frac{1}{T\left(md+s\right)} \mathbf{Q}\left(0, md+s-1\right) - \frac{1}{T} \mathbf{Q}_{s-1}^{(\infty)} \right\|$$

$$\leq \ \left| \frac{1}{T\left(md+s\right)} - \frac{1}{T} \right| \left\| \mathbf{Q}\left(0, md+s-1\right) \right\| + \left| \frac{1}{T} \right| \left\| \mathbf{Q}\left(0, md+s-1\right) - \mathbf{Q}_{s-1}^{(\infty)} \right\|$$

$$= \ \text{(from (5.15) and (5.16))} \leq c_2 b_2^m \ \text{ with } c_2 > 0 \text{ and } 0 < b_2 < 1.$$

Now we have that

$$\| \frac{1}{T\left(ms+s\right)} \sum_{\tau=0}^{m-1} \sum_{r=0}^{s-1} \Delta T\left(\tau d+r\right) \mathbf{p}_0\left(\tau d+r\right) \mathbf{Q}\left(\tau d+r, md+s-1\right)$$

$$- \frac{1}{T} \sum_{\tau=0}^{m-1} \sum_{r=0}^{s-1} \Delta T\left(\tau d+r\right) \mathbf{p}_0\left(r\right) \mathbf{Q}_r^{(\infty)} \left(\prod_{j=r}^{s-1} \mathbf{Q}\left(j\right) \right) \| \tag{5.18}$$

$$\leq \| \frac{1}{T\left(ms+s\right)} \sum_{\tau=0}^{m-1} \sum_{r=0}^{s-1} \Delta T\left(\tau d+r\right) \mathbf{p}_0\left(\tau d+r\right) \mathbf{Q}\left(\tau d+r, md+s-1\right)$$

$$- \frac{1}{T} \sum_{\tau=0}^{m-1} \sum_{r=0}^{s-1} \Delta T\left(\tau d+r\right) \mathbf{p}_0\left(\tau d+r\right) \mathbf{Q}\left(\tau d+r, md+s-1\right) \|$$

$$+ \| \frac{1}{T} \sum_{\tau=0}^{m-1} \sum_{r=0}^{s-1} \Delta T\left(\tau d+r\right) \mathbf{p}_0\left(\tau d+r\right) \mathbf{Q}\left(\tau d+r, md+s-1\right)$$

$$- \frac{1}{T} \sum_{\tau=0}^{m-1} \sum_{r=0}^{s-1} \Delta T\left(\tau d+r\right) \mathbf{p}_0\left(r\right) \mathbf{Q}_r^{(\infty)} \left(\prod_{j=r}^{s-1} \mathbf{Q}\left(j\right) \right) \| = I_1 + I_2 \tag{5.20}$$

From relation (5.19) we get that

$$I_1 \leq \left|\frac{1}{T(md+s)} - \frac{1}{T}\right| \sum_{\tau=0}^{m-1}\sum_{r=0}^{s-1} \parallel \Delta T(\tau d+r)\,\mathbf{p}_0(\tau d+r)\,\mathbf{Q}(\tau d+r, md+s-1) \parallel$$

$$\leq \left|\frac{1}{T(md+s)} - \frac{1}{T}\right| \sum_{\tau=0}^{m-1}\sum_{r=0}^{s-1} \Delta T(\tau d+r) \parallel \mathbf{p}_0(\tau d+r) \parallel\parallel \mathbf{Q}(\tau d+r, md+s-1) \parallel$$

$$\leq \left|\frac{1}{T(md+s)} - \frac{1}{T}\right| [T - T(0)] \leq c_2 b_2^{md+s}. \tag{5.21}$$

Also

$$\begin{aligned} I_2 &\leq \frac{1}{T}\sum_{\tau=0}^{m-1}\sum_{r=0}^{s-1} \Delta T(\tau d+r)\,\|\mathbf{p}_0(r)\| \left\| \mathbf{Q}(\tau d+r, md+s-1) - \mathbf{Q}_r^{(\infty)} \left(\prod_{j=r}^{s-1} \mathbf{Q}(j)\right)\right\| \\ &\leq \frac{1}{T}\sum_{\tau=0}^{m-1}\sum_{r=0}^{s-1} \Delta T(\tau d+r) \left\|\mathbf{Q}_r^{(m-\tau)} - \mathbf{Q}_r^{(\infty)}\right\|. \end{aligned} \tag{5.22}$$

Assume that for $m \geq t_0$: $\left\|\mathbf{Q}_r^{(m-\tau)} - \mathbf{Q}_r^{(\infty)}\right\| \leq c_3 b_3^{m-t_0}$ then

(5.23)

$$I_2 \leq \frac{1}{T}\sum_{\tau=0}^{m-t_0}\sum_{r=0}^{s-1} \Delta T(\tau d+r) \left\|\mathbf{Q}_r^{(m-\tau)} - \mathbf{Q}_r^{(\infty)}\right\| + \frac{1}{T}\sum_{\tau=m-t_0+1}^{m-1}\sum_{r=0}^{s-1} \Delta T(\tau d+r) \left\|\mathbf{Q}_r^{(m-\tau)} - \mathbf{Q}_r^{(\infty)}\right\|,$$

from which we get that I_2 goes geometrically fast to zero. Therefore relation (5.18) converges geometrically fast to zero. In a similar way one could prove, that the convergence in (4.22) is geometrically fast. Hence, we get that

$$\mathbb{E}[0, \mathbf{q}(md+s)] \to_{m\to\infty} \mathbf{q}_s(\infty) \quad \text{geometrically fast.} \tag{5.24}$$

Now following the steps of Theorem 14 it is easy to show that

$$\lim_{t\to\infty} \left\| \frac{1}{t}\sum_{n=0}^{t} \mathbb{E}[\mathbf{q}(0,n)] - \frac{1}{d}\sum_{s=0}^{d-1} \mathbf{q}_s(\infty)\right\| = 0,$$

in a geometrical rate. □

Having proved this basic result, we are now in a position following the steps of the proof of Theorem 12 where the role of Theorems 9 and 10 is now played by Theorem16 to arrive at the following theorem.

Theorem 17. *Let a probability space $(\Omega, \mathcal{F}, \mathbb{P})$ and a Cyc-NHMS. If (a) $\mathbf{Q}_0 = \mathbf{Q}(0)\mathbf{Q}(1)...\mathbf{Q}(d-1)$ is a regular stochastic matrix and $lim_{t\to\infty}\frac{\Delta T(t)}{T(t)} = 0$ geometrically fast then*

$$\boldsymbol{\nu}(t) \overset{a.s}{\to} \frac{1}{d}\sum_{s=0}^{d-1} \mathbf{q}_s(\infty) \quad as \quad t \to \infty.$$

6. Applications

6.1. **Geriatric and Stroke Patients.** In the present section we present two types of applications. The first one in the present subsection is a general Coxian phase type model, special forms of which has been used as stochastic models for geriatric patients and stroke patients by McClean and her co-authors (McClean et.al. (1998a, 1998b, 2007, 2009), Taylor et.al. (2000),Marshall and McClean (2002,2003,2004), Lalit et.al. (2010), McClean et.al. (2014, 2014b). In these applications in the basic model, we distinguish three states which are called hospital pathways. In the case of geriatric patients the states are the "Acute Care", the "Rehabilative" and the "Long Stay". From each state we have movements outside the hospital due to discharge or death. Also, geriatric patiens may be thought of as progressing through stages of acute care, rehabilitation and long-stay care, where most patients are eventually rehabilitated and discharged. Geriatric medical services are an important asset in the care of the elderly, while at the same time they can be easy victims of the political pressure on savings in health care expenditure. Note that the number of pathways could be increased and the criterion is what best fits the data. However, there is no reason to consider a larger number of states in here due to the restriction of space. It is of importance in the best management of hospital resources and certainly to the benefit of geriatric patients to know the tendencies of the system in the long run. That is, what proportion of the total population is going to be in each state. In the case of stroke patients there are more types of transitions due to the nature of stroke, which allows for relapses and hence more transitions among the hospital pathways. The model we will illustrate in what follows could be easily adjusted for both cases.

Consider a hospital which starts with $T(0) = 400$ patients and in a very short time reaches its full capacity of 435 patients. That is $T(1) = 420$, $T(2) = 430$, $T(3) = 435$. Assume three hospital pathways and let that the initial relative population structure is

$$\mathbf{q}(0) = \begin{pmatrix} 0.5 & 0.25 & 0.25 \end{pmatrix}.$$

The vast majority of new patients enter the system in hospital pathway one, either by taking an empty place or as a virtual replacement of a discharged patient, that is $q_{11}(t) = p_{11}(t) + p_{14}(t) p_{01}(t)$. In here state 4 expresses the external enviroment. The entrance probabilities are

$$\mathbf{p}_0(0) = \begin{pmatrix} 0.6 & 0.3 & 0.1 \end{pmatrix}; \ \mathbf{p}_0(1) = \begin{pmatrix} 0.5 & 0.3 & 0.2 \end{pmatrix};$$

$$\mathbf{p}_0(2) = \begin{pmatrix} 0.75 & 0.25 & 0.1 \end{pmatrix} \text{ and } \mathbf{p}_0 = \mathbf{p}_0(t) = \begin{pmatrix} 0.7 & 0.2 & 0.1 \end{pmatrix};$$

for $t = 3, 4, ...$ The form of the transition probability matrices according to the stochastic model for movements in the hospital is the following

$$\mathbf{P}(t) = \begin{pmatrix} p_{11}(t) & p_{12}(t) & p_{13}(t) \\ 0 & p_{22}(t) & p_{23}(t) \\ 0 & 0 & p_{33}(t) \end{pmatrix},$$

also the inherent non-homogeneous Markov chain will evolve with the sequence of stochastic matrices $\mathbf{Q}(t) = \{q_{ij}(t)\}_{i,j \in S}$ where $q_{ij}(t) = p_{ij}(t) + p_{i4}(t) p_{0j}(t)$. We get the following typical set of $\mathbf{Q}(t)$'s which are easily estimated from the data by

its maximum likelihood estimates:

$$\mathbf{Q}(0)=\begin{pmatrix}0.7 & 0.2 & 0.1\\ 0.2 & 0.6 & 0.2\\ 0.6 & 0.1 & 0.3\end{pmatrix};\quad \mathbf{Q}(1)=\begin{pmatrix}0.65 & 0.25 & 0.1\\ 0.1 & 0.7 & 0.2\\ 0.5 & 0.1 & 0.4\end{pmatrix};$$

$$\mathbf{Q}(2)=\begin{pmatrix}0.5 & 0.3 & 0.2\\ 0.2 & 0.5 & 0.3\\ 0.4 & 0.2 & 0.4\end{pmatrix};\quad \mathbf{Q}(t)=\mathbf{Q}=\begin{pmatrix}0.6 & 0.3 & 0.1\\ 0.14 & 0.6 & 0.26\\ 0.49 & 0.14 & 0.37\end{pmatrix},$$

for $t=2,3,....$ The row of the stable matrix $\lim_{t\to\infty}\mathbf{Q}^t=\mathbf{Q}(\infty)=\begin{pmatrix}\mathbf{q}(\infty) & \mathbf{q}(\infty) & \mathbf{q}(\infty)\end{pmatrix}^\top$ is

$$\mathbf{q}(\infty)=\begin{pmatrix}0.41 & 0.37 & 0.22\end{pmatrix},$$

where the convergence is geometrically fast, that is for $t=5$ it already converges. Now simulating Theorem 11 we find that

$Time$	$\mathbb{E}\left[\left(\nu_1(t)-q_1(\infty)\right)^2\right]$
$t=5$	0.01380
$t=6$	0.0007

From the above table it is apparent that

$$\nu_1(t)\overset{L^2}{\to}0.41$$

Analogous results are found also for the remaining of the hodpital pathways. That is

$$\boldsymbol{\nu}(t)\overset{L^2}{\to}\begin{pmatrix}0.41 & 0.37 & 0.22\end{pmatrix}.$$

Now, since as we have seen $\Delta T(t)/T(t)\to 0$ geometrically fast, that is, for $t=3$, and since as we have seen $\lim_{t\to\infty}\mathbf{Q}^t$ conveges to $\mathbf{Q}(\infty)$ geometrically fast, that is, for $t=5$, then according to Theorem 12 we have

$$\boldsymbol{\nu}(t)\overset{a.s}{\to}\begin{pmatrix}0.41 & 0.37 & 0.22\end{pmatrix}.$$

One of the useful for hospital planning physical meanings of the above result is, that a membesrship of a patient remains in hospital pathway 1, in the long run, almost surely the 0.41 of the time the hospital is in operation. Another useful physical meaning for hospital planning, is that the relative population structure of the memberships in the various hospital pathways tends asymptotically almost surely to $\begin{pmatrix}0.41 & 0.37 & 0.22\end{pmatrix}$.

6.2. **A University System.** In this subsection we illustrate an application of a cyclic non-homogeneous Markov system in a University system. The importance of cyclic behavior was firstly stressed in Bartholomew (1982), p.71, where he also provided an interesting application of this concept which arose in Gani's (1963) study of student enrolment at Michigan State University. We consider the university system in Vassiliou and Tsantas (1984) with 3 years of study where the students that fail their year repeat it in the following year. The estimates of the transition

probability matrices taken from Tsantas and Vassiliou (1984) assuming a cyclic repetition are

$$\mathbf{P}(3t) = \begin{pmatrix} 0.17188 & 0.81875 & 0 \\ 0 & 0.29873 & 0.68644 \\ 0 & 0 & 0.32303 \end{pmatrix},$$

$$\mathbf{P}(3t+1) = \begin{pmatrix} 0.19379 & 0.7726 & 0 \\ 0 & 0.33503 & 0.65482 \\ 0 & 0 & 0.53563 \end{pmatrix},$$

$$\mathbf{P}(3t+2) = \begin{pmatrix} 0.16631 & 0.81641 & 0 \\ 0 & 0.34318 & 0.64557 \\ 0 & 0 & 0.50860 \end{pmatrix}.$$

Also

$$p_4(3t) = \begin{pmatrix} 0.00937 & 0.01483 & 0.67697 \end{pmatrix},$$

$$p_4(3t+1) = \begin{pmatrix} 0.03361 & 0.01015 & 0.46437 \end{pmatrix},$$

and

$$p_4(3t+2) = \begin{pmatrix} 0.01728 & 0.01125 & 0.49140 \end{pmatrix},$$

and $\mathbf{p}_0(t) = \begin{pmatrix} 1 & 0 & 0 \end{pmatrix}$ for every $t = 0, 1, 2, ...$ The total population of students is $T(0) = 8970$, $T(1) = 9000$, $T(2) = 9050$ and $T(t) = 9050$ for $t = 3, 4, ...$ Then we have

$$\mathbf{Q}(3t) = \begin{pmatrix} 0.181 & 0.819 & 0 \\ 0.015 & 0.299 & 0.686 \\ 0.677 & 0 & 0.323 \end{pmatrix}, \quad \mathbf{Q}(3t+1) = \begin{pmatrix} 0.227 & 0.773 & 0 \\ 0.010 & 0.335 & 0.655 \\ 0.464 & 0 & 0.536 \end{pmatrix},$$

$$\mathbf{Q}(3t+2) = \begin{pmatrix} 0.184 & 0.816 & 0 \\ 0.011 & 0.343 & 0.646 \\ 0.491 & 0 & 0.509 \end{pmatrix}, \quad \text{for } t = 0, 1, 2, ...$$

Then

$$\mathbf{Q}_0 = \begin{pmatrix} 0.277 & 0.182 & 0.541 \\ 0.388 & 0.303 & 0.359 \\ 0.147 & 0.427 & 0.426 \end{pmatrix}, \quad \mathbf{Q}_1 = \begin{pmatrix} 0.354 & 0.176 & 0.470 \\ 0.433 & 0.305 & 0.262 \\ 0.253 & 0.399 & 0.348 \end{pmatrix},$$

$$\mathbf{Q}_2 = \begin{pmatrix} 0.274 & 0.167 & 0.559 \\ 0.308 & 0.381 & 0.311 \\ 0.179 & 0.470 & 0.351 \end{pmatrix}.$$

Applying equation (2.3) recurssivelly using the above data we get

$$\mathbf{q}(0) = \begin{pmatrix} 0.32 & 0.30 & 0.38 \end{pmatrix}, \quad \mathbb{E}[\mathbf{q}(0,3)] = \begin{pmatrix} 0.242 & 0.315 & 0.443 \end{pmatrix},$$

$$\mathbb{E}[\mathbf{q}(0,6)] = \begin{pmatrix} 0.238 & 0.329 & 0.433 \end{pmatrix}, \quad \mathbb{E}[\mathbf{q}(0,9)] = \begin{pmatrix} 0.241 & 0.328 & 0.431 \end{pmatrix},$$

$$\mathbb{E}[\mathbf{q}(0,12)] = \begin{pmatrix} 0.241 & 0.328 & 0.431 \end{pmatrix}.$$

We observe that $\mathbb{E}[\mathbf{q}(0,3t)]$ converges. Since, $\Delta T(t) = 0$ for $t = 3, 4, ...$ and $\mathbf{Q}_0$ is a regular stochastic matrix then the conditions of Theorem 13b are satisfied and hence $\mathbf{q}_0(\infty)$ as given by Theorem 13b should coincide with $\mathbb{E}[\mathbf{q}(0,3t)]$. This was found to be true. The same was found with $\mathbb{E}[\mathbf{q}(0,3t+1)] \to_{t\to\infty} \begin{pmatrix} 0.340 & 0.295 & 0.365 \end{pmatrix}$, $\mathbb{E}[\mathbf{q}(0,3t+1)] \to_{t\to\infty} \begin{pmatrix} 0.340 & 0.295 & 0.365 \end{pmatrix}$, which were found equal with $\mathbf{q}_1(\infty)$ and $\mathbf{q}_2(\infty)$ given by Theorem 13b.

The Cezaro sum

$$\frac{1}{t}\sum_{n=0}^{t-1}\mathbb{E}\left[0,n\right]$$

was found to converge as early as $t=12$ to $\begin{pmatrix}0.278 & 0.331 & 0.391\end{pmatrix}$. The two conditions of Theorem 14 are valid in this case since for the model used $\mathbf{Q}_0$ is regular and $\Delta T\left(t\right)=0$ for $t=3,4,....$ According to Theorem 14 the strong run distribution was found to be equal with the limit of the Cezaro sum.

The conditions of Theorem 15 are satisfied for the present problem again since $\mathbf{Q}_0$ is regular and $\Delta T\left(t\right)=0$ for $t=3,4,....$ In order to find $\boldsymbol{\nu}\left(t\right)$ and verify that

$$\boldsymbol{\nu}\left(t\right)\overset{L^2}{\to}\frac{1}{d}\sum_{s=0}^{d-1}\mathbf{q}_s\left(\infty\right),$$

it is equivalent according to relation (5.1) in the proof of Theorem 15 to verify that

$$\lim_{t\to\infty}\mathbb{E}\left[\left(\boldsymbol{\nu}\left(t\right)-\frac{1}{d}\sum_{s=0}^{d-1}\mathbf{q}_s\left(\infty\right)\right)^2\right]=0.$$

For the present University System it was found that

$$\lim_{t\to\infty}\mathbb{E}\left[\left(\boldsymbol{\nu}\left(t\right)-\begin{pmatrix}0.278 & 0.331 & 0.391\end{pmatrix}\right)^2\right]=0.$$

Hence,

$$\boldsymbol{\nu}\left(t\right)\overset{L^2}{\to}\begin{pmatrix}0.278 & 0.331 & 0.391\end{pmatrix}\ \text{ as }\ t\to\infty.$$

Now, since $\mathbf{Q}_0$ is regular and $\Delta T\left(t\right)=0$ for $t=3,4,...,$ that is, the convergence is in geometric rate, the conditions of Theorem 17 are satisfied and thus

$$\boldsymbol{\nu}\left(t\right)\overset{a.s.}{\to}\begin{pmatrix}0.278 & 0.331 & 0.391\end{pmatrix}\ \text{ as }\ t\to\infty.$$

One of the useful for University planning physical meanings of the above result is, that a membesrship of a student remains in the first year of study, in the long run, almost surely the 0.41 of the time the University is working. Another useful physical meaning for University planning, is that the relative population structure of the memberships in the various years of study tends asymptotically almost surely to $\begin{pmatrix}0.41 & 0.37 & 0.22\end{pmatrix}$.

7. References

[1] .Bartholomew, D.J. (1963). A multistage renewal process. *J.R. Stat. Soc. Soc.* B25, 150-168.

[2] .Bartholomew, D.J. (1967) . *Stochastic models for Social processes.* First Edition. J. Wiley.

[3] .Bartholomew, D.J. (1982) . *Stochastic models for Social processes.* Third Edition. J. Wiley.

[4] . Faddy, M., McClean, S.I. (2005). Markov chain modeling for geriartic patient care. *Methods Archive 44,* (3), 369-373.

[5] . Foucher, Y., Mathew, E., Saint Pierre, P., Durand, J.-F., Daures, J.P. (2005). A semi-Markov model based on Weibull distribution with an illustration for HIV disease. *Biometri. J.* 47 (6): 1-9.

[6]. Gani, J. (1963). Formula for projecting enrollments and degrees awarded in Universities. *Journal of the Royal Statistical Society A,* 126, 400-409.

[7] .Garg, L., McClean, S.I., Meenan, B. Millard, P. (2009). Non homogeneous Markov models for sequential pattern mining of health care data. *IMA Journal of Management Mathematics* 20, (4), 327-344.

[8] .Garg, L., McClean, S.I., Meenan, B. Millard, P. (2010). A non-homogeneous discrete time Markov model for admission scheduling and resource planning in a cost capacity constraint healthcare system. *Health care Management Science 13 (2) 155-169.*

[9] . Georgiou, A.C. and P.-C.G. Vassiliou. (1992). Periodicity of Asymptotically Attainable Structures in Nonhomogeneous Markov systems. *Linear Algebra and its Applications* 176 : 137-174.

[10] . Georgiou, A.C. and N. Tsantas (1996). Non-stationary cyclic behavior in Markov systems. *Linear Algebra and its Applications* 237, 549-587.

[11] .Grimmet, G. and D. Stirzaker (2001). *Probability and Random Processes.* Third Edition.Oxford University Press. Oxford.

[12] .Hall, P. and C.C. Heyde (1980). *Martingale Limit Theorem and its Applications.* Academic Press, New York.

[13] .Huang, C., D.L. Isaacson and B. Vinograde (1976). The rate of convergence of certain nonhomogeneous Markov chains. Z. Wahrscheinlichkeitstheorie verw. Gabiete 35, 141-146.

[14] . Isaacson, D.L. and R.W. Madsen (1976). *Markov Chains Theory and Applications. J.* Wiley. New York.

[15] .Kemeny, J.G. and J.L. Snell. (1981). *Finite Markov Chains.* Springer Verlag. New York.

[16] . Kemeny, J.G., J.L. Snell and A.W. Knapp. (1976). *Denumerable Markov Chains.* Springer Verlag. New York.

[17] . Mathiew, E., Foucher, Y., Dellamonica, P., Daures, J.-P. (2006). Parametric and non-homogeneous semi-Markov process for HIV control. Working paper. Archer Hospital. Nice, France.

[18] . Lalit, G., McClean, S. I., Meenan, B., Millard, P.(2010). A non-homogeneous discrete time Markov model for admission scheduling and resource planning in a cost or capacity constrained healthcare system. *Health Care Management Science* **13**, 155-169.

[19]. Marshal, A.H., McClean, S. I., Shapcott. C.M., Millard, P. (2002). Modelling patient duration of stay to facilitate resource management of geriatric hospitals. *Health Care Management Science* **5**, 313-319.

[20] . Marshal, A.H. and McClean, S. I. (2003). Conditional phase-type distributions for modelling patient length of stay in hospital. *Int. Trans. in Op. Res.* **10**, 565-576.

[21] . Marshal, A.H. and McClean, S. I. (2004). Using Coxian Phase-Type Distributions to Identify Patient Characteristics for Duration of Stay in Hospital. *Health Care Management Science* **7**, 285-289.

[22] . McClean, S. I. and Millard, P. (1998a). A three compartment model of the patient flows in a geriatric department: a decision support approach. *Health Care Management Science* **1,** 159-163.

[23]. McClean, S. I., McAlea, B. and Millard, P. (1998b). Using a Markov reward model to estimate spend-down costs for geriatric department. *Journal of the Operational Research Society* **49**, 1021-1025.

[24] . McClean, S. I., Scotney, B., Robinson, S. (2003). Conceptual clustering of heterogeneous gene expressions sequences. *Artif. Intell. Rev.* 20:53-73.

[25] .McClean, S. I. and Millard, P. (2007). Where to treat the older patient? Can Markov models help us better understand the relationship between hospital and community care? *Journal of the Operational Research Society* 58, (2), 255-261.

[26] .McClean, S. I., Garg, L., Meenan, B., Millard, P. (2007). Non-Homogeneous Markov models for performance monitoring in healthcare. *Recent advances in Stochastic Modelling and Data Analysis, 146-153.*

[27] .McClean, S. I., Garg, L., Barton, M., Fullerton, K., Millard, P. (2009). Using Markov systems to plan stroke services. *Intelligent Patient Management, 241-256.*

[28] .McClean, S. I., Gillespie, J. Garg, L., Barton, M., Scotney, B., Fullerton, K., (2014). Using phase-type models to cost stroke patient care across health, social and community services. *European Journal of Operations Research 236 (1) 190-199.*

[29] .McClean, S. I., Garg, L., Fullerton, K. (2014b). Costing mixed Coxian phase-type systems with Poisson arrivals. *Communications in Statistics-Theory and Methods 43 (*7), 1437-1452.

[30] .Meyn, S. and R. Tweedie (2009). *Markov Chains and Stochastic Stability.* Cambridge University Press, Cambridge.

[31] . Vadori N. and A. Swishchuk. (2015). Strong Law of Large Numbers and Central Limit theorems for functionals of inhomogeneous Semi-Markov Processe. *Stochastic Analysis and Applications,* 33, 213-243.

[32] . Taylor, G.J., McClean, S. I. and Millard, P. (2000). Stochastic models of geriatric patient bed occupancy behaviour. *J.R. Statist. Soc. A* **163**, Part 1, 39-48.

[33] . Vassiliou, P.-C.G. (1982) .Asymptotic behavior of Markov systems. *J. Appl. Prob.* 19, 851-857.

[34] .Vassiliou, P.-C.G. (1984) . Cyclic behavior and asymptotic stability of nonhomogeneous Markov systems. *Journal of Applied Probability,* 21, 315-325.

[35] .Vassiliou, P.-C.G. (1986) . Asymptotic variability of nonhomogeneous Markov systems under cyclic behavior. *European Journal of Operational Research* 27, 215-228.

[36] .Vassiliou, P.-C.G. and A.C. Georgiou (1990). Asymptotically attainable structures in nonhomogeneous Markov systems. *Operations Research,* 38, 3, 537-545.

[37] .Vassiliou, P.-C.G. (1981). On the limiting behavior of a nonhomogeneous Markov chain model in manpower systems. *Biometrika* 68, 2, 557-561.

[38] . Vassiliou, P.-C.G. and Tsantas N. (1984). Maintainability of structures in nonhomogeneous Markov systems under cyclic behavior and input control. SIAM J. APPL. MATH. **44,** 5, 1014-1022.

[39] . Vassiliou, P.-C.G. (1997). The evolution of the theory of non-homogeneous Markov systems. *Applied Stochastic Models Data Anal.* 13, 159-176.

[40] . Ugwuowo F.I. and S.I. McClean (2000). Modelling heterogeneity in a manpower system : a review. *Appl. Stoch. Models Bus. Ind.* 2: 99-100.

[41] .Young, A. and G. Almond (1961). Predicting distributions of staff. *Comp. J.* 3, 246-250.

Department of Statistical Sciences, University College London.
E-mail address: vasiliou@math.auth.gr

S-weighted instrumental variables

Jan Ámos Víšek[1]

Inst. of Economic Studies, Fac. of Social Sciences, Charles University in Prague
(E-mail: visek@fsv.cuni.cz)

Abstract. The paper deals with two problems - with the situation when the orthogonality condition is broken and with the problem when an atypical data sets contains a significant amount of information in a group of good leverage points but includes also a "troublesome" group of outliers.

Several robust methods were recently modified in order to overcome problem with the broken orthogonality condition, employing typically the idea of instrumental variables. In an analogous way modified S-weighted estimator is able to cope with broken orthogonality condition, too. We prove its consistency and we offer a small pattern of results of simulations.

It is believed that the bad leverage points are a more challenging problem in identification of underlying regression model than outliers. We show that sometimes outliers can represent also an intricate task.

Keywords: Regression model, broken orthogonality condition, contamination of data .

1 Summarizing the previous relevant results

The median is the only classical statistics which is able to cope with high contamination, even 50%, and to give reasonable information about the location parameter of data set. When Peter Bickel [1] opened the problem of possibility to construct an analogy of median in the framework of regression model, i. e. an estimator of regression coefficients with 50% breakdown point, nobody had an idea how long and painful way to the solution we would have to go.

It seemed several times that we had achieved solution but finally always a bitter disappointment arrived. For instance, as the median is in fact the 50% quantile, we hoped that Koenker and Bassett's *regression quantiles* [15] are the solution. However, result by Richard Maronna and Victor Yohai [16], establishing the maximal value of breakdown point of M-estimators, ruined our dreams.

By proposing the *repeated median* Andrew Siegel [21] has broken this long-years-lasting nightmare. But only proposals of the *least median of squares* (LMS) and the *least trimmed squares* (LTS) by Peter Rousseeuw [18], [19] and [10] brought feasible methods. In fact he "rediscovered" the power of such statistical notion as the *order statistics of (squared) residuals*, see [9]. Unfortunately, at those days we have not at hand a proper tool for studying the asymptotic properties of these estimators (the proof of consistency of LTS arrived after the twenty years from its proposal, see [27]) and this technical problem was (except of others) an impuls for proposing S-estimator [20] with an immediately available proof of consistency and the simultaneous preservation of high breakdown point.

17^{th} *ASMDA Conference Proceedings, 6 – 9 June 2017, London, UK*

The algorithms for all these estimators were also successfully found. For LTS it was based on repeated application of algorithm for the *ordinary least squares* and it was so simple that it was not never published (as such, see [22]) until the moment when an improvement for large data set became inevitable ([6], [12], [13]). The algorithm for the S-estimator was a bit more complicated but feasible, see [4].

Nevertheless, results by Thomas Hettmansperger and Simon Sheater [14], although they were wrong (due to the bad algorithm they used for LMS - for efficient algorithm see [2]), they warned us that the situation need not be so simple as we had assumed. It led to a return to the order statistics of squared residuals and to the proposal of the *least weighted squares* (LWS) in [24]. It profited from extremely simple algorithm, basically the same as the algorithm for LTS (see [29]), however the study of its properties was tiresome and clumsy, see [25]. A significant simplification came with generalization of Kolmogorov-Smirnov result for the regression scheme, see [31], together with the fact that the rank of given order statistic is given by the value of empirical distribution function of these order statistics at given order statistic, see [32]. It opened a way for defining an estimator covering all above mentioned estimators as special cases - *S-weighted estimator* - and to describe its asymptotics, see [33] and [34].

Due to the character of data in the social sciences we can expect that the orthogonality condition is frequently broken. That was the reason why there are several attempts to modify the robust methods to be able to cope with the broken orthogonality condition, similarly as the *ordinary least squares* were "transformed" into the *instrumental variables*, see e. g. [5], [7], [8], [11], [23], [26], [28], [29], [35] or [36]. The present paper offers a similar modification of the *S-weighted estimator* which is able to cope with the broken orthogonality condition - *S-weighted instrumental variables*.

At the end of papers we answer to the problem whether the leverage points represent always more complicated problem than outliers. And the answer is a bit surprising.

2 The notations, framework, conditions and main tool

Let $\mathcal{N}$ denote the set of all positive integers, R the real line and R^p the p-dimensional Euclidean space. All random variables are assumed to be defined on a basic probability space $(\Omega, \mathcal{A}, P)$. (We will not write - as the mathematical rigor would ask it - the random variable as $X(\omega)$ (say) but sometimes by including (ω) we emphasize the exact state of things.) For a sequence of $(p+1)$-dimensional random variables (r. v.'s) $\{(X_i', e_i)'\}_{i=1}^{\infty}$, for any $n \in \mathcal{N}$ and a fixed $\beta^0 \in R^p$ the linear regression model given as

$$Y_i = X_i'\beta^0 + e_i = \sum_{j=1}^{p} X_{ij}\beta_j^0 + e_i, \quad i = 1, 2, ..., n \tag{1}$$

will be considered. (It is clear that the results of paper can be applied for the panel data - the model (1) will be used to keep the explanation as simple as possible.) We will need some conditions on the explanatory variables and the disturbances.

Conditions $\mathcal{C}1$. *The sequence* $\left\{(X_i', e_i)'\right\}_{i=1}^{\infty}$ *is sequence of independent* $p+1$*-dimensional random variables (r.v.'s) distributed according to distribution functions (d. f.)* $F_{X,e_i}(x,r) = F_{X,e}(x, r\sigma_i^{-1})$ *where* $F_{X,e}(x,r)$ *is a parent d. f. and* $\sigma_i^2 = \mathrm{var}\,(e_i)$. *Further,* $I\!Ee_i = 0$ *and*

$$0 < \underset{i\to\infty}{lim\,inf}\sigma_i \leq \underset{i\to\infty}{lim\,sup}\,\sigma_i < \infty.$$

Denote $F_{e|X}(r|X_1 = x)$ *the conditional d.f. corresponding to the parent d.f.* $F_{X,e}(x,r)$. *Then, for all* $x \in R^p$ $F_{e|X}(r|X_1 = x)$ *is absolutely continuous with density* $f_{e|X}(r|X_1 = x)$ *bounded by* U_e *(which does not depend on* x*).*

In what follows $F_X(x)$ and $F_e(r)$ will denote the corresponding marginal d. f.'s of the *parent d. f.* $F_{X,e}(x,r)$. Then, assuming that e is a *"parent" r. v.* distributed according to *parent d. f.* $F_e(r)$, we have, e. g., $F_{e_i}(r) = P(e_i < r) = P(\sigma_i \cdot e < r) = P(e < \sigma_i^{-1} \cdot r) = F_e(\sigma_i^{-1} \cdot r)$, etc.. Conditions $\mathcal{C}1$ imply that the marginal d. f. $F_X(x)$ does not depend on i, i. e. the sequence $\{X_i\}_{i=1}^{\infty}$ is sequence of independent and identically distributed (i.i.d.) r.v.'s.

Let for any $\beta \in R^p$ $a_i = |Y_i - X_i'\beta|$ be absolute values of the i-th residual and $F_{i,\beta}(v)$ its d. f., i. e. $F_{i,\beta}(v) = P(a_i(\beta) < v)$. Then put

$$\overline{F}_{\beta}^{(n)}(v) = \frac{1}{n}\sum_{i=1}^{n} F_{i,\beta}(v). \tag{2}$$

Further, let $F_{\beta}^{(n)}(v)$ be the empirical distribution function (e. d. f.) of the absolute values of residuals, i. e.

$$F_{\beta}^{(n)}(v) = \frac{1}{n}\sum_{i=1}^{n} I\left\{a_i(\beta) < v\right\}. \tag{3}$$

It seems strange to consider the e. d. f. of a_i's, as they are heteroscedastic, but the Lemma 1 shows that it makes a sense. Finally, let $a_{(1)} \leq a_{(2)} \leq ... \leq a_{(n)}$ denote the order statistics of absolute values of residuals and $\tilde{F}_{\beta}^{(n)}(v)$ be a continuous and strictly increasing modification of $F_{\beta}^{(n)}(v)$ defined as follows: Let $\tilde{F}_{\beta}^{(n)}(v)$ coincide with $F_{\beta}^{(n)}(v)$ at $a_i(\beta)$, $i = 1, 2, ..., n$ and let it be continuous and strictly monotone between any pair of $a_{(i)}(\beta)$ and $a_{(i+1)}(\beta)$. Then it holds:

Lemma 1. *Let Condition* $\mathcal{C}1$ *hold. Then for any* $\varepsilon > 0$ *there is a constant* K_ε *and* $n_\varepsilon \in \mathcal{N}$ *so that for all* $n > n_\varepsilon$

$$P\left(\left\{\omega \in \Omega : \sup_{r\in R^+}\sup_{\beta\in R^p}\sqrt{n}\left|\tilde{F}_{\beta}^{(n)}(v) - \overline{F}_{\beta}^{(n)}(v)\right| < K_\varepsilon\right\}\right) > 1-\varepsilon. \tag{4}$$

The proof which employs Skorohod's embedding into Wiener process, see [3], is a slight generalization of Lemma 1 of [31] and it is based on the fact that $R^p \times R^+$ is separable space and that $\tilde{F}_{\beta}^{(n)}(v)$ is monotone.

The **Conditions** $\mathcal{C}2$ specifies the character of objective and weight functions.

Conditions $\mathcal{C}2$

- $w : [0,1] \to [0,1]$ *is a continuous, non-increasing weight function with* $w(0) = 1$. *Moreover,* w *is Lipschitz in absolute value, i. e. there is* L *such that for any pair* $u_1, u_2 \in [0,1]$ *we have* $|w(u_1) - w(u_2)| \leq L\times$ $\times\,|u_1 - u_2|$.

- $\rho : (0,\infty) \to (0,\infty)$, $\rho(0) = 0$, *non-decreasing on* $(0,\infty)$ *and differentiable (denote the derivative of* ρ *by* ψ*).*
- $\psi(v)/v$ *is non-increasing for* $v \geq 0$ *with* $\lim_{v\to 0_+} \frac{\psi(v)}{v} = 1$.

3 *S*-weighted estimator and its consistency

Definition 1. Let $w : [0,1] \to [0,1]$ and $\rho : [0,\infty] \to [0,\infty]$ be a weight function and an objective function, respectively. Then

$$\hat{\beta}^{(SW,n,w,\rho)} = \underset{\beta\in R^p}{\arg\min} \left\{ \sigma(\beta) \in R^+ : \frac{1}{n}\sum_{i=1}^{n} w\left(\frac{i-1}{n}\right)\rho\left(\frac{a_{(i)}(\beta)}{\sigma}\right) = b \right\} \quad (5)$$

where $b = I\!E_{F_e}\left\{w(F_{\beta^0}(|e|))\rho(e)\right\}$, is called the *S-weighted estimator*, see [33].

Remark 1. Notice please that we cannot write in (5) simply $\rho\left(\frac{a_i(\beta)}{\sigma}\right)$ because then we would assign the weight $w\left(\frac{i-1}{n}\right)$ to other residual. (Let's recall that $\mathrm{var}_{F_e}(e) = 1$, so that the scale of e need not appear in the definition of b.)

Employing a bit modified argument of Peter Rousseeuw and Victor Yohai [20], we can show that $\hat{\beta}^{(SW,n,w,\rho)}$ has to be solution of

$$\sum_{i=1}^{n} w\left(\frac{i-1}{n}\right) X_{j_i}\psi\left(\frac{|Y_{j_i} - X'_{j_i}\beta|}{\hat{\sigma}_n}\right)\cdot \mathrm{sign}(Y_{j_i} - X'_{j_i}\beta) = 0$$

where j_i is the index of observation corresponding to $a_{(i)}$ and $\hat{\sigma}_n$ fulfills the constraint

$$\frac{1}{n}\sum_{i=1}^{n} w\left(\frac{i-1}{n}\right)\rho\left(\frac{a_{(i)}(\beta)}{\hat{\sigma}_n}\right) = b. \quad (6)$$

Then having followed Hájek and Šidák [9] and putting

$$\pi(\beta, j) = i \in \{1,2,...,n\} \qquad \Leftrightarrow \qquad a_j(\beta) = a_{(i)}(\beta), \quad (7)$$

we arrive at

$$\sum_{i=1}^{n} w\left(\frac{\pi(\beta,i)-1}{n}\right) X_i\psi\left(\frac{|Y_i - X'_i\beta|}{\hat{\sigma}_n}\right)\cdot \mathrm{sign}(Y_i - X'_i\beta) = 0 \quad (8)$$

and utilizing the equality $n^{-1}\left(\pi(\beta,i)-1\right) = F_\beta^{(n)}(a_i(\beta))$ (see [32]), we finally obtain

$$\sum_{i=1}^{n} w\left(F_\beta^{(n)}(a_i(\beta))\right) X_i\psi\left(\frac{|Y_i - X'_i\beta|}{\hat{\sigma}_n}\right)\cdot \mathrm{sign}(Y_i - X'_i\beta) = 0. \quad (9)$$

Then the fact that $\psi(0) = 0$ allows to write the normal equations (8) as

$$\sum_{\{i\,:\,r_i(\beta)\neq 0\}} w\left(F_\beta^{(n)}(a_i(\beta))\right)\left[\psi\left(\frac{a_i(\beta)}{\hat{\sigma}_n}\right)\cdot\frac{\hat{\sigma}_n}{a_i(\beta)}\right] X_i\left(Y_i - X'_i\beta\right)$$
$$= \sum_{i=1}^{n} \tilde{w}\left(\tilde{F}_\beta^{(n)}(a_i(\beta)), \hat{\sigma}_n\right) X_i\left(Y_i - X'_i\beta\right) = 0. \quad (10)$$

Notice please, that if w and ρ fulfill Conditions $\mathcal{C}2$ then $\tilde{w}$ is well defined and it also fulfill $\mathcal{C}2$ for any fixed $\sigma > 0$. Notice also that (10) coincides with the

normal equations of the *least weighted squares* only if $\rho(v) = v^2$ - compare with [32]. Otherwise, firstly, $\tilde{w}(v)$ is implicitly modified by $\psi(v)$ and secondly, $\tilde{w}(v)$ depends also on $\hat{\sigma}_n$. As the S-weighted estimator controls the influence of residuals by the weight and objective functions, the Euclidean metrics is substituted by a riemannian one and the consequence is that - contrary to the *ordinary least squares* - we need an identification condition.

Conditions $\mathcal{C}3$ *There is the only solution of the equation*

$$\beta' I\!E \left[\sum_{i=1}^{n} w \left(\overline{F}_{\beta}^{(n)}(|e_i|) \right) \cdot X_i \cdot \psi(e_i - X_i'\beta) \right] = 0, \tag{11}$$

(for $\tilde{w}$ *see (9)) at* $\beta = \beta^0$.

Remark 2. Notice that (11) is for the classical *ordinary least squares* fulfilled because $\tilde{w} \equiv 1$. Similarly, it can be shown that when w is zero-one function and ρ is quadratic function (as for the *least trimmed squares*) that (11) also holds but in that case it is technically rather complicated, see [27].

Theorem 1. *Let* **Conditions** $\mathcal{C}1$*,* $\mathcal{C}2$ *and* $\mathcal{C}3$ *be fulfilled and* $\hat{\sigma}_n$ *be a weakly consistent estimator of* $\mathrm{var}_{F_e}(e)$ *fulfilling the constraint (6). Then any sequence* $\left\{ \hat{\beta}^{(SW,w,\rho,\hat{\sigma}_n,n)} \right\}_{n=1}^{\infty}$ *of the solutions of sequence of normal equations (9) for* $n = 1, 2, ...,$ *is weakly consistent.*

The proof is a slight generalization of the proof of Theorem 1 from [33].

4 *S*-weighted instrumental variables and their consistency

Due to Euclidean geometry the solution of the extremal problem which defines the *ordinary least squares*, namely

$$\hat{\beta}^{(OLS,n)} = \underset{\beta \in R^p}{\arg\min} \sum_{i=1}^{n} \left(Y_i - X_i'\beta \right)^2, \tag{12}$$

is given as the solution of *normal equations*

$$\sum_{i=1}^{n} X_i \left(Y_i - X_i'\beta \right) = 0. \tag{13}$$

Having performed a straightforward algebra and the substitution from (1), we arrive at

$$\hat{\beta}^{(OLS,n)} = \beta^0 + \left(\frac{1}{n} \sum_{i=1}^{n} \left[X_i \cdot X_i' \right] \right)^{-1} \cdot \frac{1}{n} \sum_{i=1}^{n} \left[X_i e_i \right] \tag{14}$$

which indicates that if the *orthogonality condition* is broken, i. e. $I\!E\left[X_1 \cdot e \right] \neq 0$ (for e see **Conditions** $\mathcal{C}1$), $\hat{\beta}^{(OLS,n)}$ is biased and inconsistent. Then we look for some instrumental variables $\{Z_i\}_{i=1}^{\infty}$, usually i. i. d. r. v.'s, such that $I\!E Z_1 = 0$, $I\!E\left[Z_1 \cdot Z_1' \right]$ positive definite matrix, $I\!E\left[Z_1 \cdot e \right] = 0$ and define the estimator by *means of the instrumental variables* (IV) as the solution of the *normal equations*

$$\sum_{i=1}^{n} Z_i \left(Y_i - X_i'\beta \right) = 0. \tag{15}$$

(An alternative way how to cope with the broken *orthogonality condition* is to utilize the *orthogonal regression* - sometimes called the *total least squares*, see e. g. [17].) There are several alternative way how to define the *instrumental*

variables - see [35] and references given there - but all of them are practically equivalent to (15) - for the discussion which summarizes also geometric background of the *instrumental variables*, see again [35]. What can be of interest - to prove the unbiasedness and consistency of classical instrumental variables we don't need (nearly) any additional assumptions except of those which are given several lines above (15).

Definition 2. Let $\{Z_i\}_{i=1}^{\infty}$ be a sequence of i. i. d. r. v.'s, such that $I\!E Z_1 = 0$, $I\!E\left[Z_1 \cdot Z_1'\right]$ positive definite matrix, $I\!E\left[Z_1 \cdot e\right] = 0$. The solution of the *normal equation*

$$I\!N E_{Y,X,Z}^{(\tilde{w},\rho,\hat{\sigma}_n,n)}(\beta) = \sum_{i=1}^{n} \tilde{w}\left(\tilde{F}_{\beta}^{(n)}(a_i(\beta)), \hat{\sigma}_n\right) Z_i \left(Y_i - X_i'\beta\right) = 0 \qquad (16)$$

will be called the estimator by *means of the S-weighted instrumental variables* (briefly, the *S-weighted instrumental variables*) and denoted by $\hat{\beta}^{(SWIV,w,\rho,\hat{\sigma}_n,n)}$.

To be able to prove the consistency of $\hat{\beta}^{(SWIV,w,\rho,\hat{\sigma}_n,n)}$, we will need some additional assumption and an identification condition, similar to **Conditions** $\mathcal{C}3$. We will start with an enlargement of notations.

Let for any $\beta \in R^p$ and $u \in R$ $F_{\beta' Z X' \beta}(u) = P(\beta' Z_1 X_1' \beta < u)$ and $F_{\beta' Z X' \beta}^{(n)}(u) = \frac{1}{n}\sum_{i=1}^{n} I\left\{\beta' Z_i(\omega) X_i'(\omega)\beta < u\right\}$ be the d. f. of $\beta' Z_1 X_1' \beta$ and e. d. f. of $\{\beta' Z_i(\omega) X_i'(\omega)\beta\}_{i=1}^{n}$, respectively. Further, for any $\lambda \in R^+$ and any $a \in R$ put

$$\gamma_{\lambda,a} = \sup_{\|\beta\|=\lambda} F_{\beta' Z X' \beta}(a) \quad \text{and} \quad \tau_{\lambda} = -\inf_{\|\beta\| \le \lambda} \beta' I\!E\left[Z_1 X_1' \cdot I\{\beta' Z_1 X_1' \beta < 0\}\right]\beta. \qquad (17)$$

Conditions $\mathcal{C}4$ *The instrumental variables $\{Z_i\}_{i=1}^{\infty}$ are independent and identically distributed with distribution function $F_Z(z)$. Further, the joint distribution function $F_{X,Z}(x,z)$ is absolutely continuous with a density $f_{X,Z}(x,z)$ bounded by $U_{ZX} < \infty$. Further for any $n \in \mathcal{N}$ we have $I\!E\sum_{i=1}^{n}\left\{w(F_{\beta^0}(|e_i|))\times\right.$ $\left.\times\psi(e_i)\cdot Z_i\right\} = 0$ and the matrices $I\!E Z_1 Z_1'$ as well as $I\!E\sum_{i=1}^{n}\left\{w(F_{\beta^0}(|e_i|))\times\right.$ $\left.\times\psi(e_i)\cdot Z_i X_i'\right\}$ are positive definite. Moreover, there is $q > 1$ so that $I\!E\left\{\|Z_1\| \times\right.$ $\left.\times\|X_1\|\right\}^q < \infty$. Finally, there is $a > 0$, $b \in (0,1)$ and $\lambda > 0$ so that*

$$a \cdot (b - \gamma_{\lambda,a}) \cdot \tilde{w}(b) > \tau_{\lambda} \qquad (18)$$

for $\gamma_{\lambda,a}$ and τ_{λ} given by (17).

Lemma 2. *Let Conditions $\mathcal{C}1$, $\mathcal{C}2$, $\mathcal{C}4$ be fulfilled and $\hat{\sigma}_n$ be a weakly consistent estimator of $\mathrm{var}_{F_e}(e)$ fulfilling the constraint (6). Then for any $\varepsilon > 0$ there is $\zeta > 0$ and $\delta > 0$ such that*

$$P\left(\left\{\omega \in \Omega : \inf_{\|\beta\| \ge \zeta} -\frac{1}{n}\beta' I\!N E_{Y,X,Z}^{(\tilde{w},\rho,\hat{\sigma}_n,n)}(\beta) > \delta\right\}\right) > 1 - \varepsilon.$$

In other words, any sequence $\left\{\hat{\beta}^{(SWIV,\tilde{w},\rho,\hat{\sigma}_n,n)}\right\}_{n=1}^{\infty}$ of the solutions of the sequence of normal equations (16) $I\!N E_{Y,X,Z}^{(\tilde{w},\rho,\hat{\sigma}_n,n)}(\beta) = 0$ is bounded in probability.

The proof is formally nearly the same as the proof of Lemma 1 in [30]. The allowance for the heteroscedasticity of disturbances requires some *formally* straightforward modifications. The fact that the modifications are relatively

simple and straightforward is due to the fact that the complicated steps were made in [32] but the background of proof is different from the proof in [30]. The approximation of empirical d. f. is not by the underlying d. f. as the limit of the empirical d. f.'s but we employ the knowledge about convergence of the difference of the empirical d. f.'s and the arithmetic mean of the d. f.'s of individual disturbances, see Lemma 1. □

Lemma 3. *Let Conditions $\mathcal{C}1$, $\mathcal{C}2$ and $\mathcal{C}4$ be fulfilled and $\hat{\sigma}_n$ be a weakly consistent estimator of $\mathrm{var}_{F_e}(e)$ fulfilling the constraint (6). Then for any $\varepsilon > 0$, $\delta \in (0,1)$ and $\zeta > 0$ there is $n_{\varepsilon,\delta,\zeta} \in \mathcal{N}$ so that for any $n > n_{\varepsilon,\delta,\zeta}$ we have*

$$P\left(\left\{\omega \in \Omega \ : \ \sup_{\|\beta\| \le \zeta} \left| \frac{1}{n}\sum_{i=1}^{n} \left\{ \tilde{w}(\tilde{F}_{\beta}^{(n)}(a_i(\beta)), \hat{\sigma}_n)\beta' Z_i \left(e_i - X_i'\beta\right) \right.\right.\right.$$
$$\left.\left.\left. -\beta' I\!E\left[\tilde{w}(\overline{F}_{\beta}^{(n)}(a_i(\beta)), \hat{\sigma}_n) Z_i \left(e_i - X_i'\beta\right)\right] \right\} \right| < \delta \right\}\right) > 1-\varepsilon$$

(for $a_i(\beta)$ see a line above (2) and for $\overline{F}_{\beta}^{(n)}(v)$ see (2)).

The proof has formally similar structure as the proof of Lemma 2 in [30]. It is a bit more complicated because again instead of employing a limiting distribution we need to estimate differences of empirical d. f. of $a_i(\beta)$'s from a sequence of the arithmetic means of underlying d. f.'s $\left\{\overline{F}_{\beta}^{(n)}(v)\right\}_{n=1}^{\infty}$, see (2). □

Lemma 4. *Let Conditions $\mathcal{C}1$, $\mathcal{C}2$ and $\mathcal{C}3$ hold and $\hat{\sigma}_n$ be a weakly consistent estimator of $\mathrm{var}_{F_e}(e)$ fulfilling the constraint (6). Then for any positive ζ*

$$\beta' I\!E\left[\tilde{w}\left(F_{\beta}(a_i(\beta)), \hat{\sigma}_n\right) Z_i \left(e_i - X_i'\beta\right)\right] \tag{19}$$

(for $\tilde{w}$ see (10)) is uniformly in $i \in \mathcal{N}$, uniformly continuous in β on $\mathcal{B} = \{\beta \in R^p : \|\beta\| \le \zeta\}$, i. e. for any $\varepsilon > 0$ there is $\delta > 0$ so that for any pair of vectors $\beta^{(1)}, \beta^{(2)} \in R^p, \left\|\beta^{(1)} - \beta^{(2)}\right\| < \delta$ we have

$$\sup_{i \in \mathcal{N}} \left| \left[\beta^{(1)}\right]' I\!E\left[\tilde{w}\left(F_{\beta^{(1)}}(a_i(\beta^{(1)})), \hat{\sigma}_n\right) Z_i \left(e_i - X_i'\beta^{(1)}\right)\right] \right.$$
$$\left. - \left[\beta^{(2)}\right]' I\!E\left[\tilde{w}\left(F_{\beta^{(2)}}(a_i(\beta^{(2)})), \hat{\sigma}_n\right) Z_i \left(e_i - X_i'\beta^{(2)}\right)\right] \right| < \varepsilon.$$

Proof is a chain of approximations utilizing simple estimates of upper bounds of differences of the values of (19) for close pair of points in R^p. □

Similarly as for the *S-weighted estimator* we need for the *S-weighted instrumenal variables* the identification condition.

Conditions $\mathcal{C}4$. *For any $n \in \mathcal{N}$ the equation*

$$\beta' \sum_{i=1}^{n} I\!E\left[w\left(\overline{F}_{\beta}^{(n)}(|e_i|)\right) \cdot Z_i \cdot \psi(e_i - X_i'\beta)\right] = 0 \tag{20}$$

in the variable $\beta \in R^p$ has a unique solution at $\beta = \beta^0$.

Theorem 2. *Let Conditions $\mathcal{C}1$, $\mathcal{C}2$, $\mathcal{C}3$ and $\mathcal{C}4$ be fulfilled and $\hat{\sigma}_n$ be a weakly consistent estimator of $\mathrm{var}_{F_e}(e)$ fulfilling the constraint (6). Then any sequence $\left\{\hat{\beta}^{(SWIV,w,\rho,\hat{\sigma}_n,n)}\right\}_{n=1}^{\infty}$ of the solutions of normal equations (16) $I\!N E_{Y,X,Z}^{(\tilde{w},\rho,\hat{\sigma}_n,n)}(\beta) = 0$ is weakly consistent.*

Proof: Without loss of generality assume that $\beta^0 = 0$ (as $\hat{\sigma}^{(SWIV,w,\rho,\hat{\sigma}_n,n)}$ is scale- and regression equivariant). To prove the consistency, we have to show that for any $\varepsilon > 0$ and $\delta > 0$ there is $n_{\varepsilon,\delta} \in \mathcal{N}$ such that for all $n > n_{\varepsilon,\delta}$

$$P\left(\left\{\omega \in \Omega : \left\|\hat{\beta}^{(SWIV,\tilde{w},\rho,\hat{\sigma}_n,n)} - \beta^0\right\| < \delta\right\}\right) > 1 - \varepsilon. \tag{21}$$

So fix $\varepsilon_1 > 0$ and $\delta_1 > 0$. According to Lemma 2 there are $\delta_1 > 0$ and $\theta_1 > 0$ so that for ε_1 there is $n_{\delta_1,\varepsilon_1} \in \mathcal{N}$ so that for any $n > n_{\delta_1,\varepsilon_1}$

$$P\left(\left\{\omega \in \Omega : \inf_{\|\beta\| \geq \theta_1} -\frac{1}{n}\beta' I\!N E_{Y,X,Z}^{(\tilde{w},\rho,\hat{\sigma}_n,n)}(\beta) > \delta_1\right\}\right) > 1 - \frac{\varepsilon_1}{2}$$

(denote the corresponding set by B_n). It means that for all $n > n_{\delta_1,\varepsilon_1}$ all solutions of the normal equations (16) $I\!N E_{Y,X,Z}^{(\tilde{w},\rho,\hat{\sigma}_n,n)}(\beta) = 0$ are inside the ball $\mathcal{B}(0,\theta_1)$ with probability at least $1 - \frac{\varepsilon_1}{2}$. If $\theta_1 \leq \delta$, we have finished the proof. Generally of course we can have $\theta_1 > \delta$.
Then, utilizing Lemma 3 we may find for ε_1, $\delta = \min\{\frac{\delta_1}{2}, \delta_1\}$ and θ_1 such $n_{\varepsilon_1,\delta,\theta_1} \in \mathcal{N}, n_{\varepsilon_1,\delta,\theta_1} \geq n_{\delta_1,\varepsilon_1}$ so that for any $n > n_{\varepsilon_1,\delta,\theta_1}$ there is a set C_n (with $P(C_n) > 1 - \frac{\varepsilon}{2}$) such that for any $\omega \in C_n$

$$\sup_{\|\beta\| \leq \theta_1} \left| \frac{1}{n}\sum_{i=1}^{n} \left\{ \tilde{w}\left(\tilde{F}_\beta^{(n)}(a_i(\beta)), \hat{\sigma}_n\right) \beta' Z_i \left(e_i - X_i'\beta\right) \right.\right.$$
$$\left.\left. -\beta' I\!E\left[\tilde{w}\left(\tilde{F}_\beta(a_i(\beta)), \hat{\sigma}_n\right) Z_i \left(e_i - X_i'\beta\right)\right] \right\} \right| < \delta.$$

But it means that

$$\inf_{\|\beta\| = \theta_1} \left\{ -\beta' \frac{1}{n}\sum_{i=1}^{n} I\!E\left[\tilde{w}\left(\tilde{F}_\beta(a_i(\beta)), \hat{\sigma}_n\right) Z_i \left(e_i - X_i'\beta\right)\right] \right\} > \frac{\delta_1}{2} > 0. \tag{22}$$

Further consider the compact set $C = \{\beta \in R^p : \delta_1 \leq \|\beta\| \leq \theta_1\}$ and find

$$\tau_C = \inf_{\beta \in C} \left\{ -\beta' \frac{1}{n}\sum_{i=1}^{n} I\!E\left[\tilde{w}\left(\tilde{F}_\beta(a_i(\beta)), \hat{\sigma}_n\right) Z_i \left(e_i - X_i'\beta\right)\right] \right\}. \tag{23}$$

Then there is a $\{\beta_k\}_{k=1}^{\infty}$ such that

$$\lim_{k\to\infty} \beta_k' \frac{1}{n}\sum_{i=1}^{n} I\!E\left[\tilde{w}\left(\tilde{F}_{\beta_k}(a_i(\beta_k)), \hat{\sigma}_n\right) Z_i \left(e_i - X_i'\beta_k\right)\right] = -\tau_C.$$

On the other hand, due to compactness of C there is a β^* and a subsequence $\left\{\beta_{k_j}\right\}_{j=1}^{\infty}$ such that

$$\lim_{j\to\infty} \beta_{k_j} = \beta^*$$

and due to the uniform continuity (uniform in $i \in \mathcal{N}$ as well as in $\beta \in C$) of $\beta' I\!E\left[\tilde{w}\left(\tilde{F}_\beta(a_i(\beta)), \hat{\sigma}_n\right) Z_i \left(e_i - X_i'\beta\right)\right]$ (see Lemma 4) we have

$$-\left[\beta^*\right]' \frac{1}{n}\sum_{i=1}^{n} I\!E\left[\tilde{w}\left(\tilde{F}_{\beta^*}(a_i(\beta^*)), \hat{\sigma}_n\right) Z_i \left(e_i - X_i'\beta^*\right)\right] = \tau_C. \tag{24}$$

Employing once again the uniform continuity (uniform in $i \in \mathcal{N}$ and $\beta \in C$) of $\beta' I\!E\left[\tilde{w}\left(F_\beta(a_i(\beta)), \hat{\sigma}_n\right) Z_i\left(e_i - X_1'\beta\right)\right]$ together with Condition $\mathcal{C}4$ and (22) we find that $\tau_C > 0$, otherwise there has to be a solution of (20) inside the compact C which does not contain $\beta = 0$.
Now, utilizing Lemma 3 once again we may find for ε_1, δ_1, θ_1 and τ_C $n_{\varepsilon_1,\delta_1,\theta_1,\tau_C} \in \mathcal{N}, n_{\varepsilon_1,\delta_1,\theta_1,\tau_C} \geq n_{\varepsilon_1,\delta,\theta_1}$ so that for any $n > n_{\varepsilon_1,\delta_1,\theta_1,\tau_C}$ there is a set D_n (with $P(D_n) > 1 - \frac{\varepsilon}{2}$) such that for any $\omega \in D_n$

$$\sup_{\|\beta\| \leq \theta_1} \left| \frac{1}{n} \sum_{i=1}^{n} \left\{ \tilde{w}\left(\tilde{F}_\beta^{(n)}(a_i(\beta)), \hat{\sigma}_n\right) \beta' Z_i\left(e_i - X_i'\beta\right) \right.\right.$$
$$\left.\left. -\beta' I\!E\left[\tilde{w}\left(\tilde{F}_\beta(a_i(\beta)), \hat{\sigma}_n\right) Z_i\left(e_i - X_i'\beta\right)\right] \right\} \right| < \frac{\tau_C}{2}. \quad (25)$$

But (23) and (25) imply that for any $n > n_{\varepsilon_1,\delta_1,\theta_1,\tau_C}$ and any $\omega \in B_n \cap D_n$ we have

$$\inf_{\|\beta\| > \delta_1} -\frac{1}{n} \beta' I\!N E_{Y,X,Z}^{(\tilde{w},\rho,\hat{\sigma}_n,n)}(\beta) > \frac{\tau_C}{2}. \quad (26)$$

Of course, $P\left(B_n \cap D_n\right) > 1 - \varepsilon_1$. But it means that all solutions of normal equations (16) are inside the ball of radius δ_1 with probability at least $1 - \varepsilon_1$, i. e. in other words, $\hat{\beta}^{(SWIV,w,\rho,\hat{\sigma}_n,n)}$ is weakly consistent. □

5 Patterns of results of simulations

In the simulations we compared *S-weighted instrumental variables* with classical *instrumental variables* (which is not robust) and with three other robust versions of *instrumental variables*, namely *instrumental weighted variables* - see [35], *S-instrumental variables* and *W-instrumental variables* - see [7] and [8] (unfortunately the description of these estimators would require rather large space, so we only refer to original papers). The best results from these three alternative estimators were achieved by *S-instrumental variables* and by the *instrumental weighted variables*, we decided to report in tables below *S-instrumental variables* (the lack of space has not allow to present more).

5.1 Generating the data

The data were generated for $i = 1, 2, .., n,\ t = 1, 2, ..., T$ according to the model

$$Y_{it} = 1 - 2 \cdot X_{it1} + 3 \cdot X_{it2} - 4 \cdot X_{it3} + 5 \cdot X_{it4} + \sigma_{it} \cdot e_{it},$$

with $X_{it+1} = 0.9 \cdot X_{it} + 0.1 \cdot v_{it} + 0.5 \cdot e_{it}$ where the initial value $\{X_{i1}\}_{i=1}^{n}$, the innovations $\{v_{it}\}_{i=1,t=1}^{n,T}$ and the disturbances $\{e_{it}\}_{i=1,t=1}^{n,T}$ were i. i d. four dimensional normal vectors with the zero means and the unit covariance matrix. Sequence $\{\sigma_{it}\}_{i=1,t=1}^{n,T}$ is i. i. d., distributed uniformly over $[0.5, 5.5]$. In the role of the objective function we have employed Tukey's ρ given for some $c > 0$ as

$$\rho_c(x) = \frac{x^2}{2} - \frac{x^4}{2 \cdot c^2} + \frac{x^6}{6 \cdot c^4} \quad \text{for} \quad abs(x) \leq c,$$
$$= \frac{c^2}{6} \qquad \text{otherwise.}$$

For $0 < h < g < 1$ the weight function $w(r) : [0, 1] \to [0, 1]$ is equal to 1 for $0 \leq r \leq h$, it is equal to 0 for $g \leq r \leq 1$ and it decreases from 1 to 0 for $h \leq r \leq g$, i. e. putting $c = g - h$ and $y = g - r$ we compute

$$w(r) = 3\frac{y^2}{c^2} - 3\frac{y^4}{c^4} + \frac{y^6}{c^6}, \quad (27)$$

i. e. between h and g the weight function borrowed the shape from Tukey's ρ.

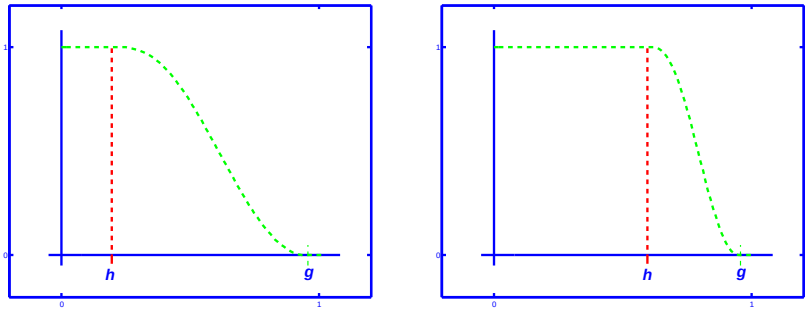

FIGURE 1

The examples of possible shapes of weight function.

The data were contaminated so that we selected randomly one block (i. e. one $t \in \{1, 2, ..., T\}$) and either the bad leverage points were created as $X^{(new)} = 5 \cdot X^{(original)}$ and $Y^{(wrong)} = -Y^{(correct)}$ or the outliers were created as $Y^{(wrong)} = -3 \cdot Y^{(correct)}$. The data contained the same number of good leverage points $X^{(new)} = 20 \cdot X^{(original)}$ (with the response Y calculated correctly) as of the bad leverage points.

5.2 Reporting the results

We have generated 500 sets, each containing $n \cdot T$ observations (it is specified in heads of tables) and the we calculated the estimates

$$\left\{\hat{\beta}^{(index,k)} = (\hat{\beta}_1^{(index,k)}, \hat{\beta}_2^{(index,k)}, \hat{\beta}_3^{(index,k)}, \hat{\beta}_4^{(index,k)}, \hat{\beta}_5^{(index,k)})'\right\}_{k=1}^{500} \quad (28)$$

where the abbreviations IV, SIV and $SWIV$ at the position of *"index"* indicate the method employed for the computation, namely IV - for the *instrumental variables*, SIV - for *S-instrumental variables estimator* and finally $SWIV$ - for *S-weighted instrumental variables estimator*. The empirical means and the empirical mean squared errors (MSE) of estimates of coefficients (over these 500 repetitions) were computed, i. e. we report values (for $j = 1, 2, 3, 4$ and 5)

$$\hat{\beta}_j^{(index)} = \frac{1}{500}\sum_{k=1}^{500}\hat{\beta}_j^{(index,k)} \text{ and } \widehat{\text{MSE}}\left(\hat{\beta}_j^{(index)}\right) = \frac{1}{500}\sum_{k=1}^{500}\left[\hat{\beta}_j^{(index,k)} - \beta_j^0\right]^2 \quad (29)$$

where $\beta^0 = [1, -2, 3, -4, 5]'$ and the index have the same role as above. The results are given in tables in the form: The first cell of each row indicates the method, e. g. $\hat{\beta}^{(IV)}$, the next 5 cells contain then just $\hat{\beta}^{(IV)}_{\left(\widehat{MSE}(\hat{\beta}^{(IV)})\right)}$ for the first, the second up to the fifth coordinate.

TABLE 1

The contamination by leverage points on the level of 1%, $n = 100$.
The values of variance of the disturbances randomly selected from $[0.5, 5.5]$.

$\boldsymbol{T = 1, \quad n \cdot T = 100, \quad h = 0.98, \quad g = 0.99}$					
$\hat{\beta}^{(IV)}_{(MSE)}$	$0.970_{(0.372)}$	$-1.924_{(0.375)}$	$2.835_{(0.419)}$	$-3.781_{(0.429)}$	$4.706_{(0.479)}$
$\hat{\beta}^{(SIV)}_{(MSE)}$	$0.993_{(0.105)}$	$-1.986_{(0.133)}$	$2.979_{(0.141)}$	$-4.021_{(0.151)}$	$4.987_{(0.142)}$
$\hat{\beta}^{(SWIV)}_{(MSE)}$	$0.992_{(0.106)}$	$-1.990_{(0.105)}$	$3.002_{(0.122)}$	$-4.000_{(0.120)}$	$4.992_{(0.105)}$

$\boldsymbol{T=2,\quad n\cdot T=200,\quad h=0.98,\quad g=0.99}$					
$\hat{\beta}^{(IV)}_{(MSE)}$	$0.966_{(0.319)}$	$-1.873_{(0.404)}$	$2.814_{(0.378)}$	$-3.808_{(0.369)}$	$4.690_{(0.605)}$
$\hat{\beta}^{(SIV)}_{(MSE)}$	$0.993_{(0.056)}$	$-2.004_{(0.082)}$	$3.007_{(0.077)}$	$-4.017_{(0.071)}$	$4.984_{(0.084)}$
$\hat{\beta}^{(SWIV)}_{(MSE)}$	$0.993_{(0.059)}$	$-1.997_{(0.069)}$	$3.009_{(0.061)}$	$-4.002_{(0.058)}$	$4.992_{(0.068)}$

$\boldsymbol{T=3,\quad n\cdot T=300,\quad h=0.98,\quad g=0.99}$					
$\hat{\beta}^{(IV)}_{(MSE)}$	$0.982_{(0.259)}$	$-1.879_{(0.323)}$	$2.795_{(0.363)}$	$-3.734_{(0.453)}$	$4.678_{(0.532)}$
$\hat{\beta}^{(SIV)}_{(MSE)}$	$1.002_{(0.037)}$	$-2.017_{(0.050)}$	$2.995_{(0.057)}$	$-4.009_{(0.057)}$	$4.989_{(0.058)}$
$\hat{\beta}^{(SWIV)}_{(MSE)}$	$0.999_{(0.039)}$	$-2.006_{(0.041)}$	$2.990_{(0.050)}$	$-3.989_{(0.046)}$	$4.995_{(0.047)}$

$\boldsymbol{T=4,\quad n\cdot T=400,\quad h=0.98,\quad g=0.99}$					
$\hat{\beta}^{(IV)}_{(MSE)}$	$0.961_{(0.213)}$	$-1.887_{(0.280)}$	$2.863_{(0.290)}$	$-3.764_{(0.403)}$	$4.743_{(0.380)}$
$\hat{\beta}^{(SIV)}_{(MSE)}$	$0.995_{(0.027)}$	$-2.022_{(0.046)}$	$2.986_{(0.052)}$	$-4.017_{(0.047)}$	$4.981_{(0.049)}$
$\hat{\beta}^{(SWIV)}_{(MSE)}$	$0.994_{(0.029)}$	$-2.013_{(0.038)}$	$2.992_{(0.042)}$	$-4.014_{(0.038)}$	$4.986_{(0.036)}$

$\boldsymbol{T=5,\quad n\cdot T=500,\quad h=0.98,\quad g=0.99}$					
$\hat{\beta}^{(IV)}_{(MSE)}$	$0.964_{(0.194)}$	$-1.859_{(0.360)}$	$2.806_{(0.393)}$	$-3.781_{(0.334)}$	$4.717_{(0.407)}$
$\hat{\beta}^{(SIV)}_{(MSE)}$	$1.003_{(0.025)}$	$-2.007_{(0.042)}$	$2.995_{(0.041)}$	$-4.006_{(0.042)}$	$4.997_{(0.045)}$
$\hat{\beta}^{(SWIV)}_{(MSE)}$	$1.002_{(0.025)}$	$-2.006_{(0.032)}$	$2.991_{(0.033)}$	$-4.000_{(0.033)}$	$5.004_{(0.036)}$

TABLE 2

The contamination by leverage points on the level of 5%, $n = 100$.
The values of variance of the disturbances randomly selected from $[0.5, 5.5]$.

$\boldsymbol{T=5,\quad n\cdot T=100, h=0.940, g=0.948}$					
$\hat{\beta}^{(IV)}_{(MSE)}$	$0.879_{(4.420)}$	$-1.505_{(6.863)}$	$2.335_{(6.609)}$	$-3.096_{(7.212)}$	$3.730_{(7.995)}$
$\hat{\beta}^{(SIV)}_{(MSE)}$	$0.992_{(0.662)}$	$-1.953_{(0.946)}$	$2.824_{(1.243)}$	$-3.920_{(1.017)}$	$4.672_{(2.158)}$
$\hat{\beta}^{(SWIV)}_{(MSE)}$	$0.982_{(0.178)}$	$-1.982_{(0.336)}$	$2.981_{(0.349)}$	$-4.018_{(0.296)}$	$4.954_{(0.362)}$

$\boldsymbol{T=10,\quad n\cdot T=200,\quad h=0.940,\quad g=0.948}$					
$\hat{\beta}^{(IV)}_{(MSE)}$	$0.862_{(2.967)}$	$-1.604_{(3.871)}$	$2.548_{(3.839)}$	$-3.227_{(4.665)}$	$4.011_{(5.258)}$
$\hat{\beta}^{(SIV)}_{(MSE)}$	$0.990_{(0.138)}$	$-2.001_{(0.349)}$	$2.971_{(0.350)}$	$-3.997_{(0.273)}$	$4.933_{(0.389)}$
$\hat{\beta}^{(SWIV)}_{(MSE)}$	$0.990_{(0.082)}$	$-1.993_{(0.140)}$	$3.010_{(0.138)}$	$-3.992_{(0.133)}$	$5.010_{(0.154)}$

$\boldsymbol{T=15,\quad n\cdot T=300,\quad h=0.940,\quad g=0.948}$					
$\hat{\beta}^{(IV)}_{(MSE)}$	$0.755_{(1.912)}$	$-1.479_{(3.644)}$	$2.431_{(3.242)}$	$-3.324_{(4.295)}$	$3.980_{(4.988)}$
$\hat{\beta}^{(SIV)}_{(MSE)}$	$0.984_{(0.053)}$	$-2.020_{(0.219)}$	$2.934_{(0.233)}$	$-4.020_{(0.236)}$	$4.897_{(0.218)}$
$\hat{\beta}^{(SWIV)}_{(MSE)}$	$0.985_{(0.048)}$	$-2.008_{(0.107)}$	$2.995_{(0.121)}$	$-4.017_{(0.104)}$	$4.975_{(0.112)}$

$\boldsymbol{T = 20, \quad n \cdot T = 400, \quad h = 0.940, \quad g = 0.948}$					
$\hat{\beta}^{(IV)}_{(MSE)}$	$0.774_{(1.463)}$	$-1.562_{(2.618)}$	$2.577_{(2.490)}$	$-3.374_{(2.845)}$	$4.220_{(2.826)}$
$\hat{\beta}^{(SIV)}_{(MSE)}$	$0.992_{(0.036)}$	$-1.988_{(0.199)}$	$2.934_{(0.191)}$	$-3.974_{(0.176)}$	$4.948_{(0.169)}$
$\hat{\beta}^{(SWIV)}_{(MSE)}$	$0.994_{(0.033)}$	$-1.986_{(0.076)}$	$3.006_{(0.078)}$	$-3.981_{(0.077)}$	$5.017_{(0.072)}$

$\boldsymbol{T = 25, \quad n \cdot T = 500, \quad h = 0.940, \quad g = 0.948}$					
$\hat{\beta}^{(IV)}_{(MSE)}$	$0.794_{(1.074)}$	$-1.629_{(1.644)}$	$2.494_{(1.923)}$	$-3.551_{(1.722)}$	$4.314_{(2.187)}$
$\hat{\beta}^{(SIV)}_{(MSE)}$	$0.990_{(0.034)}$	$-1.983_{(0.168)}$	$2.930_{(0.172)}$	$-3.991_{(0.151)}$	$4.944_{(0.209)}$
$\hat{\beta}^{(SWIV)}_{(MSE)}$	$0.993_{(0.028)}$	$-1.985_{(0.062)}$	$2.984_{(0.069)}$	$-3.995_{(0.060)}$	$4.996_{(0.065)}$

As we already said at the abstract, it is believed that the leverage points are more complicated problem than outliers. The next table offers results indicating that the "classical" estimators as the *least median of squares*, the *least trimmed squares* or the *S-estimator* can exhibit a problem when data contain a group of good leverage points (far away from the main bulk of data) and some outliers (not very far from the bulk of data). As the mean squared errors of the *S-estimates* below indicate, the *S-estimator* have used the information in data less efficiently than *S-weighted estimator* (see (5)). (Due to the lack of space we present only the results for the *S-estimator* - which were the best among the "classical" estimators (LMS, LTS, LWS and *S-estimator*). The reason for large MSE of the *S-estimates* is the depression of the information brought by good leverage points. It happened due to the implicit estimation of variance of disturbances.

Generally, the implicit estimation of variance of the disturbances (e. g. by LMS, LTS or LWS) is the significant advantage (from the computational point of view) because the estimators do not need any studentization - contrary to M-estimators - see [1]. Sometimes it can betray us.

TABLE 3

Contamination by outliers: For randomly selected observations we put $Y_i = 5 * Y_i^{original}$ *and data contained also good leverage points* $X_i = 10 * X_i^{original}$ *and responses* Y_i*'s were computed correctly.*

Number of observations in each dataset = 500					
Contamination level = 1%, $h = 0.973$, $g = 0.989$					
$\hat{\beta}^{(S)}_{(MSE)}$	$1.010_{(0.024)}$	$2.003_{(0.031)}$	$-3.021_{(0.032)}$	$3.975_{(0.035)}$	$-4.974_{(0.023)}$
$\hat{\beta}^{(SW)}_{(MSE)}$	$1.002_{(0.022)}$	$2.001_{(0.013)}$	$-3.012_{(0.011)}$	$3.986_{(0.010)}$	$-4.990_{(0.011)}$
Contamination level = 2%, $h = 0.963$, $g = 0.978$					
$\hat{\beta}^{(S)}_{(MSE)}$	$0.993_{(0.027)}$	$2.014_{(0.032)}$	$-2.973_{(0.027)}$	$3.985_{(0.028)}$	$-4.996_{(0.023)}$
$\hat{\beta}^{(SW)}_{(MSE)}$	$0.992_{(0.030)}$	$2.008_{(0.005)}$	$-3.000_{(0.004)}$	$4.000_{(0.005)}$	$-5.003_{(0.004)}$

Contamination level = 5%, $h = 0.921$, $g = 0.942$					
$\hat{\beta}^{(S)}_{(MSE)}$	$0.985_{(0.028)}$	$1.948_{(0.040)}$	$-2.967_{(0.034)}$	$3.919_{(0.038)}$	$-4.955_{(0.030)}$
$\hat{\beta}^{(SW)}_{(MSE)}$	$1.014_{(0.027)}$	$2.002_{(0.002)}$	$-3.006_{(0.002)}$	$3.998_{(0.002)}$	$-5.003_{(0.001)}$

ACKNOWLEDGEMENT

The paper was written with the support of the Czech Science Foundation project P402/12/G097 DYME - Dynamic Models in Economics.

References

1. Bickel, P. J. (1975): One-step Huber estimates in the linear model. *J. Amer. Statist. Assoc. 70, 428–433.*
2. Boček, P., Lachout, P. (1993): Linear programming approach to LMS-estimation. *Memorial volume of Comput. Statist. & Data Analysis 19(1995), 129 - 134.*
3. Breiman, L. (1968): *Probability.* Addison-Wesley Publishing Company, London 1968.
4. Campbell, N. A., Lopuhaa, H. P. and Rousseeuw, P. J. (1998): On calculation of a robust S-estimator if a covariance matrix. *Statistics in medcine, 17, 2685 - 2695.*
5. Carroll, R. J., Stefanski, L. A. (1994): Measurement error, instrumental variables and correction for attenuation with applications to meta-analyses. *Statistics in Medicine 13, 1265 - 1282.*
6. Čížek, P., Víšek, J. Á. (2000): The least trimmed squares. *User Guide of Explore, Humboldt University, Berlin.*
7. Cohen-Freue, G. V., Ortiz-Molina, H., Zamar, R. H. (2013): Natural robustification of the ordinary instrumental variables estimator. *Biometrics 69 641 - 650.*
8. Desborges, R., Verardi, V. (2012): A robust instrumental-variable estimator. *The Stata Journal (2012) 12, 169 -181.*
9. Hájek, J., Šidák, Z. (1967): *Theory of Rank Test.* Academic Press, New York.
10. Hampel, F. R., Ronchetti, E. M., Rousseeuw, P. J., Stahel, W. A. (1986): *Robust Statistics – The Approach Based on Influence Functions.* New York: J.Wiley & Son.
11. Heckman, J., Urza, S., Vytlacil, E. J. (2006): Understanding instrumental variables in models with essential heteroscedasticity. *Working papers 12574, National Bureau of Economic Research, 2006.*
12. Hawkins, D. M. (1994): The feasible solution algorithm for least trimmed squares regression. *Computational Statistics and Data Analysis 17, 185 - 196.*
13. Hawkins, D. M., Olive, D. J. (1999): Improved feasible solution algorithms for breakdown estimation. *Computational Statistics & Data Analysis 30, 1 - 12.*
14. Hettmansperger, T. P., Sheather, S. J. (1992): A Cautionary Note on the Method of Least Median Squares. *The American Statistician 46, 79–83.*
15. Koenker, R., Bassett, G. (1978): Regression quantiles. *Econometrica, 46, 33-50.*
16. Maronna, R. A., Yohai, V. (1981): Asymptotic behaviour of general M–estimates for regression and scale with random carriers. *Z. Wahrscheinlichkeitstheorie verw. Gebiete 58, 7–20.*
17. Paige, C. C., Strakoš, Z. (2002): Scaled total least squares fundamentals. *Numerische Mathematik 91, 117 - 146.*
18. Rousseeuw, P. J.(1983). Multivariate estimation with high breakdown point. In *Mathematical Statistics and Applications B (W. Grossmann, G. Pflug, I. Vincze and W. Wertz, eds.) Reidel, Dordrecht, 283-297.*

19. Rousseeuw, P. J. (1984): Least median of square regression. *Journal of Amer. Statist. Association 79, 871-880.*
20. Rousseeuw, P. J., Yohai, V. (1984): Robust regression by means of *S*-estimators. In: *Robust and Nonlinear Time Series Analysis. eds. J. Franke, W. Hárdle and R. D. Martin, Lecture Notes in Statistics No. 26 Springer Verlag, New York, 256-272.*
21. Siegel, A. F. (1982): Robust regression using repeated medians. *Biometrica 69, 242 - 244.*
22. Víšek, J. Á.(1990): Empirical study of estimators of coefficients of linear regression model. *Technical report of Institute of Information Theory and Automation, Czechoslovak Academy of Sciences (1990), number 1699.*
23. Víšek, J. Á. (1998): Robust instruments. *Robust'98 (eds. J. Antoch & G. Dohnal, published by Union of Czech Mathematicians and Physicists), Prague: matfyzpress, 195 - 224.*
24. Víšek, J. Á.(2000): Regression with high breakdown point. *ROBUST 2000 (J. Antoch & G. Dohnal, eds.), The Union of the Czech Mathematicians and Physicists and the Czech Statistical Society 2001, Prague: matfyzpress, 324 - 356.*
25. Víšek, J. Á.(2002): The least weighted squares II. Consistency and asymptotic normality. *Bulletin of the Czech Econometric Society 9, 1 - 28.*
26. Víšek, J. Á.(2004): Robustifying instrumental variables. *Proceedings of COMPSTAT'2004 (J. Antoch, ed.), Physica-Verlag/Springer, 1947 - 1954.*
27. Víšek, J. Á. (2006): The least trimmed squares. Part I - Consistency. Part II - $\sqrt{n}$-consistency. Part III - Asymptotic normality and Bahadur representation. *Kybernetika (2006) 42, 1 - 36, 181 - 202, 203 - 224.*
28. Víšek, J. Á.(2006): Instrumental weighted variables. *Austrian Journal of Statistics 35(2006), 379 - 387.*
29. Víšek, J. Á.(2006): Instrumental Weighted Variables - algorithm. *Proceedings of the COMPSTAT 2006 (A. Rizzi & M. Vichi, eds.), Physica-Verlag, Springer Company, Heidelberg, 777-786.*
30. Víšek, J. Á. (2009): Consistency of the instrumental weighted variables. *Annals of the Institute of Statistical Mathematics 61, 543 - 578.*
31. Víšek, J. Á.(2011): Empirical distribution function under heteroscedasticity. *Statistics 45, 497-508.*
32. Víšek, J. Á.(2011): Consistency of the least weighted squares under heteroscedasticity. *Kybernetika 47 , 179-206.*
33. Víšek, J.Á.(2015): *S*-weighted estimators. *Proceedings of the 16th Conference on the Applied Stochastic Models, Data Analysis and Demographics 2015 (C. H. Skiadas, ed.), 1031 - 1042* (or *Stochastic and Data Analysis Methods and Applications in Statistics and Demography (J. R. Bozeman, T. Oliveira & C. H. Skiadas, eds.), 437 - 448.*)
34. Víšek, J. Á.(2016): Representation of *SW*-estimators. *Proceedings of the 4th Stochastic Modeling Techniques and Data Analysis International Conference with Demographics Workshop, SMTDA 2016, (C. H. Skiadas,ed.), 425 - 438.*
35. Víšek, J. Á.(2017): Instrumental weighted variables under heteroscedasticity. Part I. Consistency. Part II. Numerical study. *Kybernetika 53 (2017), 1 - 25, 26 - 58.*
36. Wagenvoort, R., and Waldmann, R. (2002). On B-robust instrumental variable estimation of the linear model with panel data. *Journal of Econometrics 106, 297-324.*

Grouping Property and Decomposition of Explained Variance in Linear Regression.

Henri Wallard

Ipsos Science Center. 35 rue du Val de Marne, 75013 Paris. France.
(E-mail: henriwallard@hotmail.com)

Abstract. The quantification of the relative importance of predictors on a response variable has been an active subject of research for many years. Regression analysis may be used for that purpose but estimating importance of predictors via (standardized) regression coefficients is not adequate in the presence of correlations between these variables. Therefore, alternative methods have been considered. Grouping property is respected when estimators of importance tend to equate for highly correlated predictors. We will analyze the respect of grouping property for several methods used to quantify the relative importance of predictors through decomposition of the explained variance in linear regression. After being criticized by several authors, CAR scores have been recommended again as estimators of importance of predictors and been presented as respecting the grouping property. We will show that CAR scores actually do not respect this property. We will explain in return why some other variance decomposition methods do respect grouping property and we will formulate recommendations for quantifying the relative importance of predictors.
Keywords: Variance decomposition, linear regression, CAR scores, random forests.

1 Introduction

The quantification of relative importance of predictors on a response variable has been a subject of research in biostatistics, psychology, economics or market research. Many methods have been investigated, sometimes reinvented by researchers across different fields, see Gromping [9], [10] and [11] for an overview. Some approaches relate to game theory (*lmg, pmvd, owen*). Others are based on regularization techniques (lasso, elasticnet). Random forests have also been proposed both for estimation of relative importance and for variable selection, see Gromping [10] and Genuer *et al.* [4] and [5]. Some methods consist in decomposing the variance explained by the linear regression among the different predictors. When the predictors are mutually de-correlated, the R^2 can be naturally decomposed by allocating to each predictor the square of the correlation coefficient between this predictor and the variable to predict, but with collinearity between predictors there is no longer a unique and natural way to decompose the explained variance. Multicollinearity designates situations in which two or more explanatory variables in a multiple regression model are highly correlated.

Several methods used to decompose the explained variance in linear regression can be presented in a unified perspective using the singular value decomposition of the matrix of (standardized) observations. One of these methods was proposed in 1962 and designated as the Gibson method [6], but has later

been criticized see [13] and [11]. These criticisms lead several authors to recommend other approaches, for instance Genizi [3] in 1993 and Johnson [13] in 2000. However in 2011 Zuber and Strimmer [16] have applied again the Gibson method under the name of CAR scores for regression analysis and variable selection and suggested that CAR scores would benefit from the grouping property as introduced by Zou and Hastie [15], in the sense that if two predictors tend to correlate their CAR scores or the square of their CAR scores would tend to equate. As a consequence this method would have interesting properties for the quantification of the importance of predictors and their selection. We will demonstrate that actually CAR scores do not respect the grouping property as defined by Zou and Hastie [15] but in return that Genizi and Johnson method do respect such grouping property. Our analysis leads to recommend against the usage of Gibson-CAR scores.

2 CAR scores.

2.1 Definition and estimators.

Presentation of CAR scores. Let Y be a random variable and $\boldsymbol{X}=(X_1,...,X_p)^T$ be a random vector of dimension p. (of finite variance). The covariance matrix is $\text{var}(\boldsymbol{X})=\boldsymbol{\Sigma}_{XX}$. Let us note also $\boldsymbol{P}_{XX}$ the correlation matrix. We can decompose the covariance matrix as:

$$\boldsymbol{\Sigma}_{XY} = \boldsymbol{V}^{1/2}\boldsymbol{P}_{XX}\boldsymbol{V}^{1/2} \tag{1}$$

where $\boldsymbol{V}$ is the diagonal matrix containing the variances of the X_i. If we note $\boldsymbol{P}_{XY}=(\rho_{X_1y},...,\rho_{X_py})^T$ the vector or marginal correlations between Y and $\boldsymbol{X}$ the vector of CAR scores is noted as $\boldsymbol{\omega}=(\omega_1,...,\omega_p)^T$ and given by:

$$\boldsymbol{\omega} = \boldsymbol{P}_{XX}^{-1/2}\boldsymbol{P}_{XY} \tag{2}$$

CAR stands for *"Correlation-Adjusted marginal coRrelation"*.

As in [16] we will also introduce the *best linear predictor* of Y, the linear combination of the explanatory variables as follows :

$$Y^* = a + \boldsymbol{b}^T\boldsymbol{X}$$

that minimizes the mean squared prediction error $\text{E}[(Y\text{-}Y^*)^2]$. In the approach used by Zuber and Strimmer [16] the coefficients a and $\boldsymbol{b}=(b_1,...,b_d)^T$ are considered as *constant* for the interpretation of the grouping property, but this restriction leads to erroneous conclusions regarding the interest of the method, as shown later.

It results from the definition of CAR scores above that the sum of the square of the CAR scores adds up to the R^2 of the linear regression (see for instance [13] or [16]). This is shown in equation 3 below:

$$\boldsymbol{\omega^T\omega} = \boldsymbol{P'}_{XY}\boldsymbol{P}_{XX}^{-1}\boldsymbol{P}_{XY} = R^2 \tag{3}$$

It is possible to use the squared CAR scores to quantify the relative importance of each predictor as follows. Formally:

$$\Phi^{CAR}(X_j) = \omega_j^2 \tag{4}$$

CAR scores with two predictors. In the case with two predictors X_1 and X_2 and if we note $(\beta std)_1$ and $(\beta std)_2$ the standardized regression coefficients of Y on X_1 and X_2 and note cor(X_1,X_2)=ρ_{12}, we can write the following result:

$$\omega_1^2 - \omega_2^2 = ((\beta std_1)^2 - (\beta std_2)^2)\sqrt{1-\rho_{12}^2} \tag{5}$$

This equation is used by Zuber and Strimmer [16] with the restriction that the coefficients βstd_i are kept constant when ρ_{12} tends towards 1 so both side of the equation 5 tend towards 0. The consequences of this restriction are discussed later in this paper.

Estimators of CAR scores using SVD. When applied to linear regression on a set of observations, CAR scores as well as some other explained variance decomposition methods can be presented using matrix calculus.

Let us consider a linear model of the form below with p predictors:

$$Y_i = \beta_0 + X_{i1}\beta_1 + ... + X_{ip}\beta_p + \varepsilon_i$$

with independent errors terms ε_i of expectation 0 and constant positive variance σ^2.

Let us note as $\boldsymbol{X}$ the matrix of n observations of the p predictors (i=1,...,n and j=1,...,p), $\boldsymbol{X}$ is a (n, p) matrix deemed to be of rank p, and let us note $\boldsymbol{Y}$ the column vector of the n observations of $\boldsymbol{Y}$.

$$\boldsymbol{X} = (\boldsymbol{x_{ij}})$$

$$\boldsymbol{Y} = (\boldsymbol{y_i})$$

We will note as $\boldsymbol{Y^*}$ the values predicted by the linear model:

$$\boldsymbol{Y^* = X\ \beta^* = (X'X)^{-1}X'Y}$$

We will assume in the rest of this article that $\boldsymbol{Y}$ and the p columns of $\boldsymbol{X}$, designated as $\boldsymbol{X_j}$, are standardized: mean of all variables equal 0 and variance equal to 1.

We will refer to the singular value decomposition (SVD) of the matrix of observations using the notations from Johnson [13] as reminded below. The singular value decomposition of $\boldsymbol{X}$ is:

$$\boldsymbol{X = P\Delta Q'} \tag{6}$$

We will define a particular matrix $\boldsymbol{Z}$ as :

$$\boldsymbol{Z = PQ'} \tag{7}$$

$\boldsymbol{Z}$ is of rank p and is the Mahalanobis transform of X. $\boldsymbol{Z_j}$ is the j_{th} column of $\boldsymbol{Z}$. Johnson [13] pointed out that the columns of $\boldsymbol{Z}$ are also characterized as the best-fitting approximations to the columns of $\boldsymbol{X}$ in the sense that they

minimize the sum of squares of the differences between the original variables and the orthogonal variables.

Estimators of the CAR scores can be calculated using the singular value decomposition of the matrix $\boldsymbol{X}$. The vector of the estimators of the CAR scores is:

$$\hat{\boldsymbol{\Omega}} = \frac{\mathbf{1}}{\boldsymbol{n-1}}(\boldsymbol{X'X})^{-\mathbf{1/2}}\boldsymbol{X'Y} = \frac{\mathbf{1}}{\boldsymbol{n-1}}\boldsymbol{Q\Delta^{-1}Q'Q\Delta P'Y} = \frac{\mathbf{1}}{\boldsymbol{n-1}}\boldsymbol{QP'Y} \tag{8}$$

We have :

$$\hat{\boldsymbol{\Omega}} = \frac{\mathbf{1}}{\boldsymbol{n-1}}\boldsymbol{QP'Y} = \frac{\mathbf{1}}{\boldsymbol{n-1}}\boldsymbol{Z'Y} \tag{9}$$

The estimator of the CAR score for predictor j is equal to $\text{cor}(\boldsymbol{Y},\boldsymbol{Z_j})$.

As $\boldsymbol{Z}$ is a unitary matrix as a consequence of the properties of singular value decomposition, the column vectors of $\boldsymbol{Z}$ are all of norm 1 and are all orthogonal and the sum of the squares of the CAR scores adds up to the R^2 of the model. We will refer to the squares of the CAR scores, called squared CAR scores, which represent the proportion of R^2 allocated to a given predictor with the CAR scores method.

2.2 Historical criticism of the CAR scores.

In 2011, Zuber and Strimmer [16] proposed the CAR scores as a way to decompose the explained variance. This method was initially proposed in 1962 by Gibson as explained by Gromping in [9] and [11]. The CAR scores were at that time called Gibson scores. Zuber and Strimmer point out that the CAR scores are computed in regressing the variable to predict on the Mahalanobis-derecorrelated predictors and that these decorrelated predictors are the "*nearest*" to the original standardized predictors. This proximity had been identified and demonstrated by Johnson in 1966 as reminded in [13] and had actually been viewed by several authors as a reason not to use the CAR scores. For instance Johnson [13] explained that these decorrelated variables Z are only approximation of the original variables and may not be close representations of the original variables if two or more of the predictor variables are highy correlated. Similarly Gromping [11] underlined that in case of relevant correlations among the X variables, the Z variables can be far from being good representatives for the corresponding X variables. Gromping reminds that in 1978 Green *et al.* [7] therefore proposed to modify the values from Gibson by relating the Z variables back to the X variables leading to the Green method. In 1993 Genizi [3] and in 2000 Johnson [13] proposed also another way to decompose the explained variance. So the literature on variance decomposition methods had been criticizing Gibson-CAR scores, and this is precisely why other methods like Green [7], Fabbris [2] or Genizi-Johnson [3] and [13] were proposed, see [11] and [12]. The usage of Singular Value Decomposition will enable to analyze the respective properties of these various methods.

3 Variance decomposition methods and SVD.

We can formalize several methods used to decompose the explained variance in linear regression as a succession of two steps, first to allocate the explained variance in p positive terms and then further reallocate these p terms back to the original predictors. We can formalize this considering a vector $\boldsymbol{A}$ of p positive terms adding up to the R^2 and a matrix of weights $\boldsymbol{\Pi}$ with all positive terms, the only additional condition required being that each column of $\boldsymbol{\Pi}$ adds up to 1:

$$\boldsymbol{A} = (a_j)$$
$$\boldsymbol{\Pi} = (\pi_{ij})$$

The relative importance estimators for the predictors can then be computed as the column vector $\boldsymbol{R_w}$:

$$\boldsymbol{R_w = \Pi A}$$

Table 1 summarizes the empirical estimators of relative importance for the methods proposed by Fabbris, Genizi-Johnson (these two being identical) and Gibson-CAR scores. We are using the notation $\boldsymbol{M^{\cdot 2}}$ for the Hadamard squared matrix obtained when each term of the matrix $\boldsymbol{M}$ is elevated to its square.

Methods	**Matrix $\boldsymbol{\Pi}$**	**Vector A**
Fabbris	$\boldsymbol{Q^{\cdot 2}}$	$(\frac{1}{n-1})^{\boldsymbol{2}}\boldsymbol{(P'Y)^{\cdot 2}}$
Genizi-Johnson	$(\frac{1}{n-1})^{\boldsymbol{2}}\boldsymbol{(Z'X)^{\cdot 2}}$	$(\frac{1}{n-1})^{\boldsymbol{2}}\boldsymbol{(Z'Y)^{\cdot 2}}$
CAR scores	$\boldsymbol{I}$	$(\frac{1}{n-1})^{\boldsymbol{2}}\boldsymbol{(Z'Y)^{\cdot 2}}$

Table 1. Allocation of explained variance.

Looking at line 2 of Table 1 we can also see that any orthogonal matrix $\boldsymbol{O}$ can be used instead of $\boldsymbol{Z}$ to generate an allocation of the explained variance, as π_{ij} is the square of cor($\boldsymbol{O_i}$,$\boldsymbol{X_j}$), so the columns of $\boldsymbol{\Pi}$ all add up to $\mathbf{1}$. The relative importance measures computed with the Genizi-Johnson method are designated as Relative Weights as in [13], RW_i for predictor i.

4 Grouping Property of variance decomposition methods.

In the perspective of regularization and variable selection via the elastic net, Zou and Hastie [15] introduced the general concept of grouping property for any given type of regression method. Qualitatively speaking a regression method will be said to exhibit the grouping property if the coefficients of a group of highly correlated variables tend to be equal (up to a change of sign if negatively correlated) and also that in the extreme situation when variables would be

identical the regression-based method should assign to each of them identical coefficients. The grouping property appears useful for a consistent estimation of variable importance in case of multicollinearity.

Zuber and Strimmer [16] claimed that variable importance derived from CAR scores respect the grouping property. We will demonstrate that this method actually does not respect the grouping property as originally defined by Zou and Hastie [15].

The grouping property as presented by Zou and Hastie [15] applies to the usual linear regression model: given p predictors $\boldsymbol{x_1}$,...,$\boldsymbol{x_p}$, the response $\boldsymbol{y}$ is predicted by:

$$\hat{\mathbf{y}} = \hat{\beta}_0 + \mathbf{x}_1\hat{\beta}_1 + ... + \mathbf{x}_p\hat{\beta}_p$$

and where a model fitting procedure produces the vector of coefficients $\hat{\boldsymbol{\beta}}$=($\hat{\beta}_1$,...,$\hat{\beta}_p$).

By comparison Zuber and Strimmer consider situations where the coefficients in $\boldsymbol{b}$=(b_1,...,b_d)^T are kept *constants*. That particular way to analyze the respect of the grouping property when using CAR scores does not align with the full generality of the original definition proposed by Zou and Hastie [15]. In reality, keeping the vector $\boldsymbol{b}$ as constant when the correlation of the predictor variables vary results in modifying also $\boldsymbol{Y^*}$. With this approach it is impossible to analyze the performance of models with variable selection to model a given and fixed variable $\boldsymbol{Y}$ against various subsets of predictors.

If we follow the original approach of Zou and Hastie [15], we can in return analyze models where several predictors will be increasingly correlated while the response $\boldsymbol{Y}$ is kept constant, and the vector of estimated coefficients $\hat{\boldsymbol{\beta}}$ will vary when we use various subsets of predictors or when we change the structure of the correlations between predictors.
This will lead to different conclusions from Zuber and Strimmer [16], and this is extremely important in practice when real data are analysed.

4.1 Analysis of grouping property for CAR scores.

Based on the formula 5 for the case with two predictors, Zuber and Strimmer [16] state that when ρ_{12} tends towards 1 the product of the two terms on the right side of the equation 5 above tends towards zero and conclude that the two squared CAR scores for X_1 and X_2 become identical with growing absolute value of the correlation between the two predictors.

But quite contrary when the variable to predict Y is fixed (and not collinear to X_1+ X_2 which is a particular case) while the correlation between X_1 and X_2 tends towards 1, the quantity $((\beta std_1)^2 - (\beta std_2)^2)$ is not capped and the product of the two quantities on the right side of equation 5 does not tend towards zero. This will be illustrated in the case with two predictors.

4.2 Demonstration with two predictors.

Let us now consider two standardized and decorrelated variables E_1 and E_2. Let us also chose two real values ϕ and ψ.

$$X_1 = cos(\phi)E_1 - sin(\phi)E_2$$
$$X_2 = cos(\phi)E_1 + sin(\phi_)E_2$$
$$Y = cos(\psi)E_1 + sin(\psi_)E_2$$

We have (with $\phi \neq 0$):

$$\beta std_1 = \frac{sin(\phi - \psi)}{sin(2\phi)}$$
$$\beta std_2 = \frac{sin(\phi + \psi)}{sin(2\phi)}$$

Let us note:

$$\boldsymbol{X} = \begin{pmatrix} cos(\phi) & cos(\phi) \\ -sin(\phi) & sin(\phi) \end{pmatrix}$$

The matrix composing the SVD of the matrix $\boldsymbol{X}$ are(cf. formulas 6 and 7) :

$$\boldsymbol{P} = \begin{pmatrix} 1 & 0 \\ 0 & 1 \end{pmatrix}$$
$$\boldsymbol{\Delta} = \begin{pmatrix} \sqrt{1+\rho_{12}} & 0 \\ 0 & \sqrt{1-\rho_{12}} \end{pmatrix}$$
$$\boldsymbol{Q} = \begin{pmatrix} cos(\frac{\pi}{4}) & -sin(\frac{\pi}{4}) \\ sin(\frac{\pi}{4}) & cos(\frac{\pi}{4}) \end{pmatrix}$$
$$\boldsymbol{Z} = \begin{pmatrix} cos(\frac{\pi}{4}) & sin(\frac{\pi}{4}) \\ -sin(\frac{\pi}{4}) & cos(\frac{\pi}{4}) \end{pmatrix}$$

We also have :

$$\rho_{12} = cos(2\phi)$$

If we come back on equation 5 we can now write:

$$((\beta std_1)^2 - (\beta std_2)^2) = -\frac{sin(2\psi)}{sin(2\phi)} \tag{10}$$

This confirms the conclusion that the first term of the product on the right of equation 10 is not capped and tends towards the infinite in the general case ($\psi \neq 0$) if ϕ tends towards 0.

Using again formula 5 we can also express the CAR scores using directly ψ and ϕ.

$$\omega_1 = cos(\psi + \frac{\pi}{4})$$
$$\omega_2 = cos(\psi - \frac{\pi}{4})$$
$$\omega_1^2 - \omega_2^2 = -sin(2\psi) \tag{11}$$

The difference of squared CAR scores for the two predictors depends only on the correlation between Y and E_1. However it does not depend of ρ_{12} which is also $\cos(2\phi)$, correlation between X_1 and X_2. In the case of two predictors $\boldsymbol{Z}$ is actually strictly constant, see also Thomas [14]. If we look at the representation of the variables in a plane Z_1 and Z_2 are symmetric around E_1 and form with E_1 and angle of $\pm \frac{\pi}{4}$.

4.3 Analysis of grouping property using SVD.

An important property of the CAR scores is that they do not depend on the matrix $\boldsymbol{\Delta}$ but just on $\boldsymbol{PQ'}$ as shown in equations 7 and 9. The matrix $\boldsymbol{P}$ and $\boldsymbol{Q'}$ are known to include the eigenvectors of $\boldsymbol{X'X}$ and $\boldsymbol{XX'}$, but they do not depend on the eigenvalues of $\boldsymbol{X'X}$ that are the terms of the diagonal matrix $\boldsymbol{\Delta^2}$. The repartition of the eigenvalues of $\boldsymbol{\Delta^2}$ describes collinearity between predictors. The fact that the CAR scores do not depend on $\boldsymbol{\Delta}$ is the underlying reason why the CAR scores will not tend to equate when the correlation between predictors increases: high or low eigenvalues of $\boldsymbol{X'X}$ can be achieved with identical matrix $\boldsymbol{P}$ and $\boldsymbol{Q'}$.
In return if we look at table 1 at the matrix $\boldsymbol{Z'X}$ involved in the variance decomposition for Genizi-Johnson this property will be respected as we will demonstrate below. We can express as follows the matrix $\boldsymbol{Z'X}$, which when elevated to the Hadamard squarer is the matrix $\boldsymbol{\Pi}$ for Genizi-Johnson as per table 1 :

$$\boldsymbol{Z'X = QP'P\Delta Q' = Q\Delta Q'} \tag{12}$$

Equation 12 shows that the matrix $\boldsymbol{Z'X}$ is symmetric: $\boldsymbol{Z'X = X'Z}$, so we can write the matrix $\boldsymbol{\Pi}$ as $\boldsymbol{X'Z}$, and each Relative Weight as follows :

$$RW_i = \sum_{k=1}^{p} cor^2(\boldsymbol{X_i}, \boldsymbol{Z_k}) cor^2(\boldsymbol{Y}, \boldsymbol{Z_k}) \tag{13}$$

The difference of Relative Weights between two predictors is:

$$RW_i - RW_j = \sum_{k=1}^{p} ((cor^2(\boldsymbol{X_i}, \boldsymbol{Z_k})) - cor^2(\boldsymbol{X_j}, \boldsymbol{Z_k})) cor^2(\boldsymbol{Y}, \boldsymbol{Z}_k) \tag{14}$$

We have :

$$cor^2(\boldsymbol{X_i}, \boldsymbol{Z_k}) - cor^2(\boldsymbol{X_j}, \boldsymbol{Z_k}) = (cor(\boldsymbol{X_i}, \boldsymbol{Z_k}) - cor(\boldsymbol{X_j}, \boldsymbol{Z_k}))(cor(\boldsymbol{X_i}, \boldsymbol{Z_k}) + cor(\boldsymbol{X_j}, \boldsymbol{Z_k}))$$

As a consequence :

$$cor^2(\boldsymbol{X_i}, \boldsymbol{Z_k}) - cor^2(\boldsymbol{X_j}, \boldsymbol{Z_k}) \leq 2\,|cor(\boldsymbol{X_i}, \boldsymbol{Z_k}) - cor(\boldsymbol{X_j}, \boldsymbol{Z_k})| \tag{15}$$

As all variables are standardized the correlations equate to the covariance and we can use the additive property of covariance to write :

$$cor^2(\boldsymbol{X_i}, \boldsymbol{Z_k}) - cor^2(\boldsymbol{X_j}, \boldsymbol{Z_k}) \leq 2\,|cov(\boldsymbol{X_i}, \boldsymbol{Z_k}) - cov(\boldsymbol{X_j}, \boldsymbol{Z_k})| \tag{16}$$

$$cor^2(\boldsymbol{X_i}, \boldsymbol{Z_k}) - cor^2(\boldsymbol{X_j}, \boldsymbol{Z_k}) \leq 2\,|(cov(\boldsymbol{X_i} - \boldsymbol{X_j}, \boldsymbol{Z_k})| \tag{17}$$

We also have :

$$|(\boldsymbol{cov}(\boldsymbol{X_i} - \boldsymbol{X_j}, \boldsymbol{Z_k})| \leq \|\boldsymbol{X_i} - \boldsymbol{X_j}\| \tag{18}$$

If we note that :

$$\|\boldsymbol{X_i} - \boldsymbol{X_j}\| = \sqrt{2(1 - \rho_{ij})} \tag{19}$$

As the sum of the $cor^2(\boldsymbol{Y}, \boldsymbol{Z}_k)$ adds up to the R^2 in the end :

$$|RW_i - RW_j| \leq 2\sqrt{2(1 - \rho_{ij})}R^2 \tag{20}$$

This proves that Relative Weights (Johnson-Genizi measures) respect the grouping property in the general sense as defined by Zou and Hastie [15], but in return as shown before CAR scores do not respect that grouping property. In addition we can see that starting from equation 13 using $\boldsymbol{Y} = \boldsymbol{Xb}$ with $\boldsymbol{b}$ fixed does not change the rest of the subsequent demonstration. This means that like the CAR scores the Relative Weights from Genizi-Johnson will also tend to equate if the coefficients $\boldsymbol{b}$ are kept constant as considered by Zuber and Strimmer [16] for highly correlated predictors. So the *restricted* property as used by Zuber and Strimmer is equally respected by Relative Weights and CAR scores. But only Relative Weights do respect the *full* original grouping property as defined by Zou and Hastie [15]. These results show why Relative Weights are to be preferred to CAR scores.

There is also an interesting result regarding the variance decomposition via an orthogonal matrix in the case of two predictors. Using $\boldsymbol{X}$ as defined above let us consider an orthonormal matrix $\boldsymbol{O}$ as defined below :

$$\boldsymbol{O} = \begin{pmatrix} cos(\omega) & -sin(\omega) \\ sin(\omega) & cos(\omega) \end{pmatrix}$$

and $\boldsymbol{Y}$ similarly as in the case above with two predictors $\boldsymbol{Y}$=$(cos(\psi), sin(\psi))^T$.

If we substitute the matrix $\boldsymbol{O}$ to the matrix $\boldsymbol{Z}$ in the computation of the relative weights (Genizi-Johnson) we can easily compute the difference between the two relative weights for variables 1 and 2 noted RW_1^O and RW_2^O when using the matrix O for decomposition :

$$RW_1^O - RW_2^O = cos(2(\phi + \omega)cos^2(\psi - \omega) + cos(2(\phi - \omega)sin^2(\psi - \omega) \tag{21}$$

When ϕ tends towards 0, $RW_1^O - RW_2^O$ tends towards $\cos(2\omega)$ as per equation 21. So the two relative weights will tend to equate in case the correlation between the two predictors tends towards 1 if and only if $\omega = \pm\pi/4$ or $\omega = \pm 3\pi/4$, which means if $\boldsymbol{O}$=$\pm\boldsymbol{Z}$ or $\boldsymbol{O}$=$\pm\boldsymbol{Z'}$. This result shows that in the case of two predictors the only variance decomposition via orthogonalization that respect grouping property is Genizi-Johnson or associated decomposition related to $\boldsymbol{Z}$.

In conclusion we have identified an important difference between CAR scores decomposition and Genizi-Johnson decomposition. Given a variable to

predict $\boldsymbol{Y}$, kept constant, if the correlation between two of the predictors tends towards 1, or if in the dataset there are highly correlated predictors, their Genizi-Johnson importance (called Relative Weights by Johnson) will always tend to equate while this is not the case with CAR scores. This has important consequences as we show below on numeric examples.

4.4 Application to the Diabetes dataset.

In the documentation associated to the R package care, Strimmer and Zuber [16] use the diabetes data from Efron *et al.* (2004). The diabetes data has 10 variables ("age","sex","bmi","bp","s1","s2","s3","s4","s5","s6") and 442 measurements. The data is standardized. We will add a new predictor variable using a parameter to adjust the correlation of this new variable with one of the original predictors. We considered one of the original variables, $\boldsymbol{bp}$ and generated a random set of 442 observations called $\boldsymbol{\epsilon}$, with a mean of 0 and a standard deviation of 0.2. We then generated a variable $\boldsymbol{bp'}$ using another of the original variable from the diabetes data, the variable $\boldsymbol{bmi}$ and adding a terms as follows:

$$\mathbf{bp'} = \mathbf{bp}\boldsymbol{cos}(\phi) + (\mathbf{bmi} + \boldsymbol{\epsilon})\boldsymbol{sin}(\phi) \tag{22}$$

By adjusting the value of $\boldsymbol{\phi}$ we can vary the correlation between $\boldsymbol{bp}$ and $\boldsymbol{bp'}$. The results of the squared CAR scores as a function of the correlation between $\boldsymbol{bp}$ and $\boldsymbol{bp'}$ are shown in figure 1. There is no convergence between the squared CAR scores of $\boldsymbol{bp}$ and $\boldsymbol{bp'}$ when the correlation between these two variables tends towards 1.

We made another analysis this time introducing a variable $\boldsymbol{bp^*}$ now computed as:

$$\mathbf{bp}^* = \mathbf{bp} + \boldsymbol{\epsilon} \tag{23}$$

In that case the correlation between $\boldsymbol{bp}$ and $\boldsymbol{bp^*}$ is 0.981. We compared the ranking of the predictors by decreasing order of their importance measure according to three different methods: Random Forest,"lmg" (cf [9]) and CAR scores. The ranks are presented in table 2. We can observe that the two highly correlated predictors $\boldsymbol{bp}$ and $\boldsymbol{bp^*}$ remain close in the ranking, and even ranked one after the other when random forest or lmg-Shapley is used, but that this is not the case with squared CAR scores.

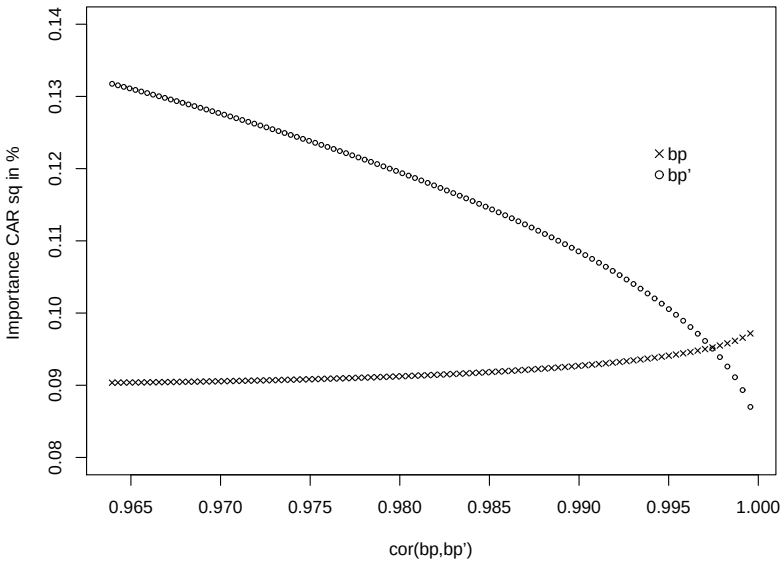

Fig. 1. Squared CAR scores. Diabetes data. Predictor bp' added correlated to bp.

Method	Random Forest	lmg-Shapley	Genizi-Johnson	CAR sores
s5	1	2	2	2
bmi	2	1	1	1
bp*	3	4	4	6
bp	4	3	3	3
s4	5	6	6	5
s3	6	5	5	4
s2	7	10	10	10
s1	8	8	8	11
s6	9	7	7	7
sex	10	9	11	8
age	11	11	9	9

Table 2. Ranking predictors by decreasing importance: random forest, lmg-Shapley, CAR scores and Genizi-Johnson.

5 Conclusions.

CAR scores have been considered since many years but were criticized by several authors because of the fact that the decorrelated predictors used to decompose the explained variance of the variable to predict can be poor representatives of the original predictors. CAR scores have been recommended again recently for the quantification of relative importance of predictors and been credited with the respect of grouping property. Using theoretical demonstrations and simulations based on datasets, we have proven that actually CAR scores do not respect the grouping property. Even when the correlation between predictors is very high and tends towards 1, the CAR scores do not tend to equate. Highly correlated predictors can be allocated very different squared CAR scores and the quantification of their importance will differ. As a consequence with CAR scores highly correlated predictor can suffer from erroneous interpretation of their relative importance and inconsistent selection in a model. In return the Relative Weights introduced by Genizi [3] and Johnson [13] do fully respect the definition of grouping property.

In the absence of proper new justification of the CAR scores, we do not see any reason to overcome the past criticisms this method had faced over a long period nor to recommend again their usage. Alternative methods should be preferred to estimate the relative importance of predictors.

For classical variance decomposition, Relative Weights can be easily implemented, see Genizi [3], Johnson [13] and Gromping [11].

Regularization and variable selection can also be implemented with elastic net including in the case of high dimensional data knowing than elastic net unlike lasso respect grouping property, see [15].

Random forests take into account non-linearities and interactions without needing to model them, see Gromping [10]. This method can be recommended to quantify the relative importance of predictors and also for variable selection including in the case of high dimensional data, see Genuer *et al.* [4] and [5]. Gregorutti [8] has also shown that they tend to respect grouping property.

Lastly, it is important to note that variance decomposition should not be seen as a substitute for linear regression models, path analytical models and models based on theory-driven explanations. However when a model based on theory is not available variance decomposition, elastic net or random forests can help identify and select important variables.

References

1. Efron, B., Hastie, T., Johnstone, I., Tibshirani, R. (2004) *Least angle regression (with discussion).* Ann. Statist.32:407?499.
2. Fabbris, L. (1980) *Measures of predictor variable importance in multiple regression.* Quality and quantity, Elsevier Scientific Publishing Company, 1980, 4,787-792
3. Genizi, A.(1993) *Decomposition of R^2 in multiple regression with correlated regressors.* Statistica Sinica 3(1993) 407-420.
4. Genuer,R., Poggi,J-M., Tuleau-Malot, C. (2012) *Variable selection using Random Forests.* Pattern Recognition Letters, Elsevier, 31 (14), pp.2225-2236. hal-00755489
5. Genuer,R., Poggi,J-M., Tuleau-Malot, C.(2015) *VSURF: An R Package for Variable Selection Using Random Forests.* The R Journal,Vol 7/2, December 2015, ISSN 2073-4589.
6. Gibson,W.A.(1962) *Orthogonal predictors: A possible solution for the Hoffman-Ward controversy.* Psychlogical Reports,11, 32-34
7. Green, P.,E., Carroll,J.D., DeSarbo, WS. (1978) *A new measure of regressor importance in multiple regression* J Marketing Res 15: 356-360.
8. Gregorutti, B., Michel, B., Saint-Pierre, P. (2015) *Grouped variable importance with random forests and application to multiple functional data analysis* Computational Statistics and Data Analysis 90: 15-35.
9. Gomping, U. (2007) *Estimators of Relative Importance in Linear Regression Based on Variance Decomposition.* The American Statistician, May 2007 Vol 61,No. 2, 139. DOI: 10.1198/000313007X188252 308-319.
10. Gromping, U. (2009) *Variable Importance Assessment in Regression: Linear Regression Versus Random Forest.* The American Statistician, November 2009, Vol 63, No. 4, 308-319. DOI: 10.1198/tast.2009.08199.
11. Gromping, U. (2015) *Variable Importance in Regression Models.* Wired Comput Stats 7:137-152. doi:10.1002/wics.
12. Gromping, U. (2016) *Variable Importance in Regression Models, corrigenda.* Wired Comput Stats 8:154-157. doi:10.1002/wics.
13. Johnson, J. W. (2000) *A heuristic method for estimating the relative weights of predictor variables in multiple regression.* Multivariate Behavioral Research 35, 1-19.
14. Thomas, R. Zumbo, B., Kwan,E., Schweitzer, L. (2014) *On Johnson?s (2000) Relative Weights Method for Assessing Variable Importance: A Reanalysis.* Multivariate Behavioral Research 49:329-338, 2014.
15. Zou, H., Hastie, T. (2005) *Regularization and variable selection via the elastic net.*Journal of the Royal Statistical Society B (2005) 67, Part2, pp.301-320.
16. Zuber, V., Strimmer, K. (2011) *High-Dimensional Regression and Variable Selection using CAR Scores.* Statistical Applications in Genetics and Molecular Biology. Volume 10, issue 1. 10:34.DOI: 10.2202/1544-6115.1730.

On GARCH models with temporary structural changes

Norio Watanabe[1] and Okihara Fumiaki[2]

[1] Department of Industrial and Systems Engineering, Chuo University
Kasuga 1-13-27, Bunkyo-ku, Tokyo 112-8551, Japan
(E-mail: watanabe@indsys.chuo-u.ac.jp)
[2] Graduate school of Science and Engineering, Chuo University
Kasuga 1-13-27, Bunkyo-ku, Tokyo 112-8551, Japan

Abstract. When an economic shock like the Lehman crash occurred, it is expected to investigate its influence based on economic time series. The intervention analysis by Box and Tiao is a method for such a purpose. Most of intervention analyses are based on ARIMA models, but some are on GARCH models. The GARCH models have been developed for analyzing time series of stock returns. Usually the expected value function of a GARCH model is assumed to be constant. However, this assumption is not appropriate when a time series includes a varying trend. Our first purpose is to propose a trend model, which can be easily taken in intervention analysis. Based on this trend model we generalize a GARCH model for an intervention analysis on both of trend and volatility. An identification method is also provided and evaluated by simulation studies. Usability of the proposed model is demonstrated by applying to real stock returns.
Keywords: intervention analysis, stock return, trend.

1 Introduction

An event such as the Lehman crash or a large modification of monetary policy causes a strong influence on economics and its effect is reflected in economic time series. It is important to analyze the influence of such an event by using time series. The intervention analysis by Box and Tiao [1] is a method for such a purpose. Most of intervention analyses are based on ARIMA models. In recent years some intervention analyses related to GARCH models have been studied. The GARCH model is used to analyze the volatility of the return of average stock prices or stock price indices. Ho and Wan [3] proposed a model which has a special GARCH structure for intervention analysis. Watanabe and Nagashima [2] proposed a GARCH model with an intervention term on volatility. These models are considered for intervention on volatility and are based on the assumption that expected values of series are not varying. However, we can find trends in some time series. For such time series we can not assume the constant expected values and we have to consider trends in models.

There two typical methods for considering trend. The first is the polynomial regression and the second is the moving average method. The former is not appropriate for stock returns, since the trend will diverge. The later is not a parametric model. The fuzzy trend model by Kuwabara and Watanabe [4] can be applied to stock returns. However, it is not easy to apply the fuzzy trend

model for intervention analysis. Though stochastic trend models are available also, it is not easy to extend them for intervention analysis. Therefore we consider the deterministic trend.

The first purpose of this paper is to propose a parametric trend model which can be applied for intervention analysis on stock returns. The second is to propose an intervention analysis on both of the mean value function and volatility in a GARCH model based on our trend model. We propose an identification method of the model and show its suitability by simulation studies. Usability of the proposed model is demonstrated by applying to practical stock returns.

2 Model

2.1 Trend model

We assume that the expected value function of stock returns can be expressed by a smoothed step function. Let $\{X_t : t = 1, 2, ..., T\}$ be a series of stock returns and μ_t be the expected value function of X_t. We divide an interval $[0, T] = \{t|0 \leq t \leq T\}$ into small segments. Let a_k be the middle point of k-th small interval. We assume that

$$a_1 = 0 \tag{1}$$

$$a_k = a_{k-1} + L_1 \qquad (2 \leq k \leq K), \tag{2}$$

where L_1 is a positive integer. The number of segments K is given by

$$K = \lfloor \frac{T + L_1}{L_1} \rfloor + 1. \tag{3}$$

where $\lfloor x \rfloor$ means the smallest integer not exceeding x.

The expected value function μ_t is defined as follows:

a) if $a_k - L_1/2 \leq t \leq a_k - d/2$

$$\mu_t = \frac{m_{k-1} - m_k}{2} \Big(- \cos \big(\frac{t - (a_k - d/2)}{L_1 - d} \big) \pi + 1 \Big) + m_k, \tag{4}$$

b) if $a_k - d/2 \leq t \leq a_k + d/2$

$$\mu_t = m_k, \tag{5}$$

c) if $a_k + d/2 \leq t \leq a_k + L_1/2$

$$\mu_t = \frac{m_{k+1} - m_k}{2} \Big(- \cos \big(\frac{t - (a_k + d/2)}{L_1 - d} \big) \pi + 1 \Big) + m_k, \tag{6}$$

except for the cases:

$$\mu_t = m_1 \qquad \text{if} \quad a_1 < t \leq a_1 + d/2, \tag{7}$$

$$\mu_t = m_K \qquad \text{if} \quad a_K - d/2 \leq t \leq T. \tag{8}$$

We call the series $\{m_k|k = 1, ..., K\}$ the latent process, since this is an unobserved process which determines the trend. We assume that d is a positive integer. The case $d = L_1$ corresponds to the step function. See Fig. 1 as an example.

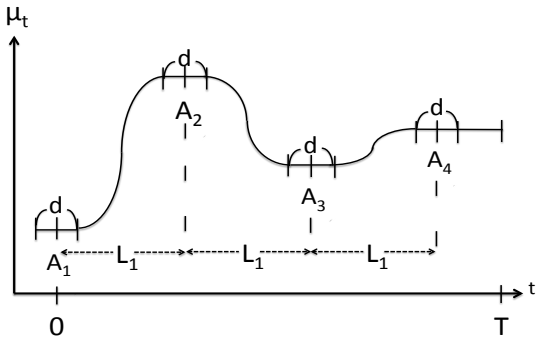

Fig. 1. An example of the trend

2.2 Intervention GARCH model

Now we introduce a GARCH(1,1) model for an intervention analysis on both of trend and volatility. Our model is defined as follows:

$$X_t = \mu_t + \varepsilon_t \tag{9}$$

$$\varepsilon_t = h_t z_t \qquad z_t \sim NID(0,1) \tag{10}$$

$$h_t^2 = \alpha_0 + \alpha_1 \varepsilon_{t-1}^2 + \beta_1 h_{t-1}^2 + I_t \tag{11}$$

$$I_t = \begin{cases} \gamma^{(v)} & (\text{if} \quad t = T_v) \\ 0 & (\text{otherwise}), \end{cases} \tag{12}$$

under the condition:

$$0 < \alpha_0 \ , \ 0 \le \alpha_0 + \gamma^{(v)} \ , \ 0 \le \alpha_1 \ , \ 0 \le \beta_1 \ , \ \alpha_1 + \beta_1 < 1. \tag{13}$$

The intervention term I_t represents a direct effect of the event on the volatility and is the simplest case among the types proposed by Watanabe and Nagashima [2]. The conditional standard deviation h_t is called volatility usually.

An intervention trend model for μ_t is a modified version of the trend model proposed in the previous section. In this paper we consider the intervention type illustrated in Fig. 2.

Let $T_m (1 \le T_m \le T)$ be the time when an effect begins to appear on the expected values, and L_2 be the length of the period when an effect continues to appear. We assume that L_2 is a positive integer. For the interval $[0, T_m]$ we consider the similar segmentation given in Section 2.1. But the direction is backward and the starting point is T_μ. The number of segments K_1 before T_m is given by

$$K_1 = \lfloor \frac{T_m + L_1 - 1}{L_1} \rfloor + 1. \tag{14}$$

The middle point a_k of the small interval is determined recursively as follows:

$$a_{-1} = T_m \tag{15}$$

$$a_k = a_{k+1} - L_1 \qquad (-2 \ge k \ge -K_1). \tag{16}$$

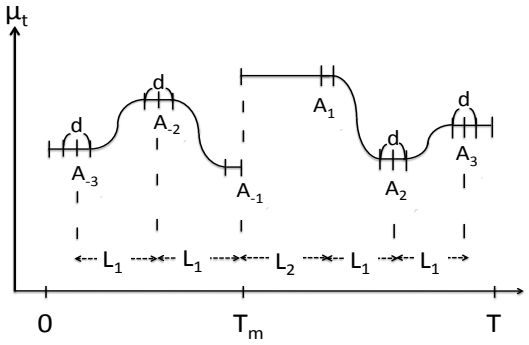

Fig. 2. An example of trend with intervention

The expected value function μ_t can be defined similarly to Section 2.1. Note that $\mu_t = m_{-1}$ when $a_{-1} - d/2 \leq t < a_{-1}$, and $\mu_t = m_{-K_1}$ when $1 \leq t \leq a_{-K_1} + d/2$.

We assume that an effect continues to appear constantly in the period $[T_\mu, T_\mu + L_2]$. That is,

$$\mu_t = m_1. \tag{17}$$

After $T_m + L_2$ we also consider the segmentation whose starting point is $T_m + L_2$. The number of segments K_2 is given by

$$K_2 = \lfloor \frac{T - (T_m + L_2) + L_1}{L_1} \rfloor + 1. \tag{18}$$

The middle point a_k is given by the recursion:

$$a_1 = T_m + L_2 \tag{19}$$

$$a_k = a_{k-1} + L_1 \quad (2 \leq k \leq K_2). \tag{20}$$

In this study the length of the segment after $T_\mu + L_2$ is the same as the one before T_μ. This assumption can be loosened easily. The expected value function μ_t is defined in the same way as Section 2.1. Note that $\mu_t = m_1$ when $a_1 < t \leq a_1 + d/2$, and $\mu_t = m_{K_2}$ when $a_{K_2} - d/2 \leq t \leq T$.

3 Identification

The parameters in the model can be estimated by the maximum likelihood method, if structural parameters T_v, T_μ, L_1, L_2 and d are given. The log likelihood function can be written as

$$\ln L = -\frac{T}{2}\ln(2\pi) - \frac{1}{2}\sum_{t=1}^{T}\ln(h_t^2) - \frac{1}{2}\sum_{t=1}^{T}\frac{(X_t - \mu_t)^2}{h_t^2} \tag{21}$$

under the condition that the initial value h_0 is given.

In this paper we adopt Akaike's Information Criterion (AIC) for selection of structural parameters. In this study we assume that T_v and T_μ are known. In many cases this assumption is natural, since the effect of event is not small in intervention analysis usually. When these are unknown, these can be estimated similarly to other parameters. For applying AIC we have to prepare sets of candidate values of L_1, L_2 and d.

When the length of the last segment is too short for trend estimation, the estimate of the last latent variable becomes unstable. In such a case the last segment should be combined with the previous segment and the definition of μ_t should be slightly modified.

In numerical calculation it is required to maximize the likelihood function under the constraints. Note that we have to pay much attention to numerical calculation, since iteration has a strong dependency on initial values of parameters. In this study we use the software MATLAB R2016a in simulation studies and applications.

4 Simulation

Simulation studies are achieved for showing suitability of AIC for our model. In this section we focus on estimation of the trend in our model.

For evaluating performance of a method we define two indices. The first is given by

$$P = \frac{\max_k (m_k) - \min_k (m_k)}{\sigma} \tag{22}$$

where m_k is the latent variable of the trend model and σ^2 is the stationary variance of $x_t - \mu_t$. The index P is a quantity on the model and shows how fluctuation of trend is large. The second is the index on the estimated result defined as follows:

$$D = \Sigma(\mu_t - \bar{x}_t)^2 - \Sigma(\mu_t - \hat{\mu}_t)^2, \tag{23}$$

where $\bar{x}_t$ is the sample mean of the series and is an estimate of the trend when the expected value function is assumed to be constant. The estimate $\hat{\mu}_t$ is the trend derived from the selected model. When the trend is varying and P is large, D becomes large if a selected model can estimate the trend well.

4.1 Simulation on trend without intervention

Trends are generated by the model in Section 2.1 by assuming latent processes follow to AR(1) processes and additive noises ϵ_t's follow to zero mean GARCH(1,1) processes. Several values of L_1 are given as true values.

The parameters in GARCH models are controlled so as to lead $\sigma^2 = 0.5$. Series following to models with different P are generated artificially by giving several coefficients of AR(1) models. For generated series we fit three models: 1) constant expected values plus Gaussian white noise, 2) constant expected

values plus GARCH(1,1) noise, and 3) trend plus GARCH(1,1) noise. The best model is selected by minimizing AIC. Fitting are done for 100 series for each case.

In the following we show a result for the case $T = 300$, $L_1 = 50$, and $d = 1$. Table 1 summarizes results for 30 cases. The index $\bar{D}$ is the mean value of 100 D's selected by AIC. The "Rate" means the rate of trend models within all selected models. The scatter plot of P and $\bar{D}$ is shown in Fig. 3.

Table 1. Simulation result ($T = 300$, $L_1 = 50$)

No.	P	Rate	$\bar{D}$	*No.*	P	Rate	$\bar{D}$	*No.*	P	Rate	$\bar{D}$
1	0.837	1.00	0.0080	11	0.671	0.96	0.0058	21	0.500	0.94	-0.0024
2	0.807	1.00	0.0615	12	0.658	1.00	0.0258	22	0.488	0.86	-0.0075
3	0.794	1.00	0.0478	13	0.636	1.00	0.0317	23	0.475	0.77	-0.0098
4	0.781	1.00	0.0415	14	0.623	0.98	0.0131	24	0.457	0.91	0.0016
5	0.763	1.00	0.0324	15	0.610	0.98	0.0117	25	0.439	0.97	0.0045
6	0.750	0.98	0.0114	16	0.592	0.99	0.0137	26	0.421	0.99	0.0154
7	0.746	0.97	0.0137	17	0.579	1.00	0.0228	27	0.409	0.88	-0.0076
8	0.728	1.00	0.0211	18	0.567	0.95	0.0143	28	0.396	0.77	-0.0120
9	0.715	0.98	0.0156	19	0.544	0.99	0.0188	29	0.365	0.77	-0.0115
10	0.702	1.00	0.0207	20	0.531	0.99	0.0154	30	0.352	0.97	0.0068

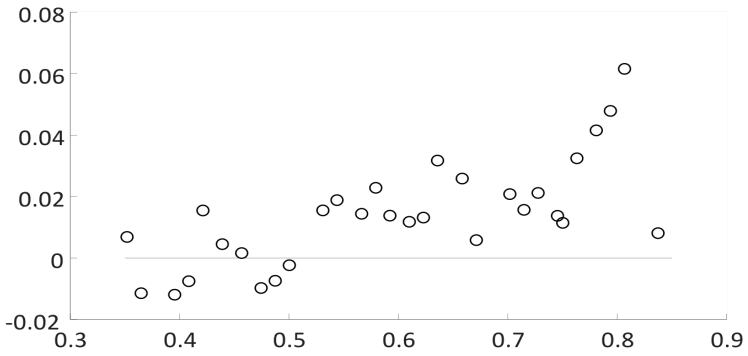

Fig. 3. Scatter plot of P and $\bar{D}$

From Table 1 and Fig. 3 we can say that trends model can be selected well by AIC, if P is not so small.

4.2 Simulation on intervention trend model

In this section we consider intervention on a trend only. Let $\gamma^{(m)}$ be the magnitude of a direct effect on trend. Then we have the equation:

$$m_1 = \gamma^{(m)} + m_{-1}. \tag{24}$$

Model setting is similar to Section 4.1. In addition several values of $\gamma^{(m)}$ are given for the intervention trend model in Section 2.2. The four models are fitted to each artificially generated series. Three are the same as Section 4.1. The fourth model is 4) intervention trend plus GARCH(1,1) noise.

Table 2 shows a result for the case $T = 400$, $T_m = 200$, $L_1 = 30$, $L_2 = 60$ and $d = 1$. The "Rate" is the rate of intervention trend models within all selected models.

Table 2. Simulation result ($T = 400$, $T_m = 200$, $L_1 = 30$,$L_2 = 60$)

No.	$\gamma^{(m)}$	P	$\bar{D}$	Rate	No.	$\gamma^{(m)}$	P	$\bar{D}$	Rate
1	1.00	0.803	0.1162	0.96	7	0.50	0.596	0.0508	0.84
2	0.75	0.791	0.1083	0.88	8	0.25	0.614	0.0299	0.69
3	0.50	0.812	0.0517	0.82	9	1.00	0.410	0.1029	0.96
4	0.25	0.809	0.0468	0.61	10	0.75	0.391	0.1028	0.88
5	1.00	0.609	0.1357	0.98	11	0.50	0.413	0.0149	0.85
6	0.75	0.624	0.1039	0.95	12	0.25	0.405	0.0020	0.65

Table 2 shows that an intervention trend model is properly selected by AIC, if $\gamma^{(m)}$ is not so small.

In intervention analysis it is important to know the value of $\gamma^{(m)}$. Fig. 4 shows the histogram of the estimated values of $\gamma^{(m)}$ for the cases when the intervention trend models are selected in No. 1 of Table 2. The vertical line in Fig 4 is the true $\gamma^{(m)}$. Our results show that $\gamma^{(m)}$ can be estimated well by the maximum likelihood method, when $\gamma^{(m)}$ is not so small.

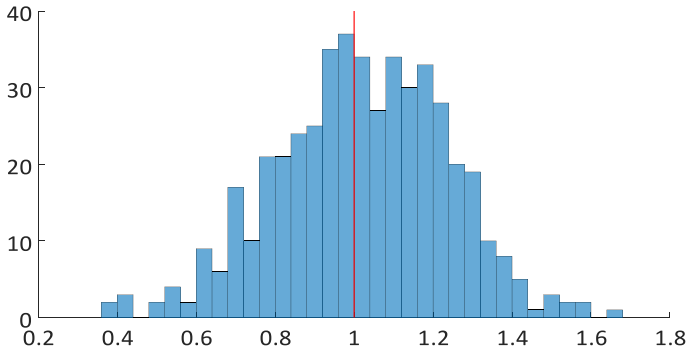

Fig. 4. Histogram of estimated value of $\gamma^{(m)}$

From simulation studies the identification method in Section 3 works well, if effect of an event is not so small.

5 Application

In this section we consider time series of TOPIX (Tokyo Stock Price Index) plotted in Fig. 5. The period is from 27 January 2012 to 20 November 2013. We apply the proposed model to the series of returns of TOPIX, which is shown in Fig. 6. The length T is 450.

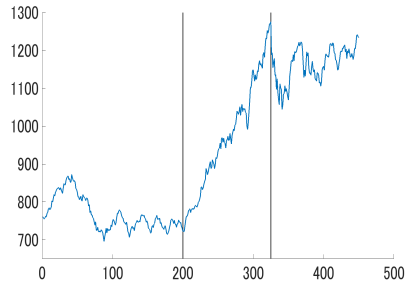

Fig. 5. TOPIX

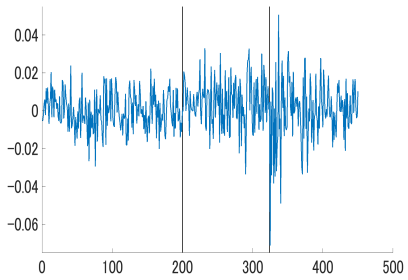

Fig. 6. Returns of TOPIX

The left vertical line in Fig. 5 or 6 indicates the day when the Japanese House of Representatives dissolved. Before this time point it seems that returns include a varying trend. Thus the trend model should be considered. After this day the level of expected values of the returns becomes higher than before. This change is an effect of the dissolution. In this case the dissolution increase the expectation on economics. Therefore we set $T_\mu = 200$ in Fig. 6 for the intervention trend model. Furthermore, after a while an effect on volatility begins to appear. We put T_v to 325, which is the time point indicated by the right vertical line in Fig. 6.

We apply three models to this data: 1) constant expected values plus GARCH(1,1), 2) the trend model in Section 2.1 plus GARCH(1,1), and 3) the intervention GARCH model in Section 2.2. In all models the intervention on volatility is commonly assumed. The results are summarized in Tables 3 – 5.

From AIC's in Table 3 it is found that model with constant expected values is not appropriate. Moreover, Table 3 implies that the intervention trend model is more suitable. Selected structural parameters of the trend and intervention trend models are shown in Table 4. In this paper, we set $d = 1$. Table 5 shows other estimated parameters of the intervention trend model.

μ_t	AIC
constant	−2688.81
trend	−2695.26
Intervention trend	−2700.46

Table 3. AIC of models

μ_t	Segment length	Segmentation size
Trend model	$L_1 = 77$	$K = 6$
Intervention trend model	$L_1 = 66, L_2 = 119$	$K_1 = 4, K_2 = 2$

Table 4. Selected structural parameters

m_{-4}	0.004786	m_{-1}	-0.001372	α_0	0.000009	$\gamma^{(v)}$	0.0016311
m_{-3}	-0.003408	m_1	0.004501	α_1	0.052395		
m_{-2}	0.000752	m_2	0.000920	β_1	0.873430		

Table 5. Parameter estimates

Figs. 7 and 8 are the plots of estimated trends. Figs. 7 and 8 are for $\{t|1 \leq t \leq T\}$ and $\{t|1 \leq t \leq 250\}$ respectively. The solid line is the estimated trend by the intervention trend model and the dotted line is by the trend model. The gray line is the sample mean of the series.

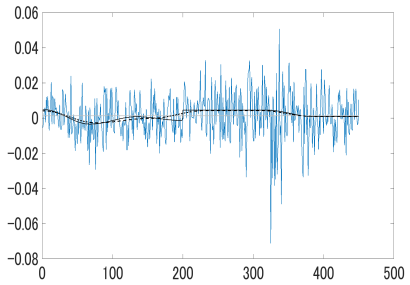

Fig. 7. Estimated trend (all)

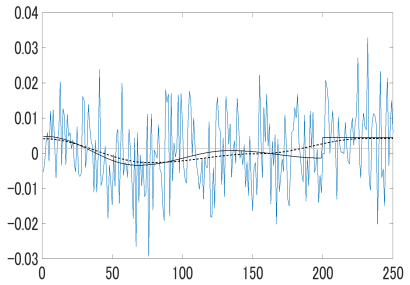

Fig. 8. Estimated trend ($t = 1, ..., 250$)

The estimated volatility are shown in Figs. 9 and 10. The meanings of lines are the same as Figs. 7 and 8.

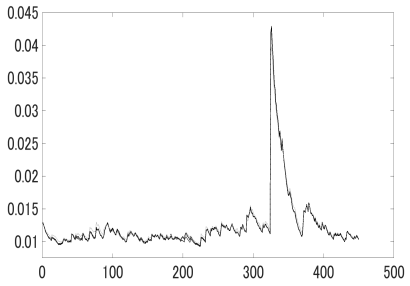

Fig. 9. Estimated volatility (all)

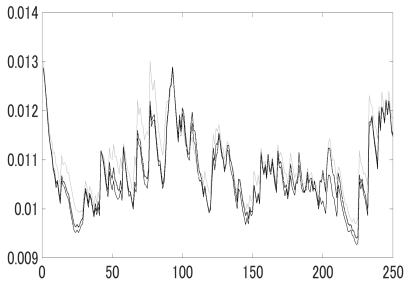

Fig. 10. Estimated volatility ($t \leq 250$)

Figs. 9 and 10 show that the model without trend overestimates volatility. Moreover, the trend model without intervention slightly overestimates volatility compared with the intervention trend model. In particular overestimation near the time point $T_\mu = 200$ is large. The main reason of overestimation is that the expected values are not estimated properly.

These results show that an appropriate estimation requires an adequate model which can represent characteristics of data well.

6 Concluding remark

In this paper we have proposed a trend model and an intervention GARCH model based on it. Our application shows that the trend should be considered properly, if expect values are not constant. In such a case usual GARCH models without intervention term tend to overestimate volatility. Our model is an intervention model on both trend and intervention, and can be applied in such a case.

The pattern of intervention in this paper is limited. Other patterns should be considered for applying our model to other kind of time series.

References

1. G.E.P. Box and G.C. Tiao. Intervention analysis with applications to economic and environmental problems. *Journal of the Statistical Association*, 70, 70–79, 1975.
2. N.Watanabe and M.Nagashima. An intervention analysis based on the GARCH model. *Proceedings of SMTDA 2016*, 515–525, 2016.
3. A. K. F. Ho and A. T. K. Wan. Testing for covariance stationary of stock returns in the presence of structural breaks : an intervention analysis. *Applied Economics Letters*, 9, 441–447, 2002.
4. Y.Kuwabara and N.Watanabe. Analysis of financial time series data by fuzzy trend model (in Japanese). *Journal of Japan Society for Fuzzy Theoretic Information*, 20, No.2, 92-10, 2008.

Investigating Southern Europeans' Perceptions of Their Employment Status

Aggeliki Yfanti[1], Catherine Michalopoulou[1], Aggelos Mimis[1], and Stelios Zachariou[2]

[1] Panteion University of Social and Political Sciences, 136 Syggrou Avenue, Athens 176 71, Greece
(E-mail: aggelikiyfanti@panteion.gr; kmichal@panteion.gr; mimis@panteion.gr)
[2] Hellenic Statistical Authority, 46 Pireos Street, Piraeus 185 10, Greece
(E-mail: s.zahariou@statistics.gr)

Abstract. The European Union Labour Force Survey (EU-LFS) measurement of the employment status is based on a synthesized economic construct computed according to the ILO conventional definitions of the employed, unemployed and inactive. Since the late 2000s, a variable measuring people's perceptions of their employment status has been included in the EU-LFS questionnaire as it is used in all large-scale sample surveys, i.e. one of the occupational background variables. These measurements are not comparable and their results will differ since a composite economic construct would normally deviate from people's perceptions. The purpose of this paper is, by obtaining a social "profile" of agreement and disagreement between Southern Europeans' declared self-perceptions of their employment status and the ILO conventional definitions, to investigate whether or not conflicting and coinciding perceptions differ overtime within-nations and cross-nationally. The analysis is based on the 2008-2014 annual datasets for Greece, Italy, Portugal and Spain. The results are reported for the age group 15-74 so as to allow for comparability with the ILO conventional definition of unemployment.
Keywords: Employment status, ILO, EU-LFS, Southern Europe.

1 Introduction

In all large-scale sample surveys, demographic and socio-economic variables are included as background variables which "in addition to providing general contextual/collateral information, they are used as independent variables, as socio-economic covariates of attitudes, behavior, or test scores, etc. and in all sorts of statistical models, in particular, as exogenous factors in causal analysis" (Braun and Mohler [2: 101]). Furthermore, background variables have been and will continue to be used in order to assess the quality of the realized sample by carrying out detailed comparisons of their distributions to the more recent available respective census data (Braun and Mohler [2]), since "it is only sound practice to test a theoretical result empirically" (Stephan and McCarthy [13: 134]). In the case of the employment status, i.e. one of the occupational

background variables, because of its great overtime variability, the census data available for such comparisons is most of the time outdated. Recognition of this fact "leads us to consider alternatives, especially the possibility of comparing the results obtained by one sample survey on such … [a variable] with the results obtained by other sample surveys" (Stephan and McCarthy [13]: 156). In this respect, the more appropriate "other [such] sample survey" that provides updated information is the Labour Force Survey (LFS) and, in this instance, the European Union Labour Force Survey (EU-LFS). However, the measurement of the employment status as a background variable included in all large-scale sample survey and the census is defined on the basis of how people perceive it, whereas the EU-LFS measurement of the employment status is based on a synthesized economic construct computed using a number of variables according to the ILO conventional definitions that classify the population of working age (15 years or more) into three mutually exclusive and exhaustive categories: employed, unemployed and inactive. These two measurements are not comparable and their results will differ since a composite economic construct would normally deviate from people's perceptions.

In the literature, the debate on the definition or concept especially of unemployment is of long standing (see for a review Yfanti et al. [14]). As Gauckler and Körner [7: 186] pointed out, "measuring the ILO employment status in household surveys and censuses is challenging in several respects…The ILO defines employment in the broadest term, whereby one hour per work counts as being employed. A small job of one hour per week is enough. Such a definition will sometimes be in conflict with the respondent's everyday life perception." Eurostat [4: 58], presenting an extensive analysis on whether the ILO definitions capture all unemployment and meet current and potential user needs, concluded that "there is no need for a revision of the ILO labour force concept when it is looked at from an economic perspective or when it is considered for international comparability… However, there is a point to make concerning the ILO definition of unemployment. It intends to capture only a restricted part of the whole labour reserve, i.e. the one showing a strong attachment to the labour market. It is not meant to measure the entire labour reserve. Jones and Riddell [9], based on their results that indicated a substantial heterogeneity within the non-employed and a distribution of degrees of labour force attachment to be separated into distinct groups that displayed different behaviour, proposed that additional information appears necessary to identify activities such as "wait unemployment." Furthermore, Brandolini *et al.* [1], discussing the heterogeneity of the labour market groups and the difficulty of a single definition of unemployment, pointed out the existence of large differences not only among countries, but also among socio-demographic groups within the same country.

All these "grey areas" of labour force attachment make the analysis difficult as the ILO conventional definitions do not reflect individuals' situation in the labour market as they perceive it. It is in this respect that Eurostat decided in 2006 to include the self-perceived employment status as a supplementary indicator to the ILO concepts intended to capture all these complexities. In

2011, de la Fuente [6] briefly discussed the coverage problems of self-perceived unemployment and the three new Eurostat indicators that were introduced as supplementary to the unemployment rate based on the results of EU-LFS for 2010. Gauckler and Körner [7] investigated the comparability of the employment status measurement in the German LFS and Census of 2011. The purpose of this paper is, by obtaining a demographic and social "profile" of agreement and disagreement between Southern Europeans' declared self-perceptions of their employment status and the ILO conventional definitions, to investigate whether or not conflicting and coinciding perceptions differ overtime within-nations and cross-nationally.

2 Method

2.1 Prerequisites for comparability

The EU-LFS is a set of independent national multipurpose large-scale sample surveys conducted by the respective statistical offices of the member countries, providing quarterly and annual results on labour participation and those outside the labour force. The survey population is defined centrally as all persons aged 15 years or more living in private households, excluding persons in compulsory military or community service and those residing in collective dwellings. Therefore, the survey population overtime within-nations and cross-national comparability is ensured (Kish [10]).

The self-perceived employment status included in the EU-LFS is an optional variable for the participating countries, provided only in the annual datasets. It is available for most countries with the exception of Germany, UK and Norway. Although this variable was first introduced in 2006, Eurostat [3] changed the reference period in 2008 and consequently there is an issue of comparability. In this respect, it was decided to base the analysis on the 2008-2014 datasets for the following Southern European countries: Greece, Italy, Portugal and Spain.

Also, the Eurostat [3] instruction that, "this question shouldn't in any case precede the questions on the labour status according to the ILO definition or the questions on the registration at the public employment office" has to be considered for comparability. Because this is a perception question, i.e. sensitive to its placement in the questionnaire (Stephan and McCarthy [13]), the questionnaires of the four countries under investigation complied with this instruction allowing for overtime within-nations and cross-national comparability. Furthermore, it was decided to report the results for the age group 15-74 so as to allow for comparability with the ILO conventional definition of unemployment (Figure 1; see also de la Fuente[6].

2.2 The ILO conventional definitions of the employment status

Figure 1 presents the detailed EU-LFS measurement of the employment status based on a number of variables according to the ILO conventional definitions.

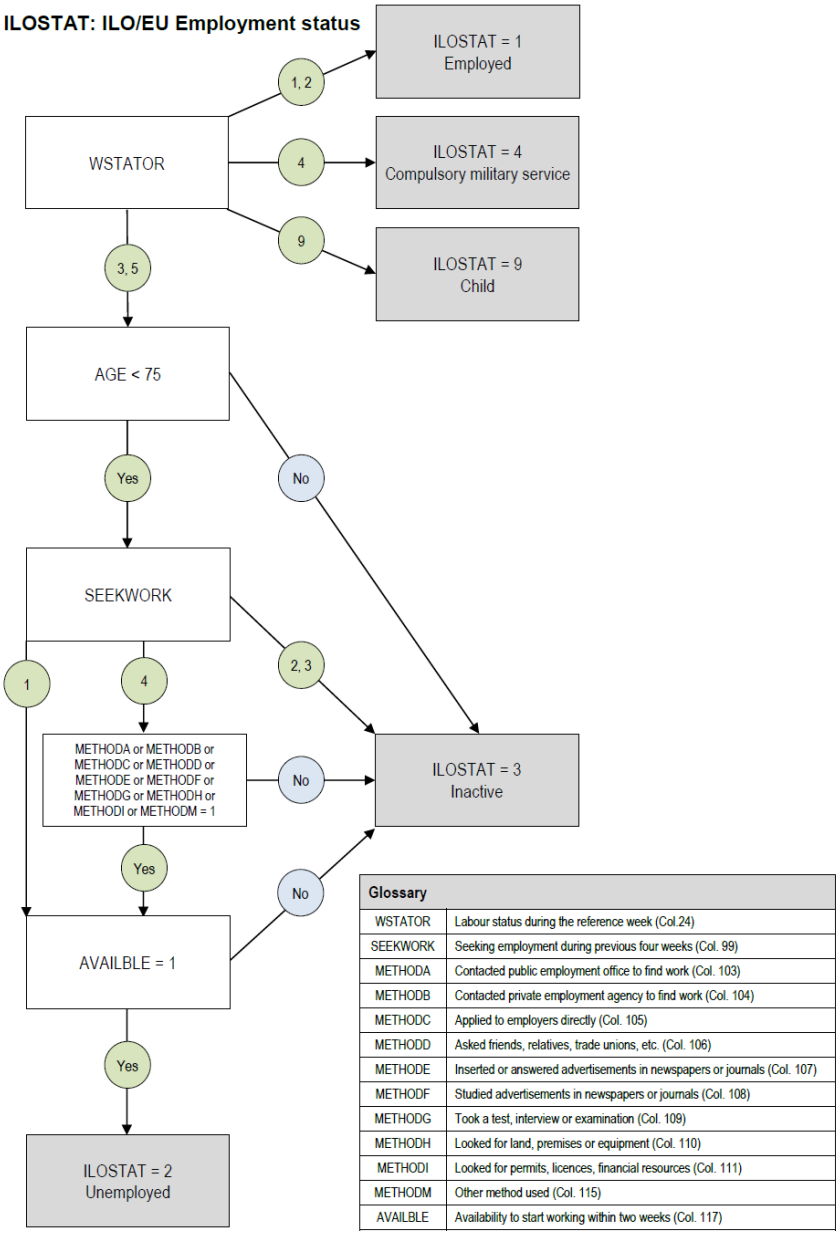

Glossary	
WSTATOR	Labour status during the reference week (Col.24)
SEEKWORK	Seeking employment during previous four weeks (Col. 99)
METHODA	Contacted public employment office to find work (Col. 103)
METHODB	Contacted private employment agency to find work (Col. 104)
METHODC	Applied to employers directly (Col. 105)
METHODD	Asked friends, relatives, trade unions, etc. (Col. 106)
METHODE	Inserted or answered advertisements in newspapers or journals (Col. 107)
METHODF	Studied advertisements in newspapers or journals (Col. 108)
METHODG	Took a test, interview or examination (Col. 109)
METHODH	Looked for land, premises or equipment (Col. 110)
METHODI	Looked for permits, licences, financial resources (Col. 111)
METHODM	Other method used (Col. 115)
AVAILBLE	Availability to start working within two weeks (Col. 117)

Figure 1. The ILO conventional definitions of the employment status used in the EU-LFS. Reproduced from "EU Labour Force Survey database user guide," by Eurostat, 2016: 55.

The variable WSTATOR measures the labour status during the reference week for all respondents aged 15 years or more according to the conventional definitions that were adopted by the ILO as agreed at the 13th and 14th International Conference of Labour Statisticians (Hussmanns *et al*. [8]). This variable takes the value one (1) when respondents did any work for pay or profit for one hour or more, including family work during the reference week. The second value (2) refers to respondents who despite of having a job or business did not work during the reference week because they were temporarily absent. The third value (3) is assigned to respondents who were not working because of lay-off. The fourth value (4) indicates the respondent who was a conscript on compulsory military service or community service. Value five (5) designates respondents who did not work nor had a job or business during the reference week. As shown in Figure 1, the definition of the unemployed applies only to respondents aged 15-74 years. Also, a number of variables is used that define whether respondents were seeking employment, the methods for doing so and their availability to start work immediately within two weeks (see for a detailed description, Eurostat [5]).

2.3 The EU-LFS self-perceived employment status definition

In Table 1, the question measuring the self-perceived employment status is presented as is the case in all large-scale sample surveys and the census which differs from the ILO multivariate definition.

Table 1. The EU-LFS self-perceived employment status definition (all respondents aged 15 years or more)

Carries out a job or profession, including unpaid work for a family business or holding, including an apprenticeship or paid traineeship, etc.	1
Unemployed	2
Pupil, student, further training, unpaid work experience	3
In retirement or early retirement or has given up business	4
Permanently disabled	5
In compulsory military service	6
Fulfilling domestic tasks	7
Other inactive person	8
Not applicable (child less than 15 years)	9
No answer	^

As shown, this is a perception question that gives the respondents the chance to identify they own employment status. The implementation rules for this variable (MAINSTAT) as defined by Eurostat [3] specify that the main activity status represents self-perception regarding the respondents' activity status. For instance, students with small jobs will in general present themselves as students. The eighth response category (value 8) includes also respondents who cannot say whether they were "carrying out a job or profession" and those who do not fit into other categories or were on an extended leave from work (Eurostat [3: 109]). The instruction for the deliverance of this question according to the

Eurostat good practices rules is that the interviewers have to read out the question and all the response categories.

2.4 Statistical analyses

In order to ensure measurement overtime within-nations and cross-national comparability, all measures-variables have to be standardized (Kish [10]). In this respect, the variable measuring self-perceived employment status is first recoded into the three categories of the employed, unemployed and inactive according to the ILO conventional definitions. Then, the recoded variable is cross-tabulated with the ILO variable that is computed as presented in Figure 1. The diagonal defines the "agreement" group, i.e. people's perceptions coinciding with the ILO conventional definitions. The off diagonal cases define the "disagreement" group, i.e., people's perceptions in conflict with the ILO conventional definitions. Then a demographic and social "profile" of both groups is obtained based on their demographic and social characteristics: gender (male, female), age (15-24, 25-34, 35-44, 45-54, 55-64 and 65-74), marital status (single, married, and other, i.e. widowed, divorced or legally separated) and highest level of educational attainment (primary, secondary and tertiary). Note that, initially, extensive checks were carried out for each category and based on these results it was decided to combine coinciding and conflicting perceptions into the before mentioned two groups.

3 Results

In Table 2, Southern Europeans' overall perceptions of their employment status as they compare to the ILO conventional definitions are presented.

Table 2. Southern Europeans' overall perceptions of their employment status as they agree or disagree to the ILO conventional definitions (15-74; *N* in 000s)

Country	2008	2009	2010	2011	2012	2013	2014
Greece							
Agree %	97.6	97.3	97.3	96.7	96.2	96.1	96.1
Disagree	2.4	2.7	2.7	3.3	3.8	3.9	3.9
N	8,328	8,303	8,305	8,308	8,313	8,184	8,135
Italy							
Agree %	93.9	93.7	93.4	93.2	93.1	92.5	92.3
Disagree	6.1	6.3	6.6	6.8	6.9	7.5	7.7
N	45,337	45,563	45,685	45,800	45,866	45,556	45,626
Portugal							
Agree %	95.0	94.7	94.8	91.7	90.6	90.0	90.9
Disagree	5.0	5.3	5.2	8.3	9.4	10.0	9.1
N	8,140	8,141	8,123	8,116	8,060	7,907	7,860
Spain							
Agree %	97.8	97.6	97.6	97.1	97.6	97.5	97.7
Disagree	2.2	2.4	2.4	2.9	2.4	2.5	2.3
N	34,650	34,809	34,673	34,683	34,494	34,602	34,477

As shown, more than 90% of Southern Europeans perceptions coincide overall with the ILO conventional definitions: 96.1 -97.6% (Greece); 92.3-93.7% (Italy); 90.0-95.0% (Portugal); 97.1- 97.8 % (Spain). However, the number of people with conflicting perceptions amounts to a considerable total ranging from 4,143,000 to 5,543,000: 202,000-319,000 (Greece); 2,759,000-3,499,000 (Italy); 407,000-791,000 (Portugal); 775,000-934,000 (Spain).

In Table 3, Southern Europeans' perceptions of their employment status coinciding with the ILO conventional definitions of the employed, unemployed and inactive are presented.

Table 3. Southern Europeans' (aged 15-74) perceptions coinciding with the ILO conventional definitions of the employed, unemployed and inactive (%)

Country	2008	2009	2010	2011	2012	2013	2014
Greece							
Employed	99.4	99.3	99.2	99.0	98.9	99.1	99.2
Unemployed	81.5	82.7	85.7	85.4	87.1	87.5	86.6
Inactive	97.3	96.9	97.4	97.4	96.9	96.8	97.0
Italy							
Employed	99.8	99.8	99.7	99.8	99.8	99.8	99.8
Unemployed	40.8	43.2	43.7	42.6	49.0	49.4	49.8
Inactive	96.9	97.2	97.4	97.7	97.4	97.7	97.7
Portugal							
Employed	99.9	100.0	99.9	99.7	99.7	99.7	99.8
Unemployed	67.0	70.6	74.1	66.0	67.3	65.4	62.5
Inactive	92.1	91.8	91.8	88.0	86.5	86.6	88.3
Spain							
Employed	99.3	99.2	99.2	98.9	98.9	98.8	99.0
Unemployed	87.6	90.6	91.8	91.3	93.8	93.6	93.8
Inactive	97.5	97.7	97.6	97.5	97.7	97.7	97.8

As shown, more than 98.8% of Southern Europeans agree with the ILO conventional definition in perceiving themselves as employed: 98.9-99.4% (Greece); 99.7-99.8% (Italy); 99.7-100.0% (Portugal); 98.8-99.3% (Spain). Also, more than 88% agree in perceiving themselves as inactive: 96.9-97.4% (Greece); 96.9-97.7% (Italy); 88.0-92.1% (Portugal); 97.5-97.8% (Spain). However, they do disagree with the ILO conventional definition in perceiving themselves as unemployed: 81.5-87.5% (Greece); 40.8-49.8% (Italy); 66.0-74.1% (Portugal); 87.6-93.8% (Spain). Italians disagree more remarked in perceiving themselves as unemployed than the Portuguese people, Greeks and Spaniards.

These findings indicate that a thorough investigation of the demographic and social characteristics of the "agreement" and "disagreement" groups is necessary in order to assess whether or not their distributions differ. In Tables 4 to 7, the demographic and social "profile" of Southern Europeans' coinciding and conflicting perceptions with the ILO conventional definitions is presented for Greece, Italy, Portugal and Spain, respectively.

Table 4. The demographic and social "profile" of coinciding and conflicting perceptions with the ILO conventional definitions: Greece (%)

Variable	2008	2009	2010	2011	2012	2013	2014
Gender							
Agree							
Male	49.6	49.6	49.6	49.6	49.7	49.2	49.3
Female	50.4	50.4	50.4	50.4	50.3	50.8	50.7
Disagree							
Male	41.6	42.9	43.2	46.9	45.9	43.9	43.8
Female	58.4	57.1	56.8	53.1	54.1	56.1	56.2
Age*							
Agree							
15-24	13.6	13.2	13.1	13.0	12.8	13.5	13.4
25-34	19.3	18.8	18.5	18.2	17.7	17.6	17.1
35-44	20.2	20.4	20.6	20.7	20.6	20.1	20.1
45-54	18.1	18.4	18.5	18.7	19.0	18.9	19.2
55-64	15.6	16.0	16.2	16.3	16.4	16.3	16.4
65-74	13.3	13.2	13.1	13.2	13.4	13.7	13.8
Disagree							
15-24	22.1	22.3	19.4	16.9	15.5	16.3	14.3
25-34	25.0	28.1	26.6	25.4	23.1	23.4	24.2
35-44	19.1	17.9	19.4	21.3	23.1	23.4	22.6
45-54	14.7	14.3	16.7	17.6	19.0	18.8	18.8
55-64	11.3	10.7	11.3	12.5	13.6	13.4	15.0
65-74	7.8	6.7	6.8	6.3	5.7	4.7	5.1
Marital status							
Agree							
Single	31.5	30.8	30.7	31.3	31.8	32.9	33.2
Married	60.9	61.3	61.2	60.5	59.8	58.7	58.5
Other	7.6	7.9	8.1	8.3	8.3	8.4	8.3
Disagree							
Single	43.1	45.5	41.0	39.3	38.0	39.4	38.1
Married	51.0	48.2	51.4	53.7	56.6	54.4	54.9
Other	5.9	6.3	7.7	7.0	5.4	6.3	7.0
Education							
Agree							
Primary	28.8	28.4	27.6	26.0	24.6	23.6	22.4
Secondary	52.9	53.1	52.9	53.2	54.0	54.1	54.4
Tertiary	18.3	18.4	19.5	20.8	21.3	22.3	23.1
Disagree							
Primary	27.2	24.1	25.7	26.6	22.4	21.0	21.0
Secondary	55.9	57.6	58.6	57.2	59.9	59.6	59.7
Tertiary	16.8	18.3	15.8	16.2	17.7	19.4	19.4

*All the results are at significant at $p<.001$.

Table 5. The demographic and social "profile" of coinciding and conflicting perceptions with the ILO conventional definitions: Italy (%)

Variable	2008	2009	2010	2011	2012	2013	2014
Gender							
Agree							
Male	49.7	49.5	49.4	49.3	49.4	49.2	49.2
Female	50.3	50.5	50.6	50.7	50.6	50.8	50.8
Disagree							
Male	46.4	48.2	49.5	50.3	49.4	50.2	50.5
Female	53.6	51.8	50.5	49.7	50.6	49.8	49.5
Age*							
Agree							
15-24	12.8	12.8	12,8	12.7	12.7	12.7	12.7
25-34	17.0	16.4	16.0	15.5	15.3	14.5	14.3
35-44	21.2	21.2	21.1	21.0	20.7	20.2	19.9
45-54	18.3	18.7	19.2	19.6	20.0	20.4	20.8
55-64	16.3	16.5	16.7	16.9	16.8	17.0	17.0
65-74	14.4	14.4	14.3	14.3	14.6	15.1	15.3
Disagree							
15-24	21.7	21.0	20.5	20.2	19.5	18.3	17.3
25-34	28.6	29.6	28.1	27.6	25.4	25.4	24.9
35-44	24.2	24.3	24.7	23.9	24.4	24.2	23.9
45-54	15.4	16.0	17.0	17.6	19.1	20.0	20.9
55-64	8.4	7.9	8.7	9.4	10.5	11.0	11.8
65-74	1.7	1.2	1.1	1.2	1.1	1.1	1.1
Marital status*							
Agree							
Single	31.0	31.2	31.3	31.6	32.3	32.5	32.9
Married	59.4	59.1	58.8	58.4	57.3	56.6	57.0
Other	9.6	9.7	9.8	10.0	10.4	10.8	10.1
Disagree							
Single	48.5	49.2	49.0	49.7	48.2	48.9	48.4
Married	45.1	44.8	44.3	43.5	44.1	43.0	44.1
Other	6.5	6.1	6.7	6.9	7.7	8.1	7.5
Education*							
Agree							
Primary	18.9	17.9	16.9	15.8	14.9	14.2	13.0
Secondary	69.3	70.2	71.0	71.8	72.0	72.1	72.8
Tertiary	11.7	11.9	12.2	12.4	13.1	13.7	14.2
Disagree							
Primary	13.1	11.8	11.6	11.1	10.6	9.8	8.9
Secondary	76.8	78.7	78.4	79.3	79.2	80.0	80.6
Tertiary	10.2	9.6	10.1	9.6	10.2	10.2	10.4

*All the results are at significant at $p<.001$.

Table 6. The demographic and social "profile" of coinciding and conflicting perceptions with the ILO conventional definitions: Portugal (%)

Variable	2008	2009	2010	2011	2012	2013	2014
Gender							
Agree							
Male	49.9	49.3	49.3	49.1	49.1	48.1	47.9
Female	50.6	50.7	50.7	50.9	50.9	51.9	52.1
Disagree							
Male	40.0	42.7	42.1	47.3	48.4	48.2	48.3
Female	60.0	57.3	57.9	52.7	51.6	51.8	51.7
Age*							
Agree							
15-24	15.2	14.9	14.5	14.2	14.1	14.2	14.1
25-34	20.3	20.0	19.7	19.4	18.6	16.8	16.2
35-44	19.7	19.9	20.0	20.6	21.0	20.9	20.9
45-54	18.0	18.2	18.5	18.7	19.0	19.4	19.4
55-64	15.1	15.3	15.4	15.3	15.4	16.1	16.4
65-74	11.7	11.6	11.9	11.9	12.0	12.7	13.1
Disagree							
15-24	11.0	10.0	10.2	12.6	13.0	13.1	13.2
25-34	15.0	15.0	14.0	13.7	13.3	12.8	12.2
35-44	13.7	14.6	14.9	13.1	14.0	14.8	14.0
45-54	15.9	15.7	16.8	17.7	17.2	17.4	18.2
55-64	21.3	21.3	21.3	22.6	23.1	23.5	23.8
65-74	23.0	23.4	22.7	20.2	19.4	18.3	18.5
Marital status							
Agree							
Single	27.3	27.4	27.4	32.7	33.8	34.1	33.6
Married	65.0	64.6	64.5	57.0	55.5	55.1	55.7
Other	7.7	8.0	8.1	10.3	10.7	10.8	10.7
Disagree							
Single	21.4	20.1	19.4	28.4	30.5	31.5	32.0
Married	69.0	69.3	69.7	59.8	57.7	56.6	56.0
Other	9.6	10.6	10.9	11.8	11.8	11.9	12.0
Education*							
Agree							
Primary	52.0	49.6	47.7	42.9	40.7	39.0	36.7
Secondary	36.0	38.0	39.2	42.0	42.8	43.9	44.4
Tertiary	11.9	12.4	13.2	15.1	16.7	17.2	18.9
Disagree							
Primary	71.5	70.4	70.9	63.2	59.8	56.6	53.8
Secondary	22.9	24.9	23.9	29.3	32.4	35.1	36.6
Tertiary	5.7	4.6	5.2	7.6	7.7	8.2	9.6

*All the results are at significant at $p<.001$.

Table 7. The demographic and social "profile" of coinciding and conflicting perceptions with the ILO conventional definitions: Spain (%)

Variable	2008	2009	2010	2011	2012	2013	2014
Gender							
Agree							
Male	50.2	50.1	50.0	49.9	49.7	49.9	49.8
Female	49.8	49.9	50.0	50.1	50.3	50.1	50.2
Disagree							
Male	43.2	45.3	45.2	45.8	46.2	45.5	44.2
Female	56.8	54.7	54.8	54.2	53.8	54.5	55.8
Age*							
Agree							
15-24	13.0	12.8	12.4	12.1	11.9	11.7	11.5
25-34	22.0	21.5	20.9	20.0	19.2	18.3	17.4
35-44	21.6	21.8	22.1	22.3	22.5	22.7	22.7
45-54	17.9	18.3	18.7	19.2	19.6	20.1	20.4
55-64	14.5	14.5	14.7	14.9	15.3	15.2	15.5
65-74	11.0	11.2	11.2	11.4	11.6	11.9	12.4
Disagree							
15-24	22.7	17.9	20.0	18.7	18.7	19.2	19.6
25-34	25.7	25.7	23.5	25.2	21.9	20.6	19.3
35-44	21.4	23.3	22.5	22.6	22.5	22.8	20.8
45-54	15.7	17.5	18.3	17.0	18.5	18.8	20.5
55-64	12.8	13.7	13.6	14.6	16.5	16.5	17.2
65-74	1.7	2.0	2.1	1.9	1.8	2.2	2.6
Marital status*							
Agree							
Single	33.7	33.9	33.9	34.0	34.4	35.7	36.1
Married	57.9	57.6	57.4	57.2	56.5	54.1	53.7
Other	8.4	8.5	8.7	8.8	9.0	10.1	10.3
Disagree							
Single	46.5	41.6	43.1	43.1	43.6	45.1	46.0
Married	47.5	49.3	49.3	48.8	49.9	47.6	44.4
Other	6.1	9.1	7.6	8.0	6.5	7.3	9.6
Education*							
Agree							
Primary	25.2	24.7	23.8	22.3	20.7	19.7	16.4
Secondary	49.0	49.1	49.9	49.9	50.8	50.9	53.1
Tertiary	25.8	26.2	26.3	27.8	28.5	29.3	30.5
Disagree							
Primary	20.0	23.6	21.6	21.6	20.2	18.3	15.3
Secondary	57.9	54.7	57.4	56.1	56.3	57.4	60.3
Tertiary	22.1	21.7	21.0	22.3	23.5	24.3	24.5

*All the results are at significant at $p<.001$.

The investigation of the "agreement" and "disagreement" groups for 2008-2014 (Tables 4 to 7) shows that they do differ in terms of their demographic and

social "profile": Greeks with conflicting perceptions are mainly women (53.1-58.4%), aged 25-34 years (23.1-28.1%), married (48.2-56.6%) with secondary education (55.9-59.9%); Italians with conflicting perceptions are mainly men and women aged 25-34 years (25.4-29.6%), single (48.2-49.7%) with secondary education (76.8-80.6%); Portuguese people with conflicting perceptions are mainly women (51.6-60.0%), aged 65-74 (20.2-23.4%) in 2008-2010 and 55-64 (22.6-23.8%) in 2011-2014, married (56.0-69.7%) with primary education (53.8-71.5%); Spaniards with conflicting perceptions are mainly women (54.2-56.8%) aged 25-34 (23.5-25.7%) in 2008-2011 and 35-44 (20.8-22.8%) in 2012-2014, married (44.4-49.9%) with secondary education (54.7-60.3%).

4 Conclusions

The surprisingly high percentages of Southern Europeans' perceptions of their employment status in agreement with the ILO conventional definitions indicate that this question should precede and not follow the questions on the labour status according to the ILO conventional definitions or the questions on the registration at the public employment office as is the Eurostat instruction to participating countries. It is common practice in social sample survey research to place perception questions before concepts are made quite clear or as Oppenheim [11] pointed out: "We try, as much as possible, to avoid putting ideas into respondents' minds". This result is in line with Gauckler and Körner [7] who proposed that the self-perceived employment status question should be asked first in their belief that this might provide radically different results. These findings have to be taken into account, since as Schwarz [12] argued, cognitive issues raised from the questionnaire may have important implications on questionnaire design and survey operations.

The demographic and social "profile" of conflicting perceptions in Greece and Spain is quite similar (young married women with secondary education). In the cases of Italy and Portugal, it differs as it is young single men and women with secondary education and older married women with primary education, respectively. However, within each country the pattern is in the main systematic overtime. These results imply that there is some kind of "bias" introduced by the ILO conventional definitions of the employed, unemployed and inactive and further research is required as Gauckler and Körner [7] carried out on the "main status effect".

References

1. A. Brandolini, P. Cipollone and E. Viviano. Does the ILO definition capture all unemployment? (Temi di discussione del Servizio Studi 529), Banca d'Italia, Roma, 2004.

2. M. Braun and P.Ph. Mohler. Background variables. In J.A. Harkness, F.J.R. Van de Vijver and P.Ph. Mohler (eds), Cross-cultural survey methods, Wiley, New Jersey, 2003.

3. Eurostat. Labour Force Survey revised explanatory notes (to be applied from 2008Q1 onwards), European Commission, 2008.

4. Eurostat. Task Force on the quality of the Labour Force Survey: Final report, European Commission, 2009.

5. Eurostat. EU Labour Force Survey database user guide, European Commission, 2016.

6. A. de la Fuente. New measures of labour market attachment: 3 new Eurostat indicators to supplement the unemployment rate (Statistics in Focus 57), Eurostat, European Commission, 2011.

7. B. Gauckler, and T. Körner. Measuring the employment status in the Labour Force Survey and the German Census 2011: Insights from recent research at Destatis, Methoden –Daten–Analysen, 5, 2, 181-205, 2011.

8. R. Hussmanns, F. Mehran and V. Verma. Surveys of economically active population, employment, unemployment and underemployment: An ILO manual on concepts and methods, International Labour Office, Geneva, 1990.

9. S.R.G. Jones and W.C Riddell. The measurement of unemployment: an empirical approach, Econometrica, 67, 1, 147-162, 1999.

10. L. Kish. Multipopulation survey designs: Five types with seven shared aspects, International Statistical Review, 62, 2, 167-186, 1994.

11. A.N. Oppenheim. Questionnaire design, interviewing and attitude measurement (new edition), Continuum, London, 1992.

12. N. Schwarz. Cognitive issues of Labour Force Surveys in a multinational context: Issues and findings, Paper prepared for the OECD Working Party on Employment and Unemployment Statistics, Paris, 14-16 April 1987.

13. F.F. Stephan and P.J. McCarthy. Sampling opinions: An analysis of survey procedure, Greenwood Press, Connecticut, 1958.

14. A. Yfanti, C. Michalopoulou and S. Zahariou. The decision of how to measure unemployment is a political and not a statistical question: Evidence from the European Labour Force Survey: 2008-2014, Manuscript in preparation, 2017.

Estimation the Key Value of Shift Cipher by Neural Networks – A Case Study

Eylem Yucel, Ruya Samli
Department of Computer Engineering, Istanbul University, Turkey

Abstract

In this study, neural networks were used to estimate the key of a Shift Cipher process which is a classical public key cryptography method. For this reason, a passage from Hamlet with 386 English letters was taken as the plaintext, it was encrypted with Shift Cipher algorithm with various keys and a backpropagation neural network model was applied by using both plaintext and ciphertext. It was seen that the success of neural networks is acceptable and it can be used for estimating encryption keys.

Keywords: Neural Networks, Public Key Cryptography, Shift Cipher.

1 Introduction

Security is an extensive concern in information and data systems of all types. One of the most important ways for keeping information secure is cryptology. Cryptology provides various algorithms to perform substitutions and transformation on the original text to produce unintelligible cipher text. This masking prevents security evasion. Cryptology can be defined as encryption science and contains two main parts: cryptography which means constituting cryptos and cryptanalysis which means breaking cryptos. There are many algorithms in cryptology field. The public and private key pair comprise of two uniquely related cryptographic keys. In private key cryptography, the key is private and it uses the same cryptographic keys for both encryption of plaintext and decryption of ciphertext. In public key cryptography, encryption and decryption parts use different keys and one of them is private while the other is public. Any person can encrypt a message using the public key

17th *ASMDA Conference Proceedings, 6 - 9 June 2017, London, UK*

of the receiver, but such a message can be decrypted only with the receiver's private key.

1.1 Shift Cipher

When a cipher method is applied to a plaintext, first of all the letters must be transformed to numbers. In the English alphabet, every letter matches to a number between 0 and 25:

A	B	C	D	E	F	G	H	I	J	K	L	M	N	O	P	Q	R	S	T	U	V	W	X	Y	Z
0	1	2	3	4	5	6	7	8	9	10	11	12	13	14	15	16	17	18	19	20	21	22	23	24	25

Here, the letters' being upper or lower case does not differ. A and a both correspond to 0; B and b both correspond to 1 and so on.

The shift cipher is a substitution cipher that involves the shifted letters of all the letters in plaintext by a specific step number which is key of the algorithm and constitutes ciphertext. So, a message that initially was quite readable, ends up in a form that can not be understood. This method is one of the methods of five classic methods which are substitution cipher, vigenere cipher, affine chipher and hill cipher. Some samples of plaintext and ciphertext in terms of English alphabet can be seen below:

Key = 0
Plaintext : A B C D E F G H I J K L M N O P Q R S T U V W X Y Z
Ciphertext:A B C D E F G H I J K L M N O P Q R S T U V W X Y Z

Key = 3 (Caesar Cipher)
Plaintext : A B C D E F G H I J K L M N O P Q R S T U V W X Y Z
Ciphertext: D E F G H I J K L M N O P Q R S T U V W X Y Z A B C

Key = 10
Plaintext : A B C D E F G H I J K L M N O P Q R S T U V W X Y Z
Ciphertext: K L M N O P Q R S T U V W X Y Z A B C D E F G H I J

The number of possible keys differs according to the character set used for plaintext. If we use English alphabet, Turkish alphabet or ASCII characters for the domain set, then the numbers of possible keys will be 26, 29, and 256 respectively. If we use upper cases and lower cases together in alphabet, it becomes twice. Thus, it is an important subject to

find the right key of the algorithm. Neural networks is a modelling and estimating method which is used in many fields. In this study we use neural networks to find the private key of Shift Cipher methodology in a specific case study. The results show that neural networks is an appropriate method for Shift Cipher cryptanalysis and in future work we will observe if the cryptanalysis of other cryptosystems can be done by neural networks or not.

1.2 Literature Review

There are many methods in the literature which uses neural networks and cryptography together. But in this study, we examined only the studies which are about classical encryption algorithms which were expressed above.

Volna et. al (2012) tried to encrypt a plaintext by dividing it into 6-bit blocks. They used a multi perceptron neural network structure. They designed the input and hidden layer of the neural network structure as 6 neurons. They transform the plaintexts in each training set to ASCII codes and these ASCII codes to binary texts. After all these operations, they encrypted the text with the neural network. In some other studies, Lonkar and Charniya (2014), Komal et. al (2015), Gujral and Pradhan (2009) used similar structures to implement encryption algorithms.

Sivagurunathan et. al (2010) encrypted files with Playfair, Vigenere and Hill Cipher Methods were used as input data. They trained the network with these files. In this training process, they implement the tests in three different manner. In the first one, they encrypted the same plaintexts with different keys; in second one, the encrypted different plaintexts with the same key and in the last one, they used both different plaintexts and different keys. The main goal of this study is to classify the texts which are encrypted with different methods by neural networks.

Tanriverdi (1993) investigated neural network structure's powerfull and poor properties by using some classical encryption methods. Tas (2002) tried to train a neural network structure with plaintexts and ciphertexts. Yayık (2013) designed a random number generator and showed that a neural network based system can make cryptanalysis independent to the algorithm.

Jagtap et. al (2015) used a neural network based sequential machine and chaotic neural networks in their study. In this study 3 bit encryption has been implemented by using sequential machine.

Kinzel and Kantel (2002) is one of the oldest general studies about neural cryptology concept. In this study, how a neural network can be trained for this type of a process and how the key can be generated were handled. Godhavari et. al (2005) is a general study which explains neural network usage in cryptology. In this study, neural cryptology concept was explained, the role of a neural network in private key generation was analyzed and cryptanalysis of this process was investigated. In another general study, Rosen-Zvi et. al presented analytical results about neural network based cryptology Rosen et. al (2002). Pointcheval presented another study about general applications of neural network in cryptology Pointcheval (1994). In this study, many applications about neural cryptology were examined.

Shibab (2006) analyzed the security of computer networks by using a back-propagation neural network model Lian (2009) offered a block encryption method over chaotic neural networks. Guo et. al (1999) also presented a novel symmetric encryption standart about chaotic neural networks too.

Crounse et. al (1996) used Cellular Neural Networks Universal Machine (CNN-UM) and generated pseudo random numbers. In Wang and Wang (2008), it was explained how Hopfield typed neural network can be used in key validation process. In another similar study Li et. al (2001), a validation process is implemented by using neural network.

In Isac and Santhi (2011), applications about images' encryption and stamping by neural network were examined. A study in which a symmetric key was designed was presented in Arvandi et. al (2006). In Dalkıran and Danisman (2010), a neural network based chaotic generator for using in cryptology applications was presented. In Laskari et. al (2006), neural network was applied to cryptology problems (Discrete Logarithm Problem, Diffie-Helman Key Exchange Problem and ElGamal Digital Signature Problem) and the performance was measured. In Al-Shakarchy (2012) and Alallayah et. al (2012), Data Encryption Standart (DES) and Simplified Data Encryption Standart (SDES) were examined respectively.

2. Material and Methods

Neural Networks are simplified models of the central nervous system. They are based on the basic model of the human brain with capability of generalization and learning. Neural networks are structured as a series of layers, each composed of one or more neurons. Each neuron produces an output, or activation, based on the outputs of the previous layer and a set of weights.

The backpropagation algorithm is a supervised learning method for multilayer feed-forward networks. Feed-forward neural networks are inspired by the information processing of one or more neural cells. This neural cells are called “neuron”. A neuron accepts input signals via its dendrites, which pass the electrical signal down to the cell body. The axon carries the signal out to synapses, which are the connections between the cells. The purpose of the backpropagation approach is to model a given function by modifying internal weightings of input signals to produce an expected output signal. The system is trained where the error between the system’s output and a known expected output is presented to the system and used to modify its internal state. Figure 1 depicts the general backpropagation neural network structure.

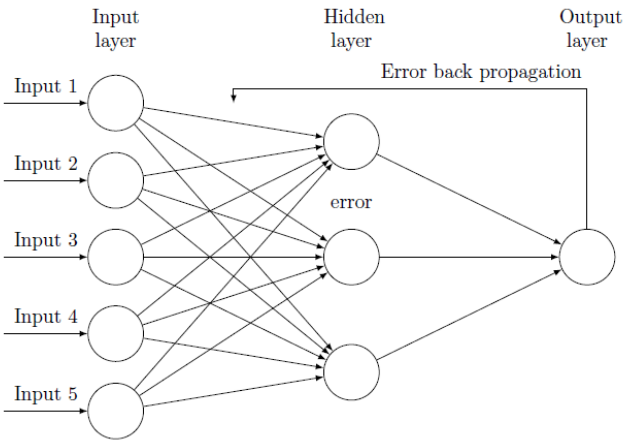

Figure 1. Backpropagation Neural Network

3. Results

We applied shift cipher to the passage of Hamlet Original Text: Act 4, Scene 1 which is given below.

O heavy deed!
It had been so with us, had we been there:
His liberty is full of threats to all;
To you yourself, to us, to every one.
Alas, how shall this bloody deed be answer’d?
It will be laid to us, whose providence
Should have kept short, restrain’d and out of haunt,
This mad young man: but so much was our love,

We would not understand what was most fit;
But, like the owner of a foul disease,
To keep it from divulging, let it feed
Even on the pith of Life. Where is he gone?

When this text was transformed to numbers, it becomes like Table 1.

Table 1. Number Transformation of the Plaintext

O	H	E	A	V	Y	D	E	E	D	I	T	H
14	7	4	0	21	24	3	4	4	3	8	19	7
A	D	B	E	E	N	S	O	W	I	T	H	U
0	3	1	4	4	13	18	14	22	8	19	7	20
S	H	A	D	W	E	B	E	E	N	T	H	E
18	7	0	3	22	4	1	4	4	13	19	7	4
R	E	H	I	S	L	I	B	E	R	T	Y	I
17	4	7	8	18	11	8	1	4	17	19	24	8
S	F	U	L	L	O	F	T	H	R	E	A	T
18	5	20	11	11	14	5	19	7	17	4	0	19
S	T	O	A	L	L	T	O	Y	O	U	Y	O
18	19	14	0	1	11	19	14	24	14	20	24	14
U	Y	O	U	R	S	E	L	F	T	O	U	S
20	24	14	20	17	18	4	11	5	19	14	20	18
T	O	E	V	E	R	Y	O	N	E	A	L	A
19	14	4	21	4	17	24	14	13	4	0	11	0
S	H	O	W	S	H	A	L	L	B	L	O	O
18	7	14	22	18	7	0	11	11	1	11	14	14
D	Y	D	E	E	D	B	E	A	N	S	W	E
3	24	3	4	4	3	1	4	0	13	18	22	4
R	D	I	T	W	I	L	L	B	E	L	A	I
17	3	8	19	22	8	11	11	1	4	11	0	8
D	T	O	U	S	W	H	O	S	E	P	R	O
3	19	14	20	18	22	7	14	18	4	15	17	14
V	I	D	E	N	C	E	S	H	O	U	L	D
21	8	3	4	13	2	4	18	7	14	20	11	3
H	A	V	E	K	E	P	T	S	H	O	R	T
7	0	21	4	10	4	15	19	18	7	14	17	19
R	E	S	T	R	A	I	N	D	A	N	D	O
17	4	18	19	17	0	8	13	3	0	13	3	14
U	T	O	H	A	U	N	T	T	H	I	S	M
20	19	14	7	0	20	13	19	19	7	8	18	12
A	D	Y	O	U	N	G	M	A	N	B	U	T
0	3	24	14	20	13	6	12	0	13	1	20	19
S	O	M	U	C	H	W	A	S	O	U	R	L
18	14	12	20	2	7	22	0	18	14	20	17	11
O	V	E	W	E	W	O	U	L	D	N	O	T
14	21	4	22	4	22	14	20	11	3	13	14	19
U	N	D	E	R	S	T	A	N	D	W	H	A
20	13	3	4	17	18	19	0	13	3	22	7	0
T	W	A	S	M	O	S	T	F	I	T	B	U
19	22	0	18	12	14	18	19	5	8	19	1	20
T	L	I	K	E	T	H	E	O	W	N	E	R

19	11	8	10	4	19	7	4	14	22	13	4	17
O	F	A	F	O	U	L	D	I	S	E	A	S
14	5	0	5	14	20	11	3	8	18	4	0	18
E	T	O	K	E	E	P	I	T	F	R	O	M
4	19	14	10	4	4	15	8	19	5	17	14	12
D	I	V	U	L	G	I	N	G	L	E	T	I
3	8	21	20	11	6	8	13	6	11	4	19	8
T	F	E	E	D	E	V	E	N	O	N	T	H
19	5	4	4	3	4	21	4	13	14	13	19	7
E	P	I	T	H	O	F	L	I	F	E	W	H
4	15	8	19	7	14	5	11	8	5	4	22	7
E	R	E	I	S	H	E	G	O	N	E		
4	17	4	8	18	7	4	6	14	13	4		

According to this table, inputs become as Table 2.

Table 2: Input Table

14	7	4	0	21	24	3	4	4	3	8	19	7
0	3	1	4	4	13	18	14	22	8	19	7	20
18	7	0	3	22	4	1	4	4	13	19	7	4
17	4	7	8	18	11	8	1	4	17	19	24	8
18	5	20	11	11	14	5	19	7	17	4	0	19
18	19	14	0	1	11	19	14	24	14	20	24	14
20	24	14	20	17	18	4	11	5	19	14	20	18
19	14	4	21	4	17	24	14	13	4	0	11	0
18	7	14	22	18	7	0	11	11	1	11	14	14
3	24	3	4	4	3	1	4	0	13	18	22	4
17	3	8	19	22	8	11	11	1	4	11	0	8
3	19	14	20	18	22	7	14	18	4	15	17	14
21	8	3	4	13	2	4	18	7	14	20	11	3
7	0	21	4	10	4	15	19	18	7	14	17	19
17	4	18	19	17	0	8	13	3	0	13	3	14
20	19	14	7	0	20	13	19	19	7	8	18	12
0	3	24	14	20	13	6	12	0	13	1	20	19
18	14	12	20	2	7	22	0	18	14	20	17	11
14	21	4	22	4	22	14	20	11	3	13	14	19
20	13	3	4	17	18	19	0	13	3	22	7	0
19	22	0	18	12	14	18	19	5	8	19	1	20
19	11	8	10	4	19	7	4	14	22	13	4	17
14	5	0	5	14	20	11	3	8	18	4	0	18
4	19	14	10	4	4	15	8	19	5	17	14	12
3	8	21	20	11	6	8	13	6	11	4	19	8
19	5	4	4	3	4	21	4	13	14	13	19	7
4	15	8	19	7	14	5	11	8	5	4	22	7
4	17	4	8	18	7	4	6	14	13	4		

There are 28 rows in total. The key numbers are 17, 4, 9, 11, 2, 22, 9, 14, 6, 5, 20, 18, 11, 15, 20, 8, 10, 4, 15, 9, 2, 8, 3, 25, 20, 11, 7 and 6 for the 28 rows respectively. These numbers were chosen randomly. So, the ciphertext is calculated as given below (Table 3).

Table 3: Ciphertext

O+17	H+17	E+17	A+17	V+17	Y+17	D+17	E+17	E+17	D+17	I+17	T+17	H+17
14+17	7+17	4+17	0+17	21+17	24+17	3+17	4+17	4+17	3+17	8+17	19+17	7+17
A+4	D+4	B+4	E+4	E+4	N+4	S+4	O+4	W+4	I+4	T+4	H+4	U+4
0+4	3+4	1+4	4+4	4+4	13+4	18+4	14+4	22+4	8+4	19+4	7+4	20+4
S+9	H+9	A+9	D+9	W+9	E+9	B+9	E+9	E+9	N+9	T+9	H+9	E+9
18+9	7+9	0+9	3+9	22+9	4+9	1+9	4+9	4+9	13+9	19+9	7+9	4+9
R+11	E+11	H+11	I+11	S+11	L+11	I+11	B+11	E+11	R+11	T+11	Y+11	I+11
17+11	4+11	7+11	8+11	18+11	11+11	8+11	1+11	4+11	17+11	19+11	24+11	8+11
S+2	F+2	U+2	L+2	L+2	O+2	F+2	T+2	H+2	R+2	E+2	A+2	T+2
18+2	5+2	20+2	11+2	11+2	14+2	5+2	19+2	7+2	17+2	4+2	0+2	19+2
S+22	T+22	O+22	A+22	L+22	L+22	T+22	O+22	Y+22	O+22	U+22	Y+22	O+22
18+22	19+22	14+22	0+22	1+22	11+22	19+22	14+22	24+22	14+22	20+22	24+22	14+22
U+9	Y+9	O+9	U+9	R+9	S+9	E+9	L+9	F+9	T+9	O+9	U+9	S+9
20+9	24+9	14+9	20+9	17+9	18+9	4+9	11+9	5+9	19+9	14+9	20+9	18+9
T+14	O+14	E+14	V+14	E+14	R+14	Y+14	O+14	N+14	E+14	A+14	L+14	A+14
19+14	14+14	4+14	21+14	4+14	17+14	24+14	14+14	13+14	4+14	0+14	11+14	0+14
S+6	H+6	O+6	W+6	S+6	H+6	A+6	L+6	L+6	B+6	L+6	O+6	O+6
18+6	7+6	14+6	22+6	18+6	7+6	0+6	11+6	11+6	1+6	11+6	14+6	14+6
D+5	Y+5	D+5	E+5	E+5	D+5	B+5	E+5	A+5	N+5	S+5	W+5	E+5
3+5	24+5	3+5	4+5	4+5	3+5	1+5	4+5	0+5	13+5	18+5	22+5	4+5
R+20	D+20	I+20	T+20	W+20	I+20	L+20	L+20	B+20	E+20	L+20	A+20	I+20
17+20	3+20	8+20	19+20	22+20	8+20	11+20	11+20	1+20	4+20	11+20	0+20	8+20
D+18	T+18	O+18	U+18	S+18	W+18	H+18	O+18	S+18	E+18	P+18	R+18	O+18
3+18	19+18	14+18	20+18	18+18	22+18	7+18	14+18	18+18	4+18	15+18	17+18	14+18
V+11	I+11	D+11	E+11	N+11	C+11	E+11	S+11	H+11	O+11	U+11	L+11	D+11
21+11	8+11	3+11	4+11	13+11	2+11	4+11	18+11	7+11	14+11	20+11	11+11	3+11
H+15	A+15	V+15	E+15	K+15	E+15	P+15	T+15	S+15	H+15	O+15	R+15	T+15
7+15	0+15	21+15	4+15	10+15	4+15	15+15	19+15	18+15	7+15	14+15	17+15	19+15
R+20	E+20	S+20	T+20	R+20	A+20	I+20	N+20	D+20	A+20	N+20	D+20	O+20
17+20	4+20	18+20	19+20	17+20	0+20	8+20	13+20	3+20	0+20	13+20	3+20	14+20
U+8	T+8	O+8	H+8	A+8	U+8	N+8	T+8	T+8	H+8	I+8	S+8	M+8
20+8	19+8	14+8	7+8	0+8	20+8	13+8	19+8	19+8	7+8	8+8	18+8	12+8
A+10	D+10	Y+10	O+10	U+10	N+10	G+10	M+10	A+10	N+10	B+10	U+10	T+10
0+10	3+10	24+10	14+10	20+10	13+10	6+10	12+10	0+10	13+10	1+10	20+10	19+10
S+4	O+4	M+4	U+4	C+4	H+4	W+4	A+4	S+4	O+4	U+4	R+4	L+4
18+4	14+4	12+4	20+4	2+4	7+4	22+4	0+4	18+4	14+4	20+4	17+4	11+4
O+15	V+15	E+15	W+15	E+15	W+15	O+15	U+15	L+15	D+15	N+15	O+15	T+15
14+15	21+15	4+15	22+15	4+15	22+15	14+15	20+15	11+15	3+15	13+15	14+15	19+15
U+9	N+9	D+9	E+9	R+9	S+9	T+9	A+9	N+9	D+9	W+9	H+9	A+9
20+9	13+9	3+9	4+9	17+9	18+9	19+9	0+9	13+9	3+9	22+9	7+9	0+9
T+2	W+2	A+2	S+2	M+2	O+2	S+2	T+2	F+2	I+2	T+2	B+2	U+2
19+2	22+2	0+2	18+2	12+2	14+2	18+2	19+2	5+2	8+2	19+2	1+2	20+2
T+8	L+8	I+8	K+8	E+8	T+8	H+8	E+8	O+8	W+8	N+8	E+8	R+8
19+8	11+8	8+8	10+8	4+8	19+8	7+8	4+8	14+8	22+8	13+8	4+8	17+8
O+3	F+3	A+3	F+3	O+3	U+3	L+3	D+3	I+3	S+3	E+3	A+3	S+3
14+3	5+3	0+3	5+3	14+3	20+3	11+3	3+3	8+3	18+3	4+3	0+3	18+3
E+25	T+25	O+25	K+25	E+25	E+25	P+25	I+25	T+25	F+25	R+25	O+25	M+25
4+25	19+25	14+25	10+25	4+25	4+25	15+25	8+25	19+25	5+25	17+25	14+25	12+25
D+20	I+20	V+20	U+20	L+20	G+20	I+20	N+20	G+20	L+20	E+20	T+20	I+20
3+20	8+20	21+20	20+20	11+20	6+20	8+20	13+20	6+20	11+20	4+20	19+20	8+20
T+11	F+11	E+11	E+11	D+11	E+11	V+11	E+11	N+11	O+11	N+11	T+11	H+11
19+11	5+11	4+11	4+11	3+11	4+11	21+11	4+11	13+11	14+11	13+11	19+11	7+11
E+7	P+7	I+7	T+7	H+7	O+7	F+7	L+7	I+7	F+7	E+7	W+7	H+7
4+7	15+7	8+7	19+7	7+7	14+7	5+7	11+7	8+7	5+7	4+7	22+7	7+7
E+6	R+6	E+6	I+6	S+6	H+6	E+6	G+6	O+6	N+6	E+6		
4+6	17+6	4+6	8+6	18+6	7+6	4+6	6+6	14+6	13+6	4+6		

Input vector is given in Table 4:

Table 4: Input Vector

31	24	21	17	38	41	20	21	21	20	25	36	24
4	7	5	8	8	17	22	18	26	12	23	11	24
27	16	9	12	31	13	10	13	13	22	28	16	13
28	15	18	19	29	22	19	12	15	28	30	35	19
20	7	22	13	13	16	7	21	9	19	6	2	21
40	41	36	22	23	33	41	36	46	36	42	46	36
29	33	23	29	26	27	13	20	14	28	23	29	27
33	28	28	35	18	31	38	28	27	18	14	25	14
24	13	20	28	24	13	6	17	17	7	17	20	20
8	29	8	9	9	8	6	9	5	18	23	27	9
37	23	28	390	42	28	31	31	21	24	31	20	28
21	37	32	38	36	40	25	32	36	22	33	35	32
32	19	14	15	24	13	15	29	18	25	31	22	14
22	15	36	19	25	19	30	34	33	22	29	32	34
37	24	38	39	37	20	28	33	23	20	33	23	34
28	27	22	15	8	28	21	27	27	15	16	26	20
10	13	34	24	30	23	16	22	10	23	11	30	29
22	18	16	24	6	11	26	4	22	18	24	21	15
29	36	19	37	19	37	29	35	26	18	28	29	34
29	22	12	13	26	27	28	9	22	12	31	16	9
21	24	2	20	14	26	20	21	7	10	21	3	22
27	19	16	18	12	27	15	12	22	30	21	12	25
17	8	3	8	17	23	14	6	11	21	7	3	21
29	44	39	35	29	29	40	33	44	30	42	39	37
23	28	41	40	31	26	28	23	26	31	24	39	28
30	16	15	15	14	15	32	15	24	25	24	30	18
11	22	15	26	14	21	12	18	15	12	11	29	14
10	23	10	14	24	13	10	12	20	19	10		

Real and estimated values are given in Table 5:

Table 5: Real and Estimated Values

17	17,65	4	4,59	11	10,90	22	21,25	9	8,65	6	5,85	20	24,99	18	18,55	15	15,62
17	17,83	4	4,61	11	10,97	22	21,25	9	8,68	6	5,89	20	20,05	11	10,93	15	15,77
17	17,83	4	4,59	11	10,85	22	21,31	9	8,68	6	5,89	20	20,17	11	10,97	15	15,60
17	17,69	4	4,61	11	10,97	22	21,30	14	14,50	6	5,83	20	20,08	11	10,89	15	15,62
17	17,65	9	8,68	11	10,93	22	21,26	14	14,47	6	5,89	20	20,08	11	10,97	15	15,62
17	17,79	9	8,72	11	10,94	22	21,25	14	22,30	6	5,90	20	20,11	11	10,90	20	20,08
17	17,75	9	8,61	11	11,09	22	21,25	14	14,48	6	5,90	20	20,26	11	10,85	20	20,26
17	17,83	9	8,61	11	10,97	22	21,32	14	14,61	5	5,13	20	20,08	11	10,97	20	20,08
17	17,83	9	8,69	2	3,67	22	21,25	14	14,49	5	5,30	20	20,12	11	10,94	20	20,07
17	17,75	9	8,67	2	3,64	22	21,24	14	14,65	5	5,13	20	20,17	11	11,01	20	20,08
17	17,76	9	8,58	2	3,68	22	21,32	14	14,47	5	5,15	18	18,65	11	10,91	20	20,12
17	17,66	9	8,67	2	3,65	22	21,25	14	14,47	5	5,15	18	18,56	11	10,94	20	20,17
17	17,83	9	8,67	2	3,65	9	8,68	14	14,61	5	5,13	18	18,55	11	10,90	20	20,07
4	4,55	9	8,64	2	3,66	9	8,82	14	14,48	5	5,13	18	18,55	11	10,89	20	20,18
4	4,52	9	8,68	2	3,64	9	8,65	14	14,47	5	5,15	18	18,56	15	15,77	20	20,12
4	4,53	9	8,72	2	3,67	9	8,68	14	14,48	5	5,15	18	18,54	15	15,62	20	20,07
4	4,55	9	8,67	2	3,66	9	8,68	6	5,92	5	5,19	18	18,72	15	15,61	20	20,18
4	4,55	11	10,93	2	3,67	9	8,68	6	5,92	5	5,21	18	18,55	15	15,76	20	20,07
4	4,58	11	10,97	2	3,62	9	8,67	6	5,90	5	5,22	18	18,56	15	15,62	8	7,67
4	4,60	11	11,01	2	3,63	9	8,64	6	5,93	20	20,08	18	18,73	15	15,76	8	7,67
4	4,59	11	10,97	2	3,67	9	8,72	6	5,92	20	20,18	18	18,55	15	15,61	8	7,63
4	4,62	11	10,94	22	21,28	9	8,68	6	5,92	20	20,17	18	18,56	15	15,62	8	7,69

8	7,59	4	4,60	15	15,67	2	12,10	3	4,06	25	22,50	11	10,93	6	5,87
8	7,67	4	4,59	15	15,60	2	3,67	3	4,04	25	22,50	11	10,97	6	5,91
8	7,63	4	4,58	15	15,60	2	3,67	3	4,06	25	22,51	11	10,90	6	5,92
8	7,67	4	4,61	15	15,62	2	3,64	3	4,08	20	20,18	11	10,91	6	5,92
8	7,67	4	4,52	9	8,68	2	3,65	3	4,10	20	20,17	11	10,90	6	5,87
8	7,69	4	4,59	9	8,64	2	3,67	3	4,07	20	20,05	11	10,94	6	5,93
8	7,66	4	4,62	9	8,61	2	3,61	3	4,02	20	20,06	11	11,01	6	5,90
8	7,66	4	4,55	9	8,67	2	3,68	3	4,08	20	20,08	7	6,70	6	5,89
8	7,62	4	4,60	9	8,68	8	7,67	3	4,09	20	20,29	7	6,72	6	5,87
10	9,72	4	4,59	9	8,68	8	7,62	3	4,04	20	20,17	7	6,73		
10	9,72	4	4,61	9	8,68	8	7,66	3	4,04	20	9,74	7	6,74		
10	9,93	4	4,60	9	8,61	8	7,63	3	4,09	20	20,29	7	6,75		
10	9,75	4	4,58	9	8,64	8	7,63	25	22,65	20	20,08	7	6,71		
10	9,78	15	15,60	9	8,61	8	7,67	25	22,49	20	20,26	7	6,74		
10	9,74	15	15,61	9	8,69	8	7,69	25	22,50	20	20,07	7	6,70		
10	9,86	15	15,76	9	8,72	8	7,63	25	22,52	20	20,17	7	6,73		
10	9,74	15	15,61	9	8,61	8	7,63	25	22,65	11	10,94	7	6,74		
10	9,72	15	15,76	2	3,67	8	7,67	25	22,65	11	11,03	7	6,70		
10	9,74	15	15,61	2	3,68	8	7,63	25	22,50	11	10,97	7	6,75		
10	9,68	15	15,60	2	3,63	8	7,63	25	22,58	11	10,97	7	6,75		
10	9,78	15	15,62	2	3,67	8	7,66	25	22,49	11	10,89	6	5,87		
10	9,78	15	15,60	2	3,65	3	4,08	25	22,68	11	10,97	6	5,92		

The neural network toolbox which is used in this study was given in Figure 2.

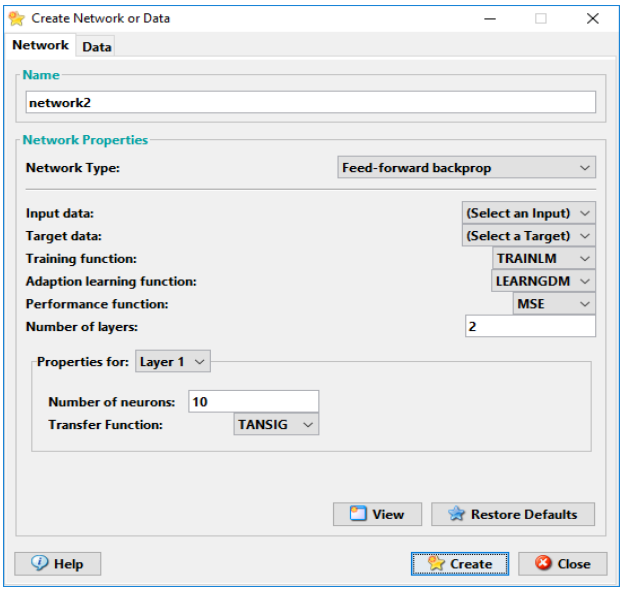

Figure 2: MATLAB Neural Network Toolbox

The neural network structure used in the study is given in Figure 3.

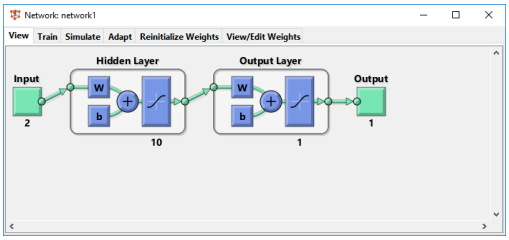

Figure 3: Neural network structure

The regression coefficients of the neural network structure is given in Figure 4. As it can be easily seen from the figure, the coefficients are very close to 1 that means the estimation process is successful.

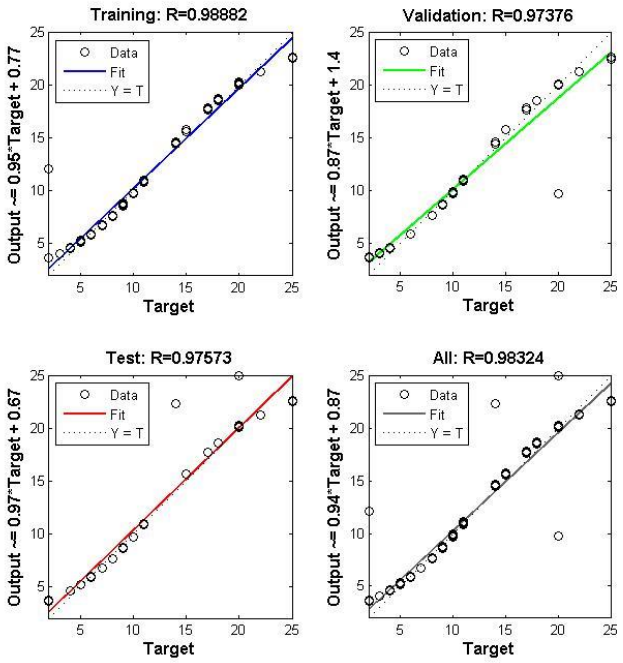

Figure 4: Regression Coefficients of Neural Network

4. Conclusion

In this study, a passage from Hamlet Original Text: Act 4, Scene 1 is encrypted by using the Shift Cipher algorithm with various keys and the keys are estimated with neural networks with the help plaintext and ciphertext. With the simulation results, it's seen that neural networks can be used for estimating encryption keys.

Acknowledgements: This work was supported by Research Fund of Istanbul University under Project YADOP-24207.

References

Alallayah, K., Amin, M, AbdElwahed, W, Alhamami A. (2012.) Applying Neural Networks for Simplified Data Encryption Standard (SDES) Cipher System Cryptanalysis, The International Arab Journal of Information Technology, 9(2), 163-169.

Al-Shakarchy, N.D.K. (2012). Simulating DES Algorithm Using Artificial Neural Network, Jouenal of Kerbala University, 10(4), 13-21.

Arvandi, M., Wu, S., Sadeghian, A., Melek, W.W., Woungang, I. (2006). Symmetric Cipher Design Using Recurrent Neural Networks, International Joint Conference on Neural Networks, July 16-21 2006 Vancouver, Canada, ISBN: 0-7803-9490-9, 2039-2046.

Crounse, K.R., Yang, T., Chua, L.O. (1996). Pseudo-Random Sequence Generation Using The CNN Universal Machine with Application to Cryptograhy, 4th IEEE Workshop on CNN and their Applications, June 24-26, Sevile, Spain, ISBN: 0-7803-3261-X, 433-438.

Dalkıran, İ., Danışman, K. (2010). Artificial Neural Network Based Chaotic Generator for Cryptology, Turk J Elec Eng & Comp Sci, 18(2), 225-240.

Godhavari, T., Alamelu, N.R., Soundararajan, R. (2005). Cryptograhy Using Neural Network, IEEE Indicon 2005 Conference, 11-13 December 2005, Chennai, India Dr.M.G.R. Educational & Research Institute, ISBN: 0-7803-9503-4, 258-261.

Gujral, V., Pradhan, S.K. (2009). Cryptography Using Artificial Neural Networks, Department of Electronics and Communications Engineering National Institute of Technology Rourkela.

Guo, D., Cheng, L.M., Cheng, L.L. (1999). A New Symmetric Probabilistic Encryption Scheme Based on Chaotic Attractors of Neural Networks, Applied Intelligence, 10, 71-84.

Isac, B., Santhi, V. (2011). A Stduy on Digital Image and Video Watermarking Schemes Using Neural Networks, International Journal of Computer Applications, 12(9), 1-6.

Jagtap, S.D., Balaramdu, P., Singh, M.K. (2015). Cryptography Based on Artificial Neural Network, International Journal of Advanced Research in Electronics and Communication Engineering, 4(11), 2785-2789.

Kinzel, W., Kanter, I. (2002). Neural Cryptograhy, Proceeding of 9th International Conference on Neural Information Processing, 1351-1354.

Komal, T., Ashutosh, R., Nalawade, S.M. (2015). Encryption and Decryption Using Artificial Neural Network, International Advanced Research Journal in Science, Engineering and Technology, 2(4), 81-83.

Laskari, E.C., Meleetiou, G.C., Tasoulis, D.K., Vrahatis, M.N. (2006). Studying the Performance of Artificial Neural Networks on Problems Related to Cryptography, Elsevier, 937-942.

Lian, S. (2009). A Block Cipher Based on Chaotic Neural Networks, Elsevier, Neurocomputing, 1296-1301.

Li, L.H., Lin, I.C., Hwang, M.S. (2001). A Remote Password Authentication Scheme for Multiserver Architecture Using Neural Networks, IEEE Transaction on Neural Networks, 12(6), 1498-1504.

Lonkar, S., Charniya, N. (2014). Neural Network Based Cryptography, International Journal of Application or Innovation in Engineering and Management, ISSN: 2319-4847.

Pointcheval, D. (1994). Neural Networks and Their Cryptographic Applications, Pascale Charpin Ed., 1-7.

Rosen-Zvi, M., Kanter, I., Kinzel, W. (2002). Cryptography based on neural networks – analytical results, Journal of Physics A: Mathematical and General, 35, 707-713.

Shihab, K. (2006). A Backpropagation Neural Network for Computer Network Security, Journal of Computer Science, 2(9), 710-715.

Sivagrunathan, G., Rajendran, V., Purusothaman, T. (2010). Classification of Substitution Ciphers Using Neural Network, International Journal of Computer Science and Network Security, 10(3), 274-279.

Tanrıverdi, H. (1993). Yapay Sinir Ağlarının Kriptolojide Kullanılması, BsC Thesis, METU, Institute of Science and Technology, Electrical – Electronical Engineering Department.

Tas, O. (2002). Yapay Sinir Ağları ile Şifreleme Algoritmalarının Çözümü, BsC Thesis, Fırat University, Institute of Science and Technology, Computer Engineering Department.

Yayık, A. (2013). Yapay Sinir Ağı ile Kriptoloji Uygulamaları, BsC Thesis, Mustafa Kemal University, Institute of Science and Technology, Informatics Department.

Volna, E., Kotyrba, M., Kocian, V., Janosek, M. (2012). Cryptography Based on Neural Network, 26th European Conference on Modelling and Simulation, ISBN: 978-0-9564944-4-3 / 978-0-9564944-5-0.

Wang, S., Wang, H. (2008). Password Authentication Using Hopfield Neural Networks, IEEE Transaction on Systems, Man and Cybernetics, 38(2), 265-268.

Health estimates for some countries of the rapid developing world

Konstantinos N. Zafeiris[1] and Christos H. Skiadas[2]

[1]Department of History and Ethnology, Laboratory of P. Anthropology, Democritus University of Thrace. P. Tsaldari 1, 69100-Komotini. Greece
(E-mail: kzafiris@he.duth.gr)
[2]Technical University of Crete, University Campus, 73100 Chania, Crete, Greece
(E-mail: skiadas@cmsim.net)

Abstract. This is a twofold paper, firstly aiming to apply a method for the calculation of healthy life expectancy to the well-known BRIICS countries. This method is based on the μx distribution of a full life table. However, for many countries of the world such data is virtually absent or problematic, and in reality, only available in the form of an abridged life table. Thus, a method for expanding these life tables into full ones was presented. This method is used by the MORTPAK software of the United Nations. It was found that the use of this application was quite problematic for our purposes. On the other hand, the μx based approach seems to be very efficient in calculating the temporal trends and levels of healthy life expectancy, given that the quality of data is good.
Keywords: life expectancy at birth, healthy life expectancy, MORTPAK, BRIICS.

1 Introduction

It was a long ago when scientists from different scientific fields tried to study the health of a population. Among the first was Chiang [1], who introduced an *"Index of health",* based on data from the Canadian Sickness Survey, 1950-1951. Others used life table techniques, like Sanders [10] who tried to construct tables of *"effective life years"*, as a measure of the current health of the population based on mortality and morbidity rates. Sullivan [19] [20] calculated the expectation of life free of disability and the expectation of disability. Torrance [21] developed a health status index model for the determination of the amount of health improvement created by a health care program. In these methods, the combined use of mortality and survey data in order for the health status of a population to be estimated was very common.

Today, one of the most important recent contributions to the problem of calculating the health status of a population is the one developed by the World Health Organization (WHO), which is based on the aforementioned Sullivan's [20] approach. In this method population data on health and disability are

17th *ASMDA Conference Proceedings, 6 - 9 June 2017, London, UK*

combined in a life table (WHO, [25]). For that the Global Burden of Disease Survey (GBD; [2] [6] [7]) is conducted aiming to quantify health loss from a high number of diseases, injuries and risk factors. However, as WHO notes, several limitations exist in this method, because of the lack of reliable data on mortality and morbidity and of the comparability of self-reported data from health interviews and the measurement of health-state preferences for such self-reporting.

In another, however very efficient, approach the stochastic theory is applied. Such a process is always described by a parent stochastic process and a boundary or barrier indicating a stopping condition for the process under consideration (see Lee and Whitmore [5]). In this case, human health is the stochastic and thus totally unpredictable process but a person dies when their health falls below a barrier. The problem then is how to model this process in order for the health status of a population to be calculated. Skiadas and Skiadas [13] [14] [15] [16] and Skiadas [11] have developed the relevant theory based only on life table data. In a series of publications Skiadas [11], Skiadas and Zafeiris [17] and Zafeiris and Skiadas [26] [27] have tested this theory and showed its validity in calculating the health status of a population or in providing accurate measurements for inter-population comparisons.

Recently, another method was developed and is based on the force of mortality μ_x (see Skiadas and Zafeiris [18] Zafeiris and Skiadas [28] .

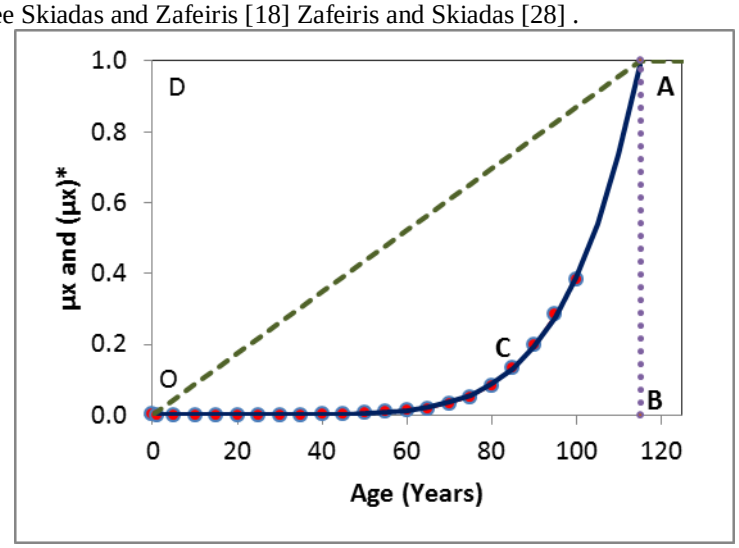

Fig. 1. The mortality diagram

This approach is based on a two parameters Gompertz-like model:

$$\mu_x = \left(\frac{x}{T}\right)^b$$

where (x) is the age and μ(x) the relevant mortality rate. T represents the age at which μ(x)=1 and b is a parameter expressing the curvature of μ(x). Then, the main idea is to divide the areas in the parallelogram OBAD, into two segments - one being the mortality effect and the other the healthy part of the population, an idea which has emerged from the First Exit Time Theory approach that was described above. Thus, the area Ex under the curve OCABO in the mortality diagram of Figure 1 is a measure of the mortality effect and can be estimated as follows:

$$E_x = \int_0^T \left(\frac{x}{T}\right)^b dx = \frac{T}{(b+1)}\left(\frac{x}{T}\right)^b$$

Based on the equation above, it is proven that the loss of healthy life years LHLY can be estimated as LHLY=λ(b+1), where λ is a correction multiplier which can be set to 1 in order for different countries to be compared. Accordingly, healthy life expectancy (HLE) is LEB-LHLY, where LEB is life expectancy at birth.

Then the problem of calculating healthy life expectancy with this method deals with the accuracy and precision of life table data. However, until now all the analyses done for such estimations are based on full life table data and in that way in cases in which such data are either problematic or absent, a usual phenomenon for many countries, this is not possible. The aim of this paper is to provide a method for estimating healthy life expectancy for such countries based on abridged life table data.

2 Methods and Data

Data come from the World's Health Organization database (WHO, http://apps.who.int/gho/data) in the form of abridged life tables. These tables contain information for the age groups <1, 1-4 and for 5-years age intervals up to the age 100 which corresponds to the open-ended one. The analysis was done for the so-called BRIICS countries: Brazil, Russia, India, Indonesia, China and South Africa. They are rapid growth economies and their population represent almost 3 billion people, nearly half the world's population (see http://www.oecd.org/tad/tradedev/globalisationandemergingeconomies.htm)/

In the analyses carried out in this paper two aspects need to be clarified further. First the method used for the estimation of healthy life expectancy and second how to expand the abridged life table into a full one.

The first aspect was confronted with the μx based method which was described in the introductory section of this paper. Thus, the parameter b must be

estimated. It was found that an excellent estimation was made according to the following estimation:

$$b=xm_x/\Sigma xm_x$$

where x is the age.

The second aspect was confronted with the aid of the UNABR application of the MORTPAK (vers. 4.3) application for Windows, of the software created by the United Nations (UN Population division) for the needs of mortality analysis. This application is based on the Heligman-Pollard [3] formula as follows:

$$1q_x = A^{(x+B)^C} + De^{-E(lnx-lnF)^2} + \frac{GH^x}{1+GH^x}$$

where x is the age and B, C, D, E, F, G and H parameters that should be estimated. However, it must be noted that the Heligman-Pollard model has proven to be quite problematic in the fitting process of mortality data (see Kostaki [4] and Zafeiris and Kostaki [29]), however it was used here as it is a widely accepted software.

3 Results

The results of the analysis are seen in the diagrams 2-7. These results are also compared with several publications from the World Health Organization's point of view, namely the World's Health reports of 2000, 2001, 2002 and 2004 [22] [23] [24] and Salomon et al.[9] and Murray et al. [8] publications. The acronym used in that case is HALE, which also corresponds to healthy life expectancy as estimated by the method applied in the time of these publications.

Such effort bears many complications. One springs from the fact that data used in this analysis are in their current and most revised form in comparison with data used for the previous publications. Thus, deviations are expected to be found because of that and also because of the differences in the methodologies used and have been revised several times in the past. Thus, the results of the analysis should be interpreted thoroughly. Also, the use of MORTPAK was quite problematic in many cases. For example, for the year 2005 in Russian males the expansion procedure of the abridged life table gave a life expectancy at birth of 81.68 years compared with 58.6 according to the estimations of the World Health Organization. But it is worth noting that the life expectancy at birth published by WHO never coincided with the estimations of MORTPAK software.

A glimpse of such problems is given by the examination of data from Brazil, where significant deviances are found in the data used by WHO in the original publications of 2000 and 2004 and the data published currently in the web page of the organization. A general trend that describes these differences, as can be

judged by life expectancy at birth, is that they become larger for the first years of the study in both genders. Thus, the estimations of WHO and related scientists are based on old data. Instead in this paper, because we have used the most recent data for the calculations, healthy life expectancy is very close to the upper confidence interval of the published estimations (Figure 2).

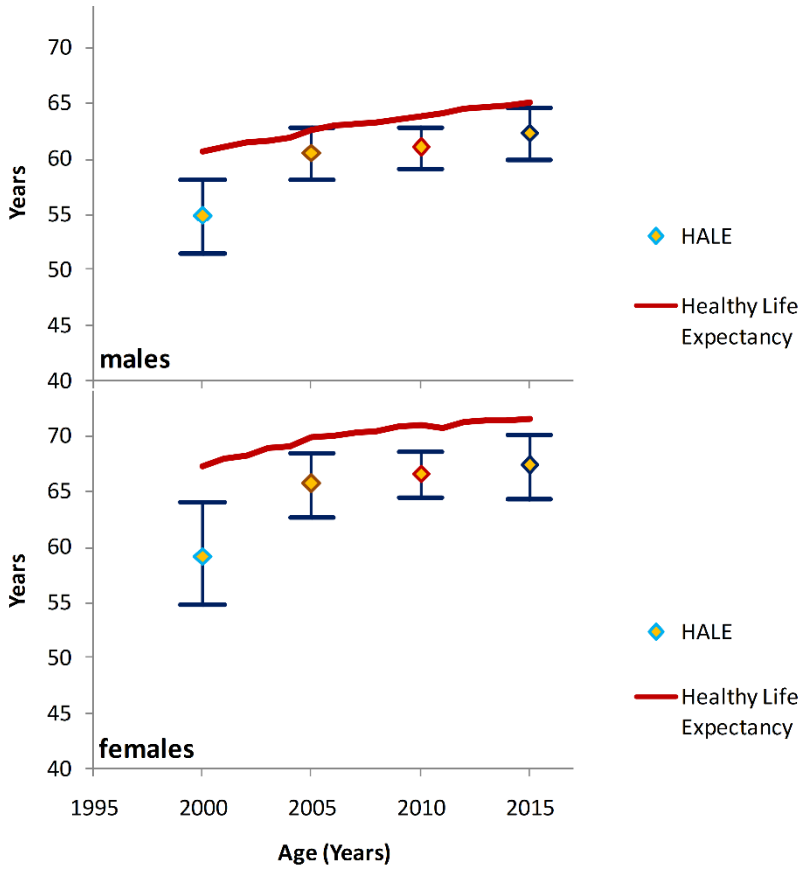

Fig. 2. HLE and HALE estimations, Brazil

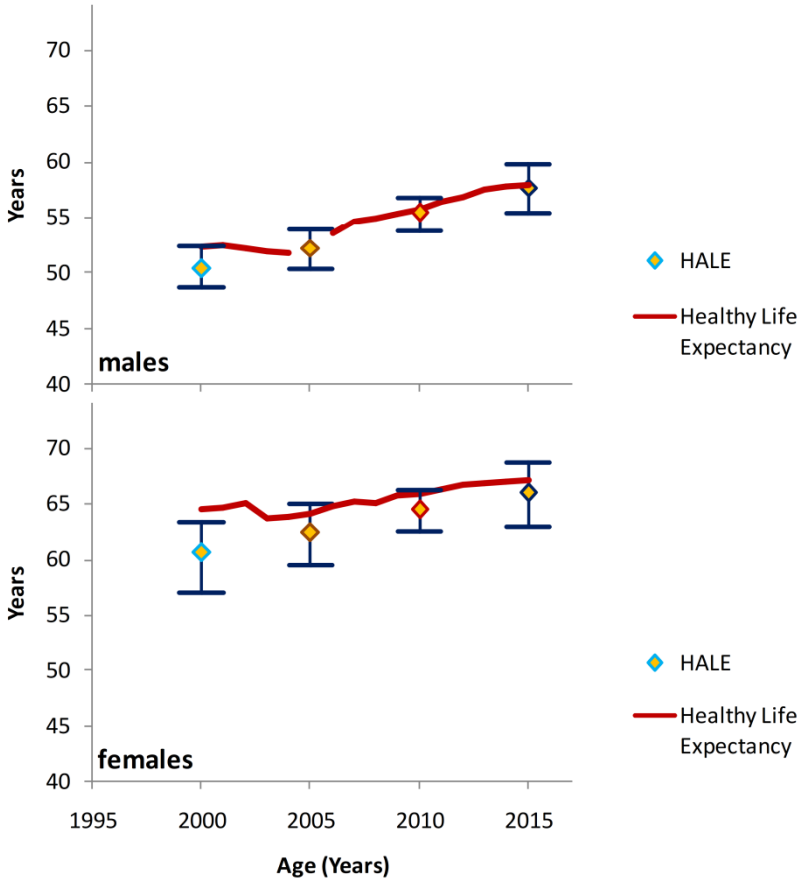

Fig. 3. HLE and HALE estimations, Russia

Population health seems to have increased almost linearly in Russia (Figure 3) in both genders and the methods compared seem to be in accordance, especially in males. It must also be noted that in Russia data revision is literally absent and the expansion software worked pretty well.

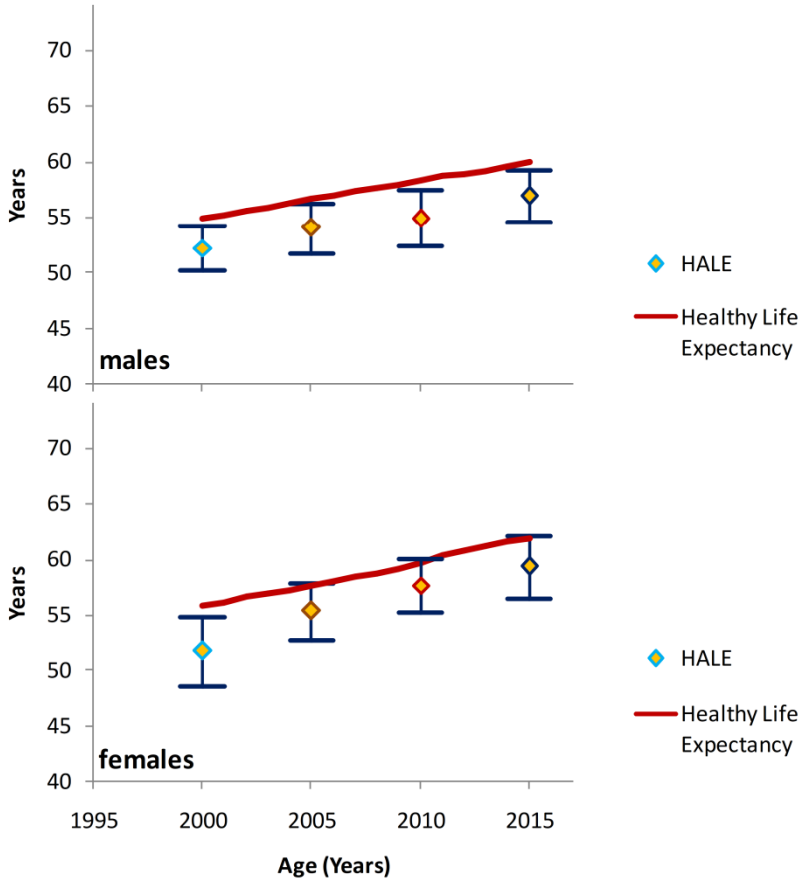

Fig. 4. HLE and HALE estimations, India

In India (Figure 4), the revision of data led to about +2 years increase in life expectancy for the majority of the calendar years studied, while in females it was almost +2 years for the older calendar years and less than 0.6 for the rest. The expanding procedure, concerning life expectancy at birth worked excellently, as the differences between the published by WHO results and those calculated by MORTPAK were less than 0.1 years for the majority of the calendar years studied. Healthy life expectancy, as calculated in this paper, were very close to the upper limit of the estimations of the World Health Organization, fact that can be attributed to the revised data used in this paper.

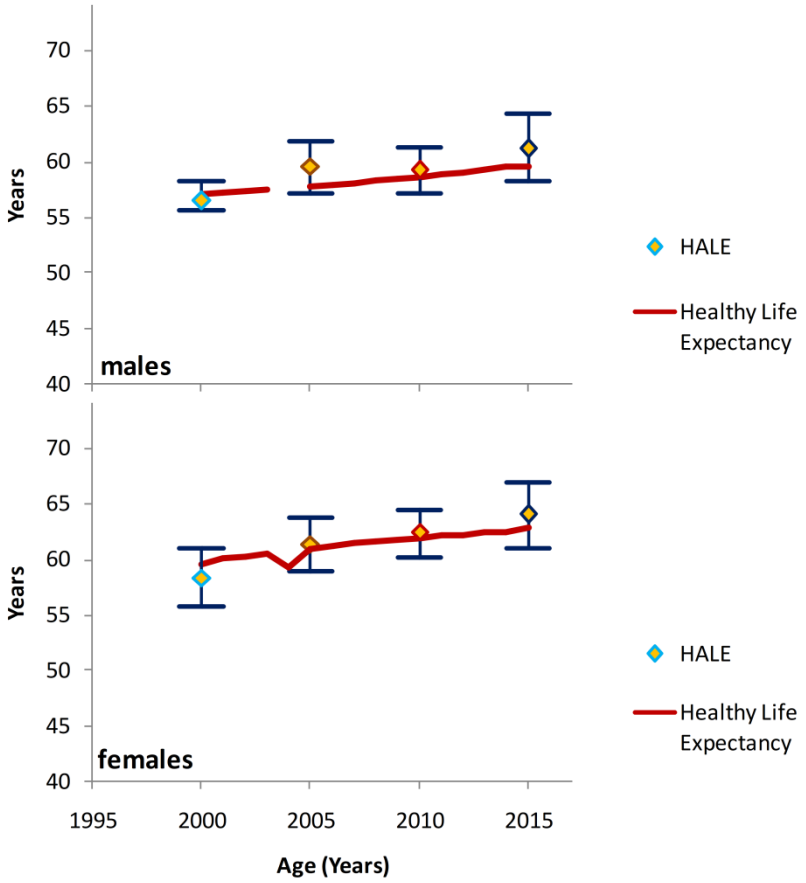

Fig. 5. HLE and HALE estimations, Indonesia

For Indonesia (Figure 5), data were revised mostly for the most recent years (almost -2 years in life expectancy). However, the expanding process led to an underestimation of life expectancy at birth from 0.4 to 2.1 years. In that scheme, the estimation of healthy life expectancy does not differ much among the methods.

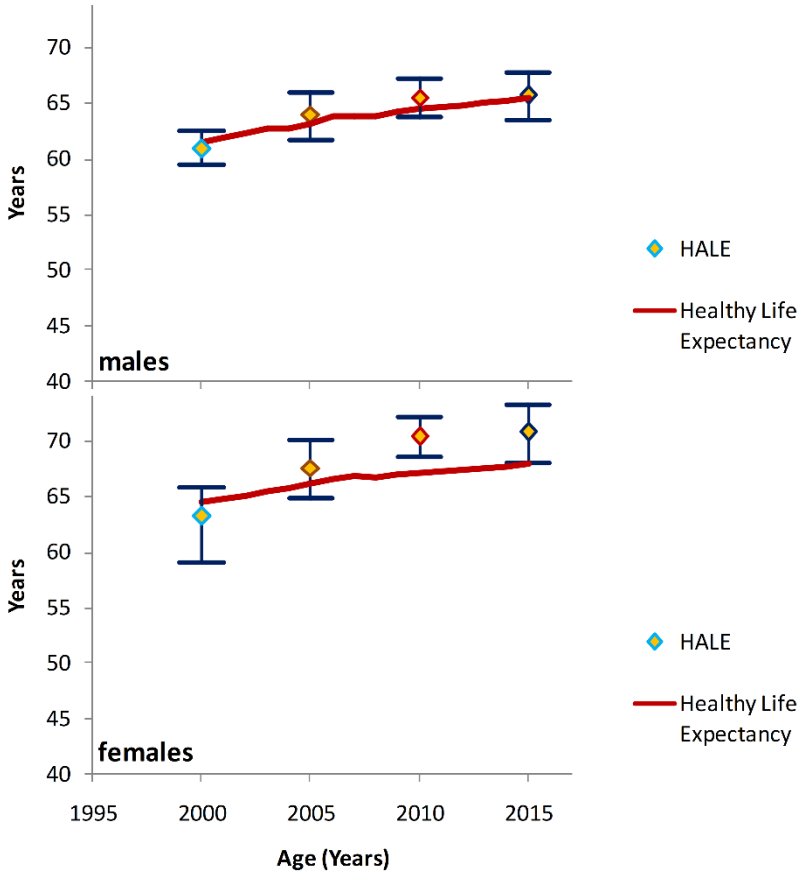

Fig. 6. HLE and HALE estimations, China

For the males from China (Figure 6) the revised life table data gave a life expectancy at birth which was 0.6-1.7 years lower than that calculated from the original data. On the contrary, life expectancy at birth from the expanding process was exactly the opposite. As a result, the healthy life expectancy calculated in this paper is almost the same estimated with the other methods. The same happened with females, though, healthy life expectancy in them is somewhat lower in the most recent years studied.

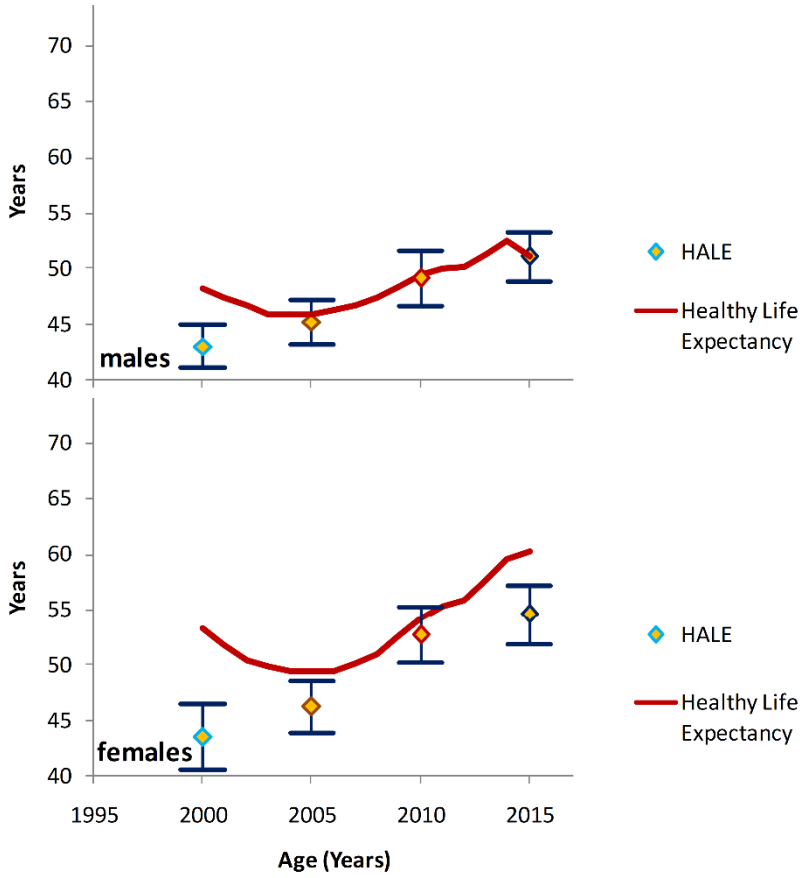

Finally, for South Africa (Figure 7) the published results by WHO and the other connected scientists have the peculiarity that HALE is increasing constantly during the 21st century even though life expectancy at birth is low and remains almost unchanged in females and decreasing in males until 2005. Instead according to the methodology used in this paper, healthy life expectancy decreases up to 2005 and increases later following the temporal trends of life expectancy at birth.

Conclusions

A method of calculating healthy life expectancy was applied in the BRIICS countries, based on abridged life table data from the World Health Organization. However, because the μx based approach described in this paper can be applied only to full life table data, the original tables were expanded to full ones with

the aid of the UNABR application of the MORTPAK software, created by the Population Division of the United Nations.

The analysis revealed that the software mentioned above is not very suitable for this purpose, as significant deviations were observed in life expectancy at birth as it was calculated by it in comparison with the published results of the World Health Organization. A further shortcoming was that the already published estimations of the World Health Organization and related agencies were made in old data, thus the ability of comparing the results of this analysis with the previous ones was problematic,

It is seen then that the μx based approach is quite efficient in estimating the healthy life expectancy and its temporal trends, as it is based solely on life table data. In that way, it is totally costless and its only limitation springs from the quality of data. In any case, it seems that a more sensitive application is needed in order for abridged life table data to be expanded and used by this method.

References

1. C. L Chiang. An Index of Health: Mathematical Models, U.S. Department of HEW, Public Health Service, Publication No. lCXK). Series 2, No. 5, 1965.
2. Global Burden of Disease Study 2010. Global Burden of Disease Study 2010 (GBD 2010) Disability Weights. Seattle, United States: Institute for Health Metrics and Evaluation (IHME), 2012.
3. L. Heligman and J.H. Pollard. The age pattern of mortality. *Journal of the Institute of Actuaries*, 107:47-80, 1980.
4. A. Kostaki. A nine parameter version of the Heligman-Pollard formula. *Mathematical Population Studies*, 3(4): 277-288, 1992.
5. M.-L T. Lee and G. A. Whitmore. Threshold regression for survival analysis: modeling event times by a stochastic process reaching a boundary. Statistical Science, 21(4), 501-513, 2006.
6. C. J. L. Murray, M. Ezzati et al. GBD 2010: a multi-investigator collaboration for global comparative descriptive epidemiology. Lancet, 380, 2055-2058, 2012.
7. C. J. L. Murray, M. Ezzati et al. GBD 2010: design, definitions, and metrics. Lancet; 380, 2063–2066, 2012b.
8. C. I. Murray et al. Global, regional, and national disability-adjusted life years (DALYs) for 306 diseases and injuries and healthy life expectancy (HALE) for 188 countries, 1990-2013 : quantifying the epidemiological transition. Lancet, 2015, available at : http://dx.doi.org/10.1016/S0140-6736(15)61340-X
9. Salomon et al. Healthy life expectancy for 187 countries, 1990-2010 : a systematic analysis for the Global Burden of Disease study. Lancet, 380,

2012.

10. B. S. Sanders. Measuring Community Health Levels. American Journal of Public Health, 54, 1063-1070, 1964.
11. C. H. Skiadas. Life expectancy at birth and forecasts in the Netherlands (females). In *The Health State function of a population.* (Skiadas, C. H. and Skiadas, C., eds). 1st ed. Athens, 47-67, 2012a.
12. C. H. Skiadas. The Health State Function, the Force of Mortality and other characteristics resulting from the First Exit Time Theory applied to Life Table Data. In *The Health State function of a population.* (Skiadas, C. H. and Skiadas, C., eds). 1st ed. Athens, 69-92, 2012b.
13. C. H. Skiadas and C. Skiadas. Estimating the Healthy Life Expectancy from the Health State Function of a Population in Connection to the Life Expectancy at Birth. In *The Health State function of a population.* (Skiadas, C. H. and Skiadas, C., eds). 1st ed. Athens, 97-109, 2012.
14. C. H. Skiadas and C. Skiadas. *Demographic and Health indicators for 193 countries of the World Health Organization and the United Nations. Second supplement of the book The Health State Function of a Population.* Athens, 2014a.
15. C. H. Skiadas and C. Skiadas. First time exit problem. In *International Encyclopedia of Statistical Science* (Miodrag, L. ed). Springer Verlag, Berlin Heilderberg, 521-523. 2014b.
16. C. H. Skiadas and C. Skiadas. The First Exit Time Theory applied to Life Table Data: the Health State Function of a Population and other Characteristics, *Communications in Statistics-Theory and Methods*, 34, 1585-1600, 2014c.
17. C. H. Skiadas and K. N. Zafeiris. Comparing WHO and First Exit Time Theory estimations of healthy life expectancy in Europe. In *Statistical, Stochastic and Data Analysis Methods and Applications* (A. Karagrigoriou, T. Oliveira and C. H. Skiadas, eds), ISAST, 261 – 266, 2015.
18. C. H. Skiadas and K. N. Zafeiris. Population aging and healthy life lessons. RELIK 2015 Conference proceedings. Reproduction and human capital. Available at: http://kdem.vse.cz/resources/relik15/download/pdf/45-SKIADAS-CHRISTOS-paper.pdf
19. D. F. Sullivan. Conceptual Problems in Developing an Index of Health, U.S. Department of HEW, Public Health Service Publication No. 1000, Series 2, No. 17, 1966
20. D. F. Sullivan. A single index of mortality and morbidity. HSMHA Health Reports, 86, 347-354, 1971
21. G. W. Torrance Health Status Index Models: A Unified Mathematical View. Management Science, 22, 9, 990-1001, 1976.
22. World Health Organization The world health report 2000 - Health systems: improving performance. Available at http://www.who.int/whr/2000/en/, France, 2000.
23. World Health Organization The world health report 2000 – Mental Health: new understanding Available at

http://www.who.int/whr/2001/en/, France, 2001.

24. World Health Organization The world health report 2004 – Changing history. Available at http://www.who.int/whr/2004/en/, France, 2004.

25. WHO. WHO methods for life expectancy and healthy life expectancy. Global Health Estimates Technical Paper WHO/HIS/HSI/GHE/2014.5. March, 2014

26. K. N. Zafeiris and C. H. Skiadas. Demographic and heath indicators in the Pomaks of Rhodopi. In *New trends in stochastic modelling and data analysis (*R. Manca, S. McClean and C. H. Skiadas, eds), ISAST, 311-324, 2015.

27. K. N. Zafeiris and C. H. Skiadas. An application of the first exit time theory in some European populations. In *Statistical, Stochastic and Data Analysis Methods and Applications* (A. Karagrigoriou, T. Oliveira and C. H. Skiadas, eds), ISAST, 229 – 249, 215.

28. K. N. Zafeiris and C. H. Skiadas. Some methods for the estimations of healthy life expectancy. RELIK 2015 Conference proceedings. Reproduction and human capital. Available at: http://kdem.vse.cz/resources/relik15/download/pdf/34-Zafeiris-Konstantinos-paper.pdf

29. K. N. Zafeiris and A. Kostaki. Recent mortality trends in Greece. Communications in Statistics-Theory and Methods, DOI 10.1080/03610926.2017.1353625

Limit Theorems for Compound Renewal Processes: Theory and Application

Nadiia Zinchenko

Department of Informatics and Applied Mathematics, Nizhyn State Mukola Gogol University, Kropyv'yanskogo 2, 16600, Nizhyn, Ukraine
(E-mail: znm@univ.kiev.ua)

Abstract. We consider a few classes of strong limit theorems for compound renewal processes (random sums, randomly stopped sums) $D(t) = \sum_{i=1}^{N(t)} X_i$ under various assumptions on the renewal counting process N(t) and random variables $\{X_i, i \geq 1\}$. First of all we present sufficient conditions for strong (a.s.) approximation of $D(t)$ by a Wiener or α-stable Lévy process under various dependent and moment conditions on summands, mainly focused on the cases of independent, φ-mixing and associated r.v. On the next step the investigation of the rate of growth of the process $D(t)$ and it's increments $D(t+a(t)) - D(t)$, when a(t) grows, is carried out. Useful applications in risk theory are investigated; particularly, non-random bounds for the rate of growth and fluctuations of the risk processes in classical Cramer-Lundberg and renewal Sparre Andersen risk models are discussed as well as the case of risk models with stochastic premiums.

Keywords: Compound Renewal Process, Random Sum, Limit Theorem, Strong Approximation, Integral Tests, Queuing Theory, Risk Process.

1 Introduction

Let $\{X_i, i \geq 1\}$ be random variables (r.v.), $S(t) = \sum_{i=1}^{[t]} X_i$, $t > 0$, $S(0) = 0$. Also suppose that $\{Z_i, i \geq 1\}$ is a sequence of non-negative i.i.d.r.v., independent of $\{X_i\}$, with common distribution function (d.f.) $F_1(x)$, characteristic function (ch.f.) $f_1(u)$ and $EZ_1 = 1/\lambda > 0$,

$$Z(x) = \sum_{i=1}^{[x]} Z_i, \quad x > 0, \quad Z(0) = 0$$

and define the *renewal (counting) process*

$$N(t) = \inf\{x \geq 0 : Z(x) > t\}.$$

Compound renewal processes (random sums, randomly stopped sums, compound sums) are defined as

$$D(t) = S(N(t)) = \sum_{i=1}^{N(t)} X_i,$$

where r.v. $\{X_i, i \geq 1\}$ and renewal process $N(t)$ are given above.

Limit theorems for $D(t) = \sum_{i=1}^{N(t)} X_i$ became rather popular during last 20 years or so (mainly they deal with weak convergence). This topic is interesting not only from theoretical point of view, but also due to numerous practical applications, since mentioned processes often appear in useful applications in queuing theory (accumulated workload input into queuing system in time interval (0,t)), in risk theory (total

claim amount to insurance company up to time t), in financial mathematics (total market price change up to time t) and in certain statistical procedures. The most popular example is compound Poisson process, when $N(t)$ is a a homogeneous Poisson process.

This paper presents a few classes of **strong** limit theorems for compound renewal processes (random sums) which summarize authors previous results obtained during last five years. The *first* class is *a strong invariance principle* (**SIP**), other terms are *strong approximation* or *almost sure approximation*.

Definition. We say that a random process $\{D(t), t \geq 0\}$ admits strong approximation by the random process $\{\eta(t), t \geq 0\}$ if $D(t)$ (or stochastically equivalent $D^*(t)$) can be constructed on the rich enough probability space together with $\eta(t)$ in such a way that a.s.

$$|D(t) - \eta(t)| = o(r(t)) \text{ or } O(r(t)) \text{ as } t \to \infty, \tag{1}$$

where approximating error (error term) $r(.)$ is a non-random function.

While week invariance principle provides the convergence of distributions, the strong invariance principle describes how "small" can be the difference between trajectories of $D(t)$ and approximating process $\eta(t)$.

Concrete assumptions on $\{X_i, i \geq 1\}$ and $\{Z_i, i \geq 1\}$ clear up the type of approximating process and the form of error term. Below we mainly focused on the case of i.i.d.r.v. $\{X_i\}$, as well as on φ-mixing and associated summands and present some general results concerning sufficient conditions for strong approximation of $D(t)$ by a Wiener or α-stable Lévy process. Corresponding proofs are based on the rather general theorems about the strong approximation of superposition of càd-làg processes, not obligatory connected with partial sums, Zinchenko ([13], [14]).

SIP-type theorems themselves can serve as a source of a number of interesting strong limit results for compound renewal processes: really, using (1) with appropriate error term one can easily transfer the results about the asymptotic behavior of the Wiener or α-stable Lévy process on the asymptotic behavior of random sums. Thus, the *second class* of limit theorems deal with the rate of growth of $D(T)$ and it's increments. For instance, a number of integral tests for investigation the rate of growth of the process $D(t)$ and it's increments $D(t + a(t)) - D(t)$, when a(t) grows, are proposed. As a consequence various modifications of the LIL and Erdös-Rényi-Csörgő-Révész -type strong law of large numbers (SLLN) are obtained.

2 SIP for compound renewal processes (random sums)

1. Independent summands. Next three theorems (Zinchenko[13], [14]) present sufficient conditions on independent summands $\{X_i\}$ and inter-occurrence intervals $\{Z_i\}$, which provide a.s. approximation of the random sums of i.i.d.r.v. with finite or infinite variance and clear up the type of approximating process and the form of error term in this case.

More precise, suppose that $\{X_i, i \geq 1\}$ are i.i.d.r.v., with common distribution function (d.f.) $F(x)$, characteristic function (ch.f.) $f(u)$, $EX_1 = m$, $VarX_1 = \sigma^2$ if $E|X_1|^2 < \infty$.

Theorem 1. *(i) Let $E|X_1|^{p_1} < \infty$, $E|Z_1|^{p_2} < \infty$, $p = \min\{p_1, p_2\} > 2$, then $\{X_i\}$ and $N(t)$ can be constructed on the same probability space together with a standard Wiener process $\{W(t), t \geq 0\}$ in such a way that a.s.*

$$\sup_{0 \leq t \leq T} |S(N(t)) - \lambda m t - \nu W(t)| = o(T^{1/p}), \quad \nu^2 = \sigma^2 \lambda + m^2 \tau^2 \lambda^3; \tag{2}$$

(ii) if $p = 2$ then right side of (12) is $o(T \ln \ln T)^{1/2}$;
(iii) if $E \exp(uX_1) < \infty$, $E \exp(uZ_1) < \infty$ for all $u \in (0, u_o)$, then right-hand side of (2) is $O(\ln T)$.

Next suppose that $\{X_i\}$ are attracted to α-stable law with $1 < \alpha < 2$, $|\beta| \le 1$, then approximating process for $S(t)$ is a stable process $Y_\alpha(t)$ (condition $\alpha > 1$ is needed to have a finite mean). Below we use following

Assumption (C) : *there are $a_1 > 0, a_2 > 0$ and $l > \alpha$ such that for $|u| < a_1$*

$$|f(u) - g_{\alpha,\beta}(u)| < a_2 |u|^l, \tag{3}$$

where $f(u)$ is a ch.f. of $(X_1 - EX_1)$ if $1 < \alpha < 2$ and ch.f. of X_1 if $0 < \alpha \le 1$, $g_{\alpha,\beta}(u)$ is a ch.f. of the stable law.

Assumption (C) not only provides normal attraction of $\{X_i, i \ge 1\}$ to the stable law $G_{\alpha,\beta}(x)$, but also leads to the rather "good" error term $q(t) = t^{1/\alpha - \varrho}, \varrho > 0$, in SIP for usual partial sums $S(t)$.

Theorem 2. *Let $\{X_i\}$ satisfy **(C)** with $1 < \alpha < 2$, $|\beta| \le 1$, $EZ_1^2 < \infty$. Then $\{X_i\}$, $\{Z_i\}$, $N(t)$ can be defined together with α-stable process $Y_\alpha(t) = Y_{\alpha,\beta}(t)$, $t \ge 0$, so that a.s.*

$$\sup_{0 \le t \le T} \left| S(N(t)) - m\lambda t - Y_{\alpha,\beta}(\lambda t) \right| = o(T^{1/\alpha - \varrho_1}), \quad \varrho_1 \in (0, \rho_0), \tag{4}$$

for some $\varrho_0 = \varrho_0(\alpha, l) > 0$.

Corollary 1 (SIP for compound Poisson process). *Theorems 1, 2 hold if $N(t)$ is a homogeneous Poisson process with intensity $\lambda > 0$, in this case $\nu^2 = \lambda E X_1^2$.*

Theorem 3. *Let $\{X_i\}$ satisfy (C) with $1 < \alpha_1 < 2$ and $\{Z_i\}$ satisfy (C) with $1 < \alpha_2 < 2$, $\alpha_1 < \alpha_2$, then*

$$\sup_{0 \le t \le T} \left| S(N(t)) - m\lambda t - Y_{\alpha_1,\beta_1}(\lambda t) \right| = o(T^{1/\alpha_1 - \varrho_2}) \ \text{a.s.} \tag{5}$$

for some $\varrho_2 = \varrho_2(\alpha_1, l) > 0$.

2. SIP for random sums of dependent r.v. Further development is connected with dependent summands: martingales, weakly dependent r.v., mixing and associated sequences. Below we present only few result in this area, connected with φ-mixing and associated summands; more results on this topic as well as detail rigorous proofs and wide bibliography can be find in the author's previous work [15].

Throughout this Section, unless otherwise stated, we suppose that inter-occurrence time intervals $\{Z_i\}$ for renewal process $N(t)$ have finite moments $E|Z_1|^p < \infty$ of order $p > 2$.

2.1. **φ-mixing sequences**. Given r.v. $\{X_i, i \ge 1\}$, let F_a^b denote the σ-field generated by $X_a, X_{a+1}, \ldots, X_b$, $a < b < \infty$, and F_b^∞ – the σ-field generated by $X_b, X_{b+1}, \ldots$.

Definition. Sequence $\{X_i, i \ge 1\}$ is said to be φ-mixing if there exist a sequence $\{\varphi(n)\}$ of real numbers, $\varphi(n) \downarrow 0$ as $n \to \infty$, such that for each $t \ge 1$, $n > 0$, $A \in F_1^t$, $B \in F_{t+n}^\infty$

$$|P(AB) - P(A)P(B)| \le \varphi(n) P(A) \tag{6}$$

Theorem 4. *Let $\{X_i, i \geq 1\}$ be strictly stationary φ-mixing sequence with $EX_1 = m$, $E|X_1|^{2+\delta} < \infty$. Suppose*

$$\sum_{n=1}^{\infty} \phi^{1/2}(n) < \infty \tag{7}$$

and

$$0 < \lim_{n\to\infty} n^{-1} E\left(\sum_{i=1}^{n}(X_i - m)\right)^2 = \sigma_1^2 < \infty. \tag{8}$$

Then $\{X_i\}$ and $N(t)$ can be constructed on the same probability space together with a Wiener process $\{W(t), t \geq 0\}$ in such a way that a.s.

$$\sup_{0\leq t\leq T} |S(N(t)) - mt\lambda - \nu W(t)| = O(T^{1/2-\vartheta_1}), \quad \nu^2 = \sigma_1^2\lambda + m^2\tau^2\lambda^3 \tag{9}$$

for some $\vartheta_1 = \vartheta_1(\delta, p)$

2.2. **Associated summands**.

Definition. R.v. $X_1, \ldots, X_n$ are **associated**, if for any two coordinate-wise nondecreasing functions $f, g : R^n \to R^1$,

$$Cov\big(f(X_1, \ldots, X_n), g(X_1, \ldots, X_n)\big) \geq 0$$

whenever the covariance is defined. A sequence $\{X_i, i \geq 1\}$ is associated, if every finite sub-collection is associated.

A lot of interesting limit theorems for partial sums of associated summands are presented by Bulinski and Shashkin [1], Yu [17]

Theorem 5. *Let $\{X_i, i \geq 1\}$ be a strictly stationary associated sequence, $EX_1 = m$. Suppose that $E|X_1|^{2+\delta} < \infty$ for some $\delta > 0$ and Cox-Grimmett coefficient*

$$u(n) = \sup_{k\geq 1} \sum_{j:|j-k|\geq n} Cov(X_j X_k) = O(e^{-\theta n}) \tag{10}$$

for some $\theta > 0$, inter-occurrence intervals $\{Z_i, i \geq 1\}$ are i.i.d.r.v. with $0 < EZ_1 = 1/\lambda < \infty$, $\tau^2 = VarZ_1 < \infty$. Denote

$$E(X_1 - m)^2 + 2\sum_{i\geq 1} E(X_1 - m)(X_i - m) = \sigma_2^2 > 0. \tag{11}$$

Then $\{X_i\}$ and $N(t)$ can be constructed on the same probability space together with a Wiener process $\{W(t), t \geq 0\}$ in such a way that a.s.

$$\sup_{0\leq t\leq T} |S(N(t)) - mt\lambda - \nu W(t)| = O(\varrho(T)), \quad \nu^2 = \sigma_2^2\lambda + m^2\tau^2\lambda^3 \tag{12}$$

where error term is $O(\varrho(T)) = O(T^{1/2-\vartheta_2})$ for some $\vartheta_2 = \vartheta_2(\delta, p)$, when $E|Z_1|^p < \infty$ for $p > 2$, and error term is $o((T \ln\ln T)^{1/2})$, if Z_1 has only second moment.

Corollary 2 (SIP for Poisson random sums). *Theorems 4, 5 hold if $N(t)$ is a homogeneous Poisson process with intensity $\lambda > 0$.*

3 SIP and rate of growth of compound renewal processes (random sums)

As it was already mentioned, SIP is a nice background for further investigation of the asymptotic behavior of compound renewal processes. Using SIP with appropriate error term one can easily extend the results about the asymptotic behavior of approximating Wiener or stable Levy process on the rate of growth of $D(t)$, when $D(t)$ admits a.s. approximation by one of the mentioned above processes. Formalizing this idea and extending the approach due to Philipp and Stout[9], we formulate rather general theorems (not obligatory connected with random sums). We start with the case, when $D(t)$ admits a.s. approximation by a standard Wiener process.

Definition. Function $f(t)$ is an *upper* function for the process $X(t)$, $t \to \infty$, if $P\{\limsup_{t\to\infty} X(t)/f(t) \le 1\} = 1$ and $f(t)$ is a *lower* function for $X(t)$, if $P\{\limsup_{t\to\infty} X(t)/f(t) \ge 1\} = 1$.

Theorem 6. *Suppose that random process $D(t)$ admits a.s. approximation by a standard Wiener process $W(t)$ with an error term $O(t^{1/p}), p > 2$, i.e.*

$$\sup_{0\le t\le T} |D(t) - Mt - \nu W(t)| = O(T^{1/p}) \text{ a.s. }, \quad M \in R^1, \nu > 0, \tag{13}$$

then function $f(t) = \nu t^{1/2} h(t)$, $h(t) \uparrow \infty$, $\nu > 0$, will be an upper function for centered process $(D(t) - Mt)$, if

$$I_1(h) = \int_1^\infty t^{-1} h(t) \exp\{-h^2(t)/2t\} dt < \infty,$$

and it will be a lower one, if $I_1(h) = \infty$.

Theorem 7. *If random process $D(t)$ admits a.s. approximation by a standard Wiener process $W(t)$ with an error term $O(t^{1/p}), p > 2$, then a.s.*

$$\limsup_{t\to\infty} \frac{|D(t) - Mt|}{\sqrt{2t \ln\ln t}} = \nu. \tag{14}$$

The proofs of these theorems easily follows from the famous Kolmogorov-Petrovski test and classical LIL for a Wiener process and form of error term in (13). For details see Zinchenko ([13] - [16]). Similarly, Chung's LIL for Wiener process obviously provides

Theorem 8. *Let $D(t)$ be as in previous Theorem, then a.s.*

$$\liminf_{T\to\infty} \left(\frac{8 \ln\ln T}{\pi^2 T}\right)^{1/2} \sup_{0\le t\le T} |D(t) - MT| = \nu. \tag{15}$$

Now consider the case of ***i.i.d.*** summands. Obviously Theorems 6 – 8 immediately yield following statements:

Corollary 3. *Let $E|X_1|^{p_1} < \infty$, $E|Z_1|^{p_2} < \infty$ for some $p_1 > 2$, $p_2 > 2$, then $f(t) = \nu t^{1/2} h(t)$, $h(t) \uparrow \infty$ will be an upper function for $D(t)$, if*

$$I_2(h) = \int_1^\infty t^{-1} h(t) \exp\{-h^2(t)/2\} dt < \infty$$

and lower function. if $I_2(h) = \infty$.

Corollary 4. ***(Classical LIL for random sums of i.i.d.r.v.)***. *Let* $\{X_i, i \geq 1\}$ *and* $\{Z_i, i \geq 1\}$ *be independent sequences of i.i.d.r.v.,* $EX_1 = m$, $0 < EZ_1 = 1/\lambda < \infty$, $\sigma^2 = VarX_1 < \infty$, $\tau^2 = VarZ_1 < \infty$. *Then a.s.*

$$\limsup_{t\to\infty} \frac{|S(N(t)) - m\lambda t|}{\sqrt{2t \ln \ln t}} = \nu, \quad \nu^2 = \lambda\sigma^2 + \lambda^3 m^2 \tau^2. \tag{16}$$

Corollary 5. ***(Chung's LIL for random sums)***. *Let* $\{X_i\}$ *and* $\{Z_i\}$ *be as in Corollary 4, then a.s.*

$$\liminf_{t\to\infty} \left(\frac{8 \ln \ln T}{\pi^2 T}\right)^{1/2} \sup_{0\leq t\leq T} |S(N(t)) - m\lambda t| = \nu, \quad \nu^2 = \lambda\sigma^2 + \lambda^3 m^2 \tau^2. \tag{17}$$

Since random sums $S(N(t))$ of ***dependent r.v.***, introduced in sub-sections 2.1 and 2.2 also satisfy (13) with $M = \lambda m$, $\nu^2 = \sigma_i^2 \lambda + m^2 \tau^2 \lambda^3$, $i = 1, 2$, $1/p = (1/2) - \vartheta$ for some $\vartheta > 0$, Theorems 6– 8 yield following Corollaries:

Corollary 6 (Classical LIL for random sums, associated summands). *Let* $\{Z_i\}$ *be i.i.d.r.v. with* $0 < EZ_1 = 1/\lambda < \infty$, $\tau^2 = VarZ_1 < \infty$, $\{X_i\}$ *constitute the strictly stationary associated sequence with mean* $EX_1 = m$ *and covariance, satisfying sufficient conditions for SIP (Theorem 5), then a.s.*

$$\limsup_{t\to\infty} \frac{|S(N(t)) - m\lambda t|}{\sqrt{2t \ln \ln t}} = \nu, \quad \nu^2 = \lambda\sigma_2^2 + \lambda^3 m^2 \tau^2. \tag{18}$$

Corollary 7 (Classical LIL for random sums, ϕ-mixing summands). *Statement analogous to (18) holds with corresponding* σ *and* ν *for strictly stationary* ϕ*-mixing summands satisfying all conditions of Theorem 4.*

On the other hand, when ***independent*** summands are attracted to the stable distribution $G_{\alpha,\beta}$, which is not concentrated on the half of the axe, from Theorem 2 and results for a stable processes (due to Donsker and Varadhan) follows

Corollary 8. *Let* $\{X_i, i \geq 1\}$ *satisfy* ***(C)*** *with* $1 < \alpha < 2$ *and* $\{Z_i, i \geq 1\}$ *be as in Corollary 4, then a.s.*

$$\liminf_{T\to\infty} \left(\frac{\ln \ln T}{T}\right)^{1/\alpha} \sup_{0\leq t\leq T} |D(t) - m\lambda t| = C_{\alpha,\beta} \lambda^{1/\alpha}. \tag{19}$$

When summands $\{X_i, i \geq 1\}$ are attracted to the asymmetric stable law $G_{\alpha,-1}$, then the approximating process for $D(t) = S(N(t))$ is a stable process $Y_{\alpha,-1}(t)$ without positive jumps, whose rate of growth can be successfully investigated with the help of certain integral test. Combining this fact with the SIP-type Theorem 2 or Theorem 3, we get

Theorem 9. *Let* $\{X_i, i \geq 1\}$ *satisfy* ***(C)*** *with* $1 < \alpha_1 < 2$, $\beta = -1$ *and* $EZ_1^2 < \infty$ *or* $\{Z_i, i \geq 1\}$ *satisfy* ***(C)*** *with* $1 < \alpha_2 < 2$, $\alpha_1 < \alpha_2$, $|\beta| \leq 1$. *Then* $f(t) = t^{1/\alpha} h(t)$, *where regular* $h(t) \uparrow \infty$, *will be an upper function for* $D(t)$, *if*

$$I_3(h) = \int_1^\infty t^{-1} h^{-\theta_1/2}(t) \exp\{-B_1 h^\theta(t)\} dt < \infty,$$

where

$$B_1 = B(\alpha_1) = (\alpha_1 - 1)\alpha_1^{-\theta_1} |\cos(\pi\alpha_1/2)|^{1/(\alpha_1 - 1)}, \quad \theta_1 = \alpha_1/(\alpha_1 - 1), \tag{20}$$

and $f(t)$ *will be a lower function if* $I_3(h) = \infty$.

As a consequence we easily obtain following modification of the LIL.

Corollary 9. *Let* $\{X_i, i \geq 1\}$ *satisfy* ***(C)*** *with* $1 < \alpha < 2$, $\beta = -1$. *Assume that* $EZ_1^2 < \infty$. *Then a.s.*

$$\limsup_{t\to\infty} \frac{S(N(t)) - m\lambda t}{t^{1/\alpha}(B^{-1}\ln\ln t)^{1/\theta}} = \lambda^{1/\alpha}, \tag{21}$$

$$B = B(\alpha) = (\alpha-1)\alpha^{-\theta}|\cos(\pi\alpha/2)|^{1/(\alpha-1)}, \quad \theta = \alpha/(\alpha-1). \tag{22}$$

Corollary 10. *Corollaries 3 – 9 are true when* $N(t)$ *is a homogeneous Poisson process with intensity* $\lambda > 0$.

4 How big are increments of the random sums?

Partial answer on this question also can be obtained with the help of the SIP-type results for compound renewal processes (as it will be demonstrated below). More precisely, we consider increments $D(T + a_T) - D(T) = S(N(T + a_T)) - S(N(T))$ and study its' asymptotics, when a_T grows as $T \to \infty$, but not faster then T. A number of results in this area (but only for *independent summands*) were obtained by Zinchenko and Safonova[10], who proved various modifications of Erdös-Rényi-Csörgő-Révész law [3] for increments of random sums using appropriate SIP-type results. Remarkable progress in studying the magnitude of increments of compound renewal processes was achieved by Frolov[6], Martikainen and Frolov[8] with the help of other methods. The case of *dependent* summands was studied in [16], where the detail proofs of the following theorems are presented. Notice that assumptions on $\{X_i, i \geq 1\}$ and $\{Z_i, i \geq 1\}$, which determine the form of approximating process and error term, have impact on the possible length of intervals a_T under consideration.

4.1. Summands with finite variance. We start with the case of i.i.d. r.v. with "light tails" , when $\{X_i\}$ and $\{Z_i\}$ satisfy Cramer's condition. In this case the approximating process is a standard Wiener process and error is the smallest, i.e. $O(\ln T)$, so a_T may increase in a slowest rate.

Theorem 10. *Let* $\{X_i, i \geq 1\}$ *and* $\{Z_i, i \geq 1\}$ *be independent sequences of i.i.d.r.v.,* $EX_1 = m$, $varX_1 = \sigma^2$, $EZ_1 = 1/\lambda > 0$, $varZ_1 = \tau^2$,

$$E\exp(uX_1) < \infty, \quad E\exp(uZ_1) < \infty, \ \text{as } |u| < u_0, u_0 > 0, \tag{23}$$

function $a_T, T \geq 0$ *satisfies following conditions:* $0 < a_T < T$ *and* T/a_T *does not decrease in* T. *Also assume that*

$$a_T/\ln T \to \infty \ \text{as } T \to \infty. \tag{24}$$

Then a.s.

$$\limsup_{T\to\infty} \frac{|D(T + a_T) - D(T) - m\lambda a_T|}{\gamma(T)} = \nu, \tag{25}$$

where $\nu^2 = \lambda\sigma^2 + \lambda^3 m^2\tau^2$, $\gamma(T) = \{2a_T(\ln\ln T + \ln T/a_T)\}^{1/2}$.

For concrete $a_T = T^\rho, 0 < \rho < 1$ or $a_T = \ln T^\rho$, $\rho > 1$ we have:

Corollary 11. *Let $\{X_i, i \geq 1\}$ and $\{Z_i, i \geq 1\}$ be the same as in Theorem 10. Then a.s.*

$$\limsup_{T\to\infty} \frac{|D(T+T^\rho) - D(T) - m\lambda T^\rho|}{(2(1-\rho)T^\rho \ln T)^{1/2}} = \nu, \quad \rho < 1,$$

$$\limsup_{T\to\infty} \frac{|D(T+(\ln T)^\rho) - D(T) - m\lambda (\ln T)^\rho|}{\left(2\ln^{(\rho+1)} T\right)^{1/2}} = \nu, \quad \rho > 1.$$

The weaker moment conditions lead to more restrictive conditions on the rate of growth of a_T.

Theorem 11. *Let $\{X_i, i \geq 1\}$, $\{Z_i, i \geq 1\}$ and a_T satisfy all conditions of previous theorem with following assumptions used instead of (26)*

$$EX_1^{p_1} < \infty, \quad p_1 > 2, \quad EZ_1^{p_2} < \infty, \quad p_2 > 2.$$

Then (28) is true if $a_T > c_1 T^{2/p}/\ln T$ for some $c_1 > 0$, $p = \min\{p_1, p_2\}$.

Auxiliary SIP-type theorems are also useful in the case of *dependent* summands (discussed in Section 2). For example, Theorem 5 or Corollary 2 yield

Theorem 12. *Let $N(T)$ be homogeneous Poisson process with intensity $\lambda > 0$ and let $\{X_i\}$ be the strictly stationary associated sequence with mean $EX_1 = m$ and covariance, satisfying sufficient conditions for SIP (Theorem 5). Suppose that function $a_T, T \geq 0$ satisfies all conditions of Theorem 10 and $a_T > c_1 T^{2/p}/\ln T$ for some $c_1 > 0$, $1/p = (1/2) - \vartheta$, $\vartheta > 0$. Then a.s.*

$$\limsup_{T\to\infty} \frac{|S(N(T+a_T)) - S(N(T)) - m\lambda a_T|}{\gamma(T)} = \nu, \tag{26}$$

where $\nu^2 = \lambda(\sigma_2^2 + m^2)$, $\gamma(T) = \{2a_T(\ln\ln T + \ln T/a_T)\}^{1/2}$.

4.2. Summands attracted to the stable law. When i.i.d.r.v. $\{X_i, i \geq 1\}$ are attracted to an asymmetric stable we have

Theorem 13. *Suppose that $\{X_i, i \geq 1\}$ satisfy (**C**) with $1 < \alpha < 2$, $\beta = -1$, $EZ_1^2 < \infty$, $EX_1 = m$, $EZ_1 = 1/\lambda > 0$. Function a_T is non-decreasing, $0 < a_T < T$, T/a_T is also non-decreasing and provides ${d_T}^{-1} T^{1/\alpha - \varrho_2} \to 0$ for certain $\varrho_2 > 0$ determined by the error term in SIP-type Theorem 2. Then a.s.*

$$\limsup_{T\to\infty} \frac{D(T+a_T) - D(T) - m\lambda a_T}{d_T} = \lambda^{1/\alpha}, \tag{27}$$

where normalizing function $d_T = a_T^{1/\alpha}\{B^{-1}(\ln\ln T + \ln T/a_T)\}^{1/\theta}$, constants B, θ are defined in (20).

5 How small are increments of the random sums?

SIP-type results can help in solution of this problem too. For instance, combining conclusions of Theorem 1 and corresponding facts for a Wiener process (Csörgő and Révész[3]), we have following statement, which holds when summands $\{X_i\}$ as well as inter-occurrence times $\{Z_i\}$ satisfy the Cramer's condition:

Corollary 12. *Assume that i.i.d.r.v. $\{X_i, i \geq 1\}$ and $\{Z_i, i \geq 1\}$ satisfy all conditions of the Theorem 10, $\nu^2 = \lambda\sigma^2 + \lambda^3 m^2 \tau^2$ and $a_T(\ln T)^{-3} \to \infty$ as $t \to \infty$, then a.s.*

$$\lim_{T\to\infty} \gamma(T, a_T) \inf_{0\leq t\leq T-a_T} \sup_{0\leq s\leq a_T} |D(t+s) - D(t) - m\lambda a_T| = \nu. \tag{28}$$

6 Applications in risk theory

6.1. Sparre-Anderssen collective risk model. Within this model (rather popular in the actuarial mathematics) the risk process, which describes the evolution of reserve capital, is defined as

$$U(t) = u + ct - \sum_{i=1}^{N(t)} X_i = u + ct - S(N(t)), \tag{29}$$

where: $u \geq 0$ denotes an initial capital; $c > 0$ stands for the gross premium rate; renewal (counting) process $N(t) = \inf\{n \geq 1 : \sum_{i=1}^{n} Z_i > t\}$ counts the number of claims to insurance company in time interval [0,t]; positive i.i.d.r.v. $\{Z_i, i \geq 1\}$ are time intervals between claim arrivals; positive i.i.d.r.v.$\{X_i\}$ with d.f. $F(x)$ denote claim sizes; the sequences $\{X_i, i \geq 1\}$ and $\{Z_i, i \geq 1\}$ are independent; $EX_1 = m$, $EZ_1 = 1/\lambda > 0$.

Classical Cramér-Lundberg risk model is model (29), where $N(t)$ is a homogeneous Poisson process with intensity $\lambda > 0$.

In the framework of collective risk model random sum $D(t) = \sum_{i=1}^{N(t)} X_i = S(N(t))$ can be interpreted as a total claim amount arising during time interval $[0, t]$, and increments

$$D(T + a_T) - D(T) = \sum_{i=N(T)+1}^{N(T+a_T)} X_i$$

as claim amounts during the time interval $[T, T + a_T]$.

Since process $D(t)$ is a typical example of the compound renewal process (compound Poisson process in Cramér-Lundberg model), main results of the Sections 2 – 5 can be applied to investigation of the risk process $U(t)$. Fist of all, Theorems 1 – 3 yield the SIP-type results for $D(t)$ and $U(t)$ under various assumptions on the claim sizes $\{X_i, i \geq 1\}$ and inter-arrival times $\{Z_i, i \geq 1\}$.

For small claims and $\{Z_i\}$ satisfying Cramér's condition, processes $D(t)$ and $U(t)$ admit strong approximation by a Wiener process with the error term $O(\ln t)$; for large claims with finite moments of order $p > 2$ the error term is $o(t^{1/p})$, if $p = 2$ then error term is $o((t \ln \ln t)^{1/2})$. For catastrophic events claims can be so large that their variance is infinite. In this case we assume that $\{X_i\}$ are in domain of normal attraction of asymmetric stable law $G_{\alpha,1}$ with $1 < \alpha < 2$, $\beta = 1$, and additionally satisfy condition (C). Then by Theorems 2,3 an approximating process for $D(t)$ is α-stable process $Y_{\alpha,1}$ with $1 < \alpha < 2$, $\beta = 1$, and risk (reserve) process $U(t)$ admits a.s. approximation by α-stable process $Y_{\alpha,-1}$, $1 < \alpha < 2$, $\beta = -1$, which has only negative jumps; the error term is presented in mentioned theorems.

The form of error term in SIP is "good" enough for investigation the rate of growth of total claims and asymptotic behavior of the reserve process. Due to results of Section 3 various modifications of the LIL for $D(T)$ can be obtained almost without a proof. So, in the case of small claims (satisfying Cramér's condition) or large claims (but with finite moments of order $p \geq 2$) for large t we can a.s. indicate upper/lower bounds for growth of total claim amounts $D(t)$ as $m\lambda t \pm \nu\sqrt{2t \ln \ln t}$ and for reserve capital $U(t)$ as $u + t\rho m\lambda \pm \nu\sqrt{2t \ln \ln t}$, where $\sigma^2 = VarX_1$, $\tau^2 = VarZ_1$, $\nu^2 = \lambda\sigma^2 + \lambda^3 m^2 \tau^2$, $\rho = (c - \lambda m)/\lambda m > 0$ is a safety loading.

For large claims in domain of normal attraction of asymmetric stable law $G_{\alpha,1}$ with $1 < \alpha < 2$, $\beta = 1$ (for instance, Pareto type r.v. with $1 < \alpha < 2$) Corollary 9 for large t provides a.s. upper bound for the risk process

$$U(t) \leq u + \rho m\lambda t + \lambda^{1/\alpha} t^{1/\alpha} (B^{-1} \ln \ln t)^{1/\theta}.$$

SIP-type results also help to answer on the question: how large can be fluctuations of the total claims/payments on the intervals whose length a_T increases as $T \to \infty$. Indeed, under appropriate conditions on claim size distributions and for rather "large" intervals a_T (but growing not faster then T) increments $D(T + a_T) - D(T)$ satisfy variants of Erdös-Rényi-Csörgő-Révész LLN similarly to (25) or (27). More results in this direction are presented in [12], [14].

Until recently, main known results concerning $U(t)$ and $D(t)$ were focused on the case of *independent* claim sizes $\{X_i, i \geq 1\}$. Our approach allows to study the case of *dependent* claims too. Thus, certain results about strong approximation of the risk process and approximation of ruin probabilities, bounds for rates of growth and fluctuations of total claim amounts in the case of weakly φ-mixing and associated r.v. (studied in Section 2) can be obtained similar to how it was done for independent summands. Our general approach also gives a possibility to study also more complicated risk models with stochastic premiums.

6.2. Risk process with stochastic premiums. Within the *risk model with stochastic premiums* the risk process $U(t)$, $t \geq 0$, is defined as

$$U(t) = u + Q(t) = u + \Pi(t) - S(t) = u + \sum_{i=1}^{N_1(t)} y_i - \sum_{i=1}^{N(t)} x_i, \tag{30}$$

where: $u \geq 0$ is an initial capital; point process $N(t)$ models the number of claims in the time interval $[0, t]$; positive r.v. $\{x_i : i \geq 1\}$ are claim sizes; $Ex_1 = \mu_1$; point process $N_1(t)$ is interpreted as a number of polices bought during $[0, t]$; r.v. $\{y_i : i \geq 1\}$ stand for sizes of premiums paid for corresponding polices, $Ey_1 = m_1$.

We call $U(t)$ (or $Q(t)$) the ***Cramér-Lundberg risk process with stochastic premiums*(CLSP)** if $N(t)$ and $N_1(t)$ are two independent *Poisson processes* with intensities $\lambda > 0$ and $\lambda_1 > 0$; $\{x_i\}$ and $\{y_i\}$ are two sequences of positive i.i.d.r.v. independent of the Poisson processes and of each other with d.f. $F(x)$ and $G(x)$, respectively, $\lambda_1 E y_1 > \lambda E x_1$.

This model, being a natural generalization of the classical Cramér -Lundberg risk model, was studied by Zinchenko and Andrusiv [11]. Korolev *et al.* [7] present an interesting example of using (30) for modeling the speculative activity of money exchange point and optimization of its profit.

Notice that process $Q(t) = \Pi(t) - S(t)$ is again a compound Poisson process with intensity $\lambda^* = \lambda + \lambda_1$ and d.f. of the jumps $G^*(x) = \frac{\lambda_1}{\lambda^*} G(x) + \frac{\lambda}{\lambda^*} F^*(x)$, where $F^*(x)$ is a d.f. of the random variable $-x_1$. In the other words

$$Q(t) = \sum_{i=1}^{N^*(t)} \xi_i, \tag{31}$$

where $N^*(t)$ is homogeneous Poisson process with intensity $\lambda^* = \lambda + \lambda_1$ and i.i.d.r.v. ξ_i have d.f. $G^*(x)$.

Thus, all results for compound Poisson process, obtained in Sections 2 – 5, are applicable to $Q(t)$. For instance, we have following SIP-type results:

Theorem 14 (SIP for CLSP, finite variance case). *(I)If in model (30) both premiums $\{y_i\}$ and claims $\{x_i\}$ have moments of order $p > 2$, then there is a standard Wiener process $\{W(t), t \geq 0\}$ such that a.s.*

$$\sup_{0 \leq t \leq T} |Q(t) - (\lambda_1 m_1 - \lambda \mu_1)t - \tilde{\sigma} W(t)| = o(T^{1/p}), \quad \tilde{\sigma}^2 = \lambda_1 m_2 + \lambda \mu_2. \tag{32}$$

(II) If premiums $\{y_i\}$ and claims $\{x_i\}$ are light-tailed with finite moment generating function in some positive neighborhood of zero, then a.s.

$$\sup_{0\le t\le T} |Q(t) - (\lambda_1 m_1 - \lambda\mu_1)t - \tilde{\sigma}W(t)| = O(\log T), \tag{33}$$

Proof immediately follows from Corollary 1 since $Q(t)$ is a compound Poisson process (see (31)) with intensity $\lambda^* = \lambda + \lambda_1$, whose jumps have mean $\frac{\tilde{a}}{\lambda^*} = \frac{\lambda_1}{\lambda^*} m_1 - \frac{\lambda}{\lambda^*}\mu_1$, and second moment $\frac{\tilde{\sigma}^2}{\lambda^*} = \frac{\lambda_1}{\lambda^*} m_2 + \frac{\lambda}{\lambda^*}\mu_2$.

For catastrophic accidents claims can be so large that they have infinite variance, i.e. belong to the domain of attraction of a certain stable law. Thus, due to Theorem 2, for Cramér-Lundberg risk process with stochastic premiums we have:

Theorem 15 (SIP for CLSP, large claims attracted to α-stable law). *Suppose that claim sizes $\{x_i\}$ satisfy **(C)** with $1 < \alpha < 2$, $\beta \in [-1, 1]$, premiums $\{y_i\}$ are i.i.d.r.v. with finite variance, then a.s.*

$$\left|Q(t) - (\lambda_1 m_1 - \lambda\mu_1)t - (\lambda + \lambda_1)^{1/\alpha} Y_{\alpha,\beta}(t)\right| = o(t^{1/\alpha - \varrho_2}), \quad \rho_2 \in (0, \rho_0), \tag{34}$$

for some $\varrho_0 = \varrho_0(\alpha, l) > 0$.

On the next step we focus on investigation the rate of growth of risk process $Q(t)$ as $t \to \infty$ and its increments $Q(t+a_t) - Q(t)$ on intervals whose length a_t grows but not faster than t. Again the key moments are representation of $Q(t)$ as compound Poisson process (31), Theorems 14, 15 and application of the results obtained in Sections 3–5, namely, various modifications of the LIL and Erdös-Rényi-Csörgő-Révész law for compound Poisson processes.

Corollary 13 (LIL for CLSP). *If in model (30) both premiums $\{y_i\}$ and claims $\{x_i\}$ have moments of order $p \ge 2$, then*

$$\limsup_{t\to\infty} \frac{|Q(t) - \tilde{a}t|}{\sqrt{2t \ln\ln t}} = \tilde{\sigma}, \text{ where } \tilde{a} = \lambda_1 m_1 - \lambda\mu_1, \quad \tilde{\sigma}^2 = \lambda_1 m_2 + \lambda\mu_2.$$

Next we shall consider the case when r.v. $\{x_i, i \ge 1\}$ in CLSP-model (30) are attracted to an asymmetric stable law $G_{\alpha,1}$, but premiums have $Ey_1^2 < \infty$. Theorem 9 and Corollary 9 yield following statement:

Corollary 14. *Let $\{x_i, i \ge 1\}$ satisfy condition **(C)** with $1 < \alpha < 2$, $\beta = 1$ and $Ey_1^2 < \infty$. Then a.s.*

$$\limsup_{t\to\infty} \frac{Q(t) - (\lambda_1 m_1 - \lambda\mu_1)t}{t^{1/\alpha}(B^{-1}\ln\ln t)^{1/\theta}} = (\lambda + \lambda_1)^{1/\alpha},$$

where $B = B(\alpha) = (\alpha - 1)\alpha^{-\theta}|\cos(\pi\alpha/2)|^{1/(\alpha-1)}$, $\theta = \alpha/(\alpha - 1)$.

Corollary 15 (Erdös-Rényi-Csörgő-Révész law for CLSP-model). *Let in CLSP-model claims $\{x_i, i \ge 1\}$ and premiums $\{y_i, i \ge 1\}$ be independent sequences of i.i.d.r.v. with $Ex_1 = m$, $Varx_1 = \sigma^2$, $Ey_1 = 1/\lambda > 0$, $Vary_1 = \tau^2$, and finite moment generating functions*

$$E\exp(ux_1) < \infty, \quad E\exp(uy_1) < \infty \text{ as } |u| < u_0, \quad u_0 > 0.$$

Assume that non-decreasing function a_T, $T \ge 0$, satisfies all conditions of Theorem 13, then a.s.

$$\limsup_{T\to\infty} \frac{|Q(T + a_T) - Q(T) - a_T(\lambda_1 m_1 - \lambda\mu_1)|}{\gamma(T)} = \tilde{\sigma},$$

where $\gamma(T) = \{2a_T(\ln\ln T + \ln T/a_T)\}^{1/2}$, $\tilde{\sigma}^2 = \lambda_1 m_2 + \lambda\mu_2$.

Remark. General Sip-type theorems give also the possibility to investigate more general cases when $\{y_i\}$ and $\{x_i\}$ are sequences of dependent r.v., for example, associated or weakly dependent, $N(t)$ and $N_1(t)$ can be renewal processes, Cox processes, ets. Partly, such problems were solved in [12].

References

1. A.V. Bulinski, A.P. Shashkin. *Limit theorems for associated random fields and related systems*, Fizmatlit, Moscow, 2008.
2. M. Csörgő, L. Horváth. *Weighted Approximation in Probability and Statistics*, Wiley, New York, 1993.
3. M. Csörgő, P. Révész. *Strong Approximation in Probability and Statistics*, Acad. Press, New York, 1981.
4. M. D. Donsker, S. R. Varadhan. On LIL for local times. *Communs. Pure and Appl. Math.* 30, N 6, 707–753, 1977.
5. B.V. Gnedenko, V.Yu. Korolev. *Random Summation: Limit Theorems and Applications*, CRT Press, Boca - Raton, Florida, 1996.
6. A. Frolov. Strong limit theorems for increments of compound renewal processes. *Journal of Math. Sciences* 152, 944–957, 2008.
7. V. Korolev, V. Bening, S. Shorgin. *Mathematical Foundations of Risk Theory*, Fizmatlit, Moscow, 2007.
8. A. Martikainen, A. Frolov. On the Chung law for compound renewal processes. *Journal of Math. Sciences*, 145, N 2, 4866–4870, 2007.
9. W. Philipp, W. Stout. Almost sure invariance principle for partial sums of weakly dependent random variables. *Mem. of Amer. Math. Society*, 161, 151p., 1975.
10. N. Zinchenko, M. Safonova. Erdös-Renyi type law for random sums with applications to claim amount process. *Journal of Numerical and Applied Mathematics* 1(96), 246–264, 2008.
11. N. Zinchenko, A. Andrusiv. Risk processes with stochastic premiums. *Theory of Stoch. Processes* 14, no 3–4 , 189–208, 2008.
12. N. Zinchenko. Strong limit theorems for the risk process with stochastic premiums. *Markov Processes and Related Fields*, 20, pp. 527-544, 2014.
13. N. Zinchenko. Strong invariance principle for a superposition of random processes. *Theory of Stoch. Processes* 16(32), 130–138, 2010.
14. N. Zinchenko. Almost sure approximation of the superposition of the random processes. *Methodology and Computing in Applied Probability*, 17, pp. 235-250, 2015.
15. N. Zinchenko. Random Sums of Dependent Random Variables: Strong Limit Theorems and Applications. *Proceedings of 16-th Applied Stochastic Models and Data Analysis International Conference (ASMDA) and the 4th Demographics Workshop*, Piraeus, Greece, 1091-1100, 2015.
16. N. Zinchenko. On the Asymptotics of the Random Sums. *Proceedings of the 4th Stochastic Modeling Techniques and Data Analysis International Conference with Demographics Workshop*, Valletta, Malta, ISAST, 565 - 575, 2016.
17. H. Yu. A strong invariance principle for associated sequences. *Annals of Probability*, 24, 4, 2079–2097, 1996.